HANDBOOK OF RADICAL POLYMERIZATION

Krzysztof Matyjaszewski

Carnegie Mellon University, Pittsburgh, Pennsylvania

Thomas P. Davis

University of New South Wales, Sydney, Australia

CONTENTS

INTRODUCTION

Free radical polymerization has been an important technological area for seventy years. As a synthetic process it has enabled the production of materials that have enriched the lives of millions of people on a daily basis. Free radical polymerization was driven by technological progress, and its commercialization often preceded scientific understanding. For example, polystyrene and poly(methyl methacrylate) were in commercial production before many of the facets of the chain polymerization process were understood.

The period 1940–1955 were particularly fruitful in laying down the basis of the subject; eminent scientists such as Mayo and Walling laid the framework that still appears in many textbooks. This success led some scientists at the time to conclude that the subject was largely understood. For example, in the preface to Volume 3 of the *High Polymers Series on the Mechanism of Polymer Reactions* in 1954, Melville stated ''In many cases it is true to say that the kinetics and chemistry of the reactions involved have been as completely elucidated as any other reaction in chemistry, and there is not much to be written or discovered about such processes.''

From 1955 through to 1980 scientific progress was incremental, bearing out (to some limited extent) the comments made by Melville. The ability to measure rate constants accurately was limited by scientific methods and equipment. Measuring molecular weights by light scattering and osmometry was time-consuming and did not provide a visualization of the shape of the molecular weight distribution. Techniques such as rotating sector were laborious, and there were significant inconsistencies among propagation and termination rate data obtained from different groups. Indeed an IUPAC working group set up under the leadership of Dr. Geoff Eastmond had great difficulty in getting agreement among experimental rate data (via dilatometry) from different laboratories. This inability to obtain accurate and consistent kinetic data has been a major impediment to developing improved control over conventional free radical polymerization, and has led to the cynical (though amusing) labeling of the *Polymer Handbook* as the 'book of random numbers.' Despite these difficulties, some notable progress was made in understanding the importance of diffusion control in termination reactions and in elucidating the mechanisms of emulsion polymerization.

In the 1980s industrial and academic attention was focused on polymerization mechanisms that offered the prospect of greater control, such as cationic and anionic chain reactions. The scope of these reactions was expanded, and group transfer polymerization was invented and heralded as a major breakthrough. At that time, major investments in research and scale up were made by polymer producing companies in

an attempt to exploit the greater control offered by these improved ionic polymerizations. However, the limitations of ionic processes—intolerance to functionality and impurities—proved too difficult to overcome, and free radical polymerization proved stubborn to displace as an industrial process. The commercial driving force behind the search for control over the polymerization mechanism was the prospect of improved materials. The ability to make specific (bespoke) polymer architectures remained a powerful incentive to develop new polymerization methods. However, the lesson learned from the failure to exploit ionic mechanisms was that improved control could not come at the expense of flexibility. Consequently, free radical polymerization remained dominant because it was (relatively) easy to introduce on an industrial plant, it was compatible with water, and it could accommodate a wide variety of functional monomers.

From the mid-1980s step changes in the understanding and exploitation of free radical polymerization began to occur. The mechanism of copolymerization came under scrutiny and the general failure of the terminal model was demonstrated. Advanced laser techniques were invented to probe propagation and termination rate coefficients. This ability to accurately measure rate constants led to the establishment of IUPAC working parties to set benchmark kinetic values, and thus enhanced the ability to create computational models to predict and control free radical polymerization reactions. The cost of computation reduced substantially, and advanced modeling methods began to be applied to free radical polymerization, leading to increased understanding of the important factors governing free radical addition and transfer reactions.

Also in the 1980s the seeds were laid for an explosion in the exploitation of free radical polymerization to make specific polymer architectures by using control agents. Catalytic chain transfer (using cobalt complexes) was discovered in the USSR and subsequently developed and exploited to produce functional oligomers by a number of companies. The use of iniferters was pioneered in Japan and alkoxyamines were patented as control agents by CSIRO.

The major growth of living (or controlled) free radical polymerization occurred in the 1990s, commencing around 1994 with the exploitation of nitroxide-mediated polymerization, atom transfer radical polymerization, degenerative transfer with alkyl iodides, and addition-fragmentation transfer approaches allowing for the facile production of a multitude of polymer architectures from simple narrow polydispersity chains to more complex stars, combs, brushes, and dendritic structures. Moreover, synthesis of block and gradient copolymers enabled preparation of many nanophase separated materials.

This book aims to capture the explosion of progress made in free radical polymerization in the past 15 years. Conventional radical polymerization (RP) and living radical polymerization (LRP) mechanisms receive extensive coverage together with all the other important methods of controlling aspects of radical polymerization. To provide comprehensive coverage we have included chapters on fundamental aspects of radical reactivity and radical methods in organic synthesis, as these are highly relevant to the chemistry and physics underpinning recent developments in our understanding and exploitation of conventional and living free radical

polymerization methods. The book concludes with a short chapter on the areas of research and commercial development that we believe will lead to further progress in the near future.

KRZYSZTOF MATYJASZEWSKI
THOMAS P. DAVIS

CONTRIBUTORS

CHRISTOPHER BARNER-KOWOLLIK,   School of Chemical Engineering and Industrial Chemistry, The University of New South Wales, UNSW Sydney NSW 2052, Australia

STEFAN A. F. BON,   Center for Supramolecular and Macromolecular Chemistry, Department of Chemistry, University of Warwick, Coventry CV4 7AL, United Kingdom

JOHN CHIEFARI,   CSIRO Molecular Science, Bag 10, Clayton South, Victoria 3169, Australia

MICHELLE COOTE,   Room 513/514, Applied Science Building, School of Chemical Engineering and Industrial Chemistry, University of New South Wales, Sydney NSW 2052, Australia

MICHAEL F. CUNNINGHAM,   P. Eng., Department of Chemical Engineering, Queen's University, Kingston, Ontario, Canada K7L 3N6

THOMAS P. DAVIS,   Room 513/514, Applied Science Building, School of Chemical Engineering and Industrial Chemistry, University of New South Wales, Sydney NSW 2052, Australia

TAKESHI FUKUDA,   Institute for Chemical Research, Kyoto University, Uji, Kyoto 611-0011, Japan

YVES GNANOU,   Director, Laboratoire de Chimie des Polymeres Organiques, Ecole Nationale de Chimie et de Physique de Bordeaux, Ave Pey-Berland, BP108, 33402, Talence Cedex, France

ATSUSHI GOTO,   Institute for Chemical Research, Kyoto University, Uji, Kyoto 611-0011, Japan

DAVID M. HADDLETON,   Center for Supramolecular and Macromolecular Chemistry, Department of Chemistry, University of Warwick, Coventry CV4 7AL, United Kingdom

CRAIG J. HAWKER,   Department K17f, IBM Almaden Research Center, 650 Harry Road, San Jose, CA 95120-6099, USA

HANS HEUTS,   School of Chemical Engineering and Industrial Chemistry, University of New South Wales, Sydney NSW 2052, Australia

ROBIN HUTCHINSON, Department of Engineering, University of Manitoba, 344A Engineering Bldg., Winnipeg R3T 5V6, Canada

AKIKAZU MATSUMOTO, Department of Applied Chemistry, Faculty of Engineering, Osaka City University, Sugimoto, Sumiyoshi-ku, Osaka 558-8585, Japan

KRZYSZTOF MATYJASZEWSKI, J. C. Warner Professor of Natural Sciences, Department of Chemistry, Carnegie Mellon University, 4400 Fifth Avenue, Pittsburgh, PA 15213, USA

MICHAEL MONTEIRO, Eindhoven University of Technology, P.O. Box 513, 5600 MB Eindhoven, The Netherlands

MARTIN NEWCOMB, LAS Distinguished Professor, Department of Chemistry (MC 111), University of Illinois at Chicago, 845 West Taylor Street, Chicago, IL 60607-7061, USA

EZIO RIZZARDO, Chief Research Scientist, CSIRO Molecular Science, Bag 10, Clayton South, Victoria 3169, Australia

DANIEL TATON, Laboratoire de Chimie des Polymeres Organiques, Ecole Nationale de Chimie et de Physique de Bordeaux, Ave Pey-Berland, BP108, 33402, Talence Cedex, France

YOSHINOBU TSUJII, Institute for Chemical Research, Kyoto University, Uji, Kyoto 611-0011, Japan

PHILIPP VANA, University of New South Wales, School of Chemical Engineering and Industrial Chemistry, Centre for Advanced Macromolecular Design, Sydney NSW 2052, Australia

ALEX M. VAN HERK, Eindhoven University of Technology, PO Box 513, 5600 MB Eindhoven, The Netherlands

JIANHUI XIA, Department of Chemistry, Carnegie Mellon University, Pittsburgh, PA 15213, USA

BUNICHIRO YAMADA, Material Chemistry Laboratory, Faculty of Engineering, Osaka City University, Sugimoto, Sumiyosaka 558, Japan

PER BO ZETTERLUND, Department of Applied Chemistry, Graduate School of Engineering, Osaka City University, 3-3-138 Sugimoto, Sumiyoshi-ku, Osaka 558-8585, Japan

1 Theory of Radical Reactions

JOHAN P. A. HEUTS

University of New South Wales, Sydney, Australia

CONTENTS

1.1 INTRODUCTION

Free-radical polymerization proceeds via a chain mechanism, which basically consists of four different types of reactions involving free radicals:[1] (1) radical generation from nonradical species (initiation), (2) radical addition to a substituted alkene (propagation), (3) atom transfer and atom abstraction reactions (chain transfer and termination by disproportionation), and (4) radical–radical recombination reactions (termination by combination). It is clear that a good process and product

control (design) requires a thorough knowledge of the respective rates of these reactions, and, preferably, a knowledge about the physics governing these rates.

In this chapter, the role that theoretical chemistry has played and can play in further elucidating the physical chemistry of these important radical reactions will be discussed. We often wish to answer questions that cannot be addressed directly through experiments, such as ''Why does this reaction follow pathway A instead of pathway B?'' or ''How will a particular substituent affect the rate of a reaction?'' In many cases, the required information needs to be extracted from elaborate experiments that address the question in an indirect way, involving many assumptions and/or simplifications; in other cases, the required information is simply impossible to obtain by current state-of-the-art experimental techniques. In such instances, theoretical chemistry, and in particular computational quantum chemistry, can provide the chemist with the appropriate tools to address the problems directly. This is particularly true for radical reactions (where the reactive intermediates are very short-lived) and for obtaining information about the transition state of a reaction; the importance and difficulties in obtaining information regarding transition structures are evidenced by the award of the 1999 Nobel Prize for Chemistry to Zewail.[2] The advent of increasingly powerful computers and user-friendly computational quantum-chemistry software make computational chemistry more accessible to the nontheoretician, and it is the aim of this chapter to provide the reader with some insight into the theory and applications of theoretical chemistry in radical polymerization. This chapter is not intended to be a rigorous introduction to theoretical chemistry, but rather aims at simple qualitative explanations of fundamental theoretical concepts so as to make the theoretical literature more accessible to the nontheoretician. The reader interested in more rigorous introductions is referred to some excellent textbooks and reviews on the various topics: transition state theory,[3–9] statistical mechanics,[10] quantum chemistry,[11–14] and organic reactivity.[15–20]

First, the framework provided by the pioneers in free-radical polymerization will be discussed, as this framework has been a guide to the polymer scientist for the past decades and has provided us with a working understanding of free-radical polymerization.[21] This discussion will then be followed by an outline of chemical dynamics and quantum-chemical models, which can provide us with a physically more realistic picture of the physics underlying the reactions of concern. With the seemingly ever-increasing computation power, these methods will become increasingly accurate and applicable to the systems of interest to the polymer chemist. Unfortunately, this ready availability may also lead to incorrect uses of theoretical models. With this in mind, the chemical dynamics and quantum-chemical sections were written in such a way to enable the nontheoretician to initiate theoretical studies and interpret their results. Realizing that many quantitative aspects of this chapter may be replaced by more accurate computational data within a few years (months?) after publication of this book, the discussion will focus on general aspects of the different computational procedures and in which situations particular procedures are useful. Several different examples will be discussed where theory has provided us with information that is not directly experimentally accessible and where future opportunities lie for computational studies in free-radical polymerization.

1.2   CLASSICAL THEORIES OF MONOMER AND RADICAL REACTIVITY

Although great progress has been made since the early 1980s in understanding radical reactivity, there seems to be a tendency among polymer chemists to think in models about radical and monomer reactivity which were laid down in the sixties and early 1970s.[21] Since these models have greatly influenced our thinking and the development of polymer science, they will be briefly discussed here.[1,21]

Traditionally, the reactivities of monomers and radicals have been studied by means of copolymerization data. In a series of monomer pairs {A, B} with fixed monomer A, the series of respective $1/r_A$ values represents a series of relative reactivities of these monomers B toward a radical $\sim A^{\bullet}$ (see Scheme 1.1).

These studies and early studies on small radicals have led to the current framework in which we tend to think about radical and monomer reactivities. The factors that govern the reactivity are generally summarized in the following four features: (1) polar effects, (2) steric effects, (3) (resonance) stabilization effects, and (4) thermodynamic effects.[1,21]

1. *Polar Effects.* From the numerous observations that nucleophilic radicals readily react with electrophilic monomers (and vice versa), it is concluded that polar effects can be very important in radical reactions. The importance of polar effects has been well established since the early 1980s through both experimental and theoretical studies.

2. *Steric Effects.* Perhaps the most convincing observations that steric effects play an important role in radical reactions is that the most common propagation reaction is a head-to-tail addition and that head-to-head additions hardly ever occur. Furthermore, several studies to date indicate that 1,2-disubstituted alkenes do not readily homopolymerize (although they might copolymerize quite readily), which could possibly be attributed to steric hindrance.

3. *Stabilization Effects.* These effects can arise if delocalization of the unpaired electron in the reactant and product radicals is possible. If the reactant radical has a highly delocalized electron, it will be relatively stable and have a relatively low reactivity. On the other hand, if the addition of a monomer will lead to a radical that has a highly delocalized electron, it is said that the monomer is relatively more reactive. In general, the order of reactivity of a range of monomers is the reverse of the order of reactivity of their respective derived radicals.

$$\left.\begin{array}{lll} \sim A^{\bullet} \;+\; A & \xrightarrow{\; k_{AA} \;} & \sim AA^{\bullet} \\[4pt] \sim A^{\bullet} \;+\; B & \xrightarrow{\; k_{AB} \;} & \sim AB^{\bullet} \end{array}\right\} \qquad r_A = \dfrac{k_{AA}}{k_{AB}}$$
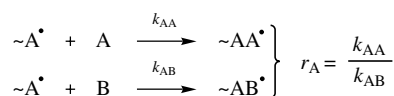
Scheme 1.1

4. *Thermodynamic Effects.* These effects can be ascribed to differences in the relative energies between reactants and products, lowering or increasing the reaction barrier. For many reactions, including propagation and transfer reactions, an approximate linear relationship exists between the activation energy, E_{act}, and reaction enthalpy, ΔH_r, the so-called Bell–Evans–Polanyi relation:[22,23]

$$E_{act} = \rho \Delta H_r + C \tag{1}$$

where ρ and C are constants.

Attempts have been made to quantify the abovementioned concepts in several semi-empirical schemes. These schemes were developed in order to predict the reaction rate coefficients of propagation and transfer reactions, and particularly to predict monomer reactivity ratios. Here, the two most interesting among these models will be briefly described: the Q–e scheme of Alfrey and Price[21,24,25] and the "patterns of reactivity" scheme of Bamford and co-workers.[21,26–28]

1.2.1   The Q–e Scheme

This scheme was one of the first to appear[21,24,25] and is probably still the most widely used for the semiquantitative prediction of monomer reactivity ratios. It is based on the assumptions that a given radical $\sim A^\bullet$ has an intrinsic reactivity P_A, a monomer A has an intrinsic reactivity Q_A, and that the polar effects in the transition state can be accounted for by a factor e_A, which is a constant for a given monomer (it is assumed that e in the radical derived from a particular monomer is the same as e for that monomer). The reaction rate coefficients of the reactions shown in Scheme 1.1 may then be represented as in Eqs. (1.2a) and (1.2b), which result in the expression of Eq. (1.2c) for the resulting monomer reactivity ratio, r_A:

$$k_{AA} = P_A Q_A \exp(-e_A^2) \tag{1.2a}$$

$$k_{AB} = P_A Q_B \exp(-e_A e_B) \tag{1.2b}$$

$$r_A = \frac{k_{AA}}{k_{AB}} = \frac{Q_A}{Q_B} \exp\{-e_A(e_A - e_B)\} \tag{1.2c}$$

After defining styrene as a reference monomer, with standard $Q = 1.00$ and $e = -0.80$,[29] the Q and e values for other monomers can be obtained by measuring the monomer reactivity ratios. This leads to a "unique" set of Q–e parameters for a wide range of monomers (there are major solvent effects on these parameters), which are relatively successful in predicting monomer reactivity ratios of any pair of comonomers. Although the scheme is fundamentally flawed in that reaction rate coefficients are not only composed of individual contributions from the two reactants but also contain a large contribution from specific interactions in the transition state of the reaction, the scheme is very successful in practical applications. The reason for this lies partially in the fact that the transition states for all propagation

reactions are rather similar, and that predictions involve the *ratios* of two rate coefficients.

1.2.2 Patterns of Reactivity

This approach, which is applicable to both propagation and transfer reactions, is based on Hammett-type relationships between the reaction rate coefficient and certain electronic substituents.[21,26–28] As in the case of the *Q–e* scheme, a general reactivity is assigned to the radical. In this case, however, it is apparently better defined and taken to be the rate coefficient, $k_{tr,T}$, of the *H* abstraction from toluene by the radical. The contribution by the substrate (i.e., a monomer or chain transfer agent) to the reaction rate in the absence of polar effects is given by a constant β. Polar effects are taken into account by using two different parameters α and σ_p for the substrate and radical, respectively (as compared to the single *e* for monomer and radical in the *Q–e* scheme). The rate coefficient can now be expressed by

$$\log k = \log k_{tr,T} + \alpha\sigma_p + \beta \tag{1.3}$$

Although this scheme does improve on some of the assumptions made in the *Q–e* scheme, it still suffers from the fundamental shortcoming that a rate coefficient is not just composed of the separate individual contributions of the two reactants, but contains their interactions in the transition state. As in the case of the *Q–e* scheme, this scheme is rather successful in predicting monomer reactivity ratios, but since the former scheme is much simpler, it seems to be more popular with the general polymer community.

1.2.3 Beyond Classical Theories

It is clear that the "classical" theories have helped us greatly advance our under-standing of free-radical polymerization and its development, however, these theories are now too limited to answer our current questions. Many studies in small-radical organic chemistry since the early 1980s have significantly improved our understand-ing of radical reactions, and together with the use of fundamental theory outlined later in this chapter, some general trends in barrier heights for radical additions have been clearly identified. The interested reader is referred to an excellent recent review article by Fischer and Radom on this topic.[30] After analysis of the available data on radical additions to alkenes to date, they identified the following trends in reactivity:

- Enthalpy effects as given by the Bell–Evans–Polanyi relationship [Eq. (1.1)]; these effects are always present, but may be obscured by the presence of other effects
- Polar effects, which can decrease the barrier beyond that indicated by the enthalpy effect

The authors further propose the following relationship between activation energy (E_{act}) on the one hand and the reaction enthalpy (ΔH_r), nucleophilic polar effects (F_n), and electophilic polar effects (F_e) on the other:

$$E_{act} = (50 + 0.22\,\Delta H_r)F_n F_e \qquad (1.4)$$

where the part between brackets corresponds to an "unperturbed" Bell–Evans–Polanyi-type relationship, and F_n and F_e are multiplicative polar factors with a value between 0 and 1, which are given by

$$F_n = 1 - \exp\left\{-\left(\frac{I(R)-EA(A)-C_n}{\gamma_n}\right)^2\right\} \qquad (1.5a)$$

and

$$F_e = 1 - \exp\left\{-\left(\frac{I(A)-EA(R)-C_e}{\gamma_e}\right)^2\right\} \qquad (1.5b)$$

where I and EA refer to ionization potential and electron affinity, respectively; A and R, refer to the alkene and radical, respectively; C_n and γ_n are the Coulomb and interaction terms for nucleophilic polar effects, respectively; and C_e and γ_e are the Coulomb and interaction terms for electrophilic polar effects, respectively. Whereas the ionization potential and electron affinity are clearly properties of the individual reactants, the Coulomb and interaction parameters are constants that can be applied to wider ranges of radical–alkene pairs. These relationships describe the experimental observations well and are shown to have some predictive quality. Since this approach is based on very fundamental aspects of reaction barrier formation (see discussion below), it has a firmer theoretical basis than either of the Q–e and Patterns schemes. However, the actual forms of Eq. (1.4) and of F_n [Eq. (1.5a)] and F_e [Eq. (1.5b)] still appear to be of an empirical nature.

It should now be clear that in order to answer some of our more fundamental questions, we will need to resort to theoretical chemistry. In what follows we briefly outline the more fundamental theories and the results obtained with these theories.

1.3   BASIC TRANSITION STATE THEORY

In order to introduce some of the concepts in chemical dynamics, it is useful to revisit our ideas about chemical reactions.[3,7,9] First, we need to realize that atoms move; that is, they translate and rotate. This occurs even within molecules, where this motion leads to vibrations, rotations, angular distortion, and other activities, of which the characteristic energies can be observed in an infrared spectrum of the molecule. The atomic motions are governed by the potential energy field, which is determined

by the electronic energy of the system. Since the electronic energy will depend on the geometric arrangement of the atoms, the potential energy field in which the atoms move will change with displacement of atoms.[*] Plotting the potential energy as a function of the atomic coordinates yields the *potential energy surface*, which is one of the most fundamental concepts in chemical dynamics.

Returning to a chemical reaction, we can now say that, simply speaking, a chemical reaction involves the rearrangement of the mutual orientation of a given set of atoms in which certain existing chemical bonds may be broken and new ones formed; thus, we move from one spot on the potential energy surface to another. This is probably best illustrated by a simple example, which is more rigorously, but still very clearly, discussed by Gilbert and Smith.[3]

Let us consider the displacement of atom A by atom C in the diatomic molecule BC:

$$AB + C \xrightarrow{k} A + BC \qquad (1.6)$$
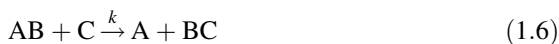
To simplify matters, the atoms are aligned in a linear fashion and will not move away from this linear rearrangement. It is simple to see that the electronic energy is determined by two coordinates, namely, the distance between atoms A and B, r_{AB}, and the distance between atoms B and C, r_{BC}. In the reactant configuration (i.e., A—B + C), r_{AB} is small and at its equilibrium value, whereas r_{BC} is rather large (i.e., large enough for C not to be considered as part of the molecule). In the product configuration (i.e., B—C + A), this situation is obviously reversed. Let us start with the reactant configuration. Any motion of the atoms causes a change in energy; for instance, compression of the A—B bond (i.e., a decrease in r_{AB}) leads to an increase in energy due to nuclear repulsion, and a stretch in the A—B bond (i.e., an increase in r_{AB}) will also lead to an increase in energy (i.e., we are trying to break a bond). Any motions of C will not affect the energy of the system until C comes close to B. When B starts to feel the electronic forces caused by the presence of C and bond formation starts, the original A—B bond needs to be stretched. Clearly, this bond-breaking process initially results in an increasing potential energy until the B—C bond-forming process starts to dominate. The net result is a decrease in energy. This process continues until the stable BC molecule is formed and the A—B bond is completely broken. We are now in the product configuration. A further decrease in r_{BC} would also lead to an increase in the potential energy, due to nuclear repulsion. The potential energy surface for this system is schematically shown in Fig. 1.1.

The potential energy surface shown in Fig. 1.1 reveals that there is a minimum energy pathway that can be followed when going from {AB + C} to {A + BC}, namely, the ''gully'' in the figure. This minimum energy pathway, which in this particular case is a combination of r_{AB} and r_{BC}, is called the *reaction coordinate*.[3,7,9] In cases in which existing bonds are broken and new bonds are formed, the energy

---

[*] This representation of atomic motion is based on the Born–Oppenheimer approximation in quantum mechanics, which states that electronic and nuclear motion can be separated.
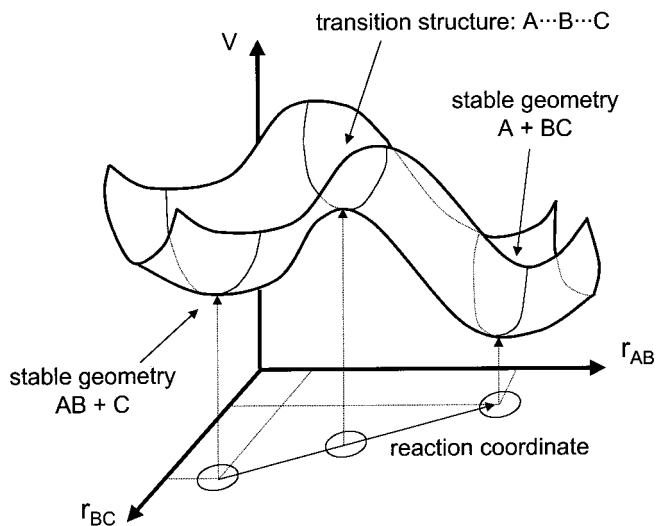
Figure 1.1   Potential energy surface for a collinear triatomic system $AB + C$ reacting to give $A + BC$.

profile along the reaction will display a maximum. The structure that corresponds to the coordinates at this maximum along the reaction coordinate is commonly known as the *transition state* (TS).[3,7,9] A plot of the potential energy against the reaction coordinate yields the very familiar picture in undergraduate textbooks defining the reaction barrier ($\Delta E^{\ddagger}$) and reaction energy ($\Delta E_{reaction}$) (see Fig. 1.2).

Before continuing with examples that are more relevant to free-radical polymerization, there is another point that deserves some attention. If we return our attention to Fig. 1.1, it can be seen that the transition state is located on a saddle point, that is, it displays a maximum in energy for only one of the coordinates (i.e., the reaction coordinate), whereas it displays a minimum for the others (in this case a coordinate perpendicular to the reaction coordinate). This is in contrast to the reactant and product configurations, which have minimal energy for all their coordinates.

This simple picture can be extended to any system with N atoms. Instead of the 2 coordinates in the previous example, we will now have $3N - 6$ internal coordinates, and we will now have a $(3N - 5)$-dimensional potential energy surface, which is obviously impossible to draw. However, the energy profile along the reaction coordinate will still be a two-dimensional picture, but it is likely that the reaction coordinate is now composed of several different internal coordinates. Figure 1.3 illustrates this point for a radical addition to an alkene. Although the reaction coordinate largely comprises the forming C⋯C bond length, it also comprises the out-of-plane bending of the hydrogen atoms attached to the C atoms forming the bond, and to some extent stretching of the C=C bond, which will end up as a C—C bond in the product radical.
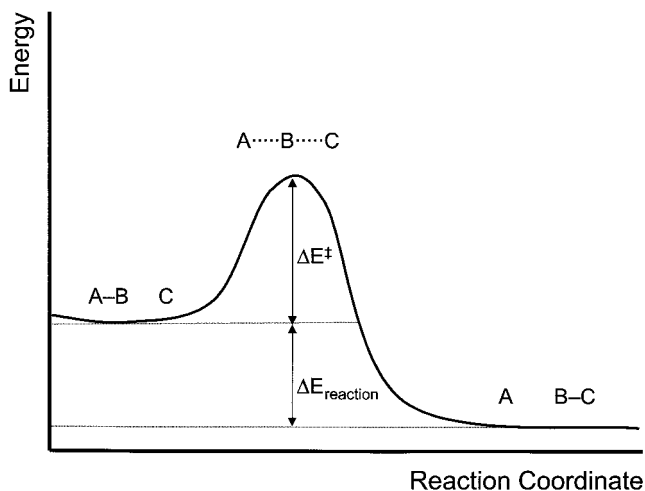
Figure 1.2   Schematic representation of the potential energy along the reaction coordinate for a collinear triatomic system $AB + C$ reacting to give $A + BC$. Clearly indicated are the reactant, product and transition state regions, as are the barrier ($\Delta E^{\ddagger}$) and reaction energy ($\Delta E_{\text{reaction}}$).

Figure 1.3   Schematic representation of the potential energy profile along the reaction coordinate for a radical addition reaction. Note that the reaction coordinate largely consists of the length of the forming C—C bond, but that it also contains some contributions from the disappearing C=C bond length and the angles of the hydrogen atoms adjacent to the forming bond.

To summarize, we can state that atoms move in a force field that is determined by the electronic energy, and that if a motion along the reaction coordinate contains sufficient energy to overcome the barrier, a chemical reaction occurs. If the energy is not large enough, then motion is still possible along the reaction coordinate, but it will not lead to a reaction.

We can evaluate the reaction rate coefficient exactly (classically) by solving the classical equations of motion of the atoms on the potential energy surface. This results in the momenta and positions of atoms at any given time, namely, a *trajectory*.[3] If we calculate a large number of trajectories, we can evaluate how many of these trajectories start in the reactant region of the potential energy surface and end in the product region on the potential energy surface in any given time. This is a lengthy and computationally demanding process, which can be greatly simplified by making the *transition state assumption*, which states that all trajectories passing through a critical geometry (i.e., the transition state) and have started as reactants will end up as products.[3] Evaluation of the mathematical description of this process leads to a relatively simple expression of the bimolecular rate coefficient, k, which depends only on the properties of the two reactants and the transition state:[3,7,9]

$$k = \frac{k_B T}{h} \frac{Q^\dagger}{Q_1 Q_2} \exp\left(-\frac{E_0}{k_B T}\right) \tag{1.7}$$

In this equation k_B is Boltzmann's constant; T is the absolute temperature in Kelvin; h is Planck's constant; $Q^\dagger$, Q_1, and Q_2 are the molecular partition functions[10] of the transition state, reactant 1, and reactant 2, respectively; and E_0 is the critical energy to reaction. In what follows, the concepts of partition functions and critical energy will be briefly discussed.

First, we consider the critical energy, E_0, which is defined as the difference in zero-point energies between reactants and transition state (see Fig. 1.4). Since there is always a motion of the atoms within a molecule, that is, the *zero-point vibration*, the energy of a molecule should not only be represented by the minimum ground-state energy, but a small additional term due to the vibrations; specifically, the *zero-point vibrational energy* (ZPVE), needs to be added.[3,7,9,10] The ZPVE contains a contribution from all $3N-6$ vibrations of the molecule ($3N-7$ in the transition state, i.e., the motion along the reaction coordinate is excluded—the corresponding frequency is imaginary!), and is defined as:

$$\text{ZPVE} = \frac{1}{2} \sum_{j=n}^{3N-6} h \nu_j \tag{1.8}$$

where $n = 1$ for a minimum-energy structure (e.g., reactants and products), $n = 2$ for a transition state, $n = m + 1$ for any mth order saddlepoint (e.g., a rotational maximum in the TS has $m = 1$), and ν_j is the harmonic frequency of the jth normal mode vibration. It is clear from this definition that the high-frequency modes (e.g., C—H bond stretches) dominate the ZPVE.

We also need to discuss the meaning of a partition function, a concept originating from statistical thermodynamics,[10] which serves as a bridge between the quantum

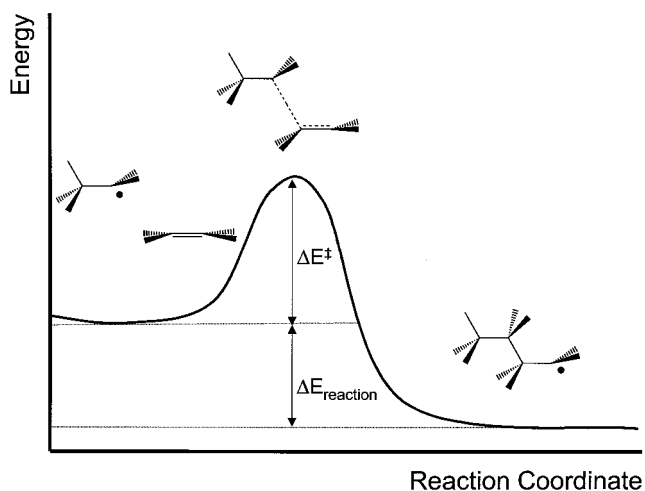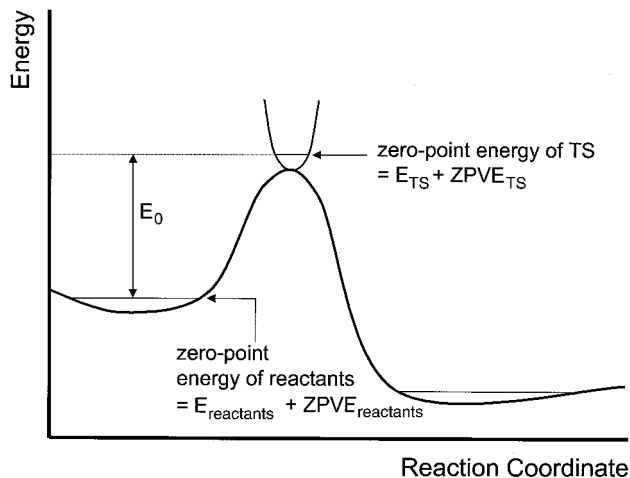**Figure 1.4** Schematic representation of the potential energy profile along the reaction coordinate. Indicated are the zero-point energy levels of the reactants and the transition state, as is the critical energy to reaction, E_0, which is defined as the difference in zero-point energy of the transition state and the reactants.

mechanical energy states of a macroscopic system and its thermodynamic properties. For example, we can express the enthalpy (H) and entropy (S) of a molecule in terms of molecular partition functions:

$$S = k_B \ln Q - \frac{k_B}{T} \frac{\partial \ln Q}{\partial T^{-1}} \tag{1.9}$$

$$H = -k_B \frac{\partial \ln Q}{\partial T^{-1}} + k_B T \tag{1.10}$$

If we use these definitions of H and S in the TST expression for the rate coefficient, we can relate the empirical parameters in the Arrhenius equation [Eq. (1.11)], namely, the frequency factor A and the activation energy E_{act}, to fundamental thermodynamic properties of the system

$$k = A \, \exp\left(-\frac{E_{act}}{k_B T}\right) \tag{1.11}$$

First, we express E_{act} and A in terms of partition functions:

$$E_{act} = -k_B \frac{\partial \ln k}{\partial T^{-1}} = E_0 - k_B \frac{\partial \ln\left(\frac{Q^\dagger}{Q_1 Q_2}\right)}{\partial T^{-1}} + k_B T \tag{1.12}$$

$$\ln A = \ln\left(\frac{e k_B T}{h}\right) - \frac{1}{T} \frac{\partial \ln\left(\frac{Q^\dagger}{Q_1 Q_2}\right)}{\partial T^{-1}} + \ln\left(\frac{Q^\dagger}{Q_1 Q_2}\right) \tag{1.13}$$

If we now define an enthalpy of activation, $\Delta H^{\ddagger}$, as

$$\Delta H^{\ddagger} = H^{\dagger} - H_1 - H_2 \qquad (1.14)$$

where $H^{\dagger}$ is the enthalpy of the transition state, and H_1 and H_2 are the enthalpies of reactants 1 and 2, respectively, and we define an entropy of activation, $\Delta S^{\ddagger}$, as

$$\Delta S^{\ddagger} = S^{\dagger} - S_1 - S_2 \qquad (1.15)$$

where $S^{\dagger}$ is the entropy of the transition state, and S_1 and S_2 are the entropies of reactants 1 and 2, respectively, then we obtain the following expressions for the Arrhenius parameters:[3,7,9]

$$E_{\mathrm{act}} = E_0 + \Delta H^{\ddagger} + 2k_{\mathrm{B}}T \qquad (1.16)$$

$$A = \frac{ek_{\mathrm{B}}T}{h} \exp\left(\frac{\Delta S^{\ddagger}}{k_{\mathrm{B}}}\right) \qquad (1.17)$$

It is clear from these expressions that the activation energy is mainly determined by enthalpic factors and the frequency factor by entropic factors.

Let us now return to the partition function and its definition. The canonical (i.e., number of particles, volume and temperature constant) partition function Q of a system is given by[10]

$$Q = \sum_i g_i \exp\left(-\frac{\varepsilon_i}{k_{\mathrm{B}}T}\right) \qquad (1.18)$$

which is a summation over all energy levels, ε_i, all with a number of degenerate states g_i. In the TST expression of the rate coefficient the molecular partition function is required, but before considering this, we will first look at the simple example of a harmonic oscillator, which is commonly used to represent a normal-mode vibration. The values for ε_i can be obtained from solving the Schrödinger equation for a particular problem:

$$\hat{H}\phi = \varepsilon\phi \qquad (1.19)$$

where $\hat{H}$ is the Hamiltonian, or energy operator, ϕ the eigenfunction, and ε the corresponding eigenvalue, that is, the energy level. The energy levels ε_i of a harmonic oscillator with a frequency of v_j are given by (see Fig. 1.5):[10]

$$\varepsilon_i = \left(i + \frac{1}{2}\right)hv_j \qquad (1.20)$$

$$\varepsilon_i = (i+1/2)\, h\nu$$

i = 6

hν

i = 5

hν

i = 4

hν

i = 3

hν

i = 2

hν

i = 1

hν

i = 0

vibrational frequency = ν

Displacement
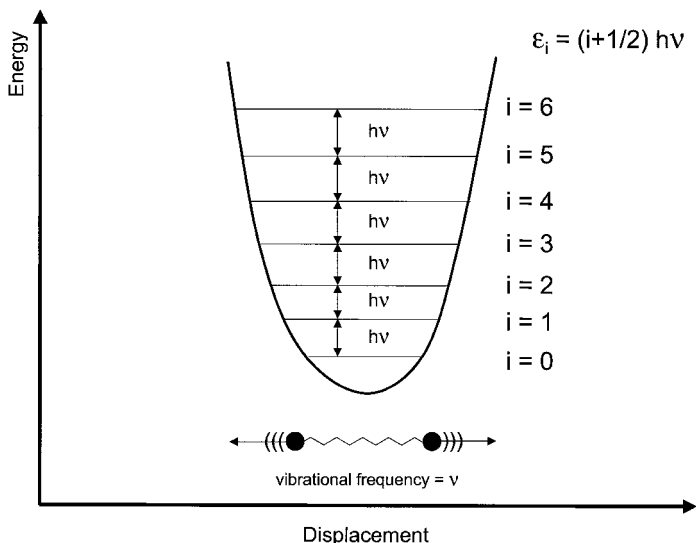
Figure 1.5   Schematic representation of the potential energy of a harmonic oscillator. The allowed quantum states and corresponding energy levels are indicated.

Substitution of this expression of the energy levels into Eq. (1.18) then yields the partition function for the harmonic oscillator, $Q_{\text{vib},\,j}$:[10]

$$Q_{\text{vib},\,j} = \left[1 - \exp\left(-\frac{h\nu_j}{k_B T}\right)\right]^{-1} \tag{1.21}$$

Let us now return to the concept of molecular partition functions. It is clear that the energy levels with corresponding energies are much more complex than those for the simple problem of a harmonic oscillator. However, if we assume that the several physical factors contributing to the overall energy—the electronic, translational, rotational and vibrational energies—are independent, the molecular partition function can be expressed as the product of the partition functions of the individual contributions:[10]

$$Q = Q_{\text{elec}} \times Q_{\text{trans}} \times Q_{\text{rot}} \times Q_{\text{int}} \tag{1.22}$$

where Q_{elec}, Q_{trans}, Q_{rot}, and Q_{int} are the electronic, translational, (external) rotational, and internal vibrational partition functions, respectively. These individual partition functions are simple and can be determined in a relatively straightforward manner as shown below. We will consider the partition functions of ideal gas molecules as a model for our current system.

The electronic partition function can be quite complex if more than one electronic pathway of the reaction is possible, for example reactions involving excited

molecules. However, the reactions that we will consider here, namely, "ordinary" radical additions and atom abstractions, do not involve excited molecules, but proceed through so-called ground-state intermediates (see section on quantum chemistry). This means that only a single energy level is accessible, and hence $Q_{\text{elec}} = 1$.

The translational partition function of an ideal gas molecule is given by[10]

$$Q_{\text{trans}} = V \left(\frac{2\pi m k_B T}{h^2} \right)^{3/2} \tag{1.23}$$

where V is the reference volume and m is the mass of the translating molecule. In the case of radical addition or abstraction reactions, the translational contribution to the frequency factor is then given by

$$\left(\frac{Q^{\dagger}}{Q_1 Q_2} \right)_{\text{trans}} = \frac{1}{V} \left(\frac{m_1 + m_2}{m_1 m_2} \right)^{3/2} \left(\frac{h^2}{2\pi k_B T} \right)^{3/2} \tag{1.24}$$

For a reaction between a small molecule, for instance, monomer or chain transfer agent, with mass m_{small} and a long radical chain with mass m_{rad}, we have in the limit of long chains that the masses of the radical and the transition state ($m^{\dagger}$) are roughly the same: $m_{\text{rad}} \approx m^{\dagger}$. Hence Eq. (1.24) will reduce to[31]

$$\left(\frac{Q^{\dagger}}{Q_{\text{very long}} Q_{\text{small}}} \right)_{\text{trans}} \approx \frac{1}{V} \left(\frac{1}{m_{\text{small}}} \right)^{3/2} \left(\frac{h^2}{2\pi k_B T} \right)^{3/2} \tag{1.25}$$

All (nonlinear) molecules exhibit an external three-dimensional rotation, for which the partition function is given by[10]

$$Q_{\text{rot}} = \frac{\sqrt{\pi}}{\sigma} \left(\frac{8\pi^2 k_B T}{h^2} \right)^{3/2} \sqrt{I_a I_b I_c} \tag{1.26}$$

where σ is the symmetry number of the molecule and I_a, I_b, and I_c are the principal moments of inertia, given by $I = \Sigma m_i r_i^2$, where m_i and r_i are the mass and the distance to the appropriate principal axis of rotation, respectively, of atom i. The principal moments of inertia can be easily calculated if the geometry of the molecule is known. In the case of a small radical adding to the monomer, the external rotations of both reactants and the TS need to be considered, but in the long-chain limit, it is only the external rotation of the small molecule that is important (since the moments of inertia of the polymeric radical and the TS will not differ significantly and will approximately cancel), leading to[31]

$$\left(\frac{Q^{\dagger}}{Q_{\text{very long}} Q_{\text{small}}} \right)_{\text{rot}} \approx \left(\frac{1}{Q_{\text{small}}} \right)_{\text{rot}} \tag{1.27}$$

Except for transition states, the geometry information required for the determination of rotational partition functions can be obtained experimentally. However, as we will discuss later, this information can also be adequately obtained by appropriate quantum-chemical calculations, including the information about the transition state.

Finally, we have to consider the internal vibrational partition function. We have already seen that the vibrational partition function of a single harmonic oscillator—the model we use for an internal vibration—is given by the following equation [=Eq. (1.21)]:[10]

$$Q_{\text{vib}, j} = \left[1 - \exp\left(-\frac{h\nu_j}{k_{\text{B}} T} \right) \right]^{-1} \tag{1.28}$$

In a polyatomic, non-linear, molecule consisting of N atoms, we have $3N - 6$ such vibrations and we can write the overall vibrational partition function (Q_{vib}) as the product of the vibrational partition functions of separate vibrational modes:

$$Q_{\text{vib}} = \prod_{j=n}^{3N-6} Q_{\text{vib}, j} \tag{1.29}$$

In this expression n is defined in the same way as for Eq. (1.8) (e.g., $n = 1$ for reactants and/or products, and $n = 2$ for the transition state).

It should be noted here that, in contrast to what we previously saw for the zero-point vibrational energy (i.e., a contribution to the critical energy E_0; see above), the low-frequency vibrations are most important, as can be seen from Eq. (1.28). Vibrational frequencies can be determined experimentally (e.g., infrared measurements) or theoretically. The experimental measurements, however, are very difficult for radicals, and virtually impossible for transition structures, which leaves theory as an important alternative. When applying theoretical methods to determine the vibrational frequencies, two factors need to be considered: (1) experience has shown that the harmonic frequencies calculated by a particular quantum-chemical method (see below) tend to be systematically out (by less than $\sim 10\%$) depending on the procedure, and will require scaling by appropriate scale factors;[32,33] and (2) the calculated frequencies are obtained by using the harmonic oscillator approximation for all the determined "vibrations." Although this is indeed an appropriate and relatively accurate description for most internal motions, it may lead to some errors for certain low-frequency modes. The actual motions of some of these low-frequency modes, as indicated by a normal-mode analysis, are better represented as internal rotations, and should be treated either as hindered or unhindered rotors (depending on the barrier to rotation).[3,31] As is shown in Fig. 1.6, the potential energy profiles of a harmonic oscillator and a hindered rotor at small displacements can be quite similar, and it is only this part that is calculated automatically by the quantum-chemistry programs.[11] These programs then automatically extrapolate with a parabola, which confines the motion to relatively small displacements. However, if the motion is really a hindered rotation, then the true potential energy profile is of a periodic
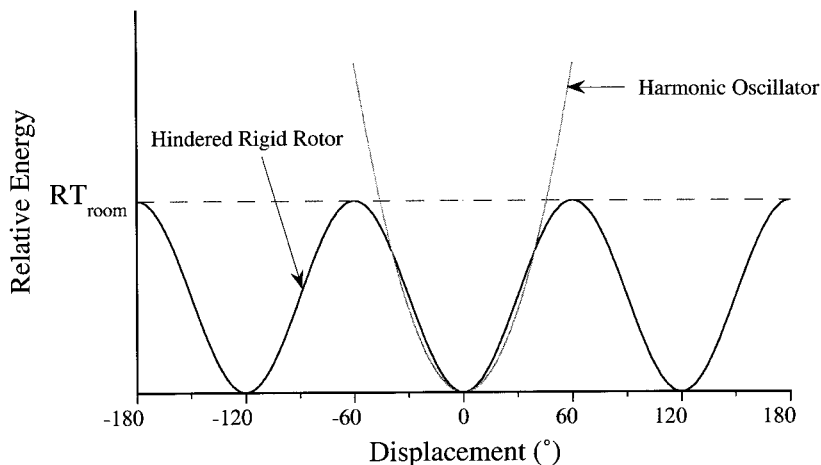
Figure 1.6   Schematic representation of the potential energy surfaces of a hindered rigid rotor and a harmonic oscillator. Note that for small displacements and energies below the thermal energy at room temperature ($R \times T_{\text{room}}$) both profiles are very similar.

nature and after overcoming a barrier, a new energy well is reached. Without going into specific details, it should be noted that because of the different potential energy profiles, the two treatments, namely, the harmonic oscillator and the hindered rotor, give different partition functions and hence it is more appropriate to treat the internal rotations as hindered rotors, rather than harmonic oscillators.[3]

The frequencies of these hindered rotors are then omitted from the vibrational partition function and enter the internal rotational partition function ($Q_{\text{int rot}}$). It is now possible to define the overall partition function of all internal motions (Q_{int}), for a system that contains r internal rotations:[3,31]

$$Q_{\text{int}} = \prod_{j=n}^{n+r} Q_{\text{int rot},j} \prod_{j=n+r+1}^{3N-6} Q_{\text{vib},j} \tag{1.30}$$

In this expression n is defined in the same way as for Eq. (1.8) (e.g., $n = 1$ for reactants and/or products, and $n = 2$ for the transition state).

Internal rotations may be described as hindered one-dimensional or two-dimensional rotors, and the corresponding partition functions can be obtained by solving the Schrödinger equation for an appropriate rigid rotor with corresponding rotational potential. Without going into details of these calculations, it should be noted that a higher barrier to rotation lowers the partition function, whereas a higher moment of inertia (mass of rotating moieties) increases the partition function.[31,34]

To conclude this section on transition state theory we should discuss the very important so-called *transitional modes*.[3,31] We have already seen that the transition

state has one imaginary frequency (which is a characteristic of the transition state), corresponding to a motion along the reaction coordinate, and which is omitted from the vibrational partition function and zero-point vibrational energy. It is clear that this motion along the reaction coordinate, such as the stretching of the forming C—C bond in radical addition, did not exist previously in the reactants (simply because this bond did not exist). A detailed examination of the vibrational modes in the transition state of a bimolecular reaction reveals that there are five more internal motions (with real frequencies) that did not exist previously in the reactants. These six extra modes (with one imaginary and five real frequencies) are the so-called *transitional modes* and arise because of the loss of three external rotational and three translational degrees of freedom of the reactants when brought together in the transition state (see Fig. 1.7).

All the other modes in the transition state correspond to modes that already existed in the reactants (they will be slightly lower because of the higher mass of the transition state). This implies that the overall contribution of the internal motions to the reaction rate coefficient, namely, $Q_{int}^{\dagger}/(Q_{1,int}Q_{2,int})$, is determined mainly by the frequencies of the five real transitional modes. These frequencies typically lie below 1000 cm^{-1} and the lowest frequencies often correspond to torsional modes.[31] Since the transition states of propagation reactions (or transfer reactions) in different monomer systems will all have similar characteristics, the differences in the overall vibrational contributions will be small.[31,35] Sterically more crowded
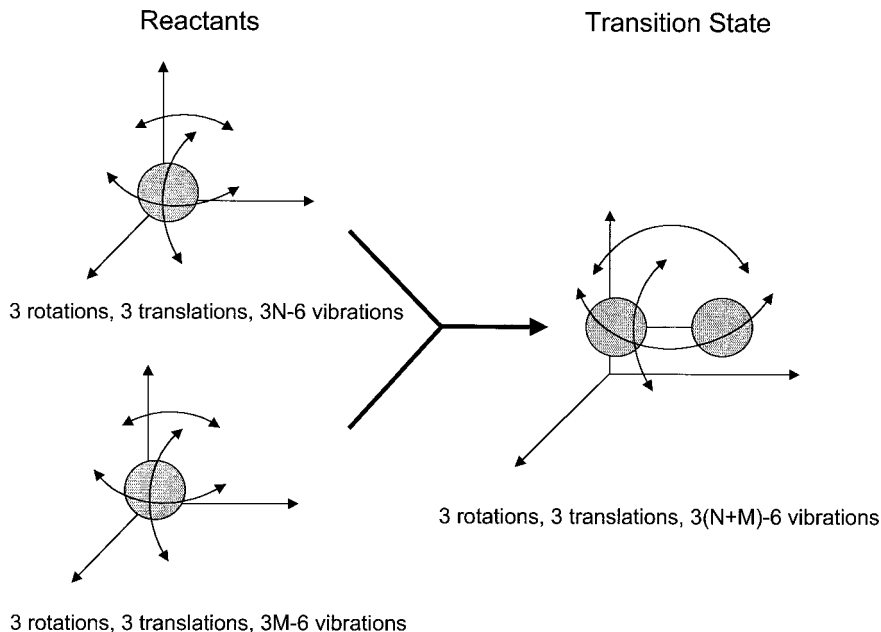

Figure 1.7 Schematic representation of the transformation of 6 external modes into 6 transitional modes when two reactants combine to form a single transition state.

monomers will probably show an increase in the frequency of a particular mode as compared with a similar mode in a less crowded monomer. Although the observed differences between different monomer systems will be significant, it is unlikely that the internal contribution to the frequency factors will show variations exceeding one order of magnitude from system to system; even an extremely large increase in frequency from 200 to 600 cm^{-1} results in a decrease in the overall vibrational contribution by a factor of only 1.6. It should be kept in mind, however, that all these small changes appear in the frequency factor as a product, so several small changes can quickly become a combined factor of, say, 5.

1.4 BASIC QUANTUM CHEMISTRY

In the previous section we saw that we need knowledge of the potential energy surface, or at least of the reactants and transition states in order to determine the reaction rate coefficient. The potential energy surface can be calculated by solving the Schrödinger equation for every possible set of atomic coordinates. The Schrödinger equation [Eq. (1.31)] is a numerical eigenvalue problem for which multiple solutions can be found, each characterised by a certain wavefunction and corresponding energy.[11-14]

$$\hat{H}\Psi = E\Psi \tag{1.31}$$

In this expression, $\hat{H}$ is the Hamilton operator (which corresponds to the total energy of the system), E is the numerical value of the energy (an eigenvalue), and Ψ is the wavefunction (an eigenfunction), which depends on the coordinates of all the particles and the spin coordinates in the system. The solutions of the Schrödinger equation are called *stationary states* and the state with the lowest energy is called the *ground state*. Stationary states with higher energies correspond to so-called excited states. These excited states are, for example, important in photochemical reactions that play a role in photoinitiation processes; in this chapter, we will discuss only the ground states, as the "ordinary" radical addition and transfer reactions involve reactions between molecules in their ground state.

In only a few simple cases do analytic solutions of the Schrödinger equation exist, and in order to solve this equation for systems of interest, certain approximations need to be made, but before we will briefly discuss the most important features of the involved calculational procedures, the actual results of quantum-chemical calculations will be discussed.

As stated before, solution of the Schrödinger equation yields the (ground state) energy and corresponding wavefunction, from which the electronic configuration of the molecule is deduced. With this information it is possible to calculate properties such as ionization energies, electron affinities, charge distributions, and dipole moments.[11] If the energy is optimized with respect to all coordinates, one obtains "stable" molecules. "Normal molecules" correspond to minima on the potential energy surface and the transition state of a reaction corresponds to a maximum in

the reaction coordinate and a minimum in all other coordinates, namely, a first-order saddle point (see also Fig. 1.1). From the second derivatives of the energy with respect to all the nuclear coordinates, the force constants of the $3N - 6$ normal-mode vibrations can be obtained for a molecule consisting of N atoms ($3N - 5$ for a linear molecule). The second derivatives, that is, the force constants, are all positive in the case of minima on the potential energy surface, which leads to $3N - 6$ real frequencies for the vibrations. In the case of a transition state of a reaction, which is characterized by a maximum in the reaction coordinate, one of the force constants is negative, and this "molecule" is now characterized by $3N - 7$ real frequencies and 1 imaginary frequency for the motion along the reaction coordinate.

To summarize, a standard quantum-chemical calculation will provide us with all the required input for a TST calculation of the rate coefficient (i.e., geometries, normal-mode vibrations and corresponding frequencies, rotational barriers, and absolute energies) and with information about the electronic structure of a molecule (i.e., important for the study of substituent effects on reaction barriers, e.g., polar effects).[11] Let us now turn our attention to the assumptions and simplifications in the actual computational procedures.

1.4.1   Ab Initio Molecular Orbital Theory

Among the procedures for obtaining (approximate) solutions to the Schrödinger equation are the molecular orbital (MO)[11] and valence bond (VB)[14] theories. Whereas both procedures yield the same results in the limiting case, MO theory is much more easily implemented in computational procedures and hence forms the basis of the great majority of theoretical studies. In this section we will focus only on MO theory; we will encounter VB theory again in the section on barrier formation.

In MO theory, the full wavefunction Ψ is approximated by one electron functions, the so-called spin orbitals (χ); the exact nature of this approximation is beyond the scope of this chapter. The spin orbitals are given by the product of *molecular orbitals* (ψ), which depend on the Cartesian coordinates x, y, and z of a single electron, and a spin function (α or β):[11–14]

$$\chi = \psi(x, y, z)\alpha \quad \text{or} \quad \chi = \psi(x, y, z)\beta \tag{1.32}$$

It is difficult to picture the actual meaning of a molecular orbital (MO), but its square, $|\psi|^2$, can be interpreted as the probability of finding the electron in a particular space. In practice, the MOs are expressed as linear combinations of M one-electron functions, the so-called *basis functions* (ϕ). Then, each individual orbital ψ_i can be written in terms of the M basis functions ϕ_μ as follows:[11–14]

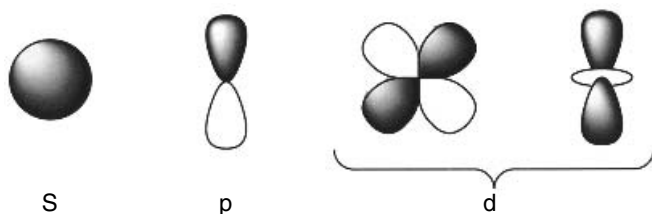$$\psi_i = \sum_{\mu=1}^{M} c_{\mu i}\phi_\mu \tag{1.33}$$

Figure 1.8   Representation of s, p, and d atomic orbitals as the boundary surface within which there is a 90% probability of finding the electron.

where the $c_{\mu i}$ are the molecular orbital expansion coefficients. The actual form of the basis functions is based on the form of the *atomic orbitals* obtained analytically for the hydrogen atom. The basis functions can then be classified as s, p, d, f, ...-type orbitals according to their angular momentum properties (see Fig. 1.8).[11–14]

At this point it is useful to recall what we are trying to achieve. We wish to solve an eigenvalue problem: the Schrödinger equation. This is basically a problem in a vector space of *infinite* dimensions, which we try to approximate by a *limited* number of basis functions. It is important to realize that the more basis functions we use, that is, the better we approximate the real vector space, the more expensive our calculations will be, and that we are therefore forced to use as few basis functions as is possible. In what follows, only the Pople–Gaussian basis sets[11] and corresponding nomenclature will be discussed for no other reasons than simplicity and their frequent usage.

We are used to thinking in such terms as that a hydrogen atom has one s electron, and a carbon atom has two electrons in its inner-shell s orbitals, two electrons in its valence s orbitals, and two electrons in its valence p orbitals. This suggests that if we allow the electrons to occupy these particular orbitals (approximated by basis functions of a similar "shape"), then we should have a fairly good description of the actual situation (i.e., the approximation of the infinite vector space), and we should get fairly good results when solving the Schrödinger equation. The so-called *minimal basis sets* (with names such as STO-3G), and to some extent the slightly better *split-valence basis sets* (with names such as 3-21G, 6-31G) are based on this philosophy.[11]

Although these minimal and split-valence basis sets do a reasonable job in certain applications, they have some major shortcomings, of which one will be briefly discussed here. These basis sets cannot take into account any distortion from atomic symmetry when placing the atoms in a molecular environment. For example, if we only allow the electron of hydrogen to occupy an orbital of s-type symmetry, then this description is clearly better for a single hydrogen atom, than when this hydrogen atom is placed in a molecule in which it forms a σ bond. In this case it is likely that the electron will have a higher probability of being found in the region of the bond, rather than away from it (which would be a consequence of the fully spherical symmetry of the s orbital). Hence, a better description would result if we
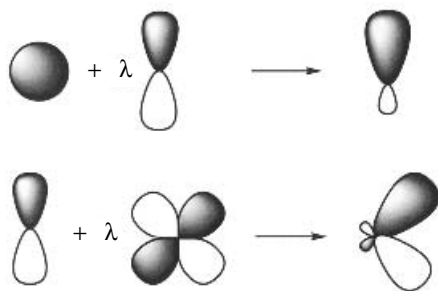
Figure 1.9   Effect of polarization functions. *Above*—addition of *p* function greatly enhances the flexibility of an *s*-type orbital; *below*—addition of a *d* function greatly enhances the flexibility of a *p*-type orbital.[11]

allowed the electron to use orbitals of different shape to create a new orbital with a better-suited shape.[11] This process can be accomplished by the addition of *polarization functions* to the basis set describing a particular atom. The effect of the addition of *p*-type functions to *s*-type functions, and of *d*-type functions to *p*-type functions is shown in Fig. 1.9. The much greater flexibility of the orbital is immediately clear from this figure.

Basis sets containing polarization functions are often denoted by symbols such as * or **, or by the addition of extra letters between brackets indicating the symmetry type of the polarization functions, such as, 6-31G(*d*) (=6-31G*), 6-311G(*d,p*) (=6-311G**), and 6-311G(*df,p*).

Additional "freedom" to the electrons can be provided by the addition of *diffuse functions*, which are very important for the description of long range behaviour with energies close to the ionisation limit, such as anions.[11] The terminology employed here is the addition of a "+" or "++" to the basis set, such as 6-311+G**.

To summarize, we can say that the approximate solution to the Schrödinger equation improves when we give a greater flexibility to where the electrons "are allowed to go," that is, the size of the basis set. However, we need to take into account that the more basis functions we use, the more computationally demanding is our problem. Hence, we will always be trading accuracy against cost. In Table 1.1, the number of basis functions for hydrogen and first-row elements is given for several commonly used basis sets. Generally we can state that the larger the name of the basis set, the larger the basis set itself.

1.4.2   "Interactions of the Electrons"

We have already seen that the size of the used basis set affects the obtained results, and in this section we will discuss briefly another factor that can greatly affect the results.[11] This factor is caused by the number of interactions between the electrons that we take into account. For example, are we describing the electrons as each individually experiencing a combined electronic field generated by the others or

TABLE 1.1 **Number of Basis Functions per Hydrogen Atom and First-Row Element in Different Basis Sets**

Basis Set	Hydrogen Atom	First-Row Elements
3-21G	2	9
6-31G* = 6-31G(d)	2	15
6-31G** = 6-31G(d,p)	5	15
6-311G** = 6-311G(d,p)	6	18
6-311G(df,p)	6	25
6-311 + G(2df,p)	6	34
6-311 + G(3df,2p)	9	39

will we also take into account individual interactions? If we consider the research output of a graduate student as an analogy, it is probably very important to consider the student's interactions with members of the research group in great detail, the interaction with the wider scientific community in some detail, and the student's night out in town as a "background force field" (using the same analogy, the research group, the wider scientific community and the nightlife can be considered as the size of the basis set). If we wish to describe the student's personal life accurately, the amount of detail would probably require the reverse. A similar situation exists for the description of electronic interactions; in certain cases, such as the description of geometries of stable molecules, no detailed interactions are required, whereas the description of absolute energies, and properties of transition structures require more detail.

The starting point in the description of electronic interactions is Hartree–Fock (HF) theory.[11–14] This theory is used to evaluate the orbital expansion coefficients $c_{\mu i}$ in Eq. (1.33), without consideration of detailed interactions between the electrons. The overall result of these calculations is a set of molecular orbitals (ψ) to which the electrons are assigned (there will also be unoccupied orbitals!); the resulting many-electron wavefunction (Ψ) now represents an electronic configuration of the system.

Although Hartree–Fock theory does a decent job in describing most properties of normal ground-state molecules, the limited interaction between the electrons leads to absolute energies that are too high, and sometimes to incorrect descriptions of more complex molecular systems. In order to take more interactions (i.e., *electron correlation*) into account, one has to invoke *configuration interaction*.[11] Instead of using a single electronic configuration to describe the many-electron wavefunction, we now use several different electronic configurations. These additional electronic configurations can be obtained by distributing the electrons over different molecular orbitals than just the lowest-energy ones as we did to obtain the HF wavefunction. Clearly, the more of these electronic configurations are added, the more accurate the overall wavefunction. However, the cost of the computations will increase dramatically.

We can roughly distinguish two different ways of introducing electron correlation; the first one is exactly the way described above, namely, configuration interaction, and the second way is via perturbation theory.[11] The best configuration interaction method is *full configuration interaction* (FCI), which takes into account all possible electronic configurations. This method, which in practice is possible only for very small systems, would result in an exact solution of the Schrödinger equation if an infinite basis set were used. Since this is in practice not possible, only a limited number of alternative configurations are often used. In general, the more alternative configurations, that is, configurations in which certain molecular orbitals are substituted for others, the better the result. Depending on the exact formulation of the procedure, we distinguish methods such as (1) CIS, CID, and CISD (i.e., configuration interaction with single, double, and single + double substitutions, respectively);[11] (2) CCSD, CCSD(T), and CCSD(T,Q) (i.e., coupled cluster with single and double; single, double and triple; and single, double, triple, and quadruple substitutions, respectively);[36] and (3) QCISD, QCISD(T), and QCISD(T,Q) (i.e., quadratic configuration interaction with single and double; single, double, and triple; and single, double, triple, and quadruple substitutions, respectively).[37] The coupled cluster (CC) and quadratic configuration interaction (QCI) methods are very similar in performance for most problems, and can currently be regarded as the best practical procedures available to describe problems of interest to the polymer chemist.

The alternative method of taking into account electron correlation is Møller–Plesset perturbation theory.[11,13] It is more difficult to provide a simple picture of the mathematics involved in these procedures, but the outcome is similar to what is achieved in the configuration interaction procedures. Instead of double substitutions, we have now second-order Møller–Plesset theory (MP2); instead of higher substitutions we now have MP3, MP4, ... The Møller–Plesset procedures are less expensive than the corresponding CC or QCI procedures, and in many cases yield comparable results. However, we will see below that certain formulations of these theories (e.g., UMP2, UMP3, UMP4, . . .) perform very poorly in radical reactions.[38–45]

We have seen that the quality of a calculation depends on both the size of the basis set and the amount of electron correlation. Depending on the problem we wish to describe, we will have to compromise on one aspect or the other, or both aspects. A clear way of depicting the quality of a calculation is a so-called Pople diagram (see Fig. 1.10),[11] which shows the size (and improvement) of the basis set in the left hand column, and the amount (and improvement) of electron correlation in the top row. The combination of the best basis set (i.e., an infinite size basis set) and full configuration interaction results in an exact solution of the Schrödinger equation. We denote the overall level of theory as the combination of procedure and basis set, for example, HF/3-21G, MP2/6-31G*, and QCISD(T)/6-311G(3*df*,2*p*).

1.4.3 Treating α and β Orbitals in MO Theory

So far, when discussing the electrons and molecular orbitals we have not paid much attention to the fact that we have α (spin up) and β (spin down) electrons.[11–14] In radicals we have a single unpaired electron, a situation that is characterized by a spin

Figure 1.10 Pople diagram showing the dependence of the performance of an ab initio method on the basis set and the amount of electron correlation.[11]

quantum number $S = \frac{1}{2}$; the wavefunction should be a pure doublet (i.e., $2S + 1 = 2$) and have an spin-squared expectation value $\langle S^2 \rangle = S(S + 1) = 0.75$. We basically have two ways of treating the α and β electrons in Hartree–Fock theory: (1) in a restricted (RHF) or (2) in an unrestricted way (UHF).[11] The former procedure, RHF, restricts the α and β electrons to the same molecular orbital leading to a single orbital with an unpaired electron and results in a wavefunction that is indeed a pure doublet with $\langle S^2 \rangle = 0.75$. Unrestricted Hartree–Fock allows the α and β electrons to occupy different molecular orbitals, thus giving the electrons a bit more freedom, and resulting in a wavefunction with a lower energy. However, because of this additional freedom, the net effect is that more than one electron remains unpaired; the wavefunction is said to be contaminated by states of higher spin multiplicity and the spin-squared expectation value $\langle S^2 \rangle > 0.75$.[44–46] This effect, which is called *spin contamination*, is especially severe in radical addition transition states.[31,38–43,47]

Correlated procedures can use both UHF and RHF wavefunctions as a starting point and for methods as quadratic configuration interaction (QCI: denoted as UQCI or RQCI, respectively) and coupled cluster (CC: denoted as UQCI or RQCI, respectively) the final results are generally not significantly different. However, the situation is very different for the Møller–Plesset procedures, which generally show very poor convergence when UHF wavefunctions are used (these Møller–Plesset procedures are denoted as UMP2, UMP3, . . .), and the results are

often erratic when using this procedure, as will be shown in a later section.[44,45] The results of the UMP procedures can often be significantly improved by so-called spin projection, a procedure that removes the contributions from the unwanted higher spin states (the resulting procedures are denoted as PMP2, PMP3, ...).[44,45] Møller–Plesset procedures using the RHF wavefunction as a starting point (i.e., RMP2, RMP3, ... or ROMP2, ROMP3, ...)[48–50] also result in significantly better results than the corresponding UMP procedures.

1.4.4   Alternative Popular Quantum Chemical Procedures

Finally, a short note should be added on two very popular alternatives to the ab initio MO procedures that we have dicussed until this point: semiempirical MO procedures[51] and density functional theory (DFT).[52]

The molecular properties that can be calculated with semiempirical MO procedures are similar to those that can be calculated using conventional ab initio procedures. However, the semiempirical procedures are less computationally demanding and hence allow, in principle, for larger systems to be studied. The semiempirical methods, for example, CNDO, INDO, MINDO, MNDO, AM1, and PM3, are computationally less demanding because they neglect several difficult integrals that need to be evaluated in the Hartree–Fock procedure;[51] recall that this was the procedure for determining the orbital coefficient and molecular orbitals. Depending on the procedure, particular interactions between certain orbitals are either completely neglected or replaced by parameters (unique for each atom) obtained by fitting against (experimental) data.[51] Furthermore, the basis sets employed in these procedures are often minimal basis sets, although some procedures try to correct for some shortcomings by the addition of a few more basis functions.[51] It is clear that the performances of these procedures will highly depend on the application and that the best results will be obtained for systems and parameters similar to those used for the parametrization and that their performance will be worse for describing more complicated electronic problems. This is not to say that semiempirical methods always lead to results of inferior quality compared to ab initio methods. Indeed, many problems, otherwise inaccessible to study using an initio methods, have been successfully studied using these procedures. However, it is always very important to establish the suitability of a method before using it to study unknown systems. This is especially true for semiempirical procedures, and we will see later on in this chapter that the AM1 procedure, which is probably together with PM3 the best-performing semiempirical procedure to date, dramatically fails in describing radical addition reactions.[42]

The solution of the Schrödinger equation yields N-electron wavefunctions Ψ, which contain very detailed information about the electronic structure of the system. However, for many properties of interest, such as the total energy, we do not require this very detailed information, and we can obtain these properties if we know the total electron density of the system, which in principle is much simpler to evaluate.[52] This realization has led to the development of density functional theory (DFT), which has been quite successful in describing and explaining many-electron systems

that have been too complicated to treat with conventional ab initio procedures, including crystal structure, metals and polymers. Density functional theory has undergone major developments since the early 1970s, and current procedures are based mostly on solving the so-called Kohn–Sham equations, which can be compared with, and are indeed similar, to the Hartree–Fock equations, which are used to evaluate the MOs in ab initio MO theory. In the case of DFT the equations are solved to obtain the electron density, and certain functionals of the electron density are used to represent electronic interactions. This procedure is in principle exact, but the exact forms of the functionals are not known and hence approximate functionals need to be used. The very similar nature of the Hartree–Fock and Kohn–Sham procedures has led to the development of hybrid methods, which generally show a great improvement over conventional Hartree–Fock procedures, because the DFT procedure contains more electron correlation. Currently popular and successful procedures are B-LYP[53,54] and B3-LYP,[54,55] which perform very well in many applications and often produce results of similar or even better quality than several higher level ab initio procedures. Since the computational demands of these procedures are generally less than those of conventional correlated ab initio methods, and they scale more favorably with increasing number of basis functions, it is likely that the popularity of these procedures, including radical reactions, will continue to rise.

1.4.4.1   Summary   From the theory outlined in this section, it is obvious that a more accurate description of the system is obtained with a high level of theory and a large and flexible basis set. It is also clear that the choice of basis set and level of theory depend on the nature of the molecular property that needs to be described. Both choices will always involve a compromise between desired accuracy and computational resources (e.g., for nearly all correlated procedures, the required amount of disk space scales as M^4, where M is the number of basis functions).

1.4.5   Pitfalls in Computational Quantum Chemistry

It is clear that, in general, the higher the level of theory, the more reliable our results. This is especially true if we wish to obtain accurate absolute energies. However, often we are interested in energy differences or certain trends, and we need not resort to these incredibly high-level and expensive methods. It is often possible to obtain adequate results at much simpler levels of theory, but it is important to establish before using these levels of theory whether they are appropriate. For example, a particular simple level procedure can introduce errors in the absolute energies of the reactants (ΔE_{reac}), transition state (ΔE_{TS}) and products (ΔE_{prod}). This situation is schematically shown in Fig. 1.11, where the calculated energies are indicated by the full lines and the real energies by dashed lines. Also the calculated and real barriers (E_0) and reaction energies (E_r) are indicated.

The description of the reactants and products is often (but not always!) not too difficult, and although we introduce an error in the absolute energies, the calculated reaction energy will be similar to the real one ($E_{\text{r,real}} \approx E_{\text{r,calc}}$) as long as the absolute error introduced in the product energies is similar to the one introduced in the
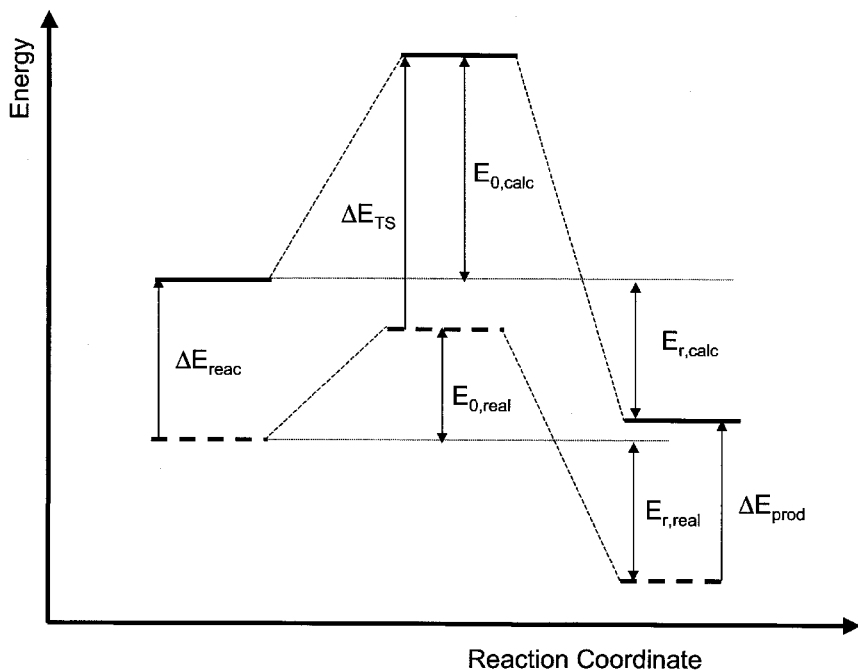
Figure 1.11 Schematic representation of the effect of computational errors on the calculated potential energy surface: full lines represent calculated energies, dashed lines represent the real energies (i.e., obtained using full CI and an infinite basis set). The situation depicted here reflects the case where the absolute error introduced in the energy of the transition state is much larger than the errors introduced in reactants and products.

reactant energies ($\Delta E_{\text{reac}} \approx \Delta E_{\text{prod}}$). However, the description of the transition state is often much more complicated than the description of the reactants, which will result in different absolute errors for the transition state and reactant energies. In Fig. 1.11 the situation is shown where the error in transition state energy is much larger than that of the reactants and products ($\Delta E_{\text{reac}} \approx \Delta E_{\text{prod}} \ll \Delta E_{\text{TS}}$), and although we found in this example that the calculated reaction energy was relatively close to the real one, the calculated barrier will be significantly too high ($E_{0,\text{calc}} \gg E_{0,\text{real}}$).

A very relevant real example of this problem is shown in Figs. 1.12 and 1.13. The data in these figures originate from an extensive study by Radom and co-workers,[42,43] who examined the effect of level of theory on the reaction energies and barriers for a range of radical additions. They established that the results for the barriers and reaction energies, respectively, converged at the QCISD(T) level of theory;[42] hence we plot the data of two different procedures against the QCISD(T) values. If the other procedures are equally good, then the data should lie on the diagonal. What we can see in Fig. 1.12 is that, except for two data points, the generally
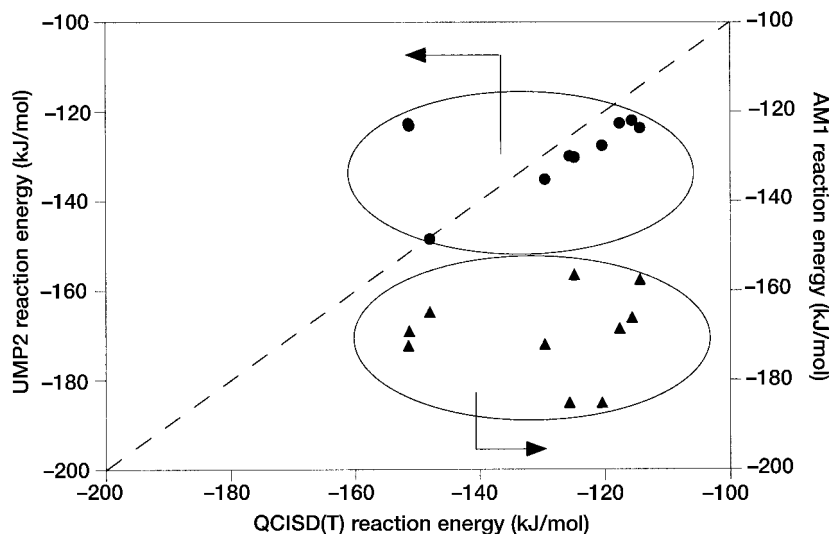
Figure 1.12   Plot of calculated UMP2/6-31G* ($\bullet$) and AM1 ($\blacktriangle$) reaction energies against calculated QCISD(T)/6-31G* reaction energies for the addition of $CH_3^{\bullet}$ radical to a range of subsituted ethylenes CH_2=CHY (Y = OH, F, H, CH_3, NH_2, SiH_3, Cl, CHO, NO_2). The erroneous UMP2 results are obtained for Y = CHO and CN, which both have UMP2/6-31G* reaction energies of about -123 kJ/mol, whereas their QCISD(T)/6-31G* reaction energies are about -151 kJ/mol. (Data are taken from the extensive study by Wong and Radom.[42])

popular (and generally accurate) UMP2 reaction energies show a reasonable, but far from perfect, agreement with the QCISD(T) results. However, the also popular semiempirical AM1 procedure gives very erratic results. Since AM1 often gives relatively good results for other types of organic reactions, we may conclude that its parametrization is incapable of providing an adequate description of radical addition reactions. Methods such as PMP2, RMP2, and QCISD showed good agreement with the QCISD(T) results.

When we consider the results for the reaction barriers obtained at the same levels of theory, we observe dramatic failures of both methods (Fig. 1.13). Clearly, the AM1 barriers are all too low and do not show any particular trend. The UMP2 results seem to look better, but all the barriers are significantly higher than those at the QCISD(T) level of theory, and furthermore the trend is quite erratic.

This poor performance of UMP2 can be ascribed to spin contamination (see discussion above).[44,45] If we have a ground state reaction such as in the reactions of most interest to us, then the electronic state does not change in going from reactants to products; in fact, it is exactly the same everywhere at the potential energy surface. Hence, everywhere on the potential energy surface we should have a single unpaired electron. However, the unrestricted procedures tend to "spread out" this single electron, and whereas this effect need not be really large when we just have a radical
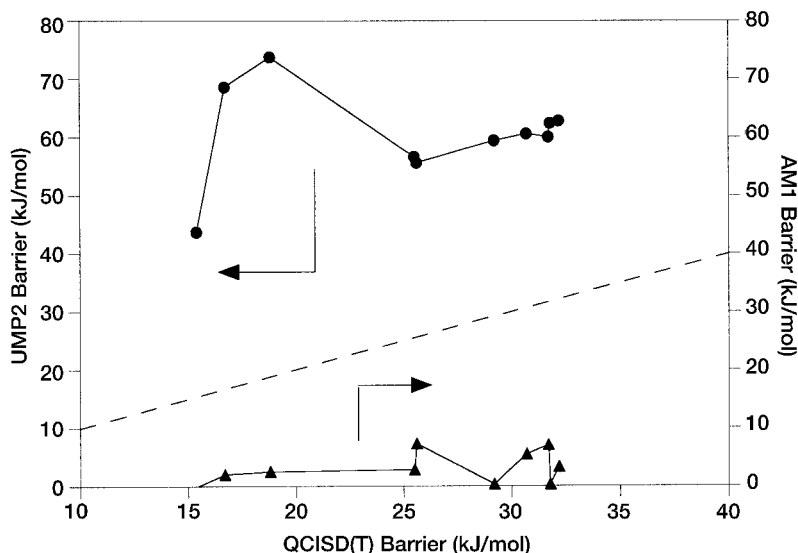
Figure 1.13   Plot of calculated UMP2/6-31G* (●) and AM1 (▲) reaction barriers against calculated QCISD(T)/6-31G* reaction barriers for the addition of $CH_3^{\bullet}$ radical to a range of subsituated ethylenes $CH_2=CHY$ ($Y = $ OH, F, H, CH_3, NH_2, SiH_3, Cl, CHO, CN, NO_2). Note that all the UMP2 results are too high, and that for $Y = $ CHO and CN not even the trend is reproduced adequately. (Data taken from the extensive study by Wong and Radom.[42])

[although several examples with severe spincontamination in simple radicals exist, e.g., cyanovinyl radical has $\langle S^2 \rangle = 1.49$],[56–59] this effect can be enormous in the electronically more complicated description of the transition state. Hence the effect of spin contamination on the calculated barrier may be huge, whereas it may be small in the case of the reaction energies. The problem of spin contamination does not exist for the restricted procedures.

In summary, it is of utmost importance to establish the suitability of the simpler levels of theory for the calculation of properties one wishes to study. Certain procedures may be cheaper and faster, and larger molecules can potentially be studied; however, one should be aware of the fact that the results may be meaningless if the chosen procedure is not appropriate. For example, the UMP2 procedure yields excellent results for many organic reactions, but we have seen it performs very poorly in radical reactions and its use should be avoided.

1.4.6   Practical Computational Quantum Chemistry

We saw in the previous part that it is essential to choose the appropriate level of theory if reliable results are to be obtained. This does not necessarily mean that one has to perform all calculations at the most expensive level of theory. For example, accurate energies for the calculation of reaction energies or barriers often

require high levels of theory, and often we cannot compromise much. However, the first cost-saving lies in geometry optimization. Although the best geometries are generally obtained at the highest levels of theory, the optimum geometries at simpler levels of theory are often very close (this is not always the case, but this can be considered as a general rule of thumb). This means that we can often optimize the geometry at a simple level of theory and then calculate the energy at the high level of theory for this geometry; this is a *single-point* energy calculation (often denoted as level of theory of single point/level of theory of geometry optimization). Naturally, one has to establish first that the geometries indeed converge with increasing level of theory; this is essential as the potential energy surface obtained at different levels of theory may differ significantly; for instance, spurious minima or transition states may occur at lower levels of theory, or essential features might be absent. This procedure of an energy calculation is shown in Fig. 1.14, in which I have attempted to reduce N atomic coordinates to a single set of coordinates. In this way we can plot the potential energy surface as a two-dimensional plot; the Y axis represents the energy and the X axis, a given set of coordinates. Three potential energy surfaces are shown, each corresponding to a different level of theory. Ultimately, we wish to calculate the energy of the molecule corresponding to the minimum on the high-level potential energy surface. However, we do not know where to start in our geometry optimization.
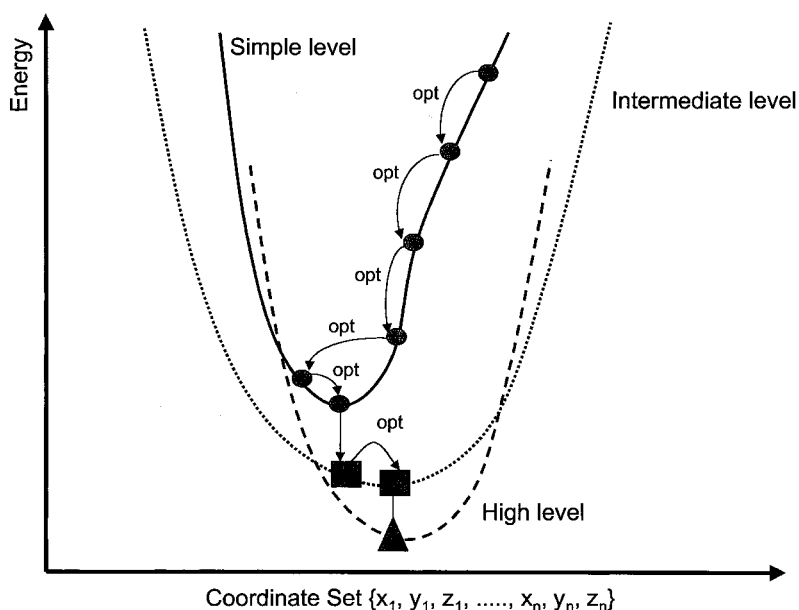

Figure 1.14   Schematic representation of the use of simple-level geometry optimizations and single-point energy calculation to approximate the energy of a high-level miminum energy conformation. Three different potential energy surfaces are shown, each at a different level of theory.

We start with the simplest level of theory and optimize until we reach the minimum on its potential energy surface, which in this particular case involves five optimization steps. Note that the potential energy surface was deliberately given a different shape than the two higher levels of theory. Since this is the case, it is not likely that the obtained geometry is sufficiently accurate, and indeed if we were to use this geometry to calculate the energy at the high level of theory, we would get a result that is significantly excessive. Hence we need to further optimize at a higher level of theory. In this example, we need only one single optimization step. It should be noted that the obtained geometry is indeed close to the optimum at the high level of theory, but that the energy is significantly higher. Finally, we use this geometry to calculate the energy at the highest level of theory, and it can be seen that the energy is indeed very close to the optimal energy. In this example, we have reduced the costs of a potentially very expensive problem significantly by not optimizing at the high level of theory, which would have involved a high-level calculation for every single optimization step; the geometry optimizations at the lower levels of theory are often only a fraction of the cost of the single-point calculation. Hence, if the same number of optimization steps at the high level of theory had been carried out as at the simpler levels, we would have had a six times more expensive calculation. Naturally, the required number of optimization steps and/or levels of theory will vary significantly from problem to problem, and will depend on the initial geometry guesses. It should be mentioned here that these procedures are often only required for the calculation of accurate energies. For example, the other properties required in a TST calculation, such as moments of inertia, rotational barriers and vibrational frequencies are often sufficiently accurate at relatively simple levels of theory, as was clearly shown for calculation of frequency factors in radical addition[47] and hydrogen abstraction reactions.[60]

The practical observations that certain properties can be adequately obtained at simpler levels of theory have led to several different additivity schemes that approximate the properties (especially the energy) at a very high level of theory by combining results obtained at simpler levels of theory. All these additivity schemes (e.g., G1,[61] G2,[62] G3,[63] CBS,[64,65] CBS-RAD[58]) have the following assumptions in common:

- Geometry at high level of theory $\approx$ geometry at simple level of theory

$$HLG \qquad \approx \qquad SLG$$

- Scaled ZPVE at high level of theory $\approx$ scaled ZPVE at simple level of theory

$$ZPVE\text{-}HL \qquad \approx \qquad ZPVE\text{-}SL$$

- Basis set effect at high level of theory $\approx$ basis set effect at simpler level of theory

$$HL/LB - HL/SB \qquad \approx \qquad SL/LB - SL/SB$$

where HL = high level of theory, SL = simple level of theory, HLG = high-level geometry, SLG = simple level geometry, LB = large basis set, SB = small basis set, ZPVE-HL = zero-point vibrational energy at high level of theory, and ZPVE-SL = zero-point vibrational energy at simple level of theory.

The energy calculated at a high level of theory of a geometry optimized at the corresponding level of theory is then in general approximated by the following equation:

$$HL/LB//HLG \approx (HL/SB//SLG) + (SL/LB//SLG)$$
$$- (SL/SB//SLG) + (ZPVE-SL) + \Omega \qquad (1.34)$$

where Ω contains some empirical corrections.

Pople and co-workers have pioneered these additivity schemes and devised the G1–G2–G3 family of theories,[61–63] in order to predict thermochemical properties of molecules within experimental errors. Others have come up with similar schemes such as the complete basis set (CBS) scheme by Petersson et al.[64,65] and the infinite basis extrapolation techniques by Martin.[66] In particular Radom and co-workers examined and optimized schemes to adequately describe radical thermochemistry and reactions.[42,43,47,56–59] Currently recommended procedures for the description of radicals are CBS-RAD and G3(MP2)-RAD.[30,43]

1.5   BASIC THEORY OF REACTION BARRIER FORMATION

So far we have discussed ways of predicting rate coefficients via transition state theory from molecular and electronic parameters, which we can calculate using, for example, ab initio molecular orbital theory. We have seen that simple geometric factors and vibrations govern the Arrhenius frequency factors and any temperature corrections to the critical energy (i.e., the barrier at 0 K). However, we have not yet discussed the factors that govern the height of a reaction barrier (and hence the activation energy) or possible ways of predicting it. A powerful theoretical framework for the discussion of reaction barrier formation is the curve-crossing model, also called the valence bond (VB) state correlation model, VB configuration mixing or state correlation diagram. This model, which has been developed by Shaik and Pross, is based on VB theory.[15–20]

In VB theory, the focus does not lie on molecular orbitals, but on electron pair bonds between atoms; VB theory assigns electrons to atomic orbitals, even in molecules.[14,17] In the limit, both VB and MO theories yield the same result; however because of the greater computational difficulties associated with VB theory, MO theory has become more interesting from a computational point of view. On the other hand, the VB descriptions allow for simple, nonmathematical representations of wavefunctions.[17] Electronic configurations described in VB theory correspond in nonmathematical terms just to the commonly used Lewis structures, and a full wavefunction with configuration interaction just corresponds to mixing of simple

resonance structures.[17] We will encounter several examples in the course of this section.

Let us return to the curve-crossing model.[15–20] We are interested in building up a reaction profile using VB theory, which we have just seen must be described in terms of electronic configurations that assign electrons to given atomic orbitals. It is clear that, in a reaction, we start with the electronic configuration of the reactants. Moving along the reaction coordinate, which involves geometric rearrangements, the electrons will start to feel increasingly uncomfortable in the atomic orbitals to which they have been assigned. The reaction involves the breaking of old and formation of new bonds, so clearly the closer the geometry resembles the product, the more the electrons wish to occupy different atomic orbitals (i.e., those making up the new bonds). Because of this effect, it is clear that the energy associated with the reactant electronic configuration (Ψ_{reac}) will continuously increase along the reaction coordinate.[17] It is clear that the appropriate electronic configuration of the products is the one in which the electrons are assigned to the atomic orbitals making up the new bonds (Ψ_{prod}). If we were now to use the product electronic configuration and move back along the reaction coordinate, we would observe the same as we did previously with the reactant electron configuration; the farther away we move from the product geometry, the worse the description of the electrons becomes if we only use the product electronic configuration (see Fig. 1.15).[17] Hence it is clear that in going from the reactants to the products along the reaction coordinate, we will, at some point, need to "switch" from Ψ_{reac} to Ψ_{prod}. This will happen in the region where the two curves "cross," and we can see that this happens at an energy that is higher than that of either the reactant or product configuration, and that it happens for a
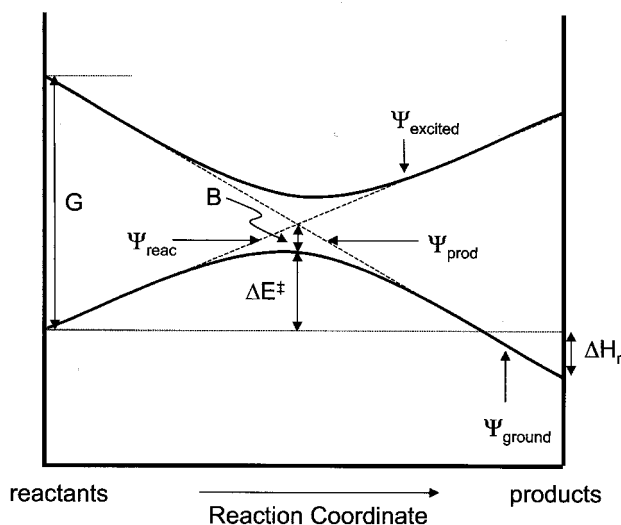

Figure 1.15 Curve-crossing diagram of reaction barrier formation through the avoided crossing of the reactant and product electronic configuration curves.

conformation between that of the reactants and that of the products.[17] Indeed, this happens in the region of the transition state.

We know from quantum mechanics [see also the discussion around Eq. (1.31)] that the ground-state wavefunction is always the lowest-energy wavefunction (for any given atomic configuration), and hence that state wavefunctions do not cross. Furthermore, we have seen in the section on configuration interaction that we often need more than a single electronic configuration to describe the state wavefunction; this situation is a very clear example of this need. The two configuration wavefunctions Ψ_{reac} and Ψ_{prod} combine to give two state wavefunctions: one for the ground state (Ψ_{ground}) and one for an excited state ($\Psi_{excited}$).[17] Since the ground state is of more interest to us, we will now focus our attention to the ground-state wavefuntion, which we can express in terms of the two configuration wavefunctions:[17]

$$\Psi_{ground} = C_1 \Psi_{reac} + C_2 \Psi_{prod} \tag{1.35}$$

where the coefficients C_1 and C_2 will depend on the position along the reaction coordinate: $C_1 \gg C_2$ close to the reactant geometry, whereas $C_2 \gg C_1$ close to the product geometry. Considering Fig. 1.15, we can also simply see that the excited-state wavefunction in the reactant geometry is determined mainly by Ψ_{prod} and in the product geometry by Ψ_{reac}. In the transition region, where we expect the electronic rearrangement to take place and where the energies of the two configurations are similar, we expect $C_1 \approx C_2$ and hence that the wavefunction in the transition state can be described as[17]

$$\Psi_{TS} \approx \frac{1}{\sqrt{2}} (\Psi_{reac} + \Psi_{prod}) \tag{1.36}$$

We have seen before that configuration interaction leads to a lowering of the energy, and hence the relative energy of the transition state; thus the barrier ($\Delta E^{\ddagger}$) is significantly lowered as compared to the energy at which the two electronic configurations cross. This lowering is indicated by the quantum-mechanical interaction parameter B in Fig. 1.15. From Fig. 1.15, we can also see that the point where the two curves cross is determined by the initial energy gap (G) between the energies of Ψ_{reac} and Ψ_{prod}. In reality, the two configuration curves are not straight lines, and hence their curvature, which is expressed in a factor $f (0 < f < 1)$, will determine the fraction of the initial energy gap that contributes to the barrier height. We can now express the barrier height as a function of these (quantum-mechanical) parameters:[17]

$$\Delta E^{\ddagger} = f \cdot G - B \tag{1.37}$$

If we compare the barriers of related reactions, the interaction parameter B is often considered to remain constant, and hence any differences in barrier heights are explained by changes in the parameters f and G.[17]

In general, reaction exothermicity affects f; a reaction that is more exothermic has a smaller f, and hence a lower barrier. This effect, which leads to
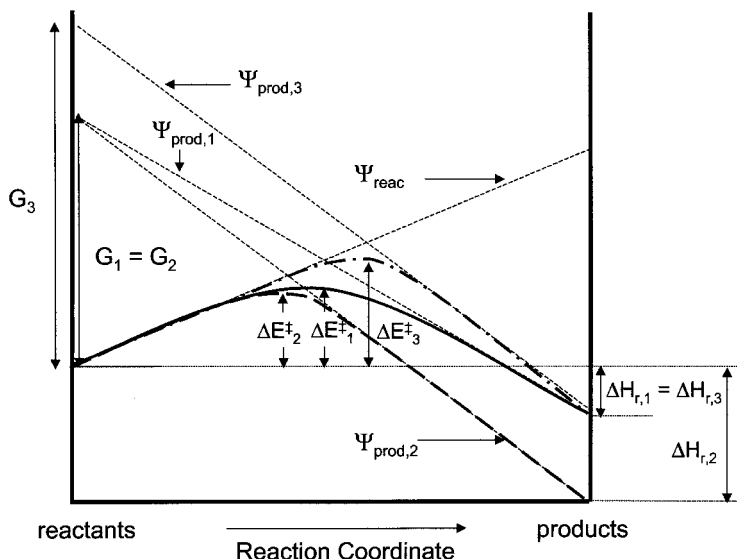
Figure 1.16   Effect of reaction exothermicilty (expressed through f) and initial energy gap (G) on barrier height and location of the transition state. For simplicity the configuration wavefunctions are depicted as straight lines. The initial situation, the effect of f, and the effect G, are characterized by the parameters with subscripts 1, 2, and 3 respectively.

Bell–Evans–Polanyi behavior,[22,23] is schematically shown in Fig. 1.16; by making the reaction more exothermic, the curves cross at a lower energy, thus lowering the barrier. Furthermore, we see that the location of the transition state has moved closer to the reactant geometry. Generally speaking, the transition state of an exothermic reaction lies closer to the reactant configuration and is said to be early, whereas an endothermic reaction lies closer to the product side and is said to be late.

A second effect on the barrier height is caused by the initial energy gap G, and we can see in Fig. 1.16 that an increase in G results in a higher barrier. This effect, which is general, need not be accompanied by a change in reaction exothermicity (see Fig. 1.16). However, in the case of radical reactions, the initial energy gap is closely related to the stability of the products (as we will see later) and hence is highly correlated with the reaction exothermicity.[17,39] This situation is depicted in Fig. 1.17, and again we expect to see a change in the location of the transition state when G changes.[17]

To summarize the discussion of the curve-crossing model to this point, we can say that in its simplest formulation, the barrier is considered to arise from an avoided crossing of the electronic configurations that correspond to reactants and products, respectively. However, it is obvious that the valence bond description in terms of single reactant and product electronic configurations will become increasingly poor on moving toward the transition state along the reaction coordinate. In order
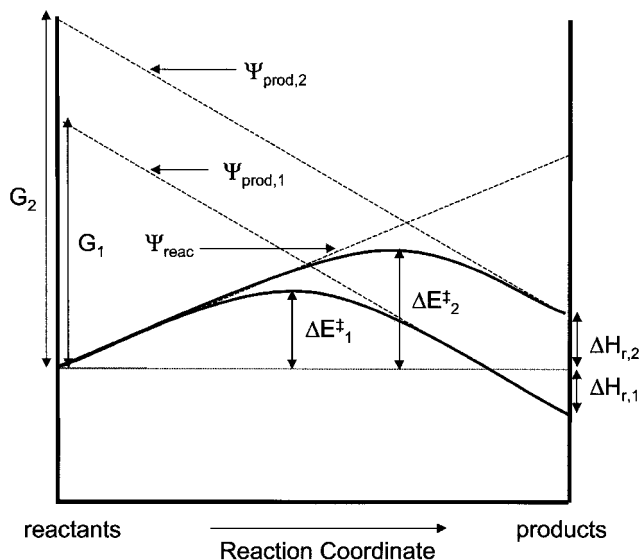
Figure 1.17   Effect of initial gap, G, on reaction barrier when G is highly correlated with the reaction exothermicity (or stability of the products). This is often the case in radical reactions, especially in radical addition reactions.

to provide a better description of the transition state region, other configurations (which are, by definition, excited-state configurations at both the reactant and product geometries) are often mixed with the ground-state descriptions of the reactant and product electronic configurations.[17] In the case of radical reactions, possible important configurations are those corresponding to polar charge transfer (CT) configurations, in which an electron has been transferred from the radical to the second reactant or vice versa. If we denote the charge transfer configuration wavefunction by Φ_{CT}, we can now express the ground state wavefunction as[17]

$$\Psi_{\text{ground}} = C_1\Psi_{\text{reac}} + C_2\Psi_{\text{prod}} + C_3\Phi_{CT} \tag{1.38}$$

and assuming that the extent of mixing of Φ_{CT} into the state wavefunction does not disturb the equal contributions of Ψ_{reac} and Ψ_{prod} to the wavefunction describing the transition state, then Ψ_{TS} can be written as[17]

$$\Psi_{TS} \approx N\left\{\frac{1}{\sqrt{2}}(\Psi_{\text{reac}} + \Psi_{\text{prod}}) + \lambda\Phi_{CT}\right\} \tag{1.39}$$

where N is a normalization constant and λ is the mixing coefficient of Φ_{CT}. The parameter γ in the model proposed by Fischer and Radom [Eq. (1.5)][30] is related to the mixing parameter λ.

$$\sim C^{\bullet} \;+\; C{=}C \;\longrightarrow\; \sim C{-}C{-}C^{\bullet}$$

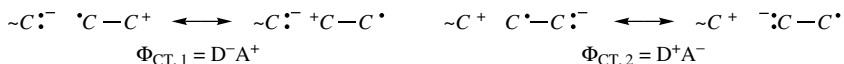$$\Psi_{reac} = DA \qquad\qquad \Psi_{prod} = D^3A^*$$
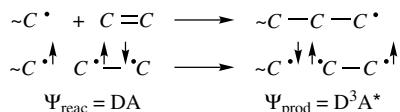
Scheme 1.2

Let us now specifically look at radical addition and abstraction reactions, beginning with radical addition reactions. In Scheme 1.2, the reaction of a radical addition is given with the corresponding electron spin shifts that accompany the reaction.[17] These schematic representations of electron pairs and electron spins are at the same time pictorial representations of the VB configurations of the reactant and product. We denote the radical in this reaction as D (donor) and the alkene as A (acceptor). Note that in the reactant configuration DA, the electrons in the π bond are of opposite spin and hence form a bond, whereas the electrons on the radical and the central carbon have the same spin (they form a triplet interaction), and do not form a bond. In the product configuration, however, the electron of the radical and the central carbon atom are paired (and have formed a new bond), whereas the electrons in the original π bond now have the same spin (and the bond is broken). Hence, the electronic configuration in the original alkene has been changed from a singlet in the reactant configuration to a triplet in the product configuration. Since the triplet is an excited state of the initial singlet, we denote the electronic state of the acceptor molecule by $^3A^*$ and the overall product configuration wavefunction by D^3A^*. Hence, in its simplest formulation, the barrier in a radical addition reaction is governed by a DA–D^3A^* avoided crossing,[17,38–41] and it is furthermore clear that the initial energy gap can be approximated by the singlet–triplet energy gap (ΔE_{ST}) of the π bond ($G \approx \Delta E_{ST} \approx 2.5 - 4.5$ eV $\approx 240 - 440$ kJ/mol, depending on the alkene substituents).[17,30,39] It can also be understood now that the reaction exothermicity and G are interrelated. If the alkene is monosubstituted, the substituent will be on the carbon with the unpaired electron in the product radical and the unpaired electron in the triplet state of the alkene. Hence, the effect of the substituent on the energies of these two species is expected to be similar, and a near-parallel shift of Ψ_{prod} is expected, as shown schematically in Fig. 1.17.

As stated before, the most important additional electronic configurations to radical reactions are the charge transfer configurations, which are shown in Scheme 1.3. The D^-A^+ configuration is generated by the electron transfer from the alkene to the radical, whereas the D^+A^- configuration is generated by the reverse reaction.

In Fig. 1.18, the curve-crossing diagram for a radical addition is shown, including all contributing electronic configurations.

$$\sim C{:}^{-}\;\;{}^{\bullet}C{-}C^{+} \;\longleftrightarrow\; \sim C{:}^{-}\;{}^{+}C{-}C^{\bullet} \qquad \sim C^{+}\;\;C^{\bullet}{-}C{:}^{-} \;\longleftrightarrow\; \sim C^{+}\;\;{:}C{-}C^{\bullet}$$

$$\Phi_{CT,\,1} = D^-A^+ \qquad\qquad\qquad \Phi_{CT,\,2} = D^+A^-$$
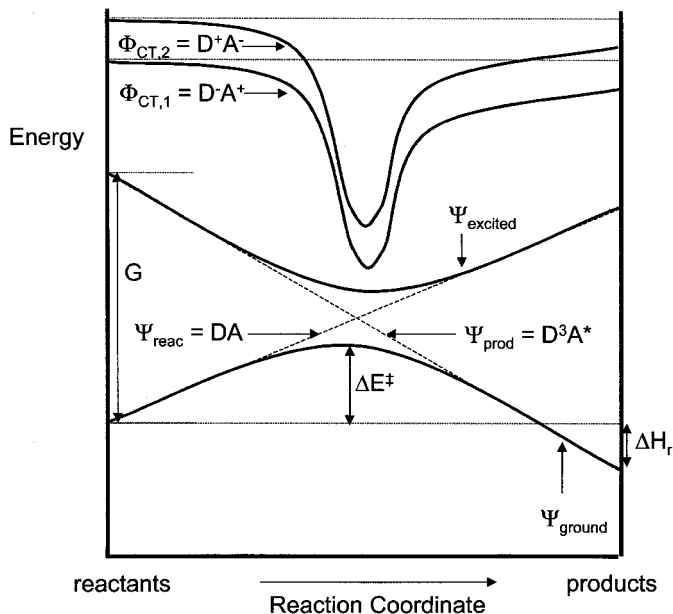
Scheme 1.3

Figure 1.18 Curve-crossing diagram for a radical addition, in which the barrier height is largely determined by a DA-D^3A* avoided crossing and a possible mixing of the D^-A^+ and D^+A^- charge transfer configurations lowers the barrier.

The shape of the two charge transfer configuration curves is explained as follows. Both configurations are excited state configurations which are generated by the electron transfer between the donor and acceptor molecules, which are neutral in the ground state. The relative energies of the charge transfer states as compared to the ground state are determined by the electron affinities (EA) and the ionization potentials (I) of the donor and acceptor molecules, which are defined as in Scheme 1.4.[17]

Hence the relative energies of D^+A^- and D^-A^+ with respect to the ground-state energy of DA can be given by[17]

$$E(D^+A^-) = I_D - EA_A \tag{1.40}$$

$$E(D^-A^+) = I_A - EA_D \tag{1.41}$$

For the addition of methyl radical, which does not seem to be significantly affected by polar effects, these energies, depending on the alkene substituent, lie roughly

$$
\begin{array}{lll}
M \longrightarrow M^+ + e^- & \Delta E = I \\
M + e^- \longrightarrow M^- & \Delta E = -EA
\end{array}
$$
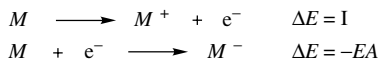
Scheme 1.4

between 8 and 12 eV ($\approx$770–1150 kJ/mol) above the ground-state energy.[39] The lowering of the energy of these configurations in the region of the transition state is caused by the Coulomb interaction ($C = e^2/r$) between the two i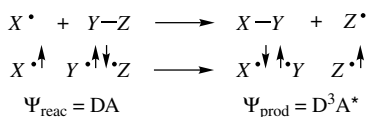onic species when they approach.[17,30,39] Mixing of a charge transfer configuration into the ground-state configuration becomes important if one or both of these charge transfer configurations is low in energy. Hence it depends on the absolute values of ($I - EA - e^2/r$) in the region of the transition state (for radical addition reactions $r \approx 2.2$ Å; hence $C \approx 6.5$ eV ≈ 630 kJ/mol; this value should be considered as an upper limit as delocalization of electrons will lower C).[30,39] In the extreme case, where $I - EA \approx C$, the barrier is likely to be very low. At this point, we should refer back again to the Fischer–Radom model [Eq. (1.5)],[30] which accounts for the polar effects using this term in their polar factors F_n and F_e. Finally, it should be pointed out that if polar effects are important and $E(D^+A^-) < E(D^-A^+)$, the radical has an electron-donating, that is, a nucleophilic, character, whereas if polar effects are important and $E(D^-A^+) < E(D^+A^-)$, the radical has electron-accepting, or an electrophilic, character.
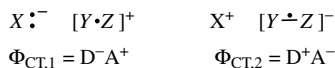
Let us now consider radical abstraction reactions (Scheme 1.5). We can see that the barrier is governed by a similar DA–D^{3}A* avoided crossing.[17] Whereas the two carbons in the alkene of the radical addition are still bound via a σ bond (we broke a π bond), in this case we break the σ bond (i.e., the only bond) between Y and Z. Possible charge transfer configurations are shown in Scheme 1.6.

As was the case in radical addition reactions, the reaction exothermicity (through G) and the magnitudes of the ionization potentials and electron affinities of the reactants (through mixing of the charge transfer configurations into the ground state) govern the height of the barrier in radical abstraction and transfer reactions.[17]

To conclude this section, it is important to note that the curve-crossing model is very useful and powerful in analysing computational results, but because it is not always clear beforehand what configurations will be important, its predictive value for unknown reaction types may be limited. Especially in the case of radical addition reactions, it has clearly demonstrated its value as will be shown in the following section, in which some of the results will be discussed on which the Fischer–Radom model [Eq. (1.5)][30] is based.

$$X^{\bullet} \; + \; Y{-}Z \; \longrightarrow \; X{-}Y \; + \; Z^{\bullet}$$

$$X^{\bullet\uparrow} \; Y^{\bullet\uparrow\downarrow\bullet}Z \; \longrightarrow \; X^{\bullet\downarrow\uparrow}Y \; Z^{\bullet\uparrow}$$

$$\Psi_{reac} = DA \qquad\qquad \Psi_{prod} = D^3A^*$$

Scheme 1.5

$$X{:}^{-} \quad [Y{\cdot}Z]^{+} \qquad\qquad X^{+} \quad [Y{\doteq}Z]^{-}$$

$$\Phi_{CT,1} = D^-A^+ \qquad\qquad \Phi_{CT,2} = D^+A^-$$

Scheme 1.6

1.6   APPLICATIONS IN FREE-RADICAL POLYMERIZATION

In this section, the theoretical concepts outlined in this chapter so far will be applied to problems of relevance to free-radical polymerization. Several different aspects of radical addition and propagation will be discussed, followed by a discussion of some problems in chain transfer reactions.

1.6.1   Radical Addition and Propagation

1.6.1.1   General Aspects   As already eluded to at several occasions in this chapter, radical additions have been widely studied using ab initio molecular orbital theory. A large number of papers have appeared since the early 1980s, but without denying the importance of many of the early papers, we will focus our discussion on a series of papers by Wong et al.,[38–43] Heuts et al.,[31,35,47,60,67,68] Coote et al.,[69–71] and Huang et al.[72] The results in these papers were obtained with current state-of-the-art levels of theory, and appear to be of most relevance to polymer chemistry. For comparisons with other theoretical studies, I refer to the original papers of which the results are discussed here. First some general aspects on suitable levels of theory will be discussed,[42,43,47] followed by a discussion of reaction barrier formation in (small) radical additions,[38–41,73] which results in formulation of the model proposed by Fischer and Radom [see Eq. (1.5)].[30] Then we will have a look at the factors that govern the frequency factors for radical addition reactions, and see how simple geometric and steric arguments can explain particular observations in free-radical polymerization.[31,35,72] Finally, we will have a look at copolymerization reactions, where theoretical chemistry has played an important role in justifying and describing the penultimate unit effect.[67,69–71] However, before we can start with all of this, one important point, which we have ignored so far, still needs to be addressed: the effect of the reaction medium.

In our theoretical descriptions, we have thus far considered only gas-phase reactions. All the described models and theories can incorporate the effect of solvents (all in a different way), but this will make the descriptions naturally more complicated. Fortunately, it is not likely that we need to incorporate medium effects for most of our mechanistic studies, as experimental gas- and liquid-phase data of radical reactions show similar trends for substituent effects with the absolute rate coefficients differing by about a factor of 10.[30] Careful analysis by Fischer and Radom suggests that calculated barriers may be a few kJ/mol higher than those of liquid-phase reactions and that frequency factors may differ by a factor of roughly 2–5. Solvent polarity can significantly affect the barrier if the charge transfer states are relatively low in energy, as polar solvents will stabilize these states, which will lead to a lowering in reaction barrier.[17] However, all these effects are relatively small compared to the effects we address using "simple" gas-phase reactions.[30] Using more complicated (and not necessarily more accurate) theories will only cloud the picture, and hence we will only focus on gas-phase theoretical results.

We have seen in previous sections that we can use ab initio molecular orbital theory to calculate all the parameters required in transition state theory to predict

the rate coefficient for radical addition (or propagation) and that we can analyze the components determining the reaction barrier formation via the curve-crossing model. We have already discussed the fact that it is of utmost importance that all the properties required in our predictions and analyses are calculated with appropriate levels of theory. It was shown in a comprehensive assessment by Heuts et al.[47] that the properties required for calculating molecular partition functions, specifically, molecular geometries, harmonic frequencies, and rotational barriers, are reliably obtained at relatively simple levels of theory, such as HF/6-31G*. Hence Arrhenius frequency factors [Eq. (1.13)] and temperature corrections to the barrier [Eq. (1.12)] and the reaction enthalpy [Eq. (1.8)] are reliably calculated at simple levels of theory. However, the situation is very different for the calculation of reaction enthalpies and reaction barriers, which need to be calculated using higher levels of theory.[42,43,47] This is caused mainly by the effect of spin contamination (see above) on the calculated energy rendering UMP methods unsuitable for adequately describing radical addition reactions. Although UHF/6-31G* geometries generally yield satisfactory results in single-point energy calculations of radical reactions and the bulk of studies regarding radical reactivity is based on these geometries, it was found that better results are obtained using B3-LYP/6-31G* geometries.[30,43] Reliable absolute reaction enthalpies are obtained using the CBS-RAD procedure, which agrees well with experimental data (showing a correlation coefficient R^2 of 0.93).[30,43] Other procedures, including RMP2, PMP2, B3-LYP, and QCISD (except for the AM1 and UMP2 procedures) yield satisfactory results (although with greater deviations from experimental data) showing good correlation with the CBS-RAD results ($R^2 = 0.98$–0.99). For barriers, methods such as CBS-RAD and G3(MP2)-RAD are recommended,[30,43] but these procedures are too expensive for many systems of interest and can currently be applied only to small systems. Comparison of CBS-RAD data with available experimental data yields good agreement, with a mean deviation of 1.7 kJ/mol.[30] Reasonable alternatives for larger systems were found to be B3-LYP/6-31G* (which gives surprisingly good agreement with CBS-RAD), B3-LYP/6-311 + G(d,p), or B3-LYP/6-311 + G(3df,2p).[30,43] Good correlations with trends observed using the CBS-RAD procedure are also observed for QCISD(T) and QCISD (both with $R^2 = 0.99$), RMP2 ($R^2 = 0.98$), and PMP2 ($R^2 = 0.96$). The interested reader is referred to the original papers for extended comparisons.[30,42,43] In what follows, general trends will be discussed.

In Fig. 1.19 a schematic representation is given for the addition of substituted methyl radicals to substituted ethylenes. Four key geometric parameters are indicated: $r(C\text{-}\text{-}\text{-}C)$ (the length of the forming CC bond), ϕ_1 and ϕ_{attack} (the angles that the two reactant fragments make with the forming bond), and ϕ_{pyr} (the deviation from planarity of the hydrogens attached to the alkene carbon forming the bond.

First we compare these parameters for the additions of methyl (X = H), ethyl (X = CH$_3$) and propyl (CH$_2$CH$_3$) radicals to ethylene (Y = H), which are listed in Table 1.2. It can be seen that except for $r(C\text{-}\text{-}\text{-}C)$, which decreases slightly in going from methyl[42] to ethyl radical,[47] all other parameters are roughly constant (further extension of the chain yields parameters very similar to those of the propyl radical
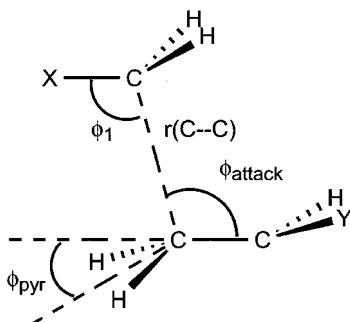
Figure 1.19   Definition of key geometric parameters for the addition of a range of substituted alkyl radicals to substituted ethylenes.

addition).[47] This result is very positive in that it allows us to use small-radical models to describe the reaction site of large polymeric radicals (see text below).

Also listed in Table 1.2 are the corresponding bond lengths and angles in the product radicals. Again, it can be seen that increasing the chain length does not significantly affect these geometric parameters. Furthermore, it can be seen that all the angles are smaller than the corresponding parameters in the product radicals. The behavior of these parameters, especially of ϕ_{pyr} (which is roughly 0° in the reactant and 56° in the product), clearly demonstrates that the reaction coordinate does not solely consist of the forming CC bond length (see also Fig. 1.3).

A final note in this section should be made regarding the conformation of the transition structure. In Fig. 1.19, the substituent X is in an anti position as compared to the substituted ethylene. However, in some cases a gauche conformation may have a lower energy (e.g., in the case of the additions of ethyl and ethylbenzene radicals to ethylene), and the pathway through this transition state structure will hence have a lower barrier.[47]

TABLE 1.2   Calculated Key Structural Parameters at the UHF/6-31G* Level of Theory for the Anti Addition of Alkyl Radicals to Ethylene[a]

X	r(C---C) (Å)	ϕ_{attack} (deg)	ϕ_{pyr} (deg)	ϕ_1 (deg)	Ref.
H	2.246	109.1	21.8	—[b]	42
	(1.537)[c]	(113.1)[c]	(55.9)[c]	(110.9)[c]	
CH_3	2.232	109.8[c]	22.8	105.9	47
	(1.539)[c]	(113.4)[c]	(56.0)[c]	(112.6)[c]	
CH_2CH_3	2.234	109.7[c]	22.7	106.4	47
	(1.539)[c]	(113.4)[c]	(56.0)[c]	(113.0)[c]	

[a] Values within parentheses apply to product radicals. For definitions, see Fig. 1.19 (Y = H).
[b] Not reported.
[c] Not reported in given reference, but part of the overall output of reported results.[60]

TABLE 1.3   Calculated Lengths (UHF/6-31G*) of the Forming CC Bond in Transition States for Addition of Four Different Substituted Methyl Radicals to a Range of Substituted Ethylenes [a]

Y	r(C---C) (Å)			
	$CH_3^{\bullet}$	$CH_2OH^{\bullet}$	$CH_2CN^{\bullet}$	$C(CH_3)_3^{\bullet}$
F	2.246	2.226	2.173	2.207
H	2.246	2.222	2.177	2.200
NH_2	2.240	2.220	2.178	2.207
Cl	2.264	2.245	2.181	2.215
CHO	2.312	2.291	2.230	2.265
CN	2.313	2.287	2.219	2.267

[a] See Fig. 1.19 for definitions. $CH_3^{\bullet}$, $CH_2OH^{\bullet}$, and $CH_2CN^{\bullet}$ data taken from Ref. 40; $C(CH_3)_3^{\bullet}$ data, from Ref. 41.

1.6.1.2   *Barrier Formation*

The effect of different substituents in methyl radicals and CH_2=CHY have also been studied, and in Tables 1.3 and 1.4, the results of key geometric parameters are listed for the transition states of the additions of $CH_3^{\bullet}$, $CH_2OH^{\bullet}$, $CH_2CN^{\bullet}$, and $C(CH_3)_3^{\bullet}$ to CH_2=CHY (Y = F, H, NH_2, Cl, CHO, CN).[40,41]

From Table 1.3 it can be seen that the length of the forming CC bond lies roughly between 2.17 and 2.31 Å (UHF/6-31G*), and it is clear that this bond length is affected by both the radical and the alkene substituent.

In Table 1.4, the calculated angles of attack and pyramidalization (UHF/6-31G*) are listed, and although their values depend on the radical and the alkene, the differences are generally small and appear to be a bit more random. Values for ϕ_{attack} range from 107.2° to 113.0°, and those for ϕ_{pyr} have a slightly wider range from 18.6° to 28.8°.

TABLE 1.4   Calculated Angles of Attack and Pyramidalization[a] **(UHF/6-31G*) in Transition States for Addition of Four Different Substituted Methyl Radicals to a Range of Substituted Ethylenes**

Y	ϕ_{attack} (deg)				ϕ_{pyr} (deg)			
	$CH_3^{\bullet}$	$CH_2OH^{\bullet}$	$CH_2CN^{\bullet}$	$C(CH_3)_3^{\bullet}$	$CH_3^{\bullet}$	$CH_2OH^{\bullet}$	$CH_2CN^{\bullet}$	$C(CH_3)_3^{\bullet}$
F	109.9	108.2	109.3	112.1	25.0	25.9	28.0	28.2
H	109.1	108.7	107.4	111.6	21.8	22.3	24.5	25.7
NH_2	111.0	109.8	109.5	113.1	25.8	26.5	27.9	28.8
Cl	108.9	107.8	107.4	113.0	22.4	23.3	26.0	27.2
CHO	107.6	107.4	106.6	110.3	18.6	19.0	22.1	22.4
CN	107.5	107.2	106.4	110.7	19.0	19.4	23.7	22.5

[a] See Fig. 1.19 for definitions. $CH_3^{\bullet}$, $CH_2OH^{\bullet}$, and $CH_2CN^{\bullet}$ data taken from Ref. 40; $C(CH_3)_3^{\bullet}$ data, from Ref. 41.

TABLE 1.5   Calculated Barriers and Enthalpies (QCISD/6-311G** + ZPVE) for Additions of Four Different Substituted Methyl Radicals to a Range of Substituted Ethylenes[a]

Y	Barrier (kJ/mol)				Reaction Enthalpy (kJ/mol)			
	$CH_3^\bullet$	$CH_2OH^\bullet$	$CH_2CN^\bullet$	$C(CH_3)_3^\bullet$	$CH_3^\bullet$	$CH_2OH^\bullet$	$CH_2CN^\bullet$	$C(CH_3)_3^\bullet$
F	39.8	35.0	42.3	21.6	−94.2	−87.5	−63.2	−89.5
H	38.9	32.7	42.5	21.4	−93.5	−87.1	−63.3	−87.8
NH_2	36.3	32.5	30.7	17.9	−100.2	−91.4	−72.1	−95.7
Cl	32.5	24.6	35.9	13.6	−105.9	−97.8	−74.5	−99.1
CHO	28.7	18.3	33.9	6.5	−120.7	−118.6	−92.9	−120.5
CN	24.3	11.7	32.6	1.9	−129.3	−123.7	−93.4	−124.5

[a] $CH_3^\bullet$, $CH_2OH^\bullet$, and $CH_2CN^\bullet$ data taken from Ref. 40; $C(CH_3)_3^\bullet$ data, from Ref. 41.

In Table 1.5, the calculated barriers and reaction enthalpies (QCISD/6-311G** + ZPVE) are listed, and it should be noted that these values deviate in an absolute sense from the better and recommended CBS-RAD procedure. However, the used procedure here has proven to have an excellent correlation with the better procedure and hence is expected to reproduce trends very well.

It can be seen from Table 1.5 that both the reaction barrier and the reaction enthalpy are greatly affected by the substituents in both the radical and the alkene. Furthermore, these effects appear to be very systematic. In general, the barriers for $CH_2CN^\bullet$ addition are highest for a given alkene as compared to the addition of the other three radicals, irrespective of the alkene substituent.[40] Similarly, the addition of $C(CH_3)_3^\bullet$ always appears to have the lowest barrier.[41] Finally, except for the addition of $CH_2CN^\bullet$, the barriers of these radical additions decrease with increasing reaction exothermicity, as is more clearly illustrated by Fig. 1.20.[41]

The data for the $CH_3^\bullet$, $CH_2OH^\bullet$, and $C(CH_3)_3^\bullet$, additions all show a linear correlation between the barrier height and reaction enthalpy with good coefficients of determination ($R^2 > 0.95$).[41] It should be noted at this point that the line of the methyl addition lies highest; for a given reaction enthalpy, the barrier is highest for methyl radical addition. This means that the barriers of all the other radical additions experience additional stabilizing effects that lower the barrier at a given reaction enthalpy. These stabilizing effects are provided by low-lying charge transfer states, which are not significantly operative in the methyl radical additions.[39–41]

The relative energies of the charge transfer states (D^+A^- and D^-A^+) for the radical additions are listed in Table 1.6, and it can immediately be seen that the charge transfer states in methyl radical addition indeed lie very high (except for the D^-A^+ state of the addition to CH_2=CHNH_2)[74] and are unlikely to play a significant role in the barrier formation. Hence it can be concluded that polar effects are relatively unimportant in the addition of a methyl radical to substituted ethylenes. For the $CH_2OH^\bullet$ and $C(CH_3)_3^\bullet$ additions, we observe that generally (again with the exception of addition to CH_2=CHNH_2) the D^+A^- states are relatively low in energy and
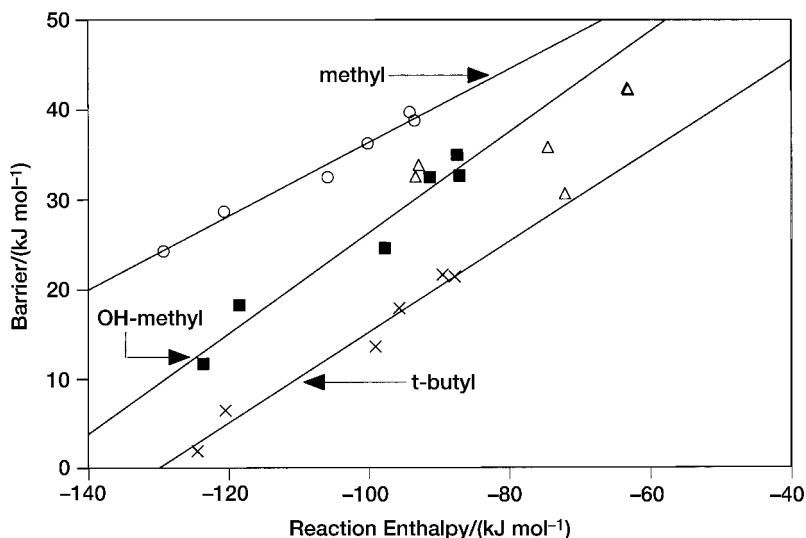
Figure 1.20 Plot of barrier height $\Delta E^{\ddagger}$ against reaction enthalpy ΔH_r (QCISD/6-311G**) for the addition of $CH_3^{\bullet}$ ($\bigcirc$), $CH_2OH^{\bullet}$ ($\blacksquare$), $CH_2CN^{\bullet}$ ($\triangle$), and $C(CH_3)_3^{\bullet}$ ($\times$) to a range of substituted alkenes $CH_2{=}CHY$, with Y = F, H, NH_2, Cl, CHO, and CN. The solid regression lines are given by $\Delta E^{\ddagger} = 77.4 + 0.41\Delta H_r$ ($CH_3^{\bullet}$ addition, $R^2 = 0.979$); $\Delta E^{\ddagger} = 82.6 + 0.56\Delta H_r$ ($CH_2OH^{\bullet}$ addition, $R^2 = 0.950$); $\Delta E^{\ddagger} = 65.9 + 0.50\Delta H_r$ [$C(CH_3)_3^{\bullet}$ addition, $R^2 = 0.972$]. Note that there is no apparent linear correlation between barrier and reaction enthalpy for $CH_2CN^{\bullet}$ addition. [$CH_3^{\bullet}$, $CH_2OH^{\bullet}$, and $CH_2CN^{\bullet}$ data taken from Ref 40; $C(CH_3)_3^{\bullet}$ data taken from Ref 41.]

TABLE 1.6   Calculated Energies of Charge Transfer States (eV), [G2(MP2)] for Additions of Four Different Substituted Methyl Radicals to a Range of Substituted Ethylenes[a]

	$CH_3^{\bullet}$		$CH_2OH^{\bullet}$		$CH_2CN^{\bullet}$		$C(CH_3)_3^{\bullet}$	
Y	D^+A^-	D^-A^+	D^+A^-	D^-A^+	D^+A^-	D^-A^+	D^+A^-	D^-A^+
F	11.39	10.33	9.05	10.51	11.78	8.78	8.40	10.36
H	11.63	10.54	9.30	10.72	12.03	8.99	8.64	10.57
NH_2	11.69	8.14	9.35	8.32	12.08	6.59	8.70	8.17
Cl	11.05	9.94	8.71	10.12	11.44	8.39	8.06	9.97
CHO	9.74	10.17	7.46	10.35	10.13	8.62	6.75	10.20
CN	10.00	10.94	7.66	11.12	10.39	9.39	7.01	10.97

[a] $CH_3^{\bullet}$, $CH_2OH^{\bullet}$, and $CH_2CN^{\bullet}$ data taken from Ref. 40; $C(CH_3)_3^{\bullet}$ data, from Ref. 41.

lower than the D^-A^+ states.[17,30,40,41,73] This indicates that the charge transfer states, in which charge has been transferred from the radical to the alkene, can interact with the ground states and hence lower the barriers for these additions; $CH_2OH^\bullet$ and $C(CH_3)_3^\bullet$ display nucleophilic behavior in the addition reactions to the studied range of substituted alkenes.[17,30,40,41,73] Similarly, the $CH_2CN^\bullet$ always displays electrophilic behaviour for the studied addition reactions $(D^-A^+ < D^+A^-)$. From the presented results, it has been concluded that energetically significant polar contributions to the transition state in radical addition reactions arise when the relative energy of one of the charge transfer configurations drops below $\sim 9 - 9.5$ eV[40,41,73] (Fischer and Radom mention values of 7–8 eV in their review, which also discusses experimental data).[30]

It is also interesting to investigate the structure of the transition state in the light of the curve-crossing model. We saw previously that if the initial energy gap G changes (see also Fig. 1.17), we expect to see a change in the location of the transition structure. Since the reaction exothermicity is directly correlated to G, we expect to see a change in the location of the transition state with changing reaction enthalpy.[17] In Fig. 1.21, the length of the forming CC bond in the transition state is plotted against the reaction enthalpy for all the reactions considered in this section
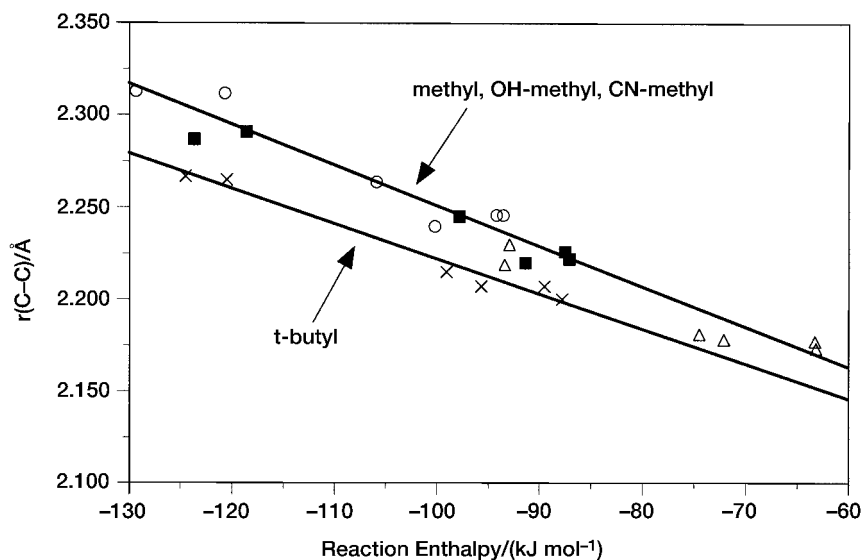

Figure 1.21   Plot of C—C bond length (UHF/6-31G*) in the transition structure against reaction enthalpy ΔH_r (QCISD/6-311G**) for the addition of $CH_3^\bullet$ ($\bigcirc$), $CH_2OH^\bullet$ ($\blacksquare$), $CH_2CN^\bullet$ ($\triangle$), and $C(CH_3^\bullet)_3$ ($\times$) to a range of substituted alkenes $CH_2{=}CHY$, with Y = F, H, NH_2, Cl, CHO, and CN. The solid regression line for t-butyl radical addition is given by $r = 2.03 - 1.92 \cdot 10^{-3}\Delta H_r$ ($R^2 = 0.975$); the solid regression line for the addition of the remaining three radicals is given by $r = 2.03 - 2.21 \cdot 10^{-3}\Delta H_r$ ($R^2 = 0.953$). [$CH_3^\bullet$, $CH_2OH^\bullet$ and $CH_2CN^\bullet$ data taken from Ref. 40; $C(CH_3)_3^\bullet$ data taken from Ref. 41.]

so far.[17,39–41] It is immediately clear that there is a linear correlation, even if we consider all the data points in a single set. The regression coefficient for the overall data set is reasonable ($R^2 = 0.869$), but better regressions are obtained when treating the $C(CH_3)_3^\bullet$ data individually.[41] We now observe two very good regression lines, with the *tert*-butyl line below that of the other studied radicals. This can be explained by the fact that the contribution from the charge transfer configurations is largest here, which leads to some additional stabilization of the transition structure (the electrostatic attraction pulls the two fragments closer together).[41] Furthermore, it may seem surprising that the $CH_2CN^\bullet$ data lie on the same line as those of the $CH_3^\bullet$ and $CH_2OH^\bullet$ radicals, whereas there was clearly no linear relationship between the barrier and the enthalpy for these additions (see Fig. 1.20).

As an explanation for this observation, it has been proposed that mixing of charge transfer configurations has an insignificant effect on the position of the barrier, but a large effect on its height; only in cases of very strong polar effects, such as seen in the $C(CH_3)_3^\bullet$ reactions, deviations will start to occur.[41] Arnaud et al.[75] studied the addition of methyl radical to a wider range of substituted ethylenes (including capto-dative alkenes) at the B3-LYP/6-311G** level of theory and found a very similar relationship, $r = 1.981 - 0.0033\,\Delta H_r$ ($R^2 = 0.984$), which further strengthens the general arguments presented by Radom and co-workers.

To summarize this part on barrier formation in radical addition reactions, we can clearly identify the following important factors which play a role in barrier formation:[17]

- *Reaction Exothermicity.* The larger the exothermicity, the lower the barrier.
- *The Singlet–Triplet Energy Gap*, G, *of the Alkene.* The smaller G, the lower the barrier. The size of G and the reaction exothermicity are closely related, as shown before; the smaller G, the larger the exothermicity. Together, they lead to Bell–Evans–Polanyi-type behavior [Eq. (1.1)], and are incorporated in the term ($50 + 0.22\,\Delta H_r$) of the Fischer–Radom model [Eq. (1.4)]. Furthermore, the overall exothermicity effects determine the position of the transition state; the larger the reaction exothermicity, the larger the length of the forming $C–C$ bond in the transition state.
- *Polar Effects.* these effects are operative when $[I(R) - EA(A)]$ or $[I(A) - EA(R)] < 9$–$9.5\,eV$ (or 7–8 eV when including experimental data), and will lower the barrier further than that given by the Bell–Evans–Polanyi relationship. They are incorporated via the terms F_n and F_e in the Fischer–Radom model [Eq. (1.4)].

1.6.1.3 Frequency Factors   In the previous section, the factors controlling barrier formation in radical addition reactions were discussed, without any discussion of the factors controlling the frequency factors for addition reactions. Since the barriers (and hence the activation energies) can vary widely, they are in general the most important factors determining the overall order of magnitude of the propagation rate coefficient k_p.

Variations in frequency factors (for long-chain propagation) are in general smaller, and from transition state theory arguments it can be concluded that they are confined to a region of about 10^5–10^7 dm^3 mol^{-1} s^{-1}. (*Note*: For a given frequency factor, a range of activation energies from 10–35 kJ/mol represents a range of k_p values over four orders of magnitude.) This has led most workers in the field of small-radical additions to focus on the activation energies and pay less attention to frequency factors; for example, Fischer and Radom lump all primary radical additions together as having a $\log[A/(\text{dm}^3 \text{ mol}^{-1} \text{ s}^{-1})] = 8.5$ and all tertiary radical additions with $\log[A/(\text{dm}^3 \text{ mol}^{-1} \text{ s}^{-1})] = 7.5$.[30] Considering the very small variations in transition state structures, this is indeed justified, however, many smaller effects (of interest to the polymer chemist) are overlooked in lumping the frequency factors. In what follows we will discuss some of these aspects in detail.

We have seen in the section on transition state theory that the frequency factor A is determined by the ratio of molecular partition functions of the transition state and the reactants, and for simplicity we will equate A to the preexponential factor in Eq. (1.7) [which means that we also equate the activation energy to the critical energy; see Eqs. (1.7), (1.12), and (1.13)]

$$A \approx \frac{k_B T}{h} \frac{Q^{\dagger}}{Q_{\text{radical}} Q_{\text{monomer}}} \tag{1.42}$$

It was shown that the ratio of partition functions is governed by masses (Q_{trans}) and overall geometries (Q_{rot}) of the reactants and transition state, and by the internal vibrations and rotations (Q_{int}). The latter contribution to A [Eq. (1.42)] was shown to be dependent largely on the transitional modes, and since this is the only "nonstraightforward" contribution in Eq. (1.42), let us now look at the transitional modes for propagation in more detail. In Fig. 1.22, the six transitional modes for the addition of ethyl radical to ethylene, namely, a model for the propagation step in ethylene polymerization, and their respective UHF/6-31G* harmonic frequencies are shown.[47]

The first transitional mode (ν_1) is the motion along the reaction coordinate and its imaginary frequency, which does not enter Q_{int}, reflects the magnitude of a C–C bond stretch in a normal molecule. The lowest real frequency transitional mode (ν_2) is the rotation of the monomer molecule about the axis through the two carbons that are forming a bond, and arises from the loss of one of the external rotations of the free ethylene molecule. This motion has been identified as the lowest real transitional mode in all published studies on radical additions to date (although it is still a limited number, i.e., the propagation reactions of ethylene,[31,35,47] acrolein,[35] acrylonitrile,[72] methacrylonitrile,[72] and the addition of ethylbenzene radical to ethylene).[34] Hence it is conceivable that this mode is in general the lowest transitional mode. As such, we should consider this motion in some more detail, as it will also be important for discussions later in this chapter.

We have seen in the section on transition state theory that rotational motions have a very different potential energy profile on displacement as compared to a harmonic oscillator, and hence should be treated as internal rotations (see Fig. 1.6).[3] Especially

$\nu_1 = 483 \, i \, cm^{-1}$ $\nu_2 = 59 \, cm^{-1}$ $\nu_3 = 178 \, cm^{-1}$

$\nu_4 = 279 \, cm^{-1}$ $\nu_5 = 403 \, cm^{-1}$ $\nu_6 = 631 \, cm^{-1}$
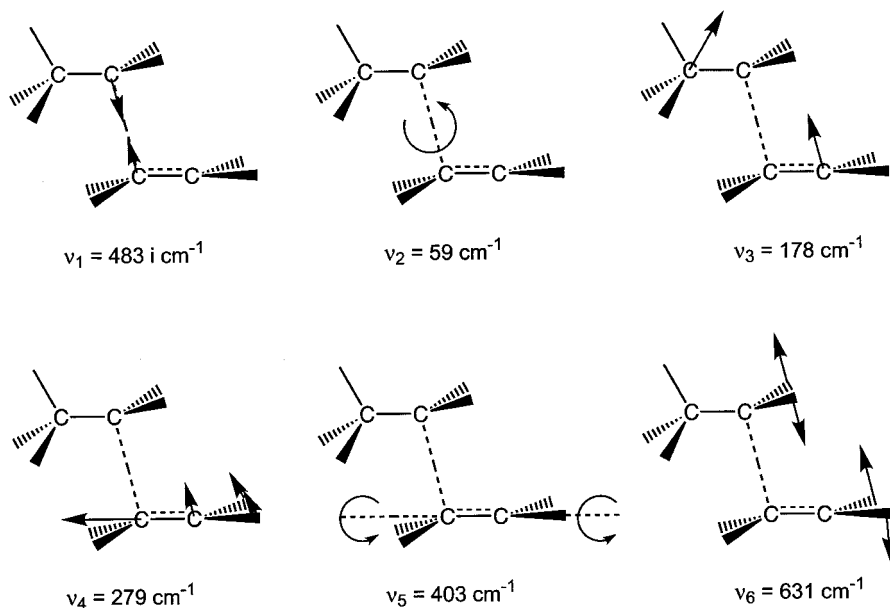
Figure 1.22 Schematic representation of the six transitional modes in the transition state for the addition of an ethyl radical to ethylene, and their respective harmonic frequencies (UHF/6-31G*).[47]

the low-frequency transitional modes, corresponding to rotational motions, and with harmonic frequencies lower than $\sim 200 \, cm^{-1}$ (i.e., the thermal energy at room temperature)[31] should not be treated as harmonic oscillators.[31] This means that we should not use the vibrational partition functions, but rather the hindered rotor partition functions; this latter approach requires us to calculate the rotational potentials, and studies thus far indicate that the results obtained at the HF/6-31G* level of theory (even within the transition state) are satisfactory,[31,35,47] but that semi-empirical methods lead to erroneous potentials.[35,72] The studies reported so far in the literature all indicate that the frequency factors calculated by treating the low-frequency torsional motions as hindered rotors are a factor of $\sim$2–6 higher than those obtained by treating all motions as harmonic oscillators.[31,34,35,72] The studies on ethylene polymerization suggest that this difference becomes smaller with increasing chain length of the radical,[31] and those on the addition of the ethylbenzene radical to ethylene that the difference becomes smaller at lower temperatures.[34] The latter result is easily explained by the fact that at lower temperatures the thermal energy is too low to "escape out of the well" (see Fig. 1.6) and that the experienced potential energy surface is very close to that of a harmonic oscillator.

The fact that the lowest real transitional mode is a rotation about the forming C—C bond is very important, as it explains certain experimental observations. Increasing the hindrance to this rotation via the introduction of substituents on the

α carbon will increase the barrier to rotation and hence will lead to a reduction in the partition function associated with this mode. However, introduction of the same substituents in the monomer will increase the moment of inertia of the rotation and hence increase the partition function. The overall effect on the partition function will be determined by the relative magnitudes of these two effects. However, in general it is expected that the effect of increasing the rotational barrier is greater than that of the increased moment of inertia, and hence a decrease in the partition function is expected, as illustrated for the propagation reactions in methacrylonitrile and acrylonitrile.[72]

The second lowest real transitional mode, i.e., a bending mode of the two fragments ($\nu_3 = 178\,\text{cm}^{-1}$) also seems to arise from the loss of external rotations of the reactants.[47] Again, it seems that this mode is also very general, as both the methacrylonitrile/acrylonitrile propagation[72] and the ethylbenzene addition to ethylene[34] studies report similar motions with low frequencies. Introduction of large substituents at the α position is likely to increase the steepness of the potential energy well and therefore reduce the contribution of this motion to the partition function (and hence the frequency factor).

The remaining three transitional modes are also likely to be general, but are more complicated in additions of substituted radicals with substituted ethylenes. However, the effect of larger substituents is likely to be smaller on these motions as the lower ones do not directly involve the α substituents in the radical and are also relatively high in frequency [the contribution to A from higher frequency modes is relatively small; see Eqs. (1.21) and (1.28)].

In the light of the preceding observations and the theory outlined in the section on transition state theory, let us now summarize how different substituents in monomer and radical will individually affect the magnitude of the frequency factors:

- Larger substituents $\Rightarrow$ monomer mass$\uparrow$ $\Rightarrow Q_{\text{trans, monomer}}\uparrow$ [Eq. (1.25)] $\Rightarrow$ A$\downarrow$ [Eq. (1.42)]
- Larger substituents $\Rightarrow$ monomer size$\uparrow$ $\Rightarrow Q_{\text{rot, monomer}}\uparrow$ [Eq. (1.27)] $\Rightarrow$ A$\downarrow$ [Eq. (1.42)]
- Larger substituents $\Rightarrow$ moment of inertia in internal rotations and vibrations$\uparrow$ $\Rightarrow Q^{\dagger}_{\text{int}}\uparrow$ [Eq. (1.30)] $\Rightarrow$ A$\uparrow$ [Eq. (1.42)]
- Larger substituents $\Rightarrow$ hindrance transitional modes $\uparrow \Rightarrow Q^{\dagger}_{\text{int}}\downarrow$ [Eq. (1.30)] $\Rightarrow$ A$\downarrow$ [Eq. (1.42)]
- The overall effect depends on the relative magnitudes of the abovementioned effects, but initial theoretical and experimental results suggest replacement of H by CH_3 in α position $\Rightarrow$ A$\downarrow$ (see below)

1.6.1.4 Chain-Length Dependence of k_p   So far, we have considered only small-radical additions to substituted ethylenes, mainly because calculations on large-radical systems are currently not feasible. A skeptical polymer chemist may say that these additions are not relevant to polymer chemistry as the chain lengths are much larger and to some extend this polymer chemist is correct. Indeed, the small

radical system may not reflect the total physical picture, but it is still a very adequate model for polymer propagation if we apply some "tricks" to introduce the polymer chain.

With respect to the reaction barrier, we are in the fortunate situation that the polymer chain is only to a small extend directly involved in the reaction, and that the largest electronic effects determining the reaction barrier are caused by the monomer and the substituents in the direct vicinity of the reaction site. This is not to say that the substituents further away from the radical site do not affect the barrier (as we will see later), but they are of minor importance as compared to the α substituent effects. Hence to a first approximation, trends in barriers observed for small-radical additions should be semi-quantitatively applicable to propagation barriers.[30]

The effect of chain length on the frequency factor is of a mechanical nature—it influences the effects of mass and size. To incorporate these effects, we just "added" a high mass to the end of the radical, which should mimic the effect of the mass of the polymer chain on the moments of inertia for torsional and vibrational motions (the higher mass of the chain will increase both Q_{vib} and $Q_{int\ rot}$).[31,35] It was found that this procedure yields adequate results when the radical is of a dimeric or larger nature, as effects of the penultimate unit in the radical on the hindrances of certain internal motions in the radical and the transition state, and in particular some of the transitional modes, cannot be taken into account when considering only a monomeric radical.[31,35] Models for polymeric radicals used by Gilbert and co-workers are schematically shown in Fig. 1.23.

This approach was tested for the propagation reaction in ethylene, where a range of alkyl and their corresponding (high-mass model) polymeric radical additions to
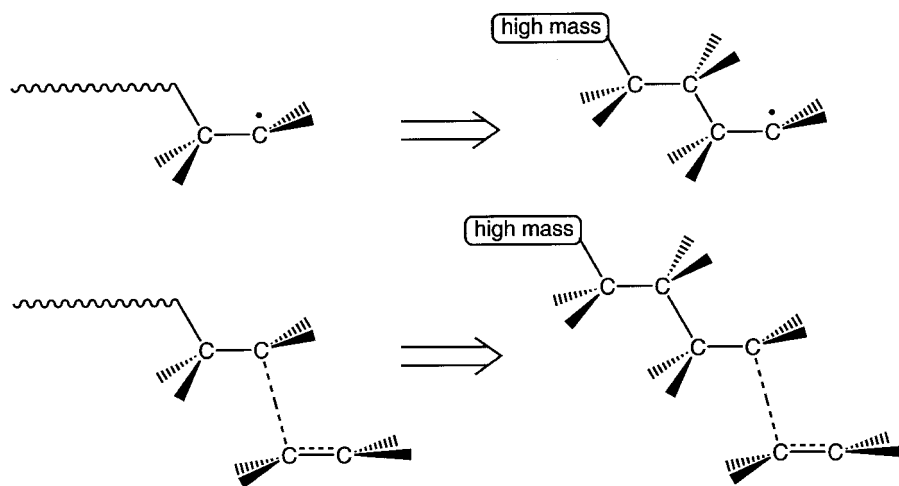

Figure 1.23 Schematic representation of the small-radical models used in transition state theory calculations of long-chain propagation reactions. The ω hydrogen atom is replaced by a high mass to mimic the mechanical effects of the polymeric chain.

ethylene was studied.[31] A decrease by a factor of 3 in frequency factor is observed when increasing the alkyl radical from ethyl (1.7×10^8 dm^3 mol^{-1} s^{-1}) to heptyl (5.0×10^7 dm^3 mol^{-1} s^{-1}) radical, and the polymeric frequency factor converges (at a dimeric "polymer" radical) toward a value in the range of $(1.0–2.2) \times 10^7$ dm^3 mol^{-1} s^{-1}, which is within the experimental uncertainty: $0.9 \times 10^7 < A < 1.9 \times 10^7$ dm^3 mol^{-1} s^{-1}.[76] These results, based on mechanical arguments within the framework of transition state theory,[31,35] thus support the idea that the rate coefficient for propagation is chain-length-dependent and that the propagation rate coefficient of the first step (k_p^1) is significantly larger than that for the propagation of polymeric radicals ($k_p : k_p^1 \approx 10 \times k_p$).[77–79]

1.6.1.5   Steric Effects on the Propagation Rate Coefficient   In Fig. 1.24, the two most important low-frequency modes (<200 cm^{-1}) in the transition state of the propagation reaction are shown. The first, τ_1, corresponds to a rotation of the monomer about the forming C—C bond, while τ_2 corresponds to a simultaneous bending of the two angles associated with the forming C—C bond. These modes were found to be important in all systems studied theoretically to date.

We have already seen that a different conformation of the transition state can lead to a different energy and hence a different barrier. From the discussion on frequency factors so far, we can now also conclude that different conformations could have different hindrances of the internal modes, and hence will lead to different frequency factors. It is therefore clear that syndiotactic and isotactic addition reactions may have significantly different activation energies and frequency factors. A clear example of the former is shown in the work by Huang et al.,[72] who studied the propagation reactions of methacrylonitrile and acrylonitrile. In the case of methacrylonitrile the activation energies were found to be about 32.5 and 43.0 kJ/mol for the syndiotactic and isotactic additions, respectively (B3-LYP/6-31G*, QCISD/6-31G*). For acrylonitrile values of 26.9 and 33.2 kJ/mol (B3-LYP/6-31G*), and 38.3 and 44.7 kJ/mol
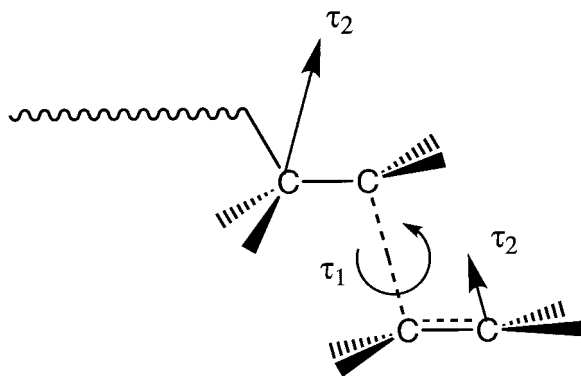

Figure 1.24   Schematic representation of the transition state for the propagation reaction in the free-radical polymerization of ethylene and its two most important low-frequency modes: the transitional modes τ_1 and τ_2.
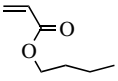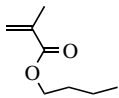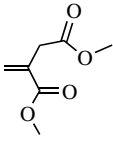
(QCISD/6-31G*) for the syndiotactic and isotactic additions, respectively were found. The results for both monomers indicate that the syndiotactic addition is favored over the isotactic addition by about 10 kJ/mol for methacrylonitrile and about 6 kJ/mol for acrylonitrile (note that these differences can affect the rate coefficients by factors of about 40 and 10, respectively, assuming an unchanged frequency factor).

A study of the effect on the frequency factor by the tacticity of the transition structure has been reported by Heuts et al.,[35] who found that the isotactic addition in acrolein polymerization had a frequency factor ($A_{isotactic} \approx 4.6 \times 10^6$ dm^3 mol^{-1} s^{-1}, HF/3-21G) about 35% higher than that of the syndiotactic addition ($A_{syndiotactic} \approx 3.4 \times 10^6$ dm^3 mol^{-1} s^{-1}, HF/3-21G). It is conceivable that this effect will be smaller for the propagation reaction of 1,1-disubstituted monomers (with substituents of similar sizes), and larger for monosubstituted monomers with a large substituent (or even 1,1-disubstituted monomers with one small and one very large substituent). Combining this with the discussion above for methacrylonitrile[72] ($A_{syndiotactic} \approx 2.2 \times 10^6$ dm^3 mol^{-1} s^{-1}, HF/6-31G*) and acrylonitrile[72] ($A_{syndiotactic} \approx 6.8 \times 10^6$ dm^3 mol^{-1} s^{-1}, HF/6-31G*) it is indeed conceivable that the k_p for syndiotactic addition in these systems is a factor of 10–40 higher than that for isotactic addition.

These theoretical studies are in line with the experimental observation that the propagating methyl methacrylate radical prefers syndiotactic over isotactic addition. Another example in the literature that could be explained with the theoretical model is the difference found between the k_p values of *cis*- and *trans*-4-*tert*-butylcyclohexyl methacrylate (BCHMA),[80] as the k_p value for *trans*-BCHMA is higher than that for the *cis* isomer. In a study on the polymerization behavior of *cis*- and *trans*-2-cyclohexyl-1,3-dioxanyl methacrylate (CHDMA),[81] however, only small differences in k_p values were found whereas larger differences in the termination rate were found.

Let us now explicitly look at the effect of an α substituent in the monomer, starting our discussion with some of the experimental results shown in Table 1.7. First, it is clear that the introduction of an α-methyl group in butyl acrylate[82] (resulting in butyl methacrylate)[83] reduces the frequency factor by a factor of ~5, whereas an increase in activation energy is observed of ~5 kJ/mol. A further increase of the size of the second α substituent (resulting in dimethyl itaconate)[84] results in an additional 20-fold decrease in frequency factor and a small increase in activation energy of about 2 kJ/mol. Moving on to the styrenic monomers, we see that the frequency factor of styrene[85] is within the same order of magnitude as butyl acrylate (about 2 times higher) with a much higher activation energy; the latter is clearly caused by different electronic substituent effects. The introduction of an α-methyl group, resulting in α-methyl styrene,[86] decreases the frequency factor by an order of magnitude and increases the activation energy by about 4 kJ/mol (it should be noted that the values reported for α-methyl styrene could not be established with great certainty, but it is expected that the reported values are indeed good estimates).[86] We can also compare the Arrhenius parameters of butyl acrylate further with those of vinyl acetate[87] and we observe a very similar frequency factor and a slightly higher activation energy (3 kJ/mol), again conceivably due to a different electronic

TABLE 1.7   Comparison of Arrhenius Parameters of Some Typical Vinyl Monomers Obtained by Pulsed Laser Polymerization

Monomer	A (dm^3 mol^{-1} s^{-1})	E_{act} (kJ/mol)	Ref.
Butyl acrylate	1.8×10^7	17.4	82
Butyl methacrylate	3.8×10^6	22.9	83
Dimethyl Itaconate	2.2×10^5	24.9	84
Styrene	4.3×10^7	32.5	85
α-Methyl Styrene	1.5×10^6	36.7	86
Vinyl Acetate	1.5×10^7	20.4	87
Methacrylonitrile	2.7×10^6	29.7	88

substituent effect. Finally, we can compare the Arrhenius parameters of butyl methacrylate with those of methacrylonitrile.[88] Again, we observe very similar frequency factors and a different activation energy due to different electronic substituent effects.

To summarize the experimental observations, we can say that the results suggest that (1) the introduction of an α-methyl group results in a 5–10-fold decrease in

the frequency factor and possibly in an increase of the activation energy by about 5 kJ/mol, (2) increasing the size of the second α substituent causes a further decrease in frequency factor, and (3) monomers with similar size substituents have similar frequency factors.

If we now compare these experimental observations with what is expected from theory, we can say that indeed we expect the observed trends for the frequency factors; the situation for the activation energies is not as obvious at this moment, but the satisfactory agreement between the activation energies of small-radical additions with corresponding polymerization reactions as reported by Fischer and Radom (E_{act} for propagation is generally about 2 kJ/mol higher than that for corresponding small-radical addition) suggests that the Fischer–Radom model also has predictive value for polymerization reactions.[30]

The only study to the author's knowledge that explicitly discusses the effect of the introduction of an α-methyl group on the Arrhenius parameters of propagation is the study by Huang et al.,[72] and their results show a $\sim$3-fold reduction of the frequency factor in going from acrylonitrile (for which no experimental Arrhenius parameters are available) to methacrylonitrile. As outlined before, the effect of the α-methyl group is operative in several different contributions to the frequency factor, but the authors conclude that the main reduction is caused by the difference in Q_{rot} of the monomers; in the studied system, the effect of greater hindrances decreasing $Q_{int}^{\dagger}$ is almost completely canceled by the effect of the greater moments of inertia increasing $Q_{int}^{\dagger}$ The authors also tried to explain the difference in activation energy of the two monomers, but this result is a bit ambiguous, because it is not clear from their study whether the activation energy for acrylonitrile is larger or smaller than that for methacrylonitrile. At the B3-LYP/6-31G* level of theory it is smaller by about 6 kJ/mol, which seems to be in accordance with what is observed experimentally for the (meth)acrylates and (α-methyl)styrene (see Table 1.7). However, the QCISD/6-31G* result is exactly the opposite; it is higher by about 6 kJ/mol. Both procedures were shown to correlate well with higher levels of theory, so it is not a priori clear which result is more appropriate.[42,43] However, in the most recent studies by Radom and co-workers, a clear preference for B3-LYP as a cost-effective alternative level of theory seems to appear as for the addition of methyl radical to a wide range of substituted ethylenes the B3-LYP/6-31G* procedure yields results in very good agreement with those obtained by the expensive and generally recommended CBS-RAD procedure.[30,43] In the light of this, the B3-LYP result, namely, the activation energy for acrylonitrile, is about 6 kJ/mol lower, is probably more likely. An analysis by the authors of the factors that possibly cause the difference in activation energies for the acrylonitrile and methacrylonitrile systems leads to the conclusion that this difference is caused mainly by differences in steric effects, comprised of angle strain and nonbonded interactions, and loss of electron delocalization in the transition state.[72]
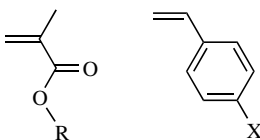
In summary, observed experimental trends in homopolymerization reactions are well explained within the theoretical framework outline above.

1.6.1.6 *Effect of Deuteration*
A small effect that can also be explained with our current theoretical understanding of propagation is the rate-enhancing effect
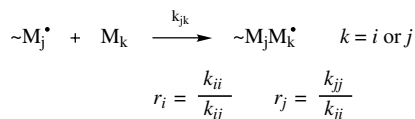
observed with deuterated monomers (excluding effects on the termination reaction, which may also be important).[31,35] Perdeuteration will have a significant effect on the frequency factor because of changes in the moments of inertia of the external rotation of monomer (Eq. (1.26)] and in the internal rotations and vibrations [Eq. (1.30)]. Since the hydrogen atoms are not involved in the reaction coordinate to any significant extent, there will be no primary isotope effect, and perdeuteration will conceivably affect only the frequency factor.[31,35] This effect has been modeled for the propagation reactions of ethylene/deuterated ethylene (A increases by $\sim 16\%$)[31] and methyl methacrylate/deuterated methyl methacrylate (A increases by $\sim 22\%$),[35] both comparing favorably with experimental rate enhancements found in the styrene/deuterated styrene (28%)[89] and methyl methacrylate/deuterated methyl methacrylate (28%)[90] systems.

1.6.1.7 *Homologous Series*

The theory outlined above also rationalizes the Arrhenius parameters for propagation in a homologous series of monomers. Of the available experimental data, those of the methacrylates and substituted styrenes are probably the most reliable. In the methacrylate series, the values of k_p seem to generally increase with increasing size of the ester group, but the data do not allow for an unambiguous conclusion whether this effect is mainly on the frequency factor or the activation energy.[91] Either way, an effect on either parameter is likely to be relatively small as the effect on activation energy should decrease with increasing distance from the radical site (both from an electronic and steric point of view), and possible hindrances of the transitional modes and an increase in $Q_{monomer}$ are counteracted by the increased moments of inertia for these modes.[72] Overall, this leads to a relatively narrow range of Arrhenius parameters for the methacrylates; taking all data into account, with substituents R (see Scheme 1.7), including susbtituents such as methyl, dodecyl, isobornyl, benzyl, and cyclohexyl groups, the following ranges of Arrhenius parameters are obtained: $A = (2-6) \times 10^6$ dm^3 mol^{-1} s^{-1} and $E_{act} = 20.5-23.5$ kJ/mol.[91] A similar situation exists for the parasubstituted styrenes, in which a slightly larger electronic effect exists; for substituents X including methoxy, methyl, fluorine, chlorine, and bromine groups, the Arrhenius parameters lie in the following range: $A = (3-9) \times 10^7$ dm^3 mol^{-1} s^{-1} and $E_{act} = 31-35$ kJ/mol.[91]

1.6.1.8 *Penultimate Unit Effects in Copolymerization*

One of the most important areas in free-radical polymerization in which the use of theoretical chemistry has been very beneficial is the copolymerization of monomers M_i and M_j, where it has yielded direct information on the existence and nature of the
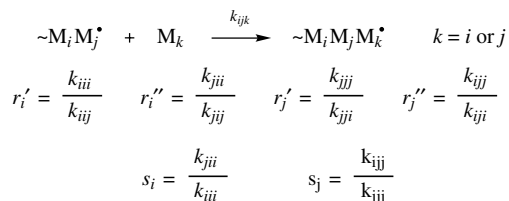

Scheme 1.7

$$\sim M_j^\bullet \; + \; M_k \xrightarrow{\; k_{jk} \;} \sim M_j M_k^\bullet \qquad k = i \text{ or } j$$

$$r_i = \frac{k_{ii}}{k_{ij}} \qquad r_j = \frac{k_{jj}}{k_{ji}}$$

Scheme 1.8

penultimate unit effect;[67,69–71] this information has not been unambiguously and directly accessible by experiment thus far.[92]

It has been known since about 1980 that the failure of the terminal model for free-radical copolymerization (Scheme 1.8) is due largely to neglect of the penultimate unit effect on the propagation rate coefficient.[93,94] The penultimate model takes the penultimate unit explicitly into account when considering the individual propagation reaction (Scheme 1.9).

Within the terminal model, both the copolymer composition and average propagation rate coefficient expressions require knowledge of the homopropagation rate coefficients k_{ii} and k_{jj} and the two monomer reactivity ratios r_i and r_j (see Scheme 1.8).[93,94] The penultimate model requires the homopropagation rate coefficients (k_{iii} and k_{jjj}) and the four monomer reactivity ratios (r_i', r_i'', r_j', and r_j') for the description of the copolymer composition and additionally the two radical reactivity ratios (s_i and s_j) for the description of the average propagation rate coefficient (see also Chapter 6).[93,94] Experimentally all these parameters are only accessible by fitting experimental data to model expressions and because so many uncertainties are involved, the physical meaning of the obtained parameters is often limited.[92] This difficulty has not facilitated the task of exploring the existence and possible causes of the penultimate unit effect. As possible causes of a penultimate unit effect factors as radical stabilization, steric and polar effects have been suggested,[93,94] but no direct experimental proof has been available for a long time, and this is where theoretical chemistry stepped in.

Let us first consider possible steric penultimate unit effects.[31,35,67] It is clear from the theory outlined above regarding the frequency factors for propagation that the partition functions of the internal motions in the transition state are highly dependent on the steric hindrances and conformation around the reaction site (see also Fig. 1.24). It is clear that if we change the penultimate unit in the radical, we will automatically change the hindrances of the internal motions and the conformation

$$\sim M_i M_j^\bullet \; + \; M_k \xrightarrow{\; k_{ijk} \;} \sim M_i M_j M_k^\bullet \qquad k = i \text{ or } j$$

$$r_i' = \frac{k_{iii}}{k_{iij}} \qquad r_i'' = \frac{k_{jii}}{k_{jij}} \qquad r_j' = \frac{k_{jjj}}{k_{jji}} \qquad r_j'' = \frac{k_{ijj}}{k_{iji}}$$

$$s_i = \frac{k_{jii}}{k_{iii}} \qquad s_j = \frac{k_{ijj}}{k_{jjj}}$$

Scheme 1.9

around the reaction site, and since all these (probably small) effects enter the overall molecular partition function in a multiplicative way [see Eqs. (1.22) and (1.30)], changes in frequency factor by a factor of 2–3 are conceivable. Hence in general it is conceivable that the following inequality is valid:[67]

$$A_{iik} \neq A_{jik} \qquad \text{with} \quad k = i \text{ or } j \tag{1.43}$$

It is clear that the closer M_i and M_j are in shape and size, the closer A_{iik} is to A_{jik}, but that if they are very different in size and shape, that A_{iik} and A_{jik} will be very dissimilar. If we apply this to the penultimate reactivity ratios, we can make a few predictions. Suppose that M_i and M_j are similar in size and shape; then the effect of a different penultimate unit may cancel in the expressions of the frequency factors of the monomer reactivity ratios, as the radical in both numerator and denominator of the expression is affected to the same (small) extent:[67]

$$\frac{A_{iii}}{A_{iij}} \approx \frac{A_{jii}}{A_{jij}} \approx \frac{A_{ii}}{A_{ij}} \tag{1.44}$$

When we compare this to the situation of the radical reactivity ratios, then the radicals in the numerator and denominator are not affected to the same extent:[67]

$$\frac{A_{jii}}{A_{iii}} \neq 1 \tag{1.45}$$

Hence, if small steric penultimate unit effects are present, it is conceivable that these are most prominently present in the radical reactivity ratios rather than the monomer reactivity ratios.[67] Let us now suppose that one of the monomers, say, M_i is much larger than M_j. We will now be able to see a marked effect on both the radical and the monomer reactivity ratios. A penultimate unit M_j will now reduce the steric hindrance and strain as compared to a M_i penultimate unit, and the overall effect on the frequency factor is likely to be largest when the terminal unit and/or the monomer are M_i. The overall effect on the monomer reactivity ratios (at least their frequency factors) is now given by[67]

$$\left.\begin{array}{l} A_{jii} \gg A_{iii} \\ A_{jij} > A_{iij} \end{array}\right\} \Rightarrow \frac{A_{jii}}{A_{jij}} > \frac{A_{iii}}{A_{iij}} \qquad (r_i'' > r_i') \tag{1.46}$$

$$\left.\begin{array}{l} A_{ijj} < A_{jjj} \\ A_{iji} \ll A_{jji} \end{array}\right\} \Rightarrow \frac{A_{ijj}}{A_{iji}} > \frac{A_{jjj}}{A_{jji}} \qquad (r_j'' > r_j') \tag{1.47}$$

We cannot directly compare this prediction with experimental data, but it is interesting to note that for the system styrene/acrylonitrile (where it is conceivable that strong polar effects also play a role) this behavior of the monomer reactivity ratios is indeed observed.[95–99] If we now turn our attention to the radical reactivity ratios, it is clear that the effect of a changing penultimate unit is most prominent in the

most congested system, that is, the system with both terminal unit and monomer being M_i:[67]

$$\frac{A_{jii}}{A_{iii}} > 1 \ (\sim s_i) \quad \text{and} \quad \frac{A_{ijj}}{A_{jjj}} \leq 1 \ (\sim s_j) \tag{1.48}$$

Because of the problems associated with the determination of radical reactivity ratios,[92] this prediction is difficult to test. However, a experimental study on the copolymerization of styrene with the highly hindered dimethyl itaconate indeed suggests the relief of hindrances and steric strain on the propagation rate coefficient of dimethyl itaconate radical when styrene is the penultimate unit.[100]

It is clear that penultimate unit effects are likely to contain an entropic contribution. Furthermore, as Coote et al. have clearly shown, the penultimate unit effect is also likely to contain a significant enthalpic contribution.[69–71] These workers studied the γ-substituent effect in the addition of α, γ-substituted propyl radicals to substituted ethylenes, which is the smallest possible model for the study of a penultimate unit effect.

First, the addition reaction of 3-X-propyl radicals to monosubstituted ethylenes (all in extended conformations and anti-addition) was studied:[69]

$$X\text{--}CH_2CH_2CH_2^{\bullet} + CH_2\text{=}CHY \rightarrow XCH_2CH_2CH_2CH_2CHY^{\bullet} \tag{1.49}$$

In Table 1.8, the calculated reaction barriers are shown for several different substituents, and it is immediately clear from these data that the penultimate unit can affect the barrier and that the magnitude of this effect depends on both the γ substituent and the alkene. For the alkenes ethylene and fluoroethylene we do not observe any significant penultimate unit effects on the barriers, whereas the other

TABLE 1.8 Calculated Radical Stabilization Energies and Reaction Barriers at 0 K for Addition of 3-X-Propyl ($XCH_2CH_2CH_2^{\bullet}$) Radicals to Substituted Ethylenes ($CH_2\text{=}CHY$)

		Barrier[b] (kJ/mol)				
X	RSE[a] (kJ/mol)	Y = H	Y = F	Y = NH₂	Y = CHO	Y = CN
H	0.00	30.3	30.8	25.7	17.8	14.6
NH₂	1.00	29.9	30.6	25.0	18.6	15.1
F	0.25	30.0	30.6	23.1	20.0	16.8
CN	−1.54	29.6	30.2	21.1	20.7	17.8

[a] Calculated as the energy change in Eq. (1.50): RMP2/6-311 + G(3df,2p)//B3-LYP/6-31G* + ZPVE (scaled B3-LYP/6-31G*).
[b] Estimated at QCISD(T)/6-311G**//HF/6-31G* + ZPVE (scaled B3-LYP/6-31G*).
Source: All data taken from Ref. 69.

three alkenes clearly show the presence of penultimate unit effects. In order to rationalize these observations, these workers investigated whether radical stabilization effects could possibly be a cause. Radical stabilization energies of the studied radicals are also listed in Table 1.8, and are calculated as the energy change of the reaction:[69]

$$X-CH_2CH_2CH_2^\bullet + CH_3CH_2CH_3 \rightarrow X-CH_2CH_2CH_3 + CH_3CH_2CH_2^\bullet \quad (1.50)$$
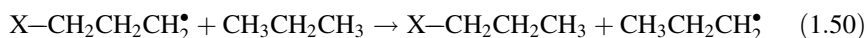
We can see from Table 1.8 that both the NH_2 and F γ substituents have a stabilizing effect and that the CN γ substituent has a destabilizing effect on the radical. However, none of these effects is particularly large, and hence are not expected to play a significant role in the penultimate unit effect on the reaction barrier.[69]

In order to investigate whether polar effects possibly play a role, the curve-crossing approach outlined before was chosen by Coote et al.,[69] and adiabatic electron affinities and vertical ionization potentials were determined for all the radicals and monomers in this study (see Table 1.9).

From Table 1.9 it can be seen that both $CH_2=CHCHO$ and $CH_2=CHCN$ have a relatively high electron affinity, and polar effects might be expected for reactions with radicals with a relatively low ionization potential. Monomer $CH_2=CHNH_2$ has a relatively low ionization potential, and hence polar effects are expected in reactions with radicals with a relatively high electron affinity. In Table 1.10, the low-lying charge transfer states (i.e., $I - EA < 9 - 9.5\,eV$) are shown, and it is immediately clear from the data that the additions to $CH_2=CHNH_2$, $CH_2=CHCHO$, and $CH_2=CHCN$ all have polar contributions to the transition state energy. If we now return to barriers listed in Table 1.8, we can see that all the reactions showing significant penultimate unit effects in the barrier also have large polar contributions. Hence we may conclude that polar effects contribute to the penultimate unit effect and that any radical stabilization effects are negligible in these systems.[69]

In order to investigate the γ-substituent effect in electronically more complicated and interesting systems (so far, we only looked at γ-substituent effects of a

TABLE 1.9   Calculated Vertical Ionization Energies (I) and Adiabatic Electron Affinities (EA) for a Range of 3-X-Propyl ($XCH_2CH_2CH_2^\bullet$) Radicals and Substituted Ethylenes ($CH_2=CHY$)^a

|	$XCH_2CH_2CH_2^\bullet$		$CH_2=CHY$	
X, Y	EA (eV)	I (eV)	EA (eV)	I (eV)
H	0.01	8.40	−1.86	10.58
NH_2	0.26	8.14	−1.92	8.18
F	0.40	8.68	−1.62	10.37
CN	0.68	9.06	−0.23	10.98
CHO	—	—	0.03	10.21

^{a} Calculated at the G2(MP2) level of theory. Data taken from Ref. 69.

TABLE 1.10   Nature and Energy Level (eV) of Relevant Charge Transfer States in Addition of 3-X-Propyl ($XCH_2CH_2CH_2^\bullet$) Radicals to Substituted Ethylenes ($CH_2{=}CHY$)[a]

X	Y = H	Y = F	Y = NH$_2$	Y = CHO	Y = CN
H	—	—	$D^-A^+ = 8.17$	$D^+A^- = 8.37$	$D^+A^- = 8.63$
NH$_2$	—	—	$D^-A^+ = 7.92$	$D^+A^- = 8.11$	$D^+A^- = 8.37$
F	—	—	$D^-A^+ = 7.78$	$D^+A^- = 8.65$	$D^+A^- = 8.91$
CN	—	—	$D^-A^+ = 7.50$	$D^+A^- = 9.03$	$D^+A^- = 9.29$
				$D^-A^+ = 9.53$	

[a] Calculated from data in Table 1.9.

propagating propyl radical), Coote et al. introduced α substituents in the γ-substituted propyl radicals and studied their additions to ethylene (additional substitution in ethylene would have made the calculations unfeasible at the time of study).[70]

$$X{-}CH_2CH_2CHZ^\bullet + CH_2{=}CH_2 \rightarrow X{-}CH_2CH_2CHZCH_2CH_2^\bullet \qquad (1.51)$$
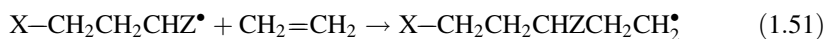
For these reactions, all calculated in fully extended conformations and anti addition, reaction barriers were calculated and the effect of radical stabilization [now defined as the energy change of the reaction shown in Eq. (1.52)] and polar contributions to the transition state were investigated. The results of this study are summarized in Table 1.11.[70]

$$X{-}CH_2CH_2CHZ^\bullet + CH_3CH_2CH_3 \rightarrow X{-}CH_2CH_2CH_3 + CH_3CH_2CHZ^\bullet \quad (1.52)$$
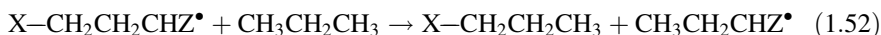
TABLE 1.11   Calculated Reaction Barriers, Radical Stabilization Energies, and Relevant Charge Transfer States in Addition of 1-Z,3-X-propyl ($XCH_2CH_2CHZ^\bullet$) Radicals to Ethylene

X	Z = H			Z = F			Z = CN		
	E_0[a]	RSE[b]	CT[c]	E_0[a]	RSE[b]	CT[c]	E_0[a]	RSE[b]	CT[c,d]
H	30.3	0.00	—	26.3	0.00	—	37.0	0.00	9.2
F	30.0	0.25	—	25.6	−2.53	—	37.0	−4.47	8.8
CN	29.6	−1.54	—	25.4	−4.50	—	34.5	−9.21	8.5

[a] Barrier at 0 K in kJ/mol, estimated at QCISD(T)/6-311G**//HF/6-31G* + ZPVE (scaled B3-LYP/6-31G*).
[b] Radical stabilization energy (kJ/mol), calculated as the energy change in Eq. (1.52): RMP2/6-311+G(3df,2p)//B3-LYP/6-31G*+ZPVE (scaled B3-LYP/6-31G*).
[c] Relative energy level of relevant charge transfer state (eV).
[d] All charge transfer states are D^-A^+ states.

Source: All data taken from Ref. 70.

As before, the addition reactions of γ-substituted propyl radicals to ethylene do not show any significant penultimate unit effect on the barrier, even though some (de)stabilization effects in the radicals are present. A similar picture is also found for the addition of γ-substituted 1-F-propyl radicals to ethylene, where even larger (de)stabilization effects are observed. The only relatively large penultimate unit effect (-2.5 kJ/mol) that is observed is for the reaction between the 1,3-dicyanopropyl radical and ethylene, which also has a large radical (de)stabilization energy (-9.2 kJ/mol). Hence, only $\sim$27% of the penultimate unit effect in radical stabilization seems to be carried over to the reaction barrier.[70] However, this reaction also has a large contribution from polar effects as evidenced by the low-lying D^-A^+ state, and hence we cannot unambiguously assign the penultimate unit effect on the barrier to the radical stabilization effect. It is interesting to note that although polar effects should also be operative in the addition of 3F,1CN-propyl radical (with a radical stabilization energy of -4.5 kJ/mol, which is similar to that of 3CN,1F-propyl radical), no penultimate unit effects in the barrier are observed.

Finally, Coote et al. studied the effect of reactant and transition state conformation on the penultimate unit effect for several γ-substituted propyl radicals to monosubstituted ethylenes.[71] They found that the penultimate unit effect on the barrier is highly dependent on the conformations of reactant and transition state. For the addition of a 3F-propyl radical to CH_2=CHF they find a range of penultimate unit effects from -3.6 to $+2.9$ kJ/mol, for the addition of 3CN-propyl to CH_2=CHCN a range from -2.1 to $+5.8$ kJ/mol and for the addition of 3CN-propyl to CH_2=CHNH$_2$ a range from -8.8 to -1.6 kJ/mol.[71] The results are explained by the fact that interactions occur between the γ substituent in the radical, the unpaired electron, and the monomer.[71] The interactions can be so strong that they can counteract the effects expected from charge transfer states based on the reactants. Furthermore, it is clear that these different conformations will all have different frequency factors, and that the overall rate coefficient will be a weighted average of all the rate coefficients of each individual pathway.[71] At present it is unclear what the overall effect on the rate coefficient will be. However, it is beyond doubt that penultimate unit effects are caused by a wide range of causes, including steric effects in the frequency factor,[67] polar effects in the barrier,[69–71] intramolecular interactions in the transition state,[67,71] and possibly radical stabilization effects.[70] Furthermore, models based on just a single effect cannot provide an adequate representation of the physical chemistry in free-radical copolymerization.[69–71]

1.6.2   Atom Abstraction and Chain Transfer

1.6.2.1   General Aspects   Most theoretical studies on radical abstraction reactions have focused on small radicals, such as hydroxyl radicals and small saturated species, often containing fluorine atoms. In general, the relevance of these studies to free-radical polymerization is limited, and for this reason the discussion of atom abstraction reactions will be much shorter than that of the radical additions, and we will focus on only two studies reported in the literature, i.e., chain transfer to monomer[60,68] and backbiting in the free-radical polymerization of ethylene.[101]

Furthermore, we will discuss the broader impact of these limited studies on our understanding of chain transfer in free-radical polymerization.

Let us start with some general aspects of the theoretical procedures involved in these studies. In principle we can calculate the rate coefficient for a hydrogen transfer reaction using conventional transition state theory, but we have to correct for a process called *quantum-mechanical tunneling*,[8,102–104] which is important when the reaction involves the transfer of light atoms. Tunneling allows the hydrogen atom to some extent to be transferred *through* the barrier rather than over it, and hence increases the rate coefficient. Many studies have and are still dealing with an accurate description of this effect, but considering the complexity of this problem, which is far beyond the scope of this chapter, we will consider only the simple Wigner tunneling correction.[104] In this case we will need to multiply the rate coefficient obtained by conventional transition state theory calculations [k_{TST}; see Eq. (1.7)] by a temperature-dependent correction factor $\kappa(T)$. The overall rate coefficient k, is now given by[104]

$$k = \kappa(T) \cdot k_{TST} \tag{1.53}$$

where the Wigner tunneling correction is given by

$$\kappa(T) = 1 - \frac{1}{24}\left(\frac{ih\nu^{\ddagger}}{k_B T}\right)^2 \tag{1.54}$$
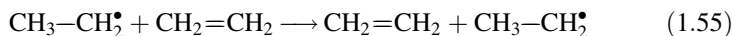
In this expression $\nu^{\ddagger}$ is the imaginary frequency of the normal mode along the reaction coordinate, which is normally left out of the expression of k_{TST}. We will see that the overall correction is relatively small in the studies that are discussed in this chapter.

Assessment of levels of theory for the problems discussed in this section is limited, but we found that the following procedures, which roughly correspond to a modified G2(MP2) level of theory,[105,106] were required for obtaining adequate results:[60,68]

- B3-LYP/6-31G* for geometry optimization, calculation of frequency factors, and calculation of ZPVE
- QCISD(T)/6-311G** for the calculation of vibrationless barriers together with a basis set correction from 6-311G** to 6-311 + G(3*df*,2*p*) at the PMP2 level of theory

1.6.2.2 Chain Transfer to Monomer in Ethylene Polymerization   Chain transfer to monomer is an important reaction in free-radical polymerization. For example, it intrinsically limits the maximum attainable molecular weight,[107] is assumed to be the kinetic event responsible for exit in emulsion polymerization,[108] and potentially limits the applicability of living radical polymerization techniques for producing narrow polydispersity polymers.[109,110] In many cases the chain transfer to monomer

reaction is assumed to proceed via a hydrogen transfer or hydrogen abstraction reaction between the growing radical and the monomer molecule. It is not always clear which hydrogen atoms are abstracted and in which direction the hydrogen transfer takes place. For example, it is often assumed that abstraction of vinylic hydrogens, which have a very strong C—H bond, is unlikely to occur.[1] One theoretical study published to date has explicitly investigated this problem for the free-radical polymerization of ethylene using the model system of an ethyl radical and ethylene.[68] The two possible reactions are a hydrogen transfer reaction from radical to monomer [Eq. (1.55), which is thermoneutral (reactants and products are the same], and a hydrogen abstraction reaction from the monomer by the radical [Eq. (1.56)]. This latter reaction involves the breaking of a strong sp^2 C—H bond and the formation of a weaker sp^3 C—H bond; the reaction is endothermic ($\Delta H_r = +40.1$ kJ/mol calculated at a modified G2(MP2) level of theory):[68]

$$CH_3{-}CH_2^\bullet + CH_2{=}CH_2 \longrightarrow CH_2{=}CH_2 + CH_3{-}CH_2^\bullet \qquad (1.55)$$

$$CH_3{-}CH_2^\bullet + CH_2{=}CH_2 \longrightarrow CH_3{-}CH_3 + CH_2{=}CH^\bullet \qquad (1.56)$$
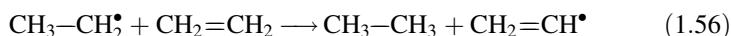
From the thermochemistry we would probably expect that the thermoneutral hydrogen transfer reaction is favored over the endothermic hydrogen abstraction reaction. However, it was shown that the activation energy of the second reaction is about 50 kJ/mol lower and hence the hydrogen abstraction of the vinylic hydrogen in the monomer is the most likely pathway for chain transfer to monomer in ethylene polymerization. This result will be discussed in more detail below. First some general and important aspects of the transition structures for both reactions will be discussed.

The transition states of the hydrogen transfer and hydrogen abstraction reactions with some key geometric parameters calculated at the UHF/6-31G* level of theory are shown in Fig. 1.25. Although there are significant differences in the conformations, the overall sizes of the transition states and the distances between the two reactant moieties in the transition states (i.e., ~2.8 and ~2.7 Å in the transfer and abstraction transition states, respectively) are very similar.[60,68] This similarity in overall geometry leads to similar overall external rotational contributions to the frequency factor. Furthermore, the overall sizes are similar to that of propagation, except that the chain transfer transition states are less tight (the two reactant moieties in the propagation transition state are separated by ~2.3 Å). It should also be noted that the hydrogen transfer reaction proceeds through a symmetrical transition state, whereas this is not the case for the hydrogen abstraction reaction. If we consider the partial C—H bonds in the abstraction transition state (Fig. 1.25b), it is clear that the forming C—H bond is shorter than the breaking C—H bond; that is, the transition state is more productlike. This is in accordance with a late transition state for an endothermic reaction.[17]

The transitional modes in the two chain transfer transition states have also been determined. Of the transitional modes, those with the lowest real frequencies are shown in Fig. 1.26.[60] As was the case in propagation, the lowest real frequency
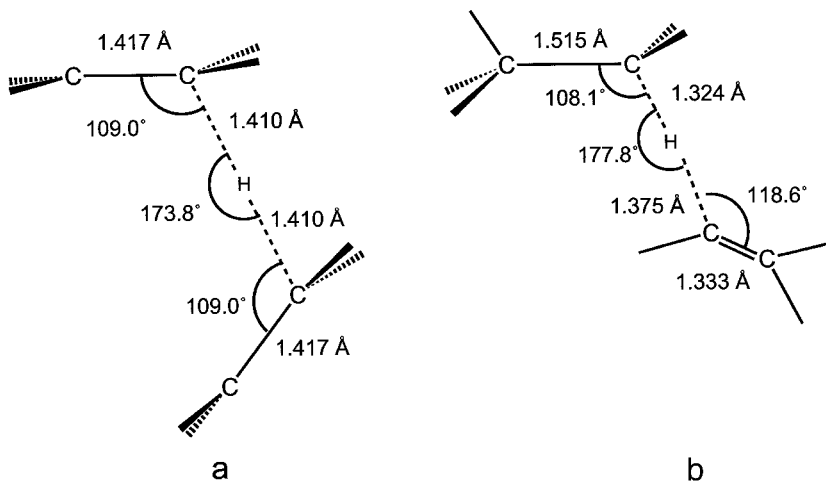
Figure 1.25 Transition structures for the hydrogen transfer (a) and hydrogen abstraction (b) reactions between ethyl radical and ethylene with some key geometrical parameters (UHF/6-31G*).[60]
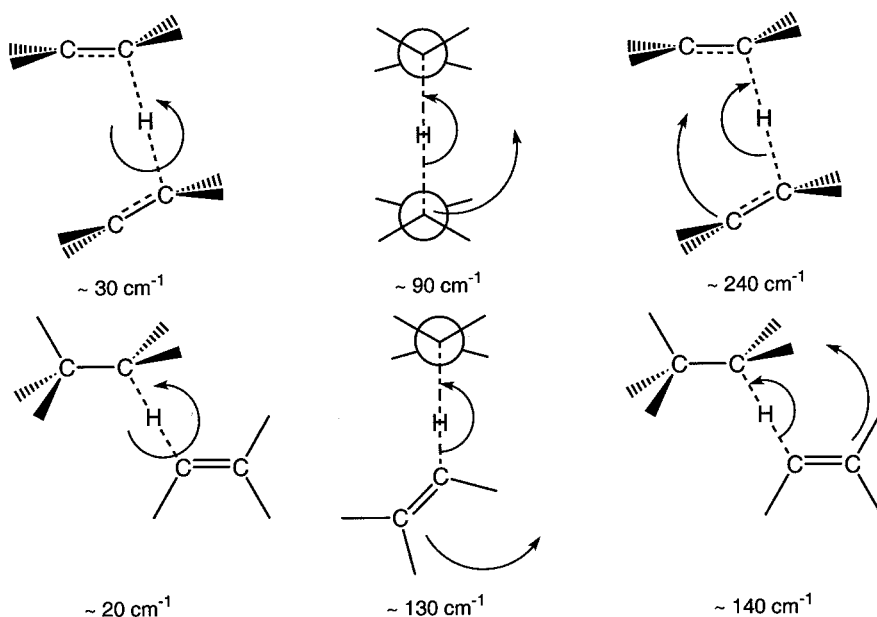

Figure 1.26 Schematic representation of the lowest real transitional modes and corresponding harmonic frequencies (HF/6-31G*) in the hydrogen-transfer (above) and hydrogen-abstraction (below) reaction between ethyl radical and ethylene. All modes correspond to external rotations in the reactants.[60]

transitional mode for both transition states is (roughly) a rotational mode in which the monomer molecule rotates about an axis connecting the two carbon atoms between which the hydrogen atom is being transferred (the partition functions for these modes in the two chain transfer transition states are very similar). Since the two reactant moieties have a greater separation in these transition states as compared to the propagation transition state, these rotational modes are virtually unhindered. This observation means that the partition functions for this rotation in the transfer transition states are larger than that in the propagation transition state.[60]

Considering the other two low-frequency modes in the chain transfer transition structures (both corresponding to external rotations in the reactants), we see again a great similarity between the two cases. Furthermore, these modes are quite similar to those previously seen in propagation (see Fig. 1.22).[35,60]

The similarities between the transition states for the two chain transfer reactions lead to very similar partition functions and frequency factors; the frequency factor for the hydrogen transfer reaction is 3.2×10^8 dm^3 mol^{-1} s^{-1}, and that for the hydrogen abstraction reaction is 7.6×10^8 dm^3 mol^{-1} s^{-1} (both values calculated without tunneling corrections).[60,68] These frequency factors are higher than that for propagation because of the smaller hindrances of the transitional modes.[31,35,68] The critical energies for the hydrogen transfer reaction [Eq. (1.55)] is 128.1 kJ/mol, and that for the hydrogen abstraction reaction [Eq. (1.56)] is 80.0 kJ/mol [both values calculated at a modified G2(MP2) level of theory]. Without tunneling corrections, these critical energies lead to activation energies of 129.8 and 81.8 kJ/mol, respectively. The effect of tunneling estimated by the Wigner tunneling correction was found to be small. The final kinetic parameters of the two reactions are listed in Table 1.12.[68]

Using the reaction between a heavy mass-substituted butyl radical (see Fig. 1.23) and ethylene as a model for chain transfer to monomer in ethylene polymerization, a frequency factor of 1.2×10^8 dm^3 mol^{-1} s^{-1} at 333 K is obtained.[35] Similar to what was discussed previously for propagation, we expect a chain length dependence for k_{tr}. If we compare the theoretical results with experimental results, a reasonable agreement is obtained. At 523 K, the calculated frequency factor is 3.8×10^8 dm^3 mol^{-1} s^{-1},[60] which compares favourably with the value reported by Buback and

TABLE 1.12   Calculated Kinetic Parameters for Hydrogen Transfer and Hydrogen Abstraction Reactions between Ethyl Radical and Ethylene

	Hydrogen Transfer	Hydrogen Abstraction
$E_0{}^a$ (kJ/mol)	128.1	80
$E_{act}{}^b$ (kJ/mol)	125.7	77.6
A^c (dm^3 mol^{-1} s^{-1})	3.7×10^8	8.5×10^8
ΔH_r^d (kJ/mol)	0	40.1

[a] Barrier at 0 K, calculated at a modified G2(MP2) level of theory.
[b] Activation energy at 298.15 K, with Wigner tunneling correction.
[c] Frequency factor at 298.15 K, with Wigner tunneling correction (HF/6-31G*).[68]
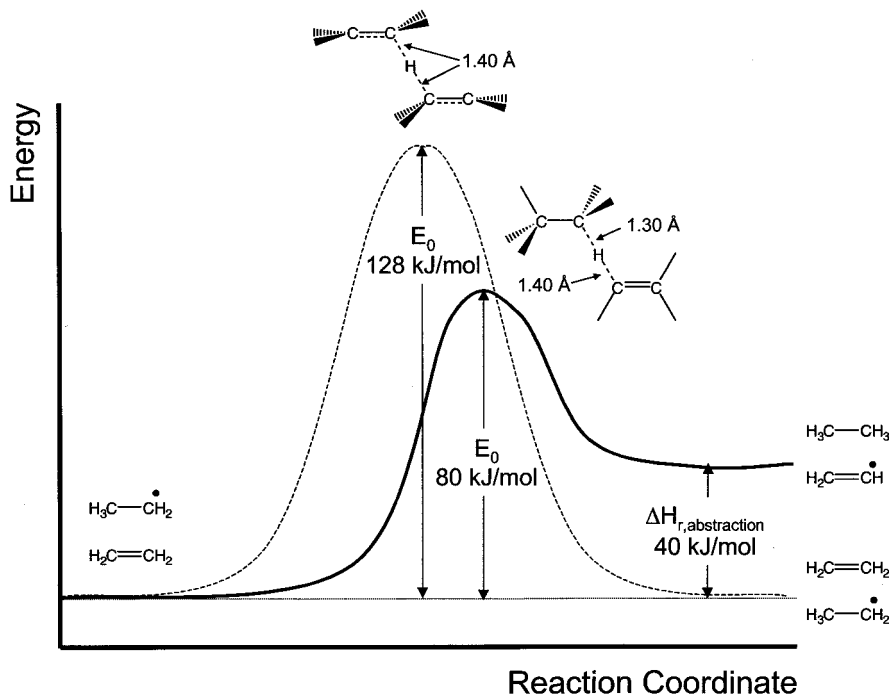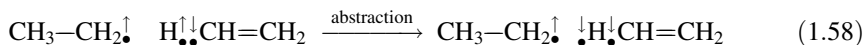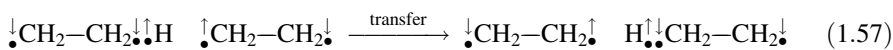
Figure 1.27 Schematic representation of the energy profiles along the reaction coordinates for the hydrogen abstraction (full line) and hydrogen transfer (dashed line) reactions between ethyl radical and ethylene.

co-workers, i.e., $(0.4–5.2) \times 10^8$ dm^3 mol^{-1} s^{-1} (recalculated from C_M data using experimental k_p data).[111] The activation energies also compare favorably at 523 K: experimental $E_{act} = 74 \pm 8$ kJ/mol,[111] theoretical $E_{act} = 82$ kJ/mol (using Wigner tunneling correction).[60]

The theoretical results clearly show that the endothermic hydrogen abstraction from the monomer is kinetically favored over the thermoneutral hydrogen transfer from radical to monomer (see Table 1.12 and Fig. 1.27). Although at first glance this result is unexpected, it can be explained in a simple way using the curve-crossing model.[68]

In Eqs. (1.57) and (1.58), the two reactions are represented in terms of the involved electronic rearrangements. Comparison of these two electronic rearrangements immediately shows why the hydrogen transfer reaction has a higher barrier. The initial energy gap G for the hydrogen transfer reaction contains two contributions, namely, the singlet–triplet excitation energies of the sp^3 C—H bond of the radical and of the π bond in the monomer; in other words, two bonds need to be broken for this reaction. In the hydrogen abstraction reaction, only the sp^2 C—H bond needs to be broken and G contains only the singlet–triplet energy gap of the

sp^2 C—H bond. Hence, the much larger value for G in the case of the hydrogen-transfer reaction causes the much larger barrier.[68]

$$\downarrow CH_2-CH_2 \uparrow \downarrow \uparrow H \quad \uparrow CH_2-CH_2 \downarrow \xrightarrow{\text{transfer}} \downarrow CH_2-CH_2 \uparrow \quad H \uparrow \downarrow CH_2-CH_2 \downarrow \quad (1.57)$$

$$CH_3-CH_2 \uparrow \quad H \uparrow \downarrow CH=CH_2 \xrightarrow{\text{abstraction}} CH_3-CH_2 \uparrow \quad \downarrow H \uparrow CH=CH_2 \quad (1.58)$$

This study clearly indicates the role that theory can play in elucidating mechanisms which are difficult to access experimentally.

1.6.2.3 Chain Transfer Constants

The discussion so far has focused on addition and hydrogen transfer reactions between a radical and a monomer. When we now consider the transition state theory expression for these two reactions, it is clear that the only differences between the two expressions are the partition function and the energy of the transition state; all reactant properties are the same. If we now consider the transition state properties, we can see from Fig. 1.19, 1.22, 1.25, and 1.26 that there are great similarities, including the overall geometries and the transitional modes (see Fig. 1.28).[35]

The main difference between the two transition structures, however, is that the transition state for hydrogen transfer is less tight; the transitional modes are less hindered and hence lead to a greater $Q_{\text{int}}^{\dagger}$, which in turn leads to a larger A (A for chain transfer to monomer in ethylene polymerization $\approx 10 \times A$ for ethylene propagation).

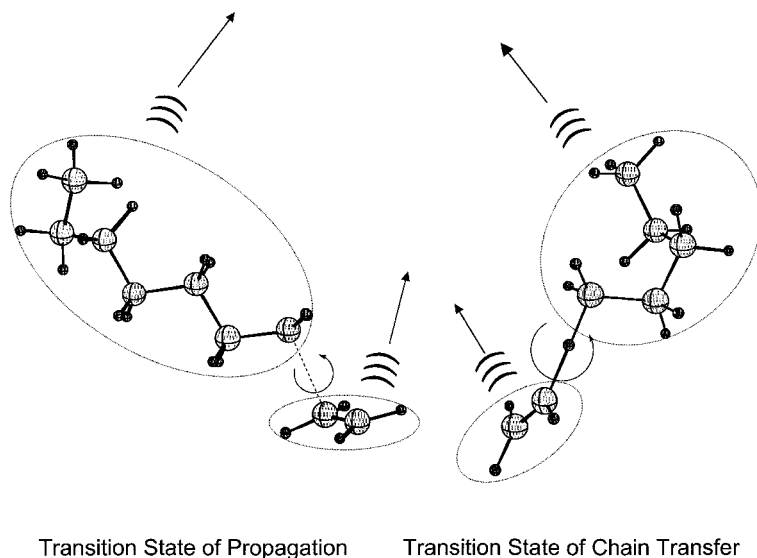Transition State of Propagation   Transition State of Chain Transfer

Figure 1.28 Schematic representation of the transition states of propagation and chain transfer to monomer in the free-radical polymerization of ethylene. The most important low-frequency modes in both transition states are also depicted. Note the similarity of the transitional modes in both cases.

This implies that the preexponential factor of the chain transfer constant (C_M), specifically, $A_{\text{chain transfer}}/A_{\text{propagation}}$, should typically have a value between 1 and 10.[35] It would be interesting to test this prediction against experimental data, but unfortunately not many reliable experimental Arrhenius parameters for chain transfer to monomer are available to date. Unfortunately, the only available reliable data available to date suggest that $A_{\text{chain transfer}} < A_{\text{propagation}}$. The preexponential factors of C_M have been reported as $\sim$0.02, $\sim$0.2, and $\sim$0.1 for butyl acrylate,[112] styrene,[113] and methyl methacrylate,[114] respectively. The main causes of these discrepancies are unclear; these results could indicate that the chain transfer to monomer reaction does not involve a reaction similar to those studied here (this argument is conceivable for styrene, where chain transfer to monomer is assumed to involve a Diels–Alder product of styrene).[115] Naturally, it could also mean that the theoretical results obtained for ethylene polymerization are not as general as they seem. It is clear that more theoretical and experimental studies are required to investigate this problem.

Since it is unlikely that the activation energies for chain transfer to monomer will significantly change within a homologous series (similar to what we have seen in propagation), and the factors governing the frequency factors for chain transfer and propagation are similar, we can expect similar behaviour of the chain transfer and propagation rate coefficients in a homologous series. This implies that chain transfer constants in a homologous series should not vary to a great extent, and might, to a first approximation, be considered constant. Insufficient reliable experimental data are currently available to test this prediction.

It is also of interest to consider what we would expect to see for chain transfer constants to chain transfer agents. First, if we consider the chain transfer reaction to dodecanethiol, we may conceivably expect a transition structure similar to the ones we discussed in detail above. We may therefore expect that within a homologous series, the chain transfer constant to this chain transfer agent should not change significantly.[35] An experimental result that indicates that this is indeed the case has been reported for the chain transfer reactions of methyl methacrylate, ethyl methacrylate, and n-butyl methacrylate, respectively, with n-dodecane thiol. The chain transfer constants at 60°C for these three systems were found to be 0.68 ± 0.02, 0.71 ± 0.02, and 0.65 ± 0.02, respectively.[116]

Finally, it is interesting to compare the chain transfer behavior with dodecanethiol and CBr_4 of methyl methacrylate[117] and dimethyl itaconate[118] (DMI; see Table 1.7). These two monomers have fairly similar activation energies for propagation[84,119] (and considering the nature of the two monomers, we conceivably expect similar activation energies for chain transfer), but DMI has a much lower frequency factor because of the steric crowding.[84] For the chain transfer reaction to CBr_4, we expect quite a crowded transition structure because of the large Br atom that is transferred, and although the transition state of hydrogen transfer is less tight, we still expect that the transitional modes will be affected by steric hindrances to an extent similar to that for the transitional modes in propagation. This implies that the additional hindrances of the large DMI as compared to methyl methacrylate are likely to cancel in the ratio $A_{\text{transfer}}/A_{\text{propagation}}$, resulting in similar chain transfer constants to CBr_4 for

methyl methacrylate and DMI. Experiment shows that they are indeed very similar; $C_S(\text{MMA}) \approx 0.2$[117] and $C_S(\text{DMI}) \approx 0.3$[118] at 60°C. A different situation exists for the chain transfer reaction with dodecanethiol, where we expect the transition state to be less tight, and hence the additional hindrances in the propagation reaction of DMI are now less felt in its chain transfer reaction. Hence the frequency factor of propagation is conceivably affected to a much larger extent than that for chain transfer, and the overall effect will be that the ratio $A_{\text{transfer}}/A_{\text{propagation}}$ for DMI increases as compared to that for MMA. Hence, we expect a larger C_S for DMI, and that is indeed what we observe experimentally: $C_S(\text{MMA}) \approx 0.8 \pm 0.1$[117] and $C_S(\text{DMI}) \approx 2.8 \pm 0.5$[118] at 60°C.

1.6.2.4 *Backbiting in Ethylene Polymerization*

As a final example of the application of theoretical chemistry in free-radical polymerization, backbiting in ethylene polymerization will be discussed.[101] This reaction, which is also very important in the free-radical polymerization of acrylates, leads to short-chain branching. A schematic representation of the overall mechanism is shown in Scheme 1.10.

The first step in this mechanism is an intramolecular hydrogen abstraction reaction from the fifth CH_2 unit in the polymer chain, leading to a midchain radical that undergoes further reactions leading to several different branch sizes.[101] This first step was investigated using transition state theory and ab initio molecular orbital theory by Gilbert and co-workers.[101] These workers used two different model systems to describe the reaction: a radical chain consisting of 6 and a radical chain consisting of 7 carbon atoms. It was found that the 6-carbon system is not sufficiently large to adequately describe the internal motions and hence the 7-carbon system was used to model the backbiting reaction using transition state theory (see Fig. 1.29). It should
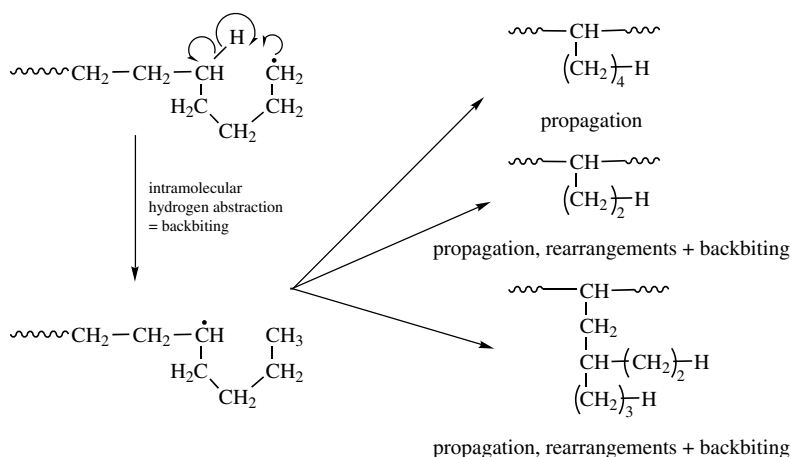
Scheme 1.10

be noted that the ratio of partition functions in Eq. (1.7) contains the partition function of only a single reactant and that transitional modes do not occur in this system.

Evaluation of the partition functions for the polymeric backbiting reaction (using a high-mass-substituted 7-carbon system) yields a frequency factor $A = 10^{12.7} \text{s}^{-1}$ (calculated at HF/6-31G*).[101] The size of the system limited the level of theory that was applied to calculate the critical energy to reaction. For the 6-carbon system, critical energies were calculated up to QCISD(T)/6-311G** and for the 7-carbon system up to QCISD(T)/6-31G*. The availability of barriers at several different levels of theory for both the 6-carbon and 7-carbon systems allows for a reasonable extrapolation to a QCISD(T)/6-311G** barrier for the 7-carbon system. However, there are some questions about the original method of extrapolation,[101] and a better extrapolation would possibly be one of the two following approximations:

$$\text{QCISD(T)}/6\text{-}311\text{G}^{**}|_{7\text{-carbon}} \approx \text{QCISD(T)}/6\text{-}31\text{G}^{*}|_{7\text{-carbon}} + \Delta_{\text{basis set}} \qquad (1.59)$$

$$\text{QCISD(T)}/6\text{-}311\text{G}^{**}|_{7\text{-carbon}} \approx \text{QCISD(T)}/6\text{-}311\text{G}^{**}|_{6\text{-carbon}} + \Delta_{\text{system}} \qquad (1.60)$$

where the subscripts 7-carbon and 6-carbon refer to the two model systems, $\Delta_{\text{basis set}}$ is a basis set correction from 6-31G* to 6-311G** obtained at lower levels of theory, and Δ_{system} is the difference between the critical energies of the 7-carbon and 6-carbon systems at lower levels of theory. If we use the following data (values in kJ/mol)
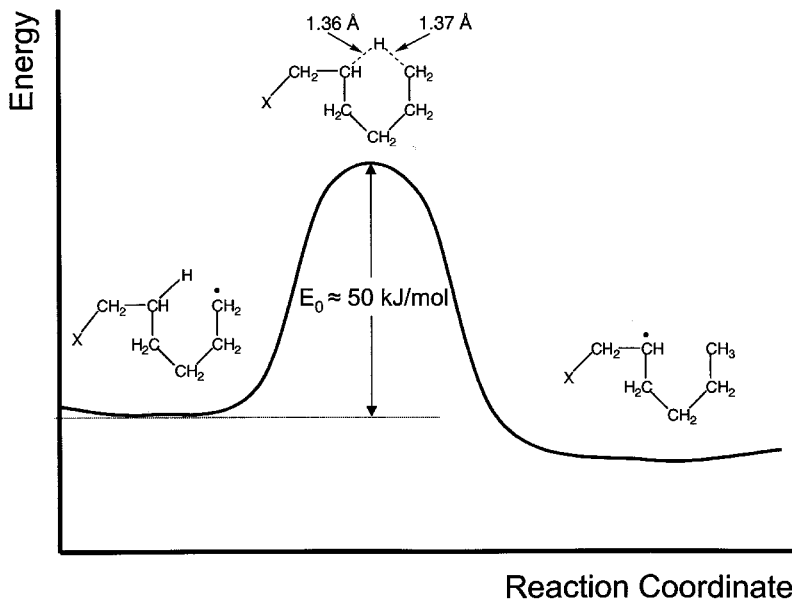
Figure 1.29 Schematic representation of the potential energy profile along the reaction coordinate for the backbiting reaction in ethylene polymerization. Indicated barrier was estimated at the QCISD(T)/6-311G** level of theory.

from the original work,[101] namely, $\{\text{QCISD(T)/6-31G*}|_{\text{7-carbon}} \approx 64, \Delta_{\text{basis set}} \approx -10\}$ and $\{\text{QCISD(T)/6-311G**}|_{\text{6-carbon}} \approx 69, \Delta_{\text{system}} \approx -16\}$, then the extrapolated QCISD(T)/6-311G** critical energy for the 7-carbon system is 50–53 kJ/mol, which is ~ 10 kJ/mol lower than the reported values. Using an experimental value for the volume of activation, which accounts for the pressure dependence of the rate coefficient, the activation energy for the 7-carbon system is given by $E_{\text{act}} \approx E_0 + 8$,[101] which, with the new estimate of E_0, would give a value ~ 60 kJ/mol.

The calculated Arrhenius parameters for the branching rate coefficients allows for the calculation of the branching ratio. Gilbert and co-workers compared their results with experimental data and observed a significant overestimation by the theoretical approach.[101] It is conceivable that the activation energy was not calculated at a sufficiently high level of theory (and the current theoretical value is too high) and that the frequency factor is incorrect by a factor of 2–5. On the other hand, the experimental procedures to determine branching ratios are very difficult, so it is not inconceivable that there is a substantial experimental error. Either way, the very large discrepancy between theory and experiment clearly indicates that additional work on short-chain branching is required. The experimental difficulties render theory to be a powerful alternative as the required information can be accessed directly. However, in order to rely on theory to guide experimental work for this particular problem, theory needs to be pushed further to its limits until we are certain that we have reached convergence with level of theory or accurate experimental data need to become available against which lower (but sufficiently high) levels of theory can be calibrated.

1.7 CONCLUDING REMARKS

This chapter was meant to bridge the apparent gap between theoretical chemistry and polymer chemistry and to highlight some successful theoretical studies of problems in free-radical polymerization. Several applications were discussed with a major emphasis on the propagation reaction. When we consider the work on radical addition reactions, we see a very beneficial interplay between experiment and theory. Although theory sometimes over- or underestimates particular effects, the deviations are often systematic, and trends are adequately reproduced. Since the underlying physics of a chemical reaction are often inaccessible by experiment, theory can be used to study these underlying aspects. A good example is the study of small-radical additions; using experimental and theoretical data, Fischer and Radom[30] were able to develop a relatively simple model for radical additions, which is fully based on fundamental theory.

Furthermore, we have seen how steric factors affect frequency factors for propagation and chain transfer, and how, on the basis of these considerations, experimental data show understandable patterns. Theory has also greatly enhanced our understanding of copolymerization kinetics, where the precise nature of the penultimate unit effect could be studied explicitly.

Some examples, of which the backbiting problem is representative, also show the great potential of theory to be used to study problems that are difficult to investigate by experiment, but for which the required computational power to push theory to its limits is currently not available.

Overall we can see that theory is a great companion to experimental chemistry and the increasing computational power will allow the study of more complex systems. It is not likely that (in the near future) theory will replace experiment, but it will be a great aid in interpreting and designing experiments that answer some of our more fundamental questions. The further development of accurate computational procedures (especially in density functional theory and hybrid semiempirical/ab initio methods) and the availability of large amounts of accurate experimental data will allow us to study more complex problems, including problems of relevance to transition-metal-mediated radical polymerizations.

In conclusion, theoretical chemistry should be considered as a helpful tool in understanding and designing experimental chemistry, and not as a separate branch of chemistry suitable only for philosophers speaking in their own language of complicated theoretical procedures and basis sets.

ACKNOWLEDGMENTS

REFERENCES

1. G. Moad and D. H. Solomon, *The Chemistry of Free Radical Polymerization*, Pergamon, Oxford, 1995.

2. A. H. Zewail, *Angew. Chem. Int. Ed.* **39**, 2586 (2000).

3. R. G. Gilbert and S. C. Smith, *Theory of Unimolecular and Recombination Reactions*, Blackwell Scientific, Oxford, 1990.

4. K. J. Laidler and M. C. King, *J. Phys. Chem.* **87**, 2657 (1983).

5. D. G. Truhlar, B. C. Garrett, and S. J. Klippenstein, *J. Phys. Chem.* **100**, 12771 (1996).

6. P. Pechukas, in *Dynamics of Molecular Collisions Part B*, W. H. Miller, ed., Plenum, New York, 1976.

7. J. I. Steinfeld, J. S. Francisco, and W. L. Hase, *Chemical Kinetics and Dynamics*, 2nd ed. Prentice-Hall, Englewood Cliffs, NJ, 1999.

8. H. S. Johnston, *Gas Phase Reaction Rate Theory*, Ronald Press, New York, 1966.

9. M. J. Pilling and P. W. Seakins, *Reaction Kinetics*, Oxford Univ. Press, Oxford, 1996.

10. D. A. McQuarrie, *Statistical Mechanics*, Harper & Row, New York, 1976.

11. W. J. Hehre, L. Radom, P. v. R. Schleyer, and J. A. Pople, *Ab Initio Molecular Orbital Theory*, Wiley, New York, 1986.

12. F. L. Pilar, *Elementry Quantum Chemistry*, 2nd ed., McGraw-Hill, Singapore, 1990.

13. A. Szabo and N. S. Ostlund, *Modern Quantum Chemistry*, 1st revised ed., McGraw-Hill, New York, 1989.

14. R. McWeeny, *Coulson's Valence*, 3rd ed., Oxford Univ. Press, Oxford, 1979.

15. A. Pross, *Acc. Chem. Res.* **18**, 212 (1985).

16. A. Pross, *Adv. Phys. Org. Chem.* **21**, 99 (1985).

17. A. Pross, *Theoretical and Physical Principles of Organic Reactivity*, Wiley, New York, 1995.

18. A. Pross and S. S. Shaik, *Acc. Chem. Res.* **16**, 363 (1983).

19. S. S. Shaik and P. C. Hiberty, in *Theoretical Models for Chemical Bonding*, Z. B. Maksic, ed., Springer-Verlag, Berlin, 1991, Vol. 4.

20. S. S. Shaik, H. B. Schlegel, and S. Wolfe, *Theoretical Aspects of Physical Organic Chemistry. The S_N2 Reaction*, Wiley-Interscience, New York, 1992.

21. C. H. Bamford, in *Comprehensive Polymer Science*, G. C. Eastmond, A. Ledwidth, S. Russo, and P. Sigwalt, eds., Pergamon, London, 1989, Vol. 3, p. 219.

22. M. G. Evans and M. Polanyi, *Trans. Faraday Soc.* **32**, 1340 (1936).

23. R. P. Bell, *Proc. Roy. Soc., Ser. A* **154**, 414 (1936).

24. T. Alfrey and C. C. Price, *J. Polym. Sci.* **2**, 101 (1947).

25. C. C. Price, *J. Polym. Sci.* **3**, 752 (1948).

26. C. H. Bamford and A. D. Jenkins, *J. Polym. Sci.* **53**, 149 (1961).

27. C. H. Bamford and A. D. Jenkins, *Trans. Faraday Soc.* **59**, 530 (1963).

28. C. H. Bamford, A. D. Jenkins, and R. Johnston, *Trans. Faraday Soc.* **55**, 418 (1959).

29. A. Brandrup and E. H. Immergut, eds., *Polymer Handbook*, 3rd ed., Wiley, New York, 1989.

30. H. Fischer and L. Radom, *Angew. Chem. Int. Ed.* **40**, 1349 (2001).

31. J. P. A. Heuts, R. G. Gilbert, and L. Radom, *Macromolecule.* **28**, 8771 (1995).

32. J. A. Pople, A. P. Scott, M. W. Wong, and L. Radom, *Isr. J. Chem.* **33**, 345 (1993).

33. A. P. Scott and L. Radom, *J. Phys. Chem.* **100**, 16502 (1996).

34. V. Van Speybroeck, D. Van Neck, M. Waroquier, S. Wauters, M. Saeys, and G. B. Marin, *J. Phys. Chem. A* **104**, 10939 (2000).

35. J. P. A. Heuts, Sudarko, and R. G. Gilbert, *Macromol. Symp.* **111**, 147 (1996).

36. R. J. Bartlett, *J. Phys. Chem.* **93**, 1697 (1989).

37. J. A. Pople, M. Head-Gordon, and K. Raghavachari, *J. Chem. Phys.* **87**, 5968 (1987).

38. M. W. Wong, A. Pross, and L. Radom, *J. Am. Chem. Soc.* **115**, 11050 (1993).

39. M. W. Wong, A. Pross, and L. Radom, *Isr. J. Chem.* **33**, 415 (1993).

40. M. W. Wong, A. Pross, and L. Radom, *J. Am. Chem. Soc.* **116**, 6284 (1994).

41. M. W. Wong, A. Pross, and L. Radom, *J. Am. Chem. Soc.* **116**, 11938 (1994).

42. M. W. Wong and L. Radom, *J. Phys. Chem.* **99**, 8582 (1995).

43. M. W. Wong and L. Radom, *J. Phys. Chem. A* **102**, 2237 (1998).

44. H. B. Schlegel, *J. Chem. Phys.* **84**, 4530 (1986).

45. H. B. Schlegel, *J. Phys. Chem.* **92**, 3075 (1988).

46. J. F. Stanton, *J. Chem. Phys.* **101**, 371 (1994).

47. J. P. A. Heuts, R. G. Gilbert, and L. Radom, *J. Phys. Chem.* **100**, 18997 (1996).

48. R. D. Amos, J. C. Andrews, N. C. Handy, and P. J. Knowles, *Chem. Phys. Lett.* **185**, 256 (1991).

49. W. J. Lauderdale, J. F. Stanton, J. Gauss, J. D. Watts, and R. J. Bartlett, *Chem. Phys. Lett.* **187**, 21 (1991).

50. P. J. Knowles, J. S. Andrews, R. D. Amos, N. C. Handy, and J. A. Pople, *Chem. Phys. Lett.* **186**, 130 (1991).

51. M. C. Zerner, In *Reviews in Computational Chemistry*, K. B. Lipkowitz and R. B. Boyd, eds., VCH Publishers, New York, 1991, Vol. 2.

52. J. M. Seminario and P. Politzer, *Modern Density Functional Theory*, Elsevier Science BV, Amsterdam, 1995.

53. A. D. Becke, *Phys. Rev. A* **38**, 3098 (1988).

54. C. Lee, W. Yang, and R. G. Parr, *Phys. Rev. B* **37**, 785 (1988).

55. A. D. Becke, *J. Chem. Phys.* **98**, 5648 (1993).

56. C. J. Parkinson, P. M. Mayer, and L. Radom, *Theor. Chem. Acc.* **102**, 92 (1999).

57. C. J. Parkinson, P. M. Mayer, and L. Radom, *J. Chem. Soc., Perkin Trans.* 2 2305 (1999).

58. P. M. Mayer, C. J. Parkinson, D. M. Smith, and L. Radom, *J. Chem. Phys.* **108**, 604 (1998).

59. P. M. Mayer, M. S. Taylor, M. W. Wong, and L. Radom, *J. Phys. Chem. A* **102**, 7074 (1998).

60. J. P. A. Heuts, Ph.D. thesis, Univ. Sydney, Sydney, Australia, 1996.

61. J. A. Pople, M. Head-Gordon, D. J. Fox, K. Raghavachari, and L. A. Curtiss, *J. Chem. Phys.* **90**, 5622 (1989).

62. L. A. Curtiss, K. Raghavachari, G. W. Trucks, and J. A. Pople, *J. Phys. Chem.* **94**, 7221 (1991).

63. L. A. Curtiss, K. Raghavachari, P. C. Redfern, V. Rassolov, and J. A. Pople, *J. Chem. Phys.* **109**, 7764 (1998).

64. G. A. Petersson and M. J. Frisch, *J. Phys. Chem. A* **104**, 2183 (2000).

65. J. W, Ochterski, G. A. Petersson, and J. A. Montgomery, *J. Chem. Phys.* **104**, 2598 (1996).

66. J. L. Martin, *Chem. Phys. Lett.* **259**, 669 (1996).

67. J. P. A. Heuts, R. G. Gilbert, and I. A. Maxwell, *Macromolecules* **30**, 726 (1997).

68. J. P. A. Heuts, A. Pross, and L. Radom, *J. Phys. Chem.* **100**, 17087 (1996).

69. M. L. Coote, T. P. Davis, and L. Radom, *J. Mol. Struct.* (THEOCHEM) **461–462**, 91 (1999).

70. M. L. Coote, T. P. Davis, and L. Radom, *Macromolecules* **32**, 2935 (1999).

71. M. L. Coote, T. P. Davis, and L. Radom, *Macromolecules* **32**, 5270 (1999).

72. D. M. Huang, M. J. Monteiro, and R. G. Gilbert, *Macromolecules* **31**, 5175 (1998).

73. L. Radom, M. W. Wong, and A. Pross, in *Controlled Radical Polymerization*, K. Matyjaszewski, ed., ACS Symposium Series, Vol. 685, American Chemical Society, Washington, DC, 1998, p. 31.

74. Wong et al. note that the ionization of $CH_2=CHNH_2$ removes an electron largely associated with the nitrogen lone pair and not with the double bond. Hence the role of D^-A^+ calculated this way is not clear.

75. R. Arnaud, N. Bugaud, V. Vetere, and V. Barone, *J. Am. Chem. Soc.* **120**, 5733 (1998).

76. J. Schweer, Ph.D. thesis, Göttingen Univ., Göttingen, 1988.

77. A. A. Gridnev and S. D. Ittel, *Macromolecules* **29**, 5864 (1996).

78. G. Moad, E. Rizzardo, D. H. Solomon, and A. L. Beckwith, *J. Polym. Bull.* **29**, 647 (1992).

79. O. F. Olaj, P. Vana, M. Zoder, A. Kornherr, and G. Zifferer, *Macromol. Rapid Commun.* **21**, 913 (2000).

80. A. Matsumoto, K. Mizuta, and T. Otsu, *Macromolecules* **26**, 1659 (1993).

81. N. Garcia, J. Guzman, E. Riande, F. Garcia, J. L. De la Pena, P. Calle, and M. L. Jimeno, *J. Polym. Sci. A, Polym. Chem.* **38**, 3883 (2000).

82. R. A. Lyons, J. Hutovic, M. C. Piton, D. I. Christie, P. A. Clay, B. G. Manders, S. H. Kable, and R. G. Gilbert, *Macromolecules* **29**, 1918 (1996).

83. S. Beuermann, M. Buback, T. P. Davis, R. G. Gilbert, R. A. Hutchinson, A. Kajiwara, B. Klumperman, and G. T. Russell, *Macromol. Chem. Phys.* **201**, 1355 (2000).

84. L. H. Yee, M. L. Coote, R. P. Chaplin, and T. P. Davis, *J. Polym. Sci. A, Polym. Chem.* **38**, 2192 (2000).

85. M. Buback, R. G. Gilbert, R. A. Hutchinson, B. Klumperman, F.-D. Kuchta, B. G. Manders, K. F. O'Driscoll, G. T. Russell, and J. Schweer, *Macromol. Chem. Phys.* **196**, 3267 (1995).

86. D. Kukulj and T. P. Davis, *Macromolecules* **31**, 5668 (1998).

87. R. A. Hutchinson, J. R. Richards, and M. T. Aronson, *Macromolecules* **27**, 4530 (1994).

88. D. A. Shipp, T. A. Smith, D. H. Solomon, and G. Moad, *Macromol. Rapid Commun.* **16**, 837 (1995).

89. P. Wittmer, H. Böck, H. Naarmann, and B. J. Schmitt, *Makromol. Chem.* **182**, 2505 (1981).

90. O. F. Olaj and I. Schnöll-Bitai, *Makromol. Chem., Rapid Commun.* **11**, 459 (1990).

91. A. M. Van Herk, *Macromol. Theory Simul.* **9**, 433 (2000).

92. J. P. A. Heuts, M. L. Coote, T. P. Davis, and L. P. M. Johnston, in *Controlled Radical Polymerization*, K. Matyjaszewski, ed., ACS Symposium Series, Vol. 685, American Chemical Society, Washington, DC, 1998, p. 120.

93. T. Fukuda, K. Kubo, and Y.-D. Ma, *Prog. Polym. Sci.* **17**, 875 (1992).

94. T. P. Davis, *J. Polym. Sci. A, Polym. Chem.* **39**, 597 (2001).

95. D. J. T. Hill, J. H. O'Donnell, and P. W. O'Sullivan, *Macromolecule* **15**, 960 (1982).

96. S. A. Jones, G. S. Prementine, and D. A. Tirrell, *J. Am. Chem. Soc.* **107**, 5275 (1985).

97. D. A. Cywar and D. A. Tirrell, *Macromolecules* **19**, 2908 (1986).

98. G. S. Prementine and D. A. Tirrell, *Macromolecules* **20**, 2034 (1987).

99. B. Klumperman and I. R. Kraeger, *Macromolecules* **27**, 1529 (1994).

100. L. H. Yee, J. P. A. Heuts, and T. P. Davis, *Macromolecules* **34**, 3581 (2001).

101. J. S.-S. Toh, D. M. Huang, P. A. Lovell, and R. G. Gilbert, *Polymer* **42**, 1915 (2001).

102. R. P. Bell, *Trans. Faraday Soc.* **55**, 1 (1959).

103. H. S. Johnston, *Adv. Chem. Phys.* **3**, 131 (1961).

104. E. Wigner, *Z. Phys. Chem.* **19**, 203 (1932).

105. L. A. Curtiss, K. Raghavachari, and J. A. Pople, *J. Phys. Chem.* **98**, 1293 (1993).

106. C. W. Bauschlicher and H. Partridge, *J. Chem. Phys.* **103**, 1788 (1995).

107. M. Farina, *Makromol. Chem., Macromol. Symp.* **10/11**, 255 (1987).

108. B. S. Casey, B. R. Morrison, I. A. Maxwell, R. G. Gilbert, and D. H. Napper, *J. Polym. Sci. A, Polym. Chem.* **32**, 605 (1994).

109. G. Litvinenko and A. H. E. Müller, *Macromolecules* **30**, 1253 (1997).

110. D. Yan, H. Dong, P. Ye, and A. H. E. Müller, *Macromolecules* **29**, 5065 (1996).

111. M. Buback, C.-R. Choe, and E.-U. Franck, *Makromol. Chem.* **185**, 1685 (1984).

112. S. Maeder and R. G. Gilbert, *Macromolecules* **31**, 4410 (1998).

113. A. V. Tobolsky and J. Offenbach, *J. Polym. Sci.* **16**, 311 (1955).

114. M. Stickler and G. Meyerhoff, *Makromol. Chem.* **179**, 2729 (1978).

115. O. F. Olaj, *Monatsh. Chem.* **102**, 648 (1971).

116. R. A. Hutchinson, D. A. Paquet, J. H. McMinn, S. Beuermann, R. E. Fuller, and C. Jackson, *DECHEMA Monographs* **131**, 467 (1995).

117. S. Harrisson, H. Kapfenstein-Doak, and T. P. Davis, *Macromolecules* **34**, 6214 (2001).

118. L. H. Yee, Ph.D. Thesis, University of New South Wales, Sydney, 2001.

119. S. Beuermann, M. Buback, T. P. Davis, R. G. Gilbert, R. A. Hutchinson, O. F. Olaj, G. T. Russell, J. Schweer, and A. M. Van Herk, *Macromol. Chem. Phys.* **198**, 1545 (1997).

2 Small-Radical Chemistry

MARTIN NEWCOMB

University of Illinois at Chicago, Chicago, Illinois

CONTENTS

This chapter contains a brief overview of small radical chemistry focusing primarily on carbon-centered radicals and their reactions.

2.1   STRUCTURES OF RADICALS

Most organic compounds are configurationally stable, and one is concerned mainly with dynamic processes that interconvert the conformations of the species. For many radicals, however, configurations interconvert by low-energy pathways. Thus, although most useful reactions of radicals are fast, configurational interconversions as well as conformational interconversions can be faster. Much of the current research in applications of radicals in synthesis is focused on controlling radical structure for diastereoselective reactions.

Radical configurations are described according to whether the odd electron is in a *p* orbital (a π radical) or in a hybrid orbital (a σ radical); examples are shown in Fig. 2.1. A trivalent π radical is planar, and a trivalent σ radical is pyramidal. Each configuration has staggered and eclipsed conformations that interconvert by bond rotation as shown for the ethyl radical in Fig. 2.2. Staggered and eclipsed conformations of a pyramidal radical are similar to those in a hydrocarbon. For a planar radical, the staggered and eclipsed terms refer to the positions of the substituents at the radical center and not to the *p* orbital containing the odd electron.
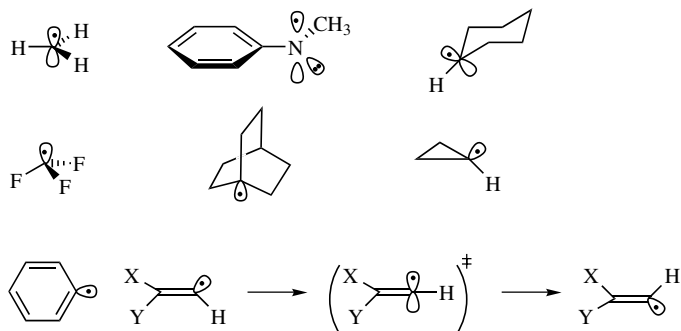

Figure 2.1   Examples of π (*top* drawings) and σ radicals. The transition state for inversion of the vinyl radical is a π radical.

eclipsed   staggered   eclipsed   staggered
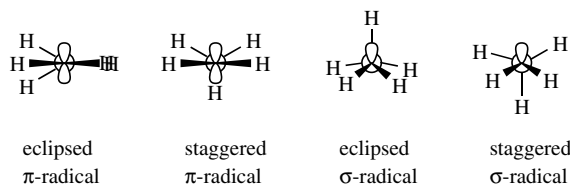π-radical   π-radical   σ-radical   σ-radical

Figure 2.2   Possible conformations and configurations for the ethyl radical.

A divalent radical can have either a linear (π-type) or bent (σ-type) configuration. As with the trivalent radical, the difference is that the odd electron is localized either in a *p* orbital (linear) or in a hybrid orbital (bent). For radicals localized on an sp^2 hybridized atom containing a lone pair, such as nitrogen or oxygen, two low-energy electronic states exist. The odd electron can be in the *p* orbital (π-type radical) or in an sp^2 hybrid orbital (σ-type radical).

In carbon-centered radicals, the energy difference between planar and pyramidal radical configurations is small. The methyl radical is planar (see Fig. 2.1), but alkyl substitution leads to a slight preference for pyramidalization that increases for the series of primary, secondary, and tertiary radicals as judged by the hyperfine couplings of the ^{13}C nucleus at the radical center. Ultimately, in the *tert*-butyl radical, the deviation from planarity is about 10°, and the barrier for interconversion is about 0.5 kcal/mol.[1]

Substitution of electronegative atoms on a trivalent carbon radical center favors pyramidalization. For example, pyramidalization increases in the series mono-, di-, and trifluoromethyl radicals, and various techniques resulted in estimates that the trifluoromethyl radical is deformed from planarity by 13–18°, close to tetrahedral (deformation of 19°). The effect is a result of the interaction between the semi-occupied molecular orbital (SOMO) containing one electron and the lowest unoccupied molecular orbital (LUMO). In a planar radical, SOMO and LUMO are orthogonal, but they interact in a pyramidal radical. Electronegative substituents increase in the energy level of SOMO by π-donation and decrease the energy level of LUMO by σ withdrawal. As the SOMO and LUMO approach one another in energy, pyramidalization is increasingly favored. Substitution of a π conjugating withdrawing group favors the planar radical structure (Fig. 2.3).

The conformational barriers in acyclic alkyl radicals are diminishingly small, resulting in very fast bond rotations. For a simple single-bond rotation as in the ethyl radical, various measurements give barriers in the range of 0.05–0.5 kcal/mol.[1–3] Heteroatoms and conjugating groups increase the rotational barriers. For example, the barrier to rotation in the methanol radical (•CH$_2$OH) is 4.6 kcal/mol, and that in the acetone radical [•CH$_2$C(=O)CH$_3$] is 9.4 kcal/mol. A state of the art ESR and computational study of a methacrylate-derived radical found a barrier for rotation of 2.9 kcal/mol.[4] The conformational barriers for radicals adjacent to a carbonyl group are high enough that the rate of rotation can be slower than the rates of unimolecular or bimolecular radical reactions, as shown for an α-amide radical,[5] and this potentially has an effect on the stereoselectivity in reactions of these types of

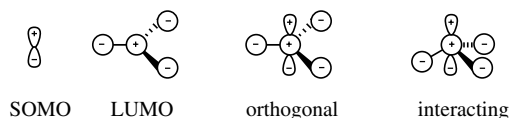
SOMO   LUMO   orthogonal   interacting

Figure 2.3   SOMO and LUMO orbitals of a trigonal radical center do not interact in a planar radical but do interact when the radical is pyramidal.

radicals. One notes that modern computational methods appear to provide highly reliable conformational barriers for radicals.[6]

The structures of cycloalkyl radicals have been studied by ESR spectroscopy.[7] The cyclohexyl radical has a nearly planar radical center with a low barrier to inversion (3.4 kcal/mol). Even the cyclobutyl radical has an essentially planar radical center, although a pyramidalized structure should have less strain. In the case of the cyclopropyl radical, a pyramidal structure is favored, but the rate of inversion through the planar structure is fast as determined by ESR line broadening studies that gave $k = 1 \times 10^{12} \, s^{-1}$ at 70°C.[8] Heteroatoms adjacent to the radical center in cyclic radicals result in anomeric effects; in the case of the 2-methyltetrahydropyran-2-yl radical, the preferred structure has the methyl group in an axial position such that the radical orbital overlaps with the oxygen lone pair.[9]

Bridgehead radicals in relatively small bicyclic structures are pyramidal by virtue of the geometry of the molecules. The fact that these radicals are readily generated from bridgehead halides is a reflection of the small energy difference between planar and pyramidal carbon-centered radicals.

Carbon radicals at unsaturated centers are σ-type radicals. That is, they are bent with an sp^2 hybridized carbon atom. This structure is enforced for the phenyl radical. In the case of the vinyl radical, a bent structure is determined by ESR spectroscopy with a low barrier for inversion of 3 kcal/mol ($k = 4 \times 10^{10} \, s^{-1}$ at 300 K).[10] Computational work on vinyl radicals indicates that sigma substituents give bent structures and pi substituents at the radical center (vinyl, phenyl, formyl) give linear vinyl radicals.[11] Formyl radicals are bent.[12]

Simple nitrogen-centered radials (dialkylaminyl, dialkylaminium) are π-type radicals. Aniline radicals are π-type unless the aromatic ring has electron-withdrawing substituents that favor π donation from nitrogen. The electronic structures of oxygen-centered radicals are quite close in energy.

2.2   RADICAL STABILITIES

2.2.1   Stabilities Evaluated by Hydrogen Atom Bond Dissociation Energies

Knowledge about the stabilities of radicals is important for understanding how readily radical reactions will occur. Hydrogen atom bond dissociation energies (BDEs) can be used to gauge the stability of a particular radical type. The BDE is the energy for homolytic cleavage of a bond at 25°C. Table 2.1 contains a list of BDE values for representative organic compounds. Most of these values are from recently published works.[13–16] For carbon-centered radicals, any type of substitution at the radical center results in increased stability as judged by a reduction in the BDE value for the parent compound. This phenomenon is a feature of the unpaired electron in a semi-occupied molecular orbital (SOMO) and the electron deficient nature of a radical. Any group that provides an orbital that can mix with the SOMO will result in stabilization. In the case of donors, a filled HOMO is close in energy to the semi-occupied MO of the radical (SOMO), and the newly formed orbitals will contain a pair of

TABLE 2.1   Bond Dissociation Energies for Selected Compounds[a]

Molecule	BDE	Molecule	BDE
CH_4	104.9 ± 0.1	H–H	104.2
CH_3CH_3	101.1 ± 0.4	H_2O	119.30 ± 0.05
$(CH_3)_2CH-H$	98.6 ± 0.4	H_2O_2	88
$(CH_3)_3C-H$	96.5 ± 0.4	CH_3O-H	104.2 ± 0.9
c-C_3H_6	106	RCO_2-H	ca. 105
$H_2C=CH_2$	111.2 ± 0.8	PhO–H	87
Ph–H	111.2 ± 0.8	CH_3S-H	87.4 ± 0.5
$HC\equiv CH$	132.8 ± 0.7	PhS–H	ca. 80–82
$H_2C=CHCH_2-H$	88.2 ± 2.1	PhSe–H	78 ± 4
$PhCH_2-H$	88.5 ± 1.5	NH_3	108.2 ± 0.3
$HOCH_2-H$	96.06 ± 0.15	Et_3Si-H	95.1
$HC(O)CH_2-H$	94.3 ± 2.2	$(Me_3Si)_3Si-H$	87.5
CH_2O	88.04 ± 0.16	Bu_3Ge-H	88.6
$CH_3C(O)-H$	89.4 ± 0.3	Bu_3Sn-H	78.6
$HOC(O)-H$	>89.5		
$NCCH_3$	94.8 ± 2.1		

[a] Bond dissociation enthalpies at 298 K. Values from Refs. 13–15. PhSeH value from Ref. 16.

electrons in the lower-energy orbital but only a single electron in the higher-energy orbital. In the case of acceptors, the LUMO orbital is close in energy to the SOMO, and a single electron will occupy the lower energy combination orbital. Delocalization of the radical center with π bonds also results in stabilization, and alkyl groups stabilize a radical by interaction of the electron pairs in the σ bonds with the radical center in π-type bonding.

2.2.2   Stability versus Persistence

Despite the stabilization afforded by various groups, most radicals react with one another with diffusion-controlled rates. Some radicals are long-lived, however, and this can be a result of either thermodynamics, sterics that prevent coupling reactions, or both. Examples of some long-lived radicals are shown in Fig. 2.4. The triphenylmethyl (or trityl) radical, the radical identified by Gomberg in 1900 in work that is typically regarded as the beginning of radical chemistry, is stabilized by extensive conjugation. If trityl radicals coupled to give hexaphenylethane, the product would be highly strained, and the actual trityl dimer is the quinoid compound shown in the figure. At equilibrium, enough trityl radical is present to give solutions a yellow color that Gomberg observed. Nitroxyl radicals, represented by 2,2,6,6-tetramethylpiperidine-N-oxyl (TEMPO), are thermodynamically favored in comparison to their dimers because of the very low energy of the O–O bond. Nitroxyl radicals with no hydrogens in the β positions to the nitroxyl are long-lived, and TEMPO is commercially available. Galvinoxyl is another well-known stable radical that is often used to calibrate signal intensities in ESR studies.
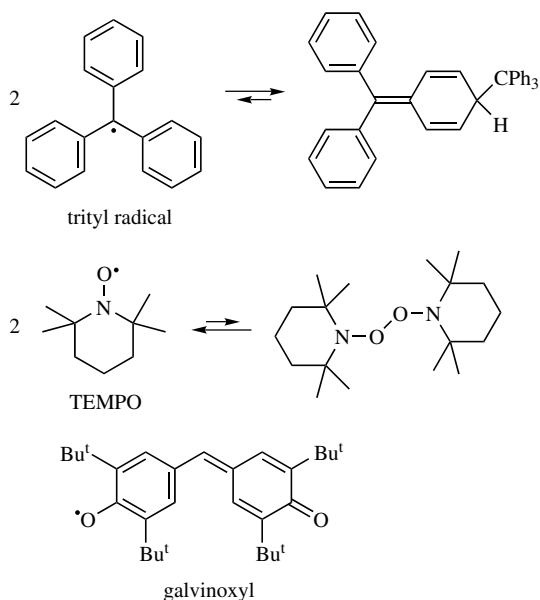
Figure 2.4   Examples of persistent radicals.

2.3   RADICAL REACTIONS

2.3.1   Elementary Radical Reactions

The elementary reactions of small-radical chemistry can be divided into three classes of reactions: those that produce radicals (initiation reactions), those in which a radical reacts to give a radical product (propagation reactions), and those in which radicals are lost (termination reactions). In most synthetic applications of radical chemistry, the propagation steps are the ones that form the desired products, but some useful radical sequences exist wherein the desired products are produced in termination steps as discussed later.

There is an important difference in the nomenclature of reactions in small-radical chemistry and those in polymer radical chemistry where reactions are divided into four elementary groups. Initiation and termination are the same in both, but the propagation reactions of small-radical chemistry are divided into two types of polymer reaction: propagations and transfers. A "propagation" reaction in polymer chemistry is one that increases the chain length of the growing polymer, whereas a "transfer" reaction is one that terminates the polymer chain but does not result in loss of radicals. Examples of polymer transfer reactions are atom and group transfer processes and radical fragmentations.

2.3.2   Initiation Reactions

Various methods can be used to initiate radical reactions, and they can be divided into the broad areas of thermolyses, photolyses, and electron transfer reactions. Most often in organic synthetic sequences, initiation involves a thermolysis reaction of an initiator that contains a weak bond, especially an azo or peroxy compound. Photolysis of many compounds will initiate radical reactions either by homolytic cleavage of a weak bond or by production of an excited state that reacts by electron transfer or atom abstraction, but synthetic chemists seldom use this method except in select cases. Electron transfer processes are involved in many reactions of metals with organic substrates, but strong reducing agents will also reduce radicals to anions or organometallic species; therefore, the method is most useful when the reductant or oxidant is not strong enough to intercept the radical rapidly.

Many thermal initiators are available commercially, and these are commonly used in synthetic conversions. In the case of chain reactions, only a small amount of initiator may be required, typically 1–5 mol% relative to substrate. A radical conversion is usually conducted in refluxing solvent (benzene or toluene have been widely used) with the initiator selected to have a half-life of about 1 hour at the reaction temperature. Figure 2.5 shows some of the more common thermal initiators and lists the approximate temperature for decomposition half-lives of 1 h.[17–19] Di-*tert*-butyl peroxide, *tert*-butyl peroxybenzoate, benzoyl peroxide, and AIBN have long shelf lives and are commercially available. The more reactive thermal initiators, di-*tert*-butyl peroxyoxalate[20] and di-*tert*-butyl hyponitrite[21] are usually used soon after preparation. Radical chain reactions are often conducted at temperatures within 10°C of the temperatures shown in Fig. 2.5 for a 1-h half-life of the initiator, but
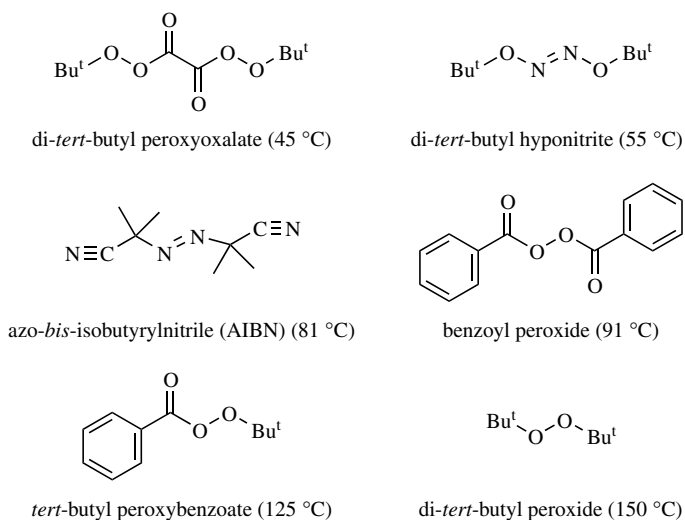

di-*tert*-butyl peroxyoxalate (45 °C)   di-*tert*-butyl hyponitrite (55 °C)

azo-*bis*-isobutyrylnitrile (AIBN) (81 °C)   benzoyl peroxide (91 °C)

tert-butyl peroxybenzoate (125 °C)   di-*tert*-butyl peroxide (150 °C)

Figure 2.5   Common thermal initiators. The temperatures in parentheses are those at which the initiator has a half-life of 1 h.

one can operate at higher temperatures by adding the initiator slowly over the course of several hours.

A relatively new thermal initiation procedure can be employed over a wide range of temperatures and has rapidly gained popularity. Admission of a small amount of oxygen and catalytic amounts of Et_3B into a reaction mixture will result in initiation.[22] In fact, adventitious oxygen often is sufficient for initiation such that Et_3B is the only necessary additive. The method has been used at temperatures ranging from -78 to $110°C$, and it appears to be especially attractive when low reaction temperatures are necessary in order to obtain high stereoselectivity in radical functionalization reactions.

Photochemical initiation of radical reactions is possible with a wide range of compounds. The photochemical event either creates a reactive state or cleaves a weak bond homolytically to produce radicals. Photochemical initiation is quite popular in polymer radical chemistry because it is readily controlled and allows the production of commercial formulations with room-temperature stability, and photoinitiators used in polymer chemistry represent a multi-million-dollar business. Many of the commercial initiators are aryl ketones and phosphine oxides that are tuned for specific wavelength initiation. Somewhat ironically, these initiators are not commonly used in small radical chemistry, despite the large amount of photochemical information available.

Photoinduced electron transfer (PET) processes are more common in small-radical chemistry.[23,24] In these reactions, an excited state is produced photochemically that is either a strong oxidant or reductant, and this excited-state species then reacts in an electron transfer reaction with another molecule. For example, chloranil is an oxidant in the ground state with an oxidation potential of 0.32 V versus NHE,[25] but triplet chloranil is a much more powerful oxidant. Irradiation of a stable solution of chloranil and an enol ether in acetonitrile with 355-nm laser light gives the chloranil triplet (lifetime of several microseconds) that oxidizes the enol ether to the corresponding radical cation in a diffusion-controlled process (Fig. 2.6).[26,27] Much of PET chemistry involves reactions of the radical cations and radical anions that are formed in the ET step, but some of these species are capable of fragmenting to give radicals. When that occurs, the PET reaction can result in the same type of initiation as one would have in a homolysis reaction.
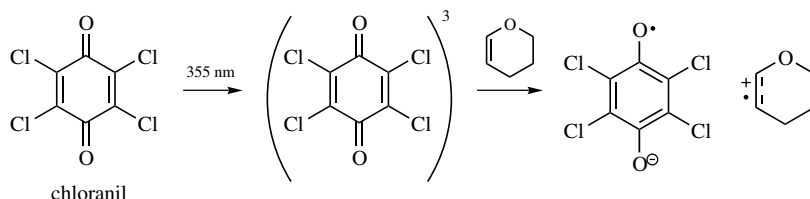

Figure 2.6   An example of photochemically induced electron transfer (PET). Chloranil is excited photochemically to give a relatively long-lived triplet state that oxidizes an enol ether to the corresponding radical cation. The chloranil radical anion is the byproduct of the reaction.

Redox initiation of radical reactions can be divided into two types of processes. One type involves either reduction or oxidation of a substrate to give a radical that reacts in one or more radical functionalization steps before a second reduction or oxidation reaction occurs. These types of processes consume two equivalents of reductant or oxidant when chemical redox is involved or are overall two-electron processes when performed electrochemically. They are discussed later in the section on nonchain radical reactions.

The second type of redox initiation also involves nonchain reactions, but the initiator serves as a catalyst. For example, a copper(I) complex will react with an alkyl halide to give a copper(II) complex and an alkyl radical in a process that is not thermodynamically favored [Eq. (2.1)]. The alkyl radical can react in a functionalization reaction, and the newly formed radical product can react with the copper(II) complex to return the thermodynamically favored copper(I) complex and a new, functionalized, alkyl halide. The reaction sequence can be employed in small-radical chemistry in, for example, formation of cyclic product from an acyclic alkene,[28] and it has been incorporated into a powerful "living radical polymerization" sequence [atom transfer radical polymerization (ATRP)][29,30] that is discussed in Chapter 11.

$$\text{Ligated Cu(I)} + \text{R−X} \rightleftarrows \text{ligated Cu(II)X} + \text{R}^{\bullet} \tag{2.1}$$
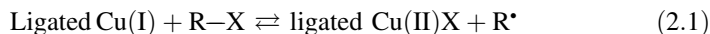
2.3.3 Elementary Propagation Reactions

Radical reactions in nature, in synthesis, and in polymerizations inevitably involve a sequence of reactions. A wide range of unimolecular and bimolecular elementary radical propagation reactions are possible, and some common ones are shown in Fig. 2.7. Note that some reaction types can occur in either a homolytic or heterolytic version, such as for the β-fragmentation reactions shown in the figure. In some cases, differentiation between homolytic and heterolytic pathways might not be obvious, and the pathway might change as a function of solvent polarity. Some concerted radical reactions (migrations and 1,3-eliminations) are implicated from computational work,[31] but they have not been documented experimentally. The concerted reactions result in the same products that would arise from a fragmentation followed by recombination or substitution, respectively, or from the stepwise rearrangement shown in Fig. 2.7, and differentiation between concerted and ion pair or radical pair reactions is subtle.

2.4 RADICAL CHAIN REACTIONS

Most useful radical processes involve a complex series of elementary reactions. In synthetic applications and in polymerizations, these sequences typically constitute chain reactions. The characteristic features of a chain reaction are (1) a series (two or more) of propagation steps exists wherein the radical product in one step is a reactant in another step and (2) the velocities of the propagation steps are fast
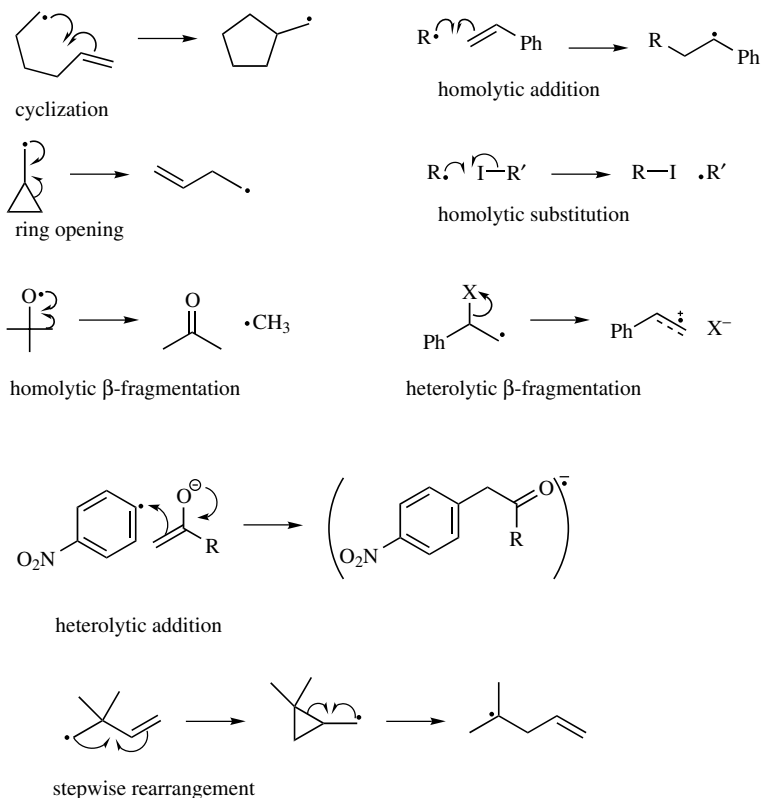
cyclization

homolytic addition

ring opening

homolytic substitution

homolytic β-fragmentation

heterolytic β-fragmentation

heterolytic addition

stepwise rearrangement

Figure 2.7   Some common radical propagation reactions.

relative to the velocity of radical–radical reactions that result in termination. The latter property is critically important; if it does not hold, the chain reaction collapses, and the reaction sequence is comprised of initiation and termination steps and may or may not contain propagation reactions. These non-chain reactions are discussed in Section 2.5.

2.4.1   Tin Hydride Radical Chain Reactions

The various components of a radical chain reaction are illustrated in one of the more common types of radical chain reactions, the tin hydride protocol, shown in Fig. 2.8. The method is named after Bu_3SnH, the reagent used almost exclusively in early studies. In this example, initiation is accomplished by thermolysis of AIBN that gives radicals that react with Bu_3SnH. In the propagation sequence, the stannyl radical reacts with an alkyl halide, pseudohalide, or other radical precursor to give Bu_3SnX and a carbon- or heteroatom-centered radical. A radical functionalization
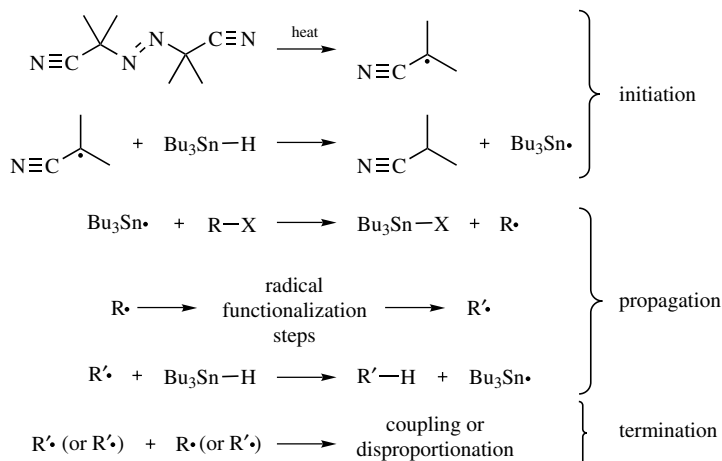
Figure 2.8 Elementary processes in the tin hydride reaction protocol.

reaction or multiple functionalization reactions follow. The final step in the propagation sequence is reaction of a radical with Bu_3SnH to generate another stannyl radical.

Radical–radical coupling and disproportionation reactions terminate the chain sequence. In principle, stannyl radicals could be involved in the termination reactions, but the velocities of the termination reactions are controlled by the radical concentrations, and, as discussed later, the stannyl radical usually is present in much smaller concentrations than alkyl radicals.

Many radical chain reactions involve halogen or pseudohalogen transfer steps that give the initial radical from a halide or pseudohalide precursor and hydrogen atom transfer steps that give the final product of the chain reaction. Bu_3SnH provides a nearly ideal combination of high reactivity of the stannane with carbon-centered radicals and high reactivity of the stannyl radical with halide and pseudo-halide precursors, but concerns about the toxicity of tin compounds resulted in a number of alternative H-atom donors that can be used in the "tin hydride" method. The success of a radical chain process is dependent on the velocities of the propagation steps that must be greater than those of the termination steps, and this places a practical limit on the alternatives to tin hydride. For example, germanium- and silicon-centered radicals will react with halides even faster than tin-centered radicals, so germanes and silanes will efficiently replace stannanes for the reactions that produce carbon-centered radicals. Bu_3GeH reacts about 4% as fast as Bu_3SnH with alkyl radicals at room temperature, and trialkylgermanes can be used successfully in chain reactions with alkyl radicals[14] (see Section 2.6.4.1 for rate constants). On the other hand, Et_3SiH reacts nearly four orders of magnitude less rapidly with alkyl radicals than does Bu_3SnH, and simple trialkylsilanes cannot be used for chain reactions with alkyl radicals. The slow reactivity of Et_3SiH with alkyl radicals is in part a

consequence of high Si—H bond energy of this silane (95 kcal/mol), and reduction of the Si—H bond energy by replacing the alkyl groups with thio and silyl groups gives silanes that react fast enough with alkyl radicals to propagate chain reactions.[14] One popular alternative to Bu$_3$SnH is *tris*-(trimethylsilyl)silane, (TMS)$_3$SiH,[32] which has an Si—H bond energy of 84 kcal/mol and reacts with alkyl radicals about 20% as fast as does Bu$_3$SnH.

Chain reactions also will fail if the halogen abstraction reaction (or other radical generation reaction) is not fast. For example, thiols and selenols react with alkyl radicals faster than Bu$_3$SnH, but the thiyl and selenyl radicals do not abstract halogen atoms rapidly from alkyl halides and cannot be used in chain reactions with alkyl halides. There is a modification that will allow the use of thiols and selenols as reducing agents in radical chain reactions with alkyl halides, however. One can successfully use a combination of a silane and a thiol (or a stannane and selenol). For example, when *t*-BuSH and Et$_3$SiH are used together, an alkyl radical reacts rapidly with the thiol to give a thiyl radical, the thiyl radical reacts rapidly with the silane to give a silyl radical, and the silyl radical rapidly abstracts halogen from an alkyl halide. Thus, although neither Et$_3$SiH nor *t*-BuSH would successfully propagate a chain reaction with an alkyl halide, the combination of them would (Fig. 2.9).

A variety of radical precursors can be used in the general tin hydride protocol. Alkyl radicals can be produced from alkyl chloride or, better, alkyl bromides; the highly reactive alkyl iodides could be used but are not necessary. One can substitute the pseudohalogens RSPh and RSePh for alkyl halides where phenyl sulfides react about as rapidly as alkyl chlorides and phenyl selenides react about as rapidly as alkyl bromides. The use of a phenyl sulfide (PhSR) instead of a dialkyl sulfide (RSR′) assures one of the desired regioselectivity of the group transfer reaction due to the "instability" of the phenyl radical. When aryl radicals are desired, aryl iodides can be employed.

2.4.2   Alkylmercuric Halide Protocol

A number of early radical studies were accomplished with alkylmercuric halides as the radical precursors reacting with NaBH$_4$. The relative ease in preparation of the precursors is an advantage of the method, but concerns about the toxicity of mercury

R• + Et$_3$Si—H ⟶ R—H + Et$_3$Si•   (A, slow)

t-BuS• + R—X ⟶ *t*-BuSX + R•   (B, slow)

R• + *t*-BuS—H ⟶ R—H + *t*-BuS•   (C, fast)

t-BuS• + Et$_3$Si—H ⟶ *t*-BuS—H + Et$_3$Si•   (D, fast)

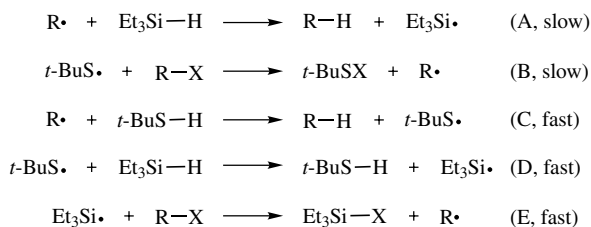Et$_3$Si• + R—X ⟶ Et$_3$Si—X + R•   (E, fast)

Figure 2.9   Sequenced reactions involving a thiol and a silane. When a thiol and silane are present in a mixture with an alkyl halide, the sequence of reactions C–E permits an efficient chain reaction.
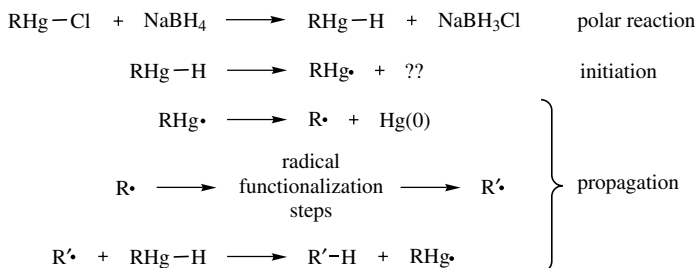
$$RHg-Cl \; + \; NaBH_4 \longrightarrow RHg-H \; + \; NaBH_3Cl \qquad \text{polar reaction}$$

$$RHg-H \longrightarrow RHg\bullet \; + \; ?? \qquad \text{initiation}$$

$$RHg\bullet \longrightarrow R\bullet \; + \; Hg(0)$$

$$R\bullet \longrightarrow \begin{array}{c}\text{radical}\\ \text{functionalization} \longrightarrow R'\bullet \\ \text{steps}\end{array} \qquad \text{propagation}$$

$$R'\bullet \; + \; RHg-H \longrightarrow R'-H \; + \; RHg\bullet$$

Figure 2.10   Initial steps in mercuric halide chain reactions.

compounds have limited its use. The radical chain sequence involved is shown in Fig. 2.10. Mercuric halides are reduced to mercuric hydrides by borohydride in a polar reaction. The radical reactions are initiated by adventitious radical production, possibly involving decomposition of the mercury hydride. Once the chain is initiated, the major reaction sequence involves reaction of a radical with an alkyl-mercury hydride to give an alkylmercury radical that decomposes to an alkyl radical. Radical functionalization reactions followed by radical trapping by another alkyl-mercury hydride complete the chain sequence. Details of this mechanism were poorly understood originally, and a speculative pathway involving electron transfer steps and reduction of radicals by $NaBH_4$ existed, but later studies found that $NaBH_4$ reacts much too slowly with alkyl radicals for this pathway to be important.[33]

2.4.3   Thione Radical Precursors

Thiones also react readily with a number of radicals such as stannyl and silyl radicals, and xanthates and related thione derivatives can be used as radical precursors in the tin hydride protocol. Successful propagation of radical chain reactions with thiones is the basis of the Barton–McCombie deoxygenation reaction shown in Fig. 2.11 as well as the Barton PTOC esters discussed in Section 2.4.4. These precursors can be used in chain reactions because the π bond in a thione is weak, the
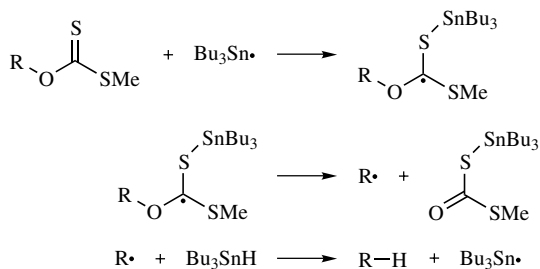
Figure 2.11   Propagation steps in the Barton–McCombie deoxygenation reaction sequence.
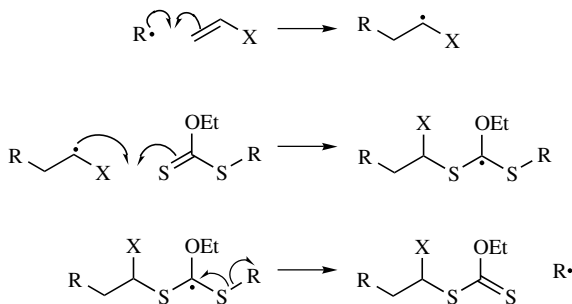
Figure 2.12   A radical chain reaction containing a ''degenerative'' xanthate transfer step.

σ bond between sulfur and the propagating radical atom (Sn or Si) is strong, and the addition reaction of the group 14 radical to the thione is fast.

One can also use the general scheme of the Barton–McCombie deoxygenation reaction in synthetically constructive sequences. When radical R$^\bullet$ reacts with an alkene faster than it reacts with tin hydride, it is possible to incorporate a radical functionalization step into the sequence as in the conventional tin hydride protocol. Furthermore, one can eliminate the tin hydride completely, in which case the radical functionalization sequence in Fig. 2.12 would be possible.[34] This sequence, termed ''degenerative'' xanthate transfer, has been incorporated into ''living'' radical polymerization reactions in a procedure known as *radical addition fragmentation transfer* (RAFT), described in Chapter 12.

2.4.4   Barton's PTOC Esters

In the mid-1980's the late Derek Barton's group introduced a new class of radical precursors based on the high reactivity of thiones with many types of radicals.[35,36] The most commonly used precursors in this group are mixed anhydrides of a carboxylic acid and the thiohydroxamic acid *N*-hydroxypyridine-2-thione. These compounds are often referred to as PTOC esters where the acronym PTOC is for pyridine-2-thione-*N*-oxycarbonyl. These carboxylic acid derivatives are readily prepared by typical acid functionalization procedures such as reaction of an acid chloride with the sodium salt of *N*-hydroxypyridine-2-thione or dicyclohexyl carbodiimide (DCC) coupling of a carboxylic acid with *N*-hydroxypyridine-2-thione. PTOC esters are isoelectronic with peroxides, but they are also activated carboxylic acid derivatives that will react reasonably efficiently with nucleophiles. Therefore, they are often prepared and immediately used in a synthetic reaction without isolation. Nonetheless, many PTOC esters have adequate stability to permit purification by silica gel chromatography.

The initiation and propagation steps in a typical chain reaction using a PTOC ester are shown in Fig. 2.9. The weak C—S π bond in the thione and the aromatization of the pyridine provide the driving force for formation of the highly unstable acyloxy radical intermediate. Rapid decarboxylation of the acyloxy radical gives
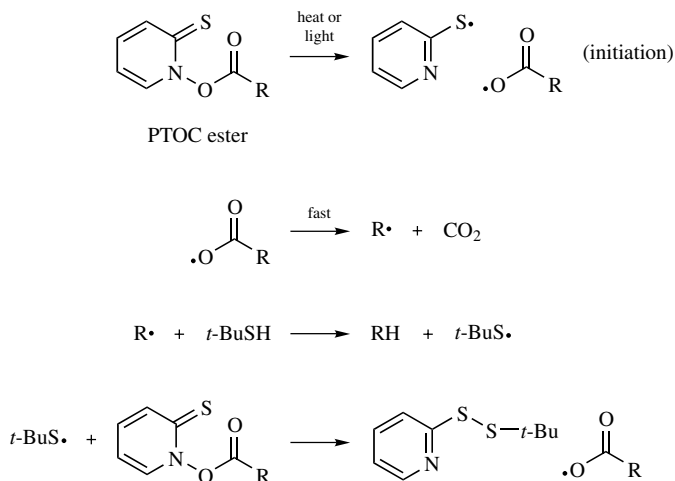
Figure 2.13   Initiation and propagation steps in reactions of a PTOC ester.

the alkyl radical in a process that will compete successfully against diffusion-controlled reactions. The alkyl radical then reacts with the H-atom donor t-BuSH in the example in Fig. 2.13 to give the thiyl radical. Of course, radical functionalization reactions, such as addition to an alkene, can be incorporated in the chain reaction. Finally, the thiyl radical adds to another PTOC ester molecule to complete the chain sequence.

The PTOC esters are reactive enough such that radical chain reactions can be conducted with thiols or selenols; that is, thiyl and selenyl radicals add efficiently to the thione group to propagate the chain sequence. In fact, chain reactions even can be propagated by addition of a carbon-centered radical to the thione. In this case, the product of the reaction sequence is an alkyl 2-pyridyl sulfide that can be further functionalized. Derivatives related to PTOC esters can be used as precursors to nitrogen-centered radicals (aminyl,[37] amidyl,[38] iminyl[39]) and to oxygen-centered radicals (hydroxyl,[40] alkoxyl,[41] oxycarbonyloxyl[42]). PTOC esters and related thiones cannot be used for production of vinyl or aryl radicals, however, because the corresponding acyloxyl radicals do not decarboxylate fast enough.

One attractive feature of PTOC esters and other thione derivatives is their instability both thermally and photochemically. This might be seen as a disadvantage, but the instability is useful because it removes the need for a radical initiator. Heating a solution containing a PTOC ester to a temperature of 60–70°C will result in thermolysis reactions (cleavage of the weak N—O bond) that initiate the chain reaction sequence. In addition, the PTOC esters have a long-wavelength absorbance centered at about 360 nm that extends into the visible spectrum, and photolysis of a solution containing a PTOC ester with visible light from a common tungsten filament bulb will also initiate reactions. The latter method of initiation allows one to perform reactions at very low temperatures in order to improve selectivity. In either

case, thermal or photochemical initiation, depletion of the PTOC ester will result in a termination of all radical processes because no initiator remains. This reduces the possibility of undesired secondary radical reactions of the products, which could be a problem when an initiator such as AIBN is used.

2.4.5   Atom and Group Transfer Chain Reactions

Another type of radical chain reaction employed in synthesis involves atom or group transfer steps in the propagation sequence. The atom can be a hydrogen atom as was the case in the earliest examples of this sequence, but in more recent applications it is commonly a halogen atom (or pseudohalogen group). A representative example is shown in Fig. 2.14. Initiation often involves a photochemical step as shown in the figure, but the Et_3B/O_2 initiation protocol also can be employed. The unusual feature of this sequence is that one of the steps is thermodynamically unfavored, in this example the addition of the diethyl methylmalonyl radical to the alkene. The sequence is successful despite the unfavorable step because few competing radical reactions are possible, and, eventually, the adduct radical abstracts a halogen atom from an iodomalonate molecule to complete the synthetic transformation. A sequence such as that shown in Fig. 2.14 would fail in the tin hydride protocol that would result in reduction of the diethyl methylmalonyl radical, but, importantly, one could follow up the atom or group transfer chain reaction with a tin hydride radical chain reduction of the crude products to achieve the addition and reduction steps.

   The reversible step in the atom transfer protocol not only precludes highly reactive H-atom transfer agents such as Bu_3SnH but also requires that the atom (or group) transfer reaction be inherently fast. In the case of simple transfer reactions such as shown in Fig. 2.14, therefore, the transferred group would be an iodine or bromine atom or an aryltelluryl or arylselenyl group. As with xanthate transfers, this method has been incorporated into polymerization chemistry as described in Chapter 12.
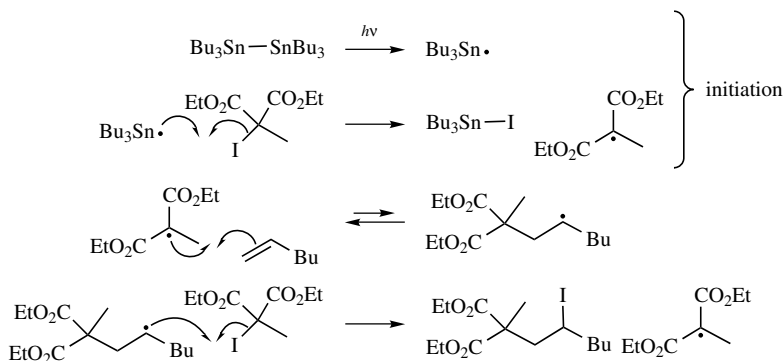
Figure 2.14   Initiation and propagation steps in an atom transfer chain reaction sequence.
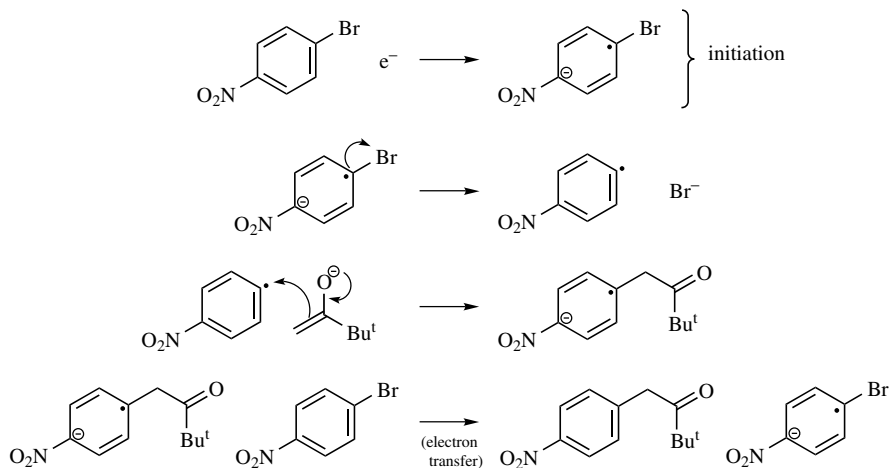
Figure 2.15   A radical anion chain reaction sequence.

2.4.6   Radical Ions in Chain Reactions

A number of radical chain reactions with synthetic potential involve radical ions in some or many of the chain propagation reactions. These can be either radical anions or radical cations. The earliest known of this general class of chain reactions involves aromatic radical anions; an example is shown in Fig. 2.15. Initiation involves an electron transfer reduction process (either thermally activated or photo-stimulated) that gives a radical anion. In the propagation reactions, the radical anion fragments heterolytically, the radical thus formed adds to a nucleophile to give a product radical anion, and the product radical anion reduces another molecule of the aromatic reagent. Depending on which step in the propagation sequence is rate controlling, the rates of these types of reactions could be independent of nucleophile concentration (first-order overall) or dependent on nucleophile concentration (second-order overall), and they have been termed $S_{RN}1$ and $S_{RN}2$ reactions, respectively.[43]

In radical anion chain reactions, an electron transfer (reduction) step precedes a heterolytic fragmentation. It is also possible to have chain reactions wherein a heterolytic fragmentation step precedes an electron transfer step; in such a case, radical cations are involved in the propagation sequence. The propagation steps in one example are shown in Fig. 2.16, where the radical precursor is a PTOC ester.[44] The initially formed radical contains a good leaving group in the β position, here a phosphatoxy group. Heterolysis of that radical gives a radical cation intermediate that reacts with a nucleophilic alcohol. Proton transfer from the adduct gives a product radical that reacts with thiol, and the thiyl radical adds to the PTOC ester radical precursor to complete the propagation sequence. The key reaction in these sequences is the heterolytic fragmentation step; it is facilitated by a good polar leaving group and radical cation stabilizing elements such as the aryl group shown
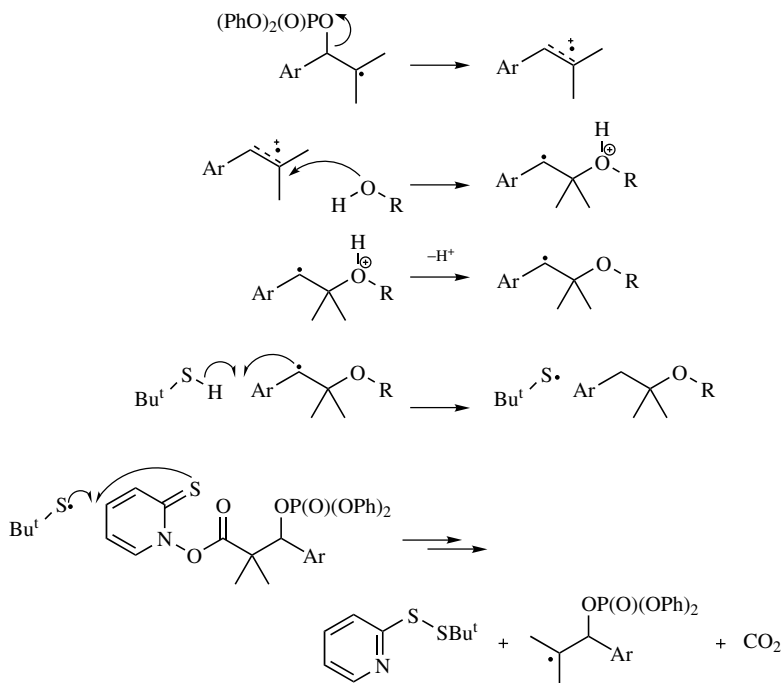
Figure 2.16   A radical chain sequence containing a radical cation.

in Fig. 2.16 or alkoxy groups that give styrene and enol ether radical cations, respectively.

2.5   NONCHAIN RADICAL PROCESSES

Radical chain reactions are the most common reaction types in synthetic applications, but some nonchain radical reactions also are useful in synthesis of small compounds and polymers, and nonchain reactions are widespread in biological radical processes. One can divide nonchain radical reactions into two classes. In one type, a persistent radical is formed in what would otherwise appear to be chain reaction conditions. The other class involves redox chemistry where a radical is produced under reductive or oxidative conditions that are adequately mild to permit a radical reaction to occur before further reduction or oxidation steps, respectively, intercept the radical.

2.5.1   Persistent Radical Effect

The persistent radical effect is the foundation of most useful nonchain radical reactions. If all possible termination reactions occur at diffusion-controlled rates,

nonchain processes inevitably lead to a mixture of products. However, if one of the termination reactions is not fast, then the concentration of one radical will accumulate, and this radical at high concentration will "steer" the reaction to give mainly the product of radical cross-termination. This phenomenon was described by Ingold[45] and by Fischer[46] and is often referred to as the *Ingold–Fischer effect*.

The persistent radical effect works in the following way. Assume that radicals X$^\bullet$ and Y$^\bullet$ are produced in a radical reaction sequence. The possible radical termination steps are self-termination of two X$^\bullet$ or two Y$^\bullet$ radicals or cross-termination of an X$^\bullet$ radical and a Y$^\bullet$ radical. Further assume that self-termination of Y$^\bullet$ and cross-termination are diffusion-controlled reactions, but self-termination of X$^\bullet$ is much slower than diffusion or is thermodynamically unfavorable. In this situation, radical X$^\bullet$ is a persistent radical, and the concentration of X$^\bullet$ will build up early in the reaction. As the X$^\bullet$ concentration becomes large, the velocity of the cross-termination between X$^\bullet$ and Y$^\bullet$ (occurring with a diffusion-controlled rate constant) increases because of the high X$^\bullet$ concentration such that this process overwhelms the self-termination reaction of two Y$^\bullet$ radicals. When this occurs, the products formed by radical–radical reactions will effectively be only those of the cross-termination reaction of X$^\bullet$ with Y$^\bullet$.

2.5.2 Nonchain Sequences Involving Persistent Radicals

One well-known example of the persistent radical effect is the Barton reaction involving the photolysis of nitrite esters to give an alkoxyl radical and NO (Fig. 2.17); the persistent radical is NO that will not couple with another NO radical. The alkoxyl radical can abstract an H atom from carbon to give a carbon-centered radical that
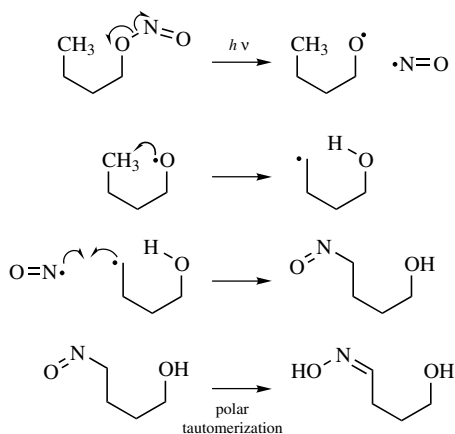

Figure 2.17   The Barton reaction, a nonchain radical process. The NO radical is persistent and effectively traps all carbon-centered radicals to give the nitroso product that rearranges to the oxime.
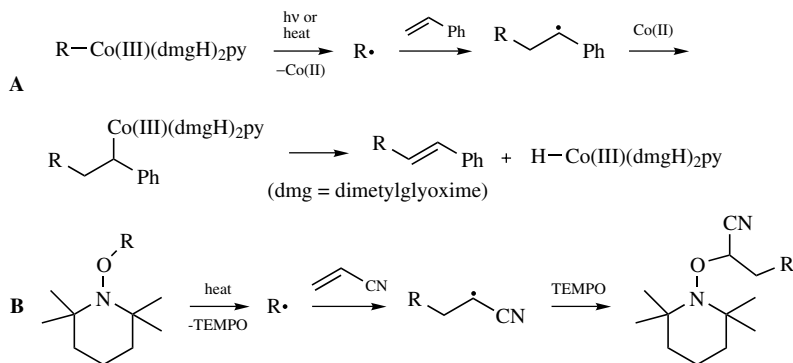
Figure 2.18 Persistent radical reactions mediated by cobalt compounds (A) and nitroxyls (B).

subsequently reacts with NO to give a nitroso compound that rearranges in a polar reaction to the oxime product.

Other nonchain radical reactions involving persistent radicals that have synthetic potential include photolyses or thermolyses of alkyl cobalt(III) species and reactions of hydroxylamine ethers (Fig. 2.18). In example **A**, homolytic cleavage of the Co—C bond in the RCo(dmgH)$_2$py complex gives a Co(II) species and an alkyl radical; the Co(II) species will not self-couple. The alkyl radical adds to styrene, and the adduct radical is trapped by the Co(II) species to give a Co(III) species that reacts by β-hydride elimination to give the product. The reaction in example **B** in Fig. 2.18 is similar; homolysis of the hydroxylamine ether gives the persistent nitroxyl radical and an alkyl radical. The nitroxyl-mediated reaction has been adapted to polymerization reactions in the form of "living" radical polymerizations as discussed in Chapter 10.

2.5.3 Nonchain Radical Sequences Involving Redox Processes

Radicals are intermediates in chemical and electrochemical reduction and oxidation processes. For example, formation of an alkyllithium reagent or Grignard reagent from reaction of an alkyl halide with lithium or magnesium metal, respectively, involves an initial reduction of the alkyl halide to give an alkyl radical and a halide anion. In these reactions, the alkyl radical is rapidly reduced to the "carbanion" or organometallic product, but, if a poorer reducing agent is used, the intermediate radical can react in a typical radical reaction before it is further reduced. The same situation applies in an oxidation reaction of, for example, an enolate anion; if the oxidizing agent is relatively poor, the intermediate radical will have time to react before a second oxidation occurs, taking the radical to a cation. Both reductive and oxidative reactions have been used in synthetic sequences where the intermediate radical reacts, often in an intramolecular reaction, to give a product radical that is then further reduced or oxidized, respectively. These nonchain processes require 2 equiv of reductant or oxidant.
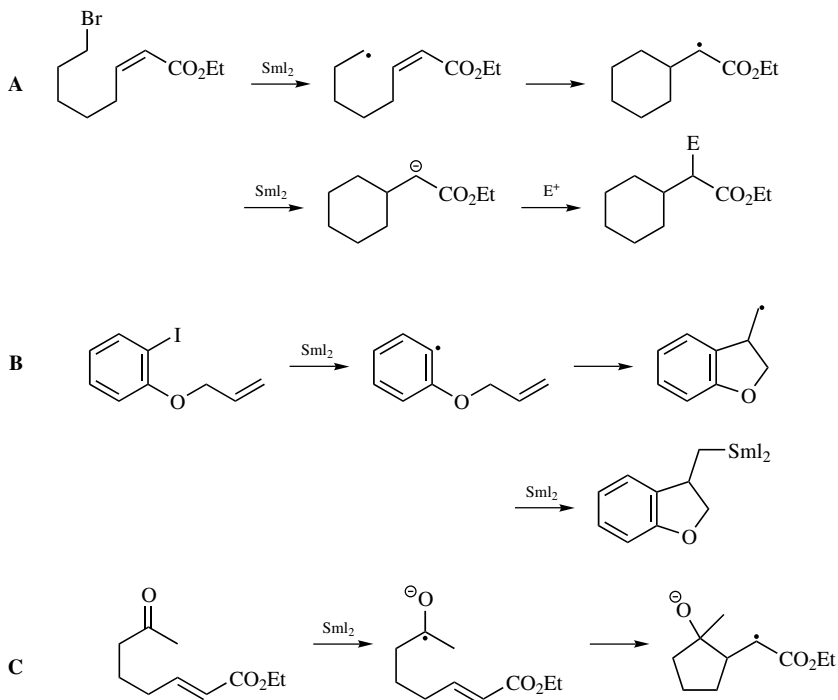
Figure 2.19   Synthetic applications of samarium diiodide.

One of the most popular reductive processes involving reaction of a radical intermediate is the samarium diiodide protocol (Fig. 2.19).[47–49] Samarium diiodide (SmI_2) will reduce alkyl chlorides or bromides and aryl iodides. The reaction is typically conducted in THF with hexamethylphosphoramide (HMPA) as an additive. Under typical conditions, a primary alkyl radical is reduced by SmI_2 to an alkylsamarium reagent with a rate constant of about $7 \times 10^6 \, M^{-1} \, s^{-1}$.[50] Thus, if the average SmI_2 concentration in a reaction is about $0.1 \, M$, a radical reaction occurring with a first-order or pseudo-first-order rate constant greater than $1 \times 10^6 \, s^{-1}$ would compete effectively with the second reduction step. In practice, such fast radical reactions are possible for an intramolecular process where the alkyl radical adds to an electron-deficient group such as an acrylate as shown in example **A** in Fig. 2.19. The adduct α-ester radical will be reduced rapidly to a samarium enolate, and this relatively stable intermediate can be functionalized by an electrophile adding to the synthetic potential of the reaction. In example **B** in Fig. 2.19, the aryl radical cyclization is exceptionally fast, and this sequence could be obtained with even stronger reducing agents than SmI_2 because the second reduction step must be at least diffusion-limited irrespective of the oxidation potential of the reducing agent. Pinacol couplings and ketyl addition reactions (example **C** in Fig. 2.19) are also possible with SmI_2.
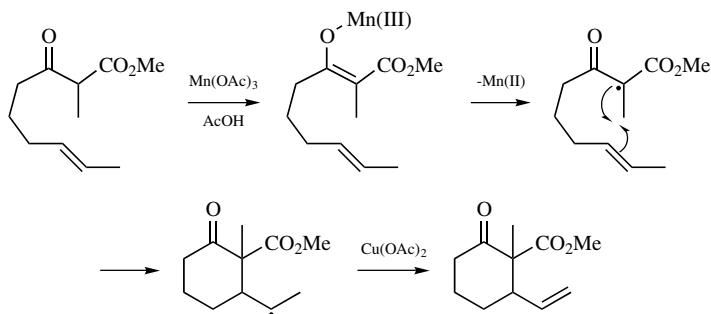
Figure 2.20   A manganese(III)-mediated radical cyclization reaction sequence.

A popular oxidative radical sequence involves manganese(III) oxidations of organic acid or, more commonly, β-keto esters; the reaction sequence for a keto ester is shown in Fig. 2.20.[51] Reaction of $Mn(OAc)_3$ with the keto ester gives a manganese enolate that is oxidized to the radical by loss of Mn(II), and the stabilized radical cyclizes to give an alkyl radical product. The cyclization reaction shown is probably reversible, but the alkyl radical is selectively trapped. Mn(III) will not oxidize a primary or secondary alkyl radical, but the reaction is typically conducted with $Cu(OAc)_2$ present, and Cu(II) oxidizes the alkyl radical to the alkene product. Other oxidizing agents that have been used in similar reaction sequences include Co(III), Fe(III), Ce(IV), Cu(II), Ag(I), Ti(IV), and V(V).

2.6   RADICAL KINETICS

2.6.1   Radical Kinetics and Chain Reactions

In order to employ radical chain reactions successfully in synthesis, one needs some information concerning the kinetics of radical reactions. In many cases, a desired reaction will compete with an unwanted one, and the yields of products can be affected by controlling the velocities of the various steps. In the case of bimolecular processes, this involves controlling the concentrations of reagents. For example, consider the reactions involved if one wished to produce the nitrile target product shown in Fig. 2.21 using the tin hydride protocol. The desired reaction sequence involves formation of the alkyl radical from an alkyl halide, addition of the alkyl radical to α-methylacrylonitrile, and tin hydride trapping of the adduct radical. Undesired reactions include reduction of the initial alkyl radical by Bu_3SnH and reaction of the adduct radical with another molecule of the acrylonitrile in a telomerization or polymerization reaction. Other undesired reactions exist, such as addition of the stannyl radical to the acrylonitrile, but those would not necessarily result in reduced yields of the desired product. Approximate second-order rate constants for each reaction at 25°C are shown in the Fig. 2.21. A high concentration of the
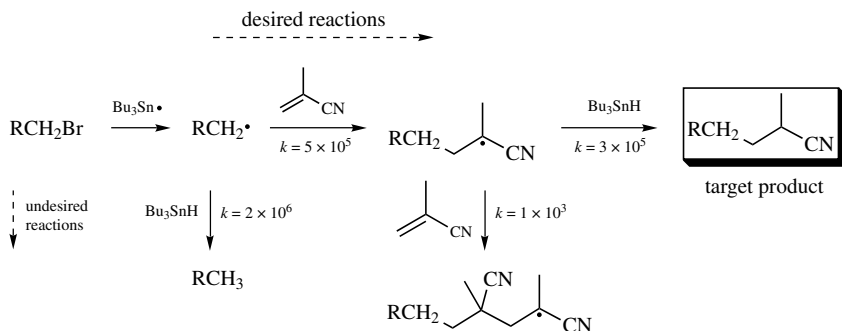
desired reactions

RCH$_2$Br $\xrightarrow{\text{Bu}_3\text{Sn}\bullet}$ RCH$_2$• $\xrightarrow[k = 5 \times 10^5]{\text{CN}}$ RCH$_2$ $\overset{\bullet}{\diagup}$ CN $\xrightarrow[k = 3 \times 10^5]{\text{Bu}_3\text{SnH}}$ RCH$_2$ $\diagup$ CN

target product

undesired reactions

$\xrightarrow[\text{Bu}_3\text{SnH}]{} \Big\downarrow k = 2 \times 10^6$

RCH$_3$

$\Big\downarrow k = 1 \times 10^3$ (CN)

RCH$_2$ $\overset{\text{CN}}{\diagup}$ $\overset{\bullet}{\diagup}$ CN

Figure 2.21 Competing reactions in a radical chain reaction.

acrylonitrile relative to that of the Bu$_3$SnH is desired so that reduction of the initial radical is prevented. However, if the concentration of acrylonitrile is too high, the telomerization reaction could become a major side reaction. In practice, maintaining a Bu$_3$SnH concentration that is only 3% that of the acrylonitrile (possibly by employing the tin hydride in catalytic amounts with regeneration from a sacrificial metal hydride) will give high yields of the desired product.

The preceding example represents one of the more difficult synthetic radical chain reactions that would be attempted synthetically because all competing processes are second-order. If the radical functionalization sequence contained a unimolecular process (such as a 5-*exo* cyclization), control of the reaction would be much easier because the reactant that gives the radical that undergoes the unimolecular radical reaction can be used in very low concentrations such that competing second-order trapping reactions are essentially eliminated.

2.6.2 What Is Fast and What Is Slow in Radical Reactions

Simple radicals react with one another with effectively no activation energy; that is, self- and cross-coupling reactions usually occur in diffusion-controlled processes. These background processes set a practical limit for the rates of desired radical reactions and suggest why an increased understanding of radical kinetics paralleled the growth of radical-based methods in synthetic applications.

In general, one can assume that radical reactions must have first-order or pseudo-first-order rate constants greater than $1 \times 10^3 \text{ s}^{-1}$ at room temperature to give high yields of a desired product. If a radical reacts less rapidly than this, undesired reactions with the solvent will become important, and radical–radical reactions will start to dominate at radical concentrations as low as $1 \times 10^{-7} \text{ M}$. In principle, one could employ radical reactions that are slower by using highly unreactive solvents and adding an initiator slowly to maintain low radical concentrations, but the reaction time would become painfully long (see Section 2.6.6 on the kinetics of radical chain processes).

2.6.3   Kinetic Methods

Rate constants for radical reactions have been determined by both direct and indirect methods. Early direct kinetic studies involved photochemical radical generation under continuous irradiation conditions, usually with ESR detection. This method requires a relatively high concentration of radicals that is achieved by studying reactions at low temperatures. The result was that many of the early kinetic determinations were at temperatures far from those that were used in applications, and the rate constants extrapolated to ambient or high temperatures contained large errors. The introduction of lasers permitted fast generation of relatively high radical concentrations (10^{-5}–10^{-4} M) at ambient temperatures, and many of the more recently measured rate constants were obtained by laser flash photolysis (LFP) methods, most commonly with UV–visible detection.

An alternative approach to measuring radical kinetics directly is to determine rate constants indirectly in competition kinetic studies. In this method, the reaction that is being calibrated competes with another reaction with a known rate constant. The experimental design is shown in Fig. 2.22. In this example, the 5-hexenyl radical (**1**) can cyclize to give the cyclopentylmethyl radical (**2**) or react with agent X–Y to give acyclic product **3**. Radical **2** also can react with agent X–Y to give the cyclic product **4**. After the reaction is complete, the yields of products **3** and **4** are determined by a conventional method such as gas or liquid chromatography or NMR spectroscopy, and the unknown rate constant (k_{XY}) is calculated from the product ratio, the concentration of agent X–Y and the known rate constant k_{cycl} by the expression in the figure. In the simplest case, with irreversible reactions and a large excess concentration of agent X–Y such that pseudo-first-order reaction conditions are maintained, the unknown rate constant can be determined with acceptable precision from a single experiment. More complicated situations, with reversible reactions and reactants that are not employed in large excess, can be studied, but multiple reactions with varying concentrations of reactants are necessary when a reaction is reversible.[19]

Because common instrumentation can be used for determining product ratios, as opposed to sophisticated laser kinetic units, the indirect kinetic method has been
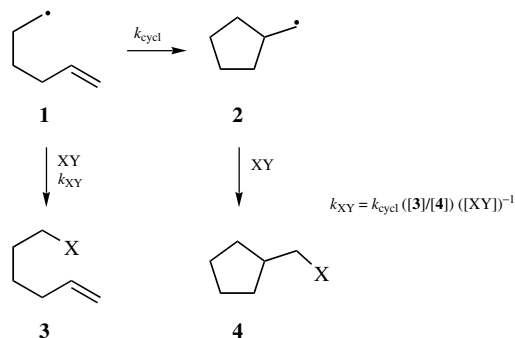

$$k_{XY} = k_{cycl} \, ([\mathbf{3}]/[\mathbf{4}]) \, ([XY])^{-1}$$

Figure 2.22   A radical clock study using the 5-hexenyl radical cyclization.

quite popular. Most of these studies are conducted in a manner similar to a synthetic sequence in that they are radical chain reactions. Rate constants for reactions of tin hydride (Bu_3SnH) and other group 14 hydrides with many types of radicals are available,[14] and it is convenient to use radical reactions with these common H-atom transfer agents as the ''basis'' reactions in the kinetic study. The major operational differences between experiments designed for indirect kinetic studies and synthetic conversions are that a large excess of the radical trapping agent usually is used in the kinetic studies to maintain pseudo-first-order kinetic conditions and the trapping agent cannot be added slowly over the course of an indirect kinetic study because the concentration of trapping agent will not be known.

One common indirect kinetic method employs a calibrated unimolecular radical reaction as the basis reaction. Such unimolecular reactions have been termed ''radical clocks.''[52,53] The example in Fig. 2.22 illustrates a typical radical clock study. The major advantages in using a radical clock is that one only needs to control the concentration of one reagent, and pseudo-first-order versus first-order reaction conditions are easy to achieve. A minor drawback is that the velocity of the unimolecular process cannot be controlled by adjusting a concentration; thus, any particular clock can be used only in a relatively limited kinetic range. For that reason, one prefers to have a large number of radical clock choices. A large repertoire of clocks is available for alkyl radicals,[19] but clocks for other types of radicals are more limited. Some representative radical clock reactions are shown in Fig. 2.23.[37,38,54–62]

Absolute rate constants have an aesthetic appeal, but relative rate constants often are just as useful. In fact, the early evolution of radical methods in fine chemical synthesis was based largely on precise relative rate constants that were determined in simple competition reactions. Subsequent refinements of the absolute kinetics of important basis reactions, such as the rate constants for reactions of Bu_3SnH with alkyl radicals,[55] have greatly improved the accuracy of radical kinetics since the early 1980s, but the precisions of relative alkyl radical rate constants generally have not improved since the fundamental works in the 1960s and 1970s.

2.6.4 Kinetics of Elementary Radical Reactions

2.6.4.1 Substitution and Atom or Group Transfer Reactions
Substitution or group transfer reactions are involved in the initial production of the reactant radical and in the ''trapping'' of the final product radical. These reactions can occur by one-step displacement processes or by addition followed by fragmentation; the difference is whether an adduct with a finite lifetime is produced. Hydrogen atom transfer reactions are examples of displacement reactions, and allyl group transfers are examples of additions that give intermediates. Simple halogen atom and chalcogen group transfers might involve formation of adducts when the atoms or groups are large, such as with iodine or phenyltelluryl, but this is not firmly established. Large leaving group rate effects in substitutions at selenium atoms suggest that the reactions do not involve intermediates.[63] The existence of an
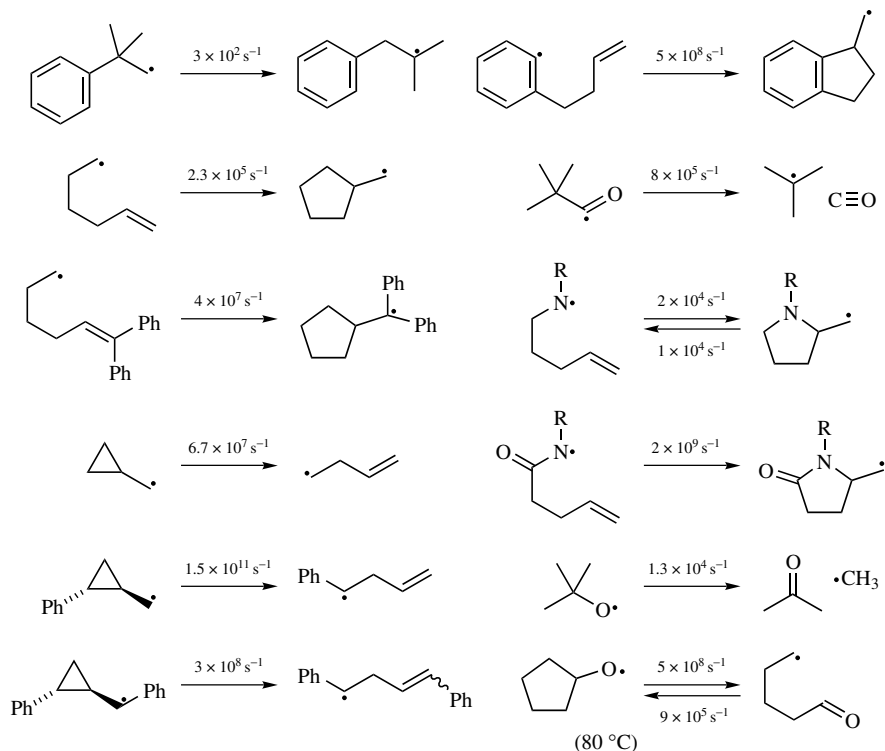
Figure 2.23 Representative radical clocks. Rate constants are for reactions at 20°C unless noted.

intermediate adduct radical is seldom of consequence in a synthetic reaction because the lifetimes of the putative intermediates would be very short.

Hydrogen atom transfer reactions are the most important in this group because so many radical sequences are completed with these reactions. The most commonly employed agents are group 14 hydrides (stannanes, germanes, silanes) and group 16 hydrides (thiols, selenols), but other H-atom donors (hydrocarbons, phosphines) have been used. The selection of the appropriate hydrogen transfer agent for a synthetic sequence is dictated mainly by the kinetics of H-atom transfer agent and the properties of the product radical with respect to the chain reaction employed. The group 14 hydrides Bu_3SnH, Et_3SiH, and $(Me_3Si)_3SiH$ have been most widely used as H-atom donors when the radical precursor is an alkyl halide because the stannyl and silyl radicals readily abstract halogen atoms. The group 16 hydrides t-BuSH, PhSH, and PhSeH have been employed frequently when halogen atom abstractions are not necessary in the radical chain sequence (as in the case of PTOC esters) or in mixtures with a group 14 hydride where the H-atom transfer is accomplished by the group 16 hydride and the thiyl or selenyl radical then reacts with the group 14 hydride.[64,65]

TABLE 2.2 Rate Constants for Reactions of H-Atom Donors with Various Radicals at 20°C in Units of $M^{-1} s^{-1}$ [a]

H-Atom Donor	$RO^{\bullet}$	$RC(O)N(R)^{\bullet}$	$Ph^{\bullet}$	$R_fCF_2^{\bullet}$	$RCH_2^{\bullet}$	$RC(O)^{\bullet}$	$R_2N^{\bullet}$
Et_3SiH	5×10^6	—	—	5×10^5	3×10^2	—	3
$(Me_3Si)_3SiH$	1.1×10^8	—	3×10^8	5×10^7	4×10^5	2×10^4	30
Bu_3SnH	2×10^8	1.3×10^9	8×10^8	2×10^8	2.5×10^6	4×10^5	4×10^5
t-BuSH	—	—	—	—	6×10^6	—	6×10^6
PhSH	—	9×10^7	—	—	9×10^7	—	1.1×10^8
PhSeH	—	—	—	—	1.2×10^9	(5×10^9)	2×10^9

[a] Group 14 hydride values from Ref. 14. Aminyl radical values from Ref. 37. Amidyl radical values from Ref. 38. Alkyl radical values with group 16 hydrides from Ref. 56. Acyl radical value with PhSeH estimated from data in Ref. 66.

Table 2.2 lists some typical kinetic values for reactions of representative radicals with common H-atom transfer agents.[14,37,38,56,66] An extensive tabulation of rate constants for reactions of group 14 hydrides with radicals has been published and should be consulted for a more detailed listing of kinetic values for this class of donors.[14] It is interesting to note the apparent "polar" contributions to rate constants. The radicals on the left side of Table 2.2 are electron-deficient or "electrophilic," whereas the carbon- and nitrogen-centered radicals on the right side are electron-rich or "nucleophilic." The H-atom donors are listed in order of increasing electronegativity of the H-atom donor from the top to the bottom, and the H atoms in this series are increasingly electron-deficient and acidic as one proceeds down the table. The "electrophilic" radicals react rapidly with the electron-rich H atom of group 14 hydrides, and "nucleophilic" radicals react rapidly with the electron-deficient H atom of group 16 hydrides.

Other synthetically important substitution reactions of carbon-centered radicals are halogen atom transfer reactions and chalcogen group transfer reactions. These reactions are involved in atom or group transfer chain reactions that give products with functionality at the former radical center (see Fig. 2.14). Table 2.3 contains rate

TABLE 2.3 Rate Constants at 50°C for Reactions of Primary Alkyl Radicals with Halides and Chalcogens in Units of $M^{-1} s^{-1}$ [a]

Compound	Cl	Br	I	SMe	SPh	SePh	TePh
RCH_2X	—	6×10^2	2×10^5	—	—	—	—
R_2CHX	—	1×10^3	5×10^5	—	—	—	—
R_3CX	6×10^2	4.6×10^3	3×10^6	—	—	—	—
EtO_2CCH_2X	—	7×10^4	3×10^7	—	—	1×10^5	2.3×10^7
$NCCH_2X$	—	—	2×10^9	—	—	2×10^5	—
$(EtO_2C)_2C(Me)X$	—	1.0×10^6	2×10^9	—	—	8×10^5	—
$(NC)_2C(Me)X$	—	—	—	$8 \times 10^{4 b}$	5×10^5	8×10^6	—
$X-X^b$	—	—	—	6×10^4	2×10^5	2.6×10^7	1.1×10^8

[a] Rate constants at 50°C unless noted otherwise. Values from Refs. 19, 63, 67, and 68.
[b] Rate constants at 25°C.

constants for halogen atom and chalcogen group transfers to primary alkyl radicals.[63,67,68] Reactivity increases down a column of the periodic table, and it is interesting to note that PhSe and PhTe group transfers are similar in rates to bromine and iodine atom transfers, respectively. These rate constants display a high degree of sensitivity to the stability of the radical leaving group.

Many radical chain reaction sequences employ alkyl halides and pseudohalides as the radical precursors. Halogen atom and chalcogen group transfer reactions of these precursors with propagating radicals from the group 14 metal hydrides must be fast enough to support the chain reactions, and one usually prefers that they are very fast. The tributylstannyl radical ($Bu_3Sn^\bullet$) reacts rapidly with alkyl iodides and alkyl bromides ($k > 1 \times 10^7\,M^{-1}\,s^{-1}$ at room temperature), but reactions with alkyl chlorides are sluggish ($k = 7 \times 10^3\,M^{-1}\,s^{-1}$ for a 1° alkyl chloride at room temperature).[69] The tributylgermyl radical ($Bu_3Ge^\bullet$) reacts slightly faster than the stannyl radical with these halides, and the triethylsilyl radical ($Et_3Si^\bullet$) reacts about an order of magnitude faster.[69] Rate constants for reactions of $Et_3Si^\bullet$ with aryl chlorides, bromides, and iodides are similar to those of the corresponding alkyl halides, and PhBr and PhI can be used in chain reactions with $Bu_3Sn^\bullet$. The *tris*-(trimethylsilyl)silyl radical reacts with alkyl halides with rate constants similar to those of $Bu_3Sn^\bullet$.[70] As a general rule of thumb, alkyl phenyl sulfides (RSPh) and alkyl phenyl selenides (RSePh) react with the group 14 trialkylmetal radicals with rate constants similar to those for RCl and RBr, respectively.[71]

Additions of alkyl radicals to the sulfur atom in thiones occurs with xanthate esters and other thione derivatives such as Barton's PTOC esters, and these reactions can be considered thio group transfers. The reactions are efficient, but few kinetic values are available. Primary alkyl radicals add to the thione group in a Barton PTOC ester with rate constants of about $1 \times 10^6\,M^{-1}\,s^{-1}$.[72]

2.6.4.2   *Radical Additions to Alkenes*

The facile formation of carbon–carbon bonds, especially in cyclizations, via radical reactions was the impetus for synthetic chemists to embrace radical chemistry as a conventional methodology in the 1970s and 1980s. In radical addition reactions, fine chemical synthesis requires that the adduct radical be successfully trapped in competition with oligomerization reactions. This is easy to accomplish in unimolecular cyclizations reactions by controlling concentrations of radical precursors. Bimolecular addition reactions are more problematical, but one generally can take advantage of the polar character of the radicals involved. That is, addition of a "nucleophilic" radical to an electron-deficient alkene, such as an acrylate ester, gives an α-ester radical product that is electron-deficient. The initial addition reaction is accelerated by polar effects, whereas addition of the product radical to a second molecule of the electron-deficient alkene will be retarded. Thus, although the kinetics of radical addition reactions can be understood mainly in terms of the thermodynamics of the overall reaction, rate enhancements due to polarized transition states exist when there is an appropriate polarity match between radical and the alkene. For example, a nucleophilic alkyl radical adds to an acrylate more rapidly than one might expect from the thermodynamics of the reaction because the favorable polarity match in the

TABLE 2.4   Second-Order Rate Constants in Units of $M^{-1}\,s^{-1}$ for Radical Addition Reactions to Substituted Alkenes at $\sim 24°C^{a}$

Alkene	$(Me)_2(OH)C^{\bullet}$	$H_3C^{\bullet}$	$NC{-}H_2C^{\bullet}$	$t\text{-}BuOC(O)H_2C^{\bullet}$
$CH_2{=}CHR$	1.1×10^3	4×10^3	1.1×10^4	5.4×10^4
$CH_2{=}CHOAc$	7.5×10^3	1.4×10^4	1.3×10^4	6.5×10^4
$CH_2{=}CHOEt$	3.2×10^2	1.4×10^4	4.3×10^4	1.5×10^5
$CH_2{=}CHCl$	—	2×10^4	1.2×10^4	7.1×10^4
$CH_2{=}CHCN$	$>1 \times 10^8$	6×10^5	1.1×10^5	5.4×10^5
$CH_2{=}CHCO_2Me$	$>1 \times 10^7$	5×10^5	1.1×10^5	4.9×10^5
$CH_2{=}CHCHO$	—	7×10^5	2.4×10^4	3.8×10^5
$CH_2{=}CHPh$	2.2×10^6	2.6×10^5	3.8×10^5	1.9×10^6

^{a} Values for 1-hydroxy-1-methylethyl radical from Ref. 73. Values for methyl radical from Ref. 74. Values for cyanomethyl radical and (*tert*-butyloxycarbonyl)methyl radical from Ref. 75.

transition state indicated by resonance contributor C below. Table 2.4 contains kinetic data that illustrates this effect for addition reactions of the nucleophilic isopropyl and methyl radicals and the electrophilic acetonitrile and *tert*-butyl acetate radials.[73–75]
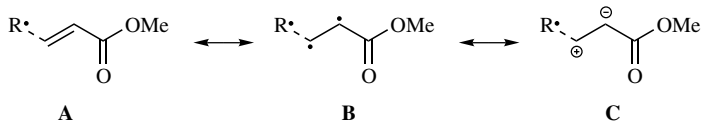
2.6.4.3   *Radical Additions to Other Unsaturated Centers*   Table 2.5 lists relative rate constants for additions of an alkyl radical to various unsaturated centers using an unsubstituted alkene as the reference point.[12,62,76–79] The controlling influence is clearly the thermodynamics of the reactions. Additions to alkynes and nitriles give relatively high energy adducts, and addition to an aldehyde gives an alkoxyl radical product. Dialkylaminyl radicals formed by addition to imines are relatively stable as

TABLE 2.5   Relative Rate Constants at 20°C for Alkyl Radical Additions to Unsaturated Compounds

Compound	Relative Rate Constant	Ref. ^{a}
$RCH{=}CH_2$	1.0	—
$R{-}C{\equiv}CH$	0.075	76
$RC{\equiv}N$	0.025	76
$RCH{=}O$	0.56	62
$RCH{=}NR$	3.75	77
$C{\equiv}O$	18	12
$RCH{=}NOMe$	24	78
$RCH{=}NNR_2$	39	78
Allyltrimethyltin	40	79

^{a} Reference for original kinetic data.

judged by the slow reactions of these radicals with H-atom donors, and the adducts from radical additions to oximes and hydrazones are further stabilized by the substituents on the nitrogen radical center.

The rate constant for alkyl radical addition to allyltrimethyltin is quite interesting. Addition of an alkyl radical to this compound gives an intermediate that expels the trimethylstannyl radical, and the overall conversion accomplishes allylation of the radical center. This sequence would not be possible if the addition reaction were not considerably faster than radical addition to an alkene. The enhanced reactivity apparently reflects a polar effect of the stannyl group, producing a more electrophilic alkene that is polarity-matched with the nucleophilic alkyl radical.

2.6.4.4 Radical Cyclizations   Radical cyclizations contain an additional element that affects the kinetics profoundly, the size of the ring being formed. In principle, cyclizations can occur in an exo or endo fashion, but only exo cyclizations are observed for small rings due to geometric constraints of these systems. In the case of unsubstituted systems, the endo cyclization product, a secondary radical, is thermodynamically favored over the exo cyclization product, a primary radical, and the amount of endo product increases as the ring size increases. Figure 2.24 lists rate constants for cyclizations of simple radicals at room temperature that show both
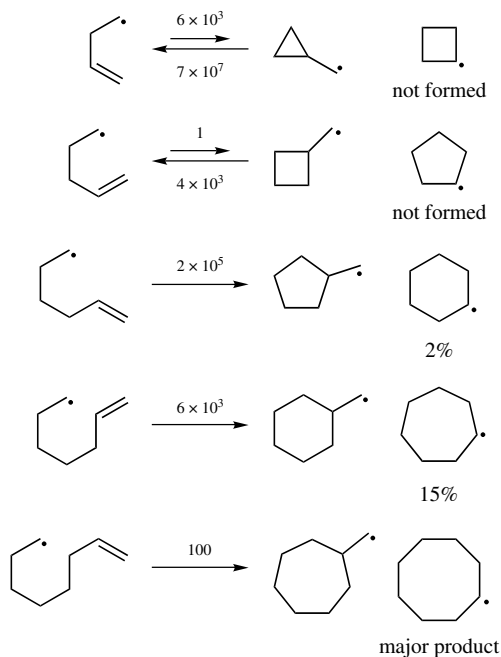
Figure 2.24   Ring size effects in alkenyl radical cyclizations. Rate constants at room temperature are listed. Data from Refs. 57, 69, 80, and 81 have been adjusted by the author for the now accepted rate constant for reaction of Bu$_3$SnH with alkyl radicals.

TABLE 2.6   Rate Constants at 20°C for 5-*exo* Cyclizations of 6-Substituted 5-Hexenyl Radicals

6-Substitutents	Rate Constant (s^{-1})	Ref.[a]
H, H	2×10^5	55
H, Me	2×10^5	82
Me, Me	5×10^5	82
H, OMe	1.4×10^6	83
H, Ph	2×10^7	56
Ph, Ph	4×10^7	56
H, CN	1.6×10^8	83
CN, OMe	2.5×10^8	83
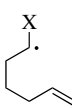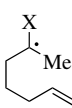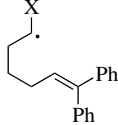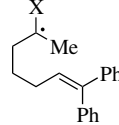
[a] Reference for kinetic data.

the ring strain and steric constraint effects.[57,69,80,81] Note that the cyclizations of the 3-butenyl and 4-pentenyl radicals are thermodynamically unfavorable; that is, the cyclopropylcarbinyl and cyclobutylcarbinyl radicals ring-open to give these radicals.

Cyclizations of 5-hexenyl radicals to give 5-membered ring products are commonly employed in synthesis and have been extensively studied. The rate constants for these cyclization reactions can be used to evaluate the effects of substituents on the cyclization reactions. In the case of substitution on position C6 of a 5-hexenyl radical, the rate constants for cyclization follow patterns similar to that seen in additions to alkenes (Table 2.6).[55,56,82,83] These reactions are primarily enthalpy-controlled, but a polar transition state effect is apparent in cyclizations of the cyano-substituted systems.

The rate constants for cyclizations of 1-substituted 5-hexenyl radicals show kinetic effects of substitution at the radical center that might at first seem counter-intuitive (Table 2.7).[56,80,84–87] In the case of cyclizations of secondary radicals, the rate constants are nearly invariant although the stability of the reacting radical center is increased by substituents as evaluated by BDE values. This demonstrates that

TABLE 2.7   Rate Constants in Units of s^{-1} for Cyclizations of 1-Substituted 5-Hexenyl Radicals at Room Temperature[a]

X	(H)	(Me)	(Ph, Ph)	(Me, Ph, Ph)
H	2×10^5	1×10^5	4×10^7	2×10^7
CH$_3$	1×10^5	1×10^5	2×10^7	1×10^7
OCH$_3$	2×10^5	—	4×10^7	6×10^7
CO$_2$Et	2×10^5	1×10^4	5×10^7	3×10^5
C(O)NEt$_2$	1×10^5	—	2×10^7	1×10^4
CN	—	—	—	2×10^5

[a] Kinetic data from Refs. 56, 80, and 84–87.

electronic effects on the cyclizations are minimal. For tertiary systems, however, substitution with a conjugative electron-withdrawing group results in dramatic kinetic reductions, and this applies even for the very "small" cyano group. These kinetic reductions in cyclizations of the substituted tertiary radicals have been ascribed to steric effects, apparently involving the forced planarity of the radical center.

2.6.4.5   Radical Fragmentations and Ring Openings   Homolytic fragmentations and ring-opening reactions of radicals are the reverse of additions and cyclizations. Fragmentations of radicals are often coupled with addition reactions and result in group transfer sequences (see text below). Cleavage of C—C bonds is not common for carbon-centered radicals except for ring opening reactions of strained cyclopropylcarbinyl and cyclobutylcarbinyl radicals, but they occur in reactions of highly reactive oxygen-centered radicals. These ring-opening reactions demonstrate the same types of enthalpic, polar, and steric effects seen in radical addition and cyclization reactions. For example, the substitution of a radical stabilizing group at C2 of a cyclopropylcarbinyl or cyclobutylcarbinyl radical results in accelerated ring-opening reactions as shown in Table 2.8 for the cyclopropylcarbinyl radical.[56–59,88–93] Substitution at the radical center by simple radical-stabilizing groups (Me, OMe) has a small retarding effect, and substitution at the radical center by an ethoxycarbonyl group results in acceleration of the ring opening because the transition state is polarized. A phenyl group at the radical center slows the ring-opening reaction due to enthalpic effects and shifts the equilibrium in favor of the cyclic product. Phenyl groups at both the radical center and C2 effectively cancel one another's effect as expected.

TABLE 2.8   Kinetic Effects of Substituents on Cyclopropylcarbinyl Radicals[a]

Y	X	k_{open}	k_{cycle}	Ref.[b]
H	H	7×10^7	6×10^3	56,57
H	Me	1×10^8	—	89
H	OMe	$\sim 1 \times 10^9$	—	88,92
H	CO$_2$Me	7×10^{10}	—	90
H	Ph	1.5×10^{11}	—	58
Me	H	4×10^7	—	89,93
OMe	H	$\sim 2 \times 10^7$	—	88
CO$_2$Et	H	2×10^8	—	91
Ph	H	6×10^4	5×10^6	57
Ph	Ph	3×10^8	—	59

[a] Rate constants in units of s^{-1} at 20°C.
[b] Reference for kinetic data.
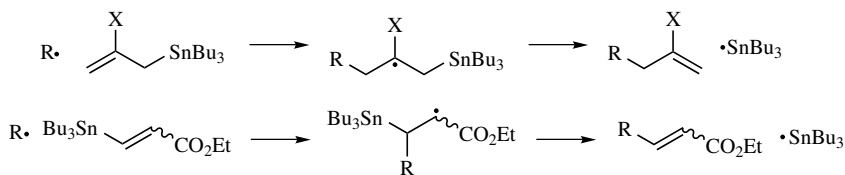
Figure 2.25   Allylation and vinylation of alkyl radicals.

2.6.4.6   *Group Transfers and Group Migrations Involving Addition–Elimination Reactions with π Bonds*

Radical additions to unsaturated groups can be followed by elimination reactions to give group transfer reactions (bimolecular processes) or group migration reactions (unimolecular processes). Unlike atom and group transfer reactions at saturated atoms that likely occur in concerted processes, these reactions give intermediate radicals. Synthetically useful addition–elimination reactions include allylations and vinylation reactions such as shown in Fig. 2.25.[94–96] Addition of an alkyl radical to an allylstannane gives the intermediate adduct that eliminates the relatively stable stannyl radical. A large number of X groups at C2 of allylstannanes have been used. The reaction also works well when the leaving group is a trialkylsilyl or alkyl- or arylthiyl. The allylation reaction has been more widely applied than the vinylation reaction that is effectively limited to substituted acrylates (as shown in Fig. 2.25) or styrenes.

When the leaving group in an allylation reactions is a stannyl or silyl radical, a chain reaction can be propagated with alkyl halides and pseudohalides just as in the case when the group 14 hydrides are used in chain reactions. Thus, in principle, allylations and vinylations can be substituted for radical reduction steps, but the rate of the initial addition reaction can be a limiting feature of this chemistry. Few rate constants for these addition reactions have been determined, but addition of an alkyl radical to allyltrimethylstannane was found to have a rate constant of about $3 \times 10^5 \, \mathrm{M^{-1} \, s^{-1}}$ at 50°C with is about 40 times faster than an alkyl radical adds to a terminal alkene.[79]

Intramolecular versions of the addition–elimination reaction result in group migrations. For example, the series of radicals shown in Fig. 2.26 rearrange by addition of the primary radical to the unsaturated group to give a 3-membered ring followed by ring opening to give the tertiary radical. Relative rates for the overall migrations are listed in the figure.[97] Note that migration of a phenyl group in the neophyl radical rearrangement involves formation of the spiro intermediate. The addition–elimination sequence in cyclic ketones is a convenient method for ring expansions as shown in Fig. 2.18 for a 1-carbon atom expansion; ring expansions for 2-carbon atoms and 4-carbon atoms also are known.[98]

2.6.5   Kinetics of Termination Reactions

Radical termination processes are involved in any composite radical reaction. Radical–radical reactions generally have very low activation energies, and most of

X=Y, rate (s^{-1}); CH=CH$_2$, 1E7; C(Bu^t)=O, 1.7E5; Ph, 760; C≡CMe$_3$; 93; C≡N, 0.9

neophyl rearrangement

ring expansion
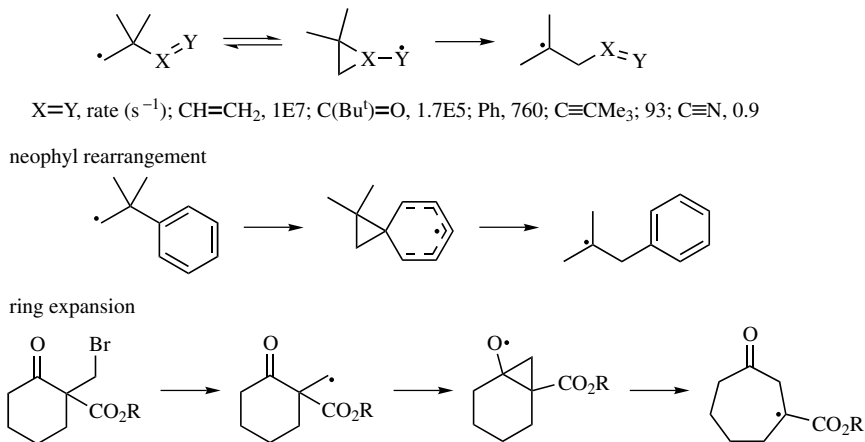
Figure 2.26   Examples of group migration reactions.

these termination processes (couplings and disproportionations) occur with diffusion-limited rate constants. When self-termination of a particular radical is slow, selective cross-coupling reactions can occur as described in Section 2.5.1.

The rates of diffusional processes are affected by the viscosity of the solvent and the size of the particular species. Generally, one can approximate diffusional rate constants for a particular solvent from self-diffusion rate constants (i.e., rate constants for diffusion of the molecules of the solvent), several of which are available. Diffusional rate constants for a specific radical R$^•$ would be more accurately estimated by determining the rate constants for its parent (R—H)[99] in the solvent of choice using sample broadening in a flowing stream or line broadening in a pulse gradient NMR experiment.[100,101] The latter can now be achieved readily on modern NMR instruments that include gradient methods.

It is noteworthy that the rate constants for reactions of organic radicals with one another will be smaller than the rate constants for diffusion-limited collision of the radicals. Two radicals with spin $\frac{1}{2}$ in a radical pair will have either a singlet or a triplet alignment of spins. The triplet radical pair will not couple because that would form an electronically excited product. As long as intersystems crossing (involving a spin flip) is slow relative to the diffusion processes, a triplet radical pair can only diffuse apart. Because the probability of formation of a singlet radical pair is one in four combinations (one singlet and three triplet states), the radical–radical termination reactions will have rate constants that are 25% of the diffusional rate constants.

The abovementioned phenomenon, known as "spin statistical selection,"[102] has some interesting ramifications. For example, if a highly exothermic radical–molecule reaction is diffusion controlled, then that radical–molecule reaction would be 4 times faster than radical–radical reactions. In addition, if one of the radicals in the radical pair is "organic" and the other "metallic," then the large difference in gyromagnetic ratios could result in "fast" intersystems crossing that, if it were faster

than diffusion, would permit selective radical cross-termination reactions without a persistent radical effect.

2.6.6 Overall Kinetics of Chain Reaction Processes

With an understanding of the kinetics of the elementary radical reactions, one can determine the velocity of the chain reaction sequence. The key simplifications that are involved are the following: (1) because each propagation step in the chain sequence gives a product radical that is the reactant radical in another propagation step, the *velocities* of all propagation steps must be equal; and (2) during the course of the chain reaction, the radicals reach steady-state concentrations, and the velocity of the initiation sequence is equal to the velocity of the termination sequence. These equalities in velocities permit the application of steady-state kinetic assumptions that eventually yield the rate law for the overall process in terms of a few key rate constants for elementary reactions.

The analysis is readily explained in the context of a simple example. Consider the tin hydride reduction of an alkyl bromide. The elementary reactions are those shown in Fig. 2.8 with the exception that no radical functionalization steps are involved. That is, the propagation sequence involves only bromine atom abstraction from RBr by the $Bu_3Sn^\bullet$ radical and H-atom abstraction from Bu_3SnH by the $R^\bullet$ radical. The rate constant for bromine atom abstraction by the tin radical is about 100 times greater than that for H-atom abstraction from the tin hydride. If the initial concentrations of RBr and Bu_3SnH are equal, it follows that during the reaction the concentration of $R^\bullet$ must be 100 times greater than the concentration of $Bu_3Sn^\bullet$ to attain equal velocities for the two propagation steps. The slower reaction in the propagation sequence is known as the ''rate-controlling step'' because the rate constant for this reaction (but not the rate constants for faster steps) appears in the rate law. Furthermore, because the $R^\bullet$ concentration is so much greater than the $Bu_3Sn^\bullet$ concentration, the only important termination reaction for this sequence is the bimolecular reaction of $R^\bullet$.

The rate of the chain process is solved starting from the simple rate law for formation of product R—H in the rate-controlling step of the chain sequence [Eq. (2.2)], where k_H is the rate constant for reaction of the alkyl radical with tin hydride. A series of steady-state approximations for $[R^\bullet]$ eventually leads to an equality for this concentration that contains the rate constant for the initiation reaction (k_{init}) and the rate constant for the termination reaction (k_{term}); the latter is usually diffusion-controlled. Substitution of that equality into the simple rate expression of Eq. (2.2) gives Eq. (2.3), where [Init] is the concentration of the initiator and f is the fraction of radicals that successfully escape the radical pair formed in the initial homolysis reaction of the initiator.

$$\frac{d[RH]}{dt} = k_H[R^\bullet][Bu_3SnH] \tag{2.2}$$

$$\frac{d[RH]}{dt} = \frac{k_{init}\,f\,[Init]^{1/2}\,k_H[Bu_3SnH]}{(2k_{term})^{1/2}} \tag{2.3}$$

For the specific example of the tin hydride reduction of an alkyl bromide in refluxing benzene, one might have the following conditions: initial concentration of Bu_3SnH and $RBr = 0.2$ M, concentration of $AIBN = 0.005$ M, and $f = 0.5$. The rate constants at $80°C$ are the following: $k_{init} = 2 \times 10^{-4}$ s^{-1}, $k_H = 6.4 \times 10^6$ M^{-1} s^{-1}, and $k_{term} = 1 \times 10^{10}$ s^{-1}. In this case, the velocity of the chain reaction is about 3×10^{-4} M/s. Thus, the reduction reaction would be complete in about 15 minutes. If the slower reacting $(Me_3Si)_3SiH$ ($k_H = 1.3 \times 10^6$ $M^{-1}s^{-1}$ at $80°C$) were substituted for tin hydride, the reduction reaction would take somewhat more than 1 h.

Rate laws for other radical chain reactions are similar to that for the tin hydride reduction discussed above. The characteristic features are that the initiator concentration is $\frac{1}{2}$ order, the only rate constant for an elementary process in the chain sequence that appears in the rate law is that for the ''slow'' propagation step, and the termination rate constant is typically that for a diffusion-controlled process. When the reactions are initiated photochemically instead of thermally, the rate constant for homolysis of the initiator is replaced by the photon flux, the quantum efficiency of the photochemical reaction, and the fraction of photons absorbed. Photochemical initiation with opaque solutions are difficult to treat because the radical concentration is not uniform throughout the solution.

It is noteworthy that these radical chain rate laws also apply to polymerization reactions but only up to a point. As long as the termination velocity is large (in a low-viscosity medium), the steady state approximations used in solving the rate laws apply. As the viscosity of the polymer mixture becomes high and the velocity of the termination reactions decreases; however, the steady-state approximation for radial concentrations no longer applies. With continued initiation, the velocity of the chain reaction will thus increase with an increase in viscosity. Eventually, termination reactions become so slow that they effectively cease as the solution ''gels,'' and the overall chain reaction becomes very fast. The phenomenon is known as a ''gel effect'' or ''Trommsdorf effect.''

2.7   WHAT IS NOT IN THIS OVERVIEW

This overview touches on several aspects of small radical chemistry, but much of that chemistry obviously is not included. For example, most of the discussion has focused on carbon-centered radicals to the exclusion of heteroatom-centered radicals. Chemoselectivity and regioselectivity of radicals reactions are illustrated by examples and rate constants, but stereoselectivity, an increasingly important aspect of small radical chemistry, is not discussed; a 1995 book nicely summarizes work involving control of stereoselectivity in radical reactions.[103] Radical chemistry is becoming increasingly important for organic synthetic conversions, and the interested reader is referred to a two-volume monograph that addresses the state of the art in this area.[104]

REFERENCES

1. J. Pacansky, W. Koch, and M. D. Miller, *J. Am. Chem. Soc.* **113**, 317–328 (1991).

2. T. J. Sears, P. M. Johnson, P. Jin, and S. Oatis, *J. Chem. Phys.* **104**, 781–792 (1996).

3. J. C. Walton, *J. Chem. Soc., Perkin Trans. 2*, 1809–1813 (1987).

4. M. Spichty, B. Giese, A. Matsumoto, H. Fischer, and G. Gescheidt, *Macromolecules* **34**, 723–726 (2001).

5. O. M. Musa, J. H. Horner, and M. Newcomb, *J. Org. Chem.* **64**, 1022–1025 (1999).

6. H. Ihee, A. H. Zewail, and W. A. Goddard, *J. Phys. Chem. A* **103**, 6638–6649 (1999).

7. K. U. Ingold and J. C. Walton, *Acc. Chem. Res.* **22**, 8–14 (1989).

8. L. J. Johnston and K. U. Ingold, *J. Am. Chem. Soc.* **108**, 2343–2348 (1986).

9. S. D. Rychnovsky, J. P. Powers, and T. J. Lepage, *J. Am. Chem. Soc.* **114**, 8375–8384 (1992).

10. R. W. Fessenden and R. H. Schuler, *J. Chem. Phys.* **39**, 2147–2195 (1963).

11. C. Galli, A. Guarnieri, H. Koch, P. Mencarelli, and Z. Rappoport, *J. Org. Chem.* **62**, 4072–4077 (1997).

12. H. Chatgilialoglu, D. Crich, M. Komatsu, and I. Ryu, *Chem. Rev.* **99**, 1991–2069 (1999).

13. J. Berkowitz, G. B. Ellison, and D. Gutman, *J. Phys. Chem.* **98**, 2744–2765 (1994).

14. C. Chatgilialoglu and M. Newcomb, *Adv. Organomet. Chem.* **44**, 67–112 (1999).

15. D. Griller, J. M. Kanabus-Kaminska, and A. Maccoll, *Theochem.* **40**, 125–131 (1988).

16. D. T. Leeck, R. M. Li, L. J. Chyall, and H. I. Kenttamaa, *J. Phys. Chem.* **100**, 6608–6611 (1996).

17. H. Kiefer and T. G. Traylor, *Tetrahedron Lett.*, 6163–6168 (1966).

18. C. Walling, *Tetrahedron* **41**, 3887–3900 (1985).

19. M. Newcomb, *Tetrahedron* **49**, 1151–1176 (1993).

20. P. G. Bartlett, E. P. Benzing, and R. E. Pincock, *J. Am. Chem. Soc.* **82**, 1762–1768 (1960).

21. G. D. Mendenhall, *Tetrahedron Lett.* **24**, 451–452 (1983).

22. K. Nozaki, K. Oshima, and K. Utimoto, *J. Am. Chem. Soc.* **109**, 2547–2549 (1987).

23. D. F. Eaton, *Pure Appl. Chem.* **56**, 1191–1202 (1984).

24. G. Pandey, in *Photoinduced Electron Transfer*, J. Mattay, ed., Springer-Verlag, Berlin, 1993, Vol. V, pp. 175–221.

25. L. Eberson, *Electron Transfer Reactions in Organic Chemistry*, Springer-Verlag, Berlin, 1987, Vol. 25.

26. M. Newcomb, N. Miranda, M. Sannigrahi, X. H. Huang, and D. Crich, *J. Am. Chem. Soc.* **123**, 6445–6446 (2001).

27. M. Newcomb, N. Miranda, X. H. Huang, and D. Crich, *J. Am. Chem. Soc.* **122**, 6128–6129 (2000).

28. A. J. Clark, F. De Campo, R. J. Deeth, R. P. Filik, S. Gatard, N. A. Hunt, D. Lastecoueres, G. H. Thomas, J. B. Verlhac, and H. Wongtap, *J. Chem. Soc., Perkin Trans. 1*, 671–680 (2000).

29. K. Matyjaszewski, T. E. Patten, and J. H. Xia, *J. Am. Chem. Soc.* **119**, 674–680 (1997).

30. K. Matyjaszewski, *J. Macromol. Sci. Pure Appl. Chem.* **A34**, 1785–1801 (1997).

31. H. Zipse, *Acc. Chem. Res.* **32**, 571–578 (1999).

32. C. Chatgilialoglu, *Acc. Chem. Res.* **25**, 188–194 (1992).

33. G. A. Russell and D. Guo, *Tetrahedron Lett.* **25**, 5239–5242 (1984).

34. S. Z. Zard, *Angew. Chem. Int. Ed.* **36**, 673–685 (1997).

35. D. H. R. Barton, D. Crich, and W. B. Motherwell, *Tetrahedron* **41**, 3901–3924 (1985).

36. D. Crich and L. Quintero, *Chem. Rev.* **89**, 1413–1432 (1989).

37. O. M. Musa, J. H. Horner, H. Shahin, and M. Newcomb, *J. Am. Chem. Soc.* **118**, 3862–3868 (1996).

38. J. H. Horner, O. M. Musa, A. Bouvier, and M. Newcomb, *J. Am. Chem. Soc.* **120**, 7738–7748 (1998).

39. M. H. Le Tadic-Biadatti, A. C. Callier-Dublanchet, J. H. Horner, B. Quiclet-Sire, S. Z. Zard, and M. Newcomb, *J. Org. Chem.* **62**, 559–563 (1997).

40. J. Boivin, E. Crepon, and S. Z. Zard, *Tetrahedron Lett.* **31**, 6869–6872 (1990).

41. J. Hartung, M. Schwarz, I. Svoboda, H. Fuess, and M. T. Duarte, *Eur. J. Org. Chem.*, 1275–1290 (1999).

42. M. Newcomb, M. U. Kumar, J. Boivin, E. Crepon, and S. Z. Zard, *Tetrahedron Lett.* **32**, 45–48 (1991).

43. R. A. Rossi and S. M. Palacios, *Tetrahedron* **49**, 4485–4494 (1993).

44. D. Crich, X. H. Huang, and M. Newcomb, *J. Org. Chem.* **65**, 523–529 (2000).

45. D. Griller and K. U. Ingold, *Acc. Chem. Res.* **9**, 13 (1976).

46. H. Fischer, *J. Am. Chem. Soc.* **108**, 3925–3927 (1986).

47. G. A. Molander and J. A. Mckie, *J. Org. Chem.* **58**, 7216–7227 (1993).

48. G. A. Molander and C. R. Harris, *Chem. Rev.* **96**, 307–338 (1996).

49. A. Gansauer and H. Bluhm, *Chem. Rev.* **100**, 2771–2788 (2000).

50. E. Hasegawa and D. P. Curran, *Tetrahedron Lett.* **34**, 1717–1720 (1993).

51. B. B. Snider, *Chem. Rev.* **96**, 339–363 (1996).

52. D. Griller and K. U. Ingold, *Acc. Chem. Res.* **13**, 317–323 (1980).

53. M. Newcomb, in *Radicals in Organic Synthesis*, P. Renaud and M. P. Sibi, eds., Wiley-VCH, Weinheim, 2001, Vol. 1, pp. 317–336.

54. M. Weber and H. Fischer, *J. Am. Chem. Soc.* **121**, 7381–7388 (1999).

55. C. Chatgilialoglu, K. U. Ingold, and J. C. Scaiano, *J. Am. Chem. Soc.* **103**, 7739–7742 (1981).

56. M. Newcomb, S. Y. Choi, and J. H. Horner, *J. Org. Chem.* **64**, 1225–1231 (1999).

57. T. A. Halgren, J. D. Roberts, J. H. Horner, F. N. Martinez, C. Tronche, and M. Newcomb, *J. Am. Chem. Soc.* **122**, 2988–2994 (2000).

58. M. Newcomb, C. C. Johnson, M. B. Manek, and T. R. Varick, *J. Am. Chem. Soc.* **114**, 10915–10921 (1992).

59. R. Hollis, L. Hughes, V. W. Bowry, and K. U. Ingold, *J. Org. Chem.* **57**, 4284–4287 (1992).

60. L. J. Johnston, J. Lusztyk, D. D. M. Wayner, A. N. Abeywickreyma, A. L. J. Beckwith, J. C. Scaiano, and K. U. Ingold, *J. Am. Chem. Soc.* **107**, 4594–4596 (1985).

61. Y. P. Tsentalovich and H. Fischer, *J. Chem. Soc., Perkin Trans. 2*, 729–733 (1994).

62. A. L. J. Beckwith and B. P. Hay, *J. Am. Chem. Soc.* **111**, 2674–2681 (1989).

63. D. P. Curran, A. A. Martin-Esker, S. B. Ko, and M. Newcomb, *J. Org. Chem.* **58**, 4691–4695 (1993).

64. R. P. Allen, B. P. Roberts, and C. R. Willis, *J. Chem. Soc., Chem. Commun.*, 1387–1388 (1989).

65. D. Crich and Q. W. Yao, *J. Org. Chem.* **60**, 84–88 (1995).

66. P. A. Simakov, F. N. Martinez, J. H. Horner, and M. Newcomb, *J. Org. Chem.* **63**, 1226–1232 (1998).

67. M. Newcomb, R. M. Sanchez, and J. Kaplan, *J. Am. Chem. Soc.* **109**, 1195–1199 (1987).

68. D. P. Curran, E. Bosch, J. Kaplan, and M. Newcomb, *J. Org. Chem.* **54**, 1826–1831 (1989).

69. K. U. Ingold, J. Lusztyk, and J. C. Scaiano, *J. Am. Chem. Soc.* **106**, 343–348 (1984).

70. C. Chatgilialoglu, D. Griller, and M. Lesage, *J. Org. Chem.* **54**, 2492–2494 (1989).

71. C. H. Schiesser and L. M. Wild, *Tetrahedron* **52**, 13265–13314 (1996).

72. M. Newcomb and J. Kaplan, *Tetrahedron Lett.* **28**, 1615–1618 (1987).

73. K. Heberger and H. Fischer, *Int. J. Chem. Kinet.* **25**, 913–920 (1993).

74. T. Zytowski and H. Fischer, *J. Am. Chem. Soc.* **119**, 12869–12878 (1997).

75. J. Q. Wu, I. Beranek, and H. Fischer, *Helv. Chim. Acta* **78**, 194–214 (1995).

76. D. Griller, P. Schmid, and K. U. Ingold, *Can. J. Chem.* **57**, 831–834 (1979).

77. S. Kim, K. S. Yoon, and Y. S. Kim, *Tetrahedron* **53**, 73–80 (1997).

78. P. Tauh and A. G. Fallis, *J. Org. Chem.* **64**, 6960–6968 (1999).

79. D. P. Curran, P. A. Vanelburg, B. Giese, and S. Gilges, *Tetrahedron Lett.* **31**, 2861–2864 (1990).

80. K. U. Ingold, B. Maillard, and J. C. Walton, *J. Chem. Soc., Perkin Trans. 2*, 970–974 (1981).

81. A. L. J. Beckwith and G. Moad, *J. Chem. Soc., Chem. Commun.*, 472–473 (1974).

82. A. L. J. Beckwith and K. U. Ingold, in *Rearrangements in Ground and Excited States*, P. de Mayo, ed., Academic, New York, 1980, Vol. 1, pp. 161–310.

83. S.-U. Park, S.-K. Chung, and M. Newcomb, *J. Am. Chem. Soc.* **108**, 240–244 (1986).

84. M. Newcomb, M. A. Filipkowski, and C. C. Johnson, *Tetrahedron Lett.* **36**, 3643–3646 (1995).

85. O. M. Musa, S. Y. Choi, J. H. Horner, and M. Newcomb, *J. Org. Chem.* **63**, 786–793 (1998).

86. C. C. Johnson, J. H. Horner, C. Tronche, and M. Newcomb, *J. Am. Chem. Soc.* **117**, 1684–1687 (1995).

87. M. Newcomb, J. H. Horner, M. A. Filipkowski, C. Ha, and S. U. Park, *J. Am. Chem. Soc.* **117**, 3674–3684 (1995).

88. F. N. Martinez, H. B. Schlegel, and M. Newcomb, *J. Org. Chem.* **63**, 3618–3623 (1998).

89. V. W. Bowry, J. Lusztyk, and K. U. Ingold, *J. Am. Chem. Soc.* **113**, 5687–5698 (1991).

90. S. Y. Choi and M. Newcomb, *Tetrahedron* **51**, 657–664 (1995).

91. J. H. Horner, N. Tanaka, and M. Newcomb, *J. Am. Chem. Soc.* **120**, 10379–10390 (1998).

92. M. H. Le Tadic-Biadatti and M. Newcomb, *J. Chem. Soc. Perkin Trans. 2*, 1467–1473 (1996).

93. F. N. Martinez, H. B. Schlegel, and M. Newcomb, *J. Org. Chem.* **61**, 8547–8550 (1996).

94. G. E. Keck and J. B. Yates, *J. Am. Chem. Soc.* **104**, 5829–5831 (1982).

95. G. E. Keck, E. J. Enholm, J. B. Yates, and M. R. Wiley, *Tetrahedron* **41**, 4079–4094 (1985).

96. G. A. Russell, H. Tashtoush, and P. Ngoviwatchai, *J. Am. Chem. Soc.* **106**, 4622–4623 (1984).

97. D. A. Lindsay, J. Lusztyk, and K. U. Ingold, *J. Am. Chem. Soc.* **106**, 7087–7093 (1984).

98. P. Dowd and W. Zhang, *Chem. Rev.* **93**, 2091–2115 (1993).

99. R. L. Donkers and D. G. Leaist, *J. Phys. Chem. B* **101**, 304–308 (1997).

100. H. S. Sandhu, *J. Mag. Res.* **17**, 34–40 (1975).

101. L. M. Li and C. H. Sotak, *J. Mag. Res. B* **101**, 8–16 (1993).

102. J. Saltiel and B. W. Atwater, *Adv. Photochem.* **14**, 1–90 (1988).

103. D. P. Curran, N. A. Porter, and B. Giese, *Stereochemistry of Radical Reactions: Concepts, Guidelines, and Synthetic Applications*, VCH, Weinheim, 1995.

104. P. Renaud and M. P. Sibi, eds., *Radicals in Organic Synthesis*, Wiley-VCH, Weinheim, 2001.

3 General Chemistry of Radical Polymerization

BUNICHIRO YAMADA and PER B. ZETTERLUND

Osaka City University, Sugimoto, Osaka, Japan

CONTENTS

3.1 INITIATION

3.1.1 General Features

The initiator-derived free radicals that initiate polymerization are generated by thermal or photochemical homolytic cleavage of covalent bonds, or by a redox process. These primary radicals add to carbon–carbon double bonds of monomer resulting in primary propagating radicals that in turn propagate further. Initiation generally occurs by tail addition to monomer of the primary radicals. However, the primary radicals do not always react with monomer in a regio- and/or chemoselective fashion, and side reactions are known to occur in many cases. The fraction of primary radicals that actually initiate a polymer chain through formation of primary propagating radicals, the initiator efficiency (f), depends on a number of factors. A low value of f is an intrinsic disadvantage as the initiator is used inefficiently, and also indicates a relatively high rate of formation of undesired byproducts, in some cases even suggesting the unsuitability of a particular compound as an initiator. Branching, crosslinking, and graft copolymerization may occur as a result of hydrogen abstraction by primary oxygen-centered radicals such as *tert*-butoxy radicals. In general, the addition of primary radicals to monomer is faster than initiator decomposition, and the rate of initiation is thus determined by the rate of decomposition of the initiator.

It has been realized that the nature of the initiator not only influences the rate of polymerization and the molecular weight of the polymer formed but also affects the polymer structure and thereby possibly polymer properties as well. The environmental stability of polymers often depends on the nature of the end groups.[1] As a direct result of the relative reactivity of the primary radicals toward different monomers, the choice of initiator in a copolymerization will determine not only the nature of the end groups but also which monomer is the most likely to be in the position next to the initiator-derived fragment at the chain end.[2]

3.1.2 Radical Generation

3.1.2.1 Homolysis

3.1.2.1.1 Azo Initiators   This class of initiators, covered in several reviews,[3–5] generate carbon-centered and oxygen-centered radicals by the homolysis of the C—N (dialkyl diazenes) and O—N (dialkyl hyponitrites) bonds. A major driving force for the dissociation is the formation of the stable nitrogen molecule. Dialkyl hyponitrites (not commercially available) are generally used at lower temperatures than dialkyldiazenes, and cannot be employed as photosensitizers.

The vast majority of commercially available aliphatic azo initiators are symmetric, and the substituted alkyl radicals generated on decomposition are usually resonance stabilized tertiary radicals to facilitate initiator decomposition. Some of the most commonly used dialkyl diazenes include 2,2′-azobisisobutyronitrile [AIBN (**1**)], dimethyl 2,2′-azobisisobutyrate (MAIB), 1,1′-azobis(1-cyclohexanenitrile) (**2**), 2,2′-azobis(2,4,4-trimethylpentane), and azobis-2,4-dimethylvaleronitrile.[6]

The decomposition of AIBN has been shown to produce the ketenimine in significant amounts.[7,8] However, confirmation of diazenyl radicals as intermediates in the case of symmetric dialkyldiazene initiators is not possible as they do not have sufficiently long lifetimes for reaction with monomer to occur or for radical trapping to be feasible.[9]

The rate of decomposition increases with increasing delocalization of the unpaired electron of the generated radical,[3,4] and it has been found that the stabilization energies of the primary radicals generated on initiator decomposition correlate fairly well with the decomposition rates.[10] Steric factors also affect the rate of decomposition; increased bulkiness of and branching on the γ-carbon results in significantly higher rates of decomposition.[5] The polarity of the solvent generally only exerts a marginal effect on the value of the rate constant for decomposition (k_d); k_d for MAIB is approximately twice as high in methanol as in cyclohexane.[6]
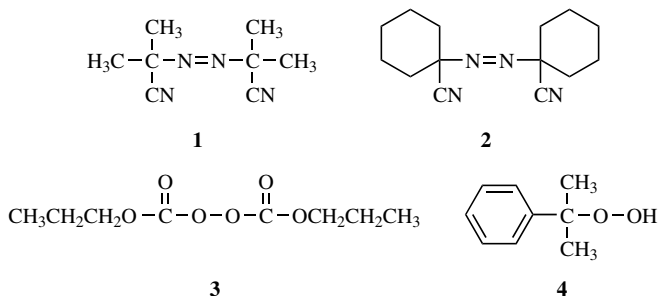
Macroazoinitiators,[11–19] polymeric or oligomeric compounds containing one or more —N=N— units, are useful for the synthesis of block copolymers. By use of macroazoinitiators, it is possible to prepare block copolymers containing polymer blocks that have been formed by different polymerization mechanisms. Macroazoinitiators are generally prepared by polycondensation of low molecular weight azoinitiators with prepolymers of suitable molecular weight and end-group functionality. An example of this synthetic strategy is the preparation of polyurethane macroazoinitiators by the polycondensation of 2,2′-azobis(2-cyanopropanol) with isocyanate-terminated prepolymer,[17] which can subsequently be employed to initiate free-radical polymerization of a vinyl monomer.

An additional interesting feature of polymers containing azo moieties along the backbone is that they are thermodegradable.[17] The thermal decomposition of macroazoinitiators proceeds by first-order kinetics, but the rate of decomposition may differ from that of the parent low molecular weight azoinitiator.[18] Both the frequency factor and the activation energy of the rate constant for the thermal decomposition of a series of azo-containing polydimethylsiloxanes have been reported to increase with increasing chain length of the polydimethylsiloxane segments.[20] Macroazoinitiators have also recently been employed in nitroxide-mediated living/controlled polymerization[13] and multimode polymerization (cationic to radical transformation).[16] For the synthesis of block copolymers of precise structure using macroinitiators in tandem with the concept of 2,2,6,6-tetramethylpiperidine-1-oxyl

(TEMPO)-based nitroxide-mediated living/controlled free-radical polymerization, azo initiators are preferred over peroxide initiators because the latter tend to undergo reaction with TEMPO, thereby altering the desired macromolecular architecture.[13,21]

Attempts have been made to initiate polymerization by the generation of a diradical species, which would result in a macroradical where both chain ends are active. This type of initiation would be a significant stride forward from an industrial point of view as high molecular weight polymer could be produced at considerably higher rates.[22] Attempts so far, usually based on cyclic azo and peroxy compounds, have met with limited success mainly as a result of the initiator efficiency being inherently low when both radical centers are located on the same molecule.[22] One study has shown that diradicals generated from bicyclic azo compounds were not successful in initiating polymerization of neither styrene nor acrylonitrile.[23] There is however experimental evidence indicative of a diradical species being involved in the spontaneous thermal copolymerization of certain electron donor and acceptor monomer pairs (Section 3.1.2.2.3). This finding is not to be confused with the situation in living/controlled systems (atom transfer radical polymerization and nitroxide-mediated living/controlled systems), where multifunctional initiators yielding chains that propagate via two or more active chain ends are readily prepared.

3.1.2.1.2 Peroxide Initiators   A wide range of peroxy compounds are being employed as initiators: acyl peroxides, alkyl peroxides, dialkyl peroxydicarbonates, hydroperoxides, peresters, and inorganic peroxides.[6,24] Examples of commonly employed peroxide initiators of each subclass are benzoyl peroxide (BPO), di-*tert*-butyl peroxide, di-*n*-propyl peroxydicarbonate (**3**), cumene hydroperoxide (**4**), di-*tert*-butyl peroxalate, and persulfate.

The oxygen-centered radicals generated on peroxide initiator decomposition can react further via the pathway of β-fragmentation. The decomposition of BPO thus results in the formation of benzoyloxy radicals, phenyl radicals, and carbon dioxide. Alkyl hydroperoxides possess a labile hydrogen atom and can therefore act as efficient chain transfer agents as well as initiators. Inorganic peroxides such as persulfate and hydrogen peroxide are used mainly in water-based applications because of their high water solubility and poor solubility in organic solvents.[25]

The rate of decomposition of peroxide initiators is a function of their chemical structure. The k_d of diacyl peroxides and peresters increase as the nature of the substituents change as in the series aryl, primary alkyl < secondary alkyl < tertiary alkyl.[26] Alkyl peroxyesters (peresters) decompose by either one-bond homolysis of the O—O bond, resulting in the formation of an acyloxy and an alkoxy radical, or by a concerted two-bond scission mechanism leading to the formation of carbon dioxide, an alkyl and alkoxy radical.[27] The nature of the substituents on the carbon connected with the $(CO)O_2$ moiety affect both the rate and the mode of decomposition. Experimental data for the decompositions of *tert*-butyl peroxyacetate (where the carbon connected with the $(CO)O_2$ moiety is primary), *tert*-butyl peroxyisobutyrate (secondary carbon), and *tert*-butyl peroxypivalate (tertiary carbon) show that the rate of decomposition increases in the order primary < secondary < tertiary carbon,

and that concerted decomposition appears to occur in the case of secondary and tertiary carbons.[27–29]

The nature of the solvent may also affect k_d; for example, the rate of thermal decomposition of *tert*-butyl peroxide is somewhat higher in acetonitrile than in cyclohexane. The rate of decomposition of the diacyl peroxide bis(3,5,5-trimethylhexanoyl)peroxide has been reported to be 7 times faster in *n*-pentadecane than in acetonitrile at 80°C and 1500 bar.[30] The rate of decomposition of diethyl peroxydicarbonate has been reported to be similar in organic solvents and supercritical carbon dioxide.[31]

The various types of peroxide initiators are suitable for different temperature ranges depending on their rates of thermal decomposition. The dialkyl peroxides and hydroperoxides are most suited for higher temperatures, whereas dialkyl peroxydicarbonates are used mainly in the lower-temperature regions.

Oxidation products of alkyl-9-borabicyclononane dissociate into alkoxyl radicals and borinate radicals at ambient temperature (in contrast to regular peroxides).[32,33] The alkoxyl radicals readily initiate polymerization, whereas the borinate radicals are relatively stable and instead tend to couple reversibly with propagating radical species, thereby inducing the characteristics of living/controlled free-radical polymerization in a manner similar to that of nitroxide-mediated living/controlled free-radical polymerization systems (Chapter 10). The polydispersity was, however, not as low as what would normally be associated with living/controlled polymerizations. A possible reason for this may be that the oxidation of alkyl-9-borabicyclononane was carried out in situ in the polymerization mixture, thereby causing chains to start growing at different times.

3.1.2.1.3 Initiators Yielding Persistent and Captodatively Substituted Radicals
Certain initiators generate persistent radicals, usually formed as a result of thermal homolysis of a C—C bond[34–40] or decomposition of azo compounds such as phenylazotriphenylmethane (**5**).[41,42] These persistent radicals exhibit relatively low reactivity toward vinyl monomers, and therefore exhibit a tendency to engage in primary radical termination to an unusually large extent. Because of the weakness of the covalent bonds thus formed at the polymer ω-ends, thermal dissociation can occur, and the polymerization might (depending on monomer type and polymerization conditions) exhibit living/controlled character as the propagating radical chain ends are reversibly end-capped by the persistent radicals.[34–42] This type of compounds are generally referred to as *iniferters*.[43] This concept, including a description of *iniferters* that also undergo extensive chain transfer (mainly dithiuram disulfides), will be treated in the section on chain transfer.

One of the first compounds to be used as a thermal iniferter was phenylazotriphenylmethane,[41,42] which on decomposition produces phenyl radicals and trityl radicals. Initiation is believed to occur by the phenyl radicals, whereas the less reactive trityl radicals partake predominantly in reversible coupling reactions with propagating radicals. The majority of thermal iniferters are 1,2-disubstituted tetraphenylethanes derivatives (**6**)[34,35,41,43–47] such as X = CN, C_2H_5, OC_6H_5, and $OSi(CH_3)_3$. The decomposition of a compound of this type generates two identical

radical species, and it is thus an inherent disadvantage of the system that both may add to monomer and thereby giving less control (this also applies to dithiuram disulfides).

5   **6**
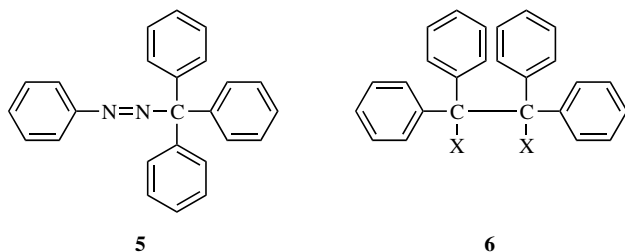
Coupling products of captodatively substituted carbon radical species dissociate at relatively low temperatures as a result of radical stabilization, and are capable of initiation of vinyl polymerization exhibiting living/controlled character similar to the 1,2-disubstituted tetraphenylethane-based systems.[39,48–51] Initiation by ethanes with captodative substituents, such as captodatively substituted morpholinosuccino-nitrile, results in higher polymerization rates of styrene and methyl methacrylate than for tetraphenylethanes.[40,49,50] The use of various selenium compounds such as benzyl phenyl selenides has also been reported.[52,53]

The systems described above tend to work fairly well with 1,1-disubstituted ethy-lenic monomers (e.g., methyl methacrylate), but not for 1-substituted ethylenic monomers (e.g., styrene)[43] as the end-capping for such monomers appears irrever-sible. Although a degree of living/controlled character is manifested (in the case of, e.g., methyl methacrylate) in linear M_n versus conversion relationships and the fact that it is possible to employ the prepolymer as a polymeric iniferter for block copo-lymer synthesis, fairly significant chain deactivation is believed to occur during the process. This gives rise to polydispersities considerably higher than those obtained in other living/controlled free-radical polymerization processes such as atom transfer radical polymerization (Chapter 11) and nitroxide-mediated (Chapter 10) and RAFT systems (Chapter 12).

3.1.2.2   Thermal Initiation

3.1.2.2.1   Styrene   The mechanism behind the thermal polymerization of styrene has been the subject of research for decades. The two main theories are those proposed by Flory and Mayo,[54] of which the latter has received the most support. It involves the formation of the Mayo dimer by the Diels–Alder reaction of two molecules of styrene and the subsequent hydrogen transfer to styrene to yield two radicals that can initiate polymerization (Scheme 3.1). The Mayo dimer has to date not been isolated, but a considerable body of evidence is in favor of this mechanism, including its detection as an end group.[22,55–58] The presence of an acid catalyst results in a decrease in the rate of initiation and formation of trimer, consistent with the expectation that the Mayo dimer, unlike the Flory dimer, would not be stable to
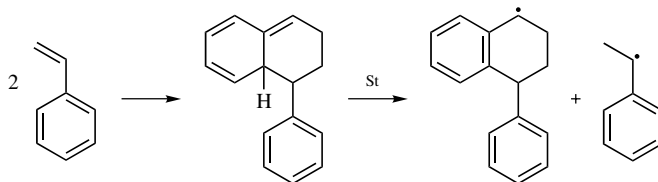
Scheme 3.1

acid.[55] The thermal initiation rate, a function of monomer concentration and temperature, can be predicted from the molecular weight of the polymer formed.

3.1.2.2.2 Acrylates   Several acrylates and methacrylates have been reported to undergo thermal polymerization, although significantly slower than styrene and styrene-related compounds.[59] It has been argued that this may in fact partly be caused by impurities present (speculated to be peroxides[60,61]), as suggested by the difficulty in obtaining reproducible data.[60] In the case of methyl methacrylate, a mechanism involving a dimeric 1,4-diradical formed by reaction of two monomer molecules is consistent with considerable experimental evidence, including the identification of dimer byproducts and the scavenging and detection of the diradical by use of a large amount of a strong transfer agent.[62–64] Certain captodatively substituted acrylates, including methyl α-acetoxyacrylate and methyl α-methoxy-acrylate, undergo spontaneous polymerization, and some experimental evidence is consistent with initiation via a diradical species.[65,66]

3.1.2.2.3 Copolymerization   Certain pairs of electron-donor and electron-acceptor olefins undergo spontaneous copolymerization in the absence of an added initiator. Examples include the monomer pairs styrene/acrylonitrile,[67,68] vinyl sulfides/maleic anhydride and acrylonitrile,[69] and styrene/maleic anhydride.[70] The styrene/acrylonitrile system was previously thought to undergo initiation via a mechanism analogous to that of the thermal homopolymerization of styrene and the Mayo initiation mechanism. However, experimental results have shown that presence of an acid catalyst (Section 3.1.2.2.1) has no effect on the rate of copolymerization, thus strongly indicating that the Mayo mechanism is not predominant in the styrene/acrylonitrile copolymerization.[68] Experimental support in favor of bond-forming initiation via a tetramethylene diradical species has been reported for the copolymerizations of trisubstituted acceptor olefins such as dimethyl cyanofumarate with various electron donating substituted styrenes such as 4-methoxystyrene.[71,72] Experimental results that may indicate initiation via an electron/hydrogen transfer mechanism have also been reported.[69,70]

*3.1.2.3   **Induced Decomposition***   Induced decomposition refers to the reaction of a radical species with an initiator molecule, resulting in a new radical species that in turn is able to initiate a chain. The net effect is that one initiator molecule is consumed while the number of radicals remains constant. The process may lead to

Scheme 3.2

the introduction of new end groups, and it lowers the molecular weight of the polymer formed. The attacking radical may be a propagating radical, and in this case the process is referred to as *chain transfer to initiator*. If the solvent molecules possess hydrogens easily abstractable by the primary radicals or propagating radicals, the solvent radicals thus generated may induce further initiator decomposition.

Diacyl and diaroyl peroxide initiators are particularly prone to induced decomposition. For example, it has been reported that for polystyrene initiated by 0.10 M BPO at 60°C, at least 75% of the chain terminating events comprise transfer to initiator (Scheme 3.2) or primary radical termination.[8] Dialkyl diazenes on the other hand only exhibit induced decomposition to a negligible extent. In the case of styrene polymerization initiated by AIBN, transfer to initiator accounts for less than 5% of the end groups at low conversion.[8] Di-*tert*-butyl and cumyl peroxide are not very prone to induced decomposition, although it has been reported to occur in the case of di-*tert*-butyl peroxide when the solvent is a primary or secondary alcohol.[9,73,74] The rate of thermal decomposition of alkyl hydroperoxides is known to partly proceed in an induced fashion. Primary and secondary hydroperoxides can undergo induced decomposition by abstraction of the α-hydrogen, resulting in β-fragmentation forming a hydroxy radical and a carbonyl compound. Peresters may undergo induced decomposition in analogy with the diacyl peroxides, although to a lesser extent.[75]

3.1.2.4   *Electron Transfer*

This mode of initiation refers to a redox reaction that is accompanied by the formation of a radical species that can initiate chain propagation.[76] A distinct difference, and often an advantage compared to initiation by the thermal decomposition of an azo or peroxide initiator, is the fact that a single initiating system can be used over a much wider temperature range because of the significantly lower activation energy of these processes. However, control of the rate of generation of primary radicals is often difficult, and dead-end polymerization is sometimes obtained. These systems can often be used at ambient temperatures or even below, and they see extensive use in emulsion and aqueous free-radical polymerization processes.

Peroxides are readily reduced by various transition metal salts resulting in the generation of an anion and a primary radical; an example is the reaction of hydrogen peroxide with Fe^{2+}. Persulfate is often used in redox formulations with transition metal ions, and generates a radical anion ($SO_4^-\cdot$) as the initiating species. Because of the low solubility in organic media, this system is used mainly in aqueous or emulsion polymerizations. Other similar systems include HSO_3^-, SO_3^{2-}, and $S_2O_3^{2-}$. Organic peroxides may form complexes with tertiary amines in nonaqueous solution generating radicals[76] and radical cations, such as *N,N*-dimethylaniline/BPO.

This form of induced decomposition has also been reported to occur with various monomers, including *N*-vinylimidazole[77] and *N*-vinylcarbazole.[78] The initiation system organic peroxide/tertiary amine is of significant practical importance in dentistry and orthopaedic surgery, for example, in the curing of acrylic resins employed in total hip replacement operations.[79] A high-viscosity mixture of poly(methyl methacrylate) and acrylic monomers (usually methyl methacrylate) is injected into the cavity, and subsequently cured at room temperature, usually by BPO and a tertiary amine such as *N,N*-dimethylaniline and *N,N*-dimethyl-4- toluidine.

Several oxidizing metal ions [e.g., Mn(III), Ce(IV), V(V), and Co(III)] in combination with reducing agents such as alcohols, thiols, ketones, aldehydes, amines, and amides constitute redox pairs suitable for initiation in free-radical polymerization.[76] Organometallic derivatives of transition metals [e.g., $Mn_2(CO)_{10}$, $Mo(CO)_6$] in low oxidation states can undergo redox reaction with, for example, an organic halide to initiate polymerization.[80] An electron is transferred from the transition metal to the halide, generating a primary alkyl radical and a halide ion.

3.1.2.5 Photoinitiation   The rapidly growing field of UV–visible light (250–450 nm)-induced polymerization refers to molecules absorbing energy from photons resulting in the formation of radical species capable of initiating free-radical polymerization, and finds the most extensive use in crosslinking processes.[81–85] This mode of initiation has a wide range of industrial applications and is also of great importance from an academic viewpoint since the rate of initiation can be conveniently controlled through the intensity and location of the light source, and high rates of initiation can be readily achieved. In addition to the photoinitiators mentioned in this section, azo and peroxy initiators also decompose photochemically.[86]

The photoinitiators are usually classified as type I and type II initiators according to the mechanism by which primary radicals are generated.[81] Photoinitiators of type I decompose via a direct unimolecular photofragmentation process, usually α-fragmentation (i.e., bond breakage occurs at a bond adjacent to the carbonyl group, as for benzoin ethers and acyl phosphine oxides) or β-fragmentation (α-haloketones). These initiators are usually aromatic carbonyl compounds with substituents that facilitate direct photofragmentation. Examples of type I photoinitiators include benzoin derivatives such as benzoin ethers, α-aminoalkylphenones, and acyl phosphine oxides. Benzoin ethers readily undergo α-fragmentation on exposure to near-UV light (Scheme 3.3) in a process that is not quenched by oxygen, thereby making them suitable for curing in air.[87] Some experimental evidence for the benzoin isobutyl ether photoinitiated polymerization of styrene suggests that initiation is occurring predominantly by benzoyl radicals at low temperature, high light intensity, and/or low
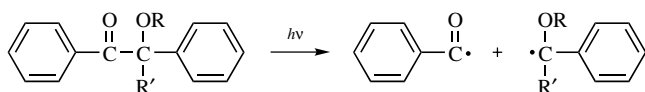
Scheme 3.3
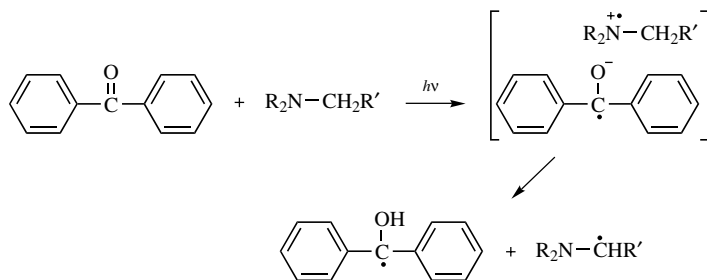
Scheme 3.4

monomer concentration.[88] The alkoxy substituted benzyl type radicals mainly engage in primary radical termination, presumably as a result of slow addition to styrene.

Aromatic ketones such as benzophenone and thioxanthone are typical photoinitiators of type II. Type II photoinitiators normally generate radicals by (1) abstracting hydrogen from the environment (e.g., the solvent, an ether or an alcohol) or (2) undergoing photoinduced electron and hydrogen transfer with a coinitiator resulting in radical ions that fragment to generate radicals (Scheme 3.4). The most commonly employed coinitiators for aromatic ketones are tertiary amines, the ionization potential of which is thought to be of crucial importance for the electron transfer process along with steric factors.[82,89–91] The tertiary amine functionality may also be located on the aromatic ketone itself; an example is Michler's ketone (**7**). Reaction product analysis after the irradiation of a typical type II system, benzophenone/N,N-dimethyl aniline, in the presence of a non-polymerising model substrate indicated that the main initiating species is the α-aminoalkyl radical, with a small contribution from the ketyl radical remaining a possibility.[92] Likewise, the alkyl radicals generated on hydrogen abstraction are believed to be the main species that initiate polymerization when alcohols or ethers are present instead of tertiary amines; the ketyl radicals undergo predominantly coupling reactions.[83,93] In the case of the system camphorquinone/amine, it has been shown that the rate of polymerization increases in the order primary < secondary < tertiary amine; the polymerizations are very slow for primary amines and amines lacking an α-hydrogen.[93]
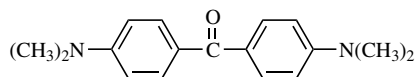
7

It is common practice in industry to employ combinations of photoinitiators of both types I and II for optimum initiator performance, for example with regards to oxygen inhibition.[94]

Considerable effort has been directed toward the development of polymeric and macromonomeric photoinitiators:[95–97] initiators that are covalently bonded to larger structures. These types of initiators are believed to offer advantages in food

packaging applications where migration of unreacted initiator molecules can pose a problem. An example is the synthesis of poly(methacrylate) containing camphorquinone as part of the side chain.[97] This photoinitiator was subsequently used to cure the system hexanediol diacrylate/*n*-butyl acrylate employing a tertiary amine as pendant functionality of a polymer chain. The photocuring rate was higher when low molecular weight tertiary amine was used as a coinitiator, presumably for steric reasons.

3.1.3   Primary Radical Reactions

Once a primary radical has escaped the solvent cage, it may undergo a variety of reactions depending on the type of the primary radical; tail/head addition to monomer, hydrogen abstraction (from monomer, solvent or polymer), aromatic addition (in the case of monomer bearing an aromatic ring), fragmentation, or primary radical termination. The relative rates of these reactions are specific to each initiator/monomer system and the reaction conditions.

By use of the nitroxide trapping technique,[98] the initiation pathways have been elucidated for a number of polymerizing systems,[99–101] including copolymerizations.[102–104] In the polymerization of styrene initiated by BPO, the benzoyloxy radicals undergo tail addition, head addition, and aromatic addition. A small fraction of the benzoyloxy radicals fragment through β-scission to yield carbon dioxide and phenyl radicals, which react with styrene predominantly by tail addition (Scheme 3.5).[7,8] *tert*-Butoxy radicals also fragment by β-scission to generate acetone and methyl radicals that can initiate polymerization.[102,103,105] The situation in a binary copolymerization is more complex; the rates of addition of primary radicals to different vinyl monomers depend on the nature of the monomer, and the relative
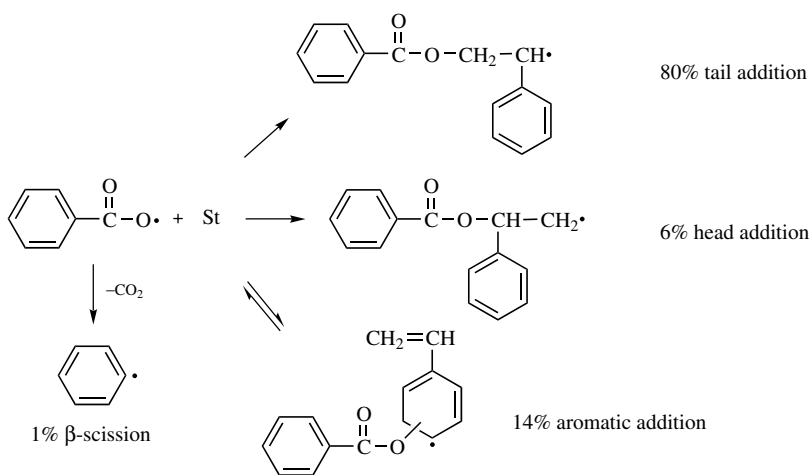
Scheme 3.5

rates of addition of primary radicals to the two monomers will affect the distribution of end groups obtained.[106] In the case of the copolymerization of styrene and acrylonitrile in bulk initiated by *tert*-butoxy radicals at 60°C, the rate of addition of *tert*-butoxy radicals to styrene is approximately 5 times greater than to acrylonitrile, whereas the addition of methyl radicals (generated from β-fragmentation of *tert*-butoxy radicals) to acrylonitrile is about 4 times more rapid than to styrene.[107] This behavior can be explained in terms of the electrophilic (*tert*-butoxy) and nucleophilic (methyl) nature of the radicals towards the electron-rich styrene and electron-poor acrylonitrile monomers.

Certain initiators generate two different types of radicals with considerably different reactivities toward vinyl monomers. These include the already mentioned photoinitiators benzoin ethers and acyl phosphine oxides (Section 3.1.2.5) and the thermal iniferter phenylazotriphenylmethane (Section 3.1.2.1.3). The absolute rate constants for the addition of diphenylphosphonyl radicals to vinyl monomers have been estimated by time-resolved ESR spectroscopic studies of the decomposition of (2,4,6-trimethylbenzoyl)diphenylphosphine oxide (**8**) (Scheme 3.6) in the presence of a variety of vinyl monomers.[108–110] The phosphorous centered radicals add to vinyl monomers about one to two orders of magnitude more rapidly than most carbon-centered radicals; the rate constant for addition is of the order $10^{6-7} \, M^{-1} \, s^{-1}$, while the 2,4,6-trimethylbenzoyl radicals also generated on decomposition of these asymmetric initiators do not undergo vinyl monomer addition rapidly enough for observation to be possible on this timescale.

Dialkyl fumarates initiated by MAIB polymerize considerably faster than when AIBN is employed, although there is only a negligible difference in k_d.[111–113] This contrasts the generally observed behavior where the rate of initiator decomposition is the rate-determining step in initiation, and has been ascribed to the difference in the rates of addition of the primary radicals to monomer.

The initiator-derived radicals may also react directly with the solvent, oxygen, or adventitious impurities. Solvents bearing easily abstractable hydrogen atoms are prone to undergoing hydrogen abstraction in the presence of mainly oxygen-centered radicals such as *tert*-butoxy radicals. In the polymerization of methyl methacrylate in toluene initiated by di-*tert*-butyl peroxalate (generating *tert*-butoxy radicals), hydrogen abstraction followed by initiation of the benzyl radical leads to a significant proportion of polymer chains with benzyl end groups.[105,106] It has been reported that 29% of *tert*-butoxy radicals react with methyl methacrylate by

8
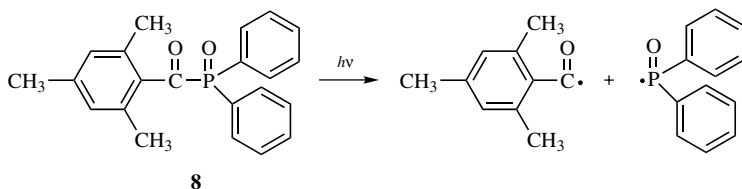
Scheme 3.6

hydrogen abstraction from the α-methyl group, and 4% by abstraction from the ester methyl group.[114] The radicals thus generated are capable of chain initiation, giving rise to a rather significant proportion of unsaturated end groups. The presence of oxygen will affect the initiation process as it reacts with carbon-centered radicals at close to diffusion-controlled rates,[115] resulting in formation of the corresponding alkyl peroxy radical. This radical may itself react with monomer, or alternatively abstract a labile hydrogen creating another radical and a hydroperoxide.

Depending on the nature of the particular monomer/initiator system and the reaction conditions, the type of solvent may exert a considerable effect on the reaction rates of the various reactions involved in the initiation process.[105,106] In the polymerization of methyl methacrylate initiated by di-*tert*-butyl peroxalate or di-*tert*-butyl hyponitrite (both yielding *tert*-butoxy radicals), major changes in the product distribution and solvent-derived products have been observed for different solvents.[105] An increase in the polarity of the solvent was found to increase the rate of hydrogen abstraction relative to *tert*-butoxy radical addition to methyl methacrylate, and the rate of β-scission of *tert*-butoxy radicals relative to both hydrogen abstraction and monomer addition.[105] Another example of solvent effects is the ratio of the rate constants for the addition of *tert*-butoxy radicals to ethyl vinyl ether and methyl methacrylate, which is less than one in both cyclohexane and acetonitrile, but approximately six in *tert*-butanol.[102]

3.1.4   Initiator Efficiency

As an initiator molecule decomposes, the resulting geminate radicals can either react with one another inside the "solvent cage" or diffuse out of the cage to participate in other reactions, mainly addition to monomer. This so called "cage effect"[116] is the main reason that the initiator efficiency f is lower than unity (another reason is primary radical termination), and usually lies somewhere between 0.3 and 0.8.[117] Inside the cage, the initiator fragments can either recombine, undergo disproportionation, or engage in other reactions. Recombination of primary radicals resulting in the regeneration of the initiator, which causes a decrease in the effective rate constant for decomposition while not affecting f, is referred to as "cage return." The cage reaction of primary radicals generated from the decomposition of AIBN leads to the formation of small amounts of methacrylonitrile, which may copolymerize with the monomer of the system.[118–120] Attempts have been made to measure the amount of recombination inside the cage by use of initiator that has been specifically labeled with ^{13}C[121] and deuterium.[122] These studies have indicated that the products from the self-reactions of the cyanoisopropyl radicals generated from AIBN (the ketenimine and tetramethylsuccinonitrile) are formed almost exclusively within the solvent cage in the presence of styrene monomer. However, in the absence of styrene (60°C in benzene), 55% of the products were formed outside the cage,[121] indicating that the addition of cyanoisopropyl radicals to styrene is sufficiently rapid to compete with the self-reaction of the radicals under these conditions.

In the case of peroxy ester initiators, the mode of decomposition will have an effect on f. Concerted two-bond scission results in an alkoxy radical and an alkyl

radical, which may couple inside the cage, leading to lower f. If concerted decomposition takes place, an alkoxy radical and an acyloxy radical are formed, the recombination of which will not affect f (cage return).[27] The application of an external magnetic field is believed to reduce the significance of the cage effect by causing a lower rate of triplet-singlet intersystem crossing of geminate radical pairs.[123–125] Experimental determination of f is most commonly carried out by use of radical scavenging techniques[126] or product and end-group analysis by NMR[121] or infrared spectroscopy.[127]

If the primary radicals can escape out of the cage, they are likely to react with monomer and initiate chain growth. The extent of cage reaction for a given initiator is a function of the rate at which the initiator fragments can diffuse apart from one another, and will thus depend on the viscosity[111,121,126–130] and thereby also on factors affecting the viscosity such as degree of conversion, temperature, and solvent type. In the polymerization of *trans*-4-*tert*-butylcyclohexyl methacrylate initiated by AIBN in benzene at 60°C, it was shown that an increase in the viscosity from 0.726 to 1.47 cP resulted in a decrease in f from 0.46 to 0.22.[126]

A strong conversion dependence can be observed in bulk polymerization; f decreases gradually until a critical point at approximately 70–80% conversion in the case of styrene and methyl methacrylate, where it falls dramatically by several orders of magnitude.[127,128,131,132] As the viscosity increases with conversion, the rate of diffusion of primary radicals out of the cage decreases, resulting in a lowering of f. At very high conversion, the decrease in monomer concentration further contributes to the fall in f. There are some data to support that the onset of the dramatic fall in f at high conversion can be correlated with the size of the diffusing initiator fragments (larger fragments diffuse at lower rates).[128] A conversion dependence of f can also be observed in solution polymerization,[121,127,129] although it is not as dramatic as in bulk systems.

Measurements of the effect of temperature on f are rare; it has been reported that in the AIBN initiated bulk polymerization of styrene at a pressure of 1000 bar, a temperature increase from 40 to 80°C leads to an increase in f by approximately 50% in the conversion range 20–40%.[127] The same study also revealed that f decreases as the pressure is increased, with f decreasing by approximately one-third in the conversion range 20–60% as the pressure increased from atmospheric to 2000 bar at 70°C.[127]

The situation is entirely different in emulsion and suspension polymerization systems since the decomposition of the initiator occurs in the continuous water phase when water-soluble initiators are used. The value of f is governed by processes occurring in the water phase, resulting in close to independence of the monomer conversion. Even at very high conversion, there is no increased tendency for radical pairs to undergo geminate recombination, and they do no enter the latex particles as pairs.[133] In emulsion polymerization employing water-soluble initiators, initiation occurs in the water phase where the monomer concentration is much lower than in bulk, and this is the main reason why f is generally significantly lower than in bulk polymerizations.

The primary radicals may also undergo various side reactions outside the cage. Primary radical termination may also occur and contribute to a decrease in f, especially under conditions of high initiator concentration and low monomer concentration.[112,134–136] The fraction of the primary radicals that manage to escape the cage that undergo side reactions is a function of monomer concentration and monomer type. The side reactions and addition to monomer are competitive reactions, and as a consequence f decreases with decreasing monomer concentration and decreasing values for the rate constant of the addition to monomer. In the case of styrene initiated by AIBN, this dependence on monomer concentration is observable for monomer concentrations lower than $\sim$0.1–0.01 M.[137] Induced initiator decomposition and chain transfer to initiator from propagating radicals also contribute to lowering f. Initiation systems that do not produce radicals in pairs (such as redox initiation systems) do not exhibit the cage effect as geminate recombination is not possible.

3.2   PROPAGATION

3.2.1   General Features

Primary radicals generated by the decomposition of initiator add to monomer to yield primary propagating radicals. This is followed by a succession of rapid propagation steps that proceed with high regioselectivity to form radical centers bearing a substituent. The reaction rates of primary propagating radicals and oligomeric radicals have been separately determined for some monomers in specially designed experiments.[138–142] The results suggest that the rate constants decrease with increasing chain length for the first few addition steps, but remain approximately constant for tetramers and longer radicals.[138,141] Recent data from pulsed-laser polymerization (PLP) have indicated a weak long chain-length dependence of the propagation rate constant (k_p) extending over several hundred degrees of polymerization.[143] Although the instantaneous degree of polymerization increases considerably with conversion during the bulk polymerization of styrene, no significant dependence of k_p on the chain length has been observed.[144] ESR quantification of the propagating radical concentration[145] and analysis of kinetic and GPC data from PLP[146,147] have been employed as modern techniques for the determination of k_p and the rate constant for termination (k_t).

The ESR spectra of various propagating radicals such as styrene and substituted styrenes,[145,148,149] methacrylic esters,[150–153] acrylic esters,[154,155] vinyl chloride,[156] α-substituted acrylic esters,[111,145,157–159] and other monomers[145,150] have revealed spin delocalization and/or the conformation of the radical with respect to the C_α—C_β bond. In general, propagation proceeds in a highly regioselective manner to yield a polymer main chain consisting of head–tail linkages. In exceptional cases, monomer bearing a nonconjugate substituent forms small amounts of head–head or tail–tail linkages because of a smaller difference in the activation energies between the head–tail and head–head or tail–tail additions. The addition of the shallow pyramidal radical center to the planar or almost planar carbon–carbon double bond cannot

be a stereospecific reaction. Consequently, propagation is not a highly stereospecific reaction except for the polymerization of monomers with sophisticated structural design.

In order for high polymer to be formed, the propagation step must occur at a sufficiently high rate in comparison with the other elementary reactions. However, several factors may prevent propagation to high molecular weight. β-Substituted vinyl monomers are in general reluctant to homopolymerize as a result of steric hindrance between the approaching radical center and the β-carbon of the monomer. Degradative chain transfer, the formation of a low reactivity radical by rapid chain transfer followed by slow reinitiation, is the main reason why allylic compounds polymerize at very low rates. The resonance stabilized radical resulting from hydrogen abstraction of the allylic hydrogen does not add to monomer because of its stability. Addition–fragmentation chain transfer[160] is responsible for the nonhomopolymerizability of α-(substituted methyl)vinyl compounds such as α-alkylthiomethylacrylate and α-bromomethylacrylate as summarized in Table 3.1.[161–172] The radical formed by addition to the carbon–carbon double bond readily undergoes β-fragmentation to form a carboalkoxy-substituted allylic end group and a small radical that rapidly reinitiates. Some of the acrylates may simultaneously behave as homopolymerizable monomers and addition–fragmentation chain transfer agents. This illustrates how the structural features of these monomers affect the chain transfer and propagation processes in different ways. The steric hindrance arising from the α-substituent suppresses propagation but facilitates fragmentation, which is one of the steps of the chain transfer process.

From a thermodynamic point of view, propagation is required to be exothermic leading to a sufficiently high ceiling temperature (T_c) for polymerization to occur.[173] T_c is governed by the thermodynamical difference between the monomer and the polymer regardless of the polymerization mechanism. α-Substituted styrenes tend

TABLE 3.1   Competition between Polymerization and AFCT of α-(Substituted methyl)acrylate [$CH_2=C(CH_2X)CO_2R$]

X	Polymerization	AFCT	Ref.
OH	Yes	No	162
OR′	Yes	No	163
OCOR′	Yes	No	164
CH(CO$_2$Me)$_2$	Yes	No	165
F	Yes	No	166
CH$_2$CO$_2$Me	Yes	Yes	167
CH$_2$C(CO$_2$Me)CH$_2$CH$_2$CO$_2$Me	Yes	Yes	168
OPh	Yes	Yes	169
Cl	Yes	Yes	170
Br	No	Yes	171
SO$_2$Ar ^{a}	No	Yes	172
SBu-t	No	Yes	161

^{a} Ar = C$_6$H$_5$ or C$_6$H$_4$-Me-p.

to have low T_c values, and polymerization is only possible at low temperatures, if at all. The T_c values of certain α-substituted acrylic esters[111,163,174–176] have been shown to be considerably lower than for methyl methacrylate by use of a convenient procedure to estimate T_c:[174]

$$\frac{d(\ln k'_p/k_t^{0.5})}{d(1/T)} = \frac{k_d E_d/R[M] - k_p E_p/R}{k_p - k_d/[M]} + \frac{E_t}{2R} \tag{3.1}$$

$$\lim_{T \to T_C} \frac{d(\ln k'_p/k_t^{0.5})}{d(1/T)} = \infty \tag{3.2}$$

where k_d denotes the rate constant for depropagation, and E with the subscripts of p, d, and t refer to the activation energies for propagation, depropagation, and termination, respectively; T and R are the polymerization temperature and the gas constant, respectively. An apparent rate constant for propagation, k'_p, is defined by Eq. (3.3). A plot of $\ln k'_p/k_t^{0.5}$ versus $1/T$ normally gives a linear relationship with a negative slope. As the temperature approaches T_c, the plot deviates from the straight line and T_c can be determined as the temperature at which the value of the slope becomes infinity. A decrease in the monomer concentration brings about a lowering of T_c according to

$$k'_p = k_p - \frac{k_d}{[M]} \tag{3.3}$$

Arrhenius plots of the k_p values for methacrylic esters determined by the PLP method at 100°C or below gave straight lines with negative slopes, but downward deviations (the magnitude of which increased with increasing temperature) from the straight lines were observed at temperatures above 140°C as a result of depropagation becoming increasingly significant.[177]

The limitation of the extent of polymerization at a certain temperature in terms of the equilibrium monomer concentration ($[M]_e$) can be estimated from polymerization data by use of Eq. (3.4):[144]

$$[M]_{t+\Delta t} = [M]_t e^{-AB\Delta t} + [M]_e(1 - e^{-AB\Delta t}) \tag{3.4}$$

where [M] with the subscripts *tert* and $t + \Delta t$ denote the monomer concentration at times *tert* and $t + \Delta t$. A and B are constants defined by the following relationships: $A = R_i^{0.5}$ and $B = k_p/k_t^{0.5}$. Although a plot of $[M]_{t+\Delta t}$ versus $[M]_t$ should give a linear relationship through the origin at $[M]_e = 0$, $[M]_e$ can be estimated as the intersection of the linear relationship with the line showing $[M]_{t+\Delta t} = [M]_t$ at $[M]_e > 0$. For the polymerization of substituted quinodimethides, high equilibrium monomer concentrations of the order of 10^0 mol/L were obtained at 50–60°C in conformity with incomplete polymerization of these monomers.[178]

The propagating radical must not be too stable in order for addition to monomer to proceed at a sufficiently high rate. When the radical center bears electron donating (dative) and electron withdrawing (capto) substituents, extra stabilization due to the captodative effect would be expected.[179] Primary radicals readily add to

captodative substituted monomers such as α-*tert*-butylsulfenyl acrylonitrile [CH$_2$=C(CN)SBu-*tert*] where the SBu-*tert* and CN groups may function as the electron donating and withdrawing groups, respectively. However, the reactivity of the resulting adduct radical is too low for propagation to occur, and the adduct radical is in equilibrium with its 4-membered cyclic dimer.[40,180,181]

A number of different strategies can be used in order to enhance the polymerizability. Exomethylene cyclic monomers corresponding to α-substituted styrene (**9–11**),[182] α-alkylacrylate (**12,13**),[183] and *N,N*-disusbtituted methacrylamide (**14,15**)[184,185] homopolymerize in spite of significant steric hindrance and low T_c of the open-chain monomers. Furthermore, the internal strain arising from the bond angle and planar structure of the cyclic structure involving the carbon–carbon double bond of the exomethylene monomer can be relieved as a result of polymerization.
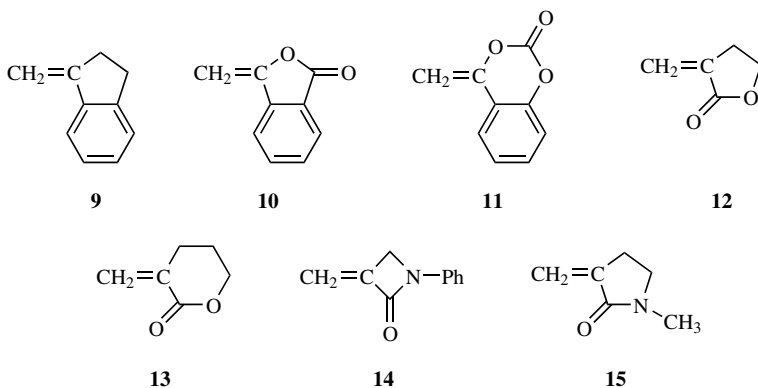
The lack of homopolymerizability arising from a low value of T_c may be overcome by decreasing the temperature and increasing the monomer concentration. The value of k_p increases with increasing pressure since propagation as a bimolecular reaction would be accelerated under conditions of high pressure.[186] However, the increase in the overall rate of polymerization may not be as significant as prediction based from the increase in the k_p value with increasing pressure as a result of simultaneous changes in the rates of initiation and termination.

Alternating copolymerizations of donor–acceptor monomer pairs are predicted to proceed readily almost regardless of the respective homopolymerizabilities of the monomers. For example, in the copolymerizations of maleic anhydride (a strong electron-accepting monomer) with α-olefins, allylic compounds, vinyl ethers, and other compounds (electron-donating monomers), the rate of cross-propagation is sufficiently fast to overcome the effect of degradative chain transfer and the lack of homopolymerizability.

3.2.2 Factors Affecting Propagation

3.2.2.1 *Polar Effects*   The rates of addition of propagating radicals to monomers are affected by polar, resonance, and steric factors resulting from the substituents

$$M_1\bullet \;+\; M_1 \;\xrightarrow{\;k_{11}\;}\; M_1\bullet \qquad\qquad M_2\bullet \;+\; M_1 \;\xrightarrow{\;k_{21}\;}\; M_1\bullet$$

$$M_1\bullet \;+\; M_2 \;\xrightarrow{\;k_{12}\;}\; M_2\bullet \qquad\qquad M_2\bullet \;+\; M_2 \;\xrightarrow{\;k_{22}\;}\; M_2\bullet$$
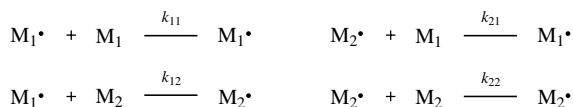
Scheme 3.7

bound to the reacting carbon–carbon double bond and the radical center. When the monomer reactivity ratios of a binary copolymerization are available ($r_1 = k_{11}/k_{12}$ and $r_2 = k_{22}/k_{21}$), the quantity $1/r_1 = k_{12}/k_{11}$ denotes the reactivity of M_2 toward the poly(M_1) radical relative to monomer M_1. Comparison of the $1/r_1$ values for copolymerizations with different M_2 monomers allows consideration of the substituent effect on monomer reactivity of M_2. The rate constants k_{11}, k_{12}, k_{21}, and k_{22} correspond to the propagation steps in a binary copolymerization system as shown in Scheme 3.7.

Hammett's polar substituent constant[187] (σ) has been employed as a measure of polar factors of substituted monomers and propagating radicals. Figure 3.1 shows the Hammett plot of the reactivities of nuclear substituted styrenes toward poly(styrene) radicals relative to styrene (M_1), where the reactivities were calculated from compiled copolymerization data.[188] The plot for the *m*-substituted monomers seems to indicate an increase in the reactivity with increasing electron-withdrawing character of the substituent, although the reactivities of the *p*-substituted styrenes cannot be correlated to σ, indicating difficulty in separation of the resonance and polar effects.

The relative reactivities of nuclear substituted styrenes toward *tert*-butoxy radicals have been evaluated using the nitroxide trapping technique.[189] A plot of the reactivities of all the monomers versus σ resulted in a linear relationship with
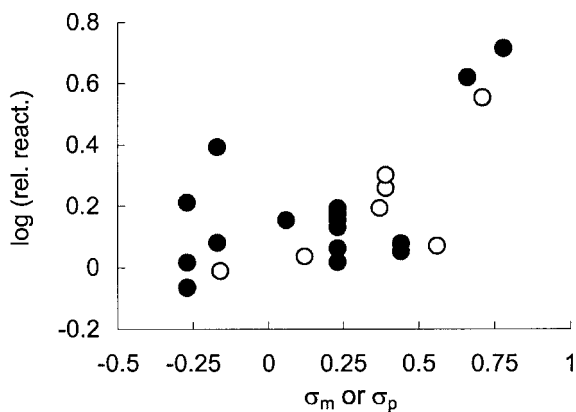
Figure 3.1 Plot of the relative reactivities of *m*-($\circ$) and *p*-substituted styrenes ($\bullet$) toward poly(styrene) radicals versus Hammett's polar substituent constant.

negative slope of -0.329, indicating the electrophilicity of the *tert*-butoxy radical. The correlation coefficient (r) was 0.74. The same plot for only the *m*-substituted styrenes gave a linear relationship with a slope of -0.309, and r was 0.98. Further improvement of the r value were observed when the reactivities of the *m*-substituted monomers were plotted against the σ^+ constants in conformity with the electrophilic nature of the *tert*-butoxy radical; slope $= -0.313$ and $r = 0.99$. However, the Hammett plot gives no linear relationship for the k_p values of substituted styrenes.[190] It is anticipated that the k_p values are affected to different extents by the substituents of both the monomer and the propagating radical.

In conformity with the definition of e according to the Q–e scheme,[191,192] a linear relationship between the electron density of the β-carbon and the e value has been established in accordance with[193,194]

$$e(\text{vinyl}) = \frac{\delta C_\beta - 113.5}{22} \tag{3.5}$$

$$e(\text{styrenes}) = \frac{\delta C_\beta - 115.5}{3.5} \tag{3.6}$$

Furthermore, a linear relationship between the e values of vinyl and vinylidene monomers versus Hammett's polar substituent constant, σ, has also been obtained by[157]

$$e_{\text{CH}_2=\text{CXY}} = 2.13(\sigma_x + \sigma_x) + 0.264 \tag{3.7}$$

In order to estimate the polar effect on the reactivities of substituted ethylenes toward a low molecular weight radical, the e values calculated from copolymerization data have been successfully employed. The rate of addition of cyclohexyl radicals to olefins was found to correlate linearly with the e values after subtraction of the Q values from the logarithm of the reaction rates to correct for the resonance effect.[195]

The addition of small carbon-centered radicals to substituted alkenes is featured by early transition states. The correlation between the activation energy and the enthalpy change is known as the *Evans–Polanyi–Semenov equation*, which disregards any polar effects. More sophisticated analyses and predictions of rate constants for the addition of carbon-centered radicals to alkenes have been reported on the basis of a large number of rate constants evaluated by modern techniques.[196] The activation energy can be calculated from the reaction enthalpy and additional factors such as polar effects, which are functions of the ionization potential and the electron affinity of the radical and the alkene, and the alkene triplet energy. Comparison of a large number of the activation parameters revealed that the frequency factors depend on whether the radical is primary, secondary, and tertiary. The activation energy, on the other hand, is a function of the substituents of both the radical and the alkene. According to these considerations, the polar effect may cause a negative deviation from the line obtained by a plot of the activation energy versus the reaction enthalpy.

This line is given by Eq. (3.8), and the polar effect can be taken into account by superimposing multiplicative polar factors as in Eq. (3.9):

$$E_a = 50 + 0.22H_r \tag{3.8}$$

$$E_a = (50 + 0.22H_r)F_nF_e \tag{3.9}$$

where E_a and $-H_r$ are referred to as the *activiation energies* and the *addition exothermicities*, respectively. F_n and F_e (the values of which are restricted between 0 and 1) denote the nucleophilic and electrophilic factors, respectively.

The validity of this approach to predict the activation energy was confirmed by the excellent agreement obtained between the predictions with experimentally obtained values for more than 200 reactions. Furthermore, the rate constants calculated from the predicted activation energies and the frequency factors were in excellent agreement with the experimental values. However, the transition state for the addition of a polymeric radical to monomer seems to be closer to the product radical, and the resonance and steric effects of the substituents of the double bond and the radical center are more important than for the addition of an alkyl radical to an alkene.

3.2.2.2 Resonance Effects

Both the monomer and the propagating radicals have the same substituent in homopolymerization, and the resonance effect of the substituent may stabilize both species, affecting their reactivities in opposite directions. The resonance stabilization is more significant in the case of the radical as exemplified by the much higher reactivity of styrene than vinyl acetate in their copolymerization. A large difference in reactivity of the radicals with styrene and vinyl acetate terminal units results in copolymer containing significantly more styrene than vinyl acetate. According to the Q–e scheme,[191] the cross-propagation rate constant can be expressed as

$$k_{ij} = P_iQ_j\exp(-e_ie_j)$$

where k_{ij} is the rate constant for addition of $M_i^{\cdot}$ to M_j, and P and Q are parameters related to resonance factors of the radical and the monomer, respectively. The values $Q = 1.0$ and $e = -0.8$ for styrene have been adopted as a standard, and the Q and e values for any monomer can be calculated from copolymerization data using the following equations:

$$r_1 = \frac{k_{11}}{k_{12}} = \left(\frac{Q_1}{Q_2}\right)\exp\{-e_1(e_1 - e_2)\}$$

$$r_2 = \frac{k_{22}}{k_{21}} = \left(\frac{Q_2}{Q_1}\right)\exp\{-e_2(e_2 - e_1)\}$$

However, P does not have a practical meaning because consistent k_p or k_{ij} values are available only in limited cases. The Q value of a monomer would increase by

the introduction of a substituent to ethylene in the order $Ph > CN > C{=}C > C{=}O > COOR$, and nonconjugative substituents such as alkyl, OCOR, Cl, and Br, cause considerably smaller increases in the Q value.[157,191]

The moderate captodative effect can facilitate propagation of α-acyloxyacrylates, of which the Q and e values should be discussed separately from those of common monomers.[159,197] The Q–e scheme is undoubtedly one of the most convenient and reliable methods to predict monomer reactivity in free-radical copolymerization. However, the Q and e values calculated from copolymerization with different reference monomers are not in good agreement, suggesting that the substituent effect depends on the monomer pair. Styrene appears to be the most preferable reference monomer for evaluation of Q and e.

The Q values for nuclear substituted styrenes primarily depend on the resonance effect of the substituent. However, the ESR hyperfine coupling constants of the α and β protons of their propagating and benzyl-type radicals are in narrow ranges,[198,199] although an increase in the Q value would signify enhanced delocalization of the unpaired electron, leading to a decrease in the coupling constants. Only a weak dependence of the coupling constants on Q has been observed.[198] The Q and e values can be calculated when $r_1 r_2 < 1$, and a significant steric effect would bias the Q and e values thus calculated.

3.2.2.3 Steric Effects

3.2.2.3.1 Rate of Propagation   Some α-substituted acrylates with substituted methyl groups larger than the ethyl group are polymerizable although the steric hindrance of the bulky substituents is undoubtedly present as evident from the reluctance of α-ethylacrylic ester to homopolymerize.[175] According to the k_p and k_t values summarized in Table 3.2, these substituents exert significant steric hindrance

TABLE 3.2   Absolute Rate Constants for Polymerization of α-Substituted Acrylic Esters and Fumaric Ester at 60°C

Monomer	k_p (L mol^{-1} s^{-1})	$k_t \times 10^{-6}$ (L mol^{-1} s^{-1})	Ref.
Ethyl α-(hydroxymethyl)acrylate	550 (THF)– 1860 (xylene)^a	—	201
Ethyl α-(benzoyloxymethyl)acrylate	990	2.9	203
Methyl α-(pivaroxymethyl)acrylate	230	0.59	164
Methyl α-(benzyloxymethyl)acrylate	182	1.6	200
Methyl α-(2-carbomethoxyethyl)acrylate	19	0.51	167
Methyl α-ethylacrylate	8.6	21	204
Methyl α-[2,2-bis(carbomethoxy)ethyl]acrylate	4.0	0.038–0.042	165
Methyl α-[2,4-bis(carbomethoxy)butyl]acrylate	2.4	0.07	168
Dimethyl itaconate	27,5.2	—, 0.36	205,206
N-tert-Butylmaleimide	100	0.021	207
Dicyclohexyl fumarate	0.60	40	213

^{a} Depends on solvent.

for both propagation and bimolecular termination, and the favorable balance of slow propagation and termination allows polymer formation.[164,165,167,168,200–207] However, the α-substituent should not be too large.[208]

The k_p value for ethyl α-(benzoyloxymethyl)acrylate,[203] which is similar to that of methyl methacrylate, is higher than what might be expected from the bulkiness of the substituent, thus suggesting the k_p value is increased as a result of some other effect. Figure 3.2 shows Arrhenius plots for k_p of common monomers and sterically congested monomers covering the approximate temperature range from 50 to 120°C. The Arrhenius plots for dimethyl itaconate and methyl methacrylate were obtained from the equations given in the respective references.[205,209] The k_p values for methyl methacrylate and diisopropyl fumarate differ by a factor of approximately 3000.[209,210] The plots for α-substituted acrylate monomers appear between the two extreme lines for methyl methacrylate and the fumarate. The two lines are almost parallel with each other, indicating that the intercept on the ordinate governs the magnitude of k_p in this temperature range.

As a mechanistic model of propagation suffering from steric hindrance, it has been proposed that the propagating radical and the monomer would attain the maximum overlapping of the orbitals of the π electron and the unpaired electron at a certain angle between the C_α—C_β bonds of the monomer and the propagating radical.[211] Bond formation is not energetically suppressed, but the possibility that the radical and the monomer approach each other such that bond formation can occur is reduced. Comparison of the k_p values for different alkyl methacrylates by inspection of the Arrhenius plots reveals differences in the A factor. However, an increase in the size of the ester alkyl group of methacrylic esters results in an increase in the k_p value.[212] This increase is much smaller than the decrease in the k_p value with increasing steric hindrance that is displayed in Fig. 3.2.
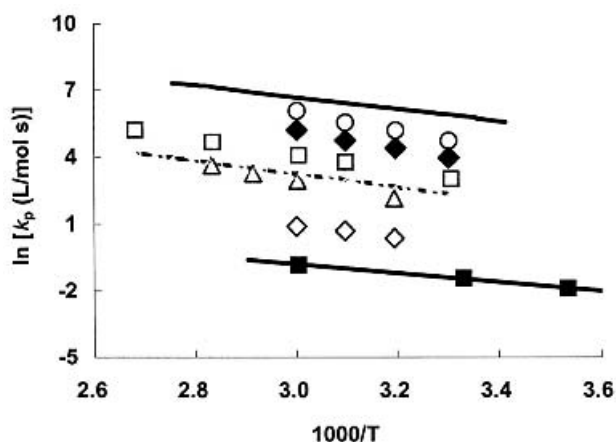
Figure 3.2 Arrhenius plots of k_p for sterically hindered monomers: ——, methyl methacrylate;[209] ○, methyl α-acetoxyacrylate;[159] ◆, methyl α-butyroxyacrylate;[159] □, methacrylonitrile;[139] - - -, dimethyl itaconate;[205] △, methyl α-(2-carbomethoxyethyl)acrylate;[167] ◇, methyl α-[2,4-bis(carbomethoxy)butyl]acrylate;[167] ■, diisopropyl fumarate.[210]

The homopolymerization of dialkyl fumarates[210,213,214] and N-substituted malei-
mides[215–217] are characterized by steric hindrance and the favorable balance
between slow propagation and slow termination as can be seen in Table 3.2. Crotonic
ester, which is usually classified as a nonpolymerizable monomer because of the
steric hindrance of the β-methyl group, may yield homopolymer when termination
is effectively suppressed by a bulky ester alkyl group.[218] Although a similar balance
arising from small k_p and k_t values is observed in the polymerization of macromo-
nomers,[219–225] no acceptable rationalization for the decrease in the rate constants is
available. If the Arrhenius parameters for k_p of macromonomers exhibit essentially
the same tendency as those in Fig. 3.2, it can be concluded that steric hindrance in
the propagation step when a resonance-stabilized radical center is surrounded by
polymer chains as substituents is the cause of the low values of k_p.

Propagation of sterically congested monomers involves the propagating radical
of which the radical center surrounded by the substituents and the monomer bearing
the bulky substituents both contribute to the steric hindrance in the propagation step.
The monomer reactivities, $1/r_1$, toward polystyrene and poly(methyl methacrylate)
radicals can be calculated from the monomer reactivity ratios for the copolymeriza-
tions with styrene and methyl methacrylate (M_1) as summarized in Table 3.3.

Most of the sterically congested monomers in Table 3.3 exhibited higher re-
activities than methyl methacrylate toward polystyrene radicals because of the
electron-withdrawing characters of the substituents bound to the α-methylene group
and the carboalkoxy group. The smaller $1/r_1$ values than those for methyl methacry-
late toward poly(methyl methacrylate) radicals in Table 3.3 can be accounted for by

**TABLE 3.3   Monomer Reactivity Ratios for Polymerization of Styrene or Methyl
Methacrylate (M_1) with Sterically Congested Monomer (M_2) at 60°C**

	M_1 = Styrene			M_1 = Methyl Methacrylate			
M_2	r_1	r_2	$1/r_1$	r_1	r_2	$1/r_1$	Ref.
Methylmethacrylate	0.52	0.46	1.92	1.00	1.00	1.00	188
Ethyl α-(benzoyloxymethyl)-acrylate	0.30	0.27	3.70	—	—	—	203
Methyl α-(methoxymethyl)-acrylate	0.42	0.69	2.38	1.20	0.52	0.88	162
Methyl α-(acetoxymethyl)-acrylate	0.34	0.19	2.94	0.91	0.24	1.10	163
Methyl α-(benzyloxymethyl)-acrylate	0.42	0.29	2.39	—	—	—	200
Methyl α-(2-carbomethoxyethyl)-acrylate	0.69	0.18	1.15	2.21	0.44	0.45	166
Methyl α-ethylacrylate	0.82	0.21	1.22	2.23[a]	0.14[a]	0.45	188,204
Methyl α-[2,2-bis-(carbomethoxy)ethyl]acrylate	0.58	0.09	1.72	3.70	0.04	0.27	28

[a] M_1 = ethyl methacrylate.

more significant steric hindrance to addition of poly(methyl methacrylate) radicals. However, the differences between the largest and smallest values of $1/r_1$ of the monomers toward both polymer radicals, less than a factor of 3–4, are much smaller than the differences in the values of k_p given in Table 3.2. The homopolymerization of α-(substituted methyl)acrylates is subject to more severe steric hindrance arising from the substituent of the monomer and the radical in comparison to attack of polymer radicals of styrene and methyl methacrylate.

3.2.2.3.2   Tacticity and Steric Structure   The structure of the radical center of the propagating radical appears to be a shallow pyramidal inverting readily, and no decisive factor to discriminate between above and below the pyramid can be anticipated. The monomer has close to a planar structure with respect to the reacting carbon–carbon double bond, and tacticities of radical polymers from common monomers are usually close to that of random propagation or that of slightly prevailing syndiotactic propagation. It is known that methyl methacrylate yields poly(methyl methacrylate) consisting predominantly of syndiotactic triad or *rr* structure, and that the syndiotacticity increases with decreasing temperature.[226] The tacticity of the polymer from ω-methacryloyloxyethyl polystyrene macromonomer was examined after removal of the polystyrene chain followed by methyl esterification to obtain poly(methyl methacrylate).[227] The tacticity of the resultant poly(methyl methacrylate) was similar to that obtained from polymerization of methyl methacrylate, showing that the polymer chains surrounding the radical center do not have any significant effect on the stereochemistry of propagation.

   Detailed studies revealed nearly complete isotactic propagation of triarylmethyl methacrylates, particularly phenyldibenzosuberyl (**16**) and pyridyldibenzosuberyl methacrylates, at room temperature or above.[228,229] The isotacticity of these polymers (>99%) has been noted to be as high as for anionically prepared polymers. Almost completely isotactic polymer (*mm*, 98.1; *mr*, 1.6; *rr*, 0.3%) of triphenylmethyl methacrylate (**17**) has been obtained at higher temperature and a lower monomer concentration because these conditions facilitate formation of the more stable structure of the propagating radical.[230] In contrast to the case of triphenylmethyl methacrylate, the tacticity of the polymers from methyl methacrylate and phenyldibenzosuberyl methacrylate was not affected by changes in the reaction conditions. In the case of methyl methacrylate, no configurational stable structure of poly(methyl methacrylate) exists, and the configuration of poly(DBSBA) is already fixed to yield highly isotactic polymer.

16   **17**   **18**   **19**
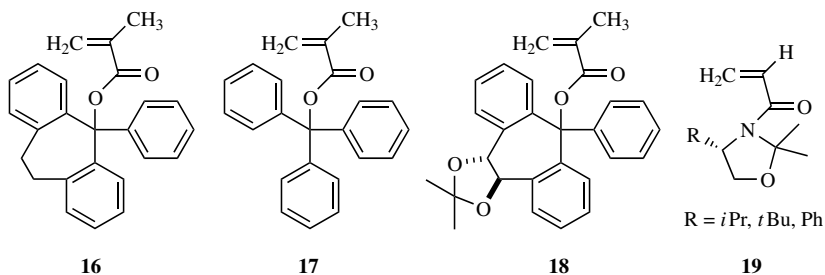
Optically active polymers of triarylmethyl methacrylates having an excess of single-handed helicity can be prepared using chiral initiators or chiral chain transfer agents. Based on GPC data, it was strongly suggested that helix-sense selection takes place during primary radical termination.[229–231] The polymerization of **18** gave polymer with an almost completely isotactic structure regardless of the enantiomeric excess (e.e.) of the monomers, and enantiomer selection during its polymerization has been observed.[232] Compound **16** can be polymerized via an asymmetric mechanism using a chiral Co(II) complex, probably as a result of some interaction between the Co complex and the propagating radical.[228,233] The resultant polymer was optically active and contained a completely single-handed helical structure. The Co complex was also employed for the polymerization of N-substituted maleimides to give optically active polymers of which chiroptical properties are ascribed to the configurational chirality of the main chain.[234] Polymerizations of N-phenylmethacrylamide,[235] N,N-disubstituted acrylamides,[236] fluoroalkyl acrylate,[237] α-(alkoxymethyl)acrylate,[238] and fluorine-containing vinyl ester[239] have been studied to examine the structural effect of the substituent in relation to the tacticity of the polymers formed.

Polymerization of acrylamide having a chiral auxiliary group such as in **19** as the substituent has been shown to control the configuration of the polymer main chain. A strong tendency to maintain the coplanarity of the carboamido group with the carbon–carbon double bond and the radical center is the dominant factor for the control of the configuration of the α-carbon in the main chain. The addition of the radical to the monomer is effectively controlled to yield highly isotactic polymer (diad isotacticity >99%) as a result of facial selectivity in the propagation step (Chapter 13).[240]

The steric interaction between the monomer and the nearest terminal unit is the dominant factor regulating the stereochemistry of propagation, and the resultant isotactic polymer would consist of carbons with the same configuration (chiral auxiliary controlled polymerization).[240–244] Interestingly, the polymerization of acrylamide with a chiral auxiliary group was found to exhibit higher selectivity of the rr structure than telomerization.[241] Chiral auxiliary control is also effective in alternating copolymerization.[243] When the chiral auxiliary of acrylamide has a carbonyl group, interaction of the carbonyl groups in penultimate and penpenultimate units of the propagating radical prefers rr configuration.[244]

3.2.2.4   Medium Effect   Although solvent effects in radical reactions are usually much less significant than for ionic reactions, the k_p values of vinyl acetate and vinyl benzoate have been known to significantly decrease in aromatic solvents depending on the nuclear substituent.[245,246] The k_p value became smaller with increasing electron-withdrawing character of the substituent. The k_p values in cyanobenzene were smaller than in benzene by factors of 11 and 7 for vinyl acetate and benzoate, respectively. These tendencies were explained by complex formation of the electron-donating propagating radicals with the solvent resulting in reduced reactivities. Furthermore, the solvent effects on the k_p values of various monomers without strong interaction of their substituents and solvents have been examined and

discussed.[203,217,245,247–254] Most of the solvent effects observed are minor, but not negligible, and can be explained by interaction of the solvent with the propagating radical. The k_p values for the polymerizations of methacrylic and acrylic acids in water are significantly affected by the solvent and monomer concentrations.[255–257] The solvent effect on the polymerization of macromonomer can be accounted for by the solubility of the polymer in the solvent.[222]

Supercritical carbon dioxide ($scCO_2$) and hybrids with organic media have also been employed for polymerization of common monomers. Smaller k_p values than for the corresponding bulk polymerizations were obtained when the local monomer concentration for propagation was decreased by lower monomer solubility in $scCO_2$.[258–262] In the case of styrene (nonpolar) and vinyl acetate (yields polymer soluble in $scCO_2$), the same k_p values were obtained in bulk and in $scCO_2$,[263] suggesting that in these cases the local monomer concentration may not be affected by the $scCO_2$.

A Lewis acid can coordinate to a site of a Lewis base in a monomer, and different reaction behaviors of the complexed monomer and the propagating radical are anticipated.[66,264,265] The polymerizations of 1 : 1 host guests complexes of methyl β-cyclodextrin with methyl methacrylate and styrene were initiated in water, a significant acceleration of the polymerizations was observed. The polymers were produced by unthreading of the complexes.[266–270] Cyclodextrin in the emulsion polymerization of hydrophobic monomers has been noted to facilitate the transfer of monomer from droplet to the particle through the aqueous phase.[271]

The effects of solvents on the tacticity of the polymers from **17** have been reported.[230] In the case of fluoroalcohols, the stereochemistry of the polymerizations of vinyl esters was affected to different extents depending on the structure of the acyl group.[272–275] The polymerization of methacrylates and vinyl acetate gave syndiotactic-rich polymer up to $rr = 50\%$ and $r = 70\%$, and heterotactic- and isotactic-rich polymers were obtained from different vinyl esters. Hydrogen bonding between the fluoroalcohol and the ester groups of the monomer and the radical has been proposed.

Although bimolecular termination is suppressed in viscous media such as in the high conversion range in bulk polymerization, the limiting conversion observed in bulk polymerizations suggests that k_p and/or the initiator efficiency also decrease to an extremely small value at the final stage of polymerization. In the case of the bulk polymerization of methyl methacrylate, both the k_p value and the initiator efficiency decrease dramatically at high conversion in the solidified polymerization mixture at 60°C.[131,132,276]

3.2.3 Reactions of Propagation

3.2.3.1 Cyclopolymerization and Ring-Opening Polymerization 1,6-Dienes containing two nonconjugated low- or nonhomopolymerizable carbon–carbon double bonds can form polymer consisting of the repeating units involving a 5- or 6-membered ring without the occurrence of crosslinking. In cyclopolymerization, intramolecular cyclization followed by intermolecular addition of the cyclized

X = O, C(CN)$_2$, C(CO$_2$R)$_2$

20
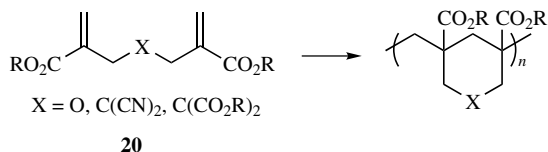
Scheme 3.8

radicals is faster than the homopropagation of the individual carbon–carbon double bonds.[277] *N*-Substituted dimethacrylamide is a typical cyclopolymerizable monomer, and the nonpolymerizability of each *N,N*-disubstituted methacrylamido group results in the formation of the 5-membered cyclic structure involving head–head linkage instead of the more commonly formed head–tail linkage.[278,279] When one of the carbon–carbon double bonds is too severely hindered to cyclopolymerize, a linear polymer with pendant double bonds is formed.[280] α-Hydroxymethylacrylate and α-halomethylacrylate have been employed as precursors of various 1,6-dienes (**20**) for cyclopolymerization. For example, an ether dimer of the hydroxymethylacrylate (X = O in Scheme 3.8)[281,282] undergoes cyclopolymerization when the ester alkyl groups of the dimer are sufficiently large to suppress the homopolymerization of each α-(substituted methyl)acryloyl group leading to the formation of a 6-membered cyclic unit by intramolecular head–tail addition in propagation (Scheme 3.8).

Additional cyclopolymerizable monomers have been derived.[283–285] Allyl compounds can homopolymerize as constituents of 1,6-dienes such as *N*-alkyl-*N*-allyl-2-(methoxycarbonyl) allylamines in cyclopolymerization, although they seldom homopolymerize separately, and 5- or 6-membered cyclic units are formed as confirmed by NMR spectroscopy.[286]

Cyclopolymerization is one of the most efficient ways to achieve structural control in radical polymerization. The copolymerization of a diacryloyl monomer involving the chiral template, 3,4-*O*-cyclohexylidene-D-mannitol, may result in the formation of new stereogenic centers and possibly four different stereoisomers.[287] Although addition of the propagating radical from the reference monomer exhibited low selectivity, the intramolecular addition to the acrylate moiety of the difunctional monomer to form a cyclic unit was highly stereoselective, resulting in a copolymer exhibiting significant optical activity.[288] In the case of a dimethacryloyl monomer bound to the optically active tartarate template, the poly(methyl methacrylate) obtained by hydrolysis followed by methylation exhibited high isotacticity suggesting helix formation.[289] The effect of complex formation with β-cyclodextrin on asymmetric cyclopolymerization has also been studied.[290]

Ring-opening polymerization is accompanied by lower shrinkage than normal vinyl polymerization, and is comparable with polycondensation as a polymerization process to form main chains involving hetereoatoms. The advantages of ring-opening polymerization over polycondensation include the fact that no small molecules are formed and milder reaction conditions. Polymerizations of 2-methylenedithiacy-

cloalkane, 2-methylene-1,3-dioxepane, vinyl cyclopropane, and other monomers undergo polymerization consisting of addition to the carbon–carbon double bond followed by ring opening of the cyclic radical to the linear radical.[161,291–295] A radical directly attacks bicyclobutanes[296] and the S—S bond involved in cyclic structure,[297,298] leading to ring-opening polymerization. The driving force for the ring opening polymerization of these monomers and some other monomers has been reviewed.[299]

3.2.3.2 *Isomerization during Propagation*

Common monomers such as styrene and methyl methacrylate give polymer consisting of the corresponding monomer units connected by head–tail linkage. However, propagating radicals from some monomers prefer to intramolecularly react with the substituent to shift the radical center to the side chain. If the newly formed radical smoothly adds to the carbon–carbon double bond of the monomer, the main chain of the resulting polymer involves the moiety from the side chain.[300–304] As an example, the polymerization of 3,3-bis(ethoxycarbonyl)propyl vinyl ether (**21**) via an addition–abstraction mechanism accompanying isomerization during propagation is shown in Scheme 3.9; the isomerisation results in 1,5-shift of the radical.[303]

During polymerization of vinyl chloride, the highly reactive poly(vinyl chloride) radical abstracts hydrogen through backbiting leading to C_4 branch formation. If addition of the resultant radical of backbiting to vinyl chloride is followed by backbiting, two C_2 branches might be formed.[305,306] The polymerization of acrylic esters tends to be accompanied by the formation of midchain radicals primarily by backbiting.[154,155] The lower reactivity and β-fragmentation of the midchain radical would affect the overall rate of polymerization and main-chain branching.[307,308] Copolymerizations of acrylic ester with ethylene and vinyl acetate exhibited rapid backbiting to the acrylate unit incorporated in the respective copolymers.[309,310]

3.2.3.3 *Chain Extension and Block Copolymer Formation*

Chain transfer is employed in order to reduce the degree of polymerization and/or to introduce a certain end group as described in Section 3.3.4. If polymerization is carried out under the conditions to minimize the contribution of bimolecular termination as an end forming reaction, the end group introduced may be used for further reaction including extension of chain and block copolymer formation.

Scheme 3.9

$$CH_3COS \left(CH_2-CH \right)_n H \nearrow HS \left(CH_2-CH \right)_n H$$

Scheme 3.10 (with structures):

CH₃COS–(CH₂–CH)ₙ–H with OCOCH₃ substituent, yielding:
- HS–(CH₂–CH)ₙ–H with OH substituent
- HS–(CH₂–CH)ₙ–H with OCOCH₃ substituent
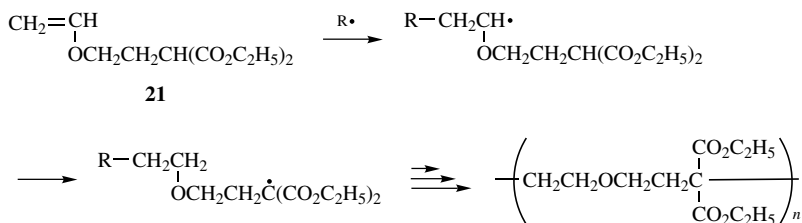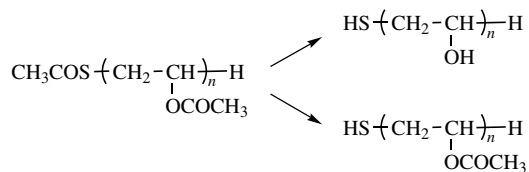
Scheme 3.10

Mercaptans (RSH) function as effective chain transfer agents yielding polymer bearing RS— and H— as the α and ω-end groups, respectively. Although these groups are not highly reactive, thioacetic acid instead of mercaptan may result in two types of polymers having the HS— end group through hydrolysis of the thioester linkage depending on reaction conditions as shown in Scheme 3.10.[311]

Polymeric mercaptan admitted to the polymerization mixture is involved as a chain transfer agent to produce block copolymer through reinitiation by the macrothiyl radical. Trichloromethyl end groups, introduced by chain transfer to carbon tetrachloride or bromotrichloromethane, can be employed for further reaction with $Mn(CO)_{10}$, $Mo(CO)_6$, ferrocene, cobaltcene, or other compounds to generate macroradicals for block copolymer formation or chain extension.[312]

Iniferters (Section Chain Transfer) can form photochemically or thermally dissociable labile bonds to the polymer end. Dissociation of the C—S bond, which is introduced using tetramethylthiuram disulfide in the presence of monomer different from the polymer chain bound to the thiocarbamoyl group [—SC(S)NR₂], can give A–B block copolymer. The block copolymer possesses a dissociable C—S bond, and photochemical dissociation of this bond can be utilized to form A–B–C block copolymer. Polyfunctional iniferter such as **22**–**24** have been employed to prepare branched, star polymer and graft copolymers.[43,313–315]

Structures **22**, **23**, **24**

22   **23**   **24**
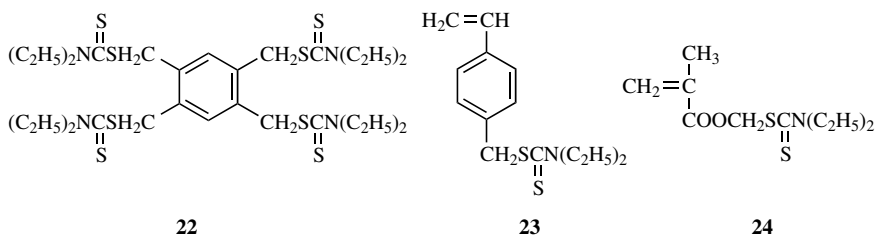
Poly(butyl acrylate) bearing a dithiocarbamate ω-end group can generate active propagating radicals, leading to increased molecular weight until reaction with the dithiocarbamyl radical results in temporary loss of activity.[316]

Some substituted tetraphenylethanes dissociating into the substituted diphenylmethyl radical initiate the polymerization of methyl methacrylate and styrene. The substituted diphenylmethyl radical, which may be less reactive than the propagating radical from conventional monomers such as methyl methacrylate and styrene, participates in primary radical termination. The bond between the poly(methyl

methacrylate) chain end and the substituted diphenylmethyl group cleaves to give an active propagating radical to extend the polymer chain at polymerization temperature.[35,36,44,46,317] Although primary radical termination introduces the diphenylmethyl group at the ω-end group of polystyrene, no dissociation and chain extension have been confirmed up to 80°C.[44,318]

The unsaturated end group can be introduced by catalytic chain transfer of methacrylic ester (Chapter 12) or addition–fragmentation chain transfer of α-(substituted methyl)acrylate (Section Chain Transfer).[157,161] Although poly(methyl methacrylate) radicals can add to this carbon–carbon double bond, the adduct radical rapidly expels the polymer radical through β-fragmentation. Initiation by the polymer radical expelled may yield block copolymer.[319] The polymerizations of methyl methacrylate and styrene in the presence of methyl α-bromomethylacrylate, functioning as an effective addition fragmentation chain transfer agent, gave low molecular weight polymers bearing the $CH_2{=}C(CO_2CH_3)CH_2{-}$ end group. An increase in conversion leads to an increase in the molecular weight of the polystyrene bearing the unsaturated end group because of the reaction of the end group with the polymer radical. However, the molecular weight of poly(methyl methacrylate) remained almost constant irrespective of conversion, showing no contribution of the polymer chain bound to the end group.[320]

3.2.3.4 *Crosslinking*

3.2.3.4 Crosslinking   A crosslinked polymer consists of a three-dimensional network, formed by the homo- or copolymerization of a system where at least one of the monomers has two or more free-radically polymerizable double bonds.[321–323] Typical monovinyl/divinyl systems include styrene/divinyl benzene and methyl methacrylate/ethylene glycol dimethacrylate. Multivinyl compounds such as unsaturated polyesters,[324] usually containing approximately 10 unsaturations per chain, also find widespread commercial application. Bulk polymerization of multifunctional monomers leads to polymers with high crosslink density that exhibit high mechanical strength and good resistance to solvent penetration.

A large body of experimental evidence suggests that the development of the polymer network during the copolymerization of a monovinyl and divinyl monomer proceeds in a nonideal manner,[325–327] deviating from the classical Flory–Stockmeyer theory,[328,329] which assumes that all polymerizable double bonds in the system exhibit identical and conversion-independent reactivities. This is clearly manifested in the underestimation of the level of conversion at the gel point by the Flory–Stockmeyer theory. This discrepancy is believed to have originated in (1) intramolecular cyclization,[330,331] (2) reduced reactivity of pendant unsaturations, (3) intramolecular crosslinking, and (4) microgelation—phenomena that are not accounted for in the Flory–Stockmeyer theory. For the system methyl methacrylate/ethylene glycol dimethacrylate, it has been reported that approximately 30% of the pendant vinyl groups take part in cyclization reactions.[331] Several studies have aimed at evaluation of the magnitude of the reduction in reactivity of the vinyl groups on incorporation in the polymer network.[327,332,333] For the system styrene/divinylbenzene, the reactivity ratio of pendant to monomer vinyls has been reported to decrease with increasing divinylbenzene content, and reach a value as low as

approximately 0.05 at 12% divinylbenzene content.[333] This suggests that the bulkiness of the chain attached to the pendant vinyl reduces its reactivity by steric hindrance.[326,327] It follows that if the reactivity of the pendant vinyl is low, crosslinking will occur only late in the reaction. Different reactivities of the double bonds of the monomers and pendant unsaturations result in conversion dependence of the degree of crosslinking and the composition of the network. The deviation from classical theory increases with the amount of divinyl compound in the feed in a monovinyl/divinyl system, and at low divinyl monomer contents, the traditional predictions approach the experimental values. In the case of the copolymerization of methyl methacrylate with 0.03% butylene dimethacrylate in the presence of a small amount of the chain transfer agent lauryl mercaptan, the gel point occurs at approximately 70% conversion, and there is only a 5% discrepancy between the Flory–Stockmeyer theory value and the actual value.[334] These nonidealities lead to a crosslinked network of inhomogeneous nature, manifested, for example, by the existence of multiple glass transition temperatures[335,336] and residual unreacted pendant vinyl groups,[337,338] and are undesirable features as they lead to a reduction in the strength of the material.

3.2.3.5 _Surface Grafting_ On many occasions in materials technology it is desirable to modify polymer surfaces, such as by transforming the usually hydrophobic surface exhibited by most industrially produced polymers into a hydrophilic one. This can be achieved by a variety of means,[339] one of which is surface grafting.[340] Most polymeric surfaces are chemically inert, and for grafting to take place, reactive groups must to be introduced, or radicals have to be generated on the polymer surface. Within the field of surface grafting, there are several vastly different techniques available: direct chemical methods,[340–342] photoinitiation using a sensitizer such as benzophenone,[343–345] ozonization,[346] use of γ-rays,[340,347] and plasma treatment.[340,348]

The techniques mentioned have the basic principle of operation in common; generation of radicals that are attached to the polymer to be grafted on, followed by polymerization with vinyl monomers (only surface grafting involving radical processes is discussed here). The methods above mainly differ in the sense that the radical generation processes are different. An example of direct chemical modification is the treatment of polymers such as polypropylene, polystyrene, polyacrylonitrile, and polyamide with an oxidizing agent such as potassium peroxydisulfate, giving hydroxylated polymer.[341] Subsequent application of a ceric salt (Ce^{4+}) redox initiation system yields oxygen-centered radicals attached to the polymer, which can initiate polymerization of vinyl monomers. In the application of photoinitiation, the photoinitiator is usually adsorbed on the polymer surface, where it initiates grafting by hydrogen abstraction from the polymer in its excited state, creating grafting points.[349–352] An example is the grafting of acrylamide onto a copolymer of styrene (ethylene-_co_-butene)styrene, which proceeded under irradiation at 350 nm in contact with an aqueous solution of monomer and a water-soluble derivative of benzophenone as photoinitiator.[353]

Pretreatment of polymer surfaces with ozone results in formation of hydroperoxides that decompose under UV irradiation, thereby initiating grafting in the presence of suitable vinyl monomers.[354,355] Grafting processes can also be induced by irradiation with γ-rays and electron beams, either in a one-step process where grafting and radical generation takes place simultaneously, or by employing irradiation pretreatment.[340,347] Cold plasma treatment can be employed for surface modification, introducing reactive groups that can be grafted and the generation of radicals on the polymer surface. This is a two-step process, where plasma treatment is followed by a grafting step in the absence of plasma.[340,348,355]

3.3   CHAIN TRANSFER

3.3.1   General Features

Chain transfer in radical polymerization is the reaction of a propagating radical ($P_i\cdot$) with a transfer agent (T) to yield dead polymer (P_i) and a small radical (T·) as shown by reactions (a) and (b) in Scheme 3.11.

The radical center is transferred from the polymer end to another molecule, and the number of unpaired electrons thus remains unchanged. By comparing the value of the rate constant for propagation (k_p) with k_{tr} and k_{ri}, ideal chain transfer can be identified when $k_{ri} \gg k_p$ and k_{tr} is sufficiently large.[312,356]

Figure 3.3 shows schematically ideal chain transfer in which the kinetic chain length is identical in the presence and absence of T. The degree of polymerization decreases and the number of polymer molecules increases as a result of chain transfer. Furthermore, a decrease in the degree of polymerization by chain transfer should not be confused with the effect of a decrease in monomer and increase in initiator concentration, both of which cause a reduction in the kinetic chain length, leading to a decrease in degree of polymerization. The contribution of initiation and bimolecular termination as end-forming reactions are reduced by chain transfer. The fragments from T are bound as α- and ω-end groups instead of the end groups otherwise resulting from initiation and termination. However, an increase in the efficiency of introduction of the end group from T always brings about a decrease in chain length, and an efficiency of 100% cannot be attained because of premature bimolecular termination.

Chain transfer can occur to all the substances present in a polymerization system, and T can be employed to effectively reduce the molecular weight or to introduce designated end groups. Allylic compounds ($CH_2{=}CHCH_2X$) are usually reluctant to homopolymerize because a highly reactive radical may be formed by addition to the

$$P_i\cdot \ + \ T \ \xrightarrow{\ k_{tr}\ } \ P_i \ + \ T\cdot \qquad (a)$$

$$T\cdot \ + \ M \ \xrightarrow{\ k_{ri}\ } \ P_i\cdot \qquad (b)$$
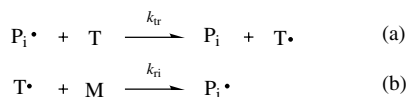
Scheme 3.11
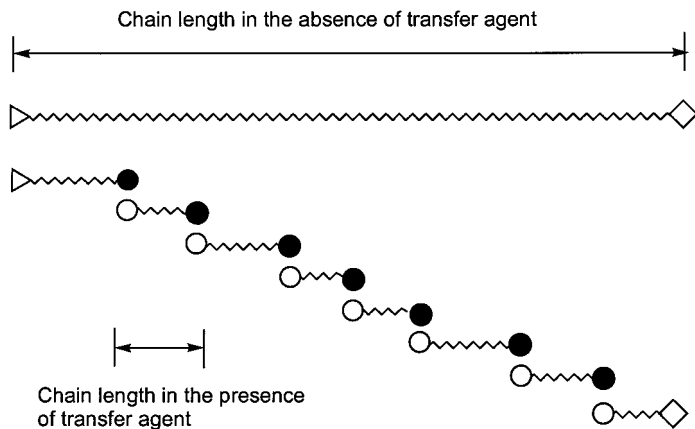
Figure 3.3 Schematic description of chain transfer: ▷ and ◇ denote end groups in the absence of transfer agent, and ○ and ● denote end groups in the presence of transfer agent. The polymer obtained in the presence of T is also polydisperse.

allylic double bond. These highly reactive radicals tend to abstract hydrogen from the methylene group adjacent to the double bond to give allylic radicals stabilized by delocalisation of the unpaired electron. The abstraction reaction competes well with propagation, resulting in only short polymer chains. The process of catalytic chain transfer, which is much more effective than conventional chain transfer to monomer, particularly to α-methyl vinyl monomers, will be described in Chapter 12.

3.3.2   Chain Transfer Constant

The effectiveness of T to reduce the degree of polymerization is given by the chain transfer constant (C), which is the ratio of k_{tr} (the overall rate constant for chain transfer) to k_p: C_I, C_M, C_P, and C_T denote C of initiator, monomer, polymer, and transfer agent, respectively. C_T is given by the following equation, and C_I, C_M, and C_P are expressed in the same way:

$$C_T = \frac{k_{trT}}{k_p}$$

The Mayo equation [Eq. (3.10)] can be employed to determine C_T based on the change in the degree of polymerization on addition of T:

$$\frac{1}{P_n} = \frac{1}{P_{n0}} + \frac{C_T[T]}{[M]} \tag{3.10}$$

where P_n and P_{n0} are the degrees of polymerization of the polymers obtained in the presence and absence of T, respectively, and $1/P_{n0}$ is given by

$$\frac{1}{P_{n0}} = \frac{k_t R_p}{k_p^2 [M]^2} + \frac{C_I [I]}{[M]} + C_M + \frac{C_P [P]}{[M]}$$
$$= \frac{R_t}{R_p} + \frac{R_{trI}}{R_p} + \frac{R_{trM}}{R_p} + \frac{R_{trP}}{R_p} \tag{3.11}$$

where R_p denotes the overall rate of polymerization, and k_t is the rate constant for termination. If $P_{n0} \gg P_n$ [Eq. (3.10)], the value of C_T can be calculated from the dependence of P_n on [T]/[M].

In order for the Mayo equation to be applicable, the propagating radical concentration and R_p must not change on the addition of T to the system. When R_p is changed in the presence of T, the Mayo equation might not give a correct C_T value. However, R_p is usually lower in the presence of T, and the determination of C_T is therefore normally carried out using low concentrations of T. If the radicals resulting from chain transfer reinitiate new chains slowly, R_p may decrease. A second requirement is that the rate constants for the elementary reactions must remain constant irrespective of the chain length of the propagating radicals. Particular attention is required when the C_T determination is carried out under conditions yielding oligomeric or shorter products. Although it has been reported that the values of k_p for the first few propagation steps are larger than the global k_p value,[138–142] any dependence of chain transfer reactivity on chain length has not been systematically investigated.

If the polymer ω-end is predominantly formed by chain transfer or disproportionation, the chain length distribution (CLD) is related to C_T as in[133,358–361]

$$\lim_{i \to \infty, [I] \to 0} p_i \propto \exp\left\{ -\frac{k_{trM}[M] + k_{trT}[T]}{k_p} \right\}$$
$$\frac{d \ln p_i}{di} = -\{C_M + C_T/[M]\} \tag{3.12}$$

where k_{trM} and k_{trT} are the rate constants for transfer to monomer and to T, respectively. p_i denotes the number fraction of chains of length i. Comparisons of the Mayo and the CLD procedures have shown that they yield essentially equivalent C_T and C_M values.[362,363] Cross-chain transfer rate constants of copolymerizations have also been estimated using more complex procedures.[364,365] When the molecular weight of T is similar to that of the resultant polymer, the Mayo equation cannot be used since the molecular weight change arising from chain transfer cannot be accurately estimated. Although C_T determination based on end-group quantification by MALDI-TOF has been attempted, this procedure has not yet been established.[366]

Except for the case when $C_T = 1$, M and T will be consumed at different rates as the polymerization proceeds leading to conversion dependence of [T]/[M]. Consequently, C_T should be obtained at the early stage of the polymerization when [T]/[M]

can be approximated by $[T]_0/[M]_0$. The concentration of T as a function of conversion (x) at constant $[M\cdot]$, is given by Eq. (3.13):[367]

$$[T]_x = [T]_0(1-x)^{C_T} \tag{3.13}$$

$$\frac{[T]_x/[M]_x}{[T]_0/[M]_0} = (1-x)^{C_T-1} \tag{3.14}$$

The ratio $[T]/[M]$ is dependent on C_T according to Eq. (3.14), where the subscripts 0 and x denote the initial concentrations and the concentrations at fractional conversion x. The molecular weight of the polymer formed in the presence of T is a function of $[T]/[M]$ as already given by Eq. (3.10). Equation (3.15) which takes the change in $[M]/[T]$ with conversion into account, can be employed to calculate chain transfer constants at nonzero conversion levels:[367]

$$\ln\left\{1 - \frac{[M]_0 x}{[T]_0} \cdot \left(\frac{1}{P_n} - \frac{1}{P_{n0}}\right)\right\} = C_T \ln(1-x) \tag{3.15}$$

3.3.3   Chain Transfer to Initiator, Monomer, Polymer, Solvent, and Transfer Agent

Chain transfer to peroxide initiators, usually by induced decomposition, might accelerate the generation of initiating radicals. Chain transfer to AIBN has been detected in styrene polymerization, whereas chain transfer to aliphatic azo initiators is believed to be negligible.[312]

The photosensitizer tetraalkylthiuram disulfide (**25**) is feasible to attack by propagating radicals at the S—S bond, resulting in polymer with an $R_2NC(S)S$ group at the ω-end and the radical $R_2NC(S)S\cdot$. The thiyl radical would either reinitiate a new chain or react with a propagating radical, leading to polymer with $R_2C(S)S$ groups at the α- and ω-terminals.[43,368,369] The C—S bond at the ω-chain end in photochemically dissociable, and the regenerated macroradical can propagate further until coupling with a thiyl radical or another propagating radical (minor pathway).[370] The cycle of dissociation of the C—S bond, propagation, and the C—S bond formation would be repeated. By generating the relatively stable thiyl radical, **25** functions as initiator, T, and terminator simultaneously, and is known as an *iniferter* as shown in Scheme 3.12.[43,369]

The reversible reaction between propagating radicals and the thiyl radicals leads to a reduction in the contribution of irreversible bimolecular termination as an end-forming event. The main process leading to loss of activity (i.e., formation of dormant species) of the propagating radicals may be reaction with thiyl radicals.

The C_M values of several monomers have been determined by use of the CLD procedure. The C_M for styrene has been shown to involve chain transfer to the Mayo dimer of styrene produced in the course of thermal initiation.[360] Although Eqs. (3.12) and (3.15) gave C_M values for methyl methacrylate and styrene
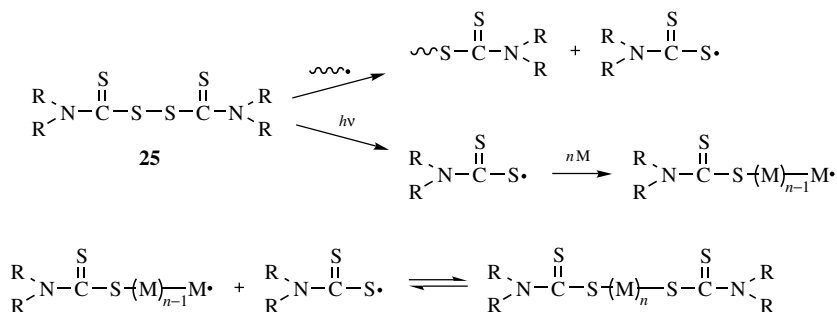
Scheme 3.12

polymerizations in agreement with those already known,[371] the value determined for *tert*-butyl acrylate was smaller than previously reported.[372] Determination of k_p for acrylic esters employing the technique of pulsed laser polymerization has resulted in considerable scatter among the reported values, and one of the reasons is considered to be chain transfer occurring during the polymerization.[373,374] The time interval between pulses needs to be sufficiently short in order to minimize the influence of chain transfer as an end-forming reaction. However, the exact nature of the chain transfer reaction has not been elucidated, and the reactivity of the reinitiating species has not been estimated.

The Mayo equation cannot be employed for the evaluation of C_P. Polymerization in the presence of polymer yields a mixture of the polymer initially present and the polymer formed, and the increase in M_n as a result of chain transfer cannot be accurately estimated. The frequency of chain transfer to polymer can however be determined by structural analysis of the polymer, provided the units arising from the chain transfer process can be identified and quantified.[375] A typical example is the evaluation of chain transfer to the side chain of poly(vinyl acetate) based on a decrease in M_n after cleavage of the side chains by saponification. Detailed structural analysis of poly(vinyl acetate) by ^{1}H and ^{13}C-NMR has revealed that hydrogen abstraction from the acetyl groups is the predominant chain transfer mechanism and abstraction from the methine groups of the main chain leads to a small amount of branching.[376,377]

The polymerization of acrylic ester is characterized by a rapid increase in molecular weight with conversion and crosslinking, probably related to the presence of midchain radicals. The midchain radical of acrylic acid and a linear tetramer have been detected by ESR spectroscopy using the flow technique with a monomer concentration low enough to prevent the formation of high polymer.[378] The midchain radical, generated by hydrogen abstraction of the α-hydrogen with respect to the carboalkoxy group, has been detected by ESR spectroscopy during the solution polymerization of acrylic esters.[154,155] The midchain radical, which is predicted to be less reactive than the propagating radical,[379] is believed to participate in branching reactions[308,380] and to undergo β-fragmentation.[381–383] Intramolecular hydrogen abstraction by a propagating radical species results in a new radical center

H₂C=CH   ∿CH₂CH−CH₂CH−CH₂CH•
    | | | |
    X   X   X   X

        X
        |
    CH₂CH•   ∿CH₂C•−CH₂CH−CH₂CH₂
    | | | |
∿CH₂C−CH₂CH−CH₂CH₂   X   X   X
    | | |
    X   X   X

        H₂C=CH   ∿CH₂C=CH₂ + •CH−CH₂CH₂
            | | | |
            X   X   X   X
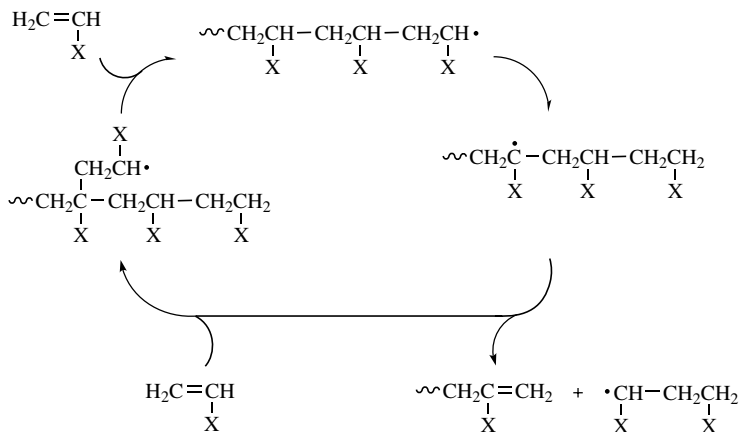
Scheme 3.13

on the same molecule and can therefore not be classified as chain transfer. Further propagation of this species would lead to the formation of a short branch. The reactions of the radicals involved in acrylate ($X = CO_2R$) polymerization are illustrated in Scheme 3.13.

Midchain radicals may be formed by intermolecular hydrogen abstraction from the polyacrylate main chain (Scheme 3.14). This pathway is favored under the conditions of low monomer and high polymer concentration such as during emulsion polymerization where the particles consist of a large amount of polymer and a small amount of monomer, and at high conversion during solution/bulk polymerization.

β-Fragmentation of this type of midchain radical is supported by the observed behavior of the structurally similar propagating radicals of the dimer and the trimer of methyl acrylate [$CH_2=C(CO_2Me)CH_2CH_2(CO_2Me)$ and $CH_2=C(CO_2Me)$-$CH_2CH(CO_2Me)CH_2CH_2CO_2Me$, respectively). However, the ESR spectra of the midchain radical and that during homopolymerization of the methyl acrylate dimer and trimer were observed as three- and five-line spectra, respectively.[154,155,167,168] The apparent three-line spectrum of the midchain radical can be explained by coupling with two of the β-methylene protons among the four, and the remaining two β-hydrogens are close to the nodal plane of the π-orbital because of the conformational requirement to intramolecular hydrogen abstraction (backbiting).[378,384]

A large number of solvents have been subjected to determination of C_T. Conjugated and nonconjugated monomers have C_T values of the order 10^{-5} and 10^{-4},

∿CH₂CH−CH₂CH−CH₂CH∿   ∿CH₂C•−CH₂CH−CH₂CH∿
    | | | | | |
    X   X   X   X   X   X

        ∿CH₂C=CH₂ + •HC−CH₂CH∿
            | | |
            X   X   X
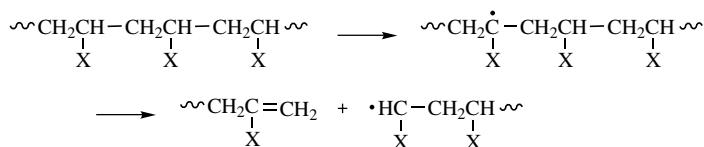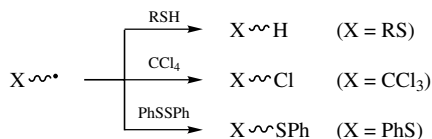
Scheme 3.14

Scheme 3.15

respectively, in most solvents commonly used for polymerization.[385] End-group analysis of the moiety from the solvent by NMR spectroscopy can be used to directly estimate chain transfer to solvent.[386,387] Solvents with large C_T values have been used for telomerization to synthesize oligomers with functional end groups.[388]

Most conventional T, such as mercaptans and carbon tetrachloride, possess labile hydrogen and halogen atoms that are easily abstracted by propagating radicals, with reinitiation occurring by the resulting radicals from these compounds to yield polymers bearing fragments from T (Scheme 3.15). Chain transfer can also proceed via a bimolecular homolytic substitution mechanism;[312] the reaction of polymer radical and diphenyl disulfide is shown as an example.

The C_T values for a variety of T have been compiled.[385] In order to be able to directly compare C_T values for different polymerizations, the difference in k_p must be considered. Although the k_p values for methyl methacrylate and styrene are relatively similar, the C_T value for carbon tetrabromide in styrene polymerization, 1.36, is larger than that in methyl methacrylate polymerization, 2.7×10^{-2}, by a factor of ~ 50.[385] The value of k_{tr} or the C_T value for the reaction of an electron accepting T with poly(methyl methacrylate) radical should be lower than that for reaction with the electron-donating polystyrene radical as a result of the polar effect on chain transfer. The enhancement of the chain transfer reactivity may be caused by a resonance effect to a limited extent because of the opposite influences on the reactivity of T and the reinitiation reactivity. The C_T value for the same compound in vinyl acetate polymerization has been evaluated to be 739,[385] indicating that the poly(vinyl acetate) radical abstracts bromine from carbon tetrabromide at a much higher rate than the radicals of styrene and methyl methacrylate. However, the extraordinary large C_T value observed in vinyl acetate polymerization suggests that chain transfer is more significant during polymerization of nonconjugated monomers.

3.3.4 Addition–Fragmentation Chain Transfer

This type of chain transfer proceeds as shown in Scheme 3.16, where X is Br, SR, SnR$_3$, SO$_2$Ar, and so on, forming a labile allyl–X bond.[160,161,171,172,294,299,320,389–400] The substituent Y is normally CO$_2$R, Ph, CN, and so forth to enhance the reactivity of the C=C toward propagating radicals. According to reaction (a) in Scheme 3.16, CH$_2$=C(Y)CH$_2$X and X may be T· and T, respectively. The activation of the reacting carbon–carbon double bond by Y = CH$_2$SR is not sufficient, and C_T values of the olefinic dithioethers (X = Y = CH$_2$SR) are not as high as those of T bearing conjugative groups.[401] The generalized structure of an addition–fragmentation chain transfer (AFCT) agent (appearing in Scheme 3.16) is a 1,1-disubstituted ethylene.

$$X\text{-}\!\!\sim\!\!\bullet \ + \ CH_2\!=\!\overset{\overset{\displaystyle CH_2X}{|}}{\underset{\underset{\displaystyle Y}{|}}{C}} \ \xrightarrow{\text{addition}} \ X\text{-}\!\!\sim\!CH_2\text{-}\overset{\overset{\displaystyle CH_2X}{|}}{\underset{\underset{\displaystyle Y}{|}}{C}}\bullet \tag{a}$$

$$X\text{-}\!\!\sim\!CH_2\text{-}\overset{\overset{\displaystyle CH_2X}{|}}{\underset{\underset{\displaystyle Y}{|}}{C}}\bullet \ \xrightarrow{\text{fragmentation}} \ X\text{-}\!\!\sim\!CH_2\text{-}\overset{\underset{\underset{\displaystyle Y}{|}}{C}}{}\!=\!CH_2 \ + \ X\bullet \tag{b}$$

$$X\bullet \ + \ CH_2\!=\!\overset{\overset{\displaystyle B}{|}}{\underset{\underset{\displaystyle A}{|}}{C}} \ \xrightarrow{\text{reinitiation}} \ X\text{-}CH_2\text{-}\overset{\overset{\displaystyle B}{|}}{\underset{\underset{\displaystyle A}{|}}{C}}\bullet \ \rightleftharpoons \ X\!\!\left(\!CH_2\text{-}\overset{\overset{\displaystyle B}{|}}{\underset{\underset{\displaystyle A}{|}}{C}}\!\right)_{\!n}\!\!CH_2\text{-}\overset{\overset{\displaystyle B}{|}}{\underset{\underset{\displaystyle A}{|}}{C}}\bullet \quad (\equiv X\text{-}\!\!\sim\!\!\bullet) \ (c)$$
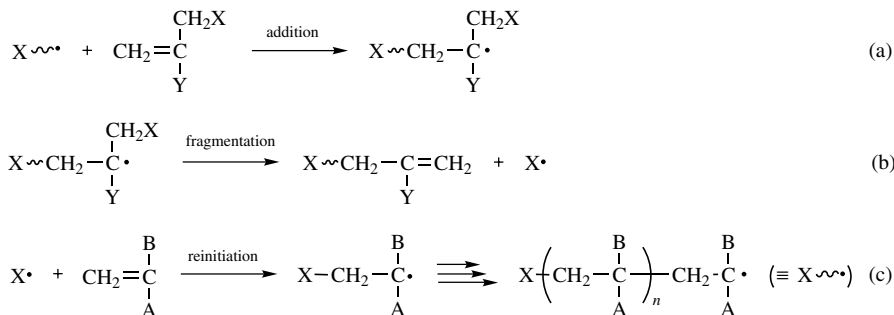
Scheme 3.16

It is believed that significant steric hindrance against propagation may increase the rate of fragmentation relative to that of propagation. The polymer formed in the presence of an AFCT agent will have X and a substituted allyl group ($-CH_2CY\!=\!CH_2$) as α- and ω-end groups, respectively. The introduction of the unsaturated end-group is readily confirmed by ^1H-NMR spectroscopy as the methoxy and methylene protons of the monomeric units adjacent to the end groups and the end group itself exhibit different chemical shifts (ppm). This is illustrated below for poly(methyl methacrylate) bearing fragments from methyl α-(bromomethyl)-acrylate.[171]
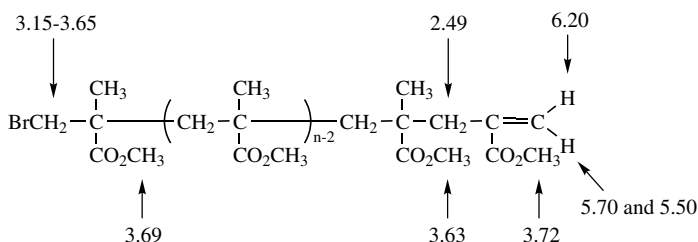
The chemical shifts of the unsaturated methylene protons depend on the adjacent monomeric unit. Copolymers prepared in the presence of chain transfer have also been structurally analyzed by NMR spectroscopy, revealing that the propagating radicals in copolymerization exhibit different reactivities toward T and that the fragmentation rate of the adduct radical depends on the penultimate unit.[170,396,402] C_T values for AFCT agents are usually of the order 10^{-1}–10^0 as summarized in Table 3.4 for several AFCT agents.[160,161,171,172,202,389,394,395,403] Their presence in a polymerizing system sometimes results in a slight reduction in R_p because addition to the carbon–carbon double bond of T is sterically hindered by the α-(substituted methyl)acryloyl structure. Although α-(substituted methyl)acrylate can be regarded as an allylic compound, examination of R_p and structural analysis indicate that no significant degradative chain transfer is taking place.

TABLE 3.4 C_T Values of Various AFCT Agents at 60°C

	C_T			
Chain Transfer Agent	Methyl Methacrylate	Styrene	Methyl Acrylate	Ref.
$CH_2=C(CH_2Br)CO_2C_2H_5$	1.45	—	2.33	160,161
$CH_2=C(CH_2Br)CO_2CH_3$	0.93	2.34	2.93	171
$CH_2=C(CH_2Br)CO_2CH_3$	1.28[a]	11.44[a]	—	389
$CH_2=CHCH=CHCH_2Br$	3.4	—	—	394
$CH_2=C(CH_2SC_4H_9\text{-}tert)CO_2C_2H_5$	0.74	0.95	—	160,161
$CH_2=CHCH=CHCH_2SC_4H_9\text{-}tert$	0.92	0.34	—	395
$CH_2=C(CH_2SO_2Ph)CO_2C_2H_5$	0.72	4.21	1.69[b]	172
$CH_2=C(CH_2SO_2C_6H_4CH_3\text{-}p)CO_2C_2H_5$	1.09	6.80	2.31[b]	172
$CH_2=CHCH=CHCH_2SO_2Ph$	3.0	—	—	394
$CH_2=C(Ph)CH_2OCH_2Ph$	0.76	0.26	5.7	403
$CH_2=C(CN)CH_2OCH_2Ph$	0.081	0.036	0.3	403
$CH_2=C(CO_2CH_3)CH_2OCH_2Ph$	0.16	0.046	0.54	403

[a] 70°C.
[b] Butyl acrylate.

A bifunctional AFCT agent (**26**) consisting of two α-(alkylthiomethyl)acryloyl groups was synthesized in order to prepare polymer bearing carbomethoxyallyl groups at both ends.[404]

However, the radical from **26** readily undergoes intramolecular addition to give a 7-membered cyclic radical without fragmentation (Scheme 3.17). This type of unde-sired reaction can be avoided by increasing the number of methylene groups between the sulfur atoms. In conventional chain transfer, an increase in the stability of X may facilitate cleavage of the C—X bond, leading to slower reinitiation with a significant decrease in R_p.[169,395] Contrary to the case of conventional chain transfer, the main and the smaller moieties of the AFCT agent may be introduced at the α- and ω-ends, respectively. When X and Y contain functional groups, this type of chain transfer can be an effective method for the introduction of functional end groups.[397,405]
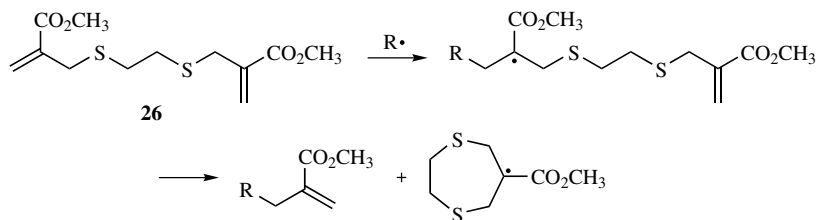
Scheme 3.17

The $CH_2CY=CH_2$ ω-end groups do not homopolymerize, and the adduct radicals formed on addition of propagating radicals appear to self-terminate at a much lower rate than the bimolecular reaction of propagating radicals. GPC analysis of the polymer formed during styrene polymerization in the presence of an AFCT agent showed that the elution curves shifted to higher molecular weight with increasing conversion since propagating radicals add to the unsaturated end groups formed by AFCT, thereby connecting polymer chains to the end groups.[320] In the case of methyl methacrylate, however, the molecular weight remained close to independent of the level of conversion, indicating the absence of any significant gel effect and addition of propagating radicals to the unsaturated end groups. The adduct radicals can be expected to either couple with propagating radical or fragment to yield polymer bearing allylic end groups, or undergo slow addition to monomer.[320,406]

A radical structurally similar to the adduct radical has been detected by ESR spectroscopy as a persistent radical during the decomposition of methyl 2,2′-azobisisobutyrate.[407] Therefore, the polymerization of vinyl acetate, which is less reactive than styrene and methyl methacrylate, is strongly retarded in the presence of an AFCT agent when Y is a conjugative group such as CO_2Me. In order to avoid this decrease in R_p, a nonconjugative substituent such as Cl should be introduced as Y.[160] However, a decrease in the reactivity of the double bond of the AFCT agent and an increase in the reactivity of the polymer radical may bring about a higher extent of hydrogen abstraction from the α-methyl group.

α-Methylstyrene dimer [X = $C(CH_3)_2Ph$ and Y = Ph] can be an effective AFCT agent at 100°C or above, resulting in the generation of a carbon-centered radical and an unsaturated end group from cleavage of the C–C bond of the adduct radical to introduce the phenylallyl end group.[408] When propagation, a bimolecular reaction, is in competition with fragmentation, a unimolecular reaction, a temperature increase would cause the rate of fragmentation to increase relative to that of propagation. The fragmentation process of α-methylstyrene dimer appears to be too slow for it to act as an AFCT agent at lower temperatures.[406] The unsaturated dimers and oligomers of methacrylic ester [**27**: X = $[C(CH_3)(CO_2CH_3)CH_2]_nH$ and Y = CO_2CH_3 as AFCT agent] are feasible to radical addition, and persistence of the adduct radicals results in regeneration of the C=C as a result of fragmentation at a temperature lower than that of the α-methylstyrene dimer.[367]

The C_T for the polymerization of methyl methacrylate in the presence of methyl methacrylate oligomers has been shown to depend on the chain length of the unsaturated oligomeric methacrylic ester (**27**): $C_T = 0.008 \pm 0.002$ $(n = 1), 0.20 \pm 0.03$ $(n = 2), 0.34 \pm 0.03$ $(n = 3)$, and 0.14 ± 0.003 (macromonomer).[367] The significant difference in C_T value between $n = 1$ and the higher oligomers has been explained by slower fragmentation of the adduct radical from the dimer because

$$CH_2=\underset{\underset{CO_2CH_3}{|}}{C}-CH_2\left(\underset{\underset{CO_2CH_3}{|}}{\overset{\overset{CH_3}{|}}{C}}-CH_2\right)_{\!n}\!\!-H$$

27

$$PhCH_2\text{\textapprox}\bullet \;+\; CH_2=\overset{\overset{\displaystyle OCH_2Ph}{|}}{C}-X \longrightarrow PhCH_2\text{\textapprox}CH_2-\overset{\overset{\displaystyle OCH_2Ph}{|}}{\underset{\bullet}{C}}-X$$

$$\longrightarrow PhCH_2\text{\textapprox}CH_2-\overset{\overset{\displaystyle O}{\|}}{C}-X \quad PhCH_2\bullet$$
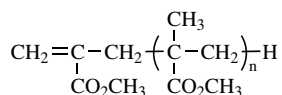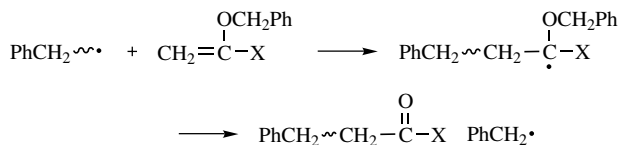
Scheme 3.18

of less steric hindrance arising from the substituent bound to the radical center. During polymerization of a methacrylic ester in the presence of polymer of different methacrylic esters bearing unsaturated end groups, the polymethacrylate radicals expelled by fragmentation could initiate new chains, leading to the formation of block copolymer consisting of two different segments of polymethacrylate with $M_w/M_n < 1.5$.[319,409] It follows that the dimer of functional methacrylates can be utilized as an AFCT agent to introduce the corresponding functional end groups.[410,411] However, the C_T value of the dimer of methyl methacrylate (**27**, $n = 1$) is not sufficiently large to attain highly efficient introduction of the end group.

α-Substituted vinyl benzyl ether ($CH_2=CYOCH_2Ph$, $Y = CO_2CH_3$, CN, Ph, $CONH_2$) undergoes another type of AFCT to form substituted ketones as the ω-end groups and benzyl radicals, which can readily initiate a new chain (Scheme 3.18).[202,411] A conjugative group is required as Y to enhance the reactivity of the C=C toward polymer radical. The C_T values determined for the benzyl vinyl ether are relatively large, as shown in Table 3.4.

Carboxylic dithioester can undergo reversible AFCT involving addition to the C=S bond if the leaving radical is properly stabilized by the substituent. Addition to the C=S bond is followed by fragmentation of the adduct radical to regenerate the C=S bond.[412–414] The reversible addition of propagating radicals to the C=S bond is the basis for the reversible addition–fragmentation chain transfer (RAFT) process, which will be discussed in detail as one of the living free radial polymerization processes in Chapter 12.

3.3.5 Addition–Substitution–Fragmentation Chain Transfer

The first step in this type of chain transfer is addition to the C=C activated by Y as in AFCT followed by 1,3-intramolecular substitution and fragmentation to yield an end group that differs from the substituted allyl end group. A typical example of an addition-substitution–fragmentation chain transfer (ASFC) process is given in Scheme 3.19, in which oxirane and small radical ·OX are produced.[294,415,416] When X is *tert*-butyl group, the butoxy radical may add to monomer to initiate a new chain. Typical ASFC agents are **28–32**.

Some of the oxygen-centered radicals expelled from the adduct radical may undergo further fragmentation to convert to carbon centered radicals as shown in Scheme 3.20 using **30** as an example. C_T values for typical ASFC agents are summarized in Table 3.5.[417–420]
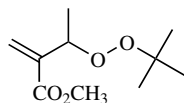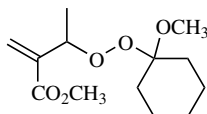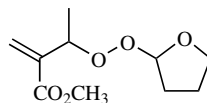
28   **29**   **30**
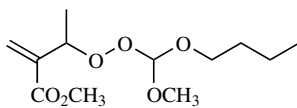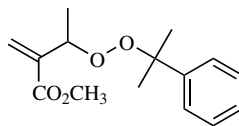
31   **32**
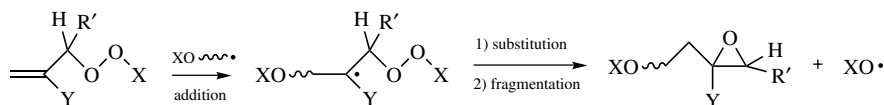
Scheme 3.19
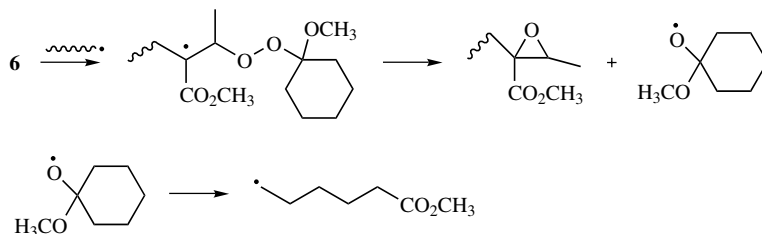
Scheme 3.20

The rate of decomposition of most peroxide type ASFC agents is considerably lower than their reactions as T, and no homo- or copolymerization occurs spontaneously. However, permethacrylic esters of which ASFT yields an α-lactone can function both as T and initiators simultaneously, and consequently Eq. (3.16) should

TABLE 3.5 C_T Values for ASFC Agents 27–30 at 60°C

ASFC Agent	C_T			Ref.
	Methyl Methacrylate	Styrene	Butyl Acrylate	
27	0.63	1.64	—	416
28	0.102	1.02	0.88	417
29	0.096	0.97	1.02	418
30	0.086	0.91	0.63	419

be used for determination of C_T instead of the conventional Mayo equation [Eq. (3.10)].[420]

$$\frac{1}{P_n} = \frac{1}{P_{n00}} \cdot \frac{\ln(1-x)}{\ln(1-x_0)} + C_T \frac{[T]}{[M]} \tag{3.16}$$

where P_n and P_{n00} denote the degree of polymerization in the absence of T and the presence of T at 0% conversion. It should be noted that the C_T values for alkyl peroxides ($2–3 \times 10^{-4}$ via direct attack of propagating radical to the O—O bond) are much smaller than those for most of the perester-type AFCT. ASFC through the mechanism of 1,5-intramolecular substitution has also been investigated.[421]

3.3.6 Temperature Dependence of Chain Transfer Reactivity

α-Methylstyrene dimer functions as an AFCT agent at temperatures of 100°C or above.[408] α-Substituted acrylates bearing CH_2Cl, CH_2OPh, $CH_2CH_2CO_2Me$, and other compounds as the α-substituent simultaneously undergo polymerization and at least a detectable amount of AFCT at lower temperatures such as 60°C.[167] The ratio of the rate constant for the fragmentation of the propagating radical, k_f, to k_p (Scheme 3.21) can be determined by quantification of the unsaturated end groups and monomeric units of the polymer formed by ^{1}H-NMR spectroscopy. Although bimolecular termination through disproportionation might produce the same unsaturated end group, chain transfer is the main end-forming reaction under conditions yielding sufficiently short kinetic chain lengths.

An Arrhenius plot of k_p/k_f gives a positive value of $(E_f - E_p)$ and a value of A_p/A_f smaller than unity: $E_f - E_p = 58.5$ kJ/mol and $A_f/A_p = 9.72 \times 10^6$ mol/L for $X = CH_2CH_2CO_2Me$ and $Y = CO_2Me$.[167] In other words, $E_f > E_p$ and $A_f > A_p$ as expected since fragmentation is a unimolecular reaction, whereas propagation is bimolecular. However, considerably smaller $A_{tr}/A_p = 0.16 - 0.41$ and $E_{tr} - E_p = 1.72 - 7.41$ kJ/mol were calculated from the Arrhenius plot of C_T for **27** ($n = 1,2,3$ and macromonomer) in MMA polymerization.[367] These tendencies indicate that the addition of the propagating radical to the sterically hindered
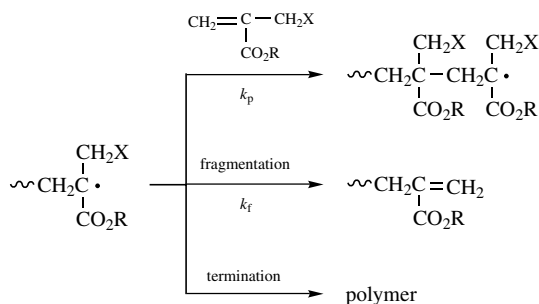
Scheme 3.21

carbon–carbon double bond of **27** is the rate-determining step in the chain transfer process.

The temperature dependence of the C_T values for the polymerization of methyl methacrylate in the presence of the ASFC agent **28** can be expressed by $E_{tr} - E_p = 11.5\,kJ/mol$ and $A_{tr}/A_p = 7.2$, in accordance with significant steric hindrance against addition of the polymer radical to the carbon–carbon double bond of T.[416] Polymerization of styrene in the presence of **32** resulted in $E_{tr} = 46.0\,kJ/mol$ and $A_{tr} = 3.87 \times 10^9\,L\,mol^{-1}\,s^{-1}$, to be compared with $E_{tr} = 12.4\,kJ/mol$ and $A_{tr} = 0.163\,L\,mol^{-1}\,s^{-1}$ in the case of methyl methacrylate.[422] More significant steric hindrance in the addition step for the chain transfer in the polymerization of methyl methacrylate is predicted particularly on the basis of the small A_{tr} value. These reaction rates of ASFC appear to be affected by the addition and the fragmentation steps depending on the attacking radical, and the reaction of poly(methyl methacrylate) radical is susceptible to more significant steric hindrance than is the polystyrene radical.

3.4   TERMINATION

3.4.1   General Features

Free-radical polymerization consists of the elementary reactions of initiation, propagation, and termination. Termination refers to the bimolecular reaction of propagating radicals by combination or disproportionation that leads to the deactivation of propagating radical chain ends. Primary radical termination, the reaction between a primary radical and a propagating species, may also contribute to the loss of propagating radicals. Reversible termination, as present in living/controlled free-radical processes, is discussed in Chapters 9–12.

Termination is perhaps the most complex of the elementary reactions in free-radical polymerization as it constitutes the consecutive events of polymer radicals undergoing translational diffusion to come into relative proximity of one another, segmental diffusion whereby the chain ends approach one another, and finally chemical reaction.[146] The rate constant for bimolecular reaction between two small carbon-centered radicals in liquid is of the order of $10^9\,M^{-1}\,s^{-1}$.[423] The termination process in a polymerizing system is usually diffusion-controlled with a rate constant significantly lower than that for small radicals in liquid.[146,424,425] Certain monomers exhibit severe steric hindrance[145,157,165,168,204,210,220,222,426–429] and consequently terminate orders of magnitude more slowly than conventional monomers such as styrene and methyl methacrylate. In most cases the chemical reactivity toward termination is not expected to affect the degree of polymerization or molecular weight distribution, except through the relative rates of termination by combination and disproportionation. Since polymer radicals may diffuse at different rates depending on the chain length, especially in viscous media, the termination rate coefficient will exhibit chain length dependence.[424,430–432] Furthermore, since the termination reaction occurs between two polymer radicals that are most likely of different degrees of polymerization, the termination rate coefficients measured by

experimental techniques currently available represent some sort of average values. The detailed kinetic aspects of termination will be discussed in Chapter 4.

The mode of termination is of great importance as it affects the molecular architecture of the polymer formed, and thereby some of its properties. The molecular weight distribution and the polydispersity are functions of the mode of termination; the polydispersity M_w/M_n is equal to 1.5 if termination is by combination only, and 2 if by disproportionation only.[433] The nature of the end groups is affected by the mode of termination; combination yields chain ends consisting of initiator fragments, whereas disproportionation results in additional chain ends in the form of unsaturated and saturated ω-end groups. The unsaturated end groups resulting from disproportionation may in some cases undergo further reaction leading to branched structures.[319,367,434–436] Combination usually results in a head–head linkage in the polymer backbone,[437] and these linkages along with terminal unsaturations from disproportionation are in some cases believed to contribute to thermal instability of the polymer.[407,438,439] At a heating rate of 10°C/min, the unsaturated portion of poly(methyl methacrylate) degrades at 230–300°C, whereas the saturated portions remain thermally stable up to 300°C.[440]

3.4.2 Bimolecular Termination

3.4.2.1 Combination versus Disproportionation

The relative extents of the two different modes of bimolecular termination, disproportionation and combination (Scheme 3.22), often expressed as the ratio of their respective rate coefficients k_{td}/k_{tc}, is difficult to measure as manifested by the spread in the data reported in the literature.[441] The techniques most commonly employed to study the mode of termination include quantification of initiator-derived end groups by NMR[204,437,442–445] and model compound studies.[118,446–449] Termination occurs mainly by combination for most vinyl monomers, although disproportionation usually makes a significant contribution when the propagating radical is sterically hindered or possesses easily abstractable β-hydrogens. It follows that styrene,[119,437,441,442,448,450] acrylonitrile,[451] and methyl acrylate[452] mainly terminate by combination, whereas disproportionation significantly contributes to the
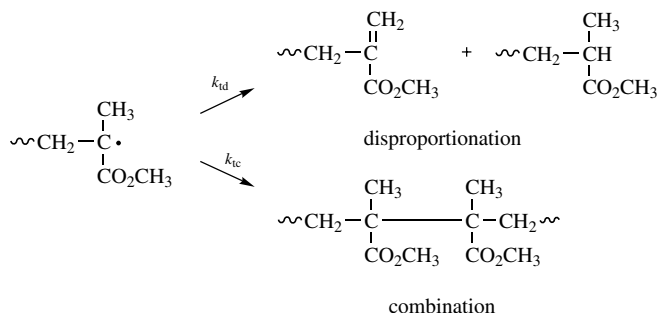
Scheme 3.22
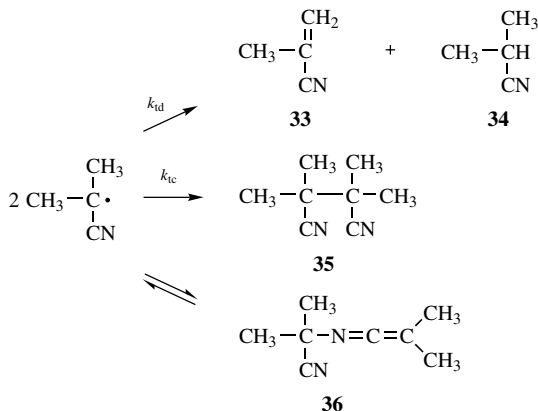
Scheme 3.23

termination step for α-methylvinyl monomers such as methyl methacrylate.[119,441,442,445] The systems that have been the most widely studied with regard to determining the dominant mode of termination are by far the polymerizations of styrene and methyl methacrylate.

A large number of termination studies involving model compounds have been carried out, often with azoinitiators employed as sources of radicals as models of propagating species.[118,446–449] For example, cyanoisopropyl radicals generated on the decomposition of AIBN can be considered as models for poly(methacrylonitrile) radicals (Scheme 3.23). The ratio k_{td}/k_{tc} as obtained from quantification of the amounts of the disproportionation products [methacrylonitrile (**33**) and isobutyronitrile (**34**)] and the combination product [tetramethylsuccinonitrile (**35**)] indicates that the cyanoisopropyl radicals terminate mainly by combination.[446] The reaction system in question also involves the reversible formation of the ketenimine (**36**), which does not affect the kinetic analysis with regard to the ratio k_{td}/k_{tc}. Model studies are useful, but caution is warranted as model systems are inherently different from polymerizing systems in a number of respects, and sometimes different results are obtained from model–polymerization investigations.[118,441,448]

Studies of the termination reactions of oligostyryl radicals,[448] as models of the polystyryl radical, have indicated that combination is the main mode of termination ($k_{td}/k_{tc} \approx 0.1$). The ratio k_{td}/k_{tc} was found to be independent of chain length, thus providing some justification for concluding that polystyryl radicals are likely to terminate in the same manner. Fewer data are available regarding a possible temperature dependence of the termination mode. Model studies of oligostyryl radicals have suggested that $E_{comb} > E_{disp}$, that is, k_{td}/k_{tc}, decreases with increasing temperature.[448] This result is, however, in disagreement with those obtained by polymerization studies, which indicate the opposite trend, and a stronger temperature dependence.[441,448]

Several studies based on end-group analysis of polystyrene have indicated termination predominantly by combination.[8,119,442–444,453] Investigations using

[13]C-enriched BPO,[441] ^{14}C-enriched AIBN,[444] fluorinated derivatives of BPO[442] and an azoinitiator,[443] and deuterated monomer[444] all pointed toward termination mainly by combination. The application of matrix-assisted laser desorption ionization time-of-flight (MALDI-TOF) mass spectrometry to the determination of the mode of termination by end group detection has been reported,[119] again indicating predominant termination by combination ($k_{td}/k_{tc} = 0.057$). The head–head linkages resulting from termination by combination have been detected by 2D-inadequate NMR, although the accuracy was not sufficiently high for the estimation of k_{td}/k_{tc} to be possible.[437]

The termination mode of poly(alkyl methacrylate) radicals has also been the subject of much research.[441] Model compound studies of the bimolecular reactions of 1-methoxycarbonyl-1-methylethyl radicals and the higher esters ethyl and butyl have resulted in $k_{td}/k_{tc} \approx 0.70$ for methyl methacrylate, 0.72 for ethyl methacrylate, and 1.17 for butyl methacrylate.[441,447] Application of MALDI-TOF to the end-group analysis of low-molecular-weight poly(methyl methacrylate) initiated by AIBN yielded $k_{td}/k_{tc} = 4.37$.[119] The use of fluorinated derivatives of BPO in connection with ^{19}F NMR analysis of poly(methyl methacrylate) also indicated that termination occurs mainly by disproportionation in this system.[442]

Quantification of initiator-derived end groups using totally deuterated methyl methacrylate and direct observation of the terminal unsaturations from disproportionation using ^{1}H-NMR showed that approximately 80% of the polymer chains have formed by disproportionation, which translates to a value of k_{td}/k_{tc} of approximately 2.[445] The termination mechanisms in the homopolymerizations of both styrene and methyl methacrylate have been investigated by employing ultrasonic scission of polymer chains followed by termination in the presence and absence of a radical trap.[454] Comparison of the molecular weights thus obtained revealed that the dominant termination modes were disproportionation for poly(methyl methacrylate) and combination for polystyrene.

Termination in copolymerization occurs by combination and disproportionation in complete analogy with homopolymerization systems. A study of the behavior of model radicals of polystyrene and poly(methyl methacrylate) radicals generated from the decomposition of an asymmetric azoinitiator (**37**) resulted in $k_{td}/k_{tc} = 0.56$ at 90°C for the cross-termination reaction, which lies in between the values obtained for the self-reactions of the two individual radicals: 0.13 for the polystyrene and 0.78 for the poly(methyl methacrylate) model radical.[441] Application of the technique of pyrolysis gas chromatography to the copolymerization of styrene and methyl
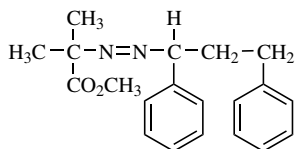
37

methacrylate resulted in k_{td}/k_{tc} values in the range 0.21–0.64, inferring that combination was favored over disproportionation at 60°C.[445]

3.4.2.2 Primary Radical Termination *Primary radical termination* refers to the bimolecular reaction between a propagating radical and a primary radical. This process leads to lower rates of initiation and propagation, thus causing a deviation from the prediction of classical kinetics (i.e., the rate of polymerization is proportional to the square root of the initiator concentration). In analogy with the termination reactions between propagating radicals, primary radical termination can also occur by either combination or disproportionation. It has been shown that primary radical termination between cyanoisopropyl radicals and polystyryl radicals occurs mainly by combination at 98°C during conditions of exceptionally high initiator concentration yielding polymers with degrees of polymerization of approximately 10 or lower.[456] For conventional free-radical initiators such as AIBN and BPO, primary radical termination normally occurs to an appreciable extent only when the concentration of primary radicals is unusually high and/or when the monomer concentration is low. In other words, the contribution of primary radical termination can be expected to be more significant at high conversion and high dilution.[112,119,134,450,457] It has been demonstrated that even under experimental conditions that would favor primary radical termination (high initiator concentration and low monomer concentration), more than 85% of termination events occur by bimolecular reaction between polymeric radicals for the styrene/AIBN system at 100°C.[8] For normal bulk polymerization conditions in the same system (initiator concentration 0.01–0.02 M), <2% of the end groups originated from primary radical termination at low conversion. In the case of BPO-initiated styrene bulk polymerization (initiator concentration 0.04 M), 8% of the chain ends had been formed through transfer to initiator or primary radical termination.[453]

Many industrial photopolymerization processes exploit unusually high initiation rates in order to achieve a rapid cure and a high final degree of conversion, and this may lead to an unusually high contribution of primary radical termination.[134] Certain primary radicals exhibit a relatively high stability and are quite unreactive toward vinyl monomers, and instead tend to engage mainly in primary radical termination reactions. This is often observed with photoinitiators such as benzoin ethers that generate two types of radicals: reactive benzoyl radicals that initiate polymerization and relatively stable benzyl ether radicals that are consumed in primary radical termination.[88] The concept of reversible primary radical termination is taken advantage of when preparing polymers and copolymers with well-controlled architecture by use of techniques such as the *iniferter* method and initiators yielding persistent and captodatively substituted radicals (Section 3.1.2.1.3). Another example of how comparatively low rates of addition of primary radicals to monomer may lead to higher rates of primary radical termination is the polymerization of fumarates (1,2-disubstituted ethylenes) initiated by AIBN.[111–113]

3.4.2.3 Sterically Hindered Monomers The propagating radicals of certain monomers that exhibit considerable steric hindrance terminate exceptionally slowly,

TABLE 3.6   Termination Rate Coefficients of Sterically Hindered Monomers Compared with Styrene and Methyl Methacrylate at 60°C

Monomer	k_t $(M^{-1} s^{-1})$	Ref.
Styrene (bulk)	1.1×10^8	111
Methyl methacrylate (bulk)	2.1×10^7	458
Methyl α-(2-carbomethoxyethyl)acrylate (bulk)	2.6×10^5	459
Diethyl itaconate (benzene)	3.2×10^4	214
Diethyl fumarate (benzene)	280	460
N-tert-Butylmaleimide (benzene)	1.2×10^4	456
Polystyrene macromonomer with methacryloyl end group[a] (benzene)	1500	457

[a] Monomer concentration 0.220 M, $M_n = 2700$, $M_w/M_n = 1.07$.

leading to an extraordinarily high propagating radical concentration in the steady state.[145] These types of monomers polymerize to high molecular weight despite significant steric hindrance as a result of a favorable balance in the magnitudes of k_p and k_t; thus, the quantity $k_p/k_t^{1/2}$ is high enough for polymerization to occur. Examples of monomers of this type include α-(substituted methyl)acrylic esters,[165,167,168,204] dialkyl itaconates,[428,429,458] N-alkylitaconimides,[426,459] dialkyl fumarates,[168,210,213,214,427,460] and N-substituted maleimides.[207,461,462] The values of k_t for many sterically hindered monomers are several orders of magnitude lower than for common monomers such as styrene and methyl methacrylate (Table 3.6).

Macromonomers[463] are oligomeric or polymeric species that contain a polymerizable group. They are usually derivatives of methacrylate esters or styrene such as polystyrene with methacryloyl end groups,[222,223] poly(methyl methacrylate) with styryl end groups,[220] and methacryloyl-terminated poly(ethylene glycol) methylether).[464] These monomers exhibit rates of bimolecular termination that are orders of magnitude lower than conventional monomers.[219,220,222,223,465] This behavior is believed to originate from low rates of segmental diffusion, which is a consequence of an excluded volume effect resulting from the multibranched structure of the propagating radicals.[220,222,223,466] The tacticity of poly(methyl methacrylate) macromonomers has been reported to influence the rate of termination by affecting the segmental mobility of the chain (the glass transition temperature of isotactic poly (methyl methacrylate) is significantly lower than that of the syndiotactic version), the *iso*-macromonomer terminating (and propagating) more rapidly than the *syn*-macromonomer.[220] The macromolecular nature of these monomers also results in a significant monomer concentration dependence of the termination rate coefficient, since an increase in the monomer concentration leads to an increase in the viscosity of the medium. For example, a reduction in monomer concentration of polystyrene macromonomer with a methacryloyl end group ($M_n = 2700$; see Table 3.6) from 0.220 to 0.0370 M in benzene at 60°C causes the termination rate coefficient to increase by approximately a factor of 125.[223]

3.4.2.4 *Effect of the Medium* The bimolecular termination process is normally diffusion-controlled from zero conversion onward, and for conventional vinyl monomers such as styrene and methyl methacrylate where the termination rate coefficient at zero conversion is of the order 10^{7-8} M^{-1} s^{-1},[467–469] the mode of diffusion control is a function of conversion.[146,470] At low conversion, segmental diffusion of the radical chain ends may be the rate-determining step. As the viscosity increases with conversion, the rate of center-of-mass diffusion of polymer radicals decreases to eventually become the rate-determining step. At intermediate to high conversion levels in bulk polymerization, the polymer radicals become so immobile that they are unable to diffuse together for bimolecular termination to take place. Under these circumstances the dominant mode of termination is thought to be that of reaction diffusion (residual termination); this refers to when the radical chain ends come into close proximity as a result of successive addition of monomer molecules.[146,470,471] For some rapidly propagating monomers such as butyl acrylate, reaction diffusion may be the dominant mode of termination starting at conversion levels as low as approximately 10%.[471] The rate of termination for most bulk polymerization systems decreases by several orders of magnitude throughout the polymerization process. Both k_t and k_p have been observed to increase with the initiator concentration in the highest conversion regime in the bulk polymerization of styrene at 70°C, probably as a result of higher monomer mobility in a matrix consisting of shorter polymer chains.[472,473] In this conversion regime, both the rate of termination (by reaction diffusion) and propagation are controlled by the rate of monomer diffusion.

Free-radical polymerization in supercritical carbon dioxide (scCO$_2$) has received considerable attention because of its unique nature and the fact that it offers environmental advantages at low cost.[474,475] Single pulse pulsed-laser polymerization experiments for styrene and butyl acrylate have shown that the value of k_t increases with scCO$_2$ content; the termination rate coefficient in scO$_2$ is significantly higher than in bulk for these two monomers.[261,476] This has been attributed to the poor solubility of the monomer in this solvent, leading to a reduction in coil size, which, in turn, results in higher rates of segmental diffusion.[261,476,477]

3.5 INHIBITION AND RETARDATION

3.5.1. General Features

In order for the quality and purity of monomer to be maintained, polymerization must not be initiated during monomer preparation, nor during the purification process and storage. However, premature radical formation from pure monomer, monomer contaminants, or impurities sometimes induces initiation to give polymer. If a substance can quantitatively scavenge the initiating radical, further propagation cannot occur. When the polymerization after consumption of the substance proceeds as rapidly as does the polymerization in its absence, such a compound is referred to as an *inhibitor*.[116,312] The induction period, the time required for complete consumption of the inhibitor, is often measured in order to calculate the initiation rate. The

ratio of the initiation rate to the decomposition rate of initiator is generally used as the definition of initiation efficiency. A *retarder* is a substance that in low concentration effectively suppresses the overall rate of polymerization without induction period.[116,312] The distinction between retarders and inhibitors is not always clear. Inhibition is one of the elementary reactions in chain reaction polymerization; however, the radical reaction of inhibition of autooxidation processes has also been studied in detail.[478]

3.5.2 Inhibition and Retardation Reactions

Stable free radicals are frequently employed as inhibitors.[479] The most commonly used species for measuring the induction period are 2,2,6,6-tetramethylpiperidinyl-1-oxyl (TEMPO) (**38**) and 1,3,5-triphenylverdazyl (**39**). During the induction period, TEMPO and the verdazyl quantitatively and rapidly scavenge the carbon-centered primary radicals to form C—O and C—N bonds, respectively. Nitroxides such as TEMPO react with carbon-centered radicals at close to diffusion-controlled rates.[480–483] The coupling of these stable radicals with carbon-centered radicals are reversible, and the coupling products dissociate into the component radicals on heating.[481,484,485] The verdazyl is less thermally stable than TEMPO.[486] Nitroxides and verdazyl do not react with oxygen-centered radicals and oxygen. If an initiator generates oxygen-centered radicals in the presence of a nitroxide, the carbon-centered radical resulting from addition of the oxygen-centered radical to monomer will be trapped by a nitroxide such as 1,1,3,3-tetramethylisoindole-2-oxyl (**40**). Galvinoxyl (**41**) and 1,3-bisdiphenylene-2-phenylallyl (Koelsch's radical) (**42**) can also be used as inhibitors. Diphenylpicrylhydrazyl (**43**) is used much less frequently because of its complicated reaction mode of inhibition.

The polymerization rate decreases with increasing amount of retarder, and as mentioned, an induction period is seldom observed. Addition to or hydrogen abstraction from the retarder by an initiating radical or a propagating radical results in a less reactive radical, leading to a decrease in the polymerization rate. The most commonly employed stabilizers of monomer are retarders such as substituted phenols (e.g. *p*-methoxyphenol and *tert*-butyl catecohol). Substituted phenols readily undergo abstraction of the labile phenolic hydrogen to yield low reactivity phenoxy radicals. The extent of retardation may depend on monomer type since the radical resulting frrom the retarder is likely to add to different monomers at different rates. An acrylic ester bearing a hindered phenol structure (**44**) has been shown to function as a retarder for the polymerizations of methyl methacrylate through addition of the propagating radical to the acrylic double bond.[485] However, 2,6-di-*tert*-butylphenol does not affect the rate of methyl methacrylate polymerization because the propagating radical of methyl methacrylate cannot abstract the sterically hindered phenolic hydrogen. The polymerization of vinyl acetate is inhibited by **44**.[485]

Benzoquinone, which may behave as a retarder, readily gives phenoxy radical as a result of rapid radical addition to the C=O bond; the addition is facilitated by aromatic stabilization.[487–491] The relative reactivities of alkyl- and methoxy-substituted
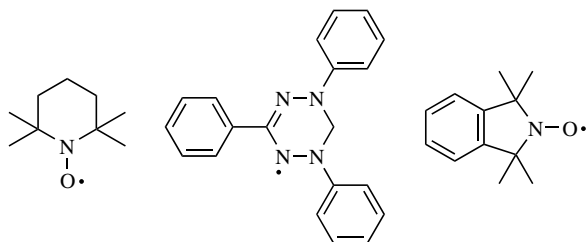
38   **39**   **40**
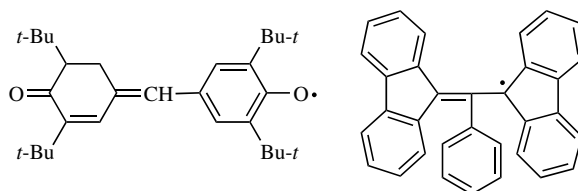
41   **42**
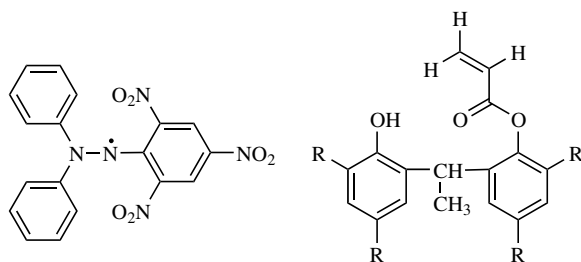
R = *iso* -C₃H₇

43   **44**

benzoquinones have been correlated to their redox potentials and a steric factor of the substituents.[488,490] The reaction of 2,6-disubstituted benzoquinones with 2-cyano-2-propyl radicals gave the monoether (1 : 1 adduct) by addition to the C=O bond followed by hydrogen abstraction of the resulting phenoxy radical, and diethers (1 : 2 adduct) by addition to the C=O bond and coupling of the resulting radical with a cyanopropyl radical (Scheme 3.24).
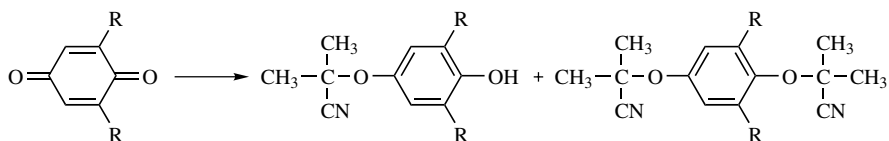
Scheme 3.24

Similarly, the 1 : 2 adduct was isolated as the reaction product of 1,1-di(*p*-tolyl) ethylene with cyanopropyl radicals.[492] However, the reaction of 2,5-di-*tert*-butylbenzoquinone gave no detectable reaction products, presumably as a result of extremely slow reaction due to the steric hindrance of the substituents.[493]

Transition metal salts such as halides or pseudohalides function as inhibitors by undergoing rapid reactions with carbon-centered radicals by an electron transfer or a ligand transfer mechanism. The carbon carrying the unpaired electron is converted to a σ-bonded carbon or ionic species.

Emulsion polymerization, which exhibits a higher polymerization rate and gives polymer of higher molecular weight than solution and bulk polymerizations, is affected by additional factors since it is a heterogeneous system. The addition of stable free radicals, such as those described, to an emulsion system would probably not lead to significnat inhibition or retardation since these water-insoluble radicals would not be able to quantitatively trap the primary radicals, including oxygen-centered radicals generated in the aqueous phase. However, water-soluble inhibitors, notably inorganic salts such as cupric chloride and sodium nitrate, can be employed.[357,494,495] Although homogeneous polymerization for quantitative analysis is usually carried out after deaeration or under vacuum, a small amount of oxygen is considered to remain in emulsion polymerization systems. The effect of oxygen on emulsion polymerization has been investigated.[496-498]

The polymerization rate of vinyl esters is remarkably reduced by a small amount of an additive such as styrene or toluene; highly reactive propagating radicals from vinyl acetate readily form styrene radicals and benzyl radicals because of resonance stabilization. These benzyl-type radicals are less reactive toward vinyl esters, because of resonance stabilization.[499] However, these compounds are not generally classified as retarders.

Buckminsterfullerene (C_{60}) has attracted interest not only because of its structure and physical properties but also because of its versatile reaction behavior exhibiting inhibition and retardation effects. It is known that C_{60} reacts rapidly with radicals to yield ESR-detectable radical species (C_{60}·).[500] The polymerization of vinyl acetate in benzene is effectively inhibited by C_{60}, and all C_{60} molecules consumed were confirmed to be incorporated into the poly(vinyl acetate).[501] During the course of the polymerization, the color of the polymerization mixture gradually changed from violet to brown and dark brown. Dark brown polymer was precipitated by pouring the polymerization mixture into *n*-hexane, on which the supernatant solution turned colorless. The violet polymerization mixture did not exhibit any color change in hexane prior to heating. The ESR-detectable C_{60}· (singlet spectrum) concentration increased with time during the induction period, reaching a threshold level corresponding to trapping of 15 radicals by each C_{60} molecule. However, a C_{60} molecule is able to react with at least 34 methyl radicals or 15 benzyl radicals.[496] The rate of polymerization of methyl methacrylate and styrene, and the molecular weight of the polymer formed, have been shown to be significantly reduced in the presence of C_{60}.[502–510] The formation of C_{60}· was confirmed by ESR spectroscopy during the polymerizations of methyl methacrylate and styrene, and a short induction period, or in some cases none at all, was observed. The concentration of C_{60}·

increased with increasing time up to the threshold concentration corresponding to that arising from trapping of 15 radicals per C_{60} molecule. The number of C_{60} molecules per polymer molecule increased with increasing concentration, suggesting coupling of polymer-$C_{60}\bullet$ to give polymer-C_{60}-C_{60}-polymer.[505,510]

3.5.3   Practical Use

Distillation is one of the most important purification methods for liquid monomers. An inhibitor that can effectively suppress premature polymerization during distillation is required. A suitable inhibitor for this purpose should remain in the distillation pot, and the distilled monomer as the final product should not be contaminated by the inhibitor. Furthermore, the inhibitor itself should be thermally stable. The nitroxides **45–49** are known to be suitable inhibitors for acrylate and methacrylate monomers as described in several patents.[511–515] In addition to these nitroxides, hydroquinone, phenothiazine, *p*-methoxyphenol, and other compounds have been employed as inhibitors to prevent polymerization during distillation.

45   **46**   **47**   **48**   **49**
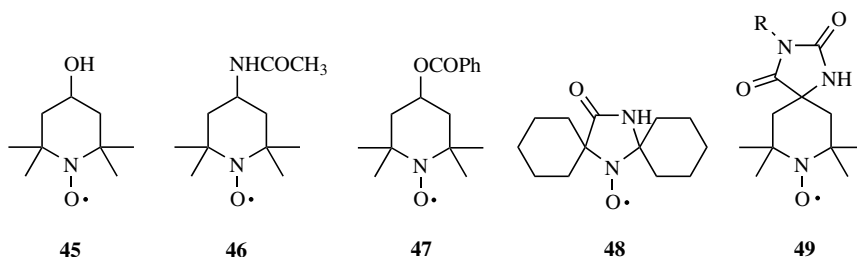
REFERENCES

1. B. Isik-Yuruksoy and O. Guven, *Polym. Degrad. Stabil.* **58**, 91 (1997).

2. M. N. Galbraith, G. Moad, D. H. Solomon, and T. H. Spurling, *Macromolecules* **20**, 675 (1987).

3. P. S. Engel, *Chem. Rev.* **80**, 99 (1980).

4. E. M. Y. Quinga and G. D. Mendenhall, *J. Org. Chem.* **50**, 2836 (1985).

5. N. Minamii and B. Yamada, in *Polymeric Materials Encyclopedia*, J. C. Salamone, ed., CRC Press, Boca Raton, FL, 1996, p. 432.

6. K. W. Dixon, in *Polymer Handbook*, 4th ed., J. Brandrup, E. H. Immergut, and E. A. Grulke, eds., Wiley, New York, 1999, p. II/12.

7. G. Moad, E. Rizzardo, and D. H. Solomon, *Macromolecules* **15**, 909 (1982).

8. G. Moad, D. H. Solomon, S. R. Johns, and R. I. Willing, *Macromolecules* **17**, 1094 (1984).

9. G. Moad and D. H. Solomon, *The Chemistry of Free Radical Polymerization*, Pergamon, Oxford, 1995, p. 66.

10. J. W. Timberlake, in *Substituent Effects in Radical Chemistry*, H. G. Viehe, Z. Janousek, and R. Merenyi, eds., Reidel, 1986, p. 271.

11. O. Nuyken, C. Scherer, A. Baindl, A. R. Brenner, U. Dahn, R. Gartner, S. Kaiser-Rohrich, R. Kollefrath, P. Matusche, and B. Voit, *Prog. Polym. Sci.* **22**, 93 (1997).

12. A. Ueda and S. Nagai, *J. Polym. Sci.; Part A: Polym. Chem.* **24**, 405 (1986).

13. E. Yoshida and S. Tanimoto, *Macromolecules* **30**, 4018 (1997).

14. A. Ueda and S. Nagai, *J. Polym. Sci.; Part A: Polym. Chem.* **22**, 1611 (1984).

15. H. Inoue, A. Ueda, and S. Nagai, *J. Polym. Sci.; Part A: Polym. Chem.* **26**, 1077 (1988).

16. M. Mishra, *Macromolecules* **29**, 5228 (1996).

17. Y. Shimura and D. Chen, *Macromolecules* **26**, 5004 (1993).

18. T. Cheikhalard, L. Tighzert, and J. P. Pascault, *Angew. Makromol. Chem.* **256**, 49 (1998).

19. T. Cheikhalard, V. Massardier, L. Tighzert, and J. P. Pascault, *J. Appl. Polym. Sci.* **70**, 613 (1998).

20. T. C. Chang, H. B. Chen, Y. C. Chen, and S. Y. Ho, *J. Polym. Sci.; Part A: Polym. Chem.* **34**, 2613 (1996).

21. R. P. N. Veregin, M. K. Georges, P. M. Kazmaier, and G. K. Hamer, *Macromolecules* **26**, 5316 (1993).

22. D. B. Priddy, *Adv. Polym. Sci.* **111**, 67 (1994).

23. E. G. Toplikar, M. S. Herman, A. B. Padias, H. K. Hall, Jr., and D. B. Priddy, *Polym. Bull.* **39**, 37 (1997).

24. G. Moad and D. H. Solomon, in *Comprehensive Polymer Science*, G. C. Eastmond, A. Ledwith, S. Russo, and P. Sigwalt, eds., Pergamon, London, 1989, p. 97.

25. C. J. Hamilton and B. J. Tighe, in *Comprehensive Polymer Science*, G. C. Eastmond, A. Ledwith, S. Russo, and P. Sigwalt, eds., Pergamon, London, 1989, Vol. 3, p. 261.

26. G. Moad and D. H. Solomon, *The Chemistry of Free Radical Polymerization*, Pergamon, Oxford, 1995, p. 67.

27. M. Buback, in *Controlled/Living Radical Polymerization*, K. Matyjaszewski, ed., ACS Symposium Series 768, 2000, p. 39.

28. M. Buback, S. Klingbeil, J. Sandmann, M.-B. Sderra, H.-P. Vogele, H. Wackerbarth, and L. Z. Wittkowski, *Phys. Chem.* (*Munich*) **210**, 199 (1999).

29. M. Buback and J. Sandmann, *Phys. Chem.* (*Munich*) **214**, 583 (2000).

30. M. Buback and C. Hinton, *Phys. Chem.* (*Munich*) **199**, 229 (1997).

31. P. A. Charpentier, J. M. DeSimone, and G. W. Roberts, *Chem. Eng. Sci.* **55**, 5341 (2000).

32. T. C. Chung and W. Janvikul, *J. Organom. Chem.* **581**, 176 (1999).

33. T. C. Chung, W. Janvikul, and H. L. Lu, *J. Am. Chem. Soc.* **118**, 705 (1996).

34. K. Tharanikkarasu, C. V. Thankam, and G. Radhakrishnan, *Eur. Polym. J.* **33**, 1771 (1997).

35. T. Otsu, A. Matsumoto, and T. Tazaki, *Polym. Bull.* **17**, 323 (1987).

36. J. V. Crivello, J. L. Lee, and D. A. Conlon, *J. Polym. Sci.; Part A: Polym. Chem.* **24**, 1251 (1986).

37. T. Otsu and T. Tazaki, *Polym. Bull.* **16**, 277 (1986).

38. X. P. Chen, K. Y. Qiu, G. Swift, D. G. Westmoreland, and S. Wu, *Eur. Polym. J.* **36**, 1547 (2000).

39. H. Tanaka, Y. Teraoka, T. Sato, and T. Ota, *Makromol. Chem.* **194**, 2719 (1993).

40. H. Tanaka, *Prog. Polym. Sci.* **17**, 1107 (1992).

41. B. Yamada, H. Tanaka, K. Konishi, and T. Otsu, *J. Macromol. Sci.-Pure Appl. Chem.* **A31**, 351 (1994).

42. J. R. Ebdon, T. N. Huckerby, B. J. Hunt, S. Rimmer, M. J. Shepherd, and M. Teodorescu, *Polym. Degrad. Stabil.* **39**, 4943 (1998).

43. T. Otsu, *J. Polym. Sci.; Part A: Polym. Chem.* **38**, 2121 (2000).

44. D. Braun, T. Skrzek, S. Steinhauer-Beiber, and H. Tretner, *Macromol. Chem. Phys.* **196**, 573 (1995).

45. A. Bledzki and D. Braun, *Polym. Bull.* **16**, 19 (1986).

46. D. Braun, H. J. Lindner, and H. Tretner, *Eur. Polym. J.* **25**, 725 (1989).

47. A. Ledzki, H. Balard, and D. Braun, *Makromol. Chem.* **189**, 2807 (1988).

48. T. Li, T. J. Willis, A. B. Padias, and H. K. Hall, Jr., *Macromolecules* **24**, 2485 (1991).

49. H. Tanaka, Y. Tezuka, and K. Fujita, *Polym. J.* **32**, 711 (2000).

50. H. Tanaka, K. Aoki, T. Hongo, and Y. Tezuka, *Polym. J.* **32**, 147 (2000).

51. H. Tanaka, *Trends Polym. Sci.* **4**, 106 (1996).

52. T. S. Kwon, K. Takagi, H. Kunisada, and Y. Yuki, *J. Macromol. Sci.–Pure Appl. Chem.* **37**, 1461 (2000).

53. T. S. Kwon, H. Ochiai, S. Kondo, K. Takagi, H. Kunisada, and Y. Yuki, *Polym. J.* **31**, 411 (1999).

54. G. Moad and D. H. Solomon, *The Chemistry of Free Radical Polymerization*, Pergamon, Oxford, 1995, p. 93.

55. W. C. Buzanowski, J. D. Graham, D. B. Priddy, and E. Shero, *Polymer* **33**, 3055 (1992).

56. B. J. Meister and M. T. Malanga, in *Encyclopedia of Polymer Science and Engineering*, J. I. Kroschwitz, ed., Wiley, New York, 1989, Vol. 16, p. 21.

57. H. Komber, M. Gruner, and H. Malz, *Macromol. Rapid Commun.* **19**, 83 (1998).

58. W. Devonport, L. Michalak, E. Malmström, M. Mate, B. Kurdi, C. J. Hawker, G. G. Barclay, and R. Sinta, *Macromolecules* **30**, 1929 (1997).

59. W. A. Pryor and L. D. Lasswell, *Adv. Free Radical Chem.* **5**, 27 (1975).

60. G. Clouet, P. Chaumont, and P. Corpart, *J. Polym. Sci.; Part A: Polym. Chem.* **31**, 2815 (1993).

61. R. S. Lehrle and A. Shortland, *Eur. Polym. J.* **24**, 425 (1988).

62. J. Lingnau and G. Meyerhoff, *Polymer* **24**, 1473 (1983).

63. J. Lingnau and G. Meyerhoff, *Macromolecules* **17**, 941 (1984).

64. M. Stickler and G. Meyerhoff, *Makromol. Chem.* **179**, 2729 (1978).

65. H. Tanaka, T. Kameshima, K. Sasai, T. Sato, and T. Ota, *Makromol. Chem.* **192**, 427 (1991).

66. H. Tanaka, Y. Kikukawa, T. Kameshima, T. Sato, and T. Ota, *Makromol. Chem., Rapid Commun.* **12**, 535 (1991).

67. D. Liu, A. B. Padias, and J. H. K. Hall, *Macromolecules* **28**, 622 (1995).

68. D. L. Hasha, D. B. Priddy, P. R. Rudolf, E. J. Stark, M. d. Pooter, and F. V. Damme, *Macromolecules* **25**, 3046 (1992).

69. T. Sato, M. Abe, and T. Otsu, *J. Makromol. Sci.—Chem.* **A15**, 367 (1981).

70. L. Eberson and O. Persson, *Acta Chem. Scand.* **53**, 680 (1999).

71. L. Eberson, O. Persson, H. K. Hall, Jr., A. B. Padias, and P. J. Steel, *Macromolecules* **33**, 2021 (2000).

72. E. A. Mash, H.-G. Korth, and S. M. DeMoss, *Tetrahedron* **53**, 15297 (1997).

73. E. S. Huyser and R. H. C. Feng, *J. Org. Chem.* **34**, 1727 (1969).

74. E. S. Huyser and C. J. Bredeweg, *J. Am. Chem. Soc.* **86**, 2401 (1964).

75. Y. Sawaki, in *Organic Peroxides*, W. Ando, ed., Wiley, Chichester, UK, 1992, p. 426.

76. A. S. Sarac, *Prog. Polym. Sci.* **24**, 1149 (1999).

77. B. B. Dambatta and J. R. Ebdon, *Eur. Polym. J.* **22**, 783 (1986).

78. S. Bottle, W. K. Busfield, I. D. Jenkins, S. Thang, E. Rizzardo, and D. H. Solomon, *Eur. Polym. J.* **25**, 671 (1989).

79. B. Vazquez, B. Levenfeld, and J. S. Roman, *Polym. Int.* **46**, 241 (1998).

80. C. H. Bamford, in *Comprehensive Polymer Science*, G. C. Eastmond, A. Ledwith, S. Russo, and P. Sigwalt, eds., Pergamon, London, 1989, p. 123.

81. H. F. Gruber, in *Polymeric Materials Encyclopedia*, J. C. Salamone, ed., CRC Press, Boca Raton, FL, 1996, p. 5190.

82. J. P. Fouassier, *Photoinitiation, Photopolymerisation and Photocuring*, Hanser Publishers, Munich, 1995.

83. N. S. Allen, *J. Photochem. Photobiol.; Part A: Chem.* **100**, 101 (1996).

84. R. S. Davidson, *J. Photochem. Photobiol.; Part A: Chem.* **73**, 81 (1993).

85. C. Decker, in *Polymeric Materials Encyclopedia*, J. C. Salamone, ed., CRC Press, Boca Raton, FL, 1996, p. 5181.

86. G. Moad and D. H. Solomon, *The Chemistry of Free Radical Polymerization*, Pergamon, Oxford, 1995, p. 43.

87. S. P. Pappas, A. K. Chattopadhyay, and L. H. Carlblom, *ACS Symp. Ser.* **25**, 12 (1976).

88. N. T. Lipscomb and Y. Tarshiani, *J. Polym. Sci.; Part A: Polym. Chem.* **26**, 529 (1988).

89. N. S. Allen, *Photopolymerisation and Photoimaging Science and Technology*, Elsevier, London, 1986.

90. D. Griller, J. A. Howard, P. R. Marriott, and J. C. Scaiano, *J. Am. Chem. Soc.* **103**, 619 (1981).

91. N. S. Allen, M. Edge, S. Sethi, F. Catalina, T. Corrales, and A. Green, *J. Photochem. Photobiol.; Part A: Chem.* **137**, 169 (2000).

92. H. J. Hageman, *Macromol. Rapid Commun.* **18**, 443 (1997).

93. W. D. Cook, *Polymer* **33**, 600 (1992).

94. H. J. Hageman and L. G. H. Jansen, *Makromol. Chem.* **189**, 2781 (1988).

95. H. F. Gruber, R. Klos, and G. Greber, *J. Macromol. Sci.—Chem.* **A28**, 925 (1991).

96. C. Carlini and L. Angiolini, in *Radiation Curing in Polymer Science and Technology*, J. P. Fouassier and J. F. Rabek, eds., Elsevier, London, 1993, p. 283.

97. L. Angiolini, D. Caretti, and E. Salatelli, *Macromol. Chem. Phys.* **201**, 2646 (2000).

98. W. K. Busfield, I. D. Jenkins, S. H. Thang, E. Rizzardo, and D. H. Solomon, *Aust. J. Chem.* **38**, 689 (1985).

99. T. Nakamura, W. K. Busfield, I. D. Jenkins, E. Rizzardo, S. H. Thang, and S. Suyama, *J. Org. Chem.* **62**, 5578 (1997).

100. W. K. Busfield, I. D. Jenkins, and P. V. Le, *J. Polym. Sci.; Part A: Polym. Chem.* **36**, 2169 (1998).

101. T. Nakamura, S. Suyama, W. K. Busfield, I. D. Jenkins, E. Rizzardo, and S. H. Thang, *Polymer* **40**, 1395 (1999).

102. W. K. Busfield, I. D. Jenkins, and M. J. Monteiro, *Aust. J. Chem.* **50**, 1 (1997).

103. W. K. Busfield, I. D. Jenkins, and M. J. Monteiro, *J. Polym. Sci.; Part A: Polym. Chem.* **35**, 263 (1997).

104. W. K. Busfield, D. I. Grice, and I. D. Jenkins, *Polym. Int.* **27**, 199 (1992).

105. R. D. Grant, P. G. Griffiths, G. Moad, E. Rizzardo, and D. H. Solomon, *Aust. J. Chem.* **36**, 2447 (1983).

106. D. Bednarek, G. Moad, E. Rizzardo, and D. H. Solomon, *Macromolecules* **21**, 1522 (1988).

107. W. K. Busfield, I. D. Jenkins, and M. J. Monteiro, *Polymer* **38**, 165 (1997).

108. A. Kajiwara, Y. Konishi, Y. Morishima, W. Schnabel, K. Kuwata, and M. Kamachi, *Macromolecules* **26**, 1656 (1993).

109. M. Kamachi, A. Kajiwara, K. Saegusa, and Y. Morishima, *Macromolecules* **26**, 7369 (1993).

110. M. Kamachi, K. Kuwata, T. Sumiyoshi, and W. Schnabel, *J. Chem. Soc. Perkin Trans.* **2**, 961 (1988).

111. T. Sato, S. Inui, H. Tanaka, T. Ota, M. Kamachi, and K. Tanaka, *J. Polym. Sci.; Part A: Polym. Chem.* **25**, 637 (1987).

112. M. Yoshioka and T. Otsu, *Macromolecules* **25**, 559 (1992).

113. M. Yoshioka and T. Otsu, *Macromolecules* **25**, 2599 (1992).

114. P. G. Griffiths, E. Rizzardo, and D. H. Solomon, *J. Macromol. Sci.–Chem.* **A17**, 45 (1982).

115. B. Maillard, K. U. Ingold, and J. C. Scaiano, *J. Am. Chem. Soc.* **105**, 5095 (1983).

116. C. H. Bamford, in *Encyclopedia of Polymer Science and Engineering*, H. F. Mark, N. M. Bikales, C. G. Overberger, and G. Menges, eds., Wiley-Interscience, New York, 1988, p. 708.

117. G. Odian, *Principles of Polymer Science*, 3rd ed., Wiley, New York, 1991, p. 234.

118. J. Krstina, G. Moad, R. I. Willing, S. K. Danek, D. P. Kelly, S. L. Jones, and D. H. Solomon, *Eur. Polym. J.* **29**, 379 (1993).

119. M. D. Zammit, T. P. Davis, D. M. Haddleton, and K. G. Suddaby, *Macromolecules* **30**, 1915 (1997).

120. W. H. Starnes, Jr., I. M. Plitz, F. C. Schilling, G. M. Villacorta, G. S. Park, and A. H. Saremi, *Macromolecules* **17**, 2507 (1984).

121. G. Moad, E. Rizzardo, D. H. Solomon, S. R. Johns, and R. I. Willing, *Makromol. Chem., Rapid Commun.* **5**, 793 (1984).

122. J. K. Fink, *J. Polym. Sci., Polym. Chem. Ed.* **21**, 1445 (1983).

123. C. I. Simionescu, A. P. Chiriac, and M. V. Chiriac, *Polymer* **34**, 3917 (1993).

124. N. J. Turro and B. Kraeutler, *Acc. Chem. Res.* **13**, 369 (1980).

125. C. I. Simionescu and A. P. Chiriac, *Prog. Polym. Sci.* **25**, 219 (2000).

126. A. Matsumoto and K. Mizuta, *Macromolecules* **27**, 5863 (1994).

127. M. Buback, B. Huckestein, F.-D. Kuchta, G. T. Russell, and E. Schmid, *Macromol. Chem. Phys.* **195**, 2117 (1994).

128. G. T. Russell, D. H. Napper, and R. G. Gilbert, *Macromolecules* **21**, 2141 (1988).

129. D. H. Solomon and G. Moad, *Makromol. Chem., Macromol. Symp.* **10/11**, 109 (1987).

130. Y. Watanabe, H. Ishigaki, H. Okada, and S. Suyama, *Polym. J.* **29**, 733 (1997).

131. J. Shen, Y. Tian, G. Wang, and M. Yang, *Makromol. Chem.* **192**, 2669 (1991).

132. T. G. Carswell, D. J. T. Hill, D. I. Londero, J. H. O'Donnell, P. J. Pomery, and C. L. Winzor, *Polymer* **33**, 137 (1992).

133. R. G. Gilbert, *Emulsion Polymerization. A Mechnistic Approach*, Academic Press, London, 1995.

134. M. D. Goodner and C. N. Bowman, *Macromolecules* **32**, 6552 (1999).

135. K. Ito, *Macromolecules* **13**, 193 (1980).

136. K. Ito, *J. Polym. Sci.; Part A: Polym. Chem.* **18**, 701 (1980).

137. G. Odian, *Principles of Polymer Science*, 3rd ed., Wiley, New York, 1991, p. 236.

138. P. B. Zetterlund, W. K. Busfield, and I. D. Jenkins, *Macromolecules* **32**, 8041 (1999).

139. D. A. Shipp, T. A. Smith, D. H. Solomon, and G. Moad, *Macromol. Rapid Commun.* **16**, 837 (1995).

140. G. Moad, E. Rizzardo, D. H. Solomon, and A. L. J. Beckwith, *Polym. Bull.* **29**, 647 (1992).

141. M. Deady, A. W. H. Mau, G. Moad, and T. H. Spurling, *Makromol. Chem.* **194**, 1691 (1993).

142. A. A. Gridnev and S. D. Ittel, *Macromolecules* **29**, 5864 (1996).

143. O. F. Olaj, P. Vana, M. Zoder, A. Kornherr, and G. Zifferer, *Macromol. Rapid Commun.* **21**, 913 (2000).

144. B. Yamada, K. Fukushima, and T. Otsu, *Polym. Bull.* **6**, 189 (1981).

145. B. Yamada, D. G. Westmoreland, S. Kobatake, and O. Konosu, *Prog. Polym. Sci.* **24**, 565 (1999).

146. S. Beuermann and M. Buback, in *Controlled Radical Polymerization*, K. Matyjaszewski, ed., ACS Symposium Series 685, 1998, p. 84.

147. M. L. Coote, M. D. Zammit, and T. P. Davis, *Trends Polym. Sci.* **4**, 189 (1996).

148. M. Kamachi and A. Kajiwara, *Macromol. Chem. Phys.* **198**, 787 (1997).

149. M. P. Tonge, A. Kajiwara, M. Kamachi, and R. G. Gilbert, *Polymer* **39**, 2305 (1998).

150. M. Kamachi, *Adv. Polym. Sci.* **82**, 207 (1987).

151. A. Matsumoto and B. Giese, *Macromolecules* **29**, 3758 (1996).

152. M. Spichty, B. Giese, A. Matsumoto, H. Fischer, and G. Gescheidt, *Macromolecules* **34**, 723 (2001).

153. M. P. Tonge, R. J. Pacce, and R. G. Gilbert, *Macromol. Chem. Phys.* **195**, 1144 (1994).

154. M. Azukizawa, B. Yamada, D. J. T. Hill, and P. J. Pomery, *Macromol. Chem. Phys.* **201**, 774 (2000).

155. B. Yamada, M. Azukizawa, H. Yamazoe, D. J. T. Hill, and P. J. Pomery, *Polymer* **41**, 5611 (2000).

156. A. Kajiwara and M. Kamachi, *Macromol. Chem. Phys.* **201**, 2165 (2000).

157. B. Yamada and S. Kobatake, *Prog. Polym. Sci.* **19**, 1089 (1994).

158. A. Matsumoto, *J. Polym. Sci.; Part A: Polym. Chem.* **37**, 1969 (1999).

159. H. Tanaka and S. Yoshida, *Macromolecules* **28**, 8117 (1995).

160. E. Rizzardo, Y. K. Chong, R. A. Evans, G. Moad, and S. H. Thang, *Macromol. Symp.* **111**, 1 (1996).

161. G. F. Meijs, E. Rizzardo, and S. H. Thang, *Macromolecules* **21**, 3122 (1988).

162. A. O. Kress, L. J. Mathias, and G. Cei, *Macromolecules* **22**, 537 (1989).

163. B. Yamada, S. Kobatake, and S. Aoki, *J. Polym. Sci.; Part A: Polym. Chem.* **31**, 3433 (1993).

164. S. Kobatake, B. Yamada, and S. Aoki, *Polymer* **36**, 413 (1995).

165. S. Kobatake and B. Yamada, *Macromolecules* **28**, 4047 (1995).

166. B. Yamada and T. Otsu, *Makromol. Chem.* **192**, 333 (1991).

167. S. Kobatake and B. Yamada, *J. Polym. Sci.; Part A: Polym. Chem.* **34**, 95 (1996).

168. S. Kobatake and B. Yamada, *Macromol. Chem. Phys.* **198**, 2825 (1997).

169. S. Kobatake, M. Satake, and B. Yamada, *J. Polym. Sci.; Part A: Polym. Chem.* **31**, 1551 (1993).

170. B. Yamada, S. Kobatake, and S. Aoki, *Macromolecules* **26**, 5099 (1993).

171. B. Yamada and S. Kobatake, *Polym. J.* **24**, 281 (1992).

172. T. Sato, M. Seno, M. Kobayashi, T. Kohono, and H. Tanaka, *Eur. Polym. J.* **31**, 29 (1995).

173. K. J. Ivin, *J. Polym. Sci.; Part A: Polym. Chem.* **38**, 2137 (2000).

174. B. Yamada, T. Tanaka, and T. Otsu, *Eur. Polym. J.* **25**, 117 (1989).

175. J. Penelle, J. Collot, and G. Rufford, *J. Polym. Sci.; Part A: Polym. Chem.* **31**, 2407 (1993).

176. E. L. Madruga, J. S. Roman, M. Angeles, and M. C. F. Moreal, *Macromolecules* **17**, 989 (1984).

177. R. A. Hutchinson, D. A. Paquet, Jr., S. Beuermann, and J. H. McMinn, *Ind. Eng. Chem. Res.* **37**, 3567 (1998).

178. T. Itoh, H. Fujinami, M. Yamahata, H. Konishi, and M. Kubo, *Macromolecules* **31**, 1501 (1998).

179. J. Fossey, D. Lefort, and J. Sorba, *Free Radicals in Organic Chemistry*, Wiley, Chichester, UK, 1995, p. 139.

180. H. Tanaka, *Trends Polym. Sci.* **1**, 361 (1993).

181. J. Penelle, A. B. Padias, H. K. Hall, Jr., and H. Tanaka, *Adv. Polym. Sci.* **102**, 74 (1992).

182. H. Ito and M. Ueda, *Macromol. Symp.* **54/55**, 551 (1992).

183. M. Ueda, M. Takahashi, Y. Imai, and C. U. Pittman, Jr., *J. Polym. Sci.; Polym. Chem. Ed.* **20**, 2819 (1982).

184. M. Ueda, M. Takahashi, T. Suzuki, Y. Imai, and C. U. Pittman, Jr., *J. Polym. Sci.; Polym. Chem. Ed.* **20**, 1139 (1983).

185. M. Ueda, H. Mori, and H. Ito, *J. Polym. Sci.; Part A: Polym. Chem.* **28**, 2597 (1990).

186. M. Buback, *Macromol. Symp.* **111**, 229 (1996).

187. C. Hansch, A. Leo, and R. W. Taft, *Chem. Rev.* **91**, 165 (1991).

188. R. Z. Greenly, in *Polymer Handbook*, 4th ed., J. Brandrup, E. H. Immergut, and E. A. Grulke, eds., Wiley-Interscience, New York, 1999, p. II/181.

189. M. J. Jones, G. Moad, E. Rizzardo, and D. H. Solomon, *J. Org. Chem.* **54**, 1607 (1989).

190. M. L. Coote and T. P. Davis, *Macromolecules* **32**, 4290 (1999).

191. T. Alfrey, Jr., J. J. Bohrer, and H. Mark, *Copolymerization*, Interscience, New York, 1952.

192. R. Z. Greenly, in *Polymer Handbook*, 4th ed., J. Brandrup, E. H. Immergut, and E. A. Grulke, eds., Wiley, New York, 1999, p. II/309.

193. A. D. Jenkins, K. Hatada, T. Kitayama, and T. Nishiura, *J. Polym. Sci.; Part A: Polym. Chem.* **38**, 4336 (2000).

194. J. J. Herman and P. Teyssie, *Macromolecules* **11**, 839 (1978).

195. A. Ghosez-Giese and B. Giese, in *Controlled Radical Polymerization*, K. Matyjaszewski, ed., ACS Symposium Series 685, 1998, p. 50.

196. H. Fischer and L. Radom, *Angew. Chem. Int. Ed.* **40**, 1340 (2000).

197. T. Hongo, S. Yoshida, T. Yamada, and H. Tanaka, *Polym. Int.* **48**, 505 (1999).

198. B. Yamada and K. Sakamoto, *Polymer* **41**, 5619 (2000).

199. D. R. Arnold, in *Substituent Effects in Radical Chemistry*, H. G. Viehe, Z. Janousek, and R. Merenyi, eds., Reidel, Dordrecht, 1986.

200. B. Yamada, S. Kobatake, and S. Aoki, *Macromol. Chem. Phys.* **195**, 933 (1994).

201. D. A. Morrison and T. P. Davis, *Macromolecules* **33**, 2128 (2000).

202. B. Yamada, S. Kobatake, and S. Aoki, *Macromol. Chem. Phys.* **195**, 581 (1994).

203. T. Sato, I. Kamiya, H. Tanaka, and T. Ota, *Eur. Polym. J.* **27**, 1087 (1991).

204. S. Kobatake and B. Yamada, *Polym. J.* **28**, 535 (1996).

205. L. H. Yee, M. L. Coote, R. P. Chaplin, and T. P. Davis, *J. Polym. Sci.; Part A: Polym. Chem.* **38**, 2909 (1991).

206. T. Sato, Y. Takahashi, M. Seno, H. Nakayama, H. Tanaka, and T. Ota, *Makromol. Chem.* **192**, 2909 (1991).

207. A. Matsumoto, Y. Oki, and T. Otsu, *Polym. J.* **25**, 237 (1993).

208. B. Yamada, S. Kobatake, and O. Konosu, *Macromol. Chem. Phys.* **197**, 901 (1996).

209. S. Beuermann, M. Buback, T. P. Davis, R. G. Gilbert, R. A. Hutchinson, O. F. Olaj, G. T. Russell, J. Schweer, and A. M. van Herk, *Macromol. Chem. Phys.* **198**, 1545 (1997).

210. B. Yamada, E. Yoshikawa, H. Miura, and T. Otsu, *Makromol. Chem., Rapid Commun.* **13**, 531 (1992).

211. H. Azuma, Y. Katagiri, and S. Yamabe, *J. Polym. Sci.; Part A: Polym. Chem.* **34**, 1407 (1996).

212. S. Beuermann, M. Buback, T. P. Davis, R. G. Gilbert, R. A. Hutchinson, A. Kajiwara, B. Klumperman, and G. T. Russell, *Macromol. Chem. Phys.* **201**, 1355 (2000).

213. A. Matsumoto, Y. Sano, M. Yoshioka, and T. Otsu, *J. Polym. Sci.; Part A: Polym. Chem.* **34**, 291 (1996).

214. A. Matsumoto and T. Otsu, *Macromol. Symp.* **98**, 139 (1995).

215. A. Matsumoto, Y. Oki, and T. Otsu, *Euro. Polym. J.* **29**, 1225 (1993).

216. T. Sato, K. Arimoto, H. Tanaka, T. Ota, K. Kato, and K. Doiuchi, *Macromolecules* **22**, 2219 (1989).

217. T. Sato, K. Masaki, M. Seno, and H. Tanaka, *Markomol. Chem.* **194**, 849 (1993).

218. A. Matsumoto, K. Shimizu, K. Mizuata, and T. Otsu, *J. Polym. Sci.; Part A: Polym. Chem.* **32**, 1957 (1994).

219. K. Hatada, T. Kitayama, and E. Masuda, *Makromol. Chem., Rapid Commun.* **11**, 101 (1990).

220. E. Masuda, S. Kishiro, T. Kitayama, and K. Hatada, *Polym. J.* **23**, 847 (1991).

221. Y. Tsukahara, K. Tsutsumi, Y. Yamashita, and S. Shimizu, *Macromolecules* **23**, 5201 (1990).

222. K. Tsutsumi, Y. Tsukahara, and Y. Okamoto, *Polym. J.* **26**, 13 (1994).

223. K. Tsutsumi, Y. Tsukahara, and Y. Okamoto, *Polymer* **35**, 2205 (1994).

224. E. Nomura, K. Ito, A. Kajiwara, and M. Kamachi, *Macromolecules* **30**, 2811 (1997).

225. K. Hatada, T. Kitayama, and O. Nakagawa, in *Polymeric Materials Encyclopedia*, J. C. Salamone, ed., CRC Press, Boca Raton, FL, 1996, p. 7956.

226. K. Hatada, T. Kitayama, and K. Ute, *Prog. Polym. Sci.* **13**, 189 (1988).

227. Y. Tsukahara, K. Yai, and K. Kaeriyama, *Polymer* **40**, 729 (1999).

228. T. Nakano and Y. Okamoto, in *Controlled Radical Polymerization*, K. Matyjaszewski, ed., ACS Symposium Series 685, 1998, p. 451.

229. T. Nakano and Y. Okamoto, *Macromol. Rapid Commun.* **21**, 603 (2000).

230. T. Nakano, A. Matsuda, and Y. Okamoto, *Polym. J.* **28**, 556 (1996).

231. T. Nakano, Y. Shikisai, and Y. Okamoto, *Polym. J.* **28**, 41 (1996).

232. T. Nakano, N. Kinjo, Y. Hidaka, and Y. Okamoto, *Polym. J.* **31**, 464 (1999).

233. T. Nakano and Y. Okamoto, *Macromolecules* **32**, 2391 (1999).

234. T. Nakano, D. Tamada, J. Miyazaki, K. Kakiuchi, and Y. Okamoto, *Macromolecules* **33**, 1489 (2000).

235. J. Zhang, W. H. Liu, T. Nakano, and Y. Okamoto, *Polym. J.* **32**, 694 (2000).

236. W. H. Liu, T. Nakano, and Y. Okamoto, *Polym. J.* **32**, 694 (2000).

237. W. H. Liu, T. Nakano, and Y. Okamoto, *J. Polym. Sci.; Part A: Polym. Chem.* **38**, 1024 (2000).

238. S. Habaue, T. Uno, H. Baraki, and Y. Okamoto, *Macromolecules* **33**, 820 (2000).

239. K. Yamada, T. Nakano, and Y. Okamoto, *Polym. J.* **30**, 641 (1998).

240. N. A. Porter, R. Breyer, E. Swan, J. Nally, J. Pradhan, T. Allen, and A. T. McPhail, *J. Am. Chem. Soc.* **113**, 7002 (1991).

241. D. P. Curran, N. A. Porter, and B. Giese, *Stereochemistry of Radical Reactions*, VCH, Weinheim, 1996, p. 178.

242. N. A. Porter, T. R. Allen, and R. A. Breyer, *J. Am. Chem. Soc.* **114**, 7676 (1992).

243. W.-X. Wu, A. T. McPhail, and N. A. Porter, *J. Org. Chem.* **59**, 1302 (1994).

244. C. L. Mero and N. A. Porter, *J. Org. Chem.* **65**, 775 (2000).

245. M. Kamachi, *Adv. Polym. Sci.* **38**, 56 (1981).

246. T. F. McKenna and A. Villanueva, *J. Polym. Sci.; Part A: Polym. Chem.* **37**, 589 (1999).

247. A. Matsumoto and Y. Mohri, *J. Polym. Sci.; Part A: Polym. Chem.* **37**, 2803 (1999).

248. T. Sato, K. Masaki, K. Kondo, M. Seno, and H. Tanaka, *Polym. Bull.* **35**, 345 (1995).

249. M. D. Zammit, T. P. Davis, G. D. Willett, and K. F. O'Driscoll, *J. Polym. Sci.; Part A: Polym. Chem.* **35**, 2311 (1997).

250. M. L. Coote and T. P. Davis, *Eur. Polym. J.* **36**, 2423 (2000).

251. K. F. O'Driscoll, M. L. Monteiro, and B. Klumperman, *J. Polym. Sci., Polym. Chem. Ed.* **35**, 515 (1997).

252. T. Sato, M. Morita, H. Tanaka, and T. Ota, *J. Polym. Sci.; Part A: Polym. Chem.* **27**, 2497 (1989).

253. T. Sato, T. Shimizu, M. Seno, H. Tanaka, and T. Ota, *Makromol. Chem.* **193**, 1439 (1992).

254. O. F. Olaj and I. Schnoll-Bitai, *Monatsh. Chem.* **130**, 731 (1999).

255. F.-D. Kuchta, A. M. V. Herk, and A. L. German, *Macromolecules* **33**, 3641 (2000).

256. S. Beuermann, D. A. Paquet, Jr., J. H. McMinn, and R. A. Hutchinson, *Macromolecules* **30**, 194 (1997).

257. C. Bunyakan, L. Armanet, and D. Hunkeler, *Polymer* **40**, 6225 (1999).

258. A. M. van Herk, B. G. Manders, D. A. Canelas, M. A. Quadir, and J. M. DeSimone, *Macromolecules* **30**, 4780 (1997).

259. M. A. Quadir, J. M. DeSimone, A. M. van Herk, and A. L. German, *Macromolecules* **31**, 6481 (1998).

260. S. Beuermann, M. Buback, C. Schmaltz, and F.-D. Kuchta, *Macromol. Chem. Phys.* **199**, 1209 (1998).

261. S. Beuermann, M. Buback, C. Isemer, and A. Wahl, *Macromol. Rapid Commun.* **20**, 26 (1999).

262. S. Beuermann, M. Buback, and C. Schmaltz, *Macromolecules* **31**, 8069 (1998).

263. F. Rindfleisch, T. DiNois, and M. McHugh, *J. Phys. Chem.* **100**, 15581 (1996).

264. M. Seno, N. Matsumura, H. Nakamura, and T. Sato, *J. Appl. Polym. Sci.* **63**, 1361 (1999).

265. H. Nakamura, M. Seno, and T. Sato, *J. Polym. Sci.; Part A: Polym. Chem.* **35**, 1361 (1999).

266. M. Fischer and H. Ritter, *Macromol. Rapid Commun.* **21**, 142 (2000).

267. P. Glockner, N. Metz, and H. Ritter, *Macromolecules* **33**, 4288 (2000).

268. J. Jeromin and H. Ritter, *Macromolecules* **32**, 5236 (1999).

269. J. Jeromin, O. Noll, and H. Ritter, *Macromol. Chem. Phys.* **199**, 2641 (1998).

270. J. Storsberg and H. Ritter, *Macromol. Rapid Commun.* **21**, 236 (2000).

271. W. Lau, *Macromol. Symp.* (in press).

272. Y. Isobe, K. Yamada, T. Nakano, and Y. Okamoto, *Macromolecules* **32**, 5979 (1999).

273. K. Yamada, T. Nakano, and Y. Okamoto, *J. Polym. Sci.; Part A: Polym. Chem.* **37**, 2677 (1999).

274. K. Yamada, T. Nakano, and Y. Okamoto, *Macromolecules* **31**, 7598 (1998).

275. Y. Okamoto, K. Yamada, and T. Nakano, in *Controlled/Living Radical Polymerization. Progress in ATRP, NMP, and RAFT*, K. Matyjaszewski, ed., ACS Symposium Series 268, 2000, p. 57.

276. J. Shen, G. Wang, Y. Zheng, and M. Yang, *Makromol. Chem. Symp.* **63**, 105 (1992).

277. G. B. Butler, *Cyclopolymerization and Cyclocopolymerization*, Marcel Dekker, New York, 1992.

278. T. Kodaira, in *Polymeric Material Encyclopedia*, J. C. Salamone, ed., CRC Press, Boca Raton, FL, 1996, p. 1750.

279. T. Kodaira, *Prog. Polym. Sci.* **25**, 627 (2000).

280. B. Yamada, M. Azukizawa, and T. Hirayama, *Polym. Bull.* **43**, 457 (2000).

281. T. Tsuda and L. J. Mathias, *Polymer* **35**, 3317 (1994).

282. T. Tsuda and L. J. Mathias, *Macromolecules* **26**, 6359 (1993).

283. D. Avci, C. Hayenes, and L. J. Mathias, *J. Polym. Sci.; Part A: Polym. Chem.* **35**, 2111 (1997).

284. D. Avci and L. J. Mathias, *J. Polym. Sci.; Part A: Polym. Chem.* **37**, 901 (1999).

285. R. D. Thompson, W. L. Jarrett, and L. J. Mathias, *Macromolecules* **25**, 6455 (1992).

286. T. Kodaira, Q.-Q. Liu, M. Satoyama, M. Urushisaki, and H. Utsumi, *Polymer* **40**, 6947 (1999).

287. G. Wulff and B. Kuhneweg, *J. Org. Chem.* **62**, 5785 (1997).

288. K. Yokota, T. Kakuchi, T. Uesaka, and M. Obata, *Acta Polymerica* **48**, 459 (1997).

289. S. Zheng and D. Y. Sogah, *Tetrahedron* **53**, 15469 (1999).

290. M. Seno, T. Ikezumi, T. Sumie, Y. Masuda, and T. Sato, *J. Polym. Sci.; Part A: Polym. Chem.* **38**, 2098 (2000).

291. T. Endo and T. Yokozawa, *New Method for Polymer Synthesis*, Plenum Press, New York, 1992, p. 155.

292. R. A. Evans and E. Rizzardo, *J. Polym. Sci.; Part A: Polym. Chem.* **39**, 202 (2000).

293. N. Moszner, F. Zeuner, T. Volkel, and V. Rheinberger, *Macromol. Chem. Phys.* **200**, 2173 (1999).

294. D. Colombani, *Prog. Polym. Sci.* **21**, 439 (1996).

295. I. Cho, *Prog. Polym. Sci.* **25**, 1043 (2000).

296. W.-S. Choi, W. Yuan, A. B. Padias, and H. K. Hall, Jr., *J. Polym. Sci.; Part A: Polym. Chem.* **37**, 1569 (1999).

297. K. Endo, T. Shiroi, and K. Murata, *J. Polym. Sci.; Part A: Polym. Chem.* **39**, 145 (2001).

298. R. Arakawa, T. Watanabe, T. Fukudo, and K. Endo, *J. Polym. Sci.; Part A: Polym. Chem.* **38**, 4403 (2000).

299. D. Colombani, *Prog. Polym. Sci.* **24**, 425 (1999).

300. T. Sato, H. Takahashi, H. Tanaka, and T. Ota, *J. Polym. Sci.; Part A: Polym. Chem.* **26**, 2839 (1988).

301. T. Sato, S. Shimooka, M. Seno, and H. Tanaka, *J. Polym. Sci.; Part A: Polym. Chem.* **33**, 2865 (1995).

302. T. Sato, S. Shimooka, M. Seno, and H. Tanaka, *J. Polym. Sci.; Part A: Polym. Chem.* **36**, 563 (1998).

303. T. Sato, D. Ito, M. Kuki, H. Tanaka, and T. Ota, *Macromolecules* **24**, 2963 (1991).

304. T. Sato, Y. Nakagawa, T. Kawachi, and M. Seno, *Eur. Polym. J.* **32**, 827 (1996).

305. W. H. Starnes, Jr., B. J. Wojciechowski, H. Chung, G. M. Benedikt, G. S. Park, and A. H. Staremi, *Macromolecules* **28**, 945 (1995).

306. W. H. Starnes, Jr., V. G. Zailkov, H. T. Chung, B. J. Wojciechowski, H. V. Tran, and K. Saylor, *Macromolecules* **31**, 1508 (1998).

307. J. S.-S. Toh, D. H. Huang, P. A. Lovell, and R. G. Gilbert, *Polymer* **42**, 1915 (2001).

308. N. M. Ahmad, F. Heatley, and P. A. Lovell, *Macromolecules* **31**, 2822 (1998).

309. E. F. McCord, W. H. Shaw, and R. A. Hutchinson, *Macromolecules* **30**, 246 (1997).

310. M. H. C. M. van-Boxtel, M. Busch, and S. Lehmann, *Macromol. Chem. Phys.* **201**, 313 (2000).

311. T. Sato, K. Terada, J. Yamauchi, and T. Okaya, *Makromol. Chem.* **194**, 175 (1993).

312. G. Odian, *Principles of Polymerization*, 3rd ed., Wiley, New York, 1991, p. 198.

313. A. Kuriyama and T. Otsu, *Polym. J.* **16** (1984).

314. T. Otsu and A. Kuriyama, *Polym. J.* **17**, 97 (1985).

315. T. Otsu, K. Yamashita, and K. Tsuda, *Macromolecules* **19**, 287 (1986).

316. J. D. Manga, M. Tardi, A. Polton, and P. Sigwalt, *Polym. Int.* **45**, 243 (1998).

317. D. Braun, *Macromol. Symp.* **111**, 63 (1996).

318. P. R. G. Santos, R. Chaumont, J. E. Herz, and G. J. Beinert, *Eur. Polym. J.* **30**, 851 (1994).

319. J. Krstina, G. Moad, E. Rizzardo, C. L. Winzor, and C. T. Berge, *Macromolecules* **28**, 5381 (1995).

320. B. Yamada, S. Kobatake, and S. Aoki, *Polym. Bull.* **31**, 263 (1993).

321. G. Odian, *Principles of Polymer Science*, 3rd ed., Wiley, New York, 1991, p. 512.

322. A. Matsumoto, *Adv. Polym. Sci.* **123**, 41 (1995).

323. S. Zhu and A. E. Hamielec, *Makromol. Chem. Macromol. Symp.* **69**, 247 (1993).

324. M. Malik, V. Choudhary, and I. K. Varma, *J. Macromol. Sci., Rev. Macromol. Chem. Phys.* **C40**, 139 (2000).

325. G. Hild and R. Okasha, *Makromol. Chem.* **186**, 93 (1985).

326. D. T. Landin and C. W. Macosko, *Macromolecules* **21**, 846 (1988).

327. N. Ide and T. Fukuda, *Macromolecules* **30**, 4268 (1997).

328. P. J. Flory, *J. Am. Chem. Soc.* **63**, 3083 (1941).

329. W. H. Stockmayer, *J. Chem. Phys.* **12**, 125 (1944).

330. J. E. Elliott and C. N. Bowman, *Macromolecules* **32**, 8621 (1999).

331. O. Okay, *Makromol. Chem.* **189**, 2201 (1988).

332. H. J. Naghash, O. Okay, and Y. Yagci, *Polymer* **38**, 1187 (1997).

333. O. Okay, D. Kaya, and O. Pekcan, *Polymer* **40**, 6179 (1999).

334. A. Matsumoto, A. Okamoto, S. Okuno, and H. Aota, *Angew. Makromol. Chem.* **240**, 275 (1996).

335. O. Okay, *Angew. Makromol. Chem.* **153**, 125 (1987).

336. T. W. Wilson, *J. Appl. Polym. Sci.* **40**, 1195 (1990).

337. L. J. Mathias, S. Steadman, K. Anderson, R. Davis, W. Jarrett, R. D. Redfearn, and A. Bunn, *Macromol. Symp.* **141**, 47 (1999).

338. P. E. M. Allen, D. J. Bennett, S. Hagias, A. M. Hounslow, G. S. Ross, G. P. Simon, D. R. G. Williams, and E. H. Williams, *Eur. Polym. J.* **25**, 785 (1989).

339. A. S. Hoffman, *Macromol. Symp.* **101**, 443 (1996).

340. Y. Uyama, K. Kato, and Y. Ikada, *Adv. Polym. Sci.* **137**, 1 (1998).

341. C. H. Bamford and K. G. Al-Lamee, *Polymer* **35**, 2844 (1994).

342. A. E. Rubtsov, V. V. Matveev, A. E. Chalykh, N. V. Smirnova, G. A. Gabrielyan, and L. S. Galbraikh, *J. Appl. Polym. Sci.* **43**, 729 (1991).

343. Z. Feng and B. Rånby, *Angew. Makromol. Chem.* **195**, 17 (1992).

344. B. Rånby and F. Z. Gao, *Polym. Adv. Techn.* **5**, 829 (1994).

345. K. Allmer, A. Hult, and B. Rånby, *J. Polym. Sci.; Polym. Chem. Ed.* **28**, 173 (1990).

346. J. F. Rabek, J. Lucki, B. Rånby, Y. Watanabe, and B. J. Qu, ACS Symposium Series, Vol. 364, 1988, p. 168.

347. Y. E. Fang, X. B. Lu, S. Z. Wang, X. Zhao, and F. Fang, *J. Appl. Polym. Sci.* **62**, 2209 (1996).

348. F. Denes, *Trends Polym. Sci.* **5**, 23 (1997).

349. G. Geuskens, A. Etoc, and P. D. Michele, *Eur. Polym. J.* **36**, 265 (2000).

350. H. Kubota and S. Ujita, *J. Appl. Polym. Sci.* **56**, 25 (1995).

351. H. Kubota and S. Suzuki, *Eur. Polym. J.* **31**, 701 (1995).

352. P. Y. Zhang and B. Rånby, *J. Appl. Polym. Sci.* **40**, 1647 (1990).

353. D. Ruckert and G. Geuskens, *Eur. Polym. J.* **32**, 201 (1996).

354. F. C. Loh, K. L. Tan, E. T. Kang, K. G. Neoh, and M. Y. Pun, *Eur. Polym. J.* **31**, 481 (1995).

355. F. Poncin-Epaillard, J. C. Brosse, and T. Falher, *Macromol. Chem. Phys.* **199**, 1613 (1998).

356. G. Moad and D. H. Solomon, *The Chemistry of Free Radical Polymerization*, Pergamon, Oxford, 1995, p. 234.

357. M. Okubo, T. Yamashita, S. T, and T. Shimizu, *Colloid Polym. Sci.* **275**, 288 (1997).

358. D. J. Christie and R. G. Gilbert, *Macromol. Chem. Phys.* **197**, 403 (1996).

359. D. I. Christie and R. G. Gilbert, *Macromol. Chem. Phys.* **198**, 663 (1997).

360. R. G. Gilbert, *Trends Polym. Sci.* **3**, 222 (1995).

361. G. Moad and C. L. Moad, *Macromolecules* **29**, 7727 (1996).

362. J. P. A. Heuts, T. P. Davis, and G. T. Russell, *Macromolecules* **32**, 6019 (1999).

363. J. L. de la Fuente and E. L. Madruga, *J. Polym. Sci.; Part A: Polym. Chem.* **38**, 170 (2000).

364. H. A. S. Schoonbrood, S. C. J. Pierik, B. van den Reijen, J. P. A. Heuts, and A. L. German, *Macromolecules* **29**, 6717 (1996).

365. J. L. de la Fuente and E. L. Madruga, *J. Polym. Sci.; Part A: Polym. Chem.* **36**, 2913 (1998).

366. H. M. Kapfenstein and T. P. Davis, *Macromol. Chem. Phys.* **199**, 2403 (1998).

367. C. L. Moad, G. Moad, E. Rizzardo, and S. H. Thang, *Macromolecules* **29**, 7717 (1996).

368. T. Otsu and M. Yoshida, *Makromol. Chem., Rapid Commun.* **29**, 127 (1982).

369. T. Otsu and A. Matsumoto, *Adv. Polym. Sci.* **136**, 75 (1998).

370. T. Doi, A. Matsumoto, and T. Otsu, *J. Polym. Sci.; Part A: Polym. Chem.* **32**, 2241 (1994).

371. D. Kukulj, T. P. Davis, and R. G. Gilbert, *Macromolecules* **31**, 994 (1998).

372. S. Maeder and R. G. Gilbert, *Macromolecules.* **31**, 4410 (1998).

373. S. Beuermann, D. A. Paquet, Jr., J. H. McMinn, and R. A. Hutchinson, *Macromolecules* **29**, 4206 (1996).

374. M. Busch and A. Wahl, *Macromol. Theory Simul.* **7**, 215 (1998).

375. D. Britton, F. Heatley, and P. A. Lovell, *Macromolecules* **31**, 2828 (1998).

376. N. M. Ahmad, D. Britton, F. Heatley, and P. A. Lovell, *Macromol. Symp.* **143**, 231 (1999).

377. K. Hatada, Y. Terawaki, T. Kitayama, M. Kamachi, and M. Tamaki, *Polym. Bull.* **4**, 451 (1981).

378. B. C. Gilbert, J. R. L. Smith, E. C. Milne, A. L. Whilwood, and P. Taylor, *J. Chem. Soc., Perkin Trans. 2*, 1759 (1994).

379. C. Plessis, G. Arzamendi, J. R. Leiza, H. A. S. Schoonbrood, D. Charmot, and J. M. Asua, *Macromoleues* **33**, 4 (2000).

380. A. Lovell, T. H. Sha, and F. Heatley, *Polym. Commun.* **32**, 98 (1991).

381. J. Chiefari, J. Jeffery, R. T. A. Mayadunne, G. Moad, E. Rizzardo, and S. H. Thang, *Macromolecules* **32**, 7700 (1999).

382. J. Chiefari, J. Jeffery, R. T. A. Maydunne, G. Moad, E. Rizzardo, and S. H. Thang, in *Controlled/Living Radical Polymerization. Progress in ATRP, NMP, and RAFT*, K. Matyjaszewski, ed., ACS Symposium Series 768, 2000, p. 297.

383. A. M. van Herk, *Macromol. Rapid Commun.* **22**, 687 (2001).

384. M. E. Best and P. H. Kasai, *Macromolecules* **22**, 2622 (1989).

385. A. Ueda and S. Nagai, in *Polymer Handbook*, 4th ed., J. Brandrup, E. H. Immergut, and E. A. Grulke, eds., Wiley, New York, 1999, p. II/169.

386. K. Hatada, T. Kitayama, K. Ute, Y. Terawaki, and T. Yanagida, *Macromolecules* **30**, 754 (1997).

387. D. J. T. Hill, L. Y. Shao, P. J. Pomery, and A. K. Whittaker, *Polymer* **42**, 4791 (2001).

388. B. Boutevin, *J. Polym. Sci.; Part A: Polym. Chem.* **38**, 3235 (2000).

389. G. F. Meijs, E. Rizzardo, and S. H. Thang, *Polym. Bull.* **24**, 501 (1990).

390. S. A. F. Bon, S. R. Morseley, C. Waterson, and D. F. M. Haddleton, *Macromolecules* **33**, 5819 (2000).

391. C. P. R. Nair, *Polym. Int.* **46**, 313 (1998).

392. C. P. R. Nair, P. Chaumont, and D. Charmot, *J. Polym. Sci.; Part A: Polym. Chem.* **37**, 2511 (1999).

393. C. P. R. Nair, P. Chaumont, and D. Charmot, *J. Polym. Sci.; Part A: Polym. Chem.* **33**, 2773 (1995).

394. D. Colombani, M. O. Zink, and P. Chaumont, *Eur. Polym. J.* **33**, 1433 (1997).

395. S. Jiang, H. Viehe, N. Oger, and D. Charmot, *Macromol. Chem. Phys.* **196**, 2349 (1995).

396. W. K. Busfield, C. I. Zayas-Holdsworth, and S. H. Thang, *Polymer* **40**, 389 (1999).

397. G. F. Meijs, T. C. Morton, E. Rizzardo, and S. H. Thang, *Macromolecules* **24**, 3689 (1991).

398. G. F. Meijs and E. Rizzardo, *Polym. Bull.* **26**, 291 (1991).

399. G. F. Meijs, E. Rizzardo, T. P. T. Le, and Y. C. Chen, *Makromol. Chem.* **193**, 369 (1992).

400. G. F. Meijs, E. Rizzardo, and T. P. T. Le, *Polym. Int.* **26**, 239 (1991).

401. A. Sunder and R. Mulhaupt, *Macromol. Chem. Phys.* **200**, 58 (1999).

402. W. K. Busfield, C. I. Zayas-Holdsworth, and S. H. Thang, *Polymer* **41**, 4409 (2000).

403. G. F. Meijs and E. Rizzardo, *Makromol. Chem., Rapid Comun.* **9**, 547 (1988).

404. K. Tanaka and B. Yamada, *Macromol. Chem. Phys.* **201**, 1565 (2000).

405. P. Chaumont, D. Colombani, L. Boitear, J. P. Lamps, M.-O. Zink, C. P. R. Nair, and D. Charmot, in *Controlled Radical Polymerization*, K. Matyjaszewski, ed., ACS Symposium Series 685, 1998, p. 362.

406. B. Yamada, S. Tagashira, and S. Aoki, *J. Polym. Sci.; Part A: Polym. Chem.* **32**, 2745 (1994).

407. H. Tanaka, H. Kawai, T. Sato, and T. Ota, *J. Polym. Sci.; Part A: Polym. Chem.* **27**, 1741 (1989).

408. Y. Watanabe, H. Ishigaki, and S. Suyama, *Chem. Lett.* **1993**, 1089 (1993).

409. J. Krstina, C. L. Moad, G. Moad, E. Rizzardo, and C. T. Berge, *Macromol. Symp.* **111**, 13 (1996).

410. D. M. Haddleton, C. T. Topping, J. J. Hastings, and K. G. Suddaby, *Macromol. Chem. Phys.* **197**, 3027 (1996).

411. D. M. Haddleton, C. T. Topping, D. Kukulj, and D. Irvine, *Polymer* **39**, 3119 (1998).

412. J. Chiefari, Y. K. Chong, F. Ercole, J. Krstina, J. Jeffery, T. P. T. Le, R. T. A. Mayadunne, G. F. Meijs, C. L. Moad, G. Moad, E. Rizzardo, and S. H. Thang, *Macromolecules* **31**, 5559 (1998).

413. E. Rizzardo, J. Chiefari, B. Y. K. Chong, F. Ercole, J. Krstina, J. Jeffery, T. P. T. Le, R. T. A. Mayadunne, G. F. Meijs, C. L. Moad, G. Moad, and S. H. Thang, *Macromol. Symp.* **143**, 291 (1999).

414. E. Rizzardo, J. Chiefari, R. T. A. Mayadunne, G. Moad, and S. H. Thang, in *Controlled/Living Radical Polymerization. Progress in ATRP, NMP, and RAFT*, K. Matyjaszewski, ed., ACS Symposium Series 768, 2000, p. 278.

415. K. S. Murthy and K. Kishore, *J. Polym. Sci.; Part A: Polym. Chem.* **34**, 1415 (1996).

416. G. F. Meijs, E. Rizzardo, and S. H. Thang, *Polym. Prepr.* (*Am. Chem. Soc., Div. Polym. Chem.*) **33**, 893 (1992).

417. D. Colombani and P. Chaumont, *Polymer* **36**, 129 (1995).

418. D. Colombani and P. Chaumont, *Macromolecules* **27**, 5972 (1994).

419. D. Colombani and P. Chaumont, *J. Polym. Sci.; Part A: Polym. Chem.* **32**, 2687 (1994).

420. P. Chaumont and D. Colombani, *Macromol. Chem. Phys.* **196**, 947 (1995).

421. D. Colombani, J. P. Lamps, and P. Chaumont, *Macromol. Chem. Phys.* **199**, 2517 (1998).

422. D. Colombani, M. O. Zink, and P. Chaumont, *Macromolecules* **29**, 819 (1996).

423. J. Fossey, D. Lefort, and J. Sorba, *Free Radicals in Organic Chemistry*, Wiley, Chichester, UK, 1995, p. 296.

424. P. A. G. M. Scheren, G. T. Russell, D. F. Sangster, R. G. Gilbert, and A. L. German, *Macromolecules* **28**, 3637 (1995).

425. G. T. Russell, R. G. Gilbert, and D. H. Napper, *Macromolecules* **26**, 3538 (1993).

426. H. Yamazaki, A. Matsumoto, and T. Otsu, *Eur. Polym. J.* **33**, 157 (1997).

427. A. Matsumoto, Y. Sano, M. Yoshioka, and T. Otsu, *Eur. Polym. J.* **32**, 1079 (1996).

428. T. Sato, K. Morino, H. Tanaka, and T. Ota, *Makromol. Chem.* **188**, 2951 (1987).

429. T. Otsu, K. Yamagishi, A. Matsumoto, M. Yoshioka, and H. Watanabe, *Macromolecules* **26**, 3026 (1993).

430. M. Buback, M. Busch, and C. Kowollik, *Macromol. Theory Simul.* **9**, 442 (2000).

431. O. F. Olaj, M. Zoder, and P. Vana, *Macromolecules* **34**, 441 (2001).

432. O. F. Olaj and P. Vana, *J. Polym. Sci.; Part A: Polym. Chem.* **38**, 697 (2000).

433. D. H. Solomon and G. Y. N. Chan, in *Polymeric Materials Encyclopedia*, J. C. Salamone, ed., CRC Press, New York, 1996, p. 2588.

434. P. Cacioli, D. G. Hawthorne, R. L. Laslett, E. Rizzardo, and D. H. Solomon, *J. Macromol. Sci., Chem.* **A23**, 839 (1986).

435. B. Yamada, O. Konosu, K. Tanaka, and F. Oku, *Polymer* **41**, 5625 (2000).

436. D. M. Haddleton, D. R. Maloney, K. G. Suddaby, A. Clarke, and S. N. Richards, *Polymer* **38**, 6207 (1997).

437. D. R. Hensley, S. D. Goodrich, A. Y. Huckstep, H. J. Harwood, and P. L. Rinaldi, *Macromolecules* **28**, 1586 (1995).

438. T. Kashiwagi, A. Inaba, J. E. Brown, K. Hatada, T. Kitayama, and E. Masuda, *Macromolecules* **19**, 2160 (1986).

439. L. E. Manring, D. Y. Sogah, and G. M. Cohen, *Macromolecules* **22**, 4654 (1989).

440. L. E. Manring, *Macromolecules* **22**, 2673 (1989).

441. G. Moad and D. H. Solomon, *The Chemistry of Free Radical Polymerization*, Pergamon, Oxford, 1995, p. 207.

442. J. C. Bevington, S. W. Breuer, T. N. Huckerby, B. J. Hunt, and R. Jones, *Eur. Polym. J.* **34**, 539 (1998).

443. J. Bessiere, B. Boutevin, and O. Loubet, *Polym. Bull.* **31**, 673 (1993).

444. K. Hatada, T. Kitayama, and E. Masuda, *Polym. J.* **17**, 985 (1985).

445. K. Hatada, T. Kitayama, and E. Masuda, *Polym. J.* **18**, 395 (1986).

446. A. K. Serelis and D. H. Solomon, *Polym. Bull.* **7**, 39 (1982).

447. S. Bizilj, D. P. Kelly, A. K. Serelis, D. H. Solomon, and K. E. White, *Aust. J. Chem.* **38**, 1657 (1985).

448. V. A. Schreck, A. K. Serelis, and D. H. Solomon, *Aust. J. Chem.* **42**, 375 (1989).

449. K. C. Berger and G. Meyerhoff, *Makromol. Chem.* **176**, 1983 (1975).

450. K. Kodaira, K. Ito, and S. Iyoda, *Polym. Commun.* **29**, 83 (1988).

451. J. C. Bevington and D. E. Eaves, *Trans Faraday Soc.* **55**, 1777 (1959).

452. G. Ayrey, M. J. Humphrey, and R. C. Poller, *Polymer* **18**, 840 (1977).

453. G. Moad, D. H. Solomon, S. R. Johns, and R. I. Willing, *Macromolecules* **15**, 1188 (1982).

454. H. Catalgil-Giz, A. Giz, and A. Oncul-Koc, *Polym. Bull.* **43**, 215 (1999).

455. H. Ohtani, A. Suzuki, and S. Tsuge, *J. Polym. Sci.; Part A: Polym. Chem.* **38**, 1880 (2000).

456. W. Konter, B. Bomer, K.-H. Kohler, and W. Heitz, *Makromol. Chem.* **182**, 2619 (1981).

457. J. C. Bevington, B. Guyot, T. N. Huckerby, B. J. Hunt, and R. Jones, *Eur. Polym. J.* **36**, 657 (2000).

458. T. Otsu, K. Yamagishi, A. Matsumoto, M. Yoshioka, and H. Watanabe, *Macromolecules* **25**, 2713 (1992).

459. H. Watanabe, A. Matsumoto, and T. Otsu, *J. Polym. Sci.; Part A: Polym. Chem.* **32**, 2073 (1994).

460. A. Matsumoto and E. Nakagawa, *Eur. Polym. J.* **35**, 2107 (1999).

461. T. Sato, K. Masaki, M. Seno, and H. Tanaka, *Makromol. Chem.* **194**, 849 (1993).

462. A. Matsumoto, Y. Oki, and T. Otsu, *Macromolecules* **25**, 3323 (1992).

463. G. F. Meijs and E. Rizzardo, *J. Macromol. Sci., Rev. Macromol. Chem. Phys.* **C30**, 305 (1990).

464. K. Ishizu, X. X. Shen, and K.-I. Tsubali, *Polymer* **41**, 2053 (2000).

465. H. Xiao, R. Pelton, and A. Hamielec, *Polymer* **37**, 1201 (1996).

466. Y. Tsukahara, K. Mizuno, A. Segawa, and Y. Yamashita, *Macromolecules* **22**, 1546 (1989).

467. M. Buback, C. Kowollik, C. Kurz, and A. Wahl, *Macromol. Chem. Phys.* **201**, 464 (2000).

468. R. W. Garrett, D. J. T. Hill, J. H. O'Donnell, P. J. Pomery, and C. L. Winzor, *Polym. Bull.* **22**, 611 (1989).

469. M. Buback and C. Kowollik, *Macromolecules* **31**, 3211 (1998).

470. M. Buback, *Macromol. Chem. Phys.* **191**, 1575 (1990).

471. M. Buback, B. Huckestein, and G. T. Russell, *Macromol. Chem. Phys.* **195**, 539 (1994).

472. P. B. Zetterlund, H. Yamazoe, B. Yamada, D. J. T. Hill, and P. J. Pomery, *Macromolecules* **34**, 7686 (2001).

473. H. Yamazoe, P. B. Zetterlund, B. Yamada, D. J. T. Hill, and P. J. Pomery, *Macromol. Chem. Phys.* **202**, 824 (2001).

474. J. M. deSimone, Z. Guan, and C. S. Elsbernd, *Science* **257**, 945 (1992).

475. K. A. Schaffer and J. M. DeSimone, *Trends Polym. Sci.* **3**, 146 (1995).

476. S. Beuermann, M. Buback, and C. Schmaltz, *Ind. Eng. Chem. Res.* **38**, 3338 (1999).

477. J. Dionisio, H. K. Mahabadi, K. F. O'Driscoll, E. Abuin, and E. A. Lissi, *J. Polym. Sci., Polym. Chem. Ed.* **17**, 1891 (1979).

478. E. T. Denisov and I. V. Khudyakov, *Chem. Rev.* **87**, 1313 (1987).

479. J. Fossey, D. Lefort, and J. Sorba, *Free Radicals in Organic Chemistry*, Wiley, Chichester, UK, 1995, p. 36.

480. G. Moad and E. Rizzardo, *Macromolecules* **28**, 8722 (1995).

481. A. L. J. Beckwith, V. W. Bowry, and K. U. Ingold, *J. Am. Chem. Soc.* **114**, 4983 (1992).

482. V. W. Bowry and K. U. Ingold, *J. Am. Chem. Soc.* **114**, 4992 (1992).

483. J. Chateauneuf, J. Lusztyk, and K. U. Ingold, *J. Org. Chem.* **53**, 1629 (1988).

484. B. Yamada, Y. Nobukane, and Y. Miura, *Polym. Bull.* **41**, 539 (1999).

485. B. Yamada, H. Tanaka, K. Konishi, and T. Otsu, *J. Macromol. Sci.–Pure Appl. Chem.* **A31**, 351 (1994).

486. A. Matsumoto, K. Yamagishi, and S. Aoki, *J. Polym. Sci.; Part A: Polym. Chem.* **32**, 917 (1994).

487. T. Zytowski and H. Fischer, *J. Am. Chem. Soc.* **119**, 12869 (1997).

488. T. L. Simandi and A. Rockenbauer, *Eur. Polym. J.* **27**, 523 (1991).

489. T. L. Simandi, A. Rockenbauer, and L. I. Simandi, *Eur. Polym. J.* **31**, 555 (1995).

490. T. L. Simandi, A. Rockenbauer, and F. Tudos, *Eur. Polym. J.* **25**, 501 (1989).

491. T. L. Simandi and F. Tudos, *Eur. Polym. J.* **21**, 865 (1985).

492. H. J. Hageman, *Eur. Polym. J.* **35**, 991 (1999).

493. H. J. Hageman, *Eur. Polym. J.* **36**, 345 (2000).

494. M. Okubo and T. Yamashita, *Colloid Polym. Sci.* **276**, 103 (1998).

495. M. Okubo, H. Yonehara, and T. Yamashita, *Colloid Polym. Sci.* **278**, 1007 (2000).

496. L. L. deArbina, L. M. Gugliotta, M. J. Barandiaran, and J. M. Asua, *Polymer* **39**, 4047 (1998).

497. M. F. Cunningham, K. Geramita, and J. W. Ma, *Polymer* **41**, 5385 (2000).

498. H. D. Bruyn, R. G. Gilbert, and B. S. Hawkett, *Polymer* **41**, 8633 (2000).

499. M. J. Monteiro, N. Subramaniam, J. R. Taylor, B. T. T. Pham, M. P. Tonge, and R. G. Gilbert, *Polymer* **42**, 2403 (2001).

500. P. J. Krusic, E. Wasserman, P. N. Keizer, J. R. Morton, and K. F. Preston, *Science* **254**, 1183 (1991).

501. M. Seno, M. Maeda, and T. Sato, *J. Polym. Sci.; Part A: Polym. Chem.* **38**, 2572 (2000).

502. A. G. Camp, A. Lary, and W. T. Ford, *Macromolecules* **28**, 7958 (1995).

503. V. Cao and S. E. Webber, *Macromolecules* **28**, 3741 (1995).

504. Y. Chen and K.-C. Lin, *J. Polym. Sci.; Part A: Polym. Chem.* **37**, 2969 (1999).

505. W. T. Ford, T. D. Graham, and T. H. Mourey, *Macromolecules* **30**, 6422 (1997).

506. K. Kirkwood, D. Stewart, and C. T. Imrie, *J. Polym. Sci.; Part A: Polym. Chem.* **35**, 3323 (1997).

507. S. Mehrotra, A. Nigam, and R. Malhortra, *Chem. Commun.* 463 (1997).

508. M. Seno, H. Fukunaga, and T. Sato, *J. Polym. Sci.; Part A: Polym. Chem.* **36**, 2905 (1998).

509. D. Stewart and C. T. Imrie, *Chem. Commun.* **11**, 1383 (1996).

510. Y.-P. Sun, G. E. Lawson, C. E. Bunker, and A. Kitaygorodsky, *Macromolecules* **29**, 8441 (1996).

511. M. Fujita, K. Taji, N. Ueno, and T. Ida (Osaka Yukikagaku), Jpn. Patent 56-010383 (1981).

512. H. Sonobe (Mitsubishi Rayon and Osaka Organic. Chem. Ind.), Jpn. Patent 11-222462 (1990).

513. H. Sonobe, J. Doi, A. Tani, S. Suzuki, and M. Miyuouga (Mitsubishi Rayon), Jpn. Patent 2001-039925 (2001).

514. T. Keil, M. Kaufhold, and K. Mori (Huels AG), Jpn. Patent 08-059524 (1996).

515. K. Murayama, T. Toda, and K. Mori (Sankyo), Jpn. Patent S51-15001 (1976).

4 The Kinetics of Free-Radical Polymerization

CHRISTOPHER BARNER-KOWOLLIK, PHILIPP VANA, and
THOMAS P. DAVIS

The University of New South Wales, Sydney, Australia

CONTENTS

4.1   INTRODUCTION

The kinetic understanding of free-radical polymerization processes is of fundamental importance for efficiently generating polymeric products for a wide variety of applications. The study of the kinetic principles involved has been a central research theme since the formulation of Hermann Staudinger's *Macromolecular Hypothesis* in the 1920s. The evaluation and analysis of reaction rates and molecular weight distributions resulting from free-radical polymerizations is far from simple, due to the coupled nature of the different reactions. The process may be described via a simplified set of fundamental reactions as given in Scheme 4.1.

   Each reaction given in Scheme 4.1 is associated with a kinetic rate law expression that contains a specific rate coefficient. It is the central task of all kinetic experiments to assess the size of these rate coefficients via a variety of experimental approaches. The experiments carried out to determine the kinetic rate coefficients can be divided into two areas, which are, however, closely linked to each other. The first approach centers on the accurate measurement of the overall polymerization rate, whereas the second one concentrates on the analysis of the resulting molecular weight distributions. If all the rate coefficients for a polymerizing system are known, it is possible to predict the kinetics of the overall polymerization process, including the full molecular weight distributions. In addition, with the increased availability of powerful computers, the simulation of complex polymerization processes contributed considerably toward a deeper understanding of the reaction kinetics.

   This chapter focuses almost exclusively on the kinetic aspects of the free-radical polymerization process and to a lesser extend on chemical considerations. Chemical principles will be introduced only when an understanding of the kinetic picture without them is impossible.

4.2   INITIATION

The initiation process constitutes the first reaction step in free-radical polymerization leading to the generation of (primary) radicals. The kinetics of the initiation

Initiator Decomposition	I_2	$\xrightarrow{k_d}$	$2\,I^\bullet$	
Chain Initiation	$I^\bullet + M$	$\xrightarrow{k_i}$	$R_1^\bullet$	
Chain Propagation	$R_i^\bullet + M$	$\xrightarrow{k_p}$	$R_{i+1}^\bullet$	
Chain Transfer	$R_i^\bullet + S$	$\xrightarrow{k_{tr}}$	$R_1^\bullet + P_i$	
Chain Termination	$R_i^\bullet + R_j^\bullet$	$\xrightarrow{k_{t,c,d}}$	P_{i+j} or $P_i + P_j$	
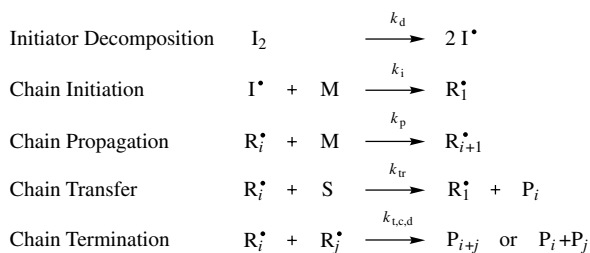
Where $R_i^\bullet$ is a radical of chain length i, I_2 is the initiator, M is the monomer, S is a transfer agent, and P is polymer

Scheme 4.1

$$\text{Initiator} \xrightarrow[hv,\, \Delta]{k_\text{d}} \text{I}_1^\bullet + \text{I}_2^\bullet$$
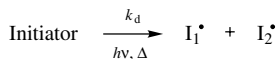
Scheme 4.2

process—its rate and effectiveness—are of fundamental importance in both theoretical studies and commercial applications. Commercial procedures rely mainly on the formation of primary radicals via thermal decomposition processes using azo- and peroxy-type compounds. Investigative kinetic studies are—to a large extent—carried out using photoinitiators, which decompose on irradiation with UV or visible light. The main reason for this choice is the possibility to define exact starting and end times of the initiation and subsequently the polymerization process.

The decomposition scheme (Scheme 4.2) is common to both thermal and photo-initiators. The measurable decrease of the initiator concentration [I] in a polymerizing systems is given by

$$-\frac{d[\text{I}]}{dt} = k_\text{d}[\text{I}] \tag{4.1}$$

However, the rate of the formation of primary radicals is of greater interest in kinetic studies. The rate of generation of radicals that are capable of initiating the polymerization process, R_d, is described via the following general first-order rate law

$$R_\text{d} = \frac{d[\text{I}^\bullet]}{dt} = -2f\frac{d[\text{I}]}{dt} = 2fk_\text{d}[\text{I}] \tag{4.2}$$

where k_d corresponds to the rate coefficient of initiator decomposition and f is the initiator efficiency (see below). It should be noted that in the case of photoinitiation, k_d is a composite of various variables. This will be discussed in detail in Section 4.2.2. Integration of Eq. (4.1) leads to Eq. (4.3), an expression that describes the decreasing initiator concentration as a function of time.

$$[\text{I}] = [\text{I}]_0 \cdot e^{-k_\text{d}\cdot t} \tag{4.3}$$

In order to initiate the polymerization process via reaction with a monomer unit, the generated primary radicals, $\text{I}_1^\bullet$ and $\text{I}_2^\bullet$, have to leave the solvent cage that surrounds them. The ability of the primary radicals to leave the solvent cage unreacted and to start the polymerization process is quantified by the initiator efficiency, f, with theoretical values between zero and unity. Not all generated primary free radicals initiate polymer growth. Shortly after decomposition, the free radicals are very close to each other and recombination can occur. In addition, they can also react in alternative ways before they can react with a monomer unit. An efficiency of zero corresponds to no initiation taking place, whereas $f = 1$ indicates that every generated primary radical escapes the solvent cage and subsequently initiates polymerization.

Typical values of f are between 0.5 and 0.8, depending on the viscosity of the reaction medium, indicating that the escaping process is diffusion-controlled. It should be noted that in the case of an unsymmetric initiator molecule, $I_1^{\bullet}$ and $I_2^{\bullet}$ do not necessarily display the same reactivity toward the monomer unit.[1,2] Hence, the initiation process may be described by Scheme 4.3:

$$I_1^{\bullet} \; + \; M \; \xrightarrow{\; k_i^{(1)} \;} \; R_1^{\bullet}$$

$$I_2^{\bullet} \; + \; M \; \xrightarrow{\; k_i^{(2)} \;} \; R_1^{\bullet}$$
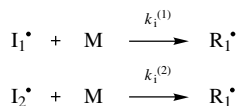
Scheme 4.3

where $I_{1,2}^{\bullet}$ represents either initiator fragment 1 or 2, M indicates a monomer unit, $R_1^{\bullet}$ corresponds to a macroradical of chain length 1, and $k_i^{(1)}$ and $k_i^{(2)}$ refer to the individual initiation rate coefficient of the respective fragments. The overall rate of initiation, R_i, is given by

$$R_i = \frac{d[R_1^{\bullet}]}{dt} = -\frac{d[I_1^{\bullet}]}{dt} - \frac{d[I_2^{\bullet}]}{dt} = k_i^{(1)} \cdot [M] \cdot [I_1^{\bullet}] + k_i^{(2)} \cdot [M] \cdot [I_2^{\bullet}] \qquad (4.4)$$

Because $[I_1^{\bullet}] = [I_2^{\bullet}] = [I^{\bullet}]/2$, the overall rate coefficient of initiation, k_i, is a composite of the individual rate coefficients of initiation for the initiator fragments $I_1^{\bullet}$ and $I_2^{\bullet}$:

$$R_i = k_i[M][I^{\bullet}] \qquad \text{with} \qquad k_i = \frac{k_i^{(1)} + k_i^{(2)}}{2} \qquad (4.5)$$

4.2.1   Thermal Initiation

Thermally decomposing initiators (mainly) fall into two classes: azo- and peroxy-type molecules. The general structures of azo- and peroxyinitiators are given in Scheme 4.4.

An important quantity of a thermal initiator is its half-life, $t_{1/2}$, (at a certain temperature), given by Eq. (4.6); the half-life is the time period during which half of the initiator molecules initially present are decomposed:

$$t_{1/2} = \frac{\ln 2}{k_d} \qquad (4.6)$$

Azoinitiator   Peroxyinitiator
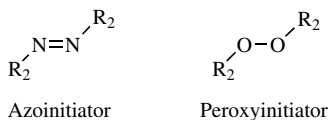
Scheme 4.4

There is an initiator for virtually any desired decomposition rate in a given solvent (or monomer). An initiator is often characterized by the temperature at which its half-life is 10 h. These temperatures range from 20 to 120° C, depending on the structure of the initiator. Extensive data on initiator decomposition rates and their activation parameters can be found in the *Polymer Handbook*.[3] When choosing an initiator for a specific application, it is important to also consider possible side reactions that monomer and initiator can undergo, as well as the transfer ability of the initiator molecule, which may limit the accessible molecular weight range (see Section 4.4).

4.2.2 Photoinitiation

An attractive alternative to thermally decomposing initiators are photoinitiators that decay on irradiation with UV or visible light. The use of photoinitiators is (in most cases) restricted to applications involving accurate kinetic measurements, whereas their usage in industrial processes is very limited because of the technical problems associated with the uniform irradiation of large reaction volumes. Some exceptions are applications involving coatings and surface polymerizations. The main advantage of photoinitiator use in polymerizing systems is the possibility to define exact start- and endpoints of the polymerization process via the duration of the irradiation period. In addition, the rate of (most) photoinitiator decomposition is almost independent of the reaction temperature, but depends strongly on the (UV) light intensity. However, weak temperature dependencies of the primary quantum yield (see text below) have long been known for the photoinduced decomposition of azoalkanes.[4] The weak dependence of the rate of decomposition on the reaction medium temperature is due to the large amount of energy that is deposited into the initiator molecules via the light source. This energy exceeds the thermal energy of the surrounding medium by orders of magnitude. An ideal photoinitiator for a specific polymerization may be defined via the following criteria:

1. The photoinitiator should decompose on iradiation with the (UV) light source; For instance, an absorption should coincide with the radiation wavelength. The monomer(s) used in the specific polymerization process should not absorb light at the selected wavelength.
2. The efficiency of the initiator should be high, preferably close to 1, which says that all radicals generated start a growing chain.
3. At best, there should be only one type of free-radical species that is formed on laser irradiation.

According to the mechanism by which initiating radicals are formed, photoinitiators are generally divided into two classes: type I photoinitiators, which undergo a unimolecular bond cleavage upon irradiation to yield free-radicals; and type II photoinitiators, which undergo a bimolecular reaction where the excited state of the photoinitiator interacts with a second molecule (a coinitiator) to generate free-radicals. However, visible light photoinitiators belong almost exclusively to the
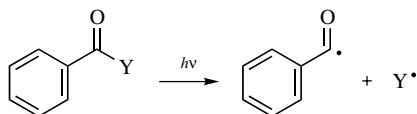
Scheme 4.5

type II class of photoinitiators. Within the type I initiator class, there are several structural variations. The most widely used class are photoinitiators containing a benzoyl group as the effective initiating moiety (acetophenone type). Their general formula and primary decomposition products are given in Scheme 4.5.

It is standard practice to show the processes that can take place on irradiation (i.e., assuming that each photoinitiator molecule absorbs a certain dose of energy) in a so-called Jablonski diagram. Such a diagram is a simplified portrayal of the relative positions of the electronic energy levels of a molecule.

On (UV) irradiation, the molecule is converted from its (singlet) ground state to its first exited state. The Jablonski diagram given in Fig. 4.1 shows that there is more than one possibility to deactivate an excited initiator molecule. This multitude of deactivation modes is summarily quantified in the quantum yield for the primary free-radical production, Φ, which is composed of three parts that can be assigned to the following reactions:

$$(\text{Ia}) \ S_0 \xrightarrow{h\nu} S_1$$
$$(\text{Ib}) \ S_1 \longrightarrow T_1 \qquad \text{with } \Phi_{\text{ISC}}$$
$$(\text{II}) \ T_1 \longrightarrow R^\bullet \qquad \text{with } \Phi_R$$
$$(\text{III}) \ R^\bullet \xrightarrow{M} RM^\bullet \qquad \text{with } \Phi_{\text{RM}}$$
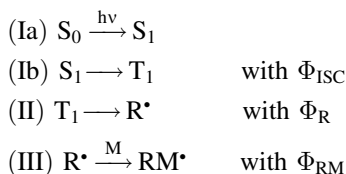
where $\Phi = \Phi_{\text{ISC}} \cdot \Phi_R \cdot \Phi_{\text{RM}} \leq 1$.
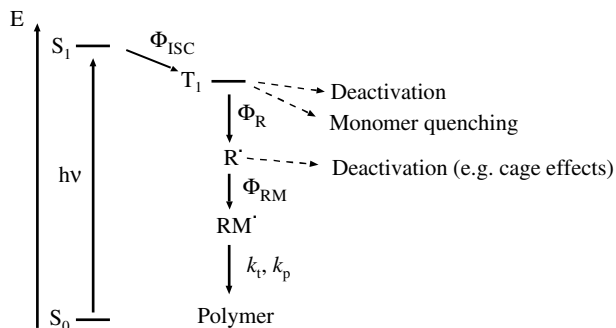
Figure 4.1 Simplified Jablonski diagram of the photochemically initiated acetophenone type initiator decomposition.

The quantum yield for intersystem crossing (Ib) is rather high for ketones,[5] so that to a good approximation Φ_{ISC} can be set to 1. Thus, the overall quantum yield of the initiation process depends only on Φ_R and Φ_{RM}. From the T_1 triplet state parallel reactions can lead to a decrease in the quantum yield Φ_R. In free-radical polymerizations these reactions are deactivation by molecular oxygen and deactivation by the monomer.[6] This is one of the reasons why the monomer mixture should be thoroughly degassed prior to the polymerization process. The longer the lifetime of the triplet state, the higher the chances that deactivation processes can reduce the quantum yield. For example, 2,2-dimethyl-2-phenylacetophenone (DMPA) has a rather short-lived T_1 state ($\tau < 0.1$ ns,[7] whereas the respective value for 1,1-dimethoxy-1-hydroxyacetophenone (Darocur 1173) is close to 20 ns[8]), which results in a high Φ_R value. The quantum yield of the third reaction, which leads to the formation of macroradicals, has been termed *initiator efficiency*, $f = \Phi_{RM}$. The initiator efficiency is influenced by the ability of the radicals formed by the laser pulse to diffuse from the solvent cage to the reaction site, and its definition is analogous to that for the efficiency factor for thermally decomposing initiators. This process has been termed the ''cage effect''. The initiator efficiency of the typical acetophenone initiator 2,2-dimethoxy-2-phenylacetophenone (DMPA) (at 30°C and ambient pressure) is close to 0.4.[9] However, the situation in the case of most acetophenone-type initiators is more complex than for a photoinitiator that yields only a single type of free-radical, $R^\bullet$, on irradiation. It is generally accepted that most acetophenone-type initiators (e.g., DMPA, Darocur 1173, or benzoin) decompose into two radical species, $R_1^\bullet$ and $R_2^\bullet$, as detailed in Scheme 4.5. Generally, both species are distinctly different in their character. The carbonyl radical is very efficient in terms of starting macromolecular growth, whereas the additional radical is not (for the example of DMPA, see the article by Fischer et al.[10]). Fischer and co-workers suggested that—in the case of DMPA—the methoxy type radical is only involved in termination steps. Initial radicals that come from a common initiator molecule, but have clearly different efficiencies, may be termed ''effective'' and ''ineffective'' (primary) initial radicals, respectively. The sum of both radical concentrations will be termed ''overall'' radical concentration and is 2 times ρ, where ρ is the concentration of primary radicals that are capable of starting macromolecular growth. The concentration of effective and ineffective initial radicals is the same and is equal to ρ. The occurrence of primary radicals with markedly different reactivities may have serious consequences for the polymerization kinetics.

Another widely used structural variation of class I photoinitiators are azoinitiators, which are also employed as thermal initiators. However, their mechanism of photodecomposition is markedly different from acetophenone-type initiators. Scheme 4.6 shows the UV induced decomposition of the widely used azoinitiator 2,2-azobisisobutyronitrile (AIBN).

On irradiation by laser light, the initiator molecule changes its stereochemical configuration from the cis to the trans isomer. This cis/trans isomerism becomes of importance if azoinitiators are employed in pulsed laser experiments (see Section 4.9). The time at which the laser pulse hits the reaction mixture is no longer identical with the generation of the primary radicals. The time delay is usually in the
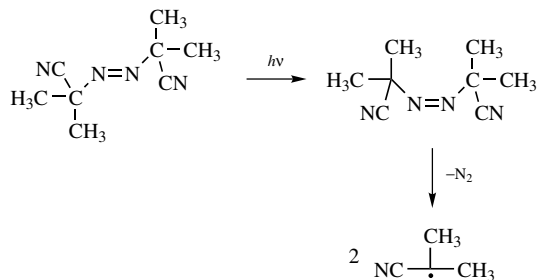
Scheme 4.6

order of microseconds and may be observed in time resolved pulsed laser experiments.

It is possible to calculate the effective primary free-radical concentration, ρ, generated by monochromatic irradiation of a reaction mixture containing a photoinitiator. The radical concentration, ρ, which is generated by a specific number of absorbed photons, is given by

$$\rho = 2\Phi \frac{n_{abs}}{V} \tag{4.7}$$

where Φ is the primary quantum yield (see text above), n_{abs} is the number of absorbed photons, and V is the irradiated volume. According to Beer–Lambert's law, the number of absorbed photons may be calculated by

$$n_{abs} = \frac{E_p}{E_\lambda} \cdot (1 - 10^{-\varepsilon \cdot c \cdot d}) \tag{4.8}$$

where E_p = energy deposited

E_λ = energy of one mole of photons at the irradiation wavelength λ

ε = molar absorption coefficient of the initiator molecule at the laser wavelength λ

c = photoinitiator concentration

d = optical pathlength

The rate of photochemical initiation is given by the product of the intensity of absorbed light (in moles of light quanta per liter and second) and the primary quantum yield. A good survey on different photoinitiators and their photo-decomposition by UV light has been given by Gruber.[11]

4.2.3 Self-Initiated Polymerization

Free-radical polymerizations can also be initiated by the monomer itself or peroxy compounds that are formed via exposure of the reaction mixture to molecular
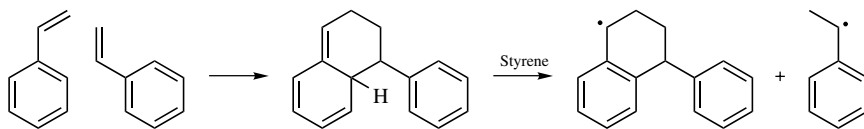
Scheme 4.7

oxygen. The processes (mainly) take place at high temperatures. However, under very pure conditions in exhaustively purified reaction vessels, few monomers tend to polymerize spontaneously by increasing the temperature. Styrene is one of the rare monomers that—also in its purest state—does exhibit initiation processes without additionally added initiator. The self-initiation of styrene has been studied in great detail with respect to its kinetics and mechanism.[12–14] The underlying reaction is a self-Diels–Alder cycloaddition of two styrene moieties as shown in Scheme 4.7.

The self-initiated polymerization of styrene has a substantial activation energy, a 50% monomer conversion needs 400 days at 29°C, but only 4 h at 127°C. However, the produced styrene is very pure due to the absence of initiators and other additives. Methyl methacrylate was also thought to undergo self-initiated polymerization, but increasing evidence indicates that this may not be the case.[15]

4.2.4 Other Methods of Initiation

Apart from the abovementioned methods of initiating free radical polymerizations, there are several more alternatives which can be selected from if required for the specific application. These techniques include (1) ionizing irradiation, (2) plasma initiation, (3) electroinitiation, (4) redox initiation, and (5) ultrasonic initiation:[16]

1. Radioactive sources and ionizing particles are used to initiate free-radical polymerization processes, such as gamma irradiation, electrons,[17] neutrons, and α-particles. The interaction of these radiations with matter are—compared to the interactions of less energetic irradiation (such as UV or visible light)—much more complex. High-energy radiation applied to vinylic monomers usually results in the formation of anions, cations, and primary free radicals. These species may then initiate chain growth. Whether this growth is of the free-radical type depends largely on the reaction conditions. Ionic chain initiation is predominant at low reaction temperatures, because the formed ions tend to dissociate into free radicals at higher reaction temperatures. High-energy radiation initiated free-radical polymerizations are much less applied in scientific and commercial applications, which is due mainly to the complex initiation mechanism and the safety issues associated with the usage of this type of irradiation.

2. When a gaseous monomer under low pressure is exposed to a high-voltage electric discharge, plasma polymerization may occur.[18] The plasma consists of ionized molecules. A large number of monomers undergo plasma polymerization

and form high-molecular-weight products. The polymerization process appears to be rather complicated but seems to involve both ionic and free-radical species. Plasma polymerization is especially attractive for the generation of thin polymer films for a variety of applications.

3. Electroinitiation—which is not to be confused with initiation by an electron beam—is done by direct electrolysis of the reaction mixture. The reaction mixture usually contains an organic solvent, the monomer and an inorganic compound that allows one to conduct the current or participates in the ionization process itself.[19] The polymerization proceeds via either free radicals or ions, depending on the reaction conditions and the substances present in the reaction mixture.

4. Redox-initiating systems consist of a reducing agent and an oxidizing agent. The reaction between those compounds generates intermediate free radicals that can initiate free-radical polymerization processes. A typical redox initiation system is given in Scheme 4.8.

$$\text{ROOH} \;+\; \text{Mt}^n \;\longrightarrow\; \text{RO}^\bullet \;+\; \text{Mt}^{n+1} \;+\; \text{OH}^-$$

Scheme 4.8

If a monomer is present in such a system, the polymerization is initiated by reaction of the alkoxy radical with a monomer unit. A typical redox system of the above-mentioned type consists of hydrogen peroxide and an iron(II) salt. It should be mentioned that there exist more possible redox initiating systems. Other water-soluble redox systems consist of $K_2S_2O_8$ and catalytic amounts of iron(II) ions, peroxides, and glucose. An alternative to these relatively oxygen-sensitive systems are peroxides in combination with amines, such as the system dibenzoyl peroxide and dimethylaniline. The decomposition of the peroxide is induced by the amine, and care has to be taken when handling this explosive mixture. Redox initiating system are of some industrial importance, because they exhibit relatively low activation energies for radical formation (on the order of 40 kJ/mol) and are therefore applicable at low and intermediate reaction temperatures.

4.3   PROPAGATION

The propagation step in free-radical polymerization has been specifically in the center of scientific interest since 1990, due to the advent of novel methods for the accurate determination of the propagation rate coefficients (for details, see Sections 4.11.2 and 4.7.3). The addition of a macroradical to a monomer unit may be described via the following rate law expression:

$$-\frac{d[\text{M}]}{dt} = \sum_i k_p^i [\text{R}_i^\bullet][\text{M}] \tag{4.9}$$

where k_p^i is the propagation rate coefficient of a macroradical with chain length i, R_i. It is generally accepted that the propagation reaction is chemically controlled up to high monomer conversions i.e. high viscosities of the reaction medium. This implies that the propagation rate coefficient is independent of monomer conversions $\leq 80\%$. The chemical control of the propagation step is impressively demonstrated when comparing the average collision frequency in the liquid phase at room temperature of $10^{12}\,s^{-1}$ to the frequency of successful propagation reactions (typically close to $10^3\,s^{-1}$). These numbers indicate that (approximately) only every 10^9 collision leads to a successful addition of a monomer unit to a macroradical. The propagation rate coefficient given in Eq. (4.9) carries the index i (representing the chain length of the growing chain), because it is beyond doubt that k_p is a true chain-length-dependent rate coefficient. This is especially true for the first few addition steps, which proceed at a markedly increased rate compared to long-chain propagation. In the case of methyl methacrylate, for example, the first propagation step at 60°C is approximately 16 times faster than the long-chain propagation limit.[20] In addition, recent evidence points toward a pronounced chain length dependence of the product of k_p times the monomer concentration, [M], up to chain lengths of hundreds of monomer units.[21] Unfortunately, up to this date there is no method to determine k_p independently from the monomer concentration. It is thus quite possible that the apparent chain length dependence of k_p reflects a structuring of the monomer concentration at the propagating chain end.

The absolute size of the propagation rate coefficient is governed by the nature of the monomer unit and the reactivity of the propagating radical. Both entropic and electronic factors influence the absolute value of the propagation rate coefficient and its activation parameters, E_A and A. It is important to notice that the reactivity of the propagating radical and the reactivity of the monomer units are close to opposite to each other. For example, ethene is a very unreactive monomer, but an ethene macroradical is highly reactive. On the contrary, styrene is a rather reactive monomer, but its propagating radical is extensively stabilized by the adjacent phenyl group. For polymerization and chain growth to take place, it is mandatory that the free macroradical lives long enough to survive the abovementioned 10^9 ineffective collisions. The addition of the monomer in a propagation reaction has to take place before any possible decomposition reaction or other side reaction. For example, acetone can not be polymerized at ambient reaction conditions—besides thermodynamic reasons, which make the polymerization unfavorable—because the associated free radicals quickly decompose into methyl free radicals and a ketone.

The substituent that is introduced into the ethene molecule to facilitate polymerization via activation of the double bond and stabilization of the propagating radical, respectively, also has the effect of adding steric hindrance to the propagation step. It is thus evident that it is close to impossible to completely separate enthalpic from entropic effects.

A separation of individual contributions using different monomers is illustrated in Scheme 4.9. While electronic effects should be reflected in the activation energy, E_A, steric effects are associated with the preexponential factor, A. When going from methyl methacrylate (MMA) to dimethyl itaconate (DMI),[22] a substantial decrease

MMA

$$CH_2=C \begin{matrix} CH_2-H \\ \\ COOCH_3 \end{matrix}$$

$E_A = 22.4 \text{ kJ mol}^{-1}$
$A = 2.7 \cdot 10^6 \text{ L mol}^{-1} \text{ s}^{-1}$

β oxygen electronic effect   large α substituent steric effect

EHMA $CH_2=C \begin{matrix} CH_2-OH \\ \\ COOC_2H_5 \end{matrix}$ $CH_2=C \begin{matrix} CH_2-\overset{\displaystyle O}{\overset{\|}{C}}-OCH_3 \\ \\ COOCH_3 \end{matrix}$ DMI

$E_A = 14–17 \text{ kJ mol}^{-1}$ Both effects $E_A = 24.9 \text{ kJ mol}^{-1}$
$A = (3\text{-}8) \cdot 10^6 \text{ L mol}^{-1} \text{ s}^{-1}$ $A = 2.2 \cdot 10^5 \text{ L mol}^{-1} \text{ s}^{-1}$

$$CH_2=C \begin{matrix} CH_2-O-\overset{\displaystyle O}{\overset{\|}{C}}-CH_3 \\ \\ COOC_2H_5 \end{matrix}$$

$E_A = 12.4 \text{ kJ mol}^{-1}$
$A = 8 \cdot 10^6 \text{ L mol}^{-1} \text{ s}^{-1}$

EAMA
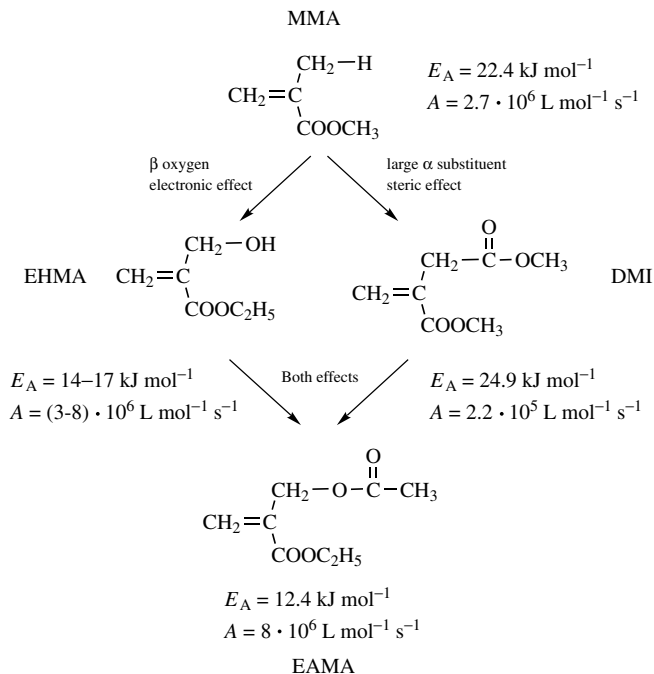
Illustrating the effect of different contributions (i.e steric and electronic) to the activation parameters using different monomers

Scheme 4.9

in the preexponential factor of about one order of magnitude is observed (r.h.s. of Scheme 4.9). This decrease is due to the sterically more demanding nature of the propagating DMI radical. When going from MMA to ethyl α-hydroxy methacrylate (EHMA), the preexponential factor remains unchanged, but the activation energy is reduced due to the electronic effect of the additional β-oxygen atom (l.h.s. of Scheme 4.9). Both effects may be combined in one monomer (ethyl α-acetoxy-methyl acrylate, bottom of Scheme 4.9) with a resulting decrease in the activation energy and the preexponential factor. The propagation rate coefficients of some monomers are very similar, which allows them to be arranged in groups or families. This is the case for structurally similar monomers such as acrylates or methacrylates. The homologous series of acrylates with linearly increasing ester groups, such as methyl, ethyl, butyl, and dodecyl acrylate, have approximately the same k_p value, as do the corresponding methacrylate systems. The propagation rate coefficients and Arrhenius parameters (determined via the PLP-SEC method) for these and additional monomers are given in Table 4.1 (data taken from Ref.[23]).

It should also be mentioned that the propagation rate coefficient for most monomers is strongly pressure-dependent with large negative activation volumes; thus an increase in pressure leads to an increased k_p value. Typical activation volumes for

TABLE 4.1   Activation Parameters for the Propagation Step for Various Monomers, Obtained via PLP-SEC [a]

Monomer	E_A (kJ/mol)	A (L mol^{-1} s^{-1})	k_p at 60°C (L mol^{-1} s^{-1})
Methyl methacrylate	22.3	2.65×10^6	833
Ethyl methacrylate	23.4	4.07×10^6	873
Butyl methacrylate	22.9	3.80×10^6	976
Isodecyl methacrylate	20.8	2.19×10^6	1,590
Dodecyl methacrylate	21.0	2.51×10^6	1,280
Methyl acrylate [b]	13.9	3.61×10^6	24,000
Butyl acrylate	17.4	1.8×10^7	33,700
Dodecyl acrylate [b]	15.8	1.09×10^7	36,400
Styrene	32.5	4.27×10^7	341
p-Me-styrene	32.4	2.84×10^7	236
p-Cl-styrene	32.1	4.48×10^7	415
p-F-styrene	32.0	3.50×10^7	336
2-Ethylhexyl methacrylate	20.4	1.87×10^6	1,190
Cyclohexyl methacrylate	22.3	4.88×10^6	1,560
Dimethyl itaconate [c]	24.9	2.20×10^5	27
Dicyclohexyl Itaconate [e]	22.0	1.74×10^4	6
Glycidyl methacrylate	21.9	4.41×10^6	1,620
Hydroxyethyl methacrylate	21.9	8.89×10^6	3,270
Hydroxypropyl methacrylate	20.8	3.51×10^6	1,900
Isobornyl methacrylate	22.5	4.28×10^6	1,290
3-[Tris(trimethylsilyloxy)silyl] propyl methacrylate [d]	19.9	1.44×10^6	1,092
Vinyl acetate	20.4	1.49×10^7	9,460

[a] All numbers are from A. M. van Herk, *Macromol. Theory Simul.* **9**, 433 (2000) unless otherwise indicated.
[b] Experiments carried out at 100 bar.
[c] L. H. Yee, M. L. Coote, T. P. Davis, and R. P. Chaplin, *J. Polym. Sci.; Part A: Polym. Chem.* **38**, 2192 (2000).
[d] L. M. Muratore, M. L. Coote, and T. P. Davis, *Polymer* **41**, 1441 (2000).
[e] P. Vana, L. H. Yee, and T. P. Davis, *Macromolecules* **35**, 3008 (2001).

some common monomers are given in Table 4.2. It should be noted that the termination rate coefficient is in contrary decreasing with increasing pressure (see Section 4.4). The opposite behavior of k_p and k_t with respect to an increase in pressure results in markedly increased overall polymerization rates at higher reaction pressures.

Since the propagation reaction is chemically controlled (up to high monomer conversions of ≤80%), there is little to no solvent influence on the propagation rate coefficients. Extensive studies have been carried out, which mainly confirm this small influence of the solvent on the propagation rate coefficient.[24–26] Larger effects in solvents have only been observed for specific monomers, including ethyl α-hydroxy methacrylate (EHMA),[27] or specific solvents such as supercritical CO_2.[28–31] In the case of the solvent effects on EHMA, where k_p falls between 580 (tetrahydrofuran) and 1860 (xylene) L mol^{-1} s^{-1}, it was proposed that the solvent is playing a

TABLE 4.2 Typical Activation Volumes, $\Delta V^{\#}$, for the Propagation Step for Some Common Monomers

	Methyl Acrylate	Dodecyl Acrylate	Methyl Methacrylate	Butyl Methacrylate	Dodecyl Methacrylate
$\Delta V^{\#}$ (cm^3 mol^{-1})	$-11.7\,^a$	$-11.7\,^a$	$-15.8\,^b$	$-16.5\,^c$	$-16.0\,^c$

[a] M. Buback, C. H. Kurz, and C. Schmaltz, *Macromol. Chem. Phys.* **199**, 1721 (1998).
[b] S. Beuermann, M. Buback, and G. T. Russell, *Macromol. Rapid Commun.* **15**, 351 (1994).
[c] M. Buback, U. Geers, C. H. Kurz, and J. Heyne, *Macromol. Chem. Phys.* **198**, 3451 (1997).

specific role in the transition state of the reaction by possibly affecting the geometry of the transition state via specific interactions. This suspicion is underpinned by the observation that the solvent also affects both the activation energy and the preexponential factor. However, it should always be kept in mind that any existing technique to asses the propagation rate coefficient (see Section 4.11.2), is only capable of measuring the product of k_p and the monomer concentration. Results obtained from free-radical polymerizations carried out in supercritical CO_2 suggest that the actual monomer concentration at the reaction site is somewhat different from the solution concentration, that is, that a structuring of the solution occurs. Since at present there is no methodology to separate the propagation rate coefficient from the monomer concentration, these interpretations are somewhat speculative.

It has been shown that for conversion exceeding 80%, the propagation reaction becomes diffusion controlled, which leads to a marked decrease of k_p. However, exact measurements in this highly viscous reaction regime are extremely difficult to carry out, and thus reliable data are scarce.

4.4 TRANSFER

The measured average molecular weights, such as those obtained from molecular weight distributions, of macromolecules generated by free-radical polymerization processes are often lower than predicted by accounting for initiation, propagation, and termination processes. This experimental observation can be attributed to chain stoppage via a chain transfer reaction. The transfer reaction can be described via Scheme 4.10.
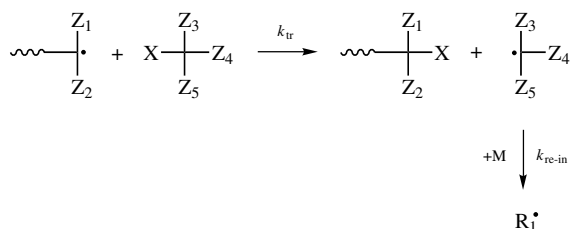
Scheme 4.10

The propagating macroradical of chain length i, R_i, abstracts a weakly bonded atom (e.g., a hydrogen or halogen, X) from the transfer agent, T. A dead polymer with a saturated end group is generated as well as a new free-radical, which in turn might react with monomer units. The transfer agent may be the monomer itself, the initiator, the solvent, or any other deliberately added transfer agent. The rate of this displacement reaction is expressed by the equation

$$-\frac{d[T]}{dt} = k_{tr}[R^\bullet][T] \tag{4.10}$$

where k_{tr} is the transfer rate coefficient and [T] is the concentration of the transfer agent. The transfer rate coefficient is often reported in a ratio with the propagation rate coefficient. The resulting quantity is called the transfer constant, C:

$$C = \frac{k_{tr}}{k_p} \tag{4.11}$$

If the chain transfer reaction has a measurable effect on the overall rate of polymerization, R_p, this rate depends on the size of the propagation, reinitiation, and transfer rate coefficients. Four cases can be distinguished: (1) $k_p \gg k_{tr}$ and $k_{re-in} \approx k_p$ leads to "normal" chain transfer, decreasing M_w and no measurable effect on R_p; (2) $k_p \ll k_{tr}$ and $k_{re-in} \approx k_p$ leads to telomerization, a large decreasing effect on M_w, and no measurable effect on R_p; (3) $k_p \gg k_{tr}$ and $k_{re-in} < k_p$ leads to retardation, a decrease in M_w and a decrease in R_p; and (4) Finally, $k_p \ll k_{tr}$ and $k_{re-in} < k_p$ results in degenerative chain transfer, a large decrease in M_w and a large decrease in R_p. It can thus be easily inferred that chain transfer may alter the properties of the polymeric product in an undesirable way, or—in contrast—may be used advantageously to specifically reduce the molecular weights obtained in a specific polymerization process. The first case discussed above (which refers to the kinetic concept of chain transfer) is assumed for the derivation of the Mayo equation, which is frequently used to derive chain transfer rate coefficients (see Section 4.11.3). This specific case does not alter the overall rate of the polymerization system because it does not change the overall free-radical concentration, but rather influences the molecular weight distribution.

The only transfer reaction that cannot be avoided is transfer to monomer. Thus, the maximum upper limit of the molecular weight that can be reached under a given set of reaction conditions is given by the transfer to monomer reaction, assuming the absence of all other transfer events (Section 4.7.1.1). Fortunately, the transfer to monomer rate coefficients are usually rather low, approximately between 3×10^{-5} and $20 \times 10^{-5}\,\mathrm{L\,mol^{-1}\,s^{-1}}$. It is important to notice that the transfer to monomer reaction cannot be decreased via a decrease in monomer concentration because the average number degree of polymerization is independent on the monomer concentration for the transfer to monomer step. This is, because the transfer to monomer effect is governed by the ratio of the transfer rate to propagation rate and both the denominator and numerator of this ratio contain the monomer concentration.

Consequently, the monomer concentrations cancel. This is illustrated in Eq. (4.55). However, the activation energy of propagation and transfer differs for most of the common monomers. Thus a decrease of the temperature normally lowers the monomer transfer constant, C_M. Table 4.3 gives the transfer to monomer constants, C_M, for some common monomers.

Also unavoidable is the transfer to the initiator molecule used to induce polymerization. However, this form of chain transfer is somewhat controllable via the choice

TABLE 4.3   Transfer Constants to Monomers C_M

Monomer	$T(°C)$	$C_M \times 10^5$
Acrylamide	60[a]	6.0[a]
Acrylonitrile	60[b]	3.3–10.2[b]
1-Butene	60	73
Butyl acrylate	60	3.33–12.5
o-Chlorostyrene	50	2.5–2.8
Ethyl acrylate	60	5.79
Ethylene	60[c]	4–42[c]
	110	11–90
	130	16–112
Methacrylonitrile	60	58.1
Methyl acrylate	60[d]	0.36–3.25[d]
Methyl methacrylate	0	1.28–1.48
	30	1.17–2.6
	50[e]	5.15[e]
	100	3.8
α-Methylstyrene	50[e]	412[e]
Styrene	25[f]	3.5[f]
	60	7.8–8.7
	90	1.5–16.5
Vinyl acetate	0	5.0–9.6
	25	9.0–107
	40	12.9–13.2
	60	18[g]
Vinylidene chloride	60	380[h]

[a] C. F. Jasso, E. Mendizabal, and M. E. Hernandez, *Rev. Plast. Mod.* **62**, 823 (1991).
[b] I. Capek, *Collect. Czech. Chem. Commun.* **51**, 2546 (1986).
[c] B. Erussalimsky, et.al., *Makromol. Chem.* **104**, 288 (1967).
[d] V. Mahadevan and M. Santhappa, *Makromol. Chem.* **16**, 119 (1955).
[e] D. Kukulj, T. P. Davis, and R. G. Gilbert, *Macromolecules* **31**, 994 (1998).
[f] H. Kapfenstein-Doak, C. Barner-Kowollik, T. P. Davis, and J. Schweer, *Macromolecules* **34**, 2822 (2001).
[g] S. P. Potnis and A. M. Deshpande, *Makromol. Chem.* **153**, 139 (1972).
[h] K. Matsuo, G. W. Nelb, R. G. Nelb, and W. H. Stockmayer, *Macromolecules* **10**, 654 (1977).

Source: Data from A. Brandrup, E. H. Immergut, and E. A. Grulke, *Polymer Handbook*, 4th ed., Wiley, 1999, unless other reference is noted.

TABLE 4.4   Transfer Constants to Initiators, C_I at 60°C

Initiator	C_I		
	Styrene	Methyl acrylate	Methyl methacrylate
2,2'-Azobis (isobutyronitrile)	0.09–0.14 [a]	—	0.02 [b]
t-Butyl peroxide	0.00023–0.0006 [c]	0.00047 (65°C)	0.0001 [d] (20°C)
2-Butanone peroxide	0.46 (50°C)	0.05 (65°C)	0.0025–0.00698 (65°C)
t-Butyl hydroperoxide	0.035	0.01	—
Ethyl peroxide	0.00066	—	—
2,2'-Azobis(2,4,4-trimethyl valeronitrile)	0.59 (25°C)	—	—
Benzoyl peroxide	0.101 [e]	0.0246 [f]	0.02 [g]

[a] J. G. Braks and R. Y. M. Huang, *J. Appl. Polym. Sci.* **22**, 3111 (1978).
[b] G. Ayrey and A. C. Haynes, *Makromol. Chem.* **175**, 1463 (1974).
[c] W. A. Pryor, A. Lee, and C. E. Witt, *J. Am. Chem. Soc.* **86**, 4229 (1964).
[d] I. M. Bel'govskii, L. S. Sakhonenko, and N. S. Enikolopyan, *Vysokomolekul. Soedin.* **8**, 369 (1966).
[e] J. A. May and W. B. Smith, *J. Phys. Chem.* **72**, 216 (1968).
[f] V. Mahadevan and M. Santhappa, *Makromol. Chem.* **16**, 119 (1955).
[g] S. Henrici-Olive and S. Olive, *Fortschr. Hochpolymer. Forsch.* **2**, 496 (1961).

Source: Data from A. Brandrup, E. H. Immergut and E. A. Grulke, *Polymer Handbook*, 4th ed., Wiley, 1999, unless other reference is noted.

of the employed initiator. In addition, the effects on the overall polymerization kinetics and on the molecular weight distribution are small, if low concentrations of initiator are employed. Typical transfer to initiator constants, C_I, are presented in Table 4.4.

In contrast to the transfer to monomer and initiator, the transfer to a solvent molecule is of considerable importance, because solvents are used in high concentrations in most industrial polymerization processes. Many organic solvents exhibit transfer constants similar to those found for common monomers, and their significant transfer effect can be attributed largely to their usage in high concentrations. There are a few solvents that show significantly higher transfer constants, such as carbon tetrachloride. In the case when the transfer constant of a solvent is too high, it may not be used as a solvent but rather as a modifier, namely a "conventional" chain transfer agent. Chain transfer agents with chain transfer constants greater than one are very useful, as they can be employed in low concentrations. These agents are important for industrial processes, because they allow for the regulation of the molecular weight of the generated polymer and thus significantly reducing the viscosity of the reaction medium and allowing for an optimum heat transfer. A similar molecular weight control can be achieved via an increase in the initial initiator concentration (see Section 4.7.1). However, such an increase in initiator concentration is associated with a considerable increase in the rate of polymerization according to Eq. (4.20), which may lead to a loss over the control of the polymerization. Typical agents with very high transfer constants are thiols and halogenated compounds such

TABLE 4.5   Transfer Constants to Solvents and Additives, C_T, at 60°C

	$C_T \times 10^4$	
Transfer Agent	Styrene	Methyl Methacrylate
2-Butanone	4.98	0.45
Acetaldehyde	8.5	6.5
Acetic acid	2.22 (40°C)	0.24 (80°C)
Acetone	0.32[a]	0.195
Acetonitrile	0.44	—
Aniline	2.0	4.2
Benzaldehyde	4.5–5.5	0.86–2.5
Benzene	0.018–0.04	0.04–0.83
Carbon tetrabromide	2,500,000[b]	1500–2700
Carbon tetrachloride	69–148	0.5–20.11
Chloroform	0.41[a]	0.45–1.77
Cumene	0.8–3.88	1.9–2.56
Cyclohexane	0.024–0.063	0.1–0.2 (80°C)
Ethyl acetate	15.5	0.1–0.46
Ethyl ether	5.64	—
Heptane	0.42	1.8 (50°C)
Iron(III) chloride	5,360,000	—
Isopropanol	3.05	0.583
Methanol	0.296–0.74	0.2
N,N-Dibenzylhydroxylamine	5000	—
N,N-Dimethyl acetamide	4.6	—
N,N-Dimethyl formamide	4.0	—
n-Butanol	1.6	0.394
n-Butanthiol	220,000	6600
n-Dodecanethiol	150,000	9700–12,300[c]
Pentaphenylethane	20,000	—
Phenyl ether	7.86	9.13
Pyridine	0.6	0.176 (70°C)
Tetrahydrofurane	0.5 (50°C)	—
Toluene	0.105–2.05	0.17–0.45
Triethylamine	1.4–7.5	8.3
Water	0.006–0.31	—

[a] N. Y. Kaloforov and E. Borsig, *J. Polym. Sci., Polym. Chem. Ed.* **11**, 2665 (1973).
[b] G. Gleixner, J. W. Breitenbach, and O. F. Olaj, *Makromol. Chem.* **178**, 2249 (1977).
[c] J. P. A. Heuts, T. P. Davis, and G. T. Russell, *Macromolecules* **32**, 6019 (1999).

Source: Data from A. Brandrup, E. H. Immergut, and E. A. Grulke, *Polymer Handbook*, 4th ed., Wiley, 1999, unless other reference is noted.

as carbon tetrabromide. A considerable disadvantage of these transfer agents is their often very unpleasant odor. The application of effective transfer agents in very high concentrations leads to so-called telomerization, namely, the formation of almost exclusively dimer and trimer species. The kinetics of such telomerizations is far from simple, due to the disparate radical reactivities displayed by the very short

TABLE 4.6   Transfer to Polymer Constants, C_P

Polymer	$T(°C)$	$C_P \times 10^4$
Poly-1,3-butadien	50	11
Polyacrylonitrile	50	4.7
Polyethylene	175	108.4
Poly(methyl methacrylate)	50	0.22–1.5
Poly-N,N-dimethyl acrylamide	50	0.61
Polystyrene	50	1.9–16.6
Polyvinylacetate	50	0.06–10.2

Source: Data from A. Brandrup, E. H. Immergut, and E. A. Grulke, *Polymer Handbook*, 4th ed., Wiley-Interscience, New York, 1999.

radicals involved; the shorter radicals show a smaller reactivity towards propagation and transfer reactions than the larger ones. In the case of carbon tetrachloride-mediated polymerizations, this has been attributed to the stabilizing effect of the CCl_3 end group.[32] A summary of the most important chain transfer agents and solvents capable of chain transfer can be found in Table 4.5.

It should be mentioned that an attractive alternative to these conventional chain transfer agents is provided by catalytic chain transfer agents. Such agents were discovered in the late 1970s and are now commonly used in industrial applications. Because of their catalytic nature, they can be employed in ultralow concentrations. At higher monomer conversion, transfer processes to the formed polymer are becoming significant. Interestingly, the transfer to polymer rate constants are considerably higher (by a factor of ~ 10) than those observed for the corresponding monomer. Transfer to polymer is resulting in so-called long-chain branching, if the reaction takes place intermolecularly. In the case of intramolecular transfer to polymer, the reaction is described as "backbiting," leading to short-chain branching (observed in ethylene polymerizations). Typical values for the transfer to polymer constant, C_p, of some common monomers are collected in Table 4.6.

The methods commonly applied for the determination of chain transfer constants are extensively described in Section 4.11.3.

4.5 TERMINATION

The termination reaction in free-radical polymerization is the most complex reaction in the polymerization process. Its termination rate coefficient, k_t, is influenced by a multitude of different factors, which are not easily separated. Only since the mid-1980s have new methods become available that allow for an accurate measurement of this rate coefficient. The scatter of the termination rate coefficients given in the *Polymer Handbook*[33] reported for the same monomer at the same reaction temperature is a direct manifestation of the influence of these various parameters on k_t. This appreciable disagreement is explainable partly by the frequent use of incorrect

values for the propagation rate coefficient, k_p, which is always needed to determine k_t from the coupled form of the two coefficients. However, the situation has improved greatly with the invention of the pulsed laser polymerization—size-exclusion chromatography (PLP-SEC) method (see Section 4.11.2.1).

It is generally accepted that the termination rate coefficient depends on the following factors and experimental parameters: (1) the system viscosity, (2) the chain length of the terminating free macroradicals, (3) the temperature, (4) the pressure, and the (5) monomer conversion.

The rate law expression for the termination step reads

$$-\frac{d[R^\bullet]}{dt} = \sum_i \sum_j 2k_t^{i,j}[R_i^\bullet][R_j^\bullet] \tag{4.12}$$

The indices i and j indicate the individual chain lengths of the terminating macroradicals. There has been considerable confusion in the past on whether to incorporate the factor 2 from the rate law expression into the termination rate coefficient. The factor 2 is necessary if the rate law describes the rate of the loss of macroradicals but unnecessary if only termination events are considered. Nevertheless, the IUPAC ruling on this is clear, termination rate coefficients are to be reported without the incorporated factor 2. All termination rate coefficients given in this chapter are in accordance to the IUPAC guideline.

There are two modes of termination: (1) direct coupling (combination) of two free macroradicals to give a dead polymer chain of chain length $i + j$, with the rate coefficient $k_{t,c}$; and (2) so-called disproportionation, where a hydrogen atom is abstracted from one of the radical chain ends, yielding two stabilized polymer chains, one of which carries a double bond, with the rate coefficient $k_{t,d}$. The process is illustrated in Scheme 4.11 on the example of polyethylene macroradicals. It is important to notice that—in the case of macroradicals derived from other monomers—in principle any β-hydrogen may be abstracted.

Which termination mode dominates depends largely on the structure of the monomer unit, but also—however to a lesser extent—on the reaction temperature and pressure. Disproportionation is (slightly) favored at higher reaction temperatures. The reasons for this behavior have yet to be clarified, but there is some evidence pointing toward a different temperature dependence of the corresponding preexponential factors in the Arrhenius expression for k_{tc} and k_{td}. However, the observed effects are small and associated with a large experimental scatter as indicated in Fig. 4.2 in the example of the temperature dependence of the contribution of
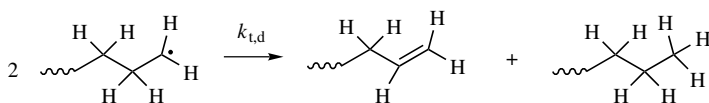
Scheme 4.11
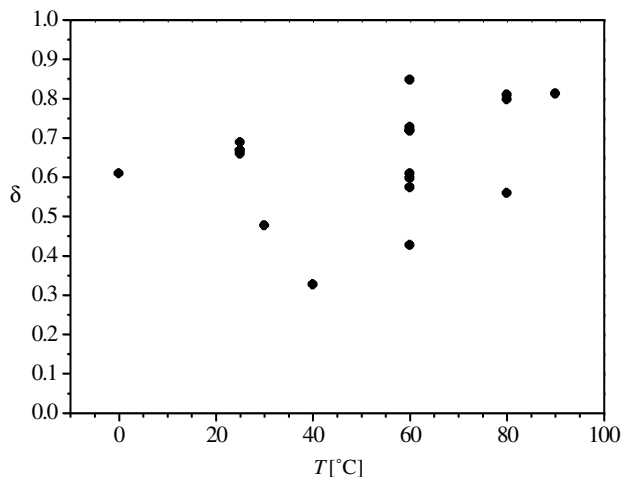
Figure 4.2 Temperature dependence of the contribution of disproportionation to the overall termination process, δ, for a methyl methacrylate polymerization at ambient pressure. [M. D. Zammit, T. P. Davis, D. M. Haddleton, and K. G. Suddaby, *Macromolecules* **30,** 1915 (1997) and references cited therein.]

disproportionation to the overall termination process, δ, for a MMA polymerization at ambient pressure.

$$\delta = \frac{k_{t,d}}{(k_{t,d} + k_{t,c})} \tag{4.13}$$

It should be noted that the mode of termination has no influence on the rate of the free-radical polymerization process. However, the generated molecular weight distributions are strongly influenced by the termination mode. Since some methods (see Section 4.11.4.2) for the determination of the termination rate coefficient rely exclusively on the analysis of the full molecular weight distributions, it is mandatory to have reliable data on the termination mode of a specific monomer. Table 4.7 gives data on termination modes for various monomers at ambient pressure and various temperatures. A comprehensive review of the literature known data on combination–disproportionation modes for various monomers can be found in Ref. 34.

Because of the abovementioned chain length dependence of the termination rate coefficient and its strong dependence on the monomer conversion, it is rather difficult to report tabulated values for k_t. However, its is possible to give chain length averaged k_t values for a specific monomer conversion, $\langle k_t \rangle$. It is important to note that for many of the reported chain length averaged k_t values, it is unclear to which chain length region they correspond. Since most measurements of the termination rate coefficient have been carried out at low monomer conversion, it is sensible to report k_t values for the low conversion regime (see below for a discussion of high conversion k_t data).

TABLE 4.7   Contribution of Disproportionation to the Overall Termination, δ, for Different Monomers

Monomer	$T(^{\circ}C)$	δ
Butyl methacrylate	80[a]	0.54[a]
Ethyl methacrylate	80[a]	0.42[a]
Methacrylonitrile	80[b]	0.091[b]
Methyl methacrylate	0[c]	0.61[c]
	25[d]	0.67[d]
	60[d]	0.73[d]
	90[i]	0.81[i]
α-Methyl styrene	55[e]	0.091[e]
Styrene	20–50[f]	0.17[f]
	50[g]	0.2[g]
	60[h]	0.1–0.2[h]
	90[i]	0.054[i]

[a] S. Bizilj, D. P. Kelly, A. K. Serelis, D. H. Solomon, and K. E. White, *Aust. J. Chem.* **38**, 1657 (1985).

[b] A. K. Serelis and D. H. Solomon, *Polym. Bull.* (Berlin) **7**, 39 (1982).

[c] J. C. Bevington, H. W. Melville, and R. P. Taylor, *J. Polym. Sci.* **14**, 463 (1954).

[d] C. H. Bamford, G. C. Eastmond, and D. Whittle, *Polymer* **10**, 771 (1969).

[e] R. C. Neuman, Jr. and M. J. Amrich, Jr. *J. Org. Chem.* **45**, 4629 (1980).

[f] O. F. Olaj, J. W. Breitenbach, and B. Wolf, *Monatsh. Chem.* **95**, 1646 (1964).

[g] K. C. Berger and G. Meyerhoff, *Makromol. Chem.* **176**, 1975 (1983); K. C. Berger, *Makromol. Chem.* **176**, 3575 (1975).

[h] G. Moad, D. H. Solomon, S. R. Johns, and R. I. Willing, *Macromolecules* **17**, 1094 (1984).

[i] M. D. Zammit, T. P. Davis, D. M. Haddleton, and K. G. Suddaby, *Macromolecules* **30**, 1915 (1997).

Average termination rate coefficients have been reported over several orders of magnitude, ranging from approximately 50 to 10^9 L mol^{-1} s^{-1}.[35] This impressive range may be explained by a shift in the rate determining step when going from one monomer to another. The termination reaction can be broken down into a three stage process:[36]

1. The center-of-mass diffusion of the individual macroradical coils toward each other through the reaction medium.

2. The so-called segmental diffusion of the radical chain ends toward each other. This segmental diffusion process brings the chain ends into a position that enables them to react.

3. The chemical reaction of the two radicals that yields the polymeric product(s).

The slowest reaction step—in a sequence of reaction steps—will always determine the rate of the overall reaction. Because of the extremely fast reaction rate of the radical combination/disproportionation reaction (i.e., strictly speaking, the

termination itself) in the order of $10^{10}\,\mathrm{L\,mol^{-1}\,s^{-1}}$, the center-of-mass and segmental diffusion steps are (in almost all the cases) the rate-determining steps. At low monomer conversions, the rate-determining step for reasonably high-molecular-weight macroradicals (of length ≥ 50) is believed to be almost exclusively segmental diffusion. Typical examples for high k_t monomers are methyl methacrylate (MMA) and styrene: $\langle k_t \rangle \approx 10^8\,\mathrm{L\,mol^{-1}\,s^{-1}}$. Differences in the (average) termination rate coefficient that can be observed when comparing different monomers are most likely due to differences in segmental diffusion coefficients. However, lower values of k_t, as observed, for example, for dodecyl methacrylate, specifically $\langle k_t \rangle \approx 10^6\,\mathrm{L}$ $\mathrm{mol^{-1}\,s^{-1}}$, have been attributed to the sterically demanding substituents, leading to a (partly) chemically controlled termination process.[37] For reported ultralow k_t monomers, such as the fumarates, specifically $\langle k_t \rangle \approx 500\,\mathrm{L\,mol^{-1}\,s^{-1}}$,[38,39] a chemically controlled termination process may also be envisaged, but evidence for this hypothesis is nonexistent, and other explanations can by no means be ruled out.

As indicated above, for most common monomers, the termination reaction is believed to be segmental diffusion controlled at low and intermediate monomer conversions and center-of-mass diffusion controlled at high conversion. If the diffusion-controlled nature of the termination reaction is accepted, this has the immediate consequence that the termination rate coefficient should be chain-length-dependent. However, the chain length dependence of k_t is markedly different for the two diffusion mechanisms.

The chain length dependence of k_t is normally quantified by the following equations. Macroscopic k_t values may be obtained by the following averaging procedure:

$$\langle k_t \rangle = \frac{\sum_i \sum_j k_t^{i,j}[\mathbf{R}_i^{\bullet}][\mathbf{R}_j^{\bullet}]}{\left(\sum_i [\mathbf{R}_i^{\bullet}]\right)^2} \tag{4.14}$$

The microscopic k_t value, $k_t^{i,j}$, corresponds to the individual termination rate coefficient involving two free macroradicals with the chain lengths i and j. The averaging procedure is advantageous because the chain length distribution of the macroradicals in free-radical polymerization is normally highly disperse. The chain length dependence of the macroscopic k_t is often expressed via the following power law

$$\langle k_t \rangle = k_t^0 \cdot \bar{P}_n^{-\alpha} \tag{4.15}$$

This power law correlates the average value for the termination rate coefficient $\langle k_t \rangle$ with the number average degree of polymerization, $\bar{P}_n$. The chain length dependence of k_t is now easily described and quantified by the exponent α in Eq. (4.15).

If center-of-mass diffusion is the rate-determining step in the termination reaction, an exponent of 0.5–0.6 results, depending on the quality of the solvent. This result can be explained by considering the translational diffusion properties of the polymer coil. The diffusion coefficient of the polymer coil is inversely proportional to its hydrodynamic radius. If the hydrodynamic radius is equated with the radius of gyration, $\langle s^2 \rangle^{0.5}$, it can be inferred[40] that for a theta solution $\langle s^2 \rangle \propto i$ and for an

athermic solution $\langle s^2 \rangle \propto i^{1.176}$. This leads directly to the chain lengths dependence of the diffusion coefficient of $D \propto i^{-0.5}$ for theta solutions and $D \propto i^{-0.59}$ for athermic solutions. According to various theories for diffusion controlled reactions, the diffusion coefficient is directly proportional to the termination rate coefficient.

The segmental diffusion coefficient is generally chain-length-independent. However, a slight chain length dependence of the termination rate coefficient of close to $\alpha = 0.16$ is predicted for athermic solvents, due to thermodynamic shielding effects of the chain. The chain shields its own reactive center because of its size from the second chain, which displays a similar shielding effect. The exponent of -0.167 has been confirmed in various theoretical studies applying the scaling theory,[41] as well as in chain statistic simulations.[42] The chain length dependence of k_t is almost negligible in theta solvents for the segmental diffusion controlled regime, where α is close to 0.05. Experimentally, evidence has been gathered for both exponents, 0.1–0.2 for segmental diffusion and 0.5–0.6 for center-of-mass diffusion, depending on the size of the macroradicals undergoing termination. Consequently, the chain length dependence of the termination rate coefficient is best described by a function featuring two (main) domains of different chain lengths dependencies as depicted in Fig. 4.3.

Domain A in Fig. 4.3 is associated with center-of-mass diffusion-controlled termination, due to the small size of the macroradicals (i.e., $\alpha \approx 0.5$–0.16), whereas domain B is controlled by segmental diffusion processes (i.e., $\alpha \approx 0.05$–0.16). The C domain represents an intermediate region associated with the change in mechanism. These numbers have been confirmed experimentally by various research groups in the past.[43] Styrene and methyl methacrylate (MMA) have been studied particularly extensively with respect to the chain length dependence of the
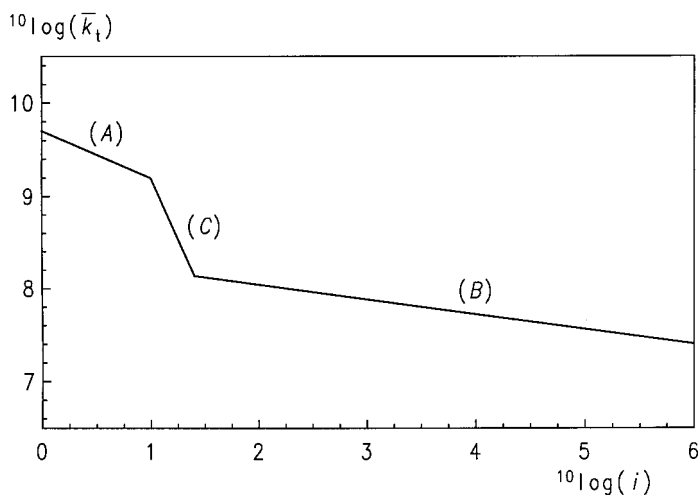
Figure 4.3   General function for the termination rate coefficient as a function of the chain length of terminating macroradicals.

termination rate coefficient in the segmental diffusion region. These chain length dependencies may be described by the following equations:[44]

$$\text{MMA}(25°C): \quad \langle k_t \rangle_i = 7.56 \cdot 10^7 \cdot i^{-0.18}$$

$$\text{Styrene}(25°C): \quad \langle k_t \rangle_i = 1.21 \cdot 10^8 \cdot i^{-0.16}$$

where $\langle k_t \rangle_i$ denotes the average experimental termination rate coefficient for a mean chain length i.

Although the termination rate coefficient of a particular monomer is influenced by the system viscosity and the chain length of the terminating free macroradicals, it is important to notice that the pressure and to a lesser extent the reaction temperature have a significant effect on its value. Especially the reaction pressure influences the absolute value of the termination rate to a far greater extent than the change in k_t associated with its chain length dependence. Table 4.8 gives activation energies and activation volumes for selected acrylate and methacrylate termination rate coefficients along with its value at 1000 bar and 40°C at low monomer conversions. The numbers given in Table 4.8 were derived mainly from SP-PLP experiments (see Section 4.11.4.1).

Inspection of Table 4.8 shows that the activation energies are rather low and between 3 and 8 kJ/mol. This observation is consistent with the diffusion (either segmental or translational) controlled nature of the termination reaction. Strictly speaking, these activation energies correspond to temperature dependence of the inverse system viscosity. To this date, there is no data on the activation energy of the actual termination reaction itself. However, it is very likely that the termination reaction itself has a close to zero activation energy. This conclusion may be deduced from the activation parameters observed for small-radical termination.[63] It is interesting to note that the activation volume of the termination reaction is positive, that is, that the value of k_t is reduced at higher reaction pressures. The activation volumes

TABLE 4.8 Activation Parameters of the Termination Step for Various Acrylates and Methacrylates

Monomer	$E_A/(\text{kJ/mol})$	$\Delta V/(\text{cm}^3/\text{mol})$	$\log[k_t(\text{L mol}^{-1}\,\text{s}^{-1})]$
MA	8.0 (1000 bar)[a]	16.0 (30°C)[a]	8.13[a]
BA	6.0 (1000 bar)[b]	16.0 (40°C)[b]	7.55[b]
DA	3.0 (1000 bar)[a]	20.0 (40°C)[a]	6.38[a]
MMA	6.0 (1000 bar)[c]	15.0[d] (40°C)[c]	7.39[c]
BMA	—	—	6.70[c]
DMA	—	10.8 (30°C)	6.22

[a] C. H. Kurz, Ph.D. thesis, Göttingen, 1995.
[b] S. Beuermann, M. Buback, and C. Schmaltz, *Ind. Eng. Chem. Rez.* **38**, 3338 (1999).
[c] C. Kowollik, Ph.D. thesis, Göttingen, 1999; M. Buback and C. Kowollik, *Macromolecules* **31**, 3211 (1998).
[d] This activation volume is pressure-dependent; the value is valid for the pressure range from 1000 to 1500 bar.

of a given reaction is defined by

$$\frac{d \ln k}{dp} = -\frac{\Delta V^{\#}}{RT} \tag{4.16}$$

where $\Delta V^{\#}$ is the activation volume and p the pressure.

This experimental observation can also be connected with the pressure dependency of the viscosity. The reaction medium tends to be more viscous at higher reaction pressures, thus slowing the rate of termination; the activation volume of the termination rate coefficient is very close to the corresponding activation volume that characterizes the pressure dependence of the inverse of the monomer viscosity.[45] It is important to note that the pressure dependencies of the termination and propagation rate coefficients display opposite behavior, allowing for increased rates of polymerization at elevated pressures.

As has been indicated above, the termination rate coefficient is—depending on the monomer in question—strongly dependent on the overall monomer conversion. The conversion dependencies of the (average) termination rate coefficient have been reported for several monomers, with most measurements being done via the SP-PLP technique, which allows one to pointwise probe the kinetics of the polymerization reaction up to high overall monomer conversions. A typical k_t/monomer conversion dependence is given in Fig. 4.4 on the example of methyl acrylate (MA) and dodecyl acrylate (DA). The data are taken from Ref. 37.

Inspection of Fig. 4.4 shows that both monomers behave very differently. Whereas in the case of methyl acrylate different regions for the change of the termination rate coefficient with conversion can be identified, dodecyl acrylate exhibits a constant (average) k_t value up to high conversions. The different regions in the
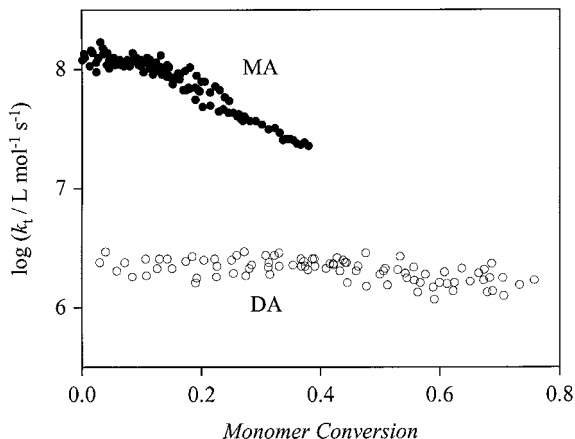
Figure 4.4 Termination rate coefficients in bulk methyl acrylate (MA) and dodecyl acrylate (DA) homopolymerizations as a function of monomer conversion. The reaction conditions were 40°C and 1000 bar.

methyl acrylate k_t versus conversion dependence may be attributed to segmental diffusion (from 0 to $\sim$15%), followed by translational diffusion and the onset of the so-called "gel effect," which is characterized by a strong auto-acceleration of the reaction. At very high monomer conversions, the reaction medium is highly viscous and the macroradicals are no longer capable of movement via translational diffusion. Instead, the addition of new monomer units to the chain end results in a change in the position of the radical chain end. This process has been termed *reaction diffusion*. Buback has introduced a model for the abovementioned dependence of the termination rate on the monomer conversion, which considers segmental, translational, and reaction diffusion processes.[46] This model has been extremely successful in describing a large set of data up to high monomer conversions.[47] In the case of dodecyl acrylate, the segmental diffusion region seems to extend to high monomer conversions, although the system viscosity changes by orders of magnitude when going from 0 to 80% conversion. Up to this point, it has not been conclusively clarified if with a monomer behaving like dodecyl acrylate (1) the entire conversion range is in the segmental or translational diffusion-controlled regime and (2) what the exact cause for a nonchanging (average) termination rate coefficient is. Figure 4.5 shows the (possible) different regimes of the termination rate coefficient in general, as outlined above.

It should be noted that it has been observed that the average k_t value slightly increases up to 5–10% conversion and then starts to decrease.[97,48] An explanation for such behavior was first offered by North and Reed who assumed faster segmental diffusion to be responsible.[36] The initial increase of k_t with increasing monomer conversion has also been associated with a change in solvent quality: k_t increases when going from a good to a poor solvent, either because of diminishing coil sizes (which
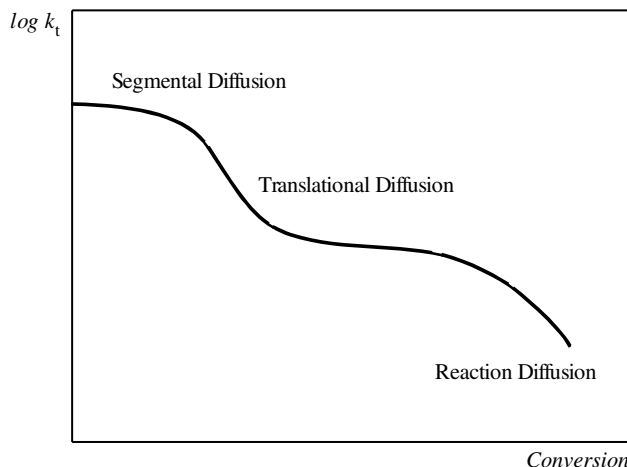
Figure 4.5 Schematic dependence of the (average) termination rate coefficient on the overall monomer conversion indicating different regimes of reaction control.

increases the segmental diffusion coefficient) or decreasing repulsions between macroradicals. This behavior of k_t not only has been observed experimentally but is also predicted theoretically.[49]

The question of the conversion dependence of the termination rate coefficient is linked to the abovementioned autoacceleration effect of the polymerization, which can be observed with some monomers at increased conversion, such as methyl methacrylate, styrene, vinyl acetate, and methyl acrylate. Also known as the *Trommsdorff, Norrish–Smith*, or *Norrish–Trommsdorff effect*, this effect can cause problems within both an industrial and scientific context ranging from a product mixture to reactor explosion, due to its exothermic nature.[50,51] It is important not to confuse the gel effect with the autoacceleration that is observed when a polymerization is carried out under nonisothermal conditions, so that the reaction temperature increases with increasing monomer conversion, due to the exothermic nature of the polymerization reaction. The gel effect is observed under isothermal reaction conditions. The cause of the gel effect has been debated over 50 years and various theories have emerged that can explain all or part of the experimental data (excellent reviews on the topic can be found in Refs. 52 and 53). In theory, any given model that links the termination rate coefficient to the increasingly difficult diffusion of macroradicals through the reaction mixture as the monomer conversion increases and thus accounts for a decrease in the termination rate, is capable of explaining the gel effect, without introducing a drastic change in the physical chemistry of the polymerizing system. The debate focuses not so much on the fact that the termination reaction becomes increasingly hindered as the mobility of the polymer chains decreases, than on the details of exactly what type of mobility is important. The main explanation for the gel effect that is offered concentrates on the formation of chain entanglements that hinders the diffusion of the macroradicals thus causing a decrease in the rate of termination.

4.6   RATE OF POLYMERIZATION

4.6.1   Stationary Polymerization

A stationary polymerization system is characterized by a constant free radical concentration as given by

$$\frac{d[R^\bullet]}{dt} = 0 \tag{4.17}$$

In the past it has been standard practice to derive a simple but general expression for the rate of polymerization, R_p. This expression correlates the rate of polymerization with the initiator and monomer concentrations on the one side and the kinetic rate coefficients k_d, k_p, and k_t on the other side. Although this expression contains many approximations, it is surprisingly successful in describing the experimental reality. Detailed kinetic studies have revealed the shortcomings of this equation. However, it remains the basis of standard free-radical polymerization kinetics. The approxima-

tions that are made in its derivation are

1. Chain-length- and conversion-independent rate coefficients k_t and k_p.
2. The instantaneous establishment of a steady-state free-radical concentration.
3. The assumption that monomer is consumed only by chain propagation and not via the initiation process or chain transfer. This assumption allows one to equate the rate of the loss of monomer with the rate of polymerization.
4. All reactions are irreversible.
5. The effective concentration of initiator derived free radicals is constant throughout the polymerization.

The core of the deviation for the rate of polymerization expression is the assumption that the rate of initiation equals the rate of termination, Eq. (4.12) in its simplified form.

This assumption is mandatory for the establishment of a constant free-radical concentration

$$2f \, k_d[I] = 2k_t[R^\bullet][R^\bullet] \tag{4.18}$$

Rearrangement of this equation and insertion into the simplified form of Eq. (4.9)

$$R_p = -\frac{d[M]}{dt} = k_p[M][R^\bullet] \tag{4.19}$$

yields the final expression for the rate of polymerization, R_p:

$$R_p = -\frac{d[M]}{dt} = k_p \left(f \frac{k_d}{k_t} \right)^{0.5} [M][I]^{0.5} \tag{4.20}$$

Equation (4.20) indicates a first-order dependence of the rate of polymerization on the monomer concentration and a square-root dependence on the concentration of the initiator. These dependencies have been confirmed on the example of many polymerizing systems. It should be pointed out that deviations from Eq. (4.20) (such as chain-length-dependent rate coefficients or primary radical termination) are manifest in a change in the exponent 0.5 associated with the initiator concentration. Extreme dilution of monomer can also change the exponents of monomer and initiator concentration. Equation (4.20) is easily integrated to yield an expression which directly correlates the monomer conversion with the observed kinetic rate coefficient, k_{obs}:

$$\ln\left(\frac{1}{1-p}\right) = k_{obs} \cdot t \quad \text{where} \quad k_{obs} = k_p \left(f \frac{k_d}{k_t}[I] \right)^{0.5} \tag{4.21}$$

where p is the conversion of monomer to polymer. The temperature dependence of the polymerization rate is given by the temperature dependencies of the individual

rate coefficients. Each rate coefficient follows its own Arrhenius law, $k = A \cdot \exp(-E_A/RT)$, where A is the preexponential factor and E_A denotes the activation energy. The overall activation energy of the rate of polymerization, $E_A^{R_p}$, equals the sum of the weighted activation energies of the elementary reactions, propagation (E_A^p), initiation (E_A^i), and termination (E_A^t).

$$E_A^{R_p} = E_A^p + \frac{1}{2}E_A^i - \frac{1}{2}E_A^t \qquad (4.22)$$

Activation energies for commonly used thermal decomposing initiators, E_A^i, are in the order of 120–150 kJ/mol. The E_A^p values for most common monomers lie within the range of 20–40 kJ/mol, and E_A^t is generally in the range of 4–10 kJ/mol. Hence, typical values for overall activation energies for the rate of polymerization initiated by a thermally decomposing initiator are close to 80 kJ/mol. This corresponds to a two or threefold rate increase for a 10°C temperature increase. Photochemical polymerization rates have a much lower activation energy of about 20 kJ/mol, according to close to zero activation energy of the photoinitiation process (see Section 4.2.2).

4.6.2 Dead-End Polymerization

To reach a steady state in free-radical polymerization, it is important that the initiator concentration is constant over a significant time span to ensure a constant rate of initiation. However, the initiator is decomposing according to Eq. (4.3) and its concentration is unavoidably decreasing. This can often be neglected when the decomposition rate of the initiator is very small in comparison to the rate of polymerization. To perform a steady-state experiment, an appropriate initiator should be chosen with a rate coefficient of decomposition, k_d, (at the given temperature) that ensures a maximum decrease in initiator concentration of no more than 10% over the entire reaction time. Especially for fast decomposing initiators or very long reaction times the decreasing initiator concentration has to be accounted for. If all initiator molecules are decomposed before the end of polymerization, the reaction ceases. However, the polymerization can be reinitiated by adding new initiator. Insertion of Eq. (4.3) in Eq. (4.20), separation of the variables and integration from $[M]_0$ to $[M]$ and from $t = 0$ to $t = t$ yields

$$-\ln\frac{[M]}{[M]_0} = -\ln(1-p) = 2k_p \left(f\frac{[I]_0}{k_d k_t} \right)^{0.5} \left(1 - e^{-(k_d t/2)} \right) \qquad (4.23)$$

where p is the extent of monomer conversion to polymer and is defined by $p = ([M]_0 - [M])/[M]_0$. At long reaction times ($t \to \infty$, the monomer concentration and conversion reach the limiting values of $[M]_\infty$ and p_∞.

$$-\ln\frac{[M]_\infty}{[M]_0} = -\ln(1-p_\infty) = 2k_p \left(\frac{f[I]_0}{k_d k_t} \right)^{0.5} \qquad (4.24)$$

The example for polymerizations of styrene using AIBN at 60°C shows how the maximum conversion depends on the concentration of the initiator: ($k_p = 341$ L mol^{-1} s^{-1}, $k_t = 5 \times 10^7$ L mol^{-1} s^{-1}, $k_d = 1.35 \times 10^{-5}$ L mol^{-1} s^{-1}, $f = 0.5$)

$$[\text{AIBN}] = 0.001 \text{ mol/L} \qquad p_\infty = 44.4\%$$
$$[\text{AIBN}] = 0.01 \text{ mol/L} \qquad p_\infty = 84.4\%$$
$$[\text{AIBN}] = 0.1 \text{ mol/L} \qquad p_\infty = 99.7\%$$

A higher initiator concentration results in a higher polymer yield However, the molecular weight of the polymer produced decreases at the same time (see Section 4.7.1).

4.6.3   Instationary Polymerization

Especially at the beginning and at the end of the polymerization process, the steady-state principle does not hold true. The generation of new free radicals by the initiator decay exceeds their consumption via termination events at early reaction times (preeffect). After the initiation process ceases, the free-radical concentration decreases according to the termination rate law expression (aftereffect). Consequently, the rate of polymerization is not constant over the entire time period of the polymerization. Measurement of the polymerization rate in the pre- and aftereffect regions allows for the determination of the coupled form of termination and propagation rate coefficients, k_p/k_t, whereas in the steady-state region, they can be accessed only as the ratio k_p^2/k_t. The individual propagation and termination rate coefficients can be calculated by combining the preceding two ratios. The determination of k_p/k_t and k_p^2/k_t via the pre- and aftereffects and stationary polymerization experiments, respectively, has long been the only possibility to determine propagation and termination rate coefficients. However, more recent studies reveal that serious problems are associated with this approach, due to the chain length dependence of k_t,[54] which is not accounted for. This may be the reason for the large discrepancies observed when comparing values for k_p and k_t from different sources. The situation has improved drastically by the invention of the pulsed laser polymerization (PLP) method, which has been introduced by Olaj and co-workers in the late 1980's (see Section 4.11.2.1). This improvement is impressively demonstrated when comparing more recent data for the propagation rate coefficient in styrene homopolymerizations with earlier data (see Fig. 4.6).

Although the steady state is reached within a couple of seconds after starting the initiation process, the generation of free radicals exceeds their loss by termination (i.e., the preeffect) in this period. Therefore, the concentration of free-radicals [R$^\bullet$] is not constant but a function of time. The rate of free-radical production is the rate of initiation minus the rate of termination as given by

$$\frac{d[\text{R}^\bullet]}{dt} = R_i - 2k_t[\text{R}^\bullet]^2 \tag{4.25}$$
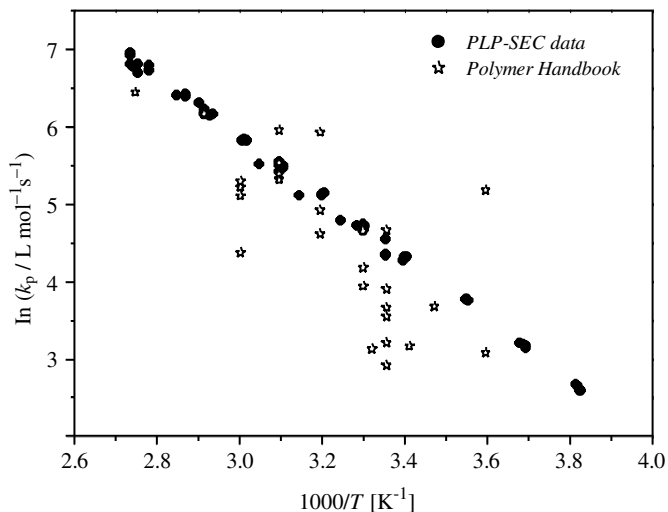
Figure 4.6 Comparison of propagation rate coefficients for bulk styrene homopolymerizations from two generations: PLP-SEC data from an IUPAC benchmark publication [M. Buback, R. G. Gilbert, R. A. Hutchinson, B. Klumperman, F.-D. Kuchta, G. B. Manders, K. F. O'Driscoll, G. T. Russell, and J. Schweer, *Macromol. Chem. Phys.* **196**, 3267 (1995)] full circles (●), and data compiled from A. Brandrup, E. H. Immergut, and E. A. Grulke, *Polymer Handbook*, Wiley-Interscience: New York, 1998, stars (☆).

Assuming a constant rate of initiation, integration leads to

$$[R^\bullet] = [R^\bullet]_S \tanh[(2k_t R_i)^{0.5} t] \tag{4.26}$$

where $[R^\bullet]_S$ represents the steady-state free-radical concentration. The example for the polymerization of styrene using AIBN at 60°C shows how fast the steady state is reached: $(k_p = 341 \, \text{L mol}^{-1} \, \text{s}^{-1}, \; k_t = 5 \times 10^7 \, \text{L mol}^{-1} \, \text{s}^{-1}, \; k_d = 1.35 \times 10^{-5} \, \text{L mol}^{-1} \, \text{s}^{-1}, f = 0.5)$:

$t = 0.5 \, \text{s}$	52% of steady-state free-radical concentration
$t = 1 \, \text{s}$	82%
$t = 2 \, \text{s}$	98%
$t = 3 \, s$	100%

After stopping the initiation process, no new free radicals are available and the concentration decreases according to a second-order rate law. Integration of Eq. (4.25) with $R_i = 0$ yields the concentration of free radicals as a function of time in the so-called aftereffect region:

$$[R^\bullet]^{-1} - [R^\bullet]_S^{-1} = 2k_t t \tag{4.27}$$

Insertion into the rate law of propagation, Eq. (4.19)—assuming that the rate of loss of monomer equals the rate of polymerization, R_p—gives

$$R_p = \frac{k_p[M]}{2k_t t + [R^\bullet]_S^{-1}} \tag{4.28}$$

which contains the individual rate coefficients k_p and k_t in a combination different from that obtained via steady-state experiments. Thus, the ratio k_p/k_t is accessible by Eq. (4.28) via the measurement of the polymerization rate in the aftereffect region.

4.6.4   Pseudostationary Polymerization

Conversions in the pre- and aftereffect regions are rather low, making it experimentally challenging to determine them accurately. To overcome this problem, a structured continuos initiation profile is chosen by which the system is facing pre- and aftereffects in sequences. This can be achieved by a photopolymerizable system, which is exposed to a succession of light and dark periods leading to a *pseudostationary* state, which provides a continuos polymerization of a system being in a nonsteady state. It is characterized by a constant mean free-radical concentration, averaged over one cycle period, but a permanently changing actual concentration of the reactive intermediates. Whereas the technique was introduced by using a rotating sector[55] (light periods are considerably long, i.e., about one-fourth of the whole cycle time t_0) the technique improved by using a pulsed laser as light source. The extremely short duration of the laser flash (on the order of nanoseconds) allows to assume an instantaneous formation of free radicals. Strictly speaking, instantaneous radical generation is equivalent to neglecting the preeffect and termination during the laser pulse, respectively. Figure 4.7 shows a typical time profile of the free-radical concentration in a pulsed laser experiment.

The maximum free-radical concentration, $[R_+^\bullet]$, is reached immediately after the laser pulse has been applied. It is the sum of the radical concentration formed at each laser flash, ρ, and the amount of free radicals still in the system, which are produced by former pulses, $[R_-^\bullet]$. This value is identical to the minimum free-radical concentration in the polymerizing system. Radical formation during the dark time is neglected. Assuming that termination is not dependent on the chain length, the rate law for termination can be written as

$$-\frac{d[R^\bullet]}{dt} = 2k_t[R^\bullet]^2 \tag{4.29}$$

Integration of Eq. (4.29) over the whole pulse period, t_0, yields

$$[R_-^\bullet]^{-1} - [R_+^\bullet]^{-1} = 2k_t t_0 \tag{4.30}$$
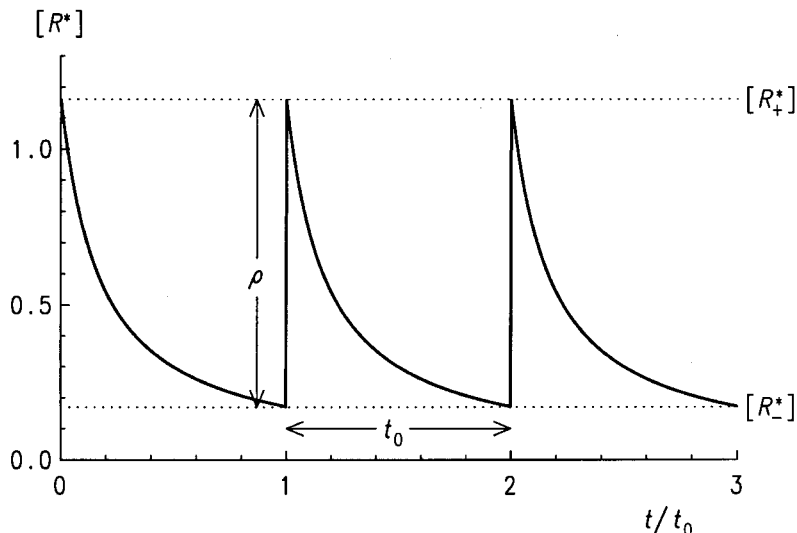
Figure 4.7   Typical radical concentration profile generated by the pulsing action of a laser on a reaction mixture of photoinitiator and monomer. The maximum free-radical concentration $[R^{\bullet}_{+}]$ is reached immediately after the laser pulse has been applied. It is the sum of the radical concentration formed at each laser flash, ρ, and the amount of free radicals still in the system produced by former pulses, $[R^{\bullet}_{-}]$.

The pseudostationary state is defined by the exact compensation of the loss of free radicals during the dark period via termination by the radical formation of the laser pulse.

$$\rho = [R^{\bullet}_{+}] - [R^{\bullet}_{-}] \tag{4.31}$$

Combination of Eq. (4.30) and (4.31) leads to

$$[R^{\bullet}_{+}] = \rho \left\{ \frac{1}{2} \pm \left(\frac{1}{4} + \frac{1}{2\rho k_t t_0} \right)^{0.5} \right\} \tag{4.32}$$

The free-radical concentration at any moment during the pulse period is

$$[R^{\bullet}] = \left(\frac{1}{[R^{\bullet}_{+}]} + 2k_t t \right)^{-1} = \frac{[R^{\bullet}_{+}]}{1 + 2[R^{\bullet}_{+}]k_t t} \tag{4.33}$$

Averaging over the whole pulse period leads to a mean value for the free-radical concentration:

$$[\bar{R}^{\bullet}] = \frac{1}{t_0} \int_0^{t_0} \frac{[R^{\bullet}_{+}]}{1 + 2[R^{\bullet}_{+}]k_t t} dt = \frac{1}{2k_t t_0} \ln(1 + 2[R^{\bullet}_{+}]k_t t_0) \tag{4.34}$$

By insertion of Eqs. (4.32) and (4.34) in Eq. (4.19), the expression for the polymerization rate in pseudostationary pulsed laser polymerizations is obtained:

$$R_p = \frac{k_p[M]}{2k_t t_0} \ln\left\{ 1 + \rho k_t t_0 \left[1 + \left(1 + \frac{2}{\rho k_t t_0} \right)^{0.5} \right] \right\} \tag{4.35}$$

This expression contains the ratio of k_p/k_t, which is typically derived from instationary polymerizations. However, the major advantage of pseudostationary polymerization does not lie within the possibility to separate the ratio of k_p^2/k_t into its individual components, but to generate structured chain length distributions. These structured distributions allow for the accurate determination of the propagation and termination rate coefficients (see Sections 4.7 and 4.11).

A special case of the pulsed laser polymerization is the single pulsed laser polymerization technique, which was introduced by Buback and co-workers in the late 1980's.[56] The equations needed to analyze the monomer conversion—time traces obtained from single-pulse–pulsed laser experiments are easily derived. Integration of the rate law expression for termination assuming a non-chain-length-dependent, average termination rate coefficient, k_t, [Eq. (4.29)] yields

$$[R^\bullet] = \left(2k_t t + \frac{1}{[R_+^\bullet]} \right)^{-1} \tag{4.36}$$

Substitution of this equation into the rate law expression for the propagation step [Eq. (4.19)] and subsequent integration yields the change in relative monomer concentration after a single laser pulse:

$$\frac{[M]}{[M]_0} = (2k_t[R_+^\bullet]t + 1)^{-k_p/2k_t} \tag{4.37}$$

This expression can be fitted to time-resolved monomer conversion–time traces obtained from SP-PLP experiments (see Section 4.11.4.1), where the two fit variables are $k_t \cdot [R_+^\bullet]$ and k_p/k_t. With knowledge of the primary free-radical concentration, $[R_+^\bullet]$, it is possible to determine k_t and k_p from a single conversion–time trace. Unfortunately, in reality, $[R_+^\bullet]$ is often not known (due to insufficient knowledge about initiator efficiencies) and k_t can be assessed only via knowledge of the propagation rate coefficient from independent experiments (e.g., PLP-SEC). However, in more recent studies the accurate determination of primary radical concentrations produced by a laser flash have been reported in nonpolymerizing systems,[57] giving promising results for future work.

4.7   THE CHAIN LENGTH DISTRIBUTION

The kinetic rate coefficients of the various steps involved in the polymerization reaction are controlling the rate of polymerization, R_p, and the overall free-radical

concentration. Keeping in mind that the polymerization is a chain mechanism leading to macromolecules, it is self-evident that the same kinetic parameters may be employed to calculate the sizes of polymeric intermediates and the polymer generated. For this purpose it is necessary to solve the complete set of coupled differential equations, one equation for each chain length plus one for the initiation step.

The rate law for the concentration change of a macroradical with chain length i can be written as

$$\frac{d[R_i^\bullet]}{dt} = k_p^{i-1}[M][R_{i-1}^\bullet] - \left(k_p^i[M] + k_{tr}^M[M] + \sum_k k_{tr}^{T_k}[T_k] \right.$$
$$\left. + 2\sum_{j=1}^{\infty} k_t^{i,j}[R_j^\bullet] \right) \cdot [R_i^\bullet] \tag{4.38}$$

This rate law reflects a polymerization process during which a free-radical with chain length i is solely formed by a propagation step from the free-radical with chain length $i - 1$. The free macroradical has then the possibility to grow by reaction with either a monomer molecule M, giving a chain length of $i + 1$, or it can undergo a transfer reaction with the monomer or any other transferring molecule T_k (e.g., transfer agent, solvent, initiator, polymer). Alternatively, it may be terminated by another free-radical. The analytical solution of this problem is obviously very difficult. However, numerical solutions of this set of equations became possible due to the rapid increase in computer power and simulations of chain length distributions of polymers are of increasing importance for academic and industrial applications.[58]

The chain length distribution of a polymer is defined as the fraction of molecules x_P that contains P basic monomer units. It should be noted that the degree of polymerization P is equivalent to the chain length i. The living macroradicals by which the dead polymer is generated through any chain stopping event show a chain length distribution, too. Both distributions are closely related to each other and the chain length distribution of the dead polymer can be calculated via the derivative of the distribution of the living macroradicals.

Like any other distribution function, the chain length distribution is described by its statistical moments, which are defined as

$$m^{(k)} = \sum_{P=1}^{\infty} P^k \cdot x_P \tag{4.39}$$

By combination of such moments one can easily calculate mean values for the degree of polymerization, $\bar{P}$, which characterize the chain length distribution. The distribution is only fully described if all moments are known. However, in practice there are two mean values calculated by the first three statistical moments, which are extensively used. The number average degree of polymerization, $\bar{P}_n$, and the weight

average degree of polymerization, $\bar{P}_w$.

$$\bar{P}_n = \frac{m^{(1)}}{m^{(0)}} = \frac{\sum_{P=1}^{\infty} P \cdot x_P}{\sum_{P=1}^{\infty} x_P} \qquad \bar{P}_w = \frac{m^{(2)}}{m^{(1)}} = \frac{\sum_{P=1}^{\infty} P^2 \cdot x_P}{\sum_{P=1}^{\infty} P \cdot x_P} \qquad (4.40)$$

4.7.1   Stationary Polymerization

4.7.1.1   Average Degree of Polymerization   To calculate the number average degree of polymerization, $\bar{P}_n$, of a polymer produced by a steady-state polymerization, it is mandatory to know how many propagation steps occur before the chain mechanism is stopped. It has to be distinguished between the term "chain" used in a molecular sense and "chain" used as a kinetic concept. The kinetic chain length, ν, (assuming that every radical $I^\bullet$ initiates polymerization) is defined as

$$\nu = \frac{\text{total number of polymerized monomer units}}{\text{total number of initiation steps}}$$
$$= -\int_0^t \frac{d[M]}{dt} dt \bigg/ \int_0^t \frac{d[I^\bullet]}{dt} dt \qquad (4.41)$$

In a system that has reached the steady state, the integrands of Eq. (4.41) may be constant over a significant timespan. By substituting with Eqs. (4.2) and (4.9)—with the assumption of chain-length-independent rate coefficients—Eq. (4.41) can therefore be rewritten as

$$\nu = \frac{R_p}{R_d} = \frac{k_p[R^\bullet][M]}{2f k_d[I]} \qquad (4.42)$$

Elimination of $[R^\bullet]$ by means of Eq. (4.18) leads to an expression for the kinetic chain length, ν, that shows the dependence of the different kinetic parameters. One important characteristic of the free-radical polymerization is well illustrated here—the sizes of the macromolecules produced are inversely proportional to the square root of initiator concentration. Increasing the initiator concentration leads to smaller-size polymer molecules:

$$\nu = \frac{k_p[M]}{2(f k_d k_t[I])^{0.5}} \qquad (4.43)$$

Disregarding any transfer effect as a first approximation correlates the kinetic chain length with the number average degree of polymerization, $\bar{P}_n$. In the case of termination by disproportionation, one polymer molecule is produced per every kinetic chain:

$$\bar{P}_n = \nu \qquad (4.44)$$

Termination by combination leads to one polymer molecule per two kinetic chains, reflecting the combination mechanism:

$$\bar{P}_n = 2\nu \tag{4.45}$$

Any mixture of these both mechanisms can be described by using the value δ [see Eq. (4.13)], the contribution of disproportionation to the overall termination process:

$$\bar{P}_n = \frac{2}{1+\delta}\nu \tag{4.46}$$

The mean kinetic chain length can be experimentally determined by using marked initiator molecules (e.g., ^{14}C radiolabeled, per-fluorinated). By these means the number of initiator fragments per weight of polymer can be measured, and therefore the number of monomer units polymerized by each initiator step may be calculated. This represents one method to determine the mode of termination (see Section 4.11.4.4). The transfer process (see Section 4.4) as a kinetic concept does not change the free-radical concentration, but the chain length of the polymer produced. This holds true when the free-radical generated by transfer has the same reactivity as the radical that is lost. Other reactivities lead to retardation or acceleration, which will be described later (see Section 4.8).

Without changing the free-radical concentration, "normal" chain transfer processes remain hidden in any experiment measuring the rate of polymerization alone (see Section 4.4). The kinetic chain length is also unaffected by the transfer process, because the growing free-radical center generated by the initiation step stays alive after any chain transfer event, although more than one polymer chains are produced. For this reason Eq. (4.46) does not hold true any longer if chain transfer reactions are taken into account. In many kinetic measurements based on the analysis of the molecular weight distributions, transfer processes are neglected and are seen as disturbing factors. However, determination of the chain length distribution of a polymer remains the only possibility of measuring the rate coefficients for transfer processes.

Taking chain transfer into account, the number average degree of polymerization, $\bar{P}_n$, can be described as

$$\bar{P}_n = \frac{\text{total number of polymerized monomer units}}{\text{half the number of formed end groups}} \tag{4.47}$$

The various reactions within the polymerization process generate different amounts of end groups per initiation step:

Initiation	1 end group
Propagation	0 end groups
Transfer	2 end groups
Termination by disproportionation	1 end group
Termination by combination	0 end groups

Again the steady state with its general approximations (see Section 4.6.1) is assumed in which the concentrations of the reactants, such as the monomer, free radicals, and transfer agent, do not vary with time. Hence, in Eq. (4.47) the number of polymerized monomer units can be substituted with the rate of polymerization and the numbers of end groups by the rate of their formation:

$$\bar{P}_n = \frac{R_p}{\frac{1}{2}(R_i + R_{t,d} + 2R_{tr})}$$
(4.48)

Insertion of the simplified rate laws of the different processes

$$\text{Initiation} \qquad R_i = 2fk_d[I] = 2(k_{t,d} + k_{t,c})[R^\bullet]^2 \qquad (4.49)$$
$$\text{Propagation} \qquad R_p = k_p[M][R^\bullet] \qquad (4.50)$$
$$\text{Termination (disproportionation)} \qquad R_{t,d} = 2k_{t,d}[R^\bullet]^2 \qquad (4.51)$$
$$\text{Chain Transfer} \qquad R_{tr} = \sum_k k_{tr}^{T_k}[T_k][R^\bullet] + k_{tr}^M[M][R^\bullet] \qquad (4.52)$$

and subsequent inversion leads to

$$\frac{1}{\bar{P}_n} = \frac{2k_{t,d} + k_{t,c}}{k_p^2[M]^2}R_p + \frac{k_{tr}^M}{k_p} + \sum_k \frac{k_{tr}^{T_k}}{k_p} \cdot \frac{[T_k]}{[M]}$$
(4.53)

where $[T_k]$ is the concentration of any molecule that is capable of taking part in a chain transfer reaction, including solvent S, initiator I, polymer P, and added chain transfer agent T. It is usual to define chain transfer constants C for the different molecules

$$C_M = \frac{k_{tr}^M}{k_p} \quad C_s = \frac{k_{tr}^S}{k_p} \quad C_I = \frac{k_{tr}^I}{k_p} \quad C_P = \frac{k_{tr}^P}{k_p} \quad C_T = \frac{k_{tr}^T}{k_p}$$
(4.54)

Thus Eq. (4.53) becomes

$$\frac{1}{\bar{P}_n} = \frac{2k_{t,d} + k_{t,c}}{k_p^2[M]^2}R_p + C_M + C_s\frac{[S]}{[M]} + C_I\frac{[I]}{[M]} + C_P\frac{[P]}{[M]} + C_T\frac{[T]}{[M]}$$
(4.55)

This equation gives the fundamental correlation of the number average degree of polymerization with the rate of polymerization and the various chain transfer constants. It constitutes the basis for determining the various chain transfer constants (see Section 4.11.3.1).

Performing a polymerization experiment with only low conversion of monomer to polymer, the concentration of polymer is often too low to show significant chain transfer. The same holds true for the initiator, which is used mainly in the range of

low concentrations. Without addition of solvent and additional chain transfer agent, Eq. (4.55) reads, after introduction of Eq. (4.13)

$$\frac{1}{\bar{P}_n} = \frac{(1+\delta)k_t}{k_p^2[M]^2} R_p + C_M \tag{4.56}$$

Hence, a plot of the inverse number average degree of polymerization $\bar{P}_n$ against the rate of polymerization R_p,—the rate of polymerization can easily varied by the concentration of the initiator—yields the monomer chain transfer constant C_M as intercept and the ratio $(1+\delta)k_t/(k_p^2[M]^2)$ as slope of a linear plot. The value of C_M entails an inevitable limit for the maximum number average degree of polymerization, $\bar{P}_n^{max}$. The value for $\bar{P}_n$ is increased by lowering the rate of polymerization R_p according to Eq. (4.56). The limit is reached when R_p becomes zero:

$$\lim_{R_p \to 0} \left(\frac{1}{\bar{P}_n} \right) = C_M \tag{4.57}$$

Hence, the maximum number average degree of polymerization, $\bar{P}_n^{max}$, which is feasible, is given by

$$\bar{P}_n^{max} = C_M^{-1} \tag{4.58}$$

Methyl methacrylate, for instance, has a monomer chain transfer constant of about $C_M = 5 \times 10^{-5}$ at 60°C, leading to a maximal mean chain length of about 20,000, whereas in a free-radical polymerization of vinyl acetate with a monomer chain transfer constant of $C_M = 2 \times 10^{-4}$ at 60°C, the limit is already reached at a number average degree of polymerization of 5000.

4.7.1.2 The Full Chain Length Distribution

So far, only the average degree of polymerization has been considered. To calculate the distribution function itself for a steady-state polymerization it is convenient to chose a statistical approach based on kinetic parameters. A probability factor α of propagation is defined as the probability that a radical will propagate rather than terminate. The factor α is the ratio of the rate of propagation over the sum of the rates of all possible reactions the macroradical can undergo:

$$\alpha = \frac{R_p}{R_p + R_{tr} + R_t} \tag{4.59}$$

First, we assume that termination is solely by disproportionation and that the propagation probability factor is equal for each chain length. The probability for the occurrence of a polymer chain—hence its distribution function—with the length P is given by the probability of $P-1$ propagation steps and the probability of

one chain stopping event (termination *or* transfer):

$$x_{P,d} = \alpha^{P-1}(1-\alpha) \tag{4.60}$$

The molecular weight averages can be evaluated by calculating the moments of this distribution function by insertion of Eq. (4.60) into Eq. (4.39)

$$m^{(0)} = \sum_{P=1}^{\infty} x_{P,d} = 1 \tag{4.61}$$

$$m^{(1)} = \sum_{P=1}^{\infty} P \cdot x_{P,d} = (1-\alpha)^{-1} \tag{4.62}$$

$$m^{(2)} = \sum_{P=1}^{\infty} P^2 \cdot x_{P,d} = (1+\alpha)(1-\alpha)^{-2} \tag{4.63}$$

and subsequent insertion into Eq. (4.40):

$$\bar{P}_{n,d} = \frac{m^{(1)}}{m^{(0)}} = (1-\alpha)^{-1} \qquad \bar{P}_{w,d} = \frac{m^{(2)}}{m^{(1)}} = (1+\alpha)(1-\alpha)^{-1} \tag{4.64}$$

The ratio of the weight average and the number average degree of polymerization, $\bar{P}_w/\bar{P}_n$, describes the polydispersity of a chain length distribution. It becomes unity if all chains have the same length—called a *monodisperse distribution*—and values greater than one, if the distribution exhibits a broader shape:

$$\frac{\bar{P}_{w,d}}{\bar{P}_{n,d}} = \frac{m^{(2)}m^{(0)}}{m^{(1)}m^{(1)}} = 1 + \alpha \tag{4.65}$$

It should be noted that the propagation step must be highly favored over chain stopping events to produce polymers with a significant chain length and the value of α must be near 1. Hence, Eq. (4.65) shows that for a chain length distribution of a polymer produced in a stationary experiment, where chain stopping events are termination by disproportionation or transfer, the polydispersity becomes nearly 2. This holds true for chain length distributions that are controlled by termination via disproportionation and also for distributions where chain transfer is the dominant chain-stopping event. Expressions may also be derived for the chain length distribution produced when the termination process is by combination. The expression for the probability of the occurrence of a chain with the chain length P is now given by the contributions of two chains with the chain length n and m, which form the desired molecule by combination. Hence, the auxiliary condition $n + m = P$ must be valid:

$$x_{P,c} = \sum_{n=1}^{P-1} \alpha^{n-1}(1-\alpha) \cdot \alpha^{m-1}(1-\alpha) = (P-1)\alpha^{P-2}(1-\alpha)^2 \tag{4.66}$$

Evaluating the moments of this distribution function by insertion of Eq. (4.66) into Eq. (4.39) as above

$$m^{(0)} = \sum_{P=1}^{\infty} x_{P,c} = 1 \tag{4.67}$$

$$m^{(1)} = \sum_{P=1}^{\infty} P \cdot x_{P,c} = 2(1-\alpha)^{-1} \tag{4.68}$$

$$m^{(2)} = \sum_{P=1}^{\infty} P^2 \cdot x_{P,c} = (4+2\alpha)(1-\alpha)^{-2} \tag{4.69}$$

leads to

$$\bar{P}_{n,c} = \frac{m^{(1)}}{m^{(0)}} = 2(1-\alpha)^{-1} \qquad \bar{P}_{w,c} = \frac{m^{(2)}}{m^{(1)}} = (2+\alpha)(1-\alpha)^{-1} \tag{4.70}$$

The breadth of the distribution is therefore given by

$$\frac{\bar{P}_{w,c}}{\bar{P}_{n,c}} = \frac{m^{(2)} m^{(0)}}{m^{(1)} m^{(1)}} = 1 + \frac{\alpha}{2} \tag{4.71}$$

Keeping in mind that α has a value close to 1, Eq. (4.71) leads to a polydispersity of 1.5 for a polymer produced in a polymerization process where termination is by combination. The corresponding chain length distribution is somewhat narrower than that generated by disproportionation, because of the statistical coupling of two chains with different sizes.

Almost every polymerization system shows both disproportionation and combination modes. In order to combine the two modes, the general expression for the polydispersity of any given termination controlled chain length distributions reads

$$\frac{\bar{P}_w}{\bar{P}_n} = \frac{1}{2}(3-\delta)(1+\delta) \tag{4.72}$$

Because the value of α is close to 1, the expression $\ln(\alpha) \approx \alpha - 1$ does hold true, leading to $\alpha \approx \exp[-(1-\alpha)]$. With this correlation in mind the combination of Eq. (4.60) with the l.h.s of Eq. (4.64) gives

$$x_P = \frac{1}{\bar{P}_n} \alpha^{P-1} \approx \frac{1}{\bar{P}_n} \exp\left[-\frac{(P-1)}{\bar{P}_n}\right] \approx \frac{1}{\bar{P}_n} \exp\left[-\frac{P}{\bar{P}_n}\right] \tag{4.73}$$

with the factor $(P-1)$ substituted by P, because the chain length P is assumed to be much larger than 1 (i.e., $P \gg 1$). Equation (4.73) demonstrates that the chain length distribution of the polymer formed by disproportionation or chain transfer follows an exponential function in the limit of infinite chain length.

The same calculation procedure, starting with Eq. (4.66), also leads to an exponential expression for the chain length distribution for termination by combination:

$$x_P = \frac{4P}{\bar{P}_n^2} \exp\left[-\frac{2P}{\bar{P}_n}\right]$$ (4.74)

However, Eq. (4.74) has the independent variable, the chain length P, in the preexponential factor, giving the chain length distribution of the polymer formed by combination a different shape.

Evaluation of Eq. (4.59) immediately leads to

$$\alpha = \frac{k_p[M]}{k_p[M] + 2(f\,k_d k_t[I])^{0.5} + k_{tr}[T]}$$ (4.75)

All derived distribution functions and average degrees of polymerization may now be expressed via the kinetic coefficients.

4.7.2 Instationary Polymerization

Calculation of chain length distributions of a polymer formed via an instationary polymerization is reasonable only, if the instationary process is not linked to another polymerization process, such as the pre- and after-effect of a steady state polymerization. One possibility to perform such an uncoupled instationary polymerization is the so-called single-pulse experiment (see Section 4.11.4.1). A single laser pulse produces a free-radical concentration, ρ; the polymerization process is started, and no new free radicals are generated. The kinetic equations for such an experiment can be solved analytically, even if a chain-length-dependent termination rate coefficient is assumed. This is the case, because in such an experiment all macroradicals have the same chain length—within a narrow Poisson distribution and neglecting chain transfer—at any given time. The free-radical concentration formed by the laser pulse, ρ, decays according to the termination rate law expression:

$$-\frac{d[R^\bullet]}{dt} = 2k_t[R^\bullet]^2$$ (4.76)

Assuming a perfect correlation of time and the degree of polymerization, $P = \Theta \cdot t$ with $\Theta = k_p \cdot [M]$, the average frequency of the propagation steps (see Section 4.7.3) and the postulated law for the chain length dependence of k_t, $k_t = k_t^0 \cdot P^{-\alpha}$, Eq. (4.76) can be written as

$$-\frac{d[R^\bullet]}{dt} = 2k_t^0 \cdot \Theta^{-\alpha} \cdot t^{-\alpha} \cdot [R^\bullet]^2$$ (4.77)

Solving this differential equation yields the concentration of free radicals as function of time, whereas ρ is the free-radical concentration at $t = 0$:

$$[R^\bullet]_t = \left(\frac{1}{\rho} + \frac{2k_t^0 \Theta^{-\alpha}}{1 - \alpha} \cdot t^{1-\alpha} \right)^{-1} \tag{4.78}$$

The termination process by disproportionation transforms the living macroradicals in dead polymer chains with exactly the same chain length. This transformation process can be written as

$$-\frac{d[R^\bullet]_t}{dt} = [P_P] \cdot \Theta \tag{4.79}$$

because the loss of free radicals must equal the generation of dead polymer. The factor Θ allows for the transformation of time to chain length. The concentration of dead polymer with chain length P, $[P_P]$, is the chain length distribution in terms of concentrations. Division of $[P_P]$ by the free radical concentration at the beginning, ρ, according to $x_{P,d} = [P_P]/\rho$—with $\sum[P_P] = \rho$—insertion of Eqs. (4.77)–(4.79) and rearrangement yields the number chain length distribution for a single-pulse experiment with termination by disproportionation:

$$x_{P,d} = \frac{2k_t^0 \rho}{\Theta} P^{-\alpha} \left(1 + \frac{2k_t^0 \rho}{(1 - \alpha)\Theta} P^{1-\alpha} \right)^{-2} \tag{4.80}$$

The combination process gives a dead polymer chain with exactly double the chain length of the living macroradical, because all macroradicals have the same size at any given time. The transformation process from time to chain length therefore reads

$$-\frac{d[R^\bullet]_t}{dt} = 4[P_{2P}]\Theta \tag{4.81}$$

Because two free radicals are leading to one dead polymer, $\sum[P_{2P}] = \rho/2$ must hold true. With this in mind and insertion of Eqs. (4.77), (4.78) and, (4.81) and subsequent rearrangement gives the number chain length distribution for a single-pulse experiment with termination by combination:

$$x_{P,c} = \frac{2k_t^0 \rho}{4\Theta} \left(\frac{P}{2} \right)^{-\alpha} \left(1 + \frac{2k_t^0 \rho}{(1 - \alpha)\Theta} \left(\frac{P}{2} \right)^{1-\alpha} \right)^{-2} \tag{4.82}$$

According to the different termination modes the overall number chain length distribution can be calculated via

$$x_P = \frac{2}{1 + \delta} (\delta x_{P,d} + (1 - \delta)x_{P,c}) \tag{4.83}$$

where δ is the contribution of disproportionation to the overall termination process.

4.7.3 Pseudostationary Polymerization

Throughout many decades the pseudostationary polymerization was carried out—mainly with a rotating sector—to measure a ratio of the individual rate coefficients k_p and k_t (see Section 4.6.4) different from that obtained from steady-state experiments. The rate of polymerization was the only measured value, and the chain length distribution of the polymer produced during such an experiment was not evaluated, mainly because of the lack of suitable analytic techniques. The invention and improvement of size-exclusion chromatography paved the way for detailed investigations of the chain length distribution formed throughout a pseudostationary polymerization experiment. This improvement eventually lead to the invention of the pulsed laser polymerization–size-exclusion chromatography (PLP-SEC) method,[59] which turned out to be the best improvement in polymerization kinetic measurements long since. This technique allows for the direct measurement of the individual propagation rate coefficient k_p.

The principle of the pulsed laser technique is simple but ingenious. A monomer/photoinitiator mixture is irradiated by a pulsed laser beam. Each laser flash generates free radicals that initiate a polymerization process. No new free radicals are formed during the dark time periods. All growing macroradicals formed by one specific laser pulse have the same chain length within a narrow Poisson distribution. As the free-radical concentration decreases due to termination processes, the rate of termination decreases according to Eq. (4.12), too. After the dark period, t_0, the next laser flash irradiates the system and instantaneously increases the free-radical concentration. Hence, the termination rate is suddenly highly increased, too, leading to a significant amount of dead polymer with the chain length L_0 where L_0 is the chain length of a macroradical that grew for one dark time period, t_0. Taking into account that the radicals have a certain probability to survive the laser flash and to terminate at any later pulse, the relative concentration of polymer with the chain lengths $2L_0$, $3L_0, \ldots$ is increased, too. The described polymerization conditions therefore produce a well-structured chain length distribution with additional peaks at the chain length of L_0 and its multiples. The radicals that are formed at the laser pulse are very small. The mode of termination is therefore not overly important for the formation of the additional peaks of the chain length distribution.

Assuming a low conversion of monomer to polymer, the monomer concentration can be expected to be constant. The propagation rate coefficient and the monomer concentration can therefore be combined into a new rate coefficient, $\tilde{k}_p = k_p[M]$, which is associated with the following pseudo first-order rate law:

$$R_p = \tilde{k}_p[R^\bullet] \qquad \text{with} \qquad \tilde{k}_p = k_p[M] \tag{4.84}$$

The average timespan between two first-order reaction steps, τ, is given by

$$\tau = k^{-1} \tag{4.85}$$

where k is the first-order rate coefficient. Insertion of Eq. (4.84) into Eq. (4.85) yields the time of an average propagation step τ_p, assuming that the monomer concentration is constant:

$$\tau_p = \frac{1}{\tilde{k}_p} = \frac{1}{k_p[M]} \tag{4.86}$$

The chain length $L_{0,n}$ of a macroradical that grows n laser periods, $n \cdot t_0$, is now easily correlated with the propagation rate coefficient, k_p:

$$L_{0,n} = nk_p[M]t_0 \tag{4.87}$$

The evaluation of the additional peaks occurring in the chain length distribution of a pulsed laser polymerization experiment and the corresponding values of $L_{0,n}$ by means of size exclusion chromatography enables the calculation of k_p, because the monomer concentration and the laser frequency are known.

Because of the statistical process of the chain growth, the macroradicals produced by the same laser pulse do not exhibit the same chain length at any given time, but rather show a narrow Poisson distribution where L is the mean value

$$x_P = e^{-L}\frac{L^P}{P!} \tag{4.88}$$

The theoretical chain length distribution is therefore subject to a broadening, losing its discontinuities (see Fig. 4.8b). It turned out that the inflection point on the low-molecular-weight side of the additional peak is in most cases the best measure for the real value of L_0.[60] Only at the so-called high termination limit, where the free-radical concentration produced by each laser pulse is extremely high, may the maximum of the additional peak be a better choice.[61] However, second or higher points of inflection can often be evaluated, even when there is no peak maximum visible. In
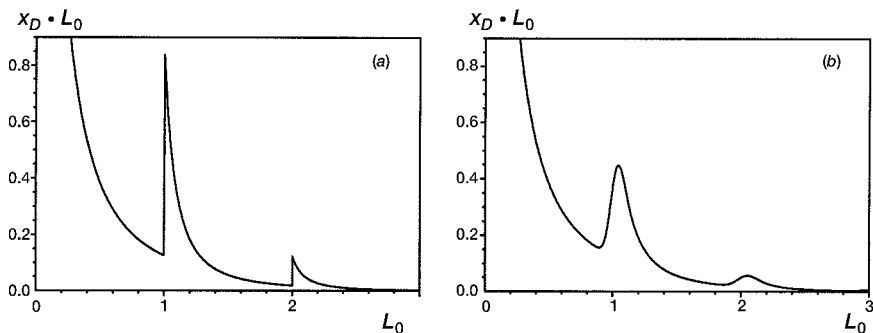
Figure 4.8   Simulated and normalized number distribution for a pulsed laser experiment with termination exclusively via disproportionation (a) without and (b) with Poisson broadening.

addition, for a point of second order, the inflection point is less affected by baseline errors occurring during the size-exclusion chromatography.

Analytic solutions for the chain length distribution generated by pulsed laser polymerization[62] are very complex, even in their simplest form, assuming no Poisson distribution, no transfer, and no initiation process during the dark time period. The chain length distribution for assuming a strict coupling of time and degree of polymerization for termination by disproportionation can be written as

$$x_{P,d}^{(n)} = \rho \left(\frac{\tilde{C}}{L_0} \cdot \left[1 + \frac{\tilde{C}}{L_0} \cdot (P - nL_0) \right]^{-2} \cdot (1 + \tilde{C})^{-n} \right) \tag{4.89}$$

$$0 \leq P \leq L_0 \qquad\qquad \text{for } n = 0$$
$$nL_0 < P \leq (n+1)L_0 \quad \text{for } n = 1, 2, 3 \ldots$$

with the definitions

$$\tilde{C} = C \cdot \frac{[R_+^{\bullet}]}{\rho} \tag{4.90}$$

$$C = 2\rho k_t t_0 \tag{4.91}$$

$$L_0 = k_p [M] t_0 \tag{4.92}$$

The value C is especially important, because it governs the overall shape of the chain length distribution. A typical value of C is 0.5–10, whereas higher values of C yield more pronounced first additional peaks (high termination limit). The shape of a PLP distribution can be (in principle) held constant by balancing the product of the laser period, t_0, and the free-radical concentration produced by each laser pulse, ρ, to give constant values of C. It should be noted that the extra peaks are the sharper the greater the value for L_0.

The expression for the chain length distribution for termination by combination reads

$$x_{P,c}^{(n)} = \rho \left(n(1 + \tilde{C})^{-n+1} \cdot \frac{\hat{x}_{P-(n-1)L_0,c}}{\rho} + (n+1)(1 + \tilde{C})^{-n} \cdot \frac{\hat{x}_{P-nL_0,c}}{\rho} \right) \tag{4.93}$$

with

$$\hat{x}_{P,c} = \frac{\rho}{2} \cdot \frac{C}{2L_0} \cdot \left(1 + \tilde{C}\frac{P}{2L_0} \right)^{-2} \tag{4.94}$$

The statistical moments of the chain length distribution in the long chain limit can be calculated by insertion of Eqs. (4.89) and (4.93) into Eq. (4.39). For termination by

disproportionation

$$m_d^{(0)} = \rho \tag{4.95}$$

$$m_d^{(1)} = \rho \left(L_0 \cdot \frac{\ln(1 + \tilde{C})}{C} \right) \tag{4.96}$$

$$m_d^{(2)} = \rho \left(2L_0 \cdot \frac{L_0}{C} \right) \tag{4.97}$$

For termination by combination

$$m_c^{(0)} = \frac{\rho}{2} \tag{4.98}$$

$$m_c^{(1)} = \rho \left(L_0 \cdot \frac{\ln(1 + \tilde{C})}{C} \right) \tag{4.99}$$

$$m_c^{(2)} = \rho \left(3L_0 \cdot \frac{L_0}{C} \right) \tag{4.100}$$

The number and weight average degree of polymerization can be calculated via combination of these moments according to Eq. (4.40). For termination by disproportionation

$$\bar{P}_{n,d} = L_0 \cdot \frac{\ln(1 + \tilde{C})}{C} \tag{4.101}$$

$$\bar{P}_{w,d} = 2L_0 \cdot \frac{1}{\ln(1 + \tilde{C})} \tag{4.102}$$

For termination by combination

$$\bar{P}_{n,c} = 2L_0 \cdot \frac{\ln(1 + \tilde{C})}{C} \tag{4.103}$$

$$\bar{P}_{w,d} = 3L_0 \cdot \frac{1}{\ln(1 + \tilde{C})} \tag{4.104}$$

The polydispersity of the chain length distribution of a polymer produced via a pulsed laser experiment for disproportionation reads

$$\frac{\bar{P}_{w,d}}{\bar{P}_{n,d}} = 2 \frac{C}{(\ln(1 + \tilde{C}))^2} \tag{4.105}$$

and for combination

$$\frac{\bar{P}_{w,c}}{\bar{P}_{n,c}} = \frac{3}{2} \cdot \frac{C}{(\ln(1 + \tilde{C}))^2} \tag{4.106}$$

As can be easily seen, the breadth of the PLP distribution is dependent not only on the termination mode, as this is the case for steady state experiments. The polydispersity is additionally controlled by the polymerization conditions such as initiator concentration and laser intensity, which both influence the value of the free-radical concentration which is produced at each laser flash, ρ. The polydispersity is also different for different pulse periods, t_0.

4.8   INHIBITION AND RETARDATION

The chain transfer process stops the chain growth process via abstraction of a hydrogen atom or some other species from another molecule. This molecule itself becomes a radical, capable of reinitiating polymerization. If the reactivity of the generated radical toward the monomer is on the order of that of the macroradical, and if the time necessary for the chain transfer process is within the range of one propagation step, "normal" chain transfer occurs. This normal or conventional chain transfer does not lead to any change in the polymerization rate (see Section 4.4). However, a generalized view of this reaction type makes the concepts of retardation and inhibition necessary. If the generated radical is less reactive than the propagating radical, *retardation* takes place, which is characterized by a decrease in the rate of polymerization. If the retardation is very effective, the polymerization process is completely suppressed and this is referred to as *inhibition*. Inhibition leads to an induction period where no polymerization takes place at all, until the inhibitor is completely consumed. The reaction then starts with the normal rate of polymerization. The kinetics of the retardation effect for a stationary polymerization can be analyzed by adding an additional reaction to the common scheme of polymerization, including initiation, propagation, and termination:

$$R_i^{\bullet} + Q \xrightarrow{k_Q} P_i + Q^{\bullet} \tag{4.107}$$

where Q is the retarder or inhibitor and k_Q is the rate coefficient of the retardation reaction.

The kinetics are simplified by assuming that the generated radical, $Q^{\bullet}$, neither reinitiates nor show any transfer behavior. There are other models that allow for reinitiation of $Q^{\bullet}$. The steady-state assumption—which is only a very rough approximation until all inhibitor is consumed[63]—can now be written as

$$-\frac{d[R^{\bullet}]}{dt} = R_i - 2k_t[R^{\bullet}]^2 - k_Q[R^{\bullet}][Q] = 0 \tag{4.108}$$

which yields in combination with Eq. (4.19), again assuming that the rate of the loss of monomer, $-d[M]/dt$, equals the rate of polymerization, R_p:

$$R_i - \frac{2k_t R_p^2}{k_p^2[M]^2} - \frac{k_Q R_p[Q]}{k_p[M]} = 0 \tag{4.109}$$

TABLE 4.9   Inhibition Constants, z, of Various Inhibitors to Selected Monomers at 50°C

Inhibitor	Monomer	z
Nitrobenzene	Methyl acrylate	0.00464
	Styrene	0.326
	Vinyl acetate	11.2
1,3,5-Trinitrobenzene	Methyl acrylate	0.204
	Styrene	64.2
	Vinyl acetate	404
Chloranil	Methyl methacrylate (44°C)	0.26
	Styrene	2040
Oxygen	Methyl methacrylate	33000
	Styrene	14600
Phenol	Methyl acrylate	0.0002
	Vinyl acetate	0.012
TEMPO	Styrene	335712 [a]

Source: Data from A. Brandrup, E. H. Immergut, and E. A. Grulke, *Polymer Handbook*, 4th ed., Wiley, 1999.
[a] D. Ereszta and K. Matyjaszewski, *Macromolecules* **29,** 7661 (1996).

The ratio of the rate coefficients for retardation, k_Q, and propagtion, k_p, is often referred to as the *inhibition constant*, $z = k_Q/k_p$, which reflects the ability of a molecule to cause inhibition. Table 4.9 gives selected values for the inhibitor constants of some inhibitors in conjunction with a specific monomer.

If the inhibition constant is large ($z \gg 1$), the second term of the l.h.s. of Eq. (4.109) will become much smaller than the third one. In this case, the rate of inhibition is much larger than the rate of termination. Equation (4.109) then reads

$$R_p = \frac{k_p[M]R_i}{k_Q[Q]} \tag{4.110}$$

This equation (4.110) shows that the polymerization rate is inversely proportional to the inhibitor concentration. It should be kept in mind that the inhibitor concentration will decrease during the reaction. Each free radical generated by the initiation process will consume one inhibitor molecule. If the inhibitor concentration finally becomes sufficiently low, propagation can become competitive with the inhibition reaction. Dividing the rate law for the loss of inhibitor, $-d[Q]/dt = k_Q[R^\bullet][Q]$, by the rate law of propagation, $-d[M]/dt = k_p[R^\bullet][M]$, leads to

$$\frac{d[Q]}{d[M]} = \frac{z[Q]}{[M]} \tag{4.111}$$

and subsequent integration where $[Q]_0$ and $[M]_0$ are the concentration of inhibitor and monomer at the beginning of the reaction:

$$\ln\left(\frac{[Q]}{[Q]_0}\right) = z \cdot \ln\left(\frac{[M]}{[M]_0}\right) \tag{4.112}$$

It is apparent from this equation that, if z is large, the monomer conversion remains nearly zero until the inhibitor is consumed.

A special type of inhibitors are stable free radicals, like nitroxides such as 2,2,6,6-tetramethylpiperidine-1-oxyl (TEMPO). They are far too stable to be able to initiate polymerization, but they are reactive enough to undergo reaction with other free radicals. These compounds are not a special type of chain transfer agent, because the reaction product is not a radical. Nitroxides are very efficient inhibitors, capable of producing induction periods when present in concentrations of less than 10^{-4} mol/L. The stoichiometry between the number of the chains terminated and the number of the nitroxide molecules consumed is 1 : 1, making these compounds very useful for quantitative measurements of free-radical concentrations.[57] The coupling process of the nitroxide with the propagating radical is reversible, especially at elevated temperatures. This equilibrium enables a living free-radical polymerization by capping the reactive chain ends. The free-radical concentration is therefore extremely decreased, suppressing the termination process. Temporarily uncapped free radicals are adding monomer leading to a very slow but controlled polymerization process.

4.9   DEPROPAGATION

Especially at elevated temperatures the propagation step can no longer be considered irreversible. The propagation step is in fact reversible, leading to a thermodynamic equilibrium. This equilibrium can be described by the magnitude of the free-energy difference, ΔG, between the polymer and the monomer. The polymerization process is thermodynamically favored if ΔG is negative. The value of the free-energy difference is given by the following fundamental equation:

$$\Delta G = \Delta H - T\Delta S \tag{4.113}$$

The polymerization heats, ΔH, of most free-radical polymerizations are negative with typical values ranging from -30 to -80 kJ/mol. The values for the polymerization entropies are negative, too, reflecting the loss of degrees of freedom of the monomer becoming a part of the polymer chain. Typical values for the polymerization entropies are -100 to -120 J K^{-1} mol^{-1}. Hence, the two terms on the r.h.s. of Eq. (4.113) are antagonistic. Under normal temperature conditions, the exothermicity of the reaction exceeds the entropic term and ΔG becomes negative. However, at elevated temperatures the entropic term becomes significantly larger and finally equals the enthalpic term at the so-called ceiling temperature, $T_c = \Delta H/\Delta S$. At this temperature the free-energy difference is zero, and no polymerization process occurs.

The kinetic interpretation of this effect describes the propagation step as reversible with a propagation and depropagation step:

$$R_i^{\bullet} + M \xrightarrow{k_p} R_{i+1}^{\bullet} \tag{4.114}$$

$$R_{i+1}^{\bullet} \xrightarrow{k_{dp}} R_i^{\bullet} + M \tag{4.115}$$

The rate coefficient of depropagation is written as k_{pd}.

For many typical free-radical polymerization systems and conditions, depropagation does not occur to any appreciable extent. However, for some 1,1-disubstituted ethylene monomers, it is possible to polymerize at conditions where the effects of the reverse reaction cannot be neglected. The classic example of such a monomer is α-methylstyrene (AMS), with a bulk monomer ceiling temperature of 60°C. Methacrylate and styrene monomers also exhibit depropagation, although at much higher temperatures (220 and 310°C, respectively, for bulk polymerizations). The depropagation process lowers the rate of polymerization according to

$$R_p = k_p[M][R^\bullet] - k_{dp}[R^\bullet] = \left(k_p - \frac{k_{dp}}{[M]}\right)[M][R^\bullet] = k_p^{eff}[M][R^\bullet] \tag{4.116}$$

The effective rate coefficient of propagation is therefore defined as

$$k_p^{eff} = k_p - \frac{k_{dp}}{[M]} \tag{4.117}$$

The depropagation effect is inversely proportional to the monomer concentration because it is part of the thermodynamic equilibrium. The effective propagation rate coefficient can be determined via the pulsed laser polymerization—size-exclusion method (see Section 4.11.2.1). Figure 4.9 shows the deviation of k_p^{eff} from the
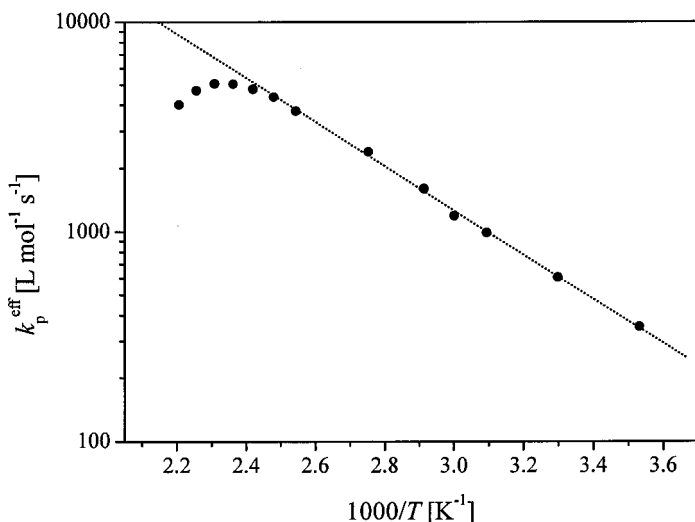
Figure 4.9   Temperature dependence of the effective propagation rate coefficient, k_p^{eff}, observed in the bulk polymerization of dodecyl methacrylate (DMA). The data are taken from R. A. Hutchinson, D. A. Paquet, Jr., S. Beuermann, and J. H. McMinn, *Ind. Eng. Chem. Res.* **37**, 3567 (1998).

linear slope of an Arrhenius plot at higher temperatures, where depropagation becomes important.[64]

The kinetic expression for the equilibrium constant, K, is the ratio of the rate coefficient of the forward reaction to the rate coefficient of the backward reaction. This can be set equal to the thermodynamical definition of K:

$$K = \frac{\vec{k}}{\overleftarrow{k}} = \frac{k_p}{k_{dp}} = \frac{[R^{\bullet}_{i+1}]}{[R^{\bullet}_i][M]_e} = \frac{1}{[M]_e} \tag{4.118}$$

where $[M]_e$ is the equilibrium monomer concentration (e.g., 10^{-6} mol/L for styrene at 25°C) By combining Eqs. (4.117) and (4.118) it can be seen that when the monomer concentration equals the equilibrium monomer concentration, the effective propagation rate coefficient, k_p^{eff}, becomes zero, which is the definition for the ceiling temperature. This implies that there exists a specific ceiling temperature for every given monomer concentration. The maximum ceiling temperature is reached for the bulk polymerization system. It has been recently demonstrated that effective molecular weight control in copolymerizations may be achieved by the judicious selection of monomers that display a low ceiling temperature.[65]

4.10   RING-OPENING POLYMERIZATION

Studies on the kinetics of ring-opening polymerizations are quite limited, and there is a paucity of data on values for absolute rate coefficients in these types of reactions. Radical ring-opening monomers may be codified according to the position of the double bond relative to the ring: vinyl, and exomethylene. The polymerizations proceed by two contiguous reactions whereby radical addition to the double bond occurs to form a ring-closed radical followed by a ring-opening isomerization to generate the propagating ring-opened radicals. This is shown in Fig. 4.10.

The relative magnitudes of k_b and k_p determine the extent of ring-opening polymerization at any given temperature. Moad and Solomon[34] have tabulated ring opening coefficients for a variety of monomers. Clearly, thermodynamics play an important role in the ring-opening process. Unfortunately it is very difficult to access k_b and k_p individually in polymerization reactions. Two attempts have been made to evaluate k_p using pulsed laser polymerization.[66] However, in both cases, chain transfer reactions were shown to play an important role in the overall kinetics, and this confounded accurate analysis of the data.

The kinetics of steady state ring-opening polymerizations can be easily analyzed.[67] The treatment is simpler if 100% ring opening can be assumed, leading to the following rate expression:

$$R_p = \left(\frac{f k_d [I]}{k_t}\right)^{0.5} \left(\frac{1}{k_\beta} + \frac{1}{k_p[M]}\right)^{-1} \tag{4.119}$$

Vinyl type
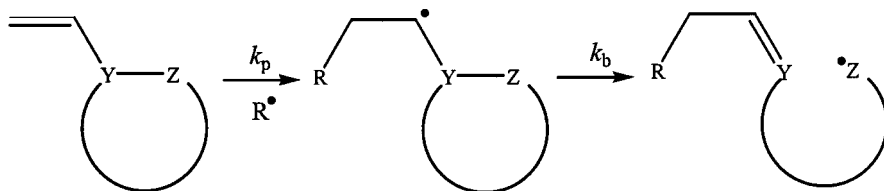
exo-methylene type
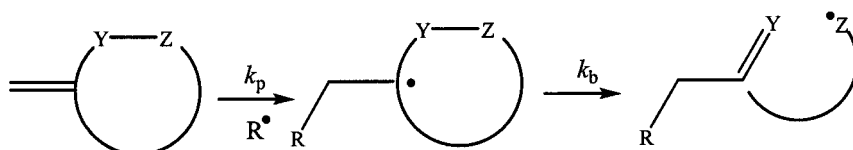
Figure 4.10

In the most recent works an extensive study was reported on chain transfer reactions in the sulfur-centered free-radical ring-opening polymerization of 3-methylene-6-methyl-1,5-dithiacyclooctane.[68] (See also Scheme 4.12.) The work showed significant differences in chain transfer activity between carbon- and sulfur-centered radicals. Currently there are very little kinetic data available on chain transfer or termination reactions in radical ring-opening polymerizations.
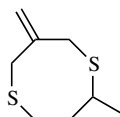
Scheme 4.12

4.11   EXPERIMENTAL METHODS

The aim of most kinetic experimental methods has always been to determine accurate values for the individual rate coefficients that govern the free-radical polymerization process, especially k_t, k_p, and k_{tr}. Up to the late 1980s termination and propagation rate coefficients were accessible only in their coupled form, $k_p/k_t^{0.5}$, or individually via combination with pseudo flickering techniques like the rotating sector or spatially intermittent polymerization methods in combination with stationary polymerization measurements (see Section 4.6.3). The only exception has been

the direct determination of the propagation rate coefficient via the measurement of the steady-state free-radical concentration by electron spin resonance (ESR) experiments in combination with rate measurements. However, the detection of such low free-radical concentrations (typically close to 10^{-8} mol/L) has always been subject to large uncertainties, leading to a large scatter in the values for the rate coefficients. The situation has dramatically improved with the invention of the pulsed laser polymerization (PLP) technique in the late 1980s. Since then, this technique [and its spinoffs such as single pulse–pulsed laser polymerization (SP-PLP)] has been extensively used to collate propagation and termination rate coefficients for various homo- and copolymerizations. Today, the PLP method is used almost exclusively to determine propagation and termination rate coefficients and has been recommended by the *Union of Pure and Applied Chemistry* (IUPAC) for the measurement of propagation rate coefficients. In contrast, the methods available for the determination of the chain transfer rate coefficient have not changed significantly. It should, however, be mentioned that the interpretation of the transfer controlled molecular weight distributions generated in stationary free-radical polymerizations have been somewhat refined with introduction of the Clay–Gilbert method (for details, see Section 4.11.3.2).

4.11.1 Methods for the Measurement of k_d

4.11.1.1 Direct Measurement of the Initiator Concentration as a Function of Time
The rate coefficients of initiator decomposition, k_d, can be assessed by various methods. A straightforward approach is to directly assess the thermal decay of the initiator via the measurement of its concentration as a function of the reaction time by Eq. (4.3). The concentration can be measured via any quantity to which it is directly proportional, such as a spectroscopic infrared absorption that can be easily followed with reaction time. The connectivity of the initiator concentration and the intensity of the absorption (at a specific wavelength) is given by the Beer–Lambert law. Infrared spectroscopy has been used extensively in the past to study the decay of organic peroxides in various reaction media (including supercritical CO_2). Organic peroxides are widely used to initiate polymerizations, and knowledge about their rate of decomposition at various temperatures and their mechanism of decomposition is vital for optimizing polymerization processes.[69]

4.11.1.2 Dead-End Polymerization
Dead-end polymerization refers to a polymerization process where the initiator concentration significantly decreases to a very low value during the polymerization (see Section 4.6.2). Measurement of the conversion of monomer to polymer, p, according to such an experiment, allows one to determine for the rate coefficient of initiator decomposition k_d, and for the calculation of the efficiency factor, f. Dividing of Eq. (4.23) by Eq. (4.24), rearranging and subsequently taking the logarithms of both sides yields

$$-\ln\left[1 - \frac{\ln(1-p)}{\ln(1-p_\infty)}\right] = \frac{k_d t}{2} \tag{4.120}$$

The value of k_d can now be easily evaluated from a slope of a plot of the l.h.s. of Eq. (4.120) against the polymerization time t. If the ratio of k_p^2/k_t is known from other studies, a value for the frequency factor f can be estimated by insertion into Eq. (4.20) or (4.24).

4.11.2   Methods for the Measurement of k_p

The determination of propagation rate coefficients was revolutionized in the late 1980s by introduction of the pulsed laser polymerization-size exclusion chromatography (PLP-SEC) method by Olaj and co-workers.[59]

4.11.2.1   *Pulsed Laser Polymerization–Size-Exclusion Chromatography (PLP-SEC)*   The careful determination of the chain length distribution of the polymer produced via a pseudostationary pulsed laser experiment allows one to obtain accurate values for the propagation rate coefficient, k_p. The polymerizable system—containing monomer and photoinitiator, occasionally solvent and transfer agents—is irradiated by a pulsed laser beam, and the chain length distribution formed is subsequently analyzed by size-exclusion chromatography. The determination of the additional peaks (see Section 4.7.3) and its points of inflection on the low-molecular-weight side, respectively, gives a value for $L_{0,n}$ that can be easily inserted into

$$L_{0,n} = nk_p[M]t_0 \tag{4.87}$$

The propagation rate coefficient k_p is now available because the monomer concentration [M] and the time interval between laser pulses, t_0, are known. This method has developed into the IUPAC recommended method for k_p determination.[70]

   Prior to the PLP experiment, the monomer should be purified to remove the stabilizer that is added to most of the commercially available monomers. This can be achieved by either distillation or column chromatography. Both methods have different advantages—distillation removes small amounts of polymer dissolved in the monomer, but many inhibitors are very volatile and distillation does not completely remove them. However, PLP experiments without cleaning the monomer were reported and have shown the robustness of this method. Photoinitiators are added in typical concentrations of mmol/L. Degassing the samples by a number of freeze–pump–thaw cycles on a high vacuum line or purging with inert gases such as nitrogen or argon makes sure that the dissolved oxygen, which disturbs the kinetic measurements by an inhibition effect, is removed.

   For a successful PLP experiment, care must be taken to ensure a homogeneous intensity profile over the whole optical cross section of the reaction cell to produce homogenous reaction conditions. In addition, absorption of the laser light by initiator and monomer molecules should be accounted for. Accurate temperature control is necessary to dissipate the heat of reaction and any possible temperature increase induced by absorbed laser energy. Typical laser sources are pulsed Nd:YAG solid state lasers (355 or 532 nm) or XeF excimer lasers (351 nm) with a pulse energy of $\leq$80 mJ/pulse and a pulse width of 5–20 ns. Laser repetition rates between 100

and 0.1 Hz have been used in the past. The value of ρ (i.e., the free-radical concentration generated by each laser pulse) can be varied by the initiator concentration and the laser pulse energy. Samples are exposed to pulsed laser irradiation to allow for a maximum conversion of monomer to polymer of about 1–3%, with typical pulsing times between 1 min and 5 h. It should be noted that a pulsed lamp or even a rotating sector in combination with a continuous lamp as a pulsed radiation source leads to well-structured molecular weight distributions allowing for the determination of k_p. However, optimum results are obtained by the use of a pulsed laser.

After the monomer solution has been irradiated, the produced polymer is analyzed by a size-exclusion chromatography system, which is calibrated by narrow polymer standards or by absolute molecular weight detection methods. The values of $L_{0,n}$ can be easily determined by differentiating the chain length distribution. The use of different types of distribution (size exclusion, mass, or number distribution) leads to slightly different values for k_p. Figure 4.11 shows a typical data sheet for styrene bulk polymerization.

4.11.2.2 Electron Spin Resonance Spectroscopy–Stationary Polymerization (ESR)   The experimental determination of k_p data usually proceeds via the
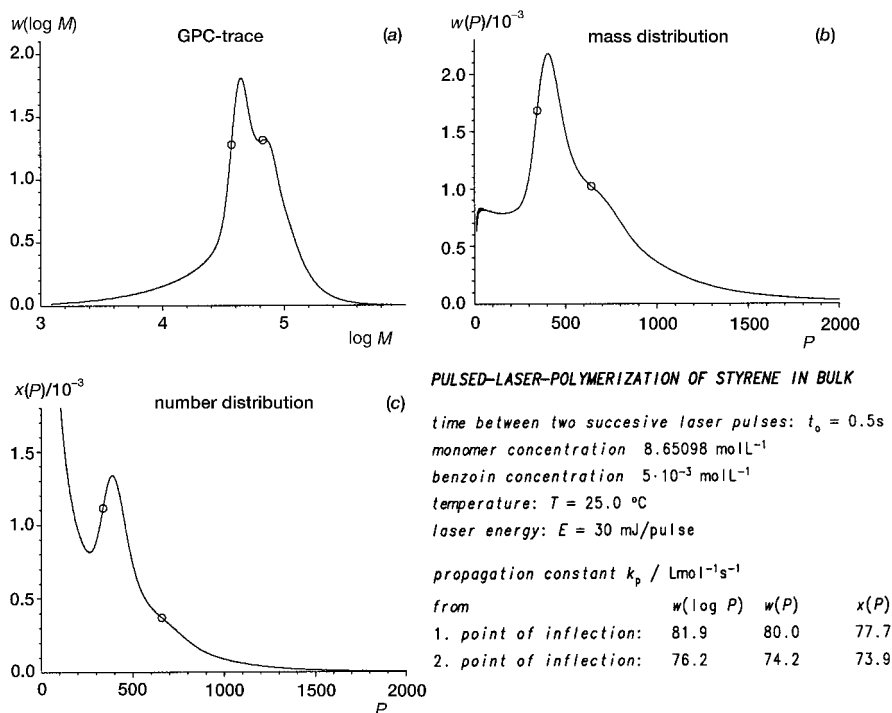
Figure 4.11   Typical data sheet detailing the outcome of a successful PLP-SEC experiment for a styrene bulk polymerization at 25°C.

IUPAC-recommended PLP-SEC procedure (see discussion above). However, under certain circumstances, k_p data are also available by direct determination of the concentration of propagating free radicals via electron spin resonance (ESR) spectroscopy accompanied by the measurement of the overall polymerization rate. The calculation of k_p then proceeds via either the differential [Eq. (4.19)] or the integrated form of the propagation rate law expression:

$$\ln \frac{[M]_2}{[M]_1} = k_p \cdot [R^\bullet] \cdot (t_1 - t_2) \qquad (4.121)$$

where $[M]_1$ and $[M]_2$ are the monomer concentrations at the reaction times t_1 and t_2, respectively. Determination of the monomer conversion at various reaction times can proceed via independent experiments (under the same experimental conditions as the ESR measurements) using, for example, NMR spectroscopy, infrared spectroscopy, gravimetry, or chromatographic methods.

Inspection of the existing literature indicates that k_p values derived from ESR are in poor agreement with k_p data from PLP-SEC measurement.[71–74] Only a few studies indicate a somewhat better agreement,[75,76] which is due partly to a significant increase in the quality of the ESR signals by using optimized ESR cavities and spectrometers.[77] The studies indicating better agreement seem to have been carried out under specific experimental conditions, allowing for a reliable measurement of the long-chain limit of the propagation rate coefficient. These studies indicate that particular attention needs to be paid to the size of the steady-state free-radical concentration, which should be in an intermediate range. The type of initiator also seems to be important, as is the fact that the only free-radical in the system is the propagating species. This point is of special importance in photochemically induced polymerizations, where, in addition to the photoinitiator, the monomer may also be excited. Furthermore, the experimental conditions must be such that the majority of propagating radicals are of sufficiently large size to avoid determination of untypically high-propagation-rate coefficients, which are known to occur with free radicals of short chain lengths. Because of this limitation, studies into higher k_p monomers may be advantageous (unless polymerization rates become too fast to allow precise determination of monomer conversion–time profiles). Moreover, it should be verified whether high-molecular-weight material is indeed produced. A specific problem of ESR spectroscopy is calibration of the spectrometer. Usually, calibration proceeds via the measurement of the signal of a known concentration of a stable radical [e.g., 2,2,6,6- tetramethylpiperidine-1-oxyl (TEMPO)] in the same medium in which the polymerization is carried out. The calibration may be the most serious drawback of the ESR method for k_p determination, since (1) it is very likely that the two different radicals—the radical used for calibration purposes and the propagating radical—are not comparable in terms of their detector signal and (2) the calibration is—strictly speaking—valid only for the hypothetical case of 0% conversion and is immediately invalidated as the polymerization process changes the bulk viscosity of the reaction medium. It should also be noted that—similar to the PLP-SEC technique—only the product of the propagation rate coefficient and the monomer concentration is the

measured quantity. To this date, no technique exists that allows the direct measurement of k_p.

With these problems kept in mind, the ESR technique remains problematic for the reliable determination of propagation rate coefficients and may be applicable in only very specific cases. However, the ESR technique also has the indisputable advantage of actually probing the propagating radicals directly and—in contrast to the PLP-SEC method—does not rely on the interpretation of secondary data material such as a molecular weight distribution. Valuable insight into the polymerization process, particularly at high conversion rates, has been deduced from ESR spectra recorded at different monomer conversions.

It should be briefly mentioned that the ESR technique may [via Eq. (4.29)] also be applied toward the measurement of termination rate coefficients. There are several publications reporting on the k_t measurements via ESR. However, these measurements are associated with same problems as the k_p determinations (for examples, see Refs. 78–80).

4.11.2.3 Quenched Instationary Polymerization Systems (QUIPS)

Quenched instationary polymerization systems[81] are characterized by the complete deactivation of all radicals by reaction with an inhibitor after a certain time. A photopolymerizable mixture passes through a capillary system, is irradiated at a specific location, and polymerizes in the capillary during a well-defined dark period until it drops into a quenching bath. The parameters determining the type of QUIPS are the duration of the initiation period (t_L) and an eventually following dark period (t_D). The method is based on the intentional limitation of the maximum active chain length $L_{act,max}$ that the radicals can achieve. For this purpose all radicals present at a certain time in the system are deactivated by reaction with an inhibitor. Therefore, the kinetic scheme for the free-radical polymerization is extended by the quench reaction with the rate constant k_q. A number of stable free radicals are known to fulfill the conditions of an extremely fast and efficient quench reaction (e.g., nitroxyl radicals below $100°C$). It is essential that the products of the quench reaction be stable and not be mediators for consecutive reactions. Experimental conditions can be chosen to ensure that the quench reaction is complete within the timespan necessary for an ordinary propagation step, namely, $1/(k_p[M])$. Under these conditions the radical spectrum present at the beginning of (the short) quench period is immediately converted into inactive products. Measuring the chain length distribution by size-exclusion chromatography reveals a structured shape that allows determination of k_p in accordance with the same equation as Eq. (4.87) used in PLP-SEC, which relates the active lifetime of a growing macroradical to its maximum active chain length.

4.11.3 Methods for the Measurement of k_{tr}

The evaluation procedures and theoretical basis for the determination of transfer constants, C, have been extended and perfected since the early 1990s, and a great number of transfer constants have been determined by various research groups (for examples, see Refs. 82 and 83 or the multiple entries in the *Polymer Handbook*[84]).

The transfer constant is defined by Eq. (4.54) as the ratio of the transfer rate coefficient, k_{tr}, to the propagation rate coefficient, k_p:

$$C = \frac{k_{tr}}{k_p} \qquad (4.122)$$

The standard procedure for transfer constant measurement (to the monomer itself, any other added substance or deliberately added transfer agent, such as a thiol or a catalytic chain transfer agent) has always been the Mayo method.[85] However, Gilbert has introduced the chain length distribution (CLD) method[86] as an alternative way to determine transfer constants. The Mayo and CLD methods in themselves also provide different choices of data analysis. Both methods have been carefully compared and thoroughly discussed with the conclusion that both are theoretically equivalent.[87]

In terms of applied experimental procedures, there are only two conceptually different methods available. The first one is the conventional or typical polymerization via thermal polymerization experiments with specific amounts of thermally decaying initiator present in the reaction mixture. Various groups have used this technique to determine transfer constants as the impressive collection of data in Ref. 84 indicates. Kukulj et al.,[88] for example, investigated the transfer to monomer constant of methyl methacrylate (MMA), styrene, and α-methyl styrene (AMS) at 50°C using thermal polymerization. To generate a sufficiently low radical flux to achieve transfer-dominated reaction conditions, the stock solution of the initiator in the monomer is successively diluted. This gives a series of solutions with decreasing initiator concentrations yielding increasing molecular weights on polymerization. In many cases and when the initiator concentrations are chosen correctly, a limiting molecular weight is reached, which may then be used to determine the transfer to monomer constant via either the Mayo or the CLD method.

A second and more recent experimental technique became possible with the advent of pulsed laser systems: pulsed laser polymerization (PLP) in combination with subsequent size-exclusion chromatography (SEC) of the resulting polymer is the standard and IUPAC-recommended technique for determination of propagation rate coefficients, k_p.[70] However, several research groups have used PLP to determine transfer rate constants to a range of chain transfer agents. For example, Hutchinson and co-workers[89] determined the transfer coefficients for transfer to n-dodecyl mercaptan in methyl methacrylate (MMA), styrene, ethyl methacrylate (EMA), and butyl methacrylate (BMA) homopolymerizations in the temperature range between 20 and 80°C. By adding sufficient transfer agent, these authors were able to generate transfer-dominated conditions, as seen by the loss of the PLP characteristics in the molecular weight distributions (MWDs) obtained by SEC analysis of the polymers. In addition, Buback and co-workers[90] designed a method to determine the value of the propagation rate coefficient, k_p, and the transfer to monomer rate coefficient (k_{tr}^M) from a single PLP experiment. Packages of high-frequency pulses separated by long dark time intervals gave rise to two polymer distributions. This procedure has been termed the "railroad" experiment, due to the characteristic pulse profile of the light

source that resembles the sounds pattern generated by a moving train. The polymer produced during the high-frequency pulse packages may be used to determine k_p, while the polymer produced in the longer dark time may be used to determine C_M.[90,91]

Pulsed laser polymerization, however, is seldom the method of choice for measuring transfer to monomer rate coefficients via the CLD method, because the CLD method requires termination to be an unimportant or even absent route of radical chain stoppage as compared to transfer to monomer. In addition, the CLD method is, like the Mayo method, derived for steady-state polymerizations. Moreover, the radical flux must be low enough so that transfer, rather than termination, is the main chain-stopping event, and the polymerization is truly transfer dominated. PLP is essentially used as a flickering termination rate technique, that is, as a technique that makes essential use of effective termination. PLP can, however, be made applicable for even studying transfer to monomer, if combined with a rotating reactor/cuvette assembly.[92] This assembly permits time-efficient experiments with very long pulse periods and thus enables high-molecular-weight material to be produced at very low radical concentrations or termination rates, respectively. The rotating reactor/cuvette allows for acceptable polymerization rates even for slowly propagating monomers such as styrene.

The mathematical methods used to analyze molecular weight distributions generated in transfer-controlled free-radical polymerization experiments, specifically, the Mayo and chain length distribution (CLD) methods, are discussed below.

4.11.3.1 *Mayo Method*

The overall chain transfer constant, C, is defined as the ratio of the chain transfer and propagation rate coefficient, k_{tr}/k_p. For example, C_T is the ratio of the rate coefficient for chain transfer to chain transfer agent, T, and the rate coefficient for propagation. It is a measure for the reactivity of a chain transfer agent. The higher the value of C_T, the lower the concentration of the chain transfer agent required for a particular molecular weight reduction. This effect on the molecular weight of the polymer is quantitatively described by the Mayo equation, Eq. (4.55), which expresses the reciprocal of $\bar{P}_n$, the number average degree of polymerization, as a function of the rates of chain growths and chain-stopping events. Neglecting chain transfer to solvent, initiator, and polymer, this assumption is nearly fulfilled in bulk polymerizations at low overall monomer conversions; Eq. (4.55) reads, after insertion of Eq. (4.13)

$$\frac{1}{\bar{P}_n} = \frac{(1+\delta)k_t}{k_p^2[M]^2}R_p + C_M + C_T\frac{[T]}{[M]} \qquad (4.123)$$

The usual procedure for measuring the chain transfer constant C_T—henceforth referred to as the *Mayo procedure*—involves determination of the number average degree of polymerization for a range of $[T]/[M]$ values and plotting the data as $(\bar{P}_n)^{-1}$ versus $[T]/[M]$, that is, a Mayo plot. The value of C_T is then determined as the straight-line slope of this plot. This procedure assumes that the intercept is independent of the variation of $[T]/[M]$. However, the chain-length-dependent termination rate coefficient implies that the first term on the r.h.s. of Eq. (4.123) is in

general not a constant, and therefore a Mayo plot is not necessarily linear. This is a principal weakness of the Mayo method. However, in practice, this effect does not seem to be significant, which suggests that in systems with added chain transfer agent, the first term on the r.h.s. of Eq. (4.123) generally makes a negligible contribution to $(\bar{P}_n)^{-1}$.

4.11.3.2 Chain Length Distribution (CLD) Method

4.11.3.2 Chain Length Distribution (CLD) Method   The transfer process shifts the chain length distribution generated by the polymerization process to lower molecular weights. The Mayo method, described above, relies on the accurate determination of the number average degree of polymerization, $\bar{P}_n$. Especially if the chain length distribution shows considerable amounts of low-molecular-weight material, application of the Mayo method is problematic. In the cases when size-exclusion chromatography is chosen to measure the number average degree of polymerization, $\bar{P}_n$, baseline errors in the low-molecular-weight region show a significant influence on its value.

To overcome this problem, Gilbert and co-workers introduced a method, that places more emphasis on the high-molecular-weight region of the polymer chain length distribution.[93]

The general rate law for the polymerization process reads as

$$\frac{d[\mathrm{R}_i^\bullet]}{dt} = k_p[\mathrm{M}][\mathrm{R}_{i-1}^\bullet] - (k_p[\mathrm{M}] + k_{tr}^{\mathrm{M}}[\mathrm{M}] + k_{tr}^{\mathrm{T}}[\mathrm{T}] + 2\sum_{j=1}^{\infty} k_t^{i,j}[\mathrm{R}_j^\bullet]) \cdot [\mathrm{R}_i^\bullet] \quad (4.124)$$

Introducing the steady-state principle, $d[\mathrm{R}^\bullet]/dt = 0$, yields an recursive expression for the concentration of macroradicals with chain length i:

$$[\mathrm{R}_i^\bullet] = \left(1 + \frac{k_{tr}^{\mathrm{M}}[\mathrm{M}] + k_{tr}^{\mathrm{T}}[\mathrm{T}] + 2\sum_{j=1}^{\infty} k_t^{i,j}[\mathrm{R}_j^\bullet]}{k_p[\mathrm{M}]}\right)^{-1} \cdot [\mathrm{R}_{i-1}^\bullet] \quad (4.125)$$

A repeated substitution leads to an expression of this free-radical concentration as a function of the concentration of radicals being composed of one monomeric unit, $[\mathrm{R}_1^\bullet]$:

$$[\mathrm{R}_i^\bullet] = \left(1 + \frac{k_{tr}^{\mathrm{M}}[\mathrm{M}] + k_{tr}^{\mathrm{T}}[\mathrm{T}] + 2\sum_{j=1}^{\infty} k_t^{i,j}[\mathrm{R}_j^\bullet]}{k_p[\mathrm{M}]}\right)^{1-i} \cdot [\mathrm{R}_1^\bullet] \quad (4.126)$$

The rate law for radicals of chain length 1, $[\mathrm{R}_1^\bullet]$, combines the rate of formation of these radicals via the initiation process, R_i, the rate of their formation by transfer, and the rate of their loss by propagation, transfer and termination events:

$$\frac{d[\mathrm{R}_1^\bullet]}{dt} = R_i + (k_{tr}^{\mathrm{M}}[\mathrm{M}] + k_{tr}^{\mathrm{T}}[\mathrm{T}]) \cdot \mu_0 - (k_p[\mathrm{M}] + k_{tr}^{\mathrm{M}}[\mathrm{M}] + k_{tr}^{\mathrm{T}}[\mathrm{T}] + 2\sum_{j=1}^{\infty} k_t^{i,j}[\mathrm{R}_j^\bullet]) \cdot [\mathrm{R}_1^\bullet]$$

$$(4.127)$$

where $\mu_0 \equiv \sum_{i=1}^{\infty}[\mathrm{R}_i^\bullet]$ is the overall free-radical concentration.

Introducing the steady-state assumption and insertion of Eq. (4.127) into Eq. (4.126) leads to

$$[R_i^{\bullet}] = \left(\frac{R_i + k_{tr}^M[M]\mu_0 + k_{tr}^T[T]\mu_0}{k_p[M]} \right) \cdot \left(1 + \frac{k_{tr}^M[M] + k_{tr}^T[T] + 2\sum_{j=1}^{\infty} k_t^{i,j}[R_j^{\bullet}]}{k_p[M]} \right)^{-i}$$

(4.128)

If transfer and termination events are much less probable than propagation, specifically, $k_{tr} \ll k_p$, and $2\sum_{j=1}^{\infty} k_t^{i,j}[R_j^{\bullet}] \ll k_p[M]$, the r.h.s. of Eq. (4.128) can be rewritten as a progression with only two terms, using $e^x \cong 1 + x$:

$$[R_i^{\bullet}] \propto \exp\left(-\frac{k_{tr}^M[M] + k_{tr}^T[T] + 2\sum_{j=1}^{\infty} k_t^{i,j}[R_j^{\bullet}]}{k_p[M]} \cdot i \right)$$

(4.129)

For transfer-dominated systems, the shape of the polymer distribution is the same as that of the free-radical distribution, $[R_i^{\bullet}] = [P_P]$, keeping in mind that the chain length i equals the degree of polymerization, P. It turns out that this situation is in fact more general: Clay and Gilbert[93] have shown that also for partly termination-controlled distributions, the following equation holds true, in which the slope of the logarithmic number distribution $(x_P \equiv [P_P]/\sum_{P=0}^{\infty}[P_P])$ is correlated with the kinetic parameters:

$$\frac{d\ln x_P}{dP} = -\frac{k_{tr}^M[M] + k_{tr}^T[T] + 2\sum_{j=1}^{\infty} k_t^{i,j}[R_j^{\bullet}]}{k_p[M]}$$

(4.130)

A plot of the logarithmic slope against the ratio of the transfer agent to monomer concentration, $[T]/[M]$, allows one to calculate the transfer constant, $C = k_{tr}/k_p$. It should be kept in mind that as a result of the chain-length-dependent termination process, Eq. (4.130) is valid only in the long-chain limit. However, reasonable results are achieved at lower molecular weights as well. This method has been studied extensively[94] and is now frequently used as an alternative to the classical Mayo method. Although it was shown that both methods are in essence the same,[95] there may be situations in which the CLD method is preferable over the Mayo method. As mentioned earlier, the number average degree of polymerization, $\bar{P}_n$, is associated with a certain degree of error. This is a difficulty of the Mayo method that therefore encounters problems with low-molecular-weight polymers. Another situation when the CLD procedure is more advantageous than the Mayo method is when one must analyze a contaminated polymer sample. A contamination (of an arbitrary nature) may alter the molecular weight distribution and will therefore significantly change the molecular weight averages, rendering the Mayo procedure useless. However, if a region in the molecular weight distribution can be identified in which the distribution is less affected by the contaminant, this region can still be used in the CLD procedure. The CLD procedure is also expected to be more robust when one

has systematic errors in SEC calibration, because then the obtained molecular weight averages will not be accurate, but the systematic error in values of x_P can be expected to cancel out to some extent when the slope of a $\ln(x_P)$ plot is taken.

4.11.4   Methods for the Measurement of k_t

4.11.4.1   *Single-Pulse–Pulsed Laser Polymerization (SP-PLP)*   Applying pulsed laser-polymerization (PLP) in conjunction with infrared or near-infrared spectroscopic measurement of monomer conversion induced by a single laser pulse (SP-PLP) allows for the determination of the ratio of termination to propagation rate coefficients, k_t/k_p, in wide ranges of temperature; pressure; and monomer conversion. The SP-PLP technique was pioneered by Buback and co-workers in the late 1980's.[56] The monomer conversion induced by a single laser pulse, typically of 20 ns width, is measured by online IR/NIR (near-infrared) spectroscopy with a time resolution of microseconds. The distribution of free-radical chain lengths after a single laser pulse is close to a Poisson distribution where chain length is linearly
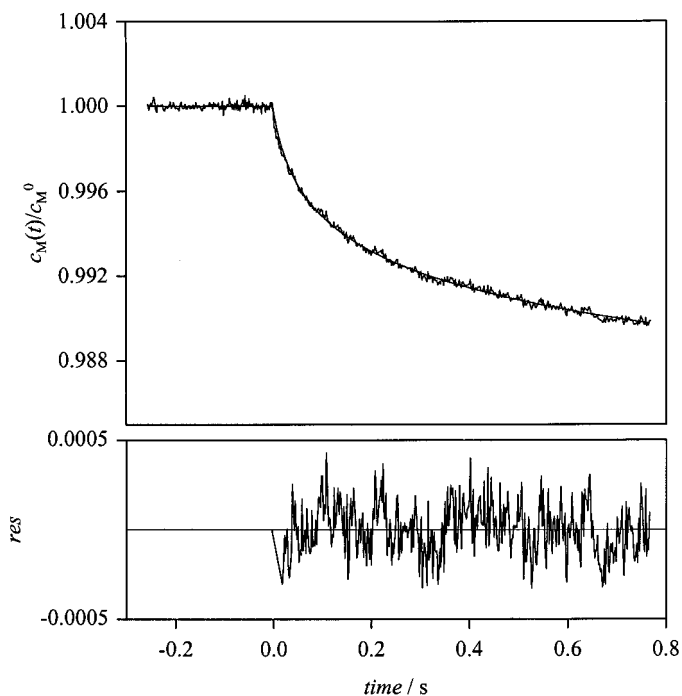
Figure 4.12   Monomer concentration versus time trace of a methyl methacrylate (MA)/ dodecyl acrylate (DA) copolymerization at equimolar amounts of both monomers measured in a reaction mixture at 40°C, 1000 bar and 5 wt% polymer concentration. The difference between measured and fitted data [Eq. (4.37)] is illustrated by plotting the residuals (*res*) in the lower part of the figure. The data ae taken from reference 37.
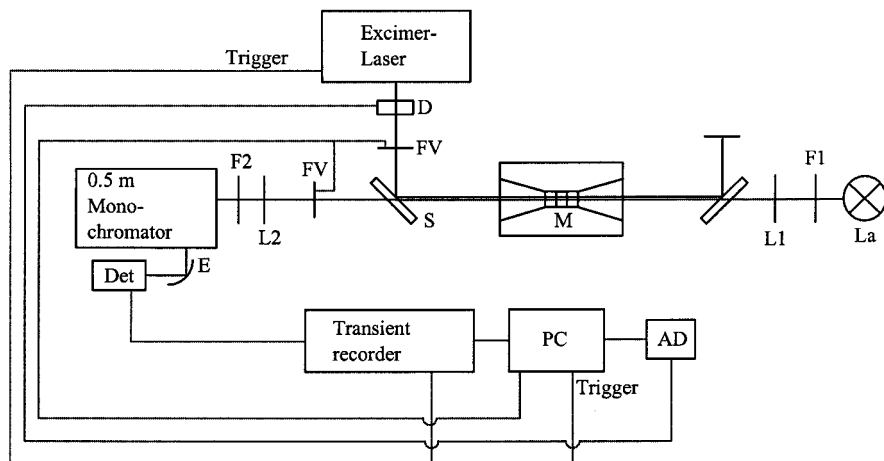
Figure 4.13 Experimental setup for the single pulse (SP)-pulsed laser polymerization (PLP). The diagram is after C. Kowollik, Ph.D. thesis, 1999.

correlated to time, unless chain transfer interferes. As a consequence, SP-PLP experiments may provide access to investigations into the chain length dependence of k_t. SP-PLP was first used for studies in ethene kinetics[56] and subsequently to measure free-radical termination of methyl acrylate (MA), butyl acrylate (BA), and dodecyl acrylate (DA).[96,97] Because of the high academic and technical interest in detailed k_t studies on slowly propagating monomers, the technique has also been applied to methyl methacrylate (MMA),[98] butyl methacrylate (BMA), and dodecyl methacrylate (DMA) and various acrylate/methacrylate binary and ternary copolymerizations.[99,37] Figure 4.12 shows the spectroscopically measured relative monomer concentration–time profile of a methyl acrylate/dodecyl acrylate copolymerization at equimolar amounts of both monomers in the reaction mixture. The relative change in overall monomer concentration induced by the single laser pulse in this particular experiment is 1% after about 600 ms. Equation (4.37) has been used to evaluate the kinetic trace. The difference between measured and fitted data is illustrated by plotting the residuals (*res*) in the lower part of the figure, indicating the excellent applicability of Eq. (4.37) to represent the kinetic data. The principal experimental setup for SP-PLP experiments is illustrated in Fig. 4.13.

For the initiation of the photopolymerization, laser pulses of an excimer laser (typically) operated on the XeF line at 351 nm are reflected on the optical axis of the sample cell by UV mirrors (S) transparent in the infrared region. A detector (D), which has to be calibrated prior to each measurement, is used to determine the intensity of the laser irradiation in front of the optical (high-pressure) cell. If needed, a second detector can be installed behind the optical high pressure cell for the measurement of the amount of photons absorbed by the sample. A photoshutter FV directly in front of the optical cell is used to intercept laser test pulses. This shutter is, just as the laser, controlled by a computer. Test pulses are used to ensure a

constant laser energy output, which is achieved only at pulse frequencies above 0.1 Hz. A tungsten–halogen lamp (La) serves as a source of infrared and near-infrared radiation. The lamp is powered by two lead accumulators to achieve a noise-free signal. A second photoshutter (FV), directly in front of the monochromator, is used to block out the analyze light to measure the detector signal without NIR radiation. Preinitiation processes by UV parts in the spectrum of the tungsten–halogen lamp are suppressed by a UV cutoff filter (F1). The analyze light is focused by a lens (L1) on the sample contained in the optical high-pressure cell. A second lens (L2) focuses the analyze light onto the lid of a monochromator.

The light is then diffracted on an interference grating and reflected on a fast NIR detector by an ellipsoid mirror (E). A silicium filter (F2) ensures that only one grating order hits the detector. The analog detector signal is recorded by a transient recorder and transferred to a computer for further evaluation. To reduce potential vibrations of the building, the entire setup is placed on solid granite board, which is supported by rubber tubes.

The majority of SP-PLP experiments reported in the literature have been carried out under high pressure to increase the conversion per single pulse. "True" single-pulse experiments can be readily carried out for the acrylates (e.g., methyl acrylate, butyl acrylate, or dodecyl acrylate). However, for slowly propagating monomers such as MMA and styrene, the signal to noise ratio of a "true" single-pulse experiment is too poor to allow a meaningful kinetic analysis of the monomer conversion–time trace. Nevertheless, slowly propagating monomers may be studied by enhancing the signal-to-noise ratio by coaddition of a larger number of individual SP-PLP signals recorded under virtually the same conditions with only a minor decrease in both monomer and photoinitiator concentration between "true" single-pulse experiments. As the concentration of free radicals originating from the previous pulse decays to a very low level and as small primary radicals are generated by each pulse, the range of chain length covered during successively recorded individual concentration–time traces is identical. The number of coadded signals is limited by the requirement of deriving k_t/k_p for a small range of monomer conversion extending over no more than $\sim 2\%$ to stay close to the intention of "pointwise" probing the kinetics. To effectively probe the kinetics of a given monomer, a minimum of 0.001% monomer conversion per single laser pulse is required for a sufficient signal-to-noise ratio after approximately 100 coadditions of single-pulse signals.

4.11.4.2 Chain Length Distribution Methods   The shape of the chain length distribution of a polymer is directly governed by the kinetic parameters of the polymerization process by which the distribution is generated. It is therefore self-evident to try to extract these parameters from such a distribution, which is convincingly realized by measuring k_p by PLP (see Section 4.11.2.1) or determining the chain transfer constant C via the Mayo or CLD methods (see Section 4.11.3). Determining the rate coefficient of termination, k_t, via the evaluation of the chain length distributions is possible only in combination with polymerization rate measurements. However, these methods also allow for determination of the chain length dependence of k_t. The chain length dependence of the termination rate

coefficient should always be taken into account if reasonable results are to be achieved.

The termination rate coefficient is, strictly speaking, not a constant, but is proven to vary with the chain length of the two radicals involved in the termination process[100] (see Section 4.4):

$$k_t^{i,j} \propto F(i,j) \tag{4.131}$$

where $k_t^{i,j}$ is the rate constant of termination between radical chains of lengths i and j. $F(i,j)$ is usually represented by a power law of the type

$$F(i,j) = (\overline{i,j})^{-\alpha} \tag{4.132}$$

where $\overline{i,j}$ denotes some average (e.g., the harmonic[101] or the geometric[102] mean) of the two chain lengths i and j involved and α a positive constant. As a consequence, the problem of determining k_t is not solved by evaluation of one specific value but rather represents the evaluation of an entire functional dependence.

Most of the methods employed to deduce k_t and k_p are based on the assumption of a chain-length-independent termination rate coefficient and yield k_p and k_t in some combination (k_p/k_t or k_p^2/k_t, respectively). In the past, before k_p could be determined directly, the usual procedure was to use two different ratios of k_p and k_t and to split them into their individual components via combination. In view of the chain length dependence of k_t, it is clear that any (single) experiment aiming at the determination of k_t will render only an average value $\bar{k}_t$ that is defined by the method used and the experimental conditions chosen (e.g., monomer and initiator concentration, type of initiation). Combination of k_p/k_t and k_p^2/k_t ratios, which are invariably taken from different experiments, therefore always involves averages of k_t that are not consistent with each other.

Any serious approach aimed at the determination of k_t should therefore avoid the shortcomings outlined above. This implies that one should (1) preferentially refer to single-point measurements, (2) avoid combinations of two different ratios of k_p and k_t, (3) take advantage of the possibility of determining k_p directly (e.g., by PLP-SEC) and (4) make sure that the average of k_t is a fair replicate of the true average $\langle k_t \rangle$ [see Eq. (4.14)], which is operative in the respective experiment.

With these premises fulfilled, it is possible to treat a k_t value originating from an experiment dealing with reactions between radicals of different chain lengths, as an average $\bar{k}_t$ specific for the experimental conditions chosen. Assuming this average $\bar{k}_t$ to be physically correct, a power law of the form

$$\bar{k}_t = k_t^0 \cdot v'^{-\alpha} \tag{4.133}$$

with the same exponent α as in Eq. (4.132) will be obtained. In order to establish the correct chain length dependence of k_t, the averages of k_t have to be correlated with a quantity characteristic of the population of terminating radicals in each experiment. The best solution to this problem appeared to chose a quantity v' that marks the

number average chain length of the radicals at the moment of their termination. ν', which is proportional to the number average degree of polymerization $\bar{P}_n$ of the polymer formed

$$\nu' = \frac{\bar{P}_n(1+\delta)}{2} \tag{4.134}$$

thus in itself is independent of the mode of termination (combination or disproportionation). The preexponential factor in Eq. (4.133), k_t^0, is not to be confused with the termination rate coefficient of two radicals of chain length 1, but is rather a proportionality factor with no physical meaning associated with it.

Two successful approaches, designed for systems with negligible chain transfer, are (1) analysis of the second moment of the chain length distribution, represented by the product of the rate of polymerization R_p and the weight average degree of polymerization, $\bar{P}_w$; and (2) the formal solution for $\bar{k}_t$ of the rate equation for polymerization with periodic laser pulses (see Section 4.6.4). Both methods were originally derived for chain-length-independent termination.[103,104] In both cases additional quantities have to be known; apart from k_p, the quantity δ (contribution of disproportionation to overall termination) must be available in the first case and the quantity ρ (the concentration of new radicals formed in each laser pulse) in the second (implicitly the knowledge of δ is necessary, too).

The two averages of k_t, $\bar{k}_t^m$ and $\bar{k}_t^*$, are calculated as follows:

1. $\bar{k}_t^m$ from the product of rate of polymerization R_p and weight average degree of polymerization $\bar{P}_w$ (which represents the second moment of the chain length distribution per time)

$$\bar{P}_w \cdot R_p = \frac{k_p^2}{2\bar{k}_t^m}[M]^2(3-\delta) \tag{4.135}$$

2. $\bar{k}_t^*$ from the rate of polymerization under the same conditions given by

$$R_p = \frac{k_p[M]}{2\bar{k}_t^* t_0}\ln\left\{1 + \rho\bar{k}_t^* t_0\left[1 + \left(1 + \frac{2}{\rho\bar{k}_t^* t_0}\right)^{0.5}\right]\right\} \tag{4.136}$$

As indicated above, both equations were originally developed for chain-length-independent termination; their use in the context of chain length dependence, however, is permissible only if the k_t data obtained are explicitly treated as averages.

The quantity ρ can be determined as follows. In systems with negligible chain transfer, the following relation holds:

$$\rho = \frac{2R_p t_0}{\bar{P}_n \cdot (1+\delta)} \tag{4.137}$$

Once $\bar{P}_n$ is known, ρ can be calculated for a given δ. A reasonable estimate of δ is sufficient because δ never appears as an isolated factor in the calculation [as either $(3 - \delta)$ or $(1 + \delta)$]. However, errors in δ do not significantly influence absolute values of k_t. The values for α, representing the chain length dependence of k_t, remains nearly unchanged.

The polymerization is performed via a PLP-SEC experiment (see Section 4.11.2.1), which allows one to control the number average degree of polymerization easily by choosing different laser frequencies and gives the exact chain length distribution of the produced polymer. The value of the propagation rate coefficient, k_p, can be obtained by the same experiment. Measuring the rate of polymerization, R_p, by determining the conversion of the polymer produced per time, and the number and weight average degree of polymerization, $\bar{P}_n$ and $\bar{P}_w$, allows calculation of the absolute values of average k_t according to Eqs. (4.135) and (4.136). Insertion into Eq. (4.133) gives values of α, which is a measure for the chain length dependence of the termination rate coefficient for macroradicals of sufficiently large size (according to region B in Fig. 4.3).

Another method used to measure the chain length dependence of k_t via evaluation of the chain length distribution of the polymer formed in a single-pulse experiment uses Eq. (4.138) to measure model-independent values of the termination rate coefficient k_t at any given chain length[105]

$$k_t^{i,i} = \frac{V k_p [M] x_{2P}}{\left(\int_0^\infty x_{2P} \, dP - \int_0^P x_{2P} \, dP \right)^2} = \frac{V k_p [M] x_{2P}}{\left(\int_P^\infty x_{2P} \, dP \right)^2} \tag{4.138}$$

where x_{2P} is the differential number distribution for termination by combination and V an arbitrary volume.

There are two uncertainties in this development that prevent a direct application of Eq. (4.138). The first one is the quantity V, which plays the role of a scaling factor; the second refers to the fact that the integration of x_{2P} cannot be carried out to infinity in practice, due to the effect of chain transfer in the high-molecular-weight region. This implies that some maximal chain length, P_{max}, has to be introduced that corresponds to a specific residual radical concentration $[R^\bullet]_{res}$ present at the moment at which integration is stopped. The calibration problem as a whole might be solved by estimating values for $[R^\bullet]_0$ as well as for $[R^\bullet]_{res}$. They may be calculated via $k_t^{1,1}$ from the Smoluchowski equation or from literature data and by combination with average $\bar{k}_t$ data linking $[R^\bullet]_0$ and $[R^\bullet]_{res}$ or alternatively from SP-PLP traces.

The chain length dependence of k_t can also be assessed by fitting a chain length distribution obtained from a single-pulse experiment to the theoretical distribution given by Eq. (4.83).[106] However, with this method it is also not possible to measure absolute termination rate coefficients, because of unknown absolute scaling factors.

4.11.4.3 Stationary Polymerization Methods

Determination of the kinetic rate coefficients k_t and k_p in their coupled form k_p^2/k_t has long proceeded via measurement of the rate of polymerization and the calculation of the k_p^2/k_t via

Eq. (4.20). With the advent of pulsed laser techniques that allows to obtain much more accurate and detailed information about the kinetic rate coefficients (such as chain length dependencies), these techniques became less important. Nevertheless, measurements of the rate of polymerization are still widely performed and are used especially for systems where the novel techniques are not applicable. This is especially true for measurements of the termination rate coefficient, k_t, where rate of polymerization measurements, in combination with independent experiments for the k_p determination, are sometimes the only possibility to get an estimate for k_t. However, it should always be kept in mind that determination of termination rate coefficients from stationary polymerization experiments yields only an average and approximate value for k_t, as has been outlined in Section 4.5. The polymerization rate can be measured via any quantity that it is directly proportional to. Possible quantities are the density (dilatometry), the refractive index (refractrometry), the heat of polymerization (calorimetry), the polymer mass (gravimetry), or a spectral absorption (IR/NIR and NMR spectroscopy).

The most two common methods are dilatometry and spectroscopic methods. Dilatometry has the advantages of being easy to perform and having low equipment costs. This technique utilizes the volume change that occurs on polymerization to follow monomer conversion versus time. It is applicable to free-radical polymerization, due to the large difference in the densities of polymer and monomer. For example, the density of methyl methacrylate changes by approximately 22% when going from its monomeric to its polymeric form. The density changes in other polymerizing systems are of the same order of magnitude. The density change is followed in a volume calibrated dilatometer. In modern dilatometers the volume change is followed by the computer-controlled observation of the meniscus of a solvent in a capillary on top of the reaction mixture. It is important that the solvent does not mix with the reaction mixture.

The spectroscopic measurement of the rate of polymerization is inherently more elegant than any other of the abovementioned methods, since it directly probes the reaction mixture on a molecular level and does not rely on the interpretation of a secondary quantity. In addition to providing the rate of polymerization, spectroscopic methods provide real-time insight into the reaction process. The major disadvantage of spectroscopic methods is the relatively large price of, for example, NMR or Fourier-transform infrared spectrometers. Kinetic spectroscopic measurements normally proceed via the recording of a part of the spectrum where a spectroscopic absorption is directly associated with the monomer in the reaction mixture. Care has to be taken that during the course of the reaction no formed product displays an absorption in the same frequency region as the monomeric species. This requirement is met for most monomers in kinetic ^{1}H NMR spectroscopic investigations, where the vinylic absorption(s) can be easily used to probe the progress of the reaction.[107] However, NMR spectroscopic investigations are limited in their time resolution. For faster proceeding reactions, NIR/IR Fourier- transform spectroscopy has been successfully performed to follow free-radical acrylate and methacrylate polymerizations, using the first overtone of the C—H stretching vibration on the double bond at roughly $6200\,\mathrm{cm}^{-1}$.[97]

4.11.4.4 Determining the Mode of Termination: Disproportionation versus Combination   Several experimental approaches have been taken to determine the mode of chain termination in free-radical polymerization. These have been extensively reviewed by Moad and Solomon.[108] In the case of termination by disproportionation, a chain is generated with one initiator fragment, whereas in the case of combination, a chain with two initiator fragments is formed. Determination of the number of end groups to the number of monomer units consumed by the polymerization process allows for the calculation of δ, via the additional knowledge of the number average degree of polymerization, $\bar{P}_n$. Unfortunately, identification and quantification of chain ends are not simple as they give only small signals (relative to the rest of the polymer chain) in a spectroscopic analysis. This can be overcome to some extent by isotopic labeling of the initiator end groups by ^{14}C or by using initiator fragments containing fluorine or phosphorus as NMR-sensitive molecules. Other complications in the analysis include isolation of the long-chain termination process from other chain-stopping mechanisms such as chain transfer and primary radical termination. Because of these experimental difficulties, there remains considerable uncertainty in existing termination mode measurements, and there is a large scatter in the obtained results. The application of the matrix-assisted laser desorption ionization time-of-flight mass spectroscopy (MALDI-TOF-MS) to the problem of end-group analysis of polymers brought some promising results to this field of polymerization kinetics.[109]

REFERENCES AND NOTES

1. M. Buback, M. Busch, and C. Kowollik, *Macromol. Theory Simul*. **9**, 442 (2000).

2. R. Kuhlmann, and W. Schnabel, *Polymer* **18**, 1163 (1977); J. Hutchison, M. C. Lamber and A. Ledwith, *Polymer* **14**, 250, (1973).

3. A. Brandrup, E. H. Immergut, and E. A. Grulke, *Polymer Handbook*, Wiley-Interscience, New York, 1999, p. II/1.

4. P. S. Engel, *Chem. Rev*. **80**, 99 (1980).

5. N. J. Turro, *Macromolecular Photochemistry*, Benjamin-Cummings, 1978.

6. N. S. Allen, ed., *Photopolymerization and Photoimaging Science and Technology*, Elsevier, 1989.

7. J. P. Fouassier, P. Jacques, D. J. Lougnot, and T. Pilot, *Polym. Photochem*. **5**, 57 (1984).

8. J. Eichler, C. P. Herz, I. Naito, and W. Schnabel, *J. Photochem*. **12**, 225 (1980).

9. C. J. Groenenboom, H. J. Hageman, T. Overeem, and A. J. M. Weber, *Makromol. Chem*. **183**, 281 (1982).

10. H. Fischer, R. Baer, R. Hany, I. Verhoolen, and M. J. Walbiner, *Chem. Soc., Perkin Trans*. **2**, 787 (1990).

11. H. F. Gruber, *Prog. Polym. Sci*. **17**, 953 (1992).

12. O. F. Olaj, H. F. Kauffmann, and J. W. Breitenbach, *Makromol. Chem*. **178**, 2707 (1977).

13. O. F. Olaj, H. F. Kauffmann, J. W. Breitenbach, and H. Bieringer, *J. Polym. Sci., Polym. Lett. Ed*. **15**, 229 (1977).

14. H. F. Kauffmann, O. F. Olaj, and J. W. Breitenbach, *Makromol. Chem*. **177**, 939 (1976).

15. R. S. Lehrle and A. Shortland, *Eur. Polym. J*. **24**, 425 (1988).

16. I. Reetz, Y. Yagci, and M. K. Mishra, *Turk. Plast. Eng.* **48**, 31 (1998).

17. J. I. M. Botman, A. T. A. Derksen, A. M. van Herk, M. Jung, F.-D. Kuchta, L. G. Manders, C. J. Timmermans, and M. J. A. de Voigt, *Nucl. Instrum. Meth. Phys. Res., Sect. B* **139**, 490 (1998).

18. H. V. Boenig, in *Encyclopedia of Polymer Science and Engineering*, Vol. 11, H. F. Mark, N. M. Bikales, C. G. Overberger, and G. Menges, eds., Wiley-Interscience, New York, 1988, pp. 248–261.

19. I. Cantero and T. F. Otero, *Rev. Plast. Mod.* **72**, 46 (1996).

20. A. A. Gridnev and S. D. Ittel, *Macromolecules* **29**, 5864 (1996); J. P. A. Heuts, R. G. Gilbert, and L. Random, *Macromolecules* **28**(26), 8771 (1995); M. Deady, A. W. H. Mau, G. Moad, and T. H. Spurling, *Makromol. Chem.* **194**(6), 1691 (1993).

21. O. F. Olaj, P. Vana, M. Zoder, A. Kornherr, and G. Zifferer, *Macromol. Rapid Commun.* **21**, 913 (2000).

22. L. H. Yee, M. L. Coote, T. P. Davis, and R. P. Chaplin, *J. Polym. Sci.; Part A: Polym. Chem.* **38**, 2192 (2000).

23. A. M. van Herk, *Macromol. Theory Simul.* **9**, 433 (2000).

24. O. F. Olaj and I. Schnöll-Bitai, *Monatshefte für Chemie* **130**, 731 (1999).

25. M. D. Zammit, T. P. Davis, G. D. Willett, and K. F. O'Driscoll, *J. Polym. Sci.; Part A: Polym. Chem.* **35**, 2311, (1997).

26. M. L. Coote, T. P. Davis, B. Klumperman, and M. J. Monteiro, *J. Macromol. Sci., Rev. Macromol. Chem. Phys.* **C38**(4), 567 (1998).

27. D. A. Morrison and T. P. Davis, *Macromol. Chem. Phys.* **201**, 2128, (2000).

28. S. Beuermann, M. Buback, C. Schmaltz, and F.-D. Kuchta, *Macromol. Chem. Phys.* **199**, 1209, (1998).

29. S. Beuermann, M. Buback, C. Isemer and A. Wahl, *Macromol. Rapid Commun.* **20**, 26 (1999).

30. M. A. Quadir, J. M. DeSimone, A. M. Van Herk, and A. L. German, *Macromolecules* **31**, 6481 (1998).

31. A. M. van Herk, B. G. Manders, D. A. Canelas, M. A. Quadir, and J. M. DeSimone, *Macromolecules* **30**, 4780 (1997).

32. J. Robb and E. Senogles, *Trans. Faraday Soc.* **58**, 708 (1962); W. Kirkham and J. Robb, *Trans. Faraday Soc.* **57**, 1757 (1961).

33. A. Brandrup, E. H. Immergut, and E. A. Grulke, *Polymer Handbook*, Wiley-Interscience, New York, 1999, p. II/77.

34. G. Moad and D. H. Solomon, *The Chemistry of Free Radical Polymerization*, Pergamon Press, Oxford, 1995.

35. A. Brandrup, E. H. Immergut, and E. A. Grulke, *Polymer Handbook*, Wiley-Interscience: New York, 1999, p. II/77.

36. A. M. North and G. A. Reed, *Trans. Faraday Soc.* **57**, 859 (1961); S. W. Benson and A. M. North, *J. Am. Chem. Soc.* **84**, 935 (1962).

37. M. Buback and C. Kowollik, *Macromolecules* **32**, 1445 (1999).

38. A. Matsumoto and T. Otsu, *Macromol. Symp.* **98**, 139 (1995).

39. A. Matsumoto and T. Otsu, *Proc. Jpn. Acad. B* **70**, 43 (1994).

40. J. C. Le Guillou and J. Zinn-Justin, *Phys. Rev. B: Condens. Matter* **21**(9), 3976 (1980).

41. A. R. Khokhlov, *Makromol. Chem., Rapid Commun.* **2**, 633 (1981); B. Friedman and B. O'Shaughnessy, *Macromolecules* **26**, 5726 (1993).

42. O. F. Olaj and G. Zifferer, *Makromol. Chem.* **189**, 1097 (1988).

43. J. B. L. de Kock, A. M. van Herk, and A. L. German, *J. Macromol. Sci.-Pol. R.* **C41**, 199 (2001); C. Kowollik, C. Ph.D. thesis Göttingen, 1999; H. K. Mahabadi, *Macromolecules* **18**, 1319 (1985); O. F. Olaj and P. Vana, *Macromol. Rapid. Commun.* **19**, 433 (1998); O. F. Olaj and P. Vana, *Macromol. Rapid. Commun.* **19**, 533 (1998).

44. O. F. Olaj and P. Vana, *Macromol. Rapid. Commun*. **19**, 433 (1998); O. F. Olaj and P. Vana, *Macromol. Rapid. Commun*. **19**, 533 (1998).

45. M. Buback and F.-D. Kuchta, *Macromol. Chem. Phys*. **198**, 1445 (1997).

46. M. Buback, *Makromol. Chem*. **191**, 1575 (1990).

47. M. Buback and J. Schweer, *Z. Phys. Chem*. **161**, 153 (1989); M. Buback, B. Degener, and B. Huckestein, *Makromol. Chem., Rapid Commun*. **10**, 311 (1989); M. Buback and B. Degener, *Makromol. Chem*. **194**, 2875 (1993).

48. J. P. Fischer, J. Mücke, and G. V. Schulz, *Ber. Bunsengesellschaft Phys. Chem*. **73**, 154 (1969); W. A. Ludwico, and S. L. Rosen, *J. Appl. Polym. Sci*. **19**, 757 (1975); W. A. Ludwico and S. L. Rosen, *J. Polym. Sci., Polym. Chem. Ed*. **14**, 2121 (1976); J. Dionisio, K. K. Mahabadi, and K. O'Driscoll, *J. Polym. Sci., Polym. Chem. Ed*. **17**, 1891 (1979).

49. K. Horie, I. Mita, and H. Kambe, *Polym. J*. **4**, 341 (1973); K. Ito, *J. Polym. Sci, Polym. Chem. Ed*. **10**, 3159 (1972).

50. R. G. W. Norrish and R. R. Smith, *Nature* **150**, 336 (1942).

51. E. Trommsdorff, H. Köhle, and P. Lagally, *Makromol. Chem*. **1**, 169 (1948).

52. G. A. O'Neil, M. B. Wisnudel, and J. M. Torkelson, *Macromolecules* **29**, 7477 (1996).

53. J. Gao and A. Penlidis, *J. Macromol. Sci., Rev. Macromol. Chem. Phys*. **C36**, 199 (1996).

54. O. F. Olaj, A. Kornherr and G. Zifferer, *Macromol. Theory Simul*. **9**, 131 (2000).

55. H. W. Melville, *Proc. Roy. Soc. London, A* **163**, 511 (1937); G. Gans and D. Duesentrieb, *Enth. J. Pol. Res*. **206**, 503 (1954); P. D. Bartlett, C. G. Swain, *J. Am. Chem. Soc*. **67**, 2273 (1945).

56. M. Buback, H. Hippler, J. Schweer, and H. P. Vögele, *Macromol. Chem. Rapid Commun*. **7**, 261 (1986).

57. G. Moad, D. A. Shipp, T. A. Smith, and D. H. Salomon, *J. Phys. Chem*. **103**, 6580 (1999).

58. M. Wulkow, *Macromol. Theory Simul*. **5**, 393 (1996).

59. O. F. Olaj, I. Bitai, and F. Hinkelmann, *Makromol. Chem*. **188**, 1689 (1987).

60. O. F. Olaj and G. Zifferer, *Makromol. Chem., Theory Simul*. **1**, 71 (1992).

61. J. Sarnecki and J. Schweer, *Macromolecules* **28**, 4080 (1995).

62. A. P. Alksandrov, V. N. Genkin, M. S. Kitai, M. Smirnova, and V. V. Sokolov, *Kvantovaya Elektron*. **4**, 976 (1977); O. F. Olaj, I. Bitai, and F. Hinkelmann, *Makromol. Chem*. **188**, 1689 (1987); A. Kornherr, G. Zifferer, and O. F. Olaj, *Macromol. Theory Simul*. **8**, 260 (1999).

63. P. E. M. Allen and C. R. Patrick, *Kinetics and Mechanisms of Polymerization Reactions*, Wiley, New York, 1974.

64. R. A. Hutchinson, D. A. Paquet, S. Beuermann, and J. H. McMinn, *Ind. Eng. Chem. Res*. **37**, 3567 (1998).

65. C. Barner-Kowollik and T. P. Davis, *Macromol. Theory Simul*. **10**(4), 255 (2001).

66. G. E. Roberts, M. L. Coote, J. P. A. Heuts, L. M. Morris, and T. P. Davis, *Macromolecules* **32**, 1332 (1999); S. Harrisson, T. P. Davis, R. A. Evans, and E. Rizzardo, *Macromolecules* **35**, 2474 (2002).

67. J. Sugiyama, N. Kayamori, and S. Shimada, *Macromolecules* **29**, 1943 (1996).

68. S. Harrison, R. A. Evans, E. Rizzardo, and T. P. Davis, *Macromolecules* **33**, 9553 (2000).

69. M. Buback and C. Hinton, *Z. Phys. Chem*. **193**, 61 (1996); M. Buback and H. Lendle, *Z. Naturforsch*. **36a**, 1371 (1981).

70. M. Buback, R. G. Gilbert, R. A. Hutchinson, B. Klumperman, F.-D. Kuchta, G. B. Manders, K. F. O'Driscoll, G. T. Russell, and J. Schweer, *Macromol. Chem. Phys*. **196**, 3267 (1995); S. Beuermann, M. Buback, T. P. Davis, R. G. Gilbert, R. A. Hutchinson, O. F. Olaj, G. T. Russell, J. Schweer, and A. M. van Herk, *Macromol. Chem. Phys*. **198**, 1545 (1997); S. Beuermann, M. Buback, T. P. Davis, R. G. Gilbert, R. A. Hutchinson, A. Kajiwara, B. Klumperman, and G. T. Russell, *Macromol. Chem. Phys*. **201**, 1355 (2000).

71. A. Kajiwara and M. Kamachi, *Macromolecules* **29**, 2378 (1996).

72. M. Buback, L.-H. Gracia-Rubio, R. G. Gilbert, D. H. Napper, J. Guillot, A. E. Hamielec, D. Hill, K. F. O'Driscoll, O. F. Olaj, J. Shen, D. Solomon, G. Moad, M. Stickler, M. Tirrell, and M. A. Winnik, *J. Polym. Sci., Polym. Lett. Ed.* **26**, 293 (1988).

73. H. P. Aleksandrov, V. N. Genkin, M. S. Kital, J. M. Smirovna, and V. V. Sokolov, *Kvantovaya Elektron.* (Moscow) **4**, 976 (1977).

74. T. P. Davis, K. F. O'Driscoll, M. C. Piton, and M. A. Winnik, *Macromolecules* **22**, 2785 (1989).

75. M. P. Tonge, A. Kajiwara, M. Kamachi, and R. G. Gilbert, *Polymer* **39**, 2305 (1998).

76. M. Buback, C. Kowollik, M. Kamachi, and A. Kajiwara, *Macromolecules* **31**, 7208 (1998).

77. A. Kajiwara and M. Kamachi, *Macromolecules* **29**, 2378 (1996).

78. J. Shen, G. Wang, Y. Zheng, and M. Yang, *Macromol. Chem., Macromol. Symp.* **63**, 105 (1992).

79. J. Shen, Y. Tian, Y. Zeng, and Z. Qiu, *Makromol. Chem., Rapid Commun.* **8**, 615 (1987).

80. T. G. Carswell, D. J. T. Hill, D. I. Londero, J. H. O'Donnell, P. J. Pomery, and C. L. Winzor, *Polymer* **33**, 137 (1992).

81. I. Schnöll-Bitai, *Macromol. Rapid Commun.* **20**, 162 (1999); I. Schnöll-Bitai, *Macromol. Theory Simul.* **9**, 230 (2000); P. Vana, L. H. Yee, and T. P. Davis, *Macromolecules* **35**, 3008 (2002).

82. L. V. Karmilova, G. V. Ponomarev, B. R. Smirnov, and I. M. Belgovskii, *Russ. Chem. Rev.* **53**, 223 (1984).

83. T. P. Davis, D. Kukulj, D. M. Haddleton, and D. R. Maloney, *Trends Polym. Sci.* **3**, 365 (1995).

84. A. Brandrup, E. H. Immergut, and E. A. Grulke, *Polymer Handbook*, Wiley-Interscience; New York, 1999, p. II/97.

85. F. R. Mayo, *J. Am. Chem. Soc.* **65**, 2324 (1943).

86. D. I. Christie and R. G. Gilbert, *Macromol. Chem. Phys.* **197**, 403 (1996); errata: *Macromol. Chem. Phys.* **198**, 663 (1997).

87. J. P. A. Heuts, T. P. Davis, and G. T. Russell, *Macromolecules* **32**, 6019 (1999).

88. D. Kukulj, T. P. Davis, and R. G. Gilbert, *Macromolecules* **31**, 994 (1998).

89. R. A. Hutchinson, D. A. Paquet, Jr., and J. H. McMinn, *Macromolecules* **28**, 5655 (1995).

90. M. Buback and R. A. Lämmel, *Macromol. Theory Simul.* **6**, 145 (1997).

91. M. Wulkow, *Macromol. Theory Simul.* **5**, 393 (1996).

92. H. Kapfenstein-Doak, C. Barner-Kowollik, T. P. Davis, and J. Schweer, *Macromolecules*, **34**, 2822 (2001).

93. P. A. Clay and R. G. Gilbert, *Macromolecules* **28**, 552 (1995); D. I. Christie and R. G. Gilbert, *Macromol. Chem. Phys.* **197**, 403 (1996); errata: D. I. Christie and R. G. Gilbert, *Macromol. Chem. Phys.* **198**, 663 (1997).

94. J. P. A. Heuts, T. P. Davis, and G. T. Russell, *Macromolecules* **32**, 6019 (1999).

95. P. A. Clay and R. G. Gilbert, *Macromolecules* **28**, 552 (1995).

96. C. H. Kurz, Ph.D. thesis, Göttingen, 1995.

97. S. Beuermann, M. Buback, and C. Schmaltz, *Ind. Eng. Chem. Res.* **38**, 3338 (1999).

98. M. Buback and C. Kowollik, *Macromolecules* **31**, 3211 (1998).

99. M. Buback and C. Kowollik, *Macromol. Chem. Phys.* **200**, 1764 (1999).

100. H. K. Mahabadi, *Macromolecules* **18**, 1319 (1985).

101. A. R. Khokhlov, *Makromol. Chem., Rapid Commun.* **2**, 633 (1981).

102. T. Yasukawa and K. Murakami, *Polymer* **12**, 1423 (1980).

103. O. F. Olaj, I. Bitai, and G. Gleixner, *Makromol. Chem.* **186**, 2569 (1985).

104. O. F. Olaj and G. Zifferer, *Eur. Polym. J.* **25**, 961 (1989).

105. J. B. L. de Kock, Ph.D. thesis, Eindhoven, 1999; J. B. L. deKock, B. Klumperman, A. M. van Herk, and A. L. German, *Macromolecules* **30**, 6743 (1997).

106. O. F. Olaj, P. Vana, A. Kornherr, and G. Zifferer, *Macromol. Chem. Phys.* **200**, 2031 (1999).

107. C. Barner-Kowollik, J. P. A. Heuts, and T. P. Davis, *J. Polym. Sci.—Chem.* **39**, 656 (2001).

108. G. Moad and D. H. Solomon, in *Azo and Peroxy Initiators* G. Moad, and D. H. Solomon, eds. Pergamon Press, London, 1989, Vol. 3, p. 97; G. Moad and D. H. Solomon, in *Chemistry of Bimolecular Termination*, G. Moad and D. H. Solomon, eds., Pergamon Press, London, 1989, Vol. 3, p. 147.

109. M. D. Zammit, T. P. Davis, D. M. Haddleton, and K. G. Suddaby, *Macromolecules* **30**, 1915 (1997).

5 Copolymerization Kinetics

MICHELLE L. COOTE* and THOMAS P. DAVIS

University of New South Wales, Sydney, Australia

CONTENTS

5.1 INTRODUCTION

In free-radical copolymerization a mixture of two or more monomers are polymerized in order to produce polymers consisting of units from each constituent monomer. This provides an extremely powerful synthetic route to a diverse range of materials. The copolymers exhibit properties combining those from the parent homopolymers. The basic kinetic model describing propagation in copolymerization was developed in the early 1940s, and scientific research into copolymerization has almost exclusively focused on a model-based approach; a model is often assumed

---

*Current address: Research School of Chemistry, Australian National University, Canberra ACT 0200, Australia.

and then model-dependent parameters are deduced and then reported and discussed. The drawback with this approach is that the model-dependent parameters can easily be overinterpreted. By definition, a model is not reality, and therefore some attention needs to be devoted to the shortcomings of models and where they fail. It is also clear that using models as a route to understanding fundamental reaction kinetics can often be flawed as the adoption of the model and its presumptions can limit the outcomes. The general adoption of the terminal model has occurred because of its overall utility in industrial applications. However, with the advent of pulsed laser polymerization, ESR methods, and ab initio calculations it has become clear that the terminal model is a crude representation of radical copolymerzation reactions, and that the widely used reactivity ratios are in fact model-dependent parameters that do not represent ratios of elementary rate constants. In this chapter, the basic models for copolymerization kinetics are outlined and a pragmatic discussion is included as a guideline on measuring and interpreting the model-dependent parameters that can be accessed via indirect approaches. The most recent advances in experimental approaches to determining termination rate coefficients in copolymerization have also led to a much clearer understanding of the important mechanistic aspects that influence kinetics of cross-termination reactions, and these are also discussed.

In essence, it is important to recognize that the years of research since the early 1940s, with the inception of the terminal model and the ensuing cross-termination factor based on chemical-controlled termination reactions, have seen considerable advances in experimental techniques for probing copolymerization kinetics. This has resulted in a more complex but richer understanding of the mechanistic features of copolymerization than that proposed in the earliest kinetic models.

5.2   GENERAL FEATURES OF POLYMERIZATION KINETICS

As in hompolymerization, free-radical copolymerization proceeds via initiation, propagation, and various types of chain-stopping reactions (such as chain transfer to various types of substrate and radical–radical termination via combination or disproportionation) (see Scheme 5.1).

$$
\begin{aligned}
\text{Initiation:} \quad & I{-}I \;\longrightarrow\; 2\,I\cdot \\[4pt]
\text{Propagation:} \quad & I\cdot && +\;M \;\longrightarrow\; I{-}M\cdot \\
& I{-}M\cdot && +\;M \;\longrightarrow\; I{-}M{-}M\cdot \\
& I{-}M{-}M\cdot && +\;M \;\longrightarrow\; I{-}M{-}M{-}M\cdot \\
& I{-}M{-}M{-}M\cdot && +\;M \;\longrightarrow\; I{-}M{-}M{-}M{-}M\cdot \\
& \quad\cdots \\[4pt]
\text{Transfer:} \quad & R{-}M\cdot \;+\; S \;\longrightarrow\; R{-}MH \;+\; S\cdot \quad \text{or} \\
& R{-}M\cdot \;+\; M \;\longrightarrow\; R{=}M \;+\; M\cdot \\[4pt]
\text{Termination:} \quad & R{-}M\cdot \;+\; R'{-}M\cdot \;\longrightarrow\; R{-}M{-}M{-}R' \quad \text{or} \\
& R{-}M\cdot \;+\; R'{-}M\cdot \;\longrightarrow\; R{=}M \;+\; M{-}R'
\end{aligned}
$$
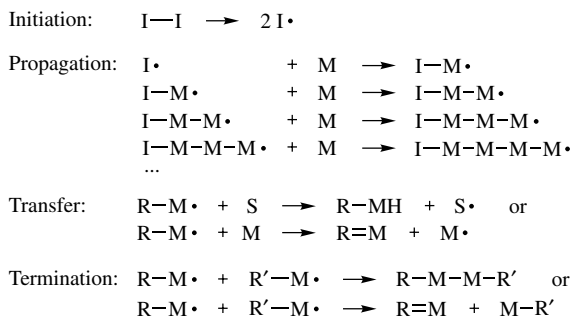
Scheme 5.1   General reaction scheme for free-radical polymerization.

As in homopolymerization, the overall steady-state polymerization rate and related quantities such as molecular weight and molecular weight distribution are a function of the rates of these individual steps, although the rate coefficients for the individual steps have to be replaced by averages over the composition of the different possible polymeric radicals. For instance, in the simplified case of no chain transfer, equations for the overall polymerization rate and number average molecular weight in terms of the average rates of the initiation, propagation and termination steps, are as follows:[1]

$$R_p = \langle k_p \rangle [M] \left(\frac{R_i}{2 \langle k_t \rangle} \right)^{1/2} \tag{5.1}$$

$$\bar{M}_n = M_0 \frac{R_p}{R_i} \qquad \text{(for termination by disproportionation)}$$

$$= 2 M_0 \frac{R_p}{R_i} \qquad \text{(for termination by combination)} \tag{5.2}$$

Even in homopolymerization, these equations can be difficult to use as there are chain length effects on the various termination rate coefficients and hence k_t has to be replaced by the average value $\langle k_t \rangle$—a weighted average of the termination rates of radicals of all different chain lengths:

$$\langle k_t \rangle = \sum_{n=1}^{\infty} \sum_{m=1}^{\infty} k_{t(n,m)} \frac{[P_n][P_m]}{[P]} \tag{5.3}$$

As can be seen in this equation, the chain-length-dependent $\langle k_t \rangle$ is a function of the molecular weight distribution of the living chains and, since this is itself a function of $\langle k_t \rangle$, this already makes modeling very complicated. The problems of modeling polymerization rates and molecular weight distributions while taking into account the chain-length-dependence of k_t were discussed in Chapter 4. In this chapter we will concentrate primarily on the additional problems posed by the presence of more than one type of monomer in the polymerization system.

In copolymerization the presence of more than one type of monomer adds an extra degree of complexity to the reaction kinetics, as can be seen in Scheme 5.2. At each propagation step, there is a choice of two different monomers that can be incorporated into the growing polymer radical and this, as is clear from Scheme 5.2, can rapidly give rise to countless different propagating radicals, each differing in their overall composition and sequence distribution and, perhaps even more importantly, their active chain-end composition. Since the rate constants of the various initiation, propagation, termination, and transfer reactions depend on the composition of the radical and (where relevant) monomer, in a free-radical copolymerization system, these various reactions may simultaneously proceed via a variety of different rate constants. Hence, for copolymerization, the kinetic equations for homopolymerization need to be modified by replacing the homopolymerization rate constants with expressions for their average values in copolymerization.
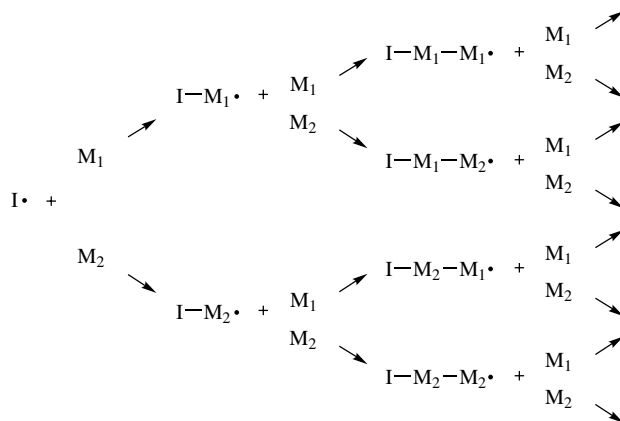
Scheme 5.2 Possible propagation sequences in free-radical copolymerization.

It is also clear from Scheme 5.2 that the presence of more than one type of structural unit adds an extra dimension to the range of possible polymers that might be assembled from a given monomer mixture. In addition to chain length and stereochemistry, copolymers can differ in their

- *Composition*—the relative amounts of each monomer unit incorporated into the copolymer.
- *Sequence distribution* or *microstructure*—the way in which these monomer units are arranged within a polymer chain. Depending on the selectivity of the propagating radicals (and the polymerization conditions), a wide range of microstructures are possible, ranging from strictly alternating copolymers (i.e., ABABABABABAB...) to block copolymers (i.e., AAAABBBBBBAA AAAA...) with any number of different random or semirandom structures (e.g., BAAABBABABBB...) in between.
- *Chain-end composition*—which monomer unit (or sequence of monomer units) is at the active chain end when it is terminated via a disproportionation reaction or via chain transfer. This is important if, as is often the case, a specific end functionality is required.

Since these quantities can have an enormous effect on the chemical and physical properties of copolymers, it is important to be able to model and hence control them. Hence, copolymerization kinetics are complicated by the need to derive expressions not only for the average values of the different primary rate constants but also for additional quantities such as copolymer composition, sequence distribution, and chain-end compositions. Expressions for these additional quantities follow directly from the kinetics of the various individual steps (see Table 5.1).

The key to copolymerization kinetics is thus to derive expressions for the average rates of the different mechanistic steps (i.e., initiation, propagation, termination, and

TABLE 5.1   Role of the Different Mechanistic Steps in Copolymerization in Determining Copolymer Properties

	Initiation	Propagation	Termination	Transfer
Overall polymerization rate	✓	✓	✓	✓
Molecular weight distribution	✓	✓	✓	✓
Composition		✓		
Sequence distribution		✓		
Chain-end composition		✓	✓	✓
Oligomer composition	✓	✓	✓	✓

transfer) as this enables modeling of not only the overall polymerization rates and resulting molecular weight distributions but also modeling (and hence control) of other important copolymer properties such as composition, sequence distribution and chain-end composition. In theory, such expressions are weighted averages of the rates of all the different possible variations on the particular mechanistic step in question, as corresponding to all the possible compositions of the radical(s), monomer(s), and/or substrate(s) involved in the reaction. However, as is clear from Scheme 5.2, in practice, such expressions would be too complicated to use as, in any given free-radical polymerization system, there are countless different possible radicals present, all of which might react with each other in any combination (in the case of termination) or with either monomer or substrate, in the case of propagation and transfer. In order to address this problem, and hence derive useful models for copolymerization kinetics, simplifying assumptions must be made as to the fundamental influences of reactivity in a given reaction.

For example, in deriving a propagation model it might be assumed that only substituents on the end unit of the propagating radical and on the monomer can affect the propagation rate. Hence, although there may be countless types of propagating radicals present in the system, it is necessary to consider only the reactions of two types of radical: those ending in each of the possible monomer units. An assumption such as this enables a family of simple equations to be derived, consisting of expressions for the average rate of the type of step (in this case a propagation rate) and expressions for any other copolymer properties that depend directly on the kinetics of this step (in the case of propagation, such properties include copolymer composition, microstructure, and radical concentrations). Such families of equations are known as a *copolymerization model*.

In this chapter we show how to derive expressions for the average initiation, propagation, termination, and transfer rate coefficients in copolymerization. These expressions can be then be substituted into the homopolymerization equations for overall polymerization rate and molecular weight distributions. We also show how these can be used in expressions for predicting copolymer composition, sequence distribution, and chain-end distribution. As noted above, to derive these expressions, various assumptions have to be made about the fundamental influences on the reaction in question, with each set of assumptions giving rise to a family of equations,

known as a *copolymerization model*. Especially in the case of the propagation reaction, many different copolymerization models have been derived, some or all of which may be applicable for certain types of copolymerization systems. In this chapter we describe some of the main copolymerization models and discuss their likely applicability to the various types of copolymerization system. We then conclude with a discussion of how such models, and other mechanistic information, may be used to achieve control of overall composition and chain-end composition, sequence distribution, and possibly even stereochemistry in free-radical copolymerization.

5.3   PROPAGATION KINETICS

Copolymerization propagation kinetics have perhaps the most significant impact on copolymer properties, for they not only form an important component of the overall rate and molecular weight distribution equations but also directly govern the copolymer composition and microstructure, and the chain-end composition of the living radicals (which, in turn, affects the chain-end composition of the dead polymer). Furthermore, it is the geometry of the transition structure in the propagation reaction that governs the stereochemistry of the resulting polymer. The ability to understand the fundamental influences on the propagation reaction (from both kinetic and mechanistic points of view) thus enables these important properties to be modeled and hence controlled, simply by manipulating the reaction conditions (such as solvent type, monomer feed composition, and temperature).

5.3.1   How to Derive Copolymerization Propagation Models

In order to model the overall propagation rate of a copolymerization, and the composition and sequence distribution of the resulting copolymer, it is necessary to kinetically model each individual propagation step. This would appear (from Scheme 5.2) to involve numerous kinetic expressions, and hence, not only would the development of an overall model be very complicated, but the resulting model would also contain numerous characteristic parameters (corresponding to the numerous kinetic constants) and would thus be of little practical value. To address this problem it is necessary to reduce the number of reactions that need to be characterized. This is achieved by making simplifying assumptions as to the fundamental influences on radical reactivity, which thereby enable the large set of chemically different reactions to be grouped into a small number of sets of kinetically different reactions. Three types of such simplifying assumptions that are made in deriving a copolymerization model are as follows:

   1. *Long-Chain Assumption.* Provided the chain length of the propagating radical is greater than around three units in length, the rate of the propagation step can usually be assumed to be chain-length-independent.[2] It is thus possible to treat the reactions of long radicals that differ only in their chain length as being kinetically equivalent. However, in any free-radical polymerization the initiation

and other small-radical addition steps will nevertheless occur. For the contribution of these kinetically different steps to be ignored, the ''long-chain assumption'' is frequently made. In other words, it is assumed that the average chain length of polymer radicals is long enough for the contributions of the short-chain reactions to be negligible. On the basis of this same assumption, it can also be assumed that the effect of selective termination or transfer reactions on the relative radical concentrations is negligible. The assumption is usually valid for polymers whose average chain length is greater than around 10 monomer units. Finally, for linear polymers, the long-chain assumption directly implies the quasi-steady-state assumption.[3] This latter assumption, which states that the relative radical concentrations are constant, is used explicitly in some of the methods for deriving copolymerization models.

2. Unimportance of Remote Substituent Effects. Although the rate of the propagation reaction depends on the composition and sequence distribution of the radical, in practice the effect on radical reactivity of all except those substituents near to the active chain-end can be considered to be negligible. Thus, by assuming that substituent effects beyond some remote position on the polymer radical are insignificant, it is possible to treat the reactions of radicals differing only in their remote substituents as being kinetically equivalent. If, for instance, it is assumed that only the terminal unit of the polymer radical can affect its reactivity, then in any free-radical copolymerization it is necessary to consider only two types of radical—corresponding to the two types of terminal units. Alternatively, if it is assumed that both the terminal and penultimate units of the polymer radical can affect its reactivity, then four types of radical need to be considered, corresponding to the possible combinations of the two types of terminal and penultimate units. And so forth.

3. Side Reactions. A number of side reactions may also affect the rates of propagation of the different types of monomer and radicals. In deriving a copolymerization model, these reactions must be taken into account. Some of the types of side reactions that may affect the copolymerization kinetics include depropagation, monomer partitioning, and various forms of complex formation. Rather than include all of these side reactions (and thus end up with an absurdly complex model containing countless characteristic parameters), simplifying assumptions as to the importance or unimportance of these various types of side reactions are made. If, for instance, spectroscopic data indicate that complex formation does not occur, side reactions involving complexes can be ignored. Alternatively, if thermodynamic data indicate that the comonomers are ideally mixed, monomer partitioning may be ignored, and so forth. Some models, such as the terminal model, ignore all of these side reactions, while other models may take into account several different side reactions.

In this section we deal with copolymerization models for which the long-chain assumption is always made—models for oligomeric systems in which this assumption is not valid will be discussed in a subsequent section. Although the alternative copolymerization models all make (1) the long-chain assumption, they differ in the particular assumptions they make with respect to (2) which substituents are capable

of affecting the propagation reaction and (3) which (if any) side reactions can occur. Once these assumptions are made, it is possible to derive expressions for the overall propagation rate constant in a free-radical copolymerization, the concentrations of the different types of radicals, and the composition and sequence distribution of the resulting copolymer, as a function of the monomer concentrations (frequently expressed as molar feed fractions) and some characteristic constants (i.e., the rate coefficients or, where relevant, equilibrium constants of the individual reactions). The general procedure for deriving such equations is outlined in the Appendix, where the derivation of the terminal model equations is used as an example.

5.3.2 Examples of Copolymerization Propagation Models

5.3.2.1 Terminal Model
In the terminal model it is assumed that the terminal unit of a propagating polymer radical is the only factor influencing its reactivity, and that side reactions are not significant. As a result, there are only four types of propagation reactions in the free-radical copolymerization of any two given monomers (M_1 and M_2):

$$RM_i^{\bullet} + M_j \xrightarrow{k_{ij}} RM_iM_j^{\bullet} \qquad (i,j = 1 \text{ or } 2)$$

From this assumption, Jenkel,[4] Mayo and Lewis,[5] and Alfrey and Goldfinger[6] all independently derived an expression for copolymer composition (F_1/F_2) as a function of the monomer feed fractions (f_1 and f_2) and the reactivity ratios (r_1 and r_2) of the monomers:

$$\frac{F_1}{F_2} = \frac{f_1}{f_2} \cdot \frac{r_1 f_1 + f_2}{r_2 f_2 + f_1} \quad \text{where} \quad r_i = \frac{k_{ii}}{k_{ij}} \quad i \neq j \quad \text{and} \quad i,j = 1 \text{ or } 2 \qquad (5.4)$$

Alfrey and Goldfinger[6] also derived expressions for the sequence distribution and the number average degree of polymerization expected for a copolymerization obeying the terminal model. They later extended the terminal model to describe polymerizations involving three or more monomers.[7,8] Fukuda et al.[9] derived the following expression for the copolymerization propagation rate constant $\langle k_p \rangle$ under the terminal model:

$$\langle k_p \rangle = \frac{r_1 f_1^2 + 2f_1 f_2 + r_2 f_2^2}{[r_1 f_1 / k_{11}] + [r_2 f_2 / k_{22}]} \qquad (5.5)$$

This equation follows from the kinetic analysis of copolymerization by Melville et al.[10] and Walling,[11] who arrived at an expression for the overall rate of copolymerization, assuming a terminal model for both propagation and termination.

5.3.2.2 Explicit and Implicit Penultimate Models
In the *explicit penultimate model*, it is assumed that both the terminal and penultimate units of a polymer

radical may affect the rate of the propagation reaction. As in the terminal model, side reactions are considered to be insignificant. The explicit penultimate model was first suggested in 1946 by Merz et al.,[12] who derived equations for predicting the composition and sequence distribution under this model. A full description of the model—including an expression for $\langle k_p \rangle$—has since been provided by Fukuda et al.,[13] whose notation is used in what follows.

In the presence of a penultimate unit effect, there are eight different types of propagation reactions to characterize:

$$RM_iM_j^{\bullet} + M_k \xrightarrow{k_{ijk}} RM_iM_jM_k^{\bullet} \quad i,j,k = 1 \text{ or } 2$$

From their eight different propagation rate constants, four different monomer reactivity ratios (r_i and r_i') and two radical reactivity ratios (s_i) can be defined as follows:

$$r_i = \frac{k_{iii}}{k_{iij}} \quad r_i' = \frac{k_{jii}}{k_{jij}} \quad s_i = \frac{k_{jii}}{k_{iii}} \quad \text{where} \quad i \neq j \quad \text{and} \quad i,j = 1 \text{ or } 2$$

These are used to calculate the adjusted parameters, $\bar{r}_i$ and $\bar{k}_{ii}$:

$$\bar{r}_i = r_i'\left(\frac{f_i r_i + f_j}{f_i r_i' + f_j}\right) \qquad \text{where} \quad i,j = 1 \text{ or } 2 \quad \text{and} \quad i \neq j \qquad (5.6)$$

$$\bar{k}_{ii} = k_{iii}\left(\frac{r_i f_i + f_j}{r_i f_i + f_j/s_i}\right) \quad \text{where} \quad i,j = 1 \text{ or } 2 \quad \text{and} \quad i \neq j \qquad (5.7)$$

These are used in place of r_i and k_{ii} in the terminal model expressions for composition and $\langle k_p \rangle$ [i.e., Eqs. (5.4), (5.5), and above].

The *implicit penultimate model* was first suggested by Fukuda et al. in 1985,[9] in order to describe their observation that the terminal model could be fitted to the composition data for the copolymerization of styrene with methyl methacrylate, although it could not simultaneously describe the propagation rate coefficients. In this model, the following restriction is placed on the explicit penultimate model:

$$r_i\left(= \frac{k_{iii}}{k_{iij}}\right) = r_i'\left(= \frac{k_{jii}}{k_{jij}}\right) = \frac{k_{ii}}{k_{ij}} \quad \text{where} \quad i \neq j \quad \text{and} \quad i,j = 1 \text{ or } 2 \qquad (5.8)$$

The penultimate unit effect is thus assumed to be absent from the monomer reactivity ratios, which are equivalent to their terminal model forms, and exist only in the radical reactivity ratios (i.e., through values of $s_i \neq 1$). This amounts to assuming that the magnitude of the penultimate unit effect on reactivity is independent of the type of monomer with which it is reacting (since the equality $k_{jii}/k_{iii} = k_{jij}/k_{iij}$ follows directly from the assumption that $r_i = r_i'$). In other words, it assumed that there is a penultimate unit effect on reactivity but not selectivity. According to

this assumption [i.e., Eq. (5.8)], Eq. (5.6) collapses into

$$\bar{r}_i = r'_i \left(= \frac{k_{jii}}{k_{jij}} \right) = r_i \left(= \frac{k_{iii}}{k_{iij}} \right) = \frac{k_{ii}}{k_{ij}} \quad \text{where} \quad i \neq j \quad \text{and} \quad i, j = 1 \text{ or } 2 \quad (5.9)$$

Thus the adjusted monomer reactivity ratios of the penultimate model are replaced simply by their corresponding terminal model values. However, since the penultimate unit effect can remain in the radical reactivity ratios (i.e., through values of $s_i \neq 1$), Eq. (5.7) does not collapse to its equivalent terminal model form (i.e., $\bar{k}_{ii} \neq k_{iii}$). Since the composition and triad/pentad fraction equations contain only $\bar{r}_i$ terms, they collapse to the corresponding terminal model equations. However, since it contains both $\bar{r}_i$ and $\bar{k}_{ii}$ terms, the propagation rate equation, unit effect on the propagation rate but not the composition or sequence distribution.

5.3.2.3 *Polarity Effects*
When polar interactions are important in the transition structure of the propagation reaction, the polarity of the solvent may affect the propagation rate. This may be explained as follows. Polar interactions are said to occur when the transition structure is stabilized by charge transfer between the reacting species.[14] The amount of charge transfer, and hence the amount of stabilisation, is inversely proportional to the energy difference between the charge transfer configuration and the product and reactant configurations that combine to make up the ground-state wavefunction of the transition structure. Now it is known that polar solvents can stabilize charged species, as seen in the favorable effect of polar solvents on both the thermodynamics and kinetics of reactions in which charge is generated.[14] Thus, when charge transfer in the transition structure is important, the relative stability of the charge transfer configuration, and thus of the transition structure, will be affected by the polarity of the solvent. Hence, when polar interactions are important in a propagation reaction, a polar solvent can stabilize the transition structure and hence lower the reaction barrier.

When such effects are important, the polarity of the solvent affects radical selectivity as well as radical reactivity. This is because the extent to which charge transfer stabilization can occur, and hence the extent to which polar solvents can further enhance these effects, depends on both reacting species. For instance, in a free-radical copolymerization, it is likely that polar interactions would be more important in the cross-propagations (when the monomer and radical bear different substituents and thus have different electronic properties) than in the homopropagations (when the monomer and radical bear the same substituents). Hence the effect of solvent polarity on the stability of the transition structure (and thus the propagation rate) would generally be expected to be greater in the cross- than in the homopropagation reactions. Thus, there would be a net effect of solvent polarity on the reactivity ratios of the copolymerization (regardless of whether these polar interactions are influenced by the penultimate unit, or merely by the terminal unit).

There are two cases to consider when predicting the effect of solvent polarity on copolymerization propagation kinetics:

1. The solvent polarity is constant as a function of the monomer feed composition for the given copolymerization system, as would be the case if the solvent polarity is dominated by an added diluent, or if the comonomers have similar dielectric constants (such as in the bulk copolymerization of styrene with methyl methacrylate[15]).

2. The solvent polarity varies with the comonomer feed mixture for the given system, as would be the case in a bulk copolymerization of monomers with significantly different dielectric constants (such as in the bulk copolymerization of styrene with acrylonitrile[15]).

In case 1, the effect on copolymerization kinetics is simple. The various reactivity ratios would vary from solvent to solvent, but, for a given copolymerization system, they would be constant as a function of the monomer feed ratios. The copolymerization kinetics would simply follow the appropriate base model for that system (according to which side reactions were assumed to be important, and which units were assumed to affect radical reactivity).

In case 2, the effect of the solvent on the copolymerization kinetics is more complicated since the various reactivity ratios would not be constant as a function of the monomer feed. To model such behavior, it would first be necessary to select an appropriate base model for the copolymerization (based on the usual assumptions). It would then be necessary to replace the various reactivity ratios (included in the base model as constants) by functions of the composition of the comonomer feed mixture. These functions would need to relate the reactivity ratios to the solvent polarity, and then relate the solvent polarity to the comonomer feed composition, and would thus vary depending on the particular chemical properties of the monomers. It is therefore difficult to suggest a general kinetic model to describe these systems, but it is clear that such effects would result in deviations from the behavior predicted by their appropriate base model.

5.3.2.4 Radical Complexes

Solvents can also interfere with the propagation step via the formation of radical–solvent complexes. When complexation occurs, the complexed radicals are generally more stable than their corresponding uncomplexed radicals as it is this stabilization that drives the complexation reaction. Thus, in general, one might expect complexed radicals to propagate more slowly than their corresponding uncomplexed radicals, if indeed they propagate at all. However, in the special case that one of the comonomers is the complexing agent, the propagation rate of the complexed radical may instead be enhanced if propagation through the complex offers an alternative less energetic reaction pathway. In any case, the complexed radicals would be expected to propagate at a rate different from their corresponding free radicals; thus, the formation of radical–solvent complexes would affect the copolymerization propagation kinetics.

A terminal radical–complex model for copolymerization was formulated by Kamachi,[16] who proposed that a complex is formed between the propagating radical and the solvent (which may be the monomer), and that this complexed radical propagates at a different rate to the corresponding uncomplexed radical. Under these

conditions (and assuming that the terminal unit is the only unit affecting radical reactivity), eight different propagation reactions are used to characterize a binary copolymerization:

$$RM_i^{\bullet} + M_j \xrightarrow{k_{ij}} RM_iM_j^{\bullet} \quad \text{or} \quad RM_iM_j^{\bullet}S \quad \text{where} \quad i,j = 1 \text{ or } 2$$

$$RM_i^{\bullet}S + M_j \xrightarrow{k_{cij}} RM_iM_j^{\bullet} \quad \text{or} \quad RM_iM_j^{\bullet}S \quad \text{where} \quad i,j = 1 \text{ or } 2$$
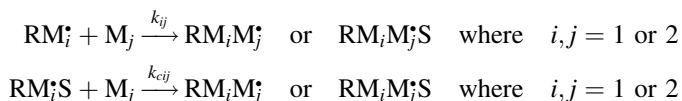
There are also two equilibrium reactions for the formation of the complex (assuming that only one complexing agent can complex with either radical):

$$RM_i^{\bullet} + S \xleftrightarrow{K_i} RM_i^{\bullet}S \quad \text{where} \quad i,j = 1 \text{ or } 2$$

On the basis of these reactions, Kamachi[16] derived expressions for the copolymer composition under this model. Later, Fukuda et al.[17] derived expressions for the composition, triad/pentad fractions, and propagation rate, by deriving expressions for $\bar{r}_i$ and $\bar{k}_{ii}$, which could be used in place of r_i and k_{ii} in the terminal model equations [Eqs. (5.4) and (5.5)]:

$$\bar{k}_{ii} = k_{ii}\frac{1 + \bar{s}_{ci}K_i[S]}{1 + K_i[S]} \tag{5.10}$$

$$\bar{r}_i = r_i\frac{1 + \bar{s}_{ci}K_i[S]}{1 + (r_i/\bar{r}_{ci}i)\bar{s}_{ci}K_i[S]} \tag{5.11}$$

where

$$r_i = \frac{k_{ii}}{k_{ij}}; \quad \bar{r}_{ic} = \frac{k_{cii}}{k_{cij}}; \quad \bar{s}_{ci} = \frac{k_{cii}}{k_{ii}}; \quad i,j = 1 \text{ or } 2, \quad \text{and} \quad i \neq j$$

Variants of this model may be derived by assuming an alternative basis model (such as the implicit or explicit penultimate model) or by making further assumptions as to the nature of the complexation reaction. For instance, in the special case that the complexed radicals do not propagate (i.e., $\bar{s}_{ci} = 0$ for all i), the reactivity ratios are not affected (i.e., $\bar{r}_i = r_i$ for all i), and the complex formation serves only to remove radicals (and monomer, if monomer is the complexing agent) from the reaction, resulting in a solvent effect that is analogous to a bootstrap effect (see Section 5.3.2.6).

5.3.2.5 Monomer Complexes   A solvent may also interfere in the propagation step via complexation with the monomer. As was the case with radical–solvent complexes, complexed monomer might be expected to propagate at a rate different from that of free monomer, since complexation might stabilize the monomer, alter its steric properties, and/or provide an alternative pathway for propagation. In examining the effect of such complexation on copolymerization kinetics, there are five different mechanisms to consider:

1. The monomer–monomer complex propagates as a single unit, competing with the propagation of free monomer.
2. The monomer–monomer complex propagates as a single unit, competing with the propagation of free monomer, but the complex dissociates during the propagation step and only one of the monomers is incorporated into the growing polymer radical.
3. The monomer–monomer complex does not propagate, and complexation serves only to alter the free monomer concentrations.
4. The monomer-solvent complex propagates, but at a rate different from that of the free monomer.
5. The monomer-solvent complex does not propagate.

Mechanisms 1–3 could apply when the complex is formed between the comonomers and mechanisms 4 and 5 should be considered in cases where the complex is formed between one of the monomers and an added solvent.

Models based on mechanisms 1 and 2 are known respectively as the monomer–monomer complex participation (MCP) and dissociation (MCD) models. Mechanisms 3 and 5 would result in a solvent effect analogous to a bootstrap effect (see discussion below), while mechanism 4 would result in a model similar to the MCD model, although it would be based on a slightly different equilibrium expression. The MCP and MCD models are outlined in the following paragraphs.

The *monomer–monomer complex participation* (MCP) *model* was first suggested by Bartlett and Nozaki,[18] later developed by Seiner and Litt,[19] and refined by Cais et al.[20] In this model, it is assumed that the two monomers can form a $1:1$ donor–acceptor complex and add to the propagating chain as a single unit in either direction. Assuming that the terminal unit is the only unit affecting radical reactivity, eight addition reactions and an equilibrium constant are required to describe the system:

$$RM_i^{\bullet} + M_j^{\circ} \xrightarrow{k_{ij}} RM_iM_j^{\bullet} \qquad \text{where} \quad i,j = 1 \text{ or } 2$$

$$RM_i^{\bullet} + M_iM_j \xrightarrow{k_{iij}} RM_iM_iM_j^{\bullet} \qquad \text{where} \quad i,j = 1 \text{ or } 2 \quad \text{and} \quad i \neq j$$

$$RM_i^{\bullet} + M_jM_i \xrightarrow{k_{iji}} RM_iM_jM_i^{\bullet} \qquad \text{where} \quad i,j = 1 \text{ or } 2 \quad \text{and} \quad i \neq j$$

$$M_1^{\circ} + M_2^{\circ} \xleftrightarrow{K} M_1M_2$$
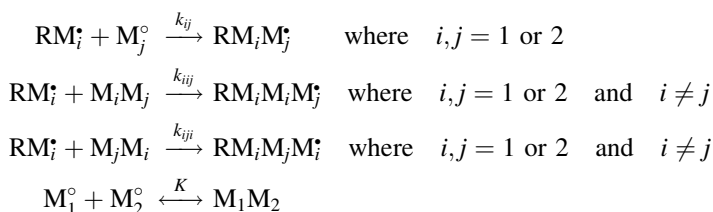
The composition and the propagation rate can be expressed in terms of the following parameters:[17]

$$\frac{F_1}{F_2} = \frac{f_1^{\circ}}{f_2^{\circ}} \frac{(A_2B_1)r_1f_1^{\circ} + (A_1C_2)f_2^{\circ}}{(A_1B_2)r_2f_2^{\circ} + (A_2C_1)f_1^{\circ}} \tag{5.12}$$

$$\langle k_p \rangle = \frac{(A_2B_1)r_1(f_1^{\circ})^2 + (A_1B_2)r_2(f_2^{\circ})^2 + (A_1C_2 + A_2C_1)f_1^{\circ}f_2^{\circ}}{(A_2r_1f_1^{\circ}/k_{11}) + (A_1r_2f_2^{\circ}/k_{22})} \tag{5.13}$$

where

$$A_1 = 1 + r_1 s_{1c} Q f_1^\circ \qquad \text{and} \quad A_2 = 1 + r_2 s_{2c} Q f_2^\circ$$

$$B_1 = 1 + s_{1c}(1 + r_{1c}^{-1}) Q f_2^\circ \qquad \text{and} \quad B_2 = 1 + s_{2c}(1 + r_{2c}^{-1}) Q f_1^\circ$$

$$C_1 = 1 + r_1 s_{1c}(1 + r_{1c}^{-1}) Q f_1^\circ \quad \text{and} \quad C_2 = 1 + r_2 s_{2c}(1 + r_{2c}^{-1}) Q f_2^\circ$$

$$2Q f_i^\circ = \{[Q(f_j - f_i) + 1]^2 + 4Q f_i\}^{1/2} - [Q(f_i - f_j) + 1] \quad \text{and} \quad Q = K[M]$$

$$f_i = \text{feed composition of } M_i \quad \text{and} \quad f_i^\circ = [M_i^\circ]/[M]$$

$$r_i = \frac{k_{ii}}{k_{ij}}; \quad r_{ic} = \frac{k_{iij}}{k_{iji}}; \quad s_{ic} = \frac{k_{iij}}{k_{iii}} \quad \text{where} \quad i, j = 1 \text{ or } 2 \quad \text{and} \quad i \neq j$$

As with all the models, variations are possible by making a different assumption as to which units can affect radical reactivity. For instance, Brown and Fujimori[21] have derived expressions for composition and sequence distribution for the "comppen" model, a complex-participation model that is based on the penultimate model.

In the *monomer–monomer complex dissociation* (MCD) *model* it is assumed that the monomer–monomer complex described in the MCP model dissociates on addition to the chain, with only one unit adding.[22] A model based on this mechanism was first formulated by Karad and Schneider[23] and later generalized by Hill et al.[24] Assuming that only the terminal unit of the radical affects the propagation step, eight rate constants and two equilibrium constants are required to describe the system:

$$\text{RM}_i^\bullet + M_j \xrightarrow{k_{ij}} \text{RM}_i M_j^\bullet \qquad \text{where} \quad i, j = 1 \text{ or } 2$$

$$\text{RM}_i^\bullet + M_j C \xrightarrow{k_{ijc}} \text{RM}_i M_j^\bullet \qquad \text{where} \quad i, j = 1 \text{ or } 2$$

$$M_i + C \xleftrightarrow{K_i} M_i C \qquad \qquad \text{where} \quad i, j = 1 \text{ or } 2$$
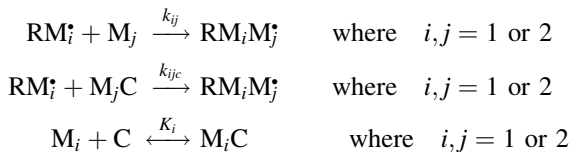
As with the penultimate and radical–complex models, it is possible to express the model in terms of equations for $\bar{r}_i$ and $\bar{k}_{ii}$, which could be used in place of r_i and k_{ii} in the terminal model equations [Eqs. (5.4) and (5.5)]:[17]

$$\bar{k}_{ii} = k_{ii} \frac{1 + s_{ic} K_i[C]}{1 + K_i[C]} \tag{5.14}$$

$$\bar{r}_i = r_i \frac{1 + s_{ic} K_i[C]}{1 + (r_i/r_{ic}) s_{ic} K_i[C]} \tag{5.15}$$

where

$$r_i = \frac{k_{ii}}{k_{ij}}; \quad r_{ic} = \frac{k_{iic}}{k_{ijc}}; \quad s_{ic} = \frac{k_{iic}}{k_{ii}}; \quad i, j = 1 \text{ or } 2 \quad \text{and} \quad i \neq j$$

This form of the model is for monomer–solvent complexes generally. Under the MCD model, the complexing agent C is the other monomer (M_j). As with all the

solvent effects models, variations are possible by making a different assumption as to which units can affect radical reactivity.

5.3.2.6 Monomer Partitioning: The Bootstrap Effect

In the bootstrap model, solvent effects on the propagation rate are attributed to solvent partitioning and the resulting difference between bulk and local monomer concentrations. In this way, a solvent could affect the measured propagation rate coefficient without changing the reactivity of the propagation step. Bootstrap effects may arise from a number of different causes. As noted above, when radical–solvent or monomer–solvent complexes form and the complexes do not propagate, the effect of complexation is to alter the effective radical or monomer concentrations, thereby causing a bootstrap effect. Alternatively, a bootstrap effect may arise from some bulk preferential sorption of one of the comonomers around the growing (and dead) polymer chains. This might be expected to occur if one of the monomers is a poor solvent for its resulting polymer. A bootstrap effect may also arise from a more localized form of preferential sorption in which one of the comonomers preferentially solvates the active chain end rather than the entire polymer chain. In all cases, the result is the same—the effective free-monomer and/or radical concentrations differ from those calculated from the monomer feed ratios, leading to a discrepancy between the predicted and actual propagation rates.

Copolymerization models based on a bootstrap effect were first proposed by Harwood[25] and Semchikov.[26] Harwood suggested that the terminal model could be extended by the incorporation of an additional equilibrium constant relating the effective and "bulk" monomer feed ratios. Different versions of this so-called bootstrap model may be derived depending on the baseline model assumed (such as the terminal model or the implicit or explicit penultimate models) and the form of equilibrium expression used to represent the bootstrap effect. In the simplest case, it is assumed that the magnitude of the bootstrap effect is independent of the comonomer feed ratios. Hence, in a bulk copolymerization, the monomer partitioning may be represented by the following equilibrium expression:

$$\frac{f_1}{f_2} = K\left(\frac{f_{1,\text{bulk}}}{f_{2,\text{bulk}}}\right) \tag{5.16}$$

The equilibrium constant K may be considered as a measure of the bootstrap effect. Using Eq. (5.16) to eliminate the effective monomer fractions (f_1 and f_2) from the terminal model equations [Eqs. (5.4) and (5.5)], replacing them with the measurable "bulk" fractions ($f_{1,\text{bulk}}$ and $f_{2,\text{bulk}}$), the following equations for composition[27] and $\langle k_p \rangle$ may be derived:[28]

$$\frac{F_1}{F_2} = \left(\frac{Kf_{1,\text{bulk}}}{f_{2,\text{bulk}}}\right)\left(\frac{r_1 Kf_{1,\text{bulk}} + f_{2,\text{bulk}}}{r_2 f_{2,\text{bulk}} + Kf_{1,\text{bulk}}}\right) \tag{5.17}$$

$$\langle k_p \rangle = \left(\frac{1}{f_{2,\text{bulk}} + Kf_{1,\text{bulk}}}\right)\left(\frac{r_1 K^2 f_{1,\text{bulk}}^2 + 2Kf_{1,\text{bulk}}f_{2,\text{bulk}} + r_2 f_{2,\text{bulk}}^2}{[r_1 Kf_{1,\text{bulk}}/k_{11}] + [r_2 f_{2,\text{bulk}}/k_{22}]}\right) \tag{5.18}$$

It should be noted that these equations are applicable to a bulk copolymerization. When modeling solution copolymerizations under the same conditions, the same equations may be used for predicting copolymer composition since it is only the relationship between bulk and local monomer feed ratios that determines the effect on the composition and microstructure of the resulting polymer. However, some additional information about the net partitioning of monomer and solvent between the bulk and local phases is required before the propagation rate can be modeled. It should be observed that in a low-conversion bulk copolymerization, knowledge of the monomer feed ratios automatically implies knowledge of the individual monomer concentrations since, as there are no other components in the system, the sum of the monomer fractions is unity. However, in a solution copolymerization there is a third component (the solvent), and the monomer concentrations depend on not only their feed ratio but also the solvent concentration. Modeling of the propagation rate in a solution copolymerization could be achieved by rewriting the preceding equilibrium expression in terms of molar concentrations (rather than comonomer feed ratios), and including the solvent concentration in this expression.

The bootstrap model may also be extended by assuming an alternative model (such as the explicit penultimate model) as the baseline model, and also by allowing the bootstrap effect to vary as a function of monomer feed ratios. Closed expressions for composition and sequence distribution under some of these extended bootstrap models may be found in papers by Klumperman and co-workers.[27,29]

5.3.2.7   *Depropagation*

All of the models discussed thus far have assumed that the propagation steps are irreversible. However, while this is usually a reasonable assumption, at high temperatures (and, for some bulky or exceptionally stable monomers, even at low temperatures) the depropagation reaction is significant. Consideration of the depropagation reactions leads to kinetic models that are quite different from the terminal model, and thus some deviations from the terminal model may be caused by the reversibility of one or more of the propagation steps. A large number of depropagation models are possible, depending on both the basis model assumed and the assumptions that are made as to the nature of the depropagation reaction (such as which units can depropagate, and which units of the polymer radical can affect the depropagation rate). Early depropagation models were derived by Barb[30] (who incorporated depropagation into a simplified terminal MCP model), and Walling[31] (who incorporated depropagation into a simplified penultimate model). Lowry[32] and later Wittmer[33,34] derived composition equations for a number of different sets of assumptions concerning the depropagation reaction, assuming the terminal model for propagation. Howell et al.[35] later generalized these equations, and provided corresponding expressions for the sequence distribution. Expressions for the propagation rate coefficient for some of these cases have been published by Martinet and Guillot[36] and by Kukulj and Davis.[37] Given the large number of possible depropagation models, the various equations will not be reproduced here but can be found in the original papers.

5.3.3   Model Discrimination: Which Model to Use for a Given System

The choice of copolymerization model for any given system is often one of great debate in the polymer literature. This, to a large extent, is caused by the fact that all the alternative models contain a number of characteristic constants (such as monomer and radical reactivity ratios). Since these are difficult to measure directly, they are usually (if not always) estimated by treating them as adjustable parameters and fitting the copolymerization model to the available data. As a result, many different models can often be made to fit the same experimental data. If the purpose of the model is merely to provide a shorthand for the existing experimental data, then, provided the model provides a good fit to that data, any of the fitted models are appropriate to use. If, however, the estimated parameters are then to be used to make other model predictions or to deduce something about the reaction mechanism, then it is necessary to select the copolymerization model with the correct assumptions.

In this section we concentrate on which assumptions are likely to be valid for different types of copolymerization system. In doing this, we make a distinction between what we refer to as a "basis model"—a model containing the set of assumptions likely to be applicable to most of the copolymerization systems—and models for "exceptional systems" in which additional system-specific influences are likely to be operating in conjunction with those accounted for by the basis model. We have reviewed and assessed the experimental evidence for the different copolymerization models for both "basis" systems[38] and exceptional systems[39] and will not attempt to reproduce these reviews here. Instead, we merely outline the main conclusions of this work and make some general comments concerning the applicability of the alternative models.

5.3.3.1   *Basis Model*   For many years people believed that the terminal model was the basis of copolymerization propagation kinetics because it could be fitted to the composition data for most systems tested. However, in 1985 Fukuda et al.[9] demonstrated that the terminal model failed to predict the propagation rate coefficients for the copolymerization of styrene with methyl methacrylate—a system for which the composition data had been widely fitted by the terminal model (see Fig. 5.1) These results were later confirmed by several independent groups for both the styrene/methyl methacrylate system (under a wide range of different conditions) and several other copolymerizations—indeed for almost all systems so far tested.[38] It now appears likely that the failure of the terminal model to describe simultaneously the composition and propagation rate coefficients of ordinary free-radical copolymerization systems is general—where the terminal model is applicable only to those exceptional systems in which the comonomers have very similar reactivities.

Although there is strong evidence against the terminal model, there has been much reluctance to abandon this model since this would also entail abandoning the 50 years of terminal model reactivity ratios that have been and continue to be published (see, e.g., the large listing of terminal model reactivity ratios in the
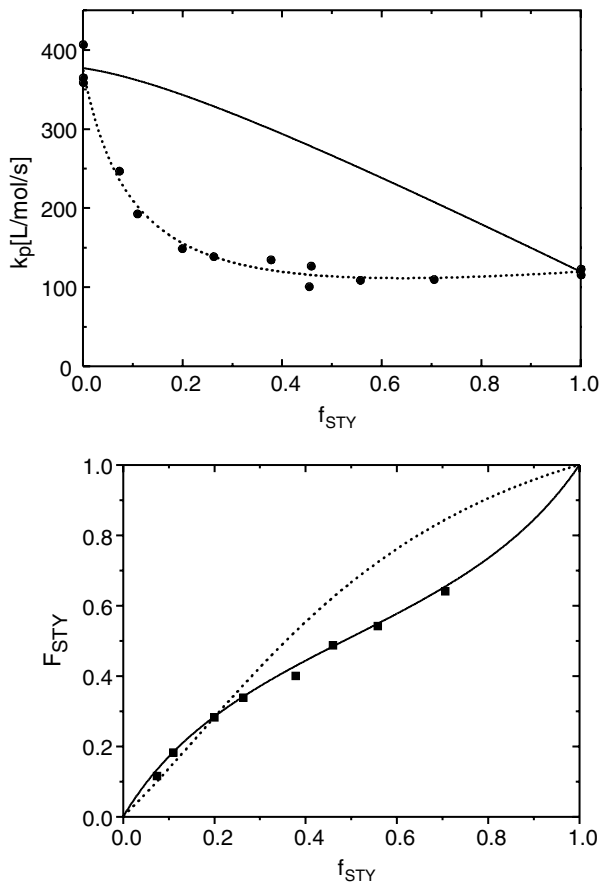
Figure 5.1   Shown here is (a) Fukuda's 40°C $\langle k_p \rangle$ data and (b) Fukuda's 40°C composition data.[9] The solid line on each graph represents the terminal model predictions using the reactivity ratios that provide the best fit to the composition data ($r_{STY} = 0.523$ and $r_{MMA} = 0.460$), while the dotted line in each graph represents the terminal model predictions using the reactivity ratios that provide the best fit to the $\langle k_p \rangle$ data ($r_{STY} = 2.5724$ and $r_{MMA} = 0.7973$). Clearly the terminal model can fit the composition or the $\langle k_p \rangle$ data but not both simultaneously.

Polymer Handbook[40]), and the various empirical schemes (such as the Patterns[41] and Q–e schemes[42]) that have been developed for predicting these parameters. The implicit penultimate model was proposed as a solution to this problem. As seen above, by assuming that the penultimate unit affected only the reactivity but not the selectivity of the propagating radical, it is possible to obtain a copolymerization model that retains the terminal model composition equation but includes a nonterminal model $\langle k_p \rangle$ equation. This thus enabled the failure of the terminal model $\langle k_p \rangle$ equation to be accounted for without abandoning the terminal model composition equation and the accompanying large database of reactivity ratios.

However, experimental and theoretical work has shown that the *assumptions* of the implicit penultimate model are unlikely to be applicable to the majority of copolymerization systems. We have published a review of this evidence,[38,43] which draws on direct experimental and theoretical measures of reactivity ratios, model testing in a range of copolymerization systems, and other tests of the mechanism of the propagation step via, for example, the examination of solvent effects on reactivity ratios. These studies provide strong evidence for penultimate unit effects but, in all cases where penultimate unit effects have been measured directly, effects on radical selectivity have been shown to be significant. In other words, all available evidence contradicts the assumption of the implicit penultimate model that the penultimate unit affects reactivity but not selectivity.

Furthermore, the most recent theoretical studies have provided a rationalisation for this result, which suggests that it is likely to be a general feature of free-radical polymerization. As noted earlier, for a penultimate unit effect in the reaction barrier to be *implicit*, it is necessary for this penultimate unit effect to occur in the absence of polar, steric, or other forms of direct interaction that, by their very nature, are dependent on and will thus vary with the chemical structure of the reacting monomer. As Fukuda argued,[13] an implicit effect could occur if the penultimate unit affected radical stability and hence the reaction enthalpy, since this radical stabilization effect would also appear in the barrier via the Evans–Polanyi rule. However, high-level ab initio molecular orbital calculations of a representative range of model propagation reactions have shown that, although penultimate unit effects in radical stability are significant, these effects largely cancel from the reaction barrier—owing to the early transition structure in these exothermic reactions.[44] As a result, for such a penultimate unit effect in the barrier to be significant, the corresponding effect on radical stability has to be enormous and thus requires substituents with very strong electron-withdrawing or electron-donating properties—substituents that are thus susceptible to polar interactions and lead to explicit penultimate unit effects. Given that the majority of copolymerization systems have highly exothermic propagation steps and thus early transition structures, it would seem that, in general, implicit radical stabilization penultimate unit effects are unlikely to occur in the absence of explicit polar or steric penultimate unit effects. An experimental paper[45] has reinforced this point by identifying significant entropic factors playing a role in the penultimate unit effect confirming predictions made in an earlier theoretical study.[46]

Finally, it should be noted that both the implicit and explicit penultimate models—and any number of other models with a suitable number of adjustable parameters—can be made to fit existing data. Hence, owing to their adjustable parameters, it is not possible to test the physical validity of these and other alternative models in this way.[47,48] Nonetheless, some direct evidence against the physical basis of the implicit penultimate model has been provided in simple model-fitting studies of para-substituted styrene systems[49] Fukuda's radical stabilisation model[13]—the theoretical justification of the implicit penultimate model—makes the further prediction that the products of the monomer and radical reactivity ratios are equal. However, in copolymerizations of sterically similar but electronically different para-substituted styrene monomers, these products were shown to be significantly

different from each other, thereby providing direct evidence against the physical basis of the implicit model in these copolymerization systems.[49]

To summarize, we know first from simple model-testing studies spanning the last two decades that, for almost all systems tested, the terminal model can be fitted to $\langle k_p \rangle$ or composition data for a copolymerization system, but not both simultaneously. More recent experimental and theoretical studies have demonstrated that the assumption of the implicit penultimate model—that the penultimate unit affects radical reactivity but not selectivity—cannot be justified. Therefore, on the basis of existing evidence, the explicit penultimate model should replace the terminal model as the basis of free-radical copolymerization propagation kinetics, and hence *the failure of the terminal model $\langle k_p \rangle$ equation must be taken as a failure of the terminal model and hence of the terminal model composition equation.* This means that the terminal model composition equation is not *physically valid* for the majority of systems to which it has been applied. As will be discussed in detail in the following section, this result has profound implications for the status of the large database of terminal model reactivity ratios that have been and continue to be published. For the remainder of the current section the likelihood of further deviations from the terminal model—arising from more system-specific side reactions—will be discussed.

5.3.3.2 Exceptional Systems

It is likely that side reactions are important in a large number of copolymerization systems. As seen above, their presence further complicates the copolymerization kinetics by adding extra parameters to the copolymerization models, thereby making model discrimination even more difficult. Indeed (with the possible exception of those few systems that have been shown to obey the terminal model in all respects), it is very difficult to find any copolymerization system for which there is consensus about the type of copolymerization model that should be applied. There is, however, strong independent evidence for the various types of side reaction in specific copolymerization systems and hence for these systems, such side reactions need to be incorporated into copolymerization models and taken into account when studying the propagation reaction. Indeed, for some systems, the presence of side reactions such as complexation may provide a means of controlling the composition and microstructure of the copolymer and, in some cases, even its stereochemistry. In what follows, we make a few general comments about the types of system in which the various side reactions are likely to be occurring.

Depropagation is known to become significant with increasing polymerization temperature and most polymerizations are known to have a ceiling temperature beyond which polymerization will not proceed. This arises because of the exothermic and exentropic nature of the propagation step for most polymerization reactions (i.e., since $\Delta G = \Delta H - T\Delta S$ and both ΔH and ΔS are negative, there will exist a temperature T_c such that for all $T > T_c, \Delta G > 0$). For most polymerization systems, these ceiling temperatures are well above ordinary operating conditions; however, for polymerizations involving exceptionally stable or bulky monomers such as CO, SO_2, and α-methyl styrene, depropagation is significant at much lower temperatures

and thus needs to be incorporated into copolymerization models. The importance of depropagation in a particular system can be determined directly from measurements of the entropy and enthalpy of the propagation reaction, or indirectly by measuring the ceiling temperature of each comonomer. The use of monomers such as α-methyl styrene to assist in the control of molecular weight by exploiting their slow propagation kinetics is often used in industry as a facile method of reaction control.[50,51]

Monomer–monomer complexes are known to form in solutions containing an electron-donor monomer with an electron-acceptor monomer. Many such complexes have been detected spectroscopically,[52] and one of the best known examples is that between maleic anhydride and styrene. There has been much dispute over the role these complexes play in the reaction mechanism, concerning, for example, whether they can propagate via an MCP or MCD mechanism, or whether they are unreactive and merely result in a bootstrap effect. For some complexes, the heat of formation is less than the heat of propagation, and hence it seems unlikely that the MCP model could be appropriate for these systems as the complex should be disrupted during the propagation step. In other systems, however, this is not the case and there is reasonable circumstantial evidence that these complexes could be propagating as a single unit. For instance, it has been observed that in the copolymerization of *N*-phenylmaleimide with chloroethyl vinyl ether, the stereochemistry at succinimide units is predominately cis (as it would be in the complex) and random elsewhere, and further that the proportion of cis linkages was correlated with the variables with which the concentration of the complex was also correlated.[53] It seems likely that, depending on factors such as the strength of the complex, the role of monomer–monomer complexes in free-radical copolymerization will vary and model discrimination should be on a case-by-case basis. However, where there is (spectroscopic) evidence for their existence, they must always be taken into account when deriving copolymerization models.

Radical–solvent complexes are more difficult to detect spectroscopically; however, they do provide a plausible explanation for many of the solvent effects observed in free-radical homopolymerization, particularly those involving unstable radical intermediates (such as vinyl acetate), where complexation can lead to stabilization. For instance, Kamachi[54] observed that the homopropagation rate of vinyl acetate in a variety of aromatic solvents was correlated with the calculated delocalization stabilization energy for complexes between the radical and the solvent. If such solvent effects are detected in the homopolymerization of one or both of the comonomers, then they are likely to be present in the copolymerization systems as well. Indeed, radical–complex models have been invoked to explain solvent effects in the copolymerization of vinyl acetate with acrylic acid. Radical–solvent complexes are probably not restricted merely to systems with highly unstable propagating radicals. In fact, these complexes have even been proposed to explain the effects of some solvents (such as benzyl alcohol, *N,N*-dimethyl formamide, and acetonitrile) on the homo- and/or copolymerizations of styrene and methyl methacrylate.[55–57] Certainly, radical–solvent complexes should be considered in systems

where there is a demonstrable solvent effect in the copolymerizations and/or in the respective homopolymerizations.

Polarity effects can also result in solvent effects in free-radical copolymerization. Theoretical studies[44,58–60] of small-radical addition reactions suggest that in a wide range of cross-propagation reactions, the transition structure is stabilized by the contribution of charge transfer configurations. When this is the case, the extent of stabilization (and hence the propagation rate) will be influenced by the dielectric constant of the reaction medium. Solvent effects on reactivity ratios have been known for a long time, and at least some of these—for instance, those for styrene-methyl methacrylate copolymerization[61–63] and styrene–acrylonitrile copolymerization[64,65] in a variety of solvents—have been shown to correlate with the dielectric constant of the reaction medium. Furthermore, it is possible that solvent effects in other systems may be in part attributable to polarity effects, although additional effects (such as radical–solvent complexes or monomer partitioning) obscure a direct correlation. As noted above, polarity effects need only be explicitly considered in a copolymerization model if the polarity of the reaction medium varies significantly as a function of the monomer feed fraction (as it would in a bulk copolymerization of two monomers with widely differing dielectric constants). However, it is worth noting that polarity effects are likely to be operating at least to some extent in copolymerizations of monomers with even moderately different electronegativities and, where such effects do occur, the reactivity ratios (and hence composition and sequence distribution) can be manipulated by varying the solvent polarity.

Bootstrap effects arise from a number of different causes. For instance, a bootstrap effect can be expected if there is preferential sorption of one of the monomers around the growing polymer chain, as might be expected if one of the monomers is a poor or nonsolvent for the resulting polymer. This can sometimes be established by examining the appropriate polymer–solvent interaction parameters. Nonideal mixing of the comonomers can also be independently established via measurements of solution thermodynamics. Indirect evidence for bootstrap effects arising from preferential solvation of the polymer chain can be obtained by examining the copolymer composition as a function of molecular weight, since it would be expected that this type of bootstrap effect would lead to chain length effects on copolymer composition, even for nonoligomeric systems that would normally be expected to satisfy the long-chain assumption. On the basis of this method and measurements of solution thermodynamics, Semchikov[26,66] has shown that such bootstrap effects do indeed operate in a number of bulk copolymerization systems, including AN-STY, STY-MA, VAC-STY, and VAc-NVP, but not in the system STY-MMA (at 298–343 K). Bootstrap effects can also be expected if unreactive monomer–monomer, monomer–solvent, radical–solvent, or radical–monomer complexes form. As noted above, there is evidence for many of these complexes in certain types of system, although there is frequently dispute as to the role these complexes play in the reaction mechanism. Bootstrap effects should be considered when attempting to model systems for which there is demonstrable existence of such complexes.

5.3.4   Practical Copolymerization Kinetics: Recommendations for the Future

Experimental and theoretical studies of copolymerization kinetics have overturned the long-held view that the majority of copolymerization systems obey the terminal model.[38,43] As outlined above, model-fitting studies since 1985 have clearly demonstrated that the terminal model may be fitted to either the composition or $\langle k_p \rangle$ data for a given system but not both simultaneously. In addition, theoretical studies have shown that the failure of the terminal model to fit simultaneously both the composition and $\langle k_p \rangle$ data of a system necessarily implies the failure of its assumptions for either. Hence, in order to provide an accurate physical description of the majority of copolymerization systems, penultimate unit effects need to be incorporated into copolymerization models. Furthermore, there is strong evidence that numerous additional effects—such as depropagation, complex formation, and partitioning—are important in specific systems, and these will further complicate the propagation kinetics.

This comprehensive failure of the terminal model has profound consequences for the status of the existing large database of terminal-model-derived reactivity ratios. In particular, their physical significance—as a measure of the selectivity of a given radical toward two alternative monomers—is severely undermined, since they are based on a physically incorrect model. At best they will provide a qualitative guide to average radical selectivities but are not suitable for quantitative mechanistic studies. Furthermore, while they can reproduce the composition data from which they were estimated, they cannot be used to make reliable predictions of composition data under different experimental conditions (such as in a different solvent) or predictions of other quantities, such as propagation rate coefficients or sequence distributions. This failure of the terminal model also raises a broader problem with regard to the status of model fitting in general, as a means of studying the reaction mechanism in free-radical polymerization. In what follows, these problems will be discussed and possible strategies for addressing them proposed. In order to do this, it is important to make a clear distinction (often neglected in the literature) between two fundamentally different goals of model fitting:

1. *Descriptive*. Using a model merely as an accurate shorthand for tables of already measured experimental data, thereby enabling a large set of data to be stored in the form of a small set of parameters.
2. *Mechanistic*. Choosing the model that provides an accurate account of the chemical processes occurring in the system so that the model parameters mean something in chemical terms (i.e., refer to actual rate coefficients, equilibrium constants, etc.) and can thus be used in their own right to deduce something about the reaction mechanism or to make reliable predictions of other as yet unmeasured quantities.

It might be suggested that this is an unnecessary distinction and that all that is necessary is to identify the mechanistically correct model that, ipso facto, is, of course, the descriptively correct model. However, for copolymerization kinetics there are two main problems with this approach.

The first problem is that choosing the mechanistically correct model is not at all a straightforward process. As noted above, the alternative copolymerization models contain a large number of characteristic constants that are not easily measured directly and are thus usually estimated as part of the model-fitting process. As a result, any number of models can be made to fit the same experimental data. Although it may be possible to rule out some of the alternative models on the basis of independent experimental and theoretical studies of the reaction mechanism (e.g., spectroscopic studies may enable one to rule out models involving complexes for a given system), it will nonetheless be difficult to be absolutely sure that the mechanistically correct model has been selected.

The second problem is that any mechanistically realistic model will contain a large number of these adjustable parameters, which makes it difficult to estimate them accurately and precisely. As was seen above, the majority of copolymerization systems require at the very least the general (or explicit) penultimate model to describe their behavior. This model contains eight different parameters, including six reactivity ratios that are not directly measured but instead estimated by fitting the model to the data. In addition, it was seen that a large number of systems also require other effects (such as solvent effects or depropagation) to be taken into account, and these add several more parameters (equilibrium constants for partitioning or complex formation, rate constants for additions involving complexes, depropagation rate coefficients, etc.) to the model. Again, most of these quantities are difficult to measure directly, and thus they further increase the number of adjustable parameters in the model-fitting process. As a result, the mechanistically correct model will usually contain more adjustable parameters than are required (mathematically) to fit the data. This is not to say that these extra parameters are superfluous in a mechanistic sense—merely that they should not be estimated in this manner. When there are more adjustable parameters than effective degrees of freedom in the data, the uncertainties in the parameter estimates are large and highly correlated with each other. Indeed this problem is regularly encountered even when applying a two-parameter fit of the mechanistically oversimplified terminal model to composition data. This can be seen in Fig. 5.2a, a plot of the 95% joint confidence intervals for the reactivity ratios of styrene with methyl methacrylate, as estimated from various sets of experimental data, plotted in Fig. 5.2b.[28]

The differences in the composition data are barely discernible, and yet the estimates of the reactivity ratio for styrene (e.g.) range from 0.4 to 0.6, and are highly dependent on the accompanying estimate for methyl methacrylate. As the number of adjustable parameters are increased, these problems only worsen. Four-parameter fits of the still-oversimplified implicit penultimate model to composition and $\langle k_p \rangle$ data regularly result in 95% joint confidence intervals of the radical reactivity ratios that are large—often even infinite (see Fig. 5.3).

When the more mechanistically realistic explicit penultimate model is fitted to simple systems such as styrene/methyl methacrylate, the problems are even more serious, as multiple sets of reactivity ratios are found to provide adequate fits to the data.
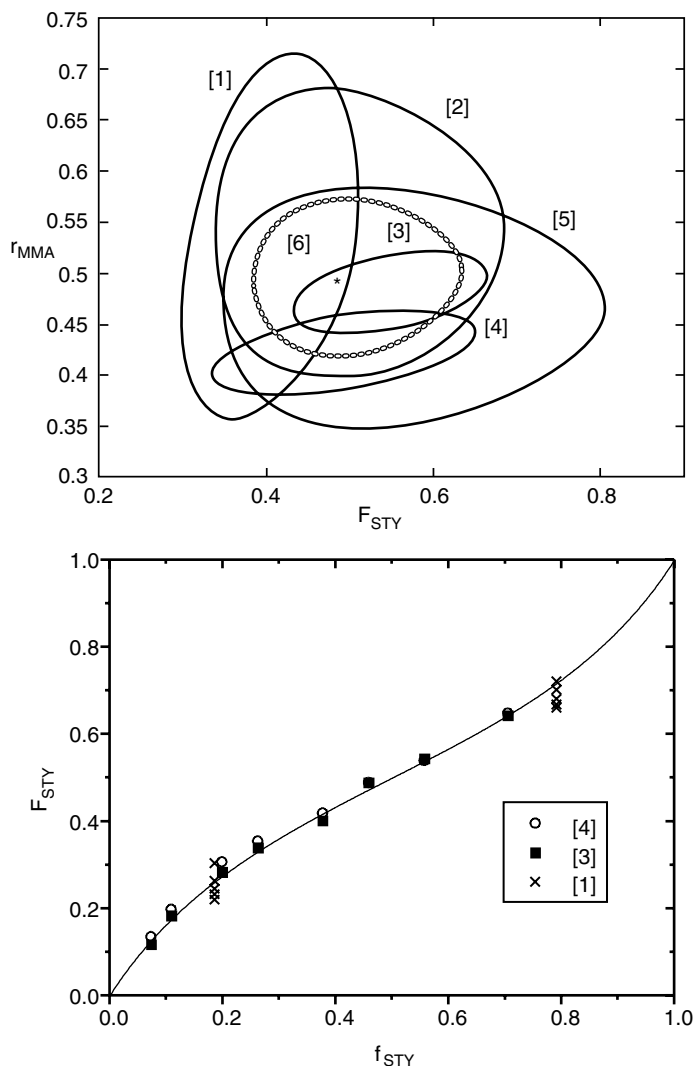
Figure 5.2 Shown here are (a) the 95% joint confidence intervals (JCIs) for the monomer reactivity ratios for individual data sets: [1] Coote et al.[28] (composition at 20°C); [2] Burke et al.[83] (sequence distribution, 60°C); [3] Fukuda et al.[9] (composition at 40°C); [4] Maxwell et al.[48] (composition, 40°C); [5] Maxwell et al.[48] (sequence distribution at 40°C). Also plotted (in bold) is [6] the 95% joint confidence interval for the combined data. Also shown are (b) the plots of the composition data used to estimate the JCIs, together with the terminal model predictions based on the overall estimates of the reactivity ratios. Only data sets [1], [3], and [4] could be plotted on this second graph as the others are sets of sequence distribution data.
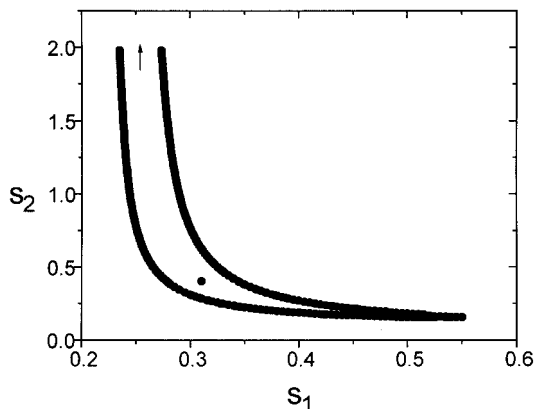
Figure 5.3 Shown here is the 95% JCI for the radical reactivity ratios of STY-MMA at 40°C, calculated from Fukuda's 40°C $\langle k_p \rangle$ data[9] for this system using the implicit penultimate model in conjunction with terminal model reactivity ratios estimated from his 40°C composition data.[9]

In summary, then, it is difficult to identify the mechanistically correct model, and, even if this were possible, the model would contain so many parameters as to render their precise and accurate estimation virtually impossible. Given this fact, we recommend that, depending on whether the intention of the model fitting is descriptive or mechanistic, the following strategies be adopted.

5.3.4.1 Descriptive Purposes If the objective of modeling copolymerization kinetics is merely to provide a convenient shorthand for tables of experimental composition or $\langle k_p \rangle$ data, then any model that can provide an adequate fit to the data is suitable. Indeed, it is desirable to choose a model with the smallest possible number of adjustable parameters compatible with providing an adequate fit to the data, as this simplifies the model-fitting process (e.g., by reducing the number of dimensions needed to represent the 95% joint confidence intervals that accompany parameter estimates). In addition, by not including more adjustable parameters than there are effective degrees of freedom in the data, the problems of multiple solutions and large and highly correlated parameter uncertainties are minimized. For the majority of copolymerization systems, it is possible to fit the composition data using the simple terminal model composition equation, and hence this model is suitable for descriptive purposes. For this reason, the large published database of terminal reactivity ratios need not be abandoned despite the overwhelming evidence for the model's failure on mechanistic grounds. However, it is important to clearly recognize that the terminal model can be used only descriptively, and that it is not legitimate to use its (physically invalid) reactivity ratios either in mechanistic studies or to predict other quantities such as propagation rate coefficients or triad/pentad fractions.

Likewise, the mechanistically unrealistic implicit penultimate model provides a convenient descriptive model for fitting $\langle k_p \rangle$ data. Provided that the terminal-model monomer reactivity ratios used in this model are estimated separately from composition data and the homopropagation rate coefficients are measured separately in homopolymerization experiments, the six-parameter $\langle k_p \rangle$ equation of this model contains only two adjustable parameters (the other four are fixed at their separately estimated values). For a large number of copolymerization systems the model can be further simplified without undermining its ability to provide an adequate fit to the data, by imposing the restriction that $s_1 = s_2 = s$ and thus creating a model that has only one adjustable parameter. Hence, as in the case of the terminal reactivity ratios, the evidence undermining the physical basis of the implicit penultimate model need not imply that the growing database of implicit penultimate model radical reactivity ratios be abandoned—merely that their status as purely descriptive parameters be clearly recognized.

5.3.4.2 *Mechanistic Purposes*

As opposed to the merely descriptive use of models, the usual objective of modeling copolymerization kinetics is to estimate parameters that have a genuine physical meaning (i.e., that are actual measures of rate constants, equilibrium constants, etc.), and that can thus be used in mechanistic studies (e.g., to assess substituent effects on radical reactivity) or to predict other as yet unmeasured quantities (e.g., using parameters obtained from composition data to predict triad/pentad fractions). In order to achieve this objective, it is of course essential that the underlying mechanistic assumptions of the model used be correct. Now, as shown above, the underlying assumptions of simple models (such as the terminal model and the implicit penultimate model) are not correct. Hence, more complex models (such as the explicit penultimate model) are required for mechanistic purposes. Unfortunately, as was also noted above, the use of these more complex models brings its own problems. Not only is there the problem of establishing which such model is correct (given that a large number of models can be made to fit the same set of data), but even if the correct model could be established, it would contain more parameters than are mathematically required to fit the data, and this results in large and highly correlated parameter uncertainties. As illustrated above, even in the unrealistically simple case of a terminal model fit to the composition data of styrene–methyl methacrylate, estimates of the reactivity ratio of styrene vary from 0.4 to 0.6. While this may not seem a large uncertainty in mathematical terms, in chemical terms it corresponds to a possible difference in selectivity of 50%.[67] And when the more realistic explicit penultimate model is fitted to the same data, the problem only gets worse, with multiple sets of parameter estimates (each providing equally good fits to the data) being obtained. These large uncertainties in the parameters clearly make it difficult to attach any physical meaning to their point estimates, and also lead to correspondingly large uncertainties when they are used to make predictions of other quantities.

It thus seems clear that model fitting is in fact not a useful method for studying the mechanism of free-radical polymerization. Instead, we recommend that more direct methods be adopted. For instance, rather than measure reactivity ratios indirectly, by

fitting a model to data, they should be measured directly from the rate constants and relative rate constants of the individual steps. While this is difficult to achieve in the context of a free-radical polymerization, these rate constants are easily accessible using small-radical models. For instance, by designing special initiator molecules, measures of initiator selectivity (from NMR studies of the resulting polymer) can be used to derive monomer reactivity ratios. Furthermore, techniques such as laser-flash photolysis and time-resolved ESR can be used to measure the rate constants for small-radical addition reactions, which can be treated as models of the propagation step in free-radical polymerization, and computer power has now advanced to a point where small-radical models of free-radical poplymerization can be examined via high-level ab initio molecular orbital calculations. In addition, there are many other ways of directly examining the mechanism of free-radical polymerization, such as via the measurement of solution thermodynamics (which can yield information about the possible presence of partitioning in a copolymerization system) and via spectroscopic studies (which can yield information concerning complex formation and direct measurements of the equilibrium constants of such complexes). Hence, although we believe that model fitting is not an appropriate technique for mechanistic studies of free-radical polymerization, this should not be seen as a despairing conclusion, for there remains a rich array of other experimental techniques that can be utilized, and which promise to give direct insights into the reaction mechanism.

5.4   TRANSFER KINETICS

The average chain transfer coefficient in copolymerization, $\langle C_s \rangle$, can be easily determined experimentally without recourse to any copolymerization kinetic model. This can be achieved by utilizing the well-known Mayo equation, over a range of different feed compositions to investigate the variation of $\langle C_s \rangle$ with feed for any given system. The primary difficulty in the experiment is to achieve rigorous molecular weight analysis of copolymer chains. The resultant average chain transfer rate coefficients are related to the average chain transfer and propagation rate coefficents, $\langle k_{tr} \rangle$ and $\langle k_p \rangle$ by

$$\langle C_s \rangle = \frac{\langle k_{tr} \rangle}{\langle k_p \rangle} \tag{5.19}$$

It is clear that in order to gain insight into the transfer process, $\langle k_{tr} \rangle$ and $\langle k_p \rangle$ need to be isolated. In a number of early studies this was achieved by predicting the values for $\langle k_p \rangle$ from the terminal model. This flawed procedure inevitably results in a misinterpretation of transfer kinetics in copolymerization. Therefore it is necessary to adopt values for $\langle k_p \rangle$ obtained by direct experimentation. This imposes a significant limit on our current understanding of transfer in copolymerization because the existing database on accurate and precise $\langle k_p \rangle$ values in copolymerization is quite limited.

One possible alternative approach is to utilize the implicit model as a descriptor for copolymerization propagation kinetics to allow access to the $\langle k_{tr} \rangle$ values. However, this can be a rigorous approach only if the s values used (which are model-dependent) are obtained directly from the correct $\langle k_p \rangle$ data (i.e., the same copolymerization and temperature), and therefore this approach does not negate the need for experimental values of $\langle k_p \rangle$.

In a study in 2001,[68] this approach was taken for the copolymerization of styrene and methyl methacrylate in the presence of carbon tetrachloride and carbon tetrabromide. This work built on a classsical approach to transfer kinetics developed by Bamford in the 1950s termed "moderated" copolymerization.[69,70] The results clearly indicated a large explicit penultimate unit effect on transfer in these reactions, resulting (at least in part) from a strong polar contribution. The widespread significance of this result and therefore the general nature of the mechanisms governing chain transfer in copolymerization remains elusive because of the limited amount of experimental data available. The preceding section on copolymerization propagation kinetics indicates that by analogy, explicit effects on transfer in copolymerization may well be extensive. Consequently, the application of either terminal or implicit models to transfer kinetics in the absence of careful experimental and theoretical studies may only serve to compound our current limited state of understanding. This clearly will have further implications in the comprehension of controlled/living radical synthetic methods in copolymerization such as catalytic chain transfer (CCT) and reversible addition fragmentation transfer (RAFT) polymerization that involve either metal centers or sulfur-based radicals where polar and steric effects would be predicted to be large.

5.5   COPOLYMERIZATION TERMINATION MODELS

In Chapter 4 the factors governing the kinetics of termination reactions are outlined, and the same picture should be valid for copolymerization kinetics. The original interpretation of termination in copolymerization was based on a chemically controlled model utilizing a cross-termination factor (commonly called the phi factor, Φ), which was defined as[11]

$$\Phi = \frac{\langle k_{t12} \rangle}{(\langle k_{t11} \rangle \langle k_{t22} \rangle)^{0.5}} \tag{5.20}$$

where $\langle k_{t11} \rangle$ and $\langle k_{t22} \rangle$ represent the termination rate coefficients of the homotermination reactions and $\langle k_{t12} \rangle$ of the cross-termination reaction. The phi factor was often combined with a terminal model for propagation to yield an overall expression for the rate of copolymerization. According to our current knowledge of propagation and termination reactions, this approach is clearly of only historical relevance.

For most copolymerization reactions the termination rate coefficient, $\langle k_t \rangle$, should be diffusion-controlled. This means that $\langle k_{t,copol} \rangle$ will be a function of properties and dimensions of the terminating chains (these can be influenced by the medium). The

issue becomes whether translational or segmental diffusion dominates as the rate-determining mechanism in low conversion termination kinetics. The simple "ideal diffusion" model[71] represents $\langle k_{t,copol} \rangle$ as a linear combination of the constituent $\langle k_{ti} \rangle s$ of the two homopolymerizations:

$$\langle k_{t,copol} \rangle = F_1 \langle k_{t1} \rangle + F_2 \langle k_{t2} \rangle \tag{5.21}$$

This relationship can be modified so that the friction coefficient of the chains is accounted for.[72] However, underpinning this type of relationship is the assumption that translational diffusion is the rate-determining step. As discussed in Chapter 4, it is far more likely that segmental diffusion plays a significant role in polyradical termination behavior at low conversion rates. Therefore it is necessary to consider the nature of the radical chain ends and their relative mobilities (and steric shielding) in any model based on segmental diffusion.

The simplest case[73] is to consider solely the terminal groups, leading to the relationship

$$\langle k_{t,copol} \rangle = \langle k_{t11} \rangle P_1^2 + 2 \langle k_{t12} \rangle P_1 P_2 + \langle k_{t22} \rangle P_2^2 \tag{5.22}$$

where k_{tii} represents the homotermination rate coefficients and P_i, the relative fraction of the two types of terminal radicals.

This simple model can be extended to account for the influence of penultimate unit groups[73,74] yielding either

$$\langle k_{t,copol} \rangle = \langle k_{t11,11} \rangle P_{11} + \langle k_{t21,21} \rangle P_{21} + \langle k_{t22,22} \rangle P_{22} + \langle k_{t12,12} \rangle P_{12} \tag{5.23}$$

or

$$\langle k_{t,copol} \rangle^{0.5} = \langle k_{t11,11}^{0.5} \rangle P_{11} + \langle k_{t21,21}^{0.5} \rangle P_{21} + \langle k_{t22,22}^{0.5} \rangle P_{22} + \langle k_{t12,12}^{0.5} \rangle P_{12} \tag{5.24}$$

where $k_{tij,kl}$ refers to the reaction of two radicals terminating in the monomer units ij and kl, respectively. The two penultimate unit equations, Eqs. (5.23) and (5.24), differ in the approximations used to simplify their derivation (arithmetic vs. geometric mean). Theoretical fits to experimental data[75,76] seem to indicate that Eq. (5.24) provides the best description of copolymerization termination kinetics.

5.6 INITIATION AND MODELS FOR OLIGOMERIC SYSTEMS

For cooligomerizations the long-chain assumption can become invalid, and the application of the terminal model for composition can fail. This is because the selectivity of initiator can play a significant role in "biasing" the composition of short chains. This was originally pointed out by Fueno and Furukawa,[77] and subsequently a number of studies demonstrated the importance of initiator selectivity to the coatings industry.[78–81]

Fueno and Furukawa showed that for a copolymer of length n, its composition, expressed as a mole fraction of enchained monomer 1, $F_1(n)$, could be written in terms of the conditional probabilities for propagation (assuming the terminal model), P_{11} and P_{22}, and the selectivity of the initiator, x:

$$F_1(n) = \left(x - \frac{1 - P_{22}}{2 - P_{11} - P_{22}} \right) (P_{11} + P_{22} - 1)^{(n-1)} + \frac{(1 - P_{22})}{(2 - P_{11} - P_{22})} \quad (5.25)$$

The implication of this equation for interpreting cooligomer propagation kinetics has been discussed in a number of studies.[78–81] Clearly, in the light of the preceding discussion in this chapter, the approach taken by Fueno and Furikawa now requires some amendment to allow for the possibility of significant penultimate unit effects. The termination reaction also becomes an important consideration as the critical chain length at which the long-chain assumption becomes invalid is determined by the kinetic chain length, and therefore the relative fraction of termination by disproportionation or combination needs to be taken into account.

5.7 CONTROL IN FREE-RADICAL COPOLYMERIZATION

Major advances have been made in the development of controlled free-radical polymerization. As can be seen throughout this book, the development of techniques such as atom transfer polymerization and radical addition–fragmentation-transfer polymerization has enabled polymers with narrow molecular weight distributions and novel molecular architectures (such as combs and stars) to be synthesized. However, these are not the only types of polymer properties that it is desirable to control. In particular, the development of stereospecific radical polymerization would be extremely useful for many commercial applications, while, in copolymerization, the control of copolymer composition and sequence distribution is extremely important, although often taken for granted. In the following section, we briefly outline possible strategies for controlling (or attempting to control) both the stereochemistry and the composition and sequence distribution in free-radical copolymerization, which have emerged as a result of studies of free-radical copolymerization kinetics.

5.7.1 Composition and Sequence Distribution

To state the obvious, determining the mechanistically correct copolymerization model and obtaining accurate and precise estimates of its parameters (via, e.g., direct measurements in small-radical studies) facilitates a large degree of control of the composition and sequence distribution of free-radical copolymerization. Such model equations can enable a specific copolymer composition to be targeted, simply by varying the monomer feed fractions, and can be used to predict the accompanying sequence distribution of the resulting polymer. However, this degree of control is nonetheless somewhat limited as the range of experimentally accessible

composition and sequence distribution combinations is fixed by the reactivity ratios of the monomers in question. However, a deeper understanding of the fundamental influences on the propagation mechanism can enable the reactivity ratios (or effective reactivity ratios) themselves to be manipulated, thereby providing even more flexibility to the range of structures that can be targeted. For instance, if the relative importance of enthalpic and entropic effects is understood, reactivity ratios can be manipulated by varying the polymerization temperature. If polar effects are known to be important, reactivity ratios can be manipulated by altering the solvent dielectric constant. If complexation is known to be occurring, this can be disrupted or enhanced using certain solvents, or by altering the temperature. Furthermore, it is probably possible to introduce the various solvent effects into most copolymerizations simply by selecting an appropriate solvent. For instance, a bootstrap effect might be introduced (and used to alter the effective reactivity ratios or achieve a tapered composition) by performing the polymerization in a poor solvent for one of the monomers, while a strong monomer–solvent interaction might be induced by choosing a solvent that is either strongly electron-donating or electron-withdrawing, depending on the electronic properties of the monomers. To summarize, then, an understanding of copolymerization propagation kinetics not only faciliates the modeling and hence the control of copolymer composition and sequence distribution, it also provides strategies for manipulating monomer and radical reactivities, thereby providing access to a broad spectrum of copolymer structures.

5.7.2   Stereochemistry

A more elusive goal for free-radical polymerization research is the control of the stereochemistry of the resulting polymer. When an alkene bearing two different substituents on one of its carbon atoms (e.g., $CH_2{=}CXY$, where $X \neq Y$) is polymerized, at each addition step two different stereoisomers are possible, depending on the side from which the growing $R{-}CXY^{\bullet}$ radical is attacked. To achieve a stereochemically pure polymer, it is necessary to control this preference so that the attack occurs either from the same side each time (resulting in an isotactic polymer) or from strictly alternating sides (resulting in a syndiotactic polymer). Now, in free-radical polymerization reactions, addition can usually occur from either side, thereby resulting in a random (or virtually random) array of stereocenters (i.e., an atactic polymer). This is because the propagating radical center is itself usually planar (or almost planar), leading to an equal or nearly equal probability of attack from either side. It is true that, for some substituents, quite large deviations from planarity do occur (e.g., the 1-F-propyl radical deviates from planarity by $\sim 35°$ based on UHF/6-31G* geometry optimizations[44]) and indeed, even in common homopolymerizations, stereospecificity of the addition step is not totally random. For example, in the free-radical polymerization of methyl methacrylate, the probability of finding a meso diad in the resulting polymer is just 20%, and hence there is a marked preference for the radical to be attacked in such a way that the new stereocenter has a configuration opposite that of the previous one.[82] However, in general, these deviations from purely random

structures are not significant enough to confer on the resulting polymer the advantageous properties of isotactic or syndiotactic polymers.

To achieve a high degree of stereospecifity in free-radical polymerization, it is necessary to manipulate the transition structure of the propagation step so as either to minimize completely the probability of attack from one side of the radical or to altogether avoid the free-radical addition pathways by providing a low-energy pathway in which the reacting species are held together (via some sort of complex) with a specific stereochemistry prior to addition. In the former case, it is not difficult to design specific monomers for which steric or electronic interactions involving the substituents on the radical and monomer lead to one pathway being completely dominant over the other.

However, unless the substituents required to achieve this objective also confer the desired physical and chemical properties on the polymer, this is not a very useful approach to control. More promising is via radical–solvent and monomer–solvent complexes. As seen above, there is strong evidence for monomer–solvent and radical–solvent complexes in free-radical polymerization, even for polymerizations involving common monomers such as styrene and methyl methacrylate. By choosing an appropriate solvent and then manipulating conditions such as temperature and monomer concentration so as to enhance the participation of the complex, it may be possible to achieve significant stereospecificity even in ordinary polymerizations. Indeed, significant progress toward stereospecific polymerization has already been made through the use of additives such as metallic complexing agents and Lewis acids. These developments are discussed in detail in Chapter 13 and are therefore not outlined here; rather, we wish to merely observe that the propagation step in free-radical polymerization can be subject to a wide range of influences that may be manipulated to achieve greater stereochemical control of radical homo- and copolymerization. It is through the study of copolymerization kinetics that a deeper understanding of these influences is attained, thereby enabling strategies to be developed for controlling this important class of reactions.

APPENDIX: HOW TO DERIVE A COPOLYMERIZATION MODEL

The objective is to eliminate the radical concentrations from the general expressions for $\langle k_p \rangle$ and composition. For a binary copolymerization, the general expressions have the form

$$\frac{F_1}{F_2} = \frac{-d[M_1]/dt}{-d[M_2]/dt} \quad \text{and} \quad \langle k_p \rangle = \frac{-d[M]/dt}{[M][R^\bullet]}$$

where $[M] = [M_1] + [M_2]$ is the overall monomer concentration and $[R^\bullet]$ is the overall radical concentration, which for the terminal model is simply $[R^\bullet] = [-M_1^\bullet] + [-M_2^\bullet]$.

Step 1   The first step is to obtain an expression for the overall rate of consumption of monomer:

$$-\frac{d[\text{M}]}{dt} = -\frac{d[\text{M}_1]}{dt} + -\frac{d[\text{M}_2]}{dt}$$

This is obtained by making the necessary assumptions as to what units influence the propagation step and what side reactions are involved, and hence writing out all the kinetically different reactions that affect the concentration of monomer. In doing this, we also make the long-chain assumption and thus ignore the initiation and termination steps. We then write out the accompanying equilibrium or rate expression.

$$\sim\sim\sim\text{M}_1^{\bullet} + \text{M}_1 \xrightarrow{k_{11}} \sim\sim\sim\text{M}_1\text{M}_1^{\bullet} \qquad \frac{-d\text{M}_1}{dt} = k_{11}[-\text{M}_1^{\bullet}][\text{M}_1]$$

$$\sim\sim\sim\text{M}_1^{\bullet} + \text{M}_2 \xrightarrow{k_{12}} \sim\sim\sim\text{M}_1\text{M}_2^{\bullet} \qquad \frac{-d\text{M}_2}{dt} = k_{12}[-\text{M}_1^{\bullet}][\text{M}_2]$$

$$\sim\sim\sim\text{M}_2^{\bullet} + \text{M}_1 \xrightarrow{k_{21}} \sim\sim\sim\text{M}_2\text{M}_1^{\bullet} \qquad \frac{-d\text{M}_1}{dt} = k_{21}[-\text{M}_2^{\bullet}][\text{M}_1]$$

$$\sim\sim\sim\text{M}_2^{\bullet} + \text{M}_2 \xrightarrow{k_{22}} \sim\sim\sim\text{M}_2\text{M}_2^{\bullet} \qquad \frac{-d\text{M}_2}{dt} = k_{22}[-\text{M}_2^{\bullet}][\text{M}_2]$$
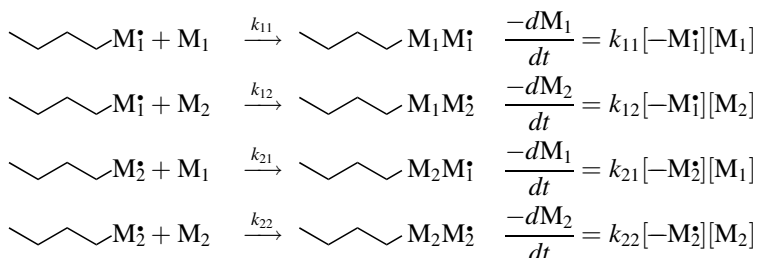
The overall rates of consumption of monomers M_1 and M_2 then follow from these expressions:

$$\frac{-d[\text{M}_1]}{dt} = k_{11}[-\text{M}_1^{\bullet}][\text{M}_1] + k_{21}[-\text{M}_2^{\bullet}][\text{M}_1]$$

$$\frac{-d[\text{M}_2]}{dt} = k_{12}[-\text{M}_1^{\bullet}][\text{M}_2] + k_{22}[-\text{M}_2^{\bullet}][\text{M}_2]$$

Step 2   The next step is to obtain expressions for the radical concentrations in terms of only monomer concentrations and characteristic constants such as rate coefficients and equilibrium constants. This is achieved by writing out all kinetically different expressions that affect the concentration of the different types of radical and their accompanying kinetic and/or equilibrium expressions:

$$\sim\sim\sim\text{M}_1^{\bullet} + \text{M}_1 \xrightarrow{k_{11}} \sim\sim\sim\text{M}_1\text{M}_1^{\bullet} \quad \text{(doesn't affect radical concentration)}$$

$$\sim\sim\sim\text{M}_1^{\bullet} + \text{M}_2 \xrightarrow{k_{12}} \sim\sim\sim\text{M}_1\text{M}_2^{\bullet} \qquad \frac{-d[-\text{M}_1^{\bullet}]}{dt} = k_{12}[-\text{M}_1^{\bullet}][\text{M}_2]$$

$$\frac{d[-\text{M}_2^{\bullet}]}{dt} = k_{12}[-\text{M}_1^{\bullet}][\text{M}_2]$$

$$\sim\sim\sim\text{M}_2^{\bullet} + \text{M}_1 \xrightarrow{k_{21}} \sim\sim\sim\text{M}_2\text{M}_1^{\bullet} \qquad \frac{-d[-\text{M}_2^{\bullet}]}{dt} = k_{21}[-\text{M}_2^{\bullet}][\text{M}_1]$$

$$\frac{d[-\text{M}_1^{\bullet}]}{dt} = k_{21}[-\text{M}_2^{\bullet}][\text{M}_1]$$

$$\sim\sim\sim\text{M}_2^{\bullet} + \text{M}_2 \xrightarrow{k_{22}} \sim\sim\sim\text{M}_2\text{M}_2^{\bullet} \quad \text{(doesn't affect radical concentration)}$$
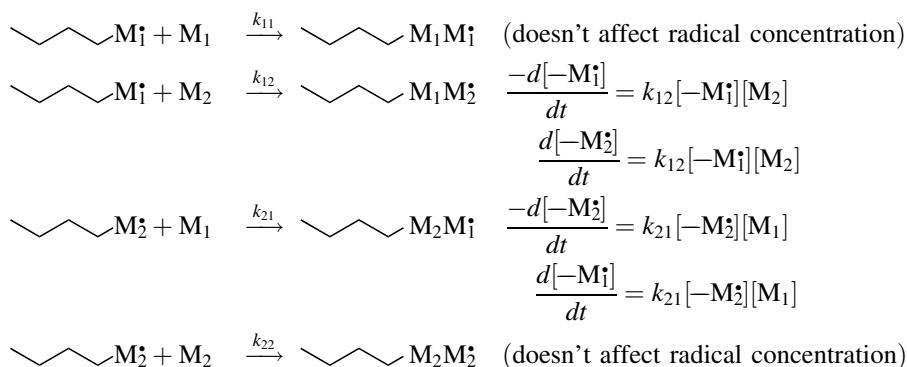
The overall rates of change of radical concentration are obtained from the following expressions:

$$\frac{d[-M_1^\bullet]}{dt} = -k_{12}[-M_1^\bullet][M_2] + k_{21}[-M_2^\bullet][M_1]$$

$$\frac{d[-M_2^\bullet]}{dt} = -k_{21}[-M_2^\bullet][M_1] + k_{12}[-M_1^\bullet][M_2]$$

Applying the quasi-steady-state assumption, the following simultaneous equations are obtained:

$$0 = -k_{12}[-M_1^\bullet][M_2] + k_{21}[-M_2^\bullet][M_1]$$

$$0 = -k_{21}[-M_2^\bullet][M_1] + k_{12}[-M_1^\bullet][M_2]$$

These can then be solved for the ratio of the radical concentrations $[-M_1^\bullet]/[-M_2^\bullet]$:

$$\frac{[-M_1^\bullet]}{[-M_2^\bullet]} = \frac{[M_1]}{[M_2]} \cdot \frac{k_{21}}{k_{12}}$$

Step 3   The expressions from steps 1 and 2 can then be substituted back into the general equations for composition and $\langle k_p \rangle$:

Composition:

$$\frac{F_1}{F_2} = \frac{-d[M_1]/dt}{-d[M_2]/dt}$$

$$= \frac{k_{11}[-M_1^\bullet][M_1] + k_{21}[-M_2^\bullet][M_1]}{k_{12}[-M_1^\bullet][M_2] + k_{22}[-M_2^\bullet][M_2]}$$

$$= \frac{k_{11}[M_1][-M_1^\bullet]/[-M_2^\bullet][M_1] + k_{21}[M_1]}{k_{12}[M_2][-M_1^\bullet]/[-M_2^\bullet] + k_{22}[M_2]}$$

$$= \frac{k_{11}[M_1]\dfrac{[M_1]}{[M_2]} \cdot \dfrac{k_{21}}{k_{12}} + k_{21}[M_1]}{k_{12}[M_2]\dfrac{[M_1]}{[M_2]} \cdot \dfrac{k_{21}}{k_{12}} + k_{22}[M_2]}$$

Propagation rate:

$$\langle k_p \rangle = \frac{-d[M]/dt}{[M][R^\bullet]} = \frac{-d[M_1]/dt + -d[M_2]/dt}{([M_1] + [M_2])([-M_1^\bullet] + [-M_2^\bullet])}$$

$$= \frac{k_{11}[-M_1^\bullet][M_1] + k_{21}[-M_2^\bullet][M_1] + k_{12}[-M_1^\bullet][M_2] + k_{22}[-M_2^\bullet][M_2]}{([M_1] + [M_2])([-M_1^\bullet] + [-M_2^\bullet])}$$

$$= \frac{k_{11}[M_1][-M_1^\bullet]/[M_2] + k_{21}[M_1] + k_{12}[M_2][-M_1^\bullet]/[-M_2^\bullet] + k_{22}[M_2]}{([M_1] + [M_2])([-M_1^\bullet]/[-M_2^\bullet] + 1)}$$

$$= \frac{k_{11}[M_1]\dfrac{[M_1]}{[M_2]} \cdot \dfrac{k_{21}}{k_{12}} + k_{21}[M_1] + k_{12}[M_2]\dfrac{[M_1]}{[M_2]} \cdot \dfrac{k_{21}}{k_{12}} + k_{22}[M_2]}{([M_1] + [M_2])\left(\dfrac{[M_1]}{[M_2]} \cdot \dfrac{k_{21}}{k_{12}} + 1\right)}$$

Step 4 Finally, the equations can be simplified by introducing monomer feed fractions instead of concentrations and reactivity ratios instead of rate coefficients.

$$\frac{F_1}{F_2} = \frac{k_{11}[M_1]\dfrac{[M_1]}{[M_2]} \cdot \dfrac{k_{21}}{k_{12}} + k_{21}[M_1]}{k_{12}[M_2]\dfrac{[M_1]}{[M_2]} \cdot \dfrac{k_{21}}{k_{12}} + k_{22}[M_2]}$$

$$= \frac{[M_1]\left([M_1] \cdot \dfrac{k_{11}}{k_{12}} + [M_2]\right)}{[M_2]\left([M_1] + \dfrac{k_{22}}{k_{21}}[M_2]\right)} = \frac{f_1}{f_2} \cdot \frac{(f_1 \cdot r_1 + f_2)}{(f_1 + r_2 \cdot f_2)}$$

$$\langle k_p \rangle = \frac{k_{11}[M_1]\dfrac{[M_1]}{[M_2]} \cdot \dfrac{k_{21}}{k_{12}} + k_{21}[M_1] + k_{12}[M_2]\dfrac{[M_1]}{[M_2]} \cdot \dfrac{k_{21}}{k_{12}} + k_{22}[M_2]}{([M_1] + [M_2])\left(\dfrac{[M_1]}{[M_2]} \cdot \dfrac{k_{21}}{k_{12}} + 1\right)}$$

$$= \frac{\dfrac{k_{11}}{k_{12}}[M_1]^2 + 2[M_1][M_2] + \dfrac{k_{22}}{k_{21}}[M_2]^2}{([M_1] + [M_2])\left([M_1]\dfrac{1}{k_{12}} + [M_2]\dfrac{1}{k_{21}}\right)}$$

$$= \frac{r_1 f_1^2 + 2f_1 f_2 + r_2 f_2^2}{f_1 \dfrac{r_1}{k_{11}} + f_2 \dfrac{r_2}{k_{22}}}$$

REFERENCES

1. G. Odian, *Principles of Polymerization*, Wiley-Interscience, New York, 1991.
2. M. Deady, A. W. H. Mau, G. Moad, and T. H. Spurling, *Makromol. Chem.* **194**, 1691 (1993).
3. M. Farina, *Makromol. Chem.* **191**, 2795 (1990).
4. E. Jenkel, *Z. Phys. Chem. Abtstr. A* **190**, 24 (1942).
5. F. R. Mayo and F. M. Lewis, *J. Am. Chem. Soc.* **66**, 1594 (1944).
6. T. Alfrey and G. Goldfinger, *J. Chem. Phys.* **12**, 205 (1944).
7. T. Alfrey and G. Goldfinger, *J. Chem. Phys.* **12**, 322 (1944).
8. T. Alfrey and G. Goldfinger, *J. Chem. Phys.* **14**, 115 (1946).
9. T. Fukuda, Y.-D. Ma, and H. Inagaki, *Macromolecules* **18**, 17 (1985).
10. H. W. Melville, B. Noble, and W. F. Watson, *J. Polym. Sci.* **2**, 229 (1947).
11. C. Walling, *J. Am. Chem. Soc.* **71**, 1930 (1949).
12. E. Merz, T. Alfrey, Jr., and G. Goldfinger, *J. Polym. Sci.* **1**, 75 (1946).
13. T. Fukuda, Y.-D. Ma, and H. Inagaki, *Makromol. Chem., Rapid Commun.* **8**, 495 (1987).
14. A. Pross, *Theoretical and Physical Principles of Organic Reactivity*, Wiley, New York, 1995.
15. D. R. Lide, in *CRC Handbook of Chemistry and Physics*, D. R. Lide, ed., CRC Press, Boca Raton, FL, 1994.

16. M. Kamachi, *Adv. Polym. Sci.* **38**, 56 (1981).

17. T. Fukuda, K. Kubo, and Y.-D. Ma, *Prog. Polym. Sci.* **17**, 875 (1992).

18. P. D. Bartlett and K. Nozaki, *J. Am. Chem. Soc.* **68**, 1495 (1946).

19. J. A. Seiner and M. Litt, *Macromolecules* **4**, 308 (1971).

20. R. E. Cais, R. G. Farmer, D. J. T. Hill, and J. H. O'Donnell, *Macromolecules* **12**, 835 (1979).

21. P. G. Brown and K. Fujimori, *J. Polym. Sci.; Part A: Polym. Chem.* **A32**, 2971 (1994).

22. E. Tsuchida and H. Tomono, *Makromol. Chem.* **141**, 265 (1971).

23. P. Karad and C. Schneider, *J. Polym. Sci.; Part A: Polym. Chem.* **16**, 1295 (1983).

24. D. J. T. Hill, J. H. O'Donnell, and P. W. O'Sullivan, *Macromolecules* **16**, 1295 (1983).

25. H. J. Harwood, *Makromol. Chem.; Macromol. Symp.* **10/11**, 331 (1987).

26. Y. D. Semchikov, *Macromol. Symp.* **111**, 317 (1996).

27. B. Klumperman and I. R. Kraeger, *Macromolecules* **27**, 1529 (1994).

28. M. L. Coote, L. P. M. Johnston, and T. P. Davis, *Macromolecules* **30**, 8191 (1997).

29. B. Klumperman and K. F. O'Driscoll, *Polymer* **34**, 1032 (1993).

30. W. G. Barb, *J. Polym. Sci.* **10**, 49 (1952).

31. C. Walling, *J. Polym. Sci.* **16**, 315 (1955).

32. G. G. Lowry, *J. Polym. Sci.* **42**, 463 (1960).

33. P. Wittmer, *Adv. Chem. Ser.* **99**, 140 (1971).

34. P. Wittmer, *Makromol. Chem.* **177**, 997 (1976).

35. J. A. Howell, M. Izu, and K. F. O'Driscoll, *J. Polym. Sci.; Part A-1* **8**, 699 (1970).

36. F. Martinet and J. Guillot, *J. Appl. Polym. Sci.* **65**, 2297 (1997).

37. D. Kukulj and T. P. Davis, *Macromolecules* **31**, 5668 (1998).

38. M. L. Coote and T. P. Davis, *Prog. Polym. Sci.* **24**, 1217–1251 (1999).

39. M. L. Coote, T. P. Davis, B. Klumperman, and M. J. Monteiro, *J. Macromol. Sci.—Rev. Macromol. Chem. Phys.* **C38**, 567 (1998).

40. J. Brandrup and E. H. Immergut, in *Polymer Handbook*; J. Brandrup and E. H. Immergut, eds., Wiley-Interscience, New York, 1989.

41. C. H. Bamford, A. D. Jenkins, and R. Johnston, *Trans. Faraday. Soc.* **55**, 418 (1959).

42. T. Alfrey and C. C. Price, *J. Polym. Sci.* **2**, 101 (1947).

43. M. L. Coote, T. P. Davis, and L. Radom, *ACS Symp. Ser.* **768 (2000).**

44. M. L. Coote, T. P. Davis, and L. Radom, *Macromolecules* **32**, 2935 (1999).

45. L. H. Yee, T. P. Davis, and J. P. A. Heuts, *Macromolecules* **34**, 3581–3586 (2001).

46. J. P. A. Heuts, R. G. Gilbert, and I. A. Maxwell, *Macromolecules* **30**, 726 (1997).

47. M. L. Coote, M. D. Zammit, T. P. Davis, and G. D. Willett, *Macromolecules* **30**, 8182 (1997).

48. I. A. Maxwell, A. M. Aerdts, and A. L. German, *Macromolecules* **26**, 1956 (1993).

49. M. L. Coote and T. P. Davis, *Macromolecules* **32**, 3626 (1999).

50. C. Barner-Kowollik and T. P. Davis, *Macromol. Theory Simul.* **10**, 255–261 (2001).

51. D. Kukulj, J. P. A. Heuts, and T. P. Davis, *Macromolecules* **31**, 6034–6041 (1998).

52. D. J. T. Hill, J. J. O'Donnell, and P. W. O'Sullivan, *Prog. Polym. Sci.* **8**, 215 (1982).

53. K. G. Olson and G. B. Butler, *Macromolecules* **16**, 707 (1983).

54. M. Kamachi, J. Satoh, and S.-I. Nozakura, *J. Polym. Sci. Polym. Chem. Ed.* **16**, 1789 (1978).

55. K. F. O'Driscoll, M. J. Monteiro, and B. Klumperman, *J. Polym. Sci.; Part A: Polym. Chem.* **A35**, 515 (1997).

56. M. D. Zammit, T. P. Davis, G. D. Willett, and K. F. O'Driscoll, *J. Polym. Sci.; Part A: Polym. Chem.* **A35**, 2311 (1997).

57. M. L. Coote and T. P. Davis, *Eur. Polym. J.* **36**, 2423–2427 (2000).

58. M. L. Coote, T. P. Davis, and L. Radom, *J. Mol. Struct. (THEOCHEM)* **461–462**, 91–96 (1999).

59. H. Fischer and L. Radom, *Angew. Chem. Int. Eng. Ed.* **40**, 1340–1371 (2001).

60. M. W. Wong, A. Pross, and L. Radom, *J. Am. Chem. Soc.* **116**, 6284 (1994).

61. T. Ito and T. Otsu, *J. Macromol. Sci.—Chem.* **A3**, 197 (1969).

62. G. Bonta, B. Gallo, and S. Russo, *Polymer* **16**, 429 (1975).

63. H. Fujihara, K. Yamazaki, Y. Matsubara, M. Yoshihara, and T. Maeshima, *J. Macromol. Sci.—Chem.* **A13**, 1081 (1979).

64. B. Sandner and E. Loth, *Faserforschung Textiltechnik* **27**, 571 (1976).

65. B. Sandner and E. Loth, *Faserforschung Textiltechnik* **27**, 633 (1976).

66. G. A. Egorochkin, Y. D. Semchikov, L. A. Smirnova, N. V. Karyakin, and A. M. Kut'in, *Eur. Polym. J.* **28**, 681 (1992).

67. T. P. Davis, *J. Polym. Sci., Part A: Polym. Chem.* **39**, 597–603 (2001).

68. H. M. Kapfenstein-Doak, S. Harrisson, and T. P. Davis, *Macromolecules* **34**, 6214–6223 (2001).

69. C. H. Bamford and S. N. Basahel, *J. Chem. Soc. Faraday Trans I* **74**, 1020 (1978).

70. C. H. Bamford and S. N. Basahel, *J. Chem. Soc. Faraday Trans I* **76**, 107 (1980).

71. J. N. Atherton and A. M. North, *Trans. Faraday Soc.* **58**, 2049 (1962).

72. K. Ito and K. F. O'Driscoll, *J. Polym. Sci: Part A: Polym. Chem.* **17**, 3913 (1979).

73. Y.-D. Ma, K.-S. Sung, Y. Tsujii, and T. Fukuda, *Macromolecules* **34**, 4749 (2001).

74. S. Russo and S. Munari, *J. Macromol. Sci., Chem.* **2**, 1321 (1968).

75. M. Buback and C. Kowollik, *Macromolecules* **32**, 1445 (1999).

76. M. Buback and C. Kowollik, *Macromol. Chem. Phys.* **200**, 1764 (1999).

77. T. Fueno and J. Furukawa, *J. Polym. Sci.* **1964**, *A2*, 3681.

78. L. W. Hill and Z. W. Wicks, *Prog. Org. Coatings* **10**, 55 (1982).

79. M. N. Galbraith, G. Moad, D. H. Solomon, and T. H. Spurling, *Macromolecules* **20**, 675 (1987).

80. K. F. O'Driscoll, *J. Coatings Tech.* **55**, 57 (1983).

81. K. F. O'Driscoll and T. P. Davis, *Polym. Commun.* **30**, 317 (1989).

82. G. Moad, D. H. Solomon, T. H. Spurling, S. R. Johns, and R. I. Willing, *Aust. J. Chem.* **39**, 43 (1986).

83. A. L. Burke, T. A. Duever, and A. Penlidis, *J. Polym. Sci. Part A: Polym. Chem.* **A34**, 2665 (1996).

6 Heterogeneous Systems

ALEX M. VAN HERK and MICHAEL MONTEIRO

Eindhoven University of Technology, Eindhoven, The Netherlands

CONTENTS

6.1 HETEROGENEOUS POLYMERIZATION TECHNIQUES

This chapter presents overviews of the different heterogeneous (or particle-forming) polymerization techniques available for radical polymerizations, both conventional radical polymerization (CRP) and ''living'' radical polymerization (LRP) in its different forms. Although the polymerization mechanism on the molecular level is the same in all cases, polymerization technique can actually have a profound impact on factors such as overall kinetics and molecular microstructure (molecular mass and chemical composition distribution, branching, etc.). Obviously in heterogeneous systems we have to deal with partitioning of, for example, monomers, the initiator, the radicals and transfer agents, and other species that play an important role in some forms of LRP.

Additionally in some applications the special morphologies that one can obtain through heterogeneous polymerizations will have major effects on the properties of the products if the morphology is retained in an application. Morphology will be touched on only briefly in this chapter (especially in Section 6.3.2, where, for example, block copolymers can be formed directly in emulsion polymerization); therefore we would like to refer to excellent reviews in this matter of, for example, Mestach and Loos,[1] Ivarsson et al.,[2] Rudin,[3] and Riess.[4]

We will emphasize especially on the differences between homogeneous and heterogeneous polymerization techniques that are relevant for molecular microstructure and rates of polymerization and product properties.

6.1.1   Basic Principles

Homogeneous polymerization techniques most often used are gasphase, bulk and solution polymerization where the monomer (a solvent) and the initiator are in one phase. The formed polymer remains soluble (either in the monomer or the solvent) till high conversion. When the polymer precipitates from the continuous phase to form polymer particles, which are not swollen with monomer, this is called *precipitation polymerization*. When the polymer particles swell with monomer, the technique is called *dispersion polymerization* and besides polymerization in the continuous phase the polymer particles are also loci of polymerization, in contrast to precipitation polymerization. Precipitation polymerization[5] is often performed in aqueous media (e.g., acrylonitrile polymerization in water).

Dispersion polymerization is usually performed in organic solvents, which are poor solvents for the formed polymer.[6] (Supercritical) liquid carbondioxide (CO_2) is now used as a continuous medium for dispersion polymerization[7] with some additional benefits. Suspension polymerization occurs in the monomer droplets, and unlike in emulsion polymerization, the initiator is oil-soluble and a non-micelle-forming stabilizing agent is also used. PVC is manufactured with this technique.

The emulsion polymerization technique comprises usually of a water-soluble initiator, water-insoluble monomer, and a micelle-forming surfactant. The main locus of polymerization, in contrast to suspension polymerization, is the monomer-swollen latex. Therefore the term *emulsion polymerization* is a misnomer; the starting point is an emulsion of monomer droplets in water, but the product is a dispersion of polymer particles. One can also form a stable microemulsion of monomer droplets (typical particle radius 10–30 nm), and usually a cosurfactant (e.g., hexanol) is applied. In a microemulsion polymerization there is no separate monomer phase anymore.[8,9] This is also the case in miniemulsion polymerization, where the thermodynamically unstable droplets have a radius between 50 and 500 nm.[10] It is also possible to perform inverse emulsion polymerizations where the continuous phase is organic in combination with a water-soluble monomer (e.g., acrylamide).[11]

The range of particle size covered by each technique is shown in Fig. 6.1. Whereas it is clear that emulsion and suspension polymerization do not cover the complete range of particle sizes, say from 30 nm till 1 mm, with the development of dispersion polymerization, spanning an interesting range of particle sizes, these
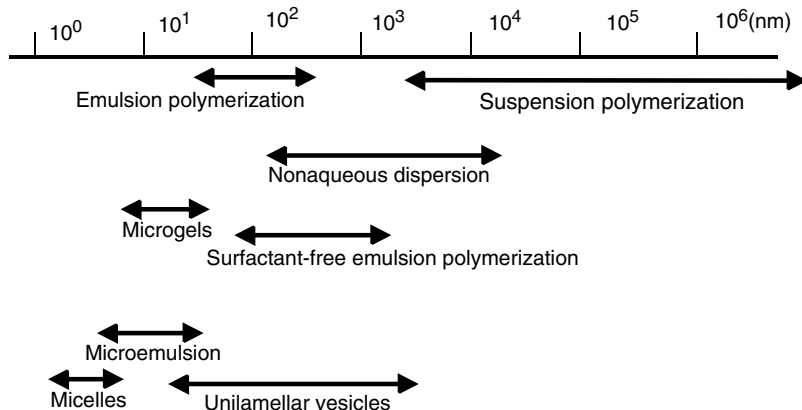
Figure 6.1 Typical particle sizes obtained in heterogeneous polymerization techniques.

three techniques cover the whole range. Control over particle size in the range of micrometer size particles can also be obtained by the so-called method of activated swelling developed by Ugelstad et al.[12] and the dynamic swelling method developed by Okubo et al.[13] Also there is a growing interest in the particle range between 5 and 30 nm, covered by microgels[14] and microemulsion polymerizations,[15] which essentially results in more or less transparent latices.

6.1.2 Suspension Polymerization

Basically suspension polymerization consists of the polymerization of small monomer droplets suspended in the medium, usually water in the normal-suspension polymerization and liquid paraffin or a chlorocarbon in the case of inverse-suspension polymerization. In normal-suspension polymerization water-insoluble monomers are suspended in water. For a methodological survey of the different heterogeneous polymerization techniques, see Arshady.[16] The initiator (azo- or peroxide initiators) is dissolved in the monomer.

Stabilization of droplets or polymer particles is done with non-micelle-forming emulsifiers such as poly(vinyl alcohol) or poly(vinyl pyrrolidone). Sometimes inorganic salts such as talc are used, either alone or in combination with the organic stabilizers. The kinetics are equivalent to bulk polymerization; we could regard the small droplets as minireactors suspended in water. The aqueous phase acts as an efficient heat transfer agent, and the viscosity in the reactor remains almost constant.

In inverse-suspension polymerization, which is mainly applied for water-soluble monomer/polymers like acrylamide and soluble acrylates, solutions of the monomer and initiator are suspended in an oil phase. The original size of the droplets is reflected in the size of the corresponding polymer beads or pearls. The size of the droplets depends on stirring speed, volume ratio of water to monomer, concentration, and type of the stabilizer and the viscosities of both phases.

The particle morphology is determined mainly by the solubility of monomer and polymer in the suspended droplet, which also may contain the so-called porogenic agents that can be solvents for either the monomer or the monomer, and the polymer. The particle pore-size distribution can be controlled in this way. The final product can be easily separated where commonly particles between 20 μm and ≤2 mm can be obtained.

Important applications include polystyrene and poly(styrene-co-divinylbenzene), poly(vinyl chloride) and polyacrylonitrile.

6.1.3   Emulsion Polymerization

Emulsion polymerization involves the emulsification of monomers in a continuous aqueous phase and stabilization of this system by a surfactant. The formation of micelles next to the stabilized monomer droplets is essential. Usually, a water-soluble initiator is used to start the free-radical polymerization. The polymerization is taking place in the monomer-swollen micelles, which, after initiation, are converted to latex particles. This results in a reaction medium consisting of submicrom-eter polymer particles swollen with monomer and dispersed in an aqueous phase. The final product, called *latex*, consists of a colloidal dispersion of polymer particles in water. Emulsion polymerization differs from suspension polymerization in the smaller size of the particles in which polymerization occurs, the applied stabilizing agents, and the kind of initiator employed and in its macroscopic mechanism and reaction characteristics. The emulsion polymerization process is often used for the (co)polymerization of monomers such as vinyl acetate, ethylene, styrene, acryloni-trile, acrylates, and methacrylates. Also conjugated dienes such as butadiene and isoprene are polymerized on a large industrial scale via the emulsion polymerization method. One advantage of emulsion polymerization is the excellent heat exchange due to the low viscosity of the continuous phase during the whole reaction. Exam-ples of applications are paints, coatings, glues, finishes, and floor polishes. Another important application is core–shell emulsion polymerization, the production of poly-mer particles with a layer structure. Core–shell products are in use by the coating industry, in photographic and printing materials, and especially in the production of high-impact materials, characterized by a core of rubber and a shell of an engi-neering plastic.

By far the most important difference as compared with other polymerization techniques is the emulsion polymerization kinetics. Emulsion polymerization is unique in the sense that an increase in molar mass can be achieved without reducing the rate of polymerization. Over a wide range the molar mass and rate of polymeri-zation can be varied independently. Emulsion polymerization is known for its relatively high rates of polymerization compared to other process strategies. A disadvantage of emulsion polymerization is the contamination of the polymer with surfactant and other additives.

6.1.4   Mini- and Microemulsion Polymerization

From a synthetic point of view, emulsion polymerization is not suitable for all mono-mers. For monomers that are highly water-soluble or, on the other hand, almost

insoluble in water, the standard emulsion polymerization technique is not suitable. For water-soluble monomers, besides emulsion polymerization, aqueous-phase polymerization can also occur.

In the case of highly water-soluble (e.g., acrylamide) or even water-miscible monomers (e.g., acrylic acid), one can resort to inverse-emulsion polymerization. In inverse-emulsion polymerization the continuous phase consists of an oil such as kerosene or paraffin in which water with dissolved monomer is emulsified, for example, with a high-shear mixer such as the Ultra Turrax in the presence of special emulsifiers (e.g., tri–block copolymers). Polyacrylamide, used as thickening in paints and pushing fluids in tertiary oil recovery, is produced industrially by inverse-emulsion polymerization.

In the case of monomers with low water solubility, another problem arises. In emulsion polymerizations, transport of monomer from monomer droplets to the growing polymer particles is needed, which demands a minimum water solubility of the monomer. For example, dodecyl methacrylate (water solubility of 0.065 mmol/L) cannot be polymerized by emulsion polymerization, and even the polymerization kinetics of vinyl-2-ethylhexanoate with a reasonable water solubility (0.01 wt% as compared to styrene with a water solubility of 0.03 wt%) reflect some diffusion limitations for the transport of the monomer[17]. Another reason for hydrophobic monomers to polymerize slowly in emulsion polymerization could be that entry of radicals is slow because the oligomers do not grow to their critical chain length[18]. A solution to the problem, which is now frequently applied, is to add cyclodextrins[19] to enhance water solubility of the hydrophobic monomers. The cyclodextrins form a more water-soluble complex with the monomer and are acting as a kind of phase transport catalyst.

Another solution to this problem is to directly polymerize in the monomer droplets, which have to be very small in order to retain the benefits of producing polymer in the form of latex. As opposed to emulsion polymerization, where the droplets are of the same size as those in suspension polymerization (10–100 µm), in mini- and microemulsion polymerization the droplets are much smaller and enable the polymerization to commence in the monomer droplets.

In miniemulsion polymerization the droplets are in the range of 50–500 nm. A mixed surfactant system consisting of an ionic surfactant (e.g., SDS) and a cosurfactant (e.g., a long-chain alkane or alcohol) stabilizes the droplets, which are formed by a high-shear field created by devices such as an ultrasonifier. The miniemulsions are thermodynamically unstable and therefore are stable for only a limited period of time ranging from hours to days.

In principle, polymerization proceeds in the monomer droplets, and the final particle number is close to the initial number of monomer droplets. However in many cases not all droplets are initiated to become polymer particles but represent only a fraction ($\leq 20\%$) of the initial number of monomer droplets. Miller et al.[20] observed that the addition of pre-formed polymer greatly increases this fraction.

In microemulsions the droplets are even smaller (5–20 nm) and the microemulsion is thermodynamically stable. Also, a mixed-emulsifier system is used here.[9] Because the polymer particles are much smaller in microemulsion polymerization, monomer partitioning in copolymerizations is affected and special structures can

be formed. Also, the apparent reactivity ratios can vary in microemulsion copolymerizations.[15]

6.1.5 Dispersion Polymerization

In dispersion polymerization the monomer dissolves in the medium but the polymer does not. This means that particles are formed early in the polymerization process. These particles are the mean locus of polymerization, leading to spherical particles between 0.1 and 10 μm. The dispersion polymerization bridges the gap between emulsion and suspension polymerization in terms of the particle sizes obtained. The kinetic features contain elements of precipitation polymerization and emulsion polymerization. Examples are the dispersion polymerization of methyl methacrylate and styrene in hydrocarbons and in various alcohols. (Supercritical) liquid carbondioxide (CO_2) is now used as a continuous medium for dispersion polymerization[7] with the additional benefits of easy product isolation. In the latter case the stabilizing agents used are block copolymers containing an anchor block and a CO_2-philic block (usually a fluor-containing segment).

6.1.6 Precipitation Polymerization

The main difference between dispersion and precipitation polymerization is the locus of polymerization. In dispersion polymerization the particles are the main locus of polymerization, whereas in precipitation polymerization the continuous phase is the locus of polymerization because the medium or the monomer does not swell the precipitated polymer. This also means that there is a continuous nucleation and the particles continue to grow in size throughout the reaction. Usually the particles are irregularly shaped. A typical example is the polymerization of acrylonitrile in bulk.

   During precipitation the environment of the polymer chain changes dramatically, and if the radical on the chain is still active, termination can be delayed, which means that precipitation polymerization leads to higher molecular masses as compared to dispersion polymerization. Precipitation polymerization can be used to obtain particles measuring 0.5–5 μm in size.

6.2   MECHANISM OF EMULSION POLYMERIZATIONS

Each heterogeneous polymerization mechanism discussed above has its own peculiarities. However, many special features of heterogeneous techniques are reflected in emulsion polymerizations, which are studied most extensively, both regarding kinetics and microstructure. Therefore we limit ourselves here to an extensive discussion of emulsion polymerization. The aspects of emulsion copolymerization such as monomer partitioning, copolymerization parameters, and composition drift are equally valid in other heterogenous polymerization techniques, but we will discuss

them only for emulsion copolymerization. The main differences can be found in particle size, an aspect that already has been discussed and radical concentrations. The radical balances in heterogeneous polymerizations will be discussed on the basis of emulsion polymerizations but will also be extended to bigger particles (pseudobulk kinetics; see Section 6.2.1.).

In this section, after a brief overview of the ingredients in an emulsion polymerization recipe, the nucleation and particle growth stage will be described. In Section 6.2.2 the special issues in an emulsion copolymerization will be discussed.

Figure 6.2 shows the basic steps in an emulsion polymerization, each of which will be discussed here.

6.2.1 Homopolymerizations

In this section the major ingredients in emulsion polymerization are reviewed. A laboratory-scale recipe for a conventional emulsion polymerization contains monomers, water, initiator, surfactant, and sometimes a buffer, salts, and/or chain transfer agents. Commercial recipes may contain 20 or more ingredients such as water, monomer (and comonomers), surfactant (often a mixture), initiation system, additives (electrolytes), pH controller, chain transfer agents (often a mixture), sequestering agents, and, unintentionally, contaminants from chemicals and from corrosion.
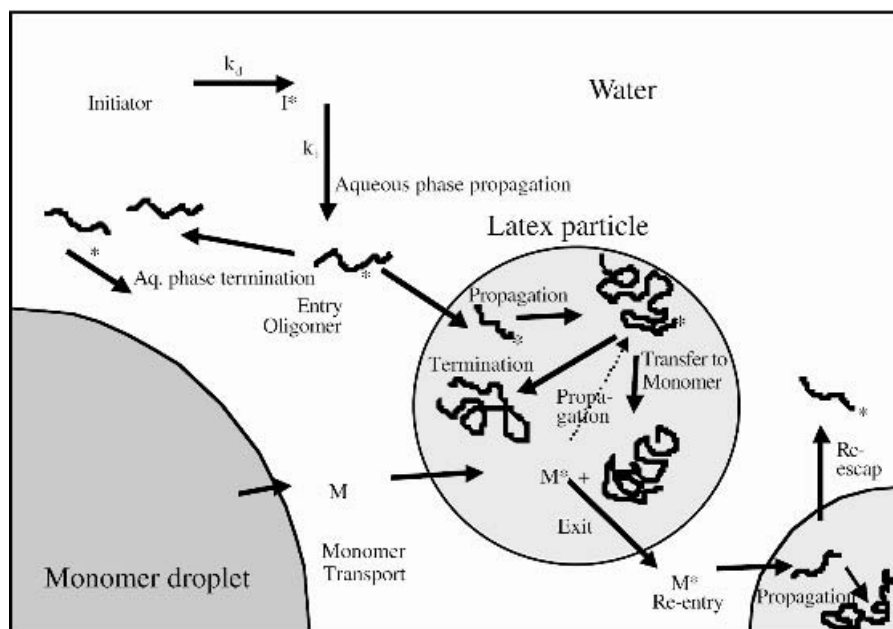
Figure 6.2 Basic steps in emulsion polymerization.

6.2.1.1   *Monomers*   The monomers used in an emulsion polymerization must have at least a minimum water solubility in relation to diffusion but also radical entry. The more hydrophobic monomers can be polymerized by using miniemulsion polymerization or adding a phase transfer catalyst such as the cyclodextrins.[19] If the monomers are too water-soluble, other problems can occur, including simultaneous solution polymerization. This water-soluble polymer formed can change rheology of the latex. Small amounts of water-soluble monomer are often added for costabilization ((meth)acrylic acid), and in some cases extensive formation of water-soluble polymer can be prevented.[21,22] Highly soluble monomer/polymer systems are usually polymerized in inverse heterogeneous polymerization techniques where an oil phase forms the continuous phase. The most common monomers are styrene, butadiene, vinyl acetate, acrylates and methacrylates, acrylic acid, and vinyl chloride.

6.2.1.2   *Initiators*   The most commonly used laboratory and industrial water-soluble initiators are potassium, sodium, and ammonia salts of persulfate. Next in line are the water-soluble azo compounds, especially those with an ionic group, such as 2,2′-azobis(2-aminopropane) dihydrochloride and redox systems with peroxides.

  Above $pH = 6$ and a temperature of $50°C$, persulfate dissociates at the O—O bond by which two identical radicals are formed; $S_2O_8^{2-} \rightarrow 2\ SO_4^{-}$. Strong evidence suggests that water molecules play a role in the dissociation to form HSO_4^{-}, which lowers the pH. Therefore, a buffer is necessary to control the pH and thus the efficiency of the initiator.

  When the polymerization should be performed at lower temperatures ($<50°C$), a redox system can be used. Lower polymerization temperature gives the advantage of lowering chain branching and crosslinking in the synthesis of rubbers, and a typical example of a redox systems is Fe(II) and cumene hydroperoxide.

  Other methods are also used to create free radicals such as γ-radiolysis, photo-initiators, and electron-beam techniques (see Section 6.3.1.)

6.2.1.3   *Surfactants*   A surfactant (*surf*ace-*act*ive *agent*) also referred to as emulsifier, soap, or stabiliser) is a molecule with both hydrophilic and hydrophobic segments. The general name for this group is *amphipatic molecules*, indicating their tendency to arrange themselves at oil–water interfaces. In emulsion polymerization surfactant serves three important purposes: stabilization of the monomer droplets, generation of micelles, and stabilization of the growing polymer particles leading to a stable end product.

  As mentioned earlier, a surfactant molecule consists of a (polar) hydrophilic and a (apolar) hydrophobic segment. Surfactants are mostly classified according to the hydrophilic group:

- *Anionic surfactants*, where the hydrophilic part is an anion
- *Cationic surfactants*, where the hydrophilic part is a cation
- *Amphoteric surfactants*, where the properties of the hydrophilic function depend on pH

- *Nonionic surfactants*, where, in addition to the hydrophobic part, the hydrophilic part is also a nonionic component, such as, polyols, sugar derivatives, or chains of ethylene oxide

Other types of surfactants are the polymeric (steric) stabilizers such as partially hydrolyzed poly(vinyl acetate). Also the oligomeric species formed in situ, when SO_4^- radicals react with some monomer units in the aqueous phase will have surface-active properties, and can even form a colloidally stable latex.[23]

Important technical emulsifiers are fatty alcohol–ethylene oxide (EO) adducts as well as nonylphenol–EO adducts. The latter type of surfactant is now replaced by others because of adverse health effects. The most commonly used anionic surfactants are sodium dodecyl sulfate (SDS), sodium dodecyl benzene sulfonate, and the Aerosol series (sodium dialkyl sulfosuccinates), such as Aerosol OT [AOT, sodium di(2-ethylhexyl)sulfosuccinate] and Aerosol MA [AMA, sodium di-(hexyl sulfosuccinate)]. These surfactants are often used when monodisperse latices are required, due to their high critical micelle concentration (CMC) and a relatively large aggregation number (number of surfactant molecules per micelle).

6.2.1.4   Other Components

6.2.1.4.1   Electrolytes   Electrolytes are added for several reasons. For example, they can control the pH, which prevents hydrolysis of the surfactant and maintains the efficiency of the initiator. Electrolytes can induce particle size monodispersity and also particle coagulation.

6.2.1.4.2   Chain Transfer Agents   Emulsion polymerization often results in an impractical high-molecular-mass polymer. Therefore, to moderate the molar mass chain transfer agents (CTA), usually mercaptans, are frequently used. The mercaptan is introduced into the reactor together with the monomer phase. The consumption of the mercaptan taking place in the loci should be properly kept in balance with monomer consumption.

A new class of chain transfer agents is introduced where metal complexes like cobaloximes are used as catalytic chain transfer agents. These complexes are not consumed and have very high activities in transfer, but the introduction in emulsion polymerizations is still not straightforward (see Chapter 12).

The physical picture of emulsion polymerization is extensively described in Gilbert[24] and Lovell and El-Aasser.[25] The main components of an emulsion polymerization recipe are the monomer(s), the dispersing medium (usually water), surfactant (combination), and initiator.

During the progress of the polymerization, three distinct intervals can be observed. *Interval I* is the initial stage where particle formation takes place. *Interval II* is characterized by a constancy of particle number, while polymerization in the particles proceeds in the presence of a separate monomer phase. The monomer-swollen particles grow at the expense of the monomer droplets. The beginning of interval II is usually taken as the conversion where the surfactant concentration

drops below its critical micelle concentration. *Interval III* begins with the disappearance of monomer droplets, after which the monomer concentration in the particles and water phase starts to decrease continuously.

6.2.1.5   *Particle Nucleation*

The nucleation stage constitutes the interval I in an emulsion polymerization, the initial period in which the particle number is changing, due to particle formation. The consequence is that in the particle formation period the rate of polymerization is not constant but will increase to a maximum value. When this value is reached, particle formation is finished and, in the ideal situation, the number of polymer particles will stay constant, which marks the beginning of Interval II.

Particle nucleation in emulsion polymerization is a complex process that is still not well understood. Numerous investigations have been conducted in attempts to clarify this phenomenon. In the so-called micellar nucleaction mechanism, the entry of a radical in a micelle produces a new polymer particle. As a result of compartmentalization of the radicals in the micellar phase and the resulting high radical concentration in the micelles and subsequent particles, the polymerization rate will be high in micelle and particle phases as compared with the rate of polymerization in the monomer droplets. This nucleation mechanism is elegantly quantified by Smith and Ewart,[26] who stated that particle nucleation will stop when the surfactant concentration drops below its CMC, due to adsorption of surfactant onto the newly formed polymer particle surface. Systems of monomers with low water solubility (e.g., styrene) partly solubilized in micelles of a surfactant with low CMC and seemed to work well for such systems.

Although the Smith–Ewart nucleation model was successful in describing the styrene system, large deviations were observed for emulsion polymerization with other monomer systems, and in some cases when the surfactant concentration was varied from above the CMC to lower concentrations, no discontinuity in, for example, particle number was observed. The situation became even more complex when it was shown that even without the use of a surfactant stable polymer particles could be formed.[23] Some important arguments against the Smith–Ewart nucleation model are: that particles are formed even when no micelles are present, more water soluble monomers do not fit the theory, and a maximum in the polymerization rate at the end of nucleation period is predicted but has rarely been observed. These observations called for alternative models. A homogeneous nucleation model was proposed[27,28] in which radicals react in the aqueous phase with solubilised monomer to form growing oligomeric species. These species will form particles when the critical water solubility length is reached. The consequence is that the water solubility of the monomer, the initiator concentration, and the water solubility of the initiator are crucial parameters in the emulsion polymerization process. This is probably one of the other reasons why very hydrophobic monomers are difficult to polymerize in emulsion. The formation of primary particles is described by the homogeneous nucleation theory of Fitch and Tsai,[28] and is known as the HUFT theory (Hanssen–Ugelstad–Fitch–Tsai), which implies that precursor particles are formed in the aqueous phase by precipitation of oligomeric radicals above a critical chain length.

No particles are nucleated before the oligomer radicals have reached a critical chain length x, and this will take some time. The precipitation of precursor particles is in fact a thermodynamic effect.

Feeney et al.[29] proposed a refinement of this theory in which it is assumed that colloidally unstable precursor particles are first formed as a result of the previously described growth of oligomers in the aqueous phase, which will precipitate after reaching a critical length and then coagulate with each other and with mature particles to form growing polymer particles. Precursor particles may coagulate with other precursor particles. Eventually the size of the coagulated entities becomes sufficient to allow appreciable monomer swelling to occur by excluding water; thus the monomer concentration in the particles increases. Thereafter, the coagulated entity is considered to be a stable polymer particle that may grow more rapidly as a result of higher monomer concentration and lower radical loss. The coagulation events involved in the nucleation mechanism explain the maximum in particle number in interval I for systems without or with low surfactant content. New insights and quantification of nucleation models reveal that in most cases micellar and homogeneous nucleation occur concurrently, which intuitively is also more acceptable, for a review, see Tauer and Kuehn.[30]

In conclusion, the determination of the nucleation mechanisms operative in a given polymerization system is very difficult. The reason is that there is no general nucleation mechanism that can describe all the aspects of a given polymerization system. Thus, the nucleation mechanism is dependent on the emulsion polymerization system characteristics. These characteristics include type of monomer, type of initiator, temperature, the importance of aqueous-phase kinetics, water solubility of monomer and initiator, and the propagation rate constant.

6.2.1.6 *Particle Growth*

Once formed and given colloidal stability, particles will take part in the polymerization process in intervals I, II, and III. The kinetics are controlled mainly by the distribution and exchange of radicals over the various phases and cannot be oversimplified. Models are numerous. The basic rate equation for homogeneous batch free-radical polymerization is [24]

$$R_{pol} = -\frac{d[M]}{dt} = k_p[M][R^\bullet] \tag{6.1}$$

where R_{pol} is the rate of polymerization per unit volume, k_p the propagation rate coefficient, [M] the monomer concentration, and [R$^\bullet$] the radical concentration. In the emulsion polymerization process the main loci of polymerization are the particles thus the rate equation must contain the number of particles, N, as well as the concentration of monomer and radicals in the particles leading to

$$R_p = \frac{k_p \bar{n} C_m N}{N_a} \tag{6.2}$$

where C_m is the monomer concentration in the particles, $\bar{n}$ is the average number of radicals per particle, and N_a is Avogadro's number. The time evolution of the

fractional conversion in a batch process, x, is then

$$\frac{dx}{dt} = \frac{k_\mathrm{p}C_\mathrm{m}N}{N_\mathrm{a}n_\mathrm{m0}}\bar{n} = A\bar{n} \tag{6.3}$$

where $A = k_\mathrm{p}C_\mathrm{m}N/N_\mathrm{a}n_\mathrm{m0}$ and n_m0 is the initially added number of moles of monomer per unit volume. Equation (6.3) is valid in intervals II and III, and in interval I, N and C_m should be replaced by $N(t)$ and $C_\mathrm{m}(t)$, respectively. In interval II k_p and C_m are constant at least to within an excellent approximation.

6.2.1.6.1   The Average Number of Radicals per Particle   The value of $\bar{n}$ is determined by three processes:

1. Absorption of radicals from the water phase into particles
2. Desorption of radicals from particles
3. Bimolecular termination of radicals in the particles

Smith and Ewart[26] were the first in formulating an equation for $\bar{n}$ in the form of a set of population balance equations describing a number of particles N_n containing n radicals:

$$\frac{dN_n}{dt} = \frac{\rho_\mathrm{a}}{N}[N_{n-1} - N_n] + k[(n+1)N_{n+1} - nN_n]$$
$$+ \frac{k_\mathrm{tp}}{v}[(n+2)(n+1)N_{n+2} - n(n-1)N_n] \tag{6.4}$$

where ρ_a is the rate coefficient of entry of free radicals, k is the rate coefficient of exit of radicals from particles, k_tp is the rate coefficient for bimolecular termination of radicals in the particles, and v is the volume of a monomer swollen particle. Several workers have reported various ways of solving this general set of equations. Smith and Ewart presented very useful solutions for three limiting cases determined by the ratios of entry, exit and termination.

Case 1: $(\rho_\mathrm{a}/N) \ll k: \bar{n} \ll 0.5.$ This situation is the result of faster desorption than absorption of radicals by particles. Consequently, particles contain at most one radical at a time and on average a number far smaller than unity. When neglecting the extremely few particles with more than one radical, Eq. (6.4) simplifies to

$$\frac{dN_0}{dt} = -N_0\frac{\rho_\mathrm{a}}{N} + N_1 k \tag{6.5}$$

and

$$\frac{\rho_\mathrm{a}}{kN} = \frac{N_1}{N} = \bar{n} \tag{6.6}$$

As in this case there will be far more N_0 particles as compared to N_1 particles it follows $N_0 \approx N$.

Case 2: $\mathbf{k} \ll (\boldsymbol{\rho_a}/N) \ll (\boldsymbol{k_{tp}}/v)\colon \bar{n} = \mathbf{0.5.}$ This situation is the result of instantaneous termination when a second radical enters a particle already containing a radical, and with negligible desorption of radicals from particles. The time interval between entries varies in a random fashion. When a radical enters a particle, this particle immediately starts to polymerize at a steady-state rate. As soon as a second radical enters, this rate abruptly falls to zero. Under these conditions it is obvious that on the average the active and inactive periods of each particle are equal in length so that $N_0 = N_1$ and $N_1/N = \bar{n} = 0.5$ ($N = N_0 + N_1$). Cases 1 and 2 are known as the zero–one systems.

Case 3: $(\boldsymbol{k_{tp}}/v) \ll (\boldsymbol{\rho_a}/N)\colon \bar{n} \gg \mathbf{0.5.}$ This situation occurs when bimolecular termination is no longer instantaneous on entry of a second radical in an active particle. This occurs, for example, in bigger particles, and in suspension polymerization we always deal with the so-called pseudobulk kinetics. Smith–Ewart neglected radical exit in their treatment of this case. With a sufficiently large $\bar{n}$, the steady-state condition is $\rho_a/N = 2k_{tp}\bar{n}^2/v$. Since the total volume of polymer per unit volume of aqueous phase is $V = N \times v$, the rate of polymerization becomes

$$R_{pol} = k_p C_m \left(\frac{\rho_a V}{2k_t} \right)^{0.5} \tag{6.7}$$

6.2.1.7   Molar Mass and Molar Mass Distribution   In the case of a homopolymer molecule the most important characteristic is its size or molar mass. The molar mass (defined by various averages and especially the molar mass distribution) determines a large range of properties of the polymer material. Naturally this applies to copolymers as well, in which case the chemical composition distribution also plays an important role.

In particular, in an emulsion polymerization the MMD is determined by the events that can start, continue, or stop the growth of a polymer chain. These events are entry of a radical in a particle, propagation, and termination. Considering termination, we can distinguish between two types of chain-stopping processes: (1) bimolecular termination and (2) transfer of the free-radical activity of the chain end to another molecule. Bimolecular termination can occur through disproportionation or combination. Transfer can occur to transfer agents, deliberately added, or to components present in the recipe (e.g., surfactant, initiator, monomer, polymer). Especially in emulsion polymerization transfer to monomer is a very important chain-stopping process because it generates a small radical that can also exit the polymer particle. Theories to predict the MMD in an emulsion polymerization have been developed by several groups.[31–33]

6.2.1.8   Particle Size Distributions   If the polymer produced by an emulsion polymerization is applied in the form of a latex, the particle size distribution is an

additional factor that determines the properties of the latex. For example, latex rheology, film formation of a latex paint, light scattering, and the appearance of a coating are influenced by the particle size and the particle size distribution. Models to predict particle size distributions have to account for not only particle nucleation and particle growth,[24] but sometimes also partial coagulation or coalescence during the emulsion polymerization.[34]

The complete modeling of emulsion polymerization is still very complicated and hampered by many factors.[35]

6.2.2   Copolymerizations

The presence of more than one monomer in an emulsion polymerization means that the monomer partitioning has to be taken into account with respect to composition drift, on top of the reactivity ratios.

6.2.2.1   *Monomer Partitioning in Emulsion Polymerization*   Because of the intrinsic heterogeneity of an emulsion polymerization system, the kinetics and mechanisms that control this polymerization are difficult to describe. To gain more insight into the kinetic processes involved in an emulsion (co)polymerization, a detailed knowledge of the partitioning of monomer(s) over the different phases present is necessary. The monomer concentration in the polymer particles directly determines the rate of polymerization, while the monomer ratio in the polymer particles determines the chemical composition of the copolymer formed. Therefore, an accurate knowledge of the concentration of the monomer in the different phases of the polymerization system is necessary to develop and test kinetic models for the emulsion polymerization process. These models can be useful in the design of polymerization reactors, process control, and product characteristics such as molar mass and chemical composition distributions of the copolymers formed. In this section a thermodynamic model based on the Flory–Huggins theory[36] of polymer solutions will be discussed and applied to experimental results on the partitioning of monomer(s) over the different phases present during an emulsion (co)polymerization. The dynamics of swelling depends on the particle size, however, not the absolute concentration, as will be discussed in this paragraph.

At equilibrium the partial molar free energy of the monomer will be equal in each phase present: the monomer swollen colloid (micelles, vesicles and/or polymer particles), the monomer droplets, and the aqueous phase:

$$\Delta G_c = \Delta G_d = \Delta G_a \qquad (6.8)$$

where ΔG_c, ΔG_d, and ΔG_a represent the partial molar free energies of the colloidal phase, monomer droplets, and the aqueous phase, respectively. Utilizing the appropriate equations for the partial molar free energy of the colloidal and aqueous phase (for derivation, see, e.g., Maxwell et al.[37]), Eq. (6.9) can be obtained, also known as the *Vanzo equation*,[38] which describes the partitioning of monomer between the

aqueous phase and the polymer particles in the absence of, in general, monomer droplets.

$$\ln(1 - v_p) + v_p * \left[1 - \frac{1}{\bar{P}_n}\right] + \chi * v_p^2 + \frac{2 * V_m * \gamma * v_p^{1/3}}{r_0 * RT} = \ln\left[\frac{[M]_{aq}}{[M]_{aq,\,sat}}\right] \quad (6.9)$$

here v_p is the volume fraction of polymer, $\bar{P}_n$ is the number average degree of polymerization of the polymer, χ is the Flory–Huggins interaction parameter between the monomer and the polymer, while R is the gas constant and T is the temperature. V_m is the molar volume of the monomer, γ is the particle–water interfacial tension and r_0 is the radius of the unswollen micelles, vesicles, and/or polymer particles. $[M]_{aq}$ is the concentration of monomer in the aqueous phase and $[M]_{aq,sat}$, the saturation concentration of monomer in the aqueous phase.

The partitioning of monomer between the aqueous phase and polymer particles, below and at saturation, can be predicted by Eq. (6.9). However, this requires that both the Flory–Huggins interaction parameter and the interfacial tension be known. These parameters may be polymer-volume-fraction dependent (see Maxwell et al.[37,39] for prediction of monomer partitioning). Equations similar to Eq. (6.9) can be derived for homopolymer, co- and terpolymer polymer particles with two or more monomers at and below saturation.[40]

The expression derived in Eq. (6.9) can describe the swelling behavior of a polymer particle with one monomer below and at saturation. In the case of saturation swelling with two monomers, substituting the appropriate expression for the partial molar free energy of the different phases into Eq. (6.8), Eq. (6.10) for monomer i can be obtained (for exact derivation, see, e.g., Maxwell et al. [37,39]):

$$\ln v_{p,i} + (1 - m_{ij}) * v_{p,j} + v_p + \chi_{ij} * v_{p,j}^2 + \chi_{ip} * v_p^2$$

$$+ v_{p,j} * v_p * (\chi_{ij} + \chi_{ip} - \chi_{jp} * m_{ij}) + \frac{2 * V_{m,i} * \gamma * v_p^{1/3}}{r_0 * RT}$$

$$= \ln v_{d,i} + (1 - m_{ij}) * v_{d,j} + \chi_{ij} * v_{d,j}^2 = \ln\left[\frac{[M_i]_{aq}}{[M_i]_{aq,sat}}\right] \quad (6.10)$$

where $v_{p,i}$ and $v_{p,j}$ are the volume fractions of monomers i and j in the polymer particles, respectively; χ_{ij} is the Flory–Huggins interaction parameter between monomer i and j, while χ_{ip} and χ_{jp} are the Flory–Huggins interaction parameters between monomers i and j and the polymer, respectively; m_{ij} is the ratio of the molar volume of monomer i over monomer j, and $v_{d,i}$ and $v_{d,j}$ represent the volume fraction of monomers i and j, respectively, in the monomer droplets. It can be shown from Eq. (6.10), that, at saturation swelling, the mole fraction of monomer i in the monomer droplets ($f_{i,d}$) is equal to the mole fraction of monomer i in the polymer particles ($f_{i,p}$). This also holds for monomer j. This is envisaged in the following equation:[39]

$$f_{i,p} = f_{i,d} \quad \text{and} \quad f_{j,p} = f_{j,d} \quad (6.11)$$

where $f_{j,d}$ and $f_{j,p}$ are the mole fractions of monomer j in the monomer droplets and in the polymer particles, respectively. Assuming that the total monomer concentration in the polymer particles is equal to the sum of the concentrations of the individual monomers, together with Eq. (6.11), the concentration of monomer i in the polymer particles can be predicted from the individual saturation concentration of monomers i and j in the polymer particles: $C_{i,\text{sat}}$ and $C_{j,\text{sat}}$, respectively. For a given seed latex, the concentration of monomer i in the polymer particles (C_i) is related to the mole fraction of monomer i in the monomer droplets ($f_{i,d}$) and given by the following equation:[37,39]

$$C_i = f_{i,d} * \left[[C_{i,\text{sat}} - C_{j,\text{sat}}] * f_{i,d} + C_{j,\text{sat}} \right] \tag{6.12}$$

A similar expression can be deduced for monomer j.

In conclusion, it can be said that the partitioning behavior of monomers between the different phases present during an emulsion polymerization can be described and predicted using a simple thermodynamic model derived from the classical Flory–Huggins theory for polymer solutions.

6.2.2.2 Composition Drift in Emulsion Co- and Terpolymerization A special aspect of (emulsion) copolymerization is the occurrence of composition drift. In combination with the instantaneous heterogeneity (statistical broadening around the average chemical composition), this phenomenon is responsible for the chemical heterogeneity of the copolymers formed. Composition drift is a consequence of the difference between instantaneous copolymer composition and overall monomer feed composition. This difference is determined by (1) the reactivity ratios of the monomers (kinetics) and (2) the monomer ratio in the main loci of polymerization (viz., polymer particles), which can differ from the overall monomer ratio of the feed (as added according to the recipe), which in turn is caused by monomer partitioning. In most cases the monomer ratio in the polymer particles equals the monomer ratio in the monomer droplets, the water solubility of the monomers is therefore the main factor in the monomer ratio in the polymer particles.

In principle, when one compares solution or bulk copolymerization to emulsion copolymerization, two situations can be distinguished: (1) if the more reactive comonomer is the less water-soluble one, then there will be a stronger composition drift as the amount of water increases in the recipe (e.g., styrene–methyl acrylate[41] and (2) if the more reactive comonomer is the more water-soluble one, then a smaller composition drift can occur as the amount of water increases (e.g., indene–methyl acrylate, methyl acrylate–vinyl 2,2-dimethyl-propanaoate.[42] In the latter cases the composition drift may even be reversed at very high water content. To describe and control an emulsion copolymerization, both the reactivity ratios and monomer partitioning have to be known.

Batch processes are known to give two-peaked distributions of copolymer composition when a strong composition drift occurs during the course of the (emulsion) copolymerization. Moreover, in emulsion copolymerization the degree of bimodality appears to depend on the monomer/water ratio.[41,43,44] Semi-continuous processes

(i.e., addition of monomer during polymerization) can be used to prepare more homogeneous copolymers. Dynamic mechanical spectroscopy or differential scanning calorimetry and transmission electron microscopy combined with preferential staining techniques have been used to determine the possible occurrence of phase separation due to double-peaked chemical composition distributions (CCDs). It has been shown that the compositional heterogeneity of the copolymer has a dramatic effect on mechanical properties.[41]

6.2.2.2.1   Ternary Emulsion Copolymerization   In the fundamental investigations described in literature dealing with emulsion copolymerization, most attention has been given to binary copolymerization, namely, polymerization of two monomers. Far less attention has been paid to ternary emulsion copolymerization (three monomers), hereafter referred to as *terpolymerization*. Emulsion terpolymerization investigations, dealing mostly with properties and applications, have been published mainly as patents.

It is obvious that the typical aspects that distinguish emulsion copolymerization from homopolymerization, including monomer partitioning and dependence of kinetics on the local monomer concentration ratio are rapidly becoming more complex when three monomers are involved, not to mention the complications in terpolymer analysis.

However, since it can easily be understood that using three monomers makes it possible to obtain an even larger variety and refinement of copolymer properties, more effort is put in research on emulsion terpolymerization, although little or no fundamental, mechanistic differences between binary and ternary emulsion copolymerization systems can be expected.

The microstructure of emulsion terpolymers of vinyl chloride, vinylidene chloride, and hydroxyethyl acrylate, prepared in batch and semicontinuous reactions, were studied by means of differential scanning calorimetry (DSC) and ^{13}C NMR (nuclear magnetic resonance).[45] Schoonbrood studied the emulsion terpolymerization of styrene, methyl methacrylate, and methyl acrylate[46] and for the first time also determined the propagation rate coefficients for this ternary system by means of pulsed laser polymerization.[47] He also determined and predicted the microstructure (in terms of CCD) of these terpolymers.[46]

In many cases one uses two relatively water-insoluble comonomers (e.g., styrene, butyl acrylate, methyl methacrylate) and small amounts of a third, highly water-soluble comonomer [e.g., (meth)acrylic acid, 2-hydroxyethyl methacrylate] or even a surface-active comonomer. These water-soluble comonomers are generally introduced to obtain functionalized lattices, for example, to improve adhesive product properties or to prepare reactive latices. The incorporation of these monomers is the subject of many studies; more recently the incorporation of acidic monomers in latex particles has been studied extensively.[21,22]

6.2.2.3   Process Strategies in Emulsion Copolymerization   The emulsion polymerization strategy, specifically, the kind of process, can have a considerable effect on the molecular structure and particle morphology. The intrinsic factors as well as

the process conditions determine the colloidal aspects of the copolymer latex (particle diameter, surface charge density, colloidal stability, etc.), the characteristics of the polymeric material in the particles (MMCCD), and the structure of the particles (copolymer composition as a function of particle radius, etc.). In turn, these factors determine the properties of the latex and the copolymer product.

The ultimate goal of most investigations on emulsion copolymerization is to be able to control the process in such a way as to produce a copolymer product (latex or coagulate) with desired properties. For this purpose the semicontinuous (sometimes called *semibatch*) emulsion copolymerization process is widely used in industry. The main advantages of this process as compared with conventional emulsion batch processes, include a convenient control of emulsion polymerization rate in relation to heat removal and control of chemical composition of the copolymer and particle morphology. These are important features in the preparation of speciality or high performance polymer latices.

Semicontinuous emulsion copolymerization processes can be performed by applying various monomer addition strategies.

6.2.2.3.1 Constant Addition Strategy The most widely investigated and described procedure is the addition of a given mixture of the monomers (sometimes preemulsified monomers) at a constant rate.[48–50]

For instance, this procedure is followed in many papers dealing with the semicontinuous emulsion copolymerization of vinyl acetate and butyl acrylate.[51] With respect to the monomer addition rate, two main situations can be distinguished: (1) *flooded conditions*, where the addition rate is higher than the polymerization rate; and (2) *starved conditions*, where the monomers are added at a rate lower than the maximum attainable polymerization rate (if more monomer would be present). The latter process (starved conditions) is often applied in the preparation of homogeneous copolymers/polymer particles. In this case after some time during the reaction, a steady state is attained because of the low addition rates in which the polymerization rate of each monomer is equal to its addition rate and a copolymer is formed with a chemical composition identical to that of the monomer feed. Sometimes semicontinuous processes with a variable feed rate (power feed) are used to obtain polymer particles with a core–shell morphology.[52]

6.2.2.3.2 Controlled Composition Reactors Intelligent monomer addition strategies in copolymerizations strongly rely on the monitoring of monomer conversions. In copolymerization, control of the copolymer composition can also be obtained when applying monomer addition profiles. These monomer addition profiles can either be (1) based on the direct translation of online measurements to monomer addition steps (controlled composition reactor) or (2) predicted by emulsion copolymerization models on a conversion basis. The required conversion-time relation is then obtained by online measurements. Online methods of determining monomer conversion are, as outlined above, important for controlling the emulsion (co)polymerization process. Excellent reviews have appeared on online sensors for polymerization reactors.[53,54] The use of online Raman spectroscopy in controlling emulsion copolymerization seems to be one of the more versatile methods.[55]

6.2.2.3.2 Optimal Addition Profile   Arzamendi and Asua[56] developed the so-called optimal monomer addition strategy. By using this method Arzamendi et al. demonstrated that within a relatively short period of time homogeneous vinyl acetate (VAc)–methyl acrylate (MA) emulsion copolymers can be prepared in spite of the large difference between the pertaining reactivity ratios. The reactor was initially charged with all of the less reactive monomer (viz., VAc) plus the amount of the more reactive monomer (viz., MA) needed to initially form a copolymer of the desired composition. Subsequently, the more reactive monomer (MA) was added at a computed (time variable) flow rate (optimal addition profile) in such a way as to ensure the formation of a homogeneous copolymer.

The key problem in this method is the calculation of the amount of methyl acrylate to be initially charged in the reactor and the optimal addition rate profile of the remaining amount of methyl acrylate. The calculations are based on the following assumptions:

1. Copolymerization is carried out starting from a monodisperse seed latex of the desired composition.
2. The number of particles remains constant during the reaction.
3. Aqueous-phase polymerization is negligible.
4. Thermodynamic equilibrium determines the various monomer concentrations.

By applying the instantaneous copolymer composition equation, the desired monomer concentration ratio inside the polymer particles is calculated. In combination with the thermodynamic equilibria equations, this ratio allows the calculation of the amount of methyl acrylate to be initially charged in the reactor. Arzamendi and Asua[56] applied a semiempirical method to calculate the time-dependent evolution of $\bar{n}$. This evolution is calculated from a semicontinuous experiment carried out under conditions similar to those of the final optimal process, but applying an estimated, constant addition rate of methyl acrylate. The evolution of $\tilde{n}$ correlated with the volume fraction (f_p) of polymer in the particles. This correlation is then used to calculate an addition profile. Another semicontinuous experiment is then carried out using this addition profile. If copolymer composition deviates too much from the desired value, another correlation of $\tilde{n}$ with f_p is then calculated from the last experiment. This procedure can be repeated until the addition profile is optimal.

Alternatively, Van Doremaele[43] applied an even more pragmatic approach. This method can be applied without actually calculating $\bar{n}(t)$ or $\bar{n}(f_p)$ and may therefore be more generally applicable. This method was applied to the emulsion copolymerization of styrene (S) and methyl acrylate (MA). The batch emulsion copolymerization of S and MA is known to often produce highly heterogeneous copolymers (where styrene is the more reactive and less water-soluble monomer).

Rather than a large difference between the reactivity ratios (VAc-MA), the large difference between the water solubilities of S and MA is the main problem here. As stated, the time evolution of $\bar{n}$ was not actually calculated but was set equal to 0.5 as a first estimation. It would be highly fortuitous if the first estimated addition profile,

based on $\bar{n} = 0.5$, would be optimal, because the average number of radicals will generally deviate from this first estimation (i.e., $\bar{n} = 0.5$). Nevertheless, a first addition profile was calculated, presuming $\bar{n} = 0.5$. Separately, the correlation between the amount of styrene to be added and the conversion was calculated from thermodynamic equilibrium data that would lead to the desired copolymer composition. Combining the results, that is, the conversion-time curve from the experiment carried out with this addition profile and the correlation between amount of styrene to be added and conversion, a new addition profile could be calculated. In the case of the S-MA system the iteration converges rapidly, only four iteration steps appeared to be required in S-MA emulsion copolymerization to arrive at indistinguishable monomer addition rate profiles.

In general it can be stated that the reactions based on the optimal addition rate profile proceed more rapidly than do those based on constant-addition-rate strategies.

6.2.2.4   Batch, Semibatch, and Continuous Emulsion Polymerization   Commercial emulsion polymerizations are usually carried out in batch or semibatch reactors. An almost complete conversion can be obtained, and the preparation of different products is possible in the same reactor.

For the production of large amounts of the same product, the use of a continuously operated stirred-tank reactor (CSTR) would be preferable because of its lower operating costs and more consistent product quality. For copolymerization, in a single CSTR a completely homogeneous copolymerization can be produced.[57] The disadvantage of polymerization in a single CSTR arise from the residence-time distribution, which lead to products with a much lower conversion, a lower particle concentration, and a much broader particle size distribution as compared to batch. Further sustained oscillations in conversion and particle concentration occur for a lot of recipes. This can be overcome in principle, by the development of a continuous reactor system where the stage of particle nucleation is spatially separated from the other stages of the process. A small plug-flow reactor as a seed reactor followed by a CSTR, or a pulsed packed column (PPC) are examples for continuous emulsion polymerization.[58] In the PPC, good local agitation is combined with lower flow rates and little backmixing, which provides the same conversion and particle concentration as the equivalent batch process.[58,59]

A proper control of the intermolecular composition distribution seem to be possible in a series of CSTRs.[60]

6.3   UNCONVENTIONAL HETEROGENEOUS POLYMERIZATIONS

6.3.1   Unconventional Free-Radical Polymerizations

6.3.1.1   Ultrasound Initiation   An unusual free-radical polymerization of vinyl monomers utilizes ultrasound to both emulsify monomer and to create free-radicals.[61] Ultrasonic cavitation in aqueous solution forms radical species by the

cleavage of chemical bonds in any vapor molecules within the cavity as it collapses. The high temperatures and pressures inside this collapsing cavity are sufficient for bond cleavage; the radicals thus formed are being expelled into the surrounding medium. It remains unclear if there is any direct formation of monomer radicals within the cavity or whether the primary radicals are formed from the cleavage of water (e.g., H•, OH•) which act as the initiating species. The first claimed emulsion polymerizations by ultrasound were those of butyl acrylate and vinyl acetate.[61] In most cases it was observed that the particle sizes obtained by ultrasound initiation are smaller than those of equivalent chemically initiated polymerizations, although they may be dependent on the energy input.

It is clear that ultrasonically initiated polymerization has many similarities with microemulsion polymerization but at a considerably reduced surfactant level and therefore appears to offer an alternative route for the synthesis of relatively small latex particles, a route that is currently under investigation in our group.

6.3.1.2 Radiation Initiation The basis of radiation processing is the ability of high-energy radiation to produce reactive cations, anions, and free radicals in materials. Radiation processing and polymerization involves mainly the use of either electron beams from electron accelerators, or gamma radiation from cobalt-60 (^{60}Co) sources. The role of reactive free radicals, cations, and anions in the production and crosslinking of synthetic polymers is well known.

Even though radiation-induced polymerization and crosslinking are usually much faster than conventional processing, the reactions that occur at the molecular level are not instantaneous. Even though many monomers can be polymerized by exposure to high-energy radiation, the industrial applications in this field have remained rather small, except for radiation curing of coatings containing acrylates.

Work on emulsion polymerization of vinyl monomers dates back to the mid-1930s in Germany, and the method has continued to grow in appeal. Typically, conventional emulsion polymerization uses chemical initiators, such as potassium persulfate. More recent work has shown that emulsion polymerization of vinyl monomers can also be brought about by radiolysis. An advantage of radiation-induced emulsion polymerization is that the process is temperature-independent and can be carried out at relatively low temperatures.

Taylor et al.[62] describe the laboratory-scale and pilot-scale studies on gamma-radiation-induced emulsion polymerization of vinyl and styrene. The industrial potential of radiation-induced emulsion polymerization remains to be exploited.

There are several important advantages compared with the use of chemical initiators, such as

1. Radiation can give an essentially unlimited range of radical fluxes from zero to those equivalent to many moles per liter of chemical initiators. Associated with this is the ease with which the fluxes can be monitored during the course of a polymerization reaction. The fluxes can be programmed, leading in principle to the orderly control of molecular weight and particle size distributions and to the elimination of residual monomer.

2. Initiation with radiation is essentially temperature-independent. This leads to comparatively low temperature dependencies for the overall reaction, with the activation energy dropping from about 84 kJ/mol for chemical initiation to only 29 kJ/mol. This difference makes the possibility of exothermic, runaway reactions extremely low. The low activation energy means that polymerizations can be conducted at will at any temperature and initiation rate. In principle this can be accomplished with chemical initiation, including redox systems. In practice, however, low-temperature initiation is especially difficult to achieve and control, particularly with polar monomers. The low-temperature polymerization of vinyl acetate is of particular interest. A study up to the pilot plant scale has been described in the literature.

3. The radicals produced by radiolysis of water are mainly hydrogen ($H^{\bullet}$) and hydroxyl ($OH^{\bullet}$) radicals. These radicals are neutral and highly reactive, which leads to efficient initiation without the need for any electrolytes and buffers, as are required for most chemical systems. No contamination with residual initiator fragments occur.

There are disadvantages to the use of radiation, for example, there are no ionic end groups such as those arising from persulfate initiation. These could lead to some stabilization of the resulting latex. In addition, the radiation attacks all the components, including the emulsifier and the polymer as it is formed. Irradiation of the emulsifier could lead to a small amount of grafting. Irradiation of the polymer could lead to branching and a small loss of functional groups. A more important problem, which could arise in flow reactors or even kettle systems, is the possible buildup of polymer on the walls of the reaction vessel, due to the diminishing flow rate near the wall.

From a fundamental point of view, it is interesting to speculate on the differences that could exist between the kinetics after initiation by gamma radiation or a chemical initiator. At radiation dose rates giving a free-radical flux comparable to those achieved with chemical initiation, the differences should be minor.

There are differences, however. Water soluble initiators generate free radicals only in the aqueous phase, whereas with radiation radicals are generated in every phase. In the case of styrene where the so-called G (radicals) is only 0.7 compared with 6 in the aqueous phase, this is not a problem, but in the case of vinyl acetate, G (radicals) may be as high as 5, and this could lead to considerable disruption of the conventional Smith–Ewart case 2 kinetics.

6.3.2 Living/Controlled Radical Polymerization in Heterogeneous Systems

Polymers with designer architectures prepared by living/controlled radical polymerization (LRP) have invoked the interest of academia and industry.[63] The various architectures that can be prepared in bulk or solution are now left up to the imagination, and moreover the applications for such architectures are slowly being realized. Three radical polymerization techniques are currently used to control molecular weight distribution, composition, and structure: nitroxide-mediated,[64,65] atom

transfer reactions catalyzed by a transition metal complex,[66,67] (ATRP), and reversible chain transfer reactions by direct exchange[68] or by addition–fragmentation[69] (RAFT). The challenge is to prepare these architectures in an environmentally friendly media, water. The purpose of this section is to examine the current literature on the use of LRP in dispersed media, to derive a mechanistic understanding of LRP and describe the advantages and limitations of the various techniques. These techniques have been applied under heterogeneous conditions such as suspension, dispersion, ab initio emulsion, seeded emulsion, and miniemulsion.

The major advantages of dispersed media over bulk or solution is that the polymerization is carried out in an environmentally friendly medium. It is a cheap and versatile process that can be used for a broad range of monomers and a wide range of experimental conditions, the heat transfer is highly efficient, high conversions with low monomer residuals can be reached, there is an absence of organic volatile compounds, and one can obtain high polymer solids ($\sim$50 wt%) in a low-viscosity environment, which means that the polymer is easy to process. Together with these advantages, LRP offers the preparation of well-defined polymer architectures with novel particle morphologies, which invariably will open a new class of polymer materials for use in the coatings industry and as speciality polymers.

Although LRP techniques are well understood in bulk or solution, in heterogeneous polymerizations the already complex kinetics are further complicated by partitioning of the activating species in the various environments, the rate of transportation of these species and larger dormant ones to the reaction locus, aqueous-phase reactions, choice of surfactant, and control of the particle size distribution (PSD). However, the major kinetic advantage of dispersion polymerizations in principle is compartmentalization of the propagating radicals in either particles or droplets, which diminishes bimolecular termination, and consequently enhances the rate of polymerization with better control of the MWD compared to both bulk and solution polymerizations. Indeed, the polymerization times are of considerable importance when scaling up to an industrial process, and dispersion polymerization offers great hope in this area.

6.3.2.1 Nitroxide-Mediated Polymerization (NMP)

The application of nitroxide-mediated polymerization (NMP) has been limited to mainly styrene using either TEMPO or alkoxyamines with a TEMPO (2,2,6,6-tetra methylpiperidine-N-oxyl) moiety. The temperatures required for control of the MWD in these systems is as high as 125°C, in which poor colloidal stability and the greater partitioning of the hydrophobic species into the aqueous phase are major factors. However, a nitroxide (SG1) has recently been synthesized that allows the use of lower temperatures ($\sim$90°C).[70]

P—O—N ⇌ P• + •O—N

Alkoxyamine   TEMPO
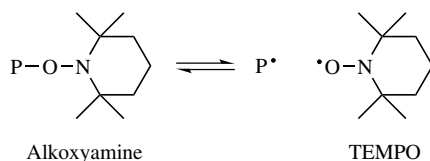
The first reported use of NMP in emulsion was by Bon et al.,[71] who wanted to study the evolution of the MWD without the mitigating complexities of the particle nucleation process, and therefore used a high molecular weight seed (with a diameter of 90 nm). The recipe was also designed such that monomer droplets were not present, thereby eliminating any transportation limitations of either the nitroxide or alkoxyamine from the droplets to the particles (i.e., interval III). The reaction was carried out at 125°C using Aerosol MA-80 surfactant, alkoxyamine, and a small amount of additional TEMPO. It was found that the reaction times to reach high conversions were as long as 36 h. The Mn and polydispersity ($\sim$1.5) were similar to that observed in bulk; however, a pronounced broadening of the low-molecular-weight tail was observed. This was ascribed to irreversible bimolecular termination or transfer and the extra thermal initiation of styrene found at these high temperatures, in which there is a greater probability of termination in smaller particles due to compartmentalization.[72]

At about the same time, Marestin et al.[73] used the NMP under ab initio conditions for a wide range of nitroxides, using potassium persulfate (KPS) as water-soluble initiator. They observed that although SDS was hydrolyzed during the polymerization, SDS in combination with an amino-TEMPO gave the best results. The obtained polydispersities were low, ranging from 1.23 to 1.7, with reaction times close to 50 h for 60% conversion, and a large average particle diameter close to 500 nm. It was suggested that the amino-TEMPO provided additional stability to the latex particles. When other nitroxides (e.g., TEMPO, hydroxy-TEMPO) were used, there was no polymerization even after considerable reactions times (78 h for tert-butoxy-TEMPO) before coagulation occurred. The reason for this is not self-evident, but does suggest that the nucleation process coupled with aqueous-phase reactions with the nitroxide play an important role.

A method to avoid the nucleation stage without the use of a seed is via a miniemulsion. In this case all the compounds are located in droplets stabilized against coalescence and Ostwald ripening by surfactant and a costabilizer (e.g., hexadecane). Charleux[72] discussed the theoretical aspects of NMP miniemulsion, relating the kinetics and MWD to the size of the droplets. The theory, neglecting partitioning, aqueous-phase reactions and chain-length-dependent termination, predicted that with large droplets the kinetics and MWD were similar to bulk, but when the particles were small enough (diameter <100 nm), the rate was increased "owing to slower terminations." Consequently, the residual nitroxide formed from termination was also lower, but the MWD was broader.

Miniemulsion of styrene in the presence of TEMPO was carried out using benzoyl peroxide (BPO) oil-soluble initiator, with anionic surfactant Dowfax 8390 with hexadecane as costabilizer at 125°C.[74] The expected living behavior as exhibited by a linear increase in Mn with conversion and low polydispersities (1.4–1.7) was observed. The average particle diameter was 121 nm, and interestingly, the rate was slower than for a corresponding bulk reaction, which is opposite to that predicted by theory. They attributed this apparent contradiction to partitioning of the active species in the aqueous phase. Importantly, the reaction times to reach >90% conversion were 12 h, much faster than observed in conventional L/CRP

emulsions. In addition, the authors postulated that bulk polydispersities were comparatively higher because of the high viscosity at high conversions, whereas in miniemulsion the hexadecane presumable acts as a plasticizer. MacLeod et al.[75] used KPS as initiator and sodium dodecyl benzene sulfonic acid, and found that there was an optimal ratio of components [surfactant to cosurfactant (hexadecane), and TEMPO to KPS] to provide stable latex particles with good MWD control and reactions times as fast as 6 h for conversions greater than 87%. The initial particle size was approximately 90 nm and was the same at final conversion, suggesting that most of the droplets were nucleated. It has been shown that the rate in traditional miniemulsion can be enhanced by the addition of polymer. In work yet to be published, Georges added a polymeric alkoxyamine and found an increased rate while maintaining a low polydispersity.

The results above suggest that caution should be taken in choice of surfactant due to the high temperatures used. A novel acyclic β-phosphonylated nitroxide (SG1) could be used at temperatures below 100°C for styrene. Styrene miniemulsions using this nitroxide in the presence of a conventional SDS surfactant, hexadecane, and initiated with KPS at 90°C were carried out.[70] Stable latex particles were produced with an average diameter of 250 nm but with a broad particle size distribution. An induction period was observed due to the formation and growth of water-soluble alkoxyamines, and their transferral to the organic phase to begin polymerization. These polymer chains were extended by further polymerization with styrene.

NMP has been shown to produce a controlled and narrow MWD in miniemulsions and seeded styrene polymerizations, but because of the sensitive nature of the kinetics and thermodynamics of heterogeneous systems, correct reaction conditions need to be selected in order to gain optimal control over rate, MWD, and colloidal stability. In particular, the partitioning of the nitroxide and alkoxyamines between the water and organic phases is a critical issue.

6.3.2.2 *Atom Transfer Radical Polymerization (ATRP)*

Unlike NMP, ATRP has been used successfully to prepare well-defined polymers and copolymers of styrenes, acrylates, methacrylates, and acrylonitrile.[66,67,76] The versatility of this technique for a range of monomers and at lower temperatures than NMP should in principle allow the production of well-defined polymer architectures in dispersed media. However, the ATRP process in conventional emulsions was initially fraught with problems when SDS was used as surfactant.[77] Molecular weights were high with broad polydispersities, which was attributed to the reaction of SDS with the copper(II) bromide to form copper(II) sulfate. The loss of copper(II) in this way resulted in little or no deactivation of the growing radical chains, and consequently behaved similarly as a redox initiated conventional radical polymerization. Nonionic surfactants solved the problem, but although well-defined poly(butyl methacrylate) was prepared using poly(ethylene glycol) as stabilizer at 90°C, the polymer latex was not stable and resulted in high amounts of coagulation. Brij 98 gave the best results, stable latex particles, well-defined polymer, and rates identical to that found in bulk. Even lower polydispersities were found by lowering the temperature to 70°C, assumed to be due to the lower rate of termination. The ideal ratio of

surfactant to monomer ranged from 1 to 5% (wt/v). Other considerations were the hydrophobicity of the ligand and the type of monomer.[78] When ligands (e.g., Me$_6$-TREN) were used that partitioned preferentially into the water phase when complexed to the copper(II), polymerizations invariably resulted in uncontrolled behavior. In contrast, changing the ligand to dNbpy allowed the production of well-defined polymers. Both polystyrene and poly(butyl acrylate) were successfully prepared by ATRP, but the rates were much slower than for butyl methacrylate. Another problem was that 1-phenylethyl bromide hydrolyzed during ultrasonication, and the stable 2-bromoisobutyrate was used. The use of this initiator gave high and broad molecular weights (Mn > 200 K, PD > 2) with fast reaction rates, attributed to the accumulation of the highly water-soluble copper(II) bromide in the water phase and thus loss of deactivation.

Similar to the NMP, partitioning is a major consideration in ATRP for both the ligand and the copper(II) complex. Chambard et al.[79] carried out ATRP emulsion polymerizations of methyl methacrylate using two ligands, dPP and dHbpy. They found that for dPP the molecular weight was high with polydispersities close to 2, whereas with dHbpy molecular weight increased linearly with conversions with a polydispersity close to 1.4 at high conversion. They concluded that once the copper(I)/dPP complex was formed, it partitioned into the aqueous phase, resulting in an increased concentration of dormant species in the particles. The use of a more hydrophobic complexing agent (dHbpy) resulted in controlled behavior and ascribed the slow rate toward the end of the reaction as due to the persistent radical effect.

Once the correct experimental conditions have been chosen, control of MWD and polymer structure can be obtained. Matyjaszewski et al.[80] synthesized statistical and block copolymers in water-borne systems. The blocks of butyl acrylate and styrene were made by addition of a poly(butyl acrylate) initiator with surfactant and styrene, polymerized at 90°C to give well-defined polymer (polydispersity <1.19). They also found that the persistent radical effect was also in operation for this system.

Although conditions have been found under which the MWD can be controlled, control of the particle size distribution proved rather difficult. Reverse ATRP using a water-soluble initiator could lend some help in the nucleation process. The choice of initiator is important for this purpose. When KPS is used in the presence of a buffer, the polymer [poly(butyl methacrylate)] is well defined but the particle size is very large close to 2510 nm.[81] This size is presumably due to the lack of colloid stability from the high concentration of salts in the system. The substitution with an azo initiator V-50 also gave well-defined polymer, but the particle diameter in this case is reduced drastically to 85 nm, which is in the range of conventional emulsion polymerizations. A mechanistic study of reverse ATRP on this monomer (butyl methacrylate) was also conducted.[82] The particle size ranged from 150 to 300 nm, and was shown to decrease from 20 to 40% conversion, after which it remained relatively constant. The nucleation behavior and the factors that govern the evolution of the particle size distribution for ATRP is an area that needs further investigation.

6.3.2.3   *Reversible Addition–Fragmentation Chain Transfer (RAFT)*   The main disadvantage of NMP and ATRP is the troublesome partitioning of the small

deactivating species over the two phases, which complicates the kinetics by altering the relative concentrations of active, persistent and dormant species inside the growing particles.[72] If the persistent species moves into the water phase, it will slow down the growth of aqueous phase radicals, hampering radical entry, while at the same time decreasing the rate of polymerization. Control of molecular weight at the main locus of polymerization (i.e., inside the particle) will be decreased because of the decrease in deactivating species. It has also been suggested that the persistent radical effect, which adds to the control in bulk and solution polymerizations, will cause a significantly greater rate of retardation due to the increased local persistent radical concentration inside the particles.[83]

Techniques based on degenerative transfer form should have rates similar to those in conventional emulsion polymerizations since the number of free propagating radicals remains theoretically unaffected. The other advantage is that the controlling species is attached to a dormant polymer chain and thus will not be able to diffuse out of the particle, negating the effect of exit and thus lack of molecular weight control. Several studies reported the successful application of such techniques in waterborne systems. All of these studies apply relatively inactive species to control the polymerization. The alkyl iodides used by several groups[83,84] have a transfer constant only slightly higher than unity. A similarly slow consumption of the compound can be expected for the reversible addition–fragmentation chain transfer (RAFT) agents because of either a poor homolytic leaving group[85] or a rather unactivated carbon–sulfur double bond,[86] respectively. Although these systems allow the preparation of architectures (e.g., block copolymers), the polydispersities are usually broad (∼2) since the transfer agent is consumed at a rate similar to that for monomer. Smulders et al.[87] studied the effect of entry and exit of RAFT agents with low transfer coefficients in seeded emulsion polymerizations. As expected as a result of the fragmentation, exit was enhanced, leading to retardation, but more surprisingly the entry rate was lowered, suggesting that these RAFT agents (xanthates) were surface-active. Zeta potential and conductivity experiments were carried out and showed that these RAFT agents were indeed pushing SDS into the aqueous phase. For the xanthates this could be due to its canonical form, which is an ionic species. Fortuitously, though, the enhanced exit rate coefficient can be used to control the particle size while maintaining the predicted MWD, which allows one to control not only the MWD but also the particle size distribution.[88]

The transition from transfer agents with low activity to those with a high activity, therefore, appears to be straightforward, but in practice this turns out to be more complicated. In previous work several RAFT agents have been applied in conventional emulsion polymerizations (SDS as surfactant), both seeded[89] and ab initio.[90] While low-activity xanthates could easily be used,[86] high reactivity agents based on the dithiobenzoate group invariably led to colloid stability problems and a conspicuous red layer.[89] A large amount of the transfer agent would be lost in the form of an (oligomeric) coagulant, resulting in a much higher molar mass than was to be expected for the emulsion material. Moad et al.[91] overcame this problem by using a semibatch process, where all the RAFT agent together with SDS and water-soluble initiator in the presence of a small amount of monomer was polymerized at 80°C for

40 min, after which monomer was fed in slowly over time. The methodology was to polymerize in the absence of monomer droplets.

This methodology led to RAFT polymerization being carried out under miniemulsion conditions. The use of SDS or for that matter any ionic stabilizer with a hydrophobe led to destabilization of the miniemulsion for polymerizations of styrene or ethyl hexyl methacrylate (EHMA).[92] However, a linear increase in Mn was found with conversion with polydispersities as high as 2. Conductivity measurements were also carried out to study the extent of surfactant migration into the aqueous phase. The results showed that SDS did migrate, but only after polymerization was initiated. The destabilization mechanism is still unknown. It was assumed, though, that it could be similar to the destabilization observed for ATRP in the presence of SDS. Therefore, ionic surfactants were substituted for nonionic surfactant (e.g., Brij 98).[93] This allowed well-defined polymer to be prepared with no stability problems. However, retardation compared to that without RAFT agent was found. This was ascribed to be due to termination of the intermediate radical species, thus lowering the propagating radical concentration considerably.[94] Although the rate is affected, this mechanism should have little or no effect on the MWD since the amount of RAFT dormant chains is less than 5%.

Brij 98 was used as surfactant to polymerize in miniemulsion a wide range of monomers and also for the preparation of block copolymers with low polydispersities (<1.2).[93] One major advantage of the RAFT process is that acidic monomers can be used, which provide very efficient stability to the polymer latex particles. For example, using Brij 98, a block copolymer of polyEHMA-block-poly(methyl methacrylate-*co*-methacrylic acid) was prepared.

In summary, the three techniques described all show that LRP in dispersed media can be carried out successfully. However, conditions need to be chosen carefully to obtain well-defined polymer architectures. It seems that the presence of droplets is the cause of many problems found in these systems. Miniemulsions offer the best method of choice to overcome this problem, but it should be realized that the amount of hexadecane (cosurfactant) required is as high as 5 wt% to monomer, and the particle size distribution is harder to control than in ab initio or seeded conventional emulsions. These miniemulsion latexes will undoubtedly have different film properties with the same polymer architectures due to the different particle morphologies, which are determined by a combination of thermodynamic and kinetic factors. The novel particle morphologies that will invariably be formed through LRP will open a new class of materials. The properties of which are being investigated and are an area of research that requires attention.

REFERENCES

1. D. E. Mestach and F. Loos, *FATIPEC Congr. 24th*, B/91–B/106 (1998).

2. L. E. Ivarsson, O. J. Karlsson, and D. C. Sundberg, *Macromol. Symp.* **151**, 407 (2000).

3. A. Rudin, *Macromol. Symp.* **92**, 53 (1995).

4. G. Riess, *Makromol. Chem.* **69**, 125 (1993).

5. A. Guyot, in *Comprehensive Polymer Science*, G. C. Eastmond, A. Ledwith, S. Russo, and P. Sigwalt, Pergamon Press, Oxford, 1989, Vol. 4, pp. 261.

6. K. E. J. Barrett, *Dispersion Polymerization in Organic Media*, Wiley, New York, (1975).

7. D. A. Canelas, D. E. Betts, and J. M. DeSimone, *Macromolecules* **29**, 2818 (1996).

8. S. L. Holt, *Microemulsions: A Contemporary Overview*, Marcel Dekker, New York, 1980.

9. J. S. Guo, E. D. Sudol, J. W. Vanderhoff, and M. S. El-Aasser, *ACS Symp. Ser. Polym. Latexes—Prep. Character. Appl.* **492**, 99 (1992).

10. H.-I. Tang, E. D. Sudol, M. E. Adams, C. A. Silebi, and M. S. El-Aasser, *ACS Symp. Ser. Polym. Latexes—Prep. Char. Appl.* **492**, 72 (1992).

11. J. W. Vanderhoff, E. B. Bradford, H. L. Tarkowski, J. B. Shaffer, and R. M. Wiley, *Adv. Chem. Ser.* **34**, 32 (1962).

12. J. Ugelstad, A. Berge, T. Ellingsen, R. Schmid, T. N. Nilsen, P. C. Moerk, P. Stenstad, E. Hornes, and D. Olsvik, *Progr. Polym. Sci.* **17**, 87 (1992).

13. M. Okubo, E. Ise, and T. Yamashita, *J. Polym. Sci.* **36**, 2513 (1998).

14. M. J. Murray and M. J. Snowden, *Adv. Colloid Interface Sci.* **54**, 73 (1995).

15. F. Candau, Z. Zekhnini, and F. Heathley, *Macromolecules* **19**, 1895 (1986).

16. R. Arshady, *Colloid Polym. Sci.* **270**, 717 (1992).

17. E. L. Kitzmiller, C. M. Miller, E. D. Sudol, and M. S. El-Aasser, *Macromol. Symp.* **92**, 157 (1995).

18. I. A. Maxwell, B. R. Morrison, D. H. Napper, and R. G. Gilbert, *Macromolecules* **24**, 1629 (1991).

19. W. Lau, U.S. Patent 5,521,266 (Rohm and Haas Company) (1996).

20. C. M. Miller, E. D. Sudol, C. A. Silebi, and M. S. El-Aasser, *Macromolecules* **28**(8), 2754 (1995).

21. M. Slawinski, M. Schellekens, J. Meuldijk, A. M. van Herk, and A. L. German, *J. Appl. Polym. Sci.* **76**, 1186 (2000).

22. M. Slawinski, J. Meuldijk, A. M. van Herk, and A. L. German, *J. Appl. Polym. Sci.* **78**, 875 (2000).

23. M. S. El-Aasser and R. M. Fitch, eds., Future Direction in Polymer Colloids, Martinus Nijhof, Dordrecht, The Netherlands, 1987.

24. R. G. Gilbert, *Emulsion Polymerization: A Mechanistic Approach*, Academic Press, London, 1995.

25. P. A. Lovell and M. S. El-Aasser, *Emulsion Polymers and Emulsion Polymerization*, Wiley, Chichester, UK, 1997.

26. W. V. Smith and R. W. Ewart, *J. Chem. Phys.* **16**, 592 (1948).

27. A. R. Goodall, M. C. Wilinson, and J. Hearn, *J. Polym. Sci.* **15**, 2193 (1977).

28. R. M. Fitch and C. H. Tsai, in *Polymer Colloids*, R. M. Fitch, ed., Plenum Press, New York, 1971, p. 73.

29. P. J. Feeney, D. H. Napper, and R. G. Gilbert, *Macromolecules* **17**, 2520 (1984).

30. K. Tauer and I. Kuehn, *NATO ASI Ser.* **335**, 49 (1997).

31. H. Tobita, Y. Takada, and M. Nomura, *Macromolecules* **27**, 3804 (1994).

32. E. Giannetti, G. Storti, and M. Morbidelli, *J. Polym. Sci.; Part A: Polym. Chem. Ed.* **26**, 1835, 2307 (1988).

33. G. Lichti, R. G. Gilbert, and D. H. Napper, in *Emulsion Polymerization*, I. Piirma, ed., Academic, Press, New York, 1982.

34. P. A. Weerts, A. L. German, and R. G. Gilbert, *Macromolecules* **24**, 1622 (1991).

35. A. M. van Herk and A. L. German, *Macromol. Theory Simul.* **7**, 557 (1998).

36. P. J. Flory, in *Principles of Polymer Science*, Cornell Univ. Press, Ithaca, NY, 1953.

37. I. A. Maxwell, J. Kurja, G. H. J. van Doremaele, A. L. German, and B. R. Morrison, *Makromol. Chem.* **193**, 2049 (1992).

38. E. Vanzo, R. H. Marchessault, and V. Stannett, *J. Colloid Sci.* **20**, 65 (1965).

39. I. A. Maxwell, J. Kurja, G. H. J. van Doremaele, and A. L. German, *Makromol. Chem.* **193**, 2065 (1992).

40. H. A. S. Schoonbrood, M. A. T. van den Boom, A. L. German, and J. Hutovic, *J. Polym. Sci., Polym. Chem. Ed.* **32**, 2311 (1994).

41. H. A. S. Schoonbrood, H. M. G. Brouns, H. A. Thijssen, A. M. van Herk, A. L. German, *Makromol. Symp.* **92**, 133 (1995).

42. L. F. J. Noel, J. L. Altveer, M. D. F. Timmermans, and A. L. German, *J. Polym. Sci., Polym. Chem. Ed.* **32**, 2223 (1994).

43a. G. H. J. Van Doremaele, Ph.D. thesis, Eindhoven Univ. Technology, The Netherlands, 1990.

43b. G. H. J. Van Doremaele, A. M. van Herk, and A. L. German, *Makromol. Chem., Macromol. Symp.* **35/36**, 231 (1990).

44. J. Guillot, *New J. Chem.* **11**, 787 (1987).

45. N. Pourahmady and P. I. Bak, *Polym. Prep., ACS, Div. Polym. Chem.* **31**(1), 603 (1990).

46. H. A. S. Schoonbrood, R. C. P. M. van Eynatten, B. van den Reijen, A. M. van Herk, and A. L. German, *J. Polym. Sci., Polym. Chem. Ed.* **34**, 935 (1996).

47. H. A. S. Schoonbrood, B. Van Den Reijen, J. B. L. de Kock, B. G. Manders, A. M. van Herk, and A. L. German, *Makromol. Chem. Rapid Commun.* **16**, 119 (1995).

48. J. Šnupárek, *Makromol. Chem. Suppl.* **10/11**, 129 (1985).

49. L. Rios, M. A. Cruz, J. Palacios, L. M. Ruiz, and A. Garcia-Rejon, *Makromol. Chem., Suppl.* **10/11**, 477 (1985).

50. S. Omi, M. Negishi, K. Kushibiki, and M. Iso, *Makromol. Chem. Suppl.* **10/11**, 149 (1985).

51. M. S. El-Aasser, T. Makgawinata, J. W. Vanderhoff, and C. Pichot, *J. Polym. Sci., Polym. Chem. Ed.* **21**, 2363 (1983).

52. D. R. Basset, in *Science and Technology of Polymer Colloids*, G. W. Poehlein, R. H. Ottewil, and J. W. Goodwin, eds., Martinus Nijhoff Publishers, The Hague, 1983, Vol. 1, p. 220.

53. F. J. Schork, in *Advances in Emulsion Polymerization and Latex Technology*, Vol. 1, 1990.

54. A. L. German, A. M. van Herk, H. A. S. Schoonbrood, and A. M. Aerdts, in *Emulsion Polymers and Emulsion Polymerization*, P. Lovell and M. S. El-Aasser, eds., Wiley, New York, 1997, Chapter 11.

55. M. van den Brink, A. M. van Herk, and A. L. German, *Makromol. Symp.* **150**, 121 (2000).

56a. G. Arzamendi and J. M. Asua, *J. Appl. Polym. Sci.* **38**, 2019 (1989).

56b. G. Arzamendi and J. M. Asua, *Makromol. Chem., Macromol. Symp.* **35/36**, 249 (1990).

57. F. H. A. M. van de Boomen, J. Meuldijk, and D. Thoenes, *Chem. Eng. Sci.* **51**, 2787 (1996).

58. G. F. M. Hoedemakers and D. Thoenes, in *Integration of Fundamental Polymer Science and Technology*, P. J. Lemstra and L. A. Kleintjes, eds., 1990, p. 182.

59. J. Meuldijk, C. J. G. van Strien, F. H. A. C. van Doormalen, and D. Thoenes, *Chem. Eng. Sci.* **47**, 263 (1992).

60. F. H. A. M. van de Boomen, Ph.D. thesis, Eindhoven Univ. Technology, The Netherlands, 1997.

61. G. Cooper, F. Grieser, and S. Biggs, *J. Colloid Interface Sci.* **184**, 52 (1996).

62. M. B. Taylor, R. D. Gilbert, V. T. Stannett, and J. L. Williams, *J. Appl. Polym. Sci.* **53**, 1385 (1994).

63. K. Matyjaszewski, *Controlled Radical Polymerization*, American Chemical Society, Washington, DC, 1998.

64. M. K. Georges, R. P. N. Veregin, P. M. Kazmaier, and G. K. Hamer, *Trends Polym. Sci.* **2**(2), 66 (1994).

65. D. H. Solomon, E. Rizzardo, and P. Cacioli, U.S. Patent 4,581,429 [*Chem. Abstr.* **102**, 221335q (1985)].

66. J.-S. Wang and K. Matyjaszewski, *Macromolecules* **28**, 7901 (1995).

67. J.-S. Wang and K. Matyjaszewski, *J. Am. Chem. Soc.* **117**, 5614 (1995).

68. A. Goto, K. Ohno, and T. Fukuda, *Macromolecules* **31**, 2809 (1998).

69. T. P. Le, G. Moad, E. Rizzardo, and S. H. Thang, RAFT_CSIRO *PCT Int. Appl.* **WO 98/01478** [Chem. Abstr. **128**, 115390 (1998)].

70. C. Farcet, M. Lansalot, B. Charleux, R. Pirri, and J. P. Vairon, *Macromolecules* **33**, 8559 (2000).

71. S. A. F. Bon, M. Bosveld, B. Klumperman, and A. L. German, *Macromolecules* **30**, 324 (1997).

72. B. Charleux, *Macromolecules* **33**, 5358 (2000).

73. C. Marestin, C. Noel, A. Guyot, and J. Claverie, *Macromolecules* **31**, 4041 (1998).

74. T. Prodpran, V. L. Dimonie, E. D. Sudol, and M. S. El-Aasser, *Macromol. Symp.* **155**, 1 (2000).

75. P. J. MacLeod, R. Barber, P. G. Odell, B. Keoshkerian, and M. K. Georges, *Macromol. Symp.* **153**, 31 (2000).

76. K. Matyjaszewski, T. Patten, J. Xia, and T. Abernathy, *Science* **272**, 866 (1996).

77. S. G. Gaynor, J. Qiu, and K. Matyjaszewski, *Macromolecules* **31**, 5951 (1998).

78. K. Matyjaszewski, J. Qiu, D. A. Shipp, and S. G. Gaynor, *Macromol. Symp.* **155**, 15 (2000).

79. G. Chambard, P. de Man, and B. Klumperman, *Macromol. Symp.* **150**, 45 (2000).

80. K. Matyjaszewski, D. A. Shipp, J. Qiu, and S. G. Gaynor, *Macromolecules* **33**, 2296 (2000).

81. J. Qiu, S. G. Gaynor, and K. Matyjaszewski, *Macromolecules* **32**, 2872 (1999).

82. J. Qiu, T. Pintauer, S. G. Gaynor, et al., *Macromolecules* **33**, 7310 (2000).

83. A. Butté, G. Storti, and M. Morbidelli, *Macromolecules* **33**, 3485 (2000).

84. M. Lansalot, C. Farcet, B. Charleux, J.-P. Vairon, and R. Pirri, *Macromolecules* **32**, 7354 (1999).

85. I. Uzulina, S. Kanagasabapathy, and J. Claverie, *Macromol. Symp.* **150**, 33 (2000).

86. M. J. Monteiro, M. Sjoberg, C. M. Gottgens, and J. van der Vlist, *J. Polym. Sci.; Part A: Polym. Chem.* **38**, 4206 (2000).

87. W. Smulders, R. G. Gilbert, and M. J. Monteiro, *Macromolecules* (in press).

88. M. J. Monteiro, J. de Barbeyrac, and A. L. German, *Macromolecules* **34**, 4416 (2001).

89. M. J. Monteiro, M. Hodgson, and H. de Brouwer, *J. Polym. Sci.; Part A: Polym. Chem.* **38**, 3864 (2000).

90. M. Hodgson, grad. thesis, Univ. Stellenbosh, South Africa, 2000.

91. G. Moad, J. Chiefari, Y. K. Chong, et al., *Polym. Int.* **49**, 993 (2000).

92. J. G. Tsavalas, F. J. Schork, H. de Brouwer, and M. J. Monteiro, *Macromolecules* **34**, 3938 (2001).

93. H. J. de Brouwer, J. G. Tsavalas, F. J. Schork, and M. J. Monteiro, *Macromolecules* **33**, 9239 (2000).

94. M. J. Monteiro and H. de Brouwer, *Macromolecules* **34**, 349 (2001).

7 Industrial Applications and Processes

MICHAEL F. CUNNINGHAM

Queen's University, Kingston, Ontario, Canada

ROBIN HUTCHINSON

Queen's University, Kingston, Ontario, Canada

CONTENTS

7.1. INTRODUCTION

''Industrial applications and processes'' of polymers is itself often a topic for entire books.[1] The reason is clear, when one considers that in the United States alone, 37×10^6 metric tons of plastics, 4.5×10^6 metric tons of synthetic fibers, 2.4×10^6 metric tons of synthetic rubber, and 5×10^6 cubic meters of paints and coatings were produced in 1999.[2] While difficult to provide an exact breakdown, it is estimated that materials made via free-radical polymerization comprise over half of this total,[1] including these major industrial polymer families:

- Low-density polyethylene (LDPE) and copolymers, used primarily in films and packaging applications. LDPE has density of $<0.94\,g/cm^3$, and is produced via high-pressure free-radical polymerization; polyethylenes of higher density (and polypropylene) are produced via transition metal catalysis.

- Poly(vinyl chloride) (PVC) and copolymers, used primarily to produce pipe and fittings, flooring material, and films and sheet.

- Polystyrene and its co- and terpolymers with acrylonitrile and butadiene. Homopolymer is used for packaging and containers, while the acrylonitrile-containing polymers are used for various molded products in the appliance, electronics, and automotive industries. Styrene–butadiene is the most widely used synthetic rubber.

- Acrylic- and methacrylic-based polymers. Polymethyl methacrylate (PMMA), because of its transparency and weatherability, is used extensively in signs, lighting fixtures, and windows. Polyacrylates and copolymers are used extensively in the adhesives and coatings markets, and are also combined with acrylonitrile to make acrylic fibers.

- Polyvinyl acetate and copolymers, used extensively in adhesives, coatings, and paper and textile treatment.

- Fluoropolymers, including polytetrafluoroethylene (PTFE) and copolymers, used widely in the wire and cable industry. They also have many specialty applications as coatings because of their inertness and low surface tension.

In addition to these major product families, there exist many other smaller-volume (but often high-value) polymeric products synthesized via free-radical chemistry.

These products are manufactured via heterogeneous (emulsion, suspension) or homogeneous (bulk, solution) polymerization in a wide range of reactor configurations ranging from tubular to well-mixed tanks (and everything in between) in processes that may be continuous, batch, or semibatch. Providing an extensive overview in this brief chapter is impossible. Instead, we focus on the aspects of polymerization systems that strongly influence the design and operation of industrial processes, such as

- The several orders-of-magnitude increase in viscosity that occurs during production of high-molecular-weight (MW) polymer in homogeneous systems. The increase in viscosity can greatly affect the reaction kinetics as well as the heat removal and quality of mixing in the system.

- The influence of reactor design on the polymer properties. Unlike many chemical systems, off-spec(ification) polymeric material cannot be easily recycled or altered by downstream unit operations. The difficulty of online characterization of polymer structure makes design of a robust easy-to-operate process especially important.

- The flexibility and economy of scale of a process. Design and operation requirements are very different for a process manufacturing several grades of a high-volume commodity homopolymer, and one that produces dozens of

different (and often new) low-volume higher-value products of varying composition and structure.

These issues, often neglected during synthesis of a new material or development of a new chemistry in the lab, become critical during process scaleup. The first half of this chapter elaborates on these important considerations, while the remainder overviews some modeling and measurement techniques that serve as important tools to help achieve robust design and operation.

This chapter is not the first treatment of this subject. Among earlier general reviews, readers might find those of Ray and Laurence[3] and Reichert and Moritz[4] of particular value. Other more specific reviews are introduced in the appropriate sections of the chapter.

7.2 POLYMERIZATION PROCESS DESIGN CONSIDERATIONS

The design of an industrial polymerization process begins with a clear understanding of objectives, as well as an appreciation of constraints, both technical and nontechnical. Typical objectives are to manufacture a product with specified physical and chemical properties at a desired production rate. Properties of interest commonly include average molecular weight and molecular weight distribution, copolymer composition and copolymer composition distribution, degree of branching distribution, and sequence length distribution. For products produced in particulate form such as emulsion polymers, additional critical properties might include mean particle size, particle size distribution, morphology (e.g., core–shell), the nature of the particle surface, and the colloidal stability of the latex under storage, transportation, handling, and usage conditions. Depending on the nature of the product, any of a number of these properties can simultaneously be product specifications. However, the polymer is ultimately not sold on these basic structural characteristics but rather on end-use properties. This poses the challenge of relating structural features to properties. Invariably the end-use properties are a product of not one but several structural features, and therefore establishing relationships is a complex task, and the ensuing relationships are usually restricted to a narrow range of materials. Establishing structure–property relationships remains an active area of research.

Together with an understanding of the key properties and their desired values is a need to quantitatively understand how much variation is acceptable for each property. In an industrial polymerization environment, there will naturally be some degree of process variability that will translate into product variability. Knowing the extent to which deviations from the target value of a property affect the manufacturer's ability to sell that product is a critical piece of design information. Design of a process involves several decisions such as the type of reactor used, the flow and contacting patterns for the reagents, and the choice of homogeneous versus heterogeneous process types. Each of these choices confers certain advantages and

disadvantages to the process, but more importantly, each choice also defines certain limits to the performance of the process. An inappropriate choice of reactor type, for example, may make it very difficult or impossible to consistently produce a desired molecular weight distribution. Major retrofitting of existing processes (e.g., changing the reactor type to one that is more suitable) is expensive and fraught with other difficulties.

Following definition of the desired properties, the technical and nontechnical constraints need to be understood. Technical constraints relate directly to inherent limitations of particular process types, while nontechnical constraints include a variety of issues such as economic considerations, process safety, health concerns, and environmental stewardship. The following discussion describes how the selection of a particular process type and/or process variables interact to determine the limitations of that process.

Robustness refers to the inherent ability of a design to consistently and reproducibly deliver the desired physical and chemical properties, while meeting the designed production rate. Poor robustness may be caused by a design that makes it difficult or impossible to consistently achieve the required properties, or is prone to various types of instability (such as fouling of reactor internal surfaces, transfer lines, heat exchangers, or other process equipment) that require the process to be frequently shut down for maintenance.

Careful consideration should be given to phenomena that introduce a high degree of variability to the process. For example, the nucleation stage in emulsion polymerization is known to be sensitive to process conditions, and can be difficult to reliably control even when considerable care is exercised. The progress of the nucleation stage determines the number of particles, and therefore directly determines the final particle size. Of more concern from an operating and safety viewpoint, the polymerization rate for many emulsion polymerizations (depending on the monomers used and the specific experimental conditions) is directly proportional to the number of particles. A process disturbance causing a 20% increase in the particle number may cause an increase in the average heat removal load of $\sim 20\%$. In a commercial size reactor (20–40 m^3), this much additional energy represents a significant potential safety issue for two reasons:

1. The reactor cooling system has likely been designed to operate near its capacity as it is most economical to run commercial processes at the maximum safe rate. There will be a margin of safety built into the cooling system design to allow for unanticipated temperature excursions resulting from process disturbances, but large surges in the heat removal load may still exceed the cooling system's maximum capacity, prompting an emergency shutdown.

2. As reactor size increases, heat transfer generally becomes slower, which increases the probability of the reactor temperature rising out of control. Product properties will almost certainly be affected. Most important is the molecular weight, which will usually depend on the particle number. However, a smaller final diameter may also affect surface and colloidal properties of the emulsion, and possibly lead to colloidal instabilities if there is insufficient surfactant to stabilize

the increased surface area. In emulsion polymerization, a common solution is the use of a seed emulsion. The nucleation stage is conducted in a smaller vessel (separate from the main polymerization reactor) where the particle number can be more reliably controlled. The seed latex is then fed into main reactor to complete the polymerization. Ideally no additional particle nucleation occurs in the main reactor.

A major concern with any free-radical polymerization is effective temperature control. Free-radical polymerizations are highly exothermic, and generally exhibit a high overall sensitivity to temperature. The overall activation energy for a radical polymerization can be calculated from the activation energies of the individual reaction steps (initiation, propagation, transfer, termination, branching). Typical overall activation energies for polymerizations initiated by thermal initiator decomposition are on the order of 84 kJ/mol.[5] However, the values of the individual activation energies should also be examined carefully. Initiator decomposition is usually far more sensitive to temperature than the other steps in the polymerization mechanism. Typical activation energies for initiator decomposition are ∼126–165 kJ/mol, for propagation ∼20–40 kJ/mol, and for termination ∼8–20 kJ/mol.[5] Some properties are known to be more sensitive to particular types of disturbance than others. For example, instantaneous molecular weight is directly influenced by the number of chains being initiated at a given time, and thus is often strongly temperature dependent. In contrast, the copolymer composition distribution, which is primarily determined by the relative rates of propagation of the monomers, tends to have less temperature sensitivity because the ratio of the activation energies for the respective propagation rates is not strongly temperature dependent.

The "controllability" of a radical polymerization is typically highly process- and monomer-dependent. Industrial processes subject to sudden or rapid changes in any of a number of relevant physical or chemical characteristics during the course of reaction may pose challenges to maintaining the desired reaction conditions (temperature, goodness of mixing, colloidal stability, etc.). For example, several monomer systems undergo an autoacceleration (gel effect) in rate during reaction. The sudden and dramatic increase in the heat of reaction can result in loss of effective temperature control. As reactor size increases, the system dynamics become increasingly slow, and therefore it takes longer for desired changes (e.g., decreasing the reactor temperature) to occur. Consequently, the reactor temperature may rise several degrees or more above its desired temperature for a prolonged period. This occurrence may in itself not be a serious problem provided the reactor cooling system is able to maintain control, albeit at a higher than desired temperature. A more serious issue may arise when a product developed using bench- or pilot-scale reactors is scaled up to manufacturing. At smaller scale, temperature excursions are less likely to be an issue, although they may be observed. However, the overall temperature *profile* during the gel effect will almost certainly vary as scale increases. For a monomer like methyl methacrylate, for which the gel effect commences at ∼20–30% conversion, most of the polymer may be produced during gel effect conditions. In this situation, large variations in the temperature profile during the

gel-effect can translate into differences in the final product properties, particularly molecular weight distribution. For more on control of polymerization reactors, see Schork.[6]

Difficulty in controlling temperature becomes even more severe if the overall viscosity increases significantly. This adversely affects controllability because mixing and heat transfer both become more difficult. Even in the absence of a gel effect, high viscosities can pose mixing and thermal control problems. Solution polymerizations offer low viscosity, but the trend in industry is to eliminate (or greatly reduce) the use of organic solvents. (Increasingly stringent VOC (volatile organic component) regulations make solvent-based processes less attractive and are promoting a conversion to water-based systems.) A key advantage of dispersed-phase polymerizations (suspension, emulsion polymerization) is a low continuous phase viscosity that facilitates heat transfer and mixing. In practice, however, economics usually dictates that emulsion polymerizations be run at the highest possible solids loadings. This naturally leads to increased overall viscosity. Furthermore, when structured emulsion particles are being produced with different monomers fed in sequence, changes in surface properties (such as how hydrophilic/ hydrophobic the surface is) can lead to increases or decreases in the overall latex viscosity.

Design of a polymerization process is best initiated at the bench-scale level, and preferably involves design and scaleup engineers from the outset. In addition to a variety of important scaleup issues, controllability needs to be considered early in the process development cycle. Since the early 1990s, most companies have adopted a more integrated team approach to process design and commercialization, in which scaleup expertise is involved at an early stage in the exploration of a promising product. This trend has been driven by pressures to reduce the time required to commercialize new products, which has often in the past required substantial redesign of processes as they were scaled up, or extensive further experimentation to clarify critical scaleup issues. In small-scale experiments, most transport phenomena (e.g., heat transfer, mixing, diffusion) occur sufficiently rapidly that overall behavior is dictated primarily by reaction kinetics. However, as scale increases, kinetic and transport effects become increasingly coupled. At large scale, transport effects can be as important as or even dominate kinetic effects. In laboratory-scale emulsion polymerizations, for example, complete conversion of styrene–methacrylate comonomers can easily be achieved in ~ 1 h. However, conducting this polymerization on an industrial scale may prove enormously challenging or costly because of the large heat removal demands. Many commercial emulsion polymerizations are run in semibatch mode, under conditions where the reaction rate is limited by the addition rate of monomers. In these situations, it is the reactor's heat removal capacity (a transport limitation) that dictates the reaction rate. From a product property perspective, a bench-scale process that can be run nearly isothermally to complete conversion in one hour will almost certainly yield very different properties (molecular weight distribution, copolymer composition distribution, branching) than a process run under monomer-starved conditions in semibatch mode. It is far

more efficient to perform the initial bench-scale design using the intended commercial-scale process, rather than attempting to redesign an existing process at pilot scale.

7.2.1 Batch, Semibatch, and Continuous Processes

There are three major classifications of chemical processes, categorized by the method in which the reactants are added to the reaction vessel. Varying the contacting pattern can dramatically alter the local reaction conditions (e.g., concentrations of individual species, including monomers, initiators, chain transfer agents, etc.), and is therefore a potentially powerful design tool for properties such molecular weight distribution, copolymer composition distribution, and degree of branching. Because of the ability to manipulate local monomer concentrations, the rate of polymerization can also be controlled, thereby providing safer and more robust operation.

7.2.1.1 *Batch Processes*   In a batch process, all the reactants are added to the reactor prior to starting the polymerization. No material is added to or removed from the reactor during operation. When the polymerization is complete, the contents are discharged and the reactor prepared for the next batch. Batch polymerizations are the simplest to run, but offer the least control over the polymerization. For polymerizations with more than one monomer, the relative consumption rates of the different monomers will be governed by their respective reactivities, possibly resulting in broad copolymer composition distributions and inhomogeneous product. Another feature of batch polymerizations is that reactant concentrations change throughout the polymerization. Molecular weight distribution drift is therefore a common phenomenon in batch polymerizations, and can lead to very broad distributions in the final product. From an economic perspective, batch polymerizations suffer from high downtime between batches, although much progress has been made in automating many of the reactant weighing, charging, and discharging steps to minimize time between batches. Automation has also improved reproducibility of batch reactions. For operations where changes to the formulation or the polymerization conditions are common, batch processes have the advantage of being flexible and readily adaptable to new products.

7.2.1.2 *Semibatch Processes*   Semibatch processes (also called *semicontinuous*) are similar to batch processes, except that reactants can be added and/or products removed during the polymerization. Usually only a portion of the total reactant charge is initially fed into the reactor. The polymerization is then started, and reactants are added during reaction in order to control a desired property (e.g., molecular weight distribution, copolymer composition distribution) or the reaction rate. Any reactant can be fed, and it is common practice to add monomer(s), initiators, chain transfer agents, and surfactant. Reactants can be added for a finite period or over the course of the entire reaction. Addition can be started and stopped at any desired time. Three of the most common applications for semibatch operation

are control of copolymer composition distribution, design of core–shell morphologies, and control of reaction rate. In a batch reaction, copolymer composition drifts according to the inherent reactivities of the monomers. However, in semibatch operation, drift can be substantially reduced by maintaining a (near) constant concentration ratio of the respective monomers in the reactor. One or both monomers is (are) fed into the reactor at rates that preserve the desired monomer concentration ratio. Although different strategies can be adopted, a common approach is to initially charge all of the less reactive monomer and a portion of the more reactive monomer so that their initial concentration ratio is at the desired value, and then during reaction feed in the more reactive monomer at a rate that preserves the target monomer concentration ratio.[7–9] Production of low-molecular-weight co- or terpolymers (e.g., coatings) is also readily done using this type of approach. The molecular weight and composition ratio can be controlled by adding initiators and monomers, and maintaining starved conditions with respect to monomer and initiator. (A system is referred to as "starved" with respect to a reactant when the concentration in the reactor is very low, and the reactant consumption rate equals the addition rate.) Molecular weight control is achieved by selecting a rapidly decomposing initiator (mean chain length is then the ratio of monomer to initiator), while the monomers are fed in the desired ratio to provide composition control.

Polymer particles with core–shell morphology are produced using semibatch processes, using either emulsion[10] or microsuspension polymerization.[11] For example, a "soft" [low-T_g (glass transition temperature)] shell can be added to a "hard" (high-T_g) core during emulsion polymerization in particles for coating applications. The core provides the required strength and most of the other bulk film properties, while a soft shell facilitates film formation. The core particles are produced in the first stage of the process, and the shell is then formed by addition of an appropriate monomer. A complex variety of morphologies can result from such a procedure[10] because the desired core–shell morphology may not be the equilibrium conformation. If this is the case, the added monomer may diffuse into the particle interior, or if the particle viscosity is sufficiently low, the core and shell polymers may mutually diffuse to yield a structure much different from the intended core–shell. To ensure that the second monomer polymerizes on the particle surface and to minimize its migration into the particle interior, the second monomer is usually added under starved conditions.

Ensuring safe operation by limiting the polymerization rate is another incentive for semibatch operation. Some free radical polymerizations are sufficiently fast that at large scale the heat of polymerization cannot be safely transferred out of the reactor. In this situation, a portion of the total monomer charge is initially fed into the reactor, and the remainder of the monomer is added during reaction at a rate that is compatible with the heat removal capacity of the cooling system. Often the reaction rate is essentially equal to the monomer addition rate, so that the factor limiting the polymerization rate is the monomer addition rate. This mode of operation also ensures that at any given time the monomer concentration in the reactor is low, and therefore the maximum potential hazard in the event of a thermal runaway

reaction is minimized. A potential concern with operating in a starved mode is that polymer concentrations are high, resulting in higher rates of transfer to polymer and branching reactions. This can have a significant effect on final product properties for monomers like vinyl acetate that exhibit high transfer to polymer.[12–14] Semibatch operation is commonly used in emulsion polymerization.

7.2.1.3 Continuous Processes In a continuous polymerization process, all reactants are fed continuously to the process, and unconsumed reactants and products are removed continuously. The process may take place in a single reactor or in a train (series) of reactors in which the monomer conversion is gradually increased. Most continuous processes are operated at ''steady state'' conditions, meaning all reactant concentrations and process conditions (temperature, pressure, etc.) are time-invariant. This can be an enormous advantage for certain types of properties. For example, because concentrations are constant, there is no molecular weight distribution drift, and no composition distribution drift. The narrowest possible molecular weight and composition distributions are produced in continuous steady-state processes. For large-volume polymers with a limited number of variations to the polymerization conditions (e.g., formulation changes), continuous processes are favored because of their low operating cost, high throughput rates, more uniform product quality, and simplicity of operation. Capital and instrumentation costs tend to be high, but operating costs are generally lower than in batch or semibatch processes. A further requirement for continuous processes that has limited their use in polymerization processes is that they must have long, uninterrupted reaction times between scheduled shutdowns for cleaning and maintenance to warrant their initial high cost. Processes prone to fouling of the reactor internals, transfer lines, or auxiliary equipment (e.g., heat exchangers) are not good candidates for continuous operation as frequent shutdowns for cleaning may be necessary. Particulate processes such as emulsion and suspension polymerization are especially prone to fouling. Continuous emulsion polymerization formulations must yield ''clean'' latexes.[15] In some processes, the inherent dynamics of the process may cause operational problems. For example, the existence of particle nucleation in emulsion polymerization can introduce periodic behavior, or a regular cycling of the conversion (and molecular weight) with time.[16] This is not aberrant behavior, but a consequence of surfactant concentrations cyclically rising to a level sufficiently high to induce a brief period of particle nucleation, which increases the reaction rate and therefore conversion. This is a dynamically stable condition, but is seldom desirable in an industrial setting.

7.2.2 Heat Transfer in Industrial Polymerizations

Free radical polymerizations are highly exothermic reactions, with adiabatic temperature rises for bulk monomers typically $\sim$200–300°C (adiabatic temperature rise is the temperature increase that would occur on complete polymerization if no heat were removed from the system). If there is a process disturbance leading to a thermal runaway condition, the heat generation rate can exceed the heat removal

rate to such an extent that the reaction behaves close to adiabatically. The resulting temperature increase can pose serious safety concerns such as reactor overpressurization and possible explosion, requiring processes to be designed to safely release the pressure prior to failure (rupture) of the process equipment.

In industrial polymerization reactors, the heat of reaction can be removed through the walls of the reactor, internal cooling coils, by using an external heat exchange loop, or by evaporative cooling. Vessels such as stirred tank reactors are usually encased in a sealed ''jacket'' through which a suitable heat transfer fluid is pumped. The temperature of the heat transfer fluid is controlled in a separate circulation loop to maintain the reactor temperature at its setpoint. A variety of different heat transfer fluids are used, depending on the required temperature range and other conditions, including steam, ethylene glycol/water mixtures, and specially designed heat transfer fluids. To increase the surface area available for heat transfer, cooling coils may be added to a reactor. Heat removal capacity may be significantly enhanced, but these coils are often prone to polymer deposition or fouling, which decreases their efficiency and can lead to product quality problems. An alternative to internal coils is an external heat exchange loop. An external circulation loop pumps reactor contents from the reactor through a heat exchanger and back into the reactor. This can be an attractive alternative for processes such as suspension and emulsion polymerization, which tend to be particularly troublesome for fouling cooling coils, but care needs to be taken in selecting the pump type and in the design of the loop to ensure that shear-induced coagulation does not become a problem. The viscosity of the reaction mixture cannot be excessively high, or pumping will become too difficult. Evaporative cooling removes heat by allowing some of the monomer (or solvent) to evaporate. The vapor is then condensed using a conventional condenser and the liquid monomer or solvent is returned to the reactor.

There are two primary modes of heat transfer relevant to radical polymerization processes: conductive heat transfer (conduction) and convective heat transfer (convection). *Conduction* involves the transfer of energy between adjacent colliding molecules. *Convection* involves the transfer of energy arising from bulk motion of the fluid in which molecules from different parts of the reaction mixture are brought into contact with each other. In a polymerization reactor, mixing promotes convective heat transfer between the cooler material near the reactor wall and the hotter material near the reactor core. Convection is also the mechanism by which heat from material flowing near the reactor wall is transferred to the reactor wall surface. Both conduction and convection act in concert. For low-viscosity mixtures that are easily mixed, convection is the dominant heat transfer mechanism. As the viscosity increases, mixing becomes more difficult and therefore the rate of convective heat transfer is reduced. For systems where there is little or no mixing, the dominant heat transfer mechanism becomes conduction. When fouling occurs on the heat exchange surface (e.g., reactor wall) or when the fluid viscosity becomes high at the surface, the rate of convective heat transfer at the surface can drop dramatically. Some processes (e.g., LDPE) use adiabatic autoclaves, and thus there is no heat transfer. The heat of reaction acts to heat the reactor feed stream, and any excess heat is removed from the reactor by the exiting product stream.

In industrial polymerizations, the cooling system's heat removal capacity often becomes a limiting factor. When a reaction is scaled up, the heat generation rate increases in direct proportion to the reaction volume, while the heat removal capacity increases in proportion to the surface area available for heat transfer. The ratio of surface area to reactor volume decreases as the reactor size increases, and therefore it can be expected that at some scale the cooling system's safe operating capacity will be exceeded by the heat generation rate from the desired polymerization reaction. The use of a nonreactive component such as the aqueous phase in suspension or emulsion polymerization, or a solvent in solution polymerization, provides a "heat sink" that absorbs some of the heat of reaction. This advantageous feature is offset by the reduction in reactor productivity caused by the relatively low overall monomer loading.

Failure to adequately control temperature can have deleterious effects on the product quality and pose serious safety issues. As previously discussed, free-radical polymerizations are highly temperature-sensitive. For an excellent discussion of thermal effects, including thermal runaway, the reader is referred to Biesenberger and Sebastian.[16]

7.2.3 Mixing Effects in Polymerization Reactors

The importance of mixing, the contacting of fluid elements from different parts of the reaction vessel with each other, has been the subject of several studies.[4,16–20] Mixing can directly affect the kinetics, molecular weight, and composition in radical polymerizations by homogenizing local concentration gradients, but can also indirectly play an important role through its role in reducing thermal gradients in a reactor. In a small laboratory reactor, good mixing is usually readily achieved and therefore the polymer properties and reaction rate are unlikely to be influenced by mixing effects. However, similar to thermal effects, mixing effects become more apparent as reactor size increases because effectively mixing the entire reaction mixture becomes more difficult.

Within the chemical process industries, polymerization reactions offer a particularly challenging problem because of the large increase in viscosity accompanying the conversion from monomer (~ 1 cP for liquids) to polymer ($>10^5$ cP). Some processes are designed to not require mixing. For example, PMMA can be polymerized in large sheets. By having large surface areas available for heat transfer, adequate temperature control is achieved without the need to provide mixing during polymerization. Heterogeneous polymerizations such as suspension and emulsion utilize an aqueous, low-viscosity continuous phase to ensure that good mixing can be maintained throughout polymerization, with the viscosity increase confined to the dispersed phase (particles). Solution polymerization provides low viscosity and can promote mixing, but requires the removal of solvent from the polymer that is typically energy-intensive and costly. Some monomers are polymerized in bulk (e.g., styrene). The processes will often employ more than one reactor in series, since different reactor configurations and agitators will be required as the viscosity increases.[21,22]

The polymerization of gaseous monomers in free-radical processes poses unique challenges. The high-pressure process for polymerizing ethylene to make low-density polyethylene (LDPE) is an established technology and still widely practiced, despite the importance of Ziegler–Natta and metallocene catalysts in producing high-density polyethylene (HDPE) and linear low-density polyethylene (LLDPE). LDPE is highly branched (with long- and short-chain branches) with a broad molecular weight distribution, and for some applications offers processing and property advantages over the HDPE and LLDPE resins, which have narrower molecular weight distributions and short-chain branches. LDPE is manufactured in high-pressure adiabatic autoclaves [<30,000 psi (lb/in.^{2})] or cooled tubular reactors (<40,000 psi). The temperature and pressure conditions are maintained to keep the polymer in solution within the reactor. Monomer conversion per pass is low (15–30%), with the unreacted ethylene separated from the solid LDPE powder as it exits the reactor and then recycled back to the inlet. The polymerizations are extremely fast and exothermic, with the potential for explosion if the radical concentration in the reactor becomes too high.

Styrene–butadiene rubber (SBR) was the first commercially important emulsion polymerization product. While styrene monomer is a liquid, butadiene is a gas under at standard temperature and pressure, and therefore the process is run under pressure to solubilize the butadiene in the monomer phase. Several commercially important fluorinated monomers (e.g., tetrafluoroethylene, vinylidene fluoride) are polymerized in aqueous dispersions or emulsion polymerization under pressure.[23]

High-impact polystyrene (HIPS) incorporates grafted polybutadiene (PBD) particles into a polystyrene matrix to increase the impact properties. To produce HIPS, PBD is dissolved in styrene (~4–8%) with a peroxide initiator(s) designed to give grafting of the PBD onto the polystyrene chains during the polymerization. Initially the mixture is homogeneous but at ~1–2% conversion two phases appear: a PBD-rich continuous phase and a styrene-rich dispersed phase. At ~5–10% conversion, there is a phase inversion, leading to a styrene-rich continuous phase and a dispersed phase rich in PBD. The phase inversion step is a critical process step in determining the size distribution of the dispersed PBD particles, an important determinant of the final physical properties (e.g., impact strength, environmental stress crack resistance). The phase inversion procedure depends on the mixing conditions in the reactor, and some manufacturers carry out this step in a separate vessel designed solely for that purpose. The HIPS process is an example of a polymerization process having relatively simple chemistry where the properties of the final product are heavily dependent on the mixing conditions during the process.

7.2.4 Economic Considerations

Economic constraints, dictated by what selling price can be realized for a given product, affect every aspect of the process design. Several questions need to be answered and many issues addressed, but ultimately, unless an adequate profit can be expected, commercialization of a product will not proceed. The minimum profit

level must exceed the return that could be realized if the development costs were invested elsewhere, to justify the risk involved in commercialization.

Several factors must be included in assessing the cost of a product, including raw-materials costs, operating costs, and capital costs. Increased product quality can often be achieved by improvements to the process design (e.g., more sophisticated process control, more on-line sensors, better product purification), but the decision to implement these must be weighed against the value they add to the selling price. This, in turn, depends very much on the type of product and its competitive position in the marketplace. Products can be broadly categorized as either commodity or specialty materials. Commodity polymers are produced in high volume in a very competitive environment where there is often only minor differentiation between your product and competitors' products. Profit margins are small and selling prices tend to be low. For these polymers (e.g., polystyrene and polyethylene for use in packaging applications), it is probably not economically justifiable to devote resources to improving the product quality beyond an acceptable level. Specialty polymers are higher-cost materials produced in smaller volumes, usually with higher profit margins and less competition, and with more opportunities to differentiate your product from your competitors on the basis of performance and properties. Users of specialty polymers are often willing to pay a higher price for increased quality, and therefore further process investments may be warranted.

Before a decision is made to invest capital for manufacture of a new product, a rigorous economic assessment is done. Companies will have internal requirements for the minimum acceptable return on investment (ROI) on the basis of projected capital costs, operating costs, raw-materials costs, and market demand over the projected lifetime of the product. Some products may have long expected lifetimes (several years), while others can be expected to be replaced by future products within a few years. While reasonably accurate estimates of capital and operating costs can usually be made, estimating raw material costs and anticipated market demand for the product is fraught with uncertainty. For example, prices of crude oil, a feedstock for many monomers, can be highly volatile. Estimates of market demand for a product is inherently a difficult activity that can be complicated by factors such as the unexpected entry into the marketplace of a similar, competing product, or a change in market conditions that renders your product less desirable.

Whenever feasible, alternatives to new capital investment will be considered. For example, if capacity needs to be expanded, what improvements can be made to the existing facility to increase its output? Operating costs vary inversely with volume, and therefore increases in throughput translate directly into reduced operating costs. Modification of existing but underutilized (or unused) equipment may allow a proposed new product to become economically viable, when it may not be if a new plant is required. Another consideration is whether by tailoring the polymer architecture of a current product, a new market could be created or an existing market expanded.

Selection of process type and operating conditions can profoundly affect the capital and operating costs. Selection of factors such as temperature, pressure, solvent concentration, solvent type, solids loading, reactor size, and postreaction purification

(e.g., catalyst removal) plays a role in determining final cost and therefore the economic viability.

7.2.5   Environmental, Health, and Safety Considerations

Environmental, health, and safety (EHS) issues should be considered from the inception of a new product design, as they will impose constraints on the types of materials that can be used in the polymer synthesis and on the reaction conditions. Major process changes to accommodate EHS issues at advanced stages of the development cycle are costly and time-consuming. Environmental concerns include the use of organic solvents in the manufacturing process, some of which will always escape into the environment (potentially through liquid, gaseous, and solid discharges, and in the actual product). Responsible environmental stewardship now includes "cradle to grave" responsibility for a product (i.e., what the eventual fate of the product is when the user no longer has use for it, and what possible environmental issues may arise). The personal health of plant workers, the community, and consumers should not be adversely affected because a polymer is being manufactured, in either the short or long term. Process safety is of paramount importance in most companies. The operation of any process should be designed to minimize the risk of explosions, runaway reactions, materials-handling mishaps and work-related injuries.

7.3   TECHNIQUES FOR FURTHERING PROCESS UNDERSTANDING

This section provides an overview of the modeling and measurement techniques that can serve as important tools to help achieve the objectives defined in the previous section. Wherever possible, examples have been selected to emphasize industrial application. Although a few historical references are included, the main focus is on advances made since the early 1990s.

7.3.1   Modeling

Mathematical modeling is a powerful methodology to improve the understanding and operation of polymer processes. A good process model can be used to

- Predict the influence of operating conditions on reaction rate and polymer properties.
- Guide (along with appropriate experimentation) the selection and optimization of "standard" operating conditions for existing and new polymer grades; a good model will reduce the required experimentation.
- Guide process development from lab to pilot-plant to full-scale production, helping to discriminate between kinetic and physical (e.g., heat and mass transfer) effects.
- Perform design and safety studies, and to train plant personnel.

- Understand and optimize transitions and other dynamic behavior (i.e., process control).

The modeling approach and level of detail should be dictated by the application. Whereas an empirical model linking measured inputs and outputs may be the best solution for control of an existing industrial reactor, it would be totally inappropriate for design of a new process or to choose operating conditions for a new polymer grade. On the other hand, it makes little sense to develop a model that can predict detailed polymer architecture for control purposes when the only measure of polymer structure is a melt index value obtained from the lab 2 h after the sample was produced. While empirical modeling has its uses, the focus of this section is on the development of fundamental models based on first-principles descriptions of chemical and physical phenomena. Although a perfect description of an actual process is, in the end, an unattainable goal, the attempt often leads to valuable insights that can aid process and product development, scaleup, and optimization.

The discussion is organized using the modeling hierarchy discussed by Ray[24] on the basis of the three principal size scales in a reaction system. Polymerization kinetics and other molecular processes take place at the *microscale*; *mesoscale* phenomena include inter- and intraphase transport (e.g., radical entry and exit in emulsion polymerization), particle morphology, and micromixing; the *macroscale* includes overall material and energy balances, reactor mixing patterns, particle population balances, and reactor dynamics and control. Separate models are usually required at each level, and simplified versions of the smaller-scale models may be required as the scale grows larger.

7.3.1.1 *Microscale Modeling of Kinetics*

The objective of kinetic modeling is to build a description of how polymer architecture and polymerization rate depend on reaction conditions (temperature, pressure) and species concentrations from a defined set of kinetic mechanisms; a dynamic model is required to examine how properties change as a function of time. The mechanisms of free-radical polymerization have been presented previously (Chapters 4 and 5), and will not be repeated here. However, it is worth emphasizing that a realistic set of mechanisms and kinetic coefficients is needed for the development of a reliable model. Tremendous progress has been made in this area, but more remains to be done.

The mechanisms to be included in a model depend on its end use. For simple mass and energy balances, it is necessary to consider only those that consume monomer, initiator, and radicals—initiation, propagation, and radical–radical termination. To track polymer molecular weight, all mechanisms that include radical transfer must also be included. Additional balances are needed to follow other molecular properties, such as the density of short- or long-chain branches, end-group functionality, and the creation and reaction of terminal double bonds.

7.3.1.1.1 *The Method of Moments*

One of the challenges in modeling polymerization systems is how to reduce a very large number of individual species (living and dead chains with lengths from 1 to $>1 \times 10^6$, often with other distributed

attributes such as the number of branch points) to a tractable solution. The classical approach to this problem is to reduce the system of equations through definition of the principal moments of the various distributions.[25] Construction of moment balances allows the tracking of *average* polymer properties; for molecular weight this would be M_n (number average), M_w (weight average) and possibly M_z, and for branched systems it is possible to track number average (B_n) and weight-average (B_w) number of branches per chain. Details of the mathematical treatment will not be given here: recent comprehensive reviews include those by Achilias and Kiparissides[26] and Dubé et al.[27]

The method of moments is flexible, and able to include most kinetic mechanisms. Furthermore, since it is easy to implement as part of larger-scale reactor modeling, it is the standard methodology used in process simulation packages.[28,29] There are numerous examples of how these models have been applied to improve understanding of industrial polymerization systems; a brief sampling of the most recent examples includes

- Apostolo et al.,[30] who study the emulsion polymerization of vinylidene fluoride with hexafluoropropylene
- Kiparissides et al.,[31] who describe a model for the industrial batch suspension of vinyl chloride
- Brandolin et al.,[32] who construct a model to represent the high-pressure free-radical polymerization of ethylene in tubular reactors

In each of these cases, the method of moments was used to represent polymerization kinetics in a more detailed multiphase or multizone reactor model.

7.3.1.1.2 Modeling of Complete Distributions The major limitation of models based on the method of moments is that they only track average quantities. While adequate for most situations, more detail may be needed if the objective of the study is to improve our knowledge of the kinetics; for example, to examine the combined effect of chain-scission and long-chain branching on polymer architecture, or to incorporate chain-length-dependent termination kinetics into the mechanistic scheme. In such cases, the kinetic and modeling assumptions can be tested more rigorously through a detailed comparison with full molecular weight distributions (MWDs) measured experimentally. More recent advances in modeling tools now make it possible to simulate the complete MWD, as well as how a second distributed quantity [e.g., long-chain branching (LCB)] varies with chain-length.

The modeling of complete MWDs has long been possible for linear polymer systems: those without any branching.[33] However, the methodology cannot be easily extended to branched systems due to the interaction of the polymer radical and dead polymer chain distributions through reaction (e.g., H abstraction, terminal double-bond polymerization, crosslinking). The methods for modeling MWDs with branching can be divided into three main groups. The first, utilizing Monte Carlo techniques, has been greatly advanced through the efforts of Tobita. Assuming a given set of mechanisms, the probabilities of connections between primary polymer

molecules (the linear chain that would exist if all of its branch points were severed) is calculated, and the resulting MWD solved using Monte Carlo techniques.[34]

A second group of models is based on the "numerical fractionation" concept developed by Teymour and Campbell.[35] This seminal work identifies a succession of branched polymer generations based on the degree of complexity of their architecture, tracking the population of chains in each generation using the method of moments. The complete MWD is approximated by combining the MWDs for individual generations that themselves are reconstructed from the leading moments assuming a distributional form. Numerical fractionation was specifically developed to examine the problem of gel formation in polymer systems. Thus, the generations were defined to follow the geometric progression in chain length caused by connection of two molecules in the same generation; while chains from the zeroth generation progress to the first generation by participating in a branching event, a chain from the first generation can progress to the second only by joining (through crosslinking, terminal double bond polymerization or termination by combination) with another molecule from the same generation.[35] One study shows that this classification scheme leads, in certain cases, to errors in the shape of the overall MWD; through comparison with distributions calculated by rigorous numerical solution, Butté et al.[36] show that the definition of generations proposed by Teymour and Campbell can create an artificial high MW shoulder due to the accumulation of chains with a wide distribution of number of branches (and thus high polydispersity) in the first branched generation. The authors conclude that a more accurate approximation is obtained by classifying the chains according to their number of branches. Both Monte Carlo[37] and a modified numerical fractionation technique[36] can also be used to calculate the LCB number as a function of chain length, an important quantity often presented experimentally.

The commercial software Predici package uses yet another numerical technique, calculating MWDs using a discrete Galerkin technique with variable grid and variable order.[38] More recently, the package has been extended to follow branch-point concentrations as a function of chain length through the introduction of balance equations.[39] The possibility to perform these tasks—calculation of complete MWD as well as LCB distribution—in a commercial software package is especially noteworthy because it makes it possible for a wider range of practitioners to perform detailed kinetic modeling.

It is hoped that these new modeling capabilities, in combination with improved characterization techniques, will hasten progress to a better understanding and representation of complex polymer architecture. Some progress in this direction has been made, such as the work of Busch[40] to model in detail the complex side reactions of high-pressure ethylene copolymerization, the efforts of Hutchinson[41] to construct a more realistic representation of how chain scission affects the LCB distribution, and the modeling by Ghielmi et al.[42,43] examining how radical compartmentalization in emulsion systems can affect development of the full MWD.

7.3.1.2 Mesoscale Particle Phenomena Modeling Polymer properties and production rate in heterogeneous polymerization systems are strongly affected by

what occurs at the particle level. This includes transport into and out of the particle, partitioning of reactants between phases, particle stabilization, possible intraparticle gradients, and morphological development (e.g., core–shell). A comprehensive review of these issues is beyond the scope of this chapter. However, some selected studies illustrate the importance of understanding and realistically modeling these phenomena for emulsion and suspension polymerization systems.

7.3.1.2.1   Emulsion Polymerization   Saldívar et al.[44] provide a good overview of particle phenomena affecting emulsion polymerization (see also Chapter 6). One of the main issues, as for suspension polymerization, is the partition of species between the continuous water phase and the polymer particles. This includes not only monomers and chain transfer agents but also growing polymer chains. Ghielmi et al.[45] develop a detailed model to illustrate that compartmentalization of radicals between particles can be important; for systems with LCB and termination by combination, it is necessary to account for the chain length distribution of both terminating chains individually to accurately predict polymer polydispersity and MWD. Other efforts focus on a better fundamental understanding of mechanisms affecting the PSD, such as the work by Melis et al.[46] to develop a better representation of how Brownian diffusion and interparticle interactions, including the effect of ionic emulsifiers, affect particle coagulation.

7.3.1.2.2   Suspension Polymerization   The same main issues—partition of species between phases, evolution of the PSD—exist in suspension as well as emulsion polymerization. However, the size of the particles involved (>10 m) means that the controlling physical phenomena are different. As an example, consider particle breakage and coalescence: unlike in emulsion systems, these mechanisms are greatly affected by the fluid dynamics in a stirred vessel. The lower interfacial particle to water surface area in suspension systems (compared to emulsion) also means that partition of monomer may not be thermodynamically controlled, but may also be affected by mass transfer limitations.[47] The reviews by Yuan et al.[48] and Vivaldo-Lima et al.[49] summarize these issues, and describe more fully how modeling has been used to improve understanding of these particle phenomena.

7.3.1.3   Macroscale Reactor Modeling   Macroscale modeling usually has quite different objectives than modeling of the smaller scale. Rather than focusing on improved understanding of the chemical and physical mechanisms and phenomena, it applies the current level of knowledge (imperfect as it is) to the more practical problems of reactor design, operation, and control. In order to efficiently solve these larger-scale issues, simplifications are often made in the kinetic and particle submodels, and engineering correlations are introduced to represent poorly understood phenomena. This section highlights advances made in the implementation of macroscale modeling, as well as providing examples of how these models are applied to industry. The categorization below is somewhat arbitrary, and is not meant to be comprehensive.

7.3.1.3.1   Complex Flowsheets   These are often constructed to represent systems with nonideal mixing and fast reaction. A classic example is the high-pressure high-temperature free-radical production of ethylene copolymers, generally in a single phase consisting largely of supercritical ethylene monomer. These conditions make for very fast reactions (e.g., initiator half-life of <1 s), promote numerous side reactions (long-chain branching, short-chain branching, and chain scission), and introduce the potential of thermal runaway. More recent models of these systems combine a detailed description of polymerization kinetics with a complex flowsheet of CSTRs in series with recycle to represent mixing in a multizone, multifeed autoclave reactor.[50–52] Models for multifeed tubular systems also include heat transfer and pressure drop along the length of the system.[32] The general strategy is to ''tune'' the model (generally based on a set of proposed kinetic mechanisms captured by the method of moments) by fitting kinetic coefficients and mixing and heat transfer parameters against a set of industrial data, and then use the model interpreting and optimizing industrial operating conditions. Advances in computing power have allowed the complexity of these models to increase.

7.3.1.3.2   Computational Fluid Dynamics (CFD) Simulation   This technique is emerging as an alternative and more fundamental approach to examine polymerization systems with complex mixing and reaction. Once again, much of the work is focused on high-pressure ethylene polymerization systems. As described by Tsai and Fox,[53] a major challenge is incorporating both macromixing (turbulent diffusion and convection) as well as micromixing (molecular diffusion) into the representation. The first efforts in this area[53,54] concern themselves with the prediction of temperature and conversion profiles in the reactors; to simplify the calculational load, they consider only initiation, propagation, and termination reactions. More recently, Kolhapure and Fox[55] incorporated a more complete kinetic scheme to allow the prediction of polymer MW, polydispersity, and average branching number. These CFD studies can point the way to improved reactor design and operation, for example, by examining the importance of initiator distribution at the injection point, and defining conditions for stable reactor operation.[55] One article discusses the implementation of CFD calculations within a process simulation package.[56] Although not yet applied to polymerization systems, this advancement shows enormous promise.

7.3.1.3.3   Heterogeneous Systems   These systems introduce an extra level of complexity to the modeling task. In suspension polymerization, it is often important to represent the full particle size distribution (PSD). Vivaldo-Lima et al.[49] provide an overview of the scaleup issues related to suspension polymerization, including the effects of mixing and energy dissipation on particle coalescence and breakage; CFD simulations and multizone flowsheet models are presented as complementary tools to improve understanding of these systems. Kiparissides et al.[31] do not model PSD, but construct a detailed representation of the complex phase equilibria and heat transfer of industrial poly(vinyl chloride) suspension systems. Generalized models for simulation of emulsion polymerization in well-mixed reactors, including

description of the full PSD, have also been developed, as described in detail by Saldívar et al.[44] The model was used to simulate dynamic phenomena in a two-reactor flowsheet, such as the formation of sustained oscillations in particle number, and the design of optimal startup policy for a methyl acrylate–vinyl acetate copolymerization.[57] Vega et al.[58] describe use of a detailed model to optimize the industrial semibatch emulsion polymerization of acrylonitrile and butadiene.

7.3.1.3.4   Model-Based Control   Model-based control of polymerization systems has also garnered its share of attention. The goal of these works, of course, is the development of robust strategies to guide and control the manufacture of polymer safely and reproducibly in the face of unmeasured disturbances and frequent product grade transitions. The main challenge in controlling polymerization systems is the lack of online measurements of polymer structure, a subject discussed later in this section. A review by Congalidis and Richards[59] provides a good summary of recent literature focusing on this difficult issue. In most cases, the implementation of detailed fundamental models is not warranted for control application. However, simple models can often be combined with limited online measurements[60–62] or empirical modeling approaches[63,64] to improve control performance. Fundamental models can also be used to test empirical models developed for control purposes.[65] Finally, Saldívar and Ray[66] use a detailed fundamental model of emulsion polymerization for control purposes.

7.3.2   Measurement

One of the challenges with studying and improving industrial systems is the lack of reliable measurements, both online and of the final polymer product. Both of these topics are active areas of research, as discussed in this section.

7.3.2.1   Polymer Structure   Accurate determination of polymer structure is a difficult task even for detailed research studies of a single product. For industrial processes that make a multitude of products supported by an on-site quality lab, sophisticated polymer analysis is simply not possible. Indeed, it can be argued that it is not even warranted, since polymer is sold not on the basis of molecular structure, but on end-use properties. While this conclusion may hold true for routine production, the development of new or modified products and processes usually benefits from improved knowledge of the polymer structure. It is for this reason, among others, that industrial groups often lead the way in the application of advanced analytical techniques. A survey of the more recent literature illustrates this fact, and also provides some insight to the problems of interest to industry.

   1. Maccone et al.[67] examine a branched fluoroelastomeric terpolymer in detail. The study examines the validity of using single-detector SEC (size-exclusion chromatography) with a branching correction based on the whole-polymer intrinsic viscosity to estimate the true MWD. Light scattering was used to provide an independent measure of weight average MW, and the branched samples were also

fractionated. Finally, a linear polymer sample was specially synthesized for SEC calibration purposes. The paper concludes that the single-detector SEC approach provides a reasonably accurate measure of the polymer MWD and average branching level. It is clear from the paper that this detailed analysis was performed in tandem with a modeling effort to support new industrial polymerization technology.

2. Thomas et al.[68] study the effect of incorporating fluorinated compounds into acrylic-based polymer films in order to change the surface activity of the coatings by reducing surface tension. They examine a series of material surfaces using contact angle measurements, X-ray photoelectron spectroscopy, time-of-flight static secondary-ion mass spectroscopy, and dynamic secondary-ion mass spectroscopy. The study concludes that only very low amounts of fluorine-modified chains were required to achieve the desired surface properties, since the fluorinated chains preferentially diffuse to the air/polymer interface. With this knowledge, it is possible to synthesis effective coatings using much smaller quantities of expensive fluorinated monomer. Surface characterization of polymer materials continues to grow in importance, not only in the area of coatings, but also in the emerging electronic and biomaterials areas.

3. Shi et al.[69] describe the application of electrospray ionization Fourier transform mass spectrometry (ESI-FTMS) which can be coupled with SEC to facilitate analysis of the complete mass distribution of lower-MW (<7000) polymers. Chains of unique polymer structure—number and type of repeat units as well as end groups—were identified for a butyl methacrylate/glycidyl methacrylate copolymer, providing insight into the kinetic mechanisms. It was possible to resolve the relative amounts of GMA and BMA in chains of identical length, an especially amazing result when the fact that GMA and BMA repeat units differ in molar mass by only 0.036 daltons is considered. Matrix-assisted-laser-desorption-ionization (MALDI) time-of-flight mass spectrometry is another emerging technique for measuring absolute MWs; it can be used to examine polymers with much higher MW than ESI-FTMS (MW $> 1 \times 10^6$), but not to the same resolution. Problems remain with quantitative analysis of unfractionated polymer with MALDI,[70] but the technique has been successfully coupled with SEC fractionation to examine acrylic copolymers.[71]

4. Folie et al.[72] examine a commercial ethylene-vinyl acetate copolymer using supercritical fluid to fractionate based on MW and crystallinity. The individual fractions were then analyzed via dual-detector SEC-LALLS (low-angle light scattering), DSC, and NMR to determine composition, short-chain branching, and long-chain branching densities. This detailed work resulted in a more fundamental understanding of the complex molecular architecture for this polymer system.

5. McCord et al.[73] describe a detailed NMR analysis focused on the short-chain branch (SCB) structures of ethylene copolymers produced via high-temperature high-pressure free-radical polymerization. It was determined that a significant number of the SCB structures contained comonomer units, and also that hydrogens from acrylate and acrylic acid methine units are particularly susceptible to abstraction.

These findings were used to illustrate the relative importance of various intramolecular transfer reactions that occur during polymer synthesis.

This selection of studies illustrates the importance of detailed polymer characterization to industrial product and process design. Even for mature industries, the application of a new analytical technique may lead to fresh insights and a competitive edge.

7.3.2.2 *Online Sensors*   The importance of on-line measurement is obvious; without a measure of when the process is deviating from expected behavior, it is not possible to prevent the production of off-spec material. Reliable measurements are also needed to ensure safe operation; without them, it is necessary to run the process at more conservative conditions. The complex nature of polymer systems has made the development and implementation of online sensors a difficult task. However, significant progress has been made, as summarized in comprehensive reviews by Chien and Penlidis[74] and Kammona et al.[75] This section does not provide such a complete treatment of the subject, but attempts to highlight the most recent advances.

7.3.2.2.1 Conversion and Copolymer Composition   Polymer composition is directly dependent on the ratio of monomers in the reactor, and molecular properties are controlled by the ratio of monomer to transfer agent (MW) or monomer to polymer (LCB density). Thus, monitoring polymer conversion is almost always necessary for robust control of a polymerization system. The task becomes more difficult in multicomponent polymerization systems, especially for processes that manufacture multiple products using a wide range of different monomers. Other challenges are faced in multiphase systems, where the monomers can be distributed among several phases. Thus, it is no surprise that many techniques have been implemented, or at least tested, for online conversion and composition measurement. Some techniques, such as densimetry and refractive index (RI) measurement, are difficult to apply to multicomponent systems. Thus, attention has more recently focused on the emergence of reliable fiberoptic probes for spectroscopic sensors such as near-IR, mid-IR, and Raman spectroscopy.[75] More recent studies also report the use of ultrasonics to monitor the emulsion copolymerization of styrene and butyl acrylate.[76] The use of calorimetry (or a dynamic energy balance) combined with another measure of overall polymer composition is also emerging as a robust method for online monitoring of multimonomer emulsion systems.[77] It is difficult to judge the extent to which these various techniques are utilized in industry.

7.3.2.2.2 Molecular Weight   An even more difficult task is the online monitoring of molecular weight. It is very common for product MW (or some easily measured indicator of MW such as viscosity or melt index) to be controlled on the basis of offline lab analyses, with measured values often lagging behind the actual process by several hours. Despite this time delay, reasonable control can be achieved in some

cases by combining online measurement and control of polymer conversion with careful control of added transfer agent. For many processes, however, there is a strong financial incentive to measure and control polymer MW on line. Viscometry, although not providing a direct measure of MW, has been coupled with conversion measurements for online control of solution polymerization systems.[62,75] There are many difficulties in obtaining a more direct MWD measure on line. SEC, for example, suffers from a long time delay in sample analysis, as well as the problem of automatically diluting the samples to the correct concentration range for the separation columns. Florenzano et al.[78] describe a more promising and robust approach: in which a diluted stream of unfractionated polymer is passed through multiple detectors (RI, UV, light scattering, viscometry) to yield on-line estimates of conversion, weight average MW, and viscosity. The extension of any of these techniques to heterogeneous systems, however, remains a challenging area of research.

7.3.2.2.3 Particle Size   In heterogeneous systems, the additional issue of particle size must be addressed. Most of the available techniques suffer from long time delays associated with sample preparation and dilution as well as the actual measurements. The broader PSDs associated with CSTR emulsion systems[44] also complicate the detection problem. As reviewed by Kammona et al.,[75] dynamic light scattering and turbidity are two techniques that show promise for online application; ultrasound spectroscopy has also been examined.[76]

7.4   SUMMARY

In addition to having desired physical and chemical properties, successful commercialization requires the product and the polymerization process to meet a variety of nontechnical constraints. Economic considerations are among the most important, and include the capital and operating costs to manufacture the product, the predicted return on investment, anticipated market demand, the competitive environment for the product, and the nature of the polymer (commodity vs. specialty). A polymer must possess a desirable set of physical and chemical properties when it is introduced to the marketplace, but maintaining strong market position usually requires continual improvement in the polymer properties and/or reduced operating costs. Each objective is best achieved through continual increases in understanding the process and the relationship between fundamental structure (e.g., molecular weight, copolymer composition) and end-use properties.

Polymer reaction engineering issues can pose major challenges for industrial-scale polymer synthesis. As reactor size increases, transport phenomena such as heat and mass transfer become more difficult, and large-scale processes are often limited by transport effects. In many cases, the final reaction rate, molecular weight, and copolymer composition will be determined by the coupled effects of reaction kinetics and transport phenomena.

Several tools are actively being developed to enhance our ability to manufacture industrial polymers. Mathematical modeling, in conjunction with a strong experimental program, is a powerful means to improve our mechanistic and process understanding. The use of empirical models has utility in the control of polymerization reactors, and can be an important contributor to product quality and process robustness. Continuing development of new measurement techniques, together with an ability to relate measurements to functional properties, will be a critical area of future research.

While many current free-radical polymerization processes have been in industrial use for years, the next several years may see the emergence of new industrial technologies. The adoption of new technology by industry requires identification of an application or product for which the new technology is clearly advantageous, and successfully overcoming the numerous scaleup challenges in converting the process to industrial scale. Promising technologies include miniemulsion polymerization, living radical polymerization, and polymerization in supercritical carbon dioxide.

Miniemulsion polymerization has been extensively studied, with the kinetics and mechanisms now reasonably well understood. A major strength is the ability to incorporate a variety of additives into submicron particles (e.g., dyes, pigments, conductive materials, medication), which cannot be done with emulsion polymerization. Miniemulsion will probably be used for specialty applications, such as ethyl cellulose latex for use in coating pharmaceutical pills.[79] Several patents on miniemulsion polymerization have been issued.[80–84]

Living (controlled) radical polymerization provides finely tuned control of microstructure and the ability to synthesize a range of morphologies, including block, star, brush, and comb polymers. Three major approaches have been used (ATRP, RAFT, SFRP). Each has its own advantages and disadvantages, and each will pose different challenges to successful commercialization. However, they are all advantaged compared to anionic living polymerization technology, which requires extensive purification of materials and is run at very low temperature ($< -50°C$). ATRP, RAFT and SFRP require no special purification, and can all be used in heterogeneous systems such as emulsion and suspension polymerization. Commercialization will likely require advances in reaction engineering technology for living radical systems. For example, Shen et al.[85] have designed a continuous packed-column reactor using a supported silica gel catalyst for the ATRP polymerization of methyl methacrylate. Another novel technique for controlling molecular weight is catalytic chain transfer. Although not a living system, this enables the facile synthesis of oligomers, and holds the promise of commercial application in the near future.

Polymerization in supercritical carbon dioxide can be used to manufacture polymers in the absence of organic solvents, and is therefore highly attractive from an environmental perspective. Because supercritical carbon dioxide has unique solvent properties, including the ability to vary the solubility of polymers by adjusting pressure and temperature, the technique is also attractive for materials such as some fluoropolymers for which good solvents are scarce. The main disadvantage is the high capital and operating cost associated with running high-pressure equipment, but niche products will likely be increasingly identified and developed.[86,87]

REFERENCES

1. H. Ulrich, *Introduction to Industrial Polymers*, Carl Hanser Verlag, Munich, 1982.

2. *Chem. Eng. News* **78**(26), 49–89 (2000).

3. W. H. Ray and R. L. Laurence, in *Chemical Reactor Theory*, L. Lapidus and N. R. Amundson, eds., Prentice Hall, Englewood Cliffs, NJ, 1977.

4. K.-H. Reichert and H.-U. Moritz, *Comprehen. Polym. Sci.* **3**, 327–363 (1989).

5. A. Rudin, *The Elements of Polymer Science and Engineering*, 2nd ed., Academic Press, New York, 1999.

6. F. J. Schork, *Control of Polymerization Reactors*, Marcel Dekker, New York, 1993.

7. G. Arzamendi and J. M. Asua, *J. Appl. Polym. Sci.* **38**, 2019–2036 (1989).

8. F. Galimberti, A. Siani, M. Morbidelli, and G. Storti, *Chem. Eng. Comm.* **163**, 69–95 (1998).

9. A. Urretabizkaia and J. M. Asua, *J. Polym. Sci.; Part A: Polym. Chem.* **32**, 1761–1778 (1994).

10. V. L. Dimonie, E. S., Daniels, Shaffer, O. L., and M. S. El-Aasser, in *Emulsion Polymerization and Emulsion Polymers*, P. A. Lovell and M. S. El-Aasser, eds., Wiley, New York, 1997, pp. 293–326.

11. M. F. Cunningham, H. K. Mahabadi, and H. M. Wright, *J. Polym. Sci.; Part A: Polym. Chem.* **38**, 345–351 (2000).

12. M. S. El-Aasser, T., Makgawinata, J. W. Vanderhoff, and C. Pichot, *J. Polym. Sci.; Part A: Polym. Chem.* **21**, 2363–2382 (1983).

13. D. Britton, F. Heatley, and P. A. Lovell, *Macromolecules* **31**, 2828–2837 (1998).

14. G. A. Vandezande, O. W. Smith, and D. R. Bassett, in *Emulsion Polymerization and Emulsion Polymers*, P. A. Lovell and M.S. El-Aasser, eds., Wiley, New York, 1997, pp. 563–587.

15. R. M. Fitch, *Polymer Colloids: A Comprehensive Introduction*, Academic Press, New York, 1997.

16. G. W. Poehlein, in *Emulsion Polymerization and Emulsion Polymers*, P. A. Lovell and M. S. El-Aasser, eds., Wiley, New York, 1997, pp. 277–292. J. A. Biesenberger and D. H. Sebastian, *Principles of Polymerization Engineering*, Wiley, New York, 1983.

17. E. Ozdeger, E. D. Sudol, M. S. El-Aasser, and A. Klein, *J. Appl. Polym. Sci.* **69**, 2277–2289 (1998).

18. P. A. Weerts, J. L. M. van der Loos, and A. L. German, *Makromol. Chem.* **192**, 1993–2008 (1991).

19. G. Tosun, *AIChE J.* **38**, 425–437 (1992).

20. E. B. Nauman, *J. Macromol. Sci.—Rev. Macromol. Chem.* **C10**, 75–112 (1974).

21. B. J. Meister and M. T. Malanga, *Encycl. Polym. Sci. Eng.* **16**, 21–62 (1989).

22. B. L. Tarmy, *Encycl. Polym. Sci. Eng.* **14**, 189–237 (1988).

23. R. E. Putnam, *Comprehen. Polym. Sci.* **3**, 321–326 (1989).

24. W. H. Ray, *Berichte der Bunsen-Gesellsh. Phys. Chem.* **90**, 947–955 (1986).

25. W. H. Ray, *J. Macromol. Sci.—Rev. Macromol. Chem.* **C8**, 1–56 (1972).

26. D. S. Achilias and C. Kiparissides, *J. Macromol. Soc.—Rev. Macromol. Chem. Phys.* **C32**, 183–234 (1992).

27. M. A. Dubé, J. B. P. Soares, A. Penlidis, and A. E. Hamielec, *Ind. Eng. Chem. Res.* **36**, 966–1015 (1997).

28. S. Ochs, P. Rosendorf, I. Hyanek, X. Zhang, and W. H. Ray, *Comp. Chem. Eng.* **20**, 657–663 (1996).

29. A. Pertsinidis, E. Papadopoulos, and C. Kiparissides, *Comp. Chem. Eng.* **20**, S449 (1996).

30. M. Apostolo, V. Arcella, G. Storti, and M. Morbidelli, *Macromolecules* **32**, 989–1003 (1999).

31. C. Kiparissides, G. Daskalakis, D. S. Achilias, and E. Sidiropoulou, *Ind. Eng. Chem. Res.* **36**, 1253–1267 (1997).

32. A. Brandolin, M. H. Lacunz, M. H., P. E. Ugrin, and N. J. Capiati, *Polym. React. Eng.* **4**, 193–241 (1996).

33. S. T. Balke and A. E. Hamielec, *J. Appl. Polym. Sci.* **17**, 905–949 (1973).

34. H. Tobita, *J. Polym. Sci.; Part B: Polym. Phys.* **31**, 1363–1371 (1993).

35. F. Teymour and J. D. Campbell, *Macromolecules* **27**, 2460–2469 (1994).

36. A. Butté, A. Ghielmi, G. Storti, and M. Morbidelli, *Macromol. Theory Simul.* **8**, 498–512 (1999).

37. H. Tobita, *Macromol. Theory Simul.* **5**, 129–144 (1996).

38. M. Wulkow, *Macromol. Theory Simul.* **5**, 393–416 (1996).

39. P. D. Iedema, M. Wulkow, and H. C. J. Hoefsloot, *Macromolecules* **33**, 498–512 (2000).

40. M. Busch, *Macromol. Theory Simul.* (in press).

41. R. A. Hutchinson, *Macromol. Theory Simul.* (in press).

42. A. Ghielmi, S. Fiorentino, G. Storti, M. Mazzotti, and M. Morbidelli, *J. Polym. Sci.; Part A: Polym. Chem.* **35**, 827–858 (1997).

43. A. Ghielmi, S. Fiorentino, G. Storti, and M. Morbidelli, *J. Polym. Sci.; Part A: Polym. Chem.* **36**, 1127–1156 (1998).

44. E. Saldívar, P. Dafniotis, and W. H. Ray, *J. Macromol. Sci.—Rev. Macromol. Chem. Phys.* **C38**, 207–325 (1998).

45. A. Ghielmi, G. Storti, M. Morbidelli, and W. H. Ray, *Macromolecules* **31**, 7172–7186 (1998).

46. S. Melis, M. Kemmere, J. Meuldijk, G. Storti, and M. Morbidelli, *Chem. Eng. Sci.* **55**, 3101–3111 (2000).

47. S. X. Zhang and W. H. Ray, *Ind. Eng. Chem. Res.* **36**, 1310–1321 (1997).

48. H. G. Yuan, G. Kalfas, and W. H. Ray, *J. Macromol. Soc.—Rev. Macromol. Chem. Phys.* **C31**, 215–299 (1991).

49. E. Vivaldo-Lima, P. E. Wood, A. E. Hamielec, and A. Penlidis, *Ind. Eng. Chem. Res.* **36**, 939–965 (1997).

50. W.-M. Chan, P. E. Gloor, and A. E. Hamielec, *AIChE J.* **39**, 111–126 (1993).

51. H. Nordhus, O. Moen, and P. Singstad, *J. Macromol. Sci.—Pure Appl. Chem.* **A34**, 1017–1043 (1997).

52. P. Pladis and C. Kiparissides, *J. Appl. Polym. Sci.* **73**, 2327–2348 (1999).

53. K. Tsai and R. O. Fox, *AIChE J.* **42**, 2926–2940 (1996).

54. N. K. Read, S. X. Zhang, and W. H. Ray, *AIChE J.* **43**, 104–117 (1997).

55. N. H. Kolhapure and R. O. Fox, *Chem. Eng. Sci.* **54**, 3233–3242 (1999).

56. F. Bezzo, S. Macchietto, and C. C. Pantelides, *Comp. Chem. Eng.* **24**, 653–658 (2000).

57. E. Saldívar and W. H. Ray, *Ind. Eng. Chem. Res.* **36**, 1322–1336 (1997).

58. J. R. Vega, L. M. Gugliotta, R. O. Bielsa, M. C. Brandolini, and G. R. Meira, *Ind. Eng. Chem. Res.* **36**, 1238–1246 (1997).

59. J. P. Congalidis, and J. R. Richards, *Polym. React. Eng.* **6**, 71–111 (1998).

60. R. K. Mutha, W. R. Cluett, and A. Penlidis, *Ind. Eng. Chem. Res.* **36**, 1036–1047 (1997).

61. H. Hammouri, T. F. McKenna, and S. Othman, *Ind. Eng. Chem. Res.* **38**, 4815–4824 (1999).

62. S.-M. Ahn, M.-J. Park, and H.-K. Rhee, *Ind. Eng. Chem. Res.* **38**, 3942–3949 (1999).

63. T. L. Clarke-Pringle, and J. F. MacGregor, *Ind. Eng. Chem. Res.* **37**, 3660–3669 (1998).

64. Y. Yabuki, T. Nagasawa, and J. F. MacGregor, *Comp. Chem. Eng.* **24**, 585–590 (2000).

65. S.-S. Na and H.-K. Rhee, *J. Appl. Polym. Sci.* **76**, 1889–1902 (2000).

66. E. Saldívar and W. H. Ray, *AIChE J.* **43**, 2021–2033 (1997).

67. P. Maccone, M. Apostolo, and G. Ajroldi, *Macromolecules* **33**, 1656–1663 (2000).

68. R. R. Thomas, D. R. Anton, W. F. Graham, M. J. Darmon, B. B. Sauer, K. M. Stika, and D. G. Swartzfager, *Macromolecules* **30**, 2883–2890 (1997).

69. S. D.-H. Shi, C. L. Hendrickson, A. G. Marshall, W. J. Simonsick, Jr., and D. J. Aaserud, *Anal. Chem.* **70**, 3220–3226 (1998).

70. H. M. Kapfenstein and T. P. Davis, *Macromol. Chem. Phys.* **199**, 2403–2408 (1998).

71. M. S. Montaudo and G. Montaudo, *Macromolecules* **32**, 7015–7022 (1999).

72. B. Folie, M. Kelchtermans, J. R. Shutt, H. Schonemann, and V. Krukonis, *J. Appl. Polym. Sci.* **64**, 2015–2030 (1997).

73. E. F. McCord, W. H. Shaw, Jr., and R. A. Hutchinson, *Macromolecules* **30**, 246–256 (1997).

74. D. C. H. Chien and A. Penlidis, *J. Macromol. Sci.—Rev. Macromol. Chem. Phys.* **C30**, 1–42 (1990).

75. O. Kammona, E. G. Chatzi, and C. Kiparissides, *J. Macromol. Chem.—Rev. Macromol. Chem. Phys.* **C39**, 57–134 (1999).

76. G. Storti, A. K. Hipp, and M. Morbidelli, *Polym. React. Eng.* **8**, 77–94 (2000).

77. T. F. McKenna, S. Othman, G. Fevotte, A. M. Santos, and H. Hammouri, *Polym. React. Eng.* **8**, 1–38 (2000).

78. F. H. Florenzano, R. Strelitzki, and W. F. Reed, *Macromolecules* **31**, 7226–7238 (1998).

79. J. W. Vanderhoff, M. S. El-Aasser, and J. Ugelstad, U.S. Patent 4,177,177 (Lehigh Univ.) (1979).

80. J. W. Vanderhoff, M. S. El-Aasser, and J. H. Hoffman, U.S. Patent 4,070,323 (Lehigh Univ.) (1978).

81. M. B. Urquiola, U.S. Patent 5,516,865 (Minnesota Mining and Manufacturing Company) (1996).

82. K. Mathauer, W. Maechtle, G. E. Kee, and H. Kroener, BASF AG, German Patent DE 19628143 A1 (1998).

83. Y. Wang, D. E. Smith, and A. B. Fant, U.S. Patent 5,866,312 (Eastman Kodak Company) (1999).

84. Y. Wang, D. E. Smith, A. B. Fant, and J. L. Muehlbauer, U.S. Patent 5,858,634 (Eastman Kodak Company) (1999).

85. Y. Shen, S. Zhu, and R. Pelton, *Macromol. Rapid Commun.* **21**, 956–959 (2000).

86. *Chem. Eng. News* **77**(17), 10 (1999).

87. *Chem. Eng. News* **77**(17), 11–13 (1999).

8 General Concepts and History of Living Radical Polymerization

KRZYSZTOF MATYJASZEWSKI

Carnegie Mellon University, Pittsburgh, Pennsylvania

CONTENTS

8.1   INTRODUCTION

As presented in previous chapters, conventional free-radical polymerization (RP) is a very important commercial process for preparing high molecular weight polymers because it can be employed for polymerization of many vinyl monomers under mild reaction conditions, requiring the absence of oxygen, but tolerant to water, and can be conducted over a large temperature range (-80 to $250°C$).[1] In addition, many monomers can easily copolymerize via a radical route, leading to an infinite number of copolymers with properties dependent on the proportion of the incorporated comonomers. The main limitation of RP is the poor control over some of the key elements of macromolecular structures such as molecular weight (MW), polydispersity, end functionality, chain architecture, and composition. Well-defined polymers with precisely controlled structural parameters are accessible by ionic living polymerization; however, ionic living polymerization requires stringent conditions and are limited to a relatively small number of monomers.[2-4] Thus, it is desirable to prepare, by free-radical means, new well-defined block and graft copolymers, stars, combs, and networks, end-functional polymers and many other materials under mild conditions and from a larger range of monomers than available for ionic living polymerizations.[5] This is the reason why we have witnessed a real explosion of academic and industrial research on controlled/"living" radical polymerizations (LRP) with over 4000 papers and hundreds of patents devoted to this area since the late 1990s.

   In this chapter, the general concepts of living polymerization will be presented, followed by peculiarities of LRP. Some attempts to systematically classify LRP will precede the discussion of historical developments of LRP. Eventually, the most efficient LRP systems will be discussed with an outlook to the future. The subsequent seven chapters will cover specific topics in greater detail: the kinetics of LRP (Chapter 9), the three currently most promising LRP techniques based on nitroxide mediated polymerization (Chapter 10), atom transfer radical polymerization (Chapter 11), chain transfer methods (Chapter 12), approaches toward stereochemical control in RP (Chapter 13), and materials formed by LRP (Chapter 14). Chapter 15 is focused on the experimental techniques used in RP and LRP and will include several typical recipes for LRP.

8.2   LIVING VERSUS CONTROLLED
RADICAL POLYMERIZATION

Living polymerization was first defined by Szwarc[6] as a chain growth process without chain breaking reactions (transfer and termination). Such a polymerization provides end-group control and enables the synthesis of block copolymers by sequential monomer addition. However, it does not necessarily provide polymers with molecular weight (MW) control and narrow molecular weight distribution (MWD). Additional prerequisites to achieve these goals include that the initiator should be consumed at early stages of polymerization and that the exchange between species of various reactivities should be at least as fast as propagation.[7–9] It has been suggested to use a term *controlled* polymerization if these additional criteria are met.[10] This term was proposed for systems, which provide control of MW and MWD but in which chain breaking reactions continue to occur as in RP. However, the term *controlled* does not specify which features are controlled and which are not controlled. Another option would be to use the term ''living'' polymerization (with quotation marks) or ''apparently living,'' which could indicate a process of preparing well-defined polymers under conditions in which chain breaking reactions undoubtedly occur, as in radical polymerization.[11,12] The term *controlled/living* could also describe the essence of these systems.[10]

This kind of nomenclature related to free-radical polymerization has been recently thoroughly discussed. The outcome of this discussion was a proposal to relax the definition of living polymerization and to encompass within this term free-radical polymerizations that share many characteristics of living systems such as relatively low polydispersities, linear growth of molecular weight with monomer conversion accompanied by essentially linear semilogarithmic kinetic plots, in spite of the occurring termination.[13] In this chapter we will follow the vox populi and use the term *living radical polymerization* (LRP) for those systems that contrast the conventional radical polymerization (RP) in several aspects, the main difference is the linear increase of molecular weight with conversion and low polydispersities, inaccessible by RP, specifically, $M_w/M_n < 1.5$ (where subscripts w and n denote weight and number averages, respectively).

The unified nomenclature may be especially useful for various computer–based literature searches. For example, a search in SciFinder Scholar on April 14, 2002 revealed 1692 entries on controlled radical polymerization (CRP) and 1479 on living radical polymerization (LRP); however, as many as 2747 entries were obtained when the two concepts were combined. The number of citations on LRP or CRP is in fact much larger, since, for example, atom transfer radical polymerization (ATRP) also had 1462 entries, and the combined three concepts had 3699 citations. Figure 8.1 illustrates the increasing number of publications per year in living radical polymerization/controlled radical polymerization; atom transfer radical polymerization; stable free-radical polymerization/nitroxide mediated polymerization; reversible addition–fragmentation transfer/degenerative transfer/catalytic chain transfer radical systems. Several reviews devoted to LRP have been already been published,
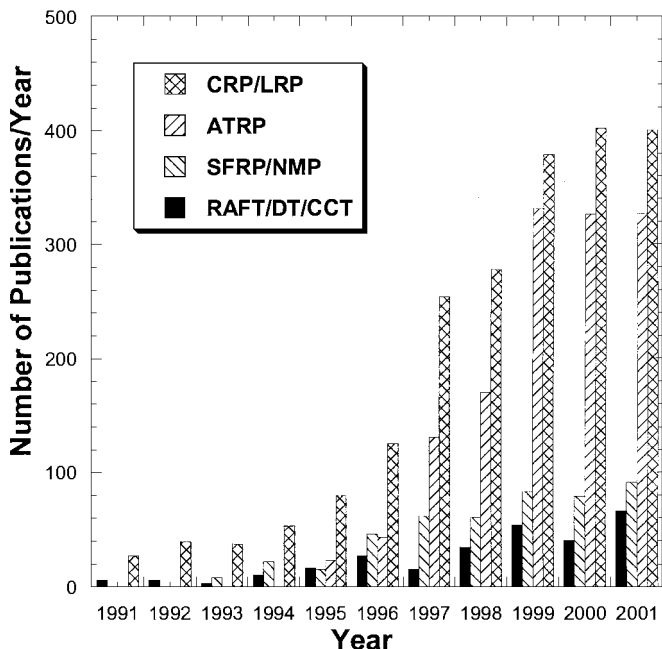
Figure 8.1 Publications on CRP/LRP, ATRP, SFRP/NMP, RAFT/DT/CCT according to SciFinder Scholar as of 04.14.2002.

and readers may refer to proceedings from ACS meetings on LRP,[14] general reviews on LRP,[15] and reviews on ATRP,[16,17] nitroxide mediated polymerization (NMP),[18] and macromolecular engineering and materials by ATRP.[19]

8.3   TYPICAL FEATURES OF A LIVING OR CONTROLLED POLYMERIZATION

A special feature of LRP, and many other new living polymerization systems, such as carbocationic, ring opening, group transfer, and ligated anionic polymerization of acrylates, is the existence of an equilibrium between active and dormant species, which will be discussed in detail later.[20] The exchange between the active and dormant species allows slow but simultaneous growth of all chains while keeping the concentration of radicals low enough to minimize termination. This exchange also enables quantitative initiation necessary for building polymers with special architectures and functionalities, presently accessible in classic living polymerizations. The importance of the exchange will be discussed later, in more detail, in this section.

Ideally, living systems lead to polymers with degrees of polymerization predetermined by the ratio of concentrations of consumed monomer to the introduced initiator $DP_n = \Delta[M]/[I]_0$, with polydispersities close to Poisson distribution ($DP_w/DP_n \approx 1 + 1/DP_n$), and with complete end functionalization. Experimentally, the best way to evaluate such systems is to follow the kinetics of polymerization
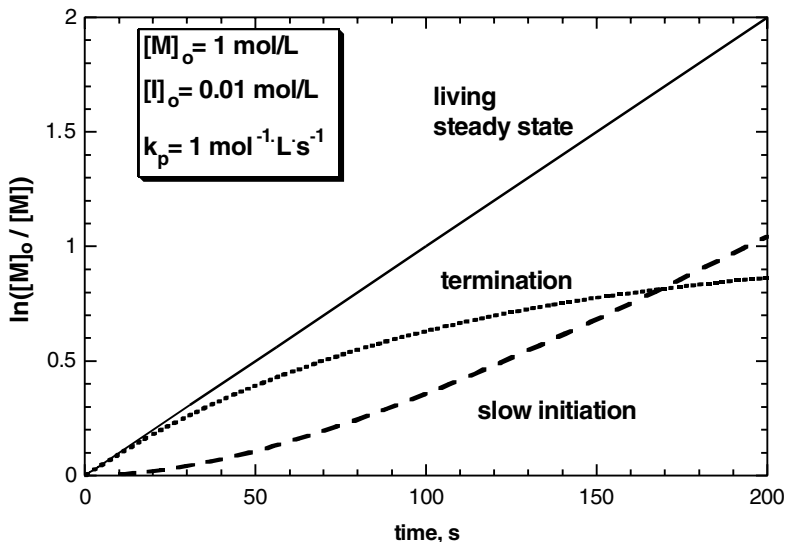
Figure 8.2 Schematic effect of slow initiation and unimolecular termination on kinetics for $[M]_0 = 1$ mol/L, $[I]_0 = 0.01$ mol/L and rate constants of initiation and termination 100 times smaller than that of propagation.

and the evolution of molecular weights, polydispersities, and functionalities with conversion. Typical behavior for living systems and the corresponding deviations are illustrated schematically in Figs. 8.2 and 8.3. To simplify the analysis, one deviation will be considered at a time. Unimolecular termination is analyzed to avoid the effect of the active-site concentration. Transfer to monomer is chosen to illustrate transfer reactions. Initial conditions are $[M]_0 = 1$ mol/L, $[I]_0 = 0.01$ mol/L, and rate constants of initiation, transfer, and termination are 100 times smaller than that of propagation ($k_p = 1$ mol^{-1} L s^{-1}).

Well-controlled systems should provide

1. Linear kinetic plot in semilogarithmic coordinates ($\ln([M]_0/[M])$ vs. time), if the reaction is first-order with respect to the monomer concentration. Acceleration on such a plot may indicate slow initiation, whereas deceleration may indicate termination or deactivation of the catalyst. Straight lines indicate only a constant number of active sites and will also be present under steady-state conditions, typical for any RP. The transfer step should have no effect on kinetics (see Fig. 8.2).

2. Linear evolution of MW with conversion. MW lower than predicted by $\Delta[M]/[I]_0$ ratio indicates transfer, while MW higher than predicted by $\Delta[M]/[I]_0$ may indicate either inefficient initiation or chain coupling (at most, twice higher than predicted MW can be formed by bimolecular radical coupling). Straight lines indicate only a constant number of all chains (dead and growing) and cannot detect unimolecular termination (or termination by disproportionation in RP) (see Fig. 8.3).
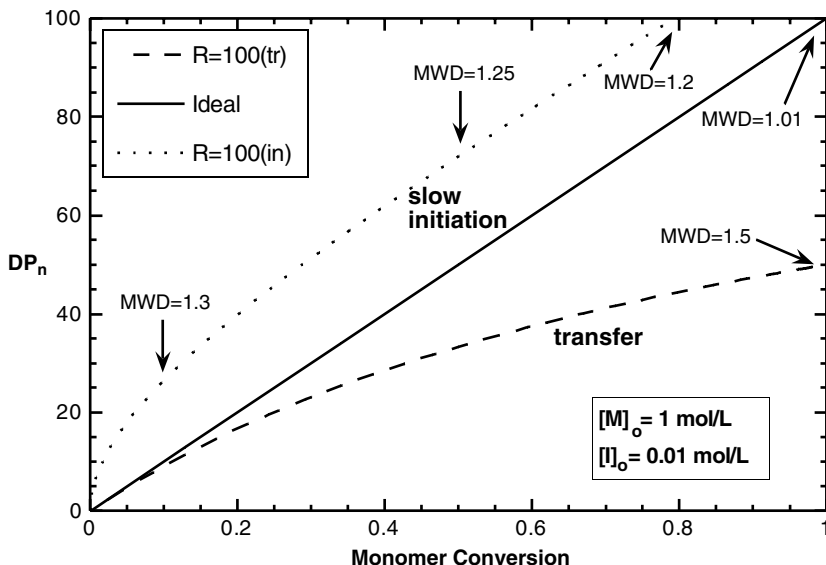
Figure 8.3 Schematic effect of slow initiation and transfer to monomer on kinetics for $[M]_0 = 1$ mol/L, $[I]_0 = 0.01$ mol/L and rate constants of initiation and transfer 100 times smaller than that of propagation.

3. Polydispersity (M_w/M_n) should decrease with conversion for systems with slow initiation and slow exchange. Polydispersities increase with conversion when the contribution of chain breaking reactions becomes significant.
4. End-functionality is not affected by slow initiation and exchange but is reduced when chain breaking reactions become important.

The effect of transfer, termination, and slow initiation on polydispersities and functionalities will be discussed first. Then, the effect of slow exchange on these parameters will be analyzed.

8.3.1 Effect of Chain Transfer and Termination on Polydispersity and End Functionality

Figures 8.4 and 8.5 show the effects of transfer and termination on the proportion of active chains (those with a preserved functionality) and polydispersities with monomer conversion for ratios of $[M]_0/[I]_0 = 1000$ and 100, in systems with instantaneous initiation.

The same ratios of rate constants of chain breaking reactions to that of propagation $[k_{t(tr)}/k_p = 10^{-3}]$ were chosen to illustrate how (pseudo)unimolecular transfer (k_{tr}), transfer to monomer (k_{trm}) and (pseudo)unimolecular termination (k_t) affect the polymerization control for targeted DP = 100 and 1000. Figure 8.4 shows that for these, arbitrarily chosen, chemoselectivities (defined as the ratio of the rate constants of chain breaking to propagation), chains progressively lose their end functionalities
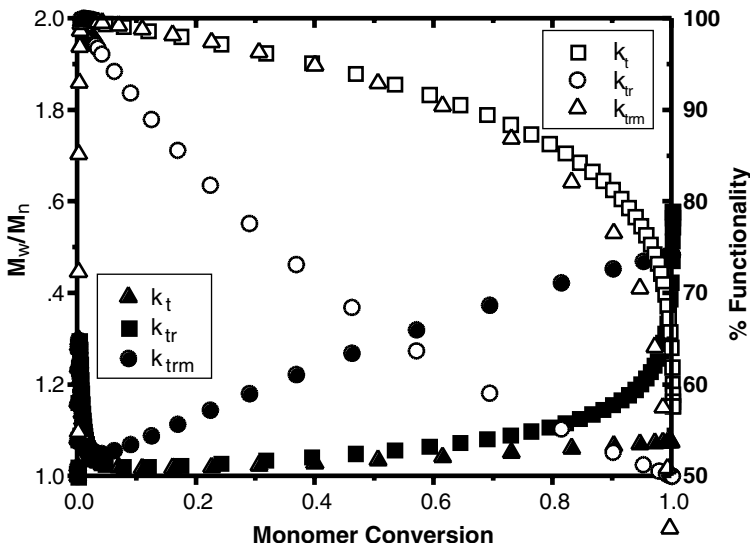
Figure 8.4 Polydispersities (closed symbols) and remaining functionalities (open symbols) as a function of monomer conversion for the ratios of $k_{t(tr)}/k_p = 0.001$, $[M]_0 = 10\,\text{mol/L}$, $[I]_0 = 0.01\,\text{mol/L}$.
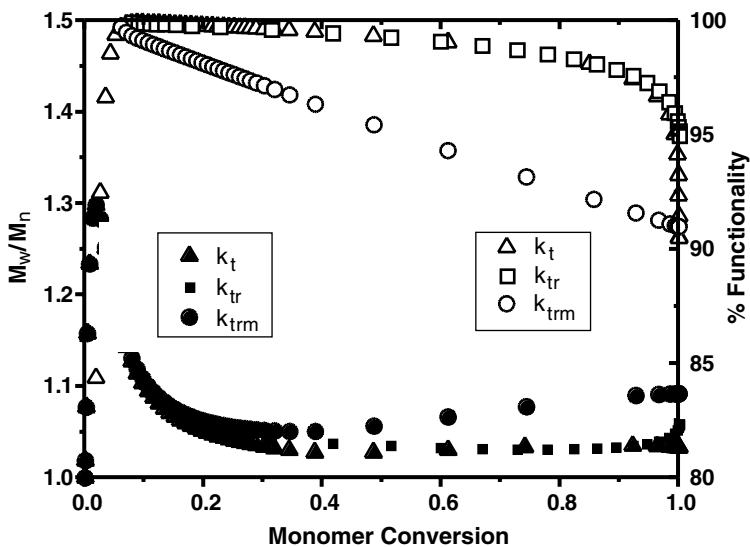
Figure 8.5 Polydispersities (closed symbols) and remaining functionalities (open symbols) as a function of monomer conversion for the ratios of $k_{t(tr)}/k_p = 0.001$, $[M]_0 = 10\,\text{mol/L}$, $[I]_0 = 0.1\,\text{mol/L}$.

and polydispersities increase with conversion. For example, if $k_{trm}/k_p = 10^{-3}$, then 50% of the chains have lost activity (open symbols) and the polydispersity reached $M_w/M_n = 1.5$ (filled symbols) at complete conversion. Nearly the same behavior is observed for (pseudo)unimolecular transfer, although the control at 80–90% conversion is much better than for transfer to monomer. The significant loss of functionalities at high conversion rates originates from the reduced rate of propagation while the rate of transfer is maintained constant. Shorter chains formed by transfer at high conversion increase polydispersity significantly. The effect of termination is quite surprising. At high conversions, chain termination has a minor influence on polydispersity, because chain growth is almost complete and only small redistributions of chain lengths can occur. However, functionalities are lost to the largest extent at high conversion. Thus, in spite of low polydispersities, conversion should be limited to retain end functionality. This is an important consideration for the synthesis of end-functionalized polymers or block copolymers.

Figure 8.5 shows that the control of shorter chains with targeted DP = 100 is much more successful, although the chemoselectivities are exactly the same as in Fig. 8.4. The only difference is 10 times higher concentration of the initiator. Whereas ill-defined polymers are formed while targeting DP = 1000, well-defined polymers with controlled functionalities and low polydispersities are obtained when aiming DP = 100.

Thus, in many new controlled/"living" polymerizations (radical systems included) it is possible to prepare well-defined polymers that are, however, limited to a certain molecular weight defined by contributions of chain breaking reactions.

8.3.2 Effect of Exchange Between Species of Different Reactivities on Polydispersity and Molecular Weight

Nearly all new controlled/"living" polymerizations (cationic, group transfer, and radical) are based on exchange between active and dormant species. The detailed kinetic analysis of these systems has been reviewed by Mueller.[9] The activation and deactivation process may take place either uni- or bimolecularly (Scheme 8.1):

The dormant species P_n—X can be activated either spontaneously (thermally) or in the presence of a catalyst (Y) to form the active species $P_n{}^\bullet$ with the rate constant of activation k_a (or k_{act}). This process is reversible, and the active species are deactivated with a rate constant of deactivation k_{da} (k_d or k_{deact}) by the deactivator X (or XY). Only active species propagate with a rate constant of propagation k_p. In such systems, MWD and MW control are defined by the relative ratios of the rates of deactivation and propagation (k_p). Active sites may also terminate (k_t) or transfer

$$\sim\!\!\sim P_n\text{-X} \quad (+Y) \quad \underset{k_{da}}{\overset{k_a}{\rightleftarrows}} \quad \sim\!\!\sim P_n{}^\bullet \;\; + \;\; X\,(\text{-Y})^\bullet$$
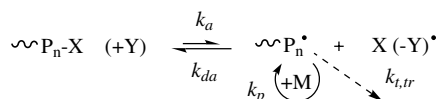
Scheme 8.1   Exchange between active and dormant species.

(k_{tr}). After all initiator ($[I]_0$) is converted into growing chains, the polydispersities for systems with slow exchange are defined by a very simple Eq. (8.1):

$$\frac{M_w}{M_n} = 1 + \frac{[I]_0 k_p}{[X] k_{da}} \left(\frac{2}{p} - 1\right)$$

(1)

where [X] is the concentration of deactivator (X or XY) and p is monomer conversion. If deactivation is unimolecular (ion pair, caged radicals), then [X] can be omitted in Eq. (8.1). This equation is valid for systems in which the equilibrium is strongly shifted toward dormant species, when sufficiently long chains are formed and initiation is completed. When deactivation is very slow and initiation is incomplete, a more complex equation, Eq. (8.2), should be used to account for the unreacted initiator:[21]

$$\frac{M_w}{M_n} = \left\{1 + \frac{[I]_0 k_p}{[X] k_{da}} \left(\frac{2}{p} - 1\right)\right\} \left\{1 - (1 - p)^{[([X]k_{da})/([I]_0 k_p)]}\right\}$$

(2)

The evolution of polydispersity and molecular weight with conversion for systems with the ratios of $([I]_0 k_p)/([X] k_{da}) = 0.01, 0.1$, and 1 are shown in Figs. 8.6 and 8.7 (circles, squares, and triangles, respectively).

Figure 8.6 shows that the polydispersities decrease with conversion (as observed in many "living" systems) and are indeed lower for both smaller initiator concentrations (longer chains) and faster deactivation (higher [X], higher k_{da}/k_p). Thus, polymers with lower polydispersity can be prepared for chains with the same length, provided the deactivation process is faster. The deactivation rate can be increased by
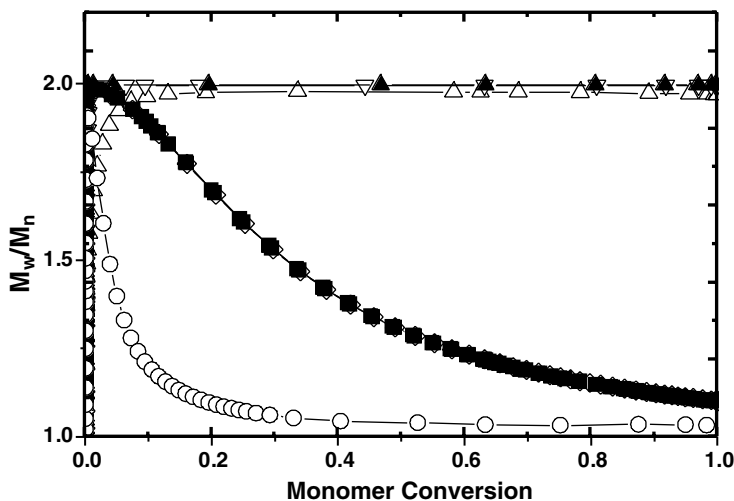
Figure 8.6 Dependence of polydispersities on conversion for systems with slow exchange and with the ratio of $([I]_0 k_p)/([X] k_{da}) = 0.01$ (○), 0.1 (variable k_a: ◇■□) and 1 (variable k_a: △▲▽).
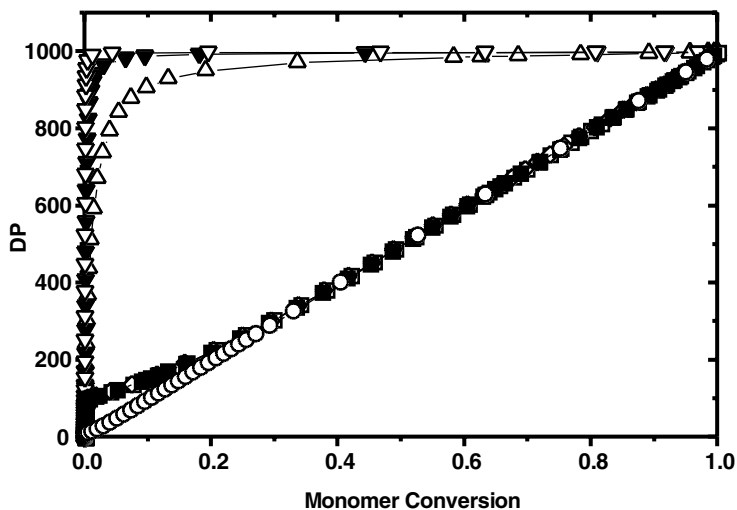
Figure 8.7   Dependence of degrees of polymerization on conversion for systems with slow exchange and with the ratio of $([I]_0 k_p)/([X]k_d) = 0.01$ (◯), 0.1 (variable k_a: ◇■□) and 1 (variable k_a: △▲▽).

using either a higher concentration of deactivator or a more reactive deactivator (higher k_{da}). The rate of activation does not affect the polydispersities when they are plotted against conversion (various filled and open symbols). However, when polydispersities are plotted against the reaction time, they scale well with the rate constants of activation.[22] As explained in much greater details in Chapter 9, using such a kinetic analysis, the evolution of polydispersities with time depends only on k_a but is totally independent of k_{da}!

When slow exchange is the only reason for the broadening MWD, its rate simply correlates with polydispersity. If chain breaking reactions (transfer, termination, etc.) are additionally present, then the polydispersity increases with conversion. This may lead to a certain "window" of degree of polymerization at which well-defined polymers can be prepared. Thus, at a low range of MW, the polydispersities may be higher than in ideal systems because of slow exchange (or slow initiation), but they may be also higher at high conversion due to progressively more noticeable side reactions.

Figure 8.7 shows the effect of slow deactivation on evolution of DP with conversion. If deactivation is relatively fast, DP increases linearly with conversion. However, for slow deactivation, such as when $([I]_0 k_p)/([X]k_{da}) = 1$ (triangles), DP is much higher than predicted, and is only slightly affected by the rate constants of activation.

Control of both DP and polydispersity improves with either faster deactivation or lower initiator concentration, when longer chains are targeted. This occurs until chain breaking reactions start to affect DP and polydispersity. In some systems, slow exchange may lead to polymers with even higher polydispersities, $M_w/M_n > 2$.

This may happen even in systems with an insignificant contribution of chain break-ing reactions when exchange is slow enough.

For the degenerative transfer process a deactivator also generates chains (it may also be considered as an initiator) and therefore simplifies to:

$$\frac{M_w}{M_n} = 1 + k_{\mathrm{p}}/k_{\mathrm{exch}} \left(\frac{2}{p} - 1 \right) \tag{3}$$

Thus, polydispersity depend only on $k_{\mathrm{p}}/k_{\mathrm{exch}}$ and conversion. However, the slow monomer addition may further reduce the polydispersity as demonstrated in addition–fragmentation reactions.[23]

8.3.3   Slow Initiation

Fast initiation is a prerequisite for the synthesis of polymers with degrees of poly-merization predetermined by $\Delta[\mathrm{M}]/[\mathrm{I}]_0$ ratios. In systems without exchange and without chain breaking reactions, the upper polydispersity limit is $M_w/M_n < 1.35$, as a result of slow initiation.[24] When slow initiation occurs and growing chains exist in dormant and active forms, polydispersity can be significantly higher. Slow initia-tion leads to slower polymerization, usually accompanied by induction periods, and to molecular weights higher than predicted by $\Delta[\mathrm{M}]/[\mathrm{I}]_0$. The effect of slow initiation is especially easy to notice when synthesizing low molar mass polymers. In degenerative transfer processes (e.g., RAFT), the aforementioned effect of slow initiation on MW and polydispersities can be translated to the slow consumption of the original transfer agent.

8.3.4   Other Factors

Control of molecular weights and polydispersities may be additionally affected by the reversibility of propagation and by inhomogeneity of the system. Heterogeneous catalytic systems may also lead to higher polydispersities. However, if the catalyst acts via activation/deactivation, then heterogeneity should not affect polydispersi-ties unless exchange reactions are too slow (e.g., concentration of deactivator X or XY is too low). Poor solubility of the initiator (e.g., macroinitiator for block copolymerization) or a growing polymer will also lead to higher polydispersities.

8.4   TYPICAL FEATURES OF CONVENTIONAL FREE-RADICAL POLYMERIZATION

In this section, the conventional free-radical polymerization (RP) is briefly summar-ized in order to compare it with LRP. Free-radical polymerization has been known for more than sixty years. The basic theory and comprehension of radical poly-merization was established by the 1950s.[25] It included a basic understanding of the mechanism of the process, encompassing the chemistry and kinetics of the

elementary reactions involved, determination of the corresponding absolute rate constants, the structure and concentrations of the growing species, and a correlation of the structure of the involved reagents with their reactivities. Since that time, significant progress has been made and a more detailed comprehensive understanding of RP has been presented in the preceding seven chapters.

Nearly all compounds with $C=C$ bonds can be either homopolymerized or copolymerized via a radical mechanism. They should fulfill two basic requirements: thermodynamic polymerizability and kinetic feasibility. The former indicates sufficient negative free energy of polymerization and the latter sufficient reactivity of monomer, stability of the derived free-radical, and a low proportion of side reactions. Most monosubstituted alkenes polymerize radically; some disubstituted alkenes either homopolymerize (methacrylates) or copolymerize (isobutene, maleic anhydride). Isobutene and α-olefins do not provide high molecular weight polymers radically since they propagate slowly and participate in transfer reactions. However, copolymerization of these monomers with electron-poor monomers is successful. Radical polymerization of unprotected hydroxyethyl (meth)acrylates, (meth)acrylic acid, and some amino derivatives lead to high molecular weight polymers, in contrast to ionic systems because radicals are tolerant to protons on heteroatoms. Monomers can be polymerized in bulk, in organic solvents and also in aqueous suspension/emulsion. The choice of solvent is limited only by potential transfer reactions.

Radical polymerization consists of four basic elementary steps: initiation, propagation, termination, and transfer. Initiation is usually composed of two processes: generation of a primary initiating radicals and reaction of these radicals with monomer. The former reaction is much slower than the latter, and it is rate determining, with typical values of $k_d \approx 10^{-5} \, s^{-1}$ and $k_i > 10^5 \, M^{-1} s^{-1}$. Typical initiators (peroxides, diazo derivatives, redox systems, organometallics, and photolabile compounds) are used at concentrations between 1 and 0.01 mol%. The reaction temperature is correlated with the initiator structure in such a way that 50% of the initiator is typically decomposed within 10 h. During that time more than 95% monomer conversion is often reached.

Propagation occurs by the repetitive addition of the growing radical to the double bond. It is considered to be chain-length-independent, with typical values of $k_p \approx 10^{3\pm1} \, M^{-1} s^{-1}$. The concentration of the propagating free radicals is established by balancing the rates of initiation and termination and is equal to ($[P^\bullet] \approx 10^{-8\pm1} \, M$).

Termination between two growing radicals can occur by either coupling (k_{tc}) or disproportionation (k_{td}) with rate constants approaching the diffusion controlled limit, $k_t > 10^7 \, M^{-1} s^{-1}$. Rate coefficients of termination are chain length and conversion dependent. If termination by coupling dominates, then polymers with higher molecular weights and lower polydispersities are formed.

The fourth elementary reaction is transfer. Transfer can occur to monomer or to polymer. In the latter case, the M_n value is not affected, but polydispersities increase as a result of formation of branched and in some cases crosslinked polymers. Transfer can also occur to a transfer agent (TA). Typically, reinitiation ($k_{trTA'}$) is fast, and

transfer has no effect on kinetics, only on molecular weights. If reinitiation is slow, then some retardation/inhibition may occur.

Polymers with molecular weights in the range of $M_n \approx 100,000$ are formed. However, in the presence of transfer agents, it is possible to prepare polymers with much lower M_n. It is also possible to prepare polymers with $M_n > 10^6$, but this is often a difficult task because of transfer and termination reactions between growing radicals. The lowest polydispersity for conventional radical polymerization is $M_w/M_n = 1.5$, which is attainable at low conversions and for termination by coupling. However, in most systems polydispersities exceed $M_w/M_n > 2$, especially at higher conversions. Typically, overall kinetics is first-order with respect to monomer and half-order with respect to initiator. The overall rate constant of polymerization is a function of the efficiency of initiation (f), the rate constant of initiation (k_d), propagation (k_p), and termination (k_t). All of these rate constants are also very important for LRP processes since control in LRP depends strongly on the delicate balance between various kinetic parameters.

8.5 LIMITATIONS OF CONVENTIONAL RADICAL POLYMERIZATION

As stated before, the main disadvantage of RP in comparison with ionic polymerization are the diffusion-controlled termination reactions between growing radicals. However, since termination is second-order, whereas propagation is first-order, with respect to growing radical concentration, by keeping the concentration of radicals very low, it is possible to build a polymer chain of appropriate molecular weight. In conventional systems this is accomplished by continuous slow initiation. Often when >90% of monomer is converted to polymer, only <20% of initiator has been consumed. Slow and continuous initiation prevents synthesis of well-defined polymers with degrees of polymerization predetermined by the ratio of concentrations of the converted monomer to the introduced initiator, with low polydispersities, with controlled topologies (stars, combs) and compositions (blocks, grafts, gradients).

The typical lifetime of a propagating chain is very short, in the range of 1 s. During that time approximately 1000 monomer units are added to the generated radicals prior to termination. Thus, macromolecular engineering is not feasible, because it is difficult during 1 s to add a sequence of another monomer to form block copolymer, or add a special terminating agent to produce end-functional polymers and so on. A hypothetical extension of the lifetime of growing radicals would require a considerable slow down of the polymerization. In such a regime, however, the molecular weights would become limited by transfer rather than by termination and remains poorly controlled.

There are two methods in RP that can provide polymers with lower molecular weights. The first method requires larger amounts of initiator and may be accompanied by a significant and uncontrolled increase of the polymerization rate. The second approach is based on transfer agents and can provide polymers, oligomers,

and telomers with well-defined end groups. However, since the rates of transfer and propagation are usually quite different, polymers with broad molecular weight distribution (MWD) are formed.

There are approaches to slow down the polymerization via retardation reactions, which may involve reversible trapping of propagating radicals. However, many of these systems are accompanied by side reactions that break the chain irreversibly.

Thus, RP has severe limitations that do not allow for the simultaneous control of rate and molecular weight (MW). It does not allow employment of any of the macromolecular engineering techniques used in ionic polymerizations in which all chains start growing at the same time and MW increases steadily and linearly with conversion.

This discussion could lead to a pessimistic conclusion that RP could never be controlled at a level observed for ionic systems, due to slow initiation and unavoidable termination. Fortunately, the concept of exchange between active and dormant species has provided a convenient tool to convert ill-defined radical systems to controlled/living polymerizations.

8.6   TOWARD LIVING OR CONTROLLED RADICAL POLYMERIZATION

The main conclusion from the last section is that living or controlled radical polymerization (LRP) should be carried out at very low concentration of growing radicals (to reduce termination reactions) but also at sufficiently high concentration of growing chains (to reduce transfer reactions). In addition, macromolecular engineering requires fast initiation to enable simultaneous growth of all chains. These requirements sound contradictory and against the general practice of RP.

Similar problems were initially faced in many other polymerization systems, including cationic, anionic, or ring opening polymerizations. Control was significantly enhanced when exchange between active species and various kinds of inactive (dormant) species was introduced. The tiny amount of growing active center was dynamically equilibrated with predominant dormant species and, provided exchange was fast, polymers with low polydispersities were obtained. Many of the initiation systems employed were bicomponent and generated active species only upon mixing. The rate of initiation was fast and comparable to propagation. Such an approach has been used in cationic ring opening polymerization;[26] group transfer (anionic) polymerization of methacrylates;[27] carbocationic polymerization of isobutene,[28] styrene[12] and vinyl ethers;[29] and anionic styrene polymerization.[30]

In ionic systems three different methods have been applied to equilibrate active and dormant species:

1. The covalent species were reversibly ionized either spontaneously or in the presence of a catalyst.
2. Ionic species were reversibly trapped by the neutral species to form unreactive ionic products such as onium cations or olate anions.

3. Active ionic centers participated in a degenerative transfer process to exchange with a dormant species in a reversible bimolecular process.

The same three approaches have been used to control radical systems. The best examples of the first approach include nitroxide mediated polymerization (NMP),[31] ATRP,[32,33] and photolabile iniferters.[34] The second approach is less common and may included some organometallic species such as $Cr^{(III)}$ or Al derivatives as well as nonpolymerizable alkenes such as stilbene or tetrathiafulvalene.[35–37] The last approach can be best exemplified by the degenerative transfer with alkyl iodides, or various addition fragmentation chemistry, via RAFT or via methacrylate macromonomers.[23,38,39]

As will be discussed in detail later, these systems can lead to well-defined polymers using free-radical intermediates. These systems can reduce the proportion of irreversibly terminated chains below 5% and assure quantitative initiation. However, because of the radical nature of intermediates, they cannot alter chemo-, regio-, and stereoselectivities observed for RP, meaning that reactivity ratios, tacticity, and head-to-tail connectivity in LRP are approximately the same as in RP.

8.7 GENERAL FEATURES OF LRP SYSTEMS AND DIFFERENCES WITH CONVENTIONAL RADICAL POLYMERIZATION (RP)

LRP closely resembles conventional radical systems, yet they have some distinct additional features. These features will be considered separately for each elementary reaction and other peculiarities discussed.

8.7.1 Propagation

The main chain building step in LRP and RP is identical and involves addition of a radical to a double bond in the monomer. This step has the same stereo-, regio- and chemoselectivity for both systems. No effect on tacticity has been observed for polymers prepared in the presence of chiral nitroxides, or with chiral ligands in ATRP.[40–42] Reactivity ratios in LRP are similar to those in RP.[43] However, some minor differences can be noted. This is due to the fact that the lifetime of propagating chain increases from <1 s to >1 h by switching from RP to LRP systems. In RP monomer is added every ~1 ms, whereas in LRP, every ~1 min. Thus, in RP, a local depletion of monomer can occur and some side reactions due to monomer starved conditions can become important. This is especially well demonstrated in copolymerization of macromonomers.[44] Conventional radical polymerization shows relatively low reactivity for macromonomers and requires a presence of a compatibilizing solvent. Without it, the monomer is consumed rapidly and forms a polymer which is not compatible with the macromonomer. Thus, unreacted macromonomer remains until the very end of the reaction. In controlled systems, on average, monomer is added very slowly and the macromonomer has enough time to diffuse to the growing chain end, to be incorporated, and compatibilize the resulting graft copolymer. This

facilitates the subsequent additions and leads to apparently higher reactivity ratios for macromonomer, very close to values observed for low molar mass monomers.

The reversible activation process should provide some isotope selectivity, accelerating cleavage of C^{12}-X versus C^{13}-X bonds, and also in some chiral species, e.g. accelerating activation of R-S versus R-R end groups. This can lead to minor increase in kinetic isotope effects in comparison with RP and also in enantiomeric enhancement when chiral monomers are used in conjunction with chiral nitroxides or chiral transition metal complexes.

8.7.2 Transfer

The contribution of transfer in LRP and RP processes is similar. This includes transfer to transfer agents, such as thiols, sulfides, phenols, and other transfer agents.[45,46] Many halogen containing transfer agents act as initiators in ATRP, since halogen transfer to the transition metal complex is faster than to a growing radical. Transfer to polymer has been also detected in LRP.[47] Transfer to monomer usually has a very low value in RP and is much more difficult to observe in LRP, especially, since most LRPs target low-molar-mass products. Monomer transfer coefficients are usually below $k_{trm}/k_p < 10^{-4}$. This means that half of all chains participate in transfer at the stage of DP = 10,000 but less than 10% of chains at DP = 1000. Thus, transfer to monomer should not interfere with the synthesis of polymers by LRP targeting $DP_n < 1000$ ($M_n \approx 100,000$). Some additives used to mediate LRP can induce additional transfer reactions. This includes nitroxides (e.g., in methacrylate polymerization),[48] or ligands in ATRP.[49] Thus, no significant difference in transfer reactions between LRP and RP has been reported, although some distinct behavior may be due to additives or monomer starvation, as discussed above for propagation.

8.7.3 Termination

Another elementary reaction, nearly identical in RP and LRP, is termination. In both systems termination does occur and cannot be avoided. Two radicals do terminate with diffusion-controlled rates. However, there are also some important subtle differences. In conventional systems, small initiating radicals are continuously generated. Because termination is chain length dependent and the rate coefficients for termination decrease with chain length, the majority of termination reactions occur not between two long chains but between a long and a short chain or two short chains.[50] On the other hand, in LRP chains grow slowly but continuously with conversion and at higher conversion, when chains become longer, termination rate coefficient drops and the rate of termination also significantly decreases since only long chains are present.[51] At the early stages termination may be more significant. This happens in ATRP and NMP and perhaps to a lesser extent in RAFT and DT, where small molecules of initiator are continuously generated, albeit in small amounts. However, in all successful LRPs, the proportion of irreversibly terminated chains is small in comparison with the total number of chains (<10%). This is in contrast to conventional systems, where all chains are essentially dead (>99%) at any moment of the reaction.

Some mediating agents for LRP may allow additional termination reactions to occur. For example, alkyl halides in ATRP may loss HX at higher temperatures,[52] or nitroxides may abstract β-H atoms, etc.[53]

8.7.4 Initiation/Radical Generation

The main difference between RP and LRP is how radicals are generated. In conventional systems, radicals are formed at low concentration, continuously and irreversibly. In LRP, radicals are formed reversibly at both the initiation and the propagation stages. At any moment of the reaction, concentration of radicals may be similar in both systems. In RP this concentration is established by balancing continuous initiation with irreversible termination. In LRP, however, this concentration is essentially established by balancing rates of activation and deactivation (also called *dissociation* and *recombination* in NMP). Degenerative transfer and RAFT rely on irreversible initiation and termination (thus resembling conventional systems), but all chains exchange activity by reversible activation/deactivation, that is, by the degenerative exchange. However, as in other LRPs, at any time only a small proportion of chains are active and the dormant species dominate.

8.7.5 Exchange Reactions

Exchange reactions are perhaps the most important reactions in LRP. They determine degree of control, polydispersities, and end functionalities. Exchange reactions are essentially absent in RP. The activation process may be spontaneous (thermal) as in NMP or cobalt-mediated systems, or may be catalyzed, as in ATRP. The deactivation reactions are perhaps even more important, since they define how many monomer molecules are added during one activation step, or how many activation/deactivation cycles (ν) occur during a buildup of the macromolecule. In the ideal case, the reciprocal value of this number defines polydispersities ($DP_w/DP_n \approx 1 + 2/\nu$). The exchange in DT and RAFT is a bimolecular reaction between a dormant and an active chain. At high conversion, the rate of exchange between two macromolecular species may be reduced more than the rate of propagation, thus increasing polydispersities.

8.7.6 Lifetime of LRP

Termination continuously occurs in all LRPs, although it is chain length dependent. Since propagation is first-order and termination is zero-order with respect to the monomer, the relative rate of termination may become more significant at high conversion. This effect is counterbalanced by the chain length dependence of the termination reactions. At the latter stage of the polymerization, when a large majority of monomer is consumed, termination may not significantly affect MW and polydispersity but it will reduce chain end functionality and the capability of forming block copolymers. This was illustrated in Fig. 8.5. Therefore, for block copolymers, it is recommended not to exceed 95% monomer conversion, especially for the first block and isolation of the macroinitiator or perhaps the addition of the second monomer, before the first one is entirely consumed, is recommended.

The shelf time of the resulting polymers may depend on the nature of the end group. Halogen-terminated polymers prepared by ATRP are relatively thermally stable, especially in the absence of catalyst. The same holds true for terminal dithioesters in RAFT process. In both systems, the chain growth can be resumed in the presence of ATRP catalysts or conventional radical initiators in the case of RAFT. Terminal alkoxyamines in NMP are thermally labile but, because of the high activation energy of dissociation, they are relatively stable at ambient temperatures.

8.7.7 Trommsdorf (Gel) Effect

Conventional bulk radical polymerization may be accompanied by an uncontrolled acceleration in the rate of polymerization at high conversion. This gel (or Trommsdorf) effect is due to a significant reduction of termination rate coefficients at high conversion, resulting from increased viscosity. Because concentration of radicals is established by balancing rates of initiation and termination, a drop in the latter rate increases the concentration of radicals and accelerates propagation. Because polymerization is exothermic, temperature increases, further enhancing initiation, and may result in an uncontrolled process, sometimes even in an explosion. ATRP and NMP behave differently and seldom exhibit a gel effect.[54] This is due to the fact that the concentration of radicals is defined by the balance between rates of activation and deactivation. At higher conversion, especially with excess persistent radical (PR), while termination slows down this has less effect on the concentration of growing radicals. High viscosity may slow down deactivation but to an extent similar to propagation, since in both cases growing radical reacts with a small molecule of either a deactivator or a monomer. DT and RAFT may behave differently, since polymerization rates are defined by the ratio of initiation and termination.

8.7.8 Contribution of Thermal Self-Initiation

In the LRP of styrene and substituted styrenes, thermal self-initiated polymerization of styrene occurs simultaneously with the controlled process. The contribution of thermal self-initiation to the overall rate and to the total number of polymer chains in the system should be carefully assessed. The rate of thermal self-initiation has been studied, and the rates of generation of new radicals are known at various temperatures.[55,56] The so-called Mayo dimer,[57] which is an intermediate in this process, is also responsible for a reduction in molecular weights since it has a very large transfer coefficient.[58]

The overall rate of self-initiated polymerization should not be confused with the rate of radical generation. For example, approximately $1\,M/h$ ($\sim 15\%/h$) of styrene is consumed at $130°C$ in bulk thermal polymerization, but less than $10^{-3}\,M/h$ of radicals are generated (which correlates to $M_n \approx 200{,}000$). Thus, in $10\,h$, less than $10^{-2}\,M$ radicals (equal to concentration of new chains) are generated. Actually this number may even be lower, because the rate of self-initiation is second- or third-order with respect to monomer.[56] Since the concentration of new chains is much smaller than the concentration of added initiator, it results in insignificant deviation from expected MW.

Self-initiation may play a beneficial role by accelerating the process and reducing the concentration of persistent radicals formed. A radical generator may be intentionally added to the system.[59,60] Some components of the catalytic system may also generate radicals.[61]

In systems based on degenerative transfer such as RAFT, polymerization rate depends on the amount of continuously generated radicals from initiators such as AIBN or BPO. However, thermal self-initiated styrene polymerization can also be used as a radical source. Well-controlled LRP of styrene using RAFT reagents without any additional initiator was observed at high temperature.[39] The control is reduced with decreasing ratio of concentration of RAFT reagent to the chains generated by self-initiation.

To summarize, self-initiation is important in the polymerization of styrene. It controls the polymerization rates for most TEMPO-mediated systems as well as some ATRP when low concentrations of either catalyst or initiator are used. Nevertheless, the exchange reactions provide good control of molecular weights in LRP systems.

8.7.9 Polymerization in (Mini)emulsion

There are several special features of LRP in heterogeneous systems, especially in (mini)emulsion, that should be considered. First, for systems with sufficiently small particles, the compartmentalization may reduce termination rate that allows increase of polymerization rate without enhanced termination.[62] Second, the nucleation process for particles is very different from classic emulsion processes. Small oligomers are formed first that may have high solubility in water and may easily exit particles. They may have a greater chance to enter droplets and reduce colloidal stability. At 5–10% monomer conversion oligomers are still formed and no irreversible nucleation is observed contrary to conventional emulsion processes. This requires use of special surfactants and cosurfactants. Additionally, since mediating species such as nitroxides or metal complexes in ATRP partition between aqueous and organic phase,[63] their structure must be carefully selected to assure predominant affinity to organic phase but also provide sufficient concentration in water to scavenge radicals and exchange between droplets and micelles.

8.7.10 Summary of Differences Between RP and LRP

The main similarity between LRP and RP is the participation of free radicals in the chain growth. This leads to essentially identical chemoselectivities, regioselectivities and stereoselectivities.

The main difference between LRP and RP is that the steady concentration of free radicals is established in LRP by balancing rates of activation and deactivation but in RP between rates of initiation and termination. Thus, in LRP rates of initiation, activation, and deactivation are much larger than that of termination. This enables initiation of all chains simultaneously, as in other living processes, and therefore control over various polymer architectures. The exchange between active and dormant

species also enables an extension of the lifetime of propagating chains from $\sim$1 s in RP to $\gg$1 h in LRP. This enables many features of macromolecular engineering, including controlled functionality, topology and composition.

8.8   BASIC PRINCIPLES OF LRP

As discussed in previous sections, LRP requires all chains to begin growing (reversibly via exchange processes) at essentially the same time and retain functionalities until the very end of the reaction. This is in contrast to RP, where all chains terminate and initiation is never completed, even when all monomer is consumed. Therefore, the three basic prerequisites for LRP are

1. Initiation should be completed at low monomer conversions.
2. Relatively low MW (DP < 1000) should be targeted to avoid transfer effects. This requires high concentration of growing chains, (e.g., $> 10^{-2}$ M for bulk polymerization).
3. Concentration of propagating radicals ($[P°] < 10^{-7}$ M) should be sufficiently low to enable growth of chains to sufficiently high MW, before they terminate.

The mismatch between concentration of growing chains and propagating radicals (10^{-2} M $\gg$ 10^{-7} M), although it seems paradoxical for RP, can be fulfilled by the exchange reactions between high concentration of growing chains in the dormant state and minute amounts (<ppm) of propagating free radicals. The exchange reactions are the very core of all LRP systems and will be discussed in depth. The other unique feature of many LRPs such as NMP and ATRP is the persistent radical effect (PRE). However, the PRE does not operate in degenerative transfer systems, such as RAFT.

8.8.1   Persistent Radical Effect

Many reactions involving free radicals exhibit surprisingly high chemoselectivities. When stable radicals, such as nitroxides, or metalloradicals [e.g., X—Cu$^{(II)}$ species] are generated together with reactive alkyl radicals, the cross-coupling is much faster than the homocoupling of alkyl radicals. Thus, in atom transfer radical addition (ATRA), >90% yields of 1 : 1 adducts of alkyl halide (RX) and alkenes are often observed. This reaction may be initiated by light or radical initiators, as in Kharasch addition, or may be catalyzed by transition metals. The former reaction is shown in Scheme 8.2. Alkyl halide, (**1**) in the presence of some radical source, generates radical (**2**). In the presence of a large excess of alkene (**3**) addition occurs resulting in product radical **4**. In the halogen transfer step with **1**, it yields the product **5** and regenerates radical **2**. This sequence resembles the degenerative transfer step in LRP. If trapping with **1** is not efficient, some oligomerization may occur. The escaped radicals 4n may then be trapped by **1** to form oligomeric covalent products **5***n*, with a structure similar to **5**.
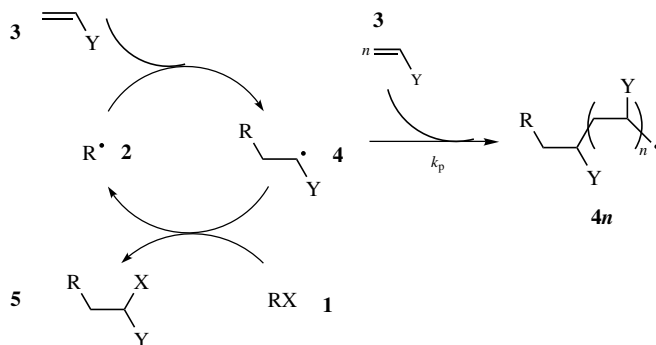
Scheme 8.2   Basic steps in Kharasch addition.
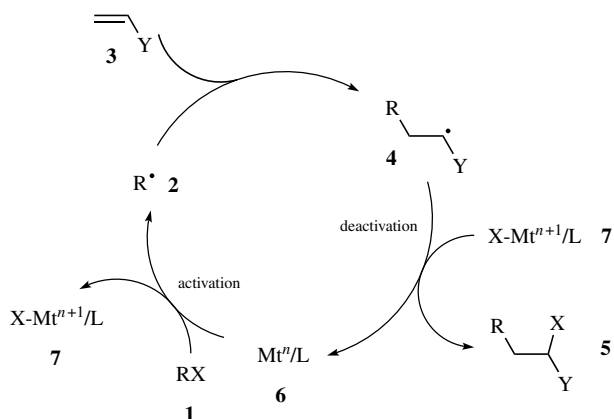
Scheme 8.3   Basic steps in metal-catalyzed ATRA.

The transition metal catalyzed ATRA is shown in Scheme 8.3. It has a similar sequence of reactions but the radicals **4** are trapped not by RX, but by much more efficient transition metal halides in higher oxidation state **7**. This may lead to different selectivities than in Kharasch addition. As an example, in the reaction with chloroform the alkene will "insert" across the H−CCl$_3$ bond under Kharasch conditions, but across the Cl−CHCl$_2$ bond in ATRA, because the C−Cl bond is more rapidly activated by the Fe(II) or Cu(I) complexes.[64] Also the deactivation step does not involve RX but proceeds by the abstraction of X from complex **7**, which may be much bulkier than RX (different regio- and stereoselectivities). Moreover, deactivation step may be much faster (different chemoselectivities).

Scheme 8.3 is simplified because in reality, both activation and deactivation steps are reversible.The correct choice of alkene and RX leads to high yield of **5**, which should be much more difficult to activate than **1**. Similar reactions have been reported for the nitroxide mediated system shown in Scheme 8.4.[65] In contrast to Scheme 8.3, this process is not catalyzed. In the activation step a reactive radical
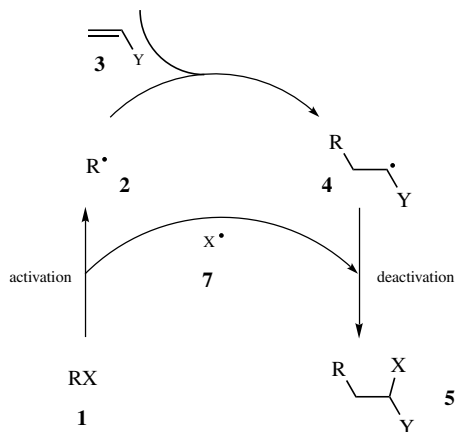
Scheme 8.4   Basic steps in alkoxyamine addition to alkenes.

2 and stable radical **7** are formed. The stable radical **7** also deactivates the product radical **4** to form **5** in high yield. Very little coupling products between radicals **2–2**, **2–4**, and **4–4** are formed, and the radicals react nearly exclusively with stable radical **7**. The unusual selectivities in this and previous systems have been explained by the persistent radical effect (PRE).[65] Its essence is that the "preference" for cross-coupling over homocoupling originates not in different rate constants of the coupling reactions (all are nearly diffusion-controlled) but in different rates. Reactive radicals **2** and **4** are present at very low concentrations, such as $\sim 10^{-8}$ M, but persistent radicals at concentration $\sim 10^{-3}$ M, thousands of times higher. With every act of termination of radical **2** or **4**, a persistent radical (PR) is accumulated. Although at the very beginning of the reaction, **2** and **7** are present at the equimolar concentrations, very soon the concentration of **2** (and **4**) drops whereas the concentration of **7** continuously increases. The amount of PR present equals the amount of homocoupling products and can be as low as 1%, effectively meaning that reactions are unusually selective.

The same principle of PRE operates in many LRP as elegantly explained by Fischer.[66] In the ideal case, when termination is chain length independent, the PRE should lead to special kinetics, in which the logarithmic monomer conversion scales with time exponent $\frac{2}{3}$ rather than linearly with time, as discussed in Chapter 9. However, many LRP were reported with linear first order kinetics. There are several possibilities for such discrepancies:

- Poor kinetic measurements
- Slow decomposition of $X^{\bullet}$ or its addition to monomer
- Self-initiated polymerization in which newly generated radicals scavenge excess $X^{\bullet}$
- Limited solubilities of $X^{\bullet}$
- Chain length dependent termination

All these factors may in some way affect kinetic studies.[67] Regardless, PRE is a very important concept, which is at the very heart of LRP. One could argue that without termination and PRE radical polymerization could not be controlled. However, it is possible to enhance PRE by additional amounts of stable radicals at the beginning of the reaction. This eliminates the need for spontaneous formation of PRE and termination of some chains. This process is also used when deactivators act relatively slowly or propagation is too fast.

8.8.2 Exchange Between Active and Dormant Species and Classification of LRPs

The exchange between growing radicals and dormant species is perhaps the most important feature of all LRP systems. The position and dynamics of the equilibrium define the observed rates as well as affect molecular weights and polydispersities of the formed polymers. It is possible to distinguish LRP systems into several categories, depending on the chemistry of exchange and structure of the dormant species. A mechanistic classification may be most appropriate, since it enables successful correlation of the rates, molecular weights, and polydispersities of the obtained polymers with the concentration of the involved reagents.

8.8.2.1 Mechanistic Classification of LRP   Mechanistically, LRP can be divided into four different cases (Scheme 8.5):
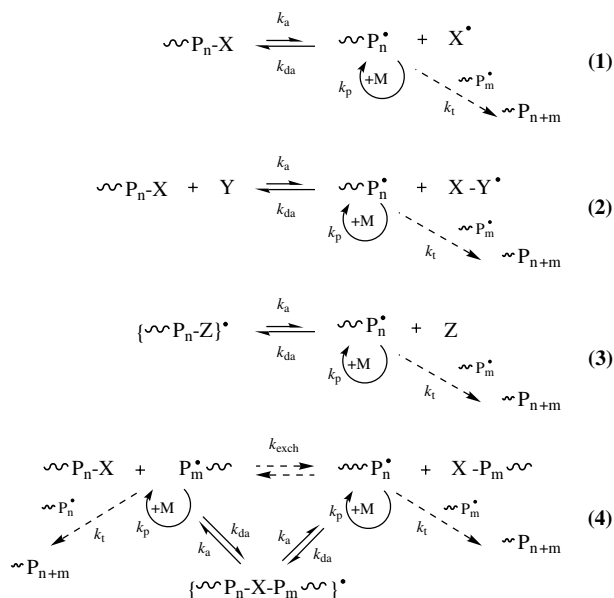
Scheme 8.5   Four general mechanisms for LRP.

In all cases dormant, nonpropagating species are reversibly activated with the rate constant of activation (k_a) to form the active species, $P_n^\bullet$, which react with monomer, M, with the propagation rate constant, k_p. The propagating radicals can be deactivated with the rate constant of deactivation, k_{da}, or can terminate with other growing radicals with the termination rate constant, k_t. Because in all LRPs the concentration of radicals is maintained very low, termination can sometimes be neglected since it does not significantly affect polymer properties. However, since in cases 1–3, each act of termination irreversibly generates radical traps ($X^\bullet$, $XY^\bullet$ or Z, respectively), these termination reactions may affect kinetics.

These methods have also been successfully applied in organic synthesis with atom transfer radical addition, of which degenerative transfer with alkyl halides and xanthates are the best examples.[68–70]

Case 1 is best exemplified by nitroxide mediated polymerization in the presence of TEMPO,[31,71] and bulky acyclic nitroxides,[72] triazolinyl radicals,[73] organoboronoxy radicals,[74] some bulky organic radicals (e.g., trityl),[75,76] photolabile C—S bonds,[34] and organometallic species.[35,77]

Case 2 is based on the catalyzed, reversible cleavage of the covalent bond in the dormant species via a redox process. Because the key step in controlling the polymerization is atom (or group) transfer between growing chains and the catalyst, this process was termed atom transfer radical polymerization (ATRP) and is catalyzed by various Ru, Cu, Fe, and other transition metal derivatives.[17,32,33]

Case 3 is not yet as successful as the systems in cases 1 and 2. This process involves the reversible formation of a PR by reaction of the growing radicals with a species containing an even number of electrons. PRs do not react with each other or with monomer. Here, the role of a reversible radical trap may be played by phosphites,[78] some reactive, but nonpolymerizable alkenes, such as tetrathiofulvalenes[79] or stilbene[36] and also metal compounds with an even number of electrons.[80] It has been proposed that it may also include some organoaluminum compounds, but the subsequent studies did not support this mechanism.[37,81] It seems that some reversible addition–fragmentation chain transfer (RAFT) systems may also behave in a similar way, especially when a strong decrease of the polymerization rate is observed. (see also case 4).

Case 4 is based on a thermodynamically neutral (at the propagation stage) exchange process between a growing radical, present at very low concentrations, and dormant species, present at much higher concentrations (at least three or four orders of magnitude). This degenerative transfer process can employ alkyl iodides,[38] tellurium compounds,[82] unsaturated methacrylate esters,[23] xanthates,[83] and dithioesters.[39] The latter three processes operate via addition–fragmentation chemistry with the redundant or degenerate loops that force radicals in the desired direction.

In the cases 1–3 the equilibrium is strongly shifted toward dormant non-propagating species and rates depend on the concentration of the persistent radical species, such as $X^\bullet$. The only difference between cases 1 and 2 is the bimolecular activation and catalyzed nature of the second system. The $X–Y^\bullet$ species plays the role of PR. Case 3 is nearly identical to case 1; the only difference is that in case 3, the dormant species has an odd number of electrons and the radical trap is not of a radical nature. Thus, formally the role of persistent radical is played by a nonradical species. Currently this is the least explored chemistry. Case 4 is very different from the other three. There is no PR in it, the equilibrium constant equals $K = 1$ ($k_a = k_{da} = k_{exch}$) and rates should conform closely to conventional radical systems with $\frac{1}{2}$ external order in radical initiator. However, rate reduction is expected if the transition state in which the atom or group being transferred from one to another chain is strongly stabilized and becomes a long-lived intermediate product.

Thus, each system has a specific dependence of the polymerization rates, molecular weights, and polydispersities on conversion and concentrations of the involved reagents. They are summarized in Table 8.1.

Polymerization rates in cases 1–3 depend on the free-radical propagation rate constant, k_p; on the equilibrium constant, $K_{eq} = k_a/k_{da}$; on the concentration of initiator, $[I]_0$; and inversely on the concentration of a radical trap ($[X^\bullet]$, $[XY^\bullet]$, or $[Z]$). The concentration of the trap —PR— changes during the polymerization, which may lead to some peculiar kinetic behavior. In case 2, rates increase with the concentration of the activator, $[Y]$. For degenerative transfer, the rate law should be similar to that for the conventional radical process, but some retardation may also be observed.

Degrees of polymerization (DP) increase linearly with conversion and depend inversely on the initiator concentration, provided the initiation is fast. DP may be higher than predicted if primary radicals terminate too soon before addition to monomer, resulting in lower initiator efficiency. In degenerative transfer, the number of chains is the sum of the used transfer agent and consumed initiator.

Polydispersities, M_w/M_n, decrease with conversion, p, and chain length, meaning that they depend inversely on the concentration of the added initiator. Polydispersities also depend on the ratio of rates of propagation and deactivation; the latter is a product of the rate constant of deactivation and the concentration of the radical trap.

TABLE 8.1 Typical Kinetic Laws and Dependence of Degree of Polymerization and Polydispersity on Conversion for LRP

No.	Example	Kinetic Law	DP_n	Polydispersity
1	NMP/TEMPO	$R_p = k_p K_{eq}[I]_0/[X^\bullet]$	$DP_n = \Delta[M]/[I]_0$	$M_w/M_n = 1+(2/p-1)(k_p[I]_0)/(k_{da}[X^\bullet])$
2	ATRP	$R_p = k_p K_{eq}[I]_0[Y]/[XY^\bullet]$	$DP_n = \Delta[M]/[I]_0$	$M_w/M_n = 1+(2/p-1)(k_p[I]_0)/(k_{da}[XY^\bullet])$
3	?	$R_p = k_p K_{eq}[I]_0/[Z]$	$DP_n = \Delta[M]/[I]_0$	$M_w/M_n = 1+(2/p-1)(k_p[I]_0)/(k_{da}[Z])$
4	DT^a/RAFT	$R_p = k_p f k_d(k_t)^{-1/2}([I]_0)^{1/2}$	$DP_n = \Delta[M]/([TA]_0+ \Delta[[I])$	$M_w/M_n = 1+(2/p-1)(k_p/k_{exch})$

^{a} Degenerative transfer.

However, in case 4, the exchange (deactivation) proceeds by the reaction with the transfer agent, which also (predominantly) defines chain length. Therefore, in this unique system, polydispersities should not depend on the chain length provided that the proportion of the added initiator is small in comparison with that of the transfer agent.[9]

If the equilibrium constants are very low and/or concentrations of the reagents are small enough, then the overall rate may be defined by the rate of the thermal process and give apparent zero orders with respect to the involved reagents. Also, when the PR is formed spontaneously, the deviations from both internal and external first orders with respect to monomer, initiator and catalysts may be observed.

8.8.2.2 Other Criteria for Classification of LRP
It is possible to further mechanistically subdivide the four systems into several additional categories, depending on the molecularity of exchange, catalytic nature of the process, occurrence of PRE, and the particular chemistry involved in the exchange.

8.8.2.2.1 The Molecularity of the Exchange
The dormant species can be converted to active species via either a unimolecular (cases 1, 3) or a bimolecular process (cases 2 and 4).

8.8.2.2.2 The Catalytic Nature of Activation of Dormant Species
In most LRP, the activation process is spontaneous and can be accelerated only by increasing the reaction temperatures. The only example of a catalytic process is ATRP, in which activation rates depend on the concentration of transition metals in their lower oxidation state (e.g., case 2). The rates in degenerative transfer systems, including RAFT, depend on the concentration of the radical initiator. Thus, although it should not be considered as a catalyst, since it is irreversibly consumed, it acts as a catalyst in affecting the polymerization rate.

8.8.2.2.3 Persistent Radical Effect
Most LRP systems conform to the PRE model: (cases 1–3). Systems based on degenerative transfer, including addition–fragmentation chemistry do *not* conform to PRE model. Hypervalent iodine-based radicals and sterically hindered tertiary radicals are considered only as short-lived intermediates (case 4). However, under some conditions they may be present at higher concentrations and retardation is plausible. These systems may behave partially like those in case 3.

8.8.2.2.4 Mechanism of Equilibration
There are three general mechanisms for the reversible formation of propagating radicals:

Bond Scission–Recombination. This is the most common mechanism, and includes all unimolecular activation systems (cases 1 and 3). One of the

most studied cases, TEMPO-mediated polymerization of styrene, is shown in equation 4.

(4)
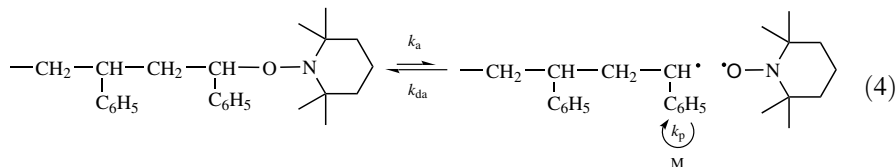
Reversible Atom or Group Transfer. This describes both iodine mediated degenerative transfer systems, equation 5; and ATRP, equation 6 (cases 2 and 4):

(5)
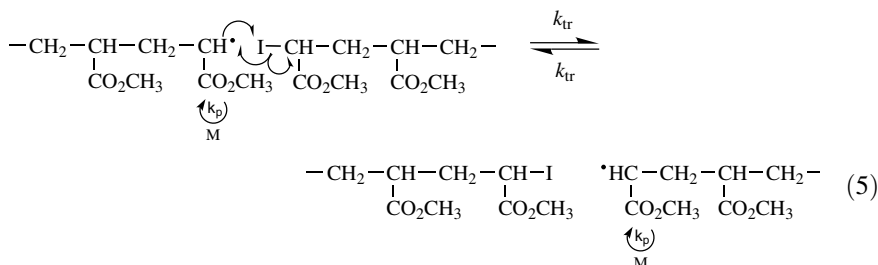
ATRP is schematically shown below together with the relevant rate constants for the styrene polymerization in bulk at 110°C catalyzed by CuBr complexed by 4,4′-di (5-nonyl)-2,2′-bipyridine (dNbpy):

$k_a = 0.45 \text{ M}^{-1} \text{ s}^{-1}$

$k_{da} = 1.1 \ 10^7 \text{ M}^{-1} \text{ s}^{-1}$

$k_t < 10^8 \text{ M}^{-1} \text{ s}^{-1}$ $k_p = 1.6 \ 10^3 \text{ M}^{-1} \text{ s}^{-1}$

(6)
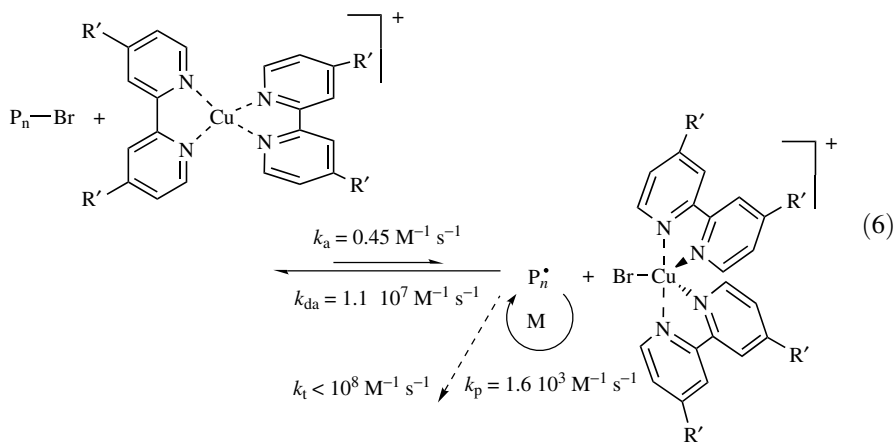
Addition–Fragmentation. This type of bimolecular exchange process employs reversible addition of the radicals to compounds with nonpolymerizable multiple bonds (case 4, and potentially case 3). It may include methacrylate oligomers prepared by catalytic chain transfer:

(7)
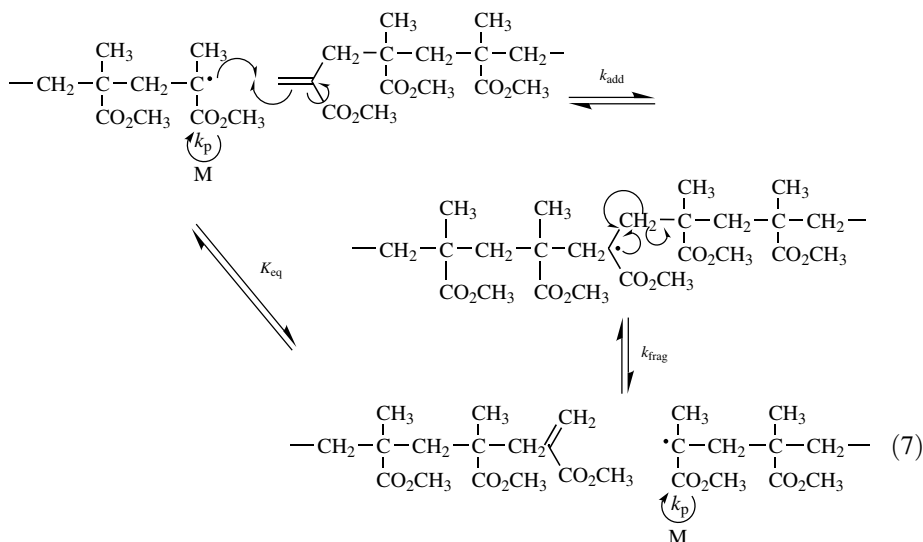
and dithioesters in polymerization of styrenes and various (meth)acrylates:

(8)
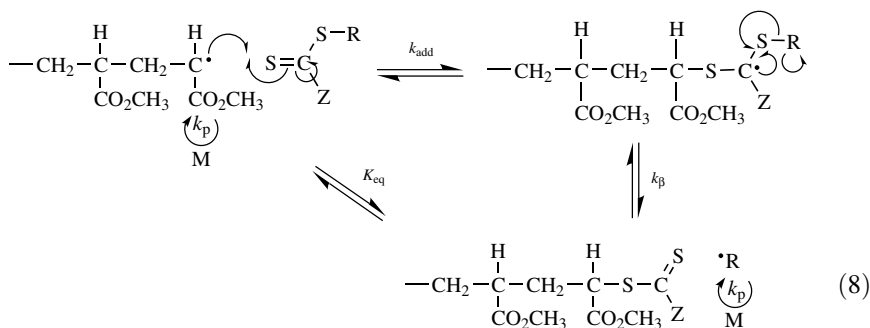
Addition–fragmentation chemistry could also be described as a reversible group transfer process.

8.8.2.2.5 Structure of Dormant Species   While the most elucidating criterion for classification of various LRP is one based on the structure of the dormant species and the type of bond that is reversibly broken mechanistically, LRP will follow one of the four examples shown as cases 1–4 and summarized in Table 8.1 (above).

C—C Bonds. The triphenylmethyl and benzhydryl radicals were first used as a reversible trap in methyl methacrylate polymerization (case 1).[75,76] Polymerization of methacrylate macromonomers mediated by the addition–fragmentation chemistry also proceeds by C—C bond cleavage (case 4).[23]

C—N Bonds. To this category belong triazolinyl[73] and verdazyl derivatives[84] (case 1). The most efficient appears triazolinyl radical with all phenyl substituents as shown below; apparently a derivative with spiroindanyl substituent at 3,3′ position is less efficient due to its higher thermal stability.

$$
\begin{array}{c}
 {}^{\bullet}\text{N}\!-\!\text{N} \\
R_1 \quad N \\
R_3
\end{array}
\tag{9}
$$

C—O Bonds. The classic example here is alkoxyamine, with TEMPO being the most common and most thoroughly studied nitroxide[71] (case 1). However, some new more bulky nitroxides provide better control and extend utility to a larger number of monomers.[72,85] Boron derivatives may also be used:[74]

$$
\tag{10}
$$
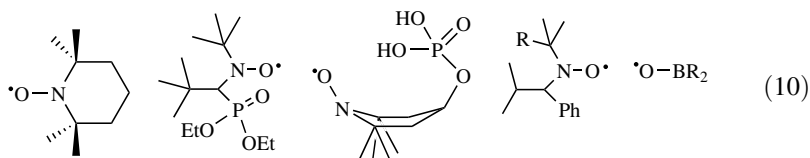
C—S Bonds. Iniferters based on dithiocarbamates were the first species with photochemically labile C—S bonds (predominantly case 1).[34] Dithioesters act as very efficient degenerative transfer reagents in the RAFT process with transfer coefficients more than 100 times higher than those of *N,N,*-dialkyl-dithiocarbamates (case 4).[39]

C—Halogen. ATRP is the most representative example (case 2).[32,33] Degenerative transfer with alkyl iodides has been successfully used for styrene, acrylates, and vinyl acetate (case 4).[38]

C—Metal Bonds. Homolytic cleavage of organometallic bonds has been successfully applied in polymerization of acrylates and styrene using cobalt derivatives, especially when complexed by sterically demanding porphyrins[35] (case 1). It is also feasible that some transition metals with even numbers of electrons (high spin) may reversibly react with organic radicals to form paramagnetic organometallic species (case 3).[80]

Other Systems. In principle, other systems can simply be formed by extrapolating the same concepts down the periodic table. Thus, C—N system can be expanded to P, As, Sb, and the C—S system to Se and Te. The latter system can act via reversible cleavage and by degenerative transfer.[82] One can also use heavier halogens and other transition metals.

8.8.3   Initiating Systems

Initiators for LRP can be either prepared in advance or formed in situ. As a rule of thumb, the structure of the initiator should resemble the dormant macromolecular

species. For example, in the TEMPO-mediated polymerization of styrene, 1-pheny-lethyl alkoxyamine is very successful.[86] In atom transfer radical polymerization (ATRP) of acrylates, 2-bromopropionates are good initiators,[40] whereas 2-bromo-propionitrile is an efficient initiator for acrylonitrile polymerization.[87] Efficient initiation occurs if the initiating precursor is more reactive than the subsequent dormant species. Thus 2-bromoisobutyrate is a good initiator for acrylates, but 2-bromopropionate is a poor initiator for ATRP of methacrylates.[88] Same rules apply for RAFT, NMP, and other LRP systems.[89] However, if the initiator is much more reactive than dormant chains, it may dimerize, reduce initiation efficiency, and significantly increase the concentration of persistent radicals, as observed for benzhydryl derivatives in ATRP.[90] There are some exceptions to this rule. For example, sulfonyl halides can be successfully used as initiators for ATRP of several monomers because radicals derived from them dimerize relatively slowly, even though they are formed in high concentrations.[91]

Initiating systems can be prepared in situ. For example, the TEMPO-mediated styrene polymerization can be thermally self-initiated in the presence of TEMPO[92] or by using BPO/TEMPO[71] or AIBN/TEMPO[85] mixtures. Reverse ATRP can be initiated using AIBN/CuX_2/bpy mixtures (bpy = 2,2′-bipyridine).[93]

8.9   ORIGIN OF LIVING RADICAL POLYMERIZATION

Table 8.2 illustrates development of fundamental concepts in organic radical processes, some concepts in living polymerization and advances in radical polymerizations, all of which have contributed to development of controlled/"living" radical polymerization (LRP). Without them, the present understanding and control of radical reactions would not be possible.

Radical addition reactions have for a long time been considered to be very difficult to control because of unavoidable termination reactions. The first successful addition of halogenated compounds to alkenes via radical intermediates under photochemical conditions [atom transfer radical addition (ATRA)] was provided by Kharash.[94] This atom transfer radical addition process was subsequently converted to a much more efficient metal-catalyzed reaction by Minisci,[95] Vofsi,[64] and others during the 1960s. At approximately the same time, various nitroxides were prepared as stable radicals but without any application to organic synthesis at that time.[96] Other types of mediators for organic reactions were also developed.[70,97]

These reactions found many synthetic applications and were summarized by Bellus in 1985.[98] It was not mechanistically clear how these reactions occurred because chemoselectivities were unusually high for free-radical reactions until the unexpected chemoselectivities were ingeniously explained by Fischer,[65] who introduced the concept of the persistent radical effect. Numerous systems based on atom transfer reactions were used for structure–reactivity comparisons[99] and for refined organic/bioorganic synthesis,[68,100] including development of many organometallic systems.[101] Atom transfer radical reactions gained increasing importance in organic

TABLE 8.2   Evolution of Controlled/"Living" Radical Polymerization

Organic Synthesis	Living Polymerization	Radical Polymerization
1940s	1950s	$\leqslant$ 1960s
Kharash: first ATRA (*h*ν)	Szwarc: living anionic, block copolymers	Bamford: inhibition/ retardation
1960s		Starks: telomerization
Minisci, Vofsi: CuX/RX/olefin	1970s	Borsig, Braun: Ar_2CH, AR_3C
Rosantsev, Volodarski: nitroxides	Penczek, Matyjaszewski: $A^{\bullet} \Leftrightarrow D$ in CROP	
Kochi: free radicals & transition metals	1980s	1970s
	Kennedy: inifers, "living" carbocationic	Kabanov: complexes with H_3PO_4
1980s	Higashimura, Sawamoto,	Farina: inclusion complexes
Fischer: persistent radical effect	Sigwalt, Matyjaszewski:	Mikulasova: emulsion
Curran, Giese, Newcomb: RI, RSnH, RSeAr	"living" carbocationic	Otsu: heterogeneous systems
Barton: thiohydroxyamate	DuPont, Müller, Quirk: GTP	Minoura: Cr(II) acetate/MMA
Kochi, Halpern, Giese, Wayland: organometallics	Grubbs, Schrock, Novak: Living ROMP & OM	
1990s	1990s	1980s
Various groups: various Mt in ATRA; stereocontrol; detailed kinetic picture	Stadler, Roovers, Quirk, Faust, Hadjichristidis: ABC, control of topologies	Otsu: iniferters, first LRP
	Matyjaszewski, Müller: ranking living systems, exchange reactions	Rizzardo et al.: TEMPO, addition–fragmentation

synthesis because of their high chemo-, regio-, and stereoselectivities and tolerance to many useful functional groups.[69,102] There are continuing attempts to improve stereocontrol in the radical addition reactions that may lead to some tacticity control in RP and LRP.[103] More detailed kinetic and mechanistic studies are needed to further optimize radical addition reactions. Future progress in this area requires developments of more efficient catalysts, which could increase the rates and selectivities of the addition, elimination and rearrangement reactions.

The concept of living polymerization as a chain growth process without chain breaking reactions was developed by Szwarc.[2] Living anionic polymerization of nonpolar monomers was the first technique used to synthesize macromolecules with controlled topologies, with predetermined molecular weight and nearly Poisson distribution of MW, and preparation of novel block copolymers with very high efficiency.[2] This system was based on entirely ionic species, although differences in reactivities of ion pairs and free ions were very significant. The first system in which both dormant and active species were clearly spectroscopically observed and kinetics and thermodynamics of exchange reactions determined was the cationic ring-opening polymerization of tetrahydrofuran.[104] The concept of equilibria

between dormant and active species that arose from this work has subsequently been successfully used in carbocationic polymerization,[4] although initially pseudocationic mechanisms,[105] invisible propagating species,[106] and stretched covalent bonds[28] were postulated. Nearly simultaneously, group transfer polymerization[27] and other approaches based on exchange between active and dormant chains were used in anionic polymerization. A similar level of control was extended to coordination polymerization.

It was realized at that time that most of these new systems were much less controlled than the original living anionic polymerization and that chain breaking reactions did occur. While it was possible to prepare well-defined polymers with $M_n = 10,000$, it was impossible to make polymers with $M_n = 100,000$ for many of these systems. It was considered useful to rank such "living" systems and to provide precise kinetic data on transfer and termination coefficients, which would define limits for control of molecular weights under particular conditions.[107] In some systems the polydispersities decreased with conversion, in contrast to general expectations from contribution of chain breaking reactions. The main reason for decreasing polydispersities was the slow exchange between species of various reactivities.[8] Kinetic treatment of such systems was very useful for improved design of controlled/"living" radical polymerization systems.[9]

The current focus of most living polymerizations is on controlling various aspects of macromolecular engineering, including polymer topologies, compositions, and functionalities in order to prepare nanophase-separated materials. Concurrently deeper understanding of the mechanism and quantification of side reactions is needed to optimize conditions and identify and expand limits of control.

Although radical polymerization has been known for a very long time, it was always difficult to control because of unavoidable termination reactions between growing radicals. It was possible to control either rates, or molecular weights, or end groups, but never all three parameters simultaneously. For example, several retarders or inhibitors were used to moderate polymerization rates; some of them, such as nitroxides and cupric halides, are now used as components of LRP systems.[108,109] Molecular weights were controlled by transfer agents; some of them are now used in LRP systems. End-functionalities were controlled by using either functional initiators, or functional transfer agents, leading to telechelic polymers.[110] Special initiating systems, which resemble ATRP components, were developed on the basis of organometallic compounds employing redox systems.[108]

However, at that time, it was impossible to prepare polymers with low polydispersities, observe a linear increase of molecular weight with conversion, and convert the initiators to growing chains quantitatively. Efficiency of initiation was always very low, and some apparent "livingness" could be attributed to dead-end systems rather than to LRP. Thus, radical polymerization has been always very far from a true living system, although some papers referred to LRP.

A more detailed and systematic discussion of controlled radical reactions will be covered in the next section. Here, only a development of some early concepts listed in Table 8.2 will be described. The first evidence for controlling radical polymerization was reported by Borsig, who used linear and cyclic tetraarylethane derivatives

to initiate polymerization of MMA and styrene. He observed a steady increase of molecular weights with conversion and also the first formation of block copolymers.[75,111] Since Borsig did not use the term *living radical polymerization*, these papers are seldom cited as part of LRP. This system was later extensively studied by Braun.[76] However, initiation efficiencies were low, polydispersities were relatively high (if measured), and molecular weight did not evolve linearly with conversion. A possible reason for these deviations from living characteristics was a slow, but continuous, initiation by the bulky organic radicals. In some cases these systems could resemble dead-end systems, in which new chains were not generated and transfer did not take place. The ideas of Borsig were later further refined via iniferter systems and nitroxides, which do not initiate polymerization themselves and reversibly reactivate the growing chains.

Another approach was taken by Kabanov.[112] The photopolymerization of MMA in the presence of phosphoric acid continued after switching off the light in a livinglike manner, with the molecular weights increasing with conversion. Complexation of the growing radicals by protonic or Lewis acid reduced radical termination due to steric and electrostatic repulsion. This approach has not been studied since that time, although it may be one of the most promising ways to reduce the rate of bimolecular termination. Another method to reduce the termination rate was to conduct the polymerization in inclusion complexes of perhydrotriphenylene.[113]

There were several approaches to LRP in emulsion polymerization. They employed the concept of intermittent irradiation and compartmentalization to reduce termination rate.[114] Initial attempts were not successful,[115] but further experiments proved that livinglike systems can be obtained in emulsion polymerization, although molecular weights were extremely high.[116] A similar situation occurred when acrylamides were polymerized in benzene and the resulting heterogeneity of the reaction provided long-lived radicals.[117] The concepts of heterogeneous reactions and compartmentalization have been extended to modern LRP in miniemulsion systems.[62]

Approximately at the same time, Minoura reported that MMA polymerization initiated by BPO in the presence of chromium(II) acetate resulted in a monotonous increase of molecular weight with conversion.[118] He also claimed the preparation of block copolymers. These phenomena, which are typical for LRP, were assigned to propagation via radicals coordinated to chromium that could not terminate. Later, this system was critically evaluated by Banderman,[119] who demonstrated that the system conformed to conventional RP. The apparent control was assigned to a combination of the dead-end and gel effects. Indeed, efficiency of initiation was very low, often below 10%. The reversible formation of organometallic species was later successfully applied to LRP of acrylates by Wayland.[35]

In 1982 Otsu, for the first time, provided a model for *living* radical polymerization to describe MMA polymerization in the presence of phenylazotriphenylmethane and benzyl dithiocarbamate.[120] By analogy with the inifers used in carbocationic systems,[121] he proposed that dithiocarbamates act as iniferters, namely, agents that *ini*tiate, trans*fer*, and *ter*minate.[122] The model that Otsu proposed is very similar to modern LRP. It consists of a reversible formation of radicals from dormant species and free-radical propagation. He did not take into account radical termination

because the concept of persistent radical effect had not yet been developed. However, the systems that Otsu studied, specifically, MMA polymerization initiated by phenylazotriphenylmethane or benzyl dithiocarbamates, were not efficient and as in the previously discussed systems, polydispersities were always high, molecular weights did not evolve linearly with conversion, and initiation efficiency was low. These systems, in comparison with currently used LRPs, has several drawbacks:

- The counter-radicals $^\bullet$S—C(S)—NR$_2$, were not really persistent radicals and were slowly initiating new chains. Otsu recognized that dithiuram had itself been used as an initiator. The same situation occurs with trityl radicals, which can slowly initiate MMA polymerization; the rate constant of initiation of MMA at 80°C is $k = 0.0011\,\mathrm{M^{-1}\,s^{-1}}$.[123]

- Benzyl dithiocarbamate was often used as initiator for MMA polymerization. According to the current state of art of LRP, benzyl derivatives are inefficient initiators for MMA.

- Degradative transfer occurred in some systems,[124] and degenerative transfer was slow, as later confirmed by RAFT methodology.[125]

- Activation required irradiation by UV light, thermal activation was relatively inefficient.

- Decomposition of dithiocarbamates radicals led to undesired irreversible termination reactions.[126]

Despite all these deficiencies, iniferters allowed synthesis of some block copolymers, although contaminated by the corresponding homopolymers. Currently used RAFT[39,125] or MADIX[127] reagents very closely resemble iniferters. However, as they are all degenerative transfer systems, they require continuous supply of radicals. Perhaps irradiation with light in Otsu's original system also helped generate more radicals. On the other hand, the slow concurrent initiation with trityl and dithiocarbamate radicals could reduce the PRE and accelerate polymerization. Unfortunately, Otsu did not extend his investigation to the polymerization of vinyl acetate and other monomers that are more suitable for dithiocarbamates iniferters than styrene and methacrylates.

A new system for controlling radical polymerizations based on nitroxides as stable radicals appeared in the patent literature in 1985.[31] The work of Rizzardo and Solomon was not sufficiently recognized at that time. Rizzardo and Moad have subsequently proposed another approach to LRP based on addition–fragmentation chemistry,[23] which can be considered as a special case of degenerative transfer. In these systems a detailed understanding of LRP was reached and the importance of termination recognized and simulated using supercomputers.[128] It was not until 1993 when Georges published his first paper on controlling the bulk radical polymerization of styrene in the presence of TEMPO, that an interest in living radical polymerization was revitalized.[71] This marked the dawn of modern LRP, which is currently best represented by stable free-radical polymerization (SFRP), with

NMP as the best example; transition-metal-catalyzed ATRP; and various degenerative transfer processes, with RAFT as the most efficient transfer system.

8.10   EXAMPLES OF CURRENT LRP

This section is focused on the historical developments of major concepts in modern LRP systems. In addition to the development of particular chemistry and structure of polymerization mediating systems, the concept of PRE was indispensable for the understanding how LRP systems work.[129]

8.10.1   Stable Free-Radical Polymerization and Nitroxides

The modern LRP era started with Georges SFRP of bulk styrene at 120–130°C, initiated by BPO in the presence of 1.3 equiv of TEMPO.[71] Good control was observed for moderate molecular weights $M_n < 10^5$ for styrene and styrene copolymers. However, it was difficult to homopolymerize other monomers. The initiation systems were expanded to other radical sources such as AIBN[85] and a pure thermal styrene polymerization.[92] Significant progress was achieved using pure alkoxyamines as initiators, which eliminated the need for adjustment of molar ratio of nitroxide and initiator.[86] This approach also enabled use of di- and multifunctional initiators and construction of novel polymer architectures.[130]

Detailed kinetic studies explained the mechanistic features of NMP, correlated them with PRE, defined the dynamics of exchange, and allowed acceleration or the rate of polymerization by scavenging access of nitroxides.[59,131]

There were several attempts to expand range of monomers by using nitroxides other than TEMPO, among them 5-member[41], nitronyl nitroxides[132] and TEMPO phosphonate derivatives,[85] but success was accomplished only when nitroxides with a H atom on α-C atom were introduced.[72,133] Such nitroxides were previously considered unstable and inappropriate for LRP. However, the combination of unique steric effects and their very slow decomposition, provided ideal conditions for fast and controlled polymerization of monomers other than styrene. Additional tuning of equilibrium constants, dynamics of exchange, and stability is possible by employing various substituents that may hydrogen bond and provide other electronic effects.[134]

Simultaneously, polymerization using other stable radicals were developed, including triazolinyl radicals,[73] verdazyl,[84] borate,[135] and organometallic species such as $Co^{(II)}$ porphyrines.[35] They were successful for the polymerization of several monomers but are not as universal as nitroxides.

Current research in SFRP and NMP is focused on development of new mediating stable radicals, expanding the range of monomers, defining reaction conditions, and macromolecular engineering.

8.10.2   Atom Transfer Radical Polymerization

SFRP and NMP systems require one mediating group per polymer chain. Thus, a catalytic process with a small amount of mediating species is especially attractive

for low-molar-mass polymers, which carry a high proportion of the end-groups. In 1995 two promising systems for controlling radical polymerizations were reported. They were based on catalytic systems used by organic chemists for ATRA and therefore were termed *atom transfer radical polymerization* (ATRP). One of these systems was based on the $RuCl_2/(PPh_3)_3$ catalyst, which was used for polymerization of MMA initiated by CCl_4.[32] This catalyst system appeared to be inactive alone and required activation by aluminum alkoxides. Another system was based on a CuX/bpy catalyst, which had also been successfully used in many ATRA reactions.[33] The Cu-based ATRP system was successful for styrene, methacrylates, acrylates, acrylonitrile, and other monomers and for copolymerization.[40,136]

The effect of varying the structures of all ATRP components has been examined. Various alkyl halides and pseudohalides[137] as well as sulfonyl halides[138] have been used as initiators. This includes many multifunctional initiators as well as macroinitiators.[139] The latter give access to hybrid systems by combining ATRP with initiators attached to natural products, inorganic surfaces, and many polymers prepared by nonradical processes.

Both metal and ligands were varied to develop new catalytic systems. Cu and Ru were expanded to other middle- and late-transition metals such as Ni, Fe, Pd, Rh, Re, and Mo.[140] In Cu-based systems, the introduction of long alkyl group to the initially employed bpy ligands considerably improved homogeneity of the systems, enhanced control, and provided polymers with polydispersities below $M_w/M_n <$ 1.05.[87,141] Later, pyridineimines[46] and various linear,[142] cyclic, and branched[143] polydentate amines, imines, pyridines, and other compounds[143,144] were used. The Ru-based system relies mostly on phosphines, but various aromatic ligands have also been used successfully.[145] Removal and recycling of the catalyst remains an important issue, especially for commercialization of ATRP.[146]

Polymerizations have been carried out in the presence of various additives to enhance control and rates of the reactions. In addition to bulk and solution systems, heterogeneous polymerization in emulsion, miniemulsion, and suspension has also been successful.

The current research in ATRP encompasses comprehensive structure–reactivity correlation for all components of the polymerization process, and structure–property correlation for materials prepared by ATRP encompassing controlled and systematically varied composition, topology, and functionality.

8.10.3   Processes Based on Degenerative Transfer

SFRP and ATRP rely on the persistent radical effect and on exchange reactions that can be considered as reversible termination (deactivation). The equilibrium constants are very small ($K \sim 10^{-10}$) and provide only a minute amount (ppm) of growing free radicals. Another approach employs a reversible transfer process in which the free radicals exchange degeneratively with the dormant species (i.e., $K = 1$).

The first system conforming to this methodology described in patent literature, employed alkyl iodides in the polymerization of fluorinated monomers.[147] Later

the degenerative transfer with alkyl iodides in the presence of AIBN or BPO was used for styrene, acrylates and vinyl chloride polymerization and allowed synthesis of block copolymers.[38,148] The polymers, however, had relatively high polydispersities $M_w/M_n \sim 1.3$, due to relatively slow exchange.[149]

Meanwhile, addition–fragmentation chemistry had been successfully employed for end functionalization by Rizzardo.[150] A degenerative system was used in polymerization of methacrylates with methacryloyl-terminated macromonomers.[23] The latter were readily accessible by catalytic chain transfer with Co complexes (CCT).[151] However, the exchange reactions were relatively slow, and high polydispersities were obtained in bulk systems. Nevertheless, slow monomer feeding improved control.

A significant advance in the field was reported when dithioesters and xanthates were applied as transfer agents (RAFT and MADIX).[39,127] The addition rate constants to $S=C(Z)-SR$ were significantly higher than propagation rate constants. The appropriate choice of substituents Z and R allowed fast fragmentation and efficient initiation. At present, RAFT can be applied to a larger range of monomers than SFRP and ATRP.

The current research directions in RAFT and other degenerative transfer processes are focused on better correlation of the structure of RAFT reagents with their reactivities to enable easier cross-propagation between various blocks, reduction of retardation in the synthesis of low-molar-mass polymers, and preparation of novel materials.

8.10.4 Comparison of NMP, ATRP, and RAFT

At present, the three most effective methods of controlling radical polymerization, all with future commercial promise include NMP (currently the most efficient of the SFRP systems), ATRP, and RAFT (the most efficient degenerative transfer process). Each of these methods has advantages as well as limitations. The advantages and limitations of each method can be illustrated by comparing four typical features. They include the range of polymerizable monomers, typical reaction conditions (temperature, time, sensitivity to impurities, etc.), the nature of transferable end groups and atoms, and various additives such as catalysts and accelerators. However, it should be remembered that the first commercialized LRP system employs a less efficient addition–fragmentation process. The plausible reason is the CCT process provides easy access to macromonomers and no byproducts. However, this process has limited ability to control many aspects of macromolecular engineering such as chain topology, composition, or preparation of hybrids.

The major aspects of the three currently most effective systems for LRP are compared in Table 8.3 and listed here. RAFT has the largest range of polymerizable monomers, although xanthates (MADIX) or dialkyldithiocarbamates should be used for vinyl acetate. RAFT reagents are not tolerant to primary amines. NMP cannot yet control polymerization of disubstituted alkenes such as methacrylates. ATRP is not yet applicable to vinyl acetate or other monomers producing nonstabilized radicals, and acid-containing monomers should be polymerized in their neutral form.

TABLE 8.3 Comparison of NMP, ATRP, and Degenerative Transfer Systems

Feature	Systems NMP	ATRP	Degenerative Transfer (RAFT)
Monomers	Styrenes with TEMPO Also acrylates and acrylamides using new nitroxides NO methacrylates	Nearly all monomers with activated double bonds NO vinyl acetate	Nearly all monomers
Conditions	Elevated T (>120°C for TEMPO) Waterborne systems OK Sensitive to oxygen	Large T range (−30–150°C) Waterborne systems OK Some tolerance to O_2 and inhibitor with Mt^0	Elevated temperatures for less reactive monomers Waterborne systems OK Sensitive to oxygen
End Groups/ Initiators	Alkoxyamines Thermally unstable Relatively expensive Requires radical chemistry for transformations May act as a stabilizer	Alkyl (pseudo)halides Thermally and photostable Inexpensive and available Either S_N, E, or radical chemistry for transformations Halogen exchange for enhanced cross-propagation	Dithioesters, iodides, and methacrylates Less thermally stable and less photo stable Relatively expensive Radical chemistry for transformations (S_N for RI) Color/odor
Additives	None NMP may be accelerated with acyl compounds	Transition metal catalyst Should be removed and recycled	Conventional radical initiator May decrease end functionality May produce too many new chains

Originally TEMPO required relatively elevated temperatures for styrene polymerization ($T > 120$°C). New nitroxides can be used at lower temperature, which enables extension of NMP to emulsions without pressurized equipment.[152] RAFT can be used at temperatures typical for any RP, although the usual temperature range is 60–110°C. ATRP is typically carried out at temperatures of 20–120°C, although there are several examples of subambient T reactions. All radical reactions are sensitive to oxygen. However, since oxygen is more rapidly scavenged by metals than by growing radicals, it is possible to carry out ATRP in the presence of Cu(0) or Fe(0), even with limited amounts of oxygen and inhibitor present in the system.[153]

Alkoxyamines are inherently thermally unstable, especially those based on new, more efficient nitroxides. They are relatively expensive, more expensive than halogens, for instance. The displacement of nitroxides requires a radical chemistry, which has limited scope. However, polymeric alkoxyamines may be used directly as polymeric stabilizers. Dithioesters are also more expensive than halogens and may give some color to lower molar mass polymers and odor if cleaved from the chain end. They can be removed from the chain end by amines or other radical chemistry.

Alkyl halides are least expensive and most abundant initiators for LRP and are often used as precursors to alkoxyamines and RAFT reagents. Halogens can be replaced by many other useful functionalities, not only via radical chemistry but also by electrophilic and nucleophilic substitution. In ATRP systems a halogen is reversibly transferred to transition metal, therefore it can be exchanged with other (pseudo)-halogens, controlling not only the structure but also the reactivity of the end groups. This enables the formation of block copolymers involving switching from acrylates to, for example, methacrylates not accessible by any other methods. NMP and ATRP can be initiated by conventional radical initiators (AIBN, BPO) in the presence of nitroxides or higher oxidation state metal halides (e.g., $CuBr_2/L$).

NMP may not require any additional additives, unless some rate acceleration is needed. On the other hand, both RAFT and ATRP rely on a radical source and a catalyst, respectively. The radical initiators in RAFT may produce too many new chains and may also decrease chain end functionality, if used in too large amounts. Catalysts in ATRP should be either removed or recycled. Perhaps, a very small amount of catalyst could be left in the final polymer, depending on the amount and also on the effect on polymer stability and mechanical properties. In principle, catalyst removal is easier than in coordination polymerization, because the catalyst is *not* bound to the chain end.

Thus, it is obvious that each system has its own advantages and its own limitations. ATRP may be best suited for low molar mass polymers with special functionalities and for preparation of some block copolymers that cannot be easily synthesized by other techniques. NMP may be best for systems that require the absolute absence of metals and other elements such as sulfur. RAFT may be most efficient system for high molecular weight polymers and less reactive monomers.

8.11 GENERAL FEATURES AND FUTURE PERSPECTIVE OF LRP

Radical polymerization has entered a renaissance stage. After reaching a certain degree of maturity in the 1960s, relatively slow progress was noted in this field since the early 1970s as major efforts were focused on cationic, anionic, ring opening, and α-olefin polymerizations, which enabled control of macromolecular structure and tacticity. However, more recent discoveries of many LRP systems have refocused the interest of many synthetic chemists on radical polymerization. Indeed, substantial progress has been achieved in the preparation of new, previously unattainable materials, in the mechanistic understanding of these reactions, in the quantitative measurements of the rate and equilibrium constants, and the concentrations of the species involved. It seems that a thorough understanding of the reactions involved in controlled radical polymerization, especially those carried out in the presence of organometallic derivatives, requires concerted efforts in various areas of chemistry, starting from theoretical/computational chemistry, kinetics, physical organic chemistry, and organic synthetic and organometallic/coordination chemistry. In addition, reliable kinetic measurements of conventional radical processes

in homogeneous and heterogeneous media are extremely important for the determination of rate and equilibrium constants of the controlled reactions. Direct observations of growing species and measurements of their concentrations are also very crucial.

It is expected that new systems will be developed; some may be transmitted from already successful or newly developed systems from organic/bioorganic synthesis. For example, ATRP has close connection to ATRA and MADIX, and RAFT has a clear foundation in xanthate chemistry efficiently used in organic synthesis, as elegantly summarized in a review entitled "Riding the tiger: Using degeneracy to tame wild radical processes."[70]

Four conditions must be fulfilled for the initiating/catalytic system to be used in controlled radical polymerization:

1. Chemoselectivity should be high. Initiating and catalytic systems should not be accompanied by side reactions such as β-H elimination or electron transfer (oxidation/reduction of radicals to carbocations or carbanions). Chemoselectivity of propagation should exceed 99.9%, meaning that propagation should occur 1000 times before a side reaction occurs. Thus, not all organic reactions can be transformed to polymer synthesis.
2. The proportion of growing radicals should be relatively low to suppress bimolecular termination. This depends on the targeted molecular weight and should be controlled by the corresponding equilibrium constant. Catalytic systems have an advantage because the position of equilibrium can be adjusted by using more or less activator or deactivator.
3. Exchange between active and dormant species must be fast to prepare polymers with low polydispersities. Higher concentrations of deactivator will accelerate deactivation and reduce polydispersities but will also slow down the polymerization. Exchange can be also accomplished by degenerative transfer, without affecting rates if fragmentation is fast.
4. Initiation should be fast and completed at low monomer conversion.

All LRP systems resemble conventional radical processes. They have chemoselectivities (reactivity ratios), regioselectivities (head-to-tail connectivity) and stereoselectivities (tacticities), and termination rate coefficients very similar to those of conventional systems. There is, however, one extremely important kinetic difference. The stationary concentration of radicals in RP is established by balancing rates of initiation and termination, whereas in NMP and ATRP the balance is established by equilibrating rates of activation and deactivation. This allows, for the first time, the rate of initiation to be similar to the rate of propagation and much higher than the rate of termination. This is the primary condition that enables simultaneous growth of all chains and macromolecular engineering. The second feature is the exchange between active and dormant species by reversible deactivation (termination) in NMP and ATRP and reversible (degenerative) transfer in RAFT. This second condition extends the time available for building up the polymer chains from a fraction of a

second to hours, facilitating many synthetic manipulations, such as sequential monomer addition and functionalization. These two conditions allow control of chain topologies, functionalities, and compositions in a way similar to living ionic polymerizations and heretofore unprecedented for RP systems.

It has to be recognized that the proportion of terminated chains and loss of functionalities increases with the chain length and concentration of growing radicals. Thus, growing long chains, especially using monomers that propagate relatively slowly, such as styrenes and methacrylates, require long reaction times during which radical termination may be suppressed but other chain breaking reactions may prevail. Therefore, LRP could be most efficiently applied to the synthesis of polymers with low and moderate molecular weights, unless propagation rate constants are very high (e.g., acrylates).

Although tremendous progress has been recently noticed in all LRP techniques, there are still many remaining challenges. They include expansion of the range of polymerizable monomers, optimization of the reaction conditions, further enhancement of polymerization control, retention of high degree of end functionality when polymerization rate (and concentration of radicals) increases, as well as other variations of chemo-, regio- and stereoselectivities in spite of propagation with radical active centers. It is possible that some inspiration from nature using template systems, selective complexation, confine space and microheterogeneity may allow further manipulation of LRPs and enhance the control, as reported for conventional RP systems.[154]

There are many interesting and unexplored structures to be prepared by LRP that these techniques should find commercial use and many new industrial applications in the very near future. It is possible to design novel surfactants, dispersants, lubricants, adhesives, gels, coatings, and many other materials that can be prepared only by controlled/living radical polymerization.

REFERENCES

1. a) G. Moad and D. H. Solomon, *The Chemistry of Free Radical Polymerization*, Oxford, Elsevier, 1995; b) K. Matyjaszewski and S. G. Gaynor, in *Applied Polymer Science*, C. D. Craver and C. E. Carraher, Jr., Pergamon Press, Oxford, 2000, p. 929.

2. M. Szwarc, *Carbanions, Living Polymers and Electron Transfer Processes*, Interscience: New York, 1968.

3. H. L. Hsieh and R. P. Quirk, *Anionic Polymerization, Principles and Practical Applications.* Marcel Dekker, New York, 1996.

4. K. Matyjaszewski, ed., *Cationic Polymerizations: Mechanisms, Synthesis and Applications.* Marcel Dekker: New York, 1996.

5. O. W. Webster, *Science* **251**, 887 (1991).

6. M. Szwarc, *Nature* **178**, 1168 (1956).

7. a) R. Quirk and B. Lee, *Polym. Int.* **27**, 359 (1992); b) K. Matyjaszewski, *J. Phys. Org. Chem.* **8**, 197 (1995).

8. K. Matyjaszewski and C.-H. Lin, *Makromol. Chem. Macromol. Symp.* **47**, 221 (1991).

9. G. Litvinienko and A. H. E. Müller, *Macromolecules* **30**, 1253 (1997).

10. K. Matyjaszewski and A. H. E. Müller, *Polym. Prepr.* (*Am. Chem. Soc., Div. Polym. Chem.*) **38**(1), 6 (1997).

11. K. Matyjaszewski, *J. Macromol. Sci., Pure Appl. Chem.* **A31**, 989 (1994).

12. K. Matyjaszewski and P. Sigwalt, *Polym. Int.* **35**, 1 (1994).

13. Special Issue, *J. Polym. Sci.; Part A: Polym. Chem.* **38**(10), 1705 (2000).

14. a) K. Matyjaszewski, ed., *Controlled Radical Polymerization*, Vol. 685, American Chemical Society, Washington, DC, 1998; b) K. Matyjaszewski, ed., *Controlled-Living Radical Polymerization: Progress in ATRP, NMP, and RAFT*, Vol. 768. American Chemical Society, Washington, DC, 2000.

15. a) H. J. Harwood, in *Encyclopedia of Polymer Science*, H Mark, ed., Wiley, New York, b) K. Matyjaszewski, *Curr. Opin. Solid State Mater. Sci.* **1**, 769 (1996); c) D. Colombani, *Progr. Polym. Sci.* **22**, 1649 (1997); d) T. Otsu and A. Matsumoto, *Adv. Polym. Sci.* **136**, 75 (1998); e) G. V. Korolev and A. P. Marchenko, *Russ. Chem. Rev.* **69**, 409 (2000).

16. a) M. Sawamoto and M. Kamigaito, *Trends Polym. Sci.* **4**(11), 371 (1996); b) M. Sawamoto and M. Kamigaito, *Chemtech* **29**, 30 (1999); c) M. Sawamoto and M. Kamigaito, in *Synthesis of Polymers*, D Schlueter, ed., VCH, Weinheim, 1999; d) K. Matyjaszewski, *ACS Symp. Ser.* **685**, 258 (1998); e) T. E. Patten and K. Matyjaszewski, *Acc. Chem. Res.* **32**, 895 (1999); f) K Matyjaszewski, J. Xia, *Chem. Rev.* **101**, 2921 (2001).

17. K. Matyjaszewski, *Chem. Eur. J.* **5**, 3095 (1999).

18. a) M. K. Georges, R. P. N. Veregin, P. M. Kazmaier, and G. K. Hamer, *Trends Polym. Sci.* **2**, 66 (1994); b) C. Hawker, *Trends Polym. Sci.* **4**, 183 (1996).

19. a) T. E. Patten and K. Matyjaszewski, *Adv. Mater.* **10**, 901 (1998); b) E. E. Malmstroem and C. J. Hawker, *Macromol. Chem. Phys.* **199**, 923 (1998).

20. K. Matyjaszewski, *Macromol. Symp.* **174**, 51 (2001).

21. K. Matyjaszewski, *ACS Symp. Ser.* **768**, 2 (2000).

22. T. Fukuda and A. Goto, *Macromol. Rapid Commun.* **18**, 683 (1997).

23. C. L. Moad, G. Moad, E. Rizzardo, and S. H. Tang, *Macromolecules* **29**, 7717 (1996).

24. L. Gold, *J. Chem. Phys.* **28**, 91 (1958).

25. a) C. Walling, *Free Radicals in Solution*, New York, Wiley, 1957; b) C. H. Bamford, W. G. Barb, A. D. Jenkins, and P. F. Onyon, *The Kinetics of Vinyl Polymerization by Radical Mechanisms*, Academic Press, New York, 1958; c) H. S. Bagdasarian, *Theory of Radical Polymerization*, Izd. Akademii Nauk, Moscow, 1959.

26. K. Matyjaszewski, P. Kubisa, and S. Penczek, *J. Polym. Sci., Polym. Chem. Ed.* **12**, 1333 (1974).

27. O. W. Webster, W. R. Hertler, D. Y. Sogah, W. B. Farnham, and T. V. RajanBabu, *J. Am. Chem. Soc.* **105**, 5706 (1983).

28. J. P. Kennedy and B. Ivan, *Designed Polymers by Carbocationic Macromolecular Engineering. Theory and Practice*, Hanser, Munich, 1992.

29. a) T. Higashimura, M. Miyamoto, and M. Sawamoto, *Macromolecules* **18**, 611 (1985); b) M. Sawamoto, S. Aoshima, and T. Higashimura, *Makromol. Chem., Macromol. Symp.* **13/14**, 513 (1988).

30. P. Desbois, M. Fontanille, A. Defieux, V. Werzelhan, S. Latsch, and C. Schade, *Macromol. Chem. Phys.* **200**, 621 (1999).

31. D. H. Solomon, E. Rizzardo, and P. Cacioli, U.S. Patent 4,581,429 (1986).

32. M. Kato, M. Kamigaito, M. Sawamoto, and T. Higashimura, *Macromolecules* **28**, 1721 (1995).

33. J. S. Wang and K. Matyjaszewski, *J. Am. Chem. Soc.* **117**, 5614 (1995).

34. T. Otsu, *J. Polym. Sci.; Part A: Polym. Chem.* **38**, 2121 (2000).

35. B. B. Wayland, G. Poszmik, S. L. Mukerjee, and M. Fryd, *J. Am. Chem. Soc.* **116**, 7943 (1994).

36. H. J. Harwood et al., *Macromol. Symp.* **111**, 25 (1996).

37. D. Mardare and K. Matyjaszewski, *Macromolecules* **27**, 645 (1994).

38. a) K. Matyjaszewski, S. G. Gaynor, and J.-S. Wang, *Macromolecules* **28**, 2093 (1995); b) P. I. Bak, G. P. Bidinger, R. J. Cozens, P. R. Klich, L. A. Mayer, U.S. Patent 5,455,319 (1995).

39. J. Chiefari, Y. K. Chong, F. Ercole, J. Krstina, J. Jeffery, T. P. T. Le, R. T. A. Mayadunne, G. F. Meijs, C. L. Moad, G. Moad, E. Rizzardo, S. H. Thang, *Macromolecules* **31**, 5559 (1998).

40. J.-S. Wang and K. Matyjaszewski, *Macromolecules* **28**, 7901 (1995).

41. R. D. Puts and D. Y. Sogah, *Macromolecules* **29**, 3323 (1996).

42. D. M. Haddleton, D. J. Duncalf, D. Kukulj, A. M. Heming, A. J. Shooter, and A. J. Clark, *J. Mater. Chem.* **8**, 1525 (1998).

43. K. Matyjaszewski, M. J. Ziegler, S. V. Arehart, D. Greszta, and T. Pakula, *J. Phys. Org. Chem.* 775 (2000).

44. a) S. G. Roos, A. H. E. Mueller, and K. Matyjaszewski, *Macromolecules* **32**, 8331 (1999); b) H. Shinoda, P. J. Miller, and K. Matyjaszewski, *Macromolecules* (in press).

45. J. P. A. Heuts, R. Mallesch, and T. P. Davis, *Macromol. Chem. Phys.* **200**, 1380 (1999).

46. D. M. Haddleton, A. J. Clark, M. C. Crossman, D. J. Duncalf, S. Heming, S. R. Morsley, C. Waterson, and A. J. Shooter, *Chem. Commun.* 1173 (1997).

47. S. G. Roos and A. H. E. Muller, *Macromol. Rapid Commun.* **21**, 864 (2000).

48. C. Burguiere, M.-A. Dourges, B. Charleux, and J.-P. Vairon, *Macromolecules* **32**, 3883 (1999).

49. M. Bednarek, T. Biedron, and P. Kubisa, *Macromol. Rapid Commun.* **20**, 59 (1999).

50. P. A. G. M. Scheren, G. T. Russell, D. F. Sangster, R. G. Gilbert, and A. L. German, *Macromolecules* **28**, 3637 (1995).

51. D. A. Shipp and K. Matyjaszewski, *Macromolecules* **32**, 2948 (1999).

52. K. Matyjaszewski, K. Davis, T. Patten, and M. Wei, *Tetrahedron* **53**, 15321 (1997).

53. I. Li, B. A. Howell, K. Matyjaszewski, T. Shigemoto, P. B. Smith, and D. B. Priddy, *Macromolecules* **28**, 6692 (1995).

54. a) M. D. Saban, M. K. Georges, R. P. N. Veregin, G. K. Hamer, and P. M. Kazmaier, *Macromolecules* **28**, 7032 (1995); b) K. Davis, H.-J. Paik, and K. Matyjaszewski, *Macromolecules* **32**, 1767 (1999); c) K. Matyjaszewski, *Macromol. Symp.* **152**, 29 (2000).

55. K. E. Russell and A. V. Tobolsky, *J. Am. Chem. Soc.* **75**, 5052 (1953).

56. A. W. Hui and A. E. Hamielec, *J. Appl. Polym. Sci.* **16**, 749 (1972).

57. a) F. R. Mayo, *J. Am. Chem. Soc.* **75**, 6133 (1953); b) Y. K. Chong, E. Rizzardo, and D. H. Solomon, *J. Am. Chem. Soc.* **105**, 7761 (1983).

58. O. F. Olaj, H. F. Kauffmann, and J. W. Breitenbach, *Makromol. Chem.* **177**, 3065 (1976).

59. D. Greszta and K. Matyjaszewski, *J. Polym. Sci.; Part A: Polym. Chem.* **35**, 1857 (1997).

60. A. Goto and T. Fukuda, *Macromolecules* **30**, 4272 (1997).

61. A. E. Acar, M. B. Yagci, and L. J. Mathias, *Macromolecules* **33**, 7700 (2000).

62. B. Charleux, *Macromolecules* **33**, 5358 (2000).

63. J. Qiu, T. Pintauer, S. G. Gaynor, K. Matyjaszewski, B. Charleux, and J.-P. Vairon, *Macromolecules* **33**, 7310 (2000).

64. M. Asscher and D. Vofsi, *J. Chem. Soc.* 3921 (1963).

65. a) H. Fischer, *J. Am. Chem. Soc.* **108**, 3925 (1986); b) A. Studer, *Chem. Eur. J.* **7**, 1159 (2001).

66. H. Fischer, *J. Polym. Sci.; Part A: Polym. Chem.* **37**, 1885 (1999).

67. D. A. Shipp and K. Matyjaszewski, *Macromolecules* **33**, 1553 (2000).

68. D. P. Curran, in *Comprehensive Organic Synthesis*, ed. B. M. Trost and I. Fleming, eds., Pergamon Press, New York, 1992.

69. J. Iqbal, B. Bhatia, and N. K. Nayyar, *Chem. Rev.* **94**, 519 (1994).

70. B. Quiclet-Sire and S. Z. Zard, *Pure & Appl. Chem.* **69**, 645 (1997).

71. M. K. Georges, R. P. N. Veregin, P. M. Kazmaier, and G. K. Hamer, *Macromolecules* **26**, 2987 (1993).

72. a) D. Benoit, V. Chaplinski, R. Braslau, C. J. Hawker, *J. Am. Chem. Soc.* **121**, 3904 (1999); b) D. Benoit, S. Grimaldi, S. Robin, J.-P. Finet, P. Tordo, and Y. Gnaou, *J. Am. Chem. Soc.* **122**, 5929 (2000).

73. M. Steenbock, M. Klapper, K. Muellen, C. Bauer, and M. Hubrich, *Macromolecules* **31**, 5223 (1998).

74. T. C. Chung, H. L. Lu, and W. Janvikul, *J. Am. Chem. Soc.* **118**, 705 (1996).

75. E. Borsig, M. Lazar, M. Capla, and S. Florian, *Angew. Makromol. Chem.* **9**, 89 (1969).

76. D. Braun, *Macromol. Symp.* **111**, 63 (1996).

77. H. J. Harwood, L. D. Arvanitopoulos, and M. P. Greuel, *Polym. Prepr.* (*Am. Chem. Soc., Div. Polym. Chem.*) **35**(2), 549 (1994).

78. D. Greszta, D. Mardare, and K. Matyjaszewski, *Polym. Prepr.* (*Am. Chem. Soc., Div. Polym. Chem.*) **35**(1), 466 (1994).

79. M. Steenbock, M. Klapper, K. Muellen, N. Pinhal, and M. Hubrich, *Acta Polym.* **47**, 276 (1996).

80. J. H. Espenson, *Acc. Chem. Res.* **25**, 222 (1992).

81. C. Granel, R. Jerome, P. Teyssie, C. B. Jasieczek, A. J. Shooter, D. M. Haddleton, J. J. Hastings, D. Gigmes, S. Grimaldi, P. Tordo, D. Greszta, K. Matyjaszewski, *Macromolecules* **31**, 7133 (1998).

82. K. Takagi, A. Soyano, T. S. Kwon, H. Kunisada, and Y. Yuki, *Polym. Bull.* **43**(2–3), 143 (1999).

83. M. Destarac, J. Alric, and B. Boutevin, *Macromol. Rapid Commun.* **21**, 1337 (2000).

84. B. Yamada, Y. Nobukane, and Y. Miura, *Polym. Bull.* **41**(5), 539 (1998).

85. K. Matyjaszewski, S. Gaynor, D. Greszta, D. Mardare, and T. Shigemoto, *J. Phys. Org. Chem.* **8**, 306 (1995).

86. C. J. Hawker, *J. Am. Chem. Soc.* **116**, 11185 (1994).

87. K. Matyjaszewski, S. M. Jo, H.-J. Paik, and S. G. Gaynor, *Macromolecules* **30**, 6398 (1997).

88. K. Matyjaszewski, D. A. Shipp, J.-L. Wang, T. Grimaud, and T. E. Patten, *Macromolecules* **31**, 6836 (1998).

89. G. Moad, J. Chiefari, Y. K. Chong, J. Krstina, R. T. A. Mayadunne, A. Postma, E. Rizzardo, and S. H. Thang, *Polym. Int.* **49**, 993 (2000).

90. K. Matyjaszewski, J.-L. Wang, T. Grimaud, and D. A. Shipp, *Macromolecules* **31**, 1527 (1998).

91. V. Percec, B. Barboiu, and H.-J. Kim, *J. Am. Chem. Soc.* **120**, 305 (1998).

92. D. Mardare and K. Matyjaszewski, *Polym. Prepr.* (*Am. Chem. Soc., Div. Polym. Chem.*) **35**(1), 778 (1994).

93. a) J. S. Wang and K. Matyjaszewski, *Macromolecules* **28**, 7572 (1995); b) J. Xia and K. Matyjaszewski, *Macromolecules* **30**, 7692 (1997).

94. M. S. Kharasch and E. V. Jensen, *Science* **102**, 128 (1945).

95. F. Minisci, *Acc. Chem. Res.* **8**, 165 (1975).

96. a) A. K. Hoffman, W. G. Hodgson, and W. H. Jura, *J. Am. Chem. Soc.* **83**, 4675 (1961); b) E. G. Rosantsev and V. D. Sholle, *Synthesis* 190 (1971).

97. D. H. R. Barton and G. Kretzschmar, *Tetrahedron Lett.* **24**, 5889 (1983).

98. D. Bellus, *Pure Appl. Chem.* **57**, 1827 (1985).

99. B. Giese, *Angew. Chem., Int. Ed. Engl.* **22**, 753 (1983).

100. D. P. Curran, *ACS Symp. Ser.* **685**, 62 (1998).

101. a) J. Halpern, F. T. T. Ng, and G. L. Rempel, *J. Am. Chem. Soc.* **101**, 7124 (1979); b) J. K. Kochi, *Organometallic Mechanisms and Catalysis*, Academic Press, New York, 1978.

102. D. P. Curran, *Synthesis* 489 (1988).

103. D. P. Curran, N. A. Porter, and B. Giese, *Sereochemistry of Radical Reactions*. VCH, Weinheim, 1996.

104. S. Penczek and K. Matyjaszewski, *J. Polym. Sci., Polym. Symp.* **56**, 255 (1976).

105. A. Gandini and P. H. Plesch, *J. Chem. Soc.* 4826 (1965).

106. M. Sawamoto and T. Higashimura, *Macromolecules* **11**, 501 (1978).

107. K. Matyjaszewski, *Macromolecules* **26**, 1787 (1993).

108. C. H. Bamford, in *Comprehensive Polymer Science*, G. Allen, S. L. Aggarwal, and S. Russo, eds., Pergamon, Oxford, 1989, p. 123.

109. W. I. Bengough and W. H. Fairservice, *Trans. Faraday Soc.* **67**, 414 (1971).

110. a) E. J. Goethals, *Telechelic Polymers: Synthesis and Applications*, CRC Press, Boca Raton, FL, 1989; b) M. Mishra, *Macromolecular Design: Concept and Practice*, Polymer Frontiers International, Inc., c) Hopewell, VA, 1994; B. Boutevin, *J. Polym. Sci.; Part A: Polym. Chem.* **38**, 3235 (2000).

111. a) E. Borsig, M. Lazar, and M. Capla, *Makromol. Chem.* **105**, 212 (1967); b) E. Borsig, M. Lazar, and M. Capla, *Collect. Czech. Chem. Commun.* **33**, 4264 (1968).

112. a) E. E. Garina, E. G. Lagutkina, V. P. Zubov, and V. A. Kabanov, *Vysokomol. Soedin., Ser. B* **14**, 563 (1972); b) V. A. Kabanov, *J. Polym. Sci., Polym. Symp.* **50**, 71 (1975).

113. M. Farina and G. Di Silvestro, *J. Chem. Soc., Chem. Commun.* 842 (1976).

114. J. P. Bianchi, F. P. Price, and B. H. Zimm, *J. Polym. Sci.; Part A: Polym. Chem.* **25**, 27 (1957).

115. G. V. Schulz and J. Romatowski, *Makromol. Chem.* **85**, 195 (1965).

116. a) V. I. Lukhovitskii, V. V. Polikarpov, A. M. Lebedeva, R. M. Lagucheva, and V. L. Karpov, *Vysokomol. Soedin., Ser. A* **10**, 835 (1968); b) D. Mikulasova, V. Chrastova, and P. Citovicky, *Eur. Polym. J.* **10**, 551 (1974).

117. H. Tanaka, T. Sato, and T. Otsu, *Makromol. Chem.* **180**, 267 (1979).

118. M. Lee and Y. Minoura, *J. Chem. Soc. Faraday Trans. 1* **74**, 1726 (1978).

119. K.-D. Hungenberg and F. Bandermann, *Makromol. Chem.* **184**, 1423 (1983).

120. T. Otsu, M. Yoshida, and T. Tazaki, *Makromol. Chem., Rapid Commun.* **3**, 133 (1982).

121. J. P. Kennedy and R. A. Smith, *J. Polym. Sci., Polym. Chem. Ed.* **18**, 1539 (1980).

122. T. Otsu and M. Yoshida, *Makromol. Chem. Rapid Commun.* **3**, 127 (1982).

123. E. V. Chernikova, Z. A. Pokataeva, E. S. Garina, M. B. Lachinov, and V. B. Golubev, *Vysokomol. Soedin., Ser. A, Ser. B* **40**, 221 (1998).

124. P. Lambrinos, M. Tardi, A. Polton, and P. Sigwalt, *Eur. Polym. J.* **26**, 1125 (1990).

125. R. T. A. Mayadunne, E. Rizzardo, J. Chiefari, Y. K. Chong, G. Moad, and S. H. Thang, *Macromolecules* **32**, 6977 (1999).

126. R. S. Turner and R. W. Blevins, *Macromolecules* **23**, 1856 (1990).

127. M. Destarac, D. Charmot, X. Franck, and S. Z. Zard, *Macromol. Rapid Comm.* **21**, 1035 (2000).

128. C. H. J. Johnson, G. Moad, D. H. Solomon, T. H. Spurling, and D. J. Vearing, *Aust. J. Chem.* **43**, 1215 (1990).

129. H. Fischer, *Macromolecules* **30**, 5666 (1997).

130. C. J. Hawker, *Angew. Chem., Int. Ed. Engl.* **34**, 1456 (1995).

131. a) J. M. Catala, F. Bubel, and S. O. Hammouch, *Macromolecules* **28**, 8441 (1995); b) T. Fukuda, T. Terauchi, A. Goto, K. Ohno, Y. Tsujii, T. Miyamoto, S. Kobatake, and B. Yamada, *Macromolecules* **29**, 6393 (1996); c) D. Greszta and K. Matyjaszewski, *Macromolecules* **29**, 7661 (1996).

132. T. Shigemoto and K. Matyjaszewski, *Macromol. Rapid Commun.* **17**, 347 (1996).

133. D. Benoit, S. Grimaldi, J. P. Finet, P. Tordo, M. Fontanille, and Y. Gnanou, *Polym. Prepr.* (*Am. Chem. Soc., Div. Polym. Chem.*) **38**(1), 729 (1997).

134. S. Marque, H. Fischer, E. Baier, and A. Studer, *J. Org. Chem.* **66**, 1146 (2001).

135. T. C. Chung, W. Janvikul, and H. L. Lu, *J. Am. Chem. Soc.* **118**, 705 (1996).

136. K. Matyjaszewski and J. S. Wang, WO 9630421; U.S. Patent 5,763,548 (1998).

137. a) J.-L. Wang, T. Grimaud, and K. Matyjaszewski, *Macromolecules* **30**, 6507 (1997); b) T. Ando, M. Kamigaito, and M. Sawamoto, *Tetrahedron* **53**, 15445 (1997).

138. V. Percec and B. Barboiu, *Macromolecules* **28**, 7970 (1995).

139. K. Matyjaszewski, S. G. Gaynor, and S. Coca, WO 9840415; U.S. Patent 5,945,491 (????).

140. a) C. Granel, P. Dubois, R. Jérôme, and P. Teyssié, *Macromolecules* **29**, 8576 (1996);
     b) K. Matyjaszewski, M. Wei, J. Xia, and N. E. McDermott, *Macromolecules* **30**, 8161 (1997);
     c) T. Ando, M. Kamigaito, and M. Sawamoto, *Macromolecules* **30**, 4507 (1997); d) Y. Kotani,
     M. Kamigaito, and M. Sawamoto, *Macromolecules* **32**, 2420 (1999); e) P. Lecomte, I. Drapier,
     P. Dubois, P. Teyssié, and R. Jérôme, *Macromolecules* **30**, 7631 (1997); f) E. Le Grognec, J. Claverie,
     R. Poli, *J. Am. Chem. Soc.* **123**, 9513 (2001).

141. a) T. E. Patten, J. Xia, T. Abernathy, and K. Matyjaszewski, *Science* **272**, 866 (1996); b) T. Grimaud
     and K. Matyjaszewski, *Macromolecules* **30**, 2216 (1997).

142. J. Xia and K. Matyjaszewski, *Macromolecules* **30**, 7697 (1997).

143. J. Xia, S. G. Gaynor, and K. Matyjaszewski, *Macromolecules* **31**, 5958 (1998).

144. B. Gobelt and K. Matyjaszewski, *Macromol. Chem. Phys.* **201**, 1619 (2000).

145. a) H. Takahashi, T. Ando, M. Kamigaito, and M. Sawamoto, *Macromolecules* **32**, 3820 (1999);
     b) F. Simal, A. Demonceau, and A. F. Noels, *Angew. Chem., Int. Ed. Engl.* **38**, 538 (1999); c) C. W.
     Bielawski, J. Louie, and R. H. Grubbs, *J. Am. Chem. Soc.* **122**, 12872 (2000).

146. a) D. M. Haddleton, D. Kukulj, and A. P. Radigue, *Chem. Commun.* 99 (1999); b) G. Kickelbick,
     H. -J. Paik, and K. Matyjaszewski, *Macromolecules* **32**, 2941 (1999).

147. Y. Yutani and M. Tatemoto, Patent EP 489370 A1 (1991).

148. S. Gaynor, J. S. Wang, and K. Matyjaszewski, *Macromolecules* **28**, 8051 (1995).

149. A. Goto, K. Ohno, and T. Fukuda, *Macromolecules* **31**, 2809 (1998).

150. E. Rizzardo, G. F. Mejis, and S. Thang, Patents WO 884304 (1988).

151. T. P. Davis, D. Kukulj, D. M. Haddleton, and D. R. Maloney, *Trends Polym. Sci*. **3**(11), 365 (1995).

152. C. Burguiere, S. Pascual, B. Coutin, A. Polton, M. Tardi, and B. Charleux, K. Matyjaszewski,
     J.-P. Vairon, *Macromol. Symp.* **150**, 39 (2000).

153. a) K. Matyjaszewski, S. Coca, S. G. Gaynor, M. Wei, and B. E. Woodworth, *Macromolecules* **30**,
     7348 (1997); b) K. Matyjaszewski, S. Coca, S. G. Gaynor, M. Wei, and B. E. Woodworth,
     Macromolecules **31**, 5967 (1998).

154. a) B. Kirci, J. Lutz, K. Matyjaszewski, *Macromolecules*, **35**, 2448 (2002); b) H. Hirai, *J. Polym. Sci.,
     Macromol. Rev.* **1976**, *11*, 47; c) T. Nakano, Y. Okamoto, *Chem. Rev.* **101**, 4013 (2001).

9 Kinetics of Living Radical Polymerization

TAKESHI FUKUDA, ATSUSHI GOTO, and YOSHINOBU TSUJII

Kyoto University, Uji, Kyoto, Japan

CONTENTS

9.1 INTRODUCTION

9.1.1 What to Study

Living radical polymerization (LRP) includes a group of radical polymerization techniques that currently attract much attention for providing simple and versatile routes to the synthesis of well-defined, low-polydispersity polymers and copolymers
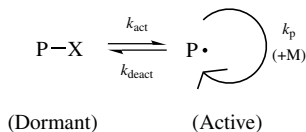
Scheme 9.1   Reversible activation (general scheme).

of simple and sophisticated structures.[1–7] As described in Chapter 8, all the members of LRP are distinguished from conventional free-radical polymerization (RP) by commonly involving a reversible activation (or deactivation) process in some form or another: in Scheme 9.1, the end-capped polymer P–X, termed a "dormant chain," is supposed to be activated (decapped) to polymer radical P• by thermal, photochemical, and/or chemical stimuli. In the presence of monomer M, P• will undergo propagation until it is deactivated back to the dormant chain P–X. Although it is not explicitly indicated in Scheme 9.1, the chain length of P–X generally becomes larger after an activation-deactivation cycle. If the reversible activation occurs frequently enough over a period of polymerization time, every dormant chain will have a nearly equal chance to grow, thus yielding a low-polydispersity polymer. Some of the main problems to be addressed in LRP kinetics are, therefore, associated with the mechanism and frequency of the reversible activation process. How is this frequency correlated with the chain length and chain length distribution of the product polymer? How is it possible to experimentally determine this frequency accurately? And how does this frequency depend on the chemical structure of the dormant chain and the thermal, photochemical, and/or chemical stimuli applied to the system? Answers to these questions are clearly important to systematically understand and evaluate the performance of individual LRP systems and design new systems of higher performance.

LRP is distinguished also from termination-free polymerizations like anionic living polymerization (in its ideal form) by the existence of bimolecular termination, chain transfer, and all other elementary reactions involved in conventional RP. While it clearly limits the degree of structural control attainable, this feature of LRP provides a variety of unique polymerization systems that are particularly interesting from the viewpoint of polymerization kinetics. Given the rate constants of all the elementary reactions, including those of the activation and deactivation reactions, and details of experimental conditions such as the concentrations of reactants and temperature, one will be able to simulate the whole process of a LRP run and predict the characteristics of the product polymer, quite accurately in principle. This, in turn, indicates the feasibility of optimizating experimental conditions for optional performance. The demerit of termination and other "side reactions" would thus be minimized in a well-designed LRP run.

With the mentioned practically important outputs in mind, in this chapter, we discuss fundamental features of the kinetics of LRP. Like all other kinetic studies, LRP kinetics primarily aims at describing the concentrations of reactants, above all those of monomer and polymeric species, as an explicit (or sometimes implicit) function

of time. Unlike in conventional RP, the products—the polymeric species in LRP—continually change their chain lengths and chain length distribution with time, so that main goals of LRP kinetics include understanding the chain length and chain length distribution as well as the monomer consumption rate (R_p) as a function of time.

This chapter is intended to be an updated and more comprehensive extension of our previous reviews on LRP kinetics.[8–10] However, general descriptions in this chapter unavoidably overlap in part with those in other chapters. The readers are referred to the relevant reviews and chapters and the references cited therein. Here we have limited citations to a necessary minimum to avoid heavy overlaps.

9.1.2 Mechanistic Classification of Reversible Activation Reactions

The rate constants of activation, k_{act}, and deactivation, k_{deact}, given in the general scheme (Scheme 9.1) are both defined as a pseudo-first-order constant, having the unit s^{-1} (reciprocal seconds). In these definitions, every dormant chain is activated once every k_{act}^{-1} s and deactivated back to the dormant state after a "transient lifetime" of k_{deact}^{-1} s, on average. Taking typical examples of successful LRP, $k_{act}^{-1} = 10$ to 10^3 s, and $k_{deact}^{-1} = 0.1$ to 10 ms. Since the steadiness of polymerization requires the following quasi-equilibrium to hold,

$$k_{act}[\text{P–X}] = k_{deact}[\text{P}^{\bullet}] \tag{9.1}$$

the equilibrium concentration of radical is, typically, around 10^{-5} times that of the dormant chain. Specifically, most potentially active chains, which we will call "living chains," are in the dormant state. In this regard, the number of living chains is practically identical to that of dormant chains.

The reversible activation reactions of the most successful LRPs currently known may be mechanistically classified into three types: which are (1) the dissociation–combination (DC), (2) the atom transfer (AT), and (3) the degenerative chain transfer (DT) mechanism (Scheme 9.2).

(a) $\text{P–X} \underset{k_c}{\overset{k_d}{\rightleftharpoons}} \text{P}\bullet \ + \ \text{X}\bullet$

(b) $\text{P–X} \ + \ \text{A} \underset{k_{da}}{\overset{k_a}{\rightleftharpoons}} \text{P}\bullet \ + \ \text{XA}\bullet$

(c) $\text{P–X} \ + \ \text{P}'\bullet \underset{k'_{ex}}{\overset{k_{ex}}{\rightleftharpoons}} \text{P}\bullet \ + \ \text{X–P}'$
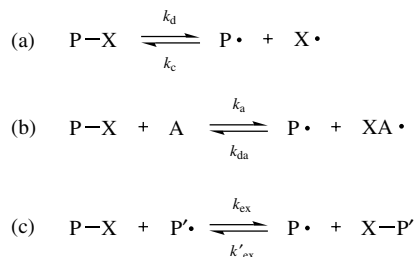
Scheme 9.2 Three main mechanisms (a, b, and c) of reversible activation: (a) dissociation–combination; (b) atom transfer; (c) degenerative chain transfer.
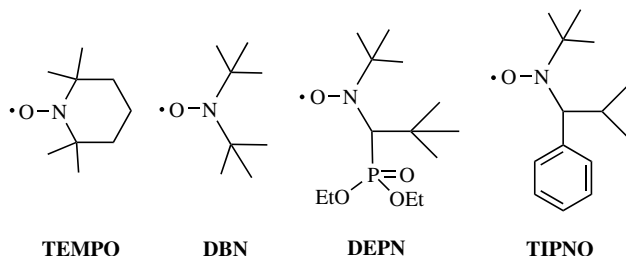
Figure 9.1   Examples of nitroxides.

9.1.2.1   *The Dissociation–Combination (DC) Mechanism*   In this mechanism, the dormant chain is dissociated by a thermal or photochemical stimulus into polymer radical P$^{\bullet}$ and capping radical X$^{\bullet}$, where X$^{\bullet}$ is assumed to be stable enough to undergo no reaction other than the combination with P$^{\bullet}$ (and other alkyl radicals, if any are present in the system). Specifically, an "ideal" stable free radical (SFR) should be the one that does not react with themselves, does not initiate polymerization, and does not undergo disproportionation with P$^{\bullet}$. The best known examples of SFR are nitroxides like TEMPO (2,2,6,6-tetramethylpiperidinyl-1-oxy) (Fig. 9.1), even though they are not perfectly ideal in the mentioned sense. The rate constants of dissociation, k_{d}, and combination, k_{c}, are related to k_{act} and k_{deact} by

$$k_{\mathrm{act}} = k_{\mathrm{d}} \qquad \text{(DC mechanism)} \qquad (9.2\mathrm{a})$$

$$k_{\mathrm{deact}} = k_{\mathrm{c}}[\mathrm{X}^{\bullet}] \qquad \text{(DC mechanism)} \qquad (9.2\mathrm{b})$$

In reference to Eq. (9.1), it is clear that the SFR concentration $[\mathrm{X}^{\bullet}]$ has to be in a suitable range dependent on k_{c} in order for k_{deact} to take suitable values.

9.1.2.2   *The Atom Transfer (AT) Mechanism*   In this mechanism, the dormant chain is activated by the catalytic action of activator A, and the capping agent is transferred to form a *stable* species AX$^{\bullet}$. All currently known successful LRPs in this category use a halogen such as Cl and Br as a capping agent and a halide complex of a transition metal like Cu and Ru as an activator A. These LRPs are often termed atom transfer radical polymerization (ATRP). The rate constants k_{a} and k_{da} defined in Scheme 9.2 are related to k_{act} and k_{deact} by

$$k_{\mathrm{act}} = k_{\mathrm{a}}[\mathrm{A}] \qquad \text{(AT mechanism)} \qquad (9.3\mathrm{a})$$

$$k_{\mathrm{deact}} = k_{\mathrm{da}}[\mathrm{AX}^{\bullet}] \qquad \text{(AT mechanism)} \qquad (9.3\mathrm{b})$$

In this mechanism, both activation and deactivation are secondary reactions depending on the concentrations of the activator A and the deactivator AX$^{\bullet}$, respectively. The relation between [A] and $[\mathrm{AX}^{\bullet}]$ is controlled, again, by Eq. (9.1).

9.1.2.3   The Degenerative Chain Transfer (DT) Mechanism   In this mechanism, the dormant chain is attacked by radical $P'^{\bullet}$ to form the active species $P^{\bullet}$ and the dormant species P'–X. This is an exchange reaction (hence the relevant rate constants in Scheme 9.2 are written k_{ex} and k'_{ex}). If the radicals P and P' are kinetically identical, then $k_{ex} = k'_{ex}$, and we can write

$$k_{act} = k_{ex}[P^{\bullet}] \qquad \text{(DT mechanism)} \qquad (9.4a)$$
$$k_{deact} = k_{ex}[P'\text{–X}] \qquad \text{(DT mechanism)} \qquad (9.4b)$$

Clearly, the equilibrium condition in Eq. (9.1) is always met in this mechanism of reversible activation.

Two types of LRPs belong to this category. One is the case in which the capping agent X is an atom or a simple group without, for instance, a double bond. In this case, X is simply transferred from radical to radical without forming any kinetically important intermediate. The so-called iodide-mediated polymerization, in which X is iodine, is a well-known example. The other is the case in which X is a group that allows addition of an alkyl radical. In this case, the exchange reaction occurs via addition of $P'^{\bullet}$ to P–X to form the intermediate radical P–$(X^{\bullet})$–P' followed by fragmentation of P–$(X^{\bullet})$–P' into $P^{\bullet}$ and P'–X. This process was named reversible addition–fragmentation chain transfer (RAFT). Hence RAFT-based polymerization has the additional prerequisites as a high-performance LRP that fragmentation should occur fast enough so that the concentration of the intermediate radical remains at a sufficiently low level, and that the intermediate radical should not effectively work as either an initiator or a radical trap.

9.1.3   Termination Reactions, Living Chains, and Dead Chains

As has been stressed, propagating radicals in LRP can be terminated by radical–radical or chain transfer reactions forming dead chains. There has been presented no plausible theoretical or experimental evidence showing that the propagation and/or termination reactions in LRP are somehow different from those in conventional RP. On the contrary, there is a body of experimental evidence indicating that the propagating radical in LRP is a "free" radical as in conventional RP, or in other words, propagation, deactivation, and termination reactions occur just competitively without giving any priority to a particular reaction. We will assume this here, or equivalently, assume that the rate constants of elementary reactions in LRP are the same as those in conventional RP, insofar as experimental conditions in the two systems are equivalent.

In conventional RP, the lifetime of the propagating radical is typically on the order of a second, in which initiation, propagation, and termination occur, giving a dead chain with a degree of polymerization (DP) of about 10^3 to 10^4. Such dead chains are produced at every instant and accumulated in the system throughout the course of polymerization that may last for hours in many cases. In LRP, polymerization is usually started with an initiating adduct P_0–X, which, in many cases, is a

low-mass homolog of the dormant polymer P–X, and is sometimes produced in situ at an early stage of polymerization.[11,12] Repeating an activation–deactivation cycle, every dormant chain grows in an intermittent fashion, or viewed in a long time scale, grows "slowly." The "transient lifetime," defined as the time segment between an activation and the subsequent deactivation event on the same chain, is typically in the range of 0.1–10 ms, as already noted. The sum of transient lifetimes of a living chain over the whole polymerization period is related to the degree of polymerization finally achieved, even though the relation is complicated by time- or conversion-dependent factors such as monomer and deactivator concentrations (see text below). For simplicity of discussion, let us assume that the monomer concentration and the activation and deactivation probabilities are independent of time, and consider the case in which the radical concentration and hence the R_p in a LRP system is the same as those in the corresponding conventional RP system. Then the chance of radical-radical termination is the same for the two systems. It follows that if the radical lifetime in the conventional system is 1 s, for example, the sum of transient lifetimes in the LRP system should be set to be sufficiently smaller than 1 s. Otherwise, an important portion of living chains will be dead at the end of the run. In other words, if the number average DP (DP_n) of the product from the conventional run is 10^4, for example, that from the LRP run should be sufficiently smaller than 10^4 in order for that polymer to have a high fraction of livingness. If, for example, the DP_n of the LRP product is 10^3, then we can expect that about 90% of the chains are living at the end of the run. If DP_n is 10^2, the fraction of dead chains would be only about 1%. A high fraction of livingness is an obvious requisite for preparing well-defined copolymers and polymers with sophisticated structures. Hence target polymers in LRP should be relatively low in DP_n, say, less than several hundreds in many cases, to yield a living-chain fraction larger than 90%, for example. Of course, such an estimate heavily depends on monomers and experimental conditions. For example, one can relax the limitation imposed on DP_n by carrying out experiments at an unusually low radical concentration, but of course, at the cost of a long polymerization time.

9.2   THEORY OF LRP KINETICS

9.2.1   Radical Concentrations and Rates of Polymerization

The existence of termination reactions gives the rate equation of LRP several unique features depending on activation–deactivation mechanisms and experimental conditions, which will be surveyed in this section from a theoretical point of view.

9.2.1.1   The Persistent Radical Effect (PRE)   Let us consider a LRP system of dissociation–combination (DC) type including only an initiating adduct P_0–X and monomer at $t = 0$. When a polymerization run is started by allowing P_0–X to dissociate, the same number of $P_0^\bullet$ and $X^\bullet$ will be produced in a unit time, and the concentrations $[P_0^\bullet]$ and $[X^\bullet]$ will linearly increase with time. The radical $P_0^\bullet$ may add to the monomer to give a polymer radical $P^\bullet$, but for a moment, $P_0^\bullet$ and $P^\bullet$ are

assumed to be kinetically identical and both of them will be written $P^\bullet$, unless otherwise noted. As $[P^\bullet]$ and $[X^\bullet]$ increase to a certain level, the reactions between $P^\bullet$ and $P^\bullet$ and those between $P^\bullet$ and $X^\bullet$ will become significant. Since the self-reaction of $P^\bullet$ results in a decrease of $[P^\bullet]$ relative to $[X^\bullet]$ or causes an accumulation of $X^\bullet$, $[X^\bullet]$ will steadily increase, and the reaction between $X^\bullet$ and $P^\bullet$ will become more and more important. For this reason, the rate of deactivation, $k_c[P^\bullet][X^\bullet]$, will eventually balance with the rate of activation $k_d[P–X]$. Namely, the quasiequilibrium in Eq. (9.1) will hold at every instance thereafter. On the other hand, in the time range where the quasiequilibrium holds, the $P^\bullet$ concentration must be a decreasing function of time, since the self-reaction of $P^\bullet$ continues to occur. This means that $[P^\bullet]$, which linearly increases with time at the onset of the reaction, will turn to a decreasing function, going through a maximum at a certain time. If the quasiequilibrium is reached fast enough, if the decreasing rate of $[P^\bullet]$ is small enough so that the main body of polymerization occurs in the time range of quasiequilibrium, and if the cumulative number of dead chains is sufficiently small compared to the number of dormant chains, or the equality $[P–X] = [P–X]_0 (= [P_0–X])$ approximately holds at all time, then the system will be an invaluable one of practical importance. In fact, a number of such systems have been found to date, and they form an important class of LRP examples.

The abovementioned work of SFR ($X^\bullet$) to adjust the radical concentrations so as to produce a high preference for cross-combinations was recognized from older times and termed the "persistent radical effect" (PRE) in the chemistry of low-mass compounds.[13–16] In the field of polymerization, such work of SFR was clearly recognized by Johnson et al.[17] in their simulation work, and subsequently by Fukuda et al.[18] and Greszta and Matyjaszewski,[19] and clear experimental evidence was presented for the inequality $[X^\bullet] \gg [P^\bullet]$ as well as the quasiequilibrium in Eq. (9.1) to hold for a nitroxide-mediated polymerization of styrene.[18] Subsequently, Fischer made a detailed theoretical analysis on the PRE in polymerization.[20–22]

9.2.1.2 *Rate Equations for SFR-Mediated Polymerization*

9.2.1.2.1 General Equations   Setting the preceding statements into equations, we have

$$\frac{d[X^\bullet]}{dt} = k_d[P–X] - k_c[P^\bullet][X^\bullet] \tag{9.5}$$

$$\frac{d[P^\bullet]}{dt} = k_d[P–X] - k_c[P^\bullet][X^\bullet] + R_i - k_t[P^\bullet]^2 \tag{9.6}$$

where R_i is the rate of *conventional* initiation (e.g., the one using a conventional radical initiator or a spontaneous initiation of monomer) and is assumed to be a constant. All other possible side reactions except those indicated in Eqs. (9.5) and (9.6) are neglected, and all the rate constants are assumed to be independent of chain length.

Equations (9.5) and (9.6) can be approximately solved analytically under the conditions already suggested. Specifically, the sum of the two equations gives

$$\frac{d[P^\bullet]}{dt} = \frac{d[X^\bullet]}{dt} + R_i - k_t[P^\bullet]^2 \tag{9.7}$$

The conditions of quasiequilibrium and of negligible fraction of dead chains allow us to write

$$[P^\bullet][X^\bullet] = K[P\text{–}X] = KI_0 \tag{9.8}$$

with

$$K = \frac{k_d}{k_c} \tag{9.9}$$

where $I_0 = [P\text{–}X]_0 = [P_0\text{–}X]$. Moreover, since it usually holds that $[P^\bullet] \ll [X^\bullet]$ for the reason mentioned above, we may neglect $d[P^\bullet]/dt$ as compared with $d[X^\bullet]/dt$ in Eq. (9.7), which, by use of Eq. (9.8), gives

$$\frac{d[X^\bullet]}{dt} = \frac{\{k_t(KI_0)^2 - R_i[X^\bullet]^2\}}{[X^\bullet]^2} \tag{9.10}$$

Equation (9.10) is easily solved to yield the analytic result

$$\ln\frac{(1+z)(1-z_0)}{(1-z)(1+z_0)} - 2(z - z_0) = bt \tag{9.11}$$

with

$$z = \left(\frac{R_i}{k_t K^2 I_0^2}\right)^{1/2}[X^\bullet] \tag{9.12}$$

$$b = \frac{2R_i^{3/2}}{(k_t K^2 I_0^2)^{1/2}} \tag{9.13}$$

where z_0 is the value of z at $t = 0$ ($[X^\bullet] = [X^\bullet]_0$ for $t = 0$).

The conditions for the existence of the quasiequilibrium were rigorously discussed.[20–22] The results show that quasiequilibrium exists in most practically interesting cases, and the time needed to reach the quasiequilibrium is much less than 1 s, typically, 1–100 ms in most cases. Equation (9.11) was first derived by us,[8] but some special cases had been treated elsewhere.

9.2.1.2.2   The Stationary-State Equation   One is the case in which $R_i > 0$, $[X^\bullet]_0 = 0$ and $bt \gg 1$. In this limit, Eq. (9.11) reduces to $z = 1$, which corresponds to the "stationary state"[18]

$$[X^\bullet] = (KI_0)\left(\frac{k_t}{R_i}\right)^{1/2} \qquad \text{(stationary state)} \qquad (9.14)$$

$$[P^\bullet] = \left(\frac{R_i}{k_t}\right)^{1/2} \qquad \text{(stationary state)} \qquad (9.15)$$

Thus, in this limit, $R_p (= k_p[P^\bullet][M])$ is independent of the reversible activation reaction, and identical with that for the conventional (SFR-free) system. The conversion index $\ln([M]_0/[M])$ follows from Eq. (9.15), and is first-order in t:

$$\ln\frac{[M]_0}{[M]} = k_p\left(\frac{R_i}{k_t}\right)^{1/2} t \qquad \text{(stationary state)} \qquad (9.16)$$

The stationary-state concentration of $X^\bullet$ depends on the reversible reaction as well as the initiation/termination parameters [Eq. (9.14)].

9.2.1.2.3   The Power-Law and Related Equations   Another special case is the one with no conventional initiation ($R_i = 0$ or $b = 0$). Expanding Eq. (9.11) around $z = z_0 = 0$, or more straightforwardly, directly solving Eq. (9.10) with $R_i = 0$, we have[9]

$$[X^\bullet]^3 - [X^\bullet]_0^3 = 3k_t K^2 I_0^2 t \qquad (R_i = 0) \qquad (9.17)$$

which, combined with Eq. (9.8), yields

$$[P^\bullet] = KI_0(3k_t K^2 I_0^2 t + [X^\bullet]_0^3)^{-1/3} \qquad (R_i = 0) \qquad (9.18)$$

Integration of the rate equation $-d[M]/dt = k_p[P^\bullet][M]$ with Eq. (6.18) gives

$$\ln\frac{[M]_0}{[M]} = \left(\frac{k_p}{2k_t KI_0}\right)\{(3k_t K^2 I_0^2 t + [X^\bullet]_0^3)^{2/3} - [X^\bullet]_0^2\} \qquad (R_i = 0) \qquad (9.19)$$

It is illuminating to consider two limiting cases with this equation. When $[X^\bullet]_0 = 0$, it gives the now-familiar power-law equation firstly derived by Fischer[20,21] from a different approach:

$$\ln\frac{[M]_0}{[M]} = \frac{3}{2}k_p\left(\frac{KI_0}{3k_t}\right)^{1/3} t^{2/3} \qquad (R_i = 0; [X^\bullet]_0 = 0) \qquad (9.20)$$

In the other limit of large $[X^\bullet]_0$ ($[X^\bullet]_0 \gg (3k_t K^2 I_0^2 t)^{1/3}$, Eq. (9.19) reduces to[9]

$$\ln \frac{[M]_0}{[M]} = \left(\frac{k_p K I_0}{[X^\bullet]_0}\right) t \qquad (R_i = 0; \text{ large } [X^\bullet]_0) \qquad (9.21)$$

In this limit, the conversion index is first-order in t as in the stationary-state system [Eq. (9.16)] or as in an ideal living polymerization system (without termination). Therefore, if the system has a finite concentration of stable radical at $t=0$, the conversion index can be linear in t to its any power between $\frac{2}{3}$ to 1, depending on $[X^\bullet]_0$ and t.

9.2.1.2.4 General Behavior and Crossover Between Power-Law and Stationary-State Kinetics

The crossover time t_{cross} between the power-law kinetics, Eq. (9.18) with $[X^\bullet]_0 = 0$, and the stationary-state kinetics, Eq. (9.15), may be estimated by equating the two relations:

$$t_{cross} = \left(\frac{K I_0}{3 k_t}\right)\left(\frac{R_i}{k_t}\right)^{-3/2} \qquad (9.22)$$

Comparison of Eqs. (9.13) and (9.22) shows that

$$t_{cross} = \frac{2}{3b} \qquad (9.23)$$

Thus, the condition for the stationary-state kinetics to hold may be restated as bt being sufficiently larger than $\frac{2}{3}$.

The solid curves in Fig. 9.2 show numerical values of $[P^\bullet]$ computed from Eq. (9.11) with $[P^\bullet] = K I_0/[X^\bullet]$ for several sets of parameter values. It may be understood that the behavior that one would experimentally observe depends basically on the magnitudes of b and z_0 or the relative magnitudes of R_i and $[X^\bullet]_0$.

The broken curves in Fig. 9.2 show the numerical solutions to Eqs. (9.5) and (9.6); hence they do not involve the assumptions used to derive Eq. (9.11). Comparison of the full and broken curves indicates that Eq. (9.11) generally gives very good approximations. In some cases, deviations from the numerical solutions are evident. This indicates the inadequacy of the assumptions on which Eq. (9.11) are based. In particular, the approximation of $[P-X] = I_0$ (constant) may be inadequate especially in a later stage of polymerization in a power-law-type system, where $[P-X]$ continuously decreases by termination. We may expect that the magnitude of errors introduced by this cause would be of the same order as that involved in the approximation of $[P-X]/I_0 = 1$. The almost exact agreement of the full and broken lines for small t (see, e.g., Fig. 9.2a) means that all the systems have reached the quasiequilibrium state before the time ranges relevant to the figures, say, < 1 min.

9.2.1.3 Rate Equations for ATRP

All the equations derived for SFR-mediated polymerization should basically be applicable to transition metal-mediated
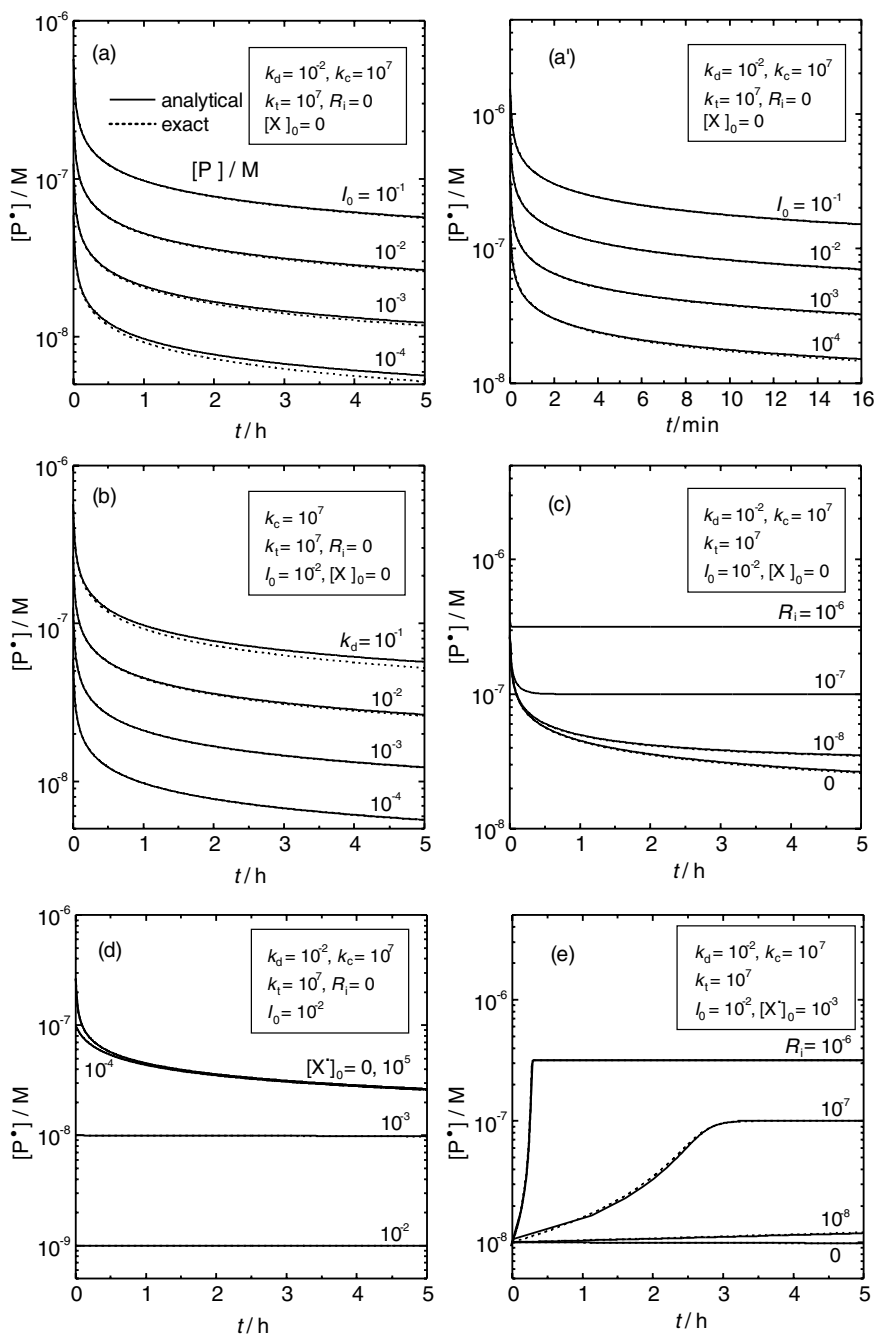
Figure 9.2 Comparison of the analytic [Eq. (9.11): full lines] and exact (broken lines) values of [P$^{\bullet}$] as a function of t; [X$^{\bullet}$] is obtained from [X$^{\bullet}$] $= KI_0/$[P$^{\bullet}$] with $K = k_d/k_c$. When only a full line is shown, it means complete overlap of full and broken lines.

polymerization (ATRP), by the reinterpretations of

$$X^\bullet = AX^\bullet, \qquad k_d = k_a[A], \qquad \text{and} \qquad k_c = k_{da} \qquad (9.24)$$

hence $K = k_a[A]/k_{da} = K_{AT}[A]$ with $K_{AT} = k_a/k_{da}$ (cf. Scheme 9.2).

9.2.1.4 Rate Equations for DT-Mediated Polymerization In this type of polymerization, radicals must be generated by a conventional initiation to start and maintain polymerization. As in conventional RP, the radical concentration would be basically unchanged by a chain transfer reaction unless it is a retarding or degrading one, or accompanies undesirable side reactions (see text below). For this reason, the stationary-state kinetics, Eq. (9.15), is expected to hold.

9.2.2 Polydispersities

9.2.2.1 Ideal LRP

9.2.2.1.1 Constant [M] To discuss the chain lengths and chain length distributions of LRP products, it will be informative to start with the "ideal" living radical polymerization in which reactions other than activation, deactivation, and propagation are absent, and the concentrations of propagating radical $P^\bullet$ and monomer M are constant. A propagating species experiences an activated and a deactivated (dormant) state alternately, and in the activated state, the chain can be added by a monomer unit with a probability p or deactivated with a probability $1-p$. Here p is related to the parameters of the reactions by

$$p = \frac{k_p[M]}{k_p[M] + k_{deact}} \qquad (9.25)$$

with k_{deact} defined as previously. The transition from the deactivated to activated state occurs with a probability density k_{act} (times per second), so that y_n given by

$$y_n = k_{act}t \qquad (9.26)$$

is the mean number of such transitions during polymerization time t. Here we have assumed that the total time during which the chain is in the activated state is much shorter than the polymerization time, $\tau y_n \ll t$, where τ is the transient lifetime. This is always met in actual LRP systems, in which the ratio $[P^\bullet]/[\text{dormant chains}]$ is on the order of 10^{-6} to 10^{-5}, typically.

The bivariable probability $N(x,y)$ that during time t, the chain experiences y activation–deactivation cycles *and* adds a total of x monomer units is given by[23]

$$N(x, y) = \frac{e^{-y_n}y_n^y}{y!}(1 - p)^y p^x \binom{x + y - 1}{x} \qquad (9.27)$$

($x, y = 0, 1, 2, \ldots$). Note that this equation is defined not only for positive integers of x and y but also for $x = y = 0$. In other words, Eq. (9.27) gives the chain length distribution of the hypothetical polymer grown from a *zero-mass* initiator. To obtain the actual distribution, the mass of the initiator should be properly added. We will come back to this point later (see Section 9.3.1.1.4). The number and weight average degrees of polymerization x_n and x_w may be calculated from Eq. (9.27) to yield

$$x_n = \frac{p y_n}{1 - p} \tag{9.28}$$

$$x_w = \frac{1 + p + p y_n}{1 - p} \tag{9.29}$$

The polydispersity index PDI $= x_w/x_n$ then reads[23]

$$\frac{x_w}{x_n} = 1 + \frac{2}{y_n} + \frac{1}{x_n} \qquad (y_n = k_{act} t) \tag{9.30}$$

Several features of this equation may be noteworthy. In the limit of $y_n \to \infty$, PDI approaches that of the Poisson distribution, i.e., PDI $= 1 + (1/x_n)$. When x_n is sufficiently large, PDI is determined only by y_n. There are comments in the literature suggesting that to achieve small values of PDI, the number of monomer units to be added per activation-deactivation cycle should be one or smaller. Those comments are misleading. What is essential in determining PDI is the number of cycles y_n, not the number of monomer units added per cycle, $k_p[M]\tau (= k_p[M]/k_{deact})$. Of course, for a fixed x_n, an increase in y_n means a decrease of the number of monomer units added per cycle, but such discussion does not quite hit the mark (see Section 9.2.2.2).

9.2.2.2.1 *Batch System*   In a batch polymerization, the monomer concentration decreases with time or conversion. Since the activation and deactivation reactions are time-independent in the system considered, the number of monomer units added per cycle decreases with conversion. This effect obviously makes PDI larger than expected by Eq. (9.30), modifying it to[8,10,24,25]

$$\frac{x_w}{x_n} = 1 + \frac{F(c)}{y_n} + \frac{1}{x_n} \qquad (y_n = k_{act} t) \tag{9.31}$$

$$F(c) = (1 - 2c^{-1})\ln(1 - c) \tag{9.32}$$

where $c = ([M]_0 - [M])/[M]_0$ is the fractional conversion. For $c \to 0$, $F(c)$ tends to 2, the value for the constant-[M] system.

Equation (9.31) with Eq. (9.32) can be expressed in two different forms: for a DT-mediated polymerization, the use of Eqs. (9.4a), (9.26), (9.31), and (9.32) along with the relation $\ln([M]_0/[M]) = -\ln(1 - c)$ with

$$\ln\frac{[M]_0}{[M]} = k_p[P^\bullet]t \tag{9.33}$$

gives

$$\frac{x_w}{x_n} = 1 + \frac{k_p}{k_{ex}}(2c^{-1} - 1) + \frac{1}{x_n} \tag{9.34}$$

Thus, in this type of polymerization, PDI is determined by the chain transfer constant $C_{ex} = k_{ex}/k_p$ and c. The theoretical minimum of PDI is $x_w/x_n = 1 + C_{ex}^{-1}$ for $c = 1$ and $x_n \to \infty$.

For ATRP, the use of Eqs. (9.1), (9.3), (9.26), and (9.33) to Eqs. (9.31) and (9.32) gives[26]

$$\frac{x_w}{x_n} = 1 + \frac{k_p}{k_{da}}\frac{I_0}{[AX^\bullet]}(2c^{-1} - 1) + \frac{1}{x_n} \tag{9.35}$$

(This equation is valid also for SFR-mediated systems by setting $k_{da}[AX^\bullet] = k_c[X^\bullet]$.) Equation (9.35) has been erroneously interpreted to be different from Eq. (9.31) (with $y_n = k_{act}t = k_a[A]t$ for ATRP),[26b] but they are equivalent, as shown above. PDIs are better discussed on the basis of Eq. (9.31) rather than Eq. (9.35), for the quantity $k_{da}[AX^\bullet]$ in Eq. (9.35) is physically less transparent, depending on many factors. On the other hand, the function $F(c)$ in Eq. (9.31) takes the values 2.00, 2.02, 2.08, and 2.41 of $c = 0$, 0.3, 0.5, and 0.8, respectively, meaning that $F(c)$ depends only weakly on c in a practically important range of c (see Fig. 9.10). Namely, excepting a region of extreme conversions, PDIs are determined predominantly by k_{act} times t. In this regard, k_{act}, or more precisely, k_d for SFR-mediated polymerization and k_a for ATRP are essential molecular or semimolecular parameters characterizing the performance of LRPs. On the contrary, the quantity $k_{da}[AX^\bullet]$ (or $k_c[X^\bullet]$) is self-adjusted by the system in many cases. The theoretical minimum of PDI is obtained from Eq. (9.35) with $c = 1$ and $x_n = \infty$: $(x_w/x_n)_{min} = 1 + (k_p/k_{da})(I_0/[AX^\bullet])$. In this limit, Eq. (9.35) works better than Eq. (9.31).

9.2.2.3 Systems Characterized by Time-Dependent Transient Lifetime (Power-Law Kinetics)

Here we still consider an idealized living radical polymerization in which termination exists, but the contribution of terminated (dead) chains to the chain length and chain length distribution of the product polymer is negligibly small: termination has an effect only on the time dependence of transient lifetime of the living chains in a quasiequilibrium system. This model, therefore, applies to those systems under PRE with no conventional initiation.

For simplicity, we consider a SFR-mediated polymerization. The concentration of stable radical, $[X^\bullet]$, increases with time because of termination, and the radical concentration $[P^\bullet]$ decreases with time, as already noted. Since the activation frequency is essentially time-independent, a decrease in $[P^\bullet]$ means a decrease in the transient lifetime. For this reason, the number of monomer units added per cycle decreases with time. This brings about an increase of PDI over the ideal values given by Eq. (9.30) (constant [M]) and Eq. (9.31) (batch). For a batch system with

$[X^\bullet]_0 = 0$, Fischer[21] has derived the following expression:

$$\frac{x_w}{x_n} = 1 + \frac{1}{x_n} + \frac{[M]_0^2}{x_n^2 I_0^2}\left(\frac{\pi k_p^3 I_0}{k_d k_c k_t}\right)^{1/2} \mathrm{erf}(u) \tag{9.36}$$

where

$$\mathrm{erf}(u) = 2(\pi)^{-1/2}\int_0^u \exp(-x^2)dx \tag{9.37}$$

$$u = (3k_p)^{1/2}(KI_0/3k_t)^{1/6}t^{1/3} \tag{9.38}$$

For $t \to \infty$, PDI approaches the limit

$$\frac{x_w}{x_n} = 1 + \frac{[M]_0}{I_0} + \left(\frac{\pi k_p^3\, I_0}{k_d k_c k_t}\right)^{1/2} \qquad (\mathrm{t} \to \infty) \tag{9.39}$$

On the other hand, for $t \to 0$, PDI approaches

$$\frac{x_w}{x_n} = 1 + \frac{1}{x_n} + \frac{8}{3}(k_d t)^{-1} \qquad (t \to 0) \tag{9.40}$$

Equation (9.40) differs from Eq. (9.30) with Eqs. (9.2a) and (9.26) in the numerical factor (2 vs. $\frac{8}{3}$). The larger factor $\frac{8}{3}$ in Eq. (9.40) arises from the $t^{-1/3}$-dependent $[P^\bullet]$ [Eq. (9.18) with $[X^\bullet]_0 = 0$], and in this regard, Eq. (9.18) suggests that the existence of the stable radical at $t = 0$ ($[X^\bullet]_0 \neq 0$) makes the time dependence of $[P^\bullet]$ less significant and hence lowers the PDI of the product. In the limit of large $[X^\bullet]_0$, $[P^\bullet]$ becomes time-independent, approaching the "ideal" limit expressed by Eq. (9.30). In fact, however, the addition of too much stable radical at $t = 0$ could make the polymerization rate impractically too small. Another important comment concerns the addition of a conventional initiator to maintain a constant radical concentration or a stationary state. Insofar as the number of the radicals originating from the initiator is in a limited range, the PDI of the product from a run with a conventional initiator can be smaller than that from a run without it. Needless to say, the above discussion is also valid for ATRP by the suitable reinterpretation of the parameters k_d and k_c.

9.2.2.4 Actual Systems

The PDIs of actual LRP products will show more or less deviations from the theoretical values for the above-described ideal systems for various reasons. First, the ideal systems consider only those chains that are living from the onset to the end of polymerization throughout. Contributions of terminated and, if necessary, initiated chains during the polymerization should be properly taken into account, when necessary. This should not be a very difficult problem to treat theoretically. Second, other side reactions, such as disproportionation between

SFR and alkyl radical and conventional chain transfer, should be taken into account, when necessary. Third, chain length dependence of the rate constants of elementary reactions can have a significant effect on PDIs as well as on rates of polymerization. Finally, the contribution from the preequilibrium or pre-stationary-state time range of polymerization was totally neglected in the discussion above, but it can be significant in some cases. A careful analysis is required in applying the theory for a quantitative discussion. At this moment, quantitative analyses may be best performed by computer simulations.[17,19,27–29]

9.3   KINETIC STUDIES ON INDIVIDUAL LRP SYSTEMS

9.3.1   Nitroxide-Mediated Polymerization (NMP)

A NMP run can be done in two ways. In one way, polymerization is initiated with a model alkoxyamine like S-TEMPO and BS-TEMPO in Fig. 9.3, which is prepared and purified independently. In the other way, the initiating alkoxyamine is prepared in situ.[11] Specifically, a conventional initiator such as benzoyl peroxide (BPO) is mixed with a nitroxyl like TEMPO in monomer in a suitable ratio, for instance, [TEMPO]/[BPO] = 1.2, and the mixture is heated at a high temperature so that all BPO molecules decompose in a short time to produce adducts of the type B-M_n-TEMPO, where B and M denote the BPO fragment and the monomer moiety with $n = 1$ or 2 in most cases, [the adduct B-TEMPO ($n = 0$) is unlikely to be formed]. These adducts will work as an initiating alkoxyamine. For kinetic studies, the use of a purified model alkoxyamine is obviously preferable to avoid unnecessary complexities.

9.3.1.1   TEMPO-Mediated Polymerization of Styrene   Since the 1993 work by Georges et al.,[11] this system has been most extensively studied of all NMP systems. The polymerization is usually carried out at a high temperature ($>120°C$) to yield a polymer with a DP_n in the order of 10^2 and DPI smaller than 1.2 or 1.1 after several hours of polymerization, in a typical case. Despite the considerable effort, the mechanism and kinetics of this system were not well understood at first, presumably because most kinetic studies were made with an initiating adduct in situ prepared in the polymerization run. In 1995, Catala et al.[30] reported the experimental data showing that R_p was independent of the concentration of the model alkoxyamine S-DBN used as an initiating adduct. Even though these authors erroneously interpreted their results, their work played an important role in shedding light into the problem. Styrene is known to undergo thermal (spontaneous) polymerization, especially at high temperatures. Combining this and Catala's observations led to the idea of stationary-state kinetics expressed by, for instance, Eq. (9.16).[18,31] In accord with that equation, the R_p values observed at different temperatures all agreed with those of thermal polymerization of styrene.[31] Qualitatively similar comments were made by Greszta and Matyjaszewski.[32] In what follows, we look into this system in more detail for its importance as a model system.
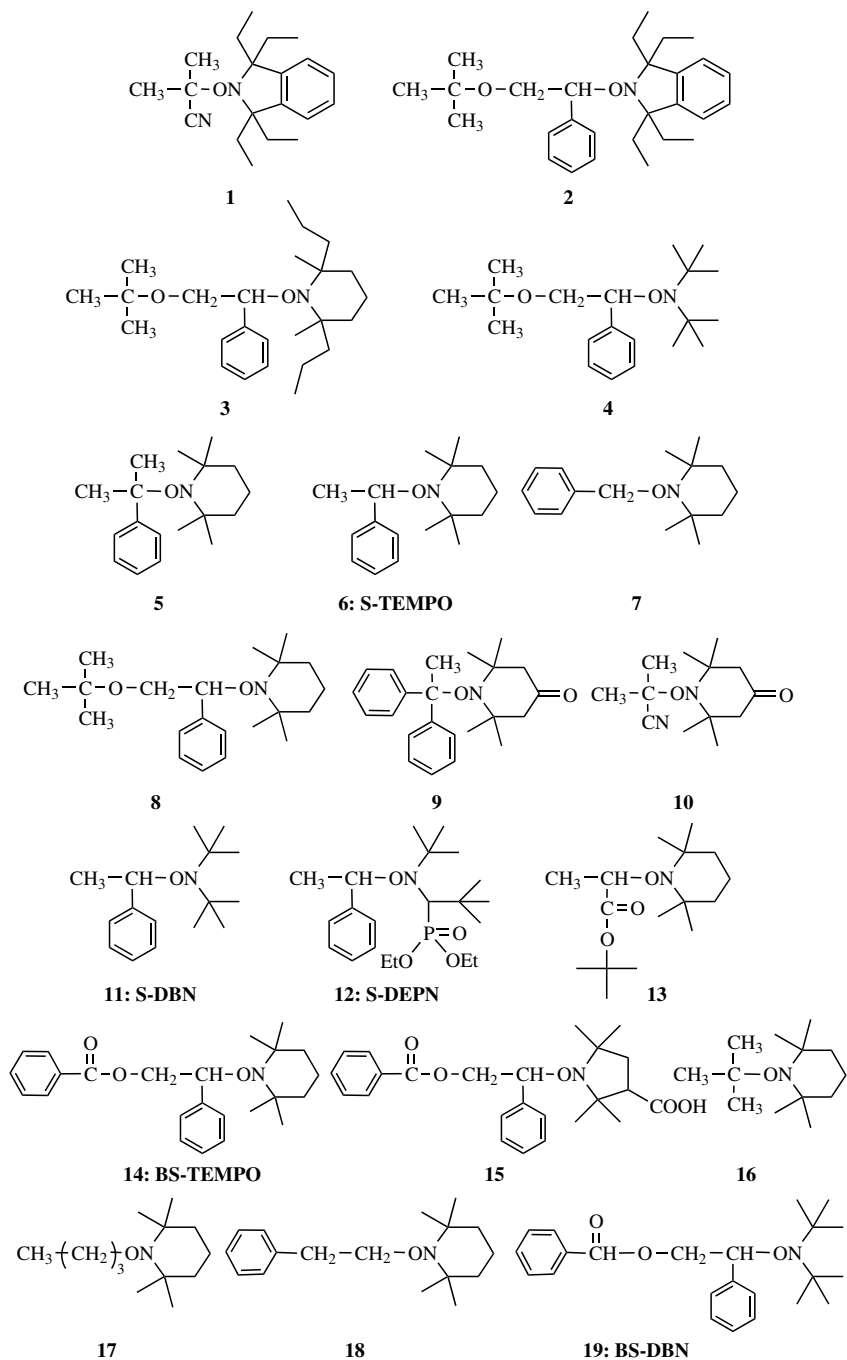
Figure 9.3 Examples of low-mass alkoxyamines, **1–19**, alkyl halides **20–24**, and alkyl dithioesters **25–31**, and model polymer adducts **32–46**.

20

21

22

23

24

25

26

27

28

29

30

31

32: PS-TEMPO

33: PS-DBN

34: PS-DEPN

35: PtBA-DBN

36: PBA-DEPN

37: PMA-Co/Porphyrin

38: PS-I

39: PS-SCSCH₃

40: PMMA-SCSCH₃

41: PS-SCSPh

42: PMMA-SCSPh

Figure 9.3 (*Continued*)

43: PS-co-PMMA-SCSPh

44: MMA-macromonomer   **45: PS-Br**   **46: PBA-Br**
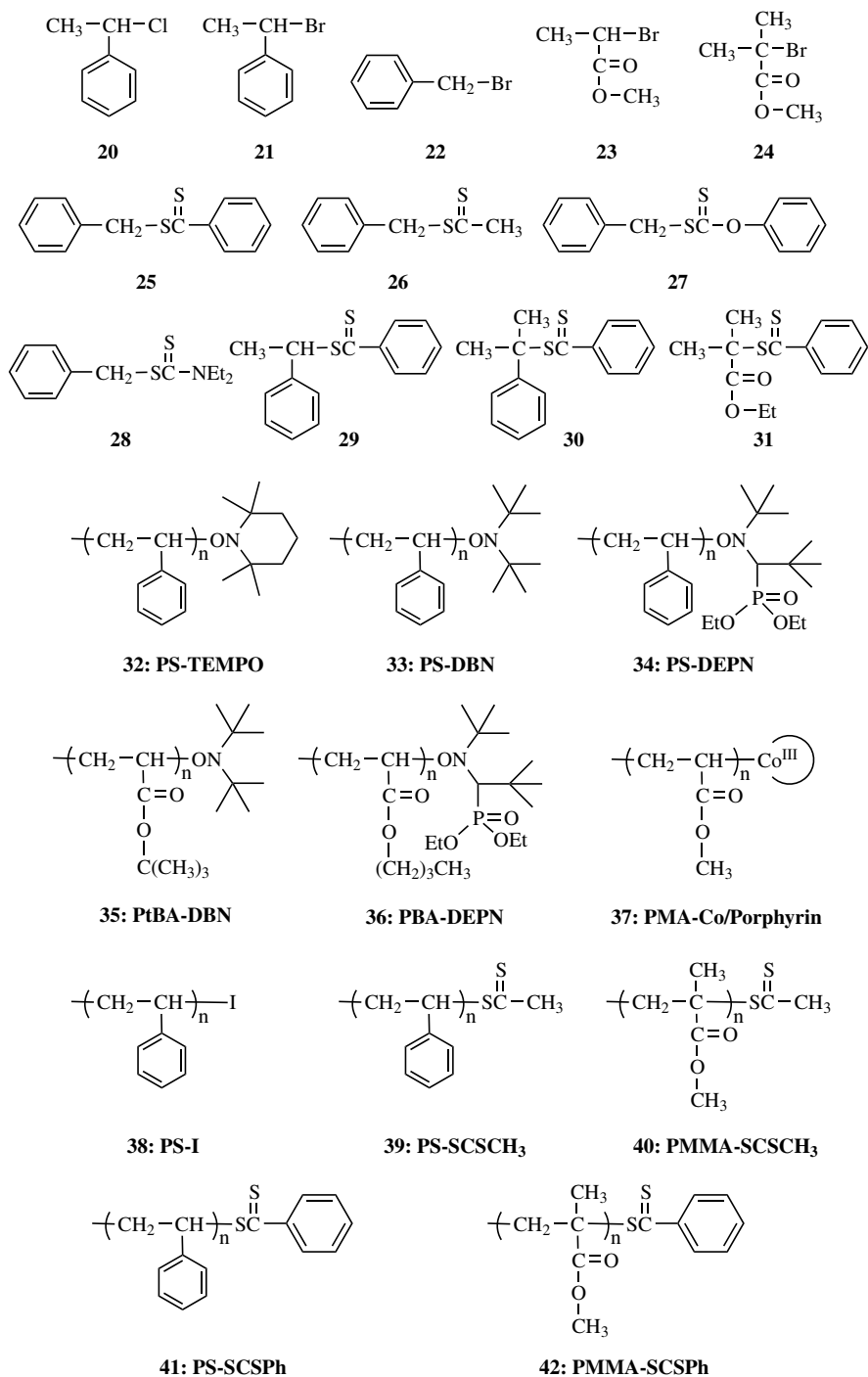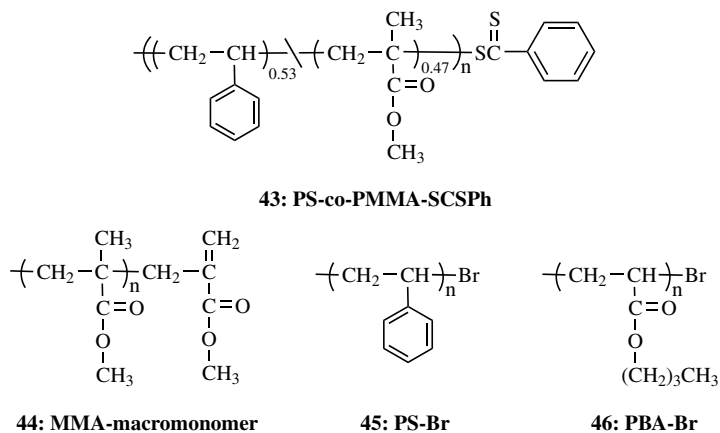
Figure 9.3   (*Continued*)

9.3.1.1.1   The Role of Conventional Initiation   Equation (9.16) was further tested in two ways. In one, the time–conversion relation was precisely followed by dilatometry.[18] Figure 9.4 compares the first-order plots for the styrene polymerizations with and without a PS-TEMPO or a BS-TEMPO adduct. Clearly, the R_p values of the nitroxide-containing systems are identical with each other, and when conversion is small ($c < 0.30$), they are equal to that of the thermal (nitroxide-free) system. Equation (9.16) was thus evidenced by this experiment. The deviations at higher c are due to changes in k_t arising from differences in chain length and viscosity. In fact, the dotted curve, which was calculated with a $[M]^3$-dependent initiation rate R_i (see below) and a constant k_t, gives the smallest R_p at large c. The marked nonlinearity of the first-order plots comes from the $[M]^3$-dependent R_i.

In the other method of testing Eq. (9.16), the conventional initiator *tert*-butyl hydroperoxide (BHP) was added to the PS-TEMPO/styrene/114°C system.[23] As in a nitroxide-free system, R_p increased with increasing [BHP]. For example, the addition of 4×10^{-3} M of BHP increased R_p by a factor ~3. Nevertheless, the chain length and its distribution were well controlled at least in this range of R_p. In Fig. 9.5, the M_n and M_w/M_n ratio are plotted against c. The fact that all M_n values fall on the same straight line indicates constancy or approximate constancy of the number of polymers throughout the course of polymerization. For a given conversion, M_w/M_n increases with increasing [BHP] or R_p, which, at first sight, may appear to indicate the loss of control over the chain length distribution with increasing [BHP]. However, this is not true. As Eqs. (9.30) or (9.31) and (9.32) imply, the PDI for an ideal (or nearly ideal) SFR-mediated system in a stationary state depends primarily on time rather than c. In fact, the PDI plotted against t is nearly independent of [BHP], as Fig. 9.6a shows (for the meaning of $x_{w,B}/x_{n,B}$ in the ordinate scale, see Section 3.1.1.4).
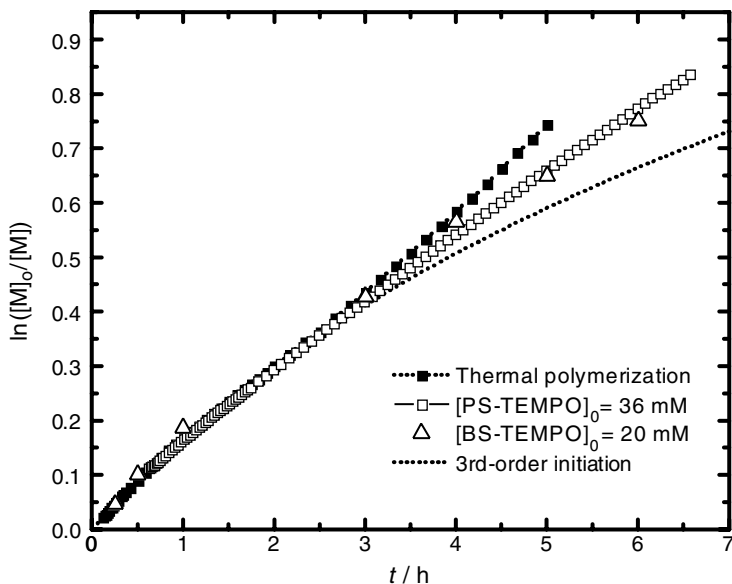
Figure 9.4   First-order plot for the polymerization of styrene at 125°C: [PS-TEMPO]$_0$ = 36 mM ($\square$); [BS-TEMPO]$_0$ = 20 mM ($\triangle$); no nitroxide ($\blacksquare$); the dotted line shows the [M]^3-dependent initiation with constant k_t (no nitroxide).
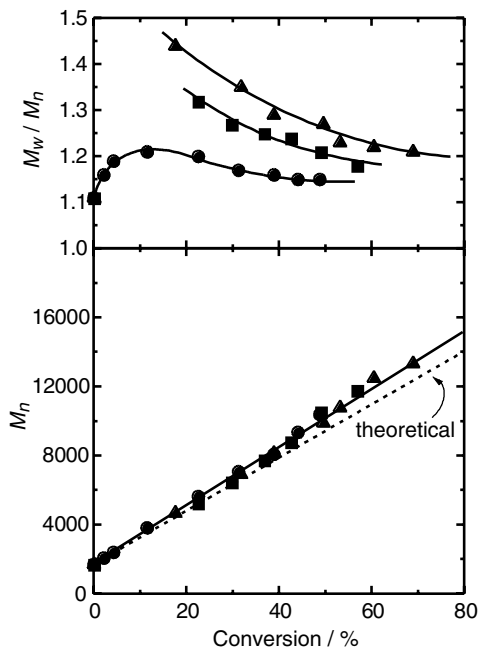
Figure 9.5.   Plot of M_w/M_n and M_n versus monomer conversion for the polymerization of styrene at 114°C with [PS-TEMPO]$_0$ = 48 mM: [BHP]$_0$ = 0 ($\bullet$), 2.0 ($\blacksquare$), and 4.0 ($\blacktriangle$) mM.
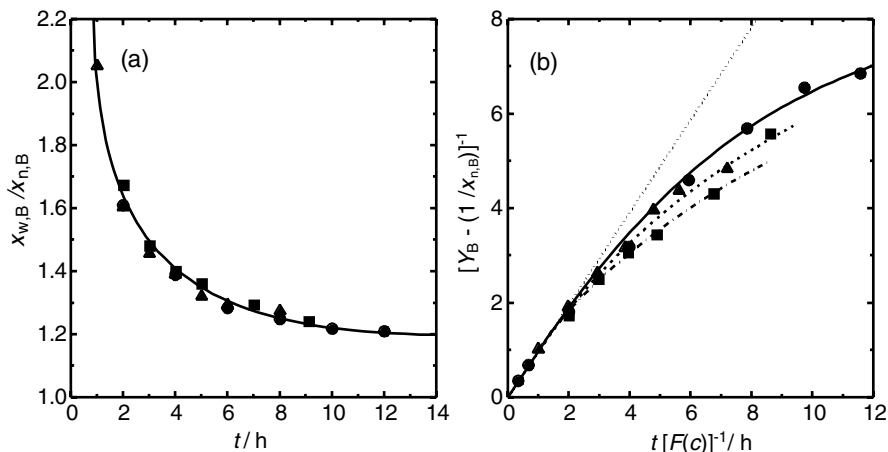
Figure 9.6 Plots of (a) $x_{w,B}/x_{n,B}$ versus t and (b) $[Y_B - x_{n,B}^{-1}]^{-1}$ versus $t\,[F(c)]^{-1}$ for the system shown in Fig. 9.5. In (b), the dotted straight line is for the "ideal" system, and the other three curves were computer-simulated (for the meaning of $x_{w,B}/x_{n,B}$, see Section 9.3.1.1.4; for symbols, see Fig. 9.5).

9.3.1.1.2 The Activation–Deactivation Equilibrium

The existence of the dissociation–combination equilibrium in the PS–TEMPO/styrene system will be evidenced by proving the relation $[P^\bullet][X^\bullet]/[P–X] = K$ (constant) [cf. Eqs. (9.8) and (9.9)], where $[P^\bullet] = [PS^\bullet]$, $[X^\bullet] = [TEMPO]$, and $[P–X] = [PS\text{-}TEMPO]$. The in situ ESR measurements[18] of $[X^\bullet]$ for the same PS-TEMPO/styrene/125°C system as that related to Fig. 9.4 showed that $[X^\bullet]$ was on the order of 10^{-5} M and gradually increased with time (Fig. 9.7a). On the other hand, the PS radical concentration $[P^\bullet]$ estimated from the data in Fig. 9.4 by use of the known k_p value[33] of 2300 $M^{-1}s^{-1}$ was on the order of 10^{-8} M and gradually decreased with time. [A comment may be due regarding the estimation of $[P^\bullet]$ using a $\ln([M]_0/[M])$ versus t curve. Since the relation $-d\ln[M]/dt = k_p[P^\bullet]$ holds independent of model, the slope of the line segment connecting two neighboring data points in Figure 9.4 approximates the slope of the curve, i.e., the value of $k_p[P^\bullet]$ there. Figure 9.7b was obtained in this manner. One group of authors[34] inappropriately estimated $k_p[P^\bullet]$ in a model-dependent manner on the basis of similar experimental data.] Since the initial concentration of the adduct, $[P–X]_0$ or $[P_0–X] = 3.6 \times 10^{-2}$ M, is much larger than both $[X^\bullet]$ and $[P^\bullet]$, $[P–X]$ may be equated to $[P–X]_0$, namely, a constant. The value of K thus estimated was 2.1×10^{-11} M, independent of time (Fig. 9.7c). The time dependence of $[P^\bullet]$ and $[X^\bullet]$ is ascribed to that of R_i and k_t as already discussed.

Clearly, the large difference between the equilibrium values of $[P^\bullet]$ and $[X^\bullet]$ was brought about by the self-termination of $P^\bullet$, which preferentially occurs until a sufficient amount of $X^\bullet$ radicals accumulate in the system and push the reversible reaction toward the undissociated state. The ratio of the equilibrium value of $[X^\bullet]$ to that of $[P–X]_0$, which is about 5×10^{-5} M$/3.6 \times 10^{-2}$ M $= 1.4 \times 10^{-3}$, suggests that the equilibrium in this system is reached after 0.14% of the living chains were
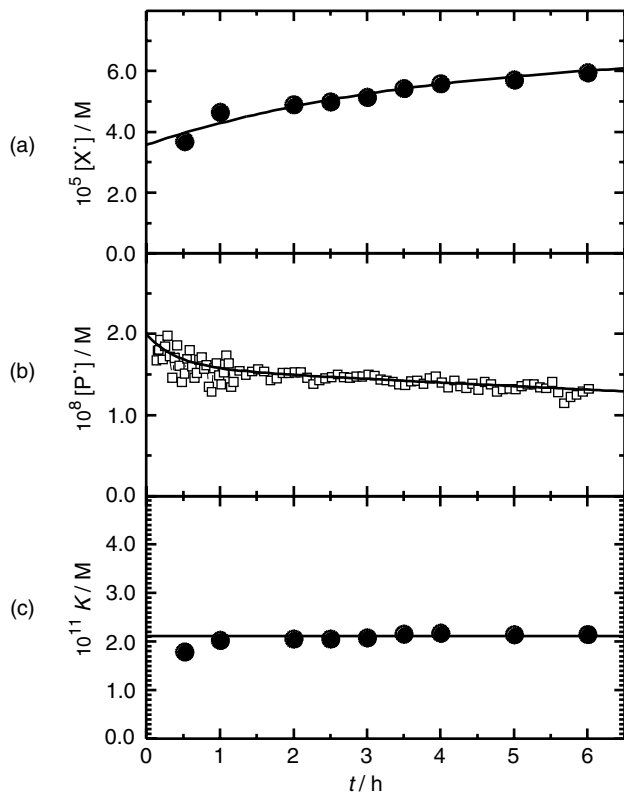
Figure 9.7   Plots of $[X^\bullet]$, $[P^\bullet]$ and K versus t for the polymerization of styrene at $125°C$ with $[\text{PS-TEMPO}]_0 = 36$ mM.

terminated, namely, at a fairly early stage of polymerization, much earlier than the stationary state of $[P^\bullet]$ was reached.[10] More quantitative discussion on this problem requires knowing the mechanism and kinetics of the reversible reactions on a quantitative basis, which is the topic of the next subsection.

9.3.1.1.3   The Activation Process   The first application of the GPC curve-resolution method (see Section 9.4.2.1) to determine the rate constant k_{act} was made to the PS-TEMPO/styrene system discussed above:[35] a styrene solution of a *constant* amount of PS-TEMPO ($[P_0-X] = 2.3 \times 10^{-2}$ M; $M_n = 1700$, and $M_w/M_n = 1.11$) and a variable amount of BHP was heated at, for instance, $110°C$ for time t, quenched to room temperature, and directly analyzed by GPC with a *constant* amount of the reaction mixture injected to the column system. Figure 9.8 shows the GPC curves of the mixtures for $t = 0$ (before reaction) and $t = 10$ min. When $[\text{BHP}]_0 = 0$, the curve slightly moves to the higher-molecular-weight side, but it is difficult to determine the fraction of the original (unactivated) species from such an
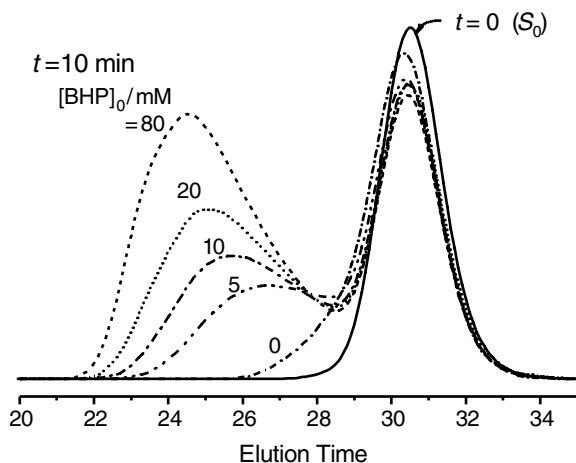
Figure 9.8 Polymeric regions of the GPC charts for the styrene/PS-TEMPO(P_0–X)/BHP mixtures heated at 110°C for 10 min: $[P_0–X]_0 = 23$ mM. The number attached on each curve indicates $[BHP]_0$ in mM. The solid curve represents the original ($t = 0$) solution containing only P_0–X as polymer species.

elution curve. For $[BHP]_0 \geq 5$ mM, the curves became bimodal, composed of two components: the first component comprising the unactivated adduct (P_0–X) and the second one comprising the once-activated adduct (P_1–X) and other minor species originating from, e.g., a further activation of P_1–X and the decomposition of BHP. Thus, BHP had an effect to lower the equilibrium concentration of X$^\bullet$, thereby increasing the transient lifetime of the propagating radical or increasing the number of monomer units to be added per activation–deactivation cycle. The monomer concentration [M] and the number density $[N_p]$ of polymer chains computed from the GPC curves showed that $[P^\bullet]$ was approximately independent of time and increased with increasing [BHP], while $[N_p]$ was approximately constant independent of both time and [BHP] in the studied experimental conditions.

The bimodal curves can be accurately resolved into the two components to give the first-order plot of S ($= [P_0–X]$) shown in Fig. 9.9. Since P_0–X originally contained 5% of potentially inactive species (without a TEMPO moiety), it was corrected by subtracting $0.05S_0$ from both S_0 and S. Figure 9.9 shows that all the experimental points for different t and different [BHP] fall on a single straight line passing through the origin. Thus this method allows accurate determination of k_{act} with no regard to kinetic details of the polymerization.

The mentioned experiment includes a particularly important implication regarding the mechanism of activation of the PS-TEMPO adduct. In Section 9.3.1.1.2, we implicitly assumed that this system was of the dissociation–combination (DC) type. However, this may not be necessarily true. The degenerative transfer (DT) mechanism can also be operative. If both the DC and DT mechanisms are important, k_{act} will
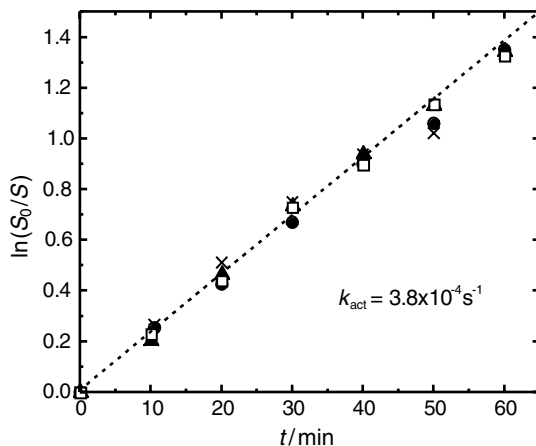
Figure 9.9 Plot of $\ln(S_0/S)$ versus t for the system in Fig. 9.8; $[BHP]_0 = 5$ ($\bullet$), 10 ($\square$), 20 ($\blacktriangle$), and 80 ($\times$) mM.

take the form

$$k_{act} = k_d + k_{ex}[P^\bullet] \tag{9.41}$$

The experiment showing the independence of k_{act} on [BHP], therefore, means that the term $k_{ex}[P^\bullet]$ is unimportant compared to k_d, specifically, $k_{act} \cong k_d$ in this system.[36]

Measurements of k_{act} (actually k_d) at various temperatures gave the following Arrhenius equation of k_d:[35]

$$k_d = 3.0 \times 10^{14} \exp(-124\ \text{KJ mol}^{-1}/RT) \tag{9.42}$$

Knowing both K and k_d, we may compute k_c from Eq. (9.9); k_c will be discussed later.

9.3.1.1.4 Polydispersities   The PDI of the polymer initiated with a low-mass or a polymeric adduct is most conveniently represented by the following relation valid for A–B diblock copolymers:[24]

$$Y = w_A^2 Y_A + W_B^2 Y_B \tag{9.43}$$

where $Y = (x_w/x_n) - 1$, $Y_K = (x_{w,K}/x_{n,K}) - 1$, $w_A = 1 - w_B = x_{n,A}/x_n$, $x_n = x_{n,A} + x_{n,B}$, and $x_{n,K}$, and $x_{w,K}$ are the number and weight average DPs of the K block ($K = A$ or B). For a monodisperse initiator with a size equivalent to DP $= m$, for example, we may simply set $Y_A = 0$ and $w_B = (x_n - m)/x_n$ in Eq. (9.43). Hence knowing x_n and x_w

of the product polymer, we may calculate Y_B from Eq. (9.43). For a polydisperse polymer initiator with known $x_{n,A}$ and $x_{w,A}$, we may similarly estimate Y_B from Eq. (9.43) by determining x_n and x_w of the product.

As already noted, $x_{n,B}$ is given by $x_{n,B} = x_n - x_{n,A} = ([M]_0 - [M])/[P-X]_0$, which obviously is *zero* for $t \to 0$ or $c \to 0$. This definition of $x_{n,B}$ is the same as those for the models discussed in Section 9.2.2, and it allows us to represent the PDI of the incremental portion of the product chain by a linear function of t; for example, application of Eq. (9.31) to the Y_B in Eq. (9.43) gives

$$\left[Y_B - \left(\frac{1}{x_{n,B}} \right) \right]^{-1} = \frac{k_{act}t}{F(c)} \tag{9.44}$$

with $F(c)$ given by Eq. (9.32). For small c (small t) or constant $[M]$, (cf. Sections 9.2.2.1 and 9.2.2.2), Eq. (9.44) reduces to

$$\left[Y_B - \left(\frac{1}{x_{n,B}} \right) \right]^{-1} = \left(\frac{1}{2} \right) k_{act}t \tag{9.45}$$

Application of Eq. (9.36) leads, after some calculations using Eqs. (9.20), (9.36), and (9.38), to

$$\left[Y_B - \left(\frac{1}{x_{n,B}} \right) \right]^{-1} = \frac{k_{act}t}{G(c)} \tag{9.46}$$

with $G(c)$ given by

$$G(c) = (\pi^{1/2}/3c^2)u^3 \mathrm{erf}(u) \tag{9.47}$$

$$u = [-2 \ln(1 - c)]^{1/2} \tag{9.48}$$

For small c or small t, Eq. (9.46) with Eqs. (9.47) and (9.48) approaches to the following limit [cf. Eq. (9.40)]:

$$\left[Y_B - \left(\frac{1}{x_{n,B}} \right) \right]^{-1} = \frac{3}{8} k_d t \tag{9.49}$$

Therefore, the plot of $F(c)[Y_B - (1/x_{n,B})]^{-1}$ versus t for a stationary-state system and the plot of $G(c)[Y_B - (1/x_{n,B})]^{-1}$ versus t for a power-law system (with zero $[X^\bullet]$ at $t = 0$) should give a linear line passing through the origin, and the slope is equal to k_{act} in both cases. Functions $F(c)$ and $G(c)$ are illustrated in Fig. 9.10. The plot of $[Y_B - (1/x_{n,B})]^{-1}$ versus t, which are suggested by both Eqs. (9.45) and (9.49), is valid for small c or small t. More importantly, this plot possibly discriminates the two models by the difference in the slope ($\frac{1}{2}$ versus $\frac{3}{8}$).
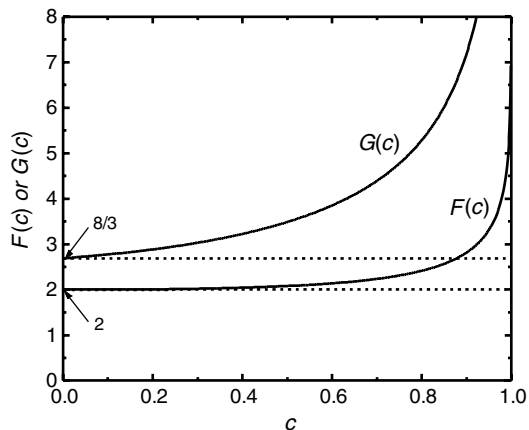
Figure 9.10   Plot of $F(c)$ and $G(c)$ versus c.

Now we examine the polydispersity of the PS-TEMPO/styrene system.[24] Figure 9.11 shows the evolution of the GPC pattern of the system with no conventional initiator. The analysis of the curves for x_n, x_w, and c revealed that both R_p (hence $[P^\bullet]$) and the number density of chains $[N_p]$ are constant in the time range ($t \leq 60$ min) studied. Figure 9.12 shows the plot of $[Y_B - (1/x_{n,B})]^{-1}$ versus t. The two lines in the figure have a slope of $\frac{1}{2}k_d$ and $\frac{3}{8}k_d$, respectively, with the k_d ($= 3.73 \times 10^{-4}$ s^{-1}) from the experimental relation (9.42). Clearly, the data points closely agree with the stationary-state Eq. (9.45) rather than Eq. (9.49), consistently with all the other observations described so far.
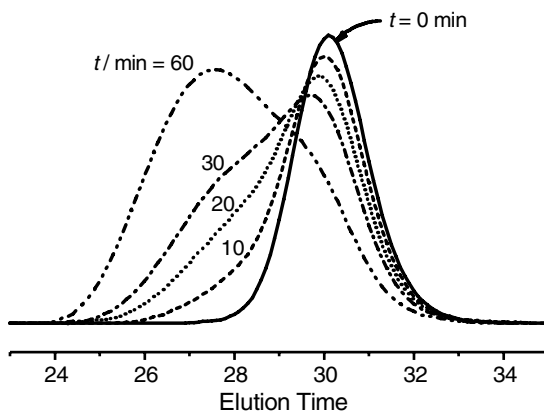
Figure 9.11   Polymeric regions of the GPC charts for the styrene/PS-TEMPO (P_0–X) mixture heated at 110°C for the time indicated in the figure: $[P_0\text{–}X]_0 = 23$ mM.
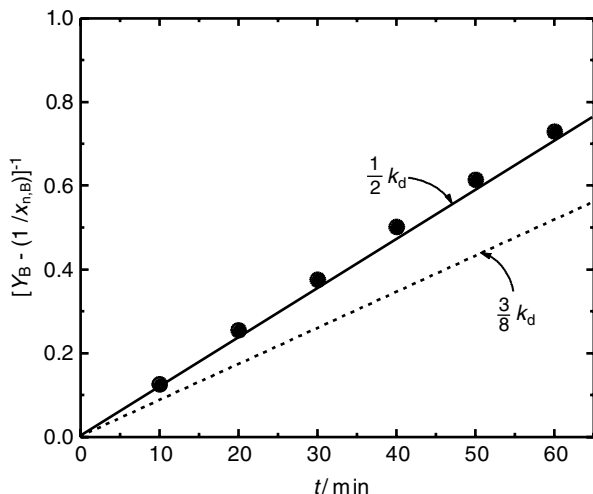
Figure 9.12 Plot of $[Y_B-x_{n,B}{}^{-1}]^{-1}$ versus t: data from Fig. 9.11. The solid line corresponds to Eq. (9.45); the broken line, to Eq. (9.49).

9.3.1.1.5 Side Reactions Equation (9.44) expects that the plot of $[Y_B-(1/x_{n,B})]^{-1}$ versus $t/F(c)$ is linear even for large t or c. Actually, this is not the case, because the effects of side reactions that are neglected in the theory will accumulate and eventually cause downward deviations from the straight line. Examples are given in Fig. 9.6b, where the experimental data were taken from Fig. 9.6a. In these examples, the linearity holds only for $t \leq 1\,\mathrm{h}$, the time range where the discussion related to Fig. 9.12 was made. As already described, the addition of the conventional initiator BHP had a remarkable effect of increasing R_p. Figure 9.6b suggests that the effect of BHP on PDI is rather minor compared with other effects.

Possible causes for the deviations of PDI from the ideal model generally include contributions of dead chains and conventionally-initiated chains, decomposition of the alkoxyamine, chain transfer to monomer and to the Diels–Alder adduct or the Mayo dimer of styrene. The most important of these for the present system may be the decomposition of alkoxyamines through the reaction in Scheme 9.3. Quantitative experimental data are available for the decomposition of PS-TEMPO and some other low-mass alkoxyamines.[37,38] It was suggested that the decomposition, namely, the abstraction of the β-proton by a TEMPO radical can occur on the occasion of dissociation as well as of combination,[38] and the rate constant of decomposition, k_{dec}, should be proportional to k_d in a system under dissociation–combination equilibrium. The activation energy of decomposition, E_{dec}, should therefore be given by the sum $E_{dec} = E_d + E_{abs}$, where E_d and E_{abs} are the activation energies of dissociation and β-proton abstraction, respectively. This means that $E_{dec} > E_d$, which was observed in fact.[38] A theoretical analysis of the kinetics of LRP was made including the alkoxyamine degradation.[39]
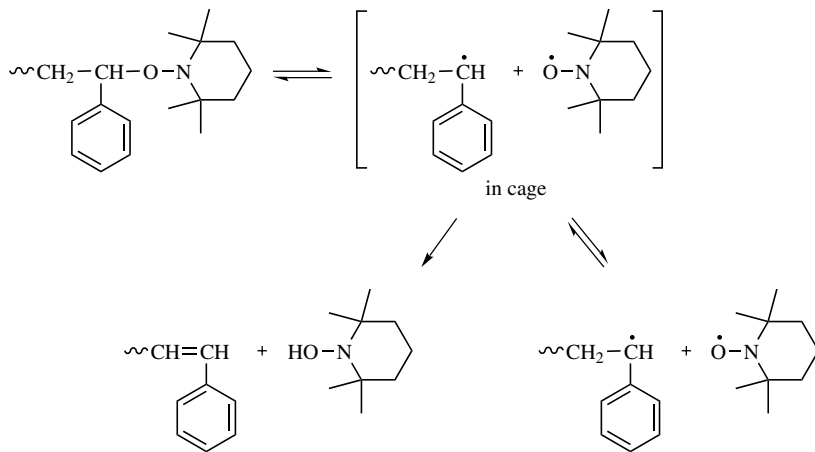
Scheme 9.3 Decomposition of an alkoxyamine.

9.3.1.2 Other NMPs

9.3.1.2.1 The NMP of a p-Substituted Styrenic Glycomonomer[40] In the absence of initiation, NMP is expected to follow the non-stationary-state kinetics. The first such example was observed for the DBN-mediated polymerization of a styrene derivative with negligible spontaneous polymerization. The polymerization rate was dependent on the concentration of the initiating adduct, I_0. According to Eq. (9.20), the plot of $I_0^{-1/3} \ln([M]_0/[M])$ versus $t^{2/3}$ for such a system should give a straight line independent of I_0. This in fact was observed, even though the experimental data were rather poorly defined at large t, due to a side reaction specific to this system. The production of low-polydispersity polymers even at small t suggested that k_d of this system is much larger than that for the PS-TEMPO system.[40]

9.3.1.2.2 DEPN-Mediated Polymerization of Styrene The polymerization of styrene mediated by DEPN was found quite different from that mediated by TEMPO. The polymerization rate was observed to increase with increasing concentration of the initiating adduct [PS$_0$-DEPN] despite the presence of significant thermal polymerization at the studied temperatures (e.g., 120°C).[34] In terms of the theory, the crossover from the power-law behavior to stationary-state kinetics was given by Eq. (9.22). For the PS-TEMPO/styrene/120°C system, for example, we may roughly put $(R_i/k_t)^{1/2} = 2 \times 10^{-8}$ M, $k_t = 10^8$ M^{-1} s^{-1}, $K = 2 \times 10^{-11}$ M, and $I_0 = 10^{-2}$ M to estimate $t_{cross} \cong 10^2$ s. This value is small compared with the polymerization time, typically on the order of 10^4 s, and explains why the PS-TEMPO system shows the stationary-state behavior from an early stage of polymerization. On the other hand, the PS-DEPN system was reported to have a K value of 6.0×10^{-9} M, about 300 times larger than that of the PS-TEMPO system.[34] This means that under the same conditions as for the PS-TEMPO system,

t_{cross} would be about 3×10^4 s. This value exceeds the usual experimental times, and explains why stationary-state kinetics is not observed in the PS-DEPN system. More recently, Boutevin et al.[41] observed a well-defined power-law behavior of the conversion factor [Eq. (9.20)] with respect to both t and I_0. Their experimental data allowed them to estimate K, on the basis of Eq. (9.20) with literature data of k_p and k_t, to be 6.1×10^{-9} M. The good agreement of this K value with the above-cited, more directly determined one is another support for the power-law kinetics.

Another piece of strong evidence for the power-law kinetics of the PS-DEPN system was recently obtained by Goto et al.,[42] who made a GPC polydispersity analysis of the polymers produced in a time rage where Eqs. (9.45) and (9.49) should hold. The observed slope of the $[Y_B - (1/x_{n,B})]^{-1}$ versus t curve was close to the value $\frac{3}{8}k_d$ predicted by Eq. (9.49) with the value of k_d determined by themselves. In this connection, Benoit et al.[34] also determined the k_d of this system by the GPC curve-resolution method. Their values of k_d are systematically smaller than those by Goto et al.[43] At 120°C, for example, they found $k_d = 3.4 \times 10^{-3}$ s^{-1}, while Goto et al. found $k_d = 1.1 \times 10^{-2}$ s^{-1}. On the other hand, Marque et al.[44] studied the low-mass homolog **12**, showing that its k_d is 5.5×10^{-3} s^{-1} at the same temperature. The reason for the largely different k_d values of PS-DEPN reported by the two groups is not clear, but the result of Goto et al. is in line with the "polymer effect" on k_d (see Section 9.4).

Combining the values of K and k_d, Benoit et al.[34] estimated the k_c of this system to be 5.7×10^5 M^{-1} s^{-1} (120°C). This value is increased to $k_c = 1.8 \times 10^6$ M^{-1} s^{-1} by the use of Goto's k_d and the same K (6.0×10^{-9} M) due to Benoit et al.[34] and Lutz et al.[41] In any case, these values of k_c are much smaller than the k_c between PS$^{\bullet}$ and TEMPO ($k_c = 7.6 \times 10^7$ M^{-1} s^{-1}), indicating that the bulkiness of nitroxides has a large effect on k_c as well as on k_d.

9.3.1.2.3 NMP of Acrylates

Di-*tert*-butyl nitroxide (DBN) was found to control the polymerization of *tert*-butyl acrylate (tBA) at a lower-temperature than that[45] mediated by a TEMPO derivative. This is in line with the observation that the k_d of PS-DBN is about 40 times larger than that of PS-TEMPO (see Section 9.4). In fact, the GPC curve-resolution method applied to a PtBA-DBN/tBA system yielded a k_d value of 1.0×10^{-3} s^{-1} at 120°C,[46] which is as large as that of PS-TEMPO at the same temperature. Since spontaneous polymerization is absent in this system, its kinetics was expected to be of the power-law type. However, the PDI of this system increased after an initial decrease to about 1.3, and the R_p markedly decreased at later stages of polymerization. This was due to the decomposition of the alkoxyamine to a macromonomer and a hydroxyamine, the latter working as an inhibitor.[47] The rate constant of decomposition, viewed as a first-order reaction, was estimated to be 1.1×10^{-5} s^{-1}, a value 4 times as large as that of PS-TEMPO at the same temperature (120°C).[46]

On the other hand, the polymerization of *n*-butyl acrylate (BA) mediated by DEPN proceeded highly satisfactorily without accompanying appreciable degradation of the alkoxyamine.[34] The k_d of a PBA-DEPN adduct was 7.1×10^{-3} s^{-1}, which calculates k_c to be 4.2×10^7 M^{-1} s^{-1} for the observed K value of 1.7×10^{-10} M.

General conditions of high-performance NMP would be a large k_d ($>10^{-3}$ s^{-1}), a reasonably small K ($K < 10^{-10}$ M) and the absence of degradation and other side reactions. When K is large, a large concentration of free nitroxide is required to achieve equilibrium. For example, putting $K = 10^{-9}$ M, $[P^{\bullet}] = 10^{-8}$ M, and $[P-X] = 10^{-2}$ M into Eq. (9.8), we have $[X^{\bullet}] = 10^{-3}$ M. Namely, to get an equilibrium, we have to wait for 10% of the living species ($[P-X]$) to be terminated to give as much $X^{\bullet}$ radical. This was nearly the case with the PS-DEPN system. In this regard, the addition of an appropriate amount of $X^{\bullet}$ to the system prior to polymerization would be useful.[34] But this amount can be deduced only by the information from a set of kinetic studies. The PBA-DEPN system may be nearly ideal with regard to the fairly large k_d, the relatively small K (or relatively large k_c), and the absence of appreciable degradation of the alkoxyamine. The nitroxide TIPNO has been reported to be powerful in controlling the polymerization of a range of monomers, including acrylates.[48] Kinetic studies on related polymerization systems would be interesting and important.

9.3.2   Atom Transfer Radical Polymerization (ATRP)

The activation–deactivation process in transition-metal-catalyzed polymerizations is supposed to involve an atom transfer (AT) process, and they are often termed ATRP. The basic kinetic features of ATRP closely resemble those of NMP in theory. In Scheme 9.4, the complex Cu(I)X/L, where X is a halogen (Br or Cl) and L is a ligand, would abstract X from the adduct P–X to generate $P^{\bullet}$ and the complex

$$P-X \ + \ Cu(I)X/L \ \underset{k_{da}}{\overset{k_a}{\rightleftarrows}} \ P^{\bullet} \ + \ Cu(II)X_2/L$$
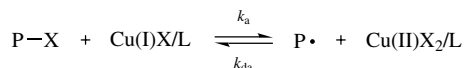
Scheme 9.4   Reversible activation process in copper-mediated ATRP.

Cu(II)X$_2$/L. This is the activation process, and the reverse reaction defines the deactivation process. If there is no Cu(II) species at the onset of polymerization, the activation process would predominate, and the concentrations of $P^{\bullet}$ and Cu(II) would monotonously increase to eventually cause a PRE effect, in which the Cu(II)X$_2$/L species plays the role of a persistent (stable) radical. Even though there are several complexing factors not allowing highly quantitative descriptions of the overall kinetics of ATRP, its qualitative features are reasonably well understood, today.

9.3.2.1   Copper-Mediated Polymerization of Styrene—a Model ATRP

9.3.2.1.1   The Activation Process   The activation process of the homogeneous ATRP of styrene at 110°C mediated by a Cu(I)Br/L complex with L = dHbipy (Fig. 9.13) and [Cu(I)]/[L] = 1/2 at 110°C was studied by the GPC curve-resolution method.[49] A PS-Br with $M_n = 1400$ and $M_w/M_n = 1.06$ was used as an initiating (probe) adduct P_0–X. Under the usual conditions of experiments, k_{act} was too large, and the transient lifetime was too short in this system to determine k_{act} accurately. To
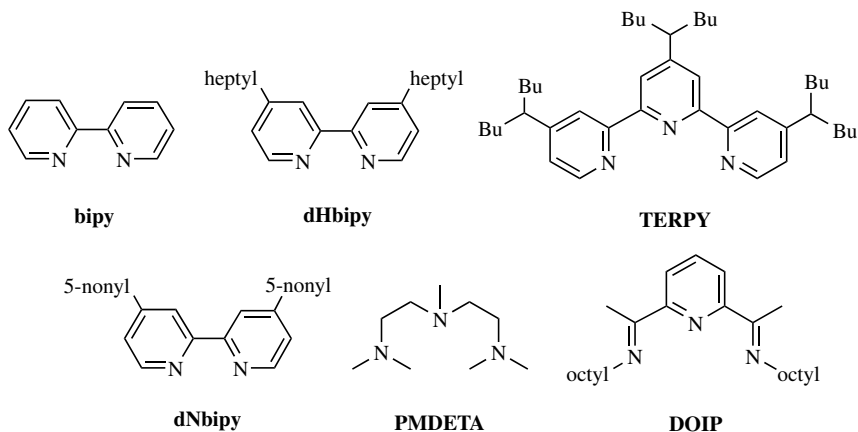
Figure 9.13 Examples of ligands.

cope with these problems, the Cu(I) concentration was about an order of magnitude lowered than usual, and the conventional initiator BHP (20 mM) was added. Example of GPC curves are given in Fig. 9.14, where the peak height S of P_0–X is observed to decrease more rapidly as [Cu(I)] increases. The first-order plot of S was linear in time in all cases to give well-defined values of k_{act}.

The activation process of this system was supposed to be atom transfer (AT), but degenerative transfer (DT) could not be a priori ruled out. When the AT and DT mechanisms coexist, k_{act} will take the from

$$k_{act} = k_a[A] + k_{ex}[P^\bullet] \tag{9.50}$$
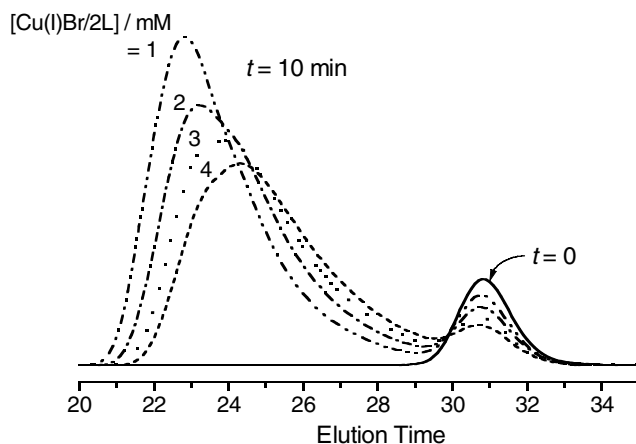
Figure 9.14 GPC charts for the PS–Br (P_0–X)/styrene/BHP mixture with different Cu(I)Br/2L concentrations heated at 110°C for 10 min: $[P_0$–X$]_0 = 12$ mM; $[BHP]_0 = 20$ mM; $[Cu(I)Br/2L]_0$ as indicated in the figure.
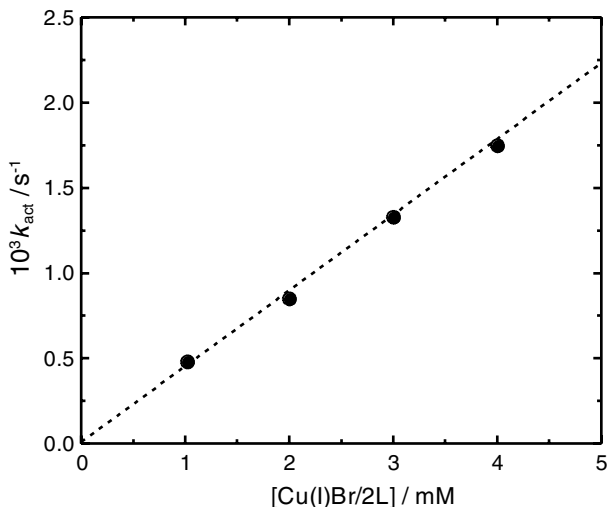
Figure 9.15   Plot of k_{act} versus $[Cu(I)Br/2L]_0$ for the system in Fig. 9.14. The slope of the straight line gives the k_a of 0.45 M^{-1} s^{-1}.

where $A = Cu(I)$ in this case. The addition of BHP had another important role of pushing the system toward the stationary state so that $[P^\bullet]$ was nearly independent of $[Cu(I)]$ (see also discussion below). As Fig. 9.15 shows, the plot of k_{act} versus $[Cu(I)]_0$ gave a linear line passing through the origin, meaning that the DT mechanism is unimportant, and the activation of this system is predominantly due to the AT mechanism.

9.3.2.1.2 The Activation and Deactivation Rate Constants   The slope of the linear line in Fig. 9.15 gives $k_a = 0.45$ M^{-1} s^{-1}. This value reasonably agrees with the k_a value of 0.43 M^{-1} s^{-1} determined in xylene (without styrene) by the ESR method using hydroxy-TEMPO as a scavenger probe for the PS radical liberated from a PS–Br adduct by the catalysis of Cu(I)Br/dHbipy.[50] Also interestingly, the k_a of the low-mass model adduct **21** with the same catalyst in toluene was 0.42 M^{-1} s^{-1},[51] indicating that the chain length dependence of k_a is insignificant. However, this is not conclusive, since k_a was reported to heavily depend on solvent.[50]

Since it holds at equilibrium that $k_a[Cu(I)][P-X] = k_{da}[P^\bullet][Cu(II)]$, the polymerization rate $R_p = k_p[P^\bullet][M]$ can be represented by

$$\frac{R_p}{[M]} = \frac{k_p K_{AT}[P-X][Cu(I)]}{[Cu(II)]} \tag{9.51}$$

where $K_{AT} = k_a/k_{da}$. To estimate K_{AT}, Matyjaszewski et al.[52] added a sufficient amount of Cu(II) to the original solution so that $[Cu(II)]$ was almost independent of time, and measured R_p. Since the changes in $[P-X]$ and $[Cu(I)]$ are generally

minor, they could thus estimate K_{AT} to be 3.9×10^{-8}. Combining this K_{AT} with the above-cited k_a value, we estimate $k_{da} = 1.1 \times 10^7 \ M^{-1} \ s^{-1}$.

9.3.2.1.3 Polymerization Rates The polymerization of styrene at 110°C initiated by 1-phenylethyl bromide **21** and mediated by a Cu(I)Br/dHbipy was studied for varying concentrations of the initiator, Cu(I), and Cu(II) species (with no conventional initiator added).[52] The ln([M]$_0$/[M])–t plot was apparently linear in all cases, indicating constancy (time independence) of [P•] or R_p/[M]. Moreover, the slope of the linear line, namely, R_p/[M], was approximately first-order with respect to both [P–X]$_0$ and [Cu(I)]$_0$, while it decreased with increasing [Cu(II)]$_0$ in a nonlinear fashion. These behaviors are contradictory to the power-law kinetics expressed in Eq. (9.20) but rather close to those predicted for the limiting case of large [Cu(II)]$_0$, specifically, Eq. (9.21).

Several factors may be responsible for these observations. An ESR study of the ATRP system did show a rapid increase of the Cu(II) concentration at an early stage of polymerization.[53] At the same time, it revealed that there is a finite concentration of Cu(II) at time zero, in many cases. This is because in the laboratory it is difficult to completely avoid a small amount of oxidized catalyst being involved in the starting materials or produced through insufficient deoxygenation. The amount of the contaminating Cu(II) species may be just a few percent of [Cu(I)]$_0$, but clearly it is important compared with the equilibrium concentrations, which are typically on the order of 10% of [Cu(I)] or even less. As already pointed out, nonzero values of [Cu(II)]$_0$ push the system toward the apparent ideality represented by Eq. (9.21).

The second factor to be considered may be the chain length dependence of the termination rate constant k_t. As the reaction proceeds, the chains become longer, the viscosity of the medium increases, and the termination reaction becomes slower, hence less significant PRE. Computer simulations of ATRP were carried out on the basis of an empirical equation describing the dependence of k_t on DP.[54] The results satisfactorily explained the observed (near) linearity of the ln([M]$_0$/[M])–t plot.

The third factor that can have a strong influence on ATRP kinetics may be the inhomogeneity of the system, in particular, with respect to the solubility of the catalyst. It is possible that not all the Cu(I) and Cu(II) species are present in solution at the concentrations involved in the system. In other words, the reactants are possibly heterogeneous, even though they may appear homogeneous to the eye. Moreover, as the reaction proceeds and the medium changes, the solubility of catalyst can change. Even though the solubility and solution state are difficult to fully specify experimentally, the effects of heterogeneity on ATRP kinetics can be predicted by simulation. If, for example, the Cu(II) species is assumed to have a limited, low solubility, the systems starting with various initial conditions would quickly reach the (same) limiting value of [Cu(II)], thereafter showing the apparent ideality of Eq. (9.21).

Shipp and Matyjaszewski[29] carried out computer simulations taking all these factors into account, showing that the kinetics of ATRP are complex. The apparent external orders of the initiator, activator, and deactivator were found to be often fractional or nonlinear and also depend heavily on other factors such as the amount of deactivator that is present or generated at the beginning. They also pointed out that

using very reactive initiators, such as benzhydryl chloride, may lead to the production of variable amounts of deactivator depending on the mode and rate of addition and therefore affect the polymerization rate. The effect of thermal (self) initiation of styrene is rather minor in the usual conditions of experiments, such as, $[Cu(I)Br/L]_0 > 1 \times 10^{-2}$ M, but at a lower level of the activator concentration, it is important (see Section 9.3.2.1.4).

9.3.2.1.4 Polydispersities

The k_a value of 0.45 M^{-1} s^{-1} for the PS–Br adduct activated by the Cu(I)Br/dHbipy complex at 110°C suggests that this system gives a low-polydispersity polymer from an early stage of polymerization or low conversion. Taking the typical value of $[Cu(I)]_0 = 0.045$ M, we find from Eq. (9.45) (with the $x_{n,B}^{-1}$ term neglected) that PDI will be smaller than 1.1 after about 17 min of polymerization. This estimates is based on the assumption of constant $[P^\bullet]$. For the power-law-type radical concentration [Eq. (9.18) with $[X^\bullet] = 0$], this polymerization time is estimated to be somewhat longer than 23 min [Eq. (9.49)]. At high conversion both types of kinetics predict that PDI approaches to 1.00, but this will never be realized, because side reactions become more and more important as conversion or time increases. In this regard, the discrimination of the kinetic models by a polydispersity analysis is possible only at an early stage of polymerization—not so early, of course, that the quasiequilibrium in [Eq. (9.8)] is still not reached. At this time, no critical experimental test has been made. The only data available now are related to the special system described in Section 9.3.2.1.1, which were characterized by an unusually low concentration of the activator (Cu(I)Br/dHbpy) and the use of the conventional initiator (BHP). The $\ln([M]_0/[M])$–t plot of this system had a marked curvature, which could not be described either by the power-law kinetics or by the stationary-state kinetics (Fig. 9.16a). However, the numerical data for this system applied to Eq. (9.22) suggested that the stationary state would be reached about 5 min after the onset of polymerization. In fact, data points after $t = 4$ min was consistent to the constant-$[P^\bullet]$ kinetics. The PDI data for this time range also conforms to the stationary-state kinetics [Eq. (9.45)] rather than the power-law kinetics [Eq. (9.49)] (Fig. 9.16b).[55]

9.3.2.2 Other ATRPs

For Cu(I)Cl/dNbipy-mediated homogeneous ATRP of methyl methacrylate (MMA), similar results to those for the abovementioned styrene system were obtained.[56] Specifically, the $\ln([M]_0/[M])$–t plot was linear, where the slope of R_p was first-order with respect to both Cu(I)Cl and initiator (alkyl or sulfonyl chloride) concentrations. Like in the styrene system, R_p did not obey simple negative first-order kinetics with respect to the concentration of the deactivator Cu(II) added at the beginning. However, unlike the styrene system, where a maximum R_p was reached at the $[ligand]_0$ to $[Cu(I)Br]_0$ (or $[Cu(I)Cl]_0$) ratio of 2, this system achieved a maximum R_p when $[ligand]_0/[Cu(I)Cl]_0 = 1$. Possible structures for Cu(I)/dNbipy in MMA was discussed. Furthermore, UV and ESR data suggested that the Cu(II) species interact with the Cu(I) species, leading to a possible mixed valence Cu(II)/Cu(I) complex with one or more structures in the monomer
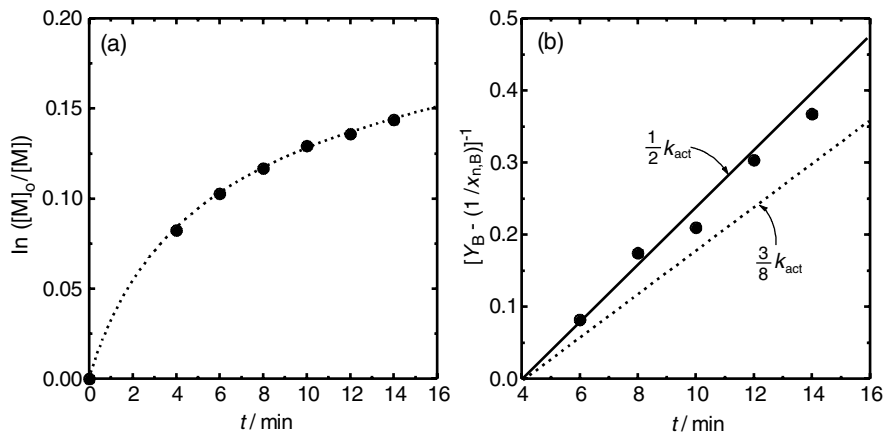
Figure 9.16 Plots of (a) $\ln([M]_0/[M])$ and (b) $[Y_B-x_{n,B}^{-1}]^{-1}$ versus t for the PS–Br (P_0–X)/styrene/BHP/Cu(I)Br/2L mixture heated at 110°C: $[P_0-X]_0 = 12$ mM; $[BHP]_0 = 20$ mM; $[Cu(I)Br/2L]_0 = 3$ mM. In (b), the solid line corresponds to Eq. (9.45); the broken line, to Eq. (9.49).

MMA. Hence the Cu(II) species at high concentrations can not only reduce R_p according to Eq. (9.51) but also deactivate the active Cu(I) catalyst.[56a]

The Cu(I)Br/dNbipy-mediated homogeneous polymerization of methyl acrylate (MA) also exhibited first-order kinetics with respect to the monomer concentration, while the dependence of R_p on I_0 was fractional (about 0.8), and that on $[Cu(I)]_0$ was nonlinear.[56b] However, it was negatively first-order with respect to the deactivator concentration $[Cu(II)]_0$.

The equilibrium constant K_{AT} ($= k_a/k_{da}$), estimated on the basis of similar experiments to the styrene system, was 1.2×10^{-9} for the Cu(I)Br/dNbipy-mediated polymerization of MA at 90°C. This value is smaller than those for either the Cu(I)Br/dNbipy-mediated polymerization of styrene ($K_{AT} = 2 \times 10^{-8}$) or the Cu(I)Cl/dNbipy-mediated polymerization of MMA ($K_{AT} = 7.0 \times 10^{-7}$) at the same temperature (90°C).

The Cu(I)Cl/bipyridine-mediated polymerization of styrene is known to be a heterogeneous one. Addition of 10% of dimethylformamide to this system was reported to achieve a homogeneous ATRP at 130°C.[57] The R_p of this system was observed to be almost independent of $[Cu(I)Cl]_0$ and I_0 when these concentrations were not too large. This behavior may be understood in terms of the stationary-state kinetics brought about by the thermal initiation of styrene. In fact, the observed values of R_p in the relevant ranges of $[Cu(I)Cl]_0$ and I_0 were about the same as that of the pure styrene system. For higher values of $[Cu(I)Cl]_0$ and I_0, the stationary state is hardly reached, and the system would behave more or less similarly to the other systems described above.

9.3.3   Degenerative Chain-Transfer-Mediated Polymerization (DTMP)

9.3.3.1   Iodide-Mediated Polymerization of Styrene   Iodide-mediated radical polymerization is a simple and robust LRP that can be performed in experimental conditions close to those of conventional radical polymerization. However, it has, at this moment, limited applicability because unlike other variants of LRP such as NMP, ATRP, and dithioester-based RAFT polymerization (see text below), it does not give polymers with a very low polydispersity.[58] This is ascribed to generally small values of k_{act} achieved by this polymerization. Mechanistically, the iodide-mediated polymerization of styrene involves a degenerative chain transfer (DT) process.[58,59] In what follows, we will describe the kinetic features of this system in some detail for its interest as a model DTMP.[59]

A polystyryl iodide PS–I with $M_n = 1500$ and $M_w/M_n = 1.26$ was used as an initiator adduct P_0–X, which had a chain-end activity of 96–98% according to spectroscopic analyses. Polymerization was carried out with a fixed amount (17 mM) of P_0–X and varying amounts of BPO (0–30 mM). The conventional initiator BPO was necessary to initiate and maintain polymerization (at the experimental temperature of 80°C, the rate of thermal initiation of styrene is very small). The GPC experiments provided all required information including the time evolutions of polymer (hence monomer) concentration, P_0–X concentration, M_n and M_w, and hence the number of polymer chains.

9.3.3.1.1   Polymerization Rates   Figure 9.17a shows that the first-order plot for the monomer concentration is linear in time, indicating that the stationary-state kinetics holds, in all cases. The values of $(R_p/[M])^2$ from Fig. 9.17a are linear in $[BPO]_0$ and
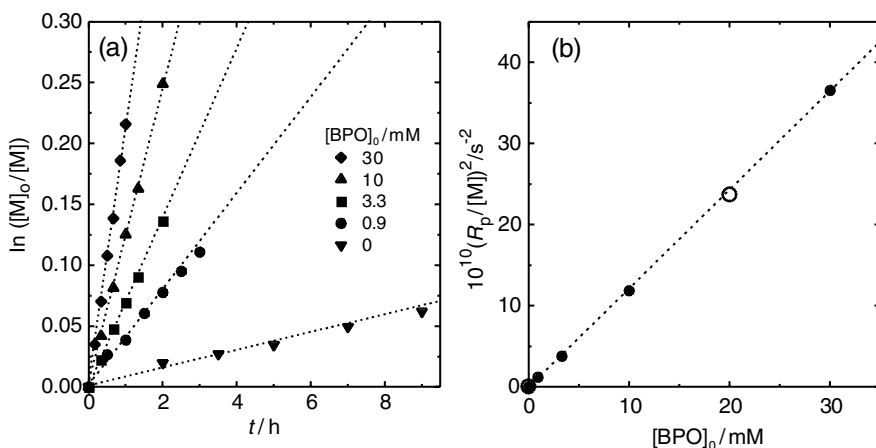
Figure 9.17   (a) Plot of $\ln([M]_0/[M])$ versus t for the PS–I (P_0–X)/styrene mixture with different BPO concentrations heated at 80°C: $[P_0–X]_0 = 17$ mM; $[BPO]_0$ as indicated in the figure; (b) plot of $(R_p/[M])^2$ versus $[BPO]_0$ in the presence of P_0–X (for the system in Fig. 9.17a, filled circles) and the absence of it (open circles).

equal to those of the conventional (iodide-free) system (Fig. 9.17b). This means that the iodide had no detectable effect on the rate of polymerization. Despite the addition of considerable amounts of BPO, the total number of polymer chains in the system was constant within $\pm 10\%$ in the studied range of $[BPO]_0$ and polymerization time ($t = 1$–9 h, depending on $[BPO]_0$). This was expectable from the calculated number of BPO-initiated chains relative to the number of active chains $[P_0-X]_0$.

9.3.3.1.2 The Activation Mechanism and Activation Rate Constants

The GPC curves obtained were composed of two well-separated peaks, from which the evolution of the concentration of $[P_0-X] = S$ was accurately followed, in all cases. The first-order plot of S is given in Fig. 9.18, showing that the plot is linear in t in all cases.

The activation—the cleavage of the C—I bond in this system—can possibly occur by a DT process and/or a thermal dissociation. When the two mechanisms are involved, k_{act} will take the form

$$k_{act} = k_d + k_{ex}[P^\bullet] \tag{9.52}$$

The values of k_{act} from Fig. 9.18 plotted as a function of $R_p/[M]$ gives a linear line passing through the origin, meaning that the k_d term is trivial and the k_{act} of the system may be identified with $k_{ex}[P^\bullet]$. Since it holds that $R_p/[M] = k_p[P^\bullet]$, the slope of the line gives $C_{ex} = k_{ex}/k_p = 3.6$. Equivalently, values of $\ln(S_0/S)$ can be plotted against $\ln[1/(1-c)]$, according to the following relation that holds for a batch DTMP:

$$\ln\left(\frac{S_0}{S}\right) = C_{ex} \ln\left(\frac{1}{1-c}\right) \tag{9.53}$$
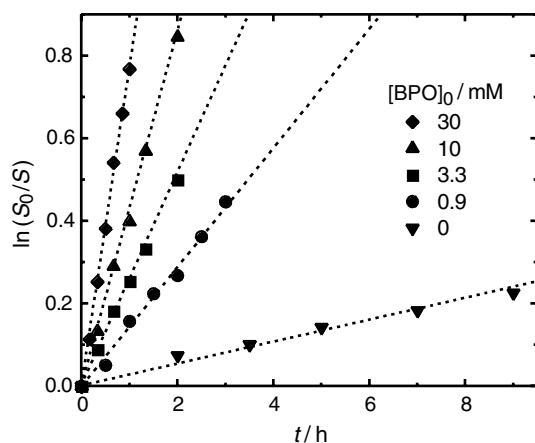
Figure 9.18 Plot of $\ln(S_0/S)$ versus t for the PS–I (P_0–X)/styrene mixture heated at 80°C: $[P_0-X]_0 = 17$ mM; $[BHP]_0$ as indicated in the figure.
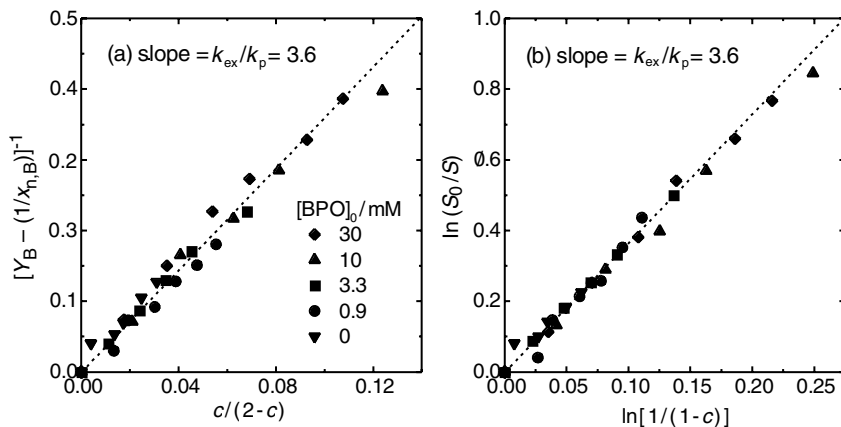
Figure 9.19 (a) Plot of $[Y_B-(1/x_{n,B})]^{-1}$ versus $c/(2-c)$ and (b) of $\ln(S_0/S)$ versus $\ln[1/(1-c)]$ for the iodide-mediated polymerization of styrene with varying $[BPO]_0$ as indicated in Fig. 9.19a (80°C).

All the data points form a single straight line, the slope of which gives $C_{ex} = 3.6$ (Fig. 9.19a). Using the IUPAC value of k_p,[33] we have $k_{ex} = 2400$ M^{-1} s^{-1}.

9.3.3.1.3 Polydispersities The PDI in a batch DTMP can be tested on the basis of Eq. (9.31), which essentially describes the time evolution, or equivalently, on the basis of Eq. (9.54), which follows the PDI as a function of c:

$$\left(Y_B - \frac{1}{x_{n,B}}\right)^{-1} = C_{ex}\left(\frac{c}{2-c}\right) \tag{9.54}$$

Figure 9.19b shows that all the data points form a single straight line passing through the origin, and the slope gives $C_{ex} = 3.6$. This beautiful agreement of the C_{ex} value with that determined by the peak-resolution method means that the chain length distribution of this system precisely obeys the stationary-state theory. Side reactions such as termination and (conventional) initiation have no important effect on PDI in the studied range of c (or t).

9.3.3.2 RAFT-Mediated Polymerization A representative RAFT system uses a dithiocarbonate as a mediator (Scheme 9.5a: $Z = CH_3$, Ph, etc.). As this scheme shows, a RAFT process involves the addition of radical $P_A^\bullet$ to the adduct P_B-X (rate constant $= k_{adAB}$) to form the intermediate radical, followed by the fragmentation of the intermediate to release either $P_A^\bullet$ (rate constant $= k_{frBA}$) or $P_B^\bullet$ (rate constant $= k_{frAB}$). This process, viewed as a degenerative chain transfer or exchange process, is simplified to Scheme 9.5b, where the rate constant of the exchange reaction, k_{exAB}, is related to those in Scheme 9.5a by

$$k_{exAB} = P_{rB}k_{adAB} \tag{9.55}$$

(a)

$P_A\bullet \; + $ (X−P_B) $\xrightleftharpoons[k_{frBA}]{k_{adAB}}$ (P_A−(X•)−P_B) $\xrightleftharpoons[k_{adBA}]{k_{frAB}}$ (P_A−X) $ + \; P_B\bullet$

(b) $P_A\bullet \; + \; X-P_B \; \xrightleftharpoons[k_{exBA}]{k_{exAB}} \; P_A-X \; + \; P_B\bullet$
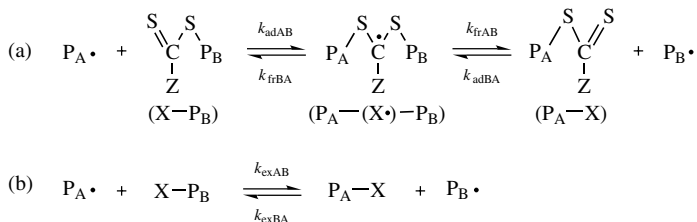
Scheme 9.5 (a) RAFT ($Z = CH_3$ or Ph) and (b) general scheme of degenerative chain transfer.

with

$$P_{rB} = \frac{k_{frAB}}{k_{frAB} + k_{frBA}} \tag{9.56}$$

Equation (9.55) assumes that the system is in a stationary state with respect to the concentration of the intermediate radical, $d[P_A-(X^\bullet)-P_B]/dt = 0$. The solution of this differential equation gives

$$[P_A-(X^\bullet)-P_B] = \frac{k_{adAB}[P_B-X][P_A^\bullet] + k_{adBA}[P_A-X][P_B^\bullet]}{k_{frAB} + k_{frBA}} \tag{9.57}$$

Equations (9.55)–(9.57) show specific features of RAFT-based polymerization kinetics.

9.3.3.2.1 Dithioacetate-Mediated Polymerization of Styrene The polymerization of styrene including a fixed amount (0.45 mM) of polystyryl dithioacetate (PS-SCSCH_3: $M_n = 1.94 \times 10^3$ and $M_w/M_n = 1.17$) as a probe adduct P_0–X and variable amounts of BPO (0–10 mM) as a radical initiator was studied.[60] In order to follow the fast exchange process in this system, the concentrations of P_0–X and BPO had to be unusually low. Figures 9.20a and 9.20b show examples of the first-order plots with respect to the concentrations of the monomer [M] and the probe adduct [P_0–X], respectively, both determined by the GPC analysis (note the exceptionally small ordinate scale in Fig. 9.20a).

The values of $R_p/[M]$ obtained from the data in Fig. 9.20a were consistent to the stationary-state rate law [Eq. (9.16); see also Section 9.2.1.4]. However, independent experiments carried out with a fixed amount of BPO and variable amounts of P_0–X revealed a decrease of R_p with increasing [P_0–X]$_0$. This was originally explained in terms of the chain length dependence of k_t,[60] since it generally holds that $x_n \propto [P_0-X]_0^{-1}$ and $k_t \propto x_n^{-m}$ with $m = 0.15-0.2$. However, it turned out later that the decrease in R_p for larger [P_0–X]$_0$ was too large to be interpreted in this way. We will come back to this point later.

The values of k_{act} obtained from Fig. 9.20b plotted against $R_p/[M]$ give a linear line passing through the origin (Fig. 9.21), meaning that the first term in Eq. (9.52) is unimportant in this system, too, and suggesting that the main mechanism of activation is the RAFT process. (There is a small possibility of the degenerative chain
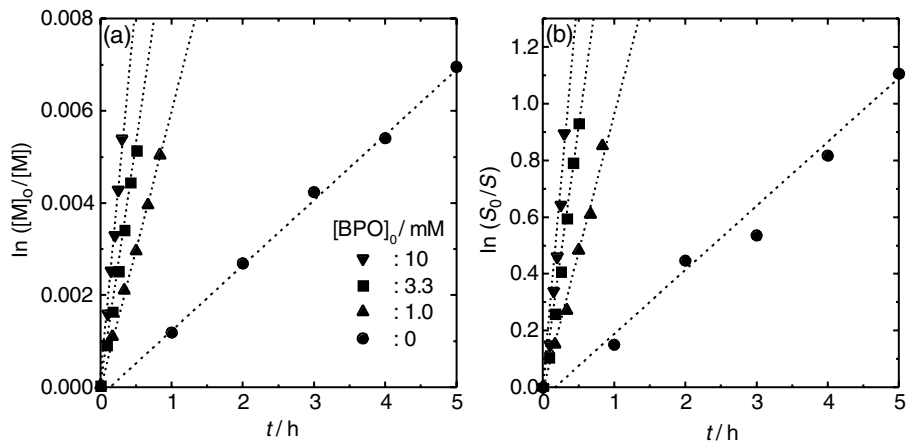
Figure 9.20   Plots of (a) $\ln([M]_0/[M])$ and (b) $\ln(S_0/S)$ versus t for the PS–SCSCH$_3$ (P$_0$–X)/ styrene mixture with different BPO concentrations heated at 80°C: $[P_0–X]_0 = 0.45$ mM; $[BPO]_0$ as indicated in Fig. 9.20a.

transfer occurring directly to the C—S bond, but this process, if any occurs, is difficult to kinetically distinguish from the RAFT process. On the other hand, the RAFT process was confirmed by the ESR observations of the intermediate radicals.[61]) The slope of the line in Fig. 9.21 gives C_{ex} ($= k_{ex}/k_p$) $= 180$. For this homopolymerization system starting with the polymeric adduct, we may put A $=$ B in Eqs. (9.55) and (9.56) to obtain

$$k_{ex} = \frac{1}{2} k_{ad} \tag{9.58}$$
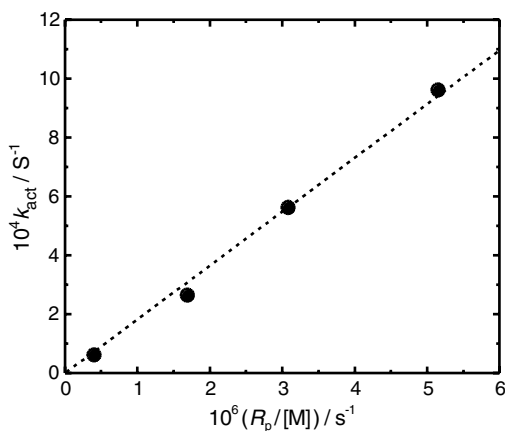
Figure 9.21   Plot of k_{act} versus $(R_p/[M])$ for the styrene/PS–SCSCH$_3$ system: by the direct (curve-resolution) method (data from Fig. 9.20).
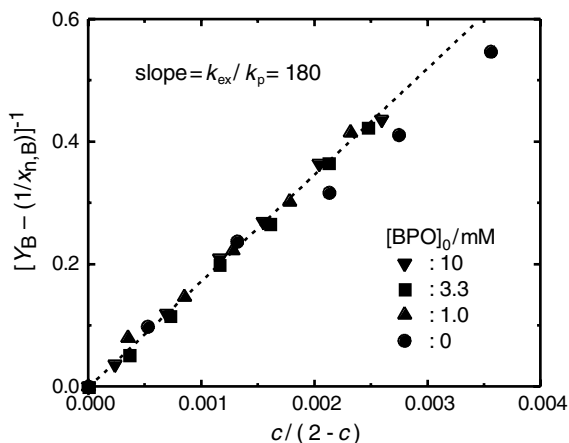
Figure 9.22   Plot of $[Y_B - (1/x_{n,B})]^{-1}$ versus $c/(2 - c)$ (60°C) for the styrene/PS–SCSCH$_3$(P$_0$–X) system: $[P_0–X]_0 = 0.45$ mM; $[BPO]_0$ as indicated in the figure. The three points for zero [BPO] show some deviation from the line, but the deviation is ascribed to the experimental error arising from the extremely small R_p for the BPO-free system.

With the abovementioned value of C_{ex} and the literature value of k_p, the value of k_{ad} is estimated to be 1.2×10^5 M^{-1} s^{-1} (60°C).

The constancy of the radical and polymer concentrations were met also in this system, and therefore the PDI of the produced polymer should obey Eq. (9.54). Figure 9.22 confirms this.

9.3.3.2.2 Other Dithiocarbonate-Mediated Polymerizations The k_{act} in the polymerization of styrene with a polystyryl dithiobenzoate (PS-SCSPh) was too large to be determined with a similar precision, but the GPC curve-resolution and polydispersity analyses provided a crude estimate of $C_{ex} = 6000 \pm 2000$ at 40°C.[60] This value is more than 30 times larger than the acetate value given above, demonstrating a large effect of the ester group on the RAFT moiety. This C_{ex} value corresponds to a k_{ad} value of about 2×10^6 M^{-1} s^{-1} (40°C), an extremely large value for an addition reaction, perhaps near the "diffusion-controlled" region.

The polymerization of MMA with a PMMA-SCSPh adduct was similarly studied to give $C_{ex} = 140$ at 60°C.[60] Comparison with the styrene/PS-SCSPh system shows a large effect of the polymer (alkyl) moiety, as well as the carbonate moiety, on k_{act}. It was also shown that the RAFT process is virtually the only mechanism of activation in the MMA system, too.

9.3.3.2.3 Comments on Copolymerizations The exchange constant (the degenerative chain transfer constant) C_{exAB} defined by $C_{exAB} = k_{exAB}/k_{pA}$, where k_{pA} is the k_p of the homopolymerization of monomer A, was determined for several systems related to styrene, MMA, and dithioacetate.[62] Now referring to Eqs. (9.55),

(9.56), and (9.58), we find

$$\frac{C_{\text{exAB}}}{C_{\text{exAA}}} = 2P_{\text{rB}}\left(\frac{k_{\text{adAB}}}{k_{\text{adAA}}}\right) \tag{9.59}$$

The experimental results (Table 9.6) shows that $C_{\text{exAB}}/C_{\text{exAA}} = 1.9$, where A and B are styrene and MMA, respectively. Since the rate constant of addition reaction should not strongly depend on the polymer (alkyl) moiety that is far apart from the C=S bond, we may assume that $k_{\text{adAB}}/k_{\text{adAA}}$ is approximately one. Hence we estimate that $P_{\text{rB}} \sim 0.95$. This estimate is supported by the other set of experimental data showing that $C_{\text{exBA}}/C_{\text{exBB}} = 0.02$, from which we estimate that $P_{\text{rA}} \sim 0.01$ or $P_{\text{rB}} = 1 - P_{\text{rA}} \sim 0.99$. In any case, fragmentation of the intermediated $P_A-(X^{\bullet})-P_B$ predominantly occurs by releasing $P_B^{\bullet}$ (PMMA radical) rather than $P_A^{\bullet}$ (PS radical). This explains why the polymerization (block copolymerization) of MMA with a PS-dithiocarbonate macroinitiator is not so satisfactory[63] as the block copolymerization of styrene with a PMMA macroinitiator.

More recent work from our laboratory on the random (statistical) copolymerization of styrene and MMA mediated by the dithioacetate suggests a pronounced penultimate unit effect[64,65] in the addition process, not in fragmentation (see Section 9.4).[62]

9.3.3.2.4 *Comments on the Intermediate Radicals*   Equation (9.57) reduces to Eq. (9.60), when P_A and P_B are kinetically identical.

$$[P-(X^{\bullet})-P] = \frac{k_{\text{ad}}}{k_{\text{fr}}}[P-X][P^{\bullet}] \tag{9.60}$$

Comparison of the homopolymerization of styrene and MMA mediated by the dithiocarbonates revealed that k_{ad} (styrene) $> k_{\text{ad}}$ (MMA). It was also indicated that k_{fr} (MMA) $\gg k_{\text{fr}}$ (styrene) (see above). Hence we expect from Eq. (9.60) that the inequality

$$[PS-(X^{\bullet})-PS] \gg [PMMA-(X^{\bullet})-PMMA] \tag{9.61}$$

holds, when comparison is made in the same conditions. Consistently, the intermediate radical for a styrene system was clearly detected by ESR, while that for a n-butyl methacrylate system was undetectable.[61]

The presence of a high concentration of intermediate radical can have significant effects on the polymerization kinetics as well as the structure of the product. If the initiation from the intermediate radical occurs fast enough, it will little affect the polymerization rate but can produce a three-armed star chain. If the intermediate radical undergoes termination with the propagating (or the primary) radical, it can retard the polymerization as well as produce a three-armed (or a double-mass) polymer. A model experiment (without monomer) has indicated the production of a triple-mass polymer, presumably by the reaction of PS–(X$^{\bullet}$)–PS and PS$^{\bullet}$ radicals.[64]

More recently, a triple-mass product was directly detected in a model polymerization run.[101] The marked decrease in R_p observed for increasing concentration of RAFT agent was interpreted in terms of the mentioned termination reaction.[65,101]

9.4   SUMMARY ON ACTIVATION AND DEACTIVATION RATE CONSTANTS

9.4.1   Low-Mass Model Adducts

Low-mass compounds such as shown in Figs. 9.3a and 9.3b have been studied with their activation/deactivation processes, and some of them are actually used as an efficient initiator of LRP. The activation and deactivation rate constants in such low-mass model systems may or may not be similar to those in homologous polymer systems, which should be experimentally established.

9.4.1.1   Activation Rate Constants for Low-Mass Alkoxyamines   Methods useful to determine the k_{act} of a low-mass alkoxyamine (R–X) (see Tables 9.1 and 9.2) are based on a common concept. Namely, the alkyl radical R$^\bullet$ formed by the activation of R–X is scavenged by a chemical agent, such as a different nitroxide (X′$^\bullet$),[66–70] oxygen,[44,70–73] or deuterated styrene,[74] and the decay of the R–X concentration is followed. A large excess of scavenger will prevent the reformation of R–X by cross-combination of the radicals, thus allowing the determination of k_{act} in a pseudo-first-order condition.

In the nitroxide exchanging method, which uses a nitroxyl radical X′$^\bullet$ as a scavenger, R–X is separated from other species and quantified by high-performance liquid chromatography (HPLC). By this method, Moad et al.[66,67] first determined the half-lives $t_{1/2}$ ($= \ln 2/k_{act}$) of various alkoxyamines, and demonstrated that k_{act} increases with an increase of the ring size for the cyclic nitroxides and that the alkoxyamines based on an open-chain nitroxide (e.g., **4**), give the largest k_{act} values. They also noted that an increase of the solvent polarity enhances the

TABLE 9.1   Half-Life Times $t_{1/2}$ of Low-Mass Model Alkoxyamines

Alkoxyamine	Solvent	$t_{1/2}$ (min)	T (°C)	Ref.
1	Hexane	38	110	67
1	Ethyl acetate	33	60	67
1	Methanol	17	110	67
2	Ethyl acetate	>1000	110	67
3	Ethyl acetate	400	80	67
4	Ethyl acetate	70	60	67
6	Styrene (in bulk)	5 ∼ 10	60	74
7	Styrene (in bulk)	150	60	74
18	Styrene (in bulk)	>300	60	74

TABLE 9.2   Arrhenius Parameters for k_{act} of Low-Mass Model Alkoxyamines

Alkoxyamine	Solvent	A_{act} (s^{-1})	E_{act} (kJ/mol)	Ref.
5	Cyclohexane	1.0×10^{14}	114	68
5	t-Butylbenzene	1.3×10^{14}	114.4	69
5	t-Butylbenzene	2.0×10^{14}	115.7	44
6	Cyclohexane	5.0×10^{13}	129	68
6	t-Butylbenzene	2.5×10^{14}	133.0	44
7	Cyclohexane	4.0×10^{13}	137	68
7	t-Butylbenzene	2.6×10^{14}	145.7	44
7	t-Butylbenzene	7.1×10^{11}	99	73
8	Toluene	1.1×10^{14}	133.2	70
8	Toluene	9.1×10^{14}	138.8	70
9	Chlorobenzene	6.3×10^{14}	102.6	71
10	Cyclohexane	1.1×10^{9}	92.1	71
10	Methanol	1.2×10^{11}	96.3	71
11	t-Butylbenzene	2.2×10^{14}	121.8	44
12	t-Butylbenzene	1.9×10^{14}	124.5	44
13	t-Butylbenzene	1.0×10^{14}	139.0	44
14	Xylene	—	130	72
15	Xylene	—	113	72
16	t-Butylbenzene	5.8×10^{10}	97	73
17	t-Butylbenzene	2.5×10^{10}	99	73

activation of alkoxyamines. Subsequently other groups employed this method to examine **5–8**.[68–70] The systematic study on **5–7** due to Scaiano et al.[68] clearly showed that the strength of the C—O bond largely depends on the steric hindrance of the alkyl moiety. In the method using oxygen as a scavenger, which is due to Howard et al.[71] and Bon et al.,[70] the alkyl radical reacts with oxygen to generate a peroxide ROOR, and the released X$^{\bullet}$ is monitored by electron spin resonance (ESR). By this method, Fischer et al.[44] examined a variety of alkoxyamines including **5–7** and **11–13**, and provided comprehensive information on k_{act}. The third method, which uses deuterated styrene as a scavenger, was proposed by Hawker et al.,[74] who determined the $t_{1/2}$ of **6**, **7**, and **18** by chasing the decay of R–X by proton magnetic resonance (^{1}H NMR).

Aside from these experimental studies, some groups have carried out semiempirical molecular orbital calculations.[67,75,76] These calculations can provide a qualitative prediction of k_{act} that is consistent with the experimentally observed trend.

9.4.1.2 Activation Rate Constants for Other Low-Mass Compounds

The k_{a} values have been determined for low-mass alkyl halide initiators in copper-catalyzed ATRP (see Tables 9.3 and 9.4). The first determination of k_{a} was due to Pascual et al.,[58] who examined the polymerization of styrene in the presence of **20** and Cu(I)Cl/2,2-bipyridine complex and followed the consumption of **20** by using vapor-phase chromatography. Fukuda et al.[51] examined **20–22** with dHbipy as a ligand,

TABLE 9.3 k_a of Low-Mass Model Alkyl Halides in Copper-Catalyzed ATRP

Alkyl Halide	CuX	Ligand	Solvent	k_a (M^{-1} s^{-1})	T (°C)	Ref.
20	CuCl	bipy	Styrene (in bulk)	0.020	110	58
20	CuCl	dHbipy	Toluene	0.018	110	51
20	CuBr	dHbipy	Toluene	0.010	110	51
21	CuBr	dHbipy	Toluene	0.42[a]	110	51
21	CuCl	dHbipy	Toluene	0.52	110	51
21	CuBr	TERPY	Acetonitrile	0.42	35	77
21	CuBr	PMDETA	Acetonitrile	0.10	35	77
21	CuBr	DOIP	Acetonitrile	0.014	35	77
22	CuBr	dHbipy	Toluene	0.18	110	51
22	CuBr	PMDETA	Acetonitrile	0.13	35	77
23	CuBr	PMDETA	Acetonitrile	0.15	35	77
24	CuBr	PMDETA	Acetonitrile	1.8	35	77

[a] k_a (M^{-1} s^{-1}) $= 2.2 \times 10^5$ exp(-42.1 kJ/mol/RT).

observing the strong dependence of k_a on the kinds of halogen and the steric factors of the alkyl group. The method used by them is analogous to the nitroxide exchanging method described above, where a nitroxide is used as a scavenger in the activation of an alkyl halide initiator and the decay of the alkyl halide concentration is chased by ^{1}H NMR. Matyjaszewski et al.[77] used this method along with HPLC to make systematic studies on **21**–**24** with various tridentate ligands, and clearly demonstrated the importance of the structures of ligands on k_a.

In the RAFT system, Moad et al.[78] determined the degenerative chain transfer constants C_{ex} ($= k_{ex}/k_p$) of various low-mass dithioester compounds by following the relative rates of consumption of transfer agent and monomer. They showed that C_{ex} of dithioesters (-SCSZ) decreases in the order of (Z =) aryl > alkyl > alkoxy > dialkylamino and that the steric factor of the alkyl leaving group is fairly important in determining C_{ex}.

9.4.1.3   Deactivation Rate Constants in Low-Mass Model Systems   The k_c values between nitroxides and low-mass alkyl radicals (Fig. 9.23; see also Table 9.5) have

TABLE 9.4 C_{ex} of Low-Mass Model Dithioester Compounds

Dithioester Compound	Monomer	C_{ex}	T (°C)	Ref.
25	Styrene	26	110	78
25	MMA	0.03	60	78
26	Styrene	10	110	78
27	Styrene	0.72	110	78
28	Styrene	0.01	80	78
29	MMA	0.16	60	78
30	MMA	10	60	78
31	MMA	2	60	78
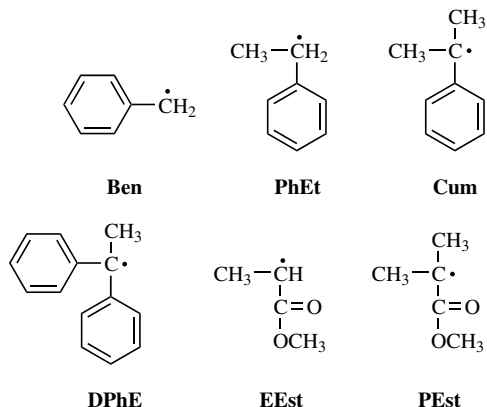
Figure 9.23 Examples of low-mass alkyl radicals.

been determined by the laser flash photolysis technique.[69,79–86] Ingold et al. performed systematic studies on k_c, showing that k_c decreases with an increase of the steric hindrance of both nitroxides and alkyl radicals,[81] and that solvents also affect k_c depending on their ability to solvate the nitroxide.[82] Scaiano et al.[83,84] examined

TABLE 9.5 Deactivation Rate Constants for Low-Mass Model Adducts[a]

	Alkyl Radical	Deactivator	Solvent	$10^{-7}k_c$ (k_{da}) ($M^{-1} s^{-1}$)	$T(°C)$	Ref.
1.	Ben	TEMPO	Isooctane	48 ± 8	18	81
2.	Ben	TEMPO	THF	23 ± 3	18	82
3.	Ben	TEMPO	THF	21	RT[b]	83
4.	Ben	TEMPO	Methanol	13 ± 1	18	82
5.	Ben	TEMPO	t-Butylbenzene	35	120	85
6.	PhEt	TEMPO	Isooctane	16 ± 4	18	81
7.	PhEt	TEMPO	Acetonitrile	13	RT[b]	84
8.	PhEt	TEMPO	t-Butylbenzene	25	120	85
9.	Cum	TEMPO	Isooctane	11.8 ± 0.1	18	81
10.	Cum	TEMPO	t-Butylbenzene	5.5	120	85
11.	DPhE	TEMPO	Isooctane	4.63 ± 0.02	18	81
12.	EEst	TEMPO	Acetonitrile	200	RT[b]	84
13.	PEst	TEMPO	Acetonitrile	25	120	85
14.	Ben	DBN	Isooctane	46 ± 2	18	81
15.	Ben	DBN	t-Butylbenzene	21	120	85
16.	PhEt	TIPNO	t-Butylbenzene	0.82	120	85
17.	PhEt	DEPN	t-Butylbenzene	0.46	120	85
18.	PhEt	CuBr$_2$/PMDETA	Acetonitrile	0.61	35	77
19.	PhEt	CuBr$_2$/DOIP	Acetonitrile	0.31	35	77
20.	PhEt	CuBr$_2$/TERPY	Acetonitrile	0.041	35	77

[a] k_c for systems 1–17 and k_{da} for systems 18–20.
[b] Room temperature.

both styrenic and acrylate systems, finding an important effect of the stability of the alkyl radical on k_c. Fischer et al.[85] determined k_c as a function of temperature for various nitroxides and alkyl radicals, and observed the unusual non-Arrhenius behavior in many cases.

In ATRP, the k_{da} values between 1-phenetyl radical and Cu(II)Br$_2$ complexes with various ligands were determined by Matyjaszewski et al.,[77] in which radical trapping with TEMPO was used as a clock reaction. The combination of the alkyl radical with TEMPO is a well-calibrated radical reaction as shown above.

9.4.2 Polymer Adducts

9.4.2.1 Methods to Study Activation Processes in Polymer Systems
The methods described in Section 9.4.1.1 are useful in determining the activation rate constants of low-mass adducts but usually difficult to apply to polymer adducts. Fukuda et al.[24,35] proposed two GPC methods generally applicable to polymer adducts in all variants of LRP.

The first method[35] is based on the GPC observation of an early stage of polymerization containing a probe (initiating) polymer adduct P$_0$–X. When P$_0$–X is activated, the released polymer radical P$_0^\bullet$ will propagate until it is deactivated by X$^\bullet$ to give a new adduct P$_1$–X, where the subscript 1 denotes one activation–deactivation cycle. Since P$_0$–X and P$_1$–X (or a mixture of P$_1$–X and other minor components) are generally different in chain length and its distribution, they may be distinguishable by GPC. By following the decay of the P$_0$–X concentration, k_{act} can be determined from the first-order plot

$$\ln\frac{S_0}{S} = k_{act}t \tag{9.62}$$

where S_0 and S are the concentrations or GPC peak areas of P$_0$–X at time zero and t, respectively. In usual experimental conditions of LRP, however, the difference between P$_0$–X and P$_1$–X may not be large enough to allow accurate resolution of the GPC curve for this purpose. A general method to increase this difference will be to decrease the rate of deactivation so that more monomers are added during a transient lifetime. In the nitroxide-mediated LRP, for example, this can be achieved by intentionally decreasing the equilibrium concentration of X$^\bullet$ (or equivalently increasing that of P$^\bullet$) by, for example, the addition of a conventional initiator. A lower initial concentration of P$_0$–X is also effective to decrease the concentrations of the deactivating species. This method is free from any kinetic details, other than the existence of activation and propagation reactions, and for this reason, it is termed the direct method.

The second approach[24] is based on the use of GPC to follow the change in polydispersity. It focuses on an early stage of polymerization started with a P$_0$–X, and analyzes the polydispersity of the product polymer on the basis of Eq. (9.43) with Eq. (9.45) or (9.46). Prerequisites for Eq. (9.43) to be valid are the constancy of [P$^\bullet$] and the number of chains [N_p], while those for Eq. (9.46) to be valid are the

TABLE 9.6   Activation Rate Constants of Polymer Adducts

	P–X	Monomer (Solvent)[a]	$10^3 k_{act}$ (s^{-1})	T(°C)	Ref.
1.	PS-TEMPO (**32**)	Styrene	1.0	120	35
2.	PS-TEMPO (**32**)	Toluene	1.9	120	70
3.	PS-DBN (**33**)	Styrene	42	120	43
4.	PS-DEPN (**34**)	Styrene	11	120	43
5.	PS-DEPN (**34**)	Styrene	3.4	120	34
6.	PtBA-DBN (**35**)	tBA	1.0	120	46
7.	PBA-DEPN (**36**)	BA	7.1	120	34
8.	PMA-Co/Porphyrin (**37**)	MA	4.0 ± 2.0	25	87
9.	PS-I (**38**)	Styrene	0.22^{b}	80	59
			($C_{ex} = 3.6$)		
10.	PS-SCSCH$_3$ (**39**)	Styrene	13^{b}	40	60
			($C_{ex} = 220$)		
11.	PS-SCSCH$_3$ (**39**)	MMA	0.050^{b}	40	62
			($C_{ex} = 0.83$)		
12.	PS-SCSCH$_3$ (**39**)	Styrene/MMA[c]	4.5^{b}	40	62
			($C_{ex} = 75$)		
13.	PMMA-SCSCH$_3$ (**40**)	Styrene	25^{b}	40	62
			($C_{ex} = 420$)		
14.	PMMA-SCSCH$_3$ (**40**)	MMA	2.4^{b}	40	62
			($C_{ex} = 40$)		
15.	PMMA-SCSCH$_3$ (**40**)	Styrene/MMA[c]	9.0^{b}	40	62
			($C_{ex} = 150$)		
16.	PS-SCSPh (**41**)	Styrene	360 ± 120^{b}	40	60
			($C_{ex} = 6000 \pm 2000$)		
17.	PMMA-SCSPh (**42**)	MMA	8.4^{b}	60	60
			($C_{ex} = 140$)		
18.	PS-co-PMMA-SCSPh (**43**)[d]	Styrene/MMA[c]	48^{b}	60	62
			($C_{ex} = 800$)		
19.	PMMA-macromonomer (**44**)	MMA	0.013^{b}	80	88
			($C_{ex} = 0.22$)		
20.	PS-Br (**45**)/CuBr/dHpipy	Styrene	23^{b}	110	49
			($k_a = 0.45$ M^{-1} s^{-1})		
21.	PS-Br (**45**)/CuBr/dHpipy	Xylene	$22^{b,e}$	110	50
			($k_a = 0.43$ M^{-1} s^{-1})		
22.	PS-Br (**45**)/CuBr/dHpipy	MMA	15^{b}	110	89
			($k_a = 0.30$ M^{-1} s^{-1})		
23.	PBA-Br (**46**)/CuBr/dHpipy	Xylene	$3.6^{b,e}$	110	50
			($k_a = 0.071$ M^{-1} s^{-1})		

[a] tBA is *t*-butyl acrylate, BA is *n*-butyl acrylate, MA is methyl acrylate, and MMA is methyl methacrylate.

[b] Value approximately estimated for $R_p = 4.8 \times 10^{-4}$ M/s. (Systems 1–8 are independent of R_p.)

[c] Mole fraction of styrene is 0.53 (azeotropic composition).

[d] Random copolymer of styrene and MMA with mole fraction of styrene unit of 0.53 (azeotropic composition).

[e] A strong solvent dependence was observed.[50]

constancy of $[N_p]$ and the power-law decay of $[P^•]$ [Eq. (9.20)]. This method, there-fore, depends on the accuracy of the theory and GPC and other kinetic details. For this reason, this method may be better used to prove or disprove the kinetic model, until its validity is established. Quite a little experimental evidence showing the validity of this method for constant-$[P^•]$ systems was presented in Section 9.3.

9.4.2.2 Activation Rate Constants for Polymer Adducts

Table 9.6 lists the values of k_{act}, C_{ex} $(= k_{ex}/k_p)$, and k_a for polymer adducts (see also Table 9.7).[34,35,43,46,49,50,59,60,62,70,87–89] Since the k_{act} for systems **9–23** is proportional to the polymerization rate R_p, the listed values for those systems are referred to a standard value of $R_p = 4.8 \times 10^{-4}$ M/s, while the k_{act} for the other systems is independent of R_p. The results show that the magnitude of k_{act} largely differs from system to system. In comparison among the nitroxide systems **1–5**, TEMPO, DBN, and DEPN attached to the same polymer (PS) give large differences in k_{act}. The open-chain nitroxides DBN and DEPN give larger k_{act} than does the less bulky ring-chain nitroxide TEMPO, meaning that steric factors are important. Also notably, DBN gives a larger k_{act} than DEPN (at 120°C) although the latter has a much bulkier side group than the former. This implies that the electron-withdrawing phosphonate group in DEPN gives an important effect on k_{act}. Thus electronic factors also impart significant contribution on k_{act}.

Comparison of the k_{act} values of the polymer adducts **32–34** (particularly systems **1**, **3**, and **5**) with those of the low-mass analog **6**, **11**, and **12** shows that the k_{act} of the former is larger than that of the latter by a factor of 2–3, stressing the importance of the effect of chain length. Such a polymer effect is even more pronounced in the RAFT system, where the C_{ex} of the polymer adduct **40** is 20 times larger than that of the low-mass homolog **31**. On the other hand, for the CuBr/dHbipy-catalyzed ATRP system, the k_a of polymer adduct **45** (0.45 M^{-1} s^{-1}) is close to that of the corresponding low-mass adduct **21** (0.42 M^{-1} s^{-1}), suggesting that k_a is nearly

TABLE 9.7   Arrhenius Parameters for k_d and k_{ex} of Polymer Adducts[a]

	P–X	Monomer (Solvent)	A_d (A_{ex})[b]	E_d (E_{ex}) (kJ/mol)	Ref.
1.	PS-TEMPO (**32**)	Styrene	3.0×10^{13}	124	35
2.	PS-TEMPO (**32**)	Toluene	1.0×10^{16}	141	70
3.	PS-DBN (**33**)	Styrene	3.8×10^{14}	120	43
4.	PS-DEPN (**34**)	Styrene	2.0×10^{15}	130	43
5.	PS-DEPN (**34**)	Styrene	1.0×10^{14}	121	34
6.	PBA-DEPN (**36**)	BA	1.7×10^{15}	130	34
7.	PS-I (**38**)	Styrene	3.1×10^{7}	27.8	59
8.	PS-SCSCH$_3$ (**39**)	Styrene	1.3×10^{8}	21.0	60
9.	PMMA-macromonomer (**42**)	MMA	2.2×10^{6}	26.2	88

[a] k_d for systems 1–6 and k_{ex} for systems 7–9.
[b] A_d and A_{ex} are in the unit of s^{-1} and M^{-1} s^{-1}, respectively.

independent of chain length. In this way, the importance of the chain length of alkyl moiety on k_{act} varies from system to system.

According to Table 9.6, the DBN-mediated polymerization of t-butyl acrylate (tBA) may be as well controlled as the TEMPO-mediated polymerization of styrene. Actually, however, the thermal degradation of the active chain end of PtBA-DBN occurs rather seriously at high temperature, not allowing the polydispersity to be lowered as in the TEMPO/styrene system.[46] Clearly, a large k_{act} is a necessary but not a sufficient condition for a high-performance living radical polymerization.

The k_{act} value for the RAFT-based system 16 with PS-SCSPh is surprisingly large, about 30 times larger than those for the system 10 with PS-SCSCH$_3$ and the system 17 with PMMA-SCSPh, showing that the RAFT velocity is strongly dependent on the structures of the dithiocarbonate group and the alkyl (polymer) moiety. Since the polymer moiety in the adduct is apart from the C=S double bond, it would have little influence on the addition of P$^\bullet$. On this assumption, it can be deduced from the results for the homo- and block copolymerization systems that PMMA$^\bullet$ undergoes a $\sim\frac{1}{2}$ times slower addition and a $\sim$100 times faster fragmentation than does PS$^\bullet$. The random copolymerization of styrene and MMA leads to the indication that P$^\bullet_{21}$ undergoes a ($\sim$0.3 times) slower addition than P$^\bullet_{11}$, while fragmentation occurs at almost the same rate for the two radicals, where P$^\bullet_{ij}$ is the propagating radical with the terminal unit j and the penultimate unit i [$i, j =$ styrene(1) or MMA(2)]. This means that there is a significant penultimate unit effect on the RAFT process in the styrene/MMA system, which is strong in the addition process, rather than in the fragmentation process.

The k_{act} value for the ATRP system 20 is also large enough to account for the experimental observations that the system provides low-polydispersity polymers even *from an early stage of polymerization*.[52] The results for systems 20–23 suggest that the polarity of solvents and the kind of polymers give important effects on k_a.

9.4.2.3 Deactivation Rate Constants for Polymer Adducts

The deactivation rate constant (see Table 9.8) can be calculated if k_{act} and K (or K_{AT}) are known. In some nitroxide systems, K was estimated, for instance, by following the concentration of

TABLE 9.8   Deactivation Rate Constants for Polymer Adducts [a]

	P$^\bullet$	Deactivator	Monomer	$10^{-7} k_c$ (k_{da}) (M^{-1} s^{-1})	T (°C)	Ref.
1.	PS$^\bullet$	TEMPO	Styrene	7.6[b]	125	35
2.	PS$^\bullet$	DEPN	Styrene	0.057[c]	120	34
3.	PS$^\bullet$	DEPN	Styrene	0.18[d]	120	34,43
4.	PBA$^\bullet$	DEPN	BA	4.2[e]	120	34
5.	PS$^\bullet$	CuBr$_2$/dHbipy	Styrene	1.1[f]	110	49

[a] k_c for systems 1–4 and k_{da} for system 5.
[b] Calculated with $K = 2.1 \times 10^{-11}$ M and $k_d = 1.6 \times 10^{-3}$ s^{-1}.
[c] Calculated with $K = 6.0 \times 10^{-9}$ M and $k_d = 3.4 \times 10^{-3}$ s^{-1}.
[d] Calculated with $K = 6.0 \times 10^{-9}$ M and $k_d = 1.1 \times 10^{-2}$ s^{-1}.[34,43]
[e] Calculated with $K = 1.7 \times 10^{-10}$ M and $k_d = 7.1 \times 10^{-3}$ s^{-1}.
[f] Calculated with $K_{AT} = 3.9 \times 10^{-8}$ and $k_a = 0.45$ M^{-1} s^{-1}.

the nitroxide by ESR and R_p.[18,34,41,90–92] The k_c value thus obtained for the PS-TEMPO combination is 7.6×10^7 M^{-1} s^{-1} at 125°C.[25] This value is about one-third that for the low-mass counterpart (16 ± 4 or 25), while it reasonably compares to those between TEMPO and radicals such as diphenylmethyl (4.63 ± 0.02) and 2-naphthylmethyl (5.7 ± 1.8),[81] where the values in parentheses are k_c in units of 10^7 M^{-1} s^{-1}. This clearly shows the strong chain length dependence on k_c due to the steric hindrance of a polystyryl radical. Such a polymer effect on k_c is more apparent for the PS-DEPN combination due to the bulkiness of DEPN.[34] A deactivation rate constant is also available for an ATRP system.[49]

9.5 CONCLUSIONS

Fundamental kinetic features of LRP were discussed. The heart of LRP is the reversible activation of the dormant species P–X (or reversible deactivation of the active species P$^\bullet$). A prerequisite for LRP is therefore the establishment of the quasiequilibrium

$$k_{act}[\text{P–X}] = k_{deact}[\text{P}^\bullet] \tag{9.63}$$

in a major part of the polymerization run ("quasi"equilibrium, because the components may change their concentrations in a longer timescale). A further prerequisite for LRP to provide a low-polydispersity polymer is a fast exchange or a sufficiently large number of activation–deactivation cycles to be experienced by every chain during the polymerization time t. Since this number is given by $k_{act} \times t$, and t is limited in practical applications, the pseudo-first-order rate constant k_{act} has to be sufficiently large. Another practically important requirement is the achievement of a high conversion in the limited time range. In other words, [P$^\bullet$] has to be sufficiently large, but, of course, not so large as to produce an important fraction of bimolecularly terminated chains. It follows that, given k_{act} and [P–X], the desirable range of k_{deact} is limited.

In SFR-mediated polymerization and ATRP with given values of k_{act} and [P–X]$_0$, the value of k_{deact} (or [P$^\bullet$]) is self-adjusted by PRE, producing characteristic time–conversion curves depending on the magnitude of conventional initiation R_i and/or the initial concentration of deactivator [D]$_0$ ($=$ [X$^\bullet$]$_0$ or [AX$^\bullet$]$_0$). Existing examples of successful LRPs were in fact found to be characterized by a sufficiently large k_{act} and a sufficiently large R_p. The stationary-state kinetics expectable for systems with a relatively large R_i was experimentally confirmed with respect to both R_p and PDI. The power-law kinetics expectable for systems with zero or small R_i was also confirmed in part, but awaits more experimental investigation. In particular, the kinetics of ATRP was found complex, not allowing simple descriptions based on the power-law kinetics.

Since k_{deact} is proportional to the deactivator concentration [D], it could be controlled by externally controlling [D]. Addition of a conventional initiator for NMP[23,93,94] and ATRP,[49] of an acid for NMP,[95–97] and of metallic copper Cu(0)

for ATRP[98] were found to be effective in decreasing the equilibrium concentration of D, even though the work of some acid[99] for NMP is not well understood.[100] The direct addition of D would be useful to adjust [D],[34,48,52] if the amount to be added is known and controllable, for which kinetic knowledge is indispensable.

In DT-mediated polymerization, the equilibrium always holds, and a sufficiently large C_{ex} $(= k_{ex}/k_p)$ is the only requirement for yielding low-polydispersity polymers. This polymerization, initiated and maintained by a conventional initiation, was confirmed to follow stationary-state kinetics with respect to both R_p and PDI. (The intermediate radicals in RAFT systems need be kinetically characterized, and their roles need be understood, more comprehensively.)

Now that the LRPs of a majority of conjugated monomers have been realized, a next big target will be those of unconjugated monomers. Systematic investigations into LRP kinetics would hopefully be useful to design more powerful SFRs, ATRP catalysts, and/or RAFT agents that are applicable even to unconjugated monomers.

9.6   ABBREVIATIONS

A	activator in ATRP (Scheme 9.2)
AX$^\bullet$	deactivator in ATRP (Scheme 9.2)
b	reduced rate of initiation [Eq. (9.13)]
c	fractional monomer conversion
C_{ex}	degenerative chain transfer constant ($C_{ex} = k_{ex}/k_p$)
D	deactivator
E_{dec}	activation energy of decomposition
E_d	activation energy of dissociation
E_{abs}	activation energy of β-proton abstraction
$F(c)$	function defined by Eq. (9.32) for a stationary-state system
$G(c)$	function defined by Eq. (9.47) for a power-law system
I_0	initial concentration of dormant species ($I_0 = [P–X]_0 = [P_0–X]_0$)
K	equilibrium constant ($K = k_d/k_c$)
k_a	activation rate constant in ATRP (Scheme 9.2)
K_{AT}	equilibrium constant in ATRP ($K_{AT} = k_a/k_{da}$)
k_{act}	pseudo-first-order activation rate constant (Scheme 9.1)
k_{ad}	addition rate constant in the RAFT process
k_c	combination rate constant (Scheme 9.2)
k_d	dissociation rate constant (Scheme 9.2)
k_{da}	deactivation rate constant in ATRP (Scheme 9.2)
k_{deact}	pseudo-first-order deactivation rate constant (Scheme 9.1)
k_{ex}	degenerative chain transfer rate constant (Scheme 9.2)
k_{fr}	fragmentation rate constant in the RAFT process
k_p	propagation rate constant
k_t	termination rate constant
L	ligand
M_n	number average molecular weight

M_w	weight average molecular weight
$[N_p]$	number density of polymer
p	probability of addition [Eq. (9.25)]
$P^\bullet$	polymer radical
PDI	polydispersity index (PDI $= x_w/x_n$)
DP	degree of polymerization
DP_n	number average degree of polymerization ($= x_n$)
$P^\bullet_{ij}$	polymer radical with the terminal unit j and the penultimate unit i
P_r	probability of fragmentation [Eq. (9.56)]
P–X	dormant species
P_0–X	initiating dormant species
R_i	(conventional) initiation rate
R_p	propagation rate
t_{cross}	cross-over time [Eq. (9.22)]
$t_{1/2}$	half-life time
τ	transient lifetime ($= k_{deact}^{-1}$)
u	variable defined by Eqs. (9.38) and (9.48)
w_K	weight fraction of the subchain K ($K =$ A or B) [Eq. (9.43)]
$X^\bullet$	stable free radical
x_n	number average degree of polymerization
x_w	weight average degree of polymerization
Y	polydispersity factor ($Y = x_w/x_n - 1$)
y_n	average number of activation–deactivation cycles ($y_n = k_{act}t$)
z	reduced stable-radical concentration [Eq. (9.12)]

REFERENCES

1. K. Matyjaszewski, ed., *ACS Symp. Ser.* **685** (1998); **768** (2000).

2. K. Matyjaszewski, *Chem. Eur. J.* **5**, 3095 (1999).

3. E. E. Malmström and C. J. Hawker, *Macromol. Chem. Phys.* **199**, 923 (1998).

4. M. Sawamoto and M. Kamigaito, *CHEMTECH* **9**(6), 30 (1999).

5. D. Colombani, *Prog. Polym. Sci.* **22**, 1649 (1997).

6. B. Quiclet-Sire and S. Z. Zard, *Pure Appl. Chem.* **69**, 645 (1997).

7. T. Otsu and A. Matsumoto, *Adv. Polym. Sci.* **136**, 75 (1998).

8. T. Fukuda and A. Goto, *ACS Symp. Ser.* **768**, 27 (2000).

9. T. Fukuda, A. Goto, and K. Ohno, *Macromol. Rapid Commun.* **21**, 151 (2000).

10. T. Fukuda, A. Goto, K. Ohno, and Y. Tsujii, *ACS Symp. Ser.* **685**, 180 (1998).

11. M. K. Georges, R. P. N. Veregin, P. M. Kazmaier, and G. K. Hamer, *Macromolecules* **26**, 2987 (1993).

12. J. Xia and K. Matyjaszewski, *Macromolecules* **30**, 7692 (1997).

13. M. J. Perkins, *J. Chem. Soc.* 5932 (1964).

14. H. Fischer, *J. Am. Chem. Soc.* **108**, 3925 (1986).

15. D. Ruegge and H. Fischer, *Int. J. Chem. Kinet.* **21**, 703 (1989).

16. E. Daikh and R. G. Finke, *J. Am. Chem. Soc.* **114**, 2939 (1992).

17. C. H. J. Johnson, G. Moad, D. H. Solomon, T. H. Spurling, and D. J. Vearing, *Aust. J. Chem.* **43**, 1215 (1990).

18. T. Fukuda, T. Terauchi, A. Goto, K. Ohno, Y. Tsujii, T. Miyamoto, S. Kobatake, and B. Yamada, *Macromolecules* **29**, 6393 (1996).

19. D. Greszta and K. Matyjaszewski, *Macromolecules* **29**, 7661 (1996).

20. H. Fischer, *Macromolecules* **30**, 5666 (1997).

21. H. Fischer, *J. Polym. Sci., Polym. Chem.* **37**, 1885 (1999).

22. M. Souaille and H. Fischer, *Macromolecules* **33**, 7378 (2000).

23. A. Goto and T. Fukuda, *Macromolecules* **30**, 4272 (1997).

24. T. Fukuda and A. Goto, *Macromol. Rapid Commun*. **18**, 683 (1997).

25. A. H. E. Müller, R. Zhuang, D. Yan, and G. Litvinenko, *Macromolecules* **28**, 4326 (1995).

26. (a) K. Matyjaszewski, *Macromol. Symp.* **111**, 47 (1996); (b) K. Matyjaszewski, *ACS Symp. Ser*. **768**, 2 (2000).

27. Y. Tsujii, T. Fukuda, and T. Miyamoto, *Polym. Prep.* (*Am. Chem. Soc. Div. Polym. Chem.*) **38**(2), 657 (1997).

28. J. He, H. Zhang, J. Chen, and Y. Yang, *Macromolecules* **30**, 8010 (1997).

29. D. A. Shipp and K. Matyjaszewski, *Macromolecules* **33**, 1553 (2000).

30. J. M. Catala, F. Bubel, and S. O. Hammouch, *Macromolecules* **28**, 8441 (1995).

31. T. Fukuda and T. Terauchi, *Chem. Lett*. 293 (1996).

32. D. Greszta and K. Matyjaszewski, *Macromolecules* **29**, 5239 (1996).

33. R. G. Gilbert, *Pure Appl. Chem*. **68**, 1491 (1996).

34. D. Benoit, S. Grimaldi, S. Robin, J.-P. Finet, P. Tordo, and Y. Gnanou, *J. Am. Chem. Soc*. **122**, 5929 (2000).

35. A. Goto, T. Terauchi, T. Fukuda, and T. Miyamoto, *Macromol. Rapid Commun*. **18**, 673 (1997).

36. A. Goto and T. Fukuda, *Macromolecules* **30**, 5183 (1997).

37. I. Li, B. A. Howell, K. Matyjaszewski, T. Shigemoto, P. B. Smith, and D. B. Priddy, *Macromolecules* **28**, 6692 (1995).

38. K. Ohno, Y. Tsujii, and T. Fukuda, *Macromolecules* **30**, 2503 (1997).

39. M. Souaille and H. Fischer, *Macromolecules* **34**, 2830 (2001).

40. K. Ohno, Y. Tsujii, T. Miyamoto, T. Fukuda, A Goto, K. Kobayashi, and A. Akaike, *Macromolecules* **31**, 1064 (1998).

41. J.-F. Lutz, P. Lacroix-Desmazes, and B. Boutevin, *Macromol. Rapid Commun*. **22**, 189 (2001).

42. A. Goto, C. Yoshikawa, and T. Fukuda, manuscript in preparation.

43. A. Goto and T. Fukuda, *Macromol. Chem. Phys*. **201**, 2138 (2000).

44. S. Marque, C. L. Mercier, P. Tordo, and H. Fischer, *Macromolecules* **33**, 4403 (2000).

45. N. A. Listigovers, M. K. Georges, P. G. Odell, and B. Keoshkerian, *Macromolecules* **29**, 8993 (1996).

46. A. Goto and T. Fukuda, *Macromolecules* **32**, 618 (1999).

47. A. A. Gridnev, *Macromolecules* **30**, 7651 (1997).

48. D. Benoit, V. Chaplinski, R. Braslau, and C. J. Hawker, *J. Am. Chem. Soc*. **121**, 3904 (1999).

49. K. Ohno, A. Goto, T. Fukuda, J. Xia, and K. Matyjaszewski, *Macromolecules* **31**, 2699 (1998).

50. G. Chambard, B. Klumperman, and A. L. German, *Macromolecules* **33**, 4417 (2000).

51. A. Goto and T. Fukuda, *Macromol. Rapid Commun*. **20**, 633 (1999).

52. K. Matyjaszewski, T. E. Patten, and J. Xia, *J. Am. Chem. Soc*. **119**, 674 (1997).

53. A. Kajiwara, K. Matyjaszewski, and M. Kamachi, *Macromolecules* **31**, 5695 (1998).

54. D. A. Shipp and K. Matyjaszewski, *Macromolecules* **32**, 2948 (1999).

55. A. Goto et al., manuscript in preparation.

56. (a) J. L. Wang, T. Grimaud, and K. Matyjaszewski, *Macromolecules* **30**, 6507 (1997); (b) K. A. Davis, H. J. Paik, and K. Matyjaszewski, *Macromolecules* **32**, 1767 (1999).

57. S. Pascual, B. Coutin, M. Tardi, A. Polton, and J.-P. Vairon, *Macromolecules* **32**, 1432 (1999).

58. S. G. Gaynor, J. S. Wang, and K. Matyjaszewski, *Macromolecules* **28**, 8051 (1995).

59. A. Goto, K. Ohno, and T. Fukuda, *Macromolecules* **31**, 2809 (1998).

60. A. Goto, K. Sato, Y. Tsujii, T. Fukuda, G. Moad, E. Rizzardo, and S. H. Thang, *Macromolecules* **34**, 402 (2001).

61. D. G. Hawthorne, G. Moad, E. Rizzardo, and S. H. Thang, *Macromolecules* **32**, 2071 (1999).

62. T. Fukuda, A. Goto, Y. Kwak, C. Yoshikawa, and Y.-D. Ma, *Macromol. Symp.*, in press (2002).

63. Y. K. Chong, T. P. T. Le, G. Moad, E. Rizzardo, and S. H. Thang, *Macromolecules* **32**, 2071 (1999).

64. H. D. Brouwer, M. A. J. Schellekens, B. Klumperman, M. J. Monteiro, and A. L. German, *J. Polym. Sci., Polym. Chem*. **38**, 3596 (2000).

65. M. J. Monteiro and H. D. Brouwer, *Macromolecules* **34**, 349 (2001).

66. D. H. Solomon, E. Rizzardo, and P. Cacioli, Eur. Patent Appl. EP135280 [*Chem. Abstr*. **102**, 221335q (1985)].

67. G. Moad and E. Rizzardo, *Macromolecules* **28**, 8722 (1995).

68. W. G. Skene, S. T. Belt, T. J. Connolly, P. Hahn, and J. C. Scaiano, *Macromolecules* **31**, 9103 (1998.).

69. T. Kothe, S. Marque, R. Martschke, M. Popov, and H. Fischer, *J. Chem. Soc., Perkin Trans.* **2**, 1553 (1998).

70. S. A. F. Bon, G. Chambard, and A. L. German, *Macromolecules* **32**, 8269 (1999).

71. D. W. Grattan, D. W. D. J. Carlsson, J. A. Howard, and D. M. Wiles, *Can. J. Chem.* **57**, 2834 (1979).

72. R. P. N. Veregin, M. K. Georges, G. K. Hamer, and P. M. Kazmaier, *Macromolecules* **28**, 4391 (1995).

73. P. Stipa, L. Greci, P. Carloni, and E. Damiani, *Polym. Degrad. Stab.* **55**, 323 (1997).

74. C. J. Hawker, G. G. Barclay, A. Orellana, J. Dao, and W. Devonport, *Macromolecules* **29**, 5245 (1996).

75. P. M. Kazmaier, K. A. Moffat, M. K. Georges, R. P. N. Veregin, and G. K. Hamer, *Macromolecules* **28**, 1841 (1995).

76. R. D. Puts, and D. Y. Sogah, *Macromolecules* **29**, 3323 (1996).

77. K. Matyjaszewski, B. Göbelt, H.-J. Paik, and C. P. Horwitz, *Macromolecules* **34**, 430 (2001).

78. G. Moad, J. Chiefari, B. Y. K. Chong, J. Krstina, R. T. A. Mayadunne, A. Postma, E. Rizzardo, and S. H. Thang, *Polym. Inter.* **49**, 993 (2000).

79. J. Chateauneuf, J. Lusztyk, and K. U. Ingold, *J. Org. Chem.* **53**, 1629 (1988).

80. A. L. J. Beckwith, V. W. Bowry, and G. Moad, *J. Org. Chem.* **53**, 1632 (1988).

81. V. W. Bowry and K. U. Ingold, *J. Am. Chem. Soc.* **114**, 4992 (1992).

82. A. L. J. Beckwith, V. W. Bowry, and K. U. Ingold, *J. Am. Chem. Soc.* **114**, 4983 (1992).

83. M. V. Baldoví, N. Mohtat, and J. C. Scaiano, *Macromolecules* **29**, 5497 (1996).

84. W. G. Skene, J. C. Scaiano, N. A. Listigovers, P. M. Kazmaier, and M. K. Georges, *Macromolecules* **33**, 5065 (2000).

85. J. Sobek, R. Martschke, and H. Fischer, *J. Am. Chem. Soc.* **123**, 2849 (2001).

86. I. W. C. E. Arends, P. Mulder K. B. Clark, and D. D. M. Wayner, *J. Phys. Chem.* **99**, 8182 (1995).

87. A. Goto, T. Fukuda, and B. B. Wayland, manuscript in preparation.

88. C. L. Moad, G. Moad, E. Rizzardo, and S. H. Thang, *Macromolecules* **29**, 7717 (1996).

89. G. Chambard and B. Klumperman, *ACS Symp. Ser.* **768**, 197 (2000).

90. R. P. N. Veregin, P. G. Odell, L. M. Michalak, and M. K. Georges, *Macromolecules* **29**, 2746 (1996).

91. P. Lacroix-Desmazes, J.-F. Lutz, and B. Boutevin, *Macromol. Chem. Phys.* **201**, 662 (2000).

92. Y. Miura, N. Nakamura, and I. Taniguchi, *Macromolecules* **34**, 447 (2001).

93. D. Greszta and K. Matyjaszewski, *J. Polym. Sci., Polym. Chem.* **35**, 1857 (1997).

94. S. O. Hammouch and J. M. Catala, *Macromol. Rapid Commun.* **17**, 683 (1996).

95. M. K. Georges, R. P. N. Veregin, P. M. Kazmaier, G. K. Hamer, and M. Saban, *Macromolecules* **27**, 7228 (1994).

96. P. G. Odell, R. P. N. Veregin, L. M. Michalak, D. Brousmiche, and M. K. Georges, *Macromolecules* **28**, 8453 (1995).

97. R. P. N. Veregin, P. G. Odell, L. M. Michalak, and M. K. Georges, *Macromolecules* **29**, 4161 (1996).

98. K. Matyjaszewski, S. Coca, S. G. Gaynor, M. Wei, and B. E. Woodworth, *Macromolecules* **30**, 7348 (1997).

99. E. Malmström, R. D. Miller, and C. J. Hawker, *Tetrahedron* **53**, 15225 (1997).

100. A. Goto, Y. Tsujii, and T. Fukuda, *Chem. Lett.* 788 (2000).

101. Y. Kwak, A. Goto, Y. Tsujii, Y. Murata, K. Komatsu, and T. Fukuda, *Macromolecules* **35**, 3026 (2002).

10 Nitroxide-Mediated Living Radical Polymerizations

CRAIG J. HAWKER

IBM Almaden Research Center, San Jose, California

CONTENTS

10.1   INTRODUCTION

10.1.1   Background

From the preceding chapters, it may be considered that radical polymerization is a mature technology with millions of tons of homopolymers and copolymers based on compounds such as styrene, acrylate, methacrylate, low-density polyethylene, and poly(vinyl chloride) produced annually. This perception is however misleading, while free-radical polymerization remains the most important industrial technology for the production of vinyl based polymeric materials this importance is due to its versatility, synthetic ease, and its compatibility with a wide variety of functional groups. A prime example is its tolerance to water and protic media, which has permitted the development of emulsion and suspension techniques, of major commercial significance at the present point in time.

It is therefore surprising to consider the contents of many of the later chapters in this book that deal with a renaissance in free-radical polymerization. Primarily this renaissance has been in the area of living free-radical procedures where major advances in the synthetic possibilities offered by these novel processes and a detailed mechanistic understanding has emerged in recent years. As detailed by Matyjaszewski in Chapter 8, the number of articles appearing in this area is increasing rapidly and was one of the most intensively studied areas in polymer science in 2001. One of the driving forces for this dramatic increase in interest has been the growing demand for functionalized, well-defined materials as building blocks in nanotechnology applications. In the preparation of well-defined macromolecules, traditional free-radical procedures have a significant drawback, which is related to the reactivity of the propagating free-radical chain end and its propensity to undergo a variety of different termination reactions. The materials obtained are therefore polydisperse with very limited control over macromolecular weight and architecture.[1] Until relatively recently, ionic polymerizations (anionic or cationic) were the only "living" techniques available that efficiently controlled the structure and architecture of vinyl polymers. Although these techniques assure low-polydispersity materials, controlled molecular weight, and defined chain ends, they are not useful for the polymerization and copolymerization of a wide range of functionalized vinylic monomers. This limitation is due to the incompatibility of the growing polymer chain end (anion or cation) with numerous functional groups and certain monomer families.[2] In addition, these polymerization techniques require stringent reaction conditions, including the use of ultrapure reagents and the total exclusion of water and oxygen. The necessity to overcome all these limitations emboldened synthetic polymer chemists to develop new concepts, which would allow for a living free-radical polymerization (LFRP) process. In addition the development of LFRP processes has opened up other areas of research that were hereto unavailable or severely restricted. A prime example is the area of block copolymers by mechanistic transformations or sequential polymerizations. One advantage of nitroxide-mediated living free-radical polymerization (NMP) is the compatibility of these systems with the stringent reaction conditions typically associated with other living polymerizations,
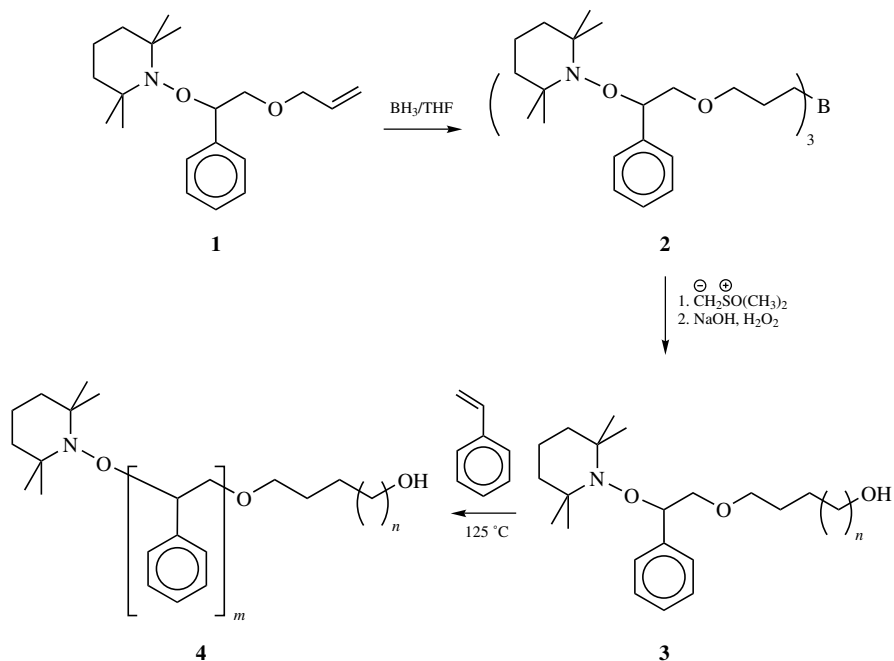
Scheme 10.1

which allows the development of dual functionalized initiators. As shown in Scheme 10.1, the alkene-terminated alkoxyamine, **1**, can be transformed into the borane derivative, **2**, which acts as an initiator for the preparation of polymethylene, **3**, and yields after the sequential living free-radical polymerization of styrene a poly (methylene-*b*-styrene) block copolymer, **4**.[3] The intriguing aspect of this material is the perfect nature of the polyethylene block, which does not contain any branches because of the nature of the ylide synthesis.[4] This is also a perfect example of the possibilities offered by LFRP and provides some justification as to why the field has witnessed explosive growth. A number of specialized reviews have been published in this general area and provide further evidence of the potential of these techniques.[5–8]

10.1.2   Scope of Review

This review covers the scientific literature from 1980 to May 2001 concerning nitroxide-mediated living free-radical polymerization. The reader should also be aware that other terms such as stable free-radical polymerization (SFRP) and controlled radical polymerization (CRP), which have been used to describe polymerizations that are mediated by nitroxides as well. Strategies for controlling polymeric structure and macromolecular architecture will be discussed in detail, with special emphasis on block copolymer synthesis. Other important synthetic considerations

such as the design of nitroxides with improved performance and the development of new synthetic approaches to alkoxyamine initiators will be examined in an effort to provide a basis for future development in the field. While mechanistic and kinetic details of the polymerization process will be examined, for a more detailed treatment the reader in directed to Chapter 9, which examines in detail the kinetics of LRP. Similarly, the relationship between nitroxide-mediated (NMP) and other living free-radical techniques, such as atom transfer radical polymerization (ATRP) and radical addition, fragmentation, and transfer (RAFT), will be discussed and examples given for each of these novel techniques; however, for an in depth analysis, the reader is directed to the Chapter 11 on atom transfer radical polymerization and Chapter 12 on degenerative transfer methods.

10.1.3 Historical Perspective

The first detailed attempt to use initiators that control radical polymerization of styrene and methyl methacrylate was reported by Werrington and Tobolsky in 1955.[9]
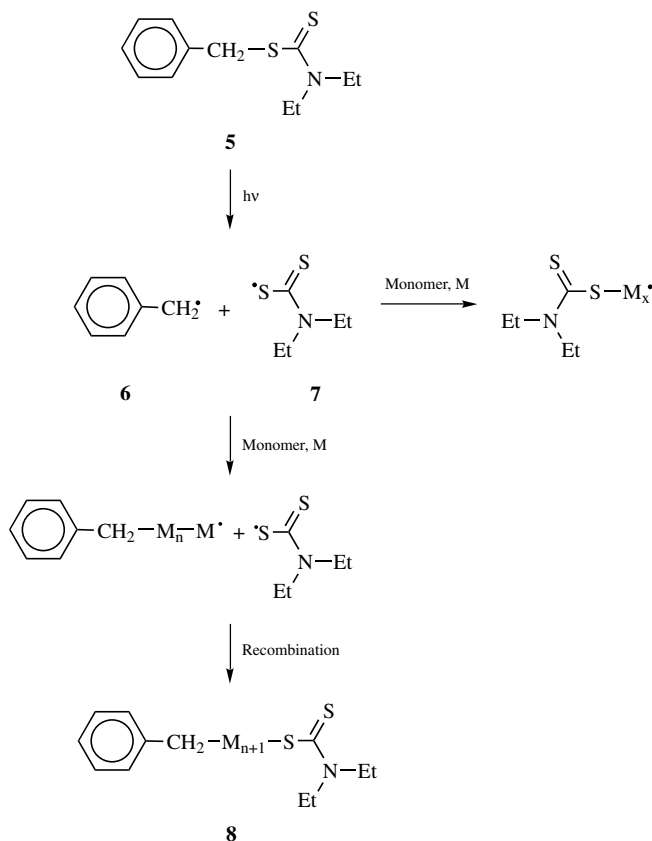
Scheme 10.2

However the dithiuram disulfides that were employed lead to high transfer constants and significant retardation of the polymerization. This promising strategy was subsequently overlooked for close to 30 years until the concept of "iniferters" (*ini*tiator–trans*fer* agent–termina*tor*) was introduced by Otsu in 1982 and constituted the first attempt to develop a LFRP technique.[10] In this case, disulfides, **5**, including diaryl and dithiuram disulfides, were proposed as photochemical initiators where cleavage can occur at the C—S bond to give a carbon-based propagating radical, **6**, and the mediating thio-radical, **7** (Scheme 10.2). While the propagating radical, **6**, can undergo monomer addition followed by recombination with the primary sulfur radical, **7**, to give a dormant species, **8**, it may also undergo chain transfer to the initiator itself.

As opposed to conventional free-radical polymerization, which results in high molecular weights, even at low conversion, this technique provides rudimentary characteristics of typical living systems, such as a linear increase in molecular weight with conversion. In addition, the monofunctional, or α,ω-bifunctional chains, can be considered as telechelic polymers, giving the possibility to prepare block copolymers. Nevertheless, other features of a true living system such as accurately controlled molecular weights and low polydispersities could not be obtained since the thio radical, **7**, can also initiate polymerization. As will be discussed below, one of the primary requirements for a mediating radical is that it undergo reversible termination of the propagating chain end without acting as an initiator or being involved in unwanted termination or side reactions. Subsequently, a wide range of stabilized radicals has been examined as mediating radicals for the development of a living free-radical system.[11–13] As with the preliminary iniferter work of Otsu, they suffer from incomplete control over both the initiation and reversible termination steps and lead to poorly controlled polymerizations; however, their structures do point to interesting features that may be relevant in future development of this technology (Fig. 10.1).
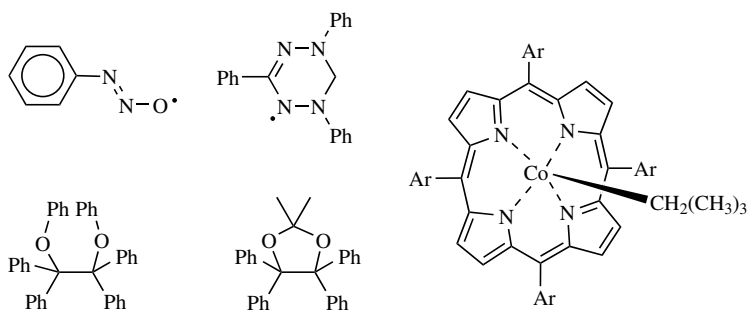
Figure 10.1   Examples of other stabilized radicals suitable for controlled radical procedures.

10.2. NITROXIDE MEDIATED LIVING FREE-RADICAL POLYMERIZATIONS

This pioneering work was one of the seminal contributions that provided the basis for the development of LFRP, and it is interesting to note the similarity between the iniferter mechanism outlined in Scheme 10.2 and the general outline of a living free-radical mechanism (Scheme 10.3). In this general mechanism, the reversible termination of the growing polymeric chain is the key step for reducing the overall concentration of the propagating radical chain end. In the absence of other reactions leading to initiation of new polymer chains (i.e., no reaction of the mediating radical with the vinylic monomer), the concentration of reactive chain ends is extremely low, minimizing irreversible termination reactions, such as combination or disproportionation. All chains would be initiated only from the desired initiating species and growth should occur in a pseudoliving fashion, allowing a high degree of control over the entire polymerization process with well-defined polymers being obtained.

The identity of the mediating radical, $X^\bullet$, is critical to the success of living free-radical procedures and a variety of different persistent, or stabilized radicals have been employed.[14–18] However the most widely studied and certainly most successful class of compounds are the nitroxides and their associated alkylated derivatives, alkoxyamines. Interestingly, the development of nitroxides as mediators for radical polymerization stems from pioneering work by Solomon, Rizzardo, and Moad into the nature of standard free-radical initiation mechanisms and the desire to efficiently trap carbon-centered free radicals.[19]

The same workers then applied a similar concept, albeit at increased temperatures (80–100°C) to the synthesis of low-molecular-weight oligomers, primarily with acrylates and nitroxides such as TEMPO.[20] It has been subsequently shown with nitroxides such as TEMPO that the polymerizations cannot be considered living at these low temperatures. In addition, the polymerization of acrylates by TEMPO leads to poorly defined materials with uncontrolled molecular weights and high

$X^\bullet$ = mediating radical
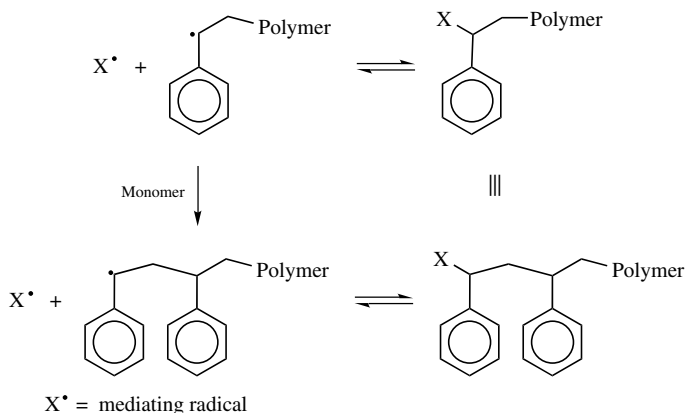
Scheme 10.3

polydispersities. Despite these drawbacks, it did provide the background information, which laid the foundation for subsequent studies.

10.2.1 Bimolecular Process

The second seminal contribution that proved conclusively that living free-radical polymerizations are a viable synthetic methodology was a report from the group of Georges at XEROX describing the preparation of low polydispersity polystyrene (PDI. $= 1.20$) and the subsequent synthesis of polystyrene-based block copolymers.[21] The key feature of this work was the realization that, while nitroxides are polymerization inhibitors at low temperatures, hence their use by Solomon to trap polymerization intermediates, at elevated temperatures they may act as polymerization mediators, not inhibitors. By increasing the temperature to 130°C and conducting the polymerizations in the bulk, a system consisting of benzoyl peroxide and a stable nitroxide, TEMPO **9**, in the molar ratio of 1.3 : 1, gave polystyrene derivatives, **10**, by a living process in which the molecular weight increased in a linear fashion with conversion (Scheme 10.4). Even more startling were the polydispersity
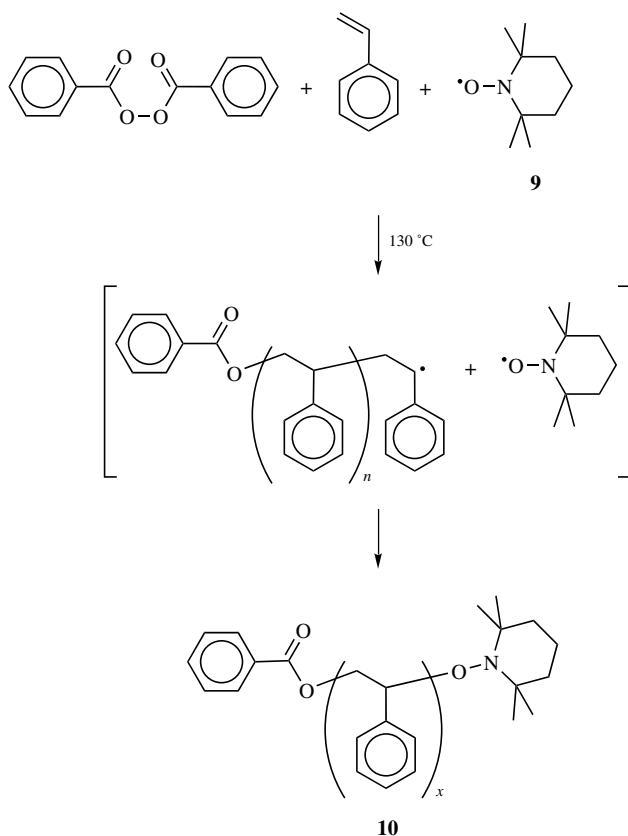
Scheme 10.4

values for **10**, PDI. $= 1.2$, which were significantly lower than the theoretical lower limit for a free-radical process of 1.5 and the typical values of ~ 2.0 for free-radical systems. While this original work by Georges displays many of the fundamental aspects of a living polymerization process, and subsequent studies have confirmed and reinforced these original observations, it must be emphasized that these are not *true* living systems.[22–25] It should also be recognized that the nature of the initiators is not crucial, while preliminary findings may have suggested that the use of peroxides is important, more detailed studies have shown that other initiators, such as AIBN can be employed in a similar fashion.[26]

While the concentration and reactivity of radicals at the propagating chain end have been significantly reduced, it is still not negligible, and therefore termination reactions can still occur. By the strictest definition, these are not living polymerizations; however, the best systems do display all the characteristics of a living system and so the term, *living* will be used throughout this chapter. For an excellent discussion of the many varied opinions on the correct terminology for living free-radical polymerizations the reader is directed to a special, "living or controlled" thematic issue of the *Journal of Polymer Science*.[27]
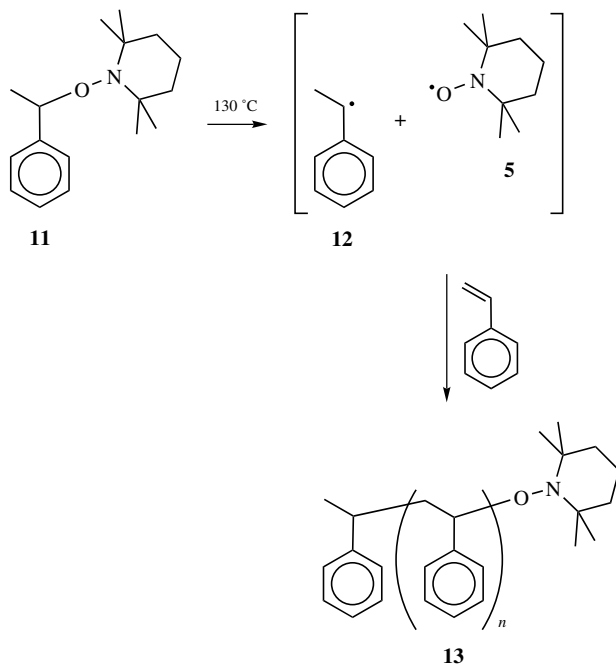
Scheme 10.5

10.2.2 Unimolecular Initiators

While successful, the poorly defined nature of the initiating species in the bimolecular process prompted the development of a single molecule initiating system. Borrowing the concept of well-defined initiators from living anionic and cationic procedures, unimolecular initiators for nitroxide mediated living free-radical polymerizations were then developed.[28] The structure of these initiators was based on the alkoxyamine functionality that is present at the chain end of the growing polymer during its dormant phase. The C—O bond of the small-molecule alkoxyamine derivative, **11**, is therefore expected to be thermolytically unstable and decompose on heating to give an initiating radical, namely, the α-methyl benzyl radical, **12**, as well as the mediating nitroxide radical, **5**, in the correct 1 : 1 stoichiometry (Scheme 10.5). Following initiation the polymerization would proceed as described previous for the bimolecular case to give the polystyrene derivative, **13**. The advantage of the unimolecular initiator approach is that the structure of the polymers prepared can be controlled to a much greater extent. Since the number of initiating sites per polymerization is known, the molecular weight can be accurately controlled. The unimolecular initiator can also be functionalized to permit the controlled introduction of functional groups at the chain ends of the macromolecules.

10.3 SYNTHETIC APPROACHES TO ALKOXYAMINES

While the abovementioned strategies proved that the concept of a living free-radical procedure was a viable process, there were a large number of problems with the use of TEMPO as the mediating nitroxide.[29] In addition, the available synthetic methods for the preparation of alkoxyamines were poor and not amenable to preparing functionalized initiators in high yield.[30] Before becoming a routine synthetic procedure for the preparation of well-defined polymers, these issues needed to be addressed.

The development of stable, readily functionalized initiators, which mimic the growing chain end for living free-radical systems, is one of the most significant achievements and advantages of LFRP. Not only does it allow the greatest degree of control over the final polymeric structure, the ready functionalization permits the development of new areas of research in polymer science and nanotechnology. In the case of nitroxide-mediated systems, the dormant chain end is a *C*-alkylated nitroxide derivative, also termed an *alkoxyamine*. Unfortunately, as a class of compounds alkoxyamines are poorly studied, and the true exploitation of their potential has been severely limited by the lack of versatile and efficient synthetic procedures for their preparation.[31–33]

The growing importance of this family of compounds for LFRP has motivated organic chemists to pursue new and more versatile synthetic approaches for their preparation. Initially the majority of synthetic approaches to alkoxyamines relied on the generation of carbon centered radicals followed by the trapping of these radicals by a nitroxide derivative. Initial examples include the reaction of benzoyl peroxide with an excess of styrene to give a benzylic radical followed by trapping of the radical intermediate with TEMPO to give the benzoyl peroxide adduct, **14**. Problems

14
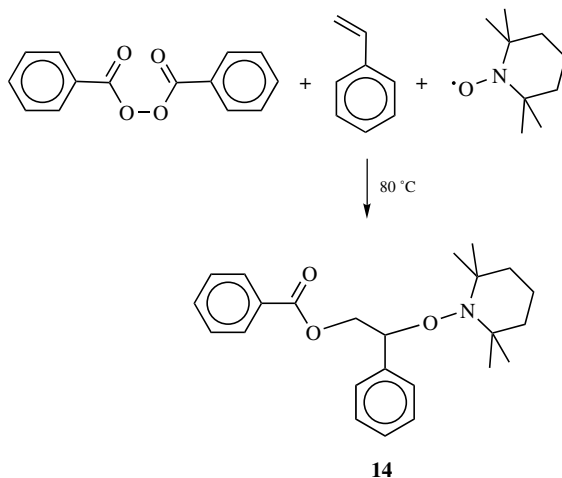
Scheme 10.6

with this synthesis include the relatively poor yield (30–40% yield) and the wide range of byproducts, which necessitated purification by repeated flash column chromatography (Scheme 10.6).[28]

In an effort to both improve the yield of the desired alkoxyamine and simplify purification, a variety of other strategies for generation of the radical intermediate have been studied. Howell has taken advantage of the low reactivity of nitroxides with oxygen-based radicals to prepare benzylic alkoxyamines, **15**, by hydrogen abstraction from ethyl benzene with di-*t*-butyl peroxide followed by nitroxide trapping (Scheme 10.7).[34,35] Generation of the intermediate radical has also been

15

16
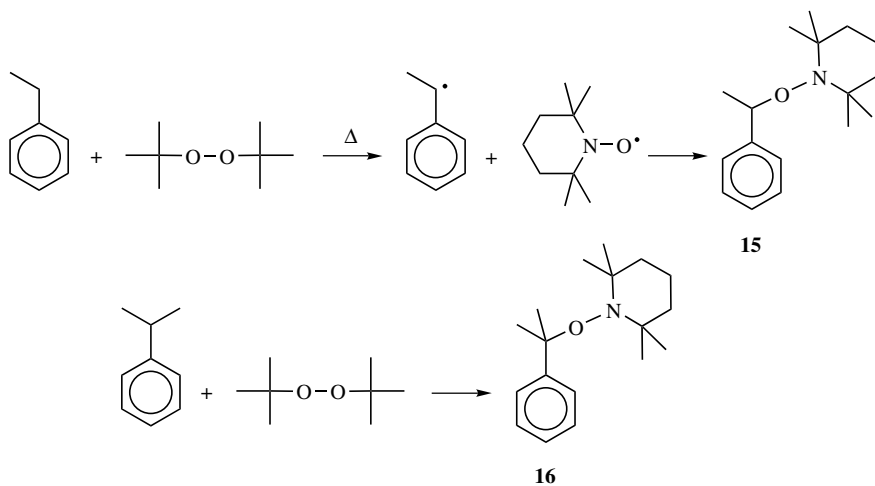
Scheme 10.7

accomplished photochemically using a similar di-*t*-butyl peroxide reaction system and irradiation with 300-nm light. In this case the mild nature of the reaction conditions allows the yields to be increased to over 90% and more importantly permits unstable alkoxyamines such as the α,α-dimethyl-substituted derivative, **16**, to be isolated. Under traditional thermal conditions, **16**, would decompose on formation due to the inherent instability of the quaternary C—ON bond.[36]

Alternative approaches have also been developed which rely on the controlled generation of carbon centered radicals followed by trapping of the radical-like intermediates. Jahn[37] has employed single electron transfer in the highly efficient generation of radicals from ester enolates, **17**, by treatment of lithium slats with ferrocenium ions, **18**, at −78°C. These radicals are then trapped by nitroxides to provide functionalized alkoxyamines, **19**, in moderate to high yields, which can then be used as precursors to other functionalized derivatives. For example, reduction with LiAlH₄ gives the hydroxy derivative, **20**, in good yield with no attack at the alkoxyamine group (Scheme 10.8). Matyjaszewski has applied techniques from atom transfer chemistry for a facile, low-temperature approach to alkoxyamines involving the treatment of suitable ATRP-based initiators, **21**, where copper complexes in the presence of a nitroxide, the resulting alkoxyamine, **22**, are obtained in very high yields (Scheme 10.9).[38]

In a similar fashion, Braslau has employed Cu^{2+}-promoted single electron transfer reactions with enolate anions to provide carbon centered free radicals that can be trapped by nitroxides at low temperatures.[39] The use of lead oxide for the oxidation of alkyl hydrazides has also been shown to be an efficient method for the synthesis of alkoxyamines and if chiral nitroxyl radicals are employed a degree of stereochemical

Scheme 10.8

21   **22**
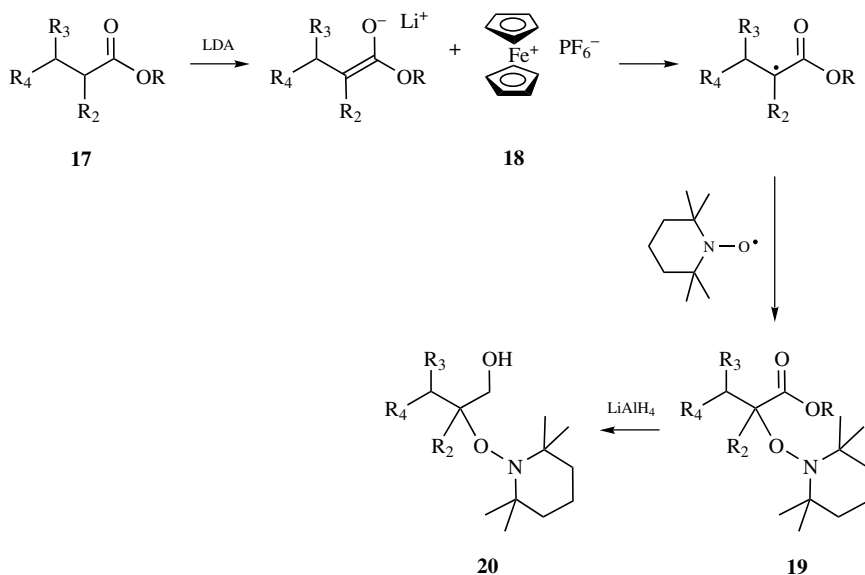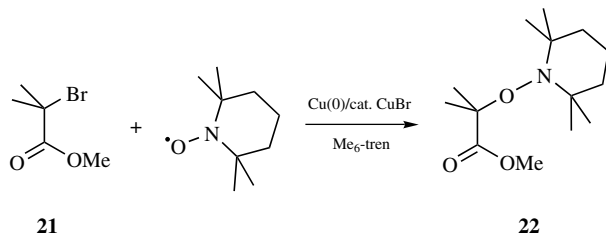
Scheme 10.9

control can be obtained.[40] Finally in a novel application of single electron transfer chemistry, Priddy[41] has employed oxoaminium slats to add across the double bond of styrenic derivatives leading to functionalized alkoxyamine initiators. In the proposed mechanism, the oxoaminium salt, **23**, undergoes a disproportionation reaction with associated electron transfer to give the corresponding nitroxide, TEMPO, and a chlorine radical. The chlorine radical then adds across the styrenic double bond to give the carbon center radical, **24**, which is then efficiently trapped by TEMPO to give the chloromethyl-substituted alkoxyamine, **25** (Scheme 10.10). The advantage of this strategy is the facile preparation of the alkoxyamine, **25**, which can be subsequently transformed into a myriad of different functionalized initiators as well as providing entry into the one-step preparation of chloromethyl terminated polymers which are useful reagents for a variety of interfacial studies.

23   **24**

25
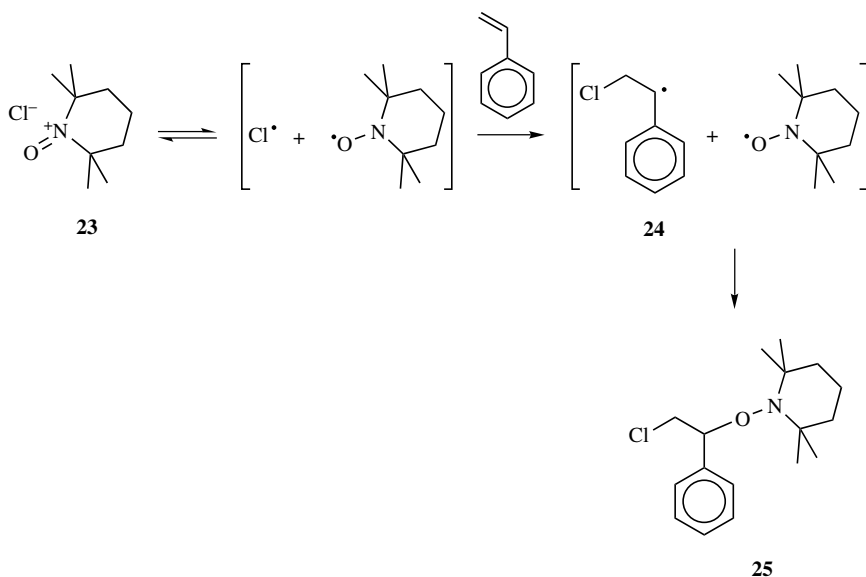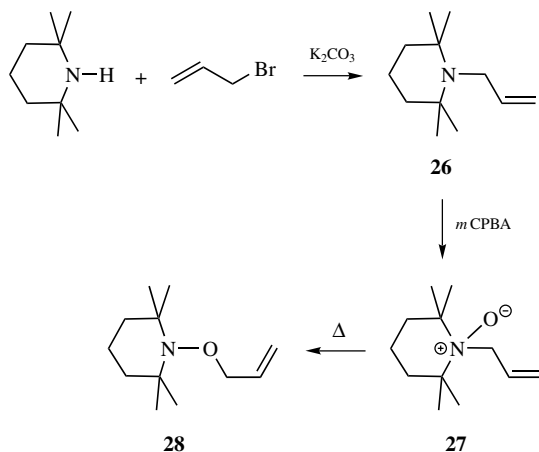
Scheme 10.10

Scheme 10.11

Alternate strategies to the trapping of carbon-centered radicals with nitroxides has been developed by a variety of groups in an effort to extend the range of functionalities that can be incorporated into the alkoxyamine structure. In an interesting application of classical organic chemistry, Bergbreiter employed a Meisenheimer rearrangement of allyl-*N*-oxides as a route to alkoxyamines.[42] As shown in Scheme 10.11, 2,2,6,6-tetramethylpiperidine is initially alkylated with allyl bromide to give the tertiary amine, **26**, which can be oxidized at low temperatures with *m*-chloroperbenzoic acid. The resulting *N*-oxide, **27**, is not isolated but allowed to undergo rearrangement on warming to room temperature to give the allyl-TEMPO
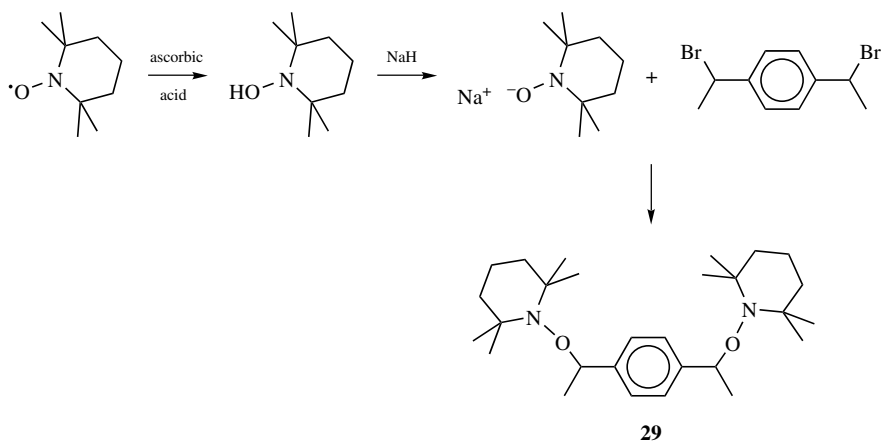
Scheme 10.12

derivative, **28**, in moderate yield (Scheme 10.11). An attractive feature of this synthetic approach to alkoxyamines is the ready availability and low cost of starting materials and reagents, which is in contrast to the high cost of many nitroxides. In addition, the controlled nature of polymerizations initiated with **28** demonstrates that an α-methylbenzyl group is not necessary for efficient initiation in these systems and a simple allyl group can be used in its place without any detrimental performance.

Taking advantage of the facile oxidation of nitroxides to hydroxylamines, Catala[43] has demonstrated that after proton abstraction with sodium hydride, the anion derived from the hydroxylamine derivative of TEMPO can nucleophilically displace
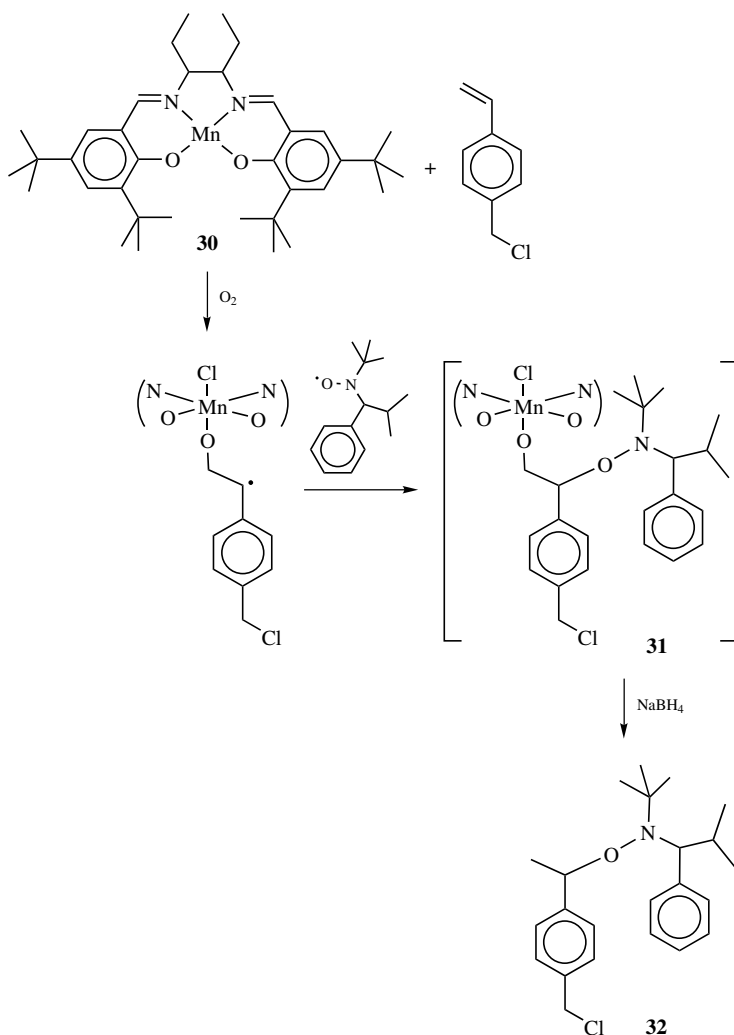
Scheme 10.13

alkyl halides to give the desired alkoxyamine. This is especially useful for multi-functional alkoxyamines such as **29**, whose synthesis from the corresponding diradical is not practical (Scheme 10.12).

The use of transition metal complexes for the synthesis of alkoxyamines has also been exploited.[44] In this case, Jacobsen's catalyst, manganese(III) salen, **30**, is employed to promote the addition of nitroxides across the double bond of olefinic derivatives,[45] specifically activated double bonds such as styrenics, leading to alkoxyamines suitable for use as initiators in living free-radical procedures. As can be seen in Scheme 10.13, the synthesis of alkoxyamines involves an intermediate organomanganese derivative, **31**, is involved, which on reduction with sodium borohydride gives the alkoxyamine, **32** (Scheme 10.13). The advantages of these methods are that a variety of functional groups can be readily introduced, large excesses of reagents are not required to trap the extremely reactive free-radical intermediates and near stoichiometric amounts of the alkene and nitroxide are required. Finally, the reactions are high-yielding and produce very few unwanted side products which greatly facilitates isolation and purification.

10.4   DEVELOPMENT OF NEW NITROXIDES

The relative cheapness and commercial availability of TEMPO motivated its initial utilization as the mediating nitroxide, however there were serious deficiencies, which readily became apparent. These included the necessity to use high polymerization temperature (125–145°C), long reaction times (24–72 h), and an incompatibility with many important monomer families. While it was shown that random copolymers of styrene and either butyl acrylate or methyl methacrylate could be readily prepared with TEMPO,[46] at high incorporations of the co-monomer (~50%+) the copolymerization and homopolymerization of (meth)acrylates is no longer living. Living polymerizations were therefore possible only with styrenic derivatives, which is a severe restriction.

To overcome this deficiency, it was apparent that changes in the structure of the nitroxide was needed. Unlike the initiating radical, which is involved only at the beginning of the polymerization, the mediating radical is involved in numerous reversible termination and activation steps, and so changes in its structure would be expected to have a substantial effect on the polymerization. Initial efforts to develop new mediating nitroxides relied on TEMPO-based derivatives. The Xerox group were able to polymerize acrylates at elevated temperatures (145–155°C) in the presence of 4-oxo-TEMPO, **33**, as the mediating nitroxide, and while this is a significant improvement when compared to TEMPO, polydispersities were still between 1.40 and 1.67 and the living nature of the polymerization was questionable.[47] Similarly, Matyjaszewski observed that the rate of polymerization of styrene could be significantly enhanced by the use of a TEMPO derivative, **34**, substituted in the 4-position with a phosphonic acid group (Fig. 10.2). Two rationale were proposed for this increase in performance, formation of an intramolecular H bond in **34** leads to a decrease in the rate of deactivation while the cleavage is accelerated.[48]
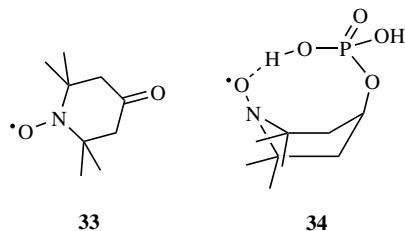
Figure 10.2 Functionalized TEMPO derivatives for accelerated living free radical polymerization of styrene.

This prompted the investigation of a wide range of other TEMPO-like structures, such as di-*t*-butyl nitroxides, and in the use of additives.[49] All of these approaches lead to an increase in the rate of polymerization, especially for additives such as camphor sulfonic acid[50] or acetic anhydride;[51] however, the improvements were not significant enough to make NMP a viable competitor to other living techniques.

The most significant breakthrough in the design of improved nitroxides was the use of alicyclic, nonquaternary nitroxides. These materials bear no structural resemblance to TEMPO, and their most striking difference was the presence of a hydrogen atom on one of the α-carbons, in contrast to the two quaternary α-carbons present in TEMPO and all the nitroxides discussed above. The best examples of these new materials are the phosphonate derivative, **35**, introduced by Gnanou and Tordo[52] and the family of arenes, **36**, introduced by Hawker (Fig. 10.3).[53] These nitroxides have subsequently been shown to be vastly superior to the original TEMPO derivatives, delegating the latter to a niche role for select styrenic derivatives. The use of nitroxides such as **35** and **36** now permits the polymerization of a wide variety of monomer families. Acrylates, acrylamides, 1,3-dienes, and acrylonitrile-based monomers can now be polymerized with accurate control of molecular weights and polydispersities as low as 1.06.[54] The versatile nature of these initiators can also be used to control the formation of random and block copolymers from a wide selection of monomer units containing reactive functional groups, such as amino, carboxylic acid, and glycidyl. The universal nature of these initiators overcomes many of the limitations typically associated with nitroxide mediated systems and leads to a level of versatility approaching atom transfer radical polymerization (ATRP) and radical addition fragmentation and transfer (RAFT) systems.[55–57] The
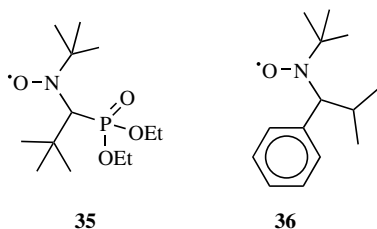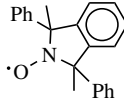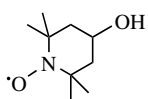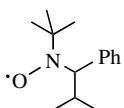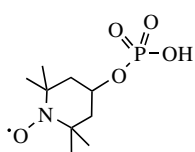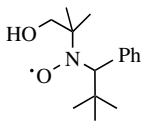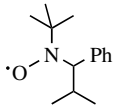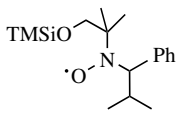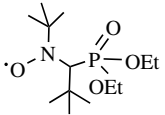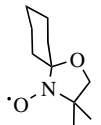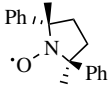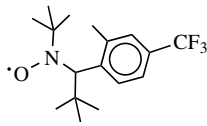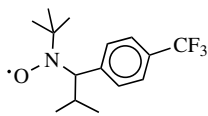
Figure 10.3   α-CH based nitroxides suitable for the living polymerization of vinyl monomers.

applicability of these systems to other monomers families will be described and demonstrated in the following sections on block copolymers and macromolecular architectures. A complete list of nitroxides that have been employed as mediators in living free-radical polymerizations are included in Table 10.1 with accompanying references.[58–91]

TABLE 10.1 Structure of Nitroxides Employed in Living Free-Radical Polymerizations

Strucutre	Ref.	Structure	Ref.
	58 66 67 72–75 82		53
	59 64 68 71 81		53
	48		53 87
	52 53 54 69 88		53
	52 53		39 53
	53 76 77		53 69
	62 63 65		53 69

(Continued)

TABLE 10.1 *(Continued)*
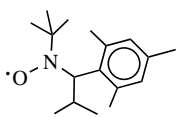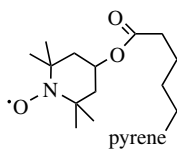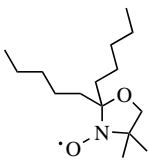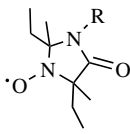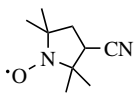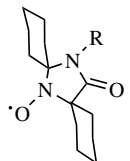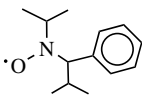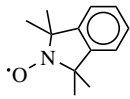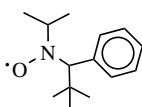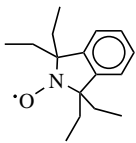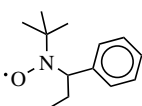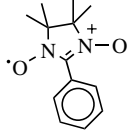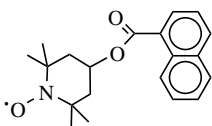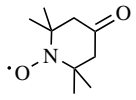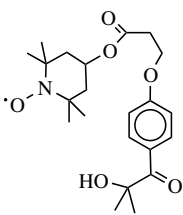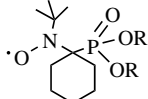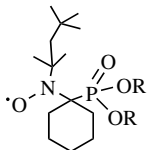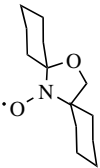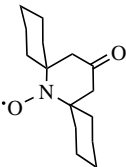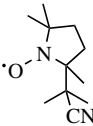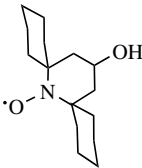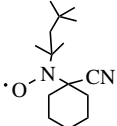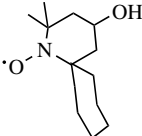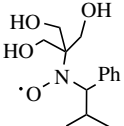
Strucutre	Ref.	Structure	Ref.
	53 69	pyrene	88
	53 69	R	91
CN	53 69	R	91
	53 69		61
	53 69		91
	53 69		78 79
	53 69		89 90
	77 84	O P—OR OR	80
HO	84	O P—OR OR	80

TABLE 10.1   *(Continued)*

Strucutre	Ref.	Structure	Ref.
	82		82
	82		83
	82		30
	82		85 86

10.5   MECHANISTIC AND KINETIC FEATURES

10.5.1   Nitroxide Exchange

The key kinetic feature of nitroxide mediated living free-radical polymerization is the operation of a special phenomena, termed the *persistent radical effect* (PRE). Fischer has developed the analytic equations for the polymerizations rates and for the polydispersities of the resulting polymers that have been shown to effectively model LFRP.[92,93]

In the initial stages of the polymerization, a small fraction of the initiating radicals, **37**, formed from decomposition of the initiator, **38**, undergo radical–radical coupling. This leads to a terminated molecule/oligomer, **39**, and the resulting removal of two initiating radicals from the system. At this early stage of the polymerization, this is a facile reaction since the diffusing radicals are sterically small and the reaction medium is not viscous. However, by nature, the mediating radical, or persistent radical, **40**, does not undergo coupling and so a small increase in the

INIT-INIT

39

↑ Coupling

INIT ⇌ INIT-rad• + Med-rad•

38   **37**   **40**

Monomer/s

Polymer

41
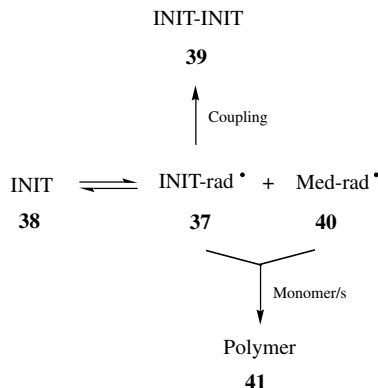
Scheme 10.14

overall concentration of **40** relative to the propagating/initiating radical, **37**, occurs. This increased level of **40** is self-limiting since a higher concentration leads to more efficient formation of the dormant chain end, **41**, and a decrease in the amount of radical–radical coupling (Scheme 10.14) leading to the persistent radical effect (PRE) and to the eventual control over the polymerization process.

The nature of the equilibrium between the dormant system, **41**, and the pair of radicals, **37** and **40**, has been probed and exploited by a number of groups. The exact nature of the radical pair, caged versus freely diffusing, was probed by a series of crossover experiments.[68,94] This is an important synthetic issue, are the nitroxide counter-radicals associated with the same polymeric chain end during the course of the polymerization, or can they diffuse freely through the reaction medium. This issue affects many aspects of the LFRP process and may influence the applicability of NMP as a macromolecular engineering tool, for example, the ability to insert functional groups at the chain ends.

The design of crossover experiments to probe the potential diffusion of the mediating radical from the propagating chain end during "living" free-radical polymerizations involves the use of two structurally similar alkoxyamines, which differ only in their substitution pattern. One derivative is unfunctionalized, **42**, while the other alkoxyamine, **43**, contains two hydroxy groups, one is attached to the TEMPO unit while the second is located at the beta-carbon atom of the ethylbenzene unit. If a 1 : 1 mixture of **42** and **43** is used to initiate the "living" free-radical polymerization of styrene, homolysis of the carbon–oxygen bond of **42** and **43** will lead to four radical species. Each radicals produced is chemically different and constitutes a pair of initiating, or propagating, radicals, **44** and **45**, and a pair of structurally similar mediating nitroxide radicals are produced, TEMPO, **46**, and 4-hydroxy-TEMPO, **47**. If no escape of the mediating nitroxide radical from propagating chain end occurs, only two polystyrene derivatives will therefore be formed; **48** and **49**. In contrast, if radical crossover does occur and the mediating nitroxide radicals are free to diffuse to the polymerization medium, four polystyrenes having different substitution patterns,

48–51, will be obtained. Significantly, the experimental result from these crossover experiments revealed a statistical mixture of all four products, even at low conversions, implying freely diffusing radicals (Scheme 10.15).

Turro[84] has elegantly taken advantage of this feature to develop a strategy for the facile preparation of chain-end functionalized macromolecules. In this approach a
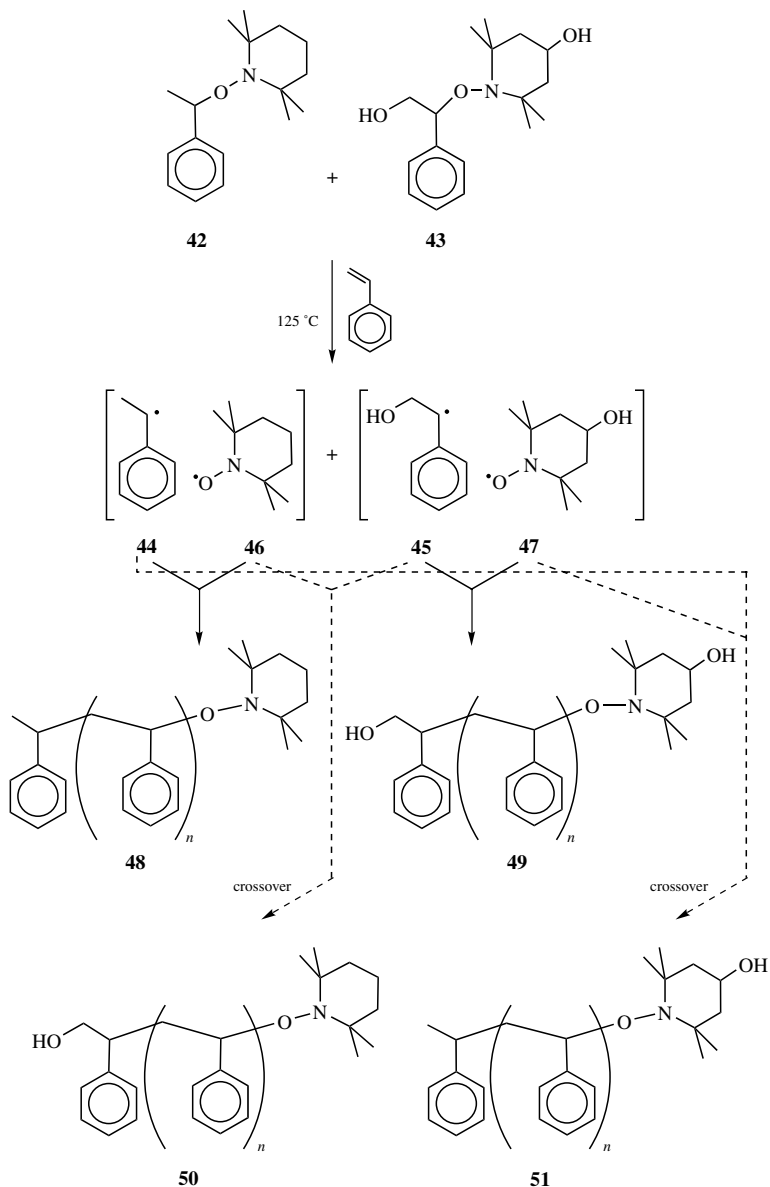
Scheme 10.15
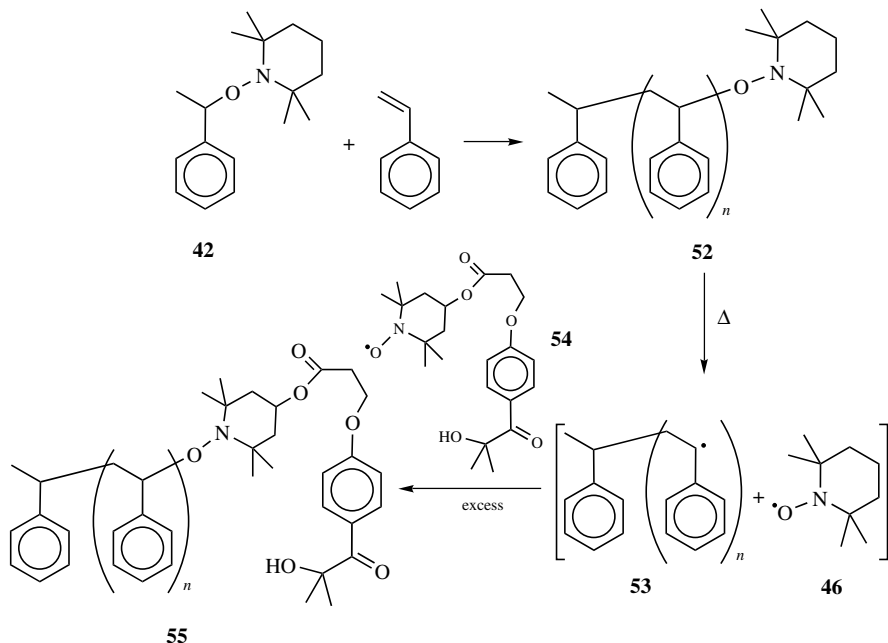
Scheme 10.16

precursor polymer, **52**, is prepared from a standard unfunctionalized initiator, such as **42**, purified and then redissolved in a high-boiling-point solvent such as chlorobenzene and heated at 125°C in the presence of a large excess of functionalized nitroxide, **54**. At this temperature the equilibrium between **53** and the two radicals is established and since the released nitroxide, **46**, is free to diffuse into the solution, exchange with the functionalized nitroxide, **54**, can occur leading to the desired chain end functionalized macromolecule, **55** (Scheme 10.16). This strategy presents a number of advantages, reactive functional groups can be introduced under mild conditions, from the same precursor polymer a variety of differently tagged macromolecules can be prepared, and the same strategy can be applied to macromolecules of different architectures. It should, however, be noted that the primary driving force for this exchange is statistics and so under normal laboratory conditions with nitroxide excesses of 1000–2000 mol%, complete exchange of the chain end does not occur. In the case where two different nitroxide families are interchanged, namely, a TEMPO derivative and a α-hydrido nitroxide, complete substitution may occur as a result of different in equilibrium constants.

10.5.2   Living/Controlled Nature

As detailed by Matyjaszewski in Chapter 8, and at the beginning of this chapter, nitroxide-mediated processes are not living by strictest definition of the term. However, they do display many of the important characteristics of living processes and
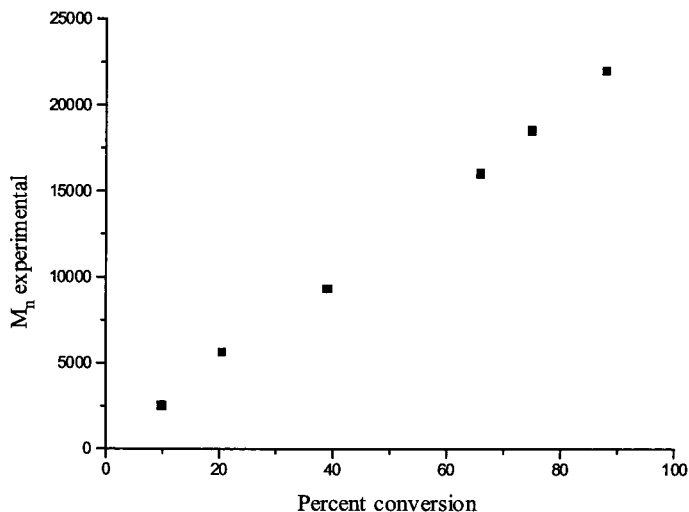
Figure 10.4 Evolution of molecular weight, M_n, with percent conversion for the polymerization of *n*-butyl acrylate (250 equiv) in the presence of **56** (X,Y $=$ H) (1.0 equiv) and **36** (0.05 equiv) at 123°C for 16 h.

typically proceed with only very limited side reactions. For monomer families other than methacrylates, the low occurrence of these side reactions and the essentially living nature of these polymerizations can be demonstrated by a variety of different techniques. A preliminary guide to the 'livingness' can be obtained by examining the relationship between the evolution of molecular weight and conversion. As shown in Fig. 10.4, the polymerization of n-butyl acrylate (250 equiv) in the presence of **59** (X $=$ Y $=$ H) (1.0 equiv) and **36** (0.05 equiv) at 123°C for 16 h results in an essentially linear relationship.[53] This demonstrates that all of the chains are initiated at the same time and grow at approximately the same rate. Following this initial screening, the efficiency of initiation and the degree of control during the polymerization can be accurately gauged by determining the correlation between the experimental molecular weight and the theoretical molecular weight. As for all living polymerizations, the theoretical molecular weight is determined by the molar ratio of monomer to initiator, taking into account the conversion of the polymeriza-tion. For an initiation efficiency of 100%, the relationship between experimental molecular weight and theoretical molecular weight should be a straight line with a slope of 1.0. As shown in Fig. 10.5, evolution of experimental molecular weight, M_n, with theoretical MW for the polymerization of styrene and **59** (X $=$ Y $=$ H) at 123°C for 8 h with no degassing or purification is essentially a straight line with initi-ating efficiencies of 95% or greater. The ability to obtain polydispersities of between 1.10 and 1.20 for these polymerization is further support for a controlled/living pro-cess. Figure 10.4 also demonstrates a critically important feature of NMP that is also true for ATRP and RAFT, no purification of monomers or rigorous polymerization
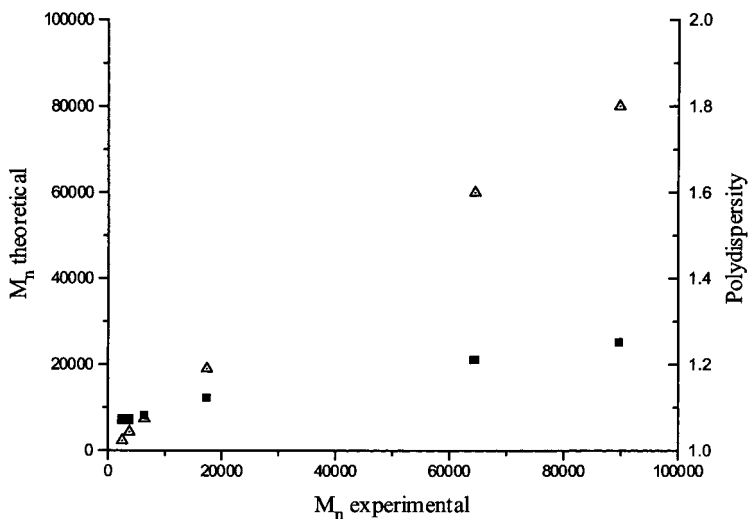
Figure 10.5   Evolution of experimental molecular weight, M_n, and polydispersity with theoretical MW for the polymerization of styrene and **56** at 123°C for 8 h with no degassing or purification.

conditions other than simple deoxygenation are required to obtain very well-defined polymers, thereby opening these synthetic techniques up to a much wider range of researchers.

As will be discussed below, the final piece of evidence that is needed to conclusively prove the living nature of NMP is to use the alkoxyamine chain end to prepare a block copolymer. Again if the polymerization is living, efficient reinitiation of the second block should be observed to give a block copolymer with no homopolymer contamination (care should be taken in analyzing homopolymer content by GPC, especially using RI detection). While this is a desired goal, it should be realized that the efficiency of reinitiation for the second block is monomer dependent and in select circumstances inefficient reinitiation may be obtained even though ~100% of the starting blocks contain an alkoxyamine chain end. This feature will be further discussed in the following section on structural control.

10.5.3   Additives

From the previous discussion it is obvious that the persistent radical effect relies on a subtle interplay between the mediating nitroxide radicals and propagating radical chain ends. The rate of polymerization and extent of termination reactions such as radical coupling can therefore be manipulated by changing the balance between all of these competing reactions and kinetic equations, which are present during the persistent radical effect. One of the best-studied strategies is to continuously add

initiator or have a slowly decomposing initiator present in the polymerization mixture.[95,96] This continuously supplies propagating/initiating radicals to the system, and as a result the system continuously tries to obtain a situation where the persistent radical effect (PRE) operates. The stationary concentration of the nitroxide is therefore reduced and correspondingly, the rate of deactivation is decreased, leading to an increase in the rate of polymerization. One negative consequence is the concomitant increase in the polydispersity of the polymers obtained. Indeed this has been shown to be the case in a number of studies. The addition of either dicumyl peroxide and *t*-butyl hydroperoxide has been shown to lead to rate enhancements of up to 300% with only moderate increases in polydispersity. In a related study, continuous slow addition of a standard low-temperature free-radical initiator, AIBN, was shown to give similar results.[97] These findings are important from a commercial viewpoint since they may allow the long reaction times and high temperatures normally associated with nitroxide mediated polymerizations, especially those involving TEMPO, to be alleviated to a certain extent without compromising the gross characteristics of the product.

These experiments are also relevant to the polymerization of styrenic derivatives. As discussed above, styrenics was the first and still arguably the easiest monomer family to polymerize under living conditions using nitroxides. Unlike acrylates and other vinyl monomers, which do not undergo self-initiation to generate radicals, it has been shown that, thermal self-initiation of styrene provides a low concentration of propagating radicals.[98,99] This is sufficient for obtaining a rate enhancement similar to the addition of excess initiator and allows a reasonable rate of polymerization under the PRE. Another consequence of autopolymerization is that the rate of polymerization of styrene in the presence of nitroxides is independent of the concentration of the alkoxyamine and remarkably close to the rate of thermal polymerization under the same conditions.[100]

10.5.4   Chain-End Stability

An extremely important side reaction in nitroxide mediated living free-radical polymerization that dramatically affects the kinetics and structural integrity of the products is decomposition of the dormant alkoxyamine chain ends. One potential pathway for loss of the alkoxyamine group is the facile reduction of the mediating nitroxide radical to give the corresponding hydroxyamine, **57**, by H transfer.

As illustrated in Scheme 10.17 for polystyrene, this results in a dead polymer chain, **57**, containing an unsaturated chain end. The hydroxylamine, **56**, can then be involved in H-transfer back to a growing radical chain end to regenerate the nitroxide while at the same time leading to a second H-terminated dead polymer chain, **58**. These termination reactions decrease the living character of the polymerization and if they are significant enough, will alter the overall kinetics and lead to a nonlinear system. To understand the system in more detail, Priddy has investigated the decomposition of alkoxyamine initiators in a variety of solvents.[101] The results clearly show that alkoxyamines undergo significant decomposition at the temperatures normally associated with living free-radical polymerization. In 1,2,4-trichlorobenzene,
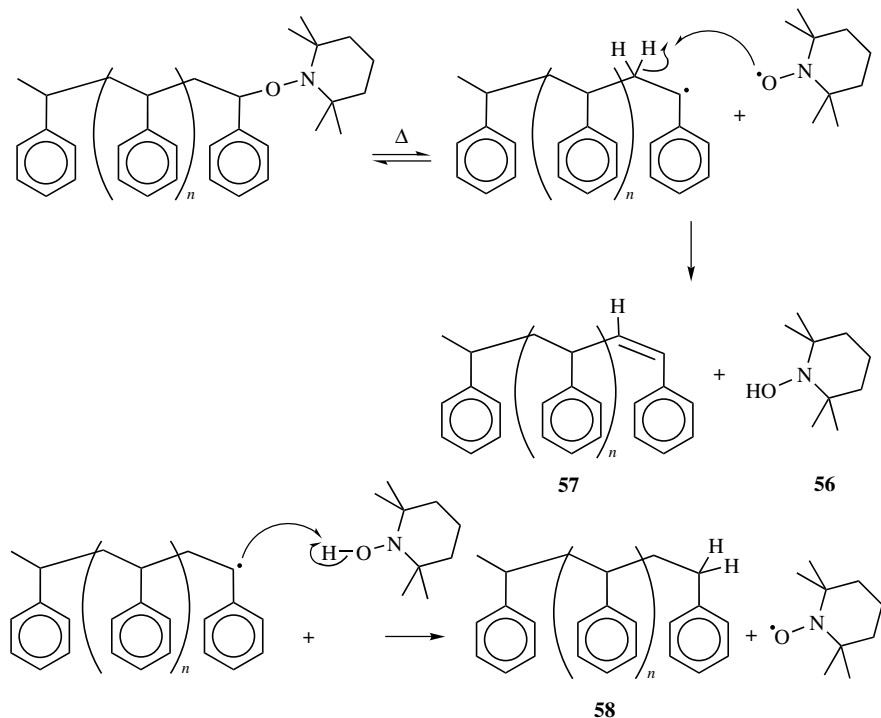
Scheme 10.17

$\sim$50% decomposition has occurred after 2 h, leading to H abstraction and the identification of styrene as a major decomposition product (Scheme 17; see also Fig 10.6). The authors concluded that significant decomposition of the alkoxyamine chain ends should occur during polymerization due to the competitive rates of polymerization and decomposition.

It is interesting to note that this effect is not experimentally observed at these levels under normal polymerization conditions that may be due to the absence of monomer in the model decomposition studies coupled with the decreased rate of H abstraction from a polymer chain compared to a small molecule. However, while reduced, this reaction is not completely absent from NMP and simulations and theoretical treatments have shown that its effect on the polymerization kinetics is slight but does result in an increase in molecular weights distribution.[102] This also explains the lower polydispersities observed for the second-generation nitroxides, **36**, ($\sim$1.05–1.10) compared to TEMPO (1.15–1.25) for polystyrene polymerizations. The shorter reaction times and lower temperatures associated with **36** leads to a decreased amount of alkoxyamine decomposition and associated broadening of the molecular weight distribution. This feature also explains the observed difference in the polymerization of styrenics and methacrylates under nitroxide mediated conditions. Styrenics are able to undergo living polymerization under the influence
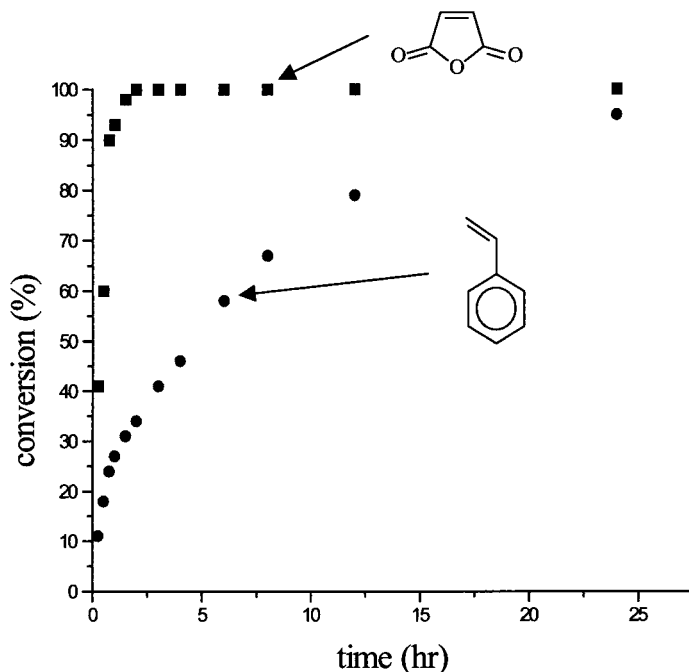
Figure 10.6 Evolution of conversion with time for the polymerization of a 9 : 1 mixture of styrene and maleic anhydride mediated by **56** and 0.05 equivs of **36** at 123°C.

of minor amounts of thermal initiation/hydrogen transfer reactions and the effect of these side reactions on the "livingness" of the system and the structure of the final products is not significant and cannot be detected in most cases. In contrast, for methacrylates there is no thermal initiation and the contribution from hydrogen transfer is significantly greater. The majority of chains therefore undergo termination reactions and effectively "die," leading to an uncontrolled, nonliving system. This has been observed experimentally with significant amounts of alkene-terminated polymer chains detected by MALDI mass spectrometry as well as NMR and UV–vis studies.[103,104]

10.5.5   Water-Based Polymerization Processes

Until the late 1990s, living radical polymerizations were studied predominantly in homogeneous systems, specifically, bulk or solution polymerizations, which are less attractive to industry, which prefers to employ aqueous dispersed media and emulsion procedures in particular. A considerable amount of recent effort has therefore been directed to the application of nitroxide-mediated polymerizations for the controlled polymerization of styrene and other monomers under heterogeneous conditions such as suspension, dispersion, seeded emulsion, batch emulsion, and

miniemulsion.[105–108] A major problem with these initial studies is that TEMPO or a derivative is employed as the mediating radical. This necessitated the use of temperatures greater than the boiling point of water, and so high-pressure reaction setups were required and stabilization of the latexes/emulsion particles at these elevated temperatures was problematic. Even with these difficulties, a basic understanding of the process is starting to emerge. The choice of the nitroxide is critical, and the compatibility of the nitroxide with water and the partition coefficients between the various phases are all critical factors.[109] Work by Charleux[110] has also shown that the choice of second-generation nitroxides which operate at lower temperatures (<100°C) may alleviate many of these difficulties and permit a viable emulsion process to be developed.

10.6   STRUCTURAL CONTROL

Given the correct conditions and with the appropriate mediating nitroxide free radical, it is now possible to design a radical-based polymerization with many of the features of a living system. On the basis of this realization, numerous groups have demonstrated that the degree of structural control normally associated with more traditional living processes, such as anionic procedures, can be equally applied to NMP. The level of control is also vastly improved when compared to normal free-radical procedures.

10.6.1   Molecular Weight Control

The initial work of Hawker[28] on the use of alkoxyamines as unimolecular initiators demonstrated that the molecular weight of polystyrene could be accurately controlled up to M_n values of ~75,000 under the assumption that one molecule of the TEMPO-based alkoxyamine, **11**, initiates the growth of one polymer chain and the length, or degree of polymerization, of that chain is governed by the molar ratio of styrene to **11**. Subsequent work by others, especially with the second-generation alkoxyamines, such as **32**, have conclusively proved this ability and, especially in the case of **32**, the upper molecular weight limit for controlled molecular weights has been increased to ~M_n of 150,000–200,000.[53] For typical monomers and polymerization conditions values of ~200,000 may represent an upper limit for NMP-, ATRP-, and RAFT-based living free-radical systems. At higher molecular weights the normally negligible influence of side reactions now becomes significant, leading to nonliving conditions and premature termination, which results in decreased molecular weight.

10.6.2   Telechelic Polymers

The ability to control molecular weight-provides good evidence that the basic reaction scheme for alkoxyamine-initiated polymerizations does operate. By analogy, it may therefore be possible to prepare telechelic polymers in a fashion similar to that
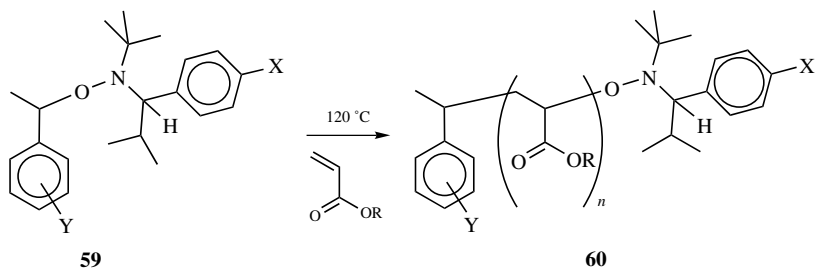
Scheme 10.18

for anionic procedures. However a major difference is that elaborate schemes for either functional group protection or efficient transformation of the anionic chain ends does not need to be developed since living free-radical procedures can tolerate a wide variety of functional groups. The ability exists to prepare functionalized alkoxyamines such as **59**, in which functional groups can be placed at either the initiating chain end, **Y**, or the nitroxide mediating chain end, **X** (Scheme 10.18). The range of functional groups that have been introduced into telechelic polymers such as **60** is wide, and a study has shown that at molecular weights of up to 50,000–75,000, the level of incorporation is very high, $\sim >95\%$.[111] This high level of incorporation for a variety of monomer families is a direct result of having the functional groups built into the initiator, coupled with the necessity for no functional group transformations at the conclusion of the polymerization. The chemistry of the single alkoxyamine chain end can also be exploited, and a number of groups have used this feature in the design of telechelic systems.[112–115]

10.6.3 Block Copolymers

One of the primary driving forces behind the desire to develop efficient living radical procedures is their potential for facile preparation of block copolymers. Not only can existing block copolymers be prepared more efficiently and in some case with a greater degree of control, but novel block copolymers can also be prepared that were not accessible using existing techniques. The synthetic versatility associated with alkoxyamine initiators and the ability to introduce a wide variety of functional groups allows block copolymers to be prepared in at least four different ways. As shown in scheme 19, vinyl block copolymers can be prepared in a traditional sequential fashion by the polymerization of one monomer followed by a second monomer (reaction 1 in Scheme 10.19). Alternatively, a functionalized alkoxyamine can be used to terminate polymerization of an initial monomer under conditions other than living free radical. The alkoxyamine-terminated macromolecule can then be used as a macroinitiator to prepare block copolymers. The interesting feature of this process is that it permits the facile introduction of a functional group or chromophore at the junction point between the two blocks (reaction 2 in Scheme 10.19). It is also possible to develop dual, or double headed, initiators in which both an

Reaction 1

Reaction 2

Reaction 3
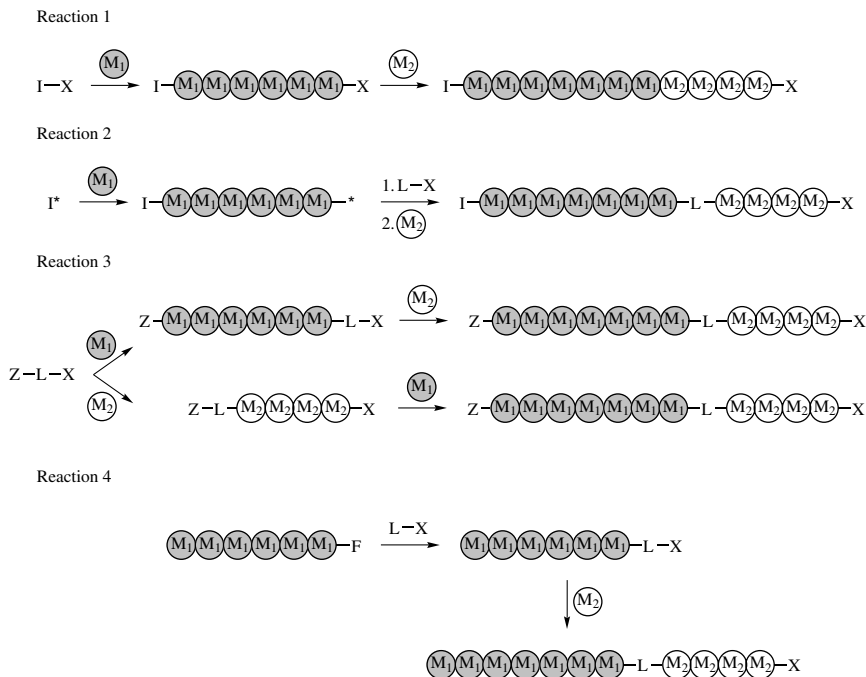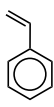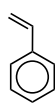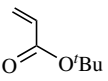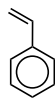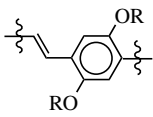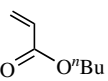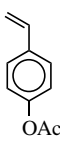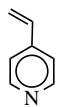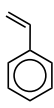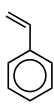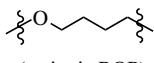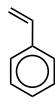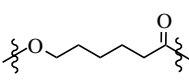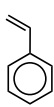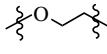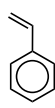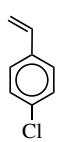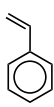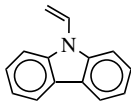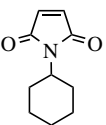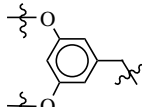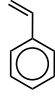
Reaction 4

Scheme 10.19

alkoxyamine initiating fragment and an initiating group for a different polymerization strategy are contained in the same molecule (reaction 3 in Scheme 10.19). Depending on the compatibility of the initiating groups and polymerization processes, the order of polymerization can be varied to give the desired block copolymer. Finally, a preexisting telechelic polymer (either mono- or difunctional) can be coupled with the appropriate alkoxyamine to give a macroinitiator from which a vinyl block can be grown under living radical conditions (reaction 4 in Scheme 10.19). While not an extensive list of all possible procedures, the multitude of synthetic strategies that have currently been explored for nitroxide-mediated living radical procedures does give an indication of the extreme versatility in block copolymer formation that is possible using this novel technique. To give a greater insight into the myriad possibilities, a list of linear block copolymers that have been prepared using nitroxide mediated processes is detailed in Table 10.2 and a number of actual examples are discussed below.[116–181]

As detailed above, two of the synthetic strategies rely on the coupling of a functionalized alkoxyamine with a telechelic or monofunctional polymer to give a macroinitiator, which can then be used in standard living free-radical procedures. Such an approach is best illustrated by the preparation of poly(ethylene glycol)-based block copolymers[129,136,150,166,167] by initial reaction of a monohydroxy-termi nated poly (ethylene glycol) with sodium hydride followed by the chloromethyl-substituted

TABLE 10.2 Structure of Monomer Employed in Synthesis of Block Copolymers by Nitroxide-Mediated Living Free-Radical Procedures

Monomer 1[a]	Monomer 2	Ref.	Monomer 1[a]	Monomer 2	Ref.
(metallocene)	(styrene)	116	(free-radical) O OMe	(styrene)	130 155
(metallocene)	O O^tBu	116	R	(styrene)	34 120 130
OR / RO (condensation)	O O^nBu	117	OAc (nitroxide)	(styrene)	131 156
(nitroxide) N	(styrene)	144 166	C_{60}	(styrene)	152 162
O OMe (Nitroxide)	(styrene)	119	O (cationic ROP)	(styrene)	148 151
O (ROP)	(styrene)	125 132 157	O (ROP)	(styrene)	129 136 150
Cl (nitroxide)	(styrene)	153	N (nitroxide)	(styrene)	146
O N O (nitroxide)	(styrene)	154	O / O (dendritic)	(styrene)	56 161

(Continued)

TABLE 10.2   *(Continued)*
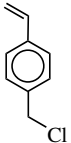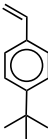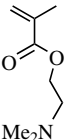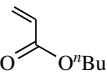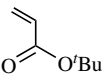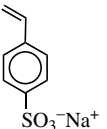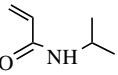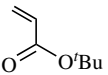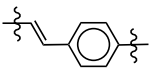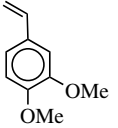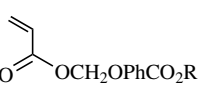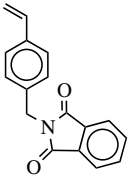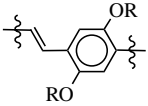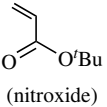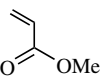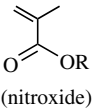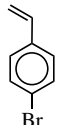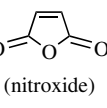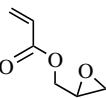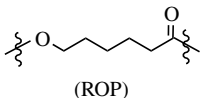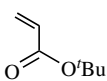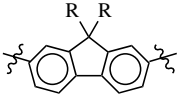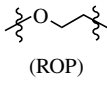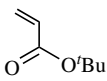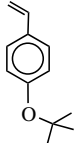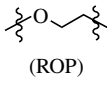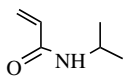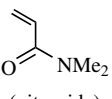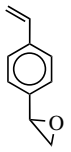
Monomer 1[a]	Monomer 2	Ref.	Monomer 1[a]	Monomer 2	Ref.
(nitroxide) [p-chloromethyl styrene]	styrene	38 118 142 149	(free-radical) [p-tert-butyl styrene]	styrene	141
(nitroxide) [Me$_2$N ethyl methacrylate]	styrene	147	(nitroxide) [vinyl ferrocene, Fe]	styrene	139
(nitroxide) O O^{n}Bu	O O^{t}Bu	38	(anionic) [butadiene]	styrene	134
(nitroxide) [SO$_3^-$Na$^+$ styrene sulfonate]	styrene	135 145	(nitroxide) [cyclic carbonate]	styrene	137
(free-radical) O NH [N-isopropyl acrylamide]	styrene	141 172	(nitroxide) [styrene]	O O^{t}Bu	38 164
(free-radical) N O [N-vinyl pyrrolidone]	styrene	141	(nitroxide) OMe [p-methoxy styrene]	styrene	164
(free-radical) OMe OMe [dimethoxy styrene]	styrene	141	(stepwise)	styrene	154
			(nitroxide) O OCH$_2$OPhCO$_2$R	styrene	168

TABLE 10.2 *(Continued)*

Monomer 1[a]	Monomer 2	Ref.	Monomer 1[a]	Monomer 2	Ref.
(nitroxide)	styrene	127	(nitroxide)	isoprene (isopropenyl)	38, 120
RO, OR (condensation)	styrene	126	O^{t}Bu acrylate (nitroxide)	isoprene	38, 121
OMe acrylate (nitroxide)	isoprene	38, 128	OR methacrylate (nitroxide)	styrene	38, 138, 158
Br styrene (nitroxide)	styrene	133	maleic anhydride (nitroxide)	styrene	159, 160, 181
glycidyl acrylate (nitroxide)	isoprene	124	CN (nitroxide)	styrene	38, 165
R R fluorene (condensation)	styrene	123	(ROP)	O^{t}Bu acrylate	165, 172
O^{t}Bu ether styrene (nitroxide)	styrene	122	(ROP)	O^{t}Bu acrylate	166, 172
NMe$_2$ acrylamide (nitroxide)	styrene	38, 121	(ROP)	NH isopropyl acrylamide	167, 172
			glycidyl styrene (nitroxide)	styrene	163

[a] Polymerization method.

Scheme 10.20

alkoxyamine, **32**. The PEG-based macroinitiator, **61**, can then be used to polymerize a variety of vinyl monomers, such as styrene, to give amphiphilic block copolymers, **62**, which have accurately controlled molecular weights and very low polydispersities, 1.05–1.10 (Scheme 10.20). An interesting feature of these macroinitiators is the observation that their use leads to lower polydispersities being obtained when compared to comparable small molecule initiators. These extremely low polydispersities may be due to the macroinitiator having a significantly reduced tendency to undergo radical coupling when compared to small molecule initiators.

The second strategy for nonvinylic block copolymer formation involves the combination of living free-radical techniques with other polymerization processes to form either linear block copolymers or graft systems. All of these processes take advantage of the compatibility and stability of alkoxyamines and NMP with a wide range of reaction conditions. For example, this permits the alkoxyamine initiating group to be copolymerized into a polyolefin backbone under metallocene conditions[169] or into a vinyl backbone under anionic[170] or normal free-radical

conditions.[171] The latter is an interesting application of the specificity of nitroxide mediated living free-radical polymerizations. Since the cleavage of the C—ON bond is thermally activated, reactions at lower temperatures ($\sim >80°C$) can be performed without any initiation occurring from the alkoxyamine sites. As a consequence, normal free-radical polymerizations, ATRP and RAFT procedures, can be performed in the presence of alkoxyamines, which permits the facile synthesis of graft and block copolymers.

The synthetic versatility associated with combining different polymerization techniques can also be demonstrated by the preparation of poly(caprolactone)-*b*-(styrene) copolymers. In this case, living ring-opening polymerization is combined with nitroxide-mediated free-radical procedures via the use of a hydroxy-substituted alkoxyamine, **63**.[173] The functionalized alkoxyamine acts as a dual, or double-headed initiator with the primary alcohol initiating the ring-opening polymerization of caprolactone to give the alkoxyamine-terminated macroinitiator, **64**, which can then be used to initiate the living polymerization of styrene to afford the well-defined block copolymer, **65**. Alternatively, the alkoxyamine group of **63** can be used to initiate the polymerization of styrene and in turn, the hydroxy-terminated polystyrene, **66**, allows the ring-opening polymerization to be initiated from the hydroxy group to give the same block copolymer, **65** (Scheme 10.21). An interesting feature of this approach is that the sequence of living polymerizations gives the same polymeric structure with similar levels of control.

The advantages of living free-radical polymerizations are not restricted to novel block copolymers with nonvinylic repeat units. The compatibility with functional groups and the inherent radical nature of the process also allows for significant progress in the synthesis of block copolymers based only on vinyl monomers. While a number of these structures can be obtained from other living processes, such as anionic procedures, in many cases they can be prepared much more readily by living free-radical techniques and the special attributes of living free-radical chemistry allow a range of new materials to be prepared.

The presence of dormant initiating centers at the chain end(s) of linear vinyl polymers prepared by NMP provides unique opportunities for the preparation of block copolymer structures. It should be noted that while the block copolymers available from ''living'' free-radical procedures may not be as well defined as the best examples available from anionic techniques, they have the advantage of greater availability and a significantly enhanced tolerance of functional groups. Technological applications that have been examined for these block copolymer include dispersants for pigments,[174,175] precursors to shell crosslinked nanoparticles for drug delivery,[176,177] supports for combinatorial chemistry,[178] and resist materials for photolithography.[179]

The advent of second generation alkoxyamines, which are suitable for the polymerization of a much wider selection of monomer families, has significantly enlarged the range of block copolymers that can be prepared using nitroxide-mediated processes. For example, block copolymers such as polystyrene-*b*-isoprene, and poly(*t*-butyl acrylate)-*b*-(*N*,*N*-dimethylacrylamide). can be readily obtained by polymerization of the first monomer, followed by isolation, and purification of the
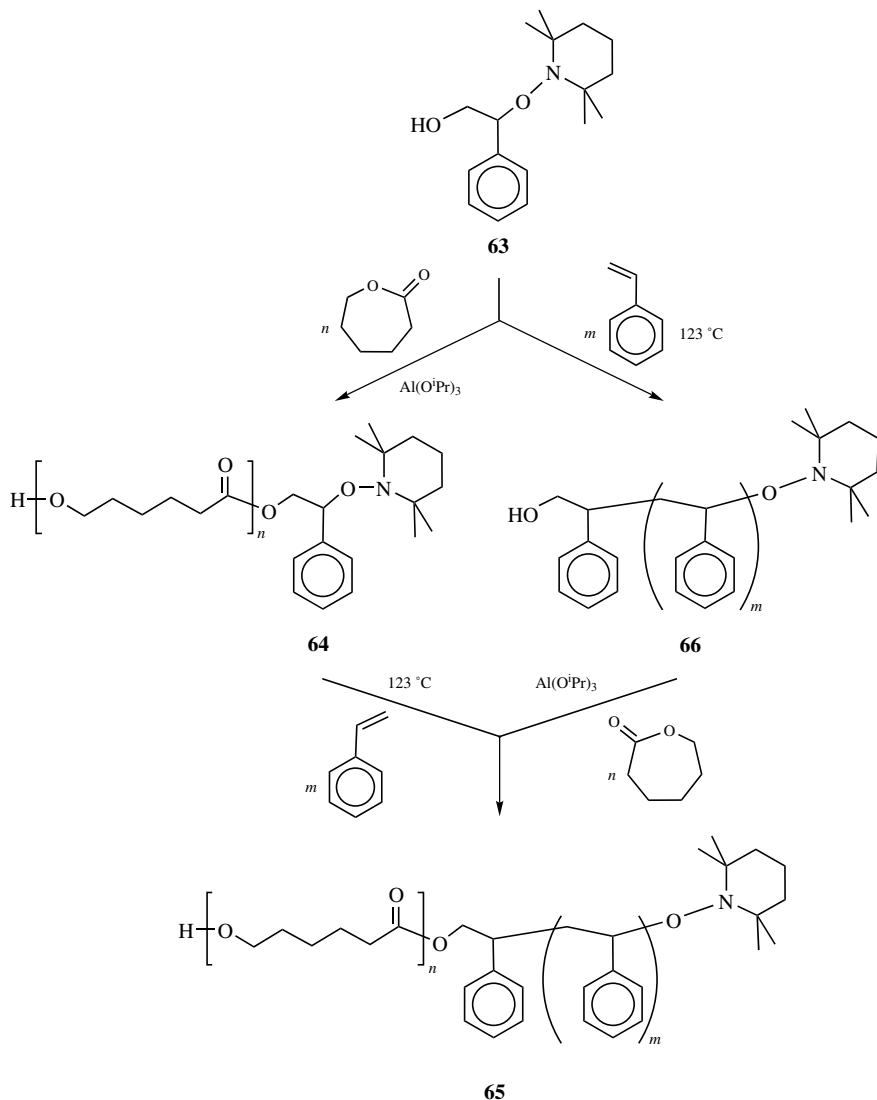
Scheme 10.21

starting block.[53] The stable starting block is then redissolved in the second mono-
mer, with or without the presence of a solvent to aid solubility, and on thermal
activation the second block is grown. One of the interesting features of preparing
block copolymers by NMP, ATRP, or RAFT procedures is that initial block can
be characterized and stored for long periods of time under normal laboratory condi-
tions before proceeding to the second block. This is totally unlike anionic procedures

and is extremely useful from a synthetic viewpoint. However, one drawback that nitroxide mediated polymerizations have in common with anionic procedures is that they both suffer from a monomer sequence issue when preparing specific block copolymers.

The classic example for living free-radical systems is the preparation of styrene-acrylate block copolymers. If a starting polystyrene macroinitiator, **67**, is used to polymerize *n*-butyl acrylate to give the block copolymer, **68**, a significant amount of a low molecular weight shoulder is observed.[53] The exact nature of this shoulder, whether it is unreacted, or terminated starting polystyrene block is unknown. Attempts to overcome this unexpected lack of reactivity by the addition of solvent and other materials have been unsuccessful and is related to the relative rates of polymerization and initiation for styrene and acrylates. The initiating ability of the starting polystyrene block is, however, not an issue since it can be used to initiate the polymerization of isoprene extremely efficiently leading to well-defined block copolymers, **69**, with no homopolymer or lower molecular weight contamination (Scheme 10.22).

In contrast, the reverse strategy, polymerization of the acrylate block followed by styrene, is extremely successful and has allowed the preparation of well-defined block copolymers with levels of control comparable to ATRP procedures. In this strategy, an alkoxyamine functionalized poly(*n*-butyl acrylate) block, **70,** is initially grown and then used to polymerize styrene at $123°C$ under argon for 8 h. This results in 92% conversion to give the block copolymer, **71**, analysis of which revealed the expected increase in molecular weight, while the polydispersity remained very low (PDI. $= 1.06–1.19$) and there were no detectable amount of unreacted starting poly(acrylate) block (Scheme 10.23).

The radical nature of nitroxide mediated processes also allows novel types of block copolymers, to be prepared. One of the simplest are block copolymers, which incorporate a random copolymer as one of the blocks.[124] The novelty of these structures is based on the inability to prepare random copolymers by living anionic or cationic procedures, in contrast to the facile synthesis of well-defined random copolymers by nitroxide-mediated systems. While similar in concept, random block copolymers are more like traditional block copolymers than random copolymers in that there are two discrete blocks, the main difference is that one or more of these blocks are composed of a random copolymer segment. An excellent example of the synthesis and application of these materials is the preparation of the functionalized block copolymer, **72**. An initial random copolymer of methyl acrylate and glycidyl methacrylate, **73**, is prepared by nitroxide mediated living free-radical polymerization and then used to initiate the polymerization of isoprene leading to the random block copolymer **72** (Scheme 10.24). The design of these macromolecules incorporates a random block that is not only miscible with thermosetting epoxies but can also undergo reaction leading to covalent linking between the copolymer microstructure and the crosslinked epoxy resin. The polyisoprene block is immiscible and thus drives the formation of a nanoscopic phase separated structure and leads to modification of the physical and mechanical properties of the thermosetting epoxy. The facile synthesis of **72**, which combines reactive epoxy functionalities
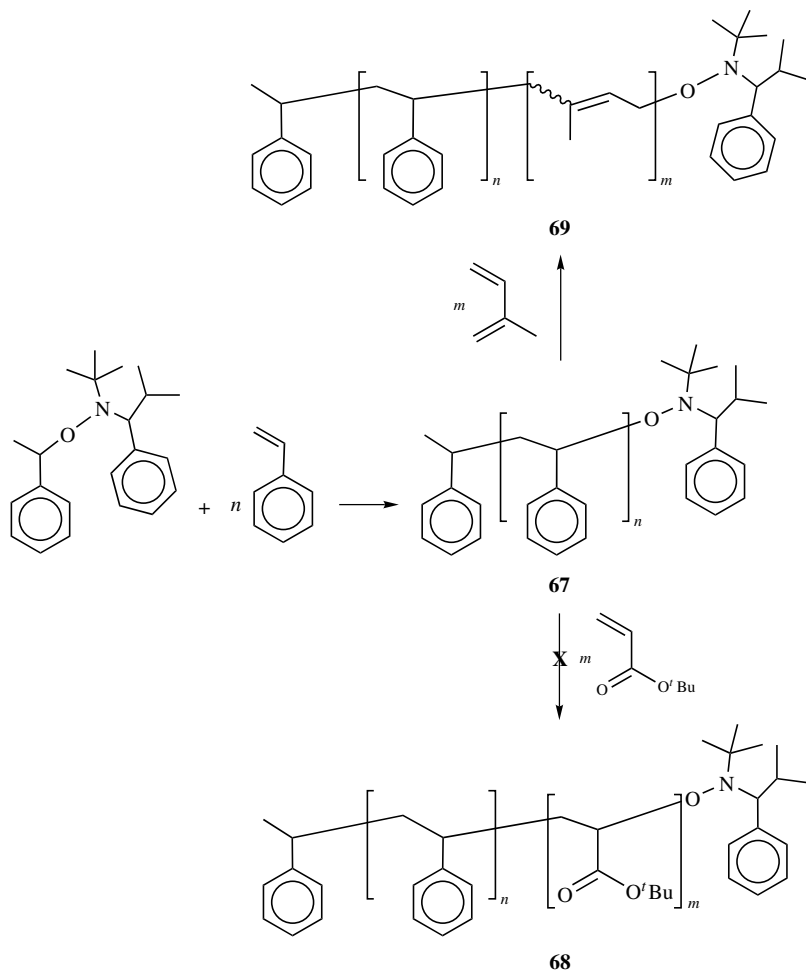
Scheme 10.22

with both a block and random copolymer structure should be compared with the difficulty in preparing **72** using other techniques.

10.6.4   Random Copolymers

One of the major advantages of normal radical procedures compared to living anionic or cationic polymerizations is the ability to prepare random copolymers. In traditional anionic or cationic procedures there are numerous problems that preclude the successful synthesis of random copolymers. For example, reactivity ratios can be large in anionic systems, and so true random copolymerizations do not occur and blocky structures are obtained. Alternatively, the polymerization conditions
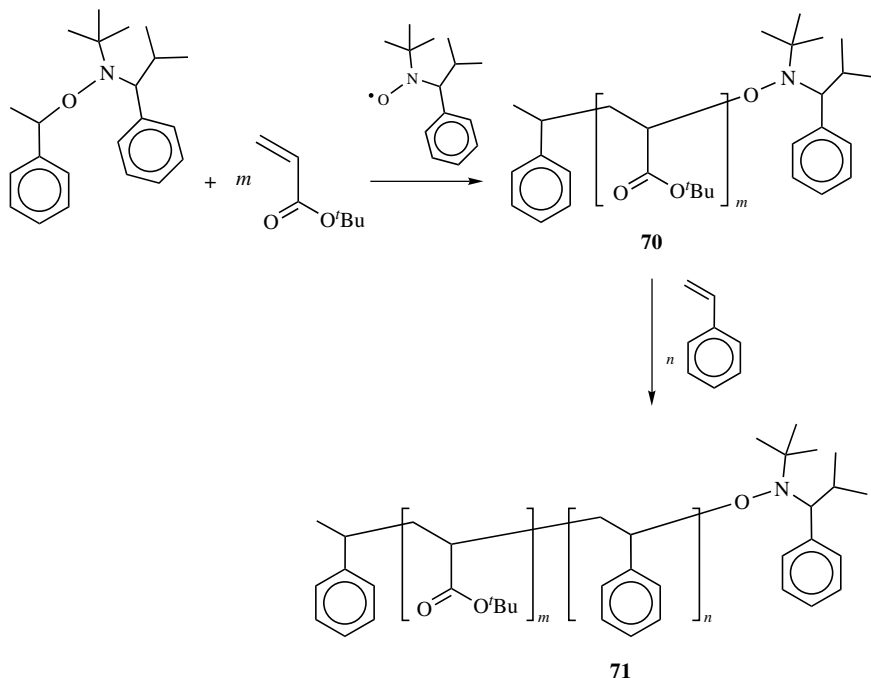
Scheme 10.23

for one monomer, or functional group may not be compatible with the second monomer and a controlled polymerization is therefore not obtained. In fact, even for a simple comonomer mixture of styrene and methyl methacrylate, well-defined random copolymers cannot be prepared using anionic or cationic procedures. This lack of synthetic versatility has prompted numerous groups to explore the extension of living radical techniques to the preparation of well-defined random copolymers. While early work with TEMPO did demonstrate that random copolymers can be prepared under NMP conditions the inability to control the homopolymerization of monomers other than styrene limited the range of monomer units and possible random copolymer structures.[31,174,180] With the advent of second generation nitroxides, such as **36**, the possibilities for well-defined random copolymers have been dramatically increased. For example, while the homopolymerization of methacrylates does not give controlled polymers, random copolymers of methacrylates with up to 90 mol% of methacylate incorporation can be prepared in a living fashion.[53] The rationale for this stark contrast may be that incorporation of a small percentage of styrene as a comonomer reduces the H-abstraction reaction that normally leads to termination in methacrylate homopolymerization, to such an extent that the polymerization can now proceed in a living fashion.

The finding that the reactivity ratios for monomers under living free-radical conditions are essentially the same as under normal free-radical conditions is

73

74
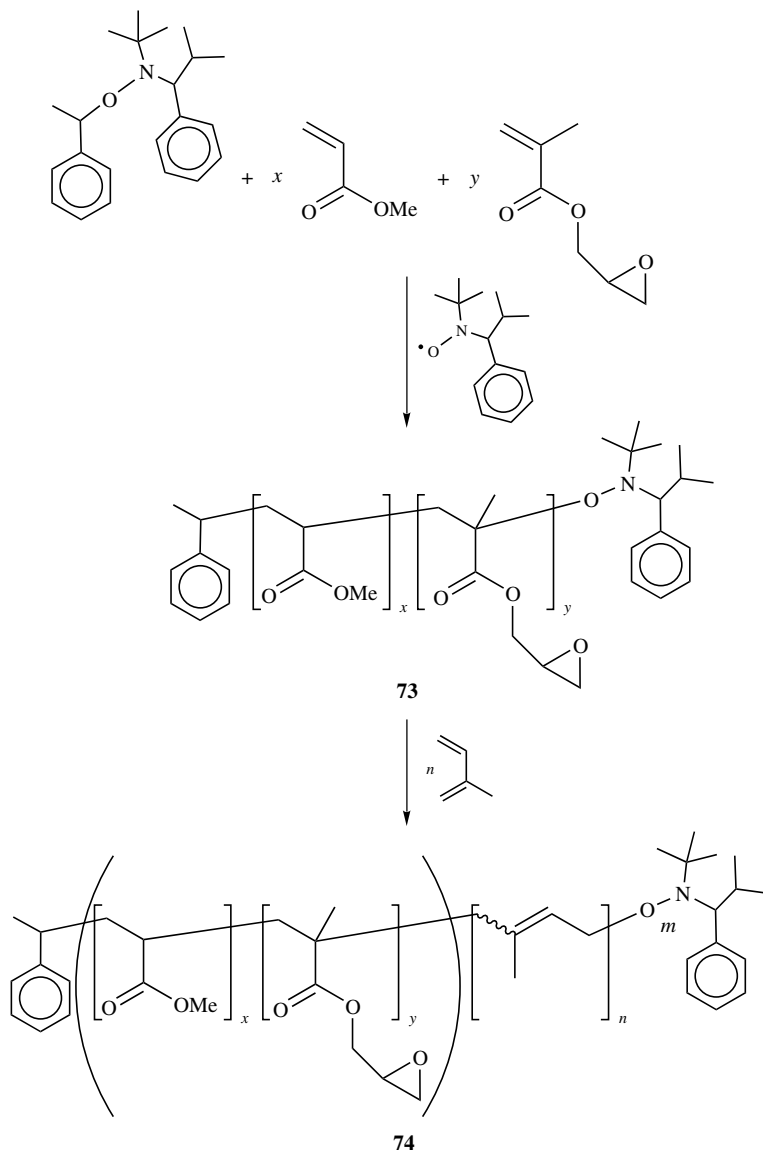
Scheme 10.24

fundamentally more important than it appears at first glance. One of the most inter-
esting consequence is that random copolymers prepared by living free-radical pro-
cesses are different on a molecular level to those prepared by normal free-radical
methods, even though they may appear the same on the macroscopic level (Scheme
10.25). In the case of normal free-radical polymerization, continuous initiation leads

Initiation at T = 0, compositionally similar

M_1 + M_2

Continuous Initiation, compositionally different
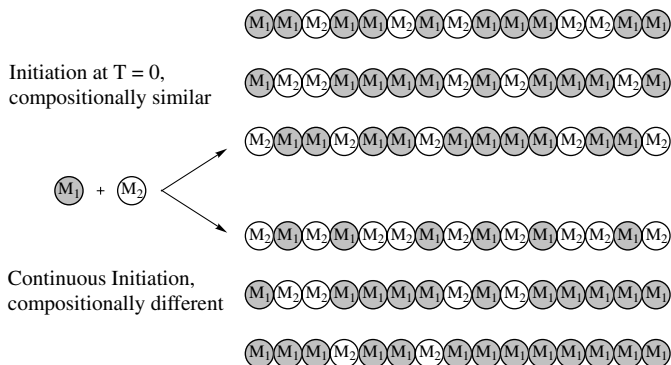
Scheme 10.25

to the growth cycle of polymer chains (initiation, propagation, termination) occurring at different stages of the polymerization. Therefore, chains that initiate, grow and terminate at low conversion experience a different monomer feed ratio compared to chains initiated at different times during the polymerization. As a result, the polymerization product is a complex mixture of random copolymers with different monomer compositions. For living radical systems the situation is totally different; all chains are initiated at the same time and grow at approximately the same rate. The growing chains therefore experience the same change in monomer concentrations due to different monomer reactivity ratios and random copolymers of the same composition are obtained. This is depicted graphically in Scheme 10.25, however it should also be pointed out that while the graphical representation suggests that all the chains are the same length, this is not the case especially for normal free-radical procedures where polydispersities of 2.0 are typically obtained (cf. 1.1 for nitroxide systems). The structural variation between chains is therefore even further exacerbated in normal radical systems.

10.6.5 Gradient Copolymers

An excellent example of using reactivity ratios and the synthetic versatility of nitroxide systems to prepare unusual block copolymers is the copolymerization of styrene/maleic anhydride mixtures.[181] In this case, the copolymerization of a mixture of styrene and maleic anhydride leads to preferential and finally total consumption of maleic anhydride at conversions of styrene significantly less than 100%. As a result, the growing polymer chains experience an initial monomer feed of styrene and maleic anhydride that gradually changes during the course of the polymerization to a monomer feed of pure styrene. These materials can be considered to be a limiting example of gradient copolymers and by carefully choosing reactivity ratios, structures intermediate between statistically random copolymers and one-step block copolymers can be prepared by living free-radical techniques.[182,183]

10.7   COMPLEX MACROMOLECULAR ARCHITECTURES

10.7.1   Branched Polymers

The robustness of the alkoxyamine functional group, coupled with the ability to pre-
pare a variety of functionalized derivatives opens up a number of possibilities for the
synthesis of complex macromolecular architectures. Again, a comparison with nor-
mal radical polymerization is educational. The use of polyfunctional initiators under
normal free-radical conditions gives crosslinked networks due to radical coupling
reactions; under living radical conditions a polyfunctional initiator may be expected
to lead to the desired graft, or star polymer with little, or no, unwanted coupling
products.

   This possibility was first tested by the synthesis and polymerization of the trifunc-
tional unimolecular initiator, **75**, and its use in the preparation of 3-arm stars.[184]
Interestingly, no detectable amounts of crosslinked or insoluble material was
observed, and degradation of the 3-arm polystyrene star, **76**, by hydrolysis of the
ester links was found to give the individual polystyrene arms, **77** (Scheme 10.26).
Analysis of **77** revealed a molecular weight comparable to that expected from the
initiator to monomer ratio and a narrow polydispersity ($\sim$1.10–1.15). These results
demonstrate that each of the initiating units in the trisalkoxyamine is "active" and
the individual polystyrene arms grow at approximately the same rate with little or no
coupling due to radical–radical reactions.

   Subsequently, this concept has been extended to more highly functionalized star
initiators as well as polymeric initiators for the synthesis of graft structures. Since
the polymerization process is still radical in nature, caution should still be exercised.
While radical–radical coupling reactions are decreased, they are not eliminated
entirely, and as the number of initiating sites per molecule increase, the probability
of coupling also increases. For example, a mixture of styrene and p-chloromethyl
styrene can be polymerized under "living" free-radical conditions to give a
well-defined linear copolymer, **78**, with controlled molecular weight and low poly-
dispersity ($\sim$1.10–1.25). Reaction of **78** with the sodium salt of the hydroxy-func-
tionalized unimolecular initiator then gives the desired polymeric initiator, **79**,
which is a precursor to a variety of graft copolymers, **80**.[185] At average grafting den-
sities of greater than six initiating sites per backbone, chain–chain coupling becomes
apparent by GPC and at densities greater than 15 it is a major process under standard
conditions; however, optimization of the star-forming reaction (temperatures of sol-
vent, monomer, etc.) may lead to a reduction in coupling (Scheme 10.27).

10.7.2   Hyperbranched and Dendritic Structures

The synthesis of these star or graft polymers has attracted much interest, and a variety
of simplified approaches to similar branched structures have been reported.[190] The
majority of work has centered on the coupling, or knitting together of preformed
linear chains by reaction with crosslinkable monomers. One of the attractive features
of this approach, which is unique to living radical systems, is that the starting linear
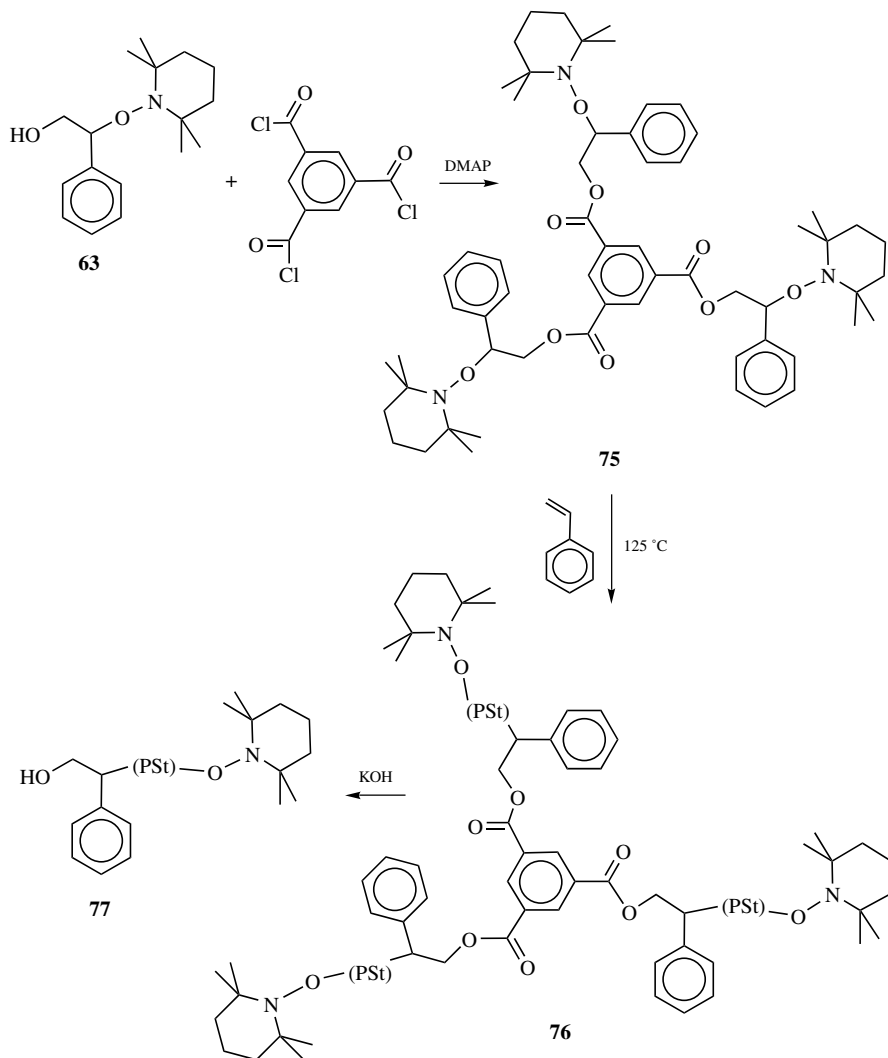
Scheme 10.26

chains, **81**, can be isolated, characterized, and stored before subsequent coupling. Additionally, a variety of different chains in terms of molecular weight, composition, and other properties can be copolymerized together to give heterogeneous star–block copolymers.[191–194] The basic strategy is outlined in Scheme 10.28, and involves the preparation of alkoxyamine terminated linear chains, **81**, and subsequent coupling of these dormant chains with crosslinking agents such as divinylbenzene or a bismaleimide derivative to give a highly branched star, **82**. Since the only requirement is an alkoxyamine chain end, the range of starting linear polymers is
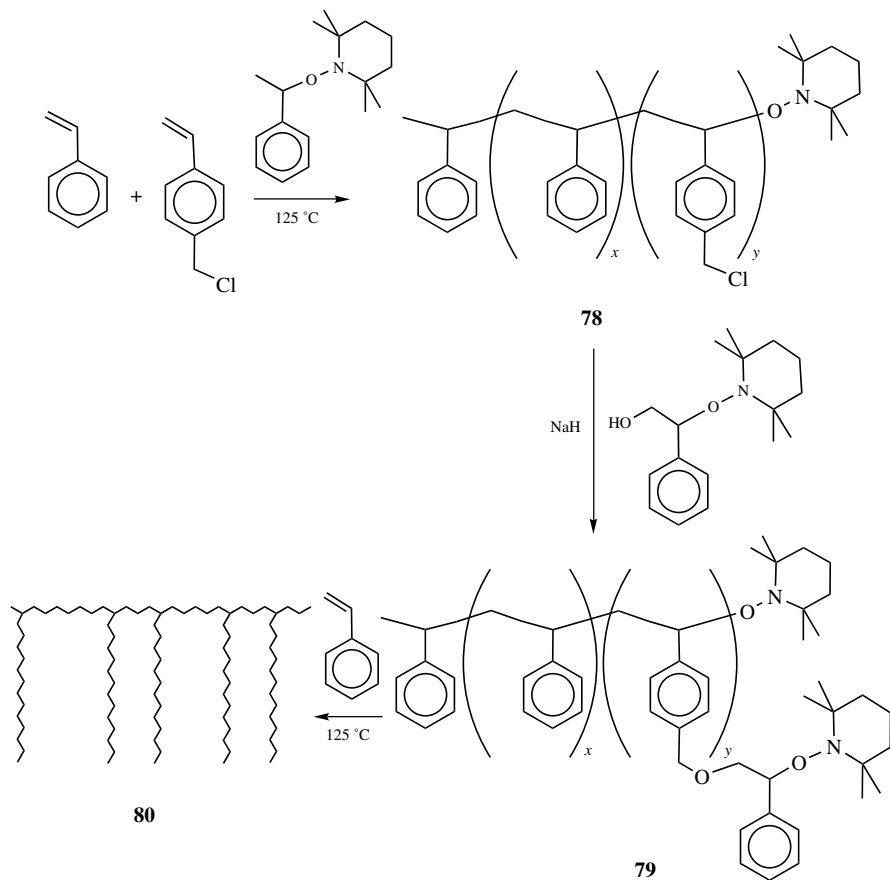
Scheme 10.27

large and not restricted to vinyl polymers or homopolymers. This permits the generation of star polymer libraries from modular polymeric building blocks.

The ability to form reactive unimolecular initiators, such as **83**, opens up a number of avenues to other unusual macromolecular architectures that are either difficult, or impossible, to prepare using traditional free-radical chemistry or living anionic procedures. In the case of the styrenic derivative, **84**, a propagating center and an initiating center are combined in the same molecule, effectively creating a self-condensing monomer. The similarity of **84** to traditional AB$_2$ monomers then permits the preparation of hyperbranched macromolecules by a novel condensation/addition process. Homopolymerization of **84** under "living" free-radical conditions then leads to initial formation of dimers, trimers, and so on and eventually hyperbranched macromolecules, **85**, with the kinetics of growth resembling a step-growth polymerization even though the polymerization occurs by a free-radical
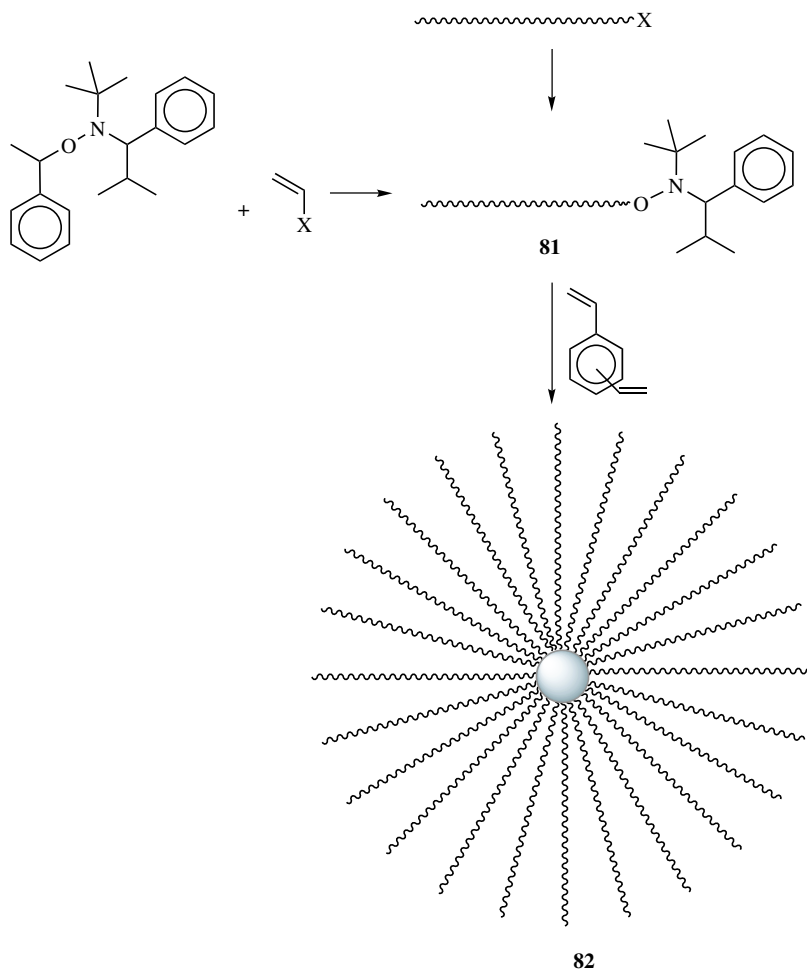
Scheme 10.28

mechanism (Scheme 10.29).[186] One interesting facet of this polymerization is that the hyperbranched polystyrene derivatives contain numerous initiating centers. These numerous initiating centers have been used to form a unique class of star macromolecules in which the central core is a highly functionalized hyperbranched polymer. Subsequently, Fréchet[187] and Matyjaszewski[188] applied a similar technique to the preparation of hyperbranched polystyrene derivatives by the homopolymerization of *p*-chloromethylstyrene using ATRP conditions, though the actual structure of the materials obtained seems to be variable.[189]

Unique dendritic–linear block copolymers have also been prepared by the coupling of functionalized initiators with dendritic macromolecules prepared by the convergent approach. In these approaches the dendrimer can be attached to either
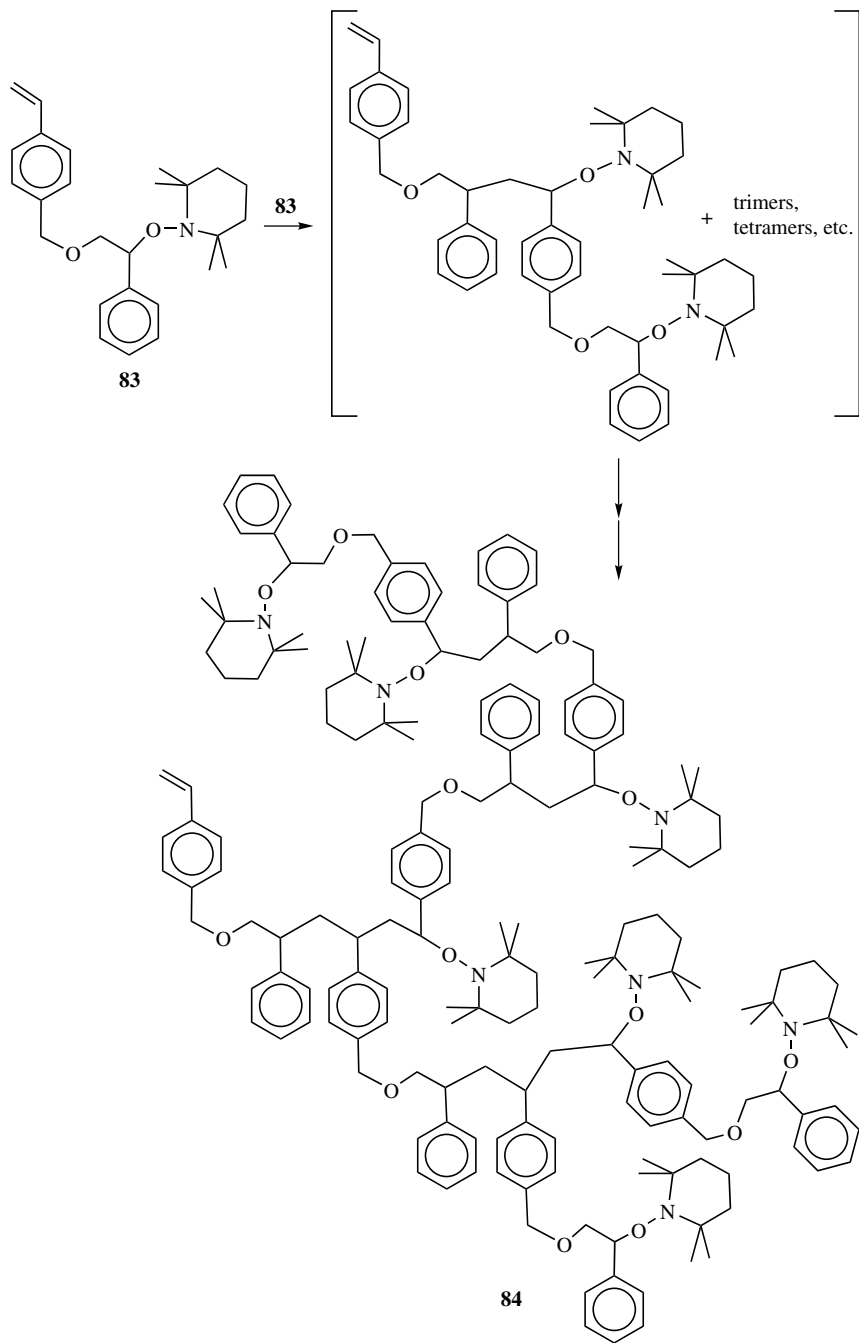
Scheme 10.29

the initiating fragment of the alkoxyamine or the mediating nitroxide and the dendritic initiator used to initiate the growth of linear vinyl blocks under controlled conditions. As demonstrated by Fréchet and co-workers, these monodisperse dendritic initiators are perfectly suited for the preparation of well-defined block copolymers; for example, coupling of the convergently prepared dendrimer, **85**, which contains a single bromomethyl group at its focal point with the hydroxy functionalized unimolecular initiators gives the dendritic initiator, **86**. Hybrid dendritic–linear block copolymers, **87**, with well-controlled molecular weights and low polydispersities are then obtained by the reaction of **86** with vinyl monomers under standard "living" free-radical polymerization conditions (Scheme 10.30).[161,195,196] Similar structures can also be prepared using ATRP chemistry and in this case the initiating group is simply a focal point chloromethyl, or bromomethyl functionality (see Chapter 11).[197] It is interesting to note that in the case[198] where the dendritic block is attached to the nitroxide functionality, the molecular weights and polydispersities for the block copolymers are not as well controlled as the case where the dendrimer is attached to the initiating fragment. This difference may be due to the increased steric bulk of the dendritic nitroxide, which would be expected to decrease its mobility and hence ability to control the polymerization. While a detailed study has not been performed, this result may have important implications especially for complex, functionalized nitroxides whose diffusion ability may be reduced.

This building block, or modular approach to the synthesis of complex macromolecular architectures can be taken a step further in the rapid synthesis of combburst, or dendritic graft copolymers by a tandem "living" free-radical approach.[185,199,200] The underlying strategy in this novel approach to highly branched linear polymers is that each layer, or generation, of linear polymers is prepared by "living" free-radical procedures and the initiating groups are either present during the polymerization or introduced in a postpolymerization functionalization step. In this way very large, highly branched combburst copolymers can be prepared in a limited number of steps using mild reaction conditions. As shown in Scheme 10.31, the initial linear backbone, **88**, is prepared by nitroxide mediated "living" free-radical polymerization of a mixture of styrene and *p*-chloromethyl styrene, **89**. At this stage TEMPO-based initiating groups can be introduced by reaction of the numerous chloromethyl groups with the sodium salt of **63** to give the polymeric initiator, **90**. A second layer, or generation, of reactive chloromethyl groups can be introduced on the grafted arms, **91**, by a second copolymerization of styrene and *p*-chloromethylstyrene. This functionalized graft copolymer can again be used as a complex polymeric initiator for ATRP polymerization that introduces a third layer of linear polymer chains, **92**. In analogy with the divergent growth approach to dendritic macromolecules, this stepwise functionalization/growth strategy can be continued to give larger and larger combburst macromolecules, and the mild reaction conditions permit a wide variety of monomer units and functional groups to be used.

The versatility associated with NMP, in terms of both monomer choice and initiator structure, also permits a wide variety of other complex macromolecular structures to be prepared. Sherrington[201] and Fukuda[202] examined the preparation of crosslinked structures by nitroxide mediated processes and in analogy with the
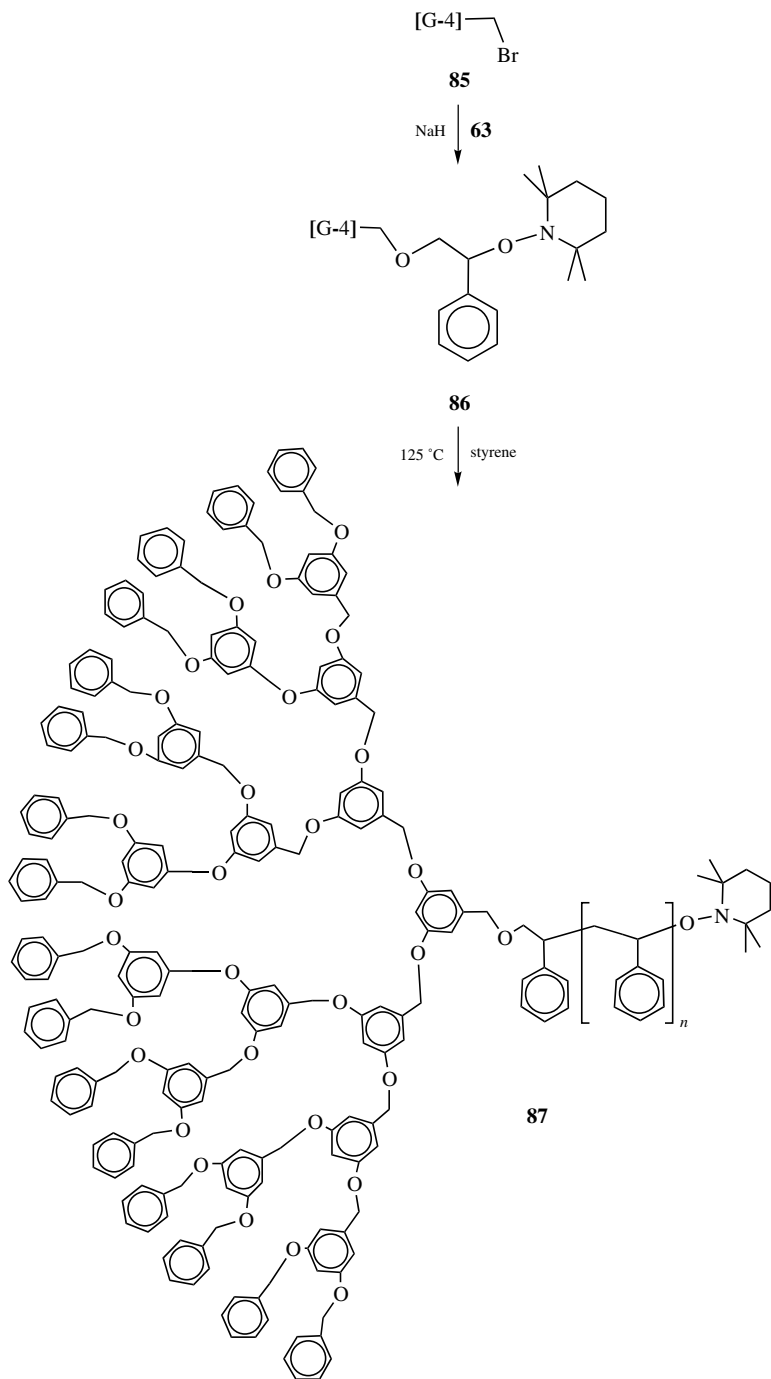
Scheme 10.30
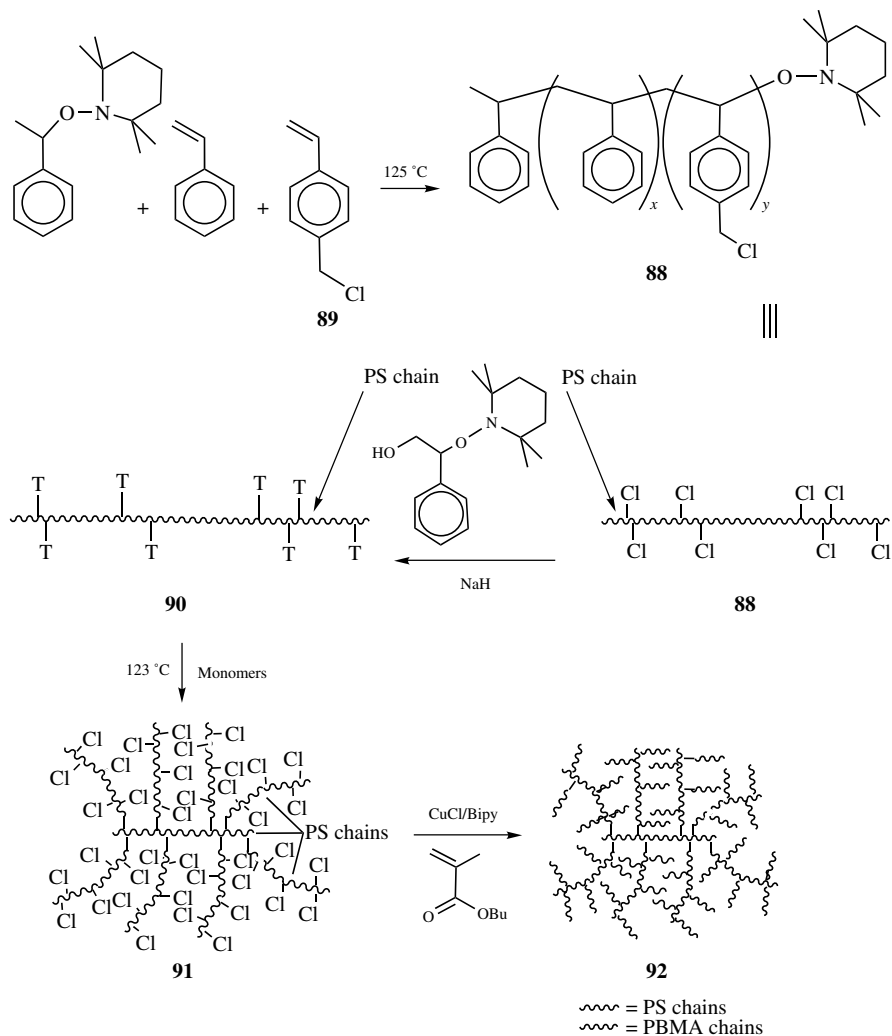
Scheme 10.31

synthesis of random copolymers, the living nature of the polymerization permits subtlety different structures to be obtained when compared to normal free-radical processes. In addition, a versatile approach to cyclic polymers has been developed by Hemery[203] that relies on the synthesis of nonsymmetric telechelic macromolecules followed by cyclization of the mutually reactive chain ends. In a similar approach, Chaumont has prepared well-defined polymer networks by the crosslinking of telechelic macromolecules prepared by nitroxide mediated processes with bifunctional small molecules.[204]
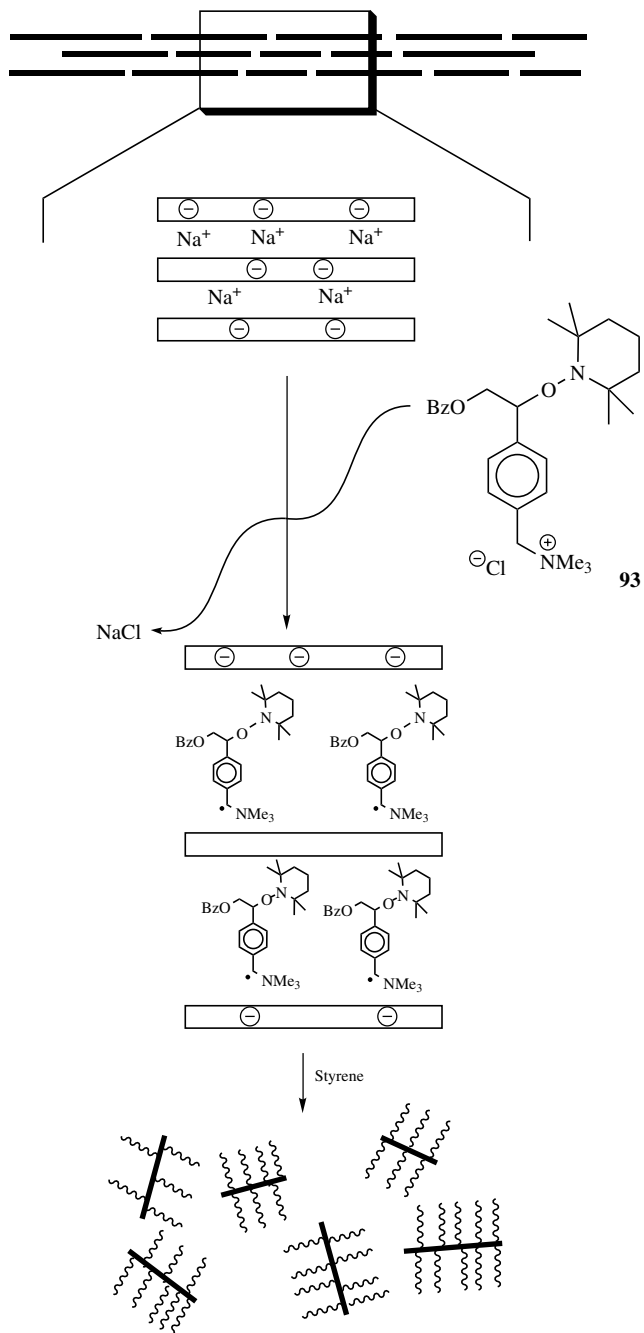
Scheme 10.32

10.8 SURFACE-INITIATED POLYMERIZATIONS

The stability of alkoxyamine initiators is a major synthetic advantage, not only in the preparation of complex macromolecular architectures, but also leads to opportunities in the area of surface modification. Functionalized initiators for living polymerizations can now be prepared and attached to a variety of surfaces and subsequently used to grow covalently attached polymer chains. The living nature of the polymerization provides an unprecedented ability to control the structure, density, functionality, and other parameters of the surface attached polymer chains and has rapidly become an area of significant importance and growth.[205] Numerous studies have appeared demonstrating the ability to control the degree of polymerization or thickness of the grafted polymer chains, achieve low polydispersities, and prepare block copolymers. The covalent nature of the surface attachment also allows either the living free-radical initiators themselves to be patterned or the resulting polymer brushes to be patterned.[206,207] Two examples that capture the essence of this area are the preparation of functionalized macroporous monoliths for advanced chromatographic separations and the design of "Rasta resins." The latter are especially interesting as ultra-high-capacity supports for combinatorial chemistry that not only utilize the increased functionality or amplification afforded by the surface initiated polymerization concept but take advantage of the more "solutionlike" environment of the functional groups attached to the solvated polymer chains when compared to functionalities at a solid–liquid interface.[208,209] Similar strategies can be performed on alternate particulate substrates such as silica[205] or carbon block[210] or via ATRP techniques.[211–214]

The future potential of surface-initiated polymerizations in nanotechnology is perhaps best illustrated by the direct synthesis of dispersed nanocomposites by Sogah.[215] In this approach the synthetic versatility of the alkoxyamine group is again exploited to prepare the quaternary amine salt, **93**, which, because of its charged nature, can intercalate readily into the intergallery spaces of a silicate matrix. These silicate-anchored alkoxyamine initiators can then be used to initiate the polymerization of a vinyl monomer such as styrene leading to a dispersed silicate nanocomposite. The advantages of this novel approach are that the intercalation of small initiating species such as **93** is orders of magnitude more facile than for similar chain-end-functionalized polystyrene derivatives. In addition, critical polymer characteristics such as molecular weight and polydispersity are controlled while block or random copolymer formation is possible (Scheme 10.32).

10.9 CONCLUSIONS

Even though the first reports of a living radical process were published in 1993, the impact on the field of polymer chemistry by early 2001 had already been immense, opening up possibilities in both polymer synthesis and polymer physics that until the late 1990s were either prohibitively difficult or impossible. The development of nitroxide-mediated living free-radical polymerizations as an important synthetic

tool has been extremely rapid and does indeed pose exciting possibilities for the future. However, a number of issues that be addressed to enable the continued evolution of this technique. A greater understanding of the relationship between nitroxide/alkoxyamine structure and polymerization efficiency needs to be developed. Specifically, mediating nitroxides or strategies must be developed that allow the polymerizations to be conducted at lower temperatures (~ 60–$80°C$) in shorter time periods (2–5 h) and with higher conversions ($\sim 99\%+$). It is also highly desirable to further increase the range of monomers that can be polymerized under living conditions, prime candidates are methacrylates and nonconjugated vinyl monomers. If these challenges can be overcome the industrial appeal of NMP will increase significantly, while also providing an extremely powerful synthetic technique for the synthesis of vinyl based polymers.

The power of living free-radical procedures as synthetic tools in polymer science can be better appreciated by considering the potential advantages when compared to traditional techniques such as anionic polymerization. The ability to accommodate functional groups and diverse families of monomers permit block, random, and gradient copolymers to be prepared without complicated, multistep reaction schemes. Complex macromolecular architectures can also be prepared; however, the low occurrence of radical–radical coupling reactions does place restrictions on the number of propagating arms per macromolecule. The radical nature of the polymerization process does limit the ability to control the stereochemistry; no evidence has been currently presented to indicate that living free-radical processes can lead to tacticity control. Presumably the generation of a planar radical at the propagating chain end during each monomer addition step is the key step in this loss of stereochemical control.

Another significant advantage of living free-radical procedures is the stability of the initiating species. In the case of nitroxide mediated processes, the discussion above clearly demonstrates that a variety of chemical transformations can be performed with no deleterious effect on the initiating ability of the alkoxyamine initiator. This not only significant improves the ability to prepare chain-end-labeled macromolecules but also permits initiating fragments to be introduced at various surfaces, interfaces, chain ends of dendrimers, along the backbone of a linear polymer chain, and so on. As more and more effort is devoted to controlling structure and function on the nanometer scale, the role of well-defined polymeric materials with controlled size, dispersity and functional group placement will become critical for the continued evolution of nanotechnology.

REFERENCES

1. G. Moad and D. H. Solomon, *The Chemistry of Free Radical Polymerization*, Pergamon, Oxford, 1995.

2. R. P. Quirk, D. J. Kinning, and L. J. Fetters, in *Comprehensive Polymer Science*, Pergamon Press, London, S. L. Aggarwal, edi., 1989; Vol. 7, p. 1.

3. X. Z. Zhou and K. J. Shea, *Macromolecules* **34**, 3111 (2001).

4. K. J. Shea, J. W. Walker, H. D. Zhu, M. Paz, and M. J. Greaves, *J. Am. Chem. Soc.* **119**, 9049 (1997).

5. M. Sawamoto and M. Kamigaito, *CHEMTECH* **29**, 30 (1999).

6. E. E. Malmstrom and C. J. Hawker, *Macromol. Chem. Phys.* **199**, 923 (1998).

7. (a) K. Matyjaszewski, *ACS Symp. Ser.* **685**, K. Matyjaszewski, ed., American Chemical Society, Washington, DC, 1998 p. 1; (b) K. Matyjaszewski, *Chem. Eur. J.* **5**, 3095 (1999).

8. D. Colombani, *Prog. Polym. Sci.* **22**, 1649 (1997).

9. T. E. Werrington and A. V. Tobolsky, *J. Am. Chem. Soc.* **77**, 4510 (1955).

10. T. Otsu and M. Yoshida, *Makromol. Chem., Rapid Commun.* **3**, 127 (1982); T. Otsu, *J. Polym. Sci., Polym. Chem.* **38**, 2121 (2000).

11. A. Bledzki, D. Braun, and K. Titzschkau, *Makromol. Chem.* **184**, 745 (1983).

12. J. V. Crivello, J. L. Lee, and D. A. Conlon, *J. Polym. Sci., Polym. Chem.* **24**, 1251 (1986).

13. T. Otsu and T. Tazaki, *Polym. Bull.* **16**, 277 (1986).

14. J. D. Druliner, *Macromolecules* **24**, 6079 (1991).

15. E. D. Leon-Saenz, G. Morales, R. Guerrero-santos, and Y. Gnanou, *Macromol. Chem. Phys.* **201**, 74 (2000).

16. B. Yamada, Y. Nobukane, and Y. Miura, *Polym. Bull.* **41**, 539 (1998).

17. M. Steenbock, M. Klapper, and K. Mullen, *Macromol. Chem. Phys.* **199**, 763 (1998).

18. R. D. Puts and D. Y. Sogah, *Macromolecules* **29**, 3323 (1996).

19. G. Moad, E. Rizzardo, and D. H. Solomon, *Macromolecules* **15**, 909 (1982).

20. D. H. Solomon, E. Rizzardo, and P. Cacioli, U.S. Patent 4,581,429 (1986).

21. M. K. Georges, R.P.N. Veregin, P. M. Kazmaier, and G. K. Hamer, *Macromolecules* **26**, 2987 (1993).

22. S. O. Hammouch and J. M. Catala, *Macromol. Rapid Commun.* **17**, 149 (1996).

23. T. Fukuda, T. Terauchi, A. Goto, K. Ohno, Y. Tsujii, and B. Yamada, *Macromolecules* **29**, 6393 (1996).

24. G. Moad and E. Rizzardo, *Macromolecules* **28**, 8722 (1995).

25. P. G. Odell, R.P.N. Veregin, L. M. Michalak, and M. K. Georges, *Macromolecules* **30**, 2232 (1997).

26. K. Matyjaszewski, S. Gaynor, D. Greszta, D. Mardare, and T. Shigemoto, *J. Phys. Org. Chem.* **8**, 306 (1995).

27. V. Percec and D. A. Tirrell, *J. Polym. Sci., Polym. Chem.* **38**, 1705 (2000).

28. C. J. Hawker, *J. Am. Chem. Soc.* **116**, 11185 (1994).

29. C. J. Hawker, G. G. Barclay, A. Orellana, J. Dao, and W. Devonport, *Macromolecules* **29**, 5245 (1996).

30. M. O. Zink, A. Kramer, and P. Nesvadba, *Macromolecules* **33**, 8106 (2000).

31. T. M. Brown, C. J. Cooksey, D. Crich, A. T. Dronsfield, and R. Ellis, *J. Chem. Soc. Perkin Trans 1* 2131 (1993).

32. V. F. Patel and G. Pattenden, *J. Chem. Soc. Perkin Trans 1* 2703 (1990).

33. T. H. Kim, P. Dokolas, N. Feeder, M. Giles, A. B. Holmes, and M. Walther, *J. Chem. Soc., Chem. Commun.* 2419 (2000).

34. I. Q. Li, B. A. Howell, M. T. Dineen, P. E. Kastl, J. W. Lyons, D. M. Meunier, P. B. Smith, and D. B. Priddy, *Macromolecules* **30**, 5194 (1997).

35. Y. Miura, K. Hirota, H. Moto, and B. Yamada, *Macromolecules* **32**, 8356 (1999).

36. T. J. Connolly, M. V. Baldovf, N. Mohtat, and J. C. Scaiano, *Tetrahedron Lett.* **37**, 4919 (1996).

37. U. Jahn, *J. Org. Chem.* **63**, 7130 (1998).

38. K. Matyjaszewski, B. E. Woodworth, X. Zhang, S. G. Gaynor, and Z. Metzner, *Macromolecules* **31**, 5955 (1998).

39. R. Braslau, L. C. Burrill, M. Siano, N. Naik, R. K. Howden, and L. K. Mahal, *Macromolecules* **30**, 6445 (1997).

40. R. Braslau, L. C. Burrill, L. K. Mahal, and T. Wedeking, *Angew. Chem., Int. Ed. Engl.* **36**, 237 (1997).

41. S. Kobatake, H. J. Harwood, R. P. Quirk, and D. B. Priddy, *J. Polym. Sci.; Part A: Polym. Chem.* **36**, 2555 (1998).

42. D. E. Bergbreiter and B. Walchuk, *Macromolecules* **31**, 6380 (1998).

43. S. O. Hammouch and J. M. Catala, *Macromol. Rapid Commun.* **17**, 149 (1996).

44. J. Dao, D. Benoit, and C. J. Hawker, *J. Polym. Sci.; Part A: Polym. Chem.* **36**, 2161 (1998).

45. T. Linker, *Angew. Chem., Int. Ed. Engl.* **36**, 2060 (1997).

46. C. J. Hawker, E. Elce, J. Dao, W. Volksen, T. P. Russell, and G. G. Barclay, *Macromolecules* **29**, 4167 (1996).

47. B. Keoshkerian, M. K. Georges, M. Quinlan, R. P. N. Veregin, and R. Goodbrand, *Macromolecules* **31**, 7559 (1998).

48. K. Matyjaszewski, S. Gaynor, D. Greszta, D. Mardare, and T. Shigemoto, *Macromol. Symp.* **95**, 217 (1995).

49. Y. K. Chong, F. Ercole, G. Moad, E. Rizzardo, and S. H. Thang, *Macromolecules* **32**, 6895 (1999).

50. M. K. Georges, R. P. N. Veregin, P. M. Kazmaier, G. K. Hamer, and M. Saban, *Macromolecules* **27**, 7228 (1994).

51. E. E. Malmstrom, C. J. Hawker, and R. D. Miller, *Tetrahedron* **53**, 15225 (1997).

52. D. Benoit, S. Grimaldi, S. Robin, J. P. Finet, P. Tordo, and Y. Gnanou, *J. Am. Chem. Soc.* **122**, 5929 (2000).

53. D. Benoit, V. Chaplinski, R. Braslau, and C. J. Hawker *J. Am. Chem. Soc.* **121**, 904 (1999).

54. D. Benoit, E. Harth, P. Fox, R. M. Waymouth, and C. J. Hawker, *Macromolecules* **33**, 363 (2000).

55. M. Kato, M. Kamigaito, M. Sawamoto, and T. Higashimura, *Macromolecules* **28**, 1721 (1995).

56. J. S. Wang and K. Matyjaszewski, *J. Am. Chem. Soc.* **117**, 5614 (1995).

57. R. T. A. Mayadunne, E. Rizzardo, J. Chiefari, J. Krstina, G. Moad, A. Postma, and S. H. Thang, *Macromolecules* **33**, 243 (2000).

58. M. Moroni, A. Hilberer, and G. Hadziioannou, *Macro. Rapid Commum.* **17**, 693 (1996).

59. E. Yoshida and T. Fujii, *J. Polym. Sci.; Part A: Polym. Chem.* **36**, 269 (1998).

60. S. Marque, C. Le Mercier, P. Tordo, and H. Fischer, *Macromolecules* **33**, 4403 (2000).

61. F. Aldabbagh, W. K. Busfield, I. D. Jenkins, and S. H. Thang, *Tetrahedron Lett.* **41**, 3673 (2000).

62. D. Greszta and K. Matyjaszewski, *Macromolecules* **29**, 7661 (1996).

63. S. Jousset, S. O. Hammouch, and J. M. Catala, *Macromolecules* **30**, 6685 (1997).

64. W. G. Skene, S. T. Belt, T. J. Connolly, P. Hahn, and J. C. Scaiano, *Macromolecules* **31**, 9103 (1998).

65. S. O. Hammouch and J. M. Catala, *Macromol. Rapid Commun.* **17**, 683 (1996).

66. M. K. Georges, R. P. N. Veregin, P. M. Kazmaier, G. K. Hamer, and M. Saban, *Macromolecules* **27**, 7228 (1994).

67. M. V. Baldovi, N. Mohtat, and J. C. Scaiano, *Macromolecules* **29**, 5497 (1996).

68. C. J. Hawker, G. G. Barclay, and J. Dao, *J. Am. Chem. Soc.* **118**, 11467 (1996).

69. M. Davey and C. J. Hawker, unpublished results.

70. C. Farcet, M. Lansalot, B. Charleux, R. Pirri, and J. P. Vairon, *Macromolecules* **33**, 8559 (2000).

71. E. Yoshida and A. Sugita, *J. Polym. Sci.; Part A: Polym. Chem.* **36**, 2059 (1998).

72. J. L. Pradel, B. Boutevin, and B. Ameduri, *J. Polym. Sci.; Part A: Polym. Chem.* **38**, 3293 (2000).

73. S. Abrol, M. J. Caulfield, G. G. Qiao, and D. H. Solomon, *Polymer* **42**, 5987 (2001).

74. M. V. Ciriano, H. G. Korth, W. B. van Scheppingen, and P. Milder, *J. Am. Chem. Soc.* **121** 6375 (1999).

75. S. Abrol, P. A. Kambouris, M. G. Looney, and D. H. Solomon, *Macromol. Rapid Commun.* **18**, 755 (1997).

76. J. Einhorn, C. Einhorn, F. Ratajczak, I. Gautier-Luneau, and J. L. Pierre, *J. Org. Chem.* **62**, 9385 (1997).

77. G. Moad, D. A. Shipp, T. A. Smith, and D. H. Solomon, *Macromolecules* **30**, 7627 (1997).

78. T. Shigemoto and K. Matyjaszewski, *Macromol. Rapid Commun.* **17**, 347 (1996).

79. S. Jousset and J. M. Catala, *Macromolecules* **33**, 4705 (2000).

80. E. Yoshida and Y. Okada, *Bull. Chem. Soc. Jpn.* **70**, 275 (1997).

81. W. G. Skene, J. C. Sciaino, N. Listigovers, P. M. Kazmaier, and M. K. Georges, *Macromolecules* **33**, 5065 (2000).

82. Y. Miura, N. Nakamura, and I. Taniguchi, *Macromolecules* **34**, 447 (2001).

83. E. Yoshida and S. Tanimoto, *Polym. J.* **33**, 221 (2001).

84. N. J. Turro, G. Lem, and I. S. Zavarine, *Macromolecules* **33**, 9782 (2000).

85. S. Marque, H. Fischer, E. Baier, and A. Studer, *J. Org. Chem.* **66**, 1146 (2001).

86. E. Harth, B. van Horn, and C. J. Hawker, *J. Chem. Soc. Chem. Commun.* 823 (2001).

87. K. S. Murthy, Q. Ma, C. G. Clark, E. E. Remsen, and K. L. Wooley, *J. Chem. Soc., Chem. Commun.* 773 (2001).

88. M. Rodlert, E. Harth, I. Rees, and C. J. Hawker, *J. Polym. Sci. Poly. Chem.* **38**, 4749 (2000).

89. C. H. Han, M. Drache, H. Baethge, and G. Schmidt-Naake, *Macromol. Chem.* **200**, 1779 (1999).

90. R. P. N. Veregin, M. K. Georges, P. M. Kazmaier, and G. K. Hamer, *Macromolecules* **26**, 5316 (1993).

91. Y. K. Chong, F. Ercole, G. Moad, E. Rizzardo, S. H. Thang, and A. G. Anderson, *Macromolecules* **32**, 6895 (1999).

92. H. Fischer, *Macromolecules* **30**, 5666 (1997).

93. H. Fischer, *J. Polym. Sci.; Part A: Polym. Chem.* **37**, 1885 (1999).

94. C. J. Hawker, *Acc. Chem. Res.* **30**, 373 (1997).

95. A. Goto and T. Fukuda, *Macromolecules* **32**, 618 (1999).

96. D. Greszta and K. Matyjaszewski, *J. Polym. Sci.; Part A: Polym. Chem.* **35**, 1857 (1997).

97. J. He, J. Chen, L. Li, J. Pan, C. Li, J. Cao, Y. Tao, F. Hua, Y. Yang, G. McKee, and S. Brinkmann, *Polymer* **41**, 4573 (2000).

98. (a) M. K. Georges, R. A. Kee, R. P. N. Veregin, G. K. Hamer, and P. M. Kazmaier, *J. Phys. Org. Chem.* **8**, 301 (1995); (b) D. Mardare and K. Matyjaszewski, *Polym. Prep.* **35**(1), 778 (1995).

99. W. Devonport, L. Michalak, E. Malmstrom, M. Mate, B. Kurdi, C. J. Hawker, G. G. Barclay, and R. Sinta, *Macromolecules* **30**, 1929 (1997).

100. D. Greszta and K. Matyjaszewski, *Macromolecules* **29**, 5239 (1996).

101. I. Q. Li, B. A. Howell, K. Matyjaszewski, T. Shigemoto, P. B. Smith, and D. B. Priddy, *Macromolecules* **28**, 6692 (1995).

102. J. He, L. Li, and Y. Yang, *Macromolecules* **33**, 2286 (2000).

103. M. A. Dourges, B. Charleux, J. P. Varion, J. C. Blais, G. Bolbach, and J. C. Tabet, *Macromolecules* **32**, 2495 (1999).

104. C. Burguiere, M. A. Dourges, B. Charleux, and J. P. Varion, *Macromolecules* **32**, 3883 (1999).

105. L. I. Gabaston, R. A. Jackson, and S. P. Armes, *Macromolecules* **31**, 2883 (1998); C. Marestin, C. Noel, A. Guyot, and J. Claverie, *Macromolecules* **31**, 4041 (1998).

106. P. J. MacLeod, R. Barber, P. G. Odell, B. Keoshkerian, and M. K. Georges, *Macromol. Symp.* **155**, 31 (2000).

107. G. Pan, E. D. Sudol, V. L. Dimonie, and M. S. El-Aasser, *Macromolecules* **34**, 481 (2001).

108. A. Butte, G. Storti, and M. Morbidelli, *Macromolecules* **33**, 3485 (2000).

109. J. W. Ma, M. F. Cunningham, K. B. McAuley, B. Keoshkerian, and M. K. Georges, *J. Polym. Sci.; Part A: Polym. Chem.* **39**, 1081 (2001).

110. B. Charleux, *Macromolecules* **33**, 5358 (2000).

111. M. Rodlert, A. Bosman, E. Harth, I. Rees, and C. J. Hawker, *Macromol. Symp.* (in press).

112. C. J. Hawker and J. L. Hedrick, *Macromolecules* **28**, 2993 (1995).

113. M. Baumert and R. Mulhaupt, *Macromol. Rapid Commun.* **18**, 787 (1997).

114. C. S. Kim, S. Oh, S. Kim, and C. G. Cho, *Macromol. Rapid Commun.* **19**, 191 (1998).

115. E. Harth, C. J. Hawker, W. Fan, and R. M. Waymouth, *Macromolecules* **34**, 3856 (2001).

116. U. M. Stehling, E. E. Malmstrom, R. M. Waymouth, and C. J. Hawker, *Macromolecules* **31**, 4396 (1998).

117. U. Stalmach, B. de Boer, A. D. Post, P.F. van Hutten, and G. Hadziioannou, *Angew. Chem., Int. Ed. Engl.* **40**, 428 (2001).

118. P. Lacroix-Desmazes, T. Delair, C. Pichot, and B. Boutevin, *J. Polym. Sci.; Part A: Polym. Chem.* **38**, 3845 (2000).

119. Z. Yousi, L. Jian, Z. Rongchuan, Y. Jianliang, D. Lizong, and Z. Lansun, *Macromolecules* **33**, 4745 (2000).

120. D. Benoit, E. Harth, P. Fox, R. M. Waymouth, and C. J. Hawker, *Macromolecules* **33**, 363 (2000).

121. D. Li and W. J. Brittain, *Macromolecules* **31**, 3852 (1998).

122. K. Ohno, M. Ejaz, T. Fukuda, T. Miyamoto, and Y. Shimizu, *Macromol. Chem. Phys.* **199**, 291 (1998).

123. G. Klaerner, M. Trollsås, A. Heise, M. Husemann, B. Atthoff, C. J. Hawker, J. L. Hedrick, and R. D. Miller, *Macromolecules* **32**, 8227 (1999).

124. R. B. Grubbs, J. M. Dean, M. E. Broz, and F. S. Bates, *Macromolecules* **33**, 9522 (2000).

125. C. J. Hawker, J. L. Hedrick, E. E. Malmstrom, M. Trollsas, D. Mecerreyes, Ph. Dubois, and R. Jerome, *Macromolecules* **31**, 213 (1998).

126. B. de Boer, U. Stalmach, H. Nijland, and G. Hadziioannou, *Adv. Mater.* **12**, 1581 (2000).

127. M. Mariani, M. Lelli, K. Sparnacci, and M. Laus, *J. Polym. Sci.; Part A: Polym. Chem.* **37**, 1237 (1999).

128. C. A. Barbosa and A. S. Gomes, *Polym. Bull.* **41**, 15 (1998).

129. X. Chen, B. Gao, J. Kops, and W. Batsberg, *Polymer* **39**, 911 (1998).

130. C. J. Hawker, J. L. Hedrick, E. E. Malmstrom, M. Trollsas, U. M. Stehling, and R. M. Waymouth, *ACS Symp. Ser.* **713**, 127 (1999).

131. G. G. Barclay, M. King, R. Sinta, E. E. Malmstrom, H. Ito, and C. J. Hawker, *Polym. Prep.* **38**(1), 902 (1997).

132. E. Yoshida and Y. Osagawa, *Macromolecules* **31**, 1446 (1998).

133. E. Yoshida, *J. Polym. Sci.; Part A: Polym. Chem.* **34**, 2937 (1996).

134. S. Kobatake, H. J. Harwood, R. P. Quirk, and D. B. Priddy, *Macromolecules* **30**, 4238 (1997).

135. M. Bouix, J. Gouzi, B. Charleux, J. P. Vairon, and P. Guinot, *Macromol. Rapid Commun.* **19**, 209 (1998).

136. Y. Wang, S. Chen, and J. Huang, *Macromolecules* **32**, 2480 (1999).

137. Y. Ei, E. J. Connors, X. Jia, and C. J. Wang, *J. Polym. Sci.; Part A: Polym. Chem.* **36**, 761 (1998).

138. S. Butz, H. Baethge, and G. Schmidt-Naake, *Macromol. Rapid Commun.* **18**, 1049 (1997).

139. M. Baumert, J. Frohlich, M. Stieger, H. Frey, R. Mulhaupt, and H. Plenio, *Macromol. Rapid Commun.* **20**, 203 (1999).

140. E. Yoshida and S. Tanimoto, *Macromolecules* **30**, 4018 (1997).

141. D. Gravert, A. Datta, P. Wentworth, and K. D. Janda, *J. Am. Chem. Soc.* **120**, 9481 (1998).

142. D. Bertin and B. Boutevin, *Polym. Bull.* **37**, 337 (1996).

143. N. A. Listigovers, M. K. Georges, P. G. Odell, and B. Keoshkerian, *Macromolecules* **29**, 8992 (1996).

144. J. Bohrisch, U. Wendler, and W. Jaeger, *Macromol. Rapid Commun.* **18**, 975 (1997).

145. B. Keoshkerian, M. K. Georges, and D. Boils-Boissier, *Macromolecules* **28**, 6381 (1995).

146. H. Baethge, S. Butz, and G. Schmidt-Naake, *Macromol. Rapid Commun.* **18**, 911 (1997).

147. J. Lokaj, P. Vlcek, and J. Kriz, *Macromolecules* **30**, 7644 (1997).

148. E. Yoshida and A. Sugita, *Macromolecules* **29**, 6422 (1996).

149. U. Wendler, J. Bohrisch, W. Jaeger, G. Rother, and H. Dautzerberg, *Macromol. Rapid Commun.* **19**, 185 (1998).

150. Y. Wang and J. Huang, *Macromolecules* **31**, 4058 (1998).

151. Y. Yagci, A. Baskan Duz, and A. Onen, *Polymer* **38**, 2861 (1997).

152. H. Okamura, T. Terauchi, M. Minoda, T. Fukuda, and K. Komatsu, *Macromolecules* **30**, 5279 (1997).

153. E. Yoshida and T. Fujii, *J. Polym. Sci.; Part A: Polym. Chem.* **35**, 2371 (1997).

154. G. Schmidt-Naake and S. Butz, *Macromol. Rapid Commun.* **17**, 661 (1996).

155. Y. Sun, D. Wan, and J. Huang, *J. Polym. Sci.; Part A: Polym. Chem.* **39**, 604 (2001).

156. G. G. Barclay, C. J. Hawker, H. Ito, A. Orellana, P. R. L. Malenfant, and R. Sinta, *Macromolecules* **31**, 1024 (1998).

157. J. L. Hedrick, B. Atthoff, K. A. Boduch, C. J. Hawker, D. Mercerreyes, R. D. Miller, and M. Trollsas, *Polym. Mat. Sci. Eng.* **80**, 104 (1999).

158. Y. Miwa, K. Yamamoto, M. Sakaguchi, and S. Shimada, *Macromolecules* **34**, 2089 (2001).

159. M. Q. Zhu, L. H. Wei, M. Li, L. Jiang, F. S. Du, Z. C. Li, and F. M. Li, *J. Chem. Soc., Chem. Commun.* 365 (2001).

160. J. Lokaj, P. Holler, and J. Kriz, *J. Appl. Polym. Sci.* **76**, 1093 (2000).

161. T. Emrick, W. Hayes, and J. M. J. Fréchet, *J. Polym. Sci.; Part A: Polym. Chem.* **37**, 3748 (1999).

162. C. Wang, J. He, S. Fu, K. Jiang, H. Cheng, and M. Wang, *Polym. Bull.* **37**, 305 (1996).

163. R. G. Jones, S. Yoon, and Y. Nagasaki, *Polymer* **40**, 2411 (1999).

164. E. Yoshida and Y. Okada, *J. Polym. Sci.; Part A: Polym. Chem.* **34**, 3631 (1996).

165. M. Baumann, A. I. Roland, G. Schmidt-Naake, and H. Fischer, *Macromol. Mater. Eng.* **280**, 1 (2000).

166. M. Baumann and G. Schmidt-Naake, *Macromol. Chem. Phys.* **201**, 2751 (2000).

167. A. W. Bosman, J. M. J. Fréchet, and C. J. Hawker, *Polym. Mat. Sci. Eng.* **84**, 376 (2001).

168. M. C. Bignozzi, C. K. Ober, and M. Laus, *Macromol. Rapid Commun.* **20**, 622 (1999).

169. B. Keoshkerian, P. J. MacLeod, and M. K. Georges, *Macromolecules* **34**, 3594 (2001).

170. T. Tsoukatos, S. Pispas, and N. Hadjichristidis, *Macromolecules* **33,** 9504 (2000).

171. R. B. Grubbs, C. J. Hawker, J. Dao, J. M. J. Fréchet, *Angew. Chem., Int. Ed. Eng.* **36**, 270 (1997).

172. A. W. Bosman, J.M.J. Fréchet, and C. J. Hawker, *Polym. Mater. Sci. Eng.* **84**, 376 (2001).

173. C. J. Hawker, J. L. Hedrick, E. E. Malmstrom, M. Trollsas, D. Mecerreyes, Ph. Dubois, and R. Jerome, *Macromolecules* **31**, 213 (1998).

174. P. M. Kazmaier, K. Daimon, M. K. Georges, G. K. Hamer, and R. P. N. Veregin, *Macromolecules,* **30**, 2228 (1997).

175. C. Farcet, B. Charleux, and R. Pirri, *Macromolecules* **34**, 3823 (2001).

176. H. Huang, E. E. Remsen, and K. L. Wooley, *J. Chem. Soc., Chem. Commun.* 1415 (1998).

177. H. Huang, T. Kowalewski, E. E. Remsen, R. Gertzmann, and K. L. Wooley, *J. Am. Chem. Soc.* **119**, 11653 (1997).

178. D. J. Gravert and K. D. Janda, *Tetrahedron Lett.* **39**, 1513 (1998).

179. G. G. Barclay, M. King, A. Orellana, P. R. F. Malenfant, R. F. Sinta, E. E. Malmstrom, H. Ito, and C. J. Hawker, *ACS Symp. Ser.* **695**, 360 (1998).

180. G. Schmidt-Naake and S. Butz, *Macromol. Rapid Commun.* **17**, 661 (1996).

181. D. Benoit, C. J. Hawker, E. E. Huang, Z. Lin, and T. P. Russell, *Macromolecules* **33**, 1505 (2000).

182. F. Annighofer and W. Gronski, *Coll. Polym. Sci.* **263**, 15 (1983).

183. (a) D. Greszta and K. Matyjaszewski, *Polym. Prep.* **37**, 569 (1996); (b) S. Arehart, D. Greszta, and K. Matyjaszewski, *Polym. Prep.* **38**, 705 (1997); (c) K. Matyjaszewski, K. M. J. Ziegler, S. Arehart, and D. Greszta, *J. Phys. Org. Chem.* **13**, 775 (2000).

184. C. J. Hawker, *Angew Chem., Int. Ed. Engl.* **34**, 1456 (1995).

185. R. B. Grubbs, C. J. Hawker, J. Dao, and J. M. J. Fréchet, *Angew. Chem., Int. Ed. Eng.* **36**, 270 (1997).

186. C. J. Hawker, J. M. J. Fréchet, R. B. Grubbs, and J. Dao, *J. Am. Chem. Soc.* **117**, 10763 (1995).

187. J. M. J. Fréchet, M. Henmi, I. Gitsov, S. Aoshima, M. Leduc, and R. B. Grubbs, *Science* **269**, 1080 (1995).

188. S. G. Gaynor, G. Edelmanm, and K. Matyjaszewski, *Macromolecules* **29**, 1079 (1996).

189. M. W. Weimer, I. Gitsov, and J. M. J. Fréchet, *J. Polym. Sci. Polym. Chem.* **36**, 955 (1998).

190. C. Li, J. He, L. Li, J. Cao, and Y. Yang, *Macromolecules* **32**, 7012 (1999); A. Niu, C. Li, J. Zhao, Y. Yang, and C. Wu, *Macromolecules* **34**, 460 (2001).

191. D. Benoit, E. Harth, C. J. Hawker, and B. Helms, *Polym. Prep.* **41**(1), 42 (2000).

192. A. W. Bosman, A. Heumann, G. G. Klaerner, D. G. Benoit, J. M. J. Fréchet, and C.J. Hawker, *J. Am. Chem. Soc.* **123**, 6461 (2001).

193. A. J. Pasquale and T. E. Long, *J. Polym. Sci.; Part A: Polym. Chem.* **39**, 216 (2001).

194. T. Tsoukatos, S. Pispas, and N. Hadjichristidis, *J. Polym. Sci.; Part A: Polym. Chem.* **39**, 320 (2001).

195. M. R. Leduc, C. J. Hawker, J. Dao, and J. M. J. Fréchet, *J. Am. Chem. Soc.* **118**, 11111 (1996).

196. R. Vestberg and C. J. Hawker, unpublished work.

197. M. R. Leduc, W. Hayes, and J. M. J. Fréchet, *J. Polym. Sci.; Part A: Polym. Chem.* **36**, 1 (1998).

198. K. Matyjaszewski, T. Shigemoto, J. M. J. Fréchet, and M. Leduc, *Macromolecule* **29**, 4167 (1996).

199. V. Percec, B. Barboiu, T. K. Bera, M. van der Sluis, R. B. Grubbs, and J. M. J. Fréchet, *J. Polym. Sci.; Part A: Polym. Chem.* **38**, 4776 (2000).

200. T. Tsoukatos, S. Pispas, and N. Hadjichristidis, *Macromolecules* **33**, 9504 (2000).

201. N. O'Brien, A. McKee, D. C. Sherrington, A. T. Slark, and A. Titterton, *Polymer* **41**, 6027 (2000).

202. N. Ide and T. Fukuda, *Macromolecules* **32**, 95 (1999).

203. B. Lepoittevin, X. Perrot, M. Masure, and P. Hemery, *Macromolecules* **34**, 425 (2001).

204. F. Asgarzadeh, P. Ourdouillie, E. Beyou, and P. Chaumont, *Macromolecules* **32**, 6996 (1999).

205. M. Husseman, E. E. Malmström, M. McNamara, M. Mate, D. Mecerreyes, D. G. Benoit, J. L. Hedrick, P. Mansky, E. Huang, T. P. Russell, and C. J. Hawker, *Macromolecules* **32**, 1424 (1999).

206. M. Husemann, M. Morrison, D. G. Benoit, J. Frommer, C. M. Mate, W. D. Hinsberg, J. L. Hedrick, and C. J. Hawker, *J. Am. Chem. Soc.* **122**, 1844 (2000).

207. U. Meyer, F. Svec, J. M. J. Fréchet, C. J. Hawker, and K. Irgum, *Macromolecules* **33**, 7769 (2000).

208. S. R. McAlpine, C. W. Lindsley, J. C. Hodges, D. M. Leonard, and G. F. Filzen, *J. Combi. Chem.* **3**, 1 (2001).

209. C. W. Lindsley, J. C. Hodges, G. F. Filzen, B. M. Watson, and A. G. Geyer, *J. Comb. Chem.* **2**, 550 (2000).

210. S. Yoshikawa, S. Machida, and N. Tsubokawa, *J. Poly. Sci.; Part A: Polym. Chem.* **36**, 3165 (1998).

211. S. Angot, N. Ayres, S. A. F. Bon, and D. M. Haddleton, *Macromolecules* **34**, 768 (2001).

212. T. von Werne and T. E. Patten, *J. Am. Chem. Soc.* **121**, 7409 (1999).

213. K. Matyjaszewski, P. J. Miller, N. Shukla, B. Immaraporn, A. Gelman, B. B. Luokala, T. M. Siclovan, G. Kickelbick, T. Vallant, H. Hoffmann, and T. Pakula, *Macromolecules* **32**, 8716 (1999).

214. S. Yamamoto, M. Ejaz, Y. Tsujii, and T. Fukuda, *Macromolecules* **33**, 5608 (2000).

215. M. W. Weimer, H. Chen, E. P. Giannelis, and D. Y. Sogah, *J. Am. Chem. Soc.* **121**, 1615 (1999).

11 Fundamentals of Atom Transfer Radical Polymerization

KRZYSZTOF MATYJASZEWSKI and JIANHUI XIA

Carnegie Mellon University, Pittsburgh, Pennsylvania

CONTENTS

11.1   INTRODUCTION

This chapter focuses on the fundamentals of transition metal catalyzed atom transfer radical polymerization (ATRP). Phenomenology, the current mechanistic understanding and some synthetic applications of ATRP will be discussed. The literature up to the beginning of 2001 is covered. Because of the limited size of the chapter, we recommend the reader refer to other chapters in this book for more in-depth analysis of kinetics (Chapter 9) and materials aspects of ATRP (Chapter 14). There are more comprehensive,[1,2] and also some short reviews,[3–6] covering ATRP available.

The name atom transfer radical polymerization (ATRP) comes from the atom transfer step, which is the key elementary reaction responsible for the uniform growth of the polymeric chains. ATRP originates in atom transfer radical addition (ATRA) reactions, which target the formation of 1 : 1 adducts of alkyl halides and alkenes, which are also catalyzed by transition metal complexes.[7] ATRA is a modification of the Kharasch addition reaction, which usually occurs in the presence of light or conventional radical initiators.[8] Because of the involvement of transition metals in the activation and deactivation steps, chemo-, regio-, and stereoselectivities in ATRA and the Kharasch addition may be different. For example, under Kharasch conditions, in the reaction with chloroform the alkene will ''insert'' across the $H-CCl_3$ bond but in ATRA, across the $Cl-CHCl_2$ bond, because the $C-Cl$ bond is rapidly activated by the Fe(II) or Cu(I) complexes.[9]

ATRP has some links to transition-metal-catalyzed telomerization reactions.[10] These reactions, however, do not proceed with efficient exchange, which results in a nonlinear evolution of the molecular weights with conversions and polymers with high polydispersities. ATRP is also related to transition metal initiated redox processes and inhibition with transition metal compounds.[11,12] These two techniques allow for either an activation or deactivation process, however, without efficient reversibility.

ATRP was developed by designing a proper catalyst (transition metal compound and ligands), using an initiator with an appropriate structure, and adjusting the polymerization conditions, such that the molecular weights increased linearly with conversion and the polydispersities were typical of a living process.[13–15] This allowed for an unprecedented control over the chain topology (stars, combs, branched), the composition (block, gradient, alternating, statistical), and the end functionality for a large range of radically polymerizable monomers.[1,5,6,15–17]

A general mechanism for ATRP is shown in Scheme 11.1. The radicals, i.e., the propagating species P_n^*, are generated through a reversible redox process catalyzed

$$P_n\text{-X} \quad + \quad M_t^n\text{-Y / Ligand} \quad \underset{k_{da}}{\overset{k_a}{\rightleftharpoons}} \quad P_n^{\bullet} \quad + \quad \text{X-}M_t^{n+1}\text{-Y / Ligand}$$

$$\overset{k_p}{\underset{\text{monomer}}{\circlearrowright}} \quad \overset{k_t}{\searrow} \quad \text{termination}$$

Scheme 11.1   General scheme of transition-metal-catalyzed ATRP.

by a transition metal complex (activator, M_t^n–Y/ligand, where Y may be another ligand or a counterion) which undergoes a one-electron oxidation with concomitant abstraction of a (pseudo)halogen atom, X, from a dormant species, P_n–X. Radicals react reversibly with the oxidized metal complexes, X–M_t^{n+1}/ligand, the deactivator, to reform the dormant species and the activator. This process occurs with a rate constant of activation, k_a, and deactivation k_{da}, respectively. Polymer chains grow by the addition of the free radicals to monomers in a manner similar to a conventional radical polymerization, with the rate constant of propagation, k_p. Termination reactions (k_t) also occur in ATRP, mainly through radical coupling and disproportionation; however, in a well-controlled ATRP, no more than a few percent of the polymer chains undergo termination. Other side reactions may additionally limit the achievable molecular weights. Typically, no more than 5% of the total growing polymer chains terminate during the initial, short, nonstationary stage of the polymerization. This process generates oxidized metal complexes, the deactivators, which behave as persistent radicals to reduce the stationary concentration of growing radicals and thereby minimize the contribution of termination at later stages.[18] A successful ATRP will have not only small contribution of terminated chains but also uniform growth of all the chains; this is accomplished through fast initiation and rapid reversible deactivation.

ATRP is among the most rapidly developing areas of chemistry. According to *SciFinder Scholar*, 13 papers were published on ATRP in 1995, 47 in 1996, 111 in 1997, 150 in 1998, 318 in 1999, and more than 300 in 2000. Not included in this list are papers, which apply the ATRP concept but use alternative nomenclature such as transition metal mediated living radical polymerization, transition metal catalyzed living free radical polymerization, etc.

11.2   BASIC PRINCIPLES

As a multicomponent system, ATRP includes the monomer, an initiator with a transferable (pseudo)halogen, and a catalyst (composed of a transition metal species with any suitable ligand). Both activating and deactivating components of the catalytic system must be simultaneously present. Sometimes an additive is used. For a successful ATRP, other factors, such as solvent, temperature, concentrations and solubility of all components, and sometimes the order of their addition must be also taken into consideration.

11.2.1   Rates

According to Scheme 11.1, and assuming that contribution of termination becomes insignificant due to the persistent radical effect[18,19] (PRE) (especially for the chain length dependent PRE[20]) and, using a fast equilibrium approximation, that is required to account for the observed low polydispersities, the rate law [Eq. (1.1)]

for ATRP can be derived as follows:

$$R_p = k_p[M][P^\bullet] = k_p K_{eq}[M][I]_0 \frac{[Cu^I]}{[X-Cu^{II}]} \tag{11.1}$$

We will often refer to the apparent rate constants being the products of the rate constants and equilibrium constants (e.g., $k_p^{app} = k_p K_{eq}$).

Figure 11.1 shows a typical linear variation of conversion with time in semilogarithmic coordinates for the ATRP of methyl acrylate (MA) initiated by methyl 2-bromopropionate (MBP) and catalyzed by CuBr/dNbpy (4,4′-di(5-nonyl)-2,2′-bipyridine).[21] Such behavior indicates that there is a constant concentration of the active species in the polymerization and first-order kinetics with respect to monomer. However, since termination occurs continuously, the concentration of the Cu(II) species increases, and deviation from linearity may be observed. For the ideal case with chain length independent termination, PRE kinetics implies the logarithmic plot of monomer conversion versus time to the $\frac{2}{3}$ exponent should be linear.[18] Nevertheless, a linear semilogarithmic plot versus time is often observed. This may be due to an excess of the Cu(II) species present initially, a chain length dependent termination rate coefficient, or heterogeneity of the reaction system due to limited solubility of the copper complexes. It is also possible that self-initiation may continuously
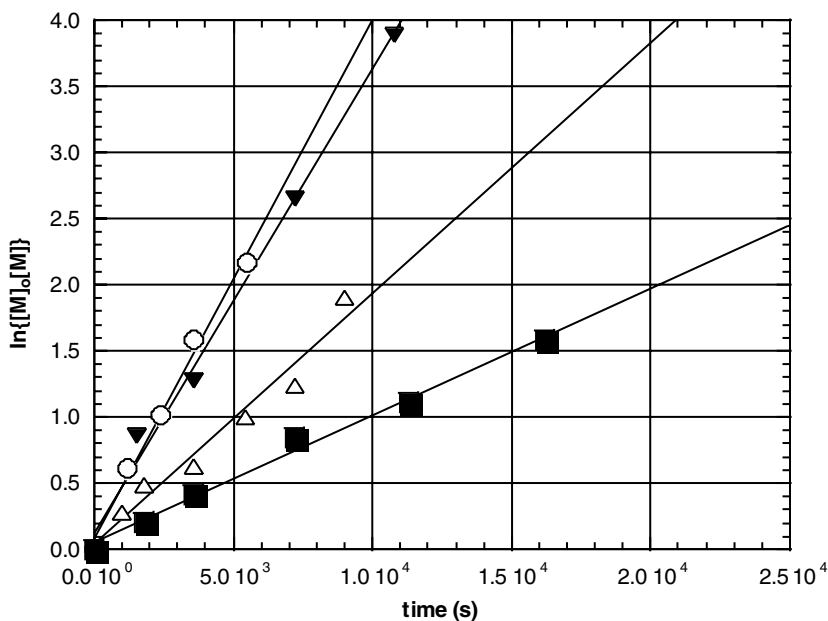
Figure 11.1 Effect of initiator concentration on kinetics of homogeneous ATRP of MA in bulk at 90°C, [MA]$_0$ = 11.2 M; [CuBr]$_0$ = [dNbpy]$_0$/2 = 0.028 M; [MBP]$_0$ = 0.083 M ($\bigcirc$), 0.056 M ($\blacktriangledown$), 0.028 M ($\triangle$), and 0.014 M ($\blacksquare$).[21]

produce radicals and compensate for termination.[22,23] Similarly, external orders with respect to initiator and the Cu(I) species may also be affected by the PRE.[24]

The precise kinetic law for the deactivator (X–Cu^{II}) is more complex due to the spontaneous generation of Cu(II) via the persistent radical effect.[18,24,25] In the atom transfer step, a reactive organic radical is generated along with a stable Cu(II) species that can be regarded as a persistent metalloradical. If the initial concentration of deactivator, the Cu(II) complex, in the polymerization is not sufficiently large to ensure a fast rate of deactivation (k_{da}[Cu(II)]), then coupling of the organic radicals will occur, leading to an increase in the Cu(II) concentration. This process has been observed experimentally using ^{1}H NMR, UV–vis, EPR, and GC-MS techniques.[25,26] Typically, a small fraction ($\sim$5%) of the total growing polymer chains terminate during the early stage of the polymerization, but the majority of the chains ($>$90%) continues to grow successfully. If a small amount of the deactivator ($\sim$10 mol% versus activator) is added initially to the polymerization, then the proportion of terminated chains can be greatly reduced.[16,26] The effect of Cu(II) on the polymerization may, however, be complicated by its poor solubility, by spontaneous dissociation of X–Cu(II) bond, by a slow reduction in the reaction with monomers leading to 1,2-dihaloadducts, or by reaction with radicals formed in self-initiated systems like styrene and other monomers.[23,27,28]

11.2.2 Molecular Weight and Molecular Weight Distribution

As in a typical living polymerization, the average molecular weight of the polymer can be predetermined by the ratio of consumed monomer and the initiator ($DP_n = \Delta[M]/[I]_0$, DP = degree of polymerization) while maintaining a relatively narrow molecular weight distribution ($1.0 < M_w/M_n < 1.5$). This occurs in a well-controlled ATRP; in addition, precise control over the chemistry and the structure of the initiator and active end group allows for the synthesis of end-functionalized polymers and block copolymers. Well-defined polymers with molecular weights ranging from 1000 to 100,000, and in some special cases even exceeding a few millions, have been successfully synthesized. However, termination and other side reactions are also present in ATRP, and they become more important as higher molecular weight polymers are targeted.

The molecular weight distribution or polydispersity (M_w/M_n) is the index of the polymer chain length distribution. In a well-controlled polymerization, M_w/M_n is usually $<$1.10. Equation (11.2) illustrates how the polydispersity index in ATRP (in the absence of chain termination and transfer) relates to the concentrations of initiator (RX) and deactivator (D), the rate constants of propagation (k_p) and deactivation (k_{deact}), and monomer conversion (p).[29] This equation is valid for the systems with constant concentration of radicals and deactivator. Polydispersities can be better correlated with the rate constant of activation rather than that of deactivation, when they are plotted against time rather than conversion (cf. Chapter 9).

$$\frac{M_w}{M_n} = 1 + \left(\frac{([RX]_0 - [RX]_t)k_p}{k_{da}[D]}\right)\left(\frac{2}{p} - 1\right) \tag{11.2}$$

Thus, for the same monomer, a catalyst that deactivates the growing chains faster will result in polymers with lower polydispersities (smaller k_p/k_{da}). Alternatively, polydispersities should decrease with an increasing concentration of the deactivator, although at the cost of lower polymerization rates. For example, the addition of a small amount of Cu(II) halides in copper-based ATRP leads to better-controlled polymerizations with decreased polymerization rates.[21,30] Higher polydispersities are usually found for polyacrylates than for polystyrene or polymethacrylates due to a much higher k_p for acrylates.[31] Other predictions from Eq. (11.2) include higher polydispersities for shorter chains (higher $[RX]_0$) and a decrease of the polydispersity with increasing monomer conversion.

Figure 11.2 shows a typical linear increase of the molecular weights with conversion in the ATRP of methyl acrylate under homogenous conditions. Since the rate constants of propagation for acrylates are relatively large, higher polydispersities are initially observed because several monomer units are added during each activation step. However, with the progress of the reaction, chains become more uniform because of random activation of the dormant chains through continuous exchange reactions and the polydispersities drop with conversion, as predicted by Eq. (11.2). If k_p and the concentrations of initiator and deactivator are known, the rate constant of deactivation can be calculated from the evolution of polydispersities with conversion. A small shoulder at higher molecular weight appears at double value of peak molecular weight, suggesting some chain coupling ($\sim$5%). However, this coupling does not significantly affect polydispersities $(M_w/M_n < 1.2)$.

11.2.3   Reverse ATRP

In a typical ATRP, the initiating radicals are generated from an alkyl halide in the presence of a transition metal in its lower oxidation state [e.g., CuBr(dNbpy)$_2$]. However, conventional radical initiators can also be employed (e.g., azobisisobutyro-

Figure 11.2 GPC traces and plot of (a) molecular weight M_w/M_n versus (b) fractional monomer conversion for different $[MBP]_0$ for bulk ATRP of MA at 90°C, $[MA]_0 = 11.2$ M; $[CuBr]_0 = [dNbpy]_0/2 = 0.028$ M; $[MBP]_0 = 0.083$ M ($\bullet$), 0.056 M ($\blacktriangledown$), 0.028 M ($\blacktriangle$), and 0.014 M ($\blacksquare$).[21]

Initiation:

$$I\text{-}I \longrightarrow 2\,I^{\bullet}$$

$$I^{\bullet} + X\,M_t^{n+1} \rightleftharpoons I\text{-}X + M_t^{n}$$

$$k_i \Big\downarrow +M \qquad\qquad \cancel{\downarrow} +M$$

$$I\text{-}P_1^{\bullet} + X\,M_t^{n+1} \rightleftharpoons I\text{-}P_1\text{-}X + M_t^{n}$$

Propagation:

$$P_n\text{-}X + M_t^{n} \rightleftharpoons P_n^{\bullet} + X\,M_t^{n+1}$$

$$\underset{M}{\bigcirc} k_p \quad\text{---}\quad k_t$$

Scheme 11.2   General scheme of reverse ATRP.

nitrile, AIBN) with the transition metal compound in its higher oxidation state [e.g., $CuBr_2(dNbpy)_2$]. This latter approach has been termed reverse ATRP, and has been successfully used for copper-based heterogeneous,[32–34] and homogeneous[35] systems in solution and in emulsion[36] as well as for iron complexes.[37] (See Scheme 11.2.)

Other conventional radical initiators have also been applied for reverse ATRP. For example, 1,1,2,2-tetraphenyl-1,2-ethanediol (TPED)[38] and diethyl 2,3-dicyano-2,3-diphenylsuccinate (DCDPS)[39] have been used successfully in the presence of $FeCl_3(PPh_3)_3$ for the reverse ATRP of MMA and styrene, respectively. For TPED, PMMA with $M_n = 171800$ and $M_w/M_n = 1.13$ was obtained, but the initiation efficiency was low (0.5). For DCDPS, the experimental molecular weights by size-exclusion chromatography (SEC) were lower than the calculated values, assuming one molecule of DCDPS generated two living polymer chains. More recently, the reverse ATRP using tetraethylthiuram disulfide and $FeCl_3(PPh_3)_3$ as the initiating system resulted in the formation of PMMA with $M_n \sim 7000$ and $M_w/M_n = 1.05$ within 8 min at 90°C in bulk.[40]

The reverse ATRP initiated by peroxides sometimes behaves quite differently from initiation based on azo compounds. For instance, no control over the polymerization was observed for initiation based on the homogeneous $BPO/CuBr_2(dNbpy)_2$ system (BPO = benzoyl peroxide). In contrast, controlled/"living" polymerization was observed when AIBN was used together with $CuBr(dNbpy)_2$. The differences between the BPO and AIBN systems were ascribed to electron transfer and the formation of a copper benzoate species.[34]

11.2.4   Experimental Setup

ATRP can be carried out either in bulk or with a solvent. Solvents are often used to reduce viscosity at high conversions. Environmentally friendly media, such as

water[36,41–45] and carbon dioxide[46] have been also used. Depending on the initial conditions, ATRP can be performed in solution, suspension,[43,47] emulsion,[36,41] miniemulsion,[48] or dispersion.[46]

Kinetics of ATRP in emulsion is quite different from conventional emulsion polymerization.[49] Because of the slow growth of MW with conversion, mechanism of nucleation changes entirely. Moreover, partition coefficients of both activators and deactivators in organic and aqueous phases become very important. The catalytic system should preferentially reside in the organic phase but should also be slightly soluble in water to transfer between monomer droplets and growing particles and also to scavenge radicals in water.[49] Both normal and reverse forms of ATRP have been successful, although colloidal stability of latexes is higher and particle size smaller for the reverse ATRP.[49] The concept of compartmentalization, which is the essence of emulsion polymerization, is strongly related to the living polymerization. Proportion of terminated chains can be smaller than in bulk at the same overall rate of monomer consumption. However, only when size of growing particles is smaller than 50 nm does the effect become significant.[50]

Originally heterogeneous catalytic systems, such as CuBr(bpy)$_3$, were used in ATRP (bpy = 2,2′-bipyridyne; here and below the notation of the complex reflects only stoichiometry of added reagents and *not* the structure of the complex). Better solubility of the transition metal complex was achieved by adding long alkyl substituents to the ligand.[25,51,52] Homogeneous systems allow for the detailed kinetic and mechanistic studies of the polymerization.[25,52,53] In addition, polymers with lower polydispersities are usually obtained with a homogeneous catalyst system due to a higher concentration of deactivator in solution.[54]

ATRP, as other free-radical polymerizations, is sensitive to oxygen. However, ATRP will proceed in the presence of a small amount of oxygen, since oxygen can be successfully scavenged by the catalyst, which is present at a much higher concentration than the growing radicals.[55] The catalyst oxidation reduces its concentration and slows down the polymerization. However, in the presence of a small amount of Cu(0), polymerization is controlled and successive addition of two monomers results in block copolymers. These reactions are so simple, they have been introduced to undergraduate laboratories.[56]

Attempts have also been made to conduct ATRP using solid-supported catalysts.[57,58] Usual laboratory procedures for removing the catalyst from a reaction involve precipitating the polymer, or filtering the polymer solution through a column of aluminum oxide, which adsorbs the catalyst. Removal of the copper-based catalyst using an ion exchange resin has also been reported.[59] The disadvantages of these techniques include cost, problems with scaleup, loss of polymer, and difficulties in separating the catalyst from functional polymers that interact with the copper complexes. Immobilization of the catalytic system on a solid support provides a more efficient way of separating, and potentially recycling, the catalyst. Thus, multidentate nitrogen donor ligands as well as Schiff base ligands have been covalently bound to silica and crosslinked polystyrene supports. In general, polymers with higher polydispersities $(M_w/M_n > 1.5)$ were obtained using the solid-supported catalysts. This was explained by slow deactivation of the growing radicals resulting

from slow diffusion toward the metal center. Lower polydispersities were obtained when the catalyst was physically absorbed onto a solid support; however, only the controlled polymerization of methacrylates has been reported so far.[58] Other approaches involve the reversible adsorption of the transition metal complex using ion exchange resins,[59] a hybrid catalyst system consisting of a majority of the immobilized catalyst and a minute amount of soluble more active catalyst[60] or using ligands whose solubility is strongly dependent on the temperature.[61]

11.3 PHENOMENOLOGY

11.3.1 Monomers

A variety of monomers have been successfully polymerized using ATRP: styrenes, (meth)acrylates, (meth)acrylamides, dienes, and acrylonitrile, which contain substituents that can stabilize the propagating radicals.[1,6,15] Ring opening polymerization is also possible.[62] Even under the same conditions using the same catalyst, each monomer has its own unique atom transfer equilibrium constant for its active and dormant species. The product of k_p and the equilibrium constant ($K_{eq} = k_a/k_{da}$) essentially determines the polymerization rate. ATRP will occur very slowly if the equilibrium constant is too small. In contrast, too large equilibrium constant will lead to a large amount of termination because of high radical concentration. This will be accompanied by production of a large amount of deactivating higher oxidation state metal complex, which will shift the equilibrium toward dormant species and may result in an apparently slower polymerization.[63] Thus, for a specific monomer, the concentration of propagating radicals and the rate of radical deactivation need to be adjusted to maintain polymerization control. However, since ATRP is a catalytic process, the overall position of the equilibrium not only depends on the radical (monomer) and the dormant species, but can also be altered by the amount and reactivity of the transition metal catalyst added to the reaction.

   The values of the equilibrium constants are lower for monosubstituted alkenes than for disubstituted alkenes (MMA $\gg$ MA). The equilibrium constant decreases in the following order with the α-substituents: CN > Ph > C(O)OR > C(O)NR$_2$ > COC(O)R. The most common monomers will now be discussed in the order of their decreasing ATRP reactivity, although under some conditions acrylonitrile may be even more reactive than MMA.

11.3.1.1 Methacrylates   The ATRP equilibrium constant for methyl methacrylate (MMA) is among the largest, and therefore even very weak ATRP catalysts have been successfully used for the polymerization of MMA. ATRP of MMA has been reported for catalytic systems based on ruthenium,[13,64] copper,[65,66] nickel,[67–69] iron,[70–72] palladium,[73] and rhodium.[74] The facile polymerizability of MMA, and the large range of suitable catalysts for the ATRP reaction, is due to the relative ease of activation of the dormant species and the high values of the ATRP equilibrium constants. The equilibrium constants can sometimes be too high to obtain a fully controlled ATRP process, as is the case for the Me$_6$TREN ligands.[63] Using

the known rate constant of propagation for MMA, typical radical concentrations for the bulk and solution controlled ATRP of MMA are estimated to be between 10^{-7} and 10^{-9} M.

Most polymerizations of MMA were carried out in solution at temperatures ranging from 70 to 90°C. Solvents are necessary to solubilize the forming poly(methyl methacrylate) (PMMA) which has a glass transition temperature, $T_g \sim 120°C$. In addition, solution polymerization helps to keep the concentration of growing radicals low. Under comparable conditions, copper-mediated ATRP of MMA displays a significantly higher equilibrium constant than does styrene or MA. As a result, higher dilution and a lower catalyst concentration should be used for the MMA polymerization.

Initiation plays an important role in the ATRP of MMA. The best initiators include sulfonyl chlorides[65] and 2-halopropionitrile[71] because these initiators have sufficiently large apparent rate constants of initiation ($k_i^{app} = K_{eq}^° k_i$). Well-defined PMMA can be prepared within the molecular weight range of 1000–200,000. A series of initiators, including multichlorinated methanes, α-chloroesters, α-chloroketones, and α-bromoesters, were studied in ruthenium-mediated ATRP of MMA.[75] CCl_3COCH_3, $CHCl_2COPh$, and dimethyl 2-bromo-2,4,4-trimethylglutarates were among the best initiators, yielding PMMA with controlled molecular weights and low polydispersities ($M_w/M_n = 1.1 \sim 1.2$). It should be noted that some of these initiators are too active for the copper-based systems and lead to excessive termination or other side reactions.[76]

Other methacrylate esters have also been successfully polymerized. These include n-butyl methacrylate,[41,52,53,77] 2-(dimethylamino)ethyl methacrylate (DMAEMA),[78] 2-hydroxyethyl methacrylate (HEMA),[64,79] silyl-protected HEMA,[80] methacrylic acid in its alkyl protected form[81] or as its sodium salt,[82] methacrylates with a long oligo(ethylene oxide) substitutent,[83] and fluorinated methacrylic esters.[46,84,85] Figure 11.3 illustrates some examples of methacrylates polymerized by ATRP.

Controlled polymerization of (meth)acrylic acid by ATRP presents a challenging problem because the acid monomers can poison the catalyst by coordinating to the transition metal. In addition, nitrogen-containing ligands can be protonated, which interferes with the metal complexation. Armes and co-workers reported the successful ATRP of sodium methacrylate in water using $CuBr(bpy)_3$ as the catalyst with a poly(ethylene oxide)-based macroinitiator.[82] Yields were moderate to good, molecular weight control was good, and the polydispersities were reasonably low
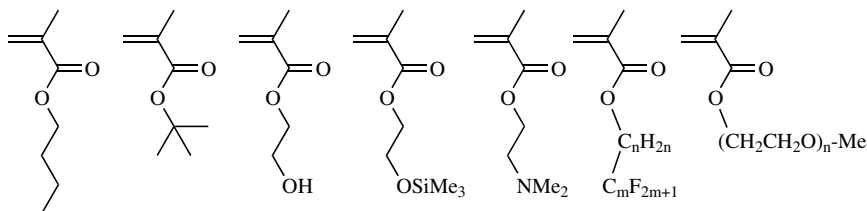
Figure 11.3   Various methacrylates polymerized by ATRP.

$(M_w/M_n = 1.30)$; however, high polydispersities were observed for the target $M_n > 10,000$. The choice of both pH and the initiator was critical. The optimum pH was determined to lie between 8 and 9, as there appears to be a balance between the reduced propagation rate at high pH and competing protonation of the ligand at low pH. In addition, low conversion and low initiator efficiency were obtained when sodium 2-bromoisobutyrate was used as the initiator. Other acidic monomers, such as sodium vinylbenzoate, were also successfully polymerized in aqueous media using a similar methodology.[86]

Alternatively, poly(meth)acrylic acids can be prepared by polymerization of protected monomers such as trimethylsilyl methacrylate, *tert*-butyl methacrylate, tetrahydropyranyl methacrylate, and benzyl methacrylate.[81,87]

11.3.1.2 Acrylonitrile

Metal-mediated controlled radical polymerization of acrylonitrile has so far been reported only for copper-mediated ATRP.[88–90] A solvent must be used because polyacrylonitrile is not soluble in its monomer. Successful polymerizations have been carried out in ethylene carbonate in the presence of the CuBr(bpy)$_2$ complex using α-bromopropionitrile as the initiator at temperatures of 44–64°C. The CuBr(bpy)$_2$ catalyst was soluble in the strongly polar polymerization medium, and the system was homogeneous. Well-defined poly-acrylonitrile with $M_w/M_n < 1.05$ has been prepared over the molecular weight range of 1000–10,000. In all polymerizations, there was significant curvature in the first-order kinetic plot of the monomer consumption. ^{1}H NMR spectroscopy and MALDI-TOF analysis showed that some halide end groups were irreversibly lost during the polymerization. It was proposed that reduction of the propagating radical by cuprous halide forming an anion was the major chain termination reaction.[90] Acrylonitrile has also been copolymerized with styrene in a well-controlled fashion to yield gradient copolymers with molecular weights ranging from 1000 to 15,000.[91,92]

11.3.1.3 Styrenes

ATRP of styrene and its derivatives has been reported for the copper,[15,25,93,94] iron,[71] ruthenium,[95] and rhenium[96] catalytic systems, with the majority of the work performed using copper-based systems.

In addition to 1-phenylethyl halide and benzylic halides, a variety of compounds, such as allylic halides and functional α-haloesters,[97] polyhalogenated alkanes,[93,98] and arenesulfonyl chlorides,[53] have been successfully used as initiators for copper-mediated styrene ATRP. One of the most extensively studied systems is the polymerization of styrene conducted at 110°C with CuBr(dNbpy)$_2$ as the catalyst and alkyl bromides as initiators. A similar system for the chloride-mediated polymerization is conducted at 130°C to obtain similar polymerization rates.[25] The reaction temperature can be lowered to 80–90°C to produce well-defined polystyrenes in a reasonable time with the use of a more active catalyst, such as CuBr/PMDETA (PMDETA = N,N,N',N'',N''-pentamethyldiethylenetriamine)[99] or CuOAc/CuBr/dNbpy.[30] However, to avoid vitrification at high conversion (for polystyrene $T_g \sim 100$°C) while maintaining a sufficiently large propagation rate, and sometimes to increase the solubility of the catalysts, higher reaction temperatures (>100°C) are preferred for styrene

ATRP. The reaction may be carried out in bulk or using a solvent, but the stability of the halide end group displays a pronounced solvent dependence as demonstrated by model studies using 1-phenylethyl bromide.[100] As a result, nonpolar solvents are recommended for styrene ATRP.

Polystyrenes with molecular weight (M_n) ranging from 1000 to 100,000 with low polydispersities have been prepared. Better molecular weight control is obtained at lower temperatures, presumably due to a lower contribution of the thermal self-initiation.[28,101] A wide range of styrene derivatives with different substituents on the aromatic ring have been polymerized in a well-controlled fashion.[102] Well-defined p-acetoxystyrene was prepared, and subsequent hydrolysis afforded water-soluble poly(vinylphenol).[103] In general, styrenes with electron-withdrawing substituents polymerize faster. The Hammett correlation for ATRP of styrene provided a $\rho = 1.5$ compared to $\rho = 0.5$ for the radical propagation constants. This indicates that the atom transfer equilibrium was further shifted toward the active species side for styrenic monomers bearing electron-withdrawing groups. This behavior can be explained by the higher ATRP reactivity of secondary benzylic halides with electron withdrawing groups.[104] Figure 11.4 shows some styrene derivatives successfully polymerized by ATRP.

11.3.1.4 Acrylates   The controlled ATRP of acrylates has been reported for copper-,[14,21,93] ruthenium-,[64] and iron-based systems.[105] Copper appears to be superior over other transition metals in producing well-defined polyacrylates with low polydispersities in a relatively short time. This is partially due to fast deactivation of the growing acrylic radicals by cupric halides. Typical polymerizations were conducted in bulk with an alkyl 2-bromopropionate initiator and well-defined polyacrylates with $M_n < o$ 100 000 and $M_w/M_n < 1.1$ were prepared. The catalyst can be selected to produce polymers within a reasonable time (e.g., $M_n = 20,000$ in ~2 h) over a wide range of polymerization temperatures. For example, using 0.05 mol% of $CuBr/Me_6TREN$ (Me_6TREN = tris[2-(dimethyl-amino)ethyl]amine) as the catalyst, poly(MA) with $M_n = 12,600$ and $M_w/M_n = 1.10$ was obtained in 1 h at ambient temperature.[106]

Acrylates with a wide range of substituents have been polymerized using ATRP (Fig. 11.5). For example, well-defined functional polymers were obtained by the ATRP of 2-hydroxyethyl acrylate (HEA)[44,107] and glycidyl acrylate.[108] Poly(tert-butyl acrylate) was also prepared in a well-controlled fashion[109,110] and subsequent
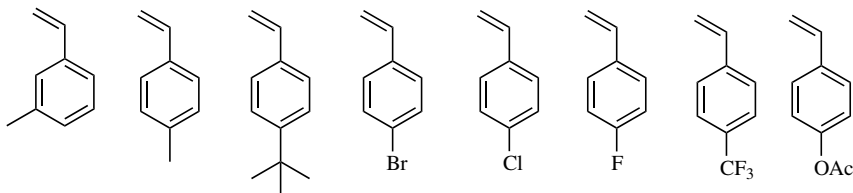
Figure 11.4   Various substituted styrenes polymerized by ATRP.
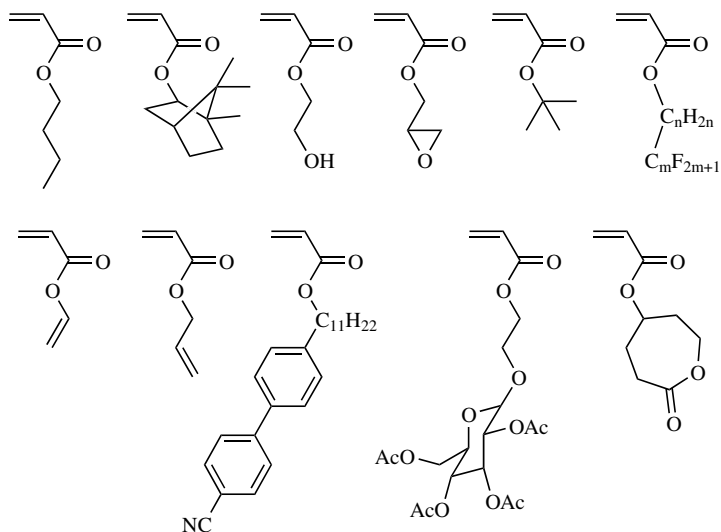
Figure 11.5   Various acrylates polymerized by ATRP.

hydrolysis yields well-defined poly(acrylic acid). In addition, well-defined homo-polymer and block copolymers with fluorocarbon side chains have been pre-pared.[46,84] When allyl acrylate was subjected to ATRP conditions with bpy or dNbpy as the ligand, crosslinking occurred, even at 0°C.[111]

11.3.1.5   (Meth)acrylamides   There are a few reports on unsuccessful ATRP of acrylamide. The use of model compounds and kinetic studies has shown that the polymerization of acrylamide under typical ATRP conditions displays a much lower ATRP equilibrium constant than acrylates or styrene.[112] Two potential side reactions are inactivation of the catalyst by complexation of copper by the forming polymer and displacement of the terminal halogen atom by the amide group. Loss of the chain-end halogen has been attributed to end-group analysis through the use of mass spectrometry.[113] The best results for the ATRP of (meth)acrylamide was obtained using one of the most powerful catalyst systems (CuCl/Me$_6$TREN) due to its high equilibrium constant. Polymerizations were carried out using alkyl chlorides as the initiators and conducted at low temperature (20°C) in a low polarity solvent (toluene) to minimize side reactions.[114] For example, poly(N,N-dimethyl metha-crylamide) with molecular weight $M_n = 8400$ and polydispersity $M_w/M_n = 1.12$ was formed at room temperature in 50% toluene solution.

Metals other than copper have also been studied for the ATRP of acrylamide. Living polymerization of dimethylacrylamide (DMAA) has been demonstrated with a bromide initiator such as CCl$_3$Br used in conjunction with RuCl$_2$(PPh$_3$)$_3$ and Al(Oi-Pr)$_3$ in toluene at 60°C.[115] Polymers with relatively low polydispersities ($M_w/M_n = 1.6$) were obtained. Improved control was achieved at lower tempera-tures, presumably due to a lower contribution of side reactions.

A unique amide monomer, N-(2-hydroxypropyl) methacrylamide, was polymerized in a controlled manner using CuBr/Me$_4$Cyclam as the catalyst.[116] The polymerization was carried out in 1-butanol and yielded a relatively well-defined polymer ($M_n = 21{,}300, M_w/M_n = 1.38$) and block copolymers.

11.3.1.6 Miscellaneous Monomers

Pyridine-containing polymers are useful as water-soluble polymers and as coordination reagents for transition metals. Both 4-vinylpyridine (4VP) and poly(4-vinylpyridine) (P4VP) can act as coordinating ligands for transition metals and compete for the binding of the metal catalysts in ATRP. However by employing a strongly coordinating ligand such as Me$_6$TREN, a well-defined P4VP has been obtained at 40°C using a copper-based catalytic system.[117]

Alternating copolymers of isobutene with MA, BA, and AN have been prepared using CuBr(bpy)$_3$ as the catalyst and 1-phenylethyl bromide as the initiator at 50°C.[118,119] Experimental molecular weights were close to the theoretical values, ranging from 4000 to 50,000, but polydispersities were relatively high ($M_w/M_n \sim 1.50$). Evidence for the alternating sequences and the tacticity of the isobutene with the MA was provided by ^{1}H NMR analysis. The alternating copolymer prepared from isobutene and MA was an elastomer with a predominately syndiotactic structure and a low glass transition temperature ($T_g \sim -30$°C).

Alternating copolymerizations of maleimides with styrene[1,120,121] and MMA[122] have been carried out using copper-based ATRP. A linear increase of M_n with conversion was observed up to $M_n \sim 13{,}000$, with $M_w/M_n \sim 1.16$–1.36. N-(2-Acetoxyethyl)-maleimide was found to copolymerize faster than N-phenylmaleimide.[121]

Polymerizations of vinylidene chloride and isoprene[15] by copper-mediated ATRP have also been carried out. Controlled polymerization of vinyl acetate (VOAc) by ATRP remains a challenge, largely because of the small atom transfer equilibrium constant.[123] However, successful copolymerization of VOAc with MA has been reported.[97] In addition, VOAc has been successfully incorporated into a block copolymer by combining ATRP with other polymerization processes.[123,124]

Ring-opening polymerization has been successful for several monomers, especially for those with radical stabilizing substituents.[125] Potential copolymerization of these monomers will lead to vinyl polymers with a hydrolyzable linkage in the main chain.[62,126] Some examples of other monomers (co)polymerized by ATRP are shown in Fig. 11.6.

In summary, a variety of monomers have been successfully polymerized under ATRP conditions to yield well-defined polymers. For a monomer to undergo ATRP, it is important that a stabilizing group (e.g., phenyl or carbonyl) be present adjacent to the carbon radicals, to produce a sufficiently large atom transfer equilibrium constant, but one that does not interfere with the growing radical and the catalytic system. In addition, it is necessary to adjust the reaction conditions (concentrations, temperature, catalyst) to obtain a suitable radical concentration for a specific monomer.
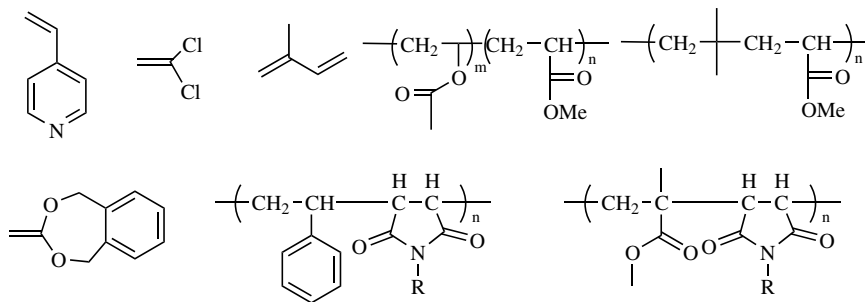
Figure 11.6   Miscellaneous monomers (co)polymerized by ATRP.

11.3.2   Initiators

The main role of the initiator is to determine the number of growing polymer chains. In ATRP, alkyl halides (RX) are typically used as initiators. To obtain well-defined polymers with narrow molecular weight distributions, the halide group, X, should rapidly and selectively migrate between the growing chain and the transition metal complex. Thus far, when X is either bromine or chlorine, the molecular weight control is best. Iodine works well for acrylate polymerizations in copper-mediated ATRP[127] and has been found to lead to controlled polymerization of styrene in ruthenium and rhenium-based ATRP.[95,96] Some pseudohalogens, specifically thiocyanates and thiocarbamates, have been used successfully in the polymerization of acrylates and styrenes.[127–129]

Initiation should be fast and quantitative with a good initiator and proper selection of group R. Any alkyl halide with activating substituents on the α-carbon, such as aryl, carbonyl, or allyl groups, can potentially be used as ATRP initiators, polyhalogenated compounds (e.g., CCl_4 and $CHCl_3$), and compounds with a weak R—X bond, such as N—X, S—X, and O—X, can also be used as ATRP initiators. When the initiating moiety is attached to a macromolecule, macroinitiators are formed, and can be used to synthesize block or graft copolymers.[17] However, the efficiency of block/graft copolymerization may be low if the apparent rate constant of cross-propagation is smaller than that of the subsequent homopolymerization.

It should be noted, however, that R—X bonds can be cleaved not only homolytically but also heterolytically; which process occurs depends mostly on the initiator structure and the choice of the transition metal catalyst. For example, the side reactions observed for copper-mediated ATRP of *p*-methoxystyrene are probably due to the heterolytic cleavage of C—X bond or oxidation of the radical to the corresponding carbocation.[12,102]

Many different types of halogenated compounds are potential initiators and their different structures form the foundation for the following discussion.

11.3.2.1   Halogenated Alkanes   Halogenated alkanes, such as $CHCl_3$ or CCl_4, are typically used in atom transfer radical addition chemistry and were among the first compounds studied as ATRP initiators.[13,14] In the ruthenium-catalyzed ATRP of MMA with CCl_4 as initiator molecular weights of the polymer increased linearly with the conversion, however, at high monomer conversion, the molecular weight deviated from the theoretical values.[77] The polymers obtained were monomodal with low polydispersities ($\sim$1.3). In contrast, use of $CHCl_3$ as the initiator resulted in uncontrolled polymerizations, and di- or monochloromethanes were not able to initiate polymerization of MMA under similar conditions.[75]

CCl_4 has also been used in other catalytic systems, including the Cu-based ATRP.[93] When $CuCl(bpy)_3$ was used as the catalyst for the ATRP of styrene at 130°C, CCl_4 was found to act as a difunctional initiator.[130] Again, deviation of the molecular weights from theoretical values was observed. This was tentatively explained by proposing that additional chains were generated resulting from activation of the central dichloromethylated moiety, which undergoes β scission.[130] Control of the molecular weight is possible using $CHCl_3$ for the $CuCl(bpy)_3$ system, whereas di- and monochloromethanes still lead to uncontrolled polymerizations.[93] In homogenous systems, CCl_4 is sometimes a less efficient initiator because of a potential outer-sphere electron transfer (OSET) reaction and the reduction of the radicals to anions (see later sections). Slow addition of the catalyst to the reaction mixture containing the initiating system apparently improves the initiation efficiency.[101] With CCl_4 and $Ni\{o,o'-(CH_2NMe_2)_2C_6H_3\}Br$ as the catalyst, the experimental molecular weight of PMMA increased with monomer conversion but showed deviation at high conversions,[67] similar to the ruthenium system.[13] Deviation of molecular weight was also observed for the $FeCl_2(PPh_3)_2$ catalytic system.[70]

CCl_3Br successfully initiated the controlled polymerization of MMA catalyzed by $RuCl_2(PPh_3)_3$,[47] $NiBr_2(PPh_3)_2$,[131] $NiBr_2(PnBu_3)_2$,[68] or $Ni(PPh_3)_4$.[132] However, with the $Ni^{(II)}/(PPh_3)_2$ system, combinations of initiators and catalysts, such as $CCl_3Br/NiCl_2(PPh_3)_2$, $CCl_4/NiBr_2(PPh_3)_2$, or $CCl_4/NiCl_2(PPh_3)_2$, resulted in bimodal molecular weight distributions at high MMA conversions.[131]

11.3.2.2   Benzylic Halides   Benzyl-substituted halides are useful initiators for the polymerization of styrene and its derivatives due to their structural resemblance. However, they fail to initiate efficiently the polymerization of more reactive monomers in ATRP such as MMA. For example, using $CuCl(dNbpy)_2$ as the catalyst, inefficient initiation was observed when 1-phenylethyl chloride was employed as the initiator for the polymerization of MMA.[76] PMMA with much higher molecular weights than the theoretical values and high polydispersities ($M_w/M_n = 1.5$ to 1.8) were obtained. In contrast, a well-controlled polymerization was accomplished with benzhydryl chloride (Ph_2CHCl) as the initiator under similar conditions. In fact, the radical generation was so fast that slow addition of benzhydryl chloride was necessary to avoid a significant contribution of the irreversible biradical termination early in the polymerization.[76] Improvement of initiation efficiency for ATRP of
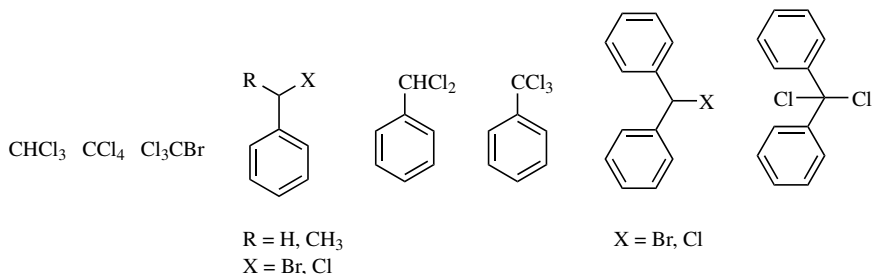
Figure 11.7   Halogenated alkanes and benzylic halides used as ATRP initiators.

MMA using primary and secondary benzylic halides is possible by employing the halogen exchange concept.[133]

Polyhalogenated benzylic halides have been used for the ATRP of MMA catalyzed by $RuCl_2(PPh_3)_3/Al(OiPr)_3$.[75] PMMA with very low polydispersities was obtained when Ph_2CCl_2 was used as the initiator. In contrast, $PhCCl_3$ led to a bimodal molecular weight distribution consisting of two narrowly distributed fractions, the higher of which was double the molecular weight of the other.[75] $PhCHCl_2$ has been also used in Cu-based ATRP of styrene and MMA, apparently providing two-directional growth of the polymeric chains.[134] Figure 11.7 illustrates some examples of halogenated alkanes and benzylic halides used successfully in ATRP.

11.3.2.3 α-Haloesters   Various α-haloesters have been successfully employed to initiate well-controlled ATRP. In general, α-haloisobutyrates produce initiating radicals faster than do the corresponding α-halopropionates because of the better stabilization of the generated radicals after the halogen abstraction step. Thus, slow initiation will generally occur if α-halopropionates are used to initiate the polymerization of methacrylates. In contrast, α-bromopropionates are good initiators for the ATRP of acrylates due to their structural resemblance.

In a search for better initiators in ruthenium-mediated ATRP, Sawamoto et al. examined three different α-bromoesters (top row in Fig. 11.8).[75] The malonate with two geminal esters generates radicals faster than 2-bromoisobutyrate and leads to polymers with lower polydispersities. The dimeric model of the dormant chain end (dimethyl 2-bromo-2,4,4-trimethylglutarate) initiates a faster polymerization and provides PMMA with lower polydispersities than α-bromoisobutyrate, likely due to the back-strain effect.[135] This effect is related to the release of the steric strain of the dormant species during rehybridization from the sp^3 to the sp^2 configuration and leads to a higher equilibrium constant.[136] The dimeric model has also been used in the ATRP of MMA catalyzed by $NiBr_2(PPh_3)_2$,[69] and the chloride analog of the dimeric model compound leads to the controlled polymerization of MMA and styrene when mediated by half-metallocene-type ruthenium complexes.[137]

Malonate derivatives are less efficient in Cu-based ATRP perhaps due to the above-mentioned OSET process. Slow addition of the catalyst to the initiator solution in monomer improves control tremendously.[101]
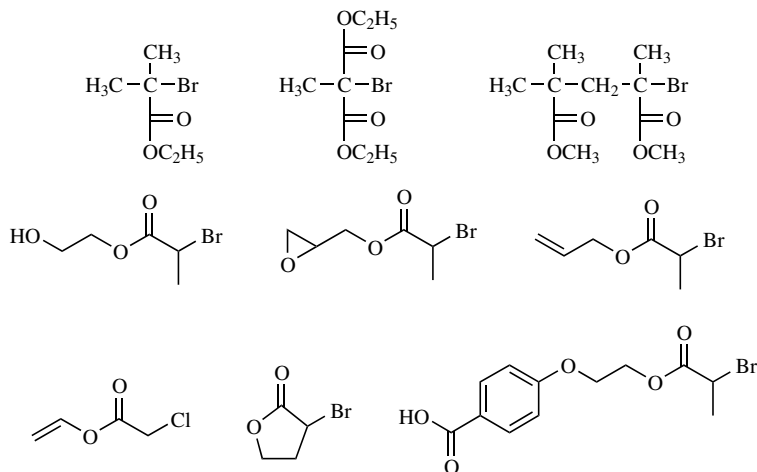
Figure 11.8   Various α-bromoesters used in ATRP.

α-Haloesters with various functional groups attached can easily be prepared through a straightforward esterification reaction of the appropriate acid halides. Since ATRP can tolerate many functional groups, well-defined end-functional polymers have been conveniently prepared without the need for additional protecting reactions. A variety of functionalities, such as hydroxy, epoxy, allyl, vinyl, γ-lactone, and carboxylic acid, have been introduced onto the α-end of the polymer by the use of a functional initiator and will be discussed in the later sections (Fig. 11.8)[97,138–140]

Polyhalogenated α-haloesters (e.g., $CCl_3CO_2CH_3$ and $CHCl_2CO_2CH_3$) have also been successful as initiators for the ATRP of MMA catalyzed by $RuCl_2(PPh_3)_3$/$Al(OiPr)_3$.[75] Mixed benzyl and ester derivatives such as methyl α-bromophenylacetate have been successfully used in the aqueous polymerization of 2-(dimethylamino) ethyl methacrylate.[141]

11.3.2.4 α-Haloketones   An α-bromoketone has been used to initiate the controlled polymerization of MMA when catalyzed by $Ni\{o,o'\text{-}(CH_2NMe_2)_2$ $C_6H_3\}Br$[67] or $Ni(PPh_3)_4$.[132] Polyhalogenated α-haloketones (e.g., CCl_3COCH_3 and $CHCl_2COPh$) are among the best initiators for the ATRP of MMA catalyzed by ruthenium complexes.[47,75,137,142,143] Well-controlled polymers with low polydispersities $(M_w/M_n < 1.20)$ were obtained. The faster initiation observed with ketones when compared with the corresponding ester counterparts is attributed to the stronger electron-withdrawing effect of the ketone carbonyl group, which induces further polarization of the carbon–chlorine bond.

11.3.2.5 α-Halonitriles   α-Halonitriles are fast radical generators in ATRP, due to the presence of the strong electron-withdrawing cyano group. Moreover, the radical formed after halogen abstraction is reactive, which leads to fast initiation through rapid addition of the radical to the monomer. Of all initiators studied for the

polymerization of acrylonitrile catalyzed by copper complexes, 2-bromopropionitrile resulted in polymers with the lowest polydispersities.[88] 2-Bromopropionitrile is also the initiator of choice when a bromine initiator is desired in the iron-mediated ATRP of MMA.[71] However, α-halonitriles are not used in ruthenium-catalyzed ATRP since it was reported that the cyano group deactivates the catalyst by forming a strong complex with ruthenium.[75]

11.3.2.6 *Sulfonyl Halides*

When used as ATRP initiators, sulfonyl chlorides yield a much faster rate of initiation than propagation.[53] The apparent rate constants of initiation are about four and three orders of magnitude higher than those for propagation for styrene and methacrylates, and for acrylates, respectively. As a result, well-controlled polymerizations of a large number of monomers have been obtained in copper-catalyzed ATRP.[53,94] End-functional polymers have been prepared using sulfonyl chlorides where functionalities were introduced onto the aromatic ring.[144] The substituent on the phenyl ring has only a negligible effect on the rate constant of initiation because the sulfonyl radical and its phenyl group are not conjugated.

A unique feature of the sulfonyl halides as initiators is that while the radicals they are easily generated, they dimerize slowly to form disulfones and slowly disproportionate. Thus, they can react with monomers and initiate the polymerization efficiently.[145] However, when sulfonyl chlorides were used in the polymerization of MMA catalyzed by $RuCl_2(PPh_3)_3/Al(OiPr)_3$, S-shaped conversion–time profiles were obtained and experimental molecular weights were higher than the theoretical values, indicating low initiator efficiency,[146] and polydispersities were around $1.2 \sim 1.5$. The low initiator efficiency was explained by the formation of sulfonyl esters from sulfonyl chlorides and $Al(OiPr)_3$ during the early stages of the polymerization. Examples of sulfonyl chlorides successfully used as ATRP initiators are shown in Fig. 11.9.

11.3.2.7 *Importance of the Initiator Structure in ATRP*

Two parameters are important for a successful ATRP initiating system: (1) initiation should be fast in comparison with propagation; and (2) the probability of side reactions should be minimized. The main factor that determines the overall rate constants are the equilibrium constants rather than the absolute rate constants of addition, as also reported for cationic processes.[147]

There are several generalities that should be considered when choosing the initiator.

1. The order for the stabilizing group in the initiator is approximately $CN > C(O)R > Ph > C(O)OR > Cl > Me$. Multiple functional groups may increase the activity of the alkyl halide, such as, carbon tetrachloride, benzhydryl derivatives, and malonates. Tertiary alkyl halides are better initiators than secondary ones, which are better than primary alkyl halides. This has been confirmed by recent measurements of activation rate constants.[148,149,222] Sulfonyl chlorides provide much faster initiation than propagation.
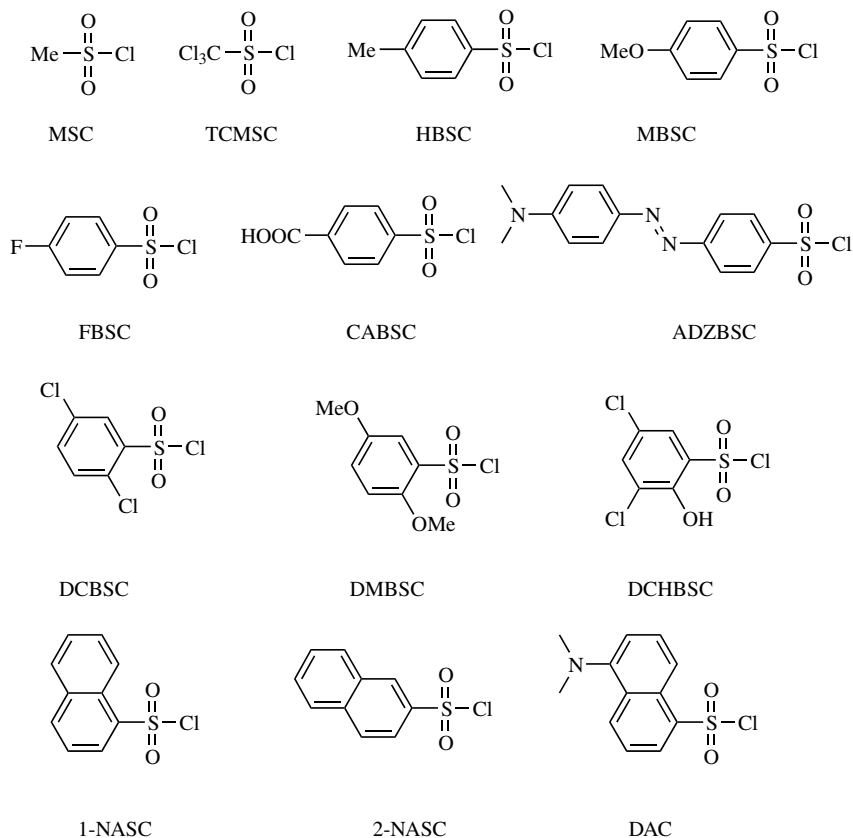
Figure 11.9   Various sulfonyl chlorides used as ATRP initiators.

2. The general order of bond strength in the alkyl halides is R—Cl > R—Br > R—I. Thus, alkyl chlorides should be the least efficient initiators and alkyl iodides the most efficient. However, the use of alkyl iodides require special precautions they are light sensitive, can form metal iodide complexes with a low stability (e.g., CuI_2 is thermodynamically unstable and has not been isolated), the R—I bond may be cleaved heterolytically, and there is a potential participation of degenerative transfer in ATRP process. Thus, transition metal may initiate polymerization but degenerative transfer is responsible for exchange reactions. By far, bromine and chlorine are the most frequently used halogens. In general, the same halogen is used in the initiator and the metal salt (e.g., RBr/CuBr); however, the halogen exchange can sometimes be used to obtain better polymerization control.[133] In a mixed halide initiating system, R—X/M_t—Y (X,Y = Br or Cl), the bulk of the polymer chains are terminated by chlorine due to the stronger alkyl–chloride bond. Thus, the rate of initiation is increased relative to propagation and ethyl 2-bromoisobutyrate/CuCl leads to a better-controlled polymerization of MMA in comparison to using ethyl 2-bromoisobutyrate/CuBr.[133] A similar result

has also been observed in Ru-based ATRP.[150] The halogen exchange method also enables the use of alkyl halides with lower reactivity in the polymerization of monomers with apparently higher equilibrium constants. This is especially important for the formation of block copolymers.[151,152] Pseudohalogens (e.g., SCN) have also been used in ATRP.[127,129] Initiation using benzyl thiocyanate is slow for both styrene and MA, and M_n values higher than the theoretical values are obtained. Better results are obtained when alkyl halides are used as the initiators and CuSCN as the catalyst. Similarly, transition metal dithiocarbamates have been employed in the presence of AIBN to induce controlled reverse ATRP of styrene at 120°C. Good agreement between theoretical and experimental M_n values were obtained with $M_w/M_n = 1.15 \sim 1.30$.[128]

3. Successful initiation in ATRP depends strongly on the choice of catalyst. For example, 2-bromoisobutyrophenone initiated the controlled polymerization of MMA when catalyzed by ruthenium or nickel complexes but had not been successful in copper-mediated ATRP.[128,133] This was ascribed to reduction of the resulting electrophilic radical by the copper(I) species since the copper catalysts have lower redox potentials.

4. The method and order of reagent addition can be crucial. For example, slow addition of the benzhydryl chloride initiator to the CuCl(dNbpy)$_2$-catalyzed ATRP of MMA generates a lower instantaneous concentration of benzhydryl radicals and thus reduces the rate of termination between the radicals. The diethyl 2-bromomalonate/CuBr system initiates the ATRP of styrene and the polymerization was well controlled when the catalyst was added slowly to the initiator/monomer solution, thus avoiding the potential reduction of the malonyl radical by the copper(I) species. Surprisingly, the heterogeneous catalytic systems may provide more efficient initiation than homogeneous systems when very reactive alkyl halide initiators are used, most likely due to slow dissolution of the catalyst, and hence its lower instantaneous concentration. For example, CCl$_4$ is a good initiator for styrene and MMA with CuBr(bpy)$_3$ as the catalyst,[93] but the same is not true using the homogeneous CuBr(dNbpy)$_2$ catalytic system. Initiation efficiency increased when the catalyst solution was added slowly to the initiator solution.[101]

11.3.3 Catalysts

Perhaps the most important component of ATRP is the catalyst. It is the key to ATRP since it determines the position of the atom transfer equilibrium and the dynamics of exchange between the dormant and active species. There are several prerequisites for an efficient transition metal catalyst.

1. The metal center must have at least two readily accessible oxidation states separated by one electron.
2. The metal center should have reasonable affinity toward a halogen.
3. The coordination sphere around the metal should be expandable on oxidation to selectively accommodate a (pseudo)halogen.
4. The ligand should complex the metal relatively strongly.

5. Eventually, the position and dynamics of the ATRP equilibrium should be appropriate for the particular system. To differentiate ATRP from the conventional redox-initiated polymerization and induce a controlled process, the oxidized transition metal should rapidly deactivate the propagating polymer chains to form the dormant species. A variety of transition metal complexes with various ligands have been studied as ATRP catalysts and will be discussed below according to their periodic groups.

11.3.3.1   Group 6: Molybdenum   A series of lithium molybdate(V) complexes [LiMo(NAr)$_2$(C–*N*)R] (C–*N* = C$_6$H$_4$(CH$_2$NMe$_2$)-2; R = (C–*N*), Me, CH$_2$SiMe$_3$, or *p*-tolyl), have been used in the ATRP of styrene using benzyl chloride as the initiator.[153] The molybdate(V) complexes were generated in situ from the reaction of the corresponding molybdenum(VI) complexes [Mo(NAr)$_2$(C–*N*)R]. Relatively high polydispersities ($M_w/M_n \sim 1.5$) were obtained, and the efficiency of the benzyl chloride initiator was rather poor (6–18%), which was attributed to the extreme air sensitivity of the lithium molybdate(V) compounds. In addition, a side reaction occurred in ATRP; the lithium molybdate(V) reacted with (α-chloroethyl) benzene and (α-bromoethyl)benzene and resulted in the formation of LiCl and LiBr, respectively. Better results obtained with Mo(III) species, CpMo(PMe$_3$)$_2$Cl$_2$, which provided relatively well-controlled ATRP of styrene.[154]

(C-N) = C⌣N =
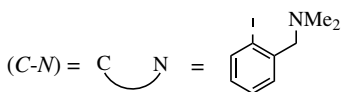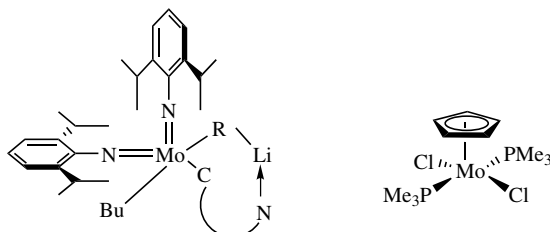
R = (C-N); Me; CH$_2$SiMe$_3$; *p*-tolyl

Chromium derivatives were successfully used in ATRA systems,[155] but not yet in ATRP.

11.3.3.2   Group 7: Manganese and Rhenium   Manganese and rhenium belongs to group 7 and shows the characteristics of both the early and late transition metals and both have been used in ATRP with limited success.[96] Manganese III (acetylacetonate) has been used for polymerization of styrene in the presence of alkyl halides. Mn(acac)$_3$ is a known thermal initiator. Apparently, it could also moderate styrene ATRP with the increasing molecular weights with conversion, although polydispersities remained relatively high. It is possible that either Mn(III)

or Mn(II) could abstract halogen atom from the initiator and chain end. Higher polydispersities could be due to either slow exchange reactions or concurrent thermal initiation process.

Rhenium(V) iododioxobis(triphenylphosphine) (ReO$_2$I(PPh$_3$)$_2$) in the presence of Al(OiPr)$_3$ was reported to be an effective catalyst for the controlled polymerization of styrene using an alkyl iodide as the initiator.[96]
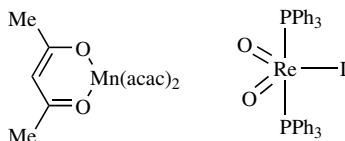
Polymerizations were carried out at temperatures of 30–100°C, with faster reactions at higher temperatures. Polydispersities were lower with decreasing temperature ($M_w/M_n \sim 1.50$ at 100°C and 1.26 at 30°C). Well-defined polystyrenes with $M_n \leq$ 40,000 and $M_w/M_n \sim 1.1$–1.2 were prepared in bulk 80°C. Of the iodide initiators studied, (CH$_3$)$_2$C(CO$_2$Et)I and CH$_3$CH(Ph)I resulted in polymers with lowest polydispersities. Quenching experiments showed that adding methanol or water did not inhibit the polymerization, while 2,2,6,6-tetramethylpiperidine-N-oxyl (TEMPO) immediately and completely terminated the reaction. Interestingly, the polystyrene quenched with TEMPO did not show any TEMPO-related peaks in the ^{1}H NMR. ^{1}H and ^{13}C NMR analysis of a mixture of ReO$_2$I(PPh$_3$)$_2$ and TEMPO indicated a possible interaction between these two compounds. It was concluded that the polymerization does not proceed via an ionic mechanism and an ATRP pathway was suggested. However, it is possible that the rhenium complexes slowly generate the initiating radicals but that control of the polymerization results from the degenerative transfer with the alkyl iodides.[156] It would be helpful to analyze the deactivation rate constants with the Re(VI) species.

In general, transition metals from groups 6 and 7 are quite oxophilic and potential coordination with (meth)acrylates may deactivate them.

11.3.3.3 Group 8: Ruthenium and Iron
Ruthenium and iron belong to the group 8 transition metals and have been well studied in atom transfer radical addition reactions.

11.3.3.3.1 Ruthenium
The polymerization of MMA via ruthenium-catalyzed ATRP was first reported by Sawamoto et al. in 1995.[13] The polymerization was carried out using CCl$_4$ as the initiator, RuCl$_2$ complexed by 3 equiv of PPh$_3$ as the catalyst, and a Lewis acid, such as methylaluminum bis(2,6-di-$tert$-butylphenoxide), as the activator in 75–80 vol% toluene at 60°C. No polymerization was observed in the absence of the Lewis acid. A linear semilogarithmic plot of conversion versus time was obtained indicating a constant number of propagating chains. The molecular weight of the polymer initially increased linearly with monomer conversion, but deviated from the theoretical values at high conversion rates. Chain extension was observed on addition of new monomer indicating the polymerization had a "living"

character. The polymers produced were monomodal and had relatively low polydispersities ($M_w/M_n \sim 1.3$). Better control was later obtained using RuCl$_2$(PPh$_3$)$_3$/Al(OiPr)$_3$ as the catalyst and α-haloesters, such as ethyl 2-bromoisobutyrate, as the initiator.[142]

The polymerization, mediated by the ruthenium complex, was proposed to follow a radical pathway based on several experimental observations.[143] First, the polymerization was inhibited in the presence of TEMPO, galvinoxyl, and 1,1-diphenyl-2-picrylhydrazyl (DPPH). The presence of H$_2$O or methanol did not affect the polymerization. In fact, well-defined PMMA was obtained in a suspension polymerization in water and alcohol.[47] The presence of the initiator moiety at both the α and ω ends was confirmed by ^{1}H NMR analysis, and the end functionality was close to 1. The tacticity of the PMMA prepared by the polymerization catalyzed by the ruthenium complex had a slight preference for syndiotacticity, which was similar to those prepared by a free-radical process. It should be noted that the intermediacy of a persistent Ru(III) radical was recently confirmed in the study of ATRP of MMA using a binuclear Ru(II) N_2-bridged complex, [{RuCl$_2$($NN'N$)}$_2$(μ-N_2)] ($NN'N$ = 2,6-bis[(dimethylamino)methyl]pyridine).[157]

More reactive ruthenium-based ATRP catalysts employing carbon-centered ligands, namely, 4-isopropyltoluene (*p*-cymene),[64,158] indenyl (Ind) and cyclopentadienyl (Cp),[137,159] have been reported. A direct relationship between the arene ligand lability and the catalyst activity suggests that the *p*-cymene ligand is released in the ATRP process. Well-defined polystyrene as well as PMMA have been obtained using the new catalysts with $M_n \sim 40,000$ and $M_w/M_n \sim 1.1$. A halogen-free Ru(II) hydride complex, RuH$_2$(PPh$_3$)$_4$, is more reactive than RuCl$_2$(PPh$_3$)$_3$, and the polymerization of MMA can be carried out at or above room temperature without the use of additional aluminum compounds.[160]

Apparently, some Ru-based ROMP catalysts can directly catalyze the ATRP process while simultaneously being active in ROMP.[161]
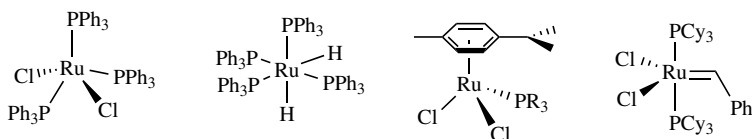
11.3.3.3.2 Iron In the presence of a preformed metal complex, FeCl$_2$(PPh$_3$)$_2$, CCl$_4$ induced the controlled polymerization of MMA at 80°C in toluene.[70] Initially the polymer molecular weights increased linearly with the monomer conversion, but deviation from the theoretical values was observed at higher conversions. Polydispersities were around 1.4. Addition of Al(OiPr)$_3$ accelerated the polymerization; however, molecular weight control was lost. The molecular weights decreased as MMA was consumed with high molecular weight polymers obtained at low conversion rates. The polydispersity was high ($M_w/M_n \sim 3.0$).

A series of organic halides, namely, CHCl$_2$COPh, (CH$_3$)$_2$CBrCO$_2$Et, and CH$_3$CBr(CO$_2$Et)$_2$, were examined as initiators in place of CCl$_4$ and led to controlled

polymerization of MMA with $M_w/M_n = 1.3$–1.5. When $CHCl_2COPh$ or $(CH_3)_2$ $CBrCO_2Et$ was used as the initiator, the molecular weights obtained were not in direct proportion to the monomer conversion and were higher than the theoretical values. When $CH_3CBr(CO_2Et)_2$ was used, a linear increase of the molecular weight with conversion was observed; however, the initiator efficiency was low. The authors attributed these observations to the interaction of $CH_3CBr(CO_2Et)_2$ with the $FeCl_2(PPh_3)_2$ catalyst to form a new iron complex.

Addition of 1 equiv of a radical inhibitor, such as galvinoxyl, completely terminated the polymerization and the tacticity of the PMMA prepared by the iron catalyst closely resembled that prepared by a conventional free-radical polymerization.

Matyjaszewski *et al.* have reported on several iron-based ATRP catalytic systems for the controlled polymerization of styrene and MMA.[71] As shown in Table 11.1, triethylphosphite, a common ligand for iron in ATRA, forms a catalyst with low efficiency in ATRP. In contrast, use of dNbpy, $N(nBu)_3$, and $P(nBu)_3$ as ligands promote controlled polymerizations with high initiator efficiencies and lead to polymers with low polydispersities.

Polymerization rate and polydispersity varied significantly depending on the catalytic system utilized for the ATRP of styrene. When dNbpy was used as the ligand, the polymerization proceeded quite slowly, with 64% monomer conversion after 21 h at 110°C. The polydispersity of the polymers obtained was quite low ($M_w/M_n < 1.2$). $P(nBu)_3$ as the ligand led to a much faster polymerization with $\sim$80% conversion of styrene in 6 h; however, the polydispersity was also higher ($M_w/M_n = 1.3$–1.4). Mixed ligands afforded an improved polymerization rate and polydispersity. For example, when a 1 : 1 mixture of dNbpy and $P(nBu)_3$ were used as the ligand, the ATRP of styrene proceeded with a comparable rate to that catalyzed by $FeBr_2/P(nBu)_3$, but with polydispersities similar to those prepared by $FeBr_2(dNbpy)$. Mixed dNbpy–$N(nBu)_3$ systems can also be successfully employed. For the mixed-ligand system, it was proposed that all the catalytic species were in dynamic equilibrium with each other and that the ligands were likely to scramble between the active centers, contributing to overall control of the polymerization.

TABLE 11.1   Results of Bulk Polymerization of Styrene with Different Fe-Based Catalytic Systems at 110°C[71]

Ligand	Time (h)	Conversion (%)	$M_{n,Cal}$	$M_{n,SEC}$	M_w/M_n
$P(OEt)_3{}^a$	15.0	87	9,200	30,500	6.14
$PPh_3{}^a$	15.0	47	5,100	4,200	1.76
dNbpy ^{b}	21.0	64	6,800	6,500	1.27
$N(nBu)_3{}^c$	10.0	78	16,800	17,000	1.24
$P(nBu)_3{}^c$	6.0	81	16,900	17,500	1.38

^{a} PEBr/$FeBr_2$/ligand/styrene = 1/1/3/100, where PEBr = 1-phenylethyl bromide.
^{b} PEBr/$FeBr_2$/ligand/styrene = 1/1/2/100.
^{c} PEBr/$FeBr_2$/ligand/styrene = 1/1/3/200.

Complexes of FeBr$_2$/dNbpy and FeBr$_2$/N(nBu)$_3$ catalyzed controlled ATRP of MMA to yield polymers with molecular weights up to 80,000 in 50 vol% o-xylene at 80°C, but lower polydispersities were observed using dNbpy ($M_w/M_n \sim 1.2$) as the ligand than using N(nBu)$_3$ ($M_w/M_n \sim 1.5$) . Similar to the FeCl$_2$(PPh$_3$)$_2$ system, discussed above, the choice of the initiator was important. Fast initiation is essential to obtain well-defined PMMA. For instance, ethyl 2-bromoisobutyrate (EBiB), 2-bromopropionitrile (BPN), and p-toluenesulfonyl chloride (pTsCl) yielded polymers with predictable molecular weights and low polydispersities.

MMA has been polymerized using AIBN as the initiator in the presence of FeCl$_3$/PPh$_3$ at 85°C either in bulk or in solution.[37] The reverse ATRP had first-order kinetics in monomer. An inhibition period was attributed to the deactivation of the initiating/growing radicals by Fe(III) to form the alkyl halide dormant species and the generation of Fe(II) as indicated by the color change from deep orange to light yellow. The molecular weight increased linearly with conversion, and the polydispersities were relatively low ($M_w/M_n < 1.3$). The initiator efficiency was lower when the polymerization was carried out in bulk rather than in solution, because of a larger proportion of termination in the bulk polymerization. The polymerization was significantly faster than that carried out using CCl$_4$/FeCl$_3$/PPh$_3$, with >95% yield after 2 h. ^{1}H NMR studies confirmed the presence of the AIBN fragment moiety as α end group ^{1}H NMR and chain extension experiments established that Cl atoms were present as the ω end groups.

X = Br, Cl
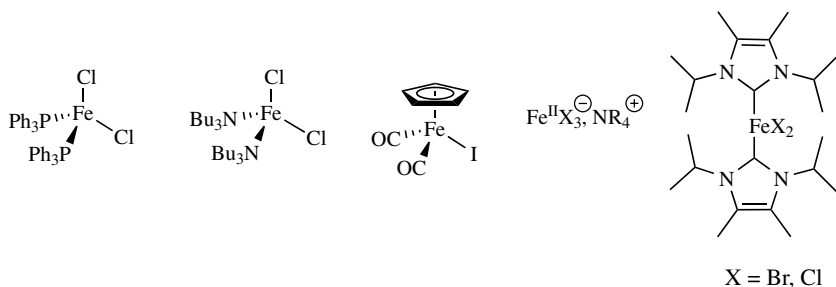
Catalyst systems with ligands other than nitrogen- and phosphine-based ones have also been studied.[105,162,163] For example, a half-metallocene catalyst, FeCp(CO)$_2$I, yielded polystyrene with low polydispersities ($M_w/M_n = 1.1$). Interestingly, the addition of a metal alkoxide, either Al(OiPr)$_3$ or Ti(OiPr)$_4$, decreased the polymerization rate.[163] In another study, FeBr$_2$ complexed with ammonium and phosphonium chloride, bromide, or iodide salts induced the controlled polymerization of both styrene and methacrylates. In addition, well-defined poly(methyl acrylate) was produced for the first time using iron-based ATRP.[105] A reverse ATRP, initiated by AIBN/FeBr$_3$/onium salts, led to a controlled polymerization of both methyl methacrylate and methyl acrylate, while for styrene uncontrolled molecular weights and high polydispersities were obtained, presumably due to the participation of a cationic polymerization mechanism.[105]

Recently, a ferrous halide complexed with 1,3-diisopropyl-4,5-dimethylimidazol-2-ylidene (PriIm) was found highly reactive and efficient in the ATRP of

MMA and styrene. The high catalyst activity was attributed to the high electron donacity of the ligand.[72]

11.3.3.4 *Group 9: Cobalt and Rhodium*   Cobalt derivatives have been successfully used in several LRP systems, however, not yet in ATRP. They have a high tendency to either form organometallic derivatives or abstract H atoms. The former system has been used for controlled polymerization of acrylates,[164,165] while the latter is used in catalytic chain transfer and addition–fragmentation chemistry.[166] Selectivity depends on spin state and steric as well as electronic effects.

Rhodium also belongs to the group 9 transition metals. The Wilkinson's catalyst, $RhCl(PPh_3)_3$, which has found wide application as a homogeneous hydrogenation catalyst in organic chemistry, has been employed in the ATRP of styrene with a sulfonyl chloride as the initiator.[51] However, poor control and polymers with high polydispersities ($M_w/M_n \sim 1.8$–3.2) were obtained. In contrast, the successful ATRP of MMA was carried out using 2,2′-dichloroacetophenone as the initiator in the presence of $RhCl(PPh_3)_3$ and 7 equiv. of PPh_3 in THF or a mixture of THF and H_2O.[74] The experimental molecular weights of PMMA agreed well with the predicted values up to 200,000 and the molecular weight distributions were relatively narrow ($M_w/M_n \sim 1.5$). A linear semilogarithmic plot of the monomer conversion versus time was observed. From the apparent polymerization rate and the propagation rate constant for MMA, the radical concentration of the polymerization reaction carried out in THF was estimated at 3.16×10^{-8} M. Interestingly, water was found to accelerate the polymerization significantly. Chain extension to *n*-butyl acrylate and MMA was successful after purification of the first block by precipitation into methanol. Lower initiator efficiency was observed when the polymerization of styrene was carried out using the same catalyst at 130°C using *p*-methoxybenzenesulfonyl chloride as the initiator. The tacticity of the PMMA, inhibition studies (galvinoxyl), and end-group analysis, indicated that radical intermediates were present in the polymerization.

11.3.3.5 *Group 10: Nickel and Palladium*   Nickel and palladium as group 10 late transition metals, have been widely used in organometallic chemistry for carbon–carbon bond formation through the oxidative addition/reductive elimination mechanism. Complexes of nickel and palladium have also been studied as ATRP catalysts.

11.3.3.5.1 Nickel   Ni{*o,o′*-$(CH_2NMe_2)_2C_6H_3$}X [denoted as Ni(NCN)Br] is one of the most reactive ATRA catalysts but initially failed to promote the ATRP of styrene because of its instability at high temperatures.[51] By lowering the reaction temperature to 80°C, Ni(NCN)Br was successfully applied to the controlled polymerization of MMA with molecular weight of $\leq$100,000. Polydispersities remained low ($M_w/M_n \sim 1.2$) throughout the reaction.[67] Interestingly, the molecular weight distribution broadened significantly when the polymerization was carried out in toluene under otherwise identical reaction conditions. Thermolysis of the obtained PMMA indicated the absence of abnormal linkages, such as the head to head linkages and vinylidene ends. Suspension polymerization of MMA was also successful, with a high conversion (rate) of MMA and reasonable

molecular weights. However, the polydispersity of the polymer was relatively high ($M_w/M_n \sim 1.7$).

Despite an earlier proposal that ATRA catalyzed by Ni(NCN)Br may not proceed via a radical mechanism, as evidenced by the high regioselectivity of the final 1 : 1 adduct,[167] a radical pathway was proposed for the ATRP of methacrylates on the basis of the following lines of evidence:[67]

1. The reaction was catalytic. When a catalyst to initiator ratio of 0.1 was used, the polymerization proceeded quite smoothly without sacrificing the molecular weight control, but with slightly higher polydispersities. The oxidative addition–insertion–reductive elimination mechanism would require a stoichiometric amount of catalyst to initiator since each transition metal center is permanently associated with the chain end.
2. The polymerization was inhibited by radical scavengers such as galvinoxyl.
3. End-group analysis indicated the presence of initiator moiety as α end group of the polymer chain, and the halogen as ω end group.
4. The tacticity of PMMA prepared using Ni(NCN)Br as the catalyst was similar to that prepared by conventional radical polymerizations.

Nickel halides complexed by phosphorous ligands have also been used for the ATRP of MMA.[68,69,131] CCl$_3$Br/NiBr$_2$(PPh$_3$)$_2$ provided a smooth polymerization, yielding polymers with predictable molecular weights and low polydispersities ($M_w/M_n \sim 1.20$) in the presence of Al(iOPr)$_3$.[131] It was reported, however, that the NiBr$_2$(PPh$_3$)$_2$ complex was not stable or soluble in organic solvents. Decomposition of the catalyst was noted after prolonged use at high temperatures (60–80°C), and the rate of polymerization decreased with time. However, Teyssié et al. reported that NiBr$_2$(PPh$_3$)$_2$ catalyzed the ATRP of MMA in the absence of any Lewis acid additive.[69] High monomer concentration and a large excess of the PPh$_3$ ligand helped preserve the control over the polymerization. The PMMA obtained from the polymerization displayed better thermal stability compared to that made by a conventional radical polymerization. In addition, the ATRP of n-butyl acrylate with $M_n \sim 35,000$ and $M_w/M_n < 1.2$ was also successfully conducted.
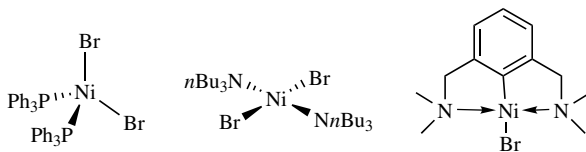
Other nickel catalysts have also been studied. NiBr$_2$(PnBu$_3$)$_2$ was more thermally stable and soluble than NiBr$_2$(PPh$_3$)$_2$ and led to the controlled ATRP of both methacrylates and acrylates.[68] In the polymerization of methacrylates, Al(iOPr)$_3$, or other additives, had no effect on the rate or the control of the polymerization. More recently, a zerovalent nickel complex, Ni(PPh$_3$)$_4$, was reported to catalyze the controlled polymerization of MMA in the presence of Al(iOPr)$_3$.[132] The polymerization profile was similar to the NiBr$_2$(PPh$_3$)$_2$/Al(iOPr)$_3$ systems; however, a bimodal

distribution was observed when a fresh feed of MMA was added to the reaction mixture after the initial monomer feed reached 90% conversion. This was attributed to excessive termination. A lower initiator efficiency was observed at a higher catalyst : initiator (Cl_3CBr) ratio, this was attributed to the possible interaction between the catalyst and the initiator through an oxidative addition reaction. It was postulated that the real catalyst was likely to be a Ni(I) species, although the involvement of Ni(II) was not excluded.

The polymerization mediated by nickel halides complexed by phosphorous ligands was proposed to proceed via a radical mechanism based on inhibition studies (TEMPO), end-group measurements, and tacticity analysis of the polymers.[68] A study of the reactivity ratios of the MMA and *n*BA copolymerization also supports a radical mechanism.[69]

11.3.3.5.2 Palladium PMMA with molecular weight of $\leq 150,000$ have been prepared using $Pd(OAc)_2$ complexed by PPh_3 as the catalyst and CCl_4 as the initiator in 63 vol% toluene at 70°C.[73] A good correlation between the theoretical and experimental molecular weights was observed when a 10-fold excess of the catalyst over the initiator was used. Lower ratios of catalyst to initiator (<10) resulted in high polydispersities and low initiator efficiencies, which was attributed to the low turnover of the palladium catalyst. Identification and use of the correct ratio of PPh_3 ligand to $Pd(OAc)_2$ were essential for the preparation of well-defined polymers. The absence of ligand led to an ill-controlled polymerization with very high molecular weights and polydispersities. In the presence of 4 equiv of ligand, the polymerization control was significantly improved. High conversion, high initiator efficiency (~ 1), and low polydispersities were obtained. However, the initiator efficiency decreased to 0.3 when a 10-fold excess of ligand relative to palladium was used. The polymerization temperature was also optimized; slow initiation was observed at low temperatures (20°C), while the catalyst was unstable at high temperatures (90°C). The optimal polymerization reaction temperature was 70°C. At this temperature, a linear increase of the experimental molecular weights versus the monomer conversion was observed with an initiator efficiency close to unity. The relatively high polydispersity obtained for the polymers was likely due to either slow initiation or slow exchange between the active and dormant species. The polymerization was insensitive to water. A suspension polymerization has been carried out to yield PMMA of $M_n = 32,500$ and $M_w/M_n = 1.55$. Inhibition studies (with 1,1-diphenyl-2-picrylhydrazyl or galvinoxyl), a composition study of poly(MMA-*b*-styrene), and the tacticity analysis of the obtained PMMA were used to support a radical mechanism for the polymerization.

11.3.3.6 **Group 11: Copper** Copper catalysts are superior in ATRP in terms of versatility and cost. According to *SciFinder Scholar* $>80\%$ of publications on ATRP employed Cu-based systems. Styrenes, (meth)acrylate esters and amides, and acrylonitrile have been successfully polymerized using copper-mediated ATRP.[1,2,5,6] The first copper-based ATRP system was reported in 1995.[14,93] Initially, cuprous halides in the presence of three equivalents of bpy were used as the catalysts. Controlled polymerizations with a linear increase of the molecular weight

with conversion were achieved for styrene, MA and MMA.[32] The polydispersities were fairly narrow ($M_w/M_n = 1.2 \sim 1.5$) and polymers with molecular weights of $\leq 100{,}000$ were prepared with good control. Well-defined polyacrylonitrile was also prepared.[88,89]

It was proposed that the polymerization proceeded via a radical pathway based on several experimental observations.[168]

1. Radical scavengers (e.g., galvinoxyl, TEMPO) terminated the polymerization. The polymerization was tolerant to a variety of functional groups, such as $-OH$ and $-NH_2$, and insensitive to additives, such as H_2O, CH_3OH, and CH_3CN.[25]

2. The tacticity of the PMMA prepared by ATRP catalyzed by copper complexes was similar to that prepared by a free-radical process.

3. Regio- and chemoselectivities were similar to those in conventional free radical polymerizations. This is related to the microstructure of the polymers and the end groups, the reactivity ratios, and the sensitivity to transfer agents.[93,169,170]

4. The PRE results in the formation of a paramagnetic Cu(II) species that was detected by EPR.[26,171]

5. ATRP equilibrium can be approached from the other side, via reverse ATRP, using a CuX_2/L species and AIBN.[32,34,35]

6. Propagating radicals were directly observed by EPR[172] in ATRP of dimethacrylates.

Various polydentate ligands, such as phenanthroline and its derivatives,[173] substituted 2,2′ : 6′,2″-*tert*-pyridine,[174] and pyridineimines[66,175] have been used for copper-mediated ATRP. The multidentate aliphatic amines as the ligands, either linear[43,99,176] or branched,[106,177] greatly reduce the cost of the catalyst and dramatically increase the rate of the polymerization while still maintaining good control. In addition, multidentate picolyl amines, which can easily be prepared and allow for further modification and tuning of the catalyst, promote well-controlled polymerizations of styrene and (meth)acrylates.[178] Branched tetradentate ligands, such as Me$_6$TREN and TPMA, provide the most strongly reducing ATRP catalysts.[106,178]

X = Br, Cl
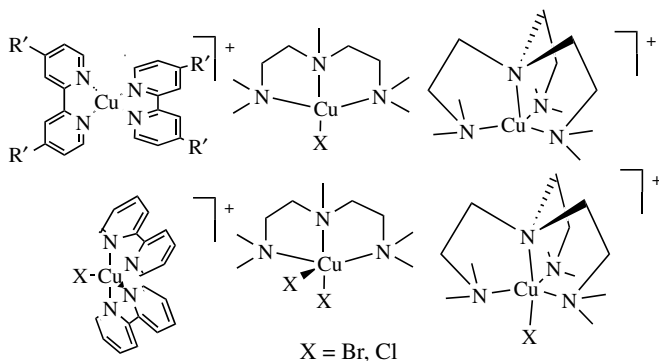
Copper(I) prefers a tetrahedral or square planar configuration, which can be achieved in cationic complexes with tetradentate ligands or with two bidentate

ligands. Tridentate ligands presumably form neutral distorted square planar complexes. On the other hand, copper(II) forms cationic trigonal bipyramidal structures with tetradentate ligands or two bidentate ligands. However, in nonpolar media, in the absence of Cu(I) species, square planar complexes $CuBr_2(dNbpy)_2$ were identified.[179] Tridentate ligands apparently form neutral square pyramidal neutral complexes with the longer Cu—X bond in the apical position.[180]

Counterions other than halides have also been used.[21,30,129,181,182] When cuprous carboxylates such as cuprous acetate (CuOAc), are used the polymerization rate is significantly increased, however, the rate increase was accompanied by a decreased control over the polymerization, as indicated by higher than calculated experimental molecular weights and an increase of the polydispersities for the CuOAc-dNbpy catalytic system. Addition of a small amount of either the Cu(II) or Cu(I) halide to the cuprous carboxylate system yielded a better controlled ATRP of styrene, while still maintaining fast polymerization.[30] A similar rate enhancement was observed for the ATRP of MA catalyzed by a $CuPF_6(dNbpy)_2$ complex.[21] Copper thiocyanate has been used in ATRP of styrene, acrylates, and MMA,[127,129] and copper triflate has been successfully used with various ligands to promote controlled polymerizations.[181] More recently, CuY/bpy systems where $Y = O,S,Se,Te$ have been successfully applied to the ATRP of MMA in conjunction with alkyl halides.[182]

11.3.4 Ligands

The main roles of the ligand in ATRP is to solubilize the transition metal salt in the organic media and to adjust the redox potential and halogenophilicity of the metal center forming a complex with an appropriate reactivity and dynamics for the atom transfer.[183,184] The ligand should complex strongly with the transition metal. It should also allow expansion of the coordination sphere and should allow selective atom transfer without promoting other reactions.

11.3.4.1 Nitrogen Ligands
Nitrogen ligands have been used in copper- and iron-mediated ATRP.[71,183] In copper-mediated ATRP, nitrogen-based ligands work particularly well. In contrast, sulfur, oxygen, or phosphorous ligands are less effective because of unsuitable electronic effects or unfavorable binding constants, however, their combination may yield good catalysts.

Both monodentate [e.g., $N(nBu)_3$] and bidentate (e.g., dNbpy) ligands have been applied to iron-mediated ATRP. In copper-based ATRP, the coordination chemistry of the transition metal complex greatly affects the catalyst activity. While monodentate ligands are suitable for most of the transition metal salts employed in ATRA, they do not promote controlled copper-mediated ATRP. In contrast, a variety of multidentate nitrogen ligands have been successfully developed.[184] The electronic and steric effects of the ligands are important. Reduced catalytic activity or efficiency is observed when there is excessive steric hindrance around the metal center or the ligand has strongly electron-withdrawing substituents. Xia *et al.* summarized different ligands employed in copper-mediated ATRP and the effect of the ligands and guidelines for ligand design were reviewed.[184]
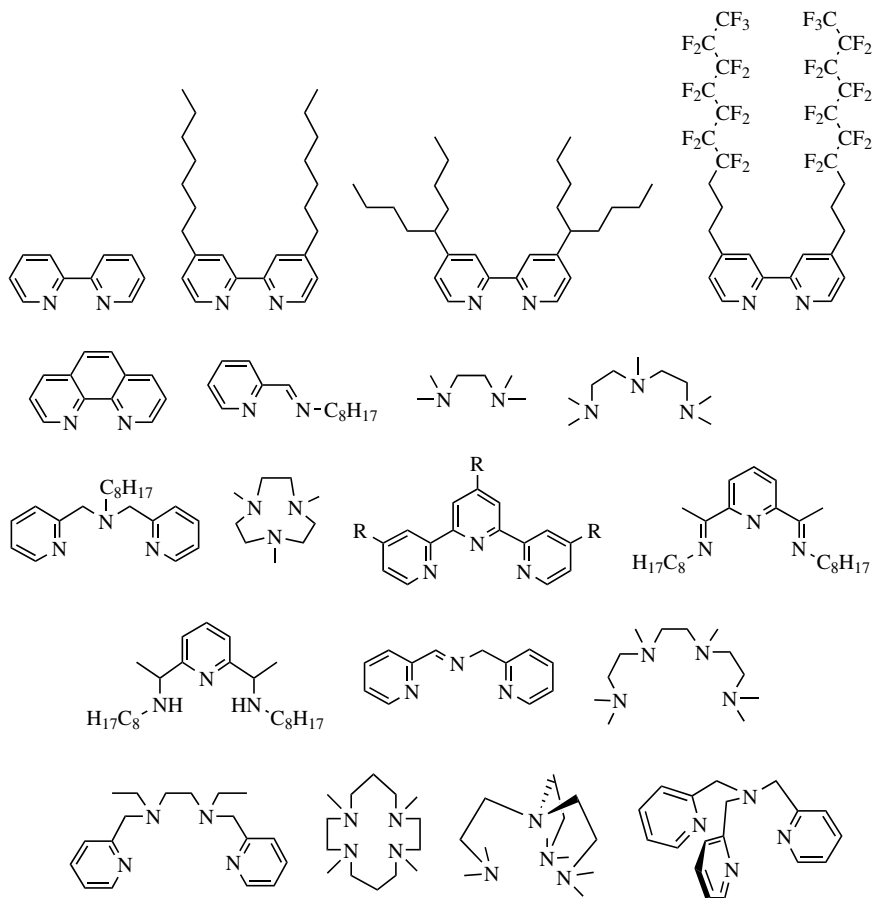
Figure 11.10 Nitrogen-containing ligands used in Cu-based ATRP.

1. Activity of N-based ligands in ATRP decreases with the number of coordinating sites: N4 > N3 > N2 ≫ N1 and with the number of linking C atoms: C2 > C3 ≫ C4.

2. It also decreases in the order: $R_2N- \sim Pyr- > R-N => Ph-$ N= > Ph−NR−.

3. Activity is usually higher for bridged and cyclic systems than for linear analogs. Examples of some N-based ligands successfully used in Cu-based ATRP are shown in Fig. 11.10.

Ligands may participate in side reactions. For example, Kubisa *et al.* studied the ATRP of several acrylates under the conditions when low molecular weight polymers ($M_n = 2,000$) were targeted using relatively high concentrations of the catalyst.[185] MALDI TOF analysis of the polymer samples isolated at different stages of the polymerization revealed that in the course of the polymerization potentially

active macromolecules terminated with bromine were gradually converted into inactive macromolecules devoid of terminal bromine. A possible chain transfer to the aliphatic amine ligand was proposed. Additionally, amines (and phosphines) can react with alkyl halides by a nucleophilic substitution reaction, with loss of HX through a Hoffman elimination process.[186,187] For example, methyl 2-bromopropionate reacts with n-butyl amine at 25°C in DMSO with the rate constant $k = 0.0046\,\mathrm{M}^{-1}\,\mathrm{s}^{-1}$; the reaction with tertiary amines is slower and with amines complexed to CuBr so slow that it could not be detected.[187]

11.3.4.2 *Phosphorous Ligands*

Phosphorous-based ligands have been used to complex most transition metals studied in ATRP, including rhenium,[96] ruthenium,[13,64] iron,[70,71] rhodium,[51,74] nickel,[68,131] and palladium,[73] however, not copper. PPh$_3$ is the most frequently used ligand and has been successfully applied to coordinate all the aforementioned transition metals. Another phosphorous ligand, P(nBu)$_3$, has been used in nickel- and iron-based systems.

A series of phosphorous ligands have been studied for the RuCl$_2$(p-cymene)PR$_3$-type catalyst.[64] Apparently, only phosphines, which are both strongly basic and possess a well-defined steric bulk ($160° < \theta < 170°$, $\theta = $ cone angle of the phosphine) form complexes that display both high catalytic activity and good control of the polymerization.

11.3.4.3 *Miscellaneous Ligands*

Cyclopentadienyl, indenyl,[137,159] and 4-isopropyltoluene[64] have been used as ligands in ruthenium-based ATRP yielding more reactive catalysts than ruthenium complexed by phosphorus alone. Similarly, 1,3-diisopropyl-4,5-dimethylimidazol-2-ylidene (PriIm) has been successfully used for iron-based ATRP.[72] Oxygen-centered ligands such as phenol or carboxylic acids have also been used.[30] It is possible that under appropriate conditions, water and polyethers may complex with transition metals. Chalcogenides, which can be considered either as ligands or counterions, may also affect the reactivity of Cu complexes.[182] In addition, iron complexed by halides also promoted the controlled polymerization of MMA.[105] Thus, under some conditions, halogens, triflate, hexafluorophosphate, and other counterions can also play a role of ligands. An interesting extension of this concept is to use charged ligands (thiophenecarboxylate, etc.).[30]

11.3.5 Additives

ATRP is tolerant to a variety of functional groups. For example, addition of water, aliphatic alcohols, or polar compounds to copper-mediated ATRP had minor effect on the control of the polymerization.[25] The same phenomenon was observed for the ruthenium/aluminum alkoxide-mediated ATRP.[47] By taking advantage of this great tolerance toward functional groups a variety of well-defined functional polymers have been prepared by ATRP without the need for protection and deprotection of functionalities.[97] These observations support the intermediacy of radicals and excludes ionic or organocuprate intermediates in ATRP. However, addition of pyridine or PPh$_3$ to the copper-mediated ATRP leads to a large decrease in the polymerization

rate and an increase in the polydispersity, presumably due to competition with the ligand for the coordination sites on the metal or the formation of less active complexes.

ATRP is moderately sensitive to oxygen. The polymerization will proceed in the presence of a small amount of oxygen, since it can be successfully scavenged by the catalyst, which is present at a much higher concentration than the growing radicals,[55] but this oxidation of the catalyst reduces the catalyst concentration and slows down the polymerization. In some cases, however, oxygen may produce peroxides that can actually catalyze the reaction. The polymerization of methacrylates in the presence of oxygen and Cu(I) or Cu(II) complexes has been reported to yield high molecular weight products with relatively low polydispersities.[23]

In some cases, additives can accelerate ATRP. For example, when a small amount of copper(0) was added to the ATRP systems for the polymerization of styrene and (meth)acrylates, a significant rate increase was observed.[188,189] For example, the polymerization of MA with a 1 : 0.2 : 0.4 ratio of MBP (MBP = methyl 2-bromo-propionate), CuBr and dNbpy in the presence of Cu(0) proceeded 10 times faster than without Cu(0), with comparable control over the molecular weights and polydispersities in both cases. The addition of copper(0) to copper(II) dibromide in the presence of a solubilizing ligand also afforded a controlled polymerization with an increased rate. Similar rate enhancements were also observed in a phase transfer catalyzed process with Cu$_2$O/copper(0)/bpy as the catalyst.[190] Presumably, copper(0) reduces "excess" copper(II), which is generated mostly during the early stage of the polymerization through irreversible radical termination, to form in situ copper(I) by a simple electron transfer process. This process reduced the concentration of copper(II) and simultaneously increased the concentration of copper(I). As a result of the significant rate enhancement, the polymerizations can be carried out with a reduced amount of catalyst. Copper(0) alone with the ligand also promotes ATRP but with less control over the polymerization. The addition of iron powder to salts of Fe(II) or Fe(III) results in a similar increased rate of polymerization.[188] Moreover, if a sufficient amount of zerovalent metal is present, the controlled radical polymerization can be carried out without the removal of any oxygen or inhibitor.[55] An induction period was observed, presumably due to the consumption of oxygen through oxidation of the catalyst. However, the presence of the zerovalent metal reduced the oxidized metal, regenerating the catalyst for a controlled polymerization. A similar effect can be achieved in the presence of other reducing agents such as sugars and aluminum alkoxides.[191]

Haddleton *et al.* investigated the ATRP of MMA catalyzed by CuBr/*N*-alkyl-2-pyridylmethanimine complexes using various phenols as additives and observed a small increase in the rate of polymerization.[192] Methylhydroquinone has a similar effect and accelerates the polymerization by a factor of 3–4 at temperatures below 40°C.[193] It appears that the rate increase is not at the expense of molecular weight control and the polydispersities were typically <1.3. Several earlier studies clearly demonstrated that although phenols do affect the polymerization of styrene, their action on radical polymerization of (meth)acrylates in the absence of oxygen is very weak. For example, less than 1% retardation was observed for MMA polymerization with 0.2 M of hydroquinone. 4-Methoxyphenol even increased the

polymerization rate when the polymerization was initiated by AIBN at 45°C. In the latter case, the transfer coefficient is $k_{tr}/k_p < 0.0005$.[194] Methyl acrylate systems were shown to be similar, and inhibition was again insignificant at 50°C: $k_x/k_p < 0.0002$.[195] Thus, weak retardation/transfer effect of phenols on the polymerization of (meth)acrylates does not contradict the radical mechanism. Phenols acceleration of the polymerization of MMA can be ascribed to a higher activity of the catalysts (larger equilibrium constants) with phenoxy ligands at the Cu center. A similar effect has been observed for Cu carboxylates and CuPF$_6$.[30,127] The observed rate enhancement could additionally result from specific interactions of the phenol or methyl hydroquinone with the metal center, such as displacement of the ligand and conversion of the Cu(II) halide to a nondeactivating Cu(II) phenoxide. Furthermore, the stereochemistry of the polymers produced was consistent with that observed for a conventional free-radical polymerization and the fraction of syndiotactic triads increased as the reaction temperature was lowered.

A similar rate increase has been observed when carboxylic acids were added to the polymerization of MMA catalyzed by (N-n-butyl-2-pyridylmethanimine)copper(I) bromide.[196] Although the polymerization rate progressively increased, the polydispersities also increased with an increase in the benzoic acid : copper ratio. It was proposed that the active catalyst species formed through complexation of the added acid to the copper. However, a rate increase was not observed with the addition of benzoic acid to the CuCl-bpy system. In contrast, addition of benzoic acid salts did result in a rate enhancement.[197] The addition of a 1 : 1 mixture of benzoic acid and sodium carbonate also enhanced the rate, although the slow *in situ* formation of sodium benzoate led to a slower polymerization than when sodium benzoate was added directly. Electron-donating groups on the benzoate also increased the rate, which was also dependent on the electronegativity of the cation and increased in the order Li < Na ~ K < Cs. This rate enhancement was attributed to the in situ formation of an active catalyst with carboxylate attached to the metal center. It was previously reported that higher rates were observed when Cu(I) carboxylates were used instead of copper(I) halides.[30]

The presence of a Lewis acid, such as aluminum alkoxide, is essential for the controlled polymerization of MMA catalyzed by RuCl$_2$(PPh$_3$)$_3$.[13] The aluminum compound can presumably activate the polymerization by coordinating to the carbonyl group of the polymer chain end and the monomer. The added aluminum alkoxide has no effect on the halogen exchange reactions.[150] Methylaluminum bis(2,6-di-*tert*-butylphenoxide), MeAl(ODBP)$_2$, led to a faster polymerization rate than did Al(*i*OPr)$_3$.[77] This was attributed to the difference in the Lewis acidity. However, the polymerization rate in the presence of MeAl(ODBP)$_2$ decreased with time at 60°C, related to the slow decomposition of the compound at this temperature. When a difunctional initiator, bis(dichloroacetoxy)ethane, was used with RuCl$_2$(PPh$_3$)$_3$ as the catalyst, transesterification between the initiator and Al(*i*OPr)$_3$ occurred.[198] This led to polymers with lower molecular weight than theoretical. To avoid this problem, a weaker Lewis acid, aluminum acetylacetonate, was used. More recently, Al(*i*OPr)$_3$ has been added to a copper-mediated ATRP.[191,199] Using 1-phenylethyl bromide as the initiator, [Cu(II)(4,4'-dimethyl-2,2'-bipyridine)$_3$](PF$_6$)$_2$/Al(*i*OPr)$_3$ successfully catalyzed the polymerization of styrene at 75°C

with $M_n \leq 50{,}000$ and $M_w/M_n = 1.1 \sim 1.5$. The actual mechanism of the reaction remains unclear, but could involve the *in situ* reduction of the Cu(II) to Cu(I) by the aluminum derivatives.

11.3.6   Solvents

ATRP can be carried out either in bulk, in solution, or in a heterogeneous system (e.g., emulsion, suspension). Various solvents, such as benzene, toluene, anisole, diphenyl ether, ethyl acetate, acetone, dimethyl formamide (DMF), ethylene carbonate, alcohol, water, carbon dioxide, and many others, have been used in the polymerization of different monomers. A solvent is sometimes necessary, especially when the polymer is insoluble in its monomer (e.g., polyacrylonitrile). ATRP has been also successfully carried under heterogeneous conditions in (mini)emulsion, suspension, or dispersion. Several factors affect the solvent choice. Chain transfer to solvent should be minimal. In addition, potential interactions between solvent and the catalytic system should be considered. Catalyst poisoning by the solvent (e.g., carboxylic acids or phosphine in copper-based ATRP)[25] and solvent-assisted side reactions, such as elimination of HX from polystyryl halides, which is more pronounced in a polar solvent,[100] should be minimized.

The possibility that the structure of the catalyst may change in different solvents should also be considered. For example, when the ATRP of *n*-butyl acrylate with CuBr(bpy)$_3$ as the catalyst was carried out in ethylene carbonate, the reaction was found to proceed much faster than in bulk.[200] A structural change from a dimeric halogen bridged Cu(I) species in the bulk system to a monomeric Cu(I) species in ethylene carbonate was proposed to explain the rate difference. A similar rate enhancement in polar media was observed at a later date in different studies.[201,202] The overall rate increase may be related to slower deactivation, when X—Cu^{II} bond is hydrolyzed. Polar media can also help to dissolve the catalyst. For example, homogeneous ATRP using CuBr(bpy)$_3$ was achieved using 10% v/v DMF.[203]

11.3.7   Temperature and Reaction Time

The rate of polymerization in ATRP increases with increasing temperature due to the increase of both the radical propagation rate constant and the atom transfer equilibrium constant. As a result of the higher activation energy for the radical propagation than for the radical termination, higher k_p/k_t ratios and better control (''livingness'') may be observed at higher temperatures. However, chain transfer and other side reactions become more pronounced at elevated temperatures.[100,101] In general, the solubility of the catalyst increases at higher temperatures; however, catalyst decomposition may also occur with an increase in temperature.[51,131] The optimal temperature depends mostly on the monomer, the catalyst, and the targeted molecular weight.

At high monomer conversions, the rate of propagation slows down considerably; however, the rate of any side reactions do not change significantly, as most of them are independent of the monomer concentration. Prolonged reaction times leading to nearly complete monomer conversion may not increase the polydispersity of the

final polymer but will induce loss of end groups.[204] Therefore, in order to obtain polymers with high end-group functionality, or when the first polymer is used to subsequently synthesize block copolymers, conversion should not exceed 95% to avoid end-group loss.

11.4   MECHANISTIC FEATURES OF ATRP

A full description of the mechanism of any polymerization should include structures of all reagents involved, correlation of those structures with reactivities, as well as kinetics and chemistry of all elementary reactions. In ATRP, there are several participating reagents: dormant species (macromolecular alkyl (pseudo)halides), propagating species (presumably growing free radicals), and a catalyst (transition metal complexes in their lower and higher oxidation states). Their structures will be discussed below, followed by their relationship with reactivities, and a discussion of the chemistry of all elementary reactions involved in ATRP.

11.4.1   Dormant Species

The NMR spectroscopy allows to examine the microstructure of the polymer obtained and also the structure of end groups for relatively low molar mass polymers. The tail group is formed from the residual alkyl part of the initiator and the head group is the remaining halogen part of the initiator attached to the more substituted part of the incorporated monomer. Figure 11.11 presents the ^{1}H NMR spectrum of polyacrylonitrile (PAN) showing the presence of the end groups originating from the initiator (2-bromopropionitrile, BPN).[88] The ratio of intensities of peaks **a** and **d** is 3 : 1, as predicted for well preserved end groups. Broad NMR signals are due to the tacticity of polyacrylonitrile. It is possible to exchange the halogens present on the chain end with catalysts. For example, using 2-bromopropionate as initiator and $CuCl(dNbpy)_2$ as catalyst in MA polymerization results to the predominant formation of a polymer with a terminal alkyl chloride and $CuBr(dNbpy)_2$.[133]

By trapping growing radicals with TEMPO, for instance, macromolecular alkoxyamines are formed, suggesting the presence of free radicals. Alkyl halides can be displaced from the chain end by other methods resulting in end-functional polymers.

MALDI-TOF-MS under appropriate conditions also allows detection of macromolecular alkyl halides. In addition a small amount of unsaturated chains and products of radical coupling can be detected. The former can result from termination but also from the loss of HX from the chain end. This loss is especially facile for the tertiary alkyl halides such as those in ATRP of MMA. Figure 11.12 presents the MALDI-TOF-MS spectrum of the same PAN whose NMR was shown in Fig. 11.11.[88] Polydispersity calculated from MALDI was $M_w/M_n = 1.01$ lower than from SEC $M_w/M_n = 1.04$.

At high conversions some side reactions could be detected, leading to the second series of MALDI peaks (B), corresponding to loss of Br and its replacement by H atoms. This reaction is plausibly induced by outer-sphere electron transfer, reduction of radical to carbanion, followed by the transfer to solvent, as shown in Fig. 11.13.[90]
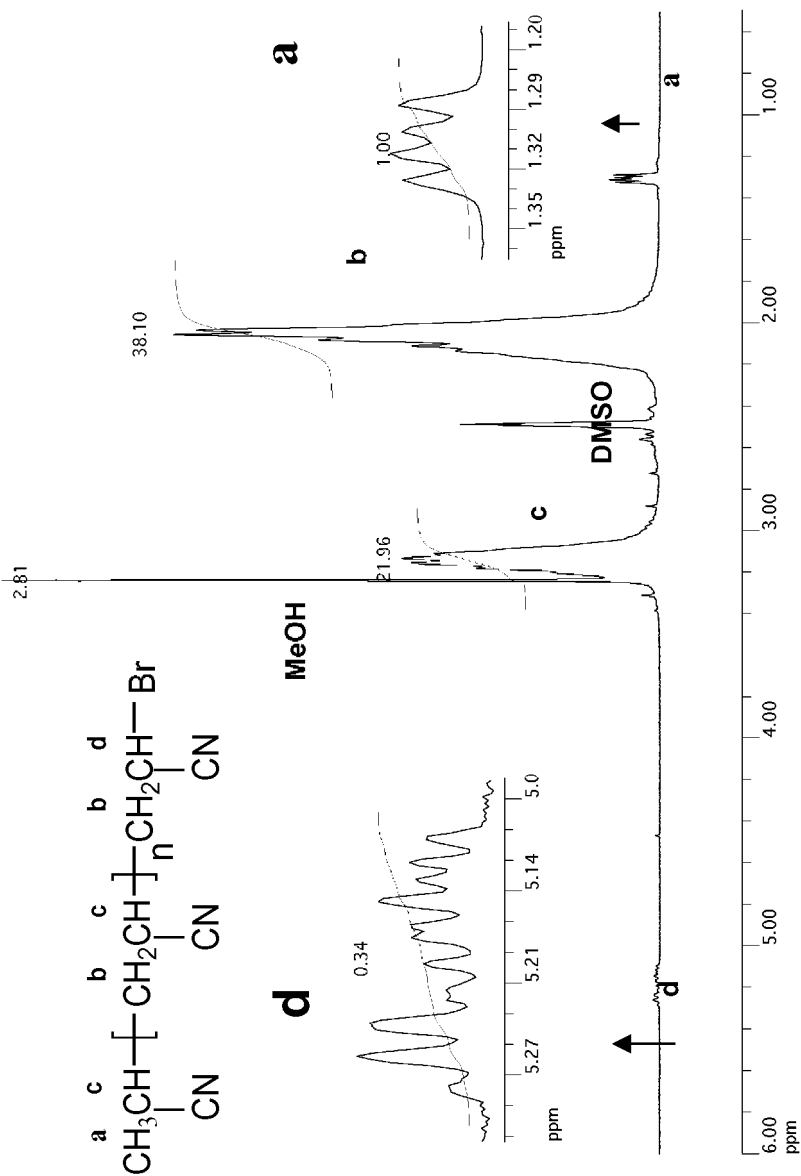
Figure 11.11 ^{1}H NMR spectrum of BPN initiated PAN in ethylene carbonate at 44°C.[368] $[AN]_0 = 5.25$ M, $[BPN]_0 = 5.53 \times 10^{-2}$ M, $[CuBr] = [bpy]_0/3 = 5.53 \times 10^{-3}$ M.[88]
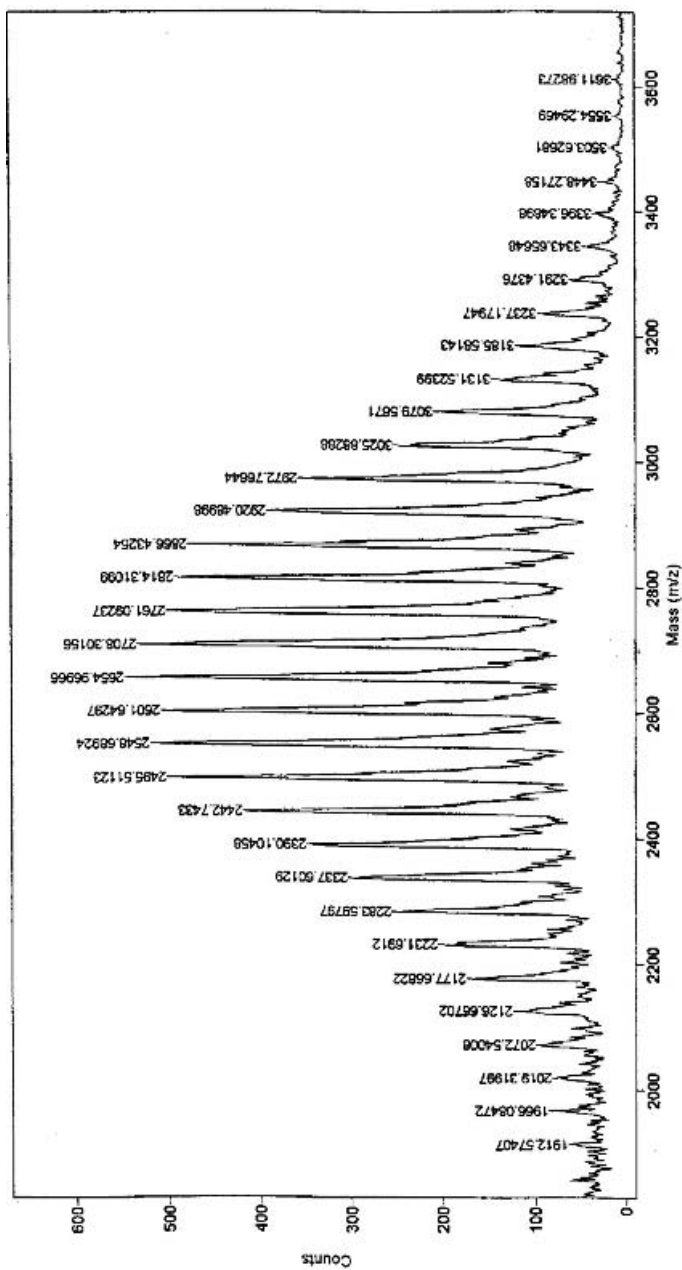
Figure 11.12 MALDI-TOF-MS of PAN prepared in ethylene carbonate at 44°C.[368] $[AN]_0 = 5.25$ M, $[BPN]_0 = 5.53 \times 10^{-2}$ M, $[CuBr] = [bpy]_0/3 = 5.53 \times 10^{-3}$ M.[88]

561
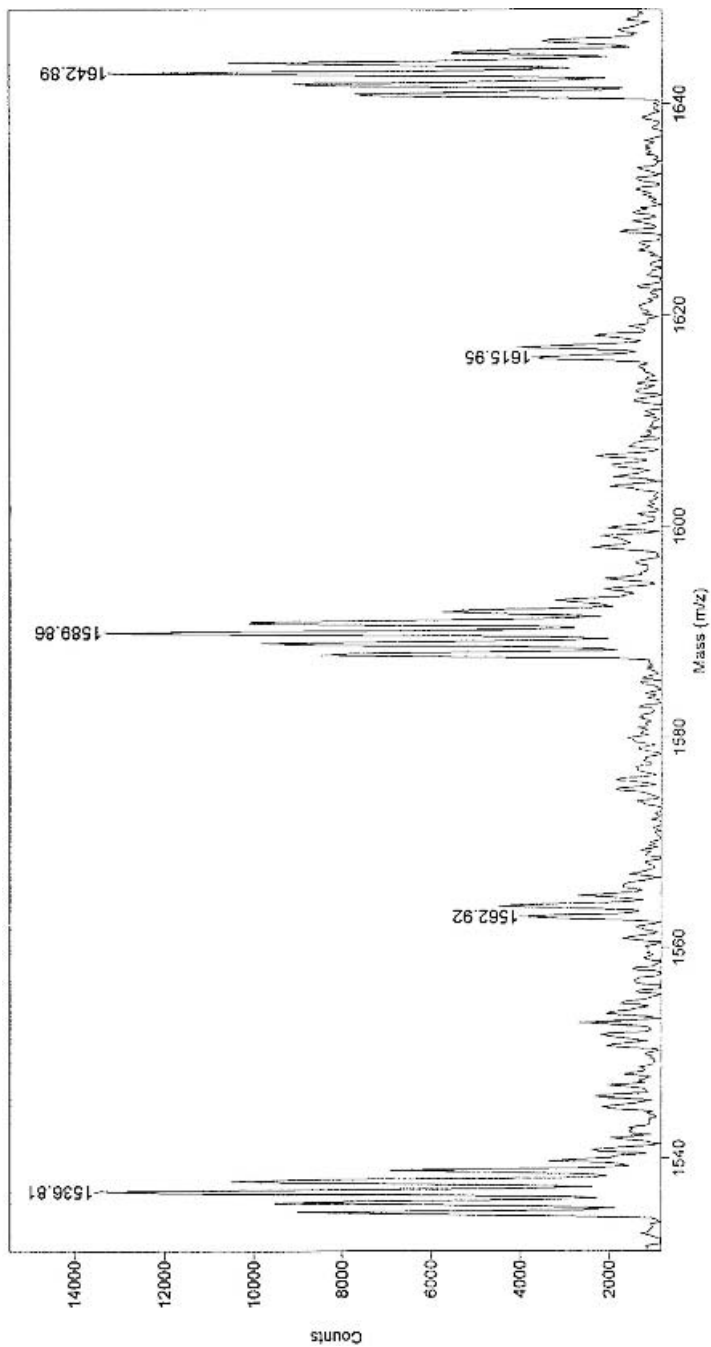
Figure 11.13 Expanded region of MALDI-TOF-MS of PAN prepared in ethylene carbonate at $44°C.^{368}$ $[AN]_0 = 5.25 M$, $[BPN]_0 = 5.53 \times 10^{-2} M$, $[CuBr] = [bpy]_0/3 = 5.53 \times 10^{-3} M$. Series A: $\{CH_3CH(CN)-[CH_2CH(CN)]_n-CH_2CH(CN)Br + Na\}^+$. Series B: $\{CH_3CH(CN)-[CH_2CH(CN)]_n-CH_2CH(CN)H + Na\}^+$.

Some catalysts may not only abstract halogen from dormant species but also form organometallic species similar to those in Co-mediated polymerization of acrylates.[164] There is some indication that this can also happen for acrylates with Cu(I) catalysts.[205] Such compounds may be considered as another type of dormant species and if they do not react directly with monomer via an insertion pathway, for instance. If they did, they should be considered as concomitant active centers. The likely outcome would be chemo-, regio-, and stereoselectivity different from those of the free-radical process. This has not been yet observed.

11.4.2 Active Species

Many indirect observations point to a free radical as the active center in ATRP. However, recently free radicals were detected by EPR in the ATRP of dimethacrylates forming a glassy network.[172] The difficulty of the EPR studies is due to the similarity of the g values of the paramagnetic transition metal complexes that are present at concentrations $>10^3$ times higher than the active growing species. Concentration of growing radicals can be deduced from the overall rate of polymerization and reported literature rate constants of propagation.[31] The concentration of radicals are in the range of 10^{-6} to 10^{-9} mol/L and can be adjusted by varying the amount and activity of the catalyst, initiator, and deactivator, as well as temperature.

The existence of free radicals has been proposed in copper-mediated ATRP on the basis of several experimental observations:[168]

1. The ATRP equilibrium has been approached from both sides: RX/M_t^n and radicals$/X–M_t^{n+1}$ species (reverse ATRP). Thus, successful polymerizations have been carried out using conventional free-radical initiators, such as AIBN and BPO, as well as using organic halides as initiators.[14,34]

2. Chemoselectivity is similar to that for conventional radical polymerizations. Typical radical inhibitors, such as galvinoxyl and TEMPO, inhibit the polymerization, and the polymerization is retarded by the presence of a small amount of oxygen. In addition, ATRP is converted into a system displaying conventional radical polymerization characteristics on the addition of octanethiol as a chain transfer reagent.[170] Chain transfer to polymer in the BA polymerization also resembles the conventional radical process.[206] ATRP can be carried out in the presence of water[36,41] or other protonogenic reagents, and is tolerant to a variety of functionalities.[97] Moreover, the reactivity ratios, which are very sensitive to the nature of the active centers, are nearly identical to those reported for the conventional radical polymerization but are very different from those for anionic, group transfer, and cationic systems.[91,92,169,207–209]

3. Regioselectivity and stereoselectivity are similar to and do not exceed that for a conventional radical polymerization. All the polymers formed by ATRP have regular head-to-tail structures, with the dormant species displaying the typical secondary/tertiary alkyl halide structures, as evidenced by NMR.[93,143] In addition, polymers have the same tacticity as those prepared by a conventional free-radical process.[13,14,93] A recent racemization study using optically active alkyl halides also supports the intermediacy of radicals.[210]

4. EPR studies have revealed the presence of X–Cu(II) species resulting from the persistent radical effect.[26,171,211] Additionally, the doubling of the molecular weight, or cross-linking in multifunctional initiator systems, as a result of radical–radical termination has been observed.[212]

5. Cross-exchange between different halogens and different polymerization systems (thermal and ATRP or nitroxide mediated and ATRP) demonstrates they have the same intermediates and supports the radical mechanism.[133] Thus, equimolar mixtures of initiators for the nitroxide-mediated polymerization and the ATRP lead to polystyrene with a unimodal molecular weight distribution (MWD).[213]

6. Direct EPR observation of propagating free radicals in ATRP of dimethacrylates catalyzed by CuBr/HMTETA.[172]

However, not all alleged ATRP processes may in reality proceed via free-radical processes since involvement of organometallic species and/or ionic intermediates is also possible. The contribution of these species will depend on monomer, catalyst, anion, temperature, solvent, and other parameters.

The reversible activation process in ATRP may alter some regio, stereo and chemoselectivity. In copolymerization, differences in activation/deactivation will effect relative concentration of active centers and overall rates. They should have minimal effects on relative rates of monomer consumption, especially, if comonomers tend to alternate. However, for reactivity ratios >1, and for much faster activation of the dormant center derived from one monomer, its faster incorporation into polymer chain is observed, especially at lower conversion. This may provide apparent reactivity ratios, different from those in the process without reversible activation. Therefore, the ''intermittent'' polymerization may also provide some isotope selectivity, accelerating cleavage of C^{12}–X versus C^{13}–X bonds, and also in stereoselectivity, e.g. accelerating activation of R—S versus R—R centers. This can lead to minor changes in kinetic isotope effects in comparison with RP and also in enantiomeric enhancement when chiral monomers are used in conjunction with chiral transition metal complexes.

11.4.3 Catalyst Structure

The determination of the active catalyst structure remains a challenging task. Even in the most thoroughly studied copper/bpy catalytic system, the exact structure of the activator and deactivator has not yet been completely elucidated. This may be due to large lability of the complexes and very easy oxidation of some activators. Preliminary UV–vis studies of the Cu(I) and Cu(II) species and electron paramagnetic resonance (EPR) studies of the Cu(II) species suggest the structure of the species in polymerization solutions are quite complex.[214] Ligands on both the Cu(I) and Cu(II) species are labile in solution and ^{1}H NMR studies indicate that there is fast exchange with the free ligand in solution on the Cu(I) coordinated by bpy.[28]

Literature data on the coordination chemistry of copper complexes in polar solvents, suggest the structures illustrated in Scheme 11.3 for the CuX/dNbpy complexes during the polymerization. In general, complexes of a one-to-one ratio
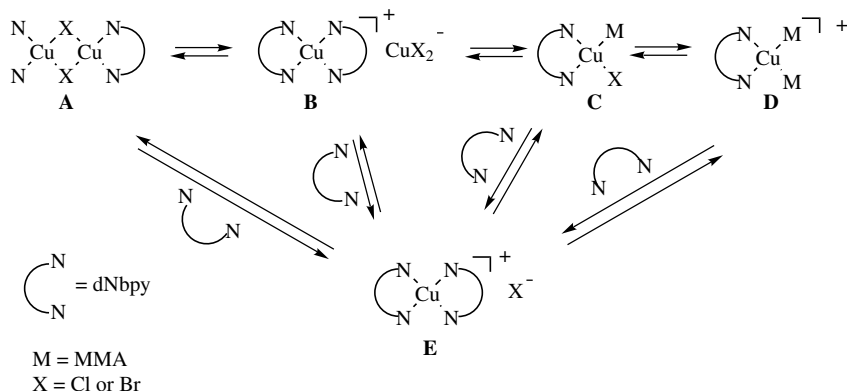
Scheme 11.3   Plausible catalyst structures of CuX/dNbpy complex.

of copper(I) halide to a bidentate ligand (e.g., bpy or phenanthroline) are either halogen-bridged dimers, LCu(μ-X)$_2$CuL (**A**), or copper(I) coordinated by two ligands with a dihalocuprate counteranion, (L$_2$Cu$^+$)CuX$_2^-$ (**B**).[215] In addition, Munakata *et al.* have suggested that the structures of CuX/bpy complexes in solution depend on the polarity of the solvent.[216] For example, in a polar solvent such as ethanol, the monomeric form L$_2$Cu$^+$X$^-$ (**E**) predominates while the bridged dimer LCu (μ-X)$_2$CuL (**A**) could exist in a less polar solvent such as acetone.

CuX$_2^-$ should not be the active catalyst during polymerization since ATRP using N(nBu)$_4^+$CuX2$^-$ is very slow and not controlled.[25] In addition, a series of polymerizations were carried out with various ratios of dNbpy to cuprous halide, and the maximum rate of polymerization for styrene and MA was obtained when the dNbpy to cuprous halide ratio was 2,[21,25] suggesting that L$_2$Cu$^+$X$^-$ (**E**) is the active form of the catalyst. On the other hand, for MMA polymerization, a dNbpy : cuprous halide ratio of 1 was sufficient to reach the maximum polymerization rate. However, when CuPF$_6$/dNbpy, which cannot form a bridged dimeric structure and cuprous anions, was used as the catalyst for the ATRP of MMA, the maximum rate of polymerization was observed with a dNbpy : copper(I) ratio of 2.[135] This implies that for CuPF$_6$/ 2dNbpy, L$_2$Cu$^+$X$^-$ (**E**) is the active form. LCu(μ-X)$_2$CuL (**A**) or Cu$^+$/2dNbpy/ CuX$_2^-$ L$_2$Cu$^+$CuX2$^-$ (**B**) may be the dominating (though not necessarily active, CuX$_2^-$ is inactive) species for the cuprous halide complex. One cannot rule out the possible coordination of one or two MMA molecules to the copper(I) species. However, more recently isolated **B** displays similar activity in styrene ATRP as the *in situ* formed CuBr(dNbpy)$_2$ catalyst.[217] The addition of 1 equiv. of ligand necessary to attain the maximum polymerization rate when using in situ catalyst formulations could be ascribed to solubility issues. Structure **B** may be the most probable structure present in nonpolar media, while structure **E** is more likely in a polar medium. The direct observation of structure **B** in styrene ATRP has been confirmed by extended X-ray absorption fine structure (EXAFS).[180,218] The equilibrium between structures **B** and **E** may strongly depend on the solvent polarity and its H-bonding
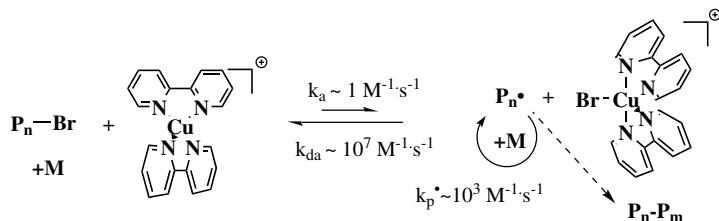
Scheme 11.4 Proposed structures for Cu(I) and Cu(II) species with bpy as the ligand.

ability. In less polar solvents, which cannot stabilize the X^- anions by hydrogen bonding, **B** and sometimes **A**, may dominate. In polar protic solvents, structure **E** is preferred.

Perhaps even more complex is the structure of the Cu(II) species. From the X-ray data and EXAFS, it appears that it should have a trigonal bipyramidal cationic structure $[X–Cu(II)(bpy)_2]^+$. However, in nonpolar media a neutral distorted square planar structure $X_2Cu(II)/bpy$ may be preferred over a pure Cu(II) species;[179] on the other hand, in the presence of Cu(I) it readily converts to $[X–Cu(II)(bpy)_2]^+$, which is accompanied by the $[X_2Cu(I)]^-$ anion. In very polar, or aqueous systems, the X–Cu(II) bond is quite labile and may be readily replaced by hydrating water molecules. Such a species will not deactivate ATRP and consequently the polymerization rate increases, as has already been experimentally observed.[83] Thus, based on the literature data and ATRP model studies,[149] it seems that the copper species complexed by bpy derivatives and actively involved in the ATRP can best be represented by a tetrahedral $Cu(I)(bpy)_2$ and a trigonal bipyramidal $XCu(II)(bpy)_2$ (Scheme 11.4).

The X-ray and EXAFS structures of the cupric halides/PMDETA complexes are shown in Fig. 11.14.[179,180,219] The longer copper(II)–Br bond compared to the copper(II)–Cl bond is proposed to be responsible for the faster exchange and lower polydispersities obtained in bromine ATRP systems.

There is more data on various bidentate, tridentate, and tetradentate copper complexes.[179,180,220] The direct observation of the dominating species in solution by EXAFS studies may help to better determine the structure of the activator and the deactivator in ATRP.[180] Nevertheless, additional spectroscopic (UV, NMR, IR, EPR,
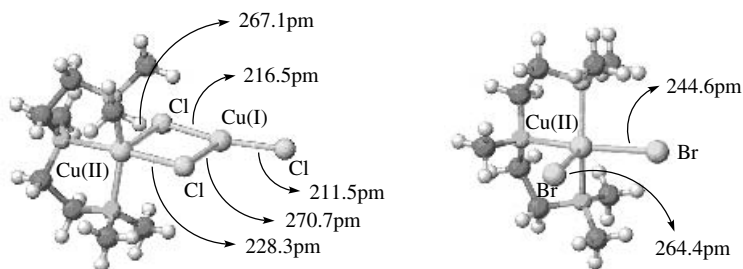
Figure 11.14 X-ray structure of the cuprous halide/PMDETA complexes.

MCD, etc.) and model kinetic studies are needed to fully understand the structures and activities of the various species that may change with temperature, solvent, and concentration.

11.4.4   Correlation of Structures with Reactivities

The basic theory of free radical polymerization correlates the structure of monomers and corresponding free radicals with the rate constants of propagation and cross-propagation. In general, more reactive monomers form less reactive free radicals. Although free radicals do not bear charge, they can be polarized and have electrophilic or nucleophilic character. Electrophilic radicals are usually more reactive than nucleophilic radicals.[221] There is a tendency for cross-propagation and electrophilic radicals prefer to react with monomers that form nucleophilic radicals and vice versa. Thus, in copolymerization of S and MMA, both reactivity ratios are smaller than unity. It is anticipated that all rules observed in the conventional free-radical polymerization (RP) apply to ATRP. This includes propagation, transfer, and termination steps and the selectivities associated with all of them. There might be a small caveat in some cases such as chain-length-dependent termination, additional side reactions with a ligand or complex but otherwise general picture remains essentially the same.

As mentioned above, the reversible activation process may have some effects on stereo- or chemoselectivity. Differences in activation rates for various dormant centers may magnify selectivities observed in the polymerization without activation/deactivation steps. Therefore, the main difference between ATRP and RP is
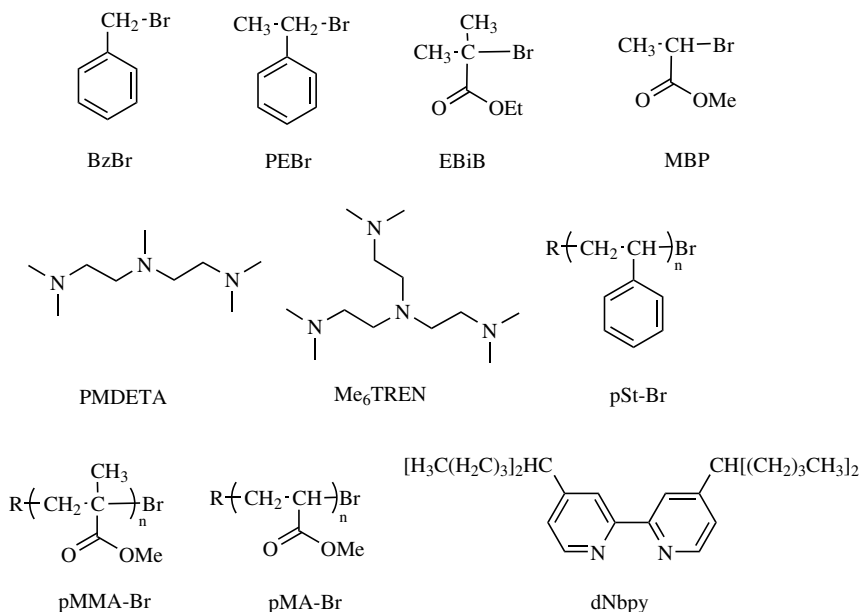
Figure 11.15 Ligands and model compounds mimicking polymeric chains used in kinetic studies.

$$R\text{-}Br \ + \ Cu^I/L^{\boxed{+}} \quad \xrightarrow{k_a} \quad R^\bullet \ + \ BrCu^{2}/L^{\boxed{+}} \qquad (1)$$

$$R^\bullet \ + \ Br\text{-}Cu^{2}/L^{\boxed{+}} \quad \dashrightarrow[k_{da}]{} \quad R\text{-}Br \ + \ Cu^I/L^{\boxed{+}} \qquad (2)$$

$$R^\bullet \ + \ T^\bullet \quad \xrightarrow{k_c} \quad R\text{-}T \qquad (3)$$

$$R\text{-}T \quad \dashrightarrow[k_{dis}]{} \quad R^\bullet \ + \ T^\bullet \qquad (4)$$

$$R^\bullet \ + \ R^\bullet \quad \dashrightarrow[k_t]{} \quad RR \qquad (5)$$
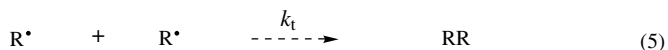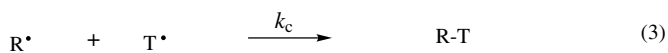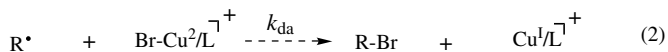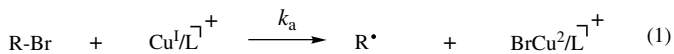
Scheme 11.5   Model reactions for the activation rate constant measurements.

the presence of atom transfer steps responsible for overall control of the process. Thus, it is extremely important to correlate rate constants of activation and deactivation with the structure of involved reagents. There have been some reports on determination of these rate constants for small-molecule models and macromolecular species.[148,222,223] The structures of the corresponding reagents are shown in Fig. 11.15.

The activation rate constants were measured using HPLC or GC under the kinetic isolation conditions achieved by trapping the generated radical with 2,2,6,6-tetramethylpiperidinyl-1-oxy (TEMPO) as shown in Scheme 11.5. The deactivation rate constants were determined by trapping 1-phenylethyl radicals using TEMPO in a competitive clock reaction (Scheme 11.6). The 1-phenylethyl radical was generated by the thermal decomposition of 1-(N,N-(2-methylpropyl-1)-(1-diethylphosphono-2,2-dimethyl-propyl-1-)-N-oxyl)-1-phenylethane (PESG1) alkoxyamine. Some values for the rate constants are shown in Tables 11.2 and 11.3.

The following conclusions can be drawn from the model studies. At 35°C, 2-bromoisobutyrate is approximately 10 times more reactive than the other alkyl halides. 1-Phenylethyl bromide is 10^3 times more reactive than the corresponding chloride. This difference dramatically decreases at higher temperatures because of the higher
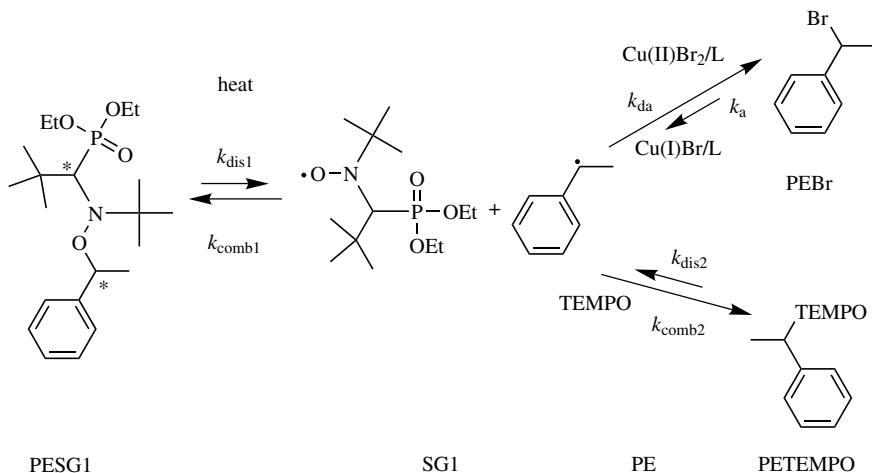
Scheme 11.6   Model reactions for the deactivation rate constant measurements.

TABLE 11.2   Activation Rate Constants Measured under Various Conditions at 35°C[222]

No.	RX	Complex	Solvent	$k_a[\text{M}^{-1}\text{s}^{-1}]$
1	PEBr	CuBr/2dNbpy	Acetonitrile	0.085
2	MBrP	CuBr/2dNbpy	Acetonitrile	0.052
3	EBriB	CuBr/2dNbpy	Acetonitrile	0.60
4	BzBr	CuBr/2dNbpy	Acetonitrile	0.043
5	PEBr	CuBr/PMDETA	Acetonitrile	0.12
6	MBrP	CuBr/PMDETA	Acetonitrile	0.11
7	EBriB	CuBr/PMDETA	Acetonitrile	1.7
8	PECl	CuCl/Me₆TREN	Acetonitrile	1.5
9	PEBr	CuBr/2dNbpy	Ethyl acetate	0.016
10	PECl	CuCl/2dNbpy	Acetonitrile	0.000056

activation energy for 1-phenylethyl chloride. PMDETA forms more reactive Cu(I) complexes than dNbpy and Me₆TREN is ~10^4 times more active than the dNbpy-based complex. The reaction is faster in acetonitrile than in ethyl acetate.[222]

In the deactivation process, the CuBr₂/dNbpy complex is more active in ethyl acetate than in acetonitrile. Deactivation is slower with CuCl₂ than with CuBr₂. The reactivity of the CuBr₂/dNbpy complex is higher than when either Me₆TREN or PMDETA is used as ligand. Among the studied ligands, Me₆TREN appears to be most attractive since it promotes very fast activation but also sufficiently fast deactivation.

A further systematic study was performed with the series of N-based tridentate complexes shown in Fig. 11.16 together with determining their reduction potentials.[224,225]

The rate constants of activation and deactivation for 1-phenylethyl bromide and the corresponding radical correlate well with the reduction potentials of the Cu(II) complexes. The good correlation between redox potentials and rate constants require nearly constant halogenophilicities of the Cu complexes which are all ligated by N-based ligands (cf. Scheme 11.8). The catalytic activity of the complexes decreases in the order: alkyl amine ≈ pyridine > alkyl imine ≫ aryl imine > aryl amine. The correlation between the activation and deactivation rate constants is approximately reciprocal, as shown in Fig. 11.17. Thus, results with Me₆TREN complex, which activates very fast but also rapidly deactivates, are quite unique, probably because of very small entropic constraints in the passage from the X–Cu(II) to the Cu(I) state.

TABLE 11.3   Deactivation Rate Constants Measured under Various Conditions at 75°C[222]

No.	Radical	Complex	Solvent	$k_{da} [\text{M}^{-1}\text{s}^{-1}]$
1	PE	Cu(II)Br₂/2dNbpy	Acetonitrile	2.5×10^7
2	PE	Cu(II)Br₂/PMDETA	Acetonitrile	6.1×10^6
3[c]	PE	Cu(II)Br₂/Me₆TREN	Acetonitrile	1.4×10^7
4	PE	Cu(II)Br₂/2dNbpy	Ethyl acetate	2.4×10^8
5	PE	Cu(II)Cl₂/2dNbpy	Acetonitrile	4.3×10^6

Figure 11.16 Reduction potentials of the series of CuBr$_2$ complexes in CH$_3$CN, 500 m V/s, 0.1 M [NBu$_4$][PF$_6$], E versus SSCE.[225]
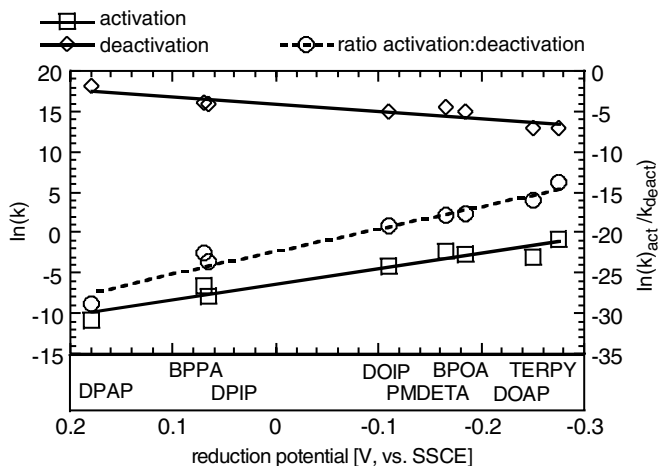
Figure 11.17 Dependence of the rate constants of activation for PEBr and deactivation for PE* as well as their ratio (k_a/k_{da}) on the reduction potential of the Cu(II) complexes. Rate constants of activation and deactivation were determined in acetonitrile at 35 and 75°C, respectively.[225]

Knowing the values of the rate constants of all the elementary reactions involved in ATRP enhances the mechanistic understanding of ATRP, facilitates the optimization of the reaction conditions for various monomers, and helps in selecting the proper initiator and catalyst structures. Without this knowledge, use of even efficient catalysts such as Me$_6$TREN-based complexes, may lead to poorly controlled ATRP processes (MMA case).[63]

11.4.5 Mechanism

The general mechanism of ATRP was shown in Schemes 11.1 and 11.4. A radical pathway has been proposed in all the ATRP systems reported so far.

ATRP is typically described as proceeding through the reversible transfer of halogen atoms between growing chains and transition metals via an inner-sphere electron transfer (ISET) process; however, as an alternative to the inner-sphere process, outer-sphere electron transfer (OSET)[101,226] may also occur. Scheme 11.7 illustrates several possible OSET processes that may occur in ATRP.

$$P_n\text{-X} + Cu(I) \rightleftharpoons P_n\text{-}\overset{\ominus}{X}^{\bullet} + Cu(II) \rightleftharpoons P_n^{\bullet} + \text{X-Cu(II)} \qquad \textbf{A}$$

$$P_n^{\bullet} + \text{X-Cu(I)} \rightleftharpoons P_n^{\ominus} + \text{X-Cu(II)} \qquad \textbf{B}$$

$$P_n^{\bullet} + \text{X-Cu(II)} \rightleftharpoons P_n^{\oplus} + \text{X-Cu(I)} \qquad \textbf{C}$$
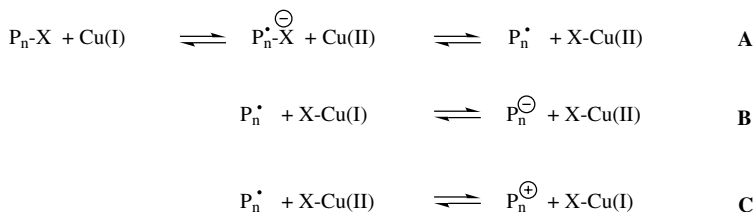
Scheme 11.7 Possible OSET processes in ATRP.

Path **A** involves the formation of intermediate radical anions followed by the halogen anion transfer to the oxidized metal. This would result in a two-step process rather than a concerted inner-sphere process for the generation of radicals from initiators or dormant polymer species. Preliminary correlation between rates of atom transfer reactions and R—X bond energies and electron affinities suggest the predominant concerted process for many initiating and propagating species. Thus, for adducts with the same radical-stabilizing substituent, tertiary alkyl halides are typically better initiators than secondary ones, which are better than primary alkyl halides. However, the unexpectedly high rates, even at low temperatures, found for some alkyl halides (e.g., haloacetonitrile) could indicate an outer-sphere electron transfer process. This may happen with initiators having very high electron affinities (e.g., diethyl 2-bromomalonate or CCl_4) and may sometimes lead to side reactions that reduce the initiation efficiency. In contrast, the formation of radical anions by the outer-sphere electron transfer process from Cu(I) to 1-phenylethyl bromide and other similar dormant species is less probable, due to unfavorable redox potentials.

Scheme 11.8 represents overall atom transfer equilibrium as a set of two redox processes, bond dissociation energy of alkyl halide, and heterolytic cleavage of halogen–metal bond in the deactivator. The latter parameter is a measure of the halogen-ophilicity of the transition metal complex. Thus, it is possible to observe similar values of atom transfer equilibrium, even if the transition metal complex is not very reducing but has high halogenophilicity (e.g., Ru complexes have redox potentials only $\sim +300$ mV vs. ~ -100 mV for Cu complexes, but may have similar ATRP activities).[159,225,227] Unfortunately, these data are not readily available in literature.

Figure 11.18 illustrates the interrelations between the electrochemical potentials of the copper complexes and the organic radicals as well as the propagating radicals in styrene and acrylate polymerizations. Depending on the redox properties of both

Atom Transfer (Overall Equilibrium)

$$R\text{-}X \ + \ M_t^n\text{-}Y\,/\,\text{Ligand} \ \underset{k_d}{\overset{k_a}{\rightleftharpoons}} \ R\bullet \ + \ X\text{-}M_t^{n+1}\text{-}Y\,/\,\text{Ligand}$$
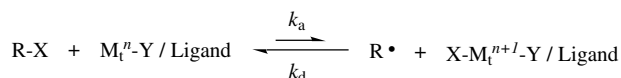
Contributing Reactions

$$M_t^n\text{-}Y\,/\,\text{Ligand} \ \rightleftharpoons \ M_t^{n+1}\text{-}Y\,/\,\text{Ligand} \ + \ e^\ominus$$

$$X\bullet \ + \ e^\ominus \ \rightleftharpoons \ X^\ominus$$

$$R\text{-}X \ \rightleftharpoons \ R\bullet \ + \ X\bullet$$

$$X^\ominus + \ M_t^{n+1}\text{-}Y\,/\,\text{Ligand} \ \rightleftharpoons \ X\text{-}M_t^{n+1}\text{-}Y\,/\,\text{Ligand}$$
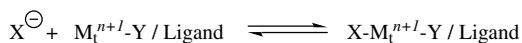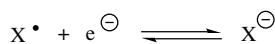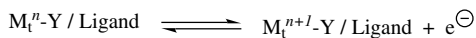
Scheme 11.8   Representation of atom transfer equilibrium as a set of two redox processes, homolytic dissociation of alkyl halide and heterolytic cleavage of $Cu^{(II)}$—X bond (i.e., halogenophilicity).
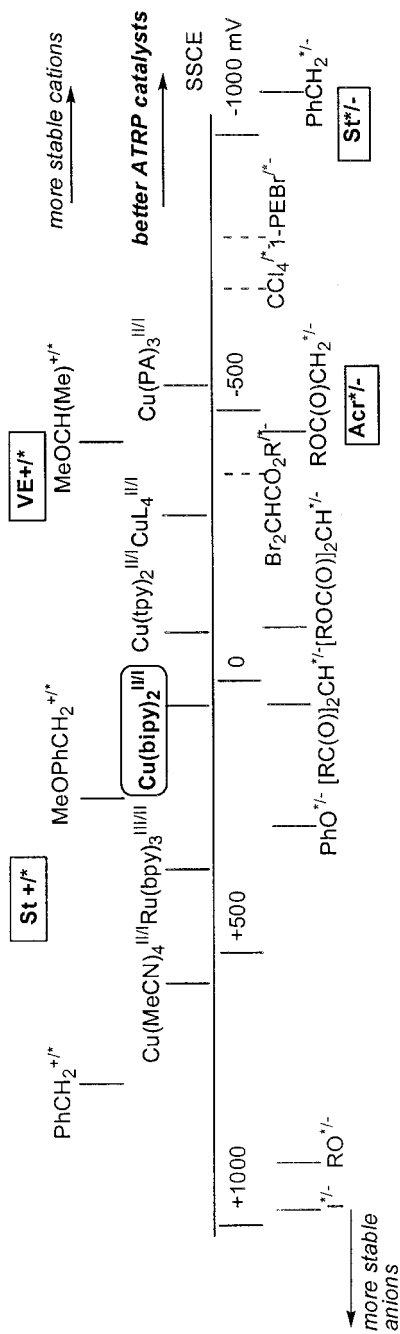
Figure 11.18 Summary of electrochemical potentials of copper complexes and organic radicals.[168]

573

the transition metal complex and the corresponding organic radicals, reduction of the growing radicals to carbanions (Scheme 11.7, path **B**) or oxidation to carbocations (Scheme 11.7, path **C**) may occur under certain conditions, and can sometimes become the dominant pathway. For example, the ATRP of p-methoxystyrene using Cu(I)/(dNbpy)$_2$ was unsuccessful.[102] Oxidation of the p-methoxystyryl radical to a cation (Scheme 11.7, path **C**) was postulated, yielding cationic intermediates responsible for an elimination process. Similarly, the presence of a large amount of cupric triflate in the polymerization of styrene reduces the molecular weight and terminates the reaction, presumably through oxidation of the growing radicals via an outer-sphere electron transfer process.[205] The observed slow termination reaction in the ATRP of styrene was attributed to the same process.[100] In addition, cationic polymerization may occur when using CuPF$_6$(CH$_3$CN)$_4$ complexes for styrene polymerizations,[228] this can be ascribed to the much stronger oxidation (and weaker reducing) power of this complex in comparison with the Cu(I)/(bpy)$_2$ complex.[229]

As shown in Fig. 11.18, the more reducing catalysts are also more active in ATRP. The activity of the catalysts in ATRP depends not only on the redox potential but also on the halogenophilicity of the transition metal complexes. Both parameters are affected by the nature of the transition metal and ligand, including the complexation constants, the nucleophilicity, back-bonding, and steric effects. Within a series of nitrogen-based ligands used in the Cu-based ATRP of methyl acrylate, a linear correlation between the polymerization rate (expressed by the apparent equilibrium constant, namely, $K_{eq}^{app} = K_{eq}/[Cu(II)]$), and the redox potential of the complex in acetonitrile was found, confirming similar halogenophilicities of Cu complexes with bpy, PMDETA, Me$_6$TREN, and other ligands.[227]

Some radicals may react reversibly with metal centers, forming organometallic species, as reported previously.[164,230] This could happen with either the Cu(I) or the Cu(II) species, especially in the absence of a ligand.[231] It seems that these reactions are not very important in styrene polymerization, since the rates of the conventional radical polymerization, initiated by azo compounds or peroxides, are not strongly affected by the addition of Cu(I)/(dNbpy)$_2$ or Cu(OTf)$_2$(dNbpy)$_2$.[205] Cupric triflate was used in these experiments instead of cupric bromide, because the latter acts as an efficient inhibitor and results in reverse ATRP. For MA, the addition of cupric salts has no effect on the rates or molecular weights when using conventional initiators. However, the reaction rates decrease in the presence of CuBr(dNbpy)$_2$ and CuOTf(dNbpy)$_2$. This observation can be explained either by the formation of organometallic R–Cu(II) species, providing an additional pathway of control and supplementing the atom transfer process, or by the reversible reduction of growing radicals to the enolate anions, as discussed previously. The contribution of these reactions is, however, relatively small, since the polymerization of 2-hydroxyethyl acrylate is well controlled, in either bulk or aqueous solution.[44] The selectivity of atom transfer over formation of organometallic species also depends on the spin state of some transition metals. Low spin species should favor atom transfer and M$_t$–X bonding, whereas high-spin species favor the formation of M$_t$–C bond and organometallic species.

Initiation

$$R\text{-}X \;+\; M_t^n\text{-}Y\,/\,Ligand \quad \underset{k_{da}^o}{\overset{k_a^o}{\rightleftarrows}} \quad R \;+\; X\text{-}M_t^{n+1}\text{-}Y\,/\,Ligand$$

$$R \;+\; M \quad \xrightarrow{k_i} \quad P_1$$

Propagation

$$P_n\text{-}X \;+\; M_t^n\text{-}Y\,/\,Ligand \quad \underset{k_{da}}{\overset{k_a}{\rightleftarrows}} \quad P_n \;+\; X\text{-}M_t^{n+1}\text{-}Y\,/\,Ligand$$

$$P_n \;+\; M \quad \xrightarrow{k_p} \quad P_{n+1}$$

Termination

$$P_n \;+\; P_m \quad \xrightarrow{k_t} \quad P_{n+m} \quad or \quad P_n^= + P_m^H$$
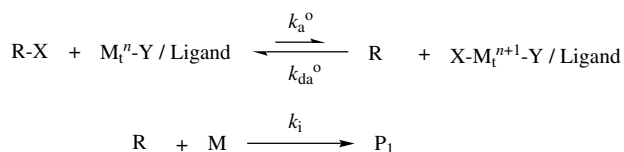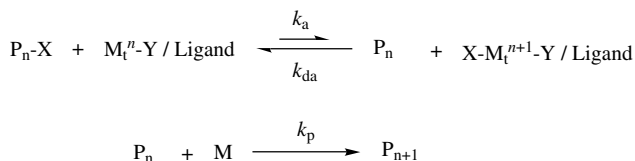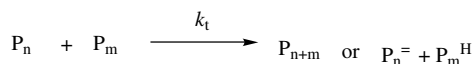
Scheme 11.9   Elementary reaction in ATRP.

11.4.6   Elementary Reactions

Similar to RP, the elementary reactions in ATRP consist of initiation, propagation, transfer, and termination (Scheme 11.9). However, successful ATRP behaves quite differently from RP. Initiation in ATRP must be fast and complete at low monomer conversion. Termination should be suppressed and should generally involve less than 10% of all chains. Polymerization rate and concentration of the propagating radicals is established by an equilibrium between activation and deactivation steps and *not* via a steady state as in RP in which rates of initiation and termination are essentially equal. In most cases transfer may be neglected because polymers with relatively low molecular weights are targeted.

For a well-controlled ATRP, initiation should be fast and quantitative. The value of the apparent initiation rate constant ($k_i^{app} = k_i K_0$, where k_i and K_0 refer to the absolute rate constant of addition of the initiating radical to the alkene and the atom transfer equilibrium constant for the initiating species, respectively) should be at least comparable to that of the apparent propagation rate constant ($k_p^{app} = k_p K_{eq}$, where k_p and K_{eq} refer to the absolute rate constant of propagation and the atom transfer equilibrium constant for the propagating species, respectively). If $k_i^{app} \ll k_p^{app}$, polymers with molecular weights higher than the theoretical values and higher polydispersities will be obtained. This behavior is based on the assumption that the system is equilibrated or there was deactivator added initially. The situation is more complex when the amount of the deactivator is small, and the rate-determining step in initiation is activation. If initiation is too fast and too many radicals are generated

during the initiation step, irreversible radical termination will reduce the initiator efficiency and slow down the polymerization. A general guideline for choosing a suitable ATRP initiator is that the initiator should have a chemical structure similar to that of the dormant polymer species.

These rules also apply to any cross-propagation step. We refer to reactivities of monomer in ATRP in terms of k_p^{app}, which does not scale with the true k_p values. Efficient cross-propagation requires $k_c^{app} > k_p^{app}$, or halogen exchange to be employed.

Polymer chains propagate by adding new monomer units to the growing chain ends. To obtain well-defined polymers with low polydispersities, it is crucial to rapidly deactivate the growing chains to form dormant species. Termination occurs through combination or disproportionation pathways and is most significant at the beginning of the polymerization. After a sufficient amount of the higher oxidation state metal complex has been built up by irreversible termination reactions, the persistent radical effect predominates and radical termination is minimized.[18,19] It has been proposed that termination rate coefficients are chain length dependent and decrease during the polymerization to result in a steady rate of polymerization.[20] This helps form well-defined polymers at higher conversions. However, as the monomer concentration becomes very low, propagation slows down but termination and other side reactions may still occur with the usual rate. Therefore, there is a certain window of concentrations and conversions where the polymerization is well controlled.

In ATRP there are the possibility of additional side reactions, not present in RP. They include loss of activity by OSET, heterolytic cleavage of R—X bond, loss of HX at elevated temperatures in polar solvents, nucleophilic displacement of X by basic solvents and additives (or monomers), and supplementary transfer with ligands and complexes. Proper choice of reaction conditions and understanding of the physical organic chemistry associated with those side reactions may diminish their contribution.

ATRP is a complex process based on several elementary reactions, and success depends on controlling all of them as well as on controlling the concentrations and reactivities of the involved species. The rate constants of radical propagation are systematically being evaluated by pulsed laser polymerization techniques.[31] The rate constants of termination are less accessible, as they depend on the chain length and the viscosity of the medium.[31] As discussed before, in ATRP perhaps most important are the rate constants for the activation and deactivation steps. They depend on the structure of monomer (i.e., the radical and the dormant species), on the halogen, and, obviously, on the transition metal complexes. The values of the rate constants of some of these reactions have been reported for the polymeric species and for some of the model systems, which mimic the structure of the dormant/active species.[148,149,222,223]

11.5 ATRP-BASED MATERIALS

Although the discovery of atom transfer radical polymerization (ATRP) is relatively recent, the number of contributions directed at preparation of materials synthesized at least in part using this technique is already quite large.[1] The discussion in this

chapter is not comprehensive, since many materials prepared by ATRP are covered in Chapter 14. In this section only a brief summary of the synthetic power of ATRP is presented and is illustrated by examples separated into broad categories based on polymer composition, topology, and functionality as well as a variety of molecular composites, which are schematically represented as follows:
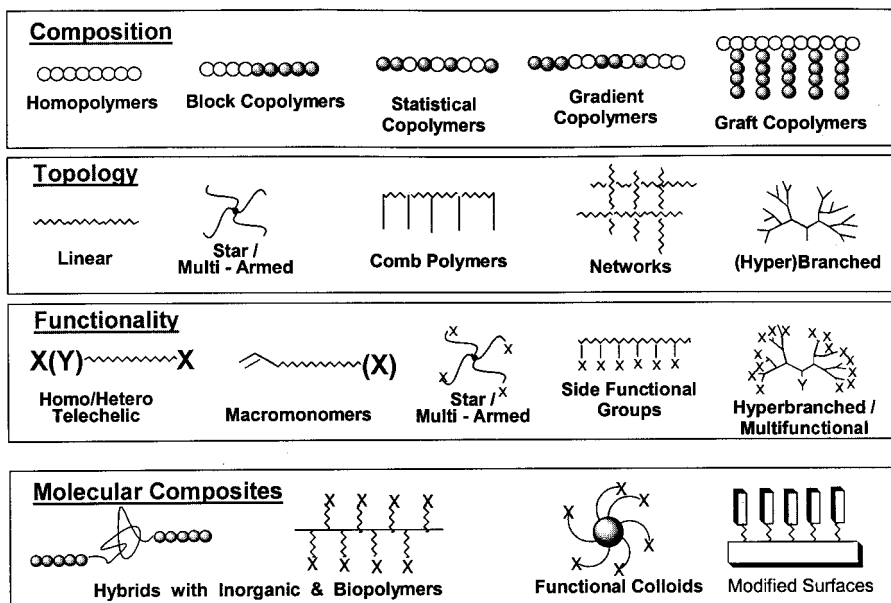
11.5.1 Functionality

Functionality can refer to many different aspects of a material when describing a polymer. Those components germane to ATRP include functional monomers, initiator fragments and polymer termini are shown in Scheme 11.10.[232]

11.5.1.1 Functional Monomers   A number of ring substituted styrenes (see Fig. 11.4) was examined to determine the correlation between the monomer structure and the polymerization rate.[102] Cu-based ATRP was well controlled for all of them except *p*-methoxystyrene. The latter produced oligomers with a structure suggesting involvement of a cationic process. Vinyl benzoic acid, in its sodium salt form, was also successfully polymerized in aqueous media.[86] 4-Vinylpyridine (VP) is structurally similar to styrene, and poly(4-vinylpyridine) can be used as polymeric multidentate ligands for the coordination of transition metals, in water purification, and in emulsification processes. VP has been successfully polymerized by ATRP using alkyl halides and CuCl/Me$_6$TREN. Other ligands were less successful. Poor control and loss of end group functionality was observed for ATRP with bromine end groups.[117]

ATRP of a number of functional (meth)acrylates have been studied. They include unprotected 2-hydroxyethyl (meth)acrylate as well as TMS-protected monomers

Scheme 11.10 Possible routes to functionalized polymers by ATRP.

and the water soluble acrylic monomer, 2-(dimethylamino)ethyl methacrylate (DMAEMA).[78] The polymerization of oligo(ethylene oxide) methacrylate by ATRP has been reported. When the reaction was conducted in aqueous media, fast and well-controlled polymerizations were obtained at ambient temperature using water-soluble initiators.[45] Methacrylic acid was polymerized in its sodium salt form at pH 8, although the reaction rate is slow even at 90°C (only 70–80% conversion is achieved after 21 h).[82] In contrast, the ATRP of sodium 4-vinylbenzoate was rapid at 20°C, with 95% yield obtained within 25 min.[86,233] Polydispersities were around 1.30 in both cases, as determined by aqueous SEC (size exclusion chromatography) studies. Several protected (meth)acrylic acids derivatives were used, for example, *tert*-butyl acrylate (tBA).[109] Derivatives with polymerizable groups were also successfully (co)polymerized by ATRP: glycidyl acrylate,[108,111] allyl,[111] and vinyl acrylate.[111]

Monomers with more specialized functionality have been polymerized such as monomers with mesogenic functionality: 11-(4′-cyanophenyl-4″-phenoxy)undecyl acrylate[234] 4-methoxyphenyl 4-{[6-(1-oxo-2-propenyloxy)-hexyl]oxy} benzoate,[235] with biologically active groups such as 5′-methacryloyluridine and 5′-methacryloyladenosine as well as sugar containing groups 3-O-methacryloyl-1,2:5,6-di-O-isopropylidene-D-glucofuranose and 2-(2′,3′,4′,6′-tetra-O-acetyl-β-D-glucopyranosyloxy) ethyl acrylate have been successful, and this has also led to the formation of the corresponding block copolymers.[236,237]

Macromonomers are polymer chains, which contain a double bond (or other polymerizable group) at one chain end that can be (co)polymerized in a separate reaction to yield graft copolymers (see Scheme 11.11). Macromonomers have been both made and copolymerized by ATRP. For example, vinyl chloroacetate was used as an initiator for the ATRP of styrene.[238] Macromonomers of molecular weights $M_n = 5,000$, 10,000, and 15,000 were synthesized with $M_w/M_n = 1.2$. No polymerization of the vinyl acetate segment was observed during the polymerization, due to the inability of that moiety to copolymerize with styrene. The macromonomers were subsequently copolymerized with N-vinylpyrrolidinone for the synthesis of hydrogels.[238] Allyl bromide and chloride were used as initiators for the ATRP of styrene using the heterogeneous copper–bipyridine complex where the halogen on the metal complex matched that on the initiator.[239] With both initiators, good agreement between the theoretical and measured molecular weights was observed. The polydispersity for the bromine system ($M_w/M_n = 1.2$) was lower than in the case of chlorine ($M_w/M_n = 1.3$), consistent with results using initiators such as benzyl bromide or chloride under similar reaction conditions.[93] Similarly, allyl end-functionalized macromonomers of DMAEMA have been prepared using either allyl 2-bromoisobutyrate or allyl trichloroacetamide.[240] Also, pyrrole containing macromonomers were prepared using 2-pyrrolethyl 2-bromoisobutyrate and several vinyl monomers in the presence of CuBr/bpy and $NiBr_2/PPh_3$.[241]

On the other hand, ATRP has been used for homopolymerization of macromonomers prepared by cationic polymerization.[242] In that study, the polymerization of methacrylate terminal poly(isobutylvinyl ether) yielded a densely grafted brush copolymer. The copolymerization of MMA-terminated polyMMA with BA by
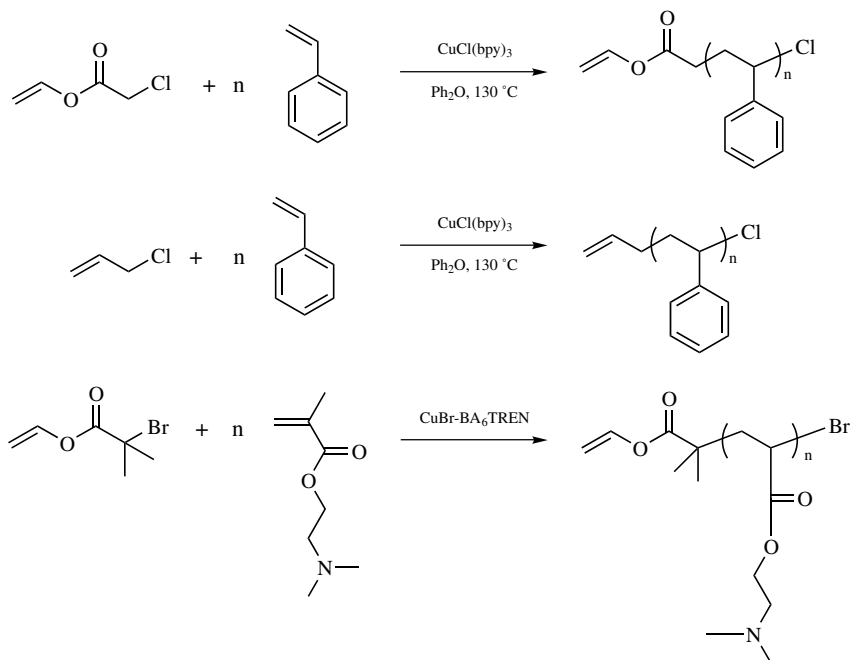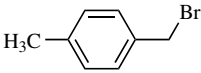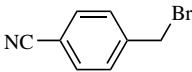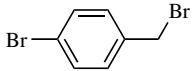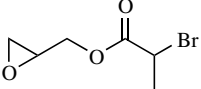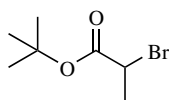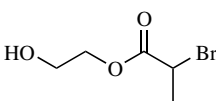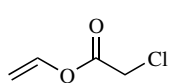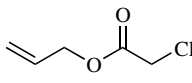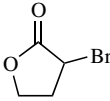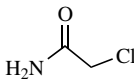
Scheme 11.11 Synthesis of macromonomers by ATRP.

ATRP lead to well defined grafts with a more uniform distribution of grafts than attainable in either a conventional radical process or an anionic polymerization.[243,244] Similar results were obtained using poly(dimethylsiloxane) macromonomers with methacrylate functionality in copolymerization with MMA.[245]

11.5.1.2 Functional Initiators   In ATRP, initiation is most often accomplished through homolytic cleavage of activated halogen-containing compounds followed by addition of the generated radical to an alkene. The radical stabilizing group should reside on the α-C atom (aryl, carbonyl, nitrile, multiple halogens) or involve weak bonding with a heteroatom (S, N, O). Direct bonding of the halogen to an aryl, vinyl, or carbonyl group does not facilitate radical generation; therefore, vinyl and acyl halides or haloarenes are poor ATRP initiators; for instance, ATRP can be carried out in chlorobenzene. The nontransferable fragment that forms the α end of the polymer chain can contain a number of functional groups tolerant to ATRP catalysts and radicals. It is also possible to incorporate several initiating sites within one molecule and initiate growth of the chain in several directions.
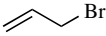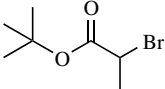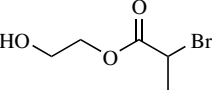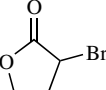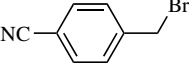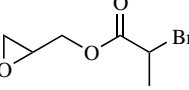
11.5.1.2.1 Activated Alkyl Halides   A number of functional initiators have been successfully used for the ATRP of styrene and methyl acrylate.[97,119] Results are collected in Tables 11.4 and 11.5. ATRP of MA was faster due to higher concentration of initiator and catalyst.

TABLE 11.4   ATRP of Styrene from Various Functionalized Initiators [a,97]

Initiator Structure	Initiator Name	$M_{n,\text{Cal}}$	$M_{n,\text{SEC}}$	M_w/M_n
	4-Methylbenzyl bromide	5110	4400	1.17
	4-Cyanobenzyl bromide	4760	5500	1.10
	4-Bromobenzyl bromide	4750	4500	1.16
	2-Bromopropionitrile	4800	5100	1.09
	Bromoacetonitrile	4750	4500	1.10
	Glycidol 2-bromopropionate	6190	6800	1.12
	tert-Butyl 2-bromopropionate	4110	4000	1.17
	Hydroxyethyl 2-bromopropionate	4810	7500	1.10
	Vinyl chloroacetate	9400	5800	1.12
	Allyl chloroacetate	1430	2600	1.77
	α-Bromo-γ-butyrolactone	4050	4000	1.17
	2-Chloroacetamide	1200	4000	1.51

[a] *Parameters*: 110°C; bulk, [styrene]$_0$/[RX]$_0$ = 96; [RX]$_0$/[CuBr]$_0$/[dNbpy]$_0$ = 1/1/2; time = 3.0 h.

TABLE 11.5   ATRP of Methyl Acrylate from Various Functionalized Initiators [a,97]

Initiator Structure	Initiator Name	$M_{n,\text{Cal}}$	$M_{n,\text{SEC}}$	M_w/M_n
	Allyl bromide	4430	6200	1.34
	tert-Butyl 2-bromopropionate	4650	4700	1.22
	Hydroxyethyl 2-bromopropionate	4850	6800	1.30
	α-Bromo-γ-butyrolactone	4165	4800	1.13
	4-Cyanobenzyl bromide	3720	4100	1.13
	Glycidol 2-bromopropionate	3710	4000	1.23
	2-Bromopropionitrile	3280	3500	1.10

[a] *Parameters*: 110°C; bulk, $[\text{MA}]_0/[\text{RX}]_0 = 58$; $[\text{RX}]_0/[\text{CuBr}]_0/[\text{dNbpy}]_0 = 1/0.3/0.6$; time $= 1.7$ h.

For successful initiation, the product of the apparent equilibrium constant and the rate constant of the addition to monomer in the initiation step should be similar to or larger than that for the propagation step. Thus 1-phenylethyl and 2-haloderivatives are good for styrene and acrylates but for methacrylates, 2-haloisobutyrates are necessary, unless halogen exchange is employed. For the MMA polymerization, 2-hydroxyethyl 2′-bromoisobutyrate was an efficient initiator.[138] MALDI-TOF-MS of a low-molecular-weight PMMA sample exclusively showed a series of peaks corresponding to PMMA oligomers containing the hydroxyl initiating fragment. Similar results were reported for a poly(methyl acrylate) sample.[246]

Functionalities in the initiator should not interfere with ATRP (i.e., should be inert toward both the catalyst and the alkyl halide). Thus, polymerizations with initiators or monomers containing carboxylic acids are more difficult because the acid functionality can poison the catalyst.[3,81,247] However, ATRP of MMA using 2-bromoisobutyric acid as initiator has been demonstrated.[196] The results indicated

a linear growth of the molecular weights with conversion, but at levels higher than those predicted by the ratio of the concentrations of monomer to initiator. The lower initiation efficiency of carboxylic acid functionalized initiators was later confirmed in the $NiBr_2(PPh_3)_2$-mediated polymerization of MMA[69] and the CuBr(PMDETA)-mediated polymerization of styrene.[139]

A number of initiators with protected carboxylic acid moieties have also been studied.[139] Hydrolysis of the protecting groups could liberate the free terminal carboxylic acid functionalities. Although the initiator efficiency was low (0.6) with trimethylsilyl as the protecting group, the initiator efficiency increased using *t*-butyl and *t*-butyldimethylsilyl groups. When carboxylic acid initiators with remote halogens such as 4-(1-bromoethyl)benzoic acid were used, well-defined polystyrene with initiator efficiencies close to 0.7 were prepared.[139] Initiators with anhydride and oxazoline functionalities have been utilized in the ATRP of styrene.[248]

Other functionalities have also been incorporated into the ATRP initiators. Through use of a thiophene-containing initiator, thiophene end-capped PMMA was prepared by ATRP.[241] The resulting polymer was subjected to electrolysis in the presence of pyrrole to result in electrically conducting graft copolymers. More recently, uridine and adenosine functionalized initiators were used to prepare polystyrene and PMMA with potential applications in the biorecognition field.[249] The same group synthesized a number of carbohydrate-based initiators that were used to prepare star polymers with a carbohydrate core, glucose end-functionalized polymer chains, and span-functionalized amphiphilic polymers efficiently.[250]

11.5.1.2.2 Activated Sulfonyl Halides   Another class of initiators for ATRP are sulfonyl halides.[53,94] Various substituted aromatic and aliphatic sulfonyl chlorides have been examined as initiators for the ATRP of styrene, MMA, and *n*-butyl methacrylate (BMA) with the heterogeneous $CuCl(bpy)_3$ system.[144] The initiators listed in Table 11.6 provided linear first-order kinetic plots with molecular weights that increased linearly with monomer conversion. Initiation, and, therefore, incorporation of the functionalities, appears to be efficient and nearly quantitative, resulting in polymers with a variety of novel moieties located at one chain end. The aryl sulfonyl chlorides can be considered as a "universal class of ATRP initiators"[53] because of their relatively high rates of initiation over propagation. They are excellent initiators for MMA and other methacrylates.[65] However, polymerization of acrylates is slow and may result in higher than predicted molecular weights and higher polydispersities.[53] Similarly, polydispersities for styrene are higher than with 1-phenylethyl halides and were generally greater than 1.3.[144] Mono-, di-, and multifunctional sulfonyl halides initiators have also been used, leading to star polymers.[145]

11.5.1.2.3 Macroinitiators   When a polymer chain contains an end group with an activated halogen atom, it can be used as ATRP initiator, or rather as a macroinitiator. Macroinitiators have been prepared via different methods, including cationic, anionic, coordination, conventional radical, and even polycondensation processes.[251] They will be discussed in detail together with mechanistic transformations.

TABLE 11.6 Experimental Rate Constants of Propagation (k_p^{exp}) and Concentration of Propagating Radicals ([P$^\bullet$]) for CuCl/bpy-Catalyzed Radical Polymerization of S (5.9 M), MMA (6.22 M), and BMA (4.9 M) Initiated with Substituted Arenesulfonyl Chlorides ^{a,144} (see Fig. 11.9 for Initiator Structures)

M	I	M_w/M_n (% Conversion)	T (°C)	k_p^{exp} ($10^{-4}s^{-1}$)	[P$^\bullet$] ($10^{-7}M$)^b
S	CABSC	1.38 (96)	130	0.50	0.19
S	DCHBSC	1.40 (85)	130	0.53	0.20
S	HBSC	1.53 (90)	130	0.36	0.14
S	MBSC	1.25 (93)	130	0.39	0.15
S	MSC	1.49 (89)	130	0.59	0.23
MMA	CABSC	1.22 (88)	90	1.83	1.13
MMA	DCHBSC	1.19 (76)	90	0.92	0.57
MMA	HBSC	1.27 (89)	90	1.50	0.93
MMA	TCMSC	1.21 (91)	90	1.50	0.93
MMA	DCBSC	1.14 (96)	90	1.58	0.98
MMA	1-NASC	1.19 (97)	90	2.44	1.51
MMA	2-NASC	1.22 (97)	90	2.97	1.84
MMA	MBSC	1.18 (94)	90	2.44	1.51
MMA	DMBSC	1.20 (92)	90	1.81	1.12
MMA	ADZBSC	1.25 (93)	90	2.08	1.29
MMA	DAC	1.60 (93)	90	0.54	0.33
MMA	MSC	1.35 (89)	90	2.87	1.76
BMA	CABSC	1.26 (92)	120	3.42	1.09
BMA	MBSC	1.24 (98)	120	3.42	1.09
BMA	MSC	1.27 (94)	120	7.50	2.40

^{a} [M]/[I]/[CuCl]/[bpy] = 200/1/1/3 molar ratio.
^{b} [P$^\bullet$] = k_p^{exp}/k_p^{rad}. For S: k_p^{rad} = 2609 L mol^{-1} s^{-1}; for MMA: k_p^{rad} =1616 L mol^{-1} s^{-1}; for BMA: k_p^{rad} = 3127 L mol^{-1} s^{-1}; recalculated using data from Ref. 374.

ATRP initiators and macroinitiators have also been immobilized on surfaces leading to a uniform growth of the chains from both flat and spherical surfaces.[252–255]

11.5.1.3 *Chain-End Functionality*   One of the criteria for the "livingness" of polymers synthesized by ATRP is the preservation of end groups throughout the polymerization. ^{1}H NMR and MALDI have been used to verify the presence of the carbon–halogen bond[77,88,90,93,94] in polymers prepared by ATRP, since essentially every chain contains a halogen atom at its head group, if termination and transfer are absent. This halogen atom can be replaced through a variety of reactions leading to end-functional polymers. Because of the increasing concern over the presence of halogens in the environment, the first consideration may be removal of those species from the chain ends after the polymerization is completed. A common method of dehalogenation of organic compounds, reaction with trialkyltin hydrides,[256] was applied to polymers prepared by ATRP.[257] Replacing tributyltin hydride in this reaction with allyl tri-*n*-butylstannane produced polymers with allyl end groups.[258]

The terminal halogen have been displaced by nucleophilic substitution, free-radical chemistry, and electrophilic addition catalyzed by Lewis acids.[259,260] Nucleophilic substitution with trimethylsilyl azide yielded the azide terminal polymer. This was followed by a reduction with lithium aluminum hydride to afford the primary amino functionalized chain end. Transformation was verified by ^{1}H NMR and as a final confirmation that the transformation had taken place, the α,ω-diamino-terminal polystyrene ($M_n = 5,100$, $M_w/M_n = 1.2$) was reacted with terephthaloyl chloride in a step-growth polymerization. This resulted in a polystyrene with several amido linkages with $M_n = 23,000$, $M_w/M_n = 2.5$.[260]

This method of end group transformation was expanded to include halo-terminated acrylates.[261] The nucleophilic displacement was carried out with NaN$_3$ in a DMF solution. Since reduction with LiAlH$_4$ cannot be performed on acrylates, conversion to phosphoranimines and subsequent hydrolysis was used to produce the amines.[261] Halogen atom displacement reactions with hyperbranched polystyrene and polyacrylate have also been reported.[119,262] On heating or UV irradiation, the hyperbranched polyacrylate with azide groups crosslinked.[119] Other examples of end-group transformation include reaction with potassium phthalimide, Gabriel synthesis, and reaction with sodium ethyl sulfide or potassium acetate under phase transfer catalysis conditions.[262] These reactions sometimes had limited yields and may be accompanied by elimination reactions. Elimination was also reported in an attempted alcoholysis reaction but better results were obtained by using functional initiators.[248] Reactions with amines and phosphines can also be accompanied by an elimination process, especially at higher temperatures and with more bulky triphenylphosphine.[186,187]

Another approach involves atom transfer radical addition reactions. This should lead exclusively to monoaddition if mono functional polymers are targeted. Thus, monomers that are nonpolymerizable by ATRP should be used. For example, addition of an excess of allyl alcohol near the end of an acrylate polymerization resulted in the monoaddition of this less reactive monomer. The new alkyl halide chain end can no longer participate in the ATRP process because of the very low reactivity of the carbon–halogen bond.[246] The concept of end functionalization through the addition of a nonpolymerizable monomer has also been applied to incorporate allyl alcohol, 1,2-epoxy-5-hexene,[258] and maleic anhydride.[263] Reacting bromo-terminated polymers with C$_{60}$ under ATRP conditions prepared C$_{60}$-terminated polystyrene and PMMA.[264] The fluorescence quenching using triethylamine or fumaronitrile showed that C$_{60}$ retained its strong electron-accepting and strong electron-donating properties after modification by the macromolecules.

Some end-group transformation reactions developed in the area of living cationic polymerizations have been applied to ATRP. One example is the reaction of an alkyl chloride with silyl enol ethers.[265] The method has been adapted for the functionalization of MMA synthesized by the ruthenium dichloride tris(triphenylphosphine) complex.[266] At the end of the polymerization, addition of either α-(trimethylsilyloxy) styrene or p-methoxy-α-(trimethylsilyloxy)styrene to the reaction mixture resulted in a ketone-functionalized polymer chain end and released chlorotrimethylsilane. The functionality of the polymers, determined by ^{1}H NMR, was >0.97. Another

example is the transformation of a halo-terminated polystyrenes to the allyl deriva-tives in the presence of allylsilanes and strong Lewis acids such as TiCl$_4$.[259]

Polymeric diols are used in step-growth copolymerizations. Inclusion of styrenes and acrylates into those copolymers could, therefore, expand the applications of materials such as polyesters and polyurethanes.[267] The first hydroxy group can be incorporated into the polymer by using hydroxy-functional initiator derivatives based on 2-bromoisobutyrates and 2-bromopropionates.[138,246] For the second group, two approaches to functionalization have been employed, the first one involved the direct substitution of the halogen with an amino alcohol such as 4-aminobutanol.[246] The other approach employed allyl alcohol. Diols can also be prepared by coupling the chains initiated by hydroxy group containing initiators. For example, a sulfide linkage between two chains with hydroxy terminal structures can be formed through the coupling of functional polymeric alkyl halides with sodium sulfide.[268] Another approach is reaction with α-methylstyrene, which leads to formation of the mono-adduct, a cumyl halide, which are thermally unstable, decompose, and react in a second addition, leading to chain coupling.[267] Coupling in the presence of Cu(0) is also possible.

The number of known transformation reactions that involve halogens (radical or ionic) is very large; therefore, the importance of transformation as a path to func-tional polymers cannot be stressed enough. A summary of several routes to displace the terminal halogen using electrophilic, nucleophilic, and radical transformations is shown in Scheme 11.12.
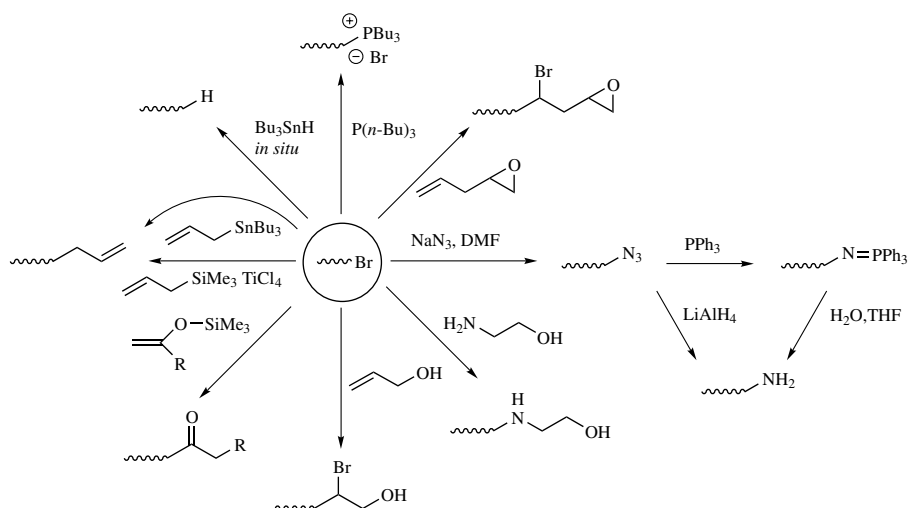
Scheme 11.12 Examples of the displacement of the terminal halogen in ATRP polymers using electrophilic, nucleophilic, and radical reactions.

11.5.2   Composition

This section covers combinations of monomers arranged in a linear polymer motif. Differentiation will be made between the relative position of monomers (i.e., statistical, gradient, or block) along a chain. Copolymers with a nonlinear structure will be discussed in a section devoted to chain topology (11.5.3).

11.5.2.1   Gradient/Statistical Copolymers   In conventional radical systems for copolymerization of two or more monomers the slow rate of initiation relative to propagation leads to chains, which have differing compositions depending on when they were grown. This results in compositional variation *among the chains* and, in the extreme cases, may result in a mixture of two homopolymers. In ATRP, all the chains are initiated early in the reaction and, under proper conditions, remain active throughout the entire course of the reaction. Therefore, changes in the instantaneous composition, arising from variations in the relative reactivity and concentration of monomers, is reflected *along the chains*. In the extreme case of very different reactivity ratios, this may lead to block copolymers. At the end of the reaction, the cumulative compositions of both conventional and controlled reactions should be the same, but in the conventional case a variety of compositions will be observed between the chains while in ATRP all chains will have a similar structure, although they may not be symmetric. This will result in a gradient of composition along the chain.[169] Such gradient copolymers are expected to have properties unlike other copolymers (block or random; see the following formula), making them candidates for applications such as blend compatibilizers and pressure sensitive adhesives:[169,269]

Random Copolymer

Block Copolymer

Gradient Copolymer

The shape of the gradient depends on the reactivity ratio and on monomer composition. In ATRP (and other controlled radical polymerization techniques) this enables the synthesis of not only spontaneous gradient but also forced gradient copolymers. In the latter system, one monomer can be metered into a reactor already containing another monomer in a semibatch mode.

Due to the relative infancy of ATRP, only a limited number of gradient copolymers have been reported.[169] They include a spontaneous and forced gradient copolymerization of styrene and MMA,[270] styrene and methyl acrylate (MA),[91] styrene and

acrylonitrile,[92] styrene and *n*-butyl acrylate,[208] and MMA with *n*-butyl acrylate.[68,69,209,271] The reactivity ratios for monomers in the two polymerization techniques were similar and independent on the structure of the catalytic system.[209] This again led to the suggestion that ATRP proceeds via a radical propagation mechanism, although some differences could arise from preferential monomer complexation by a catalyst. Differences may also appear as a result of noncomparable reaction conditions such as conversion, temperature, solvent, and methods of measurement and data analysis, which can differ significantly between the conventional and ATRP experiments.[168] Thermal and mechanical properties of block, statistical, and forced gradient copolymers with similar gross composition were compared. The DSC traces show that the forced gradient copolymer behavior depends on the thermal history. The lower modulus (G') of the forced gradient compared to the statistical gradient copolymer demonstrates that materials with different properties were produced.

Several examples of spontaneous copolymerization of monomers belonging to the same class have been reported in the literature. Because of similar reactivity ratios, no gradient should be observed such as in copolymerization of styrene with 4-acetoxystyrene[272] or epoxystyrene,[273] or MMA with *n*-butyl methacrylate (BMA) and others.[207]

A series of sequential styrene/MMA statistical copolymerizations were directed toward the synthesis of ABC "block-random" copolymers.[274] Over the course of the reaction, the feed composition of styrene/MMA was changed from 3/1 to 1/1 to 1/4 by the addition of more MMA. The polydispersity of the copolymer was $M_w/M_n \sim 1.5$.[77]

The synthesis of both spontaneous and forced gradient copolymers is in its infancy using controlled free-radical polymerization techniques and significant contributions are anticipated in the future since these macromolecules are novel materials whose bulk properties remain unexamined for utility.

11.5.2.2   Block Copolymers   The presence of an activated alkyl halide at a polymer chain end enables ATRP to be employed to synthesize di-, tri-, or multiblock copolymers. Block copolymers can be generated from a macroinitiator synthesized by either ATRP or by a different mechanism altogether.[17] Furthermore, the growth of subsequent blocks can be achieved through use of an isolated macroinitiator or by *in situ* addition of a second monomer to a reaction nearing completion.

11.5.2.2.1   Block Copolymers Formed Exclusively by ATRP   Shortly after the discovery of ATRP, it was recognized that the ability to polymerize a wide variety of monomers, with conservation of end groups and control over molecular weights and polydispersities, could facilitate the synthesis of block copolymers.[15] The first example of such a reaction was the synthesis of poly(methyl acrylate)-*b*-polystyrene and polystyrene-*b*-poly(methyl acrylate).[14,270] Since then, a number of di- and triblock copolymers have been well documented and will be discussed in more detail.

The switch from one block to another may sometimes be difficult and should be performed according to certain rules. The simplest is block copolymerization within the same class of monomers such as methacrylates, acrylates, or styrenes. Two early examples were the syntheses of poly(butyl methacrylate)-*b*-poly(methyl methacrylate) diblock[67] and poly(methyl methacrylate)-*b*-poly(butyl methacrylate)-*b*-poly(methyl methacrylate) triblock[77] copolymers prepared by sequential monomer addition. The polydispersities of the homo- and diblock copolymers were both low: $M_w/M_n < 1.2$.[67] In order to produce amphiphilic triblock copolymers, the acetate groups in polystyrene-*b*-poly(4-acetoxystyrene)-*b*-polystyrene and poly(4-acetoxystyrene)-*b*-polystyrene-*b*-poly(4-acetoxystyrene) were hydrolyzed.[272] Diblock and triblock copolymers of *n*-butyl acrylate and HEA were prepared by chain extension of poly(*n*-butyl acrylate) with HEA-TMS.[107] The amphiphilic materials were obtained by deprotection of the trimethylsilyl group with HCl in THF. ATRP was also used to produce amphiphilic block copolymers as stabilizers for suspension polymerization in supercritical carbon dioxide.[275] These diblock copolymers consist of a CO_2-phillic block, poly(perfluorooctyl methacrylate) (PFOMA), and a CO_2-phobic segment. ATRP was used to prepare block copolymers composed of fluorinated (meth)acrylates and PMMA and PDMAEMA (DMAEMA = 2-(dimethylamino)ethyl methacrylate) using bpy ligands with long fluoroalkyl groups in homogeneous sc CO_2.[46]

A series of experiments was designed to examine the blocking efficiency in methacrylate and acrylate polymerizations as a function macroinitiator composition, end group, and activating transition metal complex,[151] and the data, depicted graphically in Fig. 11.19, show that initiation of MMA from a chlorine terminal poly(methyl acrylate) macroinitiator results in poor initiation efficiency. The ''small'' tail in the weight distribution detected by SEC (Fig. 11.19a), can be much better visualized by the number distribution obtained of dividing the RI traces by MW, as shown in Fig. 11.19b. However, when PMMA was used to initiate the polymerization of acrylates, a uniform shift of the entire SEC trace to higher molecular weight occurred. Chain extension of this diblock copolymer with MMA again showed poor initiation efficiency. However, ATRP of MMA from bromine terminal poly-(methyl acrylate) mediated by a copper chloride complex showed fast initiation. When the acrylate macroinitiator contains a chlorine end group, propagation of MMA is faster than initiation, leading to a bimodal molecular weight distribution. The rate of cross-propagation from a bromine-terminated polyacrylate is at least comparable to that of propagation of MMA mediated by chlorine. Since previous model studies had shown that, in a mixed-halogen environment, the alkyl halide will contain predominantly chlorine,[133] chain extension of the bromine terminal polyacrylate with MMA mediated by a copper chloride complex provides high initiation efficiency. This study enabled the efficient synthesis of poly(methyl methacrylate-*b*-*n*-butyl acrylate-*b*-methyl methacrylate) ABA triblock copolymer by polymerization of the MMA segments from a difunctional poly(*n*-butyl acrylate) macroinitiator.[151] The halogen exchange improved the efficiency of block copolymerization significantly. The polydispersities of the hard block in all acrylic thermoplastic elastomers have reported to have a great effect on the morphology and rheological properties.[152]
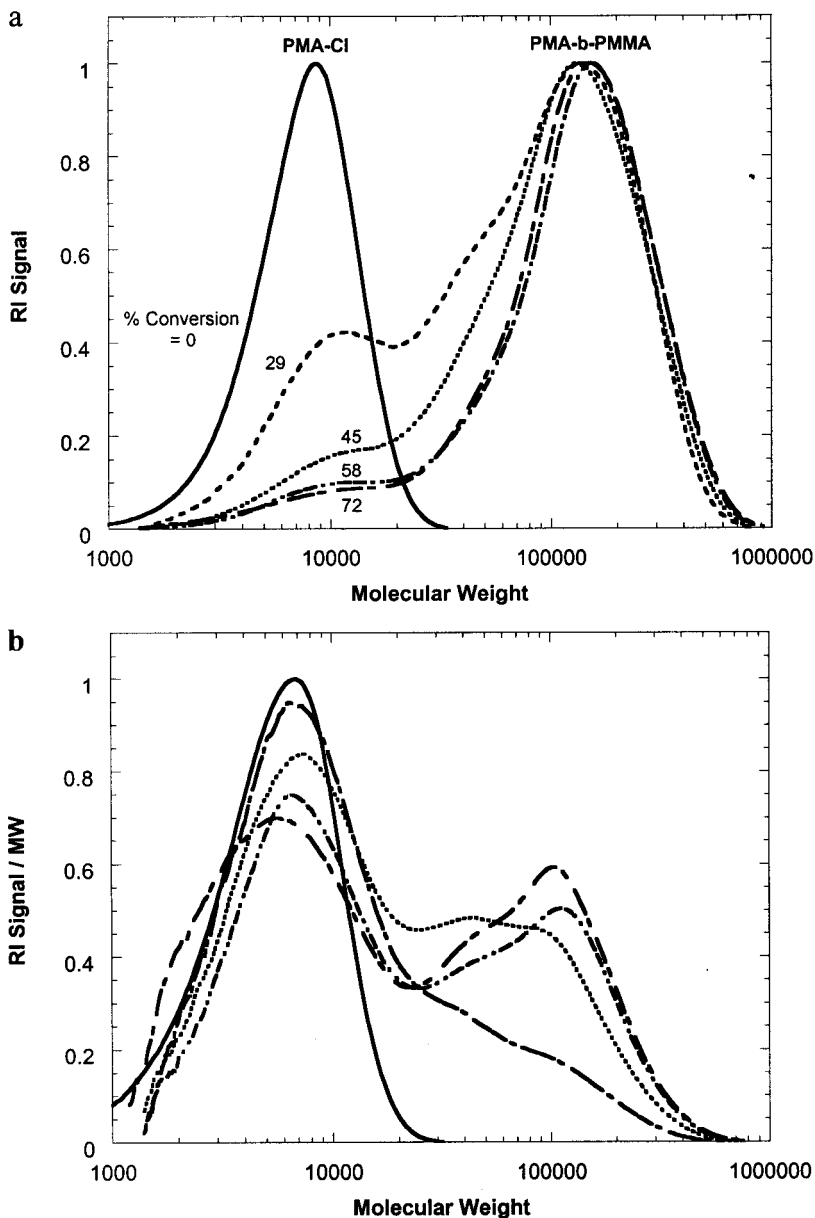
Figure 11.19 Weight (a) and number (b) distributions of PMA macroinitiator and PMA-*b*-PMMA diblock copolymer as a function of MMA conversion when not using halogen exchange. PMA $(8.3\,\text{mM}, M_n = 6,060, M_w/M_n = 1.36)$, MMA $(5.0\,\text{M})$, CuCl $(16.6\,\text{mM})$ dNbpy $(33.2\,\text{mM})$ in diphenylether at $90°\text{C}$. After $4.5\,\text{h}$ (72% conversion), the resulting polymer had $M_n = 41,400$ and $M_w/M_n = 3.63$.[276]

A possibility for avoiding halogen exchange is to add the second more reactive comonomer before the first one is consumed. A small amount of the first, less reactive, comonomer in the reaction mixture can act as a kinetic "compatibilizer," preventing an uncontrolled growth of the second block. This results in the formation of the random outer block (it may have a tapered structure). Mechanical properties of the resulting block copolymers with outer tapered segments are dramatically different from those of the pure block copolymers as presented in Fig. 11.20.[276] Hence, although this approach simplifies synthesis it leads to entirely different products.

Thus, chain extension is efficient if the product of the equilibrium constant and the rate constant of addition for the switch is at least comparable to that for
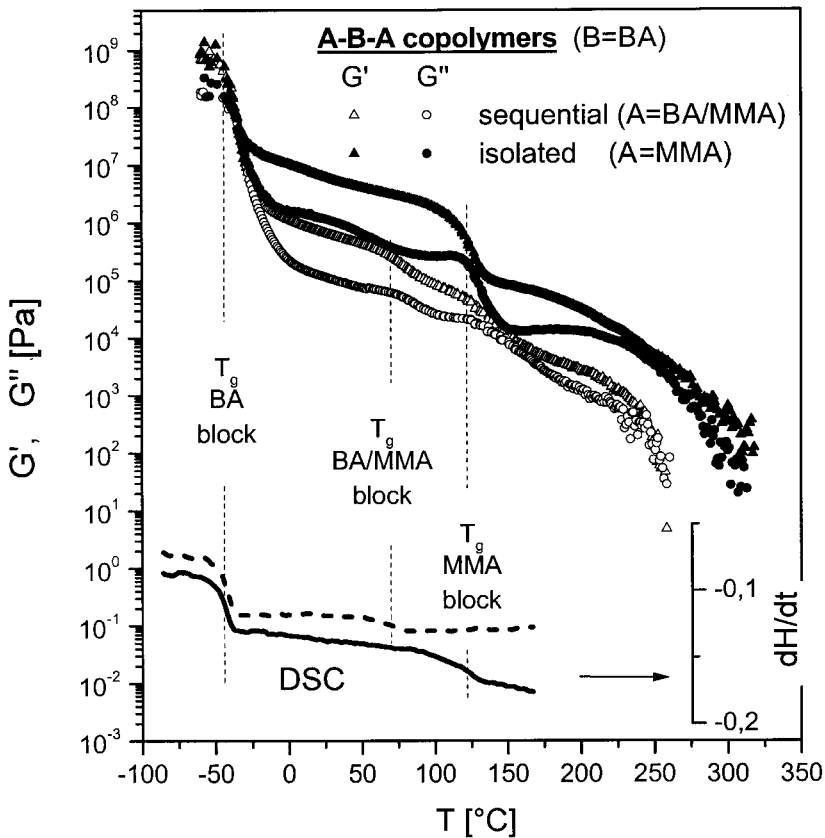
Figure 11.20   Temperature dependencies of the real (G') and imaginary (G'') component of the shear modulus measured at the deformation frequency of 10 rad/s for the pure and tapered triblock copolymers PMMA-b-pBA-b-PMMA and P(MMA-$grad$-BA)-b-PBA-b-P(MMA-$grad$-BA) of approximately the same overall composition, MW and polydispersity. For comparison DSC traces are shown that help localize the glass transition temperatures (T_g) of the microphases.[276]

continuation of growth for the second block. According to the homopolymerization and model studies the following order can be proposed; AN > MMA > St ~ MA. Here the structure of the ester group (e.g., methyl vs. butyl) is less important. This indicates that for the formation of block copolymers the order of addition for styrenes and acrylates is not important but formation of methacrylates and acrylonitrile blocks should not follow polystyrene or polyacrylate blocks. If for some reason such an order of block introduction is required, a halogen exchange should be used. Halogen exchange was also useful for the block copolymerization of DMAEMA using well-defined PMMA, PMA, or polystyrene as macroinitiators. The polydispersities of the block copolymers are lower with halogen exchange ($M_w/M_n = 1.2$).[277] On the other hand, exchange was not necessary for the block copolymerization of styrene with n-butyl acrylate[278] or polymerization of 4-vinylpyridine from PMMA-Cl. Me$_6$TREN was used as a ligand to avoid decomplexation in the presence of polyvinylpyridine.[117] PMMA-b-PS, PMMA-b-PHEMA and PS-b-PHEMA block copolymers were synthesized with polydispersities below 1.5 at high conversion of the second block without halogen exchange.[201]

Synthesis of triblock copolymers composed of polyacrylonitrile (PAN) peripheral blocks was challenging because of the relative insolubility of PAN in common organic solvents.[89] Triblock copolymers were formed in diphenyl ether from difunctional poly(n-butyl acrylate) and from poly(ethylhexyl acrylate). The polymerization of acrylonitrile from the macroinitiator resulted in a block copolymer whose molecular weight increased linearly with conversion.

Polystyrene and polyacrylate block copolymers can be grown from either type of macroinitiator. This has been demonstrated for the synthesis of various SA, AS, SAS, and ASA diblock and triblock copolymers between styrene and *tert*-butyl acrylate.[87,110] The latter triblock has been prepared using either a difunctional initiator with chain extension from both ends of the polystyrene to the polyacrylate (**A**) or by crossing from a monofunctional acrylate to styrene and back to the acrylate (**B**) which can provide unsymmetric triblock copolymer, as illustrated here:

A   Br — (···)$_m$ — (···)$_n$ — ··· — (···)$_n$ — (···)$_m$ — Br
O'Bu   OCH$_3$ H$_3$CO   O'Bu

B   (···)$_n$ — (···)$_x$ — (···)$_y$ — Br
H$_3$CO   O'Bu   O'Bu
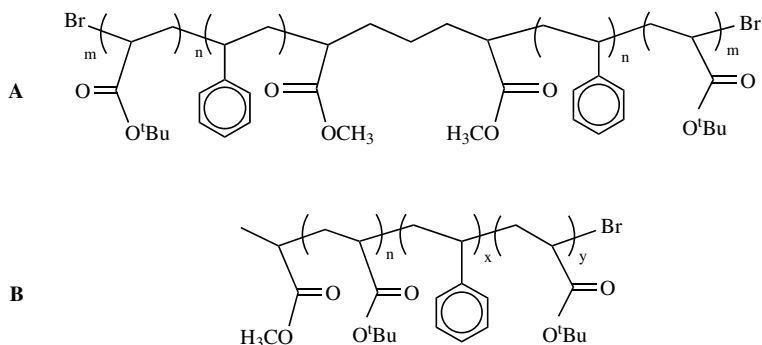
The SEC traces of final structures and intermediates in **B** are shown in Fig. 11.21.[87]

ATRP has been used successfully for the preparation of ABC triblock copolymers (terpolymers) as well as the corresponding ABCBA pentablocks and even (ABC)$_3$Z
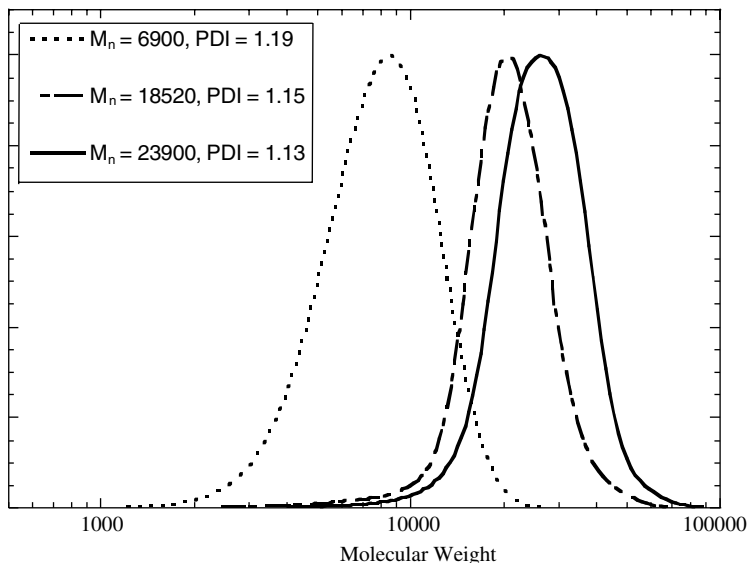
Figure 11.21 SEC traces of P*t*BA (dotted line), P*t*BA-*b*-PS (dashed line), and P*t*BA-*b*-PS-*b*-P*t*BA (solid line) in THF at 35°C.[87]

nonablock copolymers (terpolymers) using trifunctional cores. In the synthesis of ABC systems, the order of block formation is important and should generally follow the order (AN $\Rightarrow$ MMA $\Rightarrow$ S, A); however, it is possible to change this order by using the halogen exchange methodology. For example, a triblock system has been prepared using a bromine-terminated difunctional poly(*t*-butyl acrylate) macroinitiator, which was chain-extended with MMA using a CuCl-based catalyst to invoke the halogen switch. This block copolymer was subsequently chain extended with 4VP using the CuCl/Me$_6$TREN catalyst system to generate the ABC-BA block copolymer.[279] In a similar way, using halogen exchange, nonablocks with the other PPMA segments was formed (PMMA-*b*-P*t*BA-*b*-PS*t*)$_3$ with $M_n = 63,800$ and $M_w/M_n = 1.25$. When halogen exchange was not efficient, the overall polydispersity increased to $M_w/M_n = 1.55$.

A novel class of well-defined hybrid (co)polymers based on polyhedral oligomeric silsesquioxanes (POSS) have also been prepared by ATRP.[280] Well-defined homopolymers of MA-POSS, poly(MA-POSS)-*b*-poly(*n*BA)-*b*-poly(MA-POSS), and a star-shaped block copolymers of poly(methyl acrylate) and poly(MA-POSS) have been synthesized.

11.5.2.2.2 Block Copolymer Mechanistic Transformations A polymer synthesized by a polymerization mechanism other than ATRP can be used, either directly or after a simple organic transformation reaction, as a macroinitiator for the ATRP of vinyl monomers. Efficient ATRP macroinitiators were prepared by cationic, anionic, ring opening metathesis (ROMP), conventional radical, and step growth polymerizations.
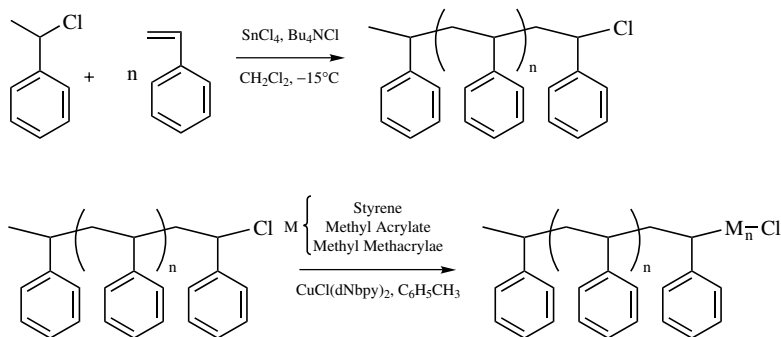
Scheme 11.13   Transformation from carbocationic polymerization to ATRP.

11.5.2.2.2.1 CATIONIC POLYMERIZATION AND ATRP   Transformation from cationic polymerization to ATRP is the simplest because the wrapping agent of the active species can be the same halogen atom. The only difference is homolytic vs. heterolytic C—X bond cleavage.

The first example of such a transformation was based on the cationic polymerization of styrene.[281] As shown in Scheme 11.13, initiation of the styrene polymerization with $SnCl_4$ produces an active species with chlorine as the counterion. Termination of the reaction yields 1-phenylalkyl chloride terminal polystyrene. After purification, ATRP with either methyl acrylate, methyl methacrylate, or styrene in conjunction with a soluble $CuCl(dNbpy)_2$ catalyst yields diblock copolymers. For all three monomers, the molecular weights increased according to the predetermined ratio of monomer to initiator. The polydispersities were quite low for styrene and methyl acrylate ($M_w/M_n = 1.2$). They were significantly higher for MMA ($M_w/M_n = 1.6$) due to slow initiation of MMA polymerization from the substituted benzyl chloride.[76] A one-pot process where methyl acrylate was added to the living polystyryl chloride to deactivate the cationic system was described.

Similar studies were performed with difunctional polyisobutene macroinitiators.[282–285] Because the *t*-butyl chloride terminal fragments are not efficient initiators for ATRP, at the end of the cationic polymerization, a small amount of styrene was added to cap the living cationic isobutene and ensure that α-phenylalkyl chloride moieties were located at the chain termini.[285] Efficient initiation was observed in methyl acrylate, methyl methacrylate, isobornyl acrylate, and styrene[281,283] polymerizations but with *p*-acetoxystyrene[283] residual macroinitiator was observed in the SEC traces.

Transformation from living cationic ring opening polymerization (CROP) to ATRP of styrene, methyl acrylate, and methyl methacrylate was realized using polyTHF as the macroinitiator.[286] The MMA polymerization was well controlled, with molecular weights less than 20% over those predicted and polydispersities reduced from $M_w/M_n = 1.71$ for the macroinitiator to $M_w/M_n = 1.34$ for the triblock copolymer. (See Scheme 11.14.)
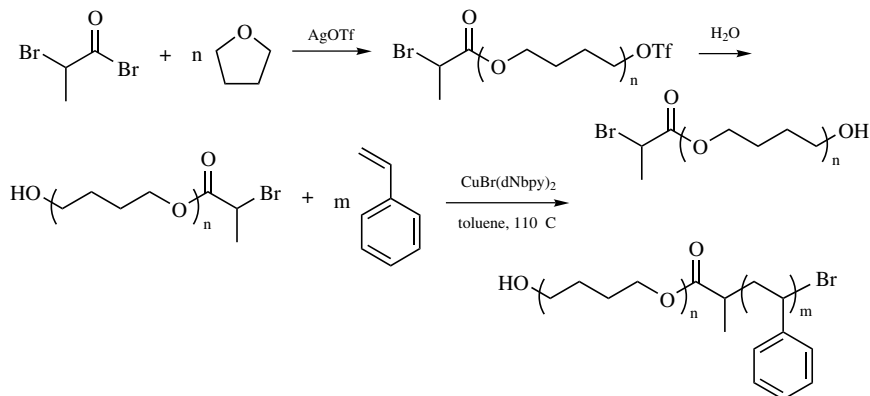
Scheme 11.14   Transformation from CROP to ATRP.

Conversely, block copolymers have also been prepared using mechanism transformation from ATRP to cationic polymerization. Thus, polystyrene (PSt) with end-terminal bromine (Br-PSt-Br) was synthesized by ATRP using the difunctional initiator 1,2-bis(2′-bromobutyryloxy)ethane. The resulting polymer was treated with silver perchlorate at −78°C to initiate the polymerization of tetrahydrofuran. Triblock poly(tetrahydrofuran)-polystyrene-poly(tetrahydrofuran) (PTHF-PSt-PTHF) diol was obtained after propagation at −15°C.[287] Similarly, polymeric radicals, generated by bromine terminated PSt under ATRP conditions, were oxidized to the corresponding carbocations using iodonium salts, such as Ph_2IPF_6, to initiate the polymerization of cyclohexene oxide.[288] The combination of cationic polymerization and ATRP can also be achieved using functional initiators capable to initiate two different types of polymerization. For example, 2-hydroxyethyl 2-bromobutyrate was first used to produce polystyrene in the presence of $CuBr(bpy)_3$. The resulting polymer was then used as a chain transfer agent in the cationic ring opening polymerization of 1,3-dioxepane with triflic acid as the initiator.[289]

11.5.2.2.2.2   ANIONIC AND ATRP   A functional initiator has been used for the anionic ring opening polymerization (AROP) of ε-caprolactone as well as the ATRP of styrene and MMA.[290] Scheme 11.15 shows two routes for the synthesis of diblock copolymers: polymerization of styrene or MMA by ATRP followed by AROP of ε-caprolactone or, conversely, AROP of the cyclic ester followed by the ATRP. In either case, diblock copolymers were produced that exhibit monomodal molecular weight distributions with little evidence of unreacted starting material.

An amphiphilic copolymer, poly(ε-caprolactone)-*b*-poly(acrylic acid), was prepared from the selective hydrolysis of a poly(ε-caprolactone)-*b*-poly(*tert*-butyl acrylate), which was synthesized by anionic ring opening polymerization (ROP) of ε-caprolactone followed by ATRP of *tert*-butyl acrylate *(t*BA). Self-assembly of PCL-*b*-PAA into polymer micelles followed by crosslinking of the hydrophilic shell via condensation reactions between the carboxylic acid functionalities of

Scheme 11.15   Simultaneous AROP and ATRP.

PAA and a diamine afforded shell-crosslinked nanoparticles. Finally, nanocage structures were produced after the selective hydrolysis of the polyester (PCL) core domain.[291]

One of the more thoroughly studied classes of block copolymers are those containing poly(ethylene oxide) (PEO). Mono-[292,293] and difunctional[294,295] PEO macroinitiators containing α-haloesters have been used in polymerizations of styrene,[292–294] methyl methacrylate[293,295] and t-butyl acrylate.[295] Polymerizations initiated with a polymer containing 2-bromopropionate end groups and a copper chloride catalyst showed lower polydispersities, in either bulk or solution, than did the corresponding bromide functional initiator/catalyst, due to halogen exchange.[294] Even more complex star and dendritic structures were prepared using this approach.[296]

Transformation from anionic vinyl polymerization is also possible. Thus, a living anionic polystyryl lithium was end-capped with styrene oxide and terminated with 2-bromoisobutyryl bromide.[297] The purified macroinitiator was then used in the ATRP of styrene, methyl acrylate, n-butyl acrylate, and a styrene/acrylonitrile mixture. In each case there was a linear increase of molecular weight with conversion, and SEC measurements of M_n were within 20% of the theoretically predicted values with $M_w/M_n < 1.2$. Using the same synthetic methodology, a polystyrene-b-polyisoprene macroinitiator was prepared and used.

Another amphiphilic block copolymer system, poly(ethylene-co-butylene)-b-poly(4-hydroxystyrene)[298] was obtained by anionic polymerization, quenching with EO, subsequent hydrogenation and esterification of monohydroxy terminal group present on the poly(ethylene-co-butylene) (Kraton polymer) with 2-bromopropionyl chloride. ATRP of styrene and 4-acetoxystyrene was conducted with a CuBr salt ligated by either bpy or 1,1,4,7,10,10-hexamethyltriethylenetetraamine, resulting in controlled polymers with $M_w/M_n < 1.3$. DSC analyses showed two glass transitions, one for the Kraton ($T_g = -63°C$) and one for either the styrene ($T_g = 93°C$) or acetoxystyrene ($T_g = 85°C$) segments. Hydrolysis of the acetoxy group to a hydroxyl fragment was demonstrated with hydrazine hydrate in xylene.

Recently, the synthesis of polyisoprene-*b*-polystyrene block copolymers bearing a fluorescent dye at the junction by the combination of living anionic polymerization and ATRP has been reported. In the synthesis, the polyisoprene carbanion was first reacted with a 1-aryl-1-phenylethylene derivative and then treated with an excess of α,α′-dihalo-*p*-xylene to generate the ATRP initiator moiety. Subsequent ATRP of styrene yielded the targeted block copolymer.[299] A similar approach was used for the block copolymers of methacrylates and acrylates.[300]

A linear increase of M_n with monomer conversion was observed with the use of well-defined monofunctional, low polydispersity PDMS macroinitiators synthesized by the anionic ring opening polymerization of hexamethylcyclotrisiloxane. In addition, a monofunctional polystyrene-*b*-poly(dimethylsiloxane) macroinitiator was used to initiate ATRP of *n*-butyl acrylate and methyl methacrylate, forming ABC organic/inorganic hybrid triblock copolymers.[301] In a similar way, 2-bromo-isobutyrate groups were attached to amino end-functional PDMS to generate a macroinitiator for growth of polymethacrylate blocks in two directions.[302] Grafting of hydrophilic polymers from PDMS backbone resulted in amphiphilic copolymers suitable for cosmetic and hair applications.[303,304]

11.5.2.2.2.3   COORDINATION POLYMERIZATION AND ATRP   There have been a few reports on the transformation from ring opening metathesis polymerization (ROMP) to ATRP. Macroinitiators were synthesized by polymerization of norbornene or dicyclopentadiene using a molybdenum Schrock carbene initiator followed by termination with *p*-(bromomethyl)benzaldehyde (Scheme 11.16). The terminal benzyl bromide moieties were then exploited in the ATRP of vinyl monomers.[305] Polymerization of styrene and methyl acrylate from a polynorbornene macroinitiator ($M_n = 30,500$, $M_w/M_n = 1.09$) yielded polynorbornene-*b*-polystyrene ($M_n = 110,400$, $M_w/M_n = 1.06$) and polynorbornene-*b*-poly(methyl acrylate) ($M_n = 85,100$, $M_w/M_n = 1.07$). In addition, the ATRP of the same two monomers from a poly(dicyclopentadiene) macroinitiator ($M_n = 12,100$, $M_w/M_n = 1.24$) produced poly(dicyclopentadiene)-*b*-polystyrene ($M_n = 20,100$, $M_w/M_n = 1.37$) and poly (dicyclopentadiene)-*b*-poly (methyl acrylate) ($M_n = 2,5300$, $M_w/M_n = 1.47$) copolymers. Two glass transition temperatures were observed for all polymers indicating microphase separation of the two segments of the blocks.

In another account, synthesis of polystyrene-*b*-polybutadiene-*b*-polystyrene and poly(methyl methacrylate)-*b*-polybutadiene-*b*-poly(methyl methacrylate) triblock copolymers with the center polybutadiene segments containing 100% 1,4-microstructure was described.[306,307] Chain transfer in the ROMP of 1,5-cyclooctadiene to vinyl compounds with ATRP initiating sites generated the difunctional macroinitiators. Triblock structure was confirmed by selective polybutadiene degradation using OsO_4/H_2O_2. ROMP catalysts are also active in ATRP, and simultaneous growth of cyclooctadiene and an acrylate was achieved using one single catalytic system.[161,307]

Other examples of combination of coordination polymerization with ATRP are discussed in Section 11.5.3.1.
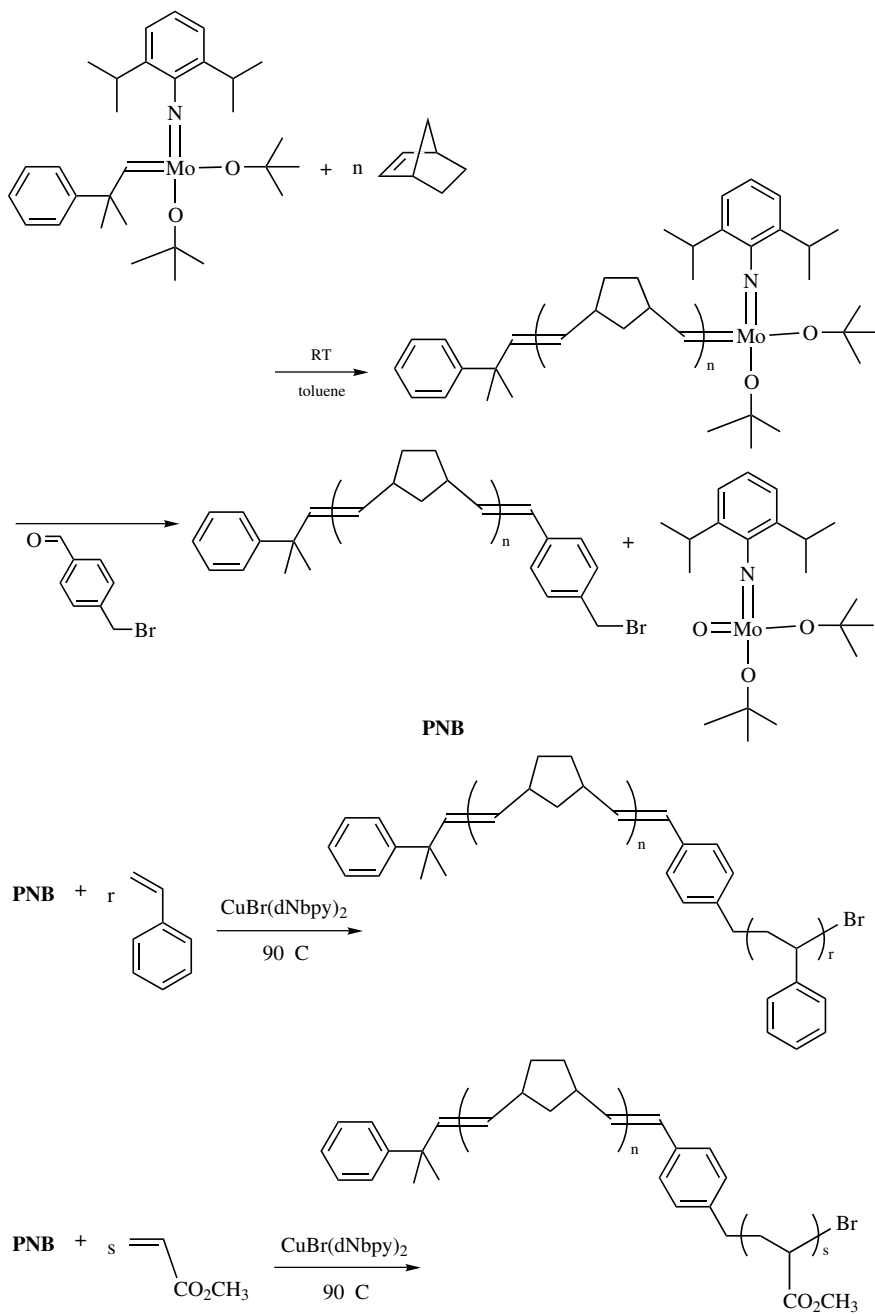
Scheme 11.16   Transformation from ROMP to ATRP.

11.5.2.2.2.4   CONVENTIONAL RADICAL POLYMERIZATION AND ATRP   Monomers without radical stabilizing substituents have not yet been successfully homopolymerized by ATRP; this group includes vinyl chloride, vinyl acetate (VOAc), and ethylene. However, these monomers have been efficiently incorporated into block and graft (see Section 11.5.3.1.1) copolymers with the second block built by ATRP. For example, block copolymers of VOAc have been prepared using four different methods.[124] The first two employed azo compounds containing activated halogen atoms. ATRP was carried before, or after, the conventional free-radical polymerization depending on the choice of initiator and reaction conditions. In the first case, low-temperature (30°C) ATRP of nBA in the presence of CuBr/Me$_6$TREN complex was completed without destroying the diazene. The resulting PnBA ($M_n = 7,500$; $M_w/M_n = 1.15$) with the preserved central azo unit was dissolved in VOAc and chain extended to a block copolymer ($M_n = 4,800$; $M_w/M_n = 3.56$).

In the second method, 2,2′-azobis[2-methyl-N-(2-(4-chloromethylbenzoyloxy) ethyl)propionamide] was first used to initiate the polymerization of VOAc at 90°C. The resulting PVOAc, with a Cl-terminal group, ($M_n = 47,900$; $M_w/M_n = 2.21$) was subsequently used as a macroinitiator for the ATRP of styrene (S) to yield PVOAc-b-PS ($M_n = 91,600$; $M_w/M_n = 1.80$).

In another route, ATRP was combined with a redox-initiated polymerization system. In this method, VOAc was polymerized in the presence of CCl$_4$/Fe(OAc)$_2$/ $N,N,N′,N″,N″$-pentamethyldiethylenetriamine (PMDETA) to yield pVOAc with trichloromethyl end groups ($M_n = 3,600$; $M_w/M_n = 1.81$). The polymer obtained was dissolved in styrene and a block copolymer, PVOAc-b-PS ($M_n = 24,300$; $M_w/M_n = 1.42$) was formed by ATRP.

In the fourth approach, a pnBA with a bromine end group ($M_n = 2,460$; $M_w/M_n = 1.32$) prepared by ATRP, was dissolved in VOAc together with CuBr/1,4,8,11-tetramethyl-1,4,8,11-tetraazacyclotetradecane (Me$_4$Cyclam) complex to initiate VOAc polymerization. A block copolymer with $M_n = 4,450$ and $M_w/M_n = 2.58$ was prepared. In the presence of 20 mol% of CuBr$_2$, the polydispersity was further reduced to 1.73.

Free radical telomerization has been combined with ATRP in several other instances. A difunctional macroinitiator was synthesized by di-$tert$-butyl peroxide–initiated radical polymerization of vinylidene fluoride in the presence of 1,2-dibromotetrafluoroethane. The difunctional bromine-terminated macroinitiator was then used for the ATRP of styrene. A linear increase of molecular weights with conversion was observed, but the polydispersity also increased from $M_w/M_n = 1.4$ to 1.7 over the course of the reaction.[308] In a similar way, vinylidene fluoride CCl$_3$-terminated telomers were synthesized and used to initiate the ATRP of styrene, MMA, MA, and nBA. By varying [CHCl$_3$]$_0$/[VDF]$_0$ and [M]$_0$/[Tm]$_0$ ratios in the telomerization and ATRP steps, the chain length of both blocks and copolymer composition was controlled.[309]

The combination of redox telomerization with ATRP has also been used in the synthesis of block copolymers of other polymers that could have been prepared solely by ATRP such as polyacrylates, polymethacrylates, and polystyrene.[130,310] During the controlled growth of the second block by ATRP, the polydispersity

decreased from 2.3 to 1.6, showing the addition of a segment with a well-defined chain length.

11.5.2.2.2.5 STEP-GROWTH POLYMERIZATION AND ATRP   There are a few examples of well-defined block copolymers composed of blocks made by step-growth polymerization and segments consisting of vinyl monomers without significant contamination by the corresponding homopolymers.

The formation of ABA triblock copolymers synthesized from a difunctional polysulfone macroinitiator has been described.[311] A α,ω-dihydroxy terminal polysulfone was synthesized by the reaction of 4-fluorophenyl sulfone with an excess (<10%) of bisphenol A in the presence potassium bicarbonate at temperatures in excess of 140°C. The polysulfone was esterified with 2-bromopropionyl bromide in the presence of pyridine to yield a difunctional ATRP macroinitiator with $M_n = 4,030$, $M_w/M_n = 1.5$. Use of this macroinitiator for the polymerization of styrene or n-butyl acrylate using the CuBr(dNbpy)$_2$ catalyst system at 110°C yielded 67% and 95% conversions of styrene and n-butyl acrylate after 7 h, respectively. Following typical ATRP behavior, the molecular weights of the triblock copolymers increased with simultaneous decreases in the molecular weight distributions: $M_n = 15,300$, $M_w/M_n = 1.2$ for polystyrene and $M_n = 10,700$, $M_w/M_n = 1.1$ for poly(n-butyl acrylate). (See Scheme 11.17.)

The triblock copolymer with a central polysulfone segment (25 wt%) organizes in supramolecular aggregates with a periodicity of 10–12 nm. According to SAXS, the periodicity remains even above 250°C, although DMA indicates that the triblock copolymer "melts" at about 100°C; this transition corresponds to a structural relaxation of a poly(n-butyl acrylate) with a molecular weight of a few million, confirming a high degree of aggregation.
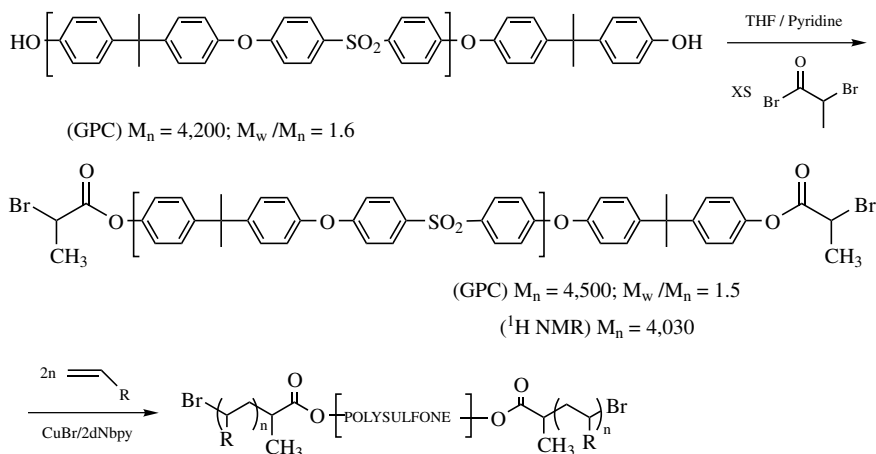
Scheme 11.17   Preparation of the polysulfone macroinitiator and triblock copolymer with polystyrene (R = Ph) and poly(n-butyl acrylate) [R = C(O)—O—nBu].

A polyester macroinitiator, prepared in a manner similar to that for synthesis of the difunctional polysulfone macroinitiator, was also used in the synthesis of block copolymers by ATRP.[312] The α,ω-dihydroxy terminal polymer was synthesized by the transesterification of 1,6-hexanediol with dimethyl adipate. The end groups were then esterified with 2-bromopropionyl bromide, and the ATRP of styrene yielded the ABA triblock copolymers.

The synthesis of rigid–flexible triblock copolymers, with a rigid central segment possessing photoluminescence, has been described.[313] First, Suzuki coupling was applied to prepare α,ω-acetoxy functionalized oligophenylenes with five or seven rings. Hydrolysis of these acetoxy end groups and esterification of the resulting hydroxy end groups with acyl chlorides led to molecules capable of acting as ATRP initiators. The final rigid–flexible copolymers of styrene displayed low polydispersities and showed blue-light emission.

Several studies on the preparation of poly(dimethylsiloxane) (PDMS) block copolymers via ATRP have been reported. Difunctional PDMS macroinitiators were synthesized by hydrosilylation of vinyl or hydrosilyl terminal PDMS with a hydrosilyl or vinyl functionalized molecule containing a benzyl chloride moiety.[119,314,315] Initiation of a number of vinyl monomers yields polymers with increased molecular weights and decreased polydispersities. The hydrosilylation of commercially available difunctional hydrosilyl terminal PDMS ($M_w/M_n > 1.3$) with allyl- or 3-butenyl 2-bromoisobutyrate results in the preparation of ATRP macroinitiators.[301]

Jones and co-workers reported the preparation of a hybrid block copolymer utilizing initiation of ATRP from telechelic chloromethylated polymethylphenyl-silylene (PMPS).[316] The attachable initiator, (4-chloromethylphenylethyl)dimethyl-chlorosilane, was added to the reductive coupling reaction of methylphenyl dichlorosilane at the end of the polymerization. The material was purified by precipitation in methanol and then used in the ATRP of styrene.[29] Si NMR showed the presence of methoxysilane species in the polymer resulting from condensation of unreacted silyl chloride with the methanol precipitant. Nevertheless, SEC confirmed the formation of the block copolymer by increasing molecular weight.

11.5.2.2.2.6   DENDRITIC INITIATORS FOR ATRP   The primary example utilizes benzyl ether dendron initiators of generations 1–4.[317] The benzyl chloride moiety is located at the focal point of the third-generation initiator. ATRP of styrene from these initiators proceeds in a controlled fashion below $M_n = 30{,}000$, $M_w/M_n < 1.3$. Above $M_n = 30{,}000$, deviations from the theoretical molecular weights are observed and polydispersities increase. This was attributed to the elimination reaction occurring early in the polymerization. However, the formation of a nonpolymerizable species is also possible because of some form of bimolecular termination resulting during establishment of the equilibrium at low monomer conversion ($<5\%$). Thermal analysis of the block copolymers reveals one T_g, indicating miscibility of the two fragments, while a blend of the homopolymer and dendron shows two glass transitions. Furthermore, for a given polystyrene block length, an increase in the dendron generation number caused a decrease in the T_g.

In a related study, benzyl ether dendrons with ethyl ester terminal groups and benzyl bromide initiator fragments at the dendron focal points were examined.[318] ATRP of styrene from initiators of generations 0-3 proceeded with slightly better control to higher molecular weights than those seen with the benzyl chloride analog. The ethyl ester moieties were then converted to carboxylic acid functionalities, [G-1]-dendron ester, butyl amide, and methyl alcohol functionalities. Interestingly, ^{1}H NMR of the block copolymers containing the hydrophilic dendron in CDCl$_3$ showed resonances only for the polystyrene segment while a spectrum measured in deuterated DMF elucidated signals for both the dendron and polystyrene protons, as a result of aggregation of the hydrophilic moieties in the nonpolar solvent with the long relaxation time.

11.5.3 Topology

The control over molecular weight and functionality obtained with ATRP has allowed for the synthesis of numerous materials with many novel topologies. With the exception of linear polymers, architectural differences lie in branched structures with regard to the number of branches and their relative placement in the macromolecule.

11.5.3.1 Graft Copolymers   The synthesis of graft copolymers can be accomplished through one of three routes: "grafting from" reactions, utilizing polymerization of grafts from a macroinitiator with pendant functionality; "grafting through" processes, operating by homo- or copolymerization of a macromonomer; and "grafting onto" reactions, occurring when the growing chain is attached to a polymer backbone. The first two methods have been used in conjunction with ATRP in the design of graft copolymers.

11.5.3.1.1 "Grafting from"   An example of graft copolymers prepared by "grafting from" utilizes the ATRP of vinyl monomers from a pendant functionalized poly(vinyl chloride) (PVC) macroinitiators.[319] The purpose of the study was to chemically incorporate another monomer into the PVC matrix to reduce the inherent brittle nature of that polymer. PVC containing 1% (mole) chloroacetate groups was prepared, and the chloroacetate moieties attached to the polymeric backbone were used in ATRP of styrene, MA, and *n*BA and MMA. (See Scheme 11.18.) The results of the study, summarized in Table 11.7 demonstrate that in each case the molecular weight of the graft copolymer increased above that of the macroinitiator yet the polydispersity remained essentially the same. The polydispersity did not decrease because of the variable quantity of initiating sites per chain. The large increase in the molecular weight distribution seen from the MMA polymerization may originate from slow ATRP initiation of MMA from the primary alkyl halide sites. The T_g of the copolymers containing MA and *n*-BA decreased, indicating that a self-plasticized PVC has been synthesized.

Another example of using ATRP to prepare useful novel copolymers by grafting from is use of ATRP of styrene,[119,320] isobornyl acrylate,[119] and MMA[321] to prepare

Scheme 11.18   Grafting from poly(vinyl chloride).

grafts from EXXPRO, a commercially available poly(isobutylene-*co*-*p*-methylstyr-ene-*co*-*p*-bromomethylstyrene). The use of ATRP for preparation of the grafts allowed for control over the composition of the copolymer. DSC analysis of the graft copolymer showed two glass transition temperatures indicative of a microphase separated system.[119,320] A graft copolymer containing 6 wt% polystyrene, displayed reversible elongations of up to 500%, indicating thermoplastic elastomeric behavior.[320]

An ATRP macroinitiator has been synthesized from an ethylene-propylene-diene terpolymer by bromination of pendant allylic groups with *N*-bromosuccinimide.[322] The allyl bromide groups served as initiating species for the polymerization of MMA. Grafting efficiencies of ≤93% were obtained. Similarly, chemical modifica-tion of commercially available low polydispersity Kraton polymer was carried out to introduce benzyl bromide ATRP initiating sites.[323] Subsequent ATRP of ethyl methacrylate produced block–graft copolymers composed of polystyrene-*b*-poly (ethylene-*co*-propylene) and poly(ethyl methacrylate).

TABLE 11.7   Characterization Data for ATRP of Vinyl Monomers from PVC Macroinitiators[319]

Second Monomer	M_n (SEC)	M_w/M_n	Mol% Second Monomer	$T_g(^\circ C)$
—	47,400	2.66	0	83
Styrene	99,500	3.72	80	80
MA	57,700	2.40	50	21
MMA	83,600	4.94	60	111
BA	81,400	2.44	65	−19

A practical application for amphiphilic graft copolymers has been disclosed in the area of personal care products. Various combinations of (meth)acrylates, methacrylic acid, and *p*-chloromethylstyrene were copolymerized by a conventional free radical copolymerization. "Grafting from" reactions using the chloromethylphenyl groups within the polysiloxane or polystyrene chains as initiators with either methacrylic acid,[303] t-BA, or HEMA-TMS[324] by ATRP yielded the amphiphilic graft copolymers. When HEMA-TMS was used, deprotection was required.[324]

The first example reported an inorganic/organic hybrid graft copolymer consisted of polystyrene grafts from a PDMS backbone.[314] The pendant functionalized PDMS macroinitiator was synthesized by hydrosilylation of poly(vinylmethylsiloxane-*co*-dimethylsiloxane) with a compound containing hydrosilyl and benzyl chloride moieties. ATRP of styrene from the macroinitiator with pendant benzyl chloride groups ($M_n = 6,600$, $M_w/M_n = 1.76$) resulted in a copolymer with $M_n = 14,800$, $M_w/M_n = 2.10$. In a similar way amphiphilic side chains were grafted from PDMS backbone.[324] An alternative method involves grafting through using PDMS macroinitiators.[245]

Polystyrene chains have also been reported to have been grafted from a polysilylene backbone by ATRP.[325] In this account, 35% of the phenyl rings of poly(methylphenylsilylene) (PMPS) were bromomethylated in a Friedel–Crafts reaction followed by ATRP of styrene from the macroinitiator using the heterogeneous $CuBr(bpy)_3$ catalyst system to provide the graft copolymers. ^{1}H NMR measurement of the purified copolymer gave a ratio of polystyrene to PMPS of 12.5 : 1.

Polyolefins were combined with ATRP by two methods. Glycidyl methacrylate units in an ethylene copolymer were transformed to benzyl halides and bromoesters used as initiators for grafting from with styrene and (meth)acrylates.[326] Another approach was based on bromination of the benzylic H atoms in a styrene ethylene copolymer, followed by grafting from with MMA and St.[326]

Densely grafted copolymers (also called "bottle–brush copolymers") contain a grafted chain at each repeat unit on the polymer backbone. As a result, the macromolecules adopt a more elongated conformation. Within the context of ATRP, examples of bottle–brush copolymers have been provided.[80,242,327] Synthesis of the macroinitiator was achieved through one of two approaches. One method used conventional radical polymerization of 2-(2-bromopropionyloxy)ethyl acrylate in the presence of CBr_4 to produce a macroinitiator with $M_n = 27,300$, and high polydispersity $M_w/M_n = 2.3$. The alternative involved ATRP of 2-trimethylsilyloxyethyl methacrylate followed by esterification of the protected alcohol with 2-bromopropionyl bromide. While synthetically more challenging, the latter method provided a macroinitiator with a well-defined structure ($M_n = 55,500$, $M_w/M_n = 1.3$) leading to a brush synthesized entirely by a controlled process (Scheme 11.19). Either macroinitiator, can be used for the ATRP of styrene or *n*-butyl acrylate leading to the desired densely grafted structures. The grafting reactions were found to be very sensitive to reaction conditions; additional deactivator, high concentrations of monomer, and reduced temperatures were all necessary to arrive at the desired materials.
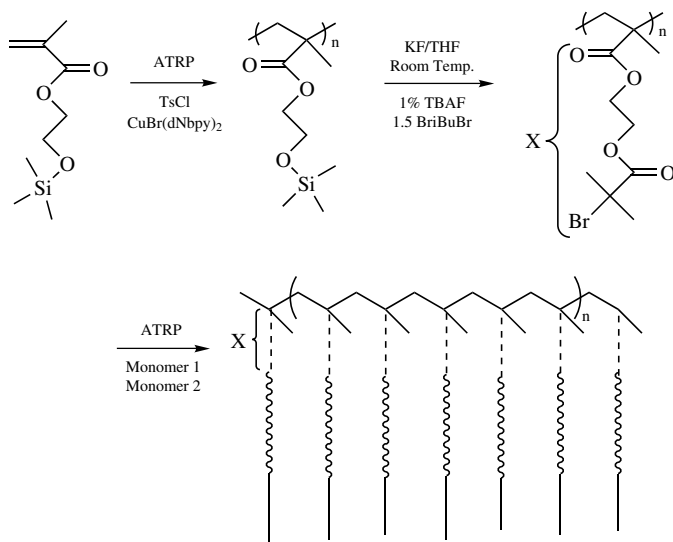
Scheme 11.19   Polymeric bottle brushes by dense grafting using ATRP.

Since the aspect ratio and size of the macromolecules are large, individual chains can be observed by atomic force microscopy (AFM) (see Fig. 11.22). The brushes with polystyrene side chains form elongated structures on a mica surface with an average length of 100 nm, a width of 10 nm, and a height of 3 nm. Poly(n-butyl acrylate) absorbs well onto the mica surface and forms spectacular single-molecule brushes in which the backbone and side chains can be visualized using tapping-mode AFM.

Similarly, core–shell cylindrical brushes were prepared via block copolymerization (see Scheme 11.19). The examples consist of the either soft poly(n-butyl acrylate) cores and hard polystyrene shells or hard cores and soft shells.[328]

The synthesis of well-defined bottle–brush block copolymers demonstrates the synthetic power of ATRP. The procedure used was to create a well-defined backbone with DP $\sim$ 500, followed by the transesterification and subsequent grafting of pnBA chains with final chain extension with St to produce the block copolymers.

Patten *et al*. have recently described a similar methodology for the formation of graft copolymers with a less densely packed backbone, where the grafted polymers (macromolecules derived from only one monomer) were prepared strictly by ATRP.[329] The copolymerization of 4-acetoxymethyl- or 4-methoxymethylstyrene with styrene yielded a pendant functional macroinitiator with "latent initiation sites." Transformation of the ester or ether to benzyl bromide substituents provided the alkyl halide necessary for initiation of the grafting reactions.

An architecturally interesting example reported is dendrigraft polymers.[330] These materials are synthesized by the combination of nitroxide mediated controlled free
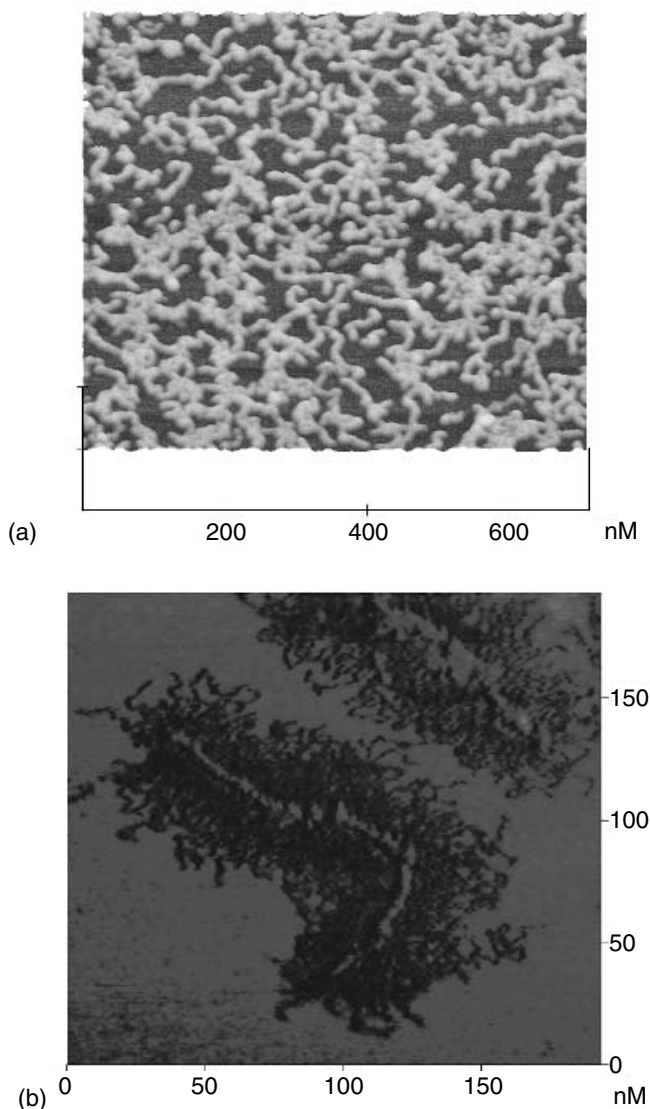
Figure 11.22   AFM images of polystyrene (a) and poly(n-butyl acrylate) brushes (b) on mica surface.[80]

radical polymerization and ATRP. Copolymerization of p-(4′-chloromethylbenzyl-oxymethyl)styrene with styrene initiated by 1-phenylethyl-TEMPO yields a linear polymer with pendant benzyl chloride moieties. Nucleophilic substitution with 2-hydroxy-1-phenylethyl-TEMPO results in a macroinitiator that will polymerize a mixture of p-(4′-chloromethylbenzyloxymethyl)styrene and styrene again. Graft

copolymers, the ATRP of styrene, and *n*-butyl methacrylate yielded dendrigraft structures with the lowest polydispersities, $M_w/M_n = 1.38$. Molecular weights measured by SEC versus linear polystyrene standards ($M_w = 480{,}000$) were significantly smaller than those from absolute methods ($M_w = 1{,}140{,}000$), indicating that the macromolecules adopted compact structures in solution.

A "tandem polymerization" technique has recently been reported where the copolymerization of 4-(2-bromoisobutyryloxy) ε-caprolactone with MMA and ε-caprolactone resulted in the synthesis of a series of architecturally complex structures.[331] When the monomer was copolymerized with ε-caprolactone, an ATRP macroinitiator was synthesized. "Grafting from" the MMA yielded the desired graft copolymer. Likewise, use of the compound to initiate the ATRP of MMA yielded a macromonomer, which was copolymerized with ε-caprolactone in a "grafting through" reaction. The authors were also able to perform these two polymerizations simultaneously to obtain a branched structure.

11.5.3.1.2 "Grafting through"   The combination of hydrophobic and hydrophilic segments in a copolymer may yield materials that swell dramatically in water without requiring chemical crosslinking. The first example of hydrogels made by ATRP involved graft copolymers of polystyrene with *N*-vinylpyrrolidinone (NVP).[238,332] The graft copolymer was formed by the copolymerization of vinyl acetate terminal polystyrene macromonomers with NVP by a conventional free-radical polymerization. Synthesis of the macromonomers was achieved by the ATRP of styrene initiated by vinyl chloroacetate. Molecular weights were predetermined, and polydispersities were low: $M_w/M_n < 1.2$. During preparation of the macromonomer, polymerization through the vinyl acetate double bond was not observed, due to low conversion of styrene during the polymerization and the reactivity ratios of the two comonomers. Three different molecular weight macromonomers were examined in the graft copolymerizations ($M_n = 5{,}000$, $10{,}000$, and $15{,}000$). Graft copolymer formation was performed using an AIBN initiated polymerization in DMF at 60°C. (See Scheme 11.20.)

Representative results for the graft copolymers are shown in Table 11.8. As the macromonomer molecular weight increased, the graft density decreased. The graft
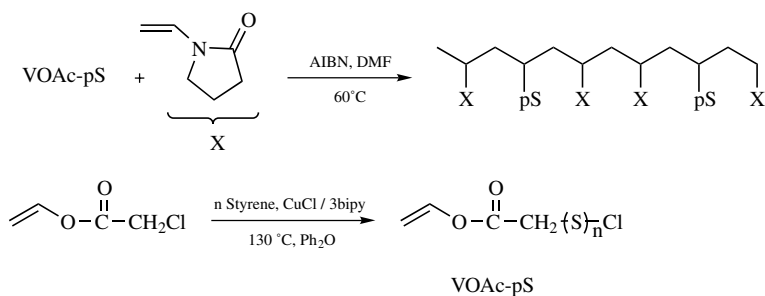
Scheme 11.20   Grafting through with macromonomers prepared by ATRP.

TABLE 11.8   Compositional Data of Copolymers Synthesized from Macromonomers ($M_n = 5800$)[238,332]

Theoretical wt% S	Actual wt% S	M_n Copolymer [a]	PDI	% Yield	$\bar{N}$[b] Grafts per Chain	% Conversion MM	NVP
50	35.4	95,500	2.80	19.6	5.8	14	25
40	34.2	316,000	5.90	48.9	18.6	42	53
30	19.2	264,000	2.36	15.8	8.7	10	18
20	13.0	219,000	2.45	20.0	4.9	12	21
10	7.73	185,000	1.81	22.1	2.5	16	23

[a] Copolymer was not isolated since it formed a surfactant.
[b] Average number of grafts per chain.

copolymers contained a higher concentration of the hydrophobic segments while maintaining the same number of grafts per chain. For the lower molecular weight macromonomer, the observed content of styrene, copolymer molecular weight, and graft density all increased with hydrophobe content. The materials behaved as hydrogels absorbing significant amounts of water, as indicated by the high equilibrium water content ($H = 97\%$) and the equilibrium state of swelling.

The "grafting through" approach using ATRP has also been applied in the copolymerization of nBA and PMMA macromonomers.[243,333] In contrast to a conventional copolymerization where the relative reactivity of the macromonomer is significantly lower than that of the MMA, the relative reactivity of the macromonomer is much closer to that of MMA in ATRP. This was explained by the much longer timescale available for monomer addition in ATRP (seconds) than in conventional polymerization (milliseconds). The graft copolymers obtained by ATRP also had lower polydispersities.[244] Similar results were obtained for PDMS macromonomers, which in ATRP, had reactivity ratios much closer to MMA than those seen in conventional processes. Even better results were obtained using PDMS macroinitiators.[245] Poly(lactic acid) macromonomers behave in a similar way.[334]

The "grafting through" approach with vinyl terminal macromonomers was also applied to the preparation of densely grafted macromolecules. Living cationic polymerization provided a methacrylate terminal poly(isobutylvinyl ether) macromonomer.[242] ATRP of the macromonomers, showed a linear increase of the molecular weights with conversion. Polydispersity remained low ($M_w/M_n < 1.2$) throughout the reaction. The study has shown that well-defined materials could be produced from components that were themselves synthesized by two living polymerization techniques.

11.5.3.2   Grafts from Surfaces   Growth of polymers at interfaces has been conducted by ATRP from either planar surfaces or spherical particles, and holds promise in lithography, lubrication, corrosion prevention, materials reinforcement, or preparation of materials for separation processes. In an ATRP process a

monofunctional initiator molecule can be attached to a surface ensuring that, in the absence of chain transfer or thermal self-initiation, chains can be grown solely from that surface. Wirth et al. confirmed by elemental analysis that polyacrylamide can be grown from functionalized silica particles.[335] They later extended the surface-initiated acrylamide polymerization to silicon wafers where they demonstrated that film thickness could be controlled by the concentration of monomer in the reaction.[252]

Spherical silica particles containing surface ethoxysilyl groups were functionalized with 2-(4-chloromethylphenyl)ethyldimethylethoxysilane by the Stöber process.[336] Following the ATRP of styrene, dynamic light scattering confirmed that the size of the particles had nearly doubled. Cleavage of the core allowed for SEC analysis of the arms relatively high molecular weight polymer was obtained with polydispersities as low as $M_w/M_n = 1.14$. Similarly, (11'-chlorodimethylsilylundecyl)-2-chloro-2-phenylacetate was attached to a silica gel surface to initiate the ATRP of styrene.[337] ATRP also enables the synthesis of block copolymers from such particles. Functional nanoparticles were prepared where approximately 1000 functional silanes bearing 2-bromoisobutyrate initiating groups were condensed onto the nanoparticle surface. The ATRP of styrene and subsequently benzyl acrylate was conducted, providing homo- and block copolymers tethered to a colloidal core.[338] Particle size increased from 24 to 30 and to 55 nm as measured by AFM and from 25 to 52 and to 106 nm by dynamic light scattering, correspondingly. SEC of the chains cleaved from the surface by destruction of particles with HF show a progressive increase of molecular weight $M_n = 5250$ to $M_n = 27,280$ on extension from polystyrene to polystyrene-b-poly(benzyl acrylate), while preserving low polydispersities.

There are several accounts of grafting from flat surfaces such as silicon wafers by ATRP. In one system, Langmuir–Blodgett techniques were used to condense a monolayer of 4-(2-trimethoxysilylethyl)phenylsulfonyl chloride onto the surface.[253] The ATRP of MMA mediated by a CuBr/alkyl bipyridine complex with a ''sacrificial'' initiator, namely, untethered p-toluenesulfonyl chloride, showed linear increases in film thickness with the molecular weight of chains in solution.

Another study utilized chlorosilanes in the self-assembly of (5'-trichlorosilyl) pentyl 2-bromoisobutyrate on an oxidized silicon wafer.[339] In the NiBr(PPh₃)₂-mediated polymerization of MMA, a linear increases of film thickness corresponding to the length of untethered chains polymerized from ethyl 2-bromoisobutyrate was observed. The authors of both studies emphasize that the free, or sacrificial, initiator was necessary to provide control of the surface polymerization as the deactivator was provided by termination of short chains very early in the reactions. A sugar-carrying methacrylate, 3-O-methacryloyl-1,2:5,6-di-O-isopropylidene-D-glucofuranose (MAIpGlc), was grafted on silica surface using a monolayer of the initiator, 2-(4-chlorosulfonylphenyl)ethyltrimethoxysilane, which had been immobilized by the Langmuir–Blodgett technique.[340]

ATRP has also been used for the synthesis of block copolymers from a modified silicon surface. A polystyrene layer was grown from the surface by living cationic polymerization.[254] The terminal secondary benzyl chloride groups were then used in the ATRP of MMA using a CuBr/PMDETA complex.[99] The efficiency of blocking

was not evaluated, although under homogeneous conditions, the blocking efficiency should be very low, because benzyl halides are poor initiators for ATRP of MMA, especially without the halogen exchange.[76] Nevertheless, incorporation of some PMMA onto the macroinitiator was confirmed by reflectance FTIR and water contact-angle measurements. The films were responsive to their environment and nanopattern formation occurred, perhaps as a result of a low brush density.[254,341] The same group also attached an azo-functional trichlorosilane to the silica surface and used reverse ATRP to prepare similar block copolymers.[342]

Block copolymers of polystyrene-b-poly(t-butyl acrylate) on silica wafer have been also prepared exclusively by ATRP.[255] Modification of the hydrophilicity of the surface layer was achieved by hydrolysis of the t-butyl ester to form poly-styrene-b-poly(acrylic acid) and confirmed by a decrease in water contact angle from 86° to 18°.[255] On the other hand, high contact angles were obtained when fluoroacrylates were polymerized from the surface (119°).[255] It was also demonstrated that the presence of a small amount of cupric halide prior to the commencement of the polymerization could result in a sufficient deactivator concentration, thus eliminating the need for the "sacrificial initiator." (See Scheme 11.21.)

Scheme 11.21   Grafting from flat surfaces by ATRP followed by block copolymerization and deprotection.

Ambient temperature ATRP of MMA using 2-bromoisobutyrates attached to the gold surface with CuBr-tris[2-(dimethylamino)ethyl]amine as the catalysts led to densely chemically bound PMMA brushes on gold surface.[343]

ATRP has also been used to amplify initiators, patterned on films of gold by microcontact printing, into polymeric barriers that can serve as robust barriers to a range of wet chemical etchants.[344] The use of ATRP permits a high level of control over the thickness and functionality of the tethered polymer brushes and makes tailoring of the physical properties of the brushes such as their wettability and etching resistance possible.

11.5.3.3 Star Polymers

The use of multifunctional small-molecule initiators to synthesize star polymers was recognized shortly after the advent of ATRP. The first example was polymerization of styrene from hexakis(bromomethyl)benzene.[270] The molecular weights correlated with the theoretical values ($M_{n,\exp} = 62,400$, $M_{n,\text{th}} = 60,000$) and the polydispersity was low ($M_w/M_n = 1.23$). Later, 3-arm star polymers with mesogenic 11-(4′-cyanophenyl-4″-phenoxy)undecyl acrylate were prepared.[234] The broadening of the isotropization temperature of the polymer prepared by conventional free-radical polymerization was due to an inhomogeneity in the chain length (polydispersity) and from contamination by branched architectures as a result of chain transfer to polymer observed at high monomer conversions.

Other star polymers were prepared from initiators bearing inorganic heterocyclic fragments such as cyclotetrasiloxanes and cyclotriphosphazenes.[315,345] Polymerizations of styrene and acrylates from these initiators yielded polymers with low polydispersities. In addition, the first 6-armed star block copolymer composed of a poly(methyl acrylate) core and poly(isobornyl acrylate) shell was synthesized.[315,345]

Two groups have reported the use of functional calixarenes as initiators for ATRP. The first study examined dichloroacetate substituted calixarenes with functionalities of 4, 6, and 8. Polymerizations of MMA and n-butyl acrylate were well-controlled as demonstrated by the agreement between the theoretical and measured arm molecular weight following cleavage of the core.[346] A star block copolymer of PMMA and poly(BMA) was synthesized from the octafunctional initiator. The ATRP of styrene from octafunctional 2-bromopropionate modified calixarenes was also studied.[347] Below 20% conversion the polymerization was controlled by agreement between measured and theoretical molecular weight. Above that conversion, high molecular weight shoulders were observed by online light scattering measurements, which the authors attributed to coupling between stars. However, under the proper conditions of high dilution and cessation of the polymerization at low conversion, stars with molecular weights as high as $M_n = 340,000$ were formed. In a similar way, multifunctional initiators with three, four, six, and eight sulfonyl halide groups were used to prepare star polymers with methacrylates and styrene.[145]

Dendrimer-forming moieties were used to synthesize hexa- and dodecafunctionalized initiators composed of 2-bromoisobutyrates.[348] Polydispersities were quite low, $M_w/M_n < 1.12$. The same initiators were used in the synthesis of star block copolymers composed of t-butyl acrylate and MMA, in both orders, extending from the core.[349] Following hydrolysis of the t-butyl esters to acrylic acid,

^{1}H NMR studies showed that the stars formed unimolecular micelles; the structure changed its conformation according to the selectivity of the solvent toward the two segments of the copolymer. Similarly, star block copolymers of MMA and HEMA were prepared.[350] It is expected that these polymers would find applications as novel templating materials for the preparation of porous low dielectric constant films.

The "dendrimerlike" star block copolymers have been synthesized from initiators produced by dendrimer techniques.[351] Synthesis of this multibranched macromolecule began with ε-caprolactone polymerization from a hexafunctional initiator. Each hydroxyl end group was then chemically transformed into two 2-bromoisobutyrate moieties, which were used to initiate the ATRP of either MMA or a mixture of MMA/HEMA. The thermal and mechanical studies of the caprolactone/MMA system showed that the material was phase-separated. The hydroxyl groups from HEMA in the statistical copolymer were used to initiate the ring opening polymerization of ethylene oxide to yield an amphiphilic star block–graft copolymer.[351]

"Tandem polymerization" was used to synthesize a 4-arm star polymer where the arms consist of PMMA synthesized by ATRP from poly(di-*n*-hexylfluorene).[352] The macroinitiator was obtained by esterification of the aryl dihydroxy terminal units of the macroinitiator with 2-bromoisobutyryl bromide.

Esterification of the natural products D-glucose and β-cyclodextrin with 2-bromoisobutyryl bromide[353] yields initiators with functionality of 5 and 21, respectively; the initiators were used for the ATRP of styrene and MMA. From the glucose derivative, both polymerizations resulted in molecular weights that were close to the theoretically predicted values based on linear standards, which is surprising for multifunctional stars. The polydispersity for the PMMA star was $M_w/M_n = 1.18$ but a higher value of $M_w/M_n = 1.70$ was obtained for the styrene polymerization. For the more highly branched β-cyclodextrin star, the SEC trace of the PMMA sample was multimodal. In the styrene polymerization, a network resulted due to coupling of the arms.

Coordination chemistry has been used in the synthesis of star polymers with up to 6 arms per molecule.[354] 4,4′-Bis(chloromethyl)-2,2′-bipyridine or mixtures of that ligand with unsubstituted bipyridine was coordinated to ruthenium(II) such that complexes with two, four, or six alkyl halide moieties per metal complex were obtained. The 4-chloromethyl groups on the ligand were then used to initiate the copper-mediated ATRP of styrene or nickel-mediated ATRP of methyl acrylate. A convergent approach has recently been reported where 2,2′-bipyridines substituted by polystyrene prepared by ATRP were made before coordination took place.[355] Using a divergent strategy, metallodendrimers were used to start ATRP and form multifunctional stars.[356]

All of the aforementioned literature reports showed star polymer formation originating from a core. The so-called "arm-first" approach has also been used (Scheme 11.22). Linear polymers of polystyrene[357] or poly(*t*-butyl acrylate)[212] were first prepared by ATRP. The resulting polymers were subsequently allowed to react with crosslinking reagents such as divinyl benzene, 1,4-butanediol diacrylate, and ethylene glycol dimethacrylate to form crosslinked cores. Several factors pertinent to star polymer formation, including the choice of the exchanging halogen
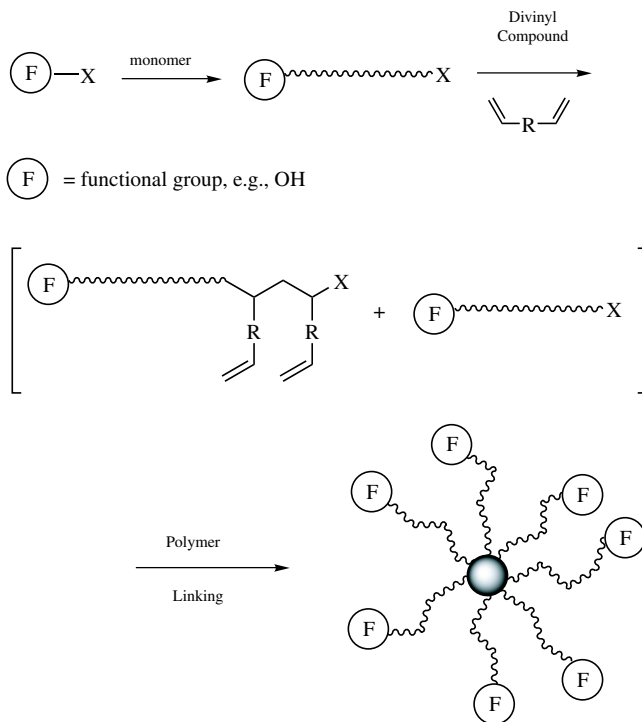
Scheme 11.22   Functional star polymers by the ''arm-first'' approach.

and solvent, the addition of a copper(II) species, the ratio of the coupling reagent to the macroinitiator, and the reaction time for the star formation are crucial for efficient star formation. The highest efficiency ($\sim$95%) was observed with 10–15-fold excess of the difunctional monomer over chain ends. Functional initiators were used to directly prepare arms with α-functionalities since ATRP is highly tolerant to functional groups. End-functional star polymers with hydroxy, epoxy, amino, cyano, and bromine groups on the outer layers have been successfully synthesized.[212] An alternative approach to end-functional stars can employ a chain end transformation process, such as a radical addition reaction to incorporate epoxy or hydroxy groups.[258]

When a difunctional initiator was first used followed by reaction with difunctional monomer, crosslinked polymer gels were formed.[358] The studies of the swelling equilibrium of different parts of the same sample showed that these gels were fairly homogeneous.

11.5.3.4 Hyperbranched Polymers   Within the context of ATRP, hyperbranched polymers are prepared by the self-condensing vinyl polymerization (SCVP)[359] of AB* monomers by a controlled free-radical process. Two examples explored in detail are vinyl benzyl chloride (VBC; *p*-chloromethylstyrene)[360] and 2-(2-bromopropionyloxy)ethyl acrylate (BPEA)[361] both depicted in Scheme 11.23. Several other
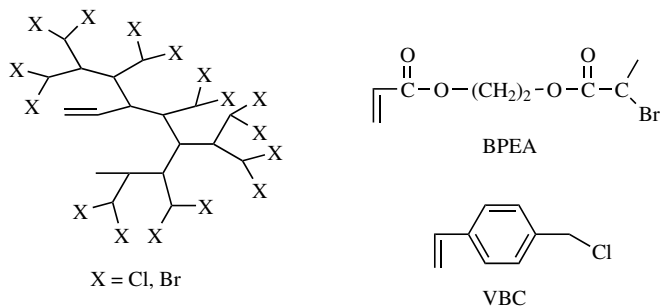
Scheme 11.23   Schematic representation of hyperbranched polymer and AB* monomers.

(meth)acrylates with either 2-bromopropionate or 2-bromoisobutyrate groups have also been used.[362] It should be noted that under certain conditions, linear homopolymers of the AB* monomers can be synthesized as intermediates on the way to other chain architectures.[80,330,361,363]

The first hyperbranched polymer synthesized by ATRP was based on VBC.[262,360] When a higher quantity of catalyst is used (>20%), more deactivator is formed, leading to faster deactivation and a higher degree of branching.[262] However, in the presence of more catalyst, more radicals are also formed, leading to more termination and resulting in an additional source of branching via radical coupling.

The synthesis of hyperbranched polymers from BPEA provides more information on conditions leading to either branched or linear polymers.[363–365] Molecular weight does not dramatically increase until conversions are greater than 50%.[363] This is in accordance with step-growth polymerization, and values predicted by theoretical treatments of the system.[365,366] A degree of branching $DB = 0.49$ was measured by ^{1}H NMR. The choice of catalyst can influence the formation of linear polymers over branched structures or produce such an active polymerization that too much irreversible termination occurs and the reaction effectively shuts down.[363] Later studies showed that inclusion of Cu(0) to reduce the excess of deactivator formed in the reaction allowed the polymerizations to continue.[362] Furthermore, the solubility of the deactivator plays a profound role in determining the topology of the polymers.[365] When more CuBr$_2$ complex was in solution, deactivation was faster, allowing for a more random initiation from the various alkyl halide species present in the macromolecules, which leads to a higher degree of branching. With less deactivator, multiple monomer additions per activation can occur, thereby decreasing the degree of branching. In a similar way, macroinitiators were used to reduce the proportion of branched units.[367]

This illustrates importance of the exchange reactions. The ratio of the rate of deactivation to that of propagation affects not only polydispersity but also the structure of the entire polymer chain by changing the degree of branching. Thus, timing of the exchange process (chronoselectivity?) may affect chain topology but in some cases also microstructure (composition, tacticity, proportion of branched units) and polydispersities.

The terminal halogens in hyperbranched polymers have been replaced by functionality more useful for downstream applications, such as azido, amino, hydroxy,

and epoxy, using radical addition reactions.[258] For example, terminal bromines in the hyperbranched poly(2-bromopropionyloxy-2-ethyl acrylate) (PBPEA) were displaced by azide anions. The resulting polyacrylates with ∼80 functional groups were thermally (200°C) or photochemically crosslinked. The labile bromines in PBPEA were used to insert functional monomers, non-polymerizable by ATRP, such as allyl alcohol and 1,2-epoxy-5-hexene via an ATRA reaction. The resulting multifunctional polyols and polyepoxides can be potentially used in thermosetting technologies.

Hydrophilic poly(ethylene glycol) or pentaerythritol ethoxylate cores with hyperbranched polystyrene arms were prepared by reacting PEG or pentaerythritol ethoxylate with 2-bromopropionyl bromide followed use of the macroinitiator for the ATRP of chloromethylstyrene to produce an amphiphilic hyperbranched polymer. Depending on the functionality of the macroinitiator, the products have either a dumbbell or 4-arm starburst structure. The dumbbell polymers tend to have higher molecular weights, while the starburst polymers have rather low molecular weights.[368]

Heat-resistant hyperbranched copolymers of VBC and N-cyclohexylmaleimide have also been synthesized by ATRP. Under the identical polymerization conditions and after the same reaction time, high monomer conversions occurred near the equimolar feed composition, indicating the formation of charge transfer complexes between VBC (electron donor) and maleimide (electron acceptor). As expected, the T_g of the copolymer increased with an increasing content of maleimide in the feed.[369]

Hyperbranched polymers can further initiate polymerizations forming dendrigraft polymers. Thus, hyperbranched polymers prepared from vinyl benzyl chloride were used to initiate the ATRP of n-butyl acrylate[370] and styrene.[371] Dendrigraft polystyrene was found to display a lower intrinsic viscosity and higher thermal stability than linear polystyrenes.[371] More recently, hyperbranched polyglycerol prepared by a ring-opening multibranching polymerization was esterified with 2-bromoisobutyryl bromide to form a macroinitiator that was used to initiate the ATRP of MA, resulting in multiarm block copolymers with polyether core and ∼50 PMA arms.[372]

By combining the concept of SCVP and "simultaneous living polymerization," hyperbranched polymers have been prepared using monomers containing both a polymerizable group and an initiating site, but the polymerizable group and the initiating site undergo different polymerization mechanisms.[373] The molecular architecture can be conveniently altered by adding monomers that can be polymerized by only one of the mechanisms.

11.6   CONCLUSIONS

This chapter presented the field of ATRP, since first reports in 1995 to approximately the end of 2000. Knowledge of the mechanism and kinetics of this process has enabled synthesis of various polymeric materials with novel functionalities, compositions, and topologies. However, since ATRP is a complex multicomponent system,

it is important to understand and to consider all of its components to make full use of this methodology and find the optimum polymerization conditions for the preparation of specific materials for particular applications. This understanding will allow ATRP processes to continue to evolve and provide lower cost commercially viable systems. A spectrum of physical properties will be developed for the expanded range of materials prepared by CRP to allow industry to target products to meet the requirements of specific applications.

A detailed knowledge of the structure and interactions of the involved reagents, and correlation between their configuration and reactivity, is needed. The desired level of information on rate constants of propagation and termination is presently available for only a few monomers from PLP measurements.[374] Precise information on the variation of the rate coefficients of termination with chain length and viscosity must be obtained to properly model ATRP and other CRP processes. Precise activation and deactivation rate constants should be measured for many catalytic systems under different conditions (monomer, solvent, temperature for both model and macromolecular systems), since only preliminary information on dynamics of atom transfer equilibria is currently available. As we start to understand the interactions of the involved reagents, alkyl group, (pseudo)halogen, transition metal, ligand, solvent, and temperature on these reactions, our ability to prepare materials with desired properties will expand.

The transition metal catalyst is the core component of ATRP systems. The search for more active and more selective catalysts will continue, and may get inspiration from enzymatic systems. Expansion of ATRP catalysts to earlier transition metals and lanthanides will require special tuning of the properties of the metal centers by suitable ligands. New catalysts are required to expand the range of monomers polymerizable by ATRP to include acidic and also less reactive monomers such as vinyl halides, esters, or even α-olefins. We are still at an embryonic stage in the development of systems for catalyst removal, regeneration and recycling. Challenges remain related to extension of ATRP to heterogeneous systems such as emulsion, suspension, or dispersion polymerization in aqueous media. Other biphasic systems such as use of supported catalysts, ionic liquids or other nonsolvents may assist in catalyst recycle.

Many new functional polymers with novel and controlled compositions and topologies have been prepared by ATRP and a complete structure–property relationship has to be developed to allow a correlation of molecular structure with macroscopic properties. The degree of end functionality must be precisely measured, although this is not an easy task, especially for higher molecular weight products. Efficiency of block and graft copolymerization must also be precisely known; perhaps 2D (two-dimensional) chromatography techniques can provide more information than currently used SEC. We still do not know how to define the quality and a shape of a gradient copolymer on the molecular level and how the gradient affects properties. More information on the effect on properties resulting from control of topologies in complex architectures such as stars, molecular brushes, hyperbranched systems and networks is also needed. A combination of this information with a systematic variation of molecular weights (perhaps also shape of molecular weight

distribution and not only overall polydispersities), composition (including gradients), end functionalities, and topologies should provide access to the needed comprehensive structure–property correlation. However, since morphologies may also be kinetically trapped, processing (i.e., mechanical stresses, solvent removal, and thermal history) may affect the final properties of the materials. Thus, processing should also be taken into consideration during the development of this comprehensive composition/property correlation. Semiempirical simulations will be employed to assist in the construction of this comprehensive picture by modeling of entire routes, including synthesis and processing to ultimately obtain materials with desired function for a targeted application. We have stressed the role of ATRP for the preparation of end-functional low molar mass polymers, "difficult" block copolymers, multiarm stars, and combs, but we also included hybrid materials with polymers prepared by different mechanisms or attached to inorganic or biomaterials, partly to define the capabilities of ATRP, in the belief that such hybrid systems can phase separate at nanoscale dimensions thereby generating entirely new materials for variety of special applications.

Although ATRP may be the most versatile system among the recently developed CRP methods, we recognize that for various targeted materials nitroxide or degenerative systems (RAFT) may be equally or even better suited. Regardless, the development of CRP techniques should have a tremendous impact on the range of commercial products prepared by a free radical method. While materials prepared by CRP may replace products made by some other techniques such as group transfer or anionic polymerization, opportunities lie in defining markets for entirely new materials. The first products prepared by controlled radical polymerization are being introduced and it is anticipated that the others will quickly follow. Patent activity indicate market targets include coatings, adhesives, elastomers, sealants, lubricants, imaging materials, powder binder compositions, pigment dispersants, personal care compositions, detergents, water treatment chemicals, and telechelic materials with hydroxy, epoxy, carboxy, and amine functionality in addition to amphiphilic block copolymers. Higher-value applications include photopaternable materials and biological sensors.

In summary, ATRP is a valuable tool for the design and synthesis of novel materials for numerous applications. They can be prepared under facile reaction conditions, using a multitude of available polymerizable monomers, with accessible chain functionalities. The types of (co)polymers produced by ATRP will be limited only by the imagination of those generating the materials.

REFERENCES

1. T. E. Patten and K. Matyjaszewski, *Adv. Mater.* **10**, 901 (1998).

2. a) K. Matyjaszewski and J. Xia, *Chem. Rev.* **101**, 2921 (2001); b) M. Kamigaito, T. Audo, M. Sawamoto, *Chem. Rev.* **101**, 3689 (2001).

3. M. Sawamoto and M. Kamigaito, *Trends Polym. Sci.* **4**, 371 (1996).

4. K. Matyjaszewski, *Curr. Opin. Solid State Mater. Sci.* **1**, 769 (1996).

5. T. E. Patten and K. Matyjaszewski, *Acc. Chem. Res.* **32**, 895 (1999).

6. K. Matyjaszewski, *Chem. Eur. J.* **5**, 3095 (1999).

7. D. P. Curran, *Synthesis* 489 (1988).

8. M. S. Kharasch and E. V. Jensen, *Science* **102**, 128 (1945).

9. a) M. Asscher and D. Vofsi, *J. Chem. Soc.* 3921 (1963); b) F. Minisci, *Acc. Chem. Res.* **8**, 165 (1975).

10. B. Boutevin, *J. Polym. Sci.; Part A: Polym. Chem.* **38**, 3235 (2000).

11. a) C. H. Bamford, in *Comprehensive Polymer Science*, G. Allen, S. L. Aggarwal, and S. Russo, eds., Pergamon, Oxford, 1989, p. 123; b) W. I. Bengough and W. H. Fairservice, *Trans. Faraday Soc.* **67**, 414 (1971).

12. J. Qiu and K. Matyjaszewski, *Acta Polym.* **48**, 169 (1997).

13. M. Kato, M. Kamigaito, M. Sawamoto, and T. Higashimura, *Macromolecules* **28**, 1721 (1995).

14. J. S. Wang and K. Matyjaszewski, *J. Am. Chem. Soc.* **117**, 5614 (1995).

15. K. Matyjaszewski and J. S. Wang, WO 9630421; U.S. Patent 5,763,548 (1998).

16. K. Matyjaszewski, S. Coca, S. G. Gaynor, D. Greszta, T. E. Patten, J. S. Wang, and J. Xia, WO 9718247; U.S. Patent 5,807,937 (1998).

17. K. Matyjaszewski, S. Coca, S. G. Gaynor, Y. Nakagawa, and S. M. Jo, WO 9801480; U.S. Patent 5,789,487 (1998).

18. H. Fischer, *J. Polym. Sci.; Part A: Polym. Chem.* **37**, 1885 (1999).

19. H. Fischer, *Macromolecules* **30**, 5666 (1997).

20. D. A. Shipp and K. Matyjaszewski, *Macromolecules* **32**, 2948 (1999).

21. K. Davis, H.-J. Paik, and K. Matyjaszewski, *Macromolecules* **32**, 1767 (1999).

22. K. Matyjaszewski, *ACS Symp. Ser.* **685**, 2 (1998).

23. A. E. Acar, M. B. Yagci, and L. J. Mathias, *Macromolecules* **33**, 7700 (2000).

24. D. A. Shipp and K. Matyjaszewski, *Macromolecules* **33**, 1553 (2000).

25. K. Matyjaszewski, T. E. Patten, and J. Xia, *J. Am. Chem. Soc.* **119**, 674 (1997).

26. A. Kajiwara, K. Matyjaszewski, and M. Kamachi, *Macromolecules* **31**, 5695 (1998).

27. A. Orochov, M. Levy, M. Asscher, and D. Vofsi, *J. Chem. Soc. Perkin II*, 857 (1974).

28. K. Matyjaszewski, *ACS Symp. Ser.* **685**, 258 (1998).

29. K. Matyjaszewski, *Macromol. Symp.* **111**, 47 (1996).

30. K. Matyjaszewski, M. Wei, J. Xia, and S. G. Gaynor, *Macromol. Chem. Phys.* **199**, 2289 (1998).

31. M. Buback, *ACS Symp. Ser.* **768**, 39 (2000).

32. J. S. Wang and K. Matyjaszewski, *Macromolecules* **28**, 7572 (1995).

33. a) W. Wang, Z. Dong, P. Xia, and Q. Zhang, *Macromol. Rapid Commun.* **19**, 647 (1998); b) W. Wang and D. Yan, *ACS Symp. Ser.* **768**, 263 (2000).

34. J. Xia and K. Matyjaszewski, *Macromolecules* **32**, 5199 (1999).

35. J. Xia and K. Matyjaszewski, *Macromolecules* **30**, 7692 (1997).

36. J. Qiu, S. Gaynor, and K. Matyjaszewski, *Macromolecules* **32**, 2872 (1999).

37. G. Moineau, P. Dubois, R. Jérôme, T. Senninger, and P. Teyssié, *Macromolecules* **31**, 545 (1998).

38. X.-P. Chen and K.-Y. Qiu, *Macromolecules* **32**, 8711 (1999).

39. S.-H. Qin, K.-Y. Qiu, G. Swift, D. G. Westmoreland, and S. Wu, *J. Polym. Sci.; Part A: Polym. Chem.* **37**, 4610 (1999).

40. X.-P. Chen and K.-Y. Qiu, *Chem. Commun.*, 233 (2000).

41. S. Gaynor, J. Qiu, and K. Matyjaszewski, *Macromolecules* **31**, 5951 (1998).

42. K. Matyjaszewski, D. A. Shipp, J. Qiu, and S. G. Gaynor, *Macromolecules* **33**, 2296 (2000).

43. X. Wan and S. Ying, *J. Appl. Polym. Sci.* **75**, 802 (2000).

44. S. Coca, C. B. Jasieczek, K. L. Beers, and K. Matyjaszewski, *J. Polym. Sci., A., Polym. Chem.* **36**, 1417 (1998).

45. X. S. Wang, S. F. Lascelles, R. A. Jackson, and S. P. Armes, *Chem. Commun.* 1817 (1999).

46. J. Xia, T. Johnson, S. Gaynor, K. Matyjaszewski, and J. DeSimone, *Macromolecules* **32**, 4802 (1999).

47. T. Nishikawa, M. Kamigaito, and M. Sawamoto, *Macromolecules* **32**, 2204 (1999).

48. K. Matyjaszewski, J. Qiu, N. V. Tsarevsky, and B. Charleux, *J. Polym. Sci.; Part A: Polym. Chem.* **38**, 4724 (2000).

49. J. Qiu, T. Pintauer, S. G. Gaynor, K. Matyjaszewski, B. Charleux, and J.-P. Vairon, *Macromolecules* **33**, 7310 (2000).

50. a) B. Charleux, *Macromolecules* **33**, 5358 (2000); b) J. Qiu, B. Charleux, and K. Matyjaszewski, *Prog. Polym. Sci.* **26**, 2083 (2001).

51. V. Percec, B. Barboiu, and A. Neumann, *Macromolecules* **29**, 3665 (1996).

52. D. M. Haddleton, C. C. Martin, B. H. Dana, D. J. Duncalf, A. M. Heming, D. Kukulj, and A. J. Shooter, *Macromolecules* **32**, 2110 (1999).

53. V. Percec, B. Barboiu, and H.-J. Kim, *J. Am. Chem. Soc.* **120**, 305 (1998).

54. T. E. Patten, J. Xia, T. Abernathy, and K. Matyjaszewski, *Science* **272**, 866 (1996).

55. K. Matyjaszewski, S. Coca, S. G. Gaynor, M. Wei, and B. E. Woodworth, *Macromolecules* **31**, 5967 (1998).

56. a) K. L. Beers, B. Woodworth, and K. Matyjaszewski, *J. Chem. Ed* **78**, 544 (2001); b) K. Matyjaszewski, K. L. Beers, B. Woodworth, and Z. Metzner, *J. Chem. Ed* **78**, 547 (2001).

57. a) G. Kickelbick, H.-J. Paik, and K. Matyjaszewski, *Macromolecules* **32**, 2941 (1999); b) D. M. Haddleton, D. J. Duncalf, D. Kukulj, and A. P. Radigue, *Macromolecules* **32**, 4769 (1999).

58. a) D. M. Haddleton, D. Kukulj, and A. P. Radigue, *Chem. Commun.* 99 (1999); b) Y. Shen, S. Zhu, and R. Pelton, *Macromolecules* **33**, 5427 (2000); c) Y. Shen, S. Zhu, and R. Pelton, *Macromol. Rapid Commun.* **21**, 956 (2000).

59. K. Matyjaszewski, T. Pintauer, and S. Gaynor, *Macromolecules* **33**, 1476 (2000).

60. S. C. Hong, H. P. Paik, and K. Matyjaszewski, *Macromolecules* **34**, 5099 (2001).

61. S. Liou, J. T. Rademacher, D. Malaba, M. E. Pallack, and W. J. Brittain, *Macromolecules* **33**, 4295 (2000).

62. C.-Y. Pan and X.-D. Lou, *Macromol. Chem. Phys.* **201**, 1115 (2000).

63. J. Queffelec, S. G. Gaynor, and K. Matyjaszewski, *Macromolecules* **33**, 8629 (2000).

64. F. Simal, A. Demonceau, and A. F. Noels, *Angew. Chem. Int. Ed. Engl.* **38**, 538 (1999).

65. T. Grimaud and K. Matyjaszewski, *Macromolecules* **30**, 2216 (1997).

66. D. M. Haddleton, C. B. Jasieczek, M. J. Hannon, and A. J. Shooter, *Macromolecules* **30**, 2190 (1997).

67. C. Granel, P. Dubois, R. Jérôme, P. Teyssié, *Macromolecules* **29**, 8576 (1996).

68. H. Uegaki, Y. Kotani, M. Kamigato, and M. Sawamoto, *Macromolecules* **31**, 6756 (1998).

69. G. Moineau, M. Minet, P. Dubois, P. Teyssié, T. Senninger, and R. Jérôme, *Macromolecules* **32**, 27 (1999).

70. T. Ando, M. Kamigaito, and M. Sawamoto, *Macromolecules* **30**, 4507 (1997).

71. K. Matyjaszewski, M. Wei, J. Xia, and N. E. McDermott, *Macromolecules* **30**, 8161 (1997).

72. J. Louie and R. H. Grubbs, *Chem. Commun.* 1479 (2000).

73. P. Lecomte, I. Drapier, P. Dubois, P. Teyssié, and R. Jérôme, *Macromolecules* **30**, 7631 (1997).

74. G. Moineau, C. Granel, P. Dubois, R. Jérôme, and P. Teyssié, *Macromolecules* **31**, 542 (1998).

75. T. Ando, M. Kamigaito, and M. Sawamoto, *Tetrahedron* **53**, 15445 (1997).

76. K. Matyjaszewski, J.-L. Wang, T. Grimaud, and D. A. Shipp, *Macromolecules* **31**, 1527 (1998).

77. Y. Kotani, M. Kato, M. Kamigaito, and M. Sawamoto, *Macromolecules* **29**, 6979 (1996).

78. X. Zhang, J. Xia, and K. Matyjaszewski, *Macromolecules* **31**, 5167 (1998).

79. K. L. Beers, S. Boo, S. G. Gaynor, and K. Matyjaszewski, *Macromolecules* **32**, 5772 (1999).

80. K. L. Beers, S. G. Gaynor, K. Matyjaszewski, S. S. Sheiko, and M. Moller, *Macromolecules* **31**, 9413 (1998).

81. X. Zhang, J. Xia, and K. Matyjaszewski, *Polym. Prep.* (*Am. Chem. Soc., Div. Polym. Chem.*) **40**(2), 440 (1999).

82. E. J. Ashford, V. Naldi, R. O'Dell, N. C. Billingham, and S. P. Armes, *Chem. Commun.* 1285 (1999).

83. X. S. Wang and S. P. Armes, *Macromolecules* **33**, 6640 (2000).

84. D. Betts, T. Johnson, C. Anderson, and J. M. DeSimone, *Polym. Prep.* (*Am. Chem. Soc., Polym. Div.*) **38**, 760 (1997).

85. a) Z. Zhang, S. Ying, and Z. Shi, *Polymer* **40**, 5439 (1999); b) Y. Li, W. Zhang, Z. Yu, and J. Huang, *Polym. Prep.* (*Am. Chem. Soc., Div. Polym. Chem.*) **41**(1), 202 (2000).

86. X. S. Wang, R. A. Jackson, and S. P. Armes, *Macromolecules* **33**, 255 (2000).

87. K. A. Davis, B. Charleux, and K. Matyjaszewski, *J. Polym. Sci.; Part A: Polym. Chem.* **38**, 2274 (2000).

88. K. Matyjaszewski, S. M. Jo, H.-J. Paik, and S. G. Gaynor, *Macromolecules* **30**, 6398 (1997).

89. S. M. Jo, S. G. Gaynor, and K. Matyjaszewski, *Polym. Prep.* (*Am. Chem. Soc., Polym. Div.*) **37**(2), 272 (1996).

90. K. Matyjaszewski, S. M. Jo, H.-J. Paik, and D. A. Shipp, *Macromolecules* **32**, 6431 (1999).

91. D. Greszta and K. Matyjaszewski, *Polym. Prep.* (*Am. Chem. Soc., Polym. Div.*) **37**(2), 569 (1996).

92. D. Greszta, K. Matyjaszewski, and T. Pakula, *Polym. Prep.* (*Am. Chem. Soc., Div. Polym. Chem.*) **38**(1), 709 (1997).

93. J.-S. Wang and K. Matyjaszewski, *Macromolecules* **28**, 7901 (1995).

94. V. Percec and B. Barboiu, *Macromolecules* **28**, 7970 (1995).

95. Y. Kotani, M. Kamigaito, and M. Sawamoto, *Macromolecules* **33**, 6746 (2000).

96. a) K. Endo and A. Yachi, *Polym. Bull.* **46**, 363 (2001); b)Y. Kotani, M. Kamigaito, and M. Sawamoto, *Macromolecules* **32**, 2420 (1999).

97. K. Matyjaszewski, V. Coessens, Y. Nakagawa, J. Xia, J. Qiu, S. Gaynor, S. Coca, and C. Jasieczek, *ACS Symp. Ser.* **704**, 16 (1998).

98. M. Destarac, J.-M. Bessiere, and B. Boutevin, *J. Polym. Sci.; A: Polym. Chem.* **36**, 2933 (1998).

99. J. Xia and K. Matyjaszewski, *Macromolecules* **30**, 7697 (1997).

100. K. Matyjaszewski, K. Davis, T. Patten, and M. Wei, *Tetrahedron* **53**, 15321 (1997).

101. K. Matyjaszewski, *Macromol. Symp.* **134**, 105 (1998).

102. J. Qiu and K. Matyjaszewski, *Macromolecules* **30**, 5643 (1997).

103. B. Gao, X. Chen, B. Ivan, J. Kops, and W. Batsberg, *Macromol. Rapid Commun.* **18**, 1095 (1997).

104. K. B. Clark and D. D. M. Wayner, *J. Am. Chem. Soc.* **113**, 9363 (1991).

105. M. Teodorescu, S. G. Gaynor, and K. Matyjaszewski, *Macromolecules* **33**, 2335 (2000).

106. J. Xia, S. G. Gaynor, and K. Matyjaszewski, *Macromolecules* **31**, 5958 (1998).

107. A. Mühlebach, S. G. Gaynor, and K. Matyjaszewski, *Macromolecules* **31**, 6046 (1998).

108. S. Coca, C. Jasieczek, and K. Matyjaszewski, *Macromol. Chem. Phys.* **198**, 4011 (1997).

109. S. Coca, K. Davis, P. Miller, and K. Matyjaszewski, *Polym. Prep.* (*Am. Chem. Soc., Div. Polym. Chem.*) **38**(1), 689 (1997).

110. K. A. Davis and K. Matyjaszewski, *Macromolecules* **33**, 4039 (2000).

111. S. Coca and K. Matyjaszewski, *Polym. Prep.* (*Am. Chem. Soc., Div. Polym. Chem.*) **38**(1), 691 (1997).

112. M. Teodorescu and K. Matyjaszewski, *Macromolecules* **32**, 4826 (1999).

113. J. T. Rademacher, M. Baum, M. E. Pallack, W. J. Brittain, and W. J. Simonsick, Jr., *Macromolecules* **33**, 284 (2000).

114. a) M. Teodorescu and K. Matyjaszewski, *Polym. Prep.* (*Am. Chem. Soc., Div. Polym. Chem.*) **40**(2), 428 (1999); b) M. Teodorescu and K. Matyjaszewski, *Macromol. Rapid Commun.* **21**, 190 (2000).

115. M. Senoo, Y. Kotani, M. Kamigaito, and M. Sawamoto, *Macromolecules* **32**, 8005 (1999).

116. a) K. Matyjaszewski, K. L. Beers, A. Muhlebach, S. Coca, X. Zhang, and S. G. Gaynor, *Polym. Mater. Sci. Eng.* **79**, 429 (1998); b) C. Konák, B. Ganchev, M. Teodorescu, K. Matyjaszewski, P. Kopecková, and J. Kopecek, *Polymer* **43**, 3753 (2002).

117. J. Xia, X. Zhang, and K. Matyjaszewski, *Macromolecules* **32**, 3531 (1999).

118. S. Coca and K. Matyjaszewski, *Polym. Prep.* (*Am. Chem. Soc., Div. Polym. Chem.*) **37**(1), 573 (1996).

119. S. G. Gaynor and K. Matyjaszewski, *ACS Symp. Ser.* **685**, 396 (1998).

120. a) G.-Q. Chen, Z.-Q. Wu, J.-R. Wu, Z.-R. Li, and F.-M. Li, *Polym. Prep.* (*Am. Chem. Soc., Div. Polym. Chem.*) **40**(2), 360 (1999); b) X. Jiang, P. Xia, W. Liu, and D. Yan, *J. Polym. Sci.; Part A: Polym. Chem.* **38**, 1203 (2000); c) F.-M. Li, G.-Q. Chen, M.-Q. Zhu, P. Zhou, F.-S. Du, and Z.-C. Li, *ACS Symp. Ser.* **768**, 384 (2000).

121. G.-Q. Chen, Z.-Q. Wu, J.-R. Wu, Z.-C. Li, and F.-M. Li, *Macromolecules* **33**, 232 (2000).

122. X. Jiang, D. Yan, Y. Zhong, and W. Liu, *Polym. Prep.* (*Am. Chem. Soc., Div. Polym. Chem.*) **41**(1), 442 (2000).

123. J. Xia, H.-J. Paik, and K. Matyjaszewski, *Macromolecules* **32**, 8310 (1999).

124. H.-J. Paik, M. Teodorescu, J. Xia, and K. Matyjaszewski, *Macromolecules* **32**, 7023 (1999).

125. X.-P. Chen, A. B. Padias, and H. K. Hall, Jr., *Macromolecules* **34**, 3514 (2001).

126. J.-Y. Yuan, C.-Y. Pan, and B. Z. Tang, *Macromolecules* **34**, 211 (2001).

127. K. Davis, J. O'Malley, H.-J. Paik, and K. Matyjaszewski, *Polym. Prep.* (*Am. Chem. Soc., Div. Polym. Chem.*) **38**(1), 687 (1997).

128. M. Nishimura, M. Kamigaito, and M. Sawamoto, *Polym. Prep.* (*Am. Chem. Soc., Div. Polym. Chem.*) **40**(2), 470 (1999).

129. N. K. Singha and B. Klumperman, *Macromol. Rapid Commun.* **21**, 1116 (2000).

130. M. Destarac, K. Matyjaszewski, and B. Boutevin, *Macromol. Chem. Phys.* **201**, 265 (2000).

131. H. Uegaki, Y. Kotani, M. Kamigato, and M. Sawamoto, *Macromolecules* **30**, 2249 (1997).

132. H. Uegaki, M. Kamigato, and M. Sawamoto, *J. Polym. Sci.; Part A: Polym. Chem.* **37**, 3003 (1999).

133. K. Matyjaszewski, D. A. Shipp, J.-L. Wang, T. Grimaud, and T. E. Patten, *Macromolecules* **31**, 6836 (1998).

134. A. Neumann, H. Keul, and H. Hocker, *Macromol. Chem. Phys.* **201**, 980 (2000).

135. J.-L. Wang, T. Grimaud, and K. Matyjaszewski, *Macromolecules* **30**, 6507 (1997).

136. a) H. C. Brown and R. S. Fletcher, *J. Am. Chem. Soc.* **71**, 1845 (1949); b) H. Mayr, M. Roth, and R. Faust, *Macromolecules* **29**, 6110 (1996).

137. H. Takahashi, T. Ando, M. Kamigaito, and M. Sawamoto, *Macromolecules* **32**, 3820 (1999).

138. D. M. Haddleton, C. Waterson, and P. J. Derrick, *Chem. Commun.*, 683 (1997).

139. X. Zhang and K. Matyjaszewski, *Macromolecules* **32**, 7349 (1999).

140. D. M. Haddleton, P. J. Derrick, M. D. Eason, and C. Waterson, *Polym. Prep.* (*Am. Chem. Soc., Div. Polym. Chem.*) **40**(2), 327 (1999).

141. F. Zeng, Y. Shen, S. Zhu, and R. Pelton, *J. Polym. Sci.; Part A: Polym. Chem.* **38**, 3821 (2000).

142. T. Ando, M. Kato, M. Kamigaito, and M. Sawamoto, *Macromolecules* **29**, 1070 (1996).

143. T. Nishikawa, T. Ando, M. Kamigaito, and M. Sawamoto, *Macromolecules* **30**, 2244 (1997).

144. V. Percec, H. J. Kim, and B. Barboiu, *Macromolecules* **30**, 8526 (1997).

145. V. Percec, B. Barboiu, T. K. Bera, M. van der Sluis, R. B. Grubbs, and J. M. J. Frechet, *J. Polym. Sci.; Part A: Polym. Chem.* **38**, 4776 (2000).

146. M. Matsuyama, M. Kamigato, and M. Sawamoto, *J. Polym. Sci.; A: Polym. Chem.* **34**, 3585 (1996).

147. a) K. Matyjaszewski, ed., *Cationic Polymerizations: Mechanisms, Synthesis and Applications*, Marcel Dekker, New York, 1996; b) K. Matyjaszewski and P. Sigwalt, *Polym. Int.* **35**, 1 (1994).

148. A. Goto and T. Fukuda, *Macromol. Rapid Commun.* **20**, 633 (1999).

149. H.-J. Paik and K. Matyjaszewski, *Polym. Prep.* (*Am. Chem. Soc., Div. Polym. Chem.*) **41**(1), 470 (2000).

150. T. Ando, M. Kamigaito, and M. Sawamoto, *Macromolecules* **33**, 2819 (2000).

151. D. A. Shipp, J.-L. Wang, and K. Matyjaszewski, *Macromolecules* **31**, 8005 (1998).

152. a) J. D. Tong, G. Moineau, P. Leclere, J. L. Bredas, R. Lazzaroni, and R. Jerome, *Macromolecules* **33**, 470 (2000); b) P. Leclere, G. Moineau, M. Minet, P. Dubois, R. Jerome, J. L. Bredas, and R. Lazzaroni, *Langmuir* **15**, 3915 (1999); c) G. Moineau, M. Minet, P. Teyssié, and R. Jerome, *Macromol. Chem. Phys.* **201**, 1108 (2000).

153. J. A. M. Brandts, P. van de Geijn, E. E. van Faassen, J. Boersma, and G. van Koten, *J. Organomet. Chem.* **584**, 246 (1999).

154. E. Le Grognec, J. Claverie, and R. Poli, *J. Am. Chem. Soc.* **123**, 9513 (2001).

155. J. H. Espenson, *Acc. Chem. Res.* **25**, 222 (1992).

156. K. Matyjaszewski, S. G. Gaynor, and J.-S. Wang, *Macromolecules* **28**, 2093 (1995).

157. I. Del Rio, G. van Koten, M. Lutz, and A. L. Spek, *Organometallics* **19**, 361 (2000).

158. a) F. Simal, A. Demonceau, and A. F. Noels, *Tetrahedron Lett.* **40**, 5689 (1999); b) F. Simal, L. Delaude, D. Jan, A. Demonceau, and A. F. Noels, *Polym. Prep.* (*Am. Chem. Soc., Div. Polym. Chem.*) **40**(2), 336 (1999).

159. T. Ando, M. Kamigaito, and M. Sawamoto, *Macromolecules* **33**, 5825 (2000).

160. H. Takahashi, T. Ando, M. Kamigaito, and M. Sawamoto, *Macromolecules* **32**, 6461 (1999).

161. C. W. Bielawski, J. Louie, and R. H. Grubbs, *J. Am. Chem. Soc.* **122**, 12872 (2000).

162. P. S. Wolfe and S. T. Nguyen, *Polym. Prep.* (*Am. Chem. Soc., Div. Polym. Chem.*) **39**(2), 552 (1998).

163. Y. Kotani, M. Kamigaito, and M. Sawamoto, *Macromolecules* **32**, 6877 (1999).

164. B. B. Wayland, G. Poszmik, S. L. Mukerjee, and M. Fryd, *J. Am. Chem. Soc.* **116**, 7943 (1994).

165. H. J. Harwood, L. D. Arvanitopoulos, and M. P. Greuel, *Polym. Prep.* (*Am. Chem. Soc., Div. Polym. Chem.*) **35**(2), 549 (1994).

166. C. L. Moad, G. Moad, E. Rizzardo, and S. H. Tang, *Macromolecules* **29**, 7717 (1996).

167. D. M. Grove, A. H. M. Verschuuren, G. van Koten, and J. A. M. van Beek, *J. Organometallic Chem.* **372 (C1)**, 83 (1989).

168. K. Matyjaszewski, *Macromolecules* **31**, 4710 (1998).

169. K. Matyjaszewski, M. J. Ziegler, S. V. Arehart, D. Greszta, and T. Pakula, *J. Phys. Org. Chem.* **13**, 775 (2000).

170. J. P. A. Heuts, R. Mallesch, and T. P. Davis, *Macromol. Chem. Phys.* **200**, 1380 (1999).

171. a) A. Kajiwara and K. Matyjaszewski, *Macromol. Rapid Commun.* **19**, 319 (1998); b) A. Kajiwara and K. Matyjaszewski, *Macromolecules* **31**, 3489 (1998); c) A. Kajiwara, K. Matyjaszewski, *Polym. J.* **31**(1), 70 (1999); d) A. Kajiwara, K. Matyjaszewski, and M. Kamachi, *ACS Symp. Ser.* **768**, 68 (2000).

172. Q. Yu, F. Zeng, and S. Zhu, *Macromolecules* **34**, 1612 (2001).

173. a) M. Destarac, J. M. Bessière, and B. Boutevin, *Macromol. Rapid Commun.* **18**, 967 (1997); b) G. L. Cheng, C. P. Hu, and S. K. Ying, *Macromol. Rapid Commun.* **20**, 303 (1999); c) G. L. Wang, C. P. Hu, and S. K. Ying, *Polymer* **40**, 2167 (1999).

174. G. Kickelbick and K. Matyjaszewski, *Macromol. Rapid Commun.* **20**, 341 (1999).

175. A. J. Amass, C. A. Wyres, E. Colclough, and I. M. Hohn, *Polymer* **41**, 1697 (1999).

176. B. Yu and E. Ruckenstein, *J. Polym. Sci.; Part A: Polym. Chem.* **37**, 4191 (1999).

177. Y. Shen, S. Zhu, F. Zeng, and R. Pelton, *Macromol. Chem. Phys.* **201**, 1169 (2000).

178. J. Xia and K. Matyjaszewski, *Macromolecules* **32**, 2434 (1999).

179. a) T. Pintauer, G. Kickelbick, and K. Matyjaszewski, *Inorg. Chem.* **40**, 2818 (2001); b) G. Kickelbick, T. Pintauer, and K. Matyjaszewski, *New J. Chem.* **26**, 462 (2002).

180. G. Kickelbick, U. Reinohl, T. S. Ertel, H. Bertagnolli, and K. Matyjaszewski, *ACS Symp. Ser.* **768**, 211 (2000).

181. B. E. Woodworth, Z. Metzner, and K. Matyjaszewski, *Macromolecules* **31**, 7999 (1998).

182. V. Percec, A. D. Asandei, F. Asgarzadeh, T. K. Bera, and B. Barboiu, *J. Polym. Sci.; Part A: Polym. Chem.* **38**, 3839 (2000).

183. J. Xia and K. Matyjaszewski, *Polym. Prep.* (*Am. Chem. Soc., Div. Polym. Chem.*) **40**(2), 442 (1999).

184. J. Xia, X. Zhang, and K. Matyjaszewski, *ACS Symp. Ser.* **760**, 207 (2000).

185. M. Bednarek, T. Biedron, and P. Kubisa, *Macromol. Chem. Phys.* **201**, 58 (2000).

186. V. Coessens and K. Matyjaszewski, *J. Macromol. Sci., Pure Appl. Chem.* **A36**, 653 (1999).

187. V. Coessens and K. Matyjaszewski, *J. Macromol. Sci., Pure Appl. Chem.* **A36**, 811 (1999).

188. K. Matyjaszewski, S. Coca, S. G. Gaynor, M. Wei, and B. E. Woodworth, *Macromolecules* **30**, 7348 (1997).

189. G. L. Cheng, C. P. Hu, and S. K. Ying, *J. Mol. Catal. A: Chem.* **144**, 357 (1999).

190. V. Percec, B. Barboiu, and M. van der. Sluis, *Macromolecules* **31**, 4053 (1998).

191. J. Guo, Z. Han, and P. Wu, *J. Mol. Catal. A: Chem.* **159**, 77 (2000).

192. D. M. Haddleton, A. J. Clark, M. C. Crossman, D. J. Duncalf, S. Heming, S. R. Morsley, C. Waterson, and A. J. Shooter, *Chem. Commun.* 1173 (1997).

193. D. M. Haddleton, D. Kukulj, D. J. Duncalf, A. M. Heming, and A. J. Shooter, *Macromolecules* **31**, 5201 (1998).

194. S. C. Barton, R. A. Bird, and K. E. Russell, *Can J. Chem.* **41**, 2737 (1963).

195. K. Bagdasarian and Z. A. Sinitsina, *J. Polym. Sci.; Part A: Polym. Chem.* **52**, 31 (1961).

196. D. M. Haddleton, A. M. Heming, D. Kukulj, D. J. Duncalf, and A. J. Shooter, *Macromolecules* **31**, 2016 (1998).

197. M. van der Sluis, B. Barboiu, N. Pesa, and V. Percec, *Macromolecules* **31**, 9409 (1998).

198. J. Ueda, M. Matsuyama, M. Kamigaito, and M. Sawamoto, *Macromolecules* **31**, 557 (1998).

199. U. S. Schubert, G. Hochwimmer, C. E. Spindler, and O. Nuyken, *Macromol. Rapid Commun.* **20**, 351 (1999).

200. K. Matyjaszewski, K. Nakagawa, and C. G. Jasieczek, *Macromolecules* **31**, 1535 (1998).

201. X. Wang, N. Luo, and S. Ying, *Polymer* **40**, 4157 (1999).

202. a) X. S. Wang and S. P. Armes, *Polym. Prep.* (*Am. Chem. Soc., Div. Polym. Chem.*) **41**(1), 413 (2000); b) D. M. Haddleton, S. Perrier, S. A. F. Bon, C. Waterson, and D. Irvine, *Polym. Prep.* (*Am. Chem. Soc., Div. Polym. Chem.*) **41**(1), 415 (2000).

203. S. Pascual, B. Coutin, M. Tardi, A. Polton, and J. P. Vairon, *Macromolecules* **32**, 1432 (1999).

204. K. Matyjaszewski, *ACS Symp. Ser.* **768**, 2 (2000).

205. K. Matyjaszewski and B. E. Woodworth, *Macromolecules* **31**, 4718 (1998).

206. S. G. Roos and A. H. E. Muller, *Macromol. Rapid Commun.* **21**, 864 (2000).

207. D. M. Haddleton, M. C. Crossman, K. H. Hunt, C. Topping, C. Waterson, and K. G. Suddaby, *Macromolecules* **30**, 3992 (1997).

208. a) S. V. Arehart, D. Greszta, and K. Matyjaszewski, *Polym. Prep.* (*Am. Chem. Soc., Div. Polym. Chem.*) **38**(1), 705 (1997); b) S. V. Arehart and K. Matyjaszewski, *Macromolecules* **32**, 5582 (1999); c) G. Chambard and B. Klumperman, *ACS Symp. Ser.* **768**, 197 (2000).

209. M. J. Ziegler and K. Matyjaszewski, *Macromolecules* **34**, 415 (2001).

210. K. Matyjaszewski, H.-J. Paik, D. A. Shipp, Y. Isobe, and Y. Okamoto, *Macromolecules* **34**, 3127 (2001).

211. a) A. Kajiwara, K. Matyjaszewski, and M. Kamachi, *ACS Symp. Ser.* **768**, 68 (2000); b) K. Matyjaszewski and A. Kajiwara, *Macromolecules* **31**, 548 (1998).

212. X. Zhang, J. Xia, and K. Matyjaszewski, *Macromolecules* **33**, 2340 (2000).

213. M. R. Korn and M. R. Gagne, *Chem. Commun.* 1711 (2000).

214. J. Qiu, T. Pintauer, S. Gaynor, and K. Matyjaszewski, *Polym. Prep.* (*Am. Chem. Soc., Div. Polym. Chem.*) **40**(2), 420 (1999).

215. a) B. J. Hathaway, *Comprehensive Inorganic Chemistry.* Pergamon, Oxford, 1987; b) P. C. Healy, C. Pakawatchai, and A. H. White, *J. Chem. Soc., Dalton. Trans.* 2531 (1985); c) A. J. Pallenberg, K. S. Koenig, and D. M. Barnhart, *Inorg. Chem.* **34**, 2833 (1995).

216. M. Munakata, S. Kitagawa, A. Asahara, and H. Masuda, *Bull. Chem. Soc. Jpn.* **60**, 1927 (1987).

217. A. T. Levy, M. M. Olmstead, and T. E. Patten, *Inorg. Chem.* **39**, 1628 (2000).

218. a) G. Kickelbick, U. Reinöh, T. S. Ertel, H. Bertagnolli, and K. Matyjaszewski, *Polym. Prep.* (*Am. Chem. Soc., Polym. Div.*) **40**(2), 334 (1999); b) G. Kickelbick, U. Reinohl, T. S. Ertel, A. Weber, H. Bertagnolli, and K. Matyjaszewski, *Inorg. Chem.* **40**, 6 (2001).

219. S. R. Breeze and S. Wang, *Inorg. Chem.* **35**, 3404 (1996).

220. D. M. Haddleton, D. J. Duncalf, D. Kukulj, C. C. Martin, S. G. Jackson, S. A. B. van, A. J. Clark, and A. J. Shooter, *Eur. J. Inorg. Chem.* 1799 (1998).

221. H. Fischer, in *Free Radicals in Biology and Environment*, F. Minisci, ed., Kluwer, Dodrecht, 1997.

222. K. Matyjaszewski, H.-J. Paik, P. Zhou, and S. J. Diamanti, *Macromolecules* **34**, 5125 (2001).

223. G. Chambard, B. Klumperman, and A. L. German, *Macromolecules* **33**, 4417 (2000).

224. B. Gobelt and K. Matyjaszewski, *Macromol. Chem. Phys.* **201**, 1619 (2000).

225. K. Matyjaszewski, B. Goebelt, H.-J. Paik, and C. P. Horwitz, *Macromolecules* **34**, 430 (2001).

226. J. K. Kochi, *Organometallic Mechanisms and Catalysis*, Academic Press, New York, 1978.

227. J. Qiu, K. Matyjaszewski, L. Thouin, and C. Amatore, *Macromol. Chem. Phys.* **201**, 1625 (2000).

228. D. M. Haddleton, A. J. Shooter, M. J. Hannon, and J. A. Barker, *Polym. Prep.* (*Am. Chem. Soc., Div. Polym. Chem.*) **38**(1), 679 (1997).

229. D. T. Sawyer, A. Sobkowiak, and J. L. Roberts, *Electrochemistry for Chemists*, Wiley, New York, 1995.

230. D. Mardare, S. Gaynor, and K. Matyjaszewski, *Polym. Prep.* (*Am. Chem. Soc., Div. Polym. Chem.*) **35**(1), 700 (1994).

231. N. Navon, G. Golub, H. Cohen, and D. Meyerstein, *Organometallics* **14**, 5670 (1995).

232. V. Coessens, T. Pintauer, and K. Matyjaszewski, *Prog. Polym. Sci.* **26**, 337 (2001).

233. X. S. Wang and S. P. Armes, *Polym. Prep.* (*Am. Chem. Soc., Div. Polym. Chem.*) **41**(1), 484 (2000).

234. A. M. Kasko, A. M. Heintz, and C. Pugh, *Macromol.* **31**, 256 (1998).

235. X. Zhang, Y. Chen, A. Gong, C. Chen, and F. Xi, *Liq. Cryst.* **25**, 767 (1998).

236. a) Y.-Z. Liang, Z.-C. Li, G.-Q. Chen, and F.-M. Li, *Polym. Int.* **48**, 739 (1999); b) K. Ohno, Y. Tsujii, and T. Fukuda, *J. Polym. Sci.; Part A: Polym. Chem.* **36**, 2473 (1998).

237. A. Marsh, A. Khan, D. M. Haddleton, and M. J. Hannon, *Macromolecules* **32**, 8725 (1999).

238. K. Matyjaszewski, K. L. Beers, A. Kern, and S. G. Gaynor, *J. Polym. Sci.; Part A: Polym. Chem.* **36**, 823 (1998).

239. Y. Nakagawa and K. Matyjaszewski, *Polym. J.* **30**, 138 (1998).

240. a) F. Zeng, Y. Shen, S. Zhu, and R. Pelton, *Macromolecules* **33**, 1628 (2000); b) D. Mecerreyes, J. A. Pomposo, M. Bengoetxea, and H. Grande, *Macromolecules* **33**, 5846 (2000).

241. S. Alkan, L. Toppare, Y. Hepuzer, and Y. Yagci, *J. Polym. Sci.; Part A: Polym. Chem.* **37**, 4218 (1999).

242. K. Yamada, M. Miyazaki, K. Ohno, T. Fukuda, and M. Minoda, *Macromolecules* **32**, 290 (1999).

243. S. G. Roos, A. H. E. Mueller, and K. Matyjaszewski, *Macromolecules* **32**, 8331 (1999).

244. S. G. Roos, A. H. E. Muller, and K. Matyjaszewski, *ACS Symp. Ser.* **768**, 361 (2000).

245. H. Shinoda, P. J. Miller, and K. Matyjaszewski, *Macromolecules* **34**, 3186 (2001).

246. V. Coessens and K. Matyjaszewski, *Macromol. Rapid Commun.* **20**, 127 (1999).

247. K. Matyjaszewski, S. Coca, Y. Nakagawa, and J. Xia, *Polym. Mater. Sci. Eng.* **76**, 147 (1997).

248. H. Malz, H. Komber, D. Voigt, I. Hopfe, and J. Pionteck, *Macromol. Chem. Phys.* **200**, 642 (1999).

249. A. Marsh, A. Khan, D. M. Haddleton, and M. J. Hannon, *Polym. Prep.* (*Am. Chem. Soc., Div. Polym. Chem.*) **41**(1), 440 (2000).

250. D. M. Haddleton and K. Ohno, *Biomacromolecules* **1**, 152 (2000).

251. K. Matyjaszewski, M. Teodorescu, M. H. Acar, K. L. Beers, S. Coca, S. G. Gaynor, P. J. Miller, and H.-J. Paik, *Macromol. Symp.* **157**, 183 (2000).

252. X. Huang and M. J. Wirth, *Macromolecules* **32**, 1694 (1999).

253. M. Ejaz, S. Yamamoto, K. Ohno, Y. Tsujii, and T. Fukuda, *Macromolecules* **31**, 5934 (1998).

254. B. Zhao and W. J. Brittian, *J. Am. Chem. Soc.* **121**, 3557 (1999).

255. K. Matyjaszewski, P. J. Miller, N. Shukla, B. Immaraporn, A. Gelman, B. B. Luokala, T. M. Siclovan, G. Kickelbick, T. Vallant, H. Hoffmann, and T. Pakula, *Macromolecules* **32**, 8716 (1999).

256. D. P. Curran, *Synthesis* 417 (1988).

257. V. Coessens and K. Matyjaszewski, *Macromol. Rapid Commun.* **20**, 66 (1999).

258. V. Coessens, J. Pyun, P. J. Miller, S. G. Gaynor, and K. Matyjaszewski, *Macromol. Rapid Commun.* **21**, 103 (2000).

259. Y. Nakagawa, S. G. Gaynor, and K. Matyjaszewski, *Polym. Prep.* (*Am. Chem. Soc., Div. Polym. Chem.*) **37**(1), 577 (1996).

260. K. Matyjaszewski, Y. Nakagawa, and S. G. Gaynor, *Macromol. Rapid Commun.* **18**, 1057 (1997).

261. V. Coessens, Y. Nakagawa, and K. Matyjaszewski, *Polym. Bull.* **40**, 135 (1998).

262. M. W. Weimer, J. M. J. Frechét, and I. Gitsov, *J. Polym. Sci.; Part A: Polym. Chem.* **36**, 955 (1998).

263. E. G. Koulouri, J. K. Kallitsis, and G. Hadziioannou, *Macromolecules* **32**, 6242 (1999).

264. a) P. Zhou, G.-Q. Chen, H. Hong, F.-S. Du, Z.-C. Li, and F.-M. Li, *Macromolecules* **33**, 1948 (2000); b) P. Zhou, G.-Q. Chen, C.-Z. Li, F.-S. Du, Z.-C. Li, and F.-M. Li, *Chem. Commun.* 797 (2000).

265. H. Fukui, M. Sawamoto, and T. Higashimura, *Macromolecules* **26**, 7315 (1993).

266. T. Ando, M. Kamigaito, and M. Sawamoto, *Macromolecules* **31**, 6708 (1998).

267. A. K. Shim, V. Coessens, T. Pintauer, S. Gaynor, and K. Matyjaszewski, *Polym. Prep.* (*Am. Chem. Soc., Div. Polym. Chem.*) **40**(2), 456 (1999).

268. M. Kusakabe and K. Kitano, EP 0 789 036 A2 (1998).

269. T. Pakula and K. Matyjaszewski, *Macromol. Theory Simul.* **5**, 987 (1996).

270. J.-S. Wang, D. Greszta, and K. Matyjaszewski, *Polym. Mater. Sci. Eng.* **73**, 416 (1995).

271. S. V. Arehart and K. Matyjaszewski, *Polym. Prep.* (*Am. Chem. Soc., Div. Polym. Chem.*) **40**(2), 458 (1999).

272. B. Gao, X. Chen, B. Ivan, J. Kops, and W. Batsberg, *Polym. Bull.* **39**(5), 559 (1997).

273. R. C. Jones, S. Yoon, and Y. Nagasaki, *Polymer* **40**, 2411 (1999).

274. Y. Kotani, K. Masami, and M. Sawamoto, *Macromolecules* **31**, 5582 (1998).

275. D. E. Betts, T. Johnson, D. LeRoux, and J. M. DeSimone, *ACS Symp. Ser.* **685**, 418 (1998).

276. K. Matyjaszewski, D. A. Shipp, G. P. McMurtry, S. G. Gaynor, and T. Pakula, *J. Polym. Sci.; Part A: Polym. Chem.* **38**, 2023 (2000).

277. X. Zhang and K. Matyjaszewski, *Macromolecules* **32**, 1763 (1999).

278. M. Cassebras, S. Pascual, A. Polton, M. Tardi, and J.-P. Vairon, *Macromol. Rapid Commun.* **20**, 261 (1999).

279. K. A. Davis and K. Matyjaszewski, *Macromolecules* **34**, 2101 (2001).

280. a) J. Pyun, P. J. Miller, G. Kickelbick, K. Matyjaszewski, J. Schwab, and J. Lichtenhan, *Polym. Prep.* (*Am. Chem. Soc., Div. Polym. Chem.*) **40**(2), 454 (1999); b) J. Pyun and K. Matyjaszewski, *Macromolecules* **33**, 217 (2000); c) J. Pyun, P. J. Miller, and K. Matyjaszewski, *Polym. Prep.* (*Am. Chem. Soc., Div. Polym. Chem.*) **41**(1), 536 (2000); d) P. T. Mather, S. B. Chun, J. Pyun, K. Matyjaszewski, and H. G. Jeon, *Polym. Prep.* (*Am. Chem. Soc., Div. Polym. Chem.*) **41**(1), 582 (2000).

281. S. Coca and K. Matyjaszewski, *Macromolecules* **30**, 2808 (1997).

282. X. Chen, B. Ivan, J. Kops, and W. Batsberg, *Polym. Prep.* (*Am. Chem. Soc., Div. Polym. Chem.*) **38**(1), 715 (1997).

283. X. Chen, B. Ivan, J. Kops, and W. Batsberg, *Macromol. Rapid Commun.* **19**, 585 (1998).

284. S. Coca and K. Matyjaszewski, *Polym. Prep.* (*Am. Chem. Soc., Div. Polym. Chem.*) **38**(1), 693 (1997).

285. a) S. Coca and K. Matyjaszewski, *J. Polym. Sci.; Part A: Polym. Chem.* **35**, 3595 (1997); b) B. Ivan, X. Chen, K. J., and W. Batsberg, *Macromol. Rapid Commun.* **19**, 15 (1998).

286. A. Kajiwara and K. Matyjaszewski, *Macromolecules* **31**, 3489 (1998).

287. Y. Xu and C. Pan, *J. Polym. Sci.; Part A: Polym. Chem.* **38**, 337 (2000).

288. A. B. Duz and Y. Yagci, *Eur. Polym. J.* **35**, 2031 (1999).

289. Y. Xu, C. Pan, and L. Tao, *J. Polym. Sci.; Part A: Polym. Chem.* **38**, 436 (2000).

290. C. J. Hawker, J. L. Hedrick, E. E. Malmström, M. Trollsås, D. Mecerreyes, G. Moineau, P. Dubois, and R. Jérôme, *Macromolecules* **31**, 213 (1998).

291. Q. Zhang, E. E. Remsen, and K. L. Wooley, *J. Am. Chem. Soc.* **122**, 3642 (2000).

292. X. Chen, B. Gao, J. Kops, and W. Batsberg, *Polymer* **39**, 911 (1998).

293. B. Reining, H. Keul, and H. Höcker, *Polymer* **40**, 3555 (1999).

294. a) K. Jankova, X. Chen, J. Kops, and W. Batsberg, *Macromolecules* **31**, 538 (1998); b) K. Jankova, J. H. Truelsen, X. Chen, J. Kops, and W. Batsberg, *Polym. Bull.* **42**, 153 (1999).

295. M. Bednarek, T. Biedron, and P. Kubisa, *Macromol. Rapid Commun.* **20**, 59 (1999).

296. S. Angot, D. Taton, and Y. Gnanou, *Macromolecules* **33**, 5418 (2000).

297. M. Acar and K. Matyjaszewski, *Macromol. Chem. Phys.* **200**, 1094 (1999).

298. K. Jankova, J. Kops, X. Chen, and W. Batsberg, *Macromol. Rapid Commun.* **20**, 219 (1999).

299. J.-D. Tong, S. Ni, and M. A. Winnik, *Macromolecules* **33**, 1482 (2000).

300. J.-D. Tong, C. Zhou, S. Ni, and M. A. Winnik, *Macromolecules* **34**, 696 (2001).

301. P. J. Miller and K. Matyjaszewski, *Macromolecules* **32**, 8760 (1999).

302. K. Huan, E. Khoshdel, and D. M. Haddleton, *Polym. Prep.* (*Am. Chem. Soc., Div. Polym. Chem.*) **41**(1), 538 (2000).

303. S. Midha and T. R. Nijakowski, WO 9851261 (1998).

304. G. Adams, E. Khoshdel, A. Moretta, Y. C. Plant, and E. S. Reid, WO 0071607 (2000).

305. S. Coca, H.-J. Paik, and K. Matyjaszewski, *Macromolecules* **30**, 6513 (1997).

306. C. W. Bielawski and R. H. Grubbs, *Polym. Prep.* (*Am. Chem. Soc., Div. Polym. Chem.*) **41**(1), 12 (2000).

307. C. W. Bielawski, T. Morita, and R. H. Grubbs, *Macromolecules* **33**, 678 (2000).

308. Z. Zhang, S. Ying, and Z. Shi, *Polymer* **40**, 1341 (1999).

309. M. Destarac, K. Matyjaszewski, E. Silverman, B. Ameduri, and B. Boutevin, *Macromolecules* **33**, 4613 (2000).

310. a) M. Destarac and B. Boutevin, *Polym. Prep.* (*Am. Chem. Soc., Polym. Div.*) **39**(2), 568 (1998); b) M. Destarac and B. Boutevin, *Macromol. Rapid Commun.* **20**, 641 (1999).

311. S. G. Gaynor and K. Matyjaszewski, *Macromolecules* **30**, 4241 (1997).

312. S. G. Gaynor, S. Z. Edelman, and K. Matyjaszewski, *Polym. Prep.* (*Am. Chem. Soc., Polym. Div.*) **38**(1), 703 (1997).

313. P. K. Tsolakis, E. G. Koulouri, and J. K. Kallitsis, *Macromolecules* **32**, 9054 (1999).

314. a) Y. Nakagawa and K. Matyjaszewski, *Polym. Prep.* (*Am. Chem. Soc., Polym. Div.*) **37**(2), 270 (1996); b) Y. Nakagawa, P. Miller, C. Pacis, and K. Matyjaszewski, *Polym. Prep.* (*Am. Chem. Soc., Polym. Div.*) **38**(1), 701 (1997); c) Y. Nakagawa, P. J. Miller, and K. Matyjaszewski, *Polymer* **39**, 5163 (1998).

315. K. Matyjaszewski, P. J. Miller, E. Fossum, and Y. Nakagawa, *Appl. Organomet. Chem.* **12**, 667 (1998).

316. L. Lusten, G. P.-G. Cordina, R. G. Jones, and F. Schue, *Eur. Polym. J.* **34**, 1829 (1998).

317. M. R. Leduc, C. J. Hawker, J. Dao, and J. M. J. Frechét, *J. Am. Chem. Soc.* **118**, 11111 (1996).

318. M. R. Leduc, W. Hayes, and J. M. J. Frechét, *J. Polym. Sci.; Part A: Polym. Chem.* **36**, 1 (1998).

319. H.-J. Paik, S. G. Gaynor, and K. Matyjaszewski, *Macromol. Rapid Commun.* **19**, 47 (1998).

320. T. Fónagy, B. Ivén, and M. Szesztay, *Macromol. Rapid Commun.* **19**, 479 (1998).

321. S. C. Hong, T. Pakula, and K. Matyjaszewski, *Macromol. Chem. Phys.* (in press).

322. X.-S. Wang, N. Luo, and S.-K. Ying, *Polymer* **40**, 4515 (1999).

323. Q. Pan, S. Liu, J. Xie, and M. Jiang, *J. Polym. Sci.; Part A: Polym. Chem.* **37**, 2699 (1999).

324. S. Midha and T. R. Nijakowski, WO 9851722 (????).

325. R. G. Jones and S. J. Holder, *Macromol. Chem. Phys.* **198**, 3571 (1997).

326. a) K. Matyjaszewski, M. Teodorescu, P. J. Miller, and M. L. Peterson, *J. Polym. Sci.; Part A: Polym. Chem.* **38**, 2440 (2000); b) S. Liu and A. Sen, *Macromolecules* **34**, 1529 (2001).

327. K. L. Beers, S. G. Gaynor, K. Matyjaszewski, S. S. Sheiko, S. A. Prokhorova, and M. Moller, *Polym. Prep.* (*Am. Chem. Soc., Div. Polym. Chem.*) **40**, 446 (1999).

328. H. G. Boerner, K. Beers, K. Matyjaszewski, S. S. Sheiko, and M. Moeller, *Macromolecules* **34**, 4375 (2001).

329. a) E. Doerffler, A. T. Levy, T. v. Werne, and T. E. Patten, *Polym. Mater. Sci. Eng.* **80**, 463 (1999); b) T. E. Patten and E. M. Doerffler, *Polym. Prep.* (*Am. Chem. Soc., Div. Polym. Chem.*) **41**(1), 87 (2000).

330. R. B. Grubbs, C. J. Hawker, J. Dao, and J. M. J. Frechet, *Angew. Chem., Int. Ed. Engl.* **36**, 270 (1997).

331. a) J. L. Hedrick, B. Atthoff, K. A. Boduch, C. J. Hawker, D. Mecerreyes, R. D. Miller, and M. Trollsas, *Polym. Mater. Sci. Eng.* **80**(1), 104 (1999); b) D. Mecerreyes, B. Atthoff, K. A. Boduch, M. Trollsas, and J. L. Hedrick, *Macromolecules* **32**, 5175 (1999).

332. K. L. Beers, A. Kern, and K. Matyjaszewski, *Polym. Prep.* (*Am. Chem. Soc., Div. Polym. Chem.*) **38**(1), 695 (1997).

333. A. H. E. Muller, S. G. Roos, and K. Matyjaszewski, *Polym. Prep.* (*Am. Chem. Soc., Div. Polym. Chem.*) **40**(2), 352 (1999).

334. H. Shinoda and K. Matyjaszewski, *Macromolecules* **34**, 6243 (2001).

335. X. Huang and M. J. Wirth, *Anal. Chem.* **69**, 4577 (1997).

336. T. Von Werne and T. E. Patten, *J. Am. Chem. Soc.* **121**, 7409 (1999).

337. H. Böttcher, M. L. Hallensleben, S. Nuss, and H. Wurm, *Polym. Bull.* **44**, 223 (2000).

338. J. Pyun, K. Matyjaszewski, T. Kowalewski, D. Savin, G. Patterson, G. Kickelbick, and N. Huesing, *J. Am. Chem. Soc.* **123**, 9445 (2001).

339. M. Husseman, E. E. Malmström, M. McNamara, M. Mate, D. Mecerreyes, D. G. Benoit, J. L. Hedrick, P. Mansky, E. Huang, T. P. Russell, and C. J. Hawker, *Macromolecules* **32**, 1424 (1999).

340. M. Ejaz, K. Ohno, Y. Tsujii, and T. Fukuda, *Macromolecules* **33**, 2870 (2000).

341. B. Zhao, W. J. Brittain, W. Zhou, and S. Z. D. Cheng, *J. Am. Chem. Soc.* **122**, 2407 (2000).

342. R. A. Sedjo, B. K. Mirous, and W. J. Brittain, *Macromolecules* **33**, 1492 (2000).

343. J.-B. Kim, M. L. Bruening, and G. L. Baker, *Polym. Prep.* (*Am. Chem. Soc., Div. Polym. Chem.*) **41**, 1300 (2000).

344. R. R. Shah, D. Merreceyes, M. Husemann, I. Rees, N. L. Abbott, C. J. Hawker, and J. L. Hedrick, *Macromolecules* **33**, 597 (2000).

345. a) G. Kickelbick, P. J. Miller, and K. Matyjaszewski, *Polym. Prep.* (*Am. Chem. Soc., Polym. Div.*) **39**(1), 284 (1998); b) K. Matyjaszewski, P. J. Miller, J. Pyun, G. Kickelbick, and S. Diamanti, *Macromolecules* **32**, 6526 (1999).

346. J. Ueda, M. Kamigaito, and M. Sawamoto, *Macromolecules* **31**, 6762 (1998).

347. S. Angot, S. Murthy, D. Taton, and Y. Gnanou, *Macromolecules* **31**, 7218 (1998); S. Angot, D. Taton, and Y. Gnanou, *Macromolecules* **33**, 7261 (2000).

348. A. Heise, J. L. Hedrick, M. Trollsås, R. D. Miller, and C. W. Frank, *Macromolecules* **32**, 231 (1999).

349. a) A. Heise, J. L. Hedrick, M. Trollsas, J. G. Hillborn, C. W. Frank, and R. D. Miller, *Polym. Prep.* (*Am. Chem. Soc., Polym. Div.*) **40**(1), 452 (1999); b) A. Heise, J. L. Hedrick, C. W. Frank, and R. D. Miller, *J. Am. Chem. Soc.* **121**, 8647 (1999).

350. A. Heise, C. Nguyen, R. Malek, J. L. Hedrick, C. W. Frank, and R. D. Miller, *Macromolecules* **33**, 2346 (2000).

351. J. L. Hedrick, M. Trollsås, C. J. Hawker, B. Atthuff, H. Claesson, A. Heise, R. D. Miller, D. Mecerreyes, R. Jérôme, and P. Dubois, *Macromolecules* **31**, 8691 (1998).

352. R. D. Miller, C. R. Hawker, J. L. Hedrick, M. Trollsas, M. Husemann, A. Heise, and G. Klaerner, *Polym. Mater. Sci. Eng.* **80**, 24 (1999).

353. D. M. Haddleton, D. Kukulj, E. J. Kelly, and C. Waterson, *Polym. Mater. Sci. Eng.* **80**, 145 (1999).

354. a) J. E. Collins and C. L. Fraser, *Polym. Prep.* (*Am. Chem. Soc., Div. Polym. Chem.*) **39**(2), 571 (1998); b) J. E. Collins and C. L. Fraser, *Macromolecules* **31**, 6715 (1998); c) C. L. Fraser, R. W. Cutts, R. M. Johnson, C. Ng, and J. E. Collins, *Polym. Prep.* (*Am. Chem. Soc., Div. Polym. Chem.*) **41**(1), 540 (2000).

355. a) C. Fraser, X. Wu, A. P. Smith, and P. S. Corbin, *Polym. Prep.* (*Am. Chem. Soc., Div. Polym. Chem.*) **41**(1), 388 (2000); b) C. L. Fraser and A. P. Smith, *J. Polym. Sci.; Part A: Polym. Chem.* **38**, 4704 (2000).

356. N. J. Hovestad, G. van Koten, S. A. F. Bon, and D. M. Haddleton, *Macromolecules* **33**, 4048 (2000).

357. J. Xia, X. Zhang, and K. Matyjaszewski, *Macromolecules* **32**, 4482 (1999).

358. F. Asgarzadeh, P. Ourdouillie, E. Beyou, and P. Chaumont, *Macromolecules* **32**, 6996 (1999).

359. J. M. J. Frechét, M. Henmi, I. Gitsov, S. Aoshima, M. Leduc, and R. B. Grubbs, *Science* **269**, 1080 (1995).

360. S. G. Gaynor, S. Edelman, and K. Matyjaszewski, *Macromolecules* **29**, 1079 (1996).

361. S. G. Gaynor, P. Balchandani, A. Kulfan, M. Podwika, and K. Matyjaszewski, *Polym. Prep.* (*Am. Chem. Soc., Div. Polym. Chem.*) **38**(1), 496 (1997).

362. K. Matyjaszewski, J. Pyun, and S. G. Gaynor, *Macromol. Rapid Commun.* **19**, 665 (1998).

363. K. Matyjaszewski and S. G. Gaynor, *Macromolecules* **30**, 7042 (1997).

364. K. Matyjaszewski, S. G. Gaynor, and A. Kulfan, *Macromolecules* **30**, 5192 (1997).

365. K. Matyjaszewski, S. G. Gaynor, and A. Mueller, *Macromolecules* **30**, 7034 (1997).

366. A. H. E. Müller, D. Yan, and M. Wulkow, *Macromolecules* **30**, 7015 (1997).

367. G. Cheng, P. F. W. Simon, M. Hartenstein, and A. H. E. Muller, *Macromol. Rapid Commun.* **21**, 846 (2000).

368. S.-G. An and C.-G. Cho, *Polym. Prep.* (*Am. Chem. Soc., Div. Polym. Chem.*) **41**(2), 1671 (2000).

369. X. Jiang, Y. Zhong, D. Yan, H. Yu, and D. Zhang, *J. Appl. Polym. Sci.* **78**, 1992 (2000).

370. S. G. Gaynor, S. Z. Edelman, A. Kulfan, and K. Matyjaszewski, *Polym. Prep.* (*Am. Chem. Soc., Div. Polym. Chem.*) **37**(2), 413 (1996).

371. X. Zhang, Y. Chen, A. Gong, C. Chen, and F. Xi, *Polym. Int.* **48**, 896 (1999).

372. S. Maier, A. Sunder, H. Frey, and R. Mulhaupt, *Macromol. Rapid Commun.* **21**, 226 (2000).

373. a) J. L. Hedrick, M. Trollsas, and D. Mecerreyes, *Polym. Prep.* (*Am. Chem. Soc., Div. Polym. Chem.*) **40**(2), 97 (1999); b) D. Mecerreyes, M. Trollsas, and J. L. Hedrick, *Macromolecules* **32**, 8753 (1999).

374. a) A. M. van Herk, *J. Macromol. Sci., Rev. Macromol. Chem. Phys.* **C37**, 633 (1997); b) S. Beuermann and M. Buback, *Prog. Pol. Sci.* **27**, 191 (2002).

12 Control of Free-Radical Polymerization by Chain Transfer Methods

JOHN CHIEFARI and EZIO RIZZARDO

CSIRO Molecular Science, Victoria, Australia

CONTENTS

This chapter describes the various chain transfer methods currently used in free-radical polymerization for the control of molecular weight, structure, and functionality. Section 12.1 introduces the basic concepts on chain transfer and illustrates some of the traditional chain transfer methodologies that are still in use today. The subsequent sections illustrate the development of chain transfer techniques toward more efficient methods of molecular weight, polydispersity, and structural control in polymers. Section 12.2 describes the principles of catalytic chain transfer with cobalt complexes and its synthetic utility in preparing oligomers with a 1,1-disubstituted alkene end group (macromonomers). Section 12.3 introduces the concept of chain transfer by addition–fragmentation and shows how macromonomers can act as chain transfer agents for reducing molecular weight and as prepolymers for preparing graft and block copolymers. The scope and versatility of addition–fragmentation chain transfer is illustrated by the use of simpler and more efficient addition–fragmentation chain transfer agents to introduce a variety of functional groups at one or both ends of the polymer chains. Section 12.4 describes a more advanced form of the chain transfer process: a living free-radical process that operates through reversible addition–fragmentation chain transfer (RAFT). Section 12.5 presents comparisons with other reversible (degenerative) chain transfer methods employing alkyl iodides and diphenyl ditellurides.

12.1 TRADITIONAL METHODS OF CHAIN TRANSFER

12.1.1 Overview

The process of chain transfer in free-radical polymerization is used to moderate the molecular weight of polymers and in some cases to introduce functionality at the ends of polymer chains. End-functional polymers have shown utility in automotive coating applications, for instance, where low-molecular-weight, end-functional oligomers are used for high-solids, low-volatile-organic content (VOC) formulations.[1] The chain transfer process is mediated by the use of a chain transfer agent (CTA) with the generic mechanism represented in Scheme 12.1. A propagating radical $P_n^\bullet$ reacts with a chain transfer agent R–X terminating the propagating chain and forming polymer P_n–X and a new radical $R^\bullet$ (step 1), which reacts with monomer to form a new propagating chain (steps 2 and 3).

$$P_n^\bullet \ + \ R{-}X \ \xrightarrow{k_{tr}} \ P_n{-}X \ + \ R^\bullet \qquad (1)$$

$$R^\bullet \ + \ M \ \longrightarrow \ R{-}M^\bullet \qquad (2)$$

$$R{-}M^\bullet \ + \ mM \ \xrightarrow{k_p} \ RP_{m+1}^\bullet \qquad (3)$$
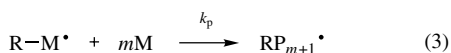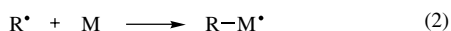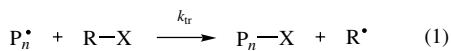
Scheme 12.1   Chain transfer reaction between propagating chain and transfer agent.

Some of the more widely used CTA include halomethanes, disulfides, thiols, and various other compounds that have a readily abstractable H-atom.[2] The chain transfer activity of the CTA is given by the chain transfer constant (C_{tr}), which is the ratio of the rate constant for chain transfer (k_{tr}) (step 1 in Scheme 12.1) to the rate constant for propagation (k_p) (step 3 in Scheme 12.1), $C_{tr} = k_{tr}/k_p$.

A C_{tr} value of 1.0 is considered ideal for batch polymerizations as this provides conditions in which the concentration of CTA relative to the concentration of monomer remains constant throughout the polymerization. This means that the average molecular weight of polymer formed at low conversion will be essentially equal to that formed at high conversion.[3]

Implicit in the mechanism of chain transfer depicted in Scheme 12.1, conditions can be devised such that the major chain terminating reaction involves chain transfer to CTA. In this situation, the majority of chains will contain end groups derived from the CTA.

12.1.2   Thiols as Chain Transfer Agents

There are many thiols that are used as CTA, and as such this class represents the one most commonly used in free-radical polymerizations. The mechanism of chain transfer is represented in Scheme 12.2. As can be seen from the overall process, a majority of polymers possess a sulfur containing end group.

The C_{tr} of thiols depends on the polymerization system and conditions. As a guide, some C_{tr} of thiols are shown in Table 12.1.

A number of functional thiols, including, mercaptoethanol and methyl thioglycolate (last two entries in Table 12.1) have been used to prepare mono end-functional polymers. These can serve as starting materials for preparing block[8,9] and graft[10] copolymers for use as emulsifiers, thermoplastic elastomers, compatibilizers, and adhesives.[11] A report detailing the preparation of a pMMA-*block*-pS using thiols as CTA highlights the usefulness of this process. When the difunctional CTA;

$$P_n^\bullet \ + \ R{-}SH \ \longrightarrow \ P_n{-}H \ + \ R{-}S^\bullet$$

$$R{-}S^\bullet \ + \ mM \ \longrightarrow \ RS{-}P_m^\bullet$$

$$\text{Overall:} \ \ R{-}SH \ + \ mM \ \longrightarrow \ RS{-}P_m{-}H$$
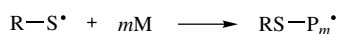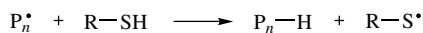
Scheme 12.2   Thiols as CTA and products formed.

TABLE 12.1 Chain Transfer Constants (C_{tr}) of Thiols (RSH) for Various Monomers at 60°C[4]

CTA	C_{tr}		
R	Methyl Methacrylate	Styrene	Vinyl Acetate
n-C_4H_9	0.67	22	48
n-$C_{12}H_{25}$	—	19	—
$H_3N^+CH_2CH_2$	0.11^a	11	—
$HOCH_2CH_2$	0.45^b	—	—
MeO_2CCH_2	0.30^c	1.4^c	0.07^c

^{a} Ref. 5.
^{b} Ref. 6.
^{c} Ref. 7.

1,6-hexanedithiol was used in MMA polymerization, a thiol-terminated pMMA oligomer was prepared. This was, in turn, used as a CTA in styrene polymerization to form the pMMA-*block*-pS diblock.[12] Thiols tend to react more rapidly with nucleophilic radicals than electrophilic radicals. Consequently, thiols have a higher C_{tr} with styrene and vinyl esters than with (meth)acrylates and acrylonitrile. The thiyl radicals produced from the transfer step are electrophilic in nature and, when used in copolymerizations, will react preferentially with electron-rich monomers.

12.1.3 Halomethanes as Chain Transfer Agents

Halomethanes, which include chloroform, carbon tetrachloride, carbon tetrabromide, and bromotrichloromethane, have been widely used as CTA (telogens) for the preparation of telomers.[13] The perhalomethanes (e.g., carbon tetrachloride, carbon tetrabromide, and bromotrichloromethane) react in the chain transfer process to exchange a halogen atom and form a perhaloalkyl radical that initiates a new propagating chain (Scheme 12.3).

For mixed halomethanes, halogen atom abstractability decreases in the series iodine > bromine > chlorine. The halohydromethanes (e.g., chloroform) can in principle react by either H-atom or halogen-atom abstraction. The preferred pathway can be usually predicted by considering the relative bond strengths, thus for chloroform H-atom abstraction is favored.[14] Some examples of C_{tr} for halomethanes in various monomers are listed in Table 12.2.

$$P_n^\bullet + X_3C\!-\!X \longrightarrow P_n\!-\!X + X_3C^\bullet$$

$$X_3C^\bullet + mM \longrightarrow X_3C\!-\!P_m^\bullet$$

$$\text{Overall:} \quad CX_4 + mM \longrightarrow X_3C\!-\!P_m\!-\!X$$
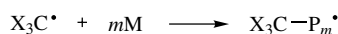
Scheme 12.3 Halomethanes as CTA and products formed.

TABLE 12.2   Chain Transfer Constants (C_{tr}) of Halomethanes for Methyl Methacrylate (MMA), Methyl Acrylate (MA), Acrylonitrile (AN), Styrene (Sty), and Vinyl Acetate (VA) at 60°C[4]

CTA	$C_{tr} \times 10^4$				
	MMA	MA	AN	Sty	VA
CBr$_4$	0.19	0.41	0.19	8.8	739
CCl$_4$	18.5	1.0[a]	0.85	92	> 800
CHCl$_3$	1.77	—	5.6	3.4	160

[a]At 40°C.

Similar to the thiols, halomethanes react faster with nucleophilic radicals compared to electrophilic radicals; hence the C_{tr} for styrene and vinyl acetate is generally higher than for acrylates. The halomethyl radicals formed from the chain transfer process are electrophilic and hence react preferentially with electron-rich monomers in copolymerizations.

12.1.4   Disulfides as Chain Transfer Agents

There are a range of disulfides[15–18] (e.g., dialkyl, diaryl, diaroyl), thiurams[19] and xanthogens[20,21] that have been utilized as CTA. Since the use of these compounds leads to incorporation of functionality at both ends of the polymer chain (see Scheme 12.4), they have found applicability in the preparation of telechelics. The C_{tr} of some disulfides with various monomers is shown in Table 12.3.

The C_{tr} of aliphatic disulfides are extremely low for MMA and styrene, but are close to ideal for VA polymerizations (i.e., $C_{tr} \sim 1$). The C_{tr} of diphenyl and dibenzoyl disulfides, although higher than the aliphatic disulfides, depends on the substitution on the aromatic ring.[16] In general, the xanthogens and thiurams have higher C_{tr} than do other disulfides (e.g., see last entry in Table 12.3), which has been attributed to an additional mechanism of decomposition through addition of propagating radicals to the C=S bond followed by fragmentation.[14]

12.1.5   Other Reagents as Chain Transfer Agents

There are many other reagents that are capable of acting as chain transfer agents in free-radical polymerizations. These are primarily common solvents used in the

$$P_n^{\bullet} \; + \; RS{-}SR \; \longrightarrow \; P_n{-}SR \; + \; RS^{\bullet}$$

$$RS^{\bullet} \; + \; mM \; \longrightarrow \; RS{-}P_m^{\bullet}$$

$$\text{Overall:} \quad RS{-}SR \; + \; mM \; \longrightarrow \; RS{-}P_m{-}SR$$
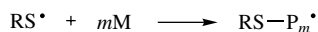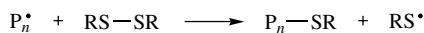
Scheme 12.4   Disulfides as CTA and products formed.

TABLE 12.3   Chain Transfer Constants (C_{tr}) of Disulfides (RS-SR) with Various Monomers at 60°C[4]

CTA	C_{tr}		
R	Methyl Methacrylate	Styrene	Vinyl Acetate
C_2H_5	0.00013	0.0045^a	—
n-C_4H_9	—	0.0024	1.0
$PhCH_2$	0.0063	0.01	—
EtO_2CH_2	0.00065	0.015	1.5
Ph	0.011	0.15	—
PhC(=O)	10	36	—
$Et_2N(C=S)$	—	0.32^b	—

^{a}At 99°C.
^{b}Ref. 19.

reaction (e.g., toluene, acetone, butan-2-one, ethyl acetate) but, in general, any compound that possesses an abstractable H atom is capable of behaving as a CTA. The accuracy of the reported chain transfer data is questionable since the C_{tr} for a given system often spans an order of magnitude.[4] However, as can be seen from Table 12.4 the ability of solvents to act as CTA depends largely on the reactivity of the propagating radicals.

The MMA propagating radical has a poor tendency to undergo chain transfer reactions whereas the more reactive propagating radical derived from vinyl acetate is more likely to abstract a H atom. The mode of chain transfer is dependent on the solvent type. A majority of solvents have abstractable hydrogens and so a favored pathway would be by H-atom abstraction. In the case of aromatic solvents such as benzene, H-atom transfer is likely to involve a two-step process. The first step is addition of propagating radical to the benzene ring to generate a cyclohexadienyl

TABLE 12.4   Chain Transfer Constants (C_{tr}) of Solvents for Methyl Methacrylate (MMA), Methyl Acrylate (MA), Acrylonitrile (AN), Styrene (Sty), and Vinyl Acetate (VA) at 60°C[4]

Solvent	$C_{tr} \times 10^4$				
	MMA	MA	AN	Sty	VA
Benzene	0.04	0.45^a	2.5	0.03	1.2
Toluene	0.20	2.7	5.8	0.21	21
Acetone	0.20	0.23	1.1	0.32	12
Butan-2-one	0.45	3.2	6.4	5.0	74
Ethyl acetate	0.15	—	2.5	0.39^b	3.0

^{a}At 80°C.
^{b}At 100°C.

radical adduct that then regains aromaticity through donation of a H atom to a second propagating radical.[14]

12.2   THE CATALYTIC CHAIN TRANSFER PROCESS

12.2.1   Overview

The concept of catalytic chain transfer (CCT) emerged in the early 1980s, when a Russian group reported that certain low-spin cobalt(II) porphyrin complexes were found to control molecular weight in free-radical polymerizations of methacrylates.[22–24] Subsequent to these initial reports, a large volume of work has shown that CCT with cobalt complexes is a highly effective method for controlling the molecular weight of polymers based on α-methylsubstituted monomers[25,26] (e.g., methacrylates), monosubstituted monomers[27,28] (e.g., styrenes, acrylates, acrylamide), and copolymers involving these two classes of monomers.[29–31] There are three factors that make this form of chain transfer attractive: (1) catalytic mode of action of the cobalt complex, (2) high transfer constant of the cobalt complex, and (3) polymers prepared by this method possess a C=C end group. As a consequence of the first two factors, only ppm quantities of the cobalt complex are required for effective molecular weight control. Polymers with a C=C end group can be further funtionalized or depending on the type of C=C end group, can be used as components in free radical polymerization.

The kinetics and mechanism of the CCT process have been topics of numerous studies.[32–36] The overall process is generally believed to occur in two steps as depicted in Scheme 12.5. The first step involves the transfer of a hydrogen atom from a propagating radical to the Co(II) complex to form a polymer and a cobalt(III) hydride. In the second step, reaction of the cobalt(III) hydride with monomer yields a monomeric radical (which continues propagation—step 3) and regenerates the cobalt(II) complex.[23,37]

Although the kinetics and mechanism of the CCT process continue to generate considerable scientific interest, there has been an increasing focus on the products of the process. The polymers from CCT are terminated with a C=C bond and have found use as chain transfer agents (CTA) in their own right as well as building blocks for preparing more complex structures such as block and graft copolymers.

$$P_n^{\bullet} \; + \; Co(II) \; \longrightarrow \; P_n \; + \; Co(III){-}H \qquad\qquad (1)$$

$$Co(III){-}H \; + \; M \; \longrightarrow \; H{-}M^{\bullet} \; + \; Co(II) \qquad\qquad (2)$$

$$H{-}M^{\bullet} \; + \; M \; \longrightarrow \; P_m^{\bullet} \qquad\qquad\qquad\qquad (3)$$
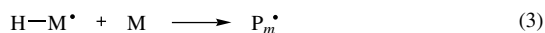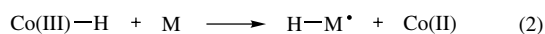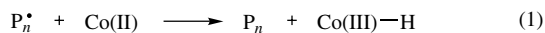
Scheme 12.5   Mechanism of catalytic chain transfer by Co(II) complexes.
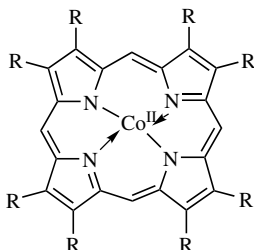
Figure 12.1   Co(II) porphyrins.

12.2.2   Cobalt Catalytic Chain Transfer Agents

The first class of cobalt(II) complexes utilized as catalytic chain transfer agents (CCTA) were cobalt(II) porphyrins as represented in Fig. 12.1.[23]

However, because of the difficulty of synthesis, poor stability, poor solubility in polar media, and the highly colored nature of these complexes, other chelates were subsequently developed.[38,39] Since Co(II) can exist in both high-spin (three unpaired electrons) and low-spin (one unpaired electron) states, the choice of ligands surrounding the central cobalt is crucial in determining the extent of spin crossover between the two spin states. In general, coordination by tetradentate nitrogen-based macrocycles enables the cobalt to adopt the low-spin state. Aside from porphyrins and the related phthalocyanins, the diaryl and dialkylglyoxime chelate have met the above criteria. In addition, the glyoxime ligand proved to be the most versatile as it was readily available and relatively inexpensive. A range of low-spin bis(glyoximato) cobalt(II) complexes have been successfully employed as CCTA, e.g., **1** and **2**.[40] Typically, the bis(glyoximato)cobalt(II) complexes are prepared and used with a bis(boron difluoride) bridge between the glyoximato units. The BF$_2$-bridged complexes have additional stability in solution, probably as a result of reduced hydrolytic susceptibility. The structure of the bis(glyoximato)cobalt(II) complex has been varified by FT-IR analysis.[41] There are many reports of synthetic approaches to these bis(glyoximato)cobalt(II) complexes but most are adapted from a procedure by Espenson et al.[37,42–44]

1   **2**
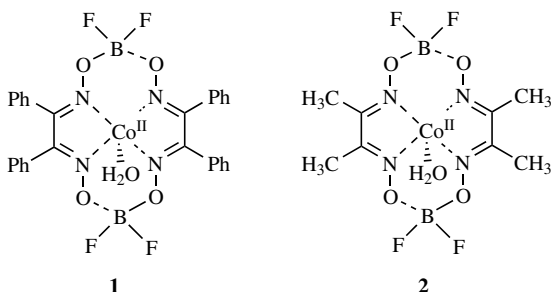
Although the bis(glyoximato)Co(II) complexes are more stable than the corresponding Co(II) porphyrin complexes, they are, nevertheless, free-radical in nature and so have a limited shelf life because of their sensitivity to air. The corresponding bis(glyoximato)Co(III) complexes, such as **3** and **4**, have a cobalt–carbon bond and are generally stable at ambient conditions, particularly in solution.[34,35,45] Current synthetic pathways to organocobalt(III) complexes are based on an original report by Schrauzer et al.[46]

3

4
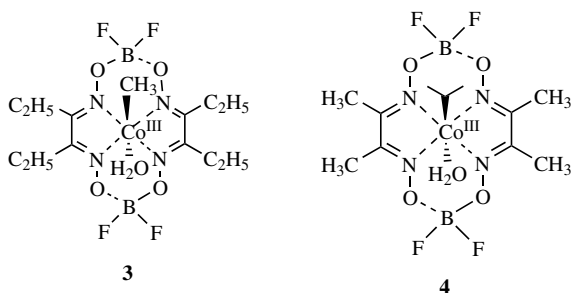
The organocobalt(III) complexes possess a weak Co—C bond and are converted in situ into the active cobalt(II) species by homolytic cleavage of the Co—C bond. The nature of the R group determines the mechanism of homolytic cleavage. It can be thermally induced, it can involve an S_H2 mechanism, or a combination of both mechanisms.[34,45,47]

12.2.3   Other Catalytic Chain Transfer Agents

To date, the most effective CCTA have been low spin Co(II) complexes. Other porphyrin complexes of Zn(II), Cu(II), Rh(III), and Ni(II) have been shown to have no catalytic activity in free-radical polymerization of vinyl monomers.[23] Certain rhodium(II) porphyrins, which exist in a low-spin state, undergo radical additions to acrylates to form mono and dimeric addition compounds.[48] These Rh(II) complexes are ineffective at initiating thermal polymerizations but have been shown to exhibit living behavior under photopromoted polymerization.[48] A bis(dimethylglyoximato) rhodium(III) compound has been prepared for X-ray analysis, but studies to determine catalytic chain transfer in free-radical polymerizations have not been reported.[49]

The known metalloradical $(\eta^5\text{-}C_5Ph_5)Cr(CO)_3$, is reported to be an effective CCTA in the polymerization of MMA.[50] A linear relationship between M_n and conversion indicates that this metalloradical imparts living behavior to the polymerization. A chain transfer constant of 984 for MMA at 100°C was measured. No studies on other vinyl monomers were reported.

12.2.4   Mechanistic Aspects of Catalytic Chain Transfer

The overall mechanism of CCT is a two-step process as shown in Scheme 12.5. The first step involves a β-elimination of a hydrogen atom by reaction of the cobalt(II)
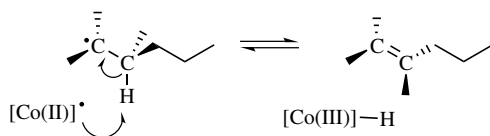
Scheme 12.6   β-Hydrogen atom abstraction via an S_H2 mechanism.

complex with the propagating radical. Evidence supporting the involvement of a H-atom transfer as the rate-determining step is from an observed deuterium kinetic isotope effect of 3.5.[51] Two possible pathways can be envisaged for a β-elimination process. In the first, an S_H2 mechanism is proposed whereby the cobalt(II) complex abstracts a β-hydrogen atom to form the alkene-terminated oligomer and a cobalt(III) hydride complex (Scheme 12.6).

The second possible mechanism is depicted in Scheme 12.7 and involves an E2-type elimination from a coordinated complex between the cobalt(II) CTA and the propagating radical.[52] The formation of these organocobalt(III) complexes by radical–radical combination has been reported[53,54] and the β-elimination from these organometallic compounds is also well known.[55] It is also likely that both mechanisms contribute to the chain transfer process with the degree of contribution depending on monomer type and reaction temperature.[52]

An alternative mechanism involving participation of monomer in the H-abstraction step, via coordination with the cobalt complex, has been discounted by a study showing that varying the monomer concentration had no effect on the chain transfer constant.[56]

The second step in the CCT process (step 2, Scheme 12.5) is addition of the cobalt(III) hydride complex to monomer. This yields a monomeric radical and regenerates the cobalt(II) species. Although a cobalt(III) hydride complex has
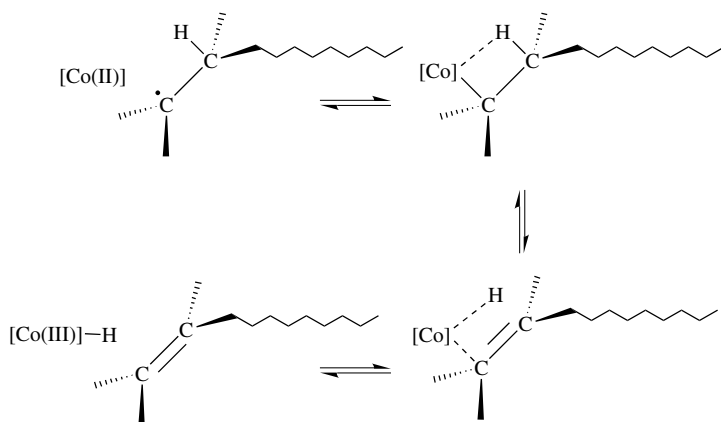
Scheme 12.7   β-Elimination mechanism of alkene formation.

TABLE 12.5   Polymerization of Methyl Methacrylate with Various Amounts of Isopropylcobalt(III) Complex (4)[71]

$[\text{Co(III)}] \times 10^6$ M	M_w	% Conversion
0.3	22,000	100
1.6	4,000	100
5.5	1,200	100

been isolated,[57] there is no direct evidence for the involvement of cobalt(III) hydrides in the hydrogen atom transfer to monomer. Nevertheless, there are many studies that support the proposal that cobalt(III) hydrides are likely intermediates in the chain transfer process.[51,58] For example, a hydridocobalt(III) porphyrin formed by treating a cobalt(II) porphyrin anion with acetic acid was shown to catalyze chain transfer in MMA polymerization.[59] Also, various trapping experiments yielded electronic spectra that suggested the presence of a cobalt(III) hydride species.[35,53,54]

It is evident from the mechanism depicted in Scheme 12.5 that chain transfer mediated by cobalt(II) complexes is "catalytic" in nature since the cobalt(II) species are regenerated. Typical C_{tr} for cobalt(II) complexes are on the order of 10^2–10^4 in styrene and methacrylate polymerizations.[23,34,37,44,60–63] Hence these two factors make this mode of chain transfer highly efficient with only ppm quantities of cobalt(II) CTA required, compared to conventional transfer agents (e.g., thiols), which require larger quantities due to their lower C_{tr} (typically 0.1–10). The C_{tr} of cobalt complexes have been measured by both the Mayo method[64] and the chain length distribution (CLD) technique,[65,66] and both methods provide similar values.[44,62] The chain transfer activity of cobalt complexes is influenced by a number of factors. These include cobalt complex structure,[60] monomer type,[23,52] reaction temperature,[37,60] solvent,[44,60,62] viscosity of the medium,[67,68] and polymer chain length.[37,38,69]

12.2.5   Synthetic Utility of Catalytic Chain Transfer Polymerization

The CCT process with cobalt complexes is an effective method for molecular weight control in polymerizations of α-methylvinyl monomers, such as methacrylate.[23,25,26,38,70] The results in Table 12.5 illustrate the dependance of polymer molecular weight on cobalt complex concentration.

An attractive feature of polymers prepared from these monomers is the 1,1-disubstitued alkene end group, as shown in **5**. This end group makes these products

5
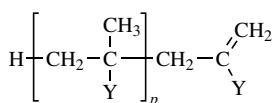
(referred to as macromonomers) suitable as CTA and as precursors to block and graft copolymers. This aspect of macromonomer chemistry will be discussed in the next section. The CCT process is compatible with a range of α-methylvinyl monomers such as α-methylstyrene (AMS), methacrylonitrile (MAN), as well as a range of methacrylates, including alkyl methacrylates, hydroxyethyl methacrylates, glycidyl methacrylates, and methacrylic acid as well as mixtures of these monomers.

There are a number of analytic techniques available to verify the structure of macromonomers. Thermal gravimetric analysis (TGA) is well suited to methacrylate macromonomers, as it distinguishes between macromonomers and oligomers formed by other mechanisms. This is because methacrylate macromonomers are prone to thermal degradation via an unzipping mechanism initiated by cleavage of the bond β to the C=C terminal bond.[72,73] A more general method of characterization involves the use of ^{1}H-NMR and ^{13}C-NMR to identify and quantify the number of alkene end groups per polymer chain.[23,30,31,74] Advances in ionization techniques coupled with sensitive detection methods have facilitated the characterization of oligomers. Approaches such as matrix assisted laser desorption ionization time-of-flight mass spectrometry[75,76] (MALDI-TOF-MS) and electrospray ionization[77] (ESI) coupled with fourier transform ion cyclotron detection (FTICR) can be used to analyze oligomers of up to 15,000 Da with a resolution of 2–5 amu. These techniques can yield information on molecular weight (M_n and M_w) and also provide a detailed analysis of polymer chain ends.[26]

The CCT process with monosubstituted monomers such as styrene, acrylates, and acrylamide has also been reported. The initial studies of the CCT polymerization of styrenes and acrylates with Co(II) porphyrins at or below 70°C resulted in inhibition periods, catalyst poisoning, and/or retardation as well as products with multimodal distributions.[23,24,35,52] In contrast, the CCT polymerization of acrylamide was reported to be successful with the correct choice of reaction conditions and type of Co(II) CCTA.[27] Similarly, styrenes and acrylates can be polymerized under CCT conditions with an appropriate CCTA, such as isopropylcobalt(III) (**4**), and reaction temperatures above 80°C to yield oligomers of **6** and **7**, respectively.[30]

6   **7**
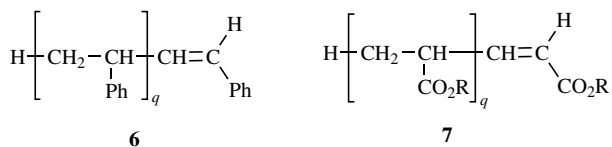
The observed problems associated with the CCT polymerization of styrene and acrylates at reaction temperatures below 70°C may be due to the formation of a polymer–cobalt(III) species that is relatively stable at lower temperatures[34,52] but is not formed (or is formed reversibly) at higher reaction temperatures.[78]

In addition, these investigations have shown that the CCT process is also effective in the preparation of styrene and acrylate oligomers (see Table 12.6). The 1,2-disubstituted alkene end groups of the resultant oligomers are easily identifiable by ^{1}H-NMR spectroscopy (Fig. 12.2).

TABLE 12.6   Polymerization of Styrene (Sty) and Butyl Acrylate (BA) in the presence of Isopropylcobalt(III) Complex (4)[28]

Monomer	Reaction Temperature (°C)	[Co(III)]× 10^4M	$\bar{M}_n$	$\bar{M}_w/\bar{M}_n$	% Conversion	% Alkene End Groups[a]
Sty	125	0.563	1,720	2.30	56	100
	125	0	33,830	1.75	46	0
BA	80	5.80	3,065	1.90	35	100
	80	0	137,200	2.30	72	0

[a] Styrene monomer gives (**6**); to a refluxing solution of 3.09 M styrene in *n*-butyl acetate and cobalt(III) complex (**4**) was fed a solution of 0.05 M 1,1′-azobis(4-cyclohexanecarbonitrile) in *n*-butyl acetate over 2 h. Butyl acrylate monomer gives (**7**): A mixture of 1.57 M butyl acrylate in *n*-butyl acetate, cobalt(III) complex (**4**) and 3.66 M 2,2′-azobis(2,4,4-trimethylpentane) were heated at 80°C for 3 h.

As synthetic precursors in free-radical polymerization, oligomers based on monosubstituted monomers with a 1,2-disubstituted alkene end group are less attractive because these end groups have substantially reduced reactivity compared to the 1,1-disubstituted alkene end group in macromonomers.

On the other hand, oligomers based primarily on monosubstituted monomers but possessing a 1,1-disubstituted alkene end group are attractive targets as they offer the potential to access a wider variety of (graft) copolymers. These macromonomers have been prepared by the CCT copolymerization of monosubstituted monomers with α-methyl-substituted monomers. Numerous synthetic studies in this area have investigated the cobalt(II)-mediated CCT copolymerization of acrylates and styrene with methyl methacrylate (MMA). These reports have centered around molecular weight reductions[23,79] as well as oligomer end-group analysis.[29–31,40]
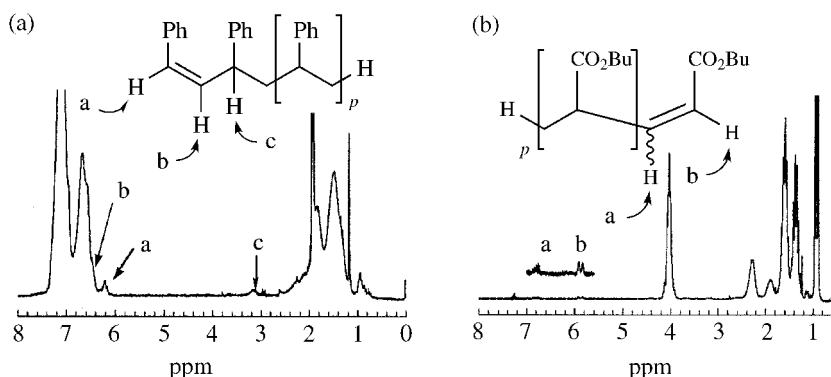
Figure 12.2 ^{1}H-NMR spectra identifying the 1,2-disubstituted alkene end group for (a) polystyrene oligomer (**6**) with signals at δ6.4 and δ6.2 and δ3.15 (backbone methine adjacent to alkene end group), in deuterated acetone, and (b) poly(butyl acrylate) oligomer (**7**) with signals at δ6.8 and δ5.85, in deuterated chloroform.

End group composition is an important consideration for copolymerizations since by the very nature of the chemistry, oligomers with two types of alkene end groups can be obtained.

The origin and identity of the two different alkene end groups is shown in Scheme 12.8 for the CCT copolymerization of monosubstituted and α-methyl-substituted monomers. Clearly, alkene end groups can be derived from the α-methyl-substituted monomer (e.g., MMA) and the monosubstituted monomer (e.g., styrene). If this product from the CCT process is to be used to build larger structures using a free-radical process (e.g., graft copolymers), then obtaining exclusively the macromonomer (i.e., the 1,1-disubstituted alkene end group) is desirable.

The alkene end group purity of the macromonomers is defined as the ratio of 1,1-disubstituted alkene end groups to 1,2-disubstituted alkene end groups. The two types of vinyl end groups can be identified by ^{1}H-NMR spectroscopy (e.g., compare Figs. 12.2a and 12.3). One of the first reports on the factors that influence the relative proportion of the two types of alkene end groups was for the CCT copolymerization of styrene and MMA.[29] In this study, the effect of the relative proportion of comonomers on the extent of macromonomer formation (i.e., oligomers with
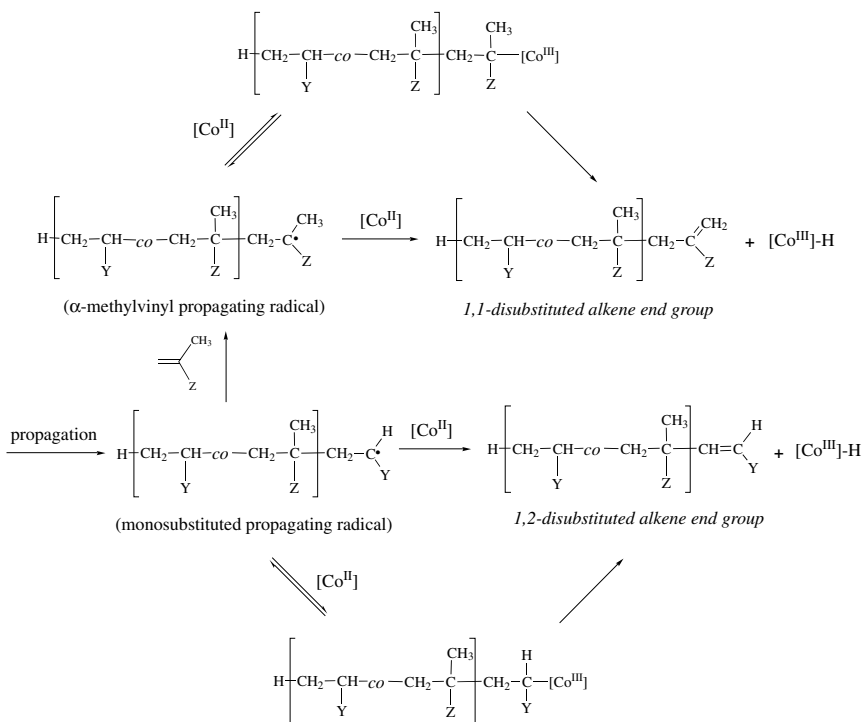
Scheme 12.8   Mechanism of CCT copolymerization and origin of 1,1-disubstituted and 1,2-disubstituted alkene end groups.
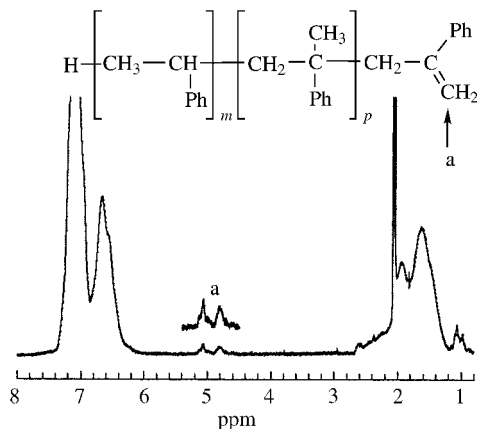
Figure 12.3 ^{1}H-NMR spectra, in deuterated acetone, of polystyrene macromonomer (**6**) identifying the 1,1-disubstituted alkene end group at δ5.2 and δ4.8.

1,1-disubstituted alkene end group) was probed. It was found that the level of 1,1-disubstituted alkene end group was proportional to the amount of MMA in the monomer feed. This meant that a styrene-based macromonomer with a high proportion of 1,1-disubstituted alkene end groups would contain a high proportion of MMA in the backbone. Subsequent studies have confirmed this observation.[30,61]

It has been shown that kinetic simulations using Monte Carlo methods[80] and numerical integrations[81] could be used to predict the molecular weight, composition, and end-group structure of multicomponent copolymers formed by free-radical polymerization in the presence of a chain transfer agent. The basis of these predictions was knowledge of the reactivity ratios, transfer constants, and relative initiation rates. These models have been extended to predict end-group structure in copolymerizations in the presence of a CCTA. When applied to the CCT copolymerization of styrene and MMA,[61] the kinetic simulation showed that end-group composition was dependant on comonomer composition. These were in general agreement with the results reported by Greuel and Harwood.[29] A subsequent report outlined results of a kinetic simulation for the CCT copolymerization of styrene and AMS.[63] The results indicated that only a small proportion of AMS ($<$5%) was required to obtain a predominant proportion of AMS derived end groups (i.e., 1,1-disubstituted alkene group). The results of this kinetic simulation appear to be inconsistent with experimental observations[30]—there is an overestimation of the proportion of AMS end groups arising from the kinetic simulation.[63] This discrepancy has been addressed and a revised kinetic model proposed that better predicts chain end structures in accordance with experimental observations.[28] From these studies a general understanding is being developed on the criteria necessary for choosing the α-methylvinyl monomer. The most critical is that the rate of reaction of the cobalt complex with the α-methylvinyl monomer derived propagating species needs to be substantially greater

than that of the propagating species derived from the monosubstituted monomer (see Scheme 12.8). The two factors that influence this are (1) the relative rate constants for chain transfer i.e., transfer constant for the α-methylvinyl propagating radical should be higher than the chain transfer constant for the monosubstituted propagating radical and (2) the relative reactivity of the propagating species, which is determined by propagation rate constants and reactivity ratios (i.e., the propagating radical should prefer to cross propagate with the α-methylvinyl monomer).[28]

The synthetic utility of the CCT process has been extended to the preparation of macromonomers based on styrenes and acrylates by the CCT copolymerization with α-methylstyrene (AMS) and methacrylates.[30] In this study it was found that the proportion of alkene end group type was affected by (1) the type of comonomer, (2) the relative amount of comonomer, (3) the type of CCTA, (4) the concentration of the CCTA, and (5) the reaction temperature. Taking these factors into account, styrene macromonomers, that are based predominantly on styrene, were prepared and isolated by copolymerizing styrene with AMS and isopropylcobalt(III) as the CCTA.[30,31] In contrast, either AMS or methacrylates have been shown to be effective α-methylvinyl comonomers for preparing acrylate macromonomers.[30,31] This methodology was extended to the preparation of functional styrene and acrylate macromonomers (**8** and **9**, respectively).[31]
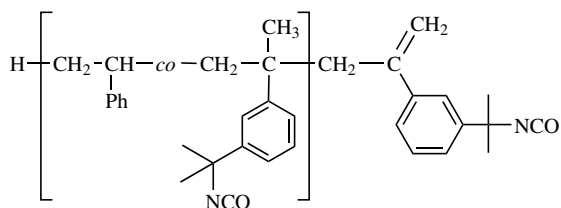
8
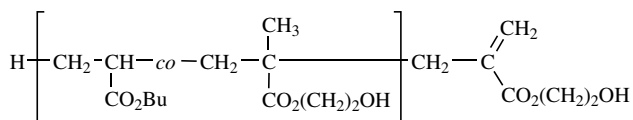
9

As judged by the volume of work published in the patent literature, there is a great deal of interest in the CCT process in free radical polymerization.[79] One of the major benefits of the CCT process is that it is a cost-effective method of controlling the molecular weight of polymers. Coupled to this, the CCT process is tolerant to a variety of functional groups and can be implemented without significant changes to conventional reaction conditions. From a synthetic point of view it also represents an attractive route to macromonomers which can be used as building blocks for well-defined macromolecules. To date, the primary industrial interest in this area appears to be for high solids coatings. In particular, the use of macromonomers to

manufacture graft copolymers for use as dispersants in automotive refinish coatings.[82] Other application areas of interest are solder masks[83] and adhesives.[84]

12.3   THE ADDITION–FRAGMENTATION CHAIN TRANSFER PROCESS

12.3.1   Overview

The addition–fragmentation chain transfer (AFCT) process in free-radical polymerization is effective in controlling molecular weight and preparing end-functional polymers. The AFCT process is induced by the addition of simple organic compounds referred to as addition–fragmentation chain transfer agents (AFCTA). The first reports of effective chain transfer utilizing the AFCT process involved the use of macromonomers of type **10** as AFCTA.[85]

$$H_2C=C \underset{CO_2R}{\overset{CH_2 \sim\sim\sim}{<}}$$

10

The utility of the AFCT was further developed by designing three classes of simple organic molecules with a general structure shown in Fig. 12.4.[86] These classes are represented by allylic compounds (Fig. 12.4, $A = Y = CH_2$), which include allylic sulfides ($X = SR$),[86–88] allylic peroxides ($X = OOR$),[89,90] allylic bromides ($X = Br$),[86,91,92] allylic sulfones ($X = S(O)R$),[86,91] allylic phosphonates ($X = P(O)(OR)_2$),[86,91] and allylic stannanes ($X = SnR$).[86,91] The other two classes are vinyl ethers (Fig. 12.4, $A = CH_2$, $Y = O$)[86,94,95] and (iii) thiocarbonyl compounds (Fig. 12.4, $A = S$, $Y = O$).[96,97] Group X is a good homolytic leaving group and Z can be varied to give an optimum C_{tr}.

AFCT is a versatile process being applicable to a range of monomers (styrene, (meth)acrylates, vinyls) and having the flexibility to introduce functionality at the α- and/or ω-terminal ends.[98,99] Mono and di end functional polymers are useful as building blocks for block, graft, segmented, and network polymer

Figure 12.4   General structure of AFCTA.

Scheme 12.9   Mechanism of AFCT process and final polymer structure.

architectures.[100–103] The general mechanism of the AFCT process is outlined in Scheme 12.9 and gives rise to polymers as depicted. The incorporation of appropriate functionality in the X and Z groups (Scheme 12.9) will result in mono and/or di end-functional oligomers.

The concept of carbon–carbon bond formation by radical addition–fragmentation has its origins in the original work by Lewis and co-workers, who reported the allylation of aldehydes utilizing radical addition–fragmentation.[104] Sometime later, the major efforts of other investigators[105–111] all helped establish radical addition–fragmentation as a useful tool for C—C bond formation. More recent works[112,113] continue to show the value of this process in organic synthesis. Although the AFCT process has its roots in these original works, there is an added dimension when applying the basic concepts of radical addition–fragmentation to free radical polymerization. In order for chain transfer by radical addition–fragmentation to operate effectively, the process must compete with propagation. To achieve this the chain transfer agent must have (1) a double bond whose reactivity toward propagating radicals is similar to that of the polymerizing monomer, (2) fast fragmentation of the resulting adduct radical, and (3) efficient re-initiation of polymerization by the expelled radical.[98,114] Important criteria for achieving optimal radical addition–fragmentation for C—C bond formation have been reviewed.[99,115]

This section will discuss how simple AFCTA are employed to control molecular weight and to prepare end-functional polymers.

12.3.2   Macromonomers as Chain Transfer Agents

The concept of chain transfer by a mechanism involving addition-fragmentation arose from observations during a study on the chemistry of methyl methacrylate macromonomers (**11**).

$$Y = CO_2Me$$
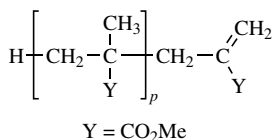
11

A detailed study of cyanoisopropyl radical addition to methyl methacrylate trimer (**11**, $p = 2$) revealed that the favored reaction of the adduct radical was β scission.[85] The major products from this pathway, which are highlighted in Scheme 12.10, are a propagating radical and a new alkene terminated oligomer, namely, a new macromonomer. The new propagating radical terminates by disproportionation to yield methyl methacrylate dimer (**11**, $p = 1$) or by combination with itself or with the cyanoisopropyl radical. In an extension to this work, the copolymerization of methacrylate-based macromonomers with acrylates, methacrylates, styrene, acrylonitrile, vinyl acetate, and acrylamide was investigated. It was observed that macromonomers copolymerize with the less sterically hindered monomers (e.g., acrylates, styrene, acrylonitrile, acrylamide) to afford graft copolymers.[85,116–119] In contrast, little[85,120] or no[116,121] copolymerization was observed with the more sterically hindered methacrylates (e.g., see Table 12.7). On the basis of all these observations, a general mechanism was proposed to explain the results of copolymerization of methacrylate macromonomers with various monomers (Scheme 12.11).[116]

The addition of propagating radical **A** to methacrylate macromonomer **B** is expected to occur readily to give adduct radical **C**.[85,116] This radical has been observed by ESR spectroscopy in the case of MMA propagating radical addition

Scheme 12.10

TABLE 12.7   Copolymerization of Methyl Methacrylate (MMA) Macromonomers with Ethyl Acrylate (EA), Styrene (Sty), and MMA[85]

Monomer	Macromonomer M_n	mol% Macromonomer in Feed	% Conversion	Product $M_n \times 10^{-3}$	Mol% Macromonomer in Product
EA	—	—	95	270.0	—
	1000	12	95	36.0	11.0
Sty	—	—	92	21.0	—
	540	7.7	51	4.8	5.3
MMA	—	—	99	26.0	—
	680	5.9	71	9.3	1.7

to MMA dimer **B** $(p = 0)$.[122] The adduct radical **C** can react by one of three different pathways: (1) it can add to monomer, which would result in the macromonomer becoming incorporated into the polymer backbone (yielding a graft copolymer); (2) it can revert to the starting species, in which case the propagating radical **A** can continue to grow by further addition of monomer; or (3) it can fragment, by β scission, and in so doing generates a polymeric reinitiating radical (**E**) and a new alkene terminated oligomer (**D**) whose backbone is based on the propagating radical (**A**). The relative rates of these pathways depend on the monomer used. For alkyl acrylates (**A**; X = H, Y = CO₂R), fragmentation of the adduct radical **C** to **D** and

Scheme 12.11   Mechanism of copolymerization of macromonomers.

E is likely to be more favourable than fragmentation by the reverse reaction to **A** and **B**. This is because the former route gives rise to a more stable tertiary radical (**E**) compared to the secondary radical of the alkyl acrylate propagating species (**A**). However, propagation of the adduct radical **C** (X = H, Y = CO$_2$R) by reaction with monomer is also favorable presumably because the alkyl acrylate monomer is relatively unhindered and so can be attacked by the bulky radical **C**. This is evident from the results in Table 12.7, which show that for ethyl acrylate, incorporation of MMA macromonomer is high. In contrast, there is little incorporation of macromonomer in copolymerizations with methyl methacrylate (i.e., propagating radical **A**; X = Me, Y = CO$_2$CH$_3$).[85] In a follow-up study, ethyl methacrylate (EMA) was polymerized in the presence of MMA dimer or trimer (**B**, $p = 0$ or $p = 1$, respectively). A ^{1}H-NMR analysis of the product revealed that only one macromonomer unit per chain was incorporated and that this resided at the chain ends, in agreement with the mechanism in Scheme 12.11.[123] The lack of macromonomer copolymerization with MMA suggests that propagation of adduct radical **C** is severely limited.[116,124] Indeed, the large van der Waals interactions between a bulky radical **C** approaching a hindered methacrylate monomer is likely to be the reason for propagation of radical **C** to be unfavorable. Ultimately, the favored route and the path forward is through fragmentation by β scission. In the case of a propagating radical derived from styrene (**A**; X = H, Y = Ph), the situation is between the methacrylate and acrylate examples with a higher level of macromonomer incorporation than methacrylates but lower than the acrylates. A more comprehensive study of chain transfer by addition–fragmentation vs copolymerization of various dimers and trimers (MMA dimer, EMA dimer, methacrylonitrile (MAN) dimer, α-methylstyrene dimer, and methyl acrylate trimer) with MMA, MA, and styrene found a similar trend. Namely, the steric bulk surrounding the radical center of the addition adduct **C** (Scheme 12.11), determined the extent of copolymerization versus chain transfer.[125,126]

It is evident from the discussion above that methacrylate macromonomers act as chain transfer agents in free radical polymerization by a mechanism of addition–fragmentation and in so doing install an olefinic group at the end of polymer chains. These products are themselves macromonomers that can react further as the polymerization progresses. For polymerization of acrylates in the presence of macromonomers the newly formed macromonomers will be branched because of concurrent copolymerization. The continued copolymerization of these would give rise to highly branched block copolymer structures.[127] The polymerization of methacrylates in the presence of methacrylate macromonomers will yield new methacrylate macromonomers that will, in turn, participate in the addition–fragmentation process. This 'recycling' is the genesis of reversible addition-fragmentation chain transfer discussed in the next section.

12.3.3 Chain Transfer Constants of Macromonomers

According to the mechanism of chain transfer of methacrylate macromonomers by addition–fragmentation, the rate constant for chain transfer, k_{tr}, is a composite term
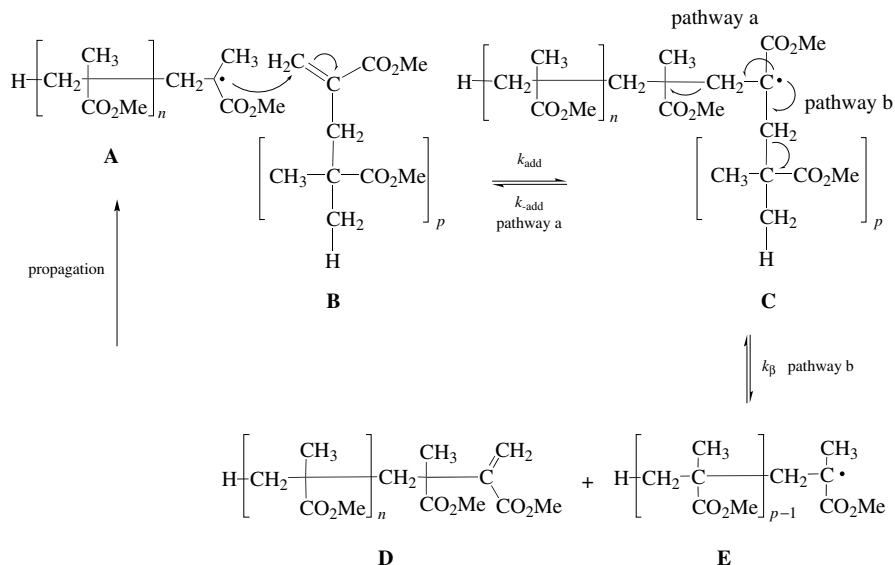
Scheme 12.12   Rate parameters that contribute to chain transfer by AF process.

consisting of a number of rate constants: k_{add}, k_β, and k_{-add} (Scheme 12.12). Hence, k_{tr} is determined by the reactivity of the alkene group and the fragmentation pathway of the adduct radical **C** (Scheme 12.12).

The C_{tr} for various macromonomers in ethyl acrylate (EA), MMA and styrene polymerization is listed in Table 12.8. In general terms, the C_{tr} for MMA trimer (Scheme 12.12, **B**, $p = 2$) is approximately an order of magnitude higher than for MMA dimer (Scheme 12.12, **B**, $p = 1$). In addition, C_{tr} for MMA macromonomers increases with chain length from dimer to tetramer (Scheme 12.12, **B**, $p = 3$) and remains constant for higher oligomers (see Table 12.8).[128]

The rate constants for addition of radicals to a double bond depends on a combination of factors which include steric, resonance, and polar terms.[130] Since any structural differences between dimer and trimer (and higher oligomers) are remote from the double bond, it has been assumed that the reactivity of the double bond, in these species is independent of chain length. This suggestion is supported by the observation that *tert*-butoxy radicals add at similar rates to the double bond of dimer and trimer but at about half the rate for addition to MMA monomer.[116] The lower reactivity of the oligomers compared to MMA monomer is attributed to steric factors. Given these observations, it would be anticipated that the reactivity of the dimer to radical addition be similar if not faster than the trimer. However, the dimer has a lower transfer constant than trimer, tetramer, and higher oligomers. This is likely to be due to the adduct radical **C** fragmenting preferentially to the starting species by pathway **a** in the case of dimer rather than fragmentation by pathway **b** (Scheme 12.12). It would appear that steric effects play a dominant role in determining the preferred fragmentation pathway. The fragmentation process, via β scission, results

TABLE 12.8   Chain Transfer Constants (C_{tr}) for Macromonomers at 60°C

Macromonomer	C_{tr}			
	EA	MMA	Styrene	Ref.
MMA dimer[a]	0.12[b]	0.013	—	128
MMA trimer[a]	0.84[b]	0.19	0.55	128
MMA tetramer[a]	—	0.31	—	128
MMA macromonomer[a]	—	0.21	—	128
BzMA dimer[c]	—	0.015	—	129
AMS-EMA dimer[d]	—	0.10	—	125
MAN-AMS dimer[e]	—	0.15	—	125
AMS-MMA dimer[f]	—	0.19	—	125
AMS dimer[g]	—	0.13	0.20	125

[a] MMA (methyl methacrylate).
[b] Ref. 123.
[c] BzMA (benzyl methacrylate), at 80°C.
[d] AMS-EMA [mixture of α-methylstyrene—ethyl methacrylate dimer and ethyl methacrylate-α-methylstyrene dimer (2.8 : 1 mole ratio), at 110°C].
[e] MAN-AMS [mixture of methacrylonitrile-α-methylstyrene dimer and α-methylstyrene-methacrylonitrile dimer (1.5 : 1 mole ratio), at 110°C].
[f] AMS-MMA [mixture of α-methylstyrene-methyl methacrylate dimer and methyl methacrylate-α-methylstyrene dimer (2.8 : 1 mole ratio), at 110°C].
[g] AMS (α-methylstyrene dimer, at 110°C).

in the breaking of C—C bonds, which relieves steric compression as the carbon hybridization moves from tetrahedral sp^3 in the radical to planar sp^2 in the products, thus allowing the substituents to move further apart from each other. Considering the case of the adduct radical (**C**, $p = 1$) from addition to dimer (see Scheme 12.12), the steric repulsion between the methyl group, a carbomethoxy group, and a polymer chain would be more than the steric repulsion between the two methyl groups and the carbomethoxy group. Hence pathway **a** would be favored over pathway **b** as the relief of steric strain would be greater if the adduct radical **C** fragments in this direction. As the size of the macromonomer increases, namely, trimer to tetramer to oligomer, the size of the attached alkyl group also increases and so the difference in steric relief between pathways **a** and **b** is diminished. In these cases fragmentation via pathway **b** is enhanced and this manifests itself as an observed increase in C_{tr} (see Table 12.8). A study involving MO calculations for the fragmentation process also show that both the enthalpy and entropy of activation are chain-length-dependent up to tetramer and these parameters also appear to favor β scission for the higher oligomers.[128]

12.3.4   Allylic Class of Addition–Fragmentation Chain Transfer Agents

The allylic class of AFCTA, represented in Fig. 12.5, encompasses a group of compounds that include the allylic sulfides (X = SR),[86–88] allylic peroxides

$$CH_2=\underset{Z}{\overset{CH_2-X}{\diagup}}$$

X = SR, Br, SO$_2$R, P(O)(OR)$_2$, SnR$_3$, SiR$_3$, OOR

Z = Ph, Ar, CO$_2$R, CN, CONH$_2$, OC(O)R, Cl, H
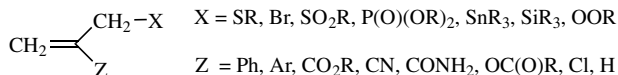
Figure 12.5 Allylic class of AFCTA.

(X = OOR),[89,90] allylic bromides (X = Br),[86,91–93] allylic sulfones (X = S(O)R),[86,91] allylic phosphonates (X = P(O)(OR)$_2$),[86,91] and allylic stannanes (X = SnR).[86,91] The allylic class of AFCTA yield macromonomers as final products via the mechanism shown in Scheme 12.13. The majority of compounds in the allylic class have been reported in a 1988 patent.[86] A summary of the different types of allylic compounds used as AFCTA, and hence the macromonomers formed (Scheme 12.13), are listed in Table 12.9. As is evident from Table 12.10, the allylic sulfides (Fig. 12.5, X = SR) are attractive AFCTA because: (1) their C_{tr} are in the range of greatest utility (an ideal C_{tr} is 1.0) for controlling molecular weight in batch polymerizations;[3] (2) they can be used to prepare a range of macromonomers based on methacrylates, styrene, and acrylates, and (3) they can provide both mono and di end-functional polymers when appropriate functionality is introduced in Z and R groups. For example, according to Scheme 12.13, utilizing a dihydroxy functional AFCTA (last entry, Table 12.10) will lead to a dihydroxy end-functional macromonomer (**12**).

$$HOCH_2CH_2S\sim\sim\sim CH_2-\underset{CO_2CH_2CH_2OH}{\overset{CH_2}{\diagup}}$$
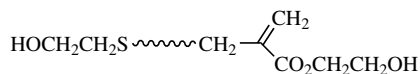
12

In a similar vein, a polymerizable allylic sulfide AFCTA (**13**) was used to prepare hyperbranched polymers and block copolymers.[135]
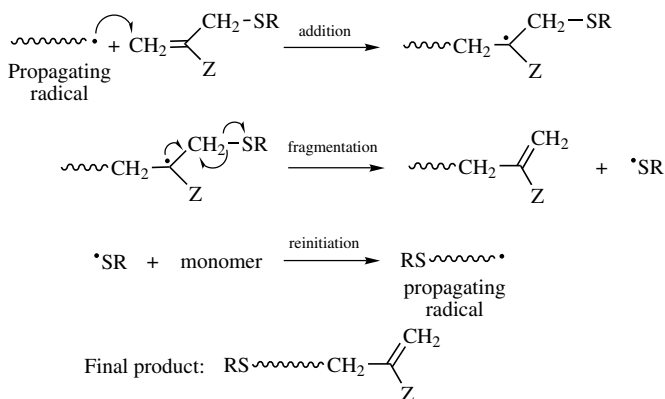
Scheme 12.13 AFCT process with allylic class as CTA and final product.

TABLE 12.9 Various AFCTA in the Allylic Class (Fig. 12.5)

Allylic	Z	X	Ref.
Bromides	CO_2Et	Br	91,131
	Ph	Br	91
	CN	Br	91
	PhCH	Br	132
Sulfides	CO_2Et	$S(tBu)$	87
	CO_2Et	SCH_2CO_2H	88
	CO_2Et	$S(CH_2)_2OH$	98
	CO_2H	$S(CH_2)_2OH$	98
	CO_2H	SCH_2CO_2H	98
	CN	$S(tBu)$	87
	Ph	$S(tBu)$	87
	Ph	$S(CH_2)_2OH$	88
	Ph	$S(CH_2)_2CO_2H$	88
	Ph	$S(CH_2)_2NH_2$	88
	Ph	$S(CH_2)_2Si(OMe)_3$	88
	H	$S(tBu)$	87
	H	Cl	114
	Cl	$S(tBu)$	114
	Cl	Cl	114,133
	Br	Br	133
Sulfonates	CO_2Et	SO_2Ph	91,134
	CO_2Et	SO_2CH_2Ph	134
	OC(O)Me	SO_2Ph	91
Sulfones	Ph	$S(O)(nBu)$	91
Stannanes	CO_2Et	$Sn(nBu)_3$	91

TABLE 12.10 Chain Transfer Constants (C_{tr}) of Allylic Sulfides (Fig. 12.5, X = SR) for Methyl Methacrylate (MMA), Styrene (Sty), Methyl Acrylate (MA), and Butyl Acrylate (BA) Polymerizations at 60°C[98]

Z	R	C_{tr}			
		MMA	Sty	MA	BA
Ph	tBu	1.2	0.8	3.9	—
CO_2Et	tBu	0.7	1.0	2.2	—
CN	tBu	1.4	1.8	1.6	—
Ph	CH_2CO_2H	1.1	1.0	—	—
Ph	$(CH_2)_2OH$	1.0	0.8	—	—
Ph	$(CH_2)_2NH_2$	0.9	0.8	—	—
CO_2Et	$(CH_2)_2OH$	0.5	1.2	—	1.3
CO_2H	$(CH_2)_2OH$	0.3	1.8	—	1.5
CO_2H	CH_2CO_2H	0.7	1.3	—	—
$CO_2(CH_2)_2OH$	$(CH_2)_2OH$	0.4	0.8	—	1.9
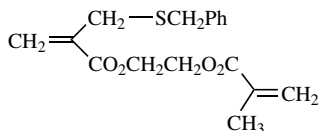
13

The other compounds in the allylic class of AFCTA (e.g., allylic bromides, allylic sulfones, allylic phosphonates, and allylic stannanes) are also useful CTA in controlling molecular weight in polymerizations as judged by their C_{tr} (Table 12.11). The allylic malonates, as represented in Fig. 12.6, are an additional group of allylic AFCTA.[136] Generally in (meth)acrylates and styrene polymerizations, the C_{tr} of allylic malonates are low, comparable to MMA dimer.[136] However, they lead to oligomers with a terminal cinnamate functionality (Fig. 12.6, R^1 = Me or Ph) which has the advantage that the oligomer is no longer a reactive macromonomer, and hence the possibility of branching in high conversion acrylic polymers is reduced.[115]

The range of allylic CTA was further supplemented by compounds shown in Fig. 12.7.[137] These compounds were designed to investigate the dependence of CTA structure on the chain transfer constant. In these structures, the fragmenting radical X• exhibits a captodative stabilization effect as it contains both electron donating and electron accepting substituents. However, although fragmentation is favored due to the stabilizing effect, the radical X• is expected to be slow to reinitiate

TABLE 12.11   Chain Transfer Constants (C_{tr}) of Allylic Bromides, Allylic Sulfones, Allylic Phosphonates, and Allylic Stannanes (Fig. 12.5) for Methyl Methacrylate (MMA), Styrene (Sty), and Methyl Acrylate (MA) Polymerizations at 60°C[98]

		C_{tr}		
Z	X	MMA	Sty	MA
Ph	Br	2.3	2.9	5.3
CO$_2$Et	Br	1.5	—	2.3
CN	Br	2.2	—	3.0
CO$_2$Et	SO$_2$Ph	1.1	5.8	—
CO$_2$Et	SO$_2$C(CH$_3$)$_3$	1.0	—	—
Ph	P(O)(OEt)$_2$	0.4	—	—
CO$_2$Et	Sn(Bu)$_3$	3.0	—	—
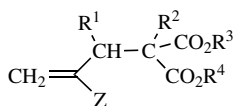
Z = Ph, CO$_2$R, CN, CONH$_2$, OC(O)R, Cl, H
R^1 = H, Me
R^2 = H, Me, PhCH$_2$
R^3,R^4 = Alkyl

Figure 12.6   Allylic malonate AFCTA.

$$CH_2 = \underset{CO_2Et}{\overset{CH_2-X}{<}} \qquad \begin{array}{l} X = CH(NMe)_2CN, CH(SMe)CN, \\ \quad OC(O)CH_2Ph \end{array}$$
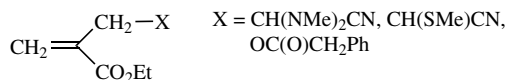
Figure 12.7

polymerization, which would explain the observed retardation.[137] The observation that captodatively stabilized radicals are slow to react with substrates has been reported.[138]

To access macromonomers with a higher reactivity toward copolymerization (e.g., to prepare graft copolymers), polystyrene and poly(methyl methacrylate) oligomers with a pentadienyl end group were prepared (Scheme 12.14) utilizing AFCTA (**14**).[137,139,140] Instances of retardation of polymerization were overcome by the correct choice of Z, Z′, X and R.[139] The retardation was presumably a result of the high stability of adduct radical **A** (Scheme 12.14). This class of AFCTA was efficient in chain transfer activity (as judged by the extent of pentadienyl end group incorporation) but exhibited limitations with poor regioselectivity and further reaction of the formed macromonomer.
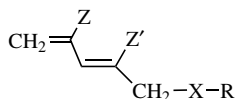
14

For an efficient AFCT process the propagating radical must undergo 1,4 addition (Scheme 12.14). However, it was found that substantial 4,1 addition of propagating radicals also occured. In this case the intermediate adduct radical does not fragment but continues propagation resulting in the copolymerization of the AFCTA.[140] Furthermore, because of the high reactivity of the pentadienyl-capped oligomers, further reaction led to the formation of highly branched polymers with an associated high polydispersity index. This problem was alleviated by stopping the polymerization at low conversion or by fractionating the products obtained at higher conversions. A
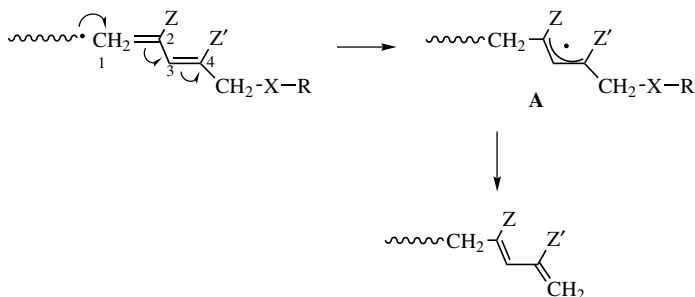
Scheme 12.14   Formation of pentadienyl-terminated oligomer.

$$CH_2 = \underset{CH_2-X^2}{\overset{CH_2-X^1}{<}} \quad \begin{array}{l} X^1 = Cl, SR, SO_2R \\ X^2 = Cl, SR, SO_2R \end{array}$$
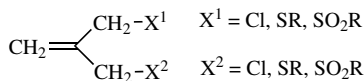
Figure 12.8

range of 1,3-disubstituted-2-methylene propanes, as represented in Fig. 12.8, have also been investigated as alternative allylic AFCTA.[133,141] As a general group, these compounds possess C_{tr} similar to those of disulfides (see Table 12.12; cf. Table 12.3). Their mode of action follows the mechanism outlined in Scheme 12.13. Hence, appropriately disubstituted 2-methylene propanes can be employed to pre-pare α,ω-functionalized polymers.[141] The allylic peroxides (**15**) fall under the allylic class of AFCTA, but yield oligomers with an oxirane end group rather than a 1,1-disubstituted alkene end group as for the general allylic class.

$$CH_2 = \underset{Z}{\overset{R'}{\underset{\displaystyle |}{<}}} CH-O-OR$$
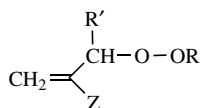
15

The mechanism by which the oxirane end group is obtained is depicted in Scheme 12.15 and is largely similar to the mechanism of action of allylic AFCTA. A propa-gating radical adds to the allylic peroxides giving an intermediate adduct radical. This radical undergoes a $1,3-S_{H}i$ intramolecular homolytic substitution, resulting in the cleavage of the weak peroxy bond. In contrast to the general allylic class of AFCTA that fragment by β scission, fragmentation for the allylic peroxides proceeds via γ scission. This results in the formation of an epoxide and the expulsion of an

TABLE 12.12   Chain Transfer Constants (C_{tr}) of 1,3-Disubstituted-2-methylene Propanes (Fig. 12.8) for Styrene and Vinyl Acetate polymerizations at 60°C

AFCTA X^1	X^2	C_{tr} Styrene	Vinyl Acetate
Cl	Cl	—	3.4
p-CH$_3$C$_6$H$_4$SO$_2$—	p-CH$_3$C$_6$H$_4$SO$_2$—	—	3.9[a]
Cl	p-CH$_3$C$_6$H$_4$SO$_2$—	—	0.05[a]
CH$_3$C(O)S—	CH$_3$C(O)S—	—	2.66 [a]
CH$_3$O$_2$CCH$_2$S—	CH$_3$O$_2$CCH$_2$S—	0.02[b]	—
HOC$_3$H$_6$S—	HOC$_3$H$_6$S—	0.04[b]	—

[a] Ref. 133.
[b] Ref. 141.
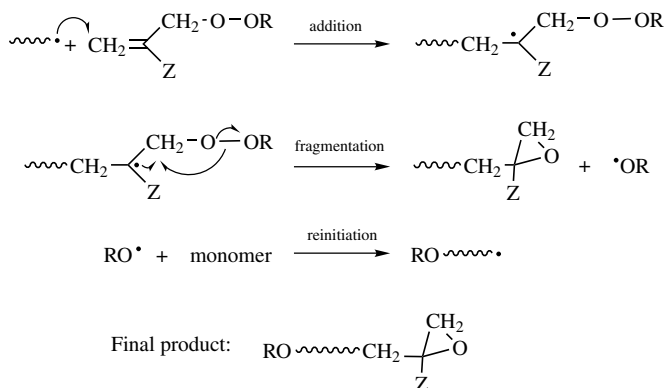
Scheme 12.15 The mechanism of action of allylic peroxides and resultant oligomer end-group structure.

alkoxyl radical (Scheme 12.15). The epoxide end-group structure has been verified by ^{1}H-NMR analysis.[98] A similar 1,3-S_Hi mechanism resulting in epoxide formation had been observed in the reaction of allyl t-butylperoxide with radicals generated from simple esters, nitriles, and amides.[142] Some allylic peroxides which have been employed as AFCTA are shown in Table 12.13. The C_{tr} of allylic peroxides determined in methyl methacrylate, styrene, and methyl acrylate (Table 12.14) show that these compounds are effective CTA. The C_{tr} of allylic peroxides is several orders of magnitude higher than simple dialkyl peroxides (compare with di-t-butyl peroxide; C_{tr} of 0.00023–0.0013 and diisopropyl peroxide; C_{tr} of 0.0003),[147] which suggested that chain transfer with the allylic peroxides is not due to direct attack at the peroxy bond.

TABLE 12.13 Various Allylic Peroxide AFCTA (15)

Z	R′	R	Ref.
H	H	t-Bu	114
CO$_2$Me	H	t-Bu	89,90,98
CO$_2$Et	Me	CH(OMe)OBu	143
CO$_2$Et	Me	CH(CH$_2$)$_3$O	144
CO$_2$Et	Me	Si(Me)$_3$	145
CO$_2$Et	Me	Si(Me)$_2$CH=CH$_2$	145
Ph	H	t-Bu	98,89,90
Ph	H	C(Me)$_2$Ph	98,89,90
Ph	OMe	C(Me)$_2$Ph	146
Ph	OOC(Me)$_2$Ph	C(Me)$_2$Ph	146

TABLE 12.14   Chain Transfer Constants (C_{tr}) of Allylic Peroxides (Fig. 12.5, X = OOR) for Methyl Methacrylate (MMA), Styrene (Sty), and Methyl Acrylate (MA) Polymerizations at 60°C[98]

		C_{tr}		
Z	R	MMA	Sty	MA
Ph	C(CH$_3$)$_3$	0.9	0.8	—
Ph	C(CH$_3$)$_2$Ph	0.8	0.8	—
CO$_2$CH$_3$	C(CH$_3$)$_3$	1.6	0.6	1.0
CN	C(CH$_3$)$_3$	2.0	0.9	0.7

12.3.5   Vinyl Ether Class of Addition–Fragmentation Chain Transfer Agents

A range of compounds in the vinyl ether class as shown in Fig. 12.9 are effective as AFCTA.[94,95] The mechanism of AFCT follows the general route discussed for allylic compounds. The vinyl ether AFCTA yield oligomers with a ketone end group structure is as shown in Scheme 12.16. In this case, the formation of the stable C—O double bond is an added driving force for the fragmentation process. Several compounds in the vinyl ether class have C_{tr} that approach the ideal value of 1.0 (Table 12.15).

Figure 12.9   Vinyl ether class of AFCTA.

Scheme 12.16   Vinyl ethers as AFCTA and oligomer end-group structure.

TABLE 12.15   Various Vinyl Ether AFCTA (Fig. 12.9) and Chain Transfer Constants (C_{tr}) for Methyl Methacrylate (MMA), Styrene (Sty), Methyl Acrylate (MA), and Vinyl Acetate (VA) Polymerizations at 60°C[98]

		C_{tr}			
Z	X	MMA	Sty	MA	VA
Ph	Ph	0.8	0.3	5.7	9.7
CN	Ph	0.08	0.04	0.3	12
CO_2Me	Ph	0.2	0.05	0.5	20
$CONH_2$	Ph	0.5	0.2	1.1	—
Ph	$4\text{-}NCC_6H_4$	0.8	0.2	—	—
H_2NCH_2Ph	$4\text{-}HOCH_2C_6H_4$	0.6	—	—	—
$p\text{-}Cl\text{-}Ph$	Ph	0.8	—	—	—

12.3.6   Thiocarbonyl Class of Addition–Fragmentation Chain Transfer Agents

The use of thiohydroxamic esters for generation of alkyl radicals in organic chemistry is well known through the work of Barton and co-workers.[148] The potential for these materials to function as AFCTA is indicated by the C_{tr} of **16** and **17** in Table 12.16.[96]

16   a. $X = C_{15}H_{31}$
         b. $X = C_6H_5CH_2$
         c. $X = C_6H_5$

17   a. $X = C_{15}H_{31}$
         b. $X = C_6H_5CH_2$
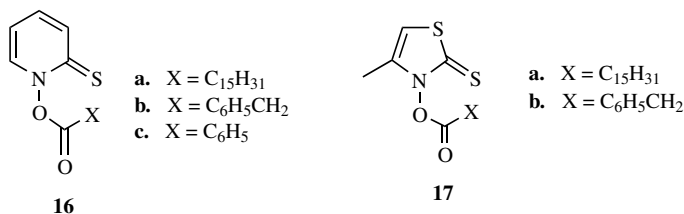
The C_{tr} shows the effectiveness of these compounds as CTA to control the polymerization of styrene, (meth)acrylates, and vinyl acetate. Compounds represented by **16**

TABLE 12.16   The Measured Chain Transfer Constant (C_{tr}) of Structures 16 and 17 at 60°C with Methyl Methacrylate (MMA), Styrene, Methyl Acrylate (MA), and Vinyl Acetate (VA).

AFCTA	C_{tr}			
(Structure)	MMA	Styrene	MA	VA
16a	4.0	3.8	20	36
16b	4.3	3.9	—	80
16c	2.8	—	—	—
17a	0.6	0.3	3.1	9.7
17b	1.0	1.0	—	18

Figure 12.10 Thionoester group of AFCTA.

have been employed to modify polymer film surfaces by grafting. Various techniques are employed to introduce a linking group, (e.g., carboxylic acid) on the polymer surface to covalently bind the thiohydroxamic acid. The first example of grafting using these compounds was illustrated by the formation of poly(acrylonitrile) grafts on polyethylene.[149] Subsequent examples have expanded the versatility of these compounds by grafting styrene onto cellulose,[150] and styrene, MMA, vinyl pyridine, and acrylamide onto poly(arylene ether sulfone).[150,151]

The thiocarbonyl class of AFCTA was broadend when thionoesters, represented in Fig. 12.10, were reported to undergo chain transfer by the AF process.[98] The use of thionoesters as AFCTA produced oligomers with a thioloester end group, as outlined in Scheme 12.17. Examples of thionoester AFCTA are listed in Table 12.17, along with their C_{tr} in styrene, methyl acrylate, and vinyl acetate.[98]

12.3.7 Applications

A common method of accessing end functional polymers is by polycondensation reactions, including preparation of polyesters.[152] An alternative procedure is by chain growth polymerization and advances in both ionic and group transfer polymerization methods have enabled some examples of end functional oligomers.[153,154] The need for stringent reaction conditions, high purity and often expensive reagents has led to severe limitations for these techniques being widely used. As an alternative chain growth polymerization technique, free radical polymerization has been employed along a number of strategies to access end functional oligomers.[152,155–157]

Scheme 12.17 Thionoesters as AFCTA and resultant oligomer end-group structure.

TABLE 12.17   Chain Transfer Constants (C_{tr}) of Thionoesters (Fig. 12.10) with Styrene, Methyl Acrylate (MA), and Vinyl Acetate (VA) Measured at 60°C[98]

		C_{tr}		
Z	X	Styrene	MA	VA
Ph	Ph	1.0	1.2	>20
Ph	4-MeOOCPh	0.6	1.4	—
4-MeOPh	Ph	0.1	1.3	—
4-MeOPh	4-MeOOCPh	0.3	1.1	—
Ph	4-HOCH$_2$Ph	0.4	0.8	—

These have included the use of iniferters,[158,159] functional initiators,[160] telomers as functional chain transfer agents[161] and incorporation of weak links along the polymer chain for cleaving.[162,163]

The AFCT process is an effective technique in the important area of controlling and reducing molecular weight of polymers. In addition, end functional oligomers are of interest since they can be used as prepolymers in coupling reactions. Typically, mono- and di- end functional oligomers can be reacted together with difunctional and multifunctional linking agents to give a variety of polymer architectures, including block and graft copolymers and crosslinked networks. The most accepted widespread use of di end-functional oligomers (telechelics) is in the preparation of polyurethanes (in foams and materials) where the terminals are hydroxyl functionalized. Other important uses include adhesives, sealants, and reactive injection moulding.[98] There is an increasing interest in targeting end-functional prepolymers as precursors in high solids coatings where low-molecular-weight oligomers are required for lowering the volatile organic content (VOC). Improved mechanical performance is achieved through molecular weight buildup by cross linking during the curing process.[164,165]

12.4   THE REVERSIBLE ADDITION–FRAGMENTATION CHAIN TRANSFER PROCESS

12.4.1   Overview

In an extension of the addition–fragmentation concept, methacrylate-based macromonomers have been shown to impart "living" behavior to free-radical polymerizations. To demonstrate this feature, narrow polydispersity block copolymers, based on methacrylates, were prepared under feed conditions.[47,70,166] The mechanism was envisaged to operate by reversible addition–fragmentation chain transfer and represented a new process for achieving living free-radical polymerization. Subsequently, it was found that simple organic compounds possessing the thiocarbonylthio moiety (S=C—S) were much more effective and versatile in inducing
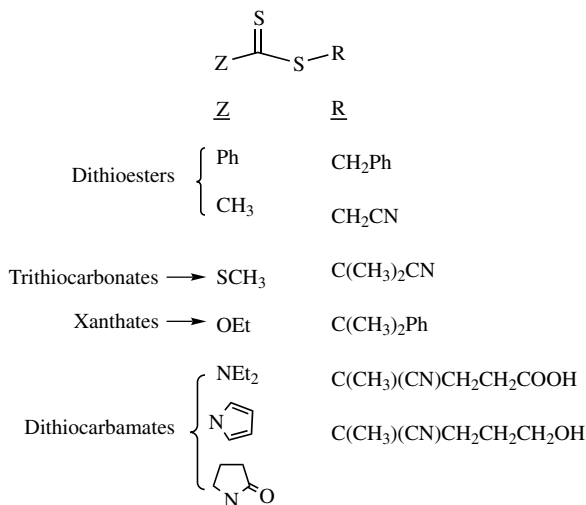
Figure 12.11   Examples of the different classes of thiocarbonylthio RAFT agents.

"livingness" by reversible addition–fragmentation chain transfer.[167–171] For convenience the terms RAFT process and RAFT agents were coined.[169] Representative examples of thiocarbonylthio RAFT agents are shown in Fig. 12.11.

There are four classes of thiocarbonylthio RAFT agents, depending on the nature of the Z group: (1) dithioesters (Z = aryl or alkyl), (2) trithiocarbonates (Z = substituted sulfur), (3) dithiocarbonates (xanthates) (Z = substituted oxygen), and (4) dithiocarbamates (Z = substituted nitrogen). A report of a controlled free-radical polymerization technique involving xanthates, referred to as MADIX (*ma*cromolecular *d*esign via *i*nterchange of *x*anthate), has been described.[172,173] The mechanism by which this technique operates has also been proposed to involve reversible addition–fragmentation chain transfer and hence any subsequent discussions which involve xanthates as RAFT agents (Fig. 12.11, Z = substituted oxygen) in the RAFT process also apply to MADIX.

RAFT polymerization is performed by adding a chosen quantity of an appropriate RAFT agent (Fig. 12.11) to a conventional free radical polymerization mixture and yields polymers of predetermined chain length and narrow polydispersity. Polydispersity indices of less than 1.1 can be usually achieved under optimal conditions. The RAFT process offers the same versatility and convenience as conventional free-radical polymerization being applicable to the same range of monomers (e.g., (meth)acrylates, styrenes, acrylamides, vinyls), solvents, functional groups (e.g., OH, CO$_2$H, NR$_2$, NCO) and reaction conditions (e.g., bulk, solution, suspension and emulsion). The RAFT process yields thiocarbonylthio-terminated polymers (or 1,1-disubstituted alkene-terminated oligomers if macromonomers are used as RAFT agents) that can be chain extended to yield a variety of copolymers (e.g., AB, ABA blocks, gradient, segmented).

12.4.2   Macromonomers as RAFT Agents

The utility of macromonomers as chain transfer agents and reagents for preparing graft copolymers has been discussed in the previous section. In addition to this, methacrylate-based macromonomers are useful as reagents for the preparation of block copolymers via the RAFT process.[47,70,166] The success of block formation was shown to be dependent on macromonomer structure, comonomer structure, and reaction conditions. The mechanism proposed for block formation is outlined in Scheme 12.18. Overall, the macromonomer forms the "A block" and the comonomer forms the "B block" in the AB diblock copolymer **5**. More specifically, the propagating species **1** derived from the comonomer, adds to the macromonomer **2** to form the adduct radical **3**. As was highlighted in Scheme 12.11, the adduct radical can react by three pathways: (1) revert back to starting species, (2) react with monomer to form a graft copolymer, or (3) fragment by β scission. The last pathway leads to a new macromonomer and a new oligomeric propagating radical that is based on
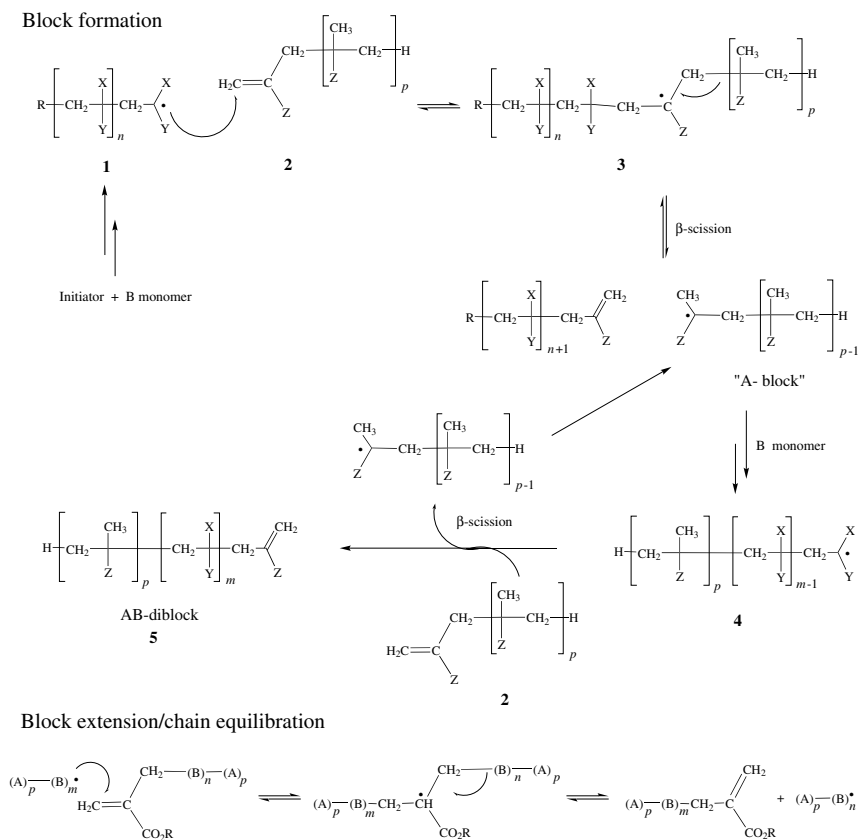
Scheme 12.18   Block formation, extension, and chain equilibration via the RAFT process with macromonomers.

the macromonomer **2**. This oligomeric radical forms the basis of the "A block." Propagation of this radical by reaction with the comonomer forms species **4**, which is the "AB diblock" propagating radical. Termination of radical **4** by reaction with macromonomer **2** results in the AB-diblock and a new "A block" propagating species.

There are two crucial factors for efficient block formation via the RAFT process with macromonomers:

1. Fragmentation of adduct radical **3** by β scission must be the predominant pathway (see Scheme 12.18). As previously discussed, for methacrylate-based macromonomers fragmentation of adduct radical **3** always dominates over reaction with monomer. The use of sterically bulky comonomers, such as methacrylates further favors fragmentation of radical species **3** over propagation. For less sterically bulky comonomers, such as styrene and acrylates, the fragmentation pathway can be made to predominate by increasing the reaction temperature.[70]

2. Chain transfer to macromonomer must be the dominant mechanism for termination and initiation. Chains formed from initiator derived radicals can give "B block" homopolymer impurity via radical–radical reactions, namely, dead polymer. Hence rates of initiation are typically minimized in accordance with acceptable rates of polymerization.

12.4.3   Thiocarbonylthio Compounds as RAFT Agents

The use of macromonomers as RAFT agents is less than ideal since the C_{tr} of macro-monomers is low ($C_{tr} < 0.5$) and hence the chain equilibration step becomes a relatively slow process (i.e., rate of transfer is slower than rate of propagation). The design and preparation of simple RAFT agents with higher C_{tr} has overcome the problems associated with slow chain equilibration. These RAFT agents, of which some are listed in Fig. 12.11, possess the thiocarbonylthio moiety that imparts the living behavior to free-radical polymerization. The facile nature of radical additions to C=S bonds contributes, in part, to faster chain equilibration than is observed when macromonomers are used as RAFT agents.

12.4.4   Mechanism of RAFT Polymerization with Thiocarbonylthio Compounds

The mechanism of RAFT polymerization with the thiocarbonylthio-based RAFT agents involves a series of addition–fragmentation steps as depicted in Scheme 12.19. As for conventional free-radical polymerization, initiation by decomposition of an initiator leads to formation of propagating chains. In the early stages, addition of a propagating radical ($P_n^\bullet$) to the RAFT agent [S=C(Z)SR] followed by fragmentation of the intermediate radical gives rise to a polymeric RAFT agent and a new radical ($R^\bullet$).

The radical $R^\bullet$ reinitiates polymerization by reaction with monomer to form a new propagating radical ($P_m^\bullet$). In the presence of monomer, the equilibrium between

Initiation and propagation

$$\text{Initiator} + \text{monomer} \longrightarrow P_n^\bullet$$
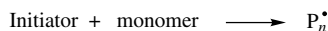
Addition to RAFT agent

Reinitiation

$$R^\bullet + \text{monomer} \longrightarrow P_m^\bullet$$
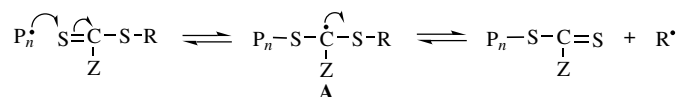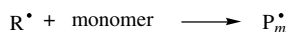
Chain equilibration by reversible addition fragmentation
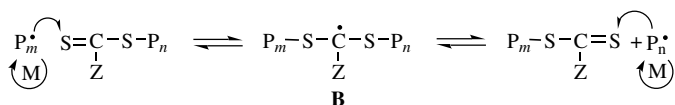
Overall
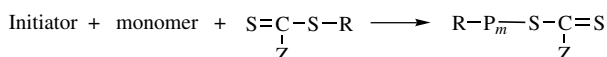
Scheme 12.19   Mechanism of RAFT polymerization with thiocarbonylthio RAFT agents.

the active propagating species ($P_n^\bullet$ and $P_m^\bullet$) with the dormant polymeric RAFT compound provides an equal probability for all the chains to grow. This feature of the RAFT process leads to the production of narrow polydispersity polymers. When the polymerization is complete, the great majority of the chains contain the thiocarbonylthio moiety as the end group (Scheme 12.19) which has been identified by ^{1}H-NMR and UV–vis spectroscopy.[169] Additional evidence for the proposed mechanism was provided by the identification of the intermediate thioketal radical (**A** and/or **B**, Scheme 12.19) by ESR spectroscopy.[174]

12.4.5   RAFT Polymerizations

In order for the RAFT process to function effectively there are certain aspects of the polymerization conditions that require consideration. The most critical considerations are choice of the RAFT agent and an appropriate rate of initiation.

12.4.5.1   Chain Transfer Constants   The RAFT agent must be chosen such that its chain transfer activity is appropriate to the monomer(s) to be polymerized. The electronic properties of the Z group and the stereoelectronic properties of the R group determine the chain transfer activity of the RAFT agents (Fig. 12.11). In general, many RAFT agents behave as ideal chain transfer agents as judged by the rates of polymerization being similar to rates of polymerization without the RAFT agent (within 20%). However, inappropriate choice of the RAFT agent can lead to significant retardation, particularly when high concentrations are employed to prepare low-molecular-weight polymers. The retardation phenomenon has been

attributed to a number of factors that have been explained in terms of the mechanism of the RAFT process (Scheme 12.19):[175] (1) slow fragmentation of the adduct radical **A** formed from addition to the original RAFT agent, (2) slow reinitiation by the expelled radical R$^\bullet$, (3) preference for the expelled radical R$^\bullet$ to add to the RAFT agent rather than to monomer, (4) slow fragmentation of the adduct radical **B** formed from addition to the polymeric RAFT agent, (5) preference for the propagating radical (P$_n^\bullet$ and P$_m^\bullet$) to add to the RAFT agent rather than to monomer. The observed retardation phenomenon has been addressed by the appropriate choice of Z and R groups. For example, in styrene polymerization with cumyl dithiobenzoate (**18a**) retardation was observed as an inhibition period accompanied by slow consumption of the RAFT agent. Since the cumyl radical is expected to be a good leaving group, the observed inhibition was attributed to Factors 2 and/or 3 mentioned above. The retardation in styrene polymerization was averted by using a RAFT agent with cyanoisopropyl as the radical leaving group (**18b**).[175] Similarly, retardation was observed in the polymerization of *n*-butyl acrylate with cumyl (**18a**) or benzyl dithiobenzoates (**18c**), even though the original RAFT agent was rapidly consumed. The observed retardation was attributed to the polymeric RAFT agent (i.e., Factors 4 and 5 listed above). The retardation was alleviated by using benzyl dithioacetate (**19**) as this RAFT agent is less active implying that addition to the C=S bond is less favored and hence occurs at a slower rate, but the resultant adduct radical is less stable thus favoring fragmentation (refer to Scheme 12.19). A possible side reaction in RAFT polymerization is termination of propagating radicals by radicals **A** and **B** (Scheme 12.19).[184] The termination of radical **B** has been postulated to be the most likely mechanism for retardation.[176] However, since retardation was observed in the early stages (<15% conversion) and not in the later stages of polymerization, the predominant path for retardation seems unlikely to involve radical **B** as this is formed throughout the polymerization. In a subsequent modelling of the polymerization of styrene in the presence of cumyl dithiobenzoate (**18a**) at 60°C, the retardation effect was explained in terms of the chain equilibration process (see Scheme 12.19). The results predicted a high concentration of adduct radicals **B** with an equilibrium constant, favoring the adduct radical, of 1.6×10^7 L/mol.[177] These predictions do not appear to be in accordance with ESR results, which show a low concentration of adduct radicals **B**, (Scheme 12.19) even though the measurements were performed under a high radical flux, that is, under more forcing conditions.[174]

a. R = C(CH$_3$)$_2$Ph
b. R = C(CH$_3$)$_2$CN
c. R = CH$_2$Ph

18

19
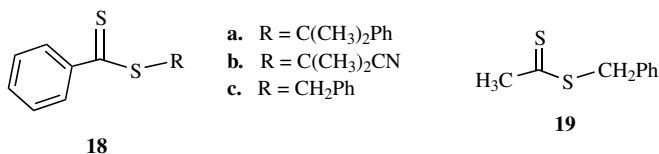
There is a similarity with the factors determining the chain transfer activity of macromonomers to those of RAFT agents (see Fig. 12.12; cf. Fig. 12.4). As with macromonomers, the Z group in the RAFT agent influences the reactivity of the double bond. As such, the Z group must be chosen so that it activates the double

reactive
thiocarbonyl
bond

radical leaving
group

$$Z-C-S-R$$

activating/stabilizing
group
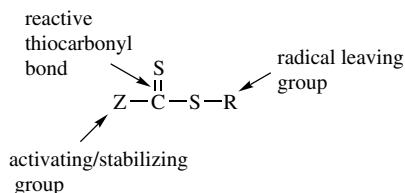
Figure 12.12

bond toward radical addition but at the same time not provide too great a stabilizing influence on the adduct radical (as this will contribute to slow fragmentation and hence retardation) (see Scheme 12.19). Similarly, the R group must be chosen such that it is a good radical leaving group relative to the radical of the propagating species.[169,178] The leaving group R$^{•}$ should also preferentially add to monomer.

In contrast to the chain transfer constants for macromonomers, which range from 0.01 to a theoretical maximum of 0.5,[128] the transfer constants of various RAFT agents have been found to span more than five orders of magnitude. The transfer constants have been measured in the range of 0.01 to above 1000 depending on the nature of Z, R, and type of monomer.[175,178–180] It has been reported that to obtain narrow polydispersity polymers $(M_w/M_n < 1.5)$ in a batch process with degenerative chain transfer (e.g., RAFT process) the C_{tr} of the transfer agent should be greater than 2.[181,182] However, it has been shown that this limitation can be overcome by the use of a monomer feed polymerization process to reduce the rate of propagation and thereby produce narrow polydispersity polymers from a less active CTA.[70,183]

The effect of various Z groups on the chain transfer activity of RAFT agents has been discussed in a published report.[180] By keeping the R group constant, a direct correlation between the chain transfer activity and the reactivity of the C=S bond was observed. The change in the reactivity of the C=S bond was related to the heats of reaction for C=S addition and the LUMO energies.[180] For the RAFT polymerization of styrene, the chain transfer constants were found to decrease in the series where Z is aryl (Ph) $\gg$ alkyl (CH$_3$) $\sim$ alkylthio (SCH$_2$Ph, SCH$_3$) $\sim$ N-pyrrolo $\gg$ N-lactam $>$ aryloxy (OC$_6$H$_5$) $>$ alkoxy $\gg$ dialkylamino. Some examples of chain transfer constants are given in Table 12.18.

As is evident from Table 12.18, the chain transfer activity of dithiocarbamates and xanthates is generally low and also dependent on the nature of the substituents on nitrogen and oxygen. For dithiocarbamates, the C_{tr} increases when the N substituent is: N,N-dialkyl $>$ N-lactam $>$ N-pyrrolo. The low activity of the N,N-dialkyl dithiocarbamates and xanthates has been explained in terms of the contributions from the zwitterionic resonance structures (Scheme 12.20).[184,185] The conjugation of the lone pair of electrons (on the nitrogen or oxygen) with the C=S double bond reduces the double bond character, thus raising the LUMO and HOMO energies and making radical addition less favorable.[180] The implications for the less reactive propagating radicals derived from styrene and MMA is that the use of N,N-dialkyl and N-phenyl,N-alkyl dithiocarbamates are ineffective as RAFT agents,

TABLE 12.18   Apparent Chain Transfer Constants (C_{tr}) for
S=C(Z)SCH$_2$Ph in Styrene Polymerization at 110°C[175]

RAFT Agent	
Z	C_{tr}
Ph	26
SCH$_2$Ph	18
CH$_3$	10
N-Pyrrolo	9
OC$_6$F$_5$	2.3
N-Lactam	1.6
OPh	0.72
NEt$_2$	0.01[a]

[a]At 80°C.

giving no significant molecular weight control. For more reactive propagating radicals such as acrylyl, these RAFT agents are mildly effective, giving molecular weight control but generally broad polydispersities. In the case of highly reactive propagating radicals, such as those derived from vinyl esters, these RAFT agents give good molecular weight control and low polydispersity indices. The xanthates are only mildly effective as RAFT agents for acrylates, styrenes, and acrylamides, giving some molecular weight control but broad polydispersities. This limitation has been overcome by attaching electron-withdrawing groups (both inductive and mesomeric) to the nitrogen and oxygen centers of dithiocarbamates and xanthates, respectively, thus reducing the conjugation of the lone pair of electrons with the C=S bond.[168,184–186] This results in an increase in the C_{tr} value, with the extent of increase depending on the extent to which the lone pair of electrons are removed from conjugation with the C=S bond (Table 12.18).

In a parallel study the Z group was kept constant and the effect of the R group on the chain transfer activity of RAFT agents was investigated.[178] It was reasoned that the C_{tr} should reflect the effect of the R group on the partitioning of the intermediate adduct radical between starting material and product (see Scheme 12.19). In the RAFT polymerization of MMA with dithiobenzoates [S=C(Ph)SR], the effectiveness of the RAFT agent (i.e., the leaving group ability of R) decreases in the order: C(Alkyl)$_2$CN ~ C(alkyl)$_2$Ph > C(CH$_3$)$_2$C(=O)OEt > C(CH$_3$)$_2$C(=O) NH(alkyl) > C(CH$_3$)$_2$CH$_2$C(CH$_3$)$_3$ ~ CH(CH$_3$)Ph > C(CH$_3$)$_3$ ~ CH$_2$Ph. In reality, only the first two groups are effective in preparing poly(MMA) of narrow polydispersity
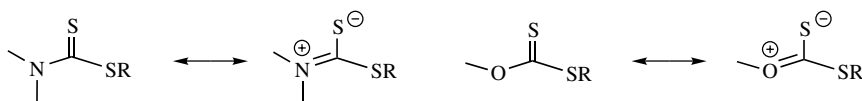
Scheme 12.20   Resonance structures of dithiocarbamates and xanthates.

TABLE 12.19   Apparent Chain Transfer Constants (C_{tr}) for S=C(Ph)SR in Methyl Methacrylate Polymerization at 60°C[175]

RAFT Agent	
R	C_{tr}
$C(CH_3)_2CN$	13
$C(CH_3)_2Ph$	10
$C(CH_3)_2CO_2Et$	2
$C(CH_3)_2CH_2C(CH_3)_3$	0.4
$CH(CH_3)Ph$	0.16
$C(CH_3)_3$	0.03
CH_2Ph	0.03

($M_w/M_n = 1.1$) and predetermined molecular weight. Some examples of C_{tr} are listed in Table 12.19. These indicate that both steric and polar factors determine the leaving group ability of R. As discussed above, when choosing an appropriate R group in the RAFT agent the polar and steric factors must be balanced with the requirement that R$^\bullet$ must be efficient in re-initiating polymerization. A report on the C_{tr} of polymeric RAFT agents indicates much higher values[179] (Table 12.20), possibly reflecting the increased leaving group ability of the bulkier polymeric group compared to the R groups of the RAFT agents in Tables 12.18 and 12.19.

12.4.5.2   Degree of Livingness   Aside from choosing an appropriate RAFT agent, an important factor in realizing an optimum RAFT polymerization process is conducting the polymerization at low radical concentration (or more precisely, low radical flux) and to use high ratios of RAFT agent to initiator consumed. As mentioned earlier, polymers that do not contain the thiocarbonylthio end group arise from initiator derived chains. Analysis of the RAFT mechanism (Scheme 12.19) reveals that the total number of polymer chains produced will be equal to the number initiated by initiator derived radicals plus the number initiated by the RAFT agent derived radicals (R$^\bullet$). A number of chains equal to the number of R$^\bullet$ will remain

TABLE 12.20   Apparent Chain Transfer Constants (C_{tr}) of Polymeric RAFT Agents Measured at 60°C[179]

Polymeric RAFT Agent	Monomer	C_{tr}
Polystyrene-SCSCH$_3$	Styrene	180
Polystyrene-SCSPh	Styrene	6000 ± 2000^a
Poly(methyl methacrylate)-SCSPh	Methyl methacrylate	140

^{a}At 40°C.

TABLE 12.21 Proportion of Dead Chains (D_c) for RAFT Polymerization of Methyl Acrylate (4.44 M), AIBN (3.3×10^{-4} M), and RAFT Agent [S=C(CH$_3$)SC(CH$_3$)$_2$CN] (3.6×10^{-3} M) at 60°C[187]

Time (h)	% Conversion	M_n(GPC)	M_w/M_n	$D_c{}^a$
2	28	39,000	1.05	0.003
4	52	67,000	1.04	0.006
8	75	97,000	1.04	0.011

^{a} Calculated from Eq. (12.1) assuming k_d for AIBN of 9.5×10^{-6} s^{-1}, an initiator efficiency of 0.5, and radical–radical termination by combination.

living, that is, will possess a thiocarbonylthio end group. It follows that the proportion of dead chains (D_c) will be given by the ratio of the number of initiator derived radicals $2f([I]_0 - [I]_t)$ to the number of RAFT agent molecules ([RA]) plus the initiatior derived radicals (equation 12.1), where $[I]_t = [I]_0 e^{-k_d t}$. The number of dead chains reduces to one half this value when termination is by combination.

$$D_c = \frac{2f([I]_0 - [I]_t)}{[RA] + 2f([I]_0 - [I]_t)} \qquad (12.1)$$

In practice, the proportion of dead chains in RAFT polymerization can be kept quite low (<5%). The data shown in Table 12.21 highlight this point.[187] As is shown, for the polymerization of methyl acrylate (MA), only 1.1% of chains are dead at 75% conversion and M_n of 97,000 (last entry in Table 12.21). For slower-propagating monomers such as styrene and MMA, the proportion of dead chains for a given molecular weight and percent conversion will be higher than for MA (Table 12.22). It should be noted that in experiments leading to lower-molecular-weight polymers, achieved by increasing the RAFT agent concentration, the number of dead chains will be proportionally lower (see last entry, Table 12.22).

TABLE 12.22 Proportion of Dead Chains (D_c) for RAFT Polymerization of Methyl Methacrylate (6.55 M), AIBN (1.8×10^{-3} M), and RAFT Agent [S=C(Ph)SC(CH$_3$)$_2$CN] (1.13×10^{-2}M) in Benzene at 60°C[187]

Time (h)	% Conversion	M_n(GPC)	M_w/M_n	$D_c{}^a$
7	27	15,100	1.15	0.022
16	61	31,900	1.12	0.042
30	~99	49,500	1.11	0.062
16^b	85	13,400	1.05	0.019

^{a} Calculated from Eq. (12.1) assuming k_d for AIBN of 9.5×10^{-6} s^{-1} and k_d for Vazo88 of 2.3×10^{-5}s^{-1}, an initiator efficiency of 0.5 and radical–radical termination by 60% disproportionation, and 40% combination.
^{b} Polymerization performed with Vazo88 (1.8×10^{-3} M) and 4.56×10^{-2} M RAFT agent at 90°C.

Operating within appropriate parameters, the RAFT process has been shown to be an efficient method for preparation of narrow polydispersity living polymers of low-, moderate-, and high-molecular-weight with moderate to high rates of polymerization.[169,171,184]

12.4.6 RAFT Polymerization of Methacrylates

The methacrylyl propagating radical is a sterically bulky radical of moderate reactivity. In choosing the requirements for a RAFT agent, group Z could be aryl, alkyl, or S(alkyl) as these groups are sufficiently radical stabilizing to allow an appropriate rate of addition of the methacrylyl propagating radical to the C=S bond. The R group should be a better leaving group than the methacrylyl radical, hence $R^{\bullet}$ should also be sterically bulky (i.e., tertiary) and possess a radical stabilizing functionality. As discussed above, RAFT agents containing $C(alkyl)_2CN$ and $C(alkyl)_2Ph$ as the R group are effective in preparing poly(MMA) of narrow polydispersity and predetermined molecular weight.[178,184] Some examples of poly(MMA) prepared with RAFT agents meeting these criteria are shown in Table 12.23.

Interestingly, when $R = C(CH_3)_2CO_2Et$, good molecular weight control was obtained but the polydispersity index was only 1.48 (second-to-last entry, Table 12.23). This indicates that this RAFT agent has relatively poor chain transfer activity, which is likely to be a reflection of the poorer leaving group ability of ethyl isobutyrate compared to, for instance, cyanoisopropyl or cumyl (first and second entries, respectively, in Table 12.23). Since the steric bulk between the three groups is likely to be similar, it may reflect the lower radical stabilizing ability if the CO_2Et group compared to CN or Ph.

The effect of reaction temperature on the RAFT polymerization of MMA has been probed.[188] The polymerization was conducted at 60 and 90°C using the same RAFT agent $[Z = Ph, R = C(CH_3)_2CN]$ and at similar rates of initiation. The higher temperature proved beneficial in all the important aspects, including faster polymerization (higher k_p/k_t), narrower polydispersity (1.04 at 90°C vs. 1.11 at 60°C) and fewer dead chains as calculated by the amounts of initiator

TABLE 12.23   RAFT Polymerization of Methyl Methacrylate at 60°C with Various RAFT agents[184]

RAFT Agents

Z	R	% Conversion	M_n(GPC)	M_n(Calc)	M_w/M_n
Ph	$C(CH_3)_2CN$	95	52,300	59,995	1.16
Ph	$C(CH_3)_2Ph$	95	6,600	4,530	1.21
SCH_3	$C(CH_3)_2CN$	95	59,300	59,995	1.14
CH_3	$C(CH_3)_2Ph$	95	53,500	59,995	1.18
Ph	$C(CH_3)_2CO_2Et$	95	52,900	59,995	1.48
Ph	$C(CH_3)(CN)(CH_2)_3OH$	92	55,300	57,100	1.05
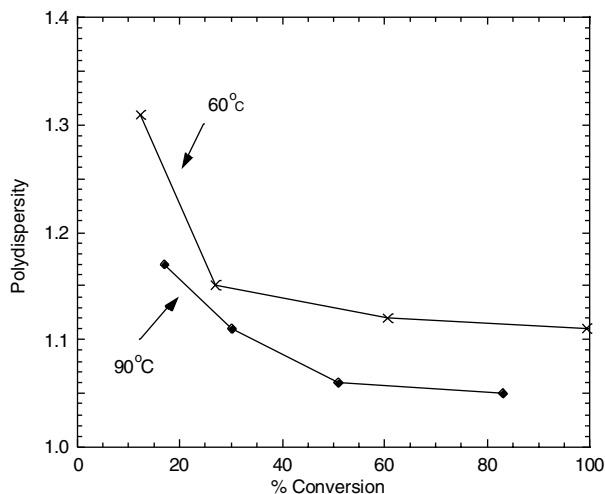
Figure 12.13   RAFT polymerization of MMA at 60°C with AIBN over 30 h and at 90°C with Vazo88 over 8 h.
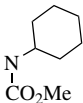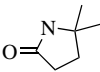
consumed. The evolution of polydispersity as conversion increases is shown in Fig. 12.13. The lower polydispersities at 90°C suggest that the C_{tr} of the RAFT agent increases with increasing temperature.

12.4.7   RAFT Polymerization of Styrenes

For the RAFT polymerization of styrene there is more freedom in the choice of the RAFT agent compared to the RAFT polymerization of methacrylates. This is particularly true in the choice of R groups. The list of RAFT agents producing narrow polydispersity polystyrene also includes groups where $R = CH_2Ph$ (Table 12.24). The greater flexibility in effective R groups is due to the less bulky nature and lower propagation rate of polystyryl radical compared to the polymethacrylyl radical. Hence the steric and electronic stabilization parameters are not as demanding as for methacrylate polymerization.

For reasons discussed previously, the low C_{tr} of *N,N*-dialkyl dithiocarbamates (Table 12.18) makes these ineffective agents for the RAFT polymerization of styrene. There is no control in molecular weight or narrowing of polydispersity in styrene polymerization when $Z = N(Et)_2$ and $R = CH_2Ph$ (Table 12.24). This is an indication that the styryl propagating radical is not adding to the RAFT agent due to the reduced reactivity of the C=S bond arising from conjugation with the nitrogen lone pair of electrons. When the extent of this conjugation is reduced, the RAFT agent is effective in styrene polymerization. This is exemplified in the last three entries in Table 12.24. Xanthates (Z = OEt) are mildly effective in controlling styrene polymerization. As shown in Table 12.24, molecular weight control is obtained

TABLE 12.24 RAFT Polymerization of Styrene with Various RAFT Agents[184]

RAFT Agents

Z	R	% Conversion	M_n(GPC)	M_n(Calc)	M_w/M_n
Ph	C(CH$_3$)$_2$Ph	81	25,200	25,100	1.12
Ph	C(CH$_3$)(CN)(CH$_2$)$_2$CO$_2$H	61	8,900	9,435	1.05
SCH$_3$	C(CH$_3$)$_2$CN	91	27,800	28,000	1.09
SCH$_3$	CH(Ph)CO$_2$H	92	29,200	28,500	1.07
OEt	C(CH$_3$)(SPh)CO$_2$Et[a]	—	4,200	3,200	1.80
N(Et)$_2$	CH$_2$Ph	15	317,100	4,590	1.86
N-Pyrrolo	CH$_2$Ph	60	15,600	18,340	1.20
(N–CO$_2$Me cyclohexyl structure)	CH(CO$_2$Et)$_2$[b]	93	19,640	18,210	1.13[c]
(O=C N ring structure)	C(CH$_3$)$_2$CN[b]	63	26,590	26,160	1.12

[a] Ref. 173.
[b] Ref. 186.
[c] Bimodal.

but the polydispersity remains relatively high, indicating a slow equilibration step (refer to Scheme 12.19).

12.4.8 RAFT Polymerization of Acrylates
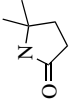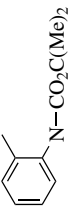
The acrylyl propagating radicals have relatively low steric bulk and high reactivity. These characteristics are ideal for addition to the C=S bond and for expulsion of the R group in RAFT agents. Consequently, there is a wider choice in both the Z and R groups available for the RAFT polymerization of acrylates. This is evident from the examples presented in Table 12.25.

The N,N-dialkyl and N-aryl,N-alkyl dithiocarbamates and the xanthates are only mildly effective RAFT agents in acrylate polymerizations, providing good molecular weight control but polydispersity remains relatively high (last four entries, Table 12.25).

12.4.9 RAFT Polymerization of Acrylamides

As for the acrylyl propagating radical, the acrylamidyl propagating radical possesses relatively low steric bulk and high reactivity. Consequently, a similarly wide range of RAFT agents would be useful in the RAFT polymerization of acrylamides. Various examples of RAFT polymerization of N,N-dimethylacrylamide (DMA) and N-isopropylacrylamide (NIPAM) have been reported to date (Table 12.26).[184,189]

TABLE 12.25 RAFT Polymerization of Acrylates with Various RAFT Agents[184]

RAFT Agents

Z	R	Monomer[a]	% Conversion	M_n(GPC)	M_n(Calc)	M_w/M_n
Ph	CH_2Ph	n-BA	40	91,700	89,300	1.14
SCH_3	$C(CH_3)_2CN$	MA	55	65,400	61,800	1.06
N-Pyrrolo	CH_2Ph	MA	74	8,800	9,500	1.17
N-Succinamido	CH_2Ph	MA	97	108,200	102,900	1.18
(cyclic N, O=)	$CH(CO_2Et)$[b]	EA	69	5,880	7,170	1.19
$N{-}CO_2C(Me)_2$ (aryl)	$CH(CH_3)CO_2Et$[b]	EA	87	7,350	7,750	1.20
Ph	$C(CH_3)_2CN$	AA	53	66,800	73,800	1.13
NEt_2	$CH(CO_2Et)_2$[c]	EA	94	7,800	9,760	2.31
N(Ph)Et	$CH(CO_2Et)_2$[c]	EA	99	8,300	8,270	1.86
OEt	$C(CH_3)(SPh)CO_2Et$[c]	MA	—	3,790	3,500	1.40
OEt	$C(CH_3)_2CN$	t-BA	72	11,000	10,100	1.77

[a] n-BA, n-butyl acrylate; MA, methyl acrylate; EA, ethyl acrylate; AA, acrylic acid; t-BA, t-butyl acrylate.
[b] Ref. 173.
[c] Ref. 186.

TABLE 12.26   RAFT Polymerization of Acrylamides.[184]

RAFT Agent						
Z	R	Monomer[a]	% Conversion	M_n(GPC)	M_n(Calc)	M_w/M_n
Ph	C(CH$_3$)$_2$Ph	DMA	64	59,500	68,300	1.05
		DMA	76	88,700	81,100	1.08
		NIPAM	56	24,500	28,700	1.15

[a] DMA, dimethyl acrylamide; NIPAM, N-isopropyl acrylamide.

12.4.10   RAFT Polymerization of Vinyl Esters

The vinyl acetate propagating radical has quite different reactivity characteristics compared to (meth)acrylate and styrene derived propagating radicals. For example, the vinyl acetate propagating radical has relatively little steric bulk and the radical is poorly stabilized making it highly reactive and, consequently, a very poor homolytic leaving group. This marked change in reactivity has severe consequences in the choice of RAFT agents for vinyl ester polymerization. The results in Table 12.27 show that the RAFT polymerization of vinyl acetate is effective only with xanthates (Z = OR) and dithiocarbamates (Z = NR$_2$).[168,172] It has been shown that the polymerization of vinyl acetate is completely inhibited in the presence of dithioesters, trithiocarbonates, and aromatic dithiocarbamates, that is, the RAFT agents, that are preferred for RAFT polymerization of (meth)acrylates, styrenes, and acrylamides.[184] The inhibition observed with these RAFT agents has been explained by a slow fragmentation of the intermediate radical **A** (Scheme 12.19). The slow fragmentation arises from the poor homolytic leaving ability of the vinyl acetate radical; thus, the intermediate radical is more stable than the products arising from fragmentation.

The RAFT process can be performed in a variety of solvents, including dimethylformamide (AA example in Table 12.25) and water. In this latter example, p-styrene

TABLE 12.27   RAFT Polymerization of Vinyl Acetate[184]

RAFT Agent					
Z	R	% Conversion	M_n(GPC)	M_n(Calc)	M_w/M_n
OEt	CH$_2$CN	66	7,000	6,190	1.18
OEt	CH(CH$_3$)CO$_2$Et[a]	—	3,080	3,200	1.30
OEt	CH$_2$CN	92	9,100	8,610	1.37
N(Ph)$_2$	CH(CO$_2$Et)$_2$[b]	86.6	2,640	2,690	1.36
N(Ph)(CH$_3$)	CH$_2$CN	96	22,700	18,000	1.24
N(Ph)(CH$_3$)	CH$_2$CN	95	7,100	5,880	1.25

[a] Ref. 173.
[b] Ref. 186.

sodium sulfonate sodium salt was polymerized in the presence of the RAFT agent, (Fig. 12.11, Z = Ph; R = C(CH$_3$)(CN)CH$_2$CH$_2$CO$_2$Na) to give a polymer of $M_n = 10,500$ [M_n(calc) $= 12,640$], $M_w/M_n = 1.20$ at 84% conversion.[169]

Examples of end functional polymers have also been reported by utilizing functional RAFT agents[190] (e.g., see last entry Table 12.23).[169,171] In these systems, since the fragmenting R group of the RAFT agent reinitiates polymerization, introducing functionality (e.g., OH or COOH group) into the R group results in end-functional polymers (see Scheme 12.19). This provides a route to telechelics as the thiocarbonylthio end group can be converted to other functionalities.[169,191,192] For example, treatment with hydroxide or an amine will produce a thiol terminated polymer. Thiols are good nucleophiles and can, in principle, be utilized to introduce a wide range of end-group functionalities. Since the thiocarbonylthio moiety induces color in the polymer, these chemical transformations have been used to decolorize the polymer. Sodium hypochlorite and hydrogen peroxide are also effective in decolorizing the polymers.[169]

12.4.11   RAFT Polymerization in Dispersed Media

It has been suggested that the RAFT process should be an ideal living free-radical polymerization (LFRP) technique for emulsion and miniemulsion systems.[193,194] Other LFRP techniques based on reversible termination (ATRP and nitroxides) suffer complications that lead to decrease in polymerization rates and loss of control of polymerization. This arises from partitioning of the deactivating species between the two phases, leading to a change in the number of radicals in the compartmentalized systems. The RAFT process (and degenerative chain transfer processes in general)[195] is better suited for dispersed media since the number of radicals per particle remains unaffected by the chain transfer process.

The RAFT process has been implemented in the emulsion polymerization of styrenes and (meth)acrylates.[167,169,173,175,196] In batch processes, the rates of polymerization are significantly retarded in the presence of RAFT agent, and polymers of broad polydispersity are typically obtained. This was attributed to a higher exit rate of propagating radicals after the fragmentation of the RAFT agent (refer to Scheme 12.19).[196] In contrast, RAFT emulsion polymerizations employing a semi-batch process do not suffer from retardation and living (meth)acrylate and styrene polymers can be prepared (Table 12.28).[167,169,173,175] In semi-batch processes the

TABLE 12.28   Emulsion Polymerization of Butyl Methacrylate (BMA), Styrene (Sty), and Butyl Acrylate (BA) with RAFT Agent S=C(Z)SR.

RAFT Agent						
Z	R	Monomer	M_n(GPC)	M_n(Calc)	M_w/M_n	Ref.
Ph	C(CH$_3$)$_2$Ph	BMA	57,700	—	1.22	169
OEt	CH(CH$_3$)CO$_2$Et	Sty	17,000	16,800	2.1	173
Ph	CH$_2$Ph	Sty	53,210	—	1.37	175
OEt	CH(CH$_3$)CO$_2$Et	BA	31,100	30,750	1.4	173

TABLE 12.29   Formation of Homo and Block Polymers via Miniemulsion Polymerization of Various Monomers with S=C(Ph)SC(CH$_3$)$_2$CN[194]

Monomer A[a]	M_n(GPC)	M_n(Calc)	M_w/M_n	Monomer B[b]	M_n(GPC)	M_n(Calc)	M_w/M_n
MMA	8,300	7,400	1.17	—	—	—	—
BMA	8,500	8,400	1.20	—	—	—	—
EHMA[c]	7,600	7,600	1.09	Sty	12,000	14,000	1.38
EHMA[d]	7,100	8,400	1.10	MMA/MA	10,000	—	1.16

[a] MMA, methyl methacrylate; BMA, butyl methacrylate; EHMA, ethylhexyl methacrylate.
[b] Sty, styrene; MMA/MA, methyl methacrylate/methacrylic acid.
[c] Seeded.
[d] Semicontinuous.

RAFT agent is consumed in the early stages of the polymerization, hence overcoming problems associated with abnormally high radical exit rates.

The usefulness of the RAFT process in emulsion polymerization was further demonstrated by the preparation of a diblock copolymer. A latex of polystyrene ($M_n = 7700 ; M_w/M_n = 1.37$), formed with RAFT agent; S=C(CH$_3$)SCH$_2$Ph, was chain extended by addition of MMA to give poly(methyl methacrylate-*block*-styrene) $M_n = 41,250 ; M_w/M_n = 1.57$.[175]

The application of the RAFT process to miniemulsions stabilized with nonionic surfactants has been reported.[194] The controlled polymerization of methacrylates and styrenes has yielded stable dispersions of low polydispersity living polymers (Table 12.29). The living character of the "latex" was demonstrated by chain extension to form block copolymers (Table 12.29).

12.4.12   Copolymerization Using the RAFT Process

12.4.12.1   *Random and Gradient Copolymers*   Analysis by ^{1}H-NMR has been used to show that the RAFT process does not alter the composition of copolymers in random copolymerizations when compared to copolymerizations without the RAFT agent.[171] Examples of random copolymers are shown in Table 12.30.

The preparation of a BA/MMA gradient copolymer by the RAFT process has been reported.[171] The results (Table 12.31) showed that using cumyl dithiobenzoate, S=C(Ph)SC(CH$_3$)$_2$Ph, as the RAFT agent gave a narrow polydispersity gradient copolymer, rich in MMA at one end and rich in BA at the other end.

12.4.12.2   *Diblock and Triblock Copolymers*   There are numerous examples utilizing the living nature of the RAFT process to prepare various AB, ABA, and

TABLE 12.30   Copolymerizations with S=C(Ph)SC(CH$_3$)$_2$Ph as RAFT Agent[169]

Monomer/Comonomer	% Conversion	M_n	M_w/M_n
MMA/HEMA[a]	75	28,000	1.21
Styrene/acrylonitrile	71	51,400	1.07

[a] MMA/HEMA, methyl methacrylate/hydroxyethyl methacrylate.

TABLE 12.31   Gradient Methyl Methacrylate/Butyl Acrylate (MMA/BA) Copolymer by the RAFT Process

MMA : BA	% Conversion	M_n	M_w/M_n
1 : 0.91	0	—	—
1 : 0.45	22	16,800	1.21
1 : 0.54	45	41,600	1.13
1 : 0.80	93	75,400	1.21

ABC blocks.[167,170,184,185] Some examples of hard–soft, hydrophilic–hydrophobic, and other AB diblocks are listed in Table 12.32.

The second last entry in Table 12.32 illustrates an alternative strategy for block synthesis—linking a condensation polymer, e.g., poly(ethylene oxide), to a functional RAFT agent and chain extending using the RAFT process. This strategy has also been applied to the preparation of novel polyolefin-based block copolymers. As shown in the last entry of Table 12.32, a functional RAFT agent was covalently linked to poly(ethylene-*co*-butylene) and chain extended with styrene/maleic anhydride to give poly(ethylene-*co*-butylene-*block*-styrene-*co*-maleic anhydride).[197]

A consideration in block synthesis with the RAFT process is that in order to obtain a narrow polydispersity block copolymer the leaving group ability of the propagating radical of the A block is greater than or at least comparable to the leaving group ability of the propagating radical of the B block.

ABC triblocks can be readily prepared by chain extending a preformed AB diblock. This has been illustrated by adding *t*-butyl methacrylate to poly(benzyl methacrylate-*block*-dimethylaminoethyl methacrylate) ($M_n = 3,500$; $M_w/M_n = 1.06$)

TABLE 12.32   AB Diblocks Prepared by the RAFT Process[170]

Z	R	A Block[a]	M_n	M_w/M_n	B Block[a]	M_n	M_w/M_n
Ph	CH₂Ph	Sty	20,300	1.15	DMA	43,000	1.24
Ph	CH(CH₃)Ph	BA	33,600	1.13	AA	52,400	1.19
Ph	C(CH₃)₂Ph	MMA	3,230	1.17	MAA	4,720	1.18
Ph	C(CH₃)₂Ph	MMA	17,400	1.20	St	35,000	1.24
Ph	C(CH₃)₂Ph	BzMA	1,800	1.13	DMAEMA	3,500	1.06
Ph	C(CH₃)(CN)(CH₂)₂CO₂H	EO	750	1.04	BzMA	10,800	1.10
Ph	C(CH₃)(CN)(CH₂)₂CO₂H[b]	p(EB)	3,800	1.04	S-*co*-MAh	11,000	1.12

The heading above spans: RAFT Agent over Z and R.

[a] Sty, styrene; BA, butyl acrylate; MMA, methyl methacrylate; BzMA, benzyl methacrylate; EO, ethylene oxide; p(EB), poly(ethylene-*co*-butylene); DMA, dimethylacrylamide; AA, acrylic acid; MAA, methacrylic acid; DMAEMA, dimethylaminoethyl methacrylate; S-*co*-MAh = styrene/maleic anhydride statistical copolymer.
[b] Reference 197.

$$\text{S}\underset{\text{Ph}}{\overset{\text{S}}{\diagdown}}\text{S}\!-\!\!\!\left[\right]\!\!\!-\!\text{S}\underset{\text{Ph}}{\overset{\text{S}}{\diagdown}}\text{S} \quad\xrightarrow{\text{BMA}}\quad \text{S}\underset{\text{Ph}}{\overset{\text{S}}{\diagdown}}\text{S}\!-\![\text{BMA}]_n\!-\!\!\!\left[\right]\!\!\!-\![\text{BMA}]_m\!-\!\text{S}\underset{\text{Ph}}{\overset{\text{S}}{\diagdown}}\text{S}$$

$$M_n = 35{,}500;\ M_w/M_n = 1.09$$

$$\Big\downarrow\ \text{MMA}$$

$$\text{S}\underset{\text{Ph}}{\overset{\text{S}}{\diagdown}}\text{S}\!-\![\text{MMA}]_p[\text{BMA}]_n\!-\!\!\!\left[\right]\!\!\!-\![\text{BMA}]_m[\text{MMA}]_q\!-\!\text{S}\underset{\text{Ph}}{\overset{\text{S}}{\diagdown}}\text{S}$$

$$M_n = 112{,}200;\ M_w/M_n = 1.14$$
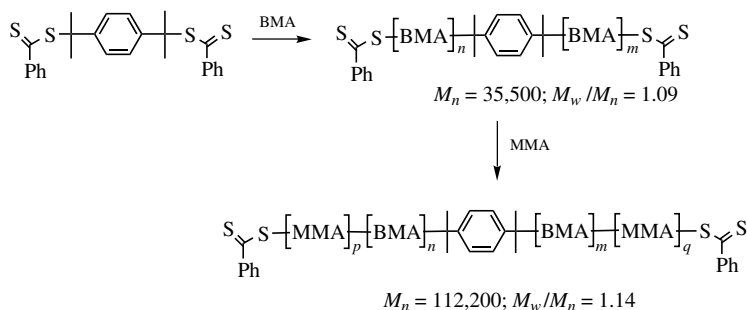
Scheme 12.21 ABA triblock synthesis using difunctional dithioester RAFT agent.

to give poly(benzyl methacrylate-*block*-dimethylaminoethyl methacrylate-*block*-t-butyl methacrylate) ($M_n = 8{,}250;\ M_w/M_n = 1.12$).[170]

ABA triblocks can be also be prepared by utilizing a difunctional RAFT agent and is exemplified by the preparation of poly(methyl methacrylate-*block*-butyl methacrylate-*block*-methyl methacrylate) ($M_n = 112{,}200;\ M_w/M_n = 1.14$) (Scheme 12.21).

The advantage of this strategy is that ABA triblocks can be prepared in two steps. An extension of this two step ABA triblock strategy is the use of symmetric trithiocarbonates as RAFT agents.[198] Several examples illustrating the utility of this approach have been reported and, in general, follow the procedure outlined in Scheme 12.22.[199]

12.4.12.3 Star Polymers Star polymers can be readily prepared by utilizing RAFT agents that contain multiple thiocarbonylthio moieties. Two distinct strategies for accessing star polymers and two classes of RAFT agents have been reported. In the first class, the representative structures depicted in Fig. 12.14 show multi-functional dithioester and trithiocarbonate RAFT agents that are designed to have the arms grow from the core (i.e., the propagating chains are attached to the core). Examples whereby these agents are used to give 4-arm and 6-arm star polystyrene

$$\text{Ph}\!\overset{\text{S}}{\diagdown}\!\text{S}\!\overset{\text{S}}{\diagdown}\!\text{S}\!\overset{}{\diagdown}\!\text{Ph} \quad\xrightarrow{\text{styrene}}\quad \text{Ph}\!-\![\text{St}]_n\!-\!\text{S}\!\overset{\text{S}}{\diagdown}\!\text{S}\!-\![\text{St}]_n\!-\!\text{Ph}$$

$$M_n = 20{,}100;\ M_w/M_n = 1.11$$

$$\xrightarrow{n\text{BA}}\quad \text{Ph}\!-\![\text{St}]_n[\text{BA}]_p\!-\!\text{S}\!\overset{\text{S}}{\diagdown}\!\text{S}\!-\![\text{BA}]_p[\text{St}]_n\!-\!\text{Ph}$$

$$M_n = 161{,}500;\ M_w/M_n = 1.16$$
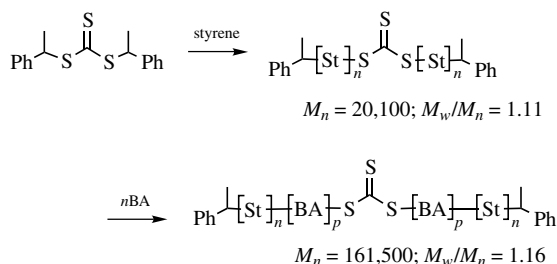
Scheme 12.22 ABA triblock synthesis using symmetrical trithiocarbonates as RAFT agents.

Dithioester RAFT agent for 4-arm star polymer   Dithioester RAFT agent for 6-arm star polymer

Trithiocarbonate RAFT agent for 4-arm star polymer
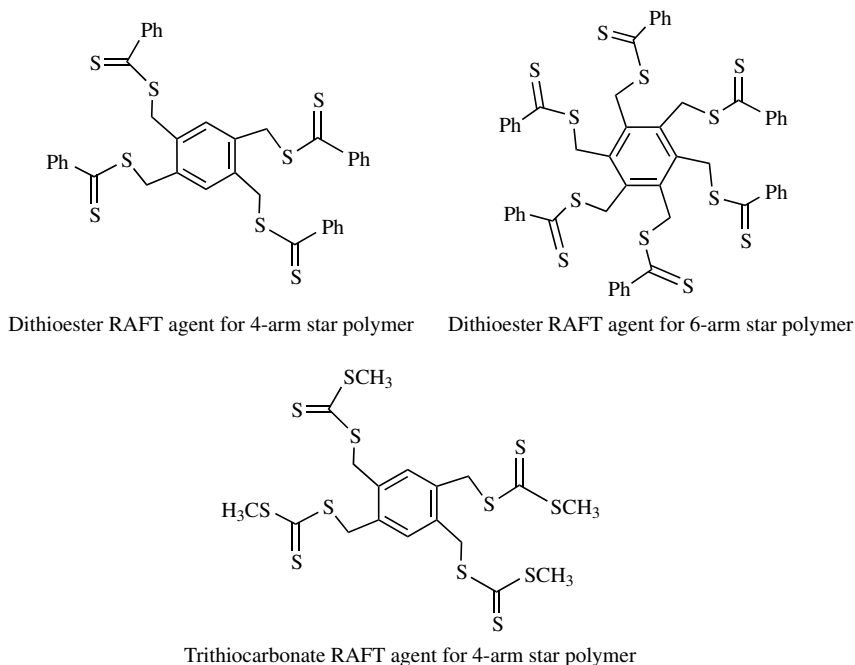
Figure 12.14   RAFT agents for growing arms from the core.

polymers have been reported.[170,200] An unavoidable consequence with this class of RAFT agent is that since the propagating chains are attached to the core, the inevitable termination coupling reactions of radicals lead to small amounts of star–star coupled products. These coupled products have been observed by GPC as peaks with two times the molecular weight of the main peak of the star polymer.[184,200]

In the second class of RAFT agents, the trithiocarbonate shown in Fig. 12.15 has been designed to have the propagating chains grow away from the core (i.e., detached from the core).

Both these approaches provide 4- and 6-arm star polymers with good molecular weight control and low polydispersity.[170,184,200] For example, the trithiocarbonate RAFT agent in Fig. 12.15 was used to prepare 4-arm polystyrene [$M_n(\text{GPC}) = 63{,}900$; $M_n(\text{calc}) = 78{,}700$; $M_w/M_n = 1.08$, 63% conversion].[200] There is a distinct
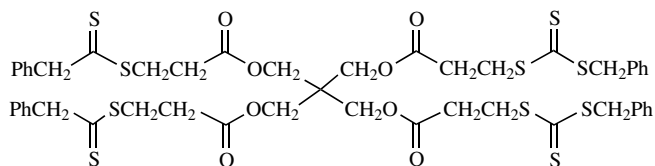
Figure 12.15   Trithiocarbonate RAFT agent for growing arms detached from the core.
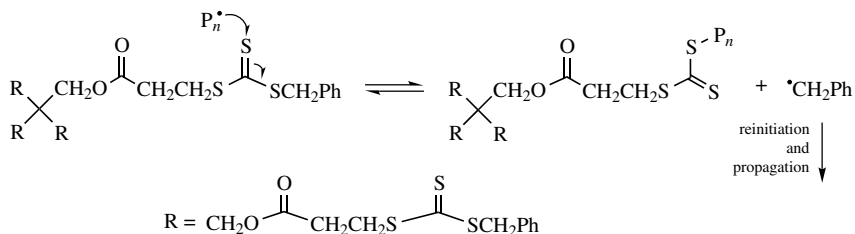
Scheme 12.23   Mechanism for chain growth detached from the core.

advantage in the use of RAFT agents of the type shown in Fig. 12.15 (i.e., where propagating chains grow detached from the core) because complications arising from star–star coupling reactions are avoided.

This is highlighted in Scheme 12.23. Since the propagating chains are detached from the core, the core remains in the "dormant" form and any radical–radical coupling reactions will yield linear polymers that are produced in lower amounts than if star–star coupling occurred. These linear termination products have been observed by GPC as peaks with approximately half the molecular weight of the star polymer.[184,200]

12.4.13   Organic Iodides and Ditellurides as Chain Transfer Agents

Appropriately substituted alkyl iodides (R–I) have been shown to undergo reversible chain transfer and impart living characteristics to free-radical polymerization.[201,202] The mechanism by which this occurs is depicted in Scheme 12.24.[203] In the early stages of the free-radical polymerization process (step 1), the exchange of iodide from the alkyl iodide (R–I) to propagating radical $P_n^\bullet$ gives an oligomeric iodide P_n–I and a new initiating radical $R^\bullet$. The inititating radical $R^\bullet$ generates a new propagating chain $P_m^\bullet$ by addition to monomer (step 2). The reversible chain transfer step involves transfer of the iodine atom between propagating radicals $P_n^\bullet$ and $P_m^\bullet$ (step 3). The details of the iodine exchange process are as yet unknown. It is plausible that a hypervalent iodine intermediate is formed during the exchange process shown in step 3 (Scheme 12.24), although no direct evidence for its formation has been reported. However, a hypervalent iodine terminated polyMMA oligomer has been proposed to explain the slight living character in the free radical polymerization of MMA with diacetoxyiodobenzene.[204]

$$P_n^\bullet \;+\; R{-}I \;\rightleftharpoons\; P_n{-}I \;+\; R^\bullet \qquad (1)$$

$$R^\bullet \;+\; mM \;\longrightarrow\; P_m^\bullet \qquad\qquad\quad (2)$$

$$P_m^\bullet \;+\; P_n{-}I \;\rightleftharpoons\; P_n^\bullet \;+\; P_m{-}I \qquad (3)$$
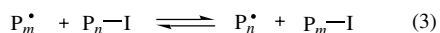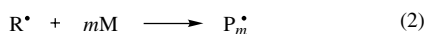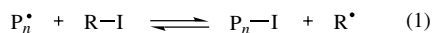
Scheme 12.24   Polymerization with reversible chain transfer mediated by alkyl iodides.

For reversible chain transfer to be successful in imparting "livingness" to free radical polymerization, the exchange process depicted in step 3 of Scheme 12.24 must be thermodynamically neutral. The fact that the propagating chains $P_n^{\bullet}$ and $P_m^{\bullet}$ are almost identical in nature lends itself to achieving a thermodynamically neutral exchange. The reversible chain transfer observed with alkyl iodides (Scheme 12.24, step 3),[205,206] and the RAFT process,[207] discussed earlier, have been classified as degenerative chain transfer processes. In addition to the thermodynamically neutral process, the rate of exchange must compete with (i.e., be at least similar to) the rate of propagation in order to obtain polymers with a low polydispersity index (viz; <1.5). An important factor for successful control by reversible chain transfer is the choice of the chain transfer agent, R–I. If large energy differences exist between the reactants, $P_n^{\bullet}$ and R–I, and the products, P_n–I and $R^{\bullet}$, as a result of chain transfer, then the equilibrium can be shifted overwhelmingly to the left or right (Scheme 12.24, step 1). If the equilibrium is shifted overwhemingly to the left, it can lead to either inhibition of polymerization or loss of control of polymerization. If the equilibrium is shifted to the right, the process is regarded as degradative chain transfer and hence control of free-radical polymerization is lost.

Of the alkyl halides (chlorides, bromides, iodides) only the C–I bond is sufficiently labile to allow efficient transfer of the iodine atom from the transfer agent to the propagating radical. The stereoelectronic properties of the R group in the chain transfer agent R–I are of critical importance. It has been shown that for effective control of styrene polymerization, 1-phenylethyl iodide is a suitable chain transfer agent (see Table 12.33).[202]

In this instance the structure of $R^{\bullet}$ resembles the structure of the propagating radical, which is ideal for a thermodynamically neutral transfer step. However, a similarity in structure need not be the over-riding requirement. In general, for step 1 in Scheme 12.24 to be favored, the R group must stabilize the resultant radical to an appropriate extent through resonance and/or inductive effects. In this context, iodoacetonitrile has been used in the polymerization of styrene to produce a polymer of $M_n(\text{Obs}) = 6550$, $M_n(\text{calc}) = 5800$, and $M_w/M_n = 1.4$.[202] In addition to bulk and solution polymerization, reversible chain transfer with alkyl iodides, and in particular, perfluoroalkyl iodides, was also shown to be effective in controlling styrene polymerization in miniemulsion systems.[195,202,208]

TABLE 12.33 Polymerization of Styrene (Sty), Butyl Acrylate (BA), Methyl Methacrylate (MMA), and Vinyl Acetate (VA) in the Presence of 1-Phenylethyl Iodide[202]

Monomer	Temperature (°C)	$M_n(\text{Obs})$	$M_n(\text{Calc})$	% Conversion	M_w/M_n
Sty	70	6,580	7,810	94	1.5
Sty	70	3,670	5,840	52	1.5
BA	50	7,320	9,160	94	2.1
MMA	60	5,080	18,800	54	2.1
VA	50	—	—	No polymer	—

TABLE 12.34   Polymerization of Styrene with Diphenyl Ditelluride (DPDTe) at 90°C for 36 hr[209]

[DPDTe]/[AIBN][a]	[DPDTe] mol%	M_n	% Conversion	M_w/M_n
0	0	16,000	90	2.46
0.5	2.5	9,500	95	1.26
1.0	5	8,200	93	1.22
2.0	10	6,200	86	1.18
—[b]	10	—	trace	—

[a] Mole ratio of DPDTe to AIBN initiator.
[b] No AIBN initiator.

In the case of faster propagating monomers such as (meth)acrylates, the phenylethyl iodide is not an effective chain transfer agent (see Table 12.33). Although molecular weight control is achieved, the polydispersity indices are broader than those obtained for styrene.[202] This is indicative of the fact that iodide exchange rate is lower than the acrylate propagation rate (step 3, Scheme 12.24).

Diphenyl ditelluride has also been reported to control the free-radical polymerization of styrene (Table 12.34).[209] The mechanism of control could not be deduced from the experimental evidence presented. However, a mechanism involving reversible chain transfer of the phenyl telluride moeity could be envisaged as it is known that homolytic substitution by carbon centered radicals on tellurium in alkyl tellurides is a facile process[210] that is believed to proceed via a hypervalent telluride intermediate.[211]

12.5   CONCLUSION

The chain transfer methods discussed here have shown utility in controlling freeradical polymerization but each method exerts "control" to varying degrees of complexity. For chain transfer that is induced by thiols, disulfides, etc. as chain transfer agents has limitations in its versatility. This traditional method is limited primarily to molecular weight control although useful functionality can be introduced at the polymer ends depending on the choice of chain transfer agent used. The process of catalytic chain transfer with cobalt complexes is a very efficient method of chain transfer for (meth)acrylates, styrenes, and acrylamides. This method is very effective in molecular weight reduction because of the high chain transfer constant of cobalt complexes as well as the regeneration of the active agent during the chain transfer process. Hence only small (catalytic) quantities of cobalt complex are required. Adding to the utility of catalytic chain transfer is the fact that the polymers obtained by this process are terminated by an alkene end group. Particularly attractive is the 1,1-disubstituted alkene end group that is derived from α-methylsubstituted vinyl monomers. These macromonomers can be used as prepolymers to prepare graft and block copolymers. In addition, macromonomers can also act as chain transfer

agents to regulate molecular weight and under certain conditions make low polydispersity block copolymers. The addition–fragmentation chain transfer process is also effective for controlling molecular weight and for preparing a wide array of end-functional polymers. This chain transfer process can be mediated by macromonomers and simple organic molecules that encompass allylic compounds (e.g., allylic sulfides, peroxides, bromides, sulfones), vinyl ethers, and thiocarbonyl compounds.

The RAFT process, operating by reversible chain transfer, is a living free-radical technique. It offers the same convenience and versatility as conventional free-radical polymerization since it is applicable to the same range of monomers, solvents, functional groups, and reaction conditions. The RAFT polymerization is performed by adding a quantity of RAFT agent (dithioester, trithiocarbonate, dithiocarbamate, or xanthate) to conventional free-radical polymerization and yields thiocarbonylthio terminated polymers of predetermined molecular weight with low polydispersity indices (<1.1 under optimal conditions). These polymers can be chain extended to give a variety of block, gradient, and segmented copolymers.

REFERENCES

1. R. A. Gray, *J. Coat. Tech.* **57**, 83 (1985).

2. C. A. Barson, in *Comprehensive Polymer Science*, G. C. Eastmond, A. Ledwith, S. Russo, and P. Sigwalt, eds., London, Pergamon, 1989, Vol. 3, p. 171.

3. T. Corner, *Adv. Polym. sci.* **62**, 95 (1984).

4. A. Ueda and S. Nagai, in *Polymer Handbook*, 4th ed., J. Brandup, E. H. Immergut, and E. A. Grulke eds., Wiley, New York, 1999, p. II/97.

5. C. P. R. Nair, M. C. Richou, P. Chaumont, and G. Clouet, *Eur. Polym. J.* **26**, 811 (1990).

6. L. J. Young, in *Polymer Handbook*, 2nd ed., J. Brandup and E. H. Immergut, eds., Wiley, New York, 1975, p. II/6.

7. L. Businelli, H. Deleuze, Y. Gnanou, and B. Maillard, *Macromol. Chem. Phys.* **201**, 1833 (2000).

8. B. Boutevin, J.-M. Lusinchi, Y. Pietrasanta, and J.-J. Robin, *Eur. Polym. J.* **30**, 615 (1994).

9. B. Boutevin, A. El Idrissi, and J. P. Parisi, *Makromol. Chem.* **191**, 445 (1990).

10. P. Gregor, D. Dolar, and G. K. Hoesche, *J. Am. Chem. Soc.* **77**, 3675 (1955).

11. G. Reiss and P. Bahadur, in *Encyclopaedia of Polymer Science and Engineering*, H. F. Mark, N. M. Bikales, C. G. Overberger, and G. Menges, eds., Wiley, New York, 1985, Vol. 2, p. 324.

12. C. P. R. Nair, P. Sivadasan, and V. P. Balagangadharan, *J. Macromol. Sci., Pure Appl. Chem.* **A36**, 51 (1999).

13. B. Boutevin, *J. Polym. Sci.; Part A: Polym. Chem.* **38**, 3235 (2000) and references cited therein.

14. G. Moad and D. H. Solomon, *The Chemistry of Free Radical Polymerization*, Pergamon, London, 1995, pp. 240–248.

15. A. J. Constanza, R. J. Coleman, R. M. Pierson, C. S. Marvel, and C. King, *J. Polym. Sci.* **17**, 319 (1955).

16. T. Otsu, Y. Kinoshita, and M. Imoto, *Makromol. Chem.* **73**, 225 (1964).

17. K. Tsuda and T. Otsu, *Bull. Chem. Soc. Japan* **39**, 2206 (1966).

18. A. J. Constanza and L. Levine, *Macromol. Synth.* **2**, 87 (1966).

19. C. P. R. Nair, G. Clouet, and P. Chaumont, *J. Polym. Sci.; Part A: Polym. Chem.* **27**, 1795 (1989).

20. C. A. Uraneck, H. L. Hsieh, and R. J. Sonnenfeld, *J. Appl. Polym. Sci.* **13**, 149 (1969).

21. K. Wendler, S. K. Verma, and M. Fedke, *Acta Polym.* **34**, 637 (1983).

22. B. R. Smirnov, I. M. Belgovskii, G. V. Ponomarev, A. P. Marchenko, and N. S. Enikolopyan, *Dokl. Akad. Nauk SSSR.* **254**, 127 (1980).

23. N. S. Enikolopyan, B. R. Smirnov, G. V. Ponomarev, and I. M. Belgovskii, *J. Polym. Sci., Polym. Chem. Ed.* **19**, 879 (1981).

24. B. R. Smirnov, V. D. Plotnikov, B. V. Ozerkovskii, V. P. Roshchupkin, and N. S. Enikolopyan, *Polym. Sci. USSR* **23**, 2807 (1981).

25. T. P. Davis, D. M. Haddleton, and S. N. Richards, *J. Macromol. Sci., Rev. Macromol. Chem. Phys.* **C34**, 274 (1994).

26. T. P. Davis, D. Kukulj, D. M. Haddleton, and D. R. Maloney, *Trends Polym. Sci.* **3**, 365 (1995).

27. A. Martchenko, T. Bremner, and K. F. O'Driscoll, *Eur. Polym. J.* **33**, 713 (1997).

28. J. Chiefari, C. L. Moad, G. Moad, and E. Rizzardo, *Macromolecules* (in press).

29. M. P. Greuel and H. J. Harwood, *Polym. Prep.* (*Am. Chem. Soc., Div. Polym. Chem.*) **32**, 545 (1990).

30. S. D. Ittel, A. A. Gridnev, C. L. Moad, G. Moad, E. Rizzardo, and L. Wilczek, WO 9731,030 [*Chem. Abstr.* **128**, 234752 (1997)].

31. J. Chiefari, J. Jeffery, R. T. A. Mayadunne, G. Moad, E. Rizzardo, and S. H. Thang, *ACS Symp. Ser.* **768**, 297 (2000).

32. L. V. Karmilova, G. V. Ponomarev, B. R. Smirnov, and I. M. Belgovskii, *Russ. Chem. Rev.* **53**, 132 (1984).

33. V. Y. Mironichev, M. M. Mogilevich, B. R. Smirnov, Y. Y. Shapiro, and I. V. Golikov, *Polym. Sci. USSR* (*Engl. transl.*) **28**, 2103 (1986).

34. A. A. Gridnev, *Polym. Sci. USSR* (*Engl. Transl.*) **31**, 2369 (1989).

35. A. A. Gridnev, *Polym. J* **24**, 613 (1992).

36. T. P. Davis and D. Kukulj, *Macromol. Theory Simul.* **4**, 195 (1995).

37. R. A. Sanayai and K. F. O'Driscoll, *J. Macromol. Sci. -Chem.* **A26**, 1137 (1989).

38. A. F. Burczyk, K. F. O'Driscoll, and G. L. Rempel, *J. Polym. Sci., Polym. Chem. ed.* **22**, 3255 (1984).

39. G. M. Carlson and K. J. Abbey, U. S. Patent 4,526,945 (1985).

40. A. H. Janowicz, U. S. Patent 4,694,054 (1987).

41. E. E. Lawson, H. G. M. Edwards, and A. F. Johnson, *Spectrochimica Acta.* **50A**, 1899 (1994).

42. A. Bakac and J. H. Espenson, *J. Am. Chem. Soc.* **106**, 5197 (1984).

43. A. Bakac, M. E. Brynildson, and J. H. Espenson, *Inorg. Chem.* **25**, 4108 (1986).

44. K. G. Suddaby, D. R. Maloney, and D. M. Haddleton, *Macromolecules* **30**, 702 (1997).

45. D. G. Hawthorne, U. S. Patent 5,324,879 (1991).

46. G. N. Schrauzer and R. J. Windgassen, *J. Am. Chem. Soc.* **88**, 3738 (1966).

47. J. Krstina, G. Moad, E. Rizzardo, C. L. Winzor, C. T. Berge, and M. Fryd, *Macromolecules* **28**, 5381 (1995).

48. B. B. Wayland, G. Poszmik, and M. Fryd, *Organometallics* **11**, 3534 (1992).

49. V. Kettmann, M. Dunaj-Jurco, D. Steinborn, and M. Ludwig, *Acta Cryst.* **C52**, 1399 (1996).

50. G. Abramo and J. R. Norton, *Macromolecules* **33**, 2790 (2000).

51. A. A. Gridnev, S. D. Ittel, B. B. Wayland, and M. Fryd, *Organometallics* **15**, 5116 (1996).

52. J. P. A. Heuts, D. J. Forster, T. P. Davis, B. Yamada, H. Yamazoe, and M. Azukizawa, *Macromolecules* **32**, 2511 (1999).

53. A. A. Gridnev, S. D. Ittel, M. Fryd, and B. B. Wayland, *Organometallics* **12**, 4871 (1993).

54. A. A. Gridnev, S. D. Ittel, M. Fryd, and B. B. Wayland, *J. Chem. Soc., Chem. Commun.*, 1010 (1993).

55. M. Brookhart, M. L. H. Green, and L. L. Wong, *Progr. Inorg. Chem.* **36**, 1 (1998).

56. J. P. A. Heuts, D. J. Forster, and T. P. Davis, *Macromol. Rapid Commun.* **20**, 299 (1999).

57. G. N. Schrauzer and R. J. Holland, *J. Am. Chem. Soc.* **93**, 1505 (1971).

58. K. G. Suddaby, K. H. Hunt, and D. M. Haddleton, *Macromolecules* **29**, 8642 (1996).

59. N. S. Enikolopyan, B. R. Smirnov, I. S. Morozova, L. M. Pushchaeva, and A. P. Marchenko, *Dokl. Chem.* (*Engl. transl.*), 542 (1980).

60. D. M. Haddleton, D. R. Maloney, K. G. Suddaby, A. V. G. Muir, and S. N. Richards, *Macromol. Symp.* **111**, 37 (1996).

61. J. P. A. Heuts, D. Kukulj, D. J. Forster, and T. P. Davis, *Macromolecules* **31**, 2894 (1998).

62. D. Kukulj and T. P. Davis, *Macromol. Chem. Phys.* **199**, 1697 (1998).

63. D. Kukulj, J. P. A. Heuts, and T. P. Davis, *Macromolecules* **31**, 6034 (1998).

64. F. R. Mayo, *J. Am. Chem. Soc.* **65**, 2324 (1943).

65. B. Y. H. Whang, M. J. Ballard, D. H. Napper, and R. G. Gilbert, *Aust. J. Chem.* **44**, 1133 (1991).

66. P. A. Clay and R. G. Gilbert, *Macromolecules* **28**, 552 (1995).

67. J. P. A. Heuts, D. J. Forster, and T. P. Davis, *Macromolecules* **32**, 3907 (1999).

68. D. J. Forster, J. P. A. Heuts, and T. P. Davis, *Polymer* **41**, 1385 (2000).

69. B. R. Smirnov, A. P. Marchenko, V. D. Plotnikov, A. I. Kuzaev, and N. S. Enikolopyan, *Polym. Sci. USSR* (*Engl. transl.*) **93**, 1016 (1981).

70. J. Krstina, C. L. Moad, G. Moad, E. Rizzardo, C. T. Berge, and M. Fryd, *Macromol. Symp.* **111**, 13 (1996).

71. C. Kowollik and T. P. Davis, *J. Polym. Sci.; Part A: Polym. Chem.* **38**, 3303 (2000).

72. P. Cacioli, G. Moad, E. Rizzardo, A. K. Serelis, and D. H. Solomon, *Polym. Bull.* **11**, 325 (1984).

73. L. E. Manring, *Macromolecules* **22**, 2673 (1989).

74. E. F. McCord, W. L. Anton, L. Wilczek, S. D. Ittel, N. T. Lissa, and K. D. Raffell. *Makromol. Chem., Macromol. Symp.* **86**, 47 (1994).

75. H. S. Creel, *Trends Polym. Sci.* **1**, 336 (1993).

76. J. E. Campana, S. Long-Shen, S. L. Shew, and B. E. Winger, *Trends Anal. Chem.* **13**, 239 (1994).

77. S. D.-H. Shi, C. L. Hendrickson, A. G. Marshall, W. J. Simonseck, Jr., and D. J. Aaserud, *Anal. Chem.* **70**, 3220 (1998).

78. B. B. Wayland, G. Poszmik, S. L. Mukerjee, and M. Fryd, *J. Am. Chem. Soc.* **116**, 7943 (1994).

79. G. M. Carlson and K. J. Abbey, U.S. Patent 4,526,945 (1985); A. H. Janowicz, EPO229481 A3 (1986); J.-C. Lin and K. J. Abbey, U.S. Patent 4,680,354 (1987); A. H. Janowicz and L. R. Melby, U.S. Patent 4,680,352 (1987); A. H. Janowicz, EPO261942 A3 (1987); A. H. Janowicz, U.S. Patent 4,722,984 (1988); A. H. Janowicz, U.S. patent 4,746,713 (1988); A. H. Janowicz, U.S. patent 4,886,861 (1989); A. H. Janowicz, L. R. Melby, and S. D. Ittel, EPO199436 (1996); A. H. Janowicz, L. R. Melby, and S. D. Ittel, EPO196783 (1996).

80. M. N. Galbraith, G. Moad, D. H. Solomon, and T. H. Spurling, *Macromolecules* **20**, 675 (1987).

81. T. H. Spurling, M. Deady, J. Krstina, and G. Moad, *Makromol. Chem., Macromol. Symp.* **51**, 127 (1991).

82. J. A. Antonelli, C. Scopazzi, and M. M. Doherty, U.S. Patent 5,010,140 (1991); B. P. Devlin and J. A. Antonelli, WO93/03081 (1993).

83. M. Fryd, M. Periyasamy, and F. L. Schadt, WO92/15628 (1992).

84. P. A. Mancinelli, EPO357229 (1990).

85. P. Cacioli, D. G. Hawthorne, R. L. Laslett, E. Rizzardo, and D. H. Solomon, *J. Macromol. Sci.— Chem.* **A23**, 839 (1986).

86. E. Rizzardo, G. F. Meijs, and S. T. Thang, WO88/4304A1 (1988).

87. G. F. Meijs, E. Rizzardo, and S. T. Thang, *Macromolecules* **21**, 3122 (1988).

88. G. F. Meijs, T. C. Morton, E. Rizzardo, and S. T. Thang, *Macromolecules* **24**, 3689 (1991).

89. E. Rizzardo, G. F. Meijs, and S. T. Thang, PCT/AU90/00523 (1990).

90. G. F. Meijs, E. Rizzardo, and S. T. Thang, *Polym. Prep.* (*Am. Chem. Soc., Div. Polym. Chem.*) **33**, 893 (1992).

91. G. F. Meijs, E. Rizzardo, and S. T. Thang, *Polym. Bull.* **24**, 501 (1990).

92. B. Yamada and T. Otsu, *Makromol. Chem., Rapid Commun.* **11**, 513 (1990).

93. B. Yamada, S. Kobatake, and S. Aoki, *Macromol. Chem. Phys.* **195**, 581 (1994).

94. G. F. Meijs and E. Rizzardo, *Makromol. Chem., Rapid Commun.* **9**, 547 (1988).

95. G. F. Meijs and E. Rizzardo, *Makromol. Chem.* **191**, 1545 (1990).

96. G. F. Meijs and E. Rizzardo, *Polym. Bull.* (*Berlin*) **26**, 291 (1991).

97. G. F. Meijs, E. Rizzardo, T. P. T. Le, and Y.-C. Chen, *Makromol. Chem.* **193**, 369 (1992).

98. E. Rizzardo, G. F. Meijs, and S. H. Thang, *Macromol. Symp.* **98**, 101 (1995).

99. D. Colombani and P. Chaumont, *Prog. Polym. Sci.* **21**, 439 (1996).

100. J. McGrath, *Pure Appl. Chem.* **55**, 1573 (1983).

101. H. A. Nguyen and E. Marechal, *J. Macromol. Sci. Rev., Macromol. Chem. Phys.* **C28**, 187 (1988).

102. J.-C. Brosse, D. Derouet, F. Epaillard, J.-C. Soutif, G. Legeay, and K. Dusek, *Adv. Polym. Sci.* **81**, 167 (1987).

103. P. V. Caeter, *Trends Polym. Sci.* **3**, 227 (1995).

104. S. N. Lewis, J. J. Miller, and S. Winstein, *J. Org. Chem.* **37**, 1478 (1972).

105. G. E. Keck and J. B. Yates, *J. Org. Chem.* **47**, 3591 (1982).

106. G. E. Keck and J. H. Byers, *J. Org. Chem.* **50**, 5442 (1985).

107. G. E. Keck, E. J. Enholm, J. B. Yates, and M. R. Wiley, *Tetrahedron* **41**, 4079 (1985).

108. G. E. Keck and A. M. Tafesh, *J. Org. Chem.* **54**, 5845 (1989).

109. J. E. Baldwin, R. M. Adlington, and A. Basak, *J. Chem. Soc., Chem. Commun.* 1339 (1988).

110. J. E. Baldwin, R. M. Adlington, D. J. Birch, J. A. Crawford, and J. B. Sweeney, *J. Chem. Soc., Chem. Commun.* 1284 (1984).

111. D. H. R. Barton and D. Crich, *J. Chem. Soc., Perkin Trans.* **1**, 1613 (1986).

112. E. J. Corey and Z. Wang, *Tetrahedron Lett.* **35**, 539 (1994).

113. B. Giese, J. Burger, T. W. Kang, C. Kesselheim, and T. Wittmer, *J. Am. Chem. Soc.* **114**, 7322 (1992).

114. E. Rizzardo, Y.-K. Chong, R. A. Evans, G. Moad, and S. H. Thang, *Macromol. Symp.* **111**, 1 (1996).

115. D. Colombani, *Prog. Polym. Sci.* **24**, 425 (1999) and references cited therein.

116. E. Rizzardo, D. S. Harrison, R. L. Laslett, G. F. Meijs, T. C. Morton, and S. H. Thang, in *Progress in Pacific Polymer Science*, B. C. Anderson and Y. Imanishi, eds., Springer-Verlag, Berlin, 1991, p. 77.

117. K. J. Abbey, D. L. Trumbo, G. M. Carlson, M. J. Masola, and R. A. Zander, *J. Polym. Sci.; Part A: Polym. Chem.* **31**, 3417 (1993).

118. D. L. Trumbo and K. J. Abbey, *J. Polym. Sci.; Part C: Polym. Lett.* **25**, 229 (1987).

119. P. Rajatapiti, V. L. Dimonie, and M. El Asser, *J. Macromol. Sci., Chem.* **A32**, 1445 (1995).

120. D. M. Haddleton, D. R. Maloney, K. G. Suddaby, A. Clarke, and S. N. Richards, *Polymer* **38**, 6207 (1997).

121. C. T. Berge, M. J. Darmon, and J. A. Antonelli, U.S. Patent 5,362,826 (1994).

122. H. Tanaka, H. Kawai, and T. Sato, *J. Polym. Sci.; Part A: Polym. Chem.* **27**, 1741 (1989).

123. D. S. Harrison, M. Sc. thesis, Swinburne Univ., Hawthorn, Australia.

124. B. Yamada, S. Kobatake, and S. Aoki, *Polym Bull.* **31**, 263 (1993).

125. B. Yamada, S. Tagashira, and S. Aoki, *J. Polym. Sci.; Part A: Polym. Chem.* **32**, 2745 (1994).

126. S. Kobatake and B. Yamada, *Macromol. Chem. Phys.* **198**, 2825 (1997).

127. L. Wilczek and E. F. McCord, U.S. patent 6,100,350 (2000).

128. C. L. Moad, G. Moad, E. Rizzardo, and S. H. Thang, *Macromolecules* **29**, 7717 (1996).

129. D. M. Haddleton, C. Topping, D Kukulj, and D. Irvine, *Polym.* **39**, 3119 (1998).

130. B. Giese, *Angew. Chem., Int. Ed. Engl.* **22**, 753 (1983).

131. B. Yamada, S. Kobatake, and T. Otsu, *Polym. J.* (*Tokyo*) **24**, 281 (1992).

132. D. Colombani and P. Chaumont, *Macromol. Chem. Phys.* **196**, 3643 (1995).

133. Y.-K. Chong, G. Moad, E. Rizzardo, and S. H. Thang, WO97/13792 (1997).

134. T. Sato, M. Seno, M. Kobayashi, T. Kohno, and H. Tanaka, *Eur. Polym. J.* **31**, 29 (1995).

135. B. Yamada, O. Konosu, K. Tanaka, and F. Oku, *Polymer* **41**, 5625 (2000).

136. E. Rizzardo, S. H. Thang, G. Moad, and C. T. Berge, U.S. Patent 5,773,543 (1998).

137. S. Jiang, H. G. Viehe, N. Oger, and D. Charmot, *Macromol. Chem. Phys.* **196**, 2349 (1995).

138. S. Mignani, Z. Janousek, R. Merenyi, H. G. Viehe, J. Riga, and J. Verbist, *Tetrahedron Lett.* **25**, 1571 (1984).

139. M. O. Zink, D. Colambani, and P. Chaumont, *Eur. Polym. J.* **33**, 1433 (1997).

140. C. P. R. Nair, P. Chaumont, and D. Charmot, *J. Polym. Sci.; Part A: Polym. Chem.* **33**, 2773 (1995).

141. A. Sunder and R. Mülhaupt, *Macromol. Chem. Phys.* **200**, 58 (1999).

142. E. Montaudon, F. Rakotomanana, and B. Maillard, *Tetrahedron*, **41**, 2727 (1985).

143. D. Colambani and P. Chaumont, *J. Polym. Sci.; Part A: Polym. Chem.* **32**, 2628 (1994).

144. D. Colambani and P. Chaumont, *Macromolecules*, **27**, 5972 (1994).

145. D. Colambani, I. Beliard, and P. Chaumont, *J. Polym. Sci.; Part A: Polym. Chem.* **34**, 893 (1996).

146. D. Colambani, M. O. Zink, and P. Chaumont, *Macromolecules* **28**, 819 (1995).

147. K. C. Berger and G. Brandrup, in *Polymer Handbook*, 3rd ed., G. Brandrup and E. H. Immergut, eds., Wiley, New York, 1989.

148. D. H. R. Barton, D. Crich, and G. Kretzchsmar, *J. Chem. Soc., Perkin Trans.* **1**, 39 (1986).

149. D. E. Bergbreiter and J. Zhou, *J. Polym. Sci.; Part A: Polym. Chem.* **30**, 2049 (1992).

150. W. H. Daly and T. S. Evenson, *ACS Symp. Ser.* **685**, 377 (1998).

151. W. H. Daly and T. S. Evenson, *Polymer* **41**, 5063 (2000).

152. E. J. Goethals, *Telechelic Polymers: Synthesis and Applications*, CRC Press, Boca Raton, FL, 1989.

153. J. R. Ebdon, in *New Methods of Polymer Synthesis*, J. R. Ebdon, ed., Blackie, Glasgow, 1991, p. 6/162.

154. M. Sawamoto and M. Kamigaito, in *New Methods of Polymer Synthesis*, J. R. Ebdon and G. C. Eastmond, eds., Blackie, Glasgow, 1995, Vol. 2, p. 2/37.

155. B. Boutevin, *Adv. Polym. Sci.* **94**, 69 (1990).

156. B. Ameduri, B. Boutevin, and P. Gramain, *Adv. Polym. Sci.* **127**, 87 (1997).

157. W. Heitz, *Makromol. Chem., Macromol. Symp.* **10/11**, 297 (1987).

158. T. Otsu and T. Tazaki, *Polym. Bull.* (*Berlin*) **16**, 277 (1986).

159. C. P. R. Nair and G. Clouet, *J. Macromol. Sci. Rev., Macromol. Chem. Phys.* **C31**, 311 (1991).

160. G. Moad and D. H. Solomon, in *Chemistry of Bimolecular Termination*, G. C. Eastmond, A. Ledwith, S. Russo, and P. Sigwalt, eds., Pergamon, Oxford, 1989, Vol. 3, p. 11/147.

161. G. Baudin, B. Boutevin, J. P. Mistral, and L. Sarraf, *Makromol. Chem.* **186**, 1445 (1985).

162. J. R. Ebdon, N. J. Flint, and P. Hodge, *Eur. Polym. J.* **25**, 759 (1989).

163. J. R. Ebdon, N. J. Flint, and S. Rimmer, *Macromol. Rep.* **A32**, 603 (1995).

164. R. D. Athey, Jr., *J. Coat. Technol.* **54**, 47 (1982).

165. R. D. Athey, Jr., *Prog. Org. Coat.* **7**, 289 (1979).

166. G. Moad, C. L. Moad, J. Krstina, E. Rizzardo, C. T. Berge, and T. R. Darling, WO 96/15157 (1996).

167. T. P. Le, G. Moad, E. Rizzardo, and S. H. Thang, WO 9801478/A1 (1998).

168. J. Chiefari, R. T. A. Mayadunne, G. Moad, E. Rizzardo, and S. H. Thang, WO 9931144 (1999).

169. J. Chiefari, Y. K. Chong, F. Ercole, J. Krstina, J. Jeffery, T. P. Le, R. T. A. Mayadunne, G. F. Meijs, C. L. Moad, G. Moad, E. Rizzardo, and S. H. Thang, *Macromolecules* **31**, 5559 (1998).

170. Y. K. Chong, T. P. Le, G. Moad, E. Rizzardo, and S. H. Thang, *Macromolecules* **32**, 2071 (1999).

171. E. Rizzardo, J. Chiefari, Y. K. Chong, F. Ercole, J. Krstina, J. Jeffery, T. P. Le, R. T. A. Mayadunne, G. F. Meijs, C. L. Moad, G. Moad, and S. H. Thang, *Macromol. Symp.* **143**, 291 (1999).

172. P. Corpart, D. Charmot, T. Biadatti, S. Z. Zard, and D. Michelet, WO 9858974 (1998).

173. D. Charmot, P. Corpart, H. Adam, S. Z. Zard, T. Biadatti, and G. Bouhadir, *Macromol. Symp.* **150**, 23 (2000).

174. D. G. Hawthorne, G. Moad, E. Rizzardo, and S. H. Thang, *Macromolecules* **32**, 5457 (1999).

175. G. Moad, J. Chiefari, Y. K. Chong, J. Krstina, R. T. A. Mayadunne, A. Postma, E. Rizzardo, and S. H. Thang, *Polymer Int.* **49**, 993 (2000).

176. M. J. Monteiro and H. de Brouwer, *Macromolecules* **34**, 349 (2001).

177. C. Barner-Kowollik, J. F. Quinn, D. R. Morsely, and T. P. Davis, *J. Polym. Sci.; Part A: Polym. Chem.* **39**, 1353 (2001).

178. Y. K. Chong, J. Krstina, T. P. Le, G. Moad, A. Postma, E. Rizzardo, and S. H. Thang, *Macromolecules* (in press).

179. A. Goto, K. Sato, Y. Tsujii, T. Fukuda, G. Moad, E. Rizzardo, and S. Thang, *Macromolecules* **34**, 402 (2001).

180. J. Chiefari, R. T. A. Mayadunne, C. L. Moad, G. Moad, A. Postma, E. Rizzardo, and S. H. Thang, *Macromolecules* (in press).

181. A. H. E. Mueller, R. Zhuang, D. Yan, and G. Litvenko, *Macromolecules* **28**, 4326 (1995).

182. A. H. E. Mueller and G. Litvenko, *Macromolecules* **30**, 1253 (1997).

183. G. Moad, F. Ercole, C. H. Johnson, J. Krstina, C. L. Moad, E. Rizzardo, T. H. Spurling, M. Fryd, and A. G. Anderson, *ACS Symp. Ser.* **685**, 332 (1998).

184. E. Rizzardo, J. Chiefari, R. T. A. Mayadunne, G. Moad, and S. H. Thang, *ACS Symp. Ser.* **768**, 278 (2000).

185. R. T. A. Mayadunne, E. Rizzardo, J. Chiefari, Y. K. Chong, G. Moad, and S. H. Thang, *Macromolecules* **32**, 6977 (1999).

186. M. Destarac, D. Charmot, X. Franck, and S. Z. Zard, *Macromol. Rapid Commun.* **21**, 1035 (2000).

187. E. Rizzardo, J. Chiefari, Y.-K. Chong, G. Moad, and S. H. Thang, *Plenary Lecture*, Pacifichem, Hawaii, 2000.

188. E. Rizzardo, J. Chiefari, Y. K. Chong, G. Moad, and S. H. Thang, unpublished results.

189. F. Ganachaud, M. J. Monteiro, R. G. Gilbert, M.-A. Dourges, S. H. Thang, and E. Rizzardo, *Macromolecules* **33**, 6738 (2000).

190. S. H. Thang, Y. K. Chong, R. T. A. Mayadunne, G. Moad, and E. Rizzardo, *Tetrahedron Lett.* **40**, 2435 (1999).

191. S. Kato and M. Ishida, *Sulfur Report* **8**, 155 (1988).

192. R. Mayer and S. Scheithauer, in *Houben-Weyl Methods of Organic Chemistry*, K. H. Buechel, J. Falbe, H. Hagemann, and M. Hanack, eds., Thieme, Stuttgart, 1985, Vol. E, p. 891.

193. A. Butté, G. Storti, and M. Morbidelli, *Macromolecules* **33**, 3485 (2000).

194. H. de Brouwer, J. G. Tsavalas, J. Schork, and M. J. Monteiro, *Macromolecules* **33**, 9239 (2000).

195. M. Lansalot, C. Farcet, B. Charleux, and J.-P. Vairon, *Macromolecules* **32**, 7354 (1999).

196. M. J. Monteiro, M. Hodgson, and H. de Brouwer, *J. Polym. Sci.; part A: Polym. Chem.* **38**, 3864 (2000).

197. H. de Brouwer, M. A. J. Schellekens, B. Klumpermann, M. J. Monteiro, and A. L. German, *J. Polym. Sci.; part A: Polym. Chem.* **38**, 3596 (2000).

198. J. Chiefari, R. T. A. Mayadunne, G. Moad, E. Rizzardo, and S. H. Thang, WO 9931144/A1 (1999).

199. R. T. A. Mayadunne, E. Rizzardo, J. Chiefari, J. Krstina, G. Moad, A. Postma, and S. H. Thang, *Macromolecules* **33**, 243 (2000).

200. R. T. A. Mayadunne, E. Rizzardo, J. Chiefari, J. Jeffery, and G. Moad, *Macromolecules* (in press).

201. K. Matyjaszewski, S. G. Gaynor, and J.-S. Wang, *Macromolecules* **28**, 2093 (1995).

202. S. G. Gaynor, J.-S. Wang, and K. Matyjaszewski, *Macromolecules* **28**, 8051 (1995).

203. A. Goto, K. Ohno, and T. Fukuda, *Macromolecules* **31**, 2809 (1998).

204. G. S. Georgiev, E. B. Kamenska, N. V. Tsarevsky, and L. K. Christov, *Polym. Int.* **50**, 313 (2001).

205. D. Greszta, D. Mardare, and K. Matyjaszewski, *Macromolecules* **27**, 638 (1994).

206. K. Matyjaszewski, S. G. Gaynor, D. Greszta, D. Mardare, T. Shigemoto, and J.-S. Wang, *Macromol. Symp.* **95**, 217 (1995).

207. K. Matyjaszewski, *ACS Symp. Ser.* **768**, 2 (1998).

208. C. Farcet, M. Lansalot, R. Pirri, J.-P. Vairon, and B. Charleux, *Macromol. Rapid Commun.* **21**, 921 (2000).

209. K. Takagi, A. Soyano, T. S. Kwon, H. Kunisada, and Y. Yuki, *Polym. Bull.* **43**, 143 (2001).

210. D. P. Curran, A. A. Martin-Esker, S.-B. Ko, and M. Newcomb, *J. Org. Chem.* **58**, 4691 (1993).

211. C. H. Schiesser and B. A. Smart, *Tetrahedron* **51**, 6051 (1995).

13 Control of Stereochemistry of Polymers in Radical Polymerization

AKIKAZU MATSUMOTO

Osaka City University, Sugimoto, Osaka, Japan

CONTENTS

13.1 INTRODUCTION

The importance of design and control of polymer chain structures in polymer synthesis can hardly be overestimated. The chemical and physical properties of polymers in a solid, melt, or solution depend significantly on their primary structures including the structure of repeating units, the chain-end structures, branching, tacticity, the molecular weight and the molecular weight distribution. Moreover,

the composition and comonomer sequence for copolymers, such as random, alternating, block, and graft copolymers, also play a major role in determining these chemical and physical properties. A variety of polymerization techniques and catalysts have been developed for the control of the primary chain structure.[1] These efforts have resulted in the successful synthesis of highly controlled chain structures for certain types of monomers and initiators under specific reaction conditions in terms of temperature and solvents. The stereochemistry of polymers has received significant attention in the fields of fundamental and applied polymer chemistry ever since the first discoveries of stereoregular polymers in the midtwentieth century.

Radical polymerization is the most important and convenient process for the production of various kinds of vinyl polymers in both fundamental and applied fields. This is as a result of more recent achievements of well-controlled polymerizations in addition to the classical advantages of the radical process.[2,3] These advantages include a high polymerization reactivity of many kinds of monomers (especially for monomers with a polar and unprotected functional group), excellent reproducibility of polymerization results due to a high tolerance to additives and impurities, the possibility of employing water as solvent and dispersant, and a generally simple overall procedure. Furthermore, several aspects of the polymerization reactions can be predicted from the established elementary reaction mechanism and monomer structure–reactivity relationships. Since the early 1980s, living radical polymerization techniques have been developed to provide polymers with well-defined structures, including well-controlled molecular weight and molecular weight distribution, chain-end structure, hyperbranched structure, and block copolymer sequences as described in preceding chapters in this book or in reviews.[4-6] In contrast, the control of polymer tacticity has been well established by coordination polymerization of olefins and diene monomers, and by anionic polymerization of certain types of polar monomers. It was previously believed that the tacticity was difficult to regulate during free-radical polymerization due to the inability of free-radical species to control propagation, except for several examples of polymerization in organized media such as inclusion polymerization. However, recent progress in free-radical chemistry now enables us to successfully control stereochemistry in radical reactions including radical polymerization.

Synthetic applications of radical reactions have become more sophisticated since the early 1980s, and nowadays, radicals are versatile intermediates in organic synthesis.[7,8] Regio- and stereoselectivity in the reactions of cyclic and acyclic radicals, as well as cyclizations, was achieved in the early 1990s through deep understanding of radical reactions. Substrate, chiral auxiliary, and chelate control provide high stereoselectivity and a stereospecific stereoisomer as the product due to the preferred conformations of cyclic and acyclic radicals. Although stereocontrol of polymers during free-radical polymerization is still immature at the present time, several clues exist for further development toward a highly efficient and more generalized method for the control of the stereochemistry of many kinds of polymers.

Commercial polymerizations are carried out in the fluid state as in solution, suspension, emulsion, gas, or melt as this provides for easy operation and control of the polymerization conditions. However, certain interesting features of solid-state polymerization have been pointed out. For example, when the monomer molecules

are themselves crystalline or are included in host crystals, the rate and selectivity of the reaction as well as the structures of the products are completely different from those obtained in an isotropic reaction medium. Many attempts to control the tacticity by free-radical polymerization have already been made in several organized media, such as liquid crystals, interfaces, micelles, vesicles, inclusion compounds, and templates.[9] The studies of solid-state organic syntheses have progressed at an accelerated speed as a result of the development of methods and equipment for crystal structure analysis. Organic reactions that proceed in the solid state without any organic solvents, including toxic and halogen-containing solvents, have recently attracted significant attention in many fields of synthetic chemistry and material science, not only due to their unique reaction mechanism features and stereospecific structure of the products but also from the standpoint of green sustainable chemistry.

In this chapter, the general features of stereocontrol during radical reactions of small molecules are described to aid the understanding of the basic concepts for the stereochemical control of polymers. The fundamental principles of the stereochemistry of vinyl and diene polymers are also briefly explained. In the subsequent sections, the stereochemical control of polymers is described during various types of radical polymerizations in isotropic solutions, as well as in organized and constrained media including micelles, vesicles, and liquid crystals, and in the solid states.

13.2 RECENT PROGRESS IN STEREOCONTROL OF FREE-RADICAL REACTIONS

Until the 1980s, organic radicals were recognized as interesting reactive intermediates, but they were used in organic syntheses with only limited potential except for some practical and important applications to bromination and polymerization. However, synthetic chemists gradually came to recognize that radicals frequently react with a high chemo- and regioselectivity. Radicals are normal organic species and experience the same classes of steric, electronic, and stereoelectronic interactions as all other organic non-radical molecules. These interactions are used for prediction and reaction design to control stereoselectivity. Before the end of the 1980s, it was believed that the high reactivity and flexibility of acyclic radicals prevented stereoselective reactions.[10–13] This changed in 1991 when Porter, Giese, and Curran proposed a new concept and guideline for the stereochemical control of acyclic systems.[14] The stereoselection of acyclic radicals can be achieved under substrate, chiral auxiliary, and chelate control, as shown in the typical examples of the stereoselective radical reactions of small molecules with the preferred conformation of the radicals leading to excellent stereoselectivity (Fig. 13.1).

For the intermolecular reaction of acyclic radicals such as the addition to a double bond or a hydrogen abstraction, a high stereoselectivity is realized when the radical center of the substrate favors conformations that correspond to an allylic strain (A-strain) model or a Felkin–Ahn model[15,16]. The concept of A strain is based on the conformation of (Z)-alkenes where allylic alkyl groups adopt preferred conformations in which the smallest substituent points in the direction of the vicinal alkene substituent. When the X substituent at the α-position of the radical is COR, CO_2R, CONR, Ar, NR_2, and NO_2, the A-strain conformations are energetically advantageous
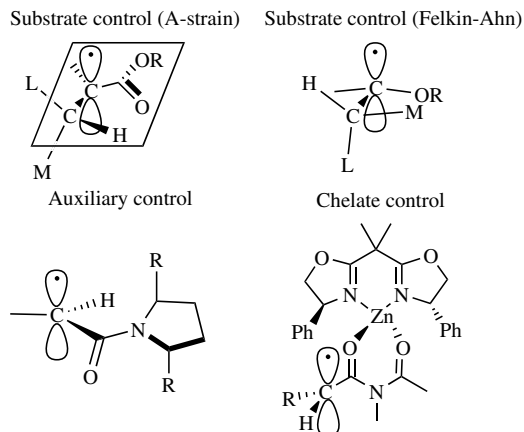
Figure 13.1 Preferred conformation of the radicals leading to excellent stereoselectivity under substrate, chiral auxiliary, and chelate control.

(Fig. 13.2). When X is OR, SR, and NHR, the radicals favor the Felkin–Ahn conformation, as shown in Fig. 13.2b. The reaction preferably occurs from the side shown with an arrow, which is opposite to the side shielded with a bulky β-substituent L.

Stereoselective reaction of an acyclic radical occurs during the reaction of a mesaconic (α-methylfumaric) ester with tBuHgCl/NaBH$_4$. The stereoselective hydrogen atom abstraction by the radical leads to products with the high diastereoselectivity of 25 : 1.[17] The existence of an α-methyl group is important for high selectivity; thus a tertiary radical is more selective than a secondary radical. The selectivity depends not only on the steric requirement of the substituents but also on the dipole interaction between the β-substituents and the X groups. In 1990,
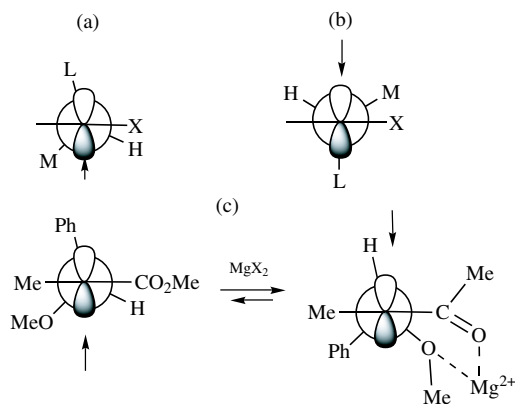
Figure 13.2 Stable conformations of radicals and the direction of attack in the following addition and abstraction reactions: (a) A-strain conformation; (b) Felkin–Ahn conformation; (c) inversion of the stereoselectivity of the radical in the absence and presence of Lewis acid.

Guindon et al.[18] suggested the existence of a dipole-dipole interaction that increases the dihedral angle between the C_β–H_β and C_α–CO_2R bonds with a polar substituent at the stereogenic center of an enolate radical, and this was later verified by quantum chemical calculations and ESR measurements.[19]

$tBuHgCl$
$NaBH_4$
20°C

$tBuHgH$

diastereoselectivity

diastereoselectivity 25 : 1

Bu_3SnH

diastereoselectivity 27 : 1 (R = CH_3)
8 : 1 (R = H, Bn_3SnD)
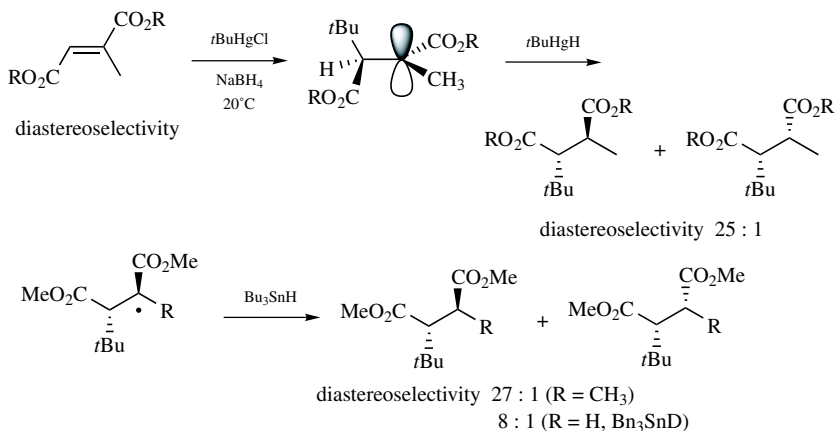
An effect of Lewis acids on the stereoselectivity of ester-substituted radicals has been detected (Fig. 13.2c). Inversion of the stereoselectivity was observed during the reduction and the allylation of a radical precursor, as shown in the following schemes.[20–23] These favorable conformations were confirmed by ab initio calculations and ESR observations. The addition of Lewis acids contributes not only to the change in the selectivity but also accelerates the reactions.

Bu_3SnH
AIBN/$h\nu$
−78°C

without MgI_2 >97 : < 3
with MgI_2 (1 eq)   < 3 : >97

Bu_3SnH
Et_3B
CH_2Cl_2, 0°C

without $MgBr_2$ 95 : < 5
with $MgBr_2$ (5 eq)   3 : 97
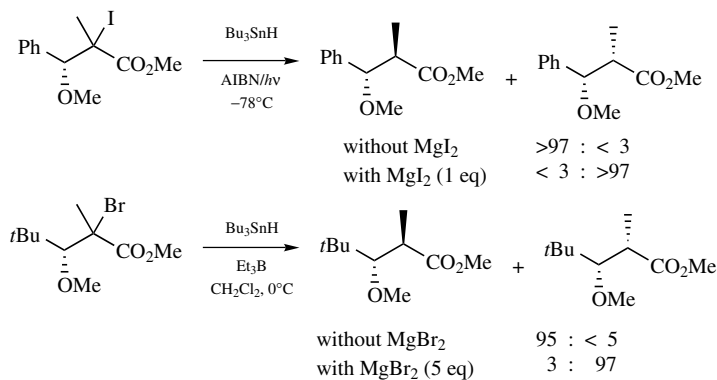
Chiral auxiliaries can also be used for control of the configuration of new stereogenic centers based on the concepts developed in carbanion and enamine chemistry. This has resulted in the design and introduction of a number of new chiral auxiliaries, including chiral Lewis acids for radical reactions.[14,24–26] For example, when two carbonyl groups of an oxazolidinone derivative are complexed with equimolar $Yb(OTf)_3$ as the Lewis acid to fix the conformation, one side of the olefin is shielded by the bulky substituent, resulting in high stereoselectivity.[27]

diastereoselectivity   45 : 1 (R = Ph)
25 : 1 (R = CH$_3$)
10 : 1 (R = CO$_2$R)
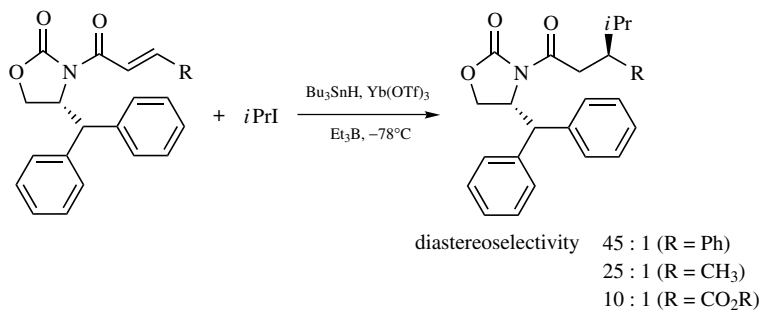
Porter et al.[28–30] reported the threo-selective and enantioselective addition of an acrylamide with an oxzolidinone ring. The oxazolidinone and oxazolidine derivatives are used for diastereoselective allylation.[31,32] Many examples of the stereoselective addition of an alkyl radical to olefins with various types of chiral auxiliaries in the presence of Lewis acid can be found in several reviews.[20,24]
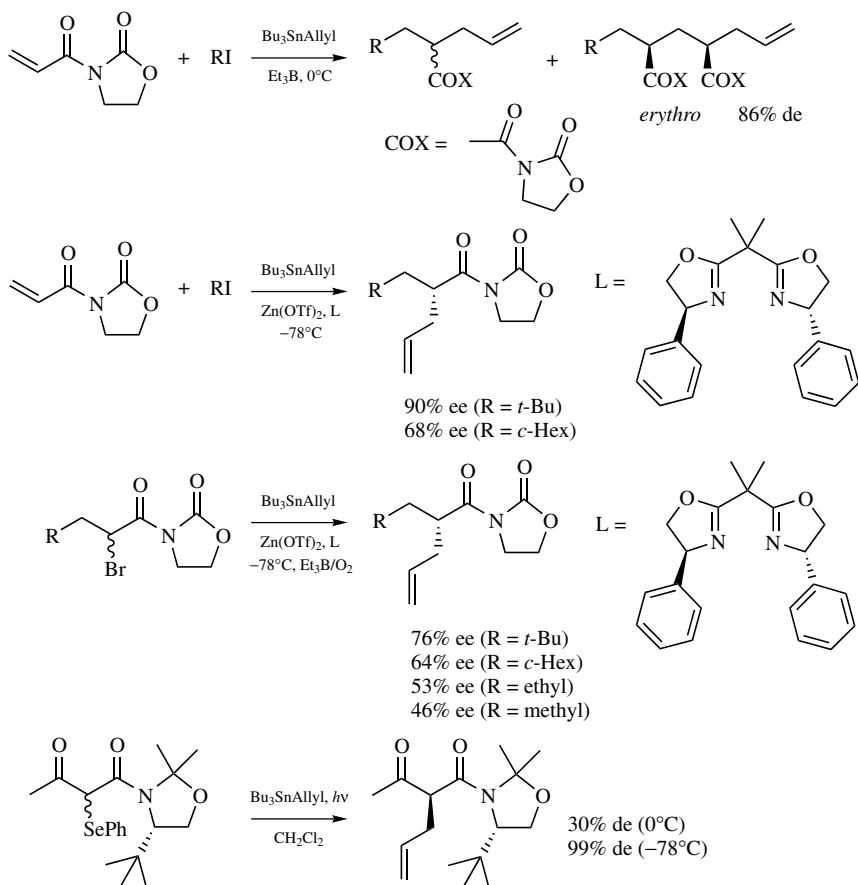
More recently, Curran et al. have developed new stereoselective reactions that capitalize on features unique to the radicals.[33] That is a conceptually new way to control stereoselection that does not use traditional competing reactions with diastereomeric transition states. The cyclization of an axially chiral amide does not go through a racemic radical intermediate because the intermediate radical is very short-lived and the cyclization is fast. Therefore, the axial chirality in the amide is faithfully transferred to the stereocenter of the product.[34]

86% ee
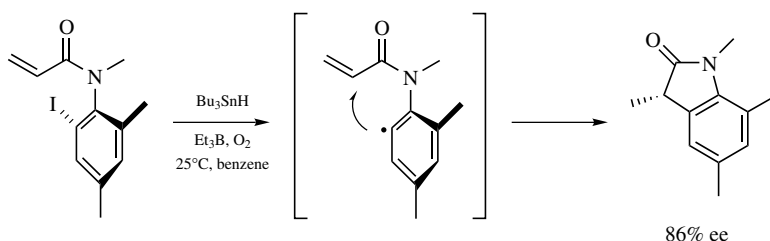
Another class of chiral auxiliaries based on axially chiral amides and imides has also been developed.[35]
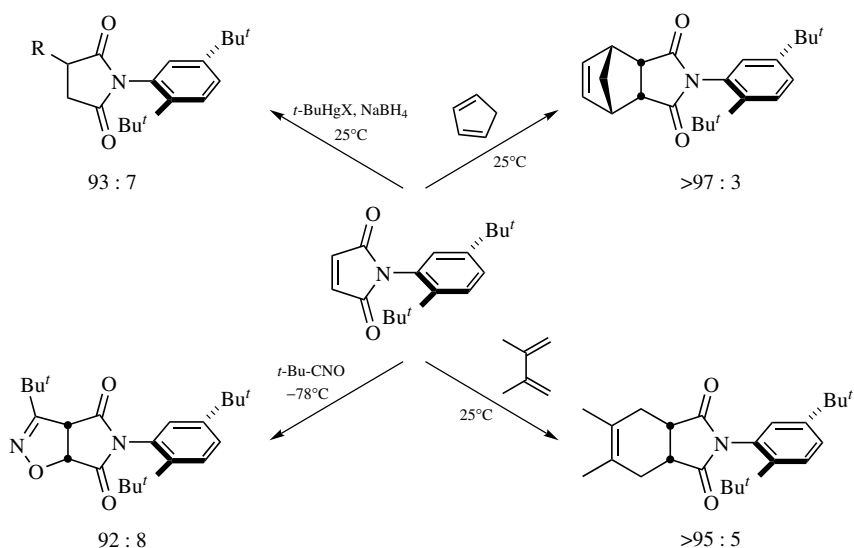
The stereoselectivity of radical–radical coupling reactions has been studied extensively.[7,36] A coupling reaction between chiral C2-symmetric nitroxide and a series of stabilized secondary prochiral radicals has been studied to reveal the factors determining stereoselectivity during the radical-radical coupling.[37] Both steric and electronic perturbations on the selectivity by the substituents of the radicals were pointed out. Highly stereoselective C—C bond formation via photolytically generated biradicals is also known to occur.[38] It has been revealed that both singlet and triplet biradicals can react with high stereoselectivity, but the outcome of the

reactions depends on the multiplicity of the biradical. It was demonstrated that the stereoselective intramolecular C—C bond formation of a biradical is governed by asymmetric induction if the reaction occurs via a triplet biradical, and by a memory effect if triplet biradicals are not intermediates in the pathway leading to the reaction products.[39]

Turro and co-workers[40,41] reported control of the lifetime of radicals using supramolecular steric effects to render reactive radicals persistent. The fate of diphenylmethyl radicals produced from photolysis of tetraphenylacetone depends on the circumstances in which they are formed. Radicals that are sucked into a hole of zeolite diffuse into the internal surface and persist, whereas radicals on the surface move away to encounter other radicals and react. The change in the reactivity of radicals under physical control is important for the design of radical reactions, including radical polymerization, although there has only been few examples of successful control except for solid-state polymerizations such as inclusion and topochemical polymerizations.

An excellent book on the topic of radicals and the radical reactions used in organic syntheses has been published.[8] It contains significant amounts of information relevant to radical polymerization that have the potential of being utilized for developments of new types of controlled radical polymerization.

13.3   STEREOCHEMICAL CONTROL IN RADICAL POLYMERIZATION OF VARIOUS MONOMERS

13.3.1   Stereochemical Structures of Vinyl and Diene Polymers

Figure 13.3a shows the structure of isotactic, syndiotactic, and heterotactic polymers as the most typical stereoregular polymers obtained from ordinary head-to-tail propagation of vinyl monomers, namely, monosubstituted ethylenes. Isotactic polymers have all the substituents on the same side of the chain; that is, the asymmetric carbon centers in the main chain have the same sign of the absolute configuration. In the case of syndiotactic polymers, the carbons with both configurations appear alternatingly along the polymer chains.

The stereochemical relationship between two successive repeating units is represented by the terms *meso* (*m*) and *racemo* (*r*) for isotactic and syndiotactic diads, respectively. In some textbooks and literature, the term *racemic* is used instead of *racemo*, although the latter is recommended by the IUPAC commission on Macromolecular Nomenclature of Macromolecular Division.[42] Nonuniform and various styles of classification and notation for stereospecific polymers are seen in the literatures. Some excellent textbooks will help us correctly understand the stereochemistry of polymers.[43–47]

An isotactic polymer contains only successive meso-diads in the chain, and a syndiotactic polymer only racemo-diads. Heterotactic polymer has a highly regulated repeating structure, in which *meso* and *racemo* diads appear alternatingly along the chain. There are few examples of actual heterotactic stereoregular polymer

(a)

isotactic

syndiotactic

heterotactic

(b)

erythro-diisotactic

meso-diisotactic

threo-diisotactic

racemo-diisotactic

disyndiotactic

disyndiotactic
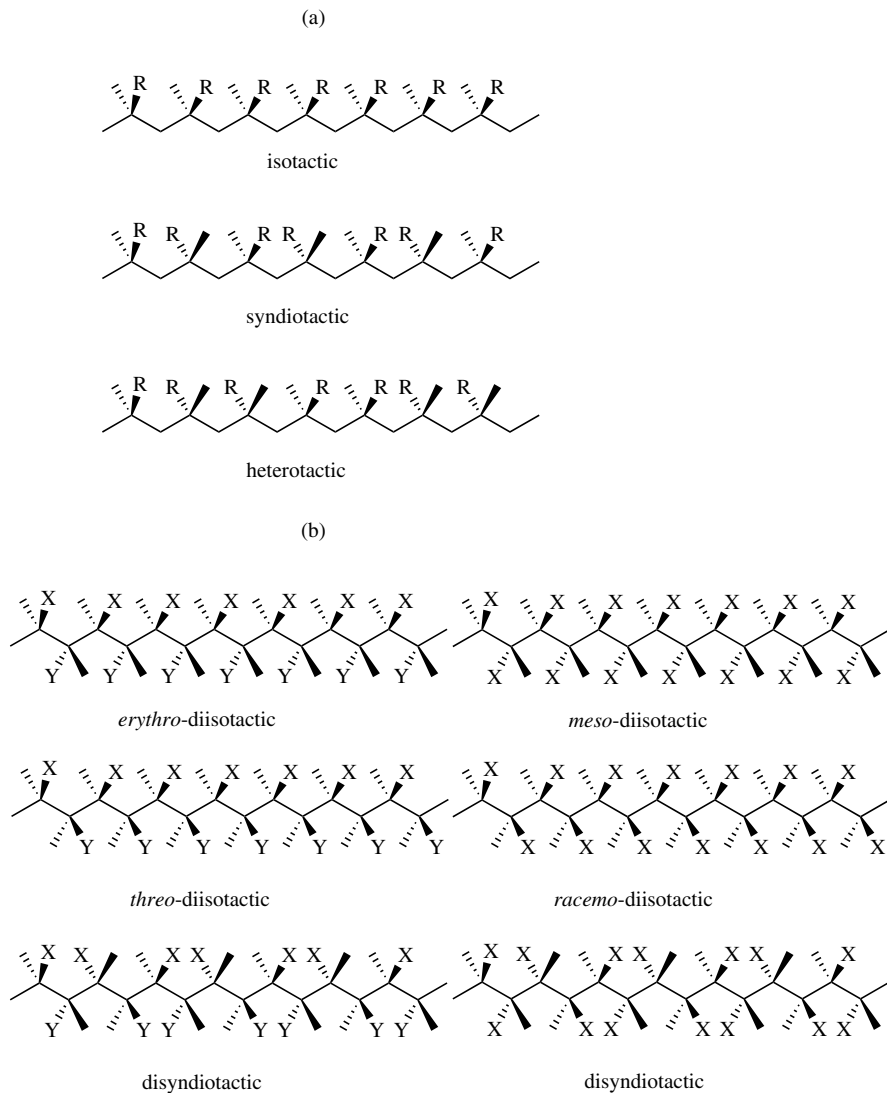
Figure 13.3   Structure of stereoregular polymers obtained from monosubstituted (a) and 1,2-disubstituted (b) ethylenes.

synthesis, except for some polymerizations under limited conditions such as anionic polymerization of methacrylates initiated by alkyl magnesium bromide combined with an alkylammonium,[48] and the alternating radical copolymerization of methyl methacrylate (MMA) with styrene in the presence of BCl_3 (see Section 13.3.2.3). Stereoregular polymers from 1,1-disubstituted ethylenes with different substituents, i.e., $CH_2=CXY$ type monomers are classified similarly.

Acyclic *cis-* or *trans*-1,2-disubstituted ethylenes (vinylene type monomers, CHX=CHY) give three kinds of stereoregular polymers; *erythro*-diisotactic, *threo*-diisotactic, and disyndiotactic polymers, as shown in Fig. 13.3b. Three types of stereoregular polymers are also obtained when the two substituents on the double bond are the same (CHX=CHX); *meso*-diisotactic, *racemo*-diisotactic, and disyndiotactic polymer. In the latter case, the stereochemistry of the polymers can also be considered on the basis of a methylene repeat unit, because each carbon atom in the main chain has the same substituent.

Two stereochemical configurations exist at the vicinal carbon atoms, meso and racemo diads as shown in Fig. 13.4, and these are represented by two kinds of projections, Fischer and planar zigzag. In the planar zigzag representation, two substituents on consecutive methylene units are located on different sides of each other when the configuration is meso. This is opposite to the case of a vinyl polymer. In the polymerization of 1,2-disubstituted ethylenes, two pseudoasymmetric centers are generated simultaneously in each propagation step. A more detailed description of the stereochemistry of substituted polymethylenes from 1,2-disubstituted ethylenes can be found in section 13.3.4. Cyclic 1,2-disubstituted ethylenes such as maleic anhydride and maleimide can give two kinds of diisotactic and two kinds of disyndiotactic polymers due to the diminished symmetry of the polymer chain structure, in contrast to the case of acyclic monomers described above.

The polymerization of diene monomers results in polymers of more complicated stereochemistry (Fig. 13.5).[46] The polymerization of butadiene may result in three kinds of configurations: 1,2-, *cis*-1,4-, and *trans*-1,4-polymers. The stereochemical structure of 1,4-polymers produced from 1,4-disubstituted butadienes is represented

(a)

meso   *racemo*

(b)

meso   *racemo*
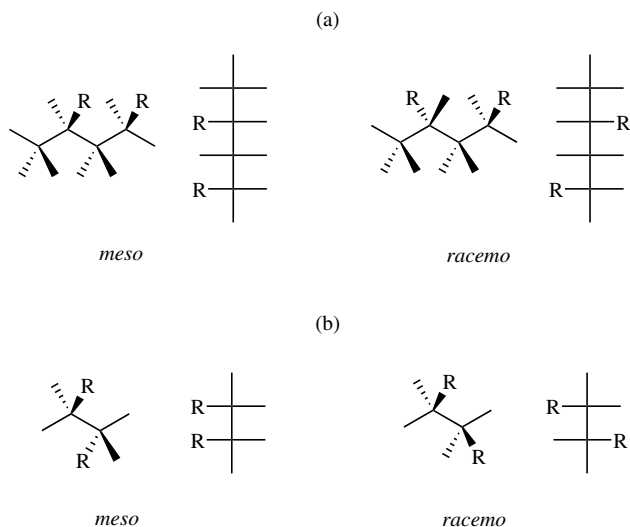
Figure 13.4 Fischer and planar zigzag projections of *meso* and *racemo* diads for poly(monosubstituted ethylene) (a) and poly(1,2-disubstituted ethylene) (b).
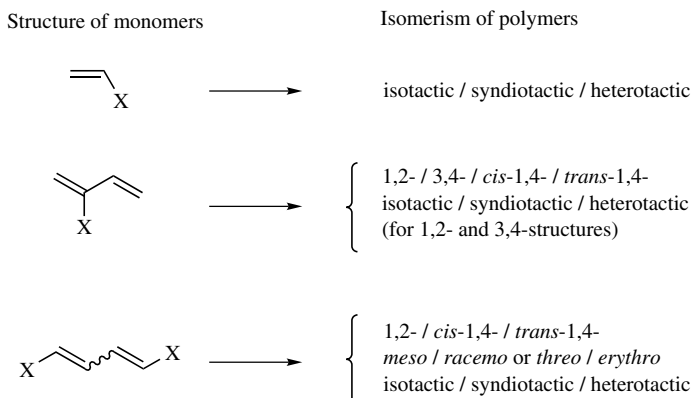
Figure 13.5   Stereochemistry of polymers obtained by polymerization of vinyl, 1,3-diene, and 1,4-disubstituted 1,3-diene monomers.

not only with cis-trans isomerism but also with isotactic-syndiotactic and erythro-threo (or meso-racemo) relationships. These polymers are referred to as *tritactic polymers* because of the presence of three elements of stereoisomerism for each monomer unit, namely, two pseudoasymmetric carbon centers and a double bond.

There are four possible stereoregular structures for *trans*-1,4-polymers of 1,4-disubstituted butadienes, and these are classified according to whether they originate from symmetric and asymmetric monomers (Fig. 13.6). The stereochemistry of these polymers is represented by two kinds of relationships, one of which is the relative configuration between the two repeating monomer units. When the configuration of all the carbons with the same substituents is identical; that is, all the repeating relationships are meso, and the polymer is diisotactic. When they are racemo, it is disyndiotactic. The other relationship is the relative configuration between the vicinal carbon centers, also represented the terms meso and racemo for a symmetric structure, and by erythro and threo for an asymmetric structure.

It is generally difficult to control the stereochemical structure of diene polymers during radical polymerization in solution. Effective control can, however, be achieved in the case of inclusion and topochemical polymerizations in the solid state (see Section 13.4.5).

13.3.2   Stereospecific Polymerization of (Meth)acrylic Monomers

13.3.2.1   Isotactic Polymerization of Triarylmethyl Methacrylates   Stereospecific polymerization of MMA and the other methacrylic esters has been intensively investigated since the first preparation of stereoregular poly(MMA) by anionic polymerization was reported in 1958.[49] Anionic and coordination polymerizations using organometallic compounds such as alkyllithiums, alkylmagnesium, and
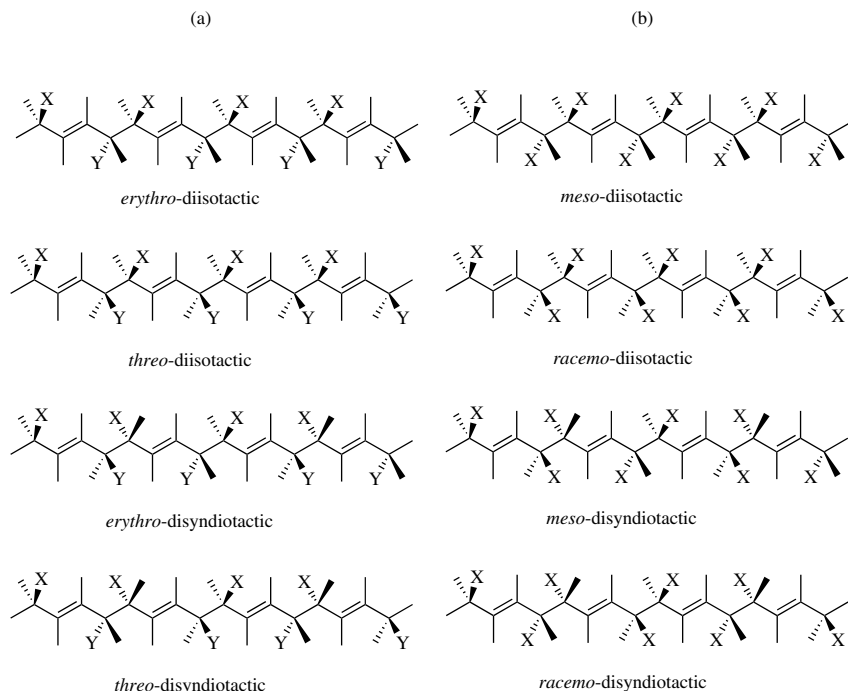
Figure 13.6 Stereoregular 1,4-*trans*-diene polymers obtained from 1,4-disubstituted 1,3-butadiene from symmetric (a) and asymmetric (b) monomers.

alkylaluminum compounds result in well-controlled stereoregular polymethacrylates (highly isotactic, syndiotactic, and heterotactic polymers[48,50]). Mainly syndiotactic polymer is obtained by radical polymerization due to the repulsion between the substituents of the propagating chain ends and less-controlled free propagation. The sequence distribution of the tacticity of poly(MMA) prepared by radical polymerization is approximately Bernoullian. Careful and precise analyses of NMR spectra have confirmed a fit of the experimental data based on the triad, pentad, and heptad sequences to a first-order Markov model with a slight deviation from Bernoullian statistics.[51,52]

It was found in the 1970s that radical polymerization of certain methacrylic esters containing aromatic groups results in polymer with different tacticity from that of poly(MMA) (Table 13.1).[49,53] The radical polymerization of triphenylmethyl methacrylate (TrMA) initiated with 2,2′-azobisisobutyronitrile (AIBN) in toluene at 60°C gave an isotactic polymer. In the earlier paper published in 1970,[54] it was reported that the polymer contained more than 60% isotactic triad. It has been considered that the observed large deviation from Bernoullian statistics is due to the bulkiness of the triphenylmethyl group preventing syndiotactic placements and favoring a helical conformation of the isotactic polymer chain.

TABLE 13.1   Triad Tacticity of Methacrylate Polymers Produced During Radical Polymerization

Ester Alkyl Group	Temperature (°C)	Tacticity		
		mm	*mr*	*rr*
Methyl	60	4	34	62
Ethyl	70	8	23	69
Isopropyl	70	7	31	62
n-Butyl	70	8	27	65
t-Butyl	70	8	40	52
1-Ethylpropyl	60	11	46	43
dl-Menthyl	60	13	47	40
Benzyl	60	7	37	56
1,1-Diphenylethyl	60	2	41	57
Triphenylmethyl	60	64	24	12
(±)-Phenyl-2-pyridyl-*o*-tolylmethyl	30	74	16	10
Diphenyl-4-pyridylmethyl	60	76	19	5
Diphenyl-2-pyridylmethyl	60	86	11	3
1-Phenyldibenzosuberyl	60	> 99	< 1	0

Sources: Refs. 49, 54–56.

It is interesting to note that the TrMA radical adds to MMA in a predominantly isotactic fashion, as evidenced by determination of the coisotactic parameters for cross-propagation in the radical copolymerization of TrMA with totally deuterated MMA.[57] The copolymer of MMA-d_8 (M_1) with a small amount of undeuterated TrMA (M_2) was converted into the copolymer of MMA-d_8 with undeuterated MMA by selective hydrolysis of TrMA units and subsequent methylation, followed by determination of the tacticity by NMR spectroscopy. Table 13.2 shows the

TABLE 13.2   Triad Tacticity and Coisotacticity Parameters for Copolymers of MMA-d_8 with Other Methacrylates [a]

Ester Alkyl Group of Methacrylate M_2	Tacticity [b]			Coisotactic Parameter		
	mm	*mr*	*rr*	σ_{12}	σ_{21}	σ_{22} [c]
Methyl (MMA)	4.4	33.2	62.4	0.20	0.22	0.21
Benzyl	3.9	34.3	61.7	0.14	0.28	0.25
Diphenylmethyl	5.2	36.0	58.8	0.19	0.27	0.23
Triphenylmethyl (TrMA)	6.3	62.0	31.7	0.10	0.65	0.75
Diphenyl-2-pyridylmethyl	7.7	62.6	29.7	0.11	0.66	0.92
(±)-Phenyl-2-pyridyl-*o*-tolylmethyl	6.7	65.2	28.1	0.10	0.69	0.84

[a] [MMA-d_8]/[M_2] = (96–97)/(3–4), with AIBN in toluene at 60°C.
[b] Tacticity of M_2-centered triad sequence.
[c] For homopolymers of M_2.

Source: Ref. 57.

triad tacticity and coisotactic parameters for the copolymers of MMA-d_8 with other methacrylates with a bulky ester alkyl group.

The coisotacticity parameters, σ_{12} and σ_{21}, were determined to be 0.10 and 0.65, respectively. Similar results have been obtained for the copolymers of MMA-d_8 with diphenyl-2-pyridylmethyl or phenyl-2-pyridyl-o-tolylmethyl methacrylate.

$$\overset{\sigma_{12}\qquad\sigma_{21}}{\underset{\underset{CO_2CD_3\quad CO_2R\quad CO_2CD_3}{|}}{\sim\!\!\sim\!\!\sim\!-CD_2-\overset{CD_3}{\underset{|}{\overset{|}{C}}}-CH_2-\overset{CH_3}{\underset{|}{\overset{|}{C}}}-CD_2-\overset{CD_3}{\underset{|}{\overset{|}{C}}}\sim\!\!\sim\!\!\sim}}$$

These results indicate that the propagating radical of the bulky methacrylate favors isotactic placement of the incoming small methacrylate monomer. Information obtained from ESR spectroscopy suggests that the isotactic placement may be controlled by the rigid conformation of the bulky methacrylate radical.[58,59]

Recently, remarkable effects of polymerization temperature and monomer concentration have been revealed by the reinvestigation of the isotactic polymerization of TrMA, giving polymers with triad tacticity ranging from 64 to 99%.[60] As shown in the results of the polymerization of TrMA in Table 13.3, a lower temperature and a higher monomer concentration results in a higher yield and a higher degree of polymerization, possibly due to the contribution of depolymerization during the propagation. Unexpected variation in tacticity depending on the conditions can be

TABLE 13.3 Isotactic Specificity for Radical Polymerization of Triarylmethyl Methacrylates Under Various Conditions [a]

Monomer	Temperature (°C)	[Monomer] (mol/L)	Yield (%)	DP	Tacticity		
					mm	*mr*	*rr*
TrMA	30	0.18	87.7	227	69.9	20.2	9.9
TrMA	40	0.18	60.7	130	81.7	13.4	4.9
TrMA	60	0.18	40.4	122	93.4	5.2	1.4
TrMA	70	0.18	3.3	102	98.1	1.6	0.3
TrMA	80	0.18	~0	—	—	—	—
TrMA	60	0.95	95.8	415	63.6	24.1	12.3
TrMA	60	0.34	69.7	244	82.6	13.1	4.3
TrMA	60	0.12	13.6	135	98.2	1.7	0.1
PDBSMA	60	0.17	75.9	337	99.9	0.1	~0
MMA	40	6.3	92.6	376	2.5	30.8	66.7
MMA	40	0.82	69.1	99	2.5	31.3	66.2
MMA	40	0.23	49.4	77	2.6	31.0	66.4

[a] *Key*: TrMA, triphenylmethyl methacrylate; PDBSMA, 1-phenyldibenzosuberyl methacrylate; MMA, methyl methacrylate; DP, degree of polymerization. *Polymerization conditions*: Solvent, toluene; [monomer]/[initiator] = 50; time, 6 h (70–80°C), 24 h (40–60°C), 144 h (30°C); initiator, AIBN at 60–80°C or (i-PrOCOO)$_2$ at 30–40°C.

Source: Ref. 60.

explained as follows. There are two types of helical propagating radicals having different conformations and different probabilities of meso addition. One of them is formed on monomer addition and is thermodynamically less stable. This radical will either propagate further with a lower probability of the meso addition than that of another, or be transformed into the other conformation by stereomutation (conformation change) at a rate comparable to that of propagation. The latter conformation results in highly isotactic propagation. At high temperature and low monomer concentration the reaction is mediated predominantly by the more stable growing radical under thermodynamic control, and under the reversed conditions predominantly by the less stable growing radical formed on monomer addition under kinetic control.

In the polymerization of 1-phenyldibenzosuberyl methacrylate (PDBSMA), designed after TrMA to improve the shortcoming of poly(TrMA) that the ester linkage is readily solvolyzed even by methanol, a highly isotactic polymer is produced independent of the conditions.[61] This is due to the rigid structure of the helical propagating radicals in the PDBSMA polymerization. Several triarylmethyl methacrylates containing a pyridyl group as the aromatic moiety also provide isotactic polymers, similarly to TrMA.[55,56,62]

TrMA   PDBSMA
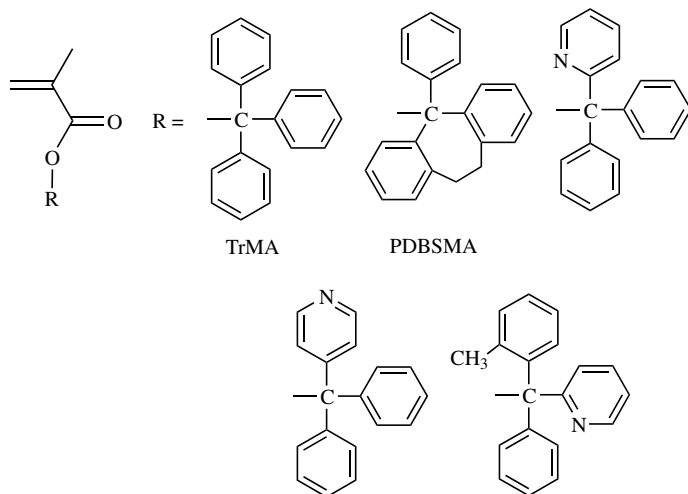
The triarylmethyl methacrylates give a one-handed helical polymer by asymmetric anionic polymerization with a chiral catalyst system.[62] PDBSMA also gives an almost perfectly isotactic polymer by radical polymerization, suggesting that the poly(PDBSMA) is an equimolar mixture of right- and left-handed helices. Radical polymerization of PDBSMA has been carried out under chiral reaction conditions based on the use of a chiral initiator, solvent, and chain transfer agent to synthesize an optically active, one-handed helical polymer. An excess of right- or left-handed helicity was confirmed as a result of the influence of the chiral materials. For example, the use of optically active chain transfer agents such as (+)- and (−)-neomethanethiol was effective in the control of helicity; the polymer showed a specific rotation of

$[\alpha]_{365}^{25} = -140°$. Fractionation by GPC provided a polymer with $[\alpha]_{365}^{25} = -750°$, which was estimated to be a ratio of (−)- and (+)-helices of 7 to 3, specifically 40% ee (enantiomeric excess). The mechanism of chiral induction involves helix-sense-selective primary radical termination and hydrogen transfer.[63] More recently, helix-sense-selective radical polymerization of PDBSMA using a cobalt(II) complex, as shown below, has been reported.[64] Several cobalt(II) complexes have been reported to act as efficient chain transfer agents during methacrylate polymerization, and to induce controlled/living radical polymerization of acrylates. The Co(II) radical may interact with the propagating radical and induce a single-handed helical structure. The polymerization proceeds with a different mechanism from typical catalytic chain transfer,[65] although the detailed mechanism of chiral induction is not clear. Another type of cobalt(II) complex has been reported to interact with the radicals more efficiently for stereocontrol during radical polymerization, giving poly(PDBSMA) with $[\alpha]_{365}^{25} = +1194°$. It has been proposed that the right- and left-handed helical radicals have different interactions or binding constants with the chiral cobalt complexes, leading to different propagation rates, specifically, different molecular weights of the helical polymers.
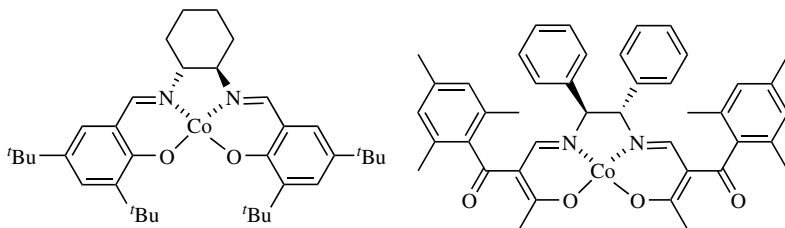
Asymmetry- and helicity-selective radical polymerization of PPyTMA has been examined, as well as anionic polymerization of the same monomer.[56] The introduction of a chiral moiety into PDBSMA was carried out in order to investigate a polymerization mechanism based on asymmetry and helicity selectivity.[66]
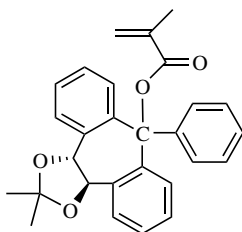
13.3.2.2 Chiral–Auxiliary Control   It has been considered that stereocontrol of acrylic derivatives during radical polymerization is difficult because of the absence of a bulky α-methyl group. Methyl acrylate gives atactic polymer regardless of the polymerization conditions (including temperature), whereas the syndiotacticity of poly(MMA) increases with decreasing temperature. Highly stereoregular poly-

TABLE 13.4   Diad Tacticity of Acrylate Polymers Produced During Radical Polymerization

| Ester Alkyl Group | Temperature (°C) | Tacticity | |
		m	*r*
Methyl	60	49	51
t-Butyl	60	46	54
Triphenylmethyl	40	49	51
Triphenylmethyl	30	45	55
1-Phenyldibenzosuberyl	40	44	56

Source: Refs. 67–69.

(MMA) can be obtained under optimized polymerization conditions in the presence of an appropriate solvent or additive. The polymerization of acrylates with a bulky ester alkyl group such as the triphenylmethyl and 1-phenyldibenzosuberyl group also yield atactic polymer (Table 13.4)[67–69] as opposed to the corresponding methacrylate polymerizations.

A cyclic α-substituted acrylic ester, α-methylene-γ-butylolactone, provides atactic polymer with a triad tacticity of *mm* : *mr* : *rr* = 14 : 44 : 42.[70] It has been reported that a racemic mixture of α-methylene-γ-methyl-γ-butylolactone provided a polymer with similar tacticity, whereas a highly isotactic polymer was produced in the polymerization of the optically active α-methylene-(*R*)-γ-methyl-γ-butylolactone.[71] This means that the microtacticity of the polymer is controlled by the chirality of the monomer. The rigid structure of the cyclic monomer may be important, because no effect of the chiral groups is observed for the polymerization of methacrylates.

In 1992, the first stereospecific radical polymerization of an acrylic monomer was reported by Porter et al.[72] They successfully achieved stereochemical control during the radical polymerization of acrylamide by introducing an oxazolidine chiral auxiliary group into the monomer.

R = *i*Pr, *t*Bu, Ph

meso propagation

X =

meso diad 92%
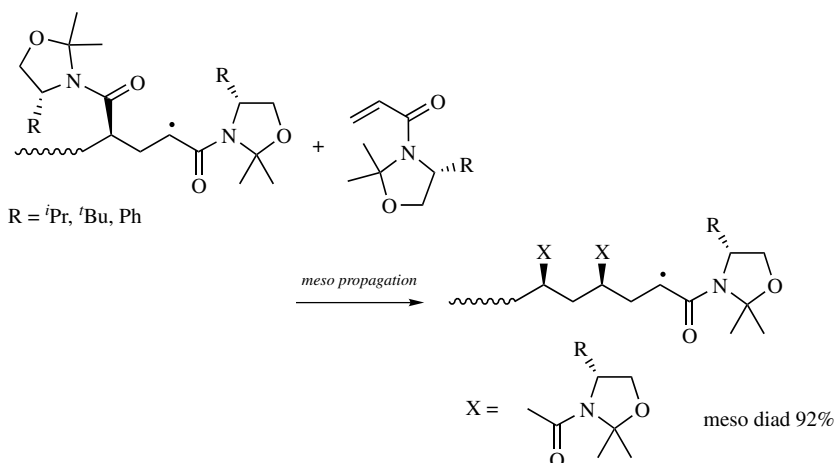
The control of stereochemistry imposed in each propagation step ensures that the configuration of each new stereogenic center is the same as all stereogenic centers in the polymer chain, giving a highly isotactic polymer. The stereogenic center is preferentially formed as the meso sequence rather than the racemo one. The obtained polyacrylamide was hydrolyzed to poly(acrylic acid) under selected conditions without detectable epimerization, and subsequently further derived to poly-(methyl acrylate) in quantitative yield. NMR analysis revealed that the polymers contained 88–92% meso diads. A stereoselectivity as high as 23 : 1 was obtained, which is substantially higher than what is observed for the reactions between small molecules, that is, the allyl transfer reaction from allyltributylstannane to radicals bearing a similar auxiliary (only 4 : 1 for the isopropyl substituent derived from (S)-valinol). Stereoselective telomerization using chain transfer agents resulting in oligomeric products with degrees of polymerization of 1–5 has also been reported.[73,74] One major diastereomer with the configuration shown below was observed for each telomer.
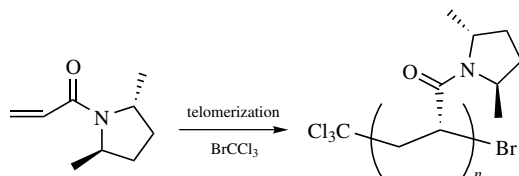
The acrylamide with the oxazolidine substituent was telomerized with different alkyl iodides and allyltributylstannane.[75]
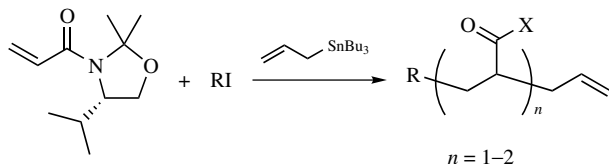
for n = 1 products
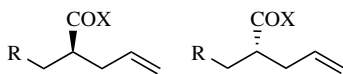
80 : 20 (R = neopentyl)

for n = 2 products
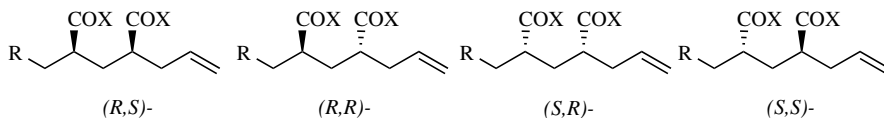
84 : 8 : 2 : 6 (R = neopentyl)

The analysis of the distribution of the $n = 2$ products shows a definite preference for *erythro* arrangements in addition to the stereocontrol provided by the auxiliary. The temperature dependence of the selectivity revealed that the stereochemistry is enthalpically controlled with little contribution from entropy for the addition of the second monomer to the $n = 1$ radical, that is, for the generation of the first stereo-center; $\Delta(\Delta H)^{\ddagger} = -7.4 \pm 0.4$ kJ/mol and $\Delta(\Delta S)^{\ddagger} = -0.9 \pm 1.3$ J K^{-1} mol^{-1}. In the cases where auxiliaries were sterically bulky, erythro preference for $n = 2$ products was observed. Four possible conformations of the major $n = 1$ radical are presented below.

threo ←

A   B   C   D   → *erythro*
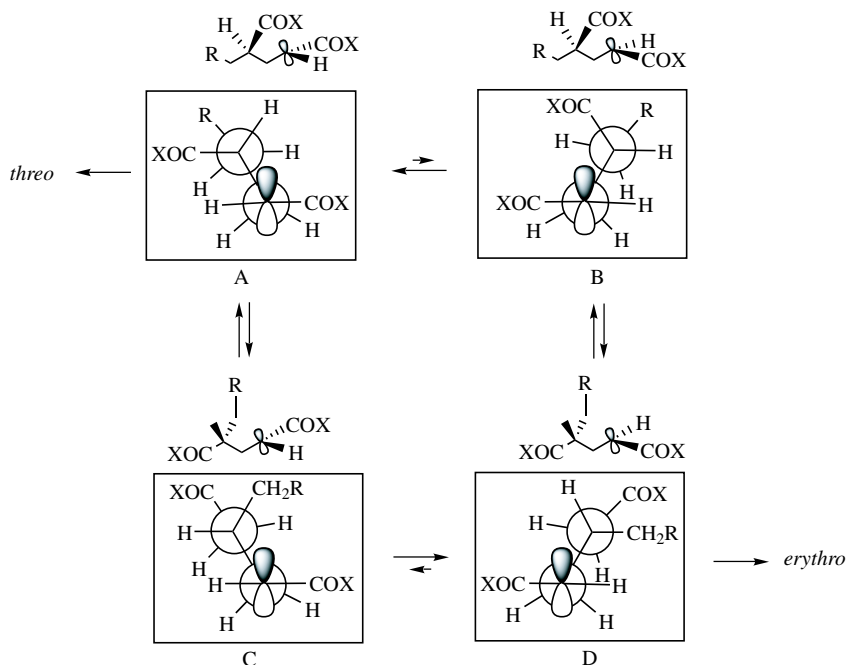
The orientation of the radical orbital is controlled by allylic strain and 1,3-steric interactions. The attack of the next monomer comes from the bottom face of the radicals because the top face is shielded by the penultimate group. The transition states for radical addition derived from the conformers A and D are energetically favored relative to those of B and C because of the 1,3-steric interactions. When the penultimate auxiliary (COX) possesses more steric bulk, as in the case of oxazolidine auxiliaries, the formation of the *erythro* product is enhanced.

Numerous attempts have been made to induce asymmetry in a polymer main chain during radical polymerization of an optically active monomer and copolymerization with other monomers. Beredjick et al.[76] reported the radical copolymerization of (S)-α-methylbenzyl methacrylate and maleic anhydride as the first example of asymmetric induction. Alternating radical copolymerization of vinyl monomers with 1,2-disubstituted ethylenes is useful for this purpose.[77] An optically

active copolymer ($[\alpha]_{435} = -2$ to $-16°$) was isolated after removing the auxiliary moiety from the copolymer of an optically-active styrene derivative with N-phenylmaleimide.[78]
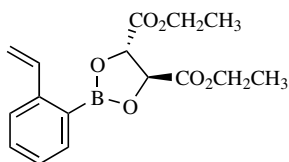
Radical cyclization polymerization of difunctional monomers has also been intensively investigated as it offers good means of controlling the stereochemistry of polymers including the chirality of asymmetric carbons in the main chain. Dimethacryl monomers with a chiral template gave poly(MMA) by hydrolysis and methylation after the polymerization.[79,80] The tacticity of the poly(MMA)s was determined to be $mm : mr : rr = 12 : 49 : 39$ and $mm : mr : rr = 14 : 51 : 33$ for the dimethacryl monomers with D-threitol and binaphtyl as the chiral templates, respectively. This is the same as the value of the tacticity for poly(MMA) derived from other nonchiral dimethacrylates. The poly(MMA) derived was optically active ($[\alpha]_{405} = -4.3°$),[79] indicating diastereoselective addition in the cyclization process during the polymerization.
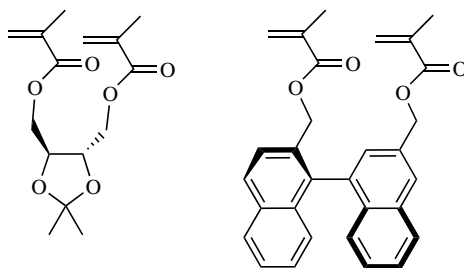
A dimethacrylate monomer with a following bulky substituent gave isotactic polymer ($mm = 86\%$) with a helical structure similar to the polymers from TrMA and PDBSMA.[81]
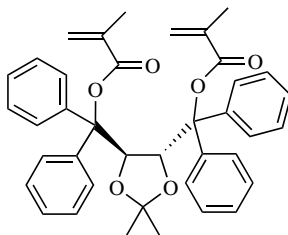
Stereochemical control of polymers from styrene derivatives using chiral templates has been reported to provide optically active polymers with high efficiency.[82–86]

When distyryl derivatives were copolymerized with MMA or styrene, asymmetry induction into the main chain of the copolymers was confirmed after removal of the chiral template in the side chains. It was pointed out that the periplanar conformation between the two styryl groups has the advantage of chirality induction as well as cyclization for the synthesis of an optically active polymer through the cyclopolymerization of these distyryl-type monomers with vinyl monomers. Asymmetric induction has also been reported for the radical cyclization polymerization of N-substituted methacrylamide derivatives in the presence of cyclodextrins and menthyl alcohol as the optically active compounds.[87,88]
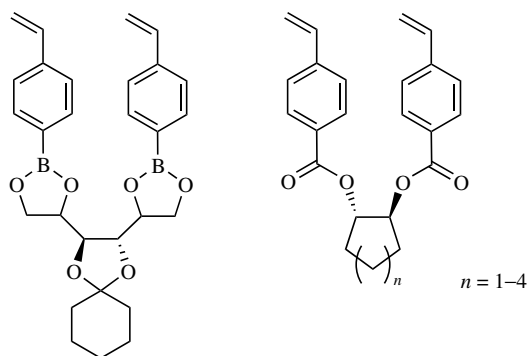
The template (matrix) polymerization of methacrylic derivatives has been investigated in the presence of optically active amines. The radical polymerization of sodium methacrylate initiated with potassium persulfate in the presence of chitosan acetate provided an isotactic-rich polymer (mm : mr : rr = 29 : 19 : 52) compared with that obtained from ordinary radical polymerization.[89] It was also reported that this polymer was optically active ($[\alpha]_{589}^{21} = +16.6°$), the sign of which was opposite to that of chitosan. The degree of polymerization and the molecular weight distribution of the polymers formed were identical to those of the chitosan used.[90–92] Polymerization of sorbic acid in the presence of chitosan has also been reported to give optically active polymer.[93] Nakano and Okamoto[94] carried out polymerizations of methacrylic acid in the presence of various kinds of amines. Polymer with microtacticity of mm : mr : rr = 16.3 : 48.8 : 34.9 was produced during the polymerization of methacrylic acid in chloroform in the presence of 0.5 equiv of (R,R)-1,2-diaminocyclohexane, to be compared with mm : mr : rr = 8.1 : 41.0 : 50.9 in the absence of the chiral amine. The hydrogen bonds between the acid and the amine and the interaction of the carboxylate and the ammonium are important for the increase in isotacticity. The formation of a highly syndiotactic polymer in the polymerization of methacrylic acid in 2-propanol at low temperature has also been reported.[95]

13.3.2.3 Control with Lewis Acids Complex formation of monomers with a Lewis acid often leads to an alteration of the polymerization reactivity.[96] In 1957, an increase in the polymerization rate and the degree of the polymerization was first reported during the polymerization of acrylonitrile in the presence of lithium

chloride as the Lewis acid.[97] Later, the accelerated propagation of MMA in the presence of zinc chloride was also reported,[98] as well as the effect on the stereoregularity in the 1960s.[99,100]

More recent extensive studies on the reactions of ester-substituted radicals of small molecules have further elucidated the effect of Lewis acids on the stereoselectivity (see Section 13.2). Inversion of the stereoselectivity was observed during reduction and allylation in the absence and in the presence of magnesium iodide. When the uncomplexed radical favors the allylic strain conformer, it is attacked from one side since the other face is shielded by a bulky substituent. The radical

Figure 13.7 Schematic models of *meso* and *racemo* addition during radical polymerization of MMA in the presence of monodentate and bidentate Lewis acids.[101]
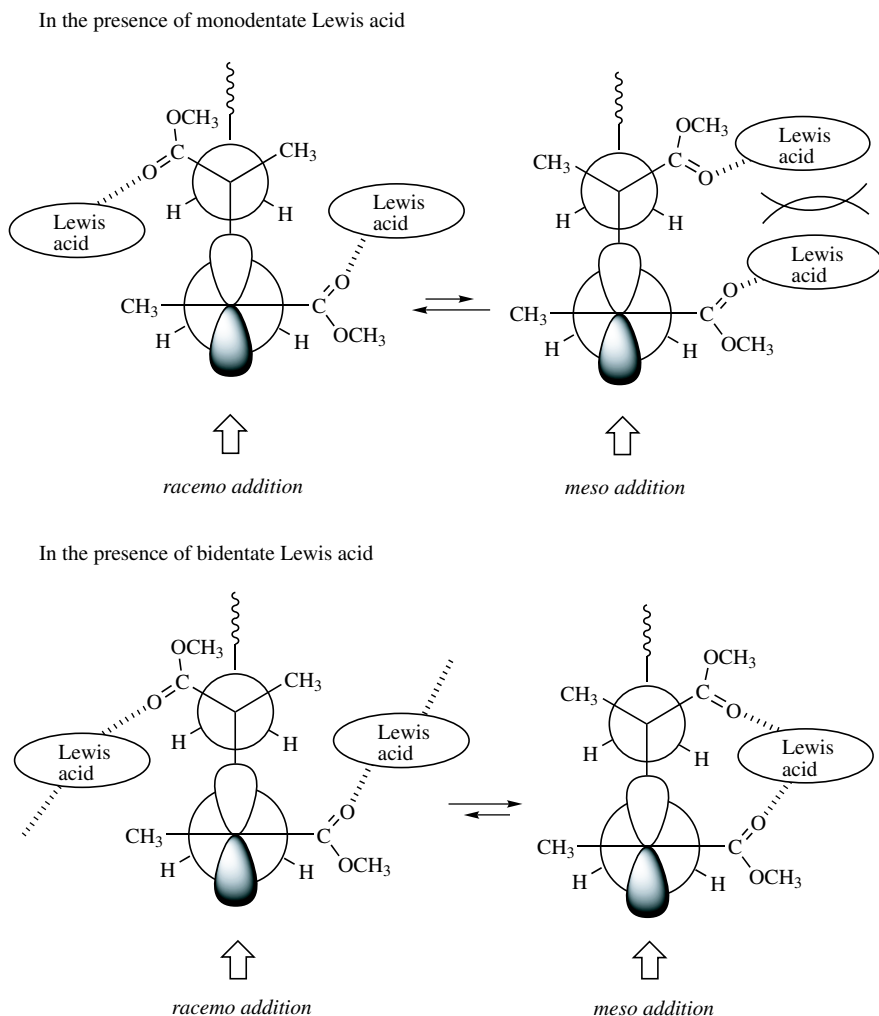
has a different conformation in the presence of magnesium iodide; the opposite face is shielded by chelate formation between the polar groups and the magnesium.

Matsumoto et al.[101] have revealed the features of magnesium bromide ($MgBr_2$) as the Lewis acid in the radical polymerization of MMA. It has been demonstrated that the addition of $MgBr_2$ to the polymerization system of MMA increases the polymerization reactivity as deduced from the yield and molecular weight of the resulting polymer. The probability of racemo addition decreased by the addition of the Lewis acid from the comparison of the microtacticity of the poly(MMA) produced from the polymerization in the presence and in the absence of $MgBr_2$. The biggest effect on the polymerization rate and the propagation manner was observed at the solid surface of the $MgBr_2$, which was partly soluble in the polymerization system, as a result of significant interaction between the Lewis acid, monomer and the propagating chain end. Other Lewis acids such as scandium trifluoromethanesulfonate ($Sc(OTf)_3$) and hafnium chloride also reduce the degree of syndiotacticity.[102]

Figure 13.7 shows schematic models of isotactic and syndiotactic propagation, namely, meso and racemo addition, during the radical polymerization of MMA in the presence of monodentate and bidentate Lewis acids.[101] When the Lewis acid interacts with the carbonyl groups as the monodentate ligand, racemo addition would be preferred because of the steric repulsion between the chain end and the penultimate unit group. On the other hand, if the Lewis acid acts as the bidentate ligand, meso propagation occurs more frequently.

The copolymerization of MMA with styrene in the presence of Lewis acids provides a highly alternating copolymer. It has been reported that a heterotactic alternating copolymer of MMA and styrene was obtained by using BCl_3 as the Lewis acid at a low temperature, for example, in toluene at $-95°C$ under UV irradiation with BCl_3 ($[BCl_3]/[MMA] = 2.0$).[103] The coisotacticity, coheterotacticity and cosyndiotacticity were 1, 89, and 10% for the MMA-centered triads, respectively, and 4, 85, and 11% for the styrene-centered triads, respectively. This is a rare example of a heterotactic polymer since heterotactic control during propagation is generally difficult, especially with a free-radical mechanism. The coisotactic parameters of two steps in the propagation process, one from the styrene unit to the MMA unit and the other from the MMA unit to the styrene unit, were experimentally determined by the use of deuterated monomers.[104] It was revealed that the step from the styrene unit to the MMA unit is highly syndiotactic ($\sigma_{12} = 0.09$) and that from the MMA unit to the styrene unit is highly isotactic ($\sigma_{21} = 0.85$), resulting in a polymer as shown below.
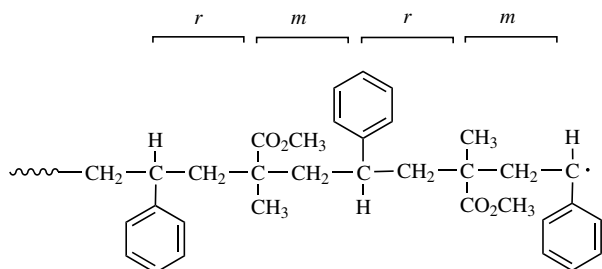
By Okamoto and co-workers realized that the polymerization of α-substituted acrylates such as benzyl α-(alkoxymethyl)acrylates in the presence of a Lewis acid results in stereochemical control.[105,106] The addition of a catalytic amount of zinc bromide resulted in the formation of syndiotactic polymer ($r = 71\%$), whereas the polymerization in the absence of Lewis acid provides atactic polymer ($r = 46\%$). Zinc trifluoromethanesulfonate, as opposed to zinc bromide, also provides atactic polymer ($r = 50\%$). Polymerization in the presence of a catalytic amount of scandium trifluoromethanesulfonate proceeds in an alternative manner to give isotactic polymer ($m = 69\%$) in a homogeneous polymerization system. They[107] also reported stereochemical control using MgBr$_2$ as the Lewis acid combined with aminoalcohols during the radical polymerization of α-alkoxyacrylates.

The polymerization of methacrylic esters with metal complexes has already been described in Section 13.3.2.1. Nakano et al.[64,108] used chiral cobalt complexes for asymmetric induction to the polymers of methacrylates and maleimides.

More recently, Okamoto et al.[109] succeeded in synthesizing isotactic polyacrylamides by radical polymerization by careful adjustment of the polymerization conditions, namely, Lewis acid, solvent, and temperature. Table 13.5 shows the results of the stereospecific radical polymerization of acrylamide, N-isopropylacrylamide, and N,N-dimethylacrylamide in the presence of Lewis acids. The temperature and nature of the solvent have only a slight influence on the tacticity during the polymerization of acrylamides in the absence of Lewis acids. In contrast, the isotactic content increases in the presence of Lewis acids and significantly depends on both the solvent and the temperature. During the polymerization of N-isopropylacrylamide in the presence of Y(OTf)$_3$ and Lu(OTf)$_3$, a higher meso content was obtained when using methanol as the solvent ($m = 80\text{–}92\%$). Similarly, isotactic polyacrylamide was obtained during polymerization in methanol at 0°C in the presence of Yb(OTf)$_3$. The isotactic-specific effect of Lewis acids has also been observed in the polymerization of N,N-dimethylacrylamide in methanol, which resulted in 84–88% meso contents at 60 and 0°C. A decrease in the isotacticity was however observed when the temperature was reduced to −78°C. Thus, efficient stereocontrol has been attained in the radical polymerization of acrylamide derivatives by the addition of a catalytic amount of Lewis acids, and the results are strongly dependent on both solvent and temperature.

TABLE 13.5 Stereospecific Radical Polymerization of *N*-Substituted Acrylamides in the Presence of Lewis Acids[a]

N-Substituent	Lewis acid (mol/L)	Solvent	Temperature (°C)	Time (h)	Yield (%)	Tacticity	
						m	r
CH(CH$_3$)$_2$	None	CHCl$_3$	60	3	65	45	55
	Yb(OTf)$_3$ (0.2)	CHCl$_3$	60	3	39	58	42
	Y(OTf)$_3$ (0.2)	CH$_3$OH	60	3	94	80	20
	Y(OTf)$_3$ (0.2)	H$_2$O	60	3	94	57	43
	Y(OTf)$_3$ (0.2)	DMSO	60	3	96	47	53
	None	CH$_3$OH	−20	24	61	44	56
	Y(OTf)$_3$ (0.2)	CH$_3$OH	−20	24	85	90	10
	Y(OTf)$_3$ (0.5)	CH$_3$OH	−20	24	72	92	8
	Lu(OTf)$_3$ (0.5)	CH$_3$OH	−20	24	62	92	8
	Y(OTf)$_3$ (0.2)	CH$_3$OH	−40	24	85	89	11
	Y(OTf)$_3$ (0.2)	CH$_3$OH	−78	24	98	80	20
H	None	CH$_3$OH	0	24	60	46	54
	Yb(OTf)$_3$ (0.1)	CH$_3$OH	0	24	50	80	20
	Y(OTf)$_3$ (0.1)	CH$_3$OH	0	24	91	75	25
(CH$_3$)$_2$	None	CH$_3$OH	60	24	73	46	54
	Yb(OTf)$_3$ (0.1)	CH$_3$OH	60	24	86	84	16
	Y(OTf)$_3$ (0.1)	CH$_3$OH	60	24	90	84	16
	Lu(OTf)$_3$ (0.1)	CH$_3$OH	60	24	85	85	15
	Yb(OTf)$_3$ (0.1)	CH$_3$OH	0	24	76	88	12
	Yb(OTf)$_3$ (0.1)	CH$_3$OH	−78	24	76	65	35

[a] [Monomer] = 1.0 or 2.4 mol/L, [AIBN] = 0.01–0.02 mol/L. UV irradiation at −20 and 0°C. In the presence of (*n*-Bu)$_3$B with air at −78°C.

Source: Ref. 109.

13.3.2.4 Solvent Effects on Stereochemistry

It is generally accepted that only weak solvent effects are present in neutral free-radical reactions, although the importance of solvent polarity and viscosity has been pointed out.[110–113] Solvent effects observed in the propagation step during radical polymerization have also been discussed. Since the early 1990s, intensive kinetic analysis of radical polymerization employing pulsed laser polymerization and ESR techniques has dramatically increased the amount of accurate and precise propagation rate coefficient data available. O'Driscoll et al.[114] reported that the value of the propagation rate coefficient increased with increasing benzyl alcohol content during homopolymerization and copolymerization of styrene and MMA based on results from pulsed laser polymerization experiments. They pointed out the possibility that benzyl alcohol forms a strong complex with the radical chain end of MMA and a weak complex with that of styrene. Zamitt et al.[115] further investigated the kinetics of homopolymerization of MMA and styrene in several solvents and detected

significant solvent effects. In some cases the enthalpic contribution was reported to suppress propagation, whereas in other cases the entropic contribution dominates resulting in an increase in the propagation rate coefficient. Beuermann et al.[116] investigated the propagation kinetics of methacrylic acid in several solvents. It is likely that significant solvent effects would be observed during the polymerization of a polar monomer having functional side groups such as a carbonyl moiety. ESR studies have also revealed solvent-dependent propagation rate coefficients during radical polymerization of several monomers.[117–119] However, no significant solvent effect on the stereochemistry has been reported except for the polymerization of methacrylic acid.[120]

More recently, stereocontrol during the radical polymerization of MMA in perfluoro-*tert*-butanol (PFTB) was reported. The use of PFTB as the solvent resulted in a significantly higher degree of syndiotacticity compared with other alcohols such as ethanol and trifluoroethanol (Table 13.6). Polymerization in PFTB at $-78°C$ provided a polymer with a triad syndiotacticity of 91%.[121] The hydrogen bonding interaction between the carbonyl group of MMA and the hydroxyl group of the fluoroalcohol, namely, an electron pair donor–acceptor interaction, is important for the stereocontrol.[122]

13.3.3 Stereospecific Polymerization of Vinyl Ester Monomers

Poly(vinyl alcohol) (PVA), produced by radical polymerization of vinyl acetate (VAc) followed by hydrolysis of the polymer, is one of the commercially most important polymers. The physical properties of PVA depend on the stereoregularity, although in general radical polymerization of VAc results in the formation of atactic polymer. Therefore, the tacticity of the polymers from vinyl ethers has been investigated, including vinyl pivarate (VPi) and vinyl benzoate (VBz).[123–127] The hydrolysis of poly(VPi) has been reported to be more difficult than that of poly(VAc). However, Otsu et al.[128] revealed in 1988 that poly(VPi) is readily hydrolyzed in

TABLE 13.6   Stereospecific Radical Polymerization of MMA in Fluoro-Containing Solvents

Solvent	Temperature (°C)	Time (h)	Yield (%)	$M_n \times 10^4$	Tacticity		
					mm	*mr*	*rr*
Benzene	60	1	11	1.68	3.5	34.1	62.4
Toluene	60	3	31	4.18	3.2	33.3	63.5
CH_3OH	60	3	52	8.34	3.6	31.9	64.4
C_2H_5OH	60	1	12	2.94	3.1	33.4	63.5
CF_3CH_2OH	60	1	24	1.34	3.6	34.3	62.0
$(CF_3)_3COH$	50	5	60	9.19	1.7	27.3	71.0
$(CF_3)_3COH$	−78	552	>99	11.7	∼0	9.0	91.0

Sources: Refs. 121, 122.

tetrahydrofuran with potassium hydroxide. The use of tetrahydrofuran as solvent is important in order to obtain a quantitative and convenient hydrolysis process. Yamamoto et al.[129] have developed the synthesis of syndiotactic PVA using syndiotactic radical polymerization of VPi at low temperature with subsequent hydrolysis. More recently, Yamada et al.[130–133] reported that the use of fluoroalcohols as solvents affects the stereoregularity of the polymers obtained during radical polymerization of VAc, VPi, and VBz, giving polymers rich in syndiotacticity, heterotacticity, and isotacticity, respectively.
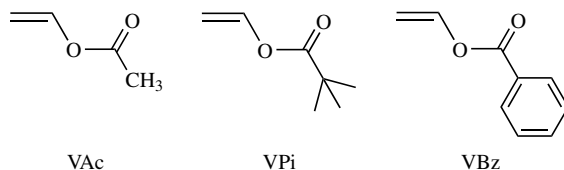
The results of the radical polymerization of vinyl esters are summarized in Table 13.7. The polymerization of VAc in PFTB resulted in higher syndiotacticity ($r = 62\%$), compared with bulk polymerization ($r = 53\%$). Polymer with a diad tacticity of 72% was obtained at a lower temperature. The steric hindrance between the repeating VAc units that interact with the bulky solvent by hydrogen bonding is very important. In contrast to the increase in syndiotactic content that is observed when VAc is polymerized in PFTB, polymerization of VPi in the same solvent gives a heterotactic rich polymer. The polymerization of VPi in PFTB at $-40°C$ resulted in a tacticity of $mm : mr : rr = 21.3 : 61.0 : 17.7$, whereas the bulk polymerization resulted in syndiotactic polymer ($mm : mr : rr = 14.2 : 49.2 : 36.6$). In the polymerization of VBz, fluorosolvents enhanced the isotacticity; for example, the mm value of the polymer obtained increased to 33% in the polymerization of VBz in

TABLE 13.7   Stereospecific Radical Polymerization of Vinyl Esters in Fluoro-Containing Solvents

Monomer[a]	Solvent	Temperature (°C)	Time (h)	Yield (%)	$M_n \times 10^{-4}$	Tacticity		
						mm	mr	rr
VAc	None	20	1	71	5.54	22.6	48.9	28.5
VAc	None	−78	600	8	7.35	22.5	48.8	28.7
VAc	CH₃OH	20	24	58	1.05	22.2	49.2	28.6
VAc	(CF₃)₃COH	20	24	94	6.15	13.0	49.4	37.6
VAc	(CF₃)₃COH	−78	168	50	8.30	5.4	44.9	49.8
VPi	(CF₃)₃COH	−40	24	83	4.17	21.3	61.0	17.7
VBz	(CF₃)₂CHOH	0	48	34	1.4	32.9	51.4	15.7

[a] Vac, vinyl acetate; VPi, vinyl pivarate; VBz, vinyl benzoate.

Sources: Refs. 131–133.

1,1,1,3,3,3-hexafluoro-2-propanol at 0°C. In this case, the stacking effects may contribute to the stereocontrol, in addition to the hydrogen bonding interaction. The stereochemistry of radical polymerization of vinyl esters in the presence of Lewis acids has also been investigated, but no significant effect of the Lewis acids has been observed.[134] Syndiotactic PVA exhibits superior thermal and mechanical properties. Syndiotactic-rich PVA ($rr = 50\%$) has a significantly higher glass transition temperature (269°C) than that of commercial atactic PVA (230–235°C).[131]

13.3.4   Stereochemistry in Polymerization of 1,2-Disubstituted Ethylenes

It has been generally accepted that 1,2-disubstituted ethylenes do not undergo radical homopolymerization because of steric hindrance of the substituents in the propagation step. Therefore, the stereochemistry of the polymers obtained from 1,2-disubstituted ethylenes has been discussed for limited polymers in relation to the propagation mechanism of ionic and coordination polymerizations.[135] Exceptions include polyhydroxymethylene derived from poly(vinylene carbonate) by hydrolysis,[136] polytetrafluoroethylene,[137,138] and alternating copolymers of maleic anhydride and maleimides with alkenes.[139,140] In 1981 Otsu and co-workers[141] began to investigate the stereochemistry of substituted polymethylenes using their finding that dialkyl fumarates (DRF) readily undergo free-radical polymerization.

$$\begin{array}{c} RO_2C \\ \diagdown\!\!=\!\!\diagup \\ CO_2R \end{array} \xrightarrow{\text{initiator}} \left(\!\!\begin{array}{c} CH \\ | \\ CO_2R \end{array}\!\!\right)_n$$

DRF
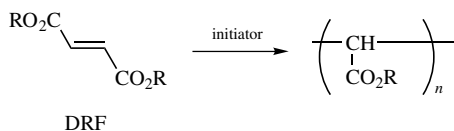
In radical polymerization of ordinary vinyl monomers, the direction of the monomer addition and the opening mode of the carbon-to-carbon double bond are not discriminated from each other. This is because the stereochemical relation of the penultimate unit at the propagating chain end is not determined until the addition of an attacking monomer to the propagating radical. In contrast, in the polymerization of 1,2-disubstituted ethylenes, the direction of the monomer addition governs the configuration of the two carbons, indicating that the determination of the tacticity of the substituted polymethylenes enables us to discuss the direction of the monomer addition and the opening mode independently.[142–145] This is an important feature of the polymer stereochemistry of 1,2-disubstituted ethylenes. In such a case, the Bernoullian probability of the formation of a meso diad is represented as P_m and P'_m, referring to the probabilities of meso addition and *meso* opening, respectively. Similarly, P_r and P'_r are the probabilities for a *racemo* diad. The tacticity of poly(DRF) should be considered on the basis of a methylene repeating unit, and it is dominated by both the opening mode and the direction of the monomer addition. In the radical polymerization of DRF, the opening of the double bond is restricted to the trans opening (meso opening). A high diastereoselectivity has also been reported in the reaction of small molecules having a similar structure, well accounted for by ESR observation and energy calculation of the conformation of the radical.[17]

Propagation of monosubstituted ethylenes
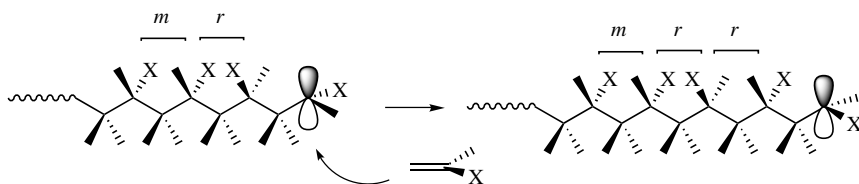
Propagation of 1,2-disubstituted ethylenes

$P'_m = 1 \ (P'_r = 0)$

$P_m \neq 1$

$a_\alpha = 20.46$ G, $a_\beta = 7.59$ G (ESR)

observed   calculated

$\theta = 18°$ $\theta = 20°$
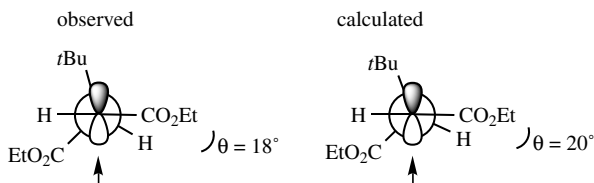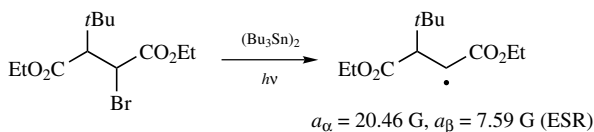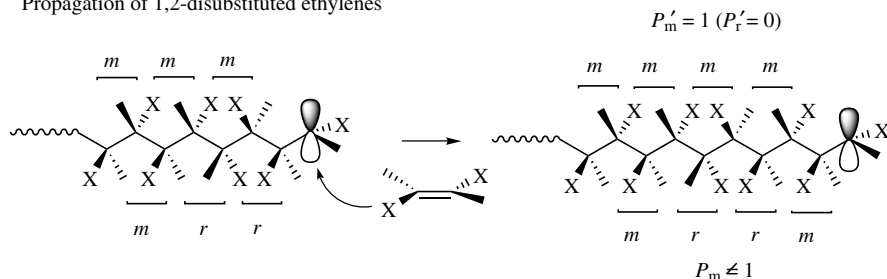
The tacticity of poly(DRF) is governed solely by the direction of addition, namely, by the probabilities of the meso and racemo additions, P_m and P_r, respectively. The P_m values have been determined to be 0.73, 0.57, 0.54, and 0.47 for the polymerization of the di-*tert*-butyl, methyl-*tert*-butyl, diisopropyl, and dimethyl esters, respectively.[143,144]

The propagation rate constant of DRF is significantly influenced by the manner of addition. The absolute rate constants for the *meso* and *racemo* additions (k_m and k_r, respectively) have been evaluated from the overall k_p and the values of P_m and P_r by use of the following equations:[146]

$$k_p = P_m k_m + P_r k_r$$

$$\frac{P_m}{P_r} = \frac{k_m}{k_r}$$

The value of k_m for the di-*tert*-butyl ester has thus been obtained as 0.74 L mol^{-1} s^{-1}, which is larger than for several other DRF; 0.054, 0.26, and 0.49 L mol^{-1} s^{-1} for dimethyl, methyl-*tert*-butyl, and diisopropyl derivatives, respectively. This suggests an energetic preference at the transition state of the meso propagation in the polymerization of di-*tert*-butyl ester on account of the particular conformation.
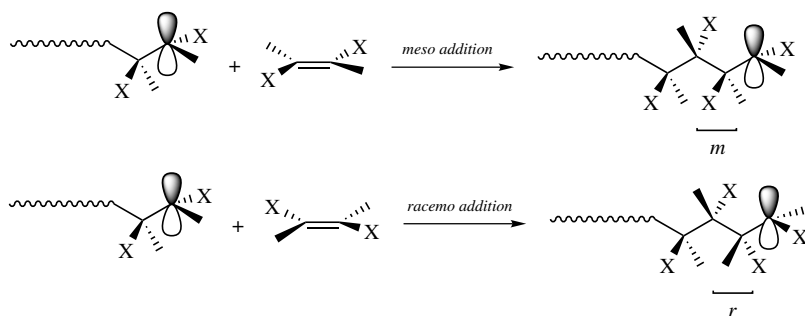
The P_m value decreased for the di-*tert*-butyl ester with an increase in the polymerization temperature; specifically, the $\Delta H_m^{\ddagger} - \Delta H_r^{\ddagger}$ value was negative (Table 13.8). The opposite tendency was observed for the diisopropyl and dimethyl esters. The tacticity of the polymer of methyl-*tert*-butyl ester was independent of the temperature.

The dissociation behavior of poly(fumaric acid) and poly(maleic acid) in solution has been revealed to depend on the structure of monomers as the precursor, that is, on the polymer tacticity.[147,148]

13.3.5 Stereochemistry of Polymers Obtained by Controlled/Living Radical Polymerization

The tacticity of polymers obtained by controlled/living radical polymerization of MMA has been investigated. The results indicate that the stereochemistry of polymers obtained by controlled/living radical polymerizations is the same as in conventional free-radical polymerization (Table 13.9). This is due to free-radical and successive (i.e., not coordinated and stepwise) propagation during controlled/living radical polymerization.[149–153] Similarly, the tacticity of polymers obtained by

TABLE 13.8 Differences in Activation Parameters for Meso and Racemo Additions in Radical Polymerization of Dialkyl Fumarates

Ester Alkyl Group	$\Delta H_m^{\ddagger} - \Delta H_r^{\ddagger}$ (kJ/mol)	$\Delta S_m^{\ddagger} - \Delta S_r^{\ddagger}$ (J mol^{-1} K^{-1})	$\Delta G_m^{\ddagger} - \Delta G_r^{\ddagger}$ at 60°C (kJ/mol)
Di-*tert*-butyl	−4.9	−6.4	−2.8
Methyl/*tert*-butyl	0	2.3	−0.77
Diisopropyl	0.6	3.2	−0.47
Dimethyl	2.6	6.5	0.43

TABLE 13.9   Tacticity of Poly(MMA) Prepared by Controlled/Living Radical Polymerization with Various Initiator and Catalyst Systems

Initiator and Catalyst System	Temperature (°C)	Tacticity		
		mm	*mr*	*rr*
$CH_3CHClPh/CuCl/bpy$	130	6	38	56
BPO	130	6	37	55
$CH_3CHBrCO_2Et/CuBr/bpy$	100	5	36	59
AIBN	100	6	34	60
CuBr/*N*-Alkyl-2-pyridylmethanimine	90	3.5	37.4	59.1
$CHCl_2COPh/RuCl_2(PPh_3)_3-Al(O\text{-}i\text{-}Pr)_3$	80	5	39	56
$CHCl_2COPh/RuH_2(PPh_3)_4-Al(O\text{-}i\text{-}Pr)_3$	80	5	37	58
$CHCl_2COPh/RuCl_2(PPh_3)_4$	80	4	37	59
$CCl_4/FeCl_2(PPh_3)_2$	80	5	37	58
$CH_3CBr(CO_2Et)_2/FeCl_2(PPh_3)_2$	80	4	38	58
$CHCl_2COPh/RuH_2(PPh_3)_4-Al(O\text{-}i\text{-}Pr)_3$	60	1	35	64
$CH_3CHBrCO_2Et/CuBr/bpy$	60	4	33	63
AIBN	60	3	35	62
CuBr/*N*-Alkyl-2-pyridylmethanimine	60	2.4	33.6	64.1
CuBr/*N*-Alkyl-2-pyridylmethanimine	40	2.8	34.4	62.8
$CHCl_2COPh/RuH_2(PPh_3)_4-Al(O\text{-}i\text{-}Pr)_3$	30	2	31	67
CuBr/*N*-Alkyl-2-pyridylmethanimine	15	1.5	28.6	70.0
CuBr/*N*-Alkyl-2-pyridylmethanimine	−15	1.8	26.7	71.5

Source: Refs. 149–153.

controlled/living radical polymerization of styrene and methyl-substituted derivatives using TEMPO has also been reported to be identical to that of conventional free-radical polymerization.[154,155]

Puts and Sogah[156] reported controlled/living radical polymerization with a chiral nitroxide, (*R,R*)-DDPO (see Fig. 13.8). They performed semiempirical calculations to draw a reaction coordinate diagram for dissociation and radical recombination of (*R,R*)-DDPO-styrene diastereomeric adducts.
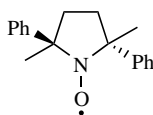
(*R,R*)-DDPO

The ground-state enthalpy ($\Delta H°$) for C—ON bond hydrolysis for DDPO-styrene adduct was found to be 118.5 kJ/mol for the (*R,R*)-*R* diastereomer and 112.9 kJ/ mol for the (*R,R*)-*S* diastereomer. The $\Delta H^{\ddagger}$ for dissociation of the diastereomeric DDPO-styryl adducts are approximately the same: 140.9 and 139.3 kJ/mol for (*R,R*)-*R* and (*R,R*)-*S* adducts, respectively. The corresponding $\Delta H^{\ddagger}$ values for the
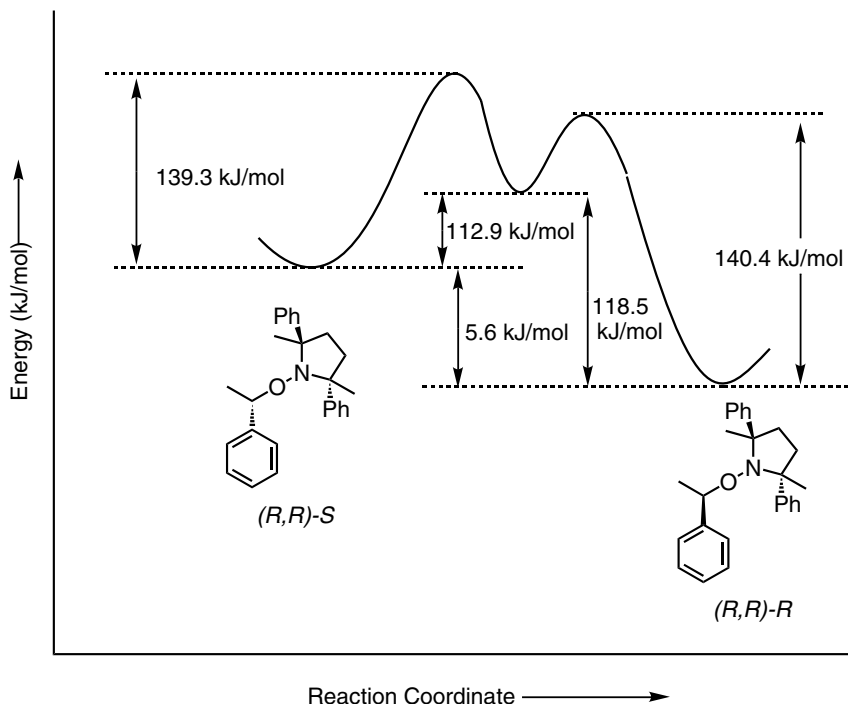
Figure 13.8   Reaction coordinate diagram for dissociation and radical recombination of (R,R)-DDPO-styrene diastereomeric adducts.[156]

reverse processes are 26.4 and 21.9 kJ/mol for the (R,R)-S and (R,R)-R diastereomers, respectively. They pointed out that the calculated $\Delta(\Delta H^{\ddagger})$ of 4.5 kJ/mol is equivalent to about a 6-fold difference in the rate at 25°C, while the rate difference will be 3- or 4-fold in favor of the (R,R)-R diastereomer at 130°C. This suggests that chiral DPPO may have an influence on the stereochemical outcome of the polymerization if the propagation step significantly involves insertion directly into the NO-styryl adduct, which would be favored by the more stable (R,R)-R diastereomer. However, any control of stereoinduction is not observed due to free propagation, not stepwise insertion of monomers to the propagation chain end during actual polymerization.
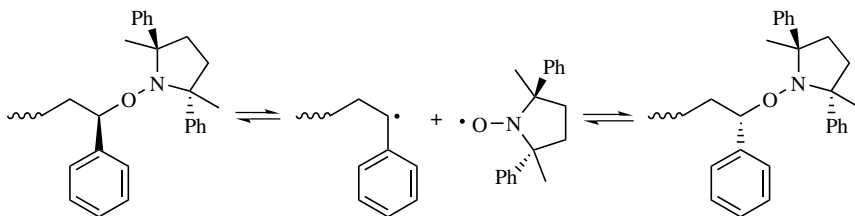
13.3.6 ESR Analysis of the Conformation of Propagating Chain Ends

The most important factor with regards to control of tacticity during radical polymerization is the conformation of the propagating chain end. Although several attempts have been made with ESR spectroscopy using different approaches to reveal a relationship between the chain-end conformation and the tacticity, this issue has not been fully clarified. This is due to the detection limit of the radicals and resolution of the obtained spectra under the polymerization conditions, as well as the complexity of the dynamic analysis of the results.

ESR spectroscopy has contributed to polymer research by revealing the structures and reactivity of polymer radicals. A large number of ESR spectra have been reported for the propagating radicals of vinyl and diene monomers during solid-state polymerization, solution polymerization by the flow method with redox initiators and the photolytic radical-generating technique, and bulk or solution polymerization using special cavities. Other examples include spectra recorded during radiation and photo- and mechanochemical degradations of polymers. The first observation of an ESR spectrum of a propagating radical was reported in 1951 for the X-ray irradiation of poly(MMA).[157] A survey of the ESR studies can be found in a book published in 1977 by Rånby and Rabek[158] and in reviews in 1987 by Kamachi[159] and 1999 by Yamada et al.[160]

A large number of ESR spectra of small enolate radicals have been reported in the literature. In particular, the 2-carboxylate-2-propyl radical having the simplest structure as the tertiary enolate radical has been most often investigated. It has been verified that this radical has a planar structure with spin delocalization since the *cis*- and *trans*-methyl groups to the carbonyl oxygen atom have been observed to be unequivalent by high-resolution ESR[161] and the µSR[162,163] experiments. Giese et al.[16] determined the coupling constant to the tertiary carbon to be 29.5 G in an experiment using a ^{13}C-enriched compound. The low value of the coupling constant supports the structure of the radical being planar. In the case of enolate radicals with a more complicated structure, the magnitude of the equivalent or unequivalent β-CH$_2$ couplings have been reported to depend on the structure of the substituents.[161,164–174] Typical examples are summarized in Table 13.10.

In the 1950–1970s, numerous workers reported independently the ESR spectra of polymethacrylate radicals, which were obtained by decomposition of the polymers or by polymerizations in the solid, namely, glassy or crystalline state and in solution. The conformation of the methacrylate radicals has been discussed relative to the splitting in the spectra, which were observed as a 5- or 9-line spectrum in many systems. In the earlier days, several workers considered that the 9-line spectrum consisted of the 5- and 4-line components.[175] Later, Harris et al.[176] reported the 9-line spectrum due to the two conformations observed for the photoinduced polymerization of methacrylates. Bresler et al.[177] observed in situ the ESR spectrum of the radical produced during bulk polymerization of MMA as a well-resolved 9-line spectrum by using a specially designed highly sensitive cavity, and they interpreted the spectra as an overlap of five lines with an intensity of 1 : 4 : 6 : 4 : 1 and four lines of 1 : 3 : 3 : 1.

TABLE 13.10   Coupling Constants for β Protons of Substituted Isobutyrate Radicals $XCH_2C \cdot (CH_3)CO_2R$ in the Literature

X	Coupling Constant (G)	Ref.
−H	21.3 (6H, CH_3)	164
−H	21.69 (3H, *trans*-CH_3), 21.44 (3H, *cis*-CH_3)	161
−OH	23.03 (3H, CH_3), 19.98 (2H, CH_2)	165,166
−OH	23.0 (3H, CH_3), 19.9 (2H, CH_2)	167
−OH	23.0 (3H, CH_3), 19.9 (2H, CH_2)	168
−CH_3	21.83 (3H, CH_3), 15.37 (2H, CH_2)	169
−CH_2OH	22.27 (3H, CH_3), 14.45 (2H, CH_2)	170
−CO_2CH_3	22.55 (3H, CH_3), 14.05 (2H, CH_2)	171
−CH_2CH_3	21.5 (3H, CH_3), 13.5 (2H, CH_2)	172
−$CH(OCOCH_3)CH_2OH$	22.4 (3H, CH_3), 15.5 (1H, CH_2), 9.5 (1H, CH_2)	167
−$C(CH_3)_2CO_2CH_3$	22.3 (3H, CH_3), 12.6 (1H, CH_2), 10.1 (1H, CH_2)	173
−$OC(CH_3)_3$	21.8 (3H, CH_3), 25.1 (1H, CH_2), ∼0 (1H, CH_2)	174
−CCl_3	23.57 (3H, CH_3), 11.17 (1H, CH_2)	188
−$C(CH_3)(CO_2CH_3)CH_2$−∿	22.46 (3H, CH_3), 13.75 (1H, CH_2), 11.04 (1H, CH_2)	180
−$C(CH_3)(CO_2CH_3)CH_2$−∿	23 (3H, CH_3), 12.5 (1H, CH_2), 10.6 (1H, CH_2)	181,182
−$C(CH_3)(CO_2CH_3)CH_2$−∿	22.2 (3H, CH_3), 14.7 (1H, CH_2), 7.5 (1H, CH_2)	183,184
−$C(CH_3)(CO_2CH_3)CH_2$−∿	22.19 (3H, CH_3), 14.18 (1H, CH_2), 9.27 (1H, CH_2)	185
−$C(CH_3)(CO_2R)CH_2$−∿	23 (3H, CH_3), 23 (1H, CH_2)	59

However, Symons[178,179] proposed as an alternative interpretation of the 9-line spectrum that two unequivalent protons of β-CH_2 resulted in the hyperfine coupling constants of 8.1 and 15.1 G, theoretically resulting in a 13-line. He argued that the 13 lines reduced to 9 lines in the observed spectrum due to broadening. In 1964, Fischer[180] observed a well-split 16-line spectrum of the polymer radicals of methacrylic acid at 320 K in aqueous solution by the flow method. He determined the coupling constants to the β-protons as follows: $a_1(\beta, CH_3, 3H) = 22.46$ G, $a_2(\beta, CH_2, 1H) = 13.75$ G, and $a_3(\beta, CH_2, 1H) = 11.04$ G. Similar coupling constants have been reported independently by other investigators, for example, $a_1 = 23$ G, $a_2 = 12.5$ G, and $a_3 = 10.6$ G by O'Donnell et al.;[181,182] $a_1 = 22.2$ G, $a_2 = 14.7$ G, and $a_3 = 7.5$ G by Sakai and Iwasaki;[183,184] and $a_1 = 22.19$ G, $a_2 = 14.18$ G, and $a_3 = 9.27$ G by Smith et al.[185] The extraordinary intensity distribution of the observed 9-line spectrum was accounted for by superposition of the spectra for two conformations of the radical, $\theta_1 = 75°$ and $\theta_2 = 45°$ and $\theta_1 = \theta_2 = 60°$ in Fig. 13.9.[186] Kamachi et al.[58,59] explained the temperature dependence of the
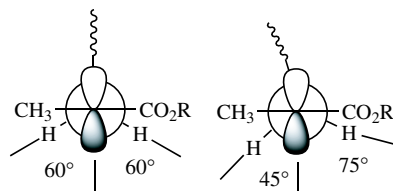
Figure 13.9   Stable conformations proposed in the literature for polymethacrylate radicals.

spectra of poly(TrMA) and other esters on the basis of two conformations: $\theta_1 = 75°$ and $\theta_2 = 45°$ for one conformation and $\theta_1 = 65°$ and $\theta_2 = 55°$ or $\theta_1 = \theta_2 = 60°$ for the other conformation. From that point onward, it has been widely accepted that the correct interpretation of the ESR spectrum of polymethacrylate radicals is that it is the result of the overlapping of a 5-line spectrum and a 9- or 13-line spectrum.

In 1996, Matsumoto et al.[187] reexamined the structure of the methacrylate radicals and obtained well-resolved ESR spectra for enolate radicals with well-defined structures over a wide range of molecular sizes ranging from small molecules to polymers, namely, adduct radicals, dimer radicals, and a trimer, as well as polymer radicals. They obtained well-resolved ESR spectra of various enolate radicals by the reduction of the corresponding bromides as the radical precursor in the presence of hexabutylditin under photoirradiation at 213–318 K. The polymer radicals were produced in the ESR tube during the radical polymerization of the corresponding
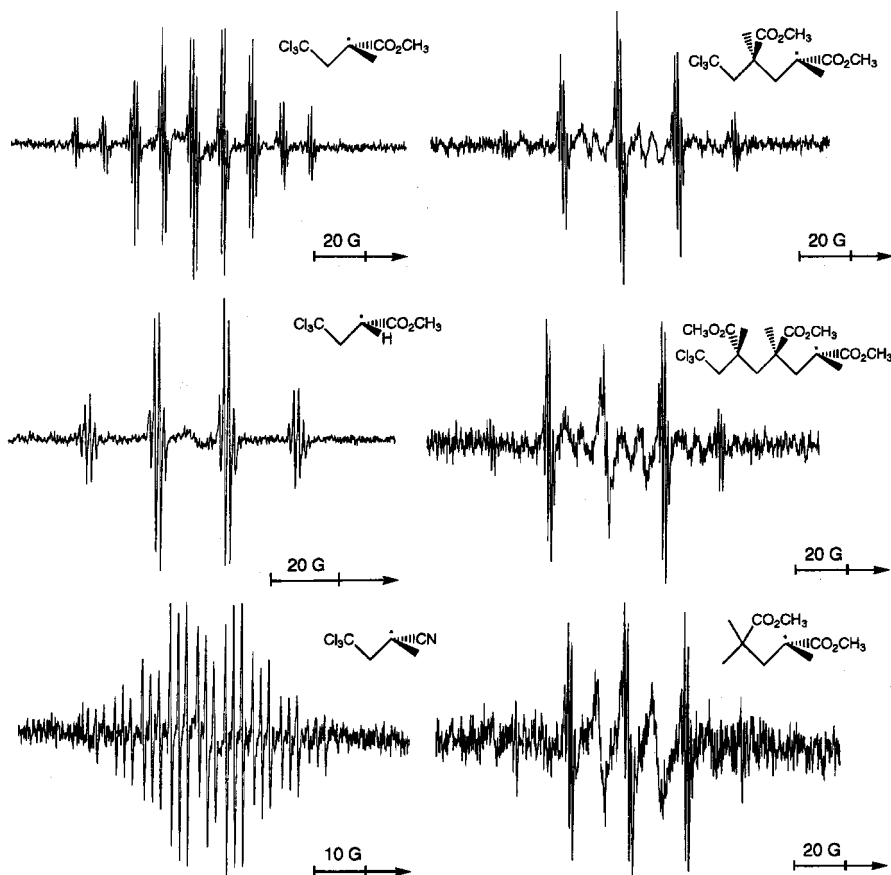
Figure 13.10 ESR spectra of the enolate radicals produced by the reduction of the corresponding bromides.[187]

methacrylate with an azo initiator at 373–393 K. Typical ESR spectra obtained are shown in Figs. 13.10–13.12.

Matsumoto et al. considered that the spectra consisted of the binary components of the radicals, and introduced the pyramidalization of the radical center in addition to the A-strain conformations to interpret the observed ESR coupling constants of methacrylate radicals. Recently, Spichty et al.[188] revealed certain dynamic phenomena of the enolate radical and consequently revised the assignment of the spectra by ESR simulations and quantum chemical calculations. Figure 13.13 shows the comparison of the simulated and experimental ESR spectra. Above 273 K, no dramatic changes in the ESR signal patterns are noticeable. A perfect match between the experimental and the simulated spectrum is obtained with the coupling constants
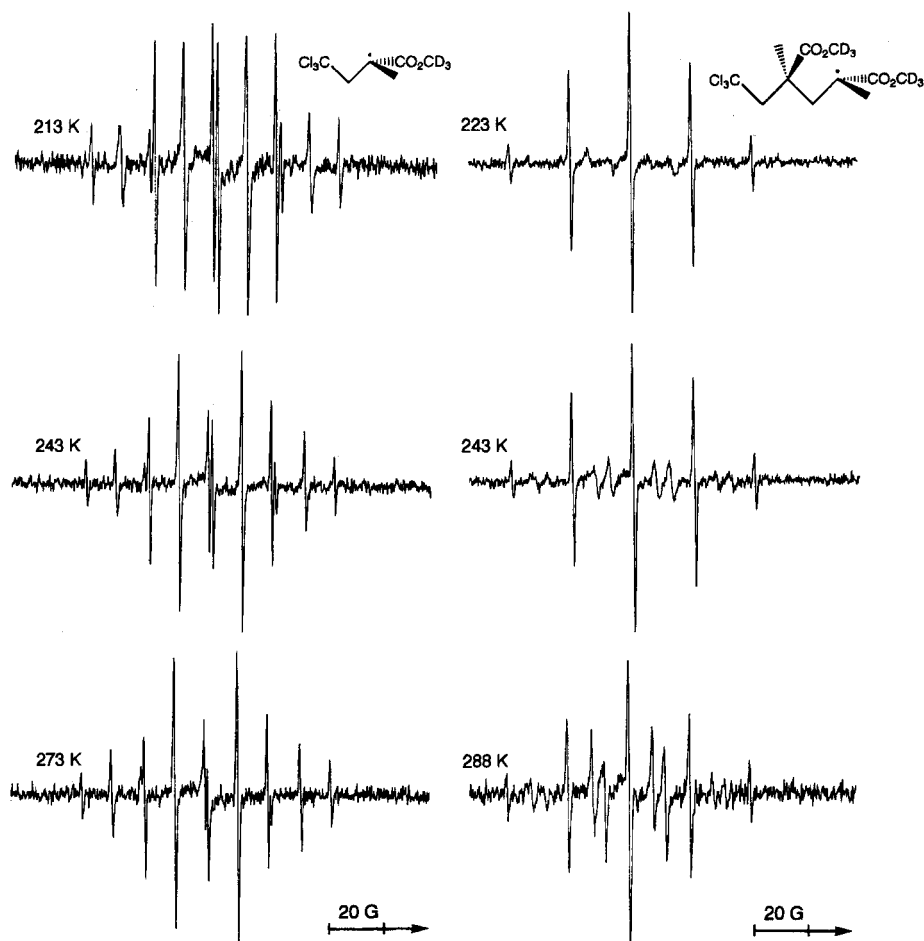
Figure 13.11   Temperature dependence of ESR spectra of the adduct and dimer radicals of methyl-d_3 methacrylate.[187]
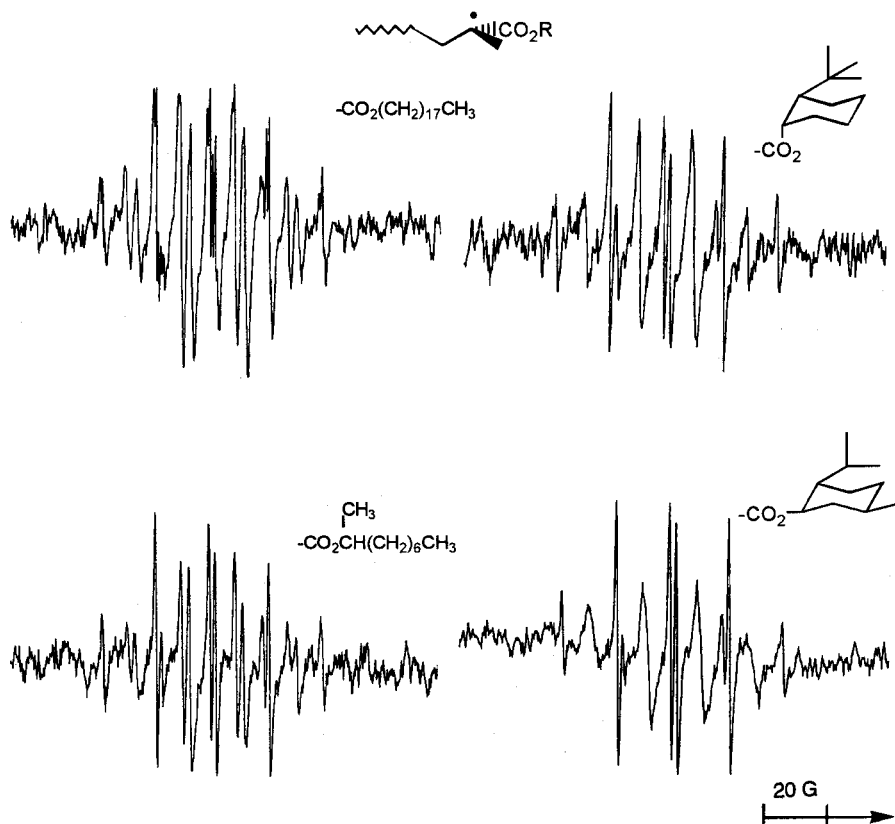
Figure 13.12 ESR spectra of the polymer radicals produced during the radical polymerization of methacrylates in *p*-xylene at 393 K.[187]

of 11.17 *G* attributable to two equivalent β-H and of 23.57 *G* of three equivalent α-CH$_3$ protons. Below 243 K, the central lines of the 1 : 2 : 1 pattern marked with an asterisk in Fig. 13.13 begin to broaden, resulting in unusual intensity ratios, while the outermost lines marked with a square remain constant. A dynamical phenomenon is the cause of the line width alteration in the ESR signals. The broadening of the signal in Fig. 13.13 is distinctive of a dynamical two-site exchange process.

It has been shown that density functional theory calculations with the hybrid functional B3LYP are able to give rather precise predictions for the minimum geometry of radicals together with the corresponding hyper fine coupling constants. Computations on the UB3LYP/6-31G* level revealed two isomers, *E*- and *Z*-isomers, for the adduct radical, as shown in Fig. 13.14. Figure 13.15 shows the energy profiles for the rotation along the CD$_3$OCOCH$_3$C$^{\bullet}$–CH$_2$CCl$_3$ bond in the *E*-isomer calculated on the UB3LYP/6-31G* level. The relative electronic energy is plotted versus the dihedral angle from 0 to 360°.
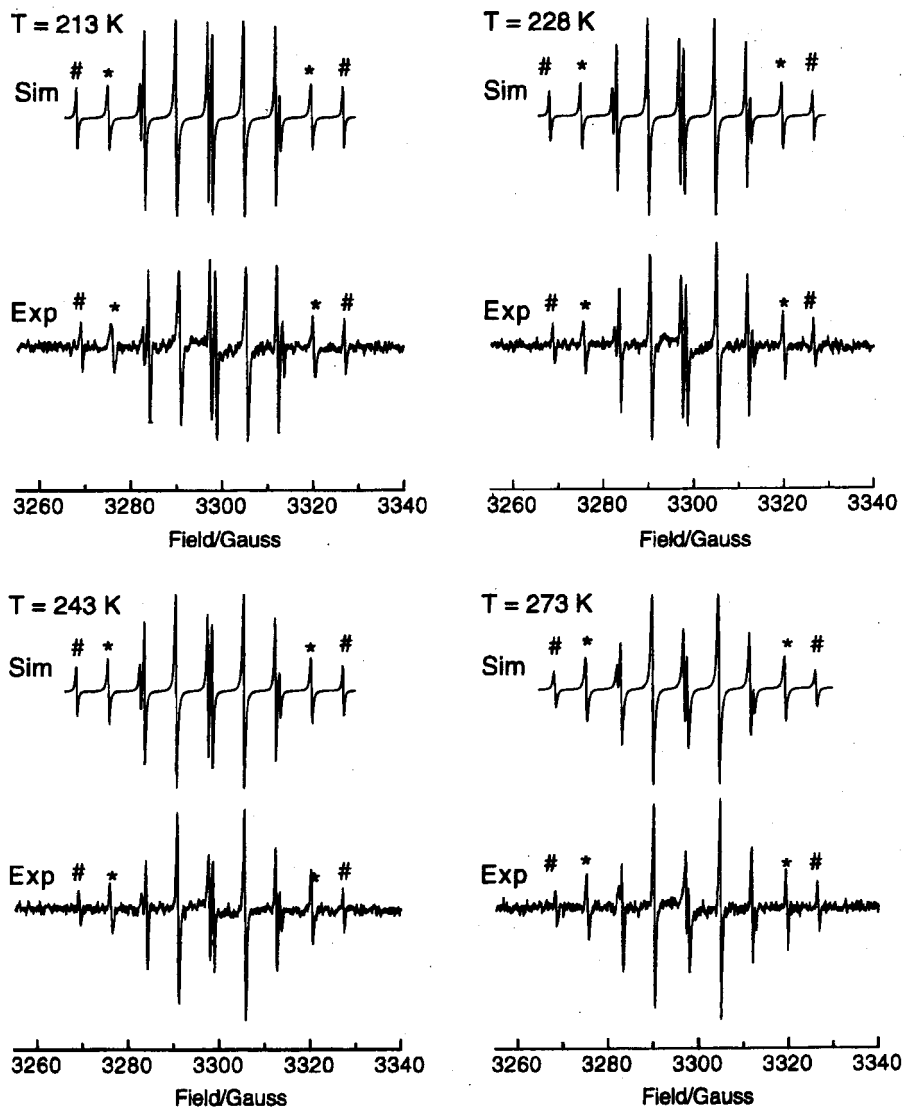
Figure 13.13 Observed and simulated ESR spectra of the adduct radical of methyl-d_3 methacrylate at 213–273 K.[188]

In both cases the radical center is planar. The calculations indicated that the *E*-isomer is more stable than the *Z*-isomer by only 1.4 kJ/mol. The calculated coupling constants for the minimum conformers of the *E*- and *Z*-isomers are summarized in Table 13.11. The calculated Boltzmann averaged coupling constants at 273 K are almost identical for both isomers and the value of 11.5–11.6 *G* is in
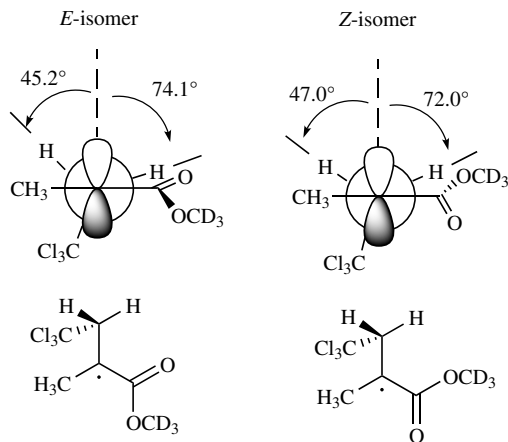
Figure 13.14 *E*- and *Z*-isomers of the adduct radical including dihedral angles of the UB3LYP/6-31G* optimized structures.[188]
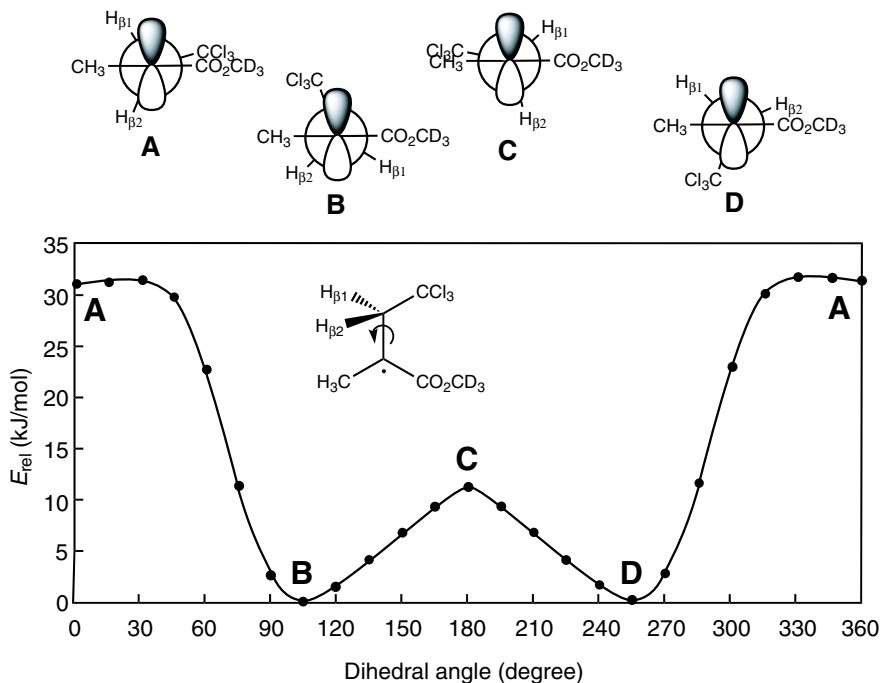
Figure 13.15 Energy profile for the rotation around the $CD_3OCOCH_3C\cdot-CH_2CCl_3$ bond in the *E*-isomer of the adduct radical.[188]

TABLE 13.11   Experimenatal and Calculated Coupling Constants for the Adduct Radical

Method	Temperature (K)	Isomer	$\alpha(\alpha\text{-CH}_3)$ (G)	$\alpha(\beta\text{-CH}_2)$ (G)
Experimental [a]	273	—	23.57	11.17
Calculation	0 [b]	E-Isomer	22.3	16.5 and 3.9
		Z-Isomer	22.1	15.3 and 4.6
	273 [c]	E-Isomer	22.3	16.5 and 3.9
		Z-Isomer	22.1	15.3 and 4.6

[a] Determined by simulation.
[b] For minimum geometry.
[c] Boltzmann distribution at 273 K.

Source: Ref. 188.

excellent agreement with the experimental counterpart of 11.2 G. Using the exchange frequencies established by the spectral simulations, the Arrhenius plot yielded an energy of 12.0 ± 1.8 kJ/mol, close to the calculated energy barrier of 11.0 and 9.7 kJ/mol for the E- and Z-isomers, respectively. Similar dynamic behavior has been observed for related radicals.[160,189,190]

The conformation of the radical directs the orientation of the incoming monomers and is also related to the penultimate unit effects in propagation.[160,191–193] The propagating radicals from 1,3-butadiene derivatives have been detected, and the coupling constants obtained by simulation reveal the direction of attack of the respective propagating radical to the monomer (Table 13.12).[194,195] The propagating radical attacks at position 1 of isoprene, as shown in the following scheme.

ESR spectroscopic studies focusing on several monomers other than methacrylate and diene monomers have also been carried out.[160,196–200]
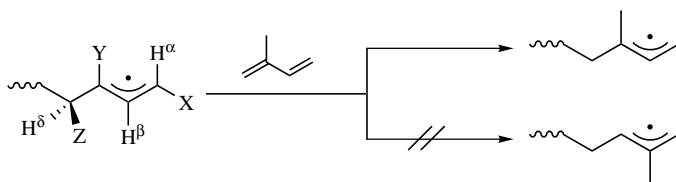
TABLE 13.12   Hyperfine Coupling Constants of Polymer Radicals from 1,3-Butadiene

Diene Monomer	$a(\alpha\text{-H})$ (G)	$a(X)$ (G)	$a(\beta\text{-H})$ (G)	$a(Y)$ (G)	$a(\delta\text{-H})$ (G)	$a(Z)$ (G)
1,3-Butadiene	16.5	14.61(H)	4.12	16.05(H)	13.50	13.53(H)
Isoprene	13.1	12.9(H)	4.3	12.9(CH_3)	14.2	11.7(H)
2-Methyl-1,3-pentadiene	15.0	12.5(CH_3)	3.1	12.5(CH_3)	16.0	15.0(H)
2,4-Hexadiene	13.0	9.5(CH_3)	3.0	13.0(H)	11.0	9.5(CH_3)

Source: Ref. 195.

13.4 STEREOCHEMICAL CONTROL DURING RADICAL POLYMERIZATION IN ORGANIZED MEDIA

13.4.1 Features of Polymerization in Organized Media

Organized and constrained reaction media have attracted much interest for controlled polymerization because of the great potential offered for the design of macromolecular architecture leading to advanced polymeric materials, including new organic materials and three-dimensional nano-composites.[9,201–203] Figure 13.16 shows a conceptual illustration of the control of the reactivity and the structure of the products in various organized polymerization media such as molecular crystals, inclusion compounds, liquid crystal, mono- and multilayers, and micelles.[201] These organized systems are classified into two groups: (1) polymerization in a vessel on the nanometer to micrometer scale and (2) polymerization of self-organized monomers such as molecular crystals. Each system exhibits different polymerization features and polymer structure. In the following sections, the features of polymerization in organized media are described not only from the viewpoint of stereocontrol of the
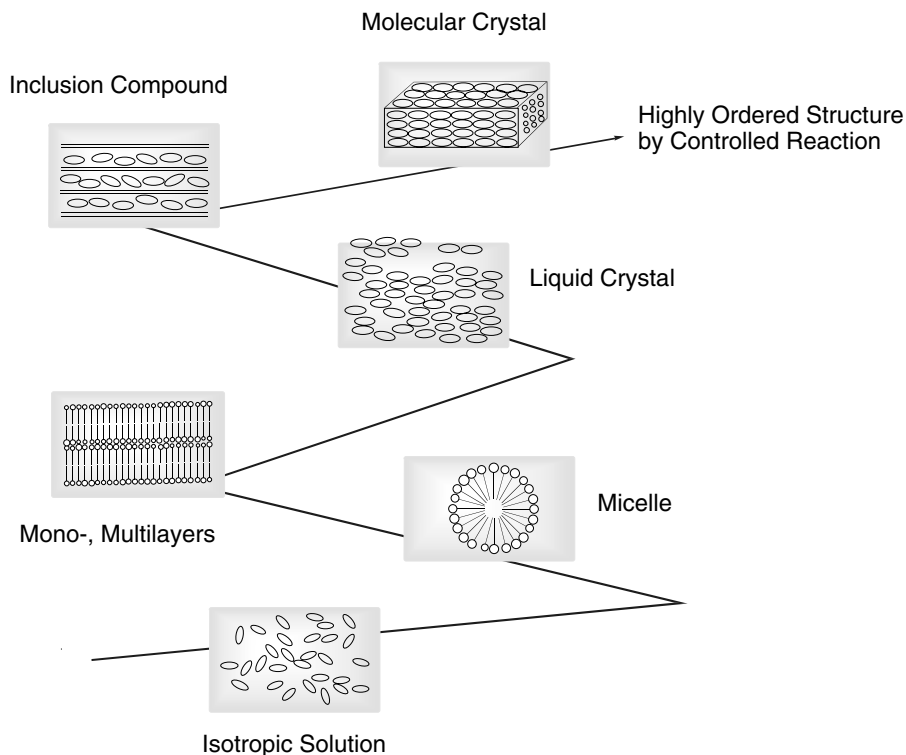
Figure 13.16   Various organized systems for the control of the polymerization reactivity and the structure of the product polymers.[201]

polymers but also considering control of the polymerization reactions and polymer architecture.

13.4.2   Polymerization in Micellar Systems

A micellar system consists of self-assembled amphiphilic molecules having both hydrophobic long alkyl chains and hydrophilic head groups in spherical shape with a diameter of several nanometers in water. Various types of monomers have been developed as polymerizable surfactants.[204] These include anionic, cationic, and nonionic surfactants that differ widely with regards to the position and structure of the polymerizable double bond, and require different conditions in terms of concentration and temperature for self-assembly to occur. Micelles are dynamic systems, in which surfactant molecules rapidly migrate between the inside and outside of micelles, and the exchange rate of surfactant molecules is greater than the propagation rate during polymerization in a micellar system. This suggests that control of the polymerization of reactive surfactants in separate micelles is difficult to achieve. For example, the degree of polymerization in a micelle is not the same as the number of aggregation in a micelle.

The most distinguished feature of radical polymerization in a micellar system, compared to isotropic solution polymerization, is the increased polymerization rate due to the condensation effect of monomer molecules. In extreme cases, spontaneous polymerization may even occur at room temperature in the absence of initiator.[205, 206]

The stereochemistry of polymers obtained in a micellar system has been investigated, but there have been few successful examples of stereochemical control. Dais et al.[207] reported the formation of syndiotactic polymer during the γ-ray radiation polymerization of dodecyl-2-methacryloyloxyethyldimethylammonium bromide at a monomer concentration above the critical micelle concentration at 25°C. Nagai et al.[208] concluded that the tacticity of the polymers from the same monomer in the presence of AIBN at 50°C was almost comparable to that of ordinary polymer formed under homogeneous conditions. Turro et al.[209] reported that poly(MMA) obtained by photoinitiated emulsion polymerization was more syndiotactic than that obtained in radical polymerization in solution under similar conditions. The tacticity was influenced by the application of a magnetic field.
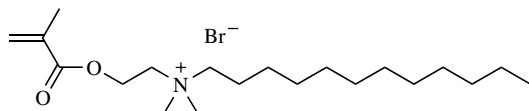
Percec et al.[210,211] reported radical polymerization of self-assembled dendritic monomers. The monomers aggregate at a concentration above 0.20 mol/L to form spherical micelles in benzene. In the interior of the aggregates, the polymerizable groups are concentrated and reacted by a free-radical initiator at a considerably accelerated rate. Polymer with a narrow molecular weight distribution is obtained, and the shape of the resulting polymer is a function of the degree of polymerization.

When the degree of polymerization is lower than 20, the polymer molecule remains spherical in shape. When it is over 20, cylindrical-shape polymer is produced. The tacticity of the polymers from these dendritic monomers is expected to be different from that of homogeneously obtained polymers because the polymerization proceeds under highly constrained circumstance, but this has not been experimentally verified.
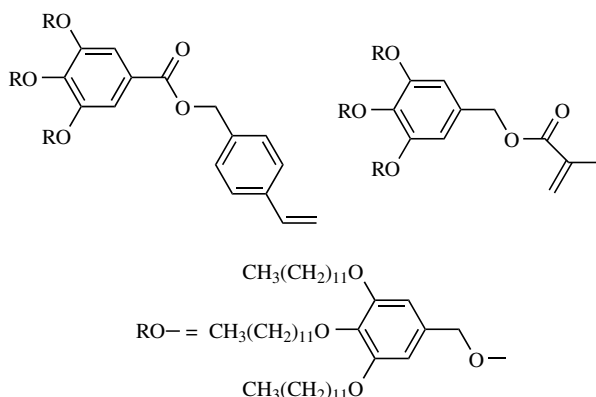
Percec et al.[211,212] have demonstrated a model for the rational design of nanoscale cylindrical and spherical macromolecules with controlled size, shape, and internal and external structure. Figure 13.17 illustrates the rational design of tapered and conical building blocks and their use in the construction of cylindrical and spherical macromolecules. Tapered building blocks self-assemble in supramolecular cylinders that self-organize in a two-dimensional columnar hexagonal *p6mm* lattice. Conical building blocks self-assemble in spherical objects which self-organize in three-dimensional *Pm3n* and *Im3n* cubic lattices. The analysis of these lattices by X-ray diffraction experiments provided information on the size of the tapered and conical building blocks that form the supramolecular objects. The polymer objects can be visualized by transition electron microscopy in a lattice,[213] or as single cylindrical and spherical macromolecules on a surface.[214,215]

13.4.3   Polymerization in Vesicles

Vesicles are liposomelike bilayer assemblies. The lipid molecules can diffuse within a layer, but have a slow changing rate of the molecules between vesicles, thus differing from the micellar systems. Extensive research has been carried out on the polymerization of synthetic bilayers to form polymerized vesicles, which are useful for many applications such as drug delivery, energy conversion, and biomimetic chemistry.[216,217]

Radical polymerization kinetics of lipid monomers in vesicles is completely different from that in isotropic solution and bulk systems. O'Brien et al.[218] studied the detailed kinetics of the radical polymerization of phosphatidylcholine derivatives, including acryloyl, methacryloyl, and sorbyl groups as the polymerizable moieties.
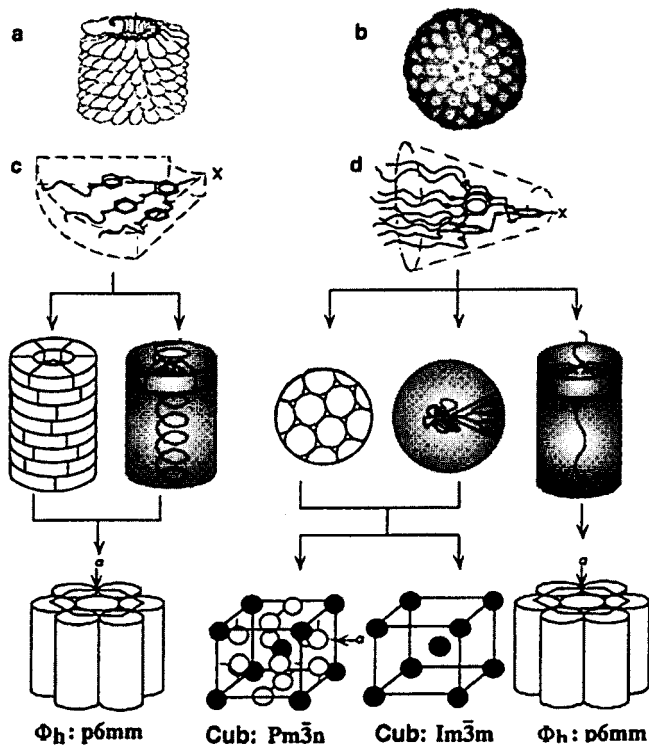
Figure 13.17 Schematic representation of the self-assembly of flat-tapered and conical monodendrons into supramolecular cylindrical and spherical dendrimers and their self-organization into hexagonal columnar and cubic lattices.[212]

The dependence of the degree of polymerization on the monomer and initiator concentration was different from what is observed in bulk polymerization, and this has been attributed to lower rates of bimolecular termination at high monomer conversion in the vesicles. The phase transition temperature of hydrophobic long alkyl chains of lipids also influences the polymerization behavior since the lipid molecules are frozen in a solidlike state below the transition temperature. The low diffusibility in vesicles is also used for the control of molecular weight of the polymer of polymerizable lipid monomers by phase separation[219] and the addition of chain transfer agent.[220]

O'Brien et al.[218,221] have reported the synthesis of a topologically interesting polymer using vesicles as templates. They carried out the radical polymerization of hetero-type bifunctional lipid monomer containing diene and dienoyl groups as the polymerizable diene moieties at the hydrophobic and hydrophilic sites, respectively. The thermal polymerization with AIBN gave rise to selective polymerization of the diene group, while the filtered UV irradiation resulted in exclusive polymerization of dienoyl group. Interestingly, a simultaneous or a sequential polymerization

under the selective conditions provided ladderlike polymer, not crosslinked network polymer. It has also been reported that the polymerization of some diacetylene amphiphiles form stable ribbons and tubules with diameters of approximately 0.5 μm and up to mm length depending on the methods of preparation of assemblies.[222,223]
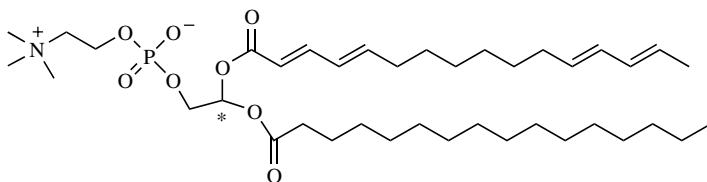
The tacticity of the polymethacrylate produced in the radical polymerization of vesicles of dioctadecyldimethylammonium methacrylate has been investigated. On UV irradiation, the methacrylate anion in the vesicles is polymerized to give highly syndiotactic poly(methacrylic acid) after hydrolysis.[224] The possibility of isotactic polymer formation reported in an earlier communication[225] was denied later by the same authors.[224]
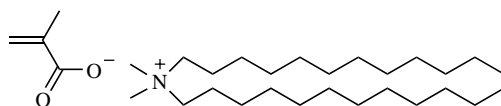
13.4.4   Polymerization in the Liquid Crystalline State

Liquid crystals have several phases depending on the molecular orientation such as nematic, smectic and cholesteric phases. Liquid crystals can be utilized for the control of polymerization via two different methods: (1) polymerization of non-mesogenic monomers in liquid-crystalline media and (2) polymerization of liquid crystalline monomers.

Amerik et al.[226] reported the radical polymerization of 4-methacryloyloxyben-zoic acid using 4-tetradecylbenzoic acid as solvent, which forms a smectic phase at 110°C in the presence or absence of a radical initiator. The polymerization rate and the molecular weight of the polymer in the liquid crystalline state were greater than what was observed in solution polymerization in dimethylformamide. When the polymerization temperature was increased above 133°C, a phase transition from the smectic phase to isotropic solution was observed. The molecular weight of the resulting polymer decreased, indicating that the arrangement of the monomer molecules in the liquid crystalline medium is an important factor for the polymerization reactivity. In a similar system, the tacticity of the resulting polymer was investigated by Blumstein et al.[227] It was found that isotactic-rich polymer was formed in the early stages of the polymerization (at conversions below 10%). However, as the conversion increased, the amount of isotactic polymer formed gradually

changed, the tacticity of the polymer formed at high conversion being similar to that obtained in isotropic solution at a high conversion. For example, the triad tacticities were reported to be $mm : mr : rr = 50 : 30 : 20$, $43 : 37 : 20$, and $27 : 36 : 37$ at 8, 55, and 80% conversion, respectively, whereas polymerizations in dimethylformamide or bulk provided polymer with $mm : mr : rr = 21 : 37 : 41$. A similar conversion dependence of the tacticity has been observed for the polymerization in a nematic phase with 4-heptyloxybenzoic acid as the solvent.
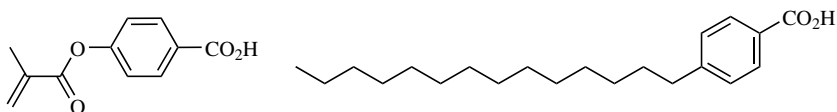
The tacticity of the polymers of a series of *n*-alkyl methacrylates obtained from radical polymerization in various liquid crystalline states was investigated in detail.[228] The polymerization of the methacrylates was carried out in *N*-(4-methoxybenzylidene)-4-butylaniline (MBA) and *N*-(4-ethoxybenzylidene)-4-butylaniline (EBA) as the nematic medium and cholesteryl octadecanoate (ChoOD) as the smectic or cholesteric medium, and compared with the results for isotropic polymerization in benzene. The results are shown in Table 13.13.

A mixture of the monomer and the solvent was heated to be isotropic, and subsequently polymerized at a desired temperature in the presence of AIBN. The viscosity numbers of the polymer produced in the liquid crystalline state were greater than those obtained in isotropic polymerizations. The tacticity of MMA and ethyl methacrylate was independent of the polymerization media, but in the polymerization of the *n*-butyl and higher alkyl esters the isotacticity increased in the liquid crystalline phases compared with solution polymerization. These results suggest that methacrylate monomers with a long alkyl ester group are arranged in the liquid crystalline state in a fashion appropriate for isotactic propagation, but the methyl and ethyl esters are too small to be in an ordered structure.

MBA   EBA

ChoOD
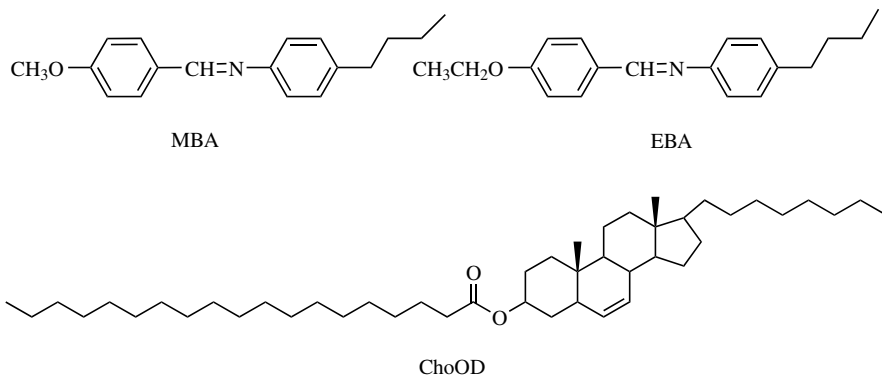
The effects of the addition of mesogenic compounds on polymer tacticity have been reported. For example, the polymerization of MMA with BPO was investigated

TABLE 13.13   Radical Polymerization of Alkyl Methacrylates in the Liquid Crystalline State[a]

Monomer	Solvent	Phase	Temperature (°C)	Tacticity		
				mm	*mr*	*rr*
MMA	Benzene	Isotropic	60	4	32	64
	EBA	Nematic	60	4	31	65
	MBA	Nematic	60	5	35	60
	ChoOD	Smectic	65	5	35	60
	ChoOD	Cholesteric	75	4	34	62
Ethyl methacrylate	Benzene	Isotropic	60	5	34	61
	EBA	Nematic	60	9	33	58
	MBA	Nematic	60	8	39	53
	ChoOD	Smectic	65	7	40	53
	ChoOD	Cholesteric	75	6	34	60
n-Butyl methacrylate	Benzene	Isotropic	60	7	33	60
	EBA	Nematic	60	20	25	55
	MBA	Nematic	60	23	32	45
	ChoOD	Smectic	65	19	34	47
	ChoOD	Cholesteric	75	15	31	54
n-Hexyl methacrylate	Benzene	Isotropic	60	12	32	56
	EBA	Nematic	55	19	38	43
	MBA	Nematic	60	27	31	42
	ChoOD	Smectic	65	28	25	47
	ChoOD	Cholesteric	74	18	30	52
Octyl methacrylate	Benzene	Isotropic	60	16	34	50
	EBA	Nematic	50	24	39	37
	MBA	Nematic	60	29	28	43
	ChoOD	Smectic	65	31	29	40
	ChoOD	Cholesteric	74	20	38	42
Dodecyl methacrylate	Benzene	Isotropic	60	23	31	46
	EBA	Nematic	50	28	32	40
	MBA	Nematic	58	33	31	36
	ChoOD	Smectic	65	29	36	35
	ChoOD	Cholesteric	73	27	31	42
Octadecyl methacrylate	Benzene	Isotropic	60	26	30	44
	EBA	Nematic	50	31	35	34
	MBA	Nematic	58	34	30	36
	ChoOD	Smectic	65	35	27	38
	ChoOD	Cholesteric	73	29	32	39

Key: EBA, *N*-(4-ethoxybenzylidene)-4-butylaniline; MBA, *N*-(4-methoxybenzylidene)-4-butylaniline; ChoOD, cholesteryl octadecanoate. Monomer 10 wt%, AIBN 1 mol%.

Source: Ref. 228.

in the presence of cholesteric liquid crystalline.[229] An increase in the molecular weight of the polymer by the addition of a small amount of the cholesteric esters of long-alkyl-chain carboxylic acids was observed. A small but detectable increase of the isotactic triads was also observed in these polymerizations, although these reaction systems are not mesomorphic. The tacticity of poly(MMA) obtained in bulk polymerization at 65°C in the presence of cholesteryl octanoate was mm : mr : $rr = 13 : 51 : 26$, different from $mm : mr : rr = 4 : 62 : 34$ obtained under similar conditions in the presence of the ester. However, cholesteryl decanoate had no effect on the tacticity. The influence of other cholesteric compounds on polymer tacticity have also been reported.[230,231] The addition of the cholesteryl esters of oleylcarbonic acid or 3-(2-ethoxyethoxy)propanoic acid enhanced the polymerization rate of MMA and influenced the tacticity of the produced poly(MMA).

The polymerization of mesogenic monomers has also been investigated. An increase in the polymerization rate in the smectic phase was reported for the γ-radiation polymerization of the vinyl ester of oleic acid.[232] The polymerization rate decreased in the order of liquid crystalline state > isotropic solution > solid state. The polymerizations of the Schiff base derivatives of styrene or (meth)acrylates[233,234] and cholesteric esters of (meth)acrylates,[235–237] as shown below, have also been investigated. The polymerization rates, the molecular weight of the resulting polymers, and the overall activation energies of the polymerization in the liquid crystalline state were examined. No definitive conclusion has been reached as the behavior is systems-dependent.
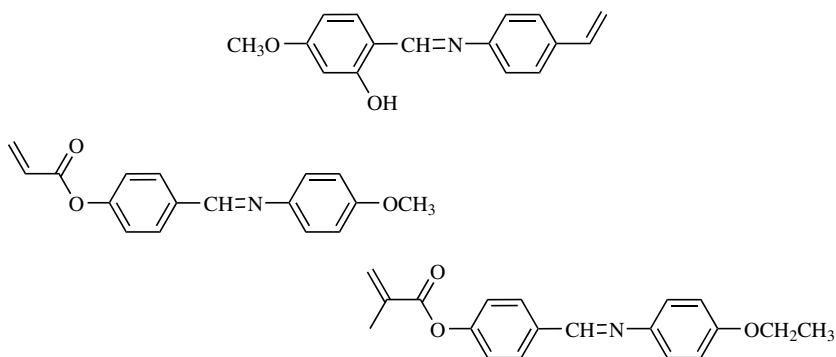
Bowman et al.[238–240] revealed that the radical polymerization of mesogenic monomer in the smectic $C*$ phase at 25°C proceeds at much higher propagation and termination rates than in an isotropic system at 70°C. For the polymerization of nonmesogenic and difunctional monomers, such acceleration was not observed. Polarized IR spectroscopy revealed the orientation of mesogenic and non-mesogenic monomers in the smectic layers of the liquid crystalline phase. The stereochemistry of the polymer has not been investigated.
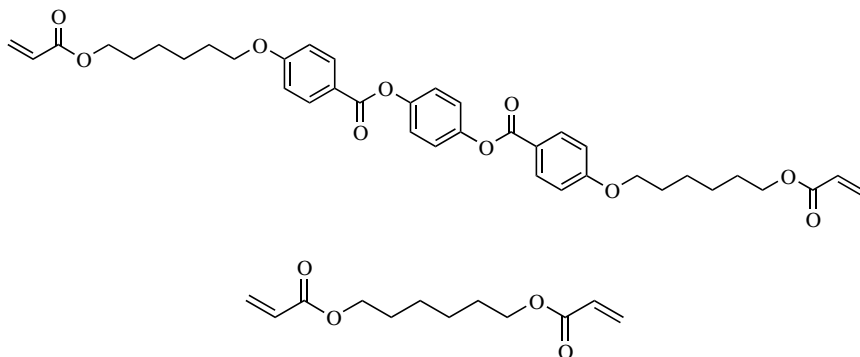
Stupp et al.[241,242] have demonstrated the synthesis of a unique two-dimensional polymer by the polymerization of a mesogenic monomer in a smectic phase. They designed a monomer having acrylic and nitrile groups as the reacting sites at the end and middle of the molecule, respectively, and a mesogenic moiety at the other terminus on the basis of their unique and new conception for the design of polymeric materials. On heating of the liquid crystalline phase, the acrylic and nitrile groups are polymerized to give a crosslinked two-dimensional network structure keeping the characteristics of the original liquid crystalline phase. GPC and TEM measurements revealed several interesting features of the crosslinked product as nanometer-sized two-dimensional object.[243,244]
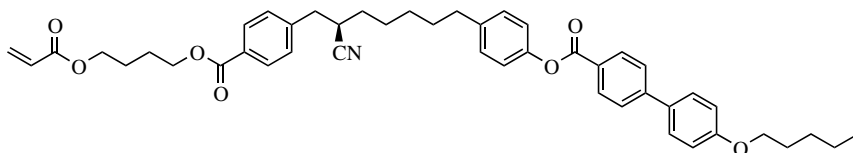
Gin and co-workers[245] reported the stabilization of a lyotropic liquid crystalline phase by crosslinked polymerization. Inverse hexagonal lyotropic liquid crystals are formed when an amphiphilic monomer is mixed with a water-soluble polymer precursor of poly(p-phenylenevinylene) in an aqueous medium. Photopolymerization was accompanied by crosslinking, and subsequent heating resulted in the formation of conjugated polymer from the polymeric precursor. This represents novel design of higher-order polymer structures, including organic–inorganic hybrids.

13.4.5 Polymerization in the Solid State

13.4.5.1 The Topochemical Principle and Crystal Engineering

Organic synthetic reactions are generally conducted in the liquid or gaseous phase. Polymerizations are also carried out in a fluid state such as in a solution, suspension, emulsion, gas, or melt. More recently, however, organic synthesis performed in the solid state has become one of the most intriguing fields of synthetic chemistry, due to

high selectivity and the specific morphology of the products. When the reactant molecules are themselves crystalline, that is, as molecular crystals, or are included in host crystals, specifically as inclusion compounds, the rate and selectivity of the reaction are different from those obtained in an isotropic reaction medium.[246–253] Solvent-free processes for organic syntheses, including solid-state polymerizations, will inevitably become more important in the future because of the advantages from an environmental point of view.

The first recognition of the features and the importance of solid-state organic reactions date back to the 1960–1970s. The idea of topochemistry or topochemical control was originally introduced in the early twentieth century for ion exchange reactions performed in the solid state, and thereafter brilliantly exploited by Schmidt and his co-workers.[254] Schmidt et al. derived the following topochemical principles on the basis of the results of the photodimerization of cinnamic acids in the solid state: (1) the product formed is governed by the environment in the crystalline state rather than by the intrinsic reactivity of the reactive bonds; (2) the proximity and degree of parallelism of the reacting centers are crucial for the dimerization, and (3) there is a one-to-one relationship between the configuration and symmetry of the product with the symmetry of the reactants in the crystals.

In the same era, Thomas[255] pointed out the importance of the distinction between topotactic and topochemical reactions, and he also stressed the problem of erroneous terminology concerning topochemical reactions. In his review article, these terms were described as follows. A reaction is said to be topotactic if the lattice of a solid product shows one or a small number of crystallographically equivalent, definite orientations relative to the lattice of the parent crystal, and the reaction has proceeded throughout the bulk of the reactant. On the other hand, the products are governed by the fact that the chemical changes proceed within the solid. Thereafter, however, the term *topochemical reaction* has been used in various situations in many fields, where its usage is not always uniform, often confusing our understanding of the concepts. For example, according to an alternative definition, a reaction that leads to a product that is crystallographically related to the precursors is called topotactic.[256] In a more favorable situation, the crystal structure and symmetry of the product materials are predictable from the crystal structural information of the starting material, and the reaction is termed topochemical. Accordingly, all topochemical reactions are topotactic, although the converse may not be true. At its simplest, we can state that a topochemical reaction is a reaction that proceeds with minimum movement of molecules and atoms in the solid state, and the symmetry of the substrate crystal is retained during the reaction; namely, the space group of the product crystal is the same as that of the starting crystal.

Schmidt et al.[246] also coined the term of crystal engineering in the context of the photodimerization in the solid state. The original objective of crystal engineering was to design organic molecules that would adopt particular crystal structures within which topochemical reactions could take place, leading to regioselective or stereoselective products. The concept of crystal engineering has recently been renewed as a strategy for the rational design of organic solid architecture utilizing supramolecular chemistry.[257–261] The study of solid-state organic synthesis has been accelerated by

the striking development of methods and apparatus for crystal structure analysis using an imaging plate and CCD camera system as a two-dimensional detector as well as the improvements in both hardware and software for computation. These measurement systems can quickly collect the X-ray diffraction data with a sufficiently quantitative intensity within a short time, being very useful for structure determination of crystalline materials that react sensitively to X-ray irradiation.

13.4.5.2 *Polymerization in Layer Compounds*   Certain amphiphilic molecules can be organized as monomolecular layers or multilayers, followed by polymerization to give oriented polymer films at interfaces. Oriented monolayers can be prepared by spreading amphiphilic molecules at the gas–liquid interface or adsorption of surfactant molecules at polar solid substrates. Multilayers are prepared by Langmuir–Blodgett (LB) deposition or a self-assembly process. The polymerization of mono- and multilayer assemblies by the LB technique has been intensively investigated.[262–264]

Ringsdorf and Schupp[265] reported the photoreactivity of amphiphilic butadiene derivatives at the air-water interface. These compounds were photoreactive under UV irradiation, but the structure of the photoproducts were unknown, although the unsaturated units can undergo either a [2 + 2] cycloaddition to form dimers and oligomers, or 1,4-addition to give a 1,4-*trans*-polymer. Fukuda et al. reported the UV polymerization of the LB membranes of octadeca-2,4-dienoic acid as the cadmium salt.[266] Laschwsky and Ringsdorf[267] described the polymerization behavior of several long-chain butadiene derivatives. Tieke[268] reported the polymerization of *N*-octadecyl-6-amino-2,4-hexadienoic acid in LB films. It was concluded from IR studies that 1,4-addition of the unsaturated units takes place on γ radiation. The polymeric LB films were extremely stable to chemical modification and exhibited a high thermal stability due to strong hydrogen bonding.

X = −CH$_2$OH, −CHO, −CO$_2$H
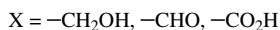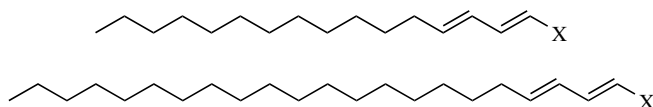
In the 1980s, Tieke et al.[269–272] investigated UV- and γ-irradiation polymerization of butadienes crystallized in a perovskite-type layer structure. They reported the solid-state polymerization of the butadienes containing aminomethyl groups as pendant substituents that form layer perovskite halide salts to yield *erythro*-diisotactic-1,4-*trans*-polymers. They determined the crystal structure of the polymerized compounds of the carboxylic acid derivatives (MtX$_2$ = CdCl$_2$) by X-ray diffraction.[272] From comparative X-ray studies of monomeric crystals, a contraction of the lattice constant parallel to the polymer chain direction by approximately 8% is evident. Both the carboxylic acid and aminomethyl substituent groups are in an isotactic arrangement, resulting in *erythro*-diisotactic polymer chains. The native halide

salt of the butadiene derivatives was also studied concerning the reactivity on UV and γ radiation.[271] It was reported that a considerable amount of polymer is formed during postpolymerization.

$$\left[R \diagdown\diagup\diagdown\diagup NH_3 \right]_2 MtX_4$$
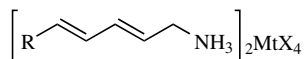
R = H, CH$_3$, CO$_2$H, CO$_2$CH$_3$,
CO$_2$CH(CH$_3$)$_2$, CO$_2$CH$_2$CH(CH$_3$)$_2$,
CO$_2$(CH$_2$)$_3$CH$_3$

MtX$_2$ = CdCl$_2$, CuCl$_2$, FeCl$_2$, MnCl$_2$

HO$_2$C $\diagup\diagdown\diagup\diagdown$ NH$_3$Cl
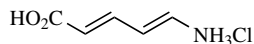
Radical polymerization of vinyl monomers in the presence of the alkaline-substituted clay Montmorillonite has also been reported. The polymerization of MMA intercalated into the layers of clay was carried out in the presence of a radical initiator or by the γ-radiation.[273,274] The resulting poly(MMA) had a higher isotacticity: $mm : mr : rr = 36 : 41 : 23$ for the polymer obtained during polymerization at 100°C with BPO. It was reported that the tacticity was independent of the polymerization temperature, but influenced by the amount of the absorbed monomer and of the metal ions, because stereocontrol was achieved at the surface of the clay used. Kyotani et al.[275] reported that the γ-radiation polymerization of acrylonitrile with Montmorillonite lamellae gave polyacrylonitrile intercalated to the layers of the clay. It was heated at 700°C to produce the precursor carbon, and subsequently treated with acid. Further heating at a higher temperature resulted in a highly oriented graphite.

13.4.5.3 Polymerization in Porous Materials

Porous crystalline compounds are classified into three groups as microporous, mesoporous, and macroporous materials, which have fine pores with a diameter of less than 2 nm, 2–50 nm, and more than 50 nm, respectively. Radical polymerizations of MMA and styrene have been studied in the presence of inorganic compounds such as silica gel, alumina, and zeolite focusing on the polymerization reactivity and the tacticity of the polymers.[276–278] The γ-radiation polymerization of MMA and acrylonitrile adsorbed to Linde zeolite 13X was investigated. The radiation was carried out at -196°C, followed by the post polymerization at a desired temperature. After post polymerization, the polymer was isolated from the zeolite by treatment with HF and subsequent extraction. The triad tacticity of poly(MMA) produced in the presence of zeolite was $mm : mr : rr = 22 : 51 : 27$, the isotactic fraction being higher than that obtained during solution polymerization.[277] Thermal polymerization of styrene was also carried out in zeolite H-ZSH-5.[278]

Recently, a variety of mesoporous silicate materials have been developed and applied to radical polymerization in a constrained medium. The radical polymerization of MMA using AIBN or BPO as radical initiators in the mesoporous silicate MCM-41 was revealed to provide a polymer with a much higher molecular weight than from solution polymerization.[279] However, zeolites with a smaller pore size, for

example, zeolite F-9 with a pore size of 0.9 nm or zeolite A-4 with 0.4 nm pore, resulted in a lower polymer yield or no polymer formation. ESR studies have revealed the formation of long-lived propagating radicals within the macroscopic channels. The molecular weight of the polymer can be controlled over a wide range by changing the initial ratio of MMA to the initiator. The tacticity of the polymer was the same as that of poly(MMA) obtained in solution polymerization. It is considered that the mesoscopic pores of MCM-41 are not small enough to affect the stereochemical course of the chain growth. Moller et al.[280] reported that poly(MMA) formed within the mesoscopic channels exhibited no glass transition temperature because of an interaction between the polymer and the internal surface of the mesopore. Wu and Bein[281,282] have reported the synthesis of a graphite-type conducting carbon wire by the radical polymerization of acrylonitrile within the mesoscopic channels of MCM-41 and the subsequent pyrolysis. The graphite/MCM-41 composite obtained by pyrolysis at 1000°C showed a noticeable microwave conductivity, greater than the properties reported for the polyaniline analog.[283,284]

Recently, mesoporous materials are more attractive than microporous materials from the viewpoint of control of the polymerization locus as well as for the fabrication of polymeric materials.[203,285]

13.4.5.4 Inclusion Polymerization

The polymerization of monomers included as the guest molecules in channellike cavities of clathrates as the host crystals is one of the most important polymerizations in organized media.[286–289] Inclusion polymerization is distinguished from solid-state polymerization of monomers themselves crystalline, because the included monomer molecules are not always in the crystalline state because of the considerably high mobility. Moreover, a wide range of monomers suited for the use in the inclusion polymerization are normally liquid or gaseous at the polymerization temperature. The monomers are arranged along the direction of the channel, and a polymer chain forms along the same direction.

The first example of inclusion polymerization was achieved in 1956, when 2,3-dimethylbutadiene included in thiourea was polymerized without using any initiator.[290] In that work, however, the polymer structure was not investigated. Not long after this achievement, inclusion polymerization was employed to control polymer structures; it was revealed that butadiene included in urea and 2,3-dimethylbutadiene included in thiourea provided pure 1,4-*trans*-polymer under irradiation with β, γ, and X-rays.[291,292] At the same time, preparation of syndiotactic poly(vinyl chloride) by inclusion polymerization with urea was also reported.[292,293] In 1963, Farina and co-workers[294] opened new areas of inclusion polymerization using *anti–trans–anti–trans–anti–trans*-perhydrotriphenylene (PHTP), a tetracyclic saturated hydrocarbon as a new host, which can form inclusion compounds with a wide variety of organic guests. In 1967, 1,4-*trans*-polybutadiene, a highly isotactic crystalline polymer, was synthesized using this host compound.[295] The first asymmetric synthesis in the solid state was also accomplished by the polymerization of 1,3-*trans*-pentadiene included in optically active PHTP.[296] Naturally originated deoxycholic acid (DCA) and apocholic acid (ACA) have been widely used as chiral

host compounds.[288] Cycophospazene compounds are also known to act as hosts; examples are tris(o-phenylenedioxy)cyclotriphosphazene (TPP) and tris(2,3-naphthalenedioxy)cyclotriphosphazene (TNP).[297–299]

urea   thiourea   PHTP

DCA   ACA

TPP   TNP
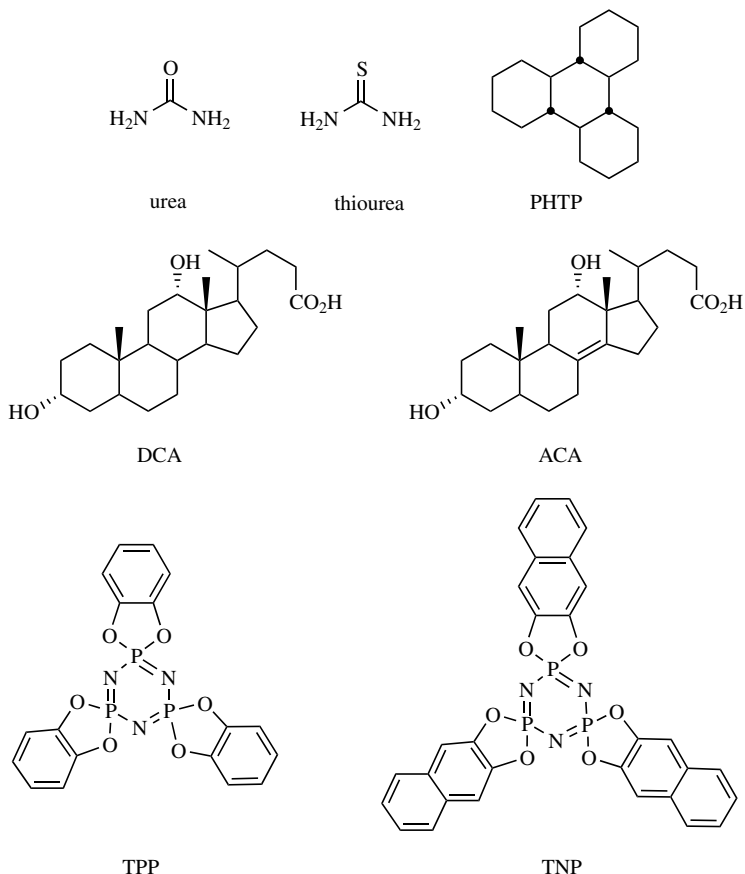
In the late 1980s and early 1990s, Miyata and co-workers[289,299] established the general aspects of inclusion polymerization of vinyl and diene monomers and revealed the intrinsic space effects of these polymerizations, in addition to the important characteristics of the stereocontrol of diene polymers discovered in 1960s. They employed several kinds of steroids including DCA and ACA to claim that inclusion polymerization should be viewed as a general space-dependent polymerization, and not only stereospecific polymerization. Figure 13.18 shows a range of diene monomers that polymerize in the channels of the hosts urea, thiourea, DAC, and ACA. The size of the space formed in the channel of the host compounds plays a decisive role in determining the polymerization reactivity of the monomer, as well as the motion of the propagating radicals and the microstructure of the resulting polymer. In larger spaces, the molecular motion is relatively unrestricted, leading to high polymerization rates and a lower degree of stereocontrol.
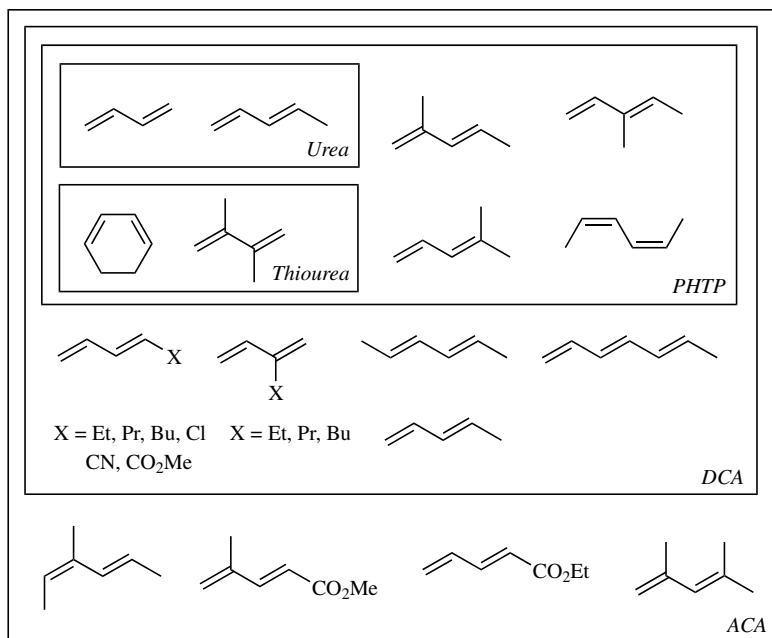
Figure 13.18   Molecular strcuture of polymerizable diene monomers in the channels of the inclusion compounds with various host molecules.

The polymerization of butadiene included in DCA and ACA resulted in polymer with a less-controlled structure of 1,2-unit up to 30%, and the fraction of 1,2-units depended on the polymerization conditions including the kind of solvent used for the crystallization of the inclusion compounds. In contrast, several methyl-substituted diene monomers such as 1,3-pentadiene, 4-methyl-1,3-pentadiene, and 2,3-dimethyl-1,3-butadiene gave highly controlled 1,4-*trans* polymers by inclusion polymerization with DCA and ACA (see Table 13.14).[300–303]

A bifunctional monomer such as divinylbenzene is converted into a soluble polymer without crosslinking during inclusion polymerization with TNP since each channel provides an isolated reaction environment.[298] Isotactic polyacrylonitrile was also reported to be formed during the γ-radiation polymerization of acrylonitrile included in urea as the host by Kamide et al.[304,305] and Minagawa et al.[306]

13.4.5.5 *Topochemical Polymerization in the Crystalline State*   Among the solid-state polymerizations of bulk monomer crystals, the polymerization that provides a polymer with a specific crystal structure formed under control of the crystal lattice of the monomer is distinguished as topotactic polymerization. In contrast to this, topochemical polymerization is described as a reaction in which the crystallographic position and symmetry of the monomer crystals as the reactant

TABLE 13.14   **Tacticity of Polymers Prepared by Radical Polymerization of Various Butadiene Derivatives in Inclusion Polymerization**

Monomer	Host	Tacticity		
		trans-1,4	cis-1,4	1,2
Butadiene	None (20°C)	58	22	20
1,3-Pentadiene	DCA	>99	0	0
4-Methyl-1,3-pentadiene	DCA	>99	0	0
4-Methyl-1,3-pentadiene	ACA	>99	0	0
2,3-Dimethyl-1,3-butadiene	ACA	>99	0	0
2,3-Dimethyl-1,3-butadiene	DCA	>99	0	0
2,3-Dimethyl-1,3-butadiene	Methyl Cholate	90	10	0
2,3-Dimethyl-1,3-butadiene	Cholic Acid	54	42	4

Source: Refs. 300–303.

are retained in the resulting polymer crystals as the product. In a topochemical polymerization process, the primary structure of a polymer chain (e.g., regioselectivity and tacticity) as well as higher order structures of chains (e.g., ordering and crystallinity) are completely controlled, resulting in the facile fabrication of polymer crystals. Furthermore, the polymerization reactivity and the solid-state properties of the resulting polymer crystals are predictable from the crystal structure of the substrates. Thus, topochemical reactions promise to yield products with highly controlled structures by the crystal lattice of the reactant, but few successful polymerizations in the crystalline state via a topochemical process have actually been reported. In the late 1960s, two typical examples of topochemical polymerization were discovered; stepwise [2 + 2] photopolymerization of 2,5-styrylpyradine and its analogous diolefins (Fig. 13.19)[307–311] and thermal or radiation polymerization of diacetylenic derivatives.[312–319]

Lauher and Fowler et al.[320,321] have proposed an elegant strategy for the control of topochemical polymerization based on the generality of the host–guest/cocrystal concept. They used the ureylene and oxalamide functionality to form layered supramolecular structures for the topochemically controlled polymerization of diacetylenes. This approach was also applied to the polymerization of 1,3-butadiene derivatives in the solid state.[322] The preliminary results indicated successful topochemical preparation of a unique polybutadiene ladder polymer.

The 1,6-polymerization of triacetylene has been unknown transformation for a long time.[323–325] It was recognized that a successful 1,6-polymerization would require preorganization of the reactants, and later Enkelmann[325] provided a more complete analysis of the criteria necessary for successful polymerization. It was a longstanding synthetic problem of considerable interest and the requirements were very well defined, but no one had been able to devise a successful synthesis. Lauher et al.[326] solved this problem by the designed 1,6-polymerization, which served as a significant test for supramolecular synthesis.

[2+2]Photopolymerization of 2,5-distyrylpyradine and its analogous derivatives
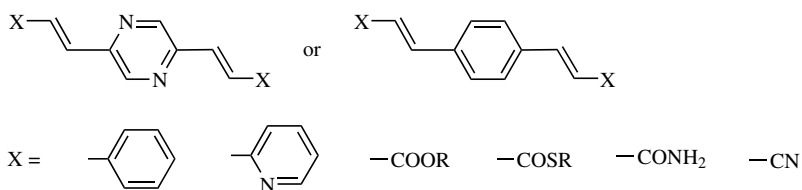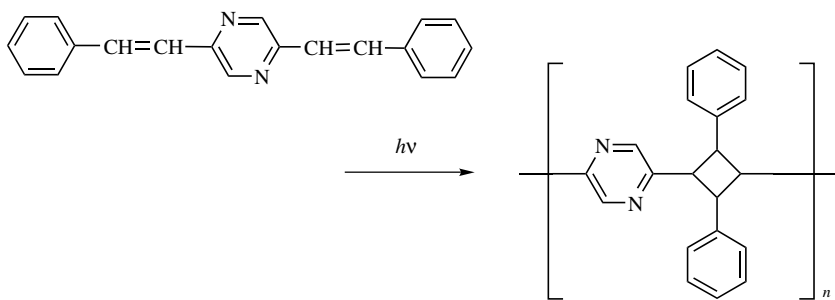
Thermal or radiation polymerization of diacetylene derivatives

$R = -(CH_2)_nCH_3$

$-(CH_2)_nCOOH$

$-(C{\equiv}C)_m(CH_2)_nCH_3$

$-(CH_2)_nOCONH-$ [benzene ring]

$-(CH_2)_nOCONHCH_2CO_2(CH_2)_3CH_3$

$-CH_2OSO_2-$ [ring] $-CH_3$

$-CH_2-N$ [carbazole ring]
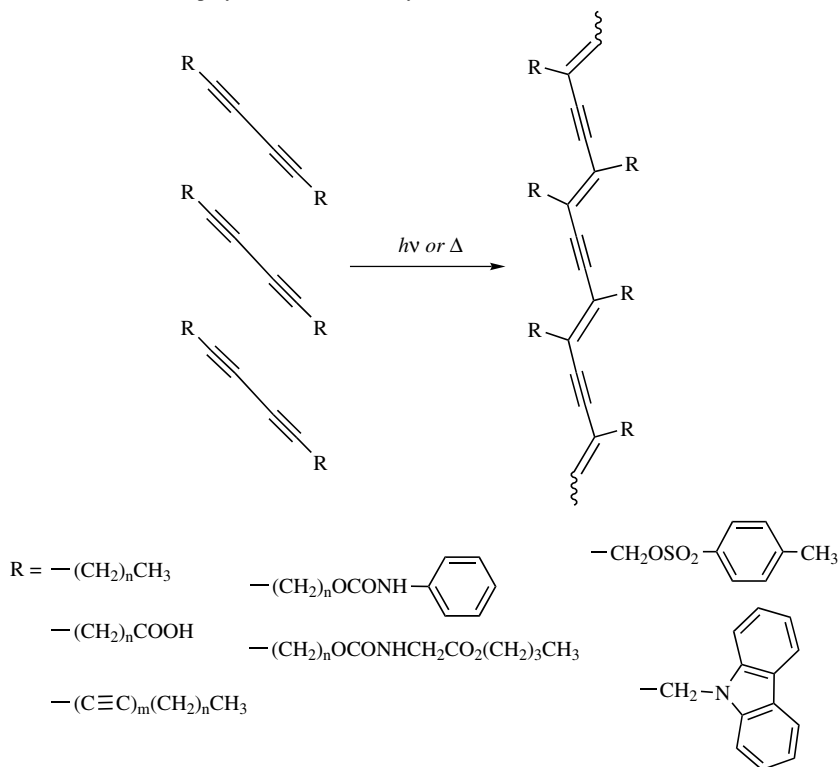
Figure 13.19 Examples of topochemical polymerization discovered in the 1960s.
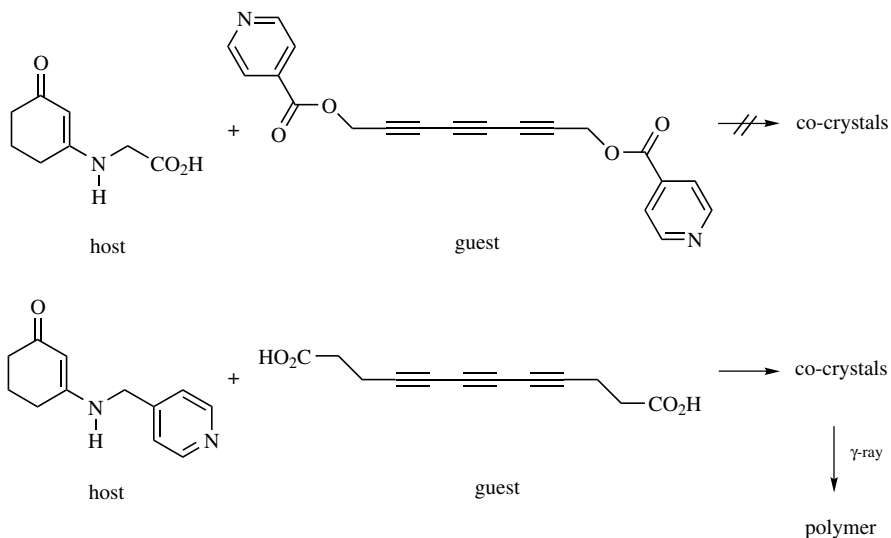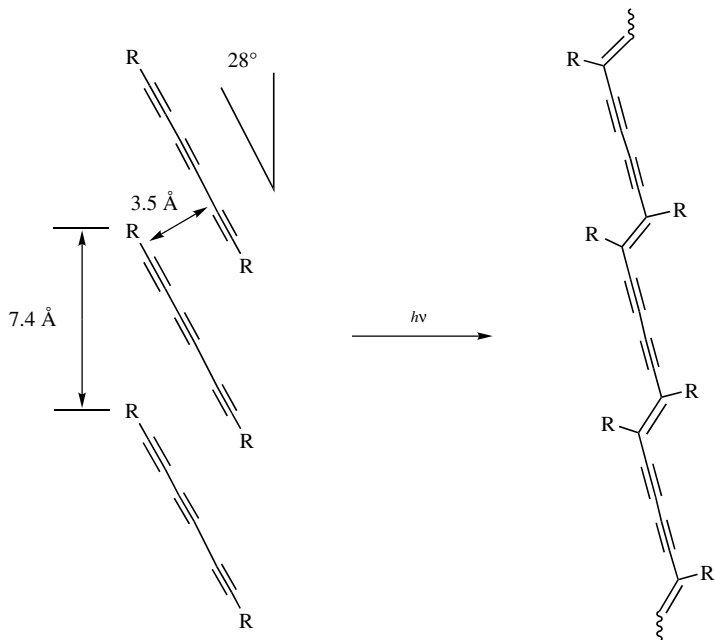
Preliminary attempts to grow cocrystals between the carboxylic acid host and the dipyridine guest were not promising because of the solubility differences. Subsequently, they turned their attention to the pyridine host, which readily cocrystallized with simple dicarboxylic acids such as succinic and adipic acids. Therefore, they prepared the triacetylene diacid as the guest molecule. The evaporation of a 2 : 1 solution of the pyridine host and the triacetylene diacid guest in methanol in fact

produced a host–guest compound as pale red crystals. A single crystal X-ray structure of the compound clearly showed that the molecules had self-assembled in accordance with their design: a stacking distance of 7.143 Å and tilt angle of 29.2°. The exposure of the host–guest crystals to γ radiation resulted in the crystals becoming dark red. The Raman spectrum of the polytriacetylene showed two intense bands in the 2500–500-cm^{-1} region at 2148 and 1552 cm^{-1}, which can be assigned to the C≡C and C=C bonds, respectively.

In 1994, Matsumoto et al. discovered a new type of topochemical polymerization of 1,3-diene monomers that gives a stereoregular polymer in the form of polymer crystals as polymerized[327]. When diethyl (Z,Z)-muconate (EMU) [diethyl (Z,Z)-2,4-hexadienedioate] was photoirradiated in the crystalline state, a tritactic polymer, specifically, the *meso*-diisotactic-*trans*-2,5-polymer, was produced in contrast to the formation of an atactic polymer by conventional radical polymerization in an isotropic state, as shown in by the NMR spectra of the polymers obtained (Fig. 13.20). During subsequent years, X-ray diffraction and IR, Raman, NMR, and ESR spectroscopic studies have revealed that this is the first clear example of the topochemical polymerization of 1,3-diene derivatives via a radical chain reaction mechanism.[201,328,329]
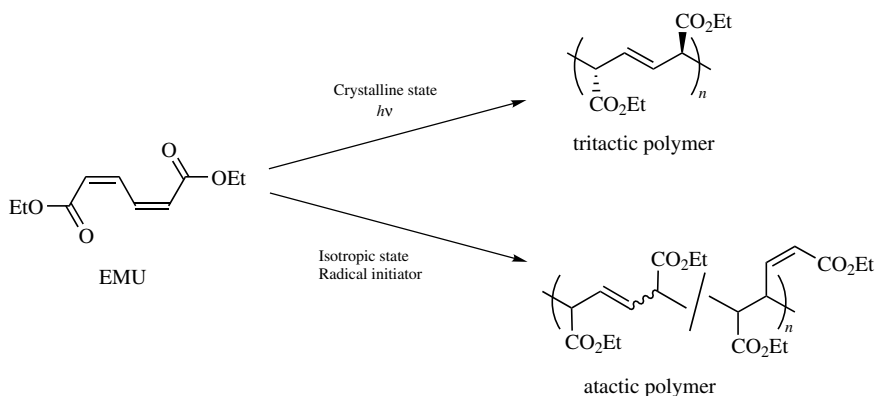
Topochemical polymerization of EMU proceeds under photo-, X-, and γ-ray irradiation.[330–334] The polymerization process is independent of the environment of the crystal: in vacuo, in air, or even in water or organic solvents as the dispersant for the crystals. When an EMU crystal was photoirradiated with sunlight or UV light, the crystal first bent in the direction of the incident light, and then it recovered to its original linear shape except for 2% shrinkage of the needle length. This is due to a heterogeneous photopolymerization process at the surface of the crystal during the initial stage of the polymerization. Such macroscopic deformation implies a considerable strain in the crystals, resulting in the formation of structural defects, such as cracking or collapse of the crystals during the photoirradiation. In contrast, X rays and γ radiation induce a polymerization that produces a high-quality polymer crystal with less structural defects, because these rays have excellent penetration and can
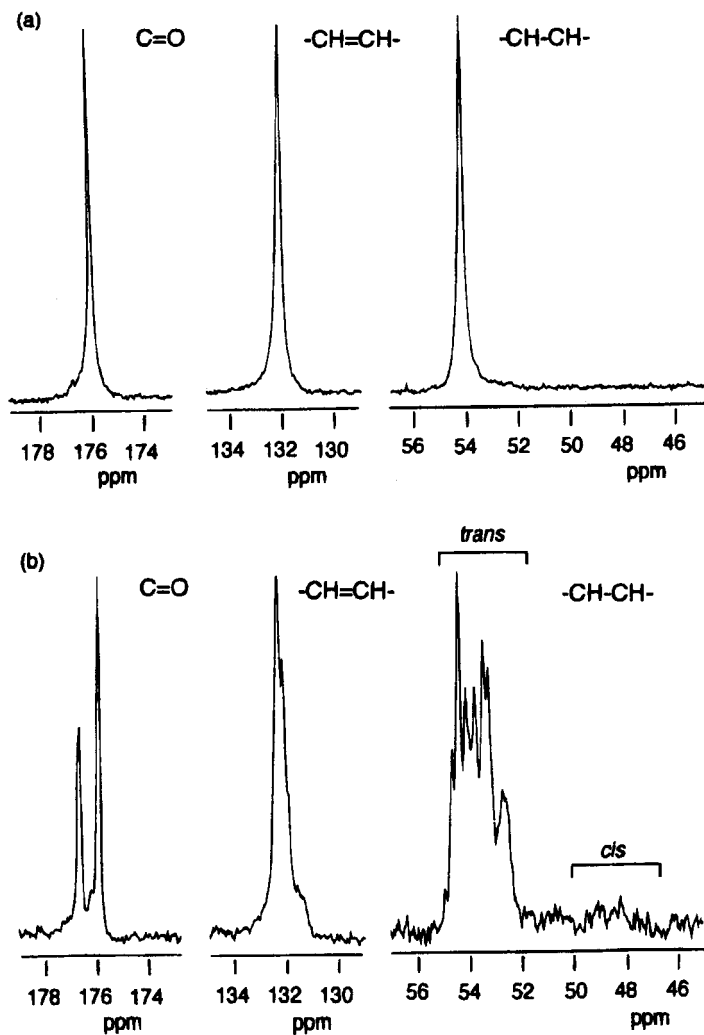
Figure 13.20   Comparison of ^{13}C NMR spectra of (a) tritactic poly(EMU) prepared by topochemical polymerization and (b) atactic poly(EMU) prepared by isotropic polymerization in the melt (measurement solvent—trifluoroacetic acid-d).[330]

initiate homogeneous polymerization in the crystals. This makes it possible to fabricate a single-polymer crystal from a single-monomer crystal.

    We can obtain poly(EMU) as needle-form crystals as polymerized under UV irradiation of the monomer crystals (Fig. 13.21a).[335] When a poly(EMU) needle was pinched by fingers, the crystal readily collapsed, and a fibril structure was observed as shown in Fig. 13.21b. It has been revealed by X-ray diffraction that the polymer chains are aligned along a specific axis of the crystal with completely extended

(a)   500 μm

(b)   250 μm

(c)   250 μm
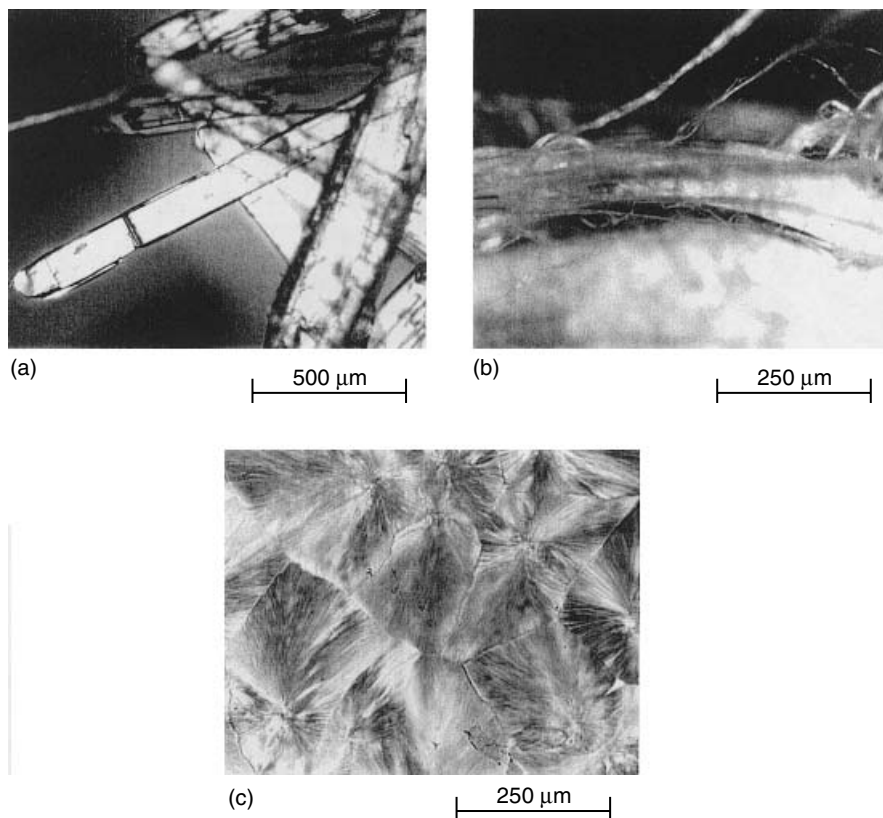
Figure 13.21 Polarized microphotographs of the poly(EMU) crystals obtained by photopolymerization of the EMU crystals recrystallized from *n*-hexane: (a) as polymerized; (b) fibril structure observed when the poly(EMU) collapsed; (c) spherulite observed in the cooling process from the melt.[335]

conformation and that the fiber period of the poly(EMU) crystal is 0.4835 nm.[331] The completely extended polymer chain conformation exists only in the polymer crystals as polymerized through the crystalline-state polymerization via a topochemical polymerization mechanism. When melted, the polymer readily crystallized during the cooling process and spherulites were formed as shown in Fig. 13.21c. This indicates that stereoregular poly(EMU) has high crystallinity, while atactic poly(EMU) is amorphous.

As expected from the characteristic of the topochemical polymerization, the size and shape of the polymer crystals depend on the monomer crystals. Propagation is very fast because of the suitable arrangement of the monomers in the crystals, resulting in the formation of a polymer with a molecular weight dependent on the crystal size.[335] When the size of the monomer crystals is regulated, control of the molecular weight and polydispersity as well as stereoregularity is also obtained. Molecular weight control was in fact attempted using microcrystals prepared by

recrystallization, milling, freeze-drying, and reprecipitation as methods for monomer crystal fabrication. Precipitation is the best method for preparation of microcrystals with a length of approximately 10–100 μm as characterized by SEM. GPC analysis also revealed that the polymer by precipitation has an M_w of 10^5 and a relatively narrow polydispersity, $M_w/M_n = 2.0$. The monomer crystal size influences not only the molecular weight but also the yield of the polymer produced, as observed for photo- and γ-ray-induced polymerization. In the case of γ-ray radiation polymerization, initiation would be expected to occur throughout the crystals because of the excellent γ-ray penetration. It has however been reported that larger crystals prepared by conventional recrystallization afforded higher polymer yields than did microcrystals prepared by freeze-drying under similar radiation conditions.[333]

Matsumoto et al.[329–331] have investigated the photoreaction of many kinds of muconic esters since the discovery of the polymerization of EMU, but it has been difficult to find other topochemical polymerizable crystals. Topochemical polymerization is so sensitive to the molecular structure that alkyl esters other than EMU do not undergo photopolymerization at all. For example, the methyl, *n*-propyl, isopropyl, cyclohexyl, and benzyl esters gave no polymer under UV irradiation in the crystalline state. Some were isomerized to the corresponding (*E,E*)-isomer, and others did not react. This sensitivity is explained by the drastic change in the packing and orientation of the monomer molecules in the crystals. Another problem was the difficulty in the isolation of the monomer crystals of many ester derivatives because of their low melting points.

In view of these findings, they turned their attention to the alkylammonium salts in the hope of finding polymerizable crystals of the muconic acid derivatives.[336] The alkylammonium salts have a number of advantages. Ammonium carboxylates are much easier to prepare than the corresponding ester derivatives, and can be isolated as crystals with higher melting points. In most cases, after mixing muconic acid and the alkylamine in methanol, an ammonium salt is isolated as the crystalline solid by precipitation with a large amount of diethyl ether. Recrystallization from an appropriate solvent, typically from methanol, provides various types of crystals, needles, plates, or prisms, depending on the monomers. Three kinds of geometric isomers are also readily synthesized from the corresponding isomers of muconic acid without isomerization during the monomer preparation and purification. There are abundant variations in the crystal structures depending on the structure of the alkyl groups and on a hydrogen bond network pattern formed between the carboxylate and ammonium groups. The classification of diverse crystal structures is important for the prediction of the reactivity and the design of a topochemically polymerizable crystal from the viewpoint of crystal engineering. Primary ammonium carboxylates have great potential as supramolecular synthons to produce robust hydrogen bond networks. The polarized hydrogen bonds formed between the primary ammonium cations and the carboxylate anions, which act as triple hydrogen bond donors or acceptors, respectively, make one-dimensional ladder-type or two-dimensional sheet-type hydrogen bond networks. The countercations in the side chain can easily be converted after polymerization. This is closely related not only to the characterization of the resulting polymer, but also to the interesting features of organic intercalation.

Figure 13.22 1,3-Diene mono- and dicarboxylic acid derivatives that proceed topochemical polymerization in the crystalline state.

During the photoreaction of muconic acid derivatives in the crystalline state, the reaction pathway observed depends significantly on the structure of the derivatives. A survey of the photoreaction behavior of various (Z,Z)-muconic acid derivatives, including esters, amides, and ammonium salts bearing different alkyl substituents, has revealed the process of the topochemical polymerization of not only EMU but also several other derivatives under photoirradiation with a high-pressure mercury lamp or sunlight. Few of the compounds give polymer, most of them isomerize to the corresponding (E,E)-isomer or do not react at all. Figure 13.22 illustrates the chemical structures of the topochemically polymerizable 1,3-diene monomers.

Here, a single photoproduct obtained from the solid-state reactions is noteworthy; either a tritactic polymer or an (E,E)-isomer is obtained as the photoproduct. The following scheme represents specific photoreaction pathways observed during the photoirradiation of (Z,Z)-muconic acid derivatives in the crystalline state. The reaction path depends on the structure of the substituent X, CO_2R, $CONHR$, and $CO_2^-{}^+NH_3R$. This is contrast to the reaction in isotropic solution which results in a mixture of several products: the unreacted (Z,Z)-derivative, the (E,Z)- and (E,E)-derivatives, and a mixture of dimers. This indicates that the reaction path is controlled exclusively by the crystal lattice in the solid state as opposed to by the chemical nature of the compounds.

After the discoveries of topochemical polymerization in the 1960s, many researchers devoted themselves to studies of solid-state polymerization of vinyl and diene monomers, only to later conclude that topochemical polymerization of vinyl and diene monomers is not possible. Schmidt and co-workers[337–340] also studied the solid-state photoreactions of (Z,Z)- and (E,E)-muconic acid and methyl esters as well as nitrile compounds in the late 1960s. They reported that the acids and their methyl esters provided a stereospecific cyclobutane as the [2 + 2] cycloaddition products under crystal lattice control. The solid-state reactions of the sorbic derivatives were also investigated.[341,342] In these reports, however, they never referred to any topochemical polymerization of the 1,3-diene compounds, including the muconic and sorbic acid derivative. Later, Tieke[162] reported the solid-state polymerization of butadiene derivatives crystallized in perovskite-type layer structures that produced *erythro*-diisotactic-1,4-*trans*-polymers, as already described in Section 13.4.5.2. He also referred to the γ-radiation polymerization of molecular crystals of the sorbic acid derivatives with long-alkyl chains as the substituents in a paper published in 1985.[268]

In crystalline-state polymerization, the molecular arrangement of the monomers determines whether topochemical polymerization proceeds. Therefore, crystal structure analysis is a key for understanding the nature of topochemical polymerization and designing the structure of polymerizable monomer crystals. However, determination of the single crystal structure of EMU was not easy using a conventional automatic four-circle diffractometer or imaging plate system because the polymerization proceeded during the X-ray irradiation before collecting reflections necessary for the analysis. Tashiro et al. successfully determined the crystal structure of EMU using a CCD camera system, which can quickly collect the X-ray diffraction data with sufficiently quantitative intensity.[334] In the case of the EMU monomer crystal, the 5260 reflections required for the structure analysis were collected within the first 13 min of the measurement. The reflections of the monomer crystal were confirmed to retain almost unchanged intensities for about 60 min after starting the X-ray irradiation. The crystal structure of EMU is shown in Fig. 13.23. A single crystal of the poly (EMU) is obtained with less strain and fewer defects by the X- and γ-ray radiation polymerizations of the single crystal of the EMU monomer. In contrast, it is difficult from UV-irradiation polymerization to obtain a single crystal of poly(EMU) of similar quality. The crystallographic parameters are very similar to the EMU monomer determined at room temperature, and the same space group before and after the polymerization indicated that this polymerization is indeed a topochemical polymerization.

X-Ray structure analyses of the substituted benzylammonium (Z,Z)-muconates were carried out by Matsumoto and Sada et al. to clarify the relationship between the crystal structure and the reaction behavior.[343] The crystals of the benzylammonium derivatives have layer structures involving two-dimensional hydrogen bond networks, which are classified into two types on the basis of the molecular arrangement of the muconate dianions: a columnar structure and a sheet-type structure. In the former structure, the muconate dianions stack to make columns, which are sandwiched between two benzylammonium cation layers. The topochemically
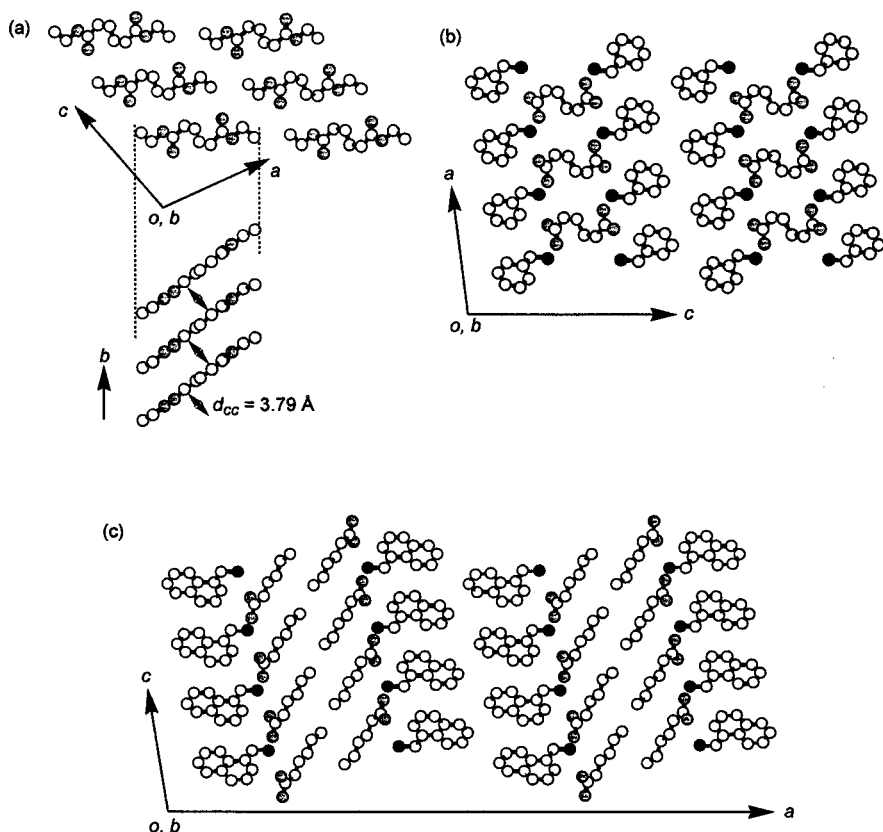
Figure 13.23 Crystal structures of (a) diethyl (*Z,Z*)-muconate, (b) di(benzylammonium) (*Z,Z*)-muconate, and (c) 1-naphthylmethylammonium (*E,E*)-sorbate. Hydrogen atoms are omitted for clarity.

polymerizable benzyl- and 2-chlorobenzylammonium derivatives belong to this category. These molecular packings in the crystals are very similar to the crystal structure of EMU (Fig. 13.23b). The other benzylammonium derivatives favor another structure, the sheet-type crystals, in which the muconate dianions are spread in a sheet and the substituents of the ammonium cations pillar the sheets.

A columnar structure is necessary for the polymerization of muconic acid derivatives in the crystalline state via a topochemical reaction mechanism. In the muconate columns, the diene moieties are arranged in a face-to-face manner. The intermolecular carbon-to-carbon distances between the reacting double bonds of the muconate anions in the column are approximately 4.2 Å for the crystals of the muconic acid derivatives, within a distance suitable for topochemical polymerization. The stereoregularity during the topochemical polymerization of this alignment of monomer molecules is expected for the formation of a polymer of

the *meso*-diisotactic-2,5-*trans* structure. This result significantly supports the stereo-regularity determined by NMR spectroscopy.

It has been demonstrated that the columnar stacking of diene moieties in the crystals is favored for the topochemical polymerization of the muconic acid derivatives. However, the stacking structures depend on the structure of the monomers. How can we design a columnar structure appropriate for topochemical polymerization without trials and errors? If there were any guide for the structural design of the diene monomers for the polymerization, it would be very useful for the control and design of not only the polymerization reaction but also the polymer crystal structure as the photoproducts. The introduction of a naphthalene ring as a substituent of the countercation was expected to effectively induce a column structure formation in the crystals because naphthalene rings favor herringbone stacking to pack the mono-mer molecules densely in a column due to π-π and CH/π interactions.[344–346]

The photoreaction of the 1-naphthylmethylammonium salts of the 1,3-diene monomers was carried out.[345] The naphthylmethylammonium salt of (*Z,Z*)-muconic acid provided a tritactic polymer, similar to the benzyl- and *n*-alkylammonium salts. The corresponding (*E,E*)-isomer also polymerized, differing from the results of the benzyl and *n*-alkylammonium salts of (*E,E*)-muconic acid that do not react under similar conditions. The stereoregularity of the polymer derived from the (*E,E*)-isomer was confirmed to be equal to that of the polymer derived from the (*Z,Z*)-isomer by ^{13}C NMR spectroscopy after polymer transformation to the triethyl-ammonium derivative. In contrast, the (*E,Z*)-isomer produced the corresponding (*E,E*)-isomer in very low yield. When the (*E,Z*)-isomer was irradiated, an atactic polymer was produced in low yield because of the isomerization of the (*E,Z*)-derivatives to the (*E,E*)-one, followed by the copolymerization of both isomers in the crystalline state.

Matsumoto et al. also found that the naphthylmethylammonium salts of mono-methyl (*E,E*)-muconate and (*E,E*)-sorbic acid polymerized in the crystalline state. The ^{13}C NMR spectra of these polymers after being transformed into soluble poly-mers indicated that the polymerization proceeded under crystal lattice control and the resulting polymers were tritactic polymers. In the powder X-ray diffraction pro-files of these polymers, sharp and intensive reflections as well as monomer crystals were observed. Thus, the introduction of a naphthylmethylammonium moiety is very effective for the induction of topochemical polymerization of 1,3-diene compounds.

During topochemical polymerization, the stereochemistry of the resulting polymer is determined by the stacking of the monomer molecules in a column formed in the crystals. Figure 13.24 shows the relationship between the monomer alignment and the stereoregular structure of the polymer.

There are two types of molecular packing configurations in the column. One is translational packing, which provides diisotactic polymer. Since most polymerizable diene monomers are translationally packed in the actual cases, both the (*Z,Z*)- and (*E,E*)-isomers provide identical polymers, the *meso*- or *erythro*-diisotactic polymer, irrespective of the monomer configuration. The other type of polymer such as *racemo*- or *threo*-diisotactic polymer could be obtained if the topochemical poly-merization of an (*E,Z*)-butadiene derivative proceeds with a similar mechanism.
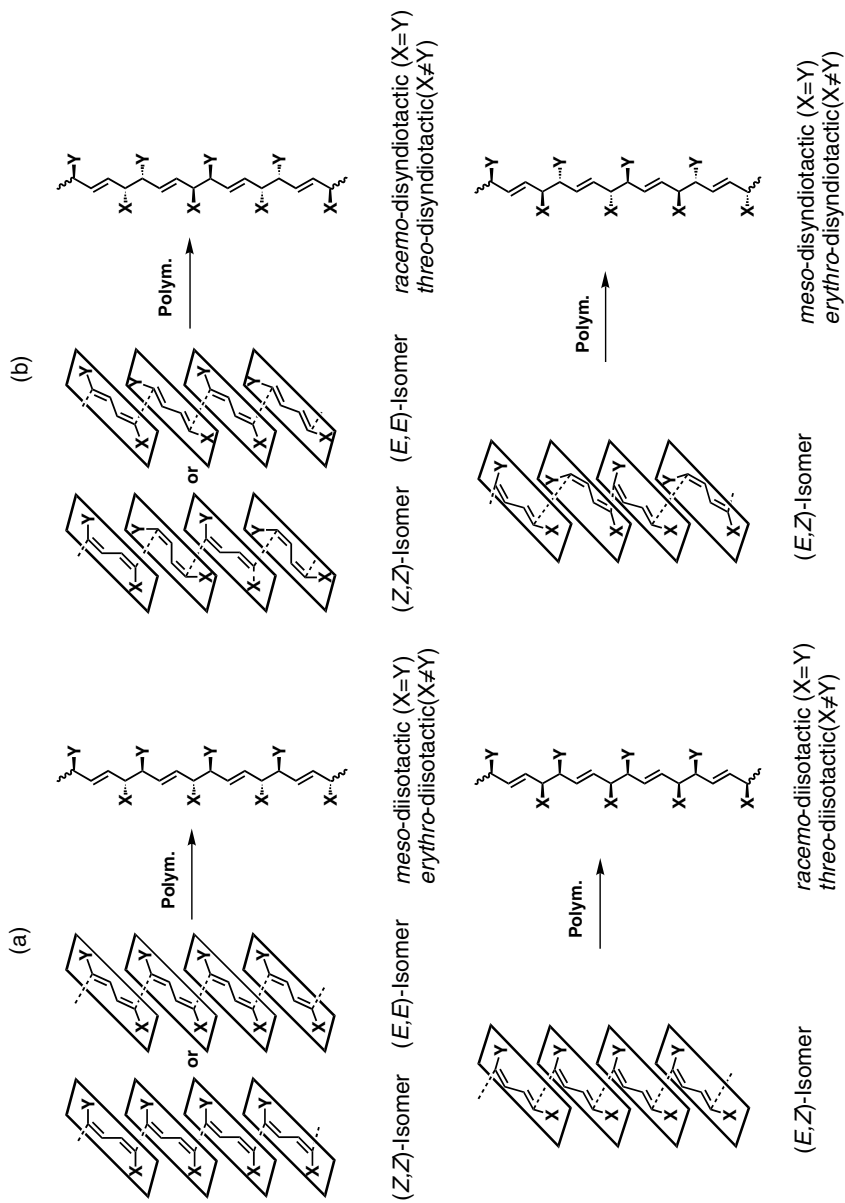
Figure 13.24 Relationship between the crystal packing of monomer molecules with different configurations and the stereochemical structures of polymers produced during topochemical polymerization of 1,4-disubstituted butadienes: (a) translational molecular packing in the column; (b) alternating molecular packing in the column.[346]

However, no successful polymerization has been found for any (E,Z)-derivative in the crystalline state. Another possible type of molecular packing is an alternating molecular packing. This sort of packing should yield disyndiotactic polymer due to the opposite direction of the diene moiety substituents in the polymerization column. Very recently, monomer crystals that provide syndiotactic stereoregular polymer have also been obtained despite the difficulty in controlling the crystal structure. In the crystals of di(4-methoxybenzyl) (Z,Z)- and (E,E)-inuconates, weak intermolecular interactions such as CH···O and CH/π interactions support the alternate molecular stacking in the column, appropriate for the syndiotactic polmer formation.[345] Based on the systematic investigation in recent years,[348–350] the topochemical polymerization principles have already been established for the polymerization of 1,3-diene derivatives,[351] and applied to the polymer architecture with a well-controlled structure in higher dimensions.[352,353] Thus, the concept of crystal engineering is very useful as a strategy for the rational design of molecular packing configuration in the crystal, although some difficulties yet have to be overcome in order to obtain the desired molecular packing in the crystals for the control of the stereoregularity of polymers.

Among the stereoregular polymers, the *racemo*-diisotactic polymer and the *erythro*- and *threo*-diisotactic polymers are chiral and possess optical activity, while the *meso*-diisotactic and *racemo*-diisotactic polymers are achiral because they have a mirror plane in the chain. Three other polymers, the *meso*-disyndiotactic, *erythro*-disyndiotactic, and *threo*-disyndiotactic polymers have no mirror plane, but they are not optically active because of the existence of a mirror glide plane. Matsumoto et al. obtained the *erythro*-diisotactic polymers prepared by the polymerization of the 1-naphthylmethylammonium salts of sorbic acid and monomethyl muconic acid. The optical rotation of these polymers was checked, but no significant value could be found. For the salt of sorbic acid, the space group of the monomer crystal is *C2/c*, which has a mirror glide plane and thus is achiral. Therefore, both optically active polymers of the right- and left-handed configurations are produced in the crystal, and the overall polymer has no optical activity. When we find a polymerizable crystal with any chiral space group, we would simultaneously succeed in an absolute asymmetric synthesis by topochemical polymerization. It will provide a polymer consisting of the main chain carbons with each sign of the absolute configuration.

13.4.5.6   Organic Intercalation into Polymer Crystals   *Intercalation* refers to the interesting phenomenon when guest species are reversibly inserted into a lamellar-host structure without altering the structural features of the host as shown by the
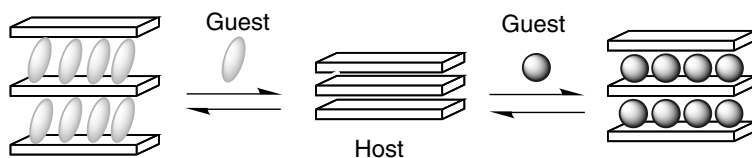
Figure 13.25   Schematic model of intercalation.[201]
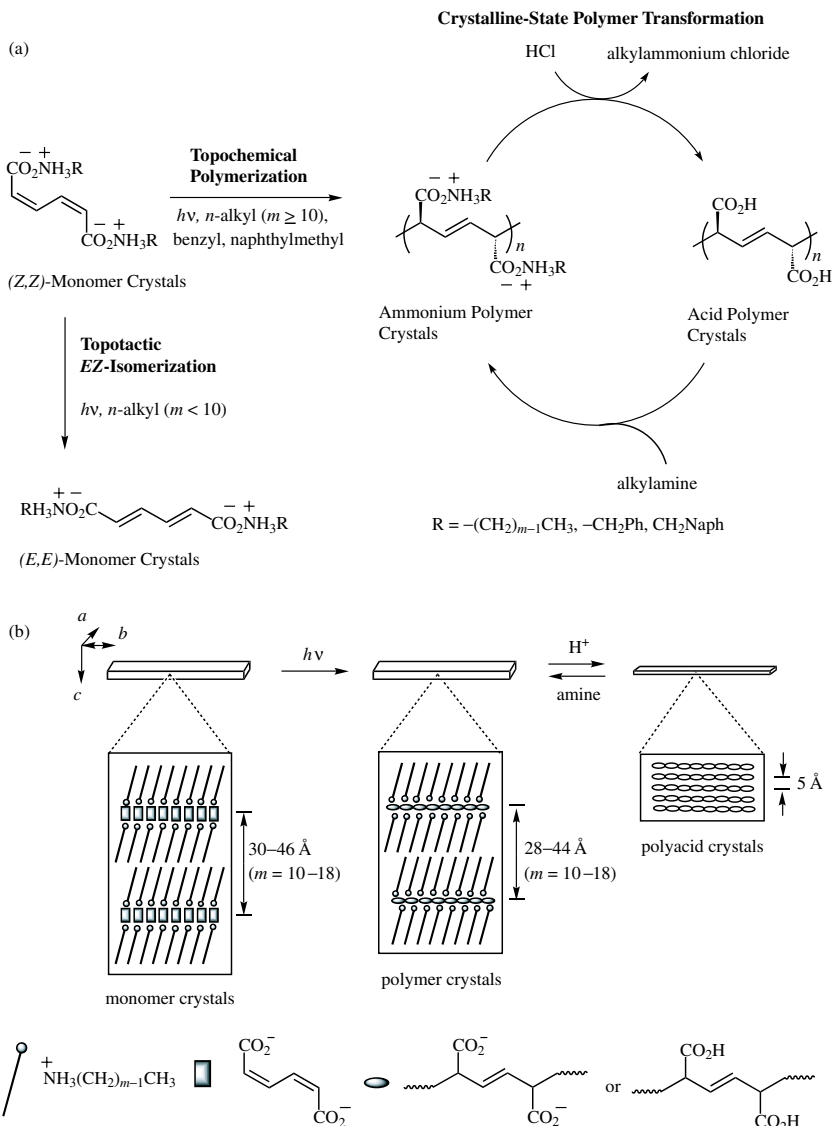
Figure 13.26 (a) Photoreactions and polymer transformation performed in the crystalline state. Depending on the carbon number of the *n*-alkylammonium group, alkylammonium (Z,Z)-muconate undergoes either topochemical polymerization or topotactic *EZ*-isomerization when exposed to photoirradiation in the crystalline state. The ammonium polymer crystals obtained by the topochemical polymerization are converted in the crystalline state to acid polymer crystals via polymer transformation. The reverse reaction from polyacid to the ammonium polymers also occurs. (b) Model of photopolymerization and polymer transformation performed in the crystalline state. The alkylamine molecules and protons are possibly introduced via the *ac* plane of the acid and ammonium polymer crystals. (*Source*: Ref. 359.)

schematic model in Fig. 13.25. The host recognizes guest species and accepts them with a reversible change using noncovalent bonding, as is typically seen in inorganic materials such as graphite, clay, and metal oxides.[354] In contrast to many kinds of intercalation materials consisting of inorganic compounds, inorganic–organic hybrids, and DNA, very few examples of intercalation by organic compounds are known.[355–358] Recently, Matsumoto et al. first reported that the alkylammonium muconate polymer crystals act as a unique intercalation compound (see also Fig. 13.26).[359,360] The ammonium polymer crystals are converted into the poly-(muconic acid) crystals by solid-state hydrolysis, and the process is reversible; an alkylamine is intercalated into the acid polymer crystals in the crystalline state.

The polymer crystals of the alkylammonium muconates have a layer structure, which is similar to that of the monomer crystals since the crystal structure is maintained during the polymerization, as well as the pattern of the hydrogen bond network. The muconate polymer sheet is sandwiched between two alkylammonium layers to make a BAB-type stacking unit, where A and B refer the acid and base layers, respectively. The BAB layers stack further in the crystals. The interface between the A and B layers is tightly fixed by the electrostatic interaction due to the salt formation and by the two-dimensional hydrogen bond network. In contrast, the B layers interact with each other by a weak interaction. Surprisingly, the ammonium layers can be removed and repeatedly inserted into the crystalline state. Polymer crystals prepared by topochemical polymerization of alkylammonium muconate are transformed into other kinds of alkylammonium salts via the poly (muconic acid) by heterogeneous reactions. Poly(muconic acid) is quantitatively obtained by the treatment of poly(alkylammonium muconate) in HCl methanol solution. After that, various alkylamines are intercalated into the poly(muconic acid) crystal by immersion in a methanol solution of the alkylamine. When *n*-alkylamines and benzylamine are used, the transformation occurs with high efficiency (94–96% conversion). These transformations are completely heterogeneous because the polymer crystals of both the acid and ammonium salts are insoluble. Repeated cycling of the ammonium-acid transformation also provides similar polymer crystals without collapse of the layer structure despite the drastic changes in the crystal volume during transformation.

The *d* value, the interplanar distance between the layers, is determined by the size of the intercalated amines. Figure 13.27 shows the relationship between the carbon number of the *n*-alkyl group and the *d* value observed for the monomer crystals, the polymer crystal without transformation, and the polymer crystal prepared by the intercalation. All the crystals produce a similar slope; the thickness of the alkylammonium layer is increased by 1.0 Å for each carbon in the *N*-alkyl substituent. This increment suggests an alkyl chain structure with a tilt angle of 38° against the stacking layers, but not an interdigitation structure. The difference between the *d* values for the monomer and polymer crystals is due to the rotation of the muconate moiety during the polymerization.

The intercalation reaction was investigated under various conditions. It was found that the type of dispersant significantly influenced the conversion, although the reaction proceeded heterogeneously. Polymer chains in the polymer crystals with
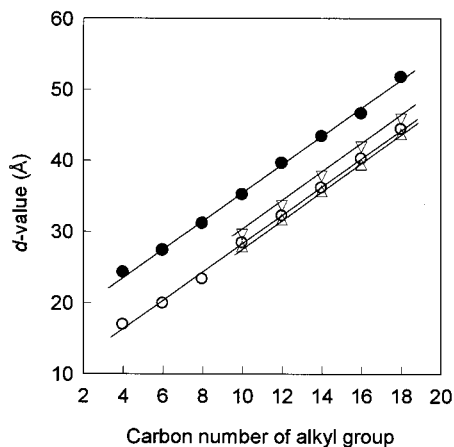
Figure 13.27   Relationship between carbon number of *n*-alkyl group of ammonium cation and the *d* value for *n*-alkylammonium (*Z,Z*)-muconates and sorbates, (∇) *n*-alkylammonium muconate monomer crystal, ($\triangle$) *n*-alkylammonium muconate polymer crystal obtained as polymerized, ($\bigcirc$) *n*-alkylammonium muconate polymer crystal obtained by intercalation, ($\bullet$) *n*-alkylammonium sorbate crystals obtained by intercalation. (*Source*: Ref. 201.)

a stereoregular structure are aligned with the *b* axis of the crystals and linked to each other by the two-dimensional hydrogen bond network. Both covalent and hydrogen bonds support the reversible crystal-to-crystal transformation. The cooperative process of the insertion of the molecules and the formation of restructured layers is indispensable for the quantitative transformation. The intercalation of secondary and tertiary amines was also attempted, but the conversion was low despite increasing basicity. The steric requirement around the polymer chain is more important than the basicity, thus resulting in failed intercalation of the secondary and tertiary amines. It is also due to the change in the fashion of the hydrogen bond network by the decrease in the number of hydrogens in the ammonium cation. In other words, poly(muconic acid) crystals memorize the crystal structure of poly-(ammonium muconate) and recognize the kinds of alkylamine. In the case of a suitable alkylamine with memorized polymer crystal structure of the ammonium salts, the intercalation reaction proceeds with quantitative conversion.

   More recently, the intercalation behavior of the polymer crystals of sorbic acid derivatives was also investigated. The alkylammonium sorbate monomer crystals as well as the corresponding polymer crystals have a BAAB-type layer structure, which is different from the BAB layer of the muconate derivatives. The interface between the A and B layers is similar to that in the muconate crystals. In the sorbate crystals, not only the B-B but also the A-A interfaces interact with each other by a weak van der Waals force.

   It has in fact been found that the polymer crystals derived from sorbic acid derivatives exhibit intercalation behavior different from that of the muconic acid derivatives. For example, the incorporation efficiency for the intercalation of
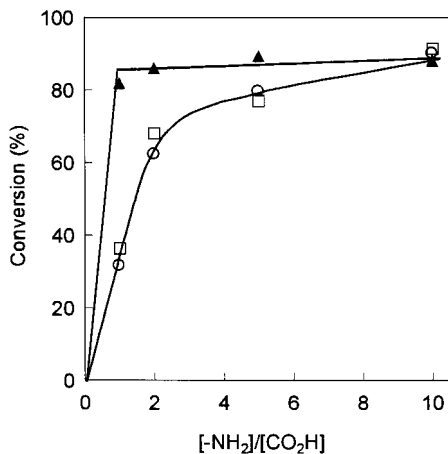
Figure 13.28   Relationship between $[-NH_2]/[-CO_2H]$ and the conversion of intercalation of dodecylamine into polymer crystals, (▲) poly(muconic acid), 1 h, (□) poly(sorbic acid), 2 h, (○) poly(sorbic acid), 5 h. (*Source*: Ref. 201.)

dodecylamine into the poly(sorbic acid) crystals was lower than the results of the intercalation into poly(muconic acid) under similar conditions. Quantitative intercalation was achieved for the poly(sorbic acid) system by use of a large excess of the amine and long reaction times, different from the rapid incorporation into poly(muconic acid) under mild conditions with an equimolar amount of the amine within a few hours (Fig. 13.28). Both polymer crystals gave a similar slope in the plots of the dependence of the carbon number of the *n*-alkyl groups on the interplanar spacing *d*, as shown in Fig. 13.27. This indicates that the alkyl chain structure stacked in the layers of these polymer crystals has a similar tilt structure, despite the differences in the polymer chain structures and the reaction behavior during the intercalation. The introduction of various functional groups that induce chemical reactions, molecular recognition, separation, and physical interactions into the specific and robust layer structures in the organic polymer crystals would be useful, thus leading to the first step in finding a new strategy for the design of functional organic solids.

13.5   CONCLUSION

In recent years, a great number of successful results have been reported on polymer structure control by radical polymerization, as described in this and previous chapters. Figure 13.29 illustrates several targets for the control of the primary chain structure of polymers, including molecular weight, molecular weight distribution, chain-end structure, branching, regioselectivity (head-to-tail structure), and stereoselectivity (tacticity) as well as comonomer sequence. The precise control of polymer chain structures is important in polymer synthesis because the chemical and
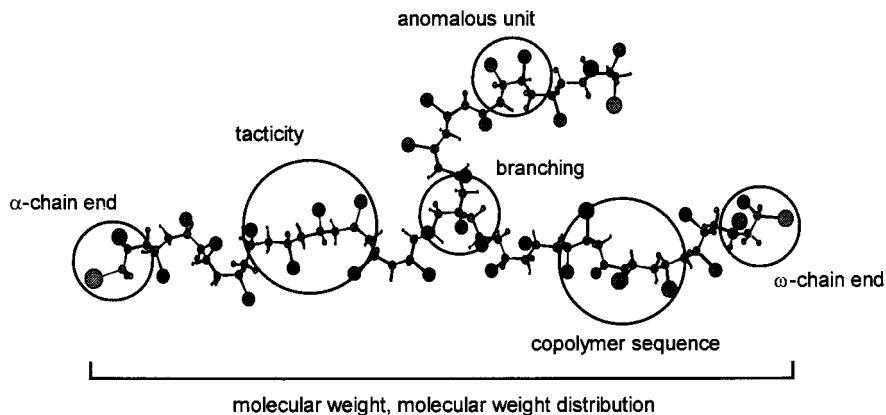
Figure 13.29 Targets for the control of primary chain structure during radical polymerization.

physical properties of polymers significantly depend on the primary chain structures. Controls of polymerization reactions as well as of polymer structures as the reaction products are indispensable for the design of new organic materials and the architecture of three-dimensional nanocomposites as advanced polymeric materials.

There are two fundamentally different approaches to stereochemical control of polymers during free-radical polymerization: (1) catalytic control of the propagating chain end using Lewis acids, solvents, and chiral auxiliaries, as described in Section 13.3, and (2) use of polymerizations in organized and constrained media, as seen in Section 13.4. The former is useful for the polymerization of many kinds of monomers, especially conventional monomers. If we can completely control the stereoregularity of polyacrylates, polymethacrylates, poly(vinyl alcohol), and the other commodity polymers obtained from polar vinyl monomers, they could be used as a new type of engineering plastics. Modern radical polymerization is clearly different from classical radical polymerization, which was the convenient but less-controlled method for the production of vinyl polymers. Modern and highly controlled radical polymerization is sophisticated and sensitive to the polymerization conditions similar to anionic and the other ionic or coordination polymerizations. We should learn much more from ionic polymerizations and organic synthetic chemistry in order to develop modified and superior radical polymerization procedures. Controlled polymerizations of organized monomers are useful not only for the control of polymer tacticity but also for the fabrication of polymer composites and materials designed on the basis of supramolecular architecture. In particular, topochemical polymerization that proceeds in the crystalline state has various merits, such as an organic solvent free system, and a synthetic process with highly selectivity and stereoselectivity without the need for separation and purification. The present methods and techniques for polymer structure control, including stereochemical control during radical polymerization, are obviously not satisfactory today and

still remain in their infancy stage. In the future, more efforts will be directed towards this field, and then new inventive methods will be developed in order to fabricate polymers with truly desired structures and properties by radical polymerization.

REFERENCES

1. D. Schlüter, ed., *Synthesis of Polymers,* Wiley-VCH, Weinheim, 1999.

2. G. Odian, *Principles of Polymerization*, 3rd ed., Wiley, New York, 1991.

3. G. Moad and D. H. Solomon, *The Chemistry of Free Radical Polymerization* Pergamon: Oxford, 1995.

4. T. Otsu and A. Matsumoto, *Adv. Polym. Sci.* **136**, 75 (1998).

5. K. Matyjaszewski, ed., *Controlled Radical Polymerization*, ACS Symposium Series 685, American Chemical Society: Washington, DC, 1998.

6. K. Matyjaszewski, ed., *Controlled/Living Radical Polymerization*, ACS Symposium Series 768, American Chemical Society: Washington, DC, 2000.

7. D. P. Curran, N. A. Porter, and B. Giese, *Stereochemistry of Radical Reactions*, VCH, Weinheim, 1996.

8. P. Renaud and M. P. Sibi, ed., *Radicals in Organic Synthesis*, Vols. 1 and 2, Wiley-VCH, Weinheim, 2001.

9. C. M. Paleos, ed., *Polymerization in Organized Media*, Gordon and Breach, Philadelphia, 1992.

10. B. Giese, *Angew. Chem. Int. Ed. Engl.* **22**, 753 (1983).

11. B. Giese, *Angew. Chem. Int. Ed. Engl.* **28**, 969 (1989).

12. D. P. Curran, *Synthesis* 417 (1988).

13. D. P. Curran, *Synthesis* 489 (1988).

14. N. A. Porter, B. Giese, and D. P. Curran, *Acc. Chem. Res.* **24**, 296 (1991).

15. B. Giese, M. Bulliard, J. Dickhaut, R. Halbach, C. Hassler, U. Hoffmann, B. Hinzer, and M. Senn, *Synlett* 116 (1995).

16. B. Giese, Vol. 1, p. 381 in Ref. 8.

17. B. Giese, W. Damm, F. Wetterich, and H.-G. Zeitz, *Tetrahedron Lett.* **33**, 1863 (1992).

18. Y. Guindon, C. Yoakim, R. Lemieux, L. Beisvert, D. Delorme, and J.-F. Lavallée, *Tetrahedron Lett.* **31**, 2845 (1990).

19. B. Giese, W. Damm, F. Wetterich, H.-G. Zeitz, J. Rancourt, and Y. Guindon, *Tetrahedron Lett.* **34**, 5855 (1993).

20. B. Guérin, W. W. Ogilve, and Y. Guindon, Vol. 1, p. 441 in Ref. 8.

21. Y. Guindon, J.-F. Lavallée, M. Llinas-Brunet, G. Horner, and J. Rancourt, *J. Am. Chem. Soc.* **113**, 9701 (1991).

22. Y. Guindon, B. Guérin, C. Chabot, N. Mackintosh, and W. W. Ogilvie, *Synlett* 449 (1995).

23. Y. Guindon and J. Rancourt, *J. Org. Chem.* **63**, 6554 (1998).

24. N. A. Porter, Vol. 1, p. 416 in Ref. 8.

25. D. P. Curran, S. J. Geib, and C. H. Lin, *Tetrahedron Asymmetry* **5**, 199 (1994).

26. M. P. Sibi and N. A. Porter, *Acc. Chem. Res.* **32**, 163 (1999).

27. M. P. Sibi, J. Ji, J. B. Sausker, and C. P. Jasperse, *J. Am. Chem. Soc.* **121**, 7517 (1999).

28. N. A. Porter, R. L. Carter, C. L. Mero, M. G. Roepel, and D. P. Curran, *Tetrahedron* **52**, 4181 (1996).

29. J. H. Wu, R. Radinov, and N. A. Porter, *J. Am. Chem. Soc.* **117**, 11029 (1995).

30. M. P. Sibi, J. G. Ji, J. H. Wu, S. Gurtler, and N. A. Porter, *J. Am. Chem. Soc.* **118**, 9200 (1996).

31. N. A. Porter, J. H. Wu, G. Zhang, and A. D. Reed, *J. Org. Chem.* **62**, 6702 (1997).

32. M. P. Sibi and T. R. Rheault, Vol. 1, p. 461 in Ref. 8.

33. (a) C. DeMello and D. P. Curran, *J. Am. Chem. Soc.* **120**, 329 (1998); (b) D. P. Curran, C.-H. Lin, N. C. DeMello, and J. Junggebauer, *J. Am. Chem. Soc.* **120**, 342 (1998).

34. D. P. Curran, W. Liu, and C. H.-T. Chen, *J. Am. Chem. Soc.* **121**, 11012 (1999).

35. D. P. Curran, H. Qi, S. J. Geib, and N. C. DeMello, *J. Am. Chem. Soc.* **116**, 3131 (1994).

36. N. A. Porter and P. J. Krebs, *Top. Stereochem.* **18**, 97 (1988).

37. R. Braslau, N. Naik, and H. Zipse, *J. Am. Chem. Soc.* **122**, 8421 (2000).

38. B. Giese, P. Wettstein, C. Stähelin, F. Barbosa, M. Neuburger, M. Zehnder, and P. Wessig, *Angew. Chem. Int. Ed. Engl.* **38**, 2586 (1999).

39. B. Giese, F. Barbosa, C. Stähelin, S. Sauer, P. Wettstein, and C. Wyss, *Pure Appl. Chem.* **72**, 1623 (2000).

40. T. Hirano, W. Li, L. Abrams, P. J. Krusic, M. F. Ottaviani, and N. J. Turro, *J. Org. Chem.* **65**, 1319 (2000).

41. N. J. Turro, *Acc. Chem. Res.* **33**, 637 (2000).

42. W. V. Metanomski, *Compendium of Macromolecular Nomenclature*, Commission on Macromolecular Nomenclature, IUPAC Macromolecular Division, Blackwell Scientific, Oxford, 1991; see also, *Pure Appl. Chem.* **53**, 733 (1981).

43. E. L. Eliel and S. H. Wilen, *Stereochemistry of Organic Compounds*, Wiley, New York, 1994.

44. S. R. Buxton and S. M. Roberts, *Guide to Organic Stereochemistry*, Pearson Education, New York, 1996.

45. F. A. Bovey, *Chain Structure and Conformation of Macromolecules*, Academic Press, New York, 1982.

46. G. Odian, Chapter 8, p. 604 in Ref. 2.

47. M. Farina, *Top. Stereochem.* **17**, 1 (1987).

48. K. Hatada and T. Kitayama, *Polym. Internal.* **49**, 11 (2000).

49. K. Hatada, T. Kitayama, and K. Ute, *Prog. Polym. Sci.* **13**, 189 (1988).

50. H. Yasuda, *Prog. Polym. Sci.* **25**, 573 (2000).

51. G. Moad, D. H. Solomon, T. H. Spurling, S. R. Jones, and R. I. Willing, *Aust. J. Chem.* **39**, 43 (1986).

52. R. Chûjô, K. Hatada, R. Kitamaru, T. Kitayama, H. Sato, and Y. Tanaka, *Polym. J.* **19**, 413 (1987).

53. Y. Okamoto and T. Nakano, *Chem. Rev.* **94**, 349 (1994).

54. H. Yuki, K. Hatada, T. Niinomi, and Y. Kikuchi, *Polym. J.* **1**, 36 (1970).

55. Y. Okamoto, M. Ishikura, K. Hatada, and H. Yuki, *Polym. J.* **15**, 851 (1983).

56. Y. Okamoto, M. Nishikawa, T. Nakano, E. Yashima, and K. Hatada, *Macromolecules* **28**, 5135 (1995).

57. K. Hatada, T. Kitayama, T. Ochi, and H. Yuki, *Polym. J.* **19**, 1105 (1987).

58. M. Kamachi, M. Kohno, D. J. Liaw, and S. Katsuki, *Polym. J.* **10**, 69 (1978).

59. M. Kamachi, Y. Kuwae, S. Nozakura, K. Hatada, and H. Yuki, *Polym. J.* **13**, 919 (1981).

60. T. Nakano, A. Matsuda, and Y. Okamoto, *Polym. J.* **28**, 556 (1996).

61. T. Nakano, Y. Shikisai, and Y. Okamoto, *Polym. J.* **28**, 51 (1996).

62. Y. Okamoto and E. Yashima, *Prog. Polym. Sci.* **15**, 263 (1990).

63. T. Nakano, Y. Shikisai, and Y. Okamoto, *Proc. Jpn. Acad. Ser. B* **71**, 251 (1995).

64. T. Nakano and Y. Okamoto, *Macromolecules* **32**, 2391 (1999).

65. A. Gridnov, *J. Polym. Sci.; Part A: Polym. Chem.* **38**, 1753 (2000).

66. T. Nakano, N. Kinjo, Y. Hidaka, and Y. Okamoto, *Polym. J.* **31**, 464 (1999).

67. K. Matsuzaki, T. Kanai, T. Kawamura, S. Matsumoto, and T. Uryu, *J. Polym. Sci., Polym. Lett. Ed.* **11**, 961 (1973).

68. K. Matsuzaki, T. Uryu T. Kanai, H. Hosonuma, T. Matsubara, H. Tachikawa, M. Yamada, and S. Okuzono, *Makromol. Chem.* **178**, 11 (1977).

69. T. Tanaka, S. Habaue, and Y. Okamoto, *Polym. J.* **27**, 1202 (1995).

70. M. K. Akkapeddi, *Macromolecules* **12**, 546 (1979).

71. J. Suenaga, D. M. Sutherlin, and J. K. Stille, *Macromolecules* **17**, 2913 (1984).

72. N. A. Porter, T. R. Allen, and R. A. Breyer, *J. Am. Chem. Soc.* **114**, 7676 (1992).

73. G. S. Miracle, S. M. Cannizzaro, and N. A. Porter, *Chemtracts Org. Chem.* **6**, 147 (1993).

74. N. A. Porter, G. S. Miracle, S. M. Cannizzaro, R. L. Carter, A. T. McPhail, and L. Liu, *J. Am. Chem. Soc.* **116**, 10255 (1994).

75. N. A. Porter, I. J. Rosenstein, R. A. Breyer, J. D. Brunhnke, W. Wu, and A. T. McPhail, *J. Am. Chem. Soc.* **114**, 7664 (1992).

76. N. Beredjik and C. Schuerch, *J. Am. Chem. Soc.* **80**, 1933 (1958).

77. B. B. De, S. Sivaram, and P. K. Dhal, *Macromolecules* **29**, 468 (1996).

78. (a) G. Wulff, *CHEMTECH* 364 (1991); (b) G. Wulff, p. 375 in Ref. 1.

79. T. Kakuchi, H. Kawai, S. Katoh, O. Haba, and Y. Yokota, *Macromolecules* **25**, 5545 (1992).

80. T. Nakano and D. Y. Sogah, *J. Am. Chem. Soc.* **117**, 534 (1995).

81. T. Nakano, Y. Okamoto, D. Y. Sogah, and S. Zheng, *Macromolecules* **28**, 8705 (1995).

82. G. Wulff, *Angew. Chem., Int. Ed., Engl.* **28**, 21 (1989).

83. G. Wulff, R. Kemmerer, and B. Vogt, *J. Am. Chem. Soc.* **109**, 7449 (1987).

84. G. Wulff and P. K. Dhal, *Angew. Chem. Int. Ed. Engl.* **28**, 196 (1989).

85. K. Yokota, T. Kakuchi, T. Uesaka, and M. Obata, *Acta Polym.* **48**, 459 (1997).

86. T. Kakuchi, A. Narumi, H. Kaga, Y. Yamauchi, M. Obata, T. Uesaka, and K. Yokota, *Macromolecules* **34**, 38 (2001).

87. M. Seno, Y. Kawamura, and T. Sato, *Macromolecules* **30**, 6417 (1997).

88. M. Seno, T. Ikezumi, T. Sumie, Y. Masuda, and T. Sato, *J. Polym. Sci.; Part A: Polym. Chem.* **38**, 2098 (2000).

89. S. Kataoka and T. Ando, *Kobunshi Ronbunshu* **37**, 185 (1980).

90. S. Kataoka and T. Ando, *Kobunshi Ronbunshu* **38**, 797 (1981).

91. S. Kataoka and T. Ando, *Kobunshi Ronbunshu* **38**, 821 (1981).

92. S. Kataoka and T. Ando, *Kobunshi Ronbunshu* **41**, 511 (1984).

93. S. Kataoka and T. Ando, *Kobunshi Ronbunshu* **37**, 375 (1980).

94. T. Nakano and Y. Okamoto, p. 451 in Ref. 5.

95. J. B. Lando, J. Semen, and B. Farmer, *Macromolecules* **3**, 524 (1973).

96. J. Barton and E. Borsig, *Complexes in Free-Radical Polymerization*, Elsevier, Amsterdam, 1988.

97. C. H. Bamford, A. D. Jenkins, and R. Johnson, *Proc. Royal Soc.* **A241**, 364 (1957).

98. C. H. Bamford, S. Brumby, and R. P. Wayne, *Nature* **209**, 202 (1966).

99. T. Otsu, B. Yamada, and M. Imoto, *J. Macromol. Chem.* **1**, 61 (1966).

100. S. Okuzawa, H. Hirai, and S. Makishima, *J. Polym. Sci.; Part A-1* **7**, 1039 (1969).

101. A. Matsumoto and S. Nakamura, *J. Appl. Polym. Sci.* **74**, 290 (1999).

102. S. Habaue and Y. Okamoto, *Chem. Record* **1**, 46 (2001).

103. Y. Gotoh, T. Iihara, N. Kanai, N. Toshima, and H. Hirai, *Chem. Lett.* 2157 (1990).

104. Y. Gotoh, M. Yamashta, M. Nakamura, N. Toshima, and H. Hirai, *Chem. Lett.* 53 (1991).

105. S. Habaue, T. Uno, and Y. Okamoto, *Polym. J.* **31**, 900 (1999).

106. S. Habaue, T. Uno, H. Baraki, and Y. Okamoto, *Macromolecules* **33**, 820 (2000).

107. H. Baraki, S. Habaue, and Y. Okamoto, *Macromolecules* **34**, 4724 (2001).

108. T. Nakano, D. Tamada, J. Miyazaki, K. Kakiuchi, and Y. Okamoto, *Macromolecules* **33**, 1489 (2000).

109. Y. Isobe, D. Fujioka, S. Habaue, and Y. Okamoto, *J. Am. Chem. Soc.* **123**, 7180 (2001).

110. C. Reichardt, *Solvents and Solvent Effects in Organic Chemistry*, 2nd ed., VCH, Weinheim, 1988, p. 121.

111. J. M. Tanko and N. K. Suleman, in *Energies of Organic Free Radicals*, J. A. M. Simoes, A. Greenberg, and J. F. Liebman, eds., Chapman and Hall, London 1996, p. 224.

112. M. Kamachi, *Ad. Polym. Sci.* **38**, 55 (1981).

113. M. L. Coote, T. P. Davis, B. Klumperman, and M. J. Monteiro, *J. Macromol. Sci., Rev. Chem. Phys.* **C38**, 567 (1998).

114. K. F. O'Driscoll, M. J. Monteiro, and B. Klumperman, *J. Polym. Sci.; Part A: Polym. Chem.* **35**, 515 (1997).

115. M. D. Zammit, T. P. Davis, G. D. Willett, and K. F. O'Driscoll, *J. Polym. Sci.; Part A: Polym. Chem.* **35**, 2311 (1997).

116. S. Beuermann, D. A. Paquet, Jr., J. H. McMinn, and R. A. Huchinson, *Macromolecules* **30**, 194 (1997).

117. T. Sato, T. Shimizu, M. Seno, H. Tanaka, and T. Ota, *Makromol. Chem.* **193**, 1439 (1992).

118. T. Sato, K. Masaki, K. Kondo, M. Seno, and H. Tanaka, *Polym. Bull.* **35**, 345 (1995).

119. A. Matsumoto, R. Hiuke, and T. Doi, *J. Polym. Sci.; Part A: Polym. Chem.* **35**, 1515 (1997).

120. M. G. Krakovyak, E. V. Annrieva, E. A. Sycheva, and T. V. Sheveleva, *Macromolecules* **26**, 7375 (1993).

121. Y. Isobe, K. Yamada, T. Nakano, and Y. Okamoto, *Macromolecules* **32**, 5979 (1999).

122. A. Matsumoto and Y. Mohri, *J. Polym. Sci.; Part A: Polym. Chem.* **37**, 2803 (1999).

123. S. Nozakura, M. Sumi, M. Uoi, T. Okamoto, and S. Murahashi, *J. Polym. Sci., Polym. Chem. Ed.* **11**, 279 (1973).

124. S. Nozakura, T. Okamoto, K. Toyora, and S. Murahashi, *J. Polym. Sci., Polym. Chem. Ed.* **11**, 1043 (1973).

125. K. Imai, T. Shiomi, N. Oda, H. Otsuka, and Y. Tezuka, *J. Polym. Sci., Polym. Chem. Ed.* **24**, 3225 (1986).

126. K. Imai, T. Shiomi, Y. Tezuka, T. Kawanishi, and T. Jin, *J. Polym. Sci., Polym. Chem. Ed.* **26**, 1961 (1988).

127. R. Fukae, T. Yamamoto, Y. Fujita, N. Kawatsuki, O. Sangen, and M. Kamachi, *Polym. J.* **29**, 293 (1997).

128. T. Otsu, A. Matsumoto, K. Endo, and H. Kataoka, *Mem. Fac. Eng., Osaka City Univ.* **29**, 161 (1988).

129. T. Yamamoto, S. Yoda, O. Sangen, R. Fukae, and M. Kamachi, *Polym. J.* **21**, 1053 (1989).

130. K. Yamada, T. Nakano, and Y. Okamoto, *Proc. Jpn. Acad., Ser. B* **74**, 46 (1998).

131. K. Yamada, T. Nakano, and Y. Okamoto, *Macromolecules* **31**, 7598 (1998).

132. K. Yamada, T. Nakano, and Y. Okamoto, *J. Polym. Sci.; Part A: Polym. Chem.* **37**, 2677 (1999).

133. K. Yamada, T. Nakano, and Y. Okamoto, *J. Polym. Sci.; Part A: Polym. Chem.* **38**, 220 (2000).

134. K. Yamada, T. Nakano, and Y. Okamoto, *Polym. J.* **32**, 707 (2000).

135. P. Pino and U. W. Suter, *Polymer* **17**, 977 (1996).

136. M. K. Akkappeddi and H. K. Reimschuessel, *Macromolecules* **11**, 1067 (1978).

137. R. E. Cais, *Macromolecules* **13**, 806 (1980).

138. A. E. Tonelli, F. C. Schilling, and R. E. Cais, *Macromolecules* **14**, 560 (1981).

139. R. Bacskai, L. P. Lindeman, and D. L. Rabenstein, *J. Polym. Sci.; A-1* **10**, 1297 (1972).

140. K. Komber, L. Jakisch, S. Zschoche, H. Mobus, M. Rätzsch, and D. Scheller, *Makromol. Chem., Rapid Commun.* **12**, 547 (1991).

141. A. Matsumoto and T. Otsu, *Macromol. Symp.* **98**, 139 (1995).

142. X. Wang, T. Komoto, I. Ando, and T. Otsu, *Makromol. Chem.* **189**, 1845 (1988).

143. M. Yoshioka, A. Matsumoto, T. Otsu, and I. Ando, *Polymer* **32**, 2741 (1991).

144. M. Yoshioka, A. Matsumoto, and T. Otsu, *Polym. J.* **23**, 1191 (1991).

145. M. Yoshioka, A. Matsumoto, and T. Otsu, *Macromolecules* **25**, 2837 (1992).

146. M. Yoshioka, A. Matsumoto, and T. Otsu, *Polym. J.* **23**, 1249 (1991).

147. T. Kitano, S. Kawaguchi, K. Ito, and A. Minakata, *Macromolecules* **20**, 1598 (1987).

148. T. Kitano, A. Ishigaki, G. Uematsu, S. Kawaguchi, and K. Ito, *J. Polym. Sci.; Part A: Polym. Chem.* **25**, 979 (1987).

149. J.-S. Wang and K. Matyjaszewski, *Macromolecules* **28**, 7901 (1995).

150. T. Ando, M. Kamigaito, and M. Sawamoto, *Macromolecules* **30**, 4507 (1997).

151. H. Takahashi, T. Ando, M. Kamigaito, and M. Sawamoto, *Macromolecules* **32**, 6461 (1999).

152. D. M. Haddleton, D. Kukulj, D. J. Duncalf, A. M. Heming, and A. J. Shooter, *Macromolecules* **31**, 5201 (1998).

153. D. M. Haddleton, D. J. Duncalf, D. Kukulj, A. M. Heming, A. J. Shooter, and A. J. Clark, *J. Mater. Chem.* **8**, 1525 (1998).

154. H. Komber, M. Gruner, and H. Malz, *Macromol. Rapid Commun.* **19**, 83 (1998).

155. E. Yoshida and T. Fujii, *J. Polym. Sci.; Part A: Polym. Chem.* **36**, 269 (1998).

156. R. D. Puts and D. Y. Sogah, *Macromolecules* **29**, 3323 (1996).

157. E. E. Schneider, M. J. Day, and G. Stein, *Nature* **168**, 645 (1951).

158. B. Rånby and J. F. Rabek, *ESR Spectroscopy in Polymer Research*, Springer, New York, 1977.

159. M. Kamachi, *Adv. Polym. Sci.* **82**, 207 (1987).

160. B. Yamada, D. Westmoreland, S. Kobatake, and O. Konosu, *Prog. Polym. Sci.* **24**, 565 (1999).

161. W. Lung-min and H. Fischer, *Helv. Chim. Acta* **66**, 138 (1983).

162. W. Strub, E. Roduner, and H. Fischer, *J. Phys. Chem.* **91**, 4379 (1987).

163. M. V. Barnabas, K. Venkateswaran, and D. C. Walker, *J. Am. Chem. Soc.* **112**, 7163 (1990).

164. P. Smith, J. T. Pearson, P. B. Wood, and T. Smith, *J. Phys. Chem.* **43**, 1535 (1965).

165. H. Fischer, *Z. Naturforsch.* **19a**, 267 (1964).

166. H. Fischer, *Z. Naturforsch.* **19a**, 866 (1964).

167. K. Takakura and B. Rånby, *J. Polym. Sci., C* **22**, 939 (1968).

168. M. J. Davies and B. C. Gilbert, *J. Chem. Soc., Perkin Trans. II* 1809 (1984).

169. H. Fischer and G. Giacometti, *J. Polym. Sci., C* **16**, 2763 (1967).

170. C. Corvaja, H. Fischer, and G. Giacometti, *Z. Phys. Chem.* (*Frankfurt*) **45**, 1 (1965).

171. S. Brumby, *J. Magn. Reson.* **10**, 203 (1973).

172. F. R. Hewill and G. M. Proudfoot, *Aust. J. Chem.* **34**, 335 (1981).

173. H. H. Keah, I. D. Rae, and D. G. Hawthrone, *Aust. J. Chem.* **45**, 659 (1992).

174. B. Yamada, A. Matsumoto, and T. Otsu, *J. Polym. Sci., Polym. Chem. Ed.* **21**, 2241 (1983).

175. L. H. Piette, *Chemical Application of EPR: In NMR and EPR Spectroscopy*, Pergamon Press, Oxford, 1960, p. 207.

176. J. A. Harris, O. Hinojosa, and J. C. Arthur, Jr., *J. Polym. Sci., Polym. Chem. Ed.* **11**, 3215 (1973).

177. S. E. Bresler, E. N. Kazbekov, and V. N. Shadrin, *Makromol. Chem.* **175**, 2875 (1974).

178. M. C. R. Symons, *J. Chem. Soc.* 277 (1959).

179. M. C. R. Symons, *J. Chem. Soc.* 1186 (1963).

180. H. Fischer, *J. Polym. Sci., B* **2**, 529 (1964).

181. J. H. O'Donnell, B. MacGarvey, and H. Morawets, *J. Am. Chem. Soc.* **86**, 2322 (1964).

182. M. J. Bowden and J. H. O'Donnell, *J. Phys. Chem.* **72**, 1577 (1964).

183. Y. Sakai and M. Iwasaki, *J. Polym. Sci.; Part A-1* **7**, 1749 (1969).

184. M. Iwasaki and Y. Sakai, *J. Polym. Sci.; Part A-1* **7**, 1537 (1969).

185. P. Smith and R. D. Stevens, *J. Phys. Chem.* **76**, 3141 (1972).

186. J. Sohma, Y. Komatsu, and H. Kashiwabara, *J. Polym. Sci.* **B3**, 287 (1965).

187. A. Matsumoto and B. Giese, *Macromolecules* **29**, 3758 (1996).

188. M. Spichty, B. Giese, A. Matsumoto, H. Fischer, and G. Gescheidt, *Macromolecules* **34**, 723 (2001).

189. B. Yamada, S. Kobatake, and O. Konosu, *Mcromol. Chem. Phys.* **197**, 901 (1996).

190. A. Matsumoto, *J. Polym. Sci.; Part A: Polym. Chem.* **37**, 1969 (1999).

191. T. Fukuda, K. Kubo, and Y. D. Ma, *Prog. Polym. Sci.* **17**, 875 (1992).

192. M. L. Coote and T. P. Davis, *Prog. Polym. Sci.* **24**, 1217 (1999).

193. H. Fischer and L. Radom, *Angew. Chem. Int. Ed.* **40**, 1340 (2001).

194. M. Kamachi, A. Kajiwara, K. Saegusa, and Y. Morishima, *Macromolecules* **26**, 7369 (1993).

195. M. Kamachi and A. Kajiwara, *Macromolecules* **29**, 2378 (1996).

196. B. Yamada, M. Fujita, and T. Otsu, *Makromol. Chem.* **192**, 1829 (1991).

197. B. Yamada, M. Kageoka, and T. Otsu, *Macromolecules* **25**, 4828 (1992).

198. A. Matsumoto and K. Mizuta, *Macromolecules* **27**, 5863 (1994).

199. M. Kamachi and A. Kajiwara, *Macromol. Chem. Phys.* **198**, 787 (1997).

200. K. Yamada, A. Kajiwara, T. Nakano, and Y. Okamoto, *Polym. J.* **44**, 313 (2001).

201. A. Matsumoto and T. Odani, *Macromol. Rapid Commun.* **22**, 1195 (2001).

202. S. I. Stupp and P. Osenar, p. 513 in Ref. 1.

203. K. Tajima and T. Aida, *Chem. Commun.* 2399 (2000).

204. K. Nagai, *Trends Polym. Sci.* **4**, 122 (1996).

205. Y. Yasuda, K. Rindo, and S. Aoki, *Makromol. Chem.* **193**, 2875 (1992).

206. S. Aoki, Y. Morimoto, and A. Nomura, *Polym. J.* **28**, 1014 (1996).

207. P. Dias, C. M. Paleos, G. Nika, and A. Malliaris, *Makromol. Chem.* **194**, 445 (1993).

208. K. Nagai and Y. Oishi, *J. Polym. Sci.; Part A: Polym. Chem.* **32**, 445 (1994).

209. N. J. Turro, I. F. Dierola, and C.-J. Chung, *J. Polym. Sci., Polym. Chem. Ed.* **21**, 1985 (1983).

210. V. Percec, C.-H. Ahn, and B. Barboiu, *J. Am. Chem. Soc.* **119**, 12978 (1997).

211. V. Percec, C.-H. Ahn, G. Unger, D. J. P. Yeardley, M. Möller, and S. S. Sheiko, *Nature* **391**, 161 (1998).

212. V. Percec and M. N. Holerca, *Biomacromolecules* **1**, 6 (2000).

213. S. D. Hudson, H.-J. Jung, V. Percec, W.-D. Cho, G. Johansson, G. Ungar, and V. S. Balagurusamy, *Science* **278**, 449 (1997).

214. V. Percec, C.-H. Ahn, W.-D. Cho, A. M. Jamieson, J. Kim, T. Leman, M. Schmidt, M. Gerle, M. Möller, S. A. Prokhorova, S. S. Sheiko, S. Z. D. Cheng, A. Zhang, G. Ungar, and D. J. P. Yeardley, *J. Am. Chem. Soc.* **120**, 8619 (1998).

215. V. Percec, W.-D. Cho, M. Möller, S. A. Prokhorova, G. Ungar, and D. J. P. Yeardley, *J. Am. Chem. Soc.* **122**, 4249 (2000).

216. J. H. Fendler, *Science* **223**, 888 (1984).

217. H. Ringsdorf, B. Schlarb, and J. Venzmer, *Angew. Chem. Int. Ed. Engl.* **27**, 113 (1988).

218. D. F. O'Brien, B. Armitage, A. Benedicto, D. E. Bennett, H. G. Lamparski, Y.-S. Lee, W. Srisiri, and T. M. Sisson, *Acc. Chem. Res.* **31**, 861 (1998).

219. N. Higashi, T. Adachi, and M. Niwa, *Macromolecules* **23**, 1475 (1990).

220. J. Lei and D. F. O'Brien, *Mecromolecules* **27**, 1381 (1994).

221. T. M. Sisson, W. Srisiri, and D. F. O'Brien, *J. Am. Chem. Soc.* **120**, 2322 (1998).

222. D. F. O'Brien, *Trends Polym. Sci.* **2**, 183 (1994).

223. J. M. Schnur, *Science* **262**, 1669 (1993).

224. H. Fukuda, T. Diem, J. Stefely, F. J. Kezdy, and S. L. Regen, *J. Am. Chem. Soc.* **108**, 2321 (1986).

225. S. L. Regen, J.-S. Shin, and K. Yamaguchi, *J. Am. Chem. Soc.* **106**, 2446 (1984).

226. Y. B. Amerik, I. I. Konstantinov, and B. A. Krentsel, *J. Polym. Sci. C* **23**, 681 (1968).

227. A. Blumstein, N. Kitagawa, and R. Blumstein, *Mol. Cryst. Liq. Cryst.* **12**, 215 (1971).

228. Y. Tanaka, F. Yamaguchi, M. Shiraki, and A. Okada, *J. Polym. Sci., Polym. Chem. Ed.* **16**, 1027 (1978).

229. D. D. Deshpande and P. Aravindakshan, *J. Macromol. Sci.—Chem.* **A21**, 509 (1984).

230. A. B. Biswas and D. D. Deshpande, *Polymer* **21**, 547 (1980).

231. D. D. Deshpande and P. Aravindakshan, *Makromol. Chem.* **184**, 1555 (1983).

232. Y. B. Amerik and K. B. Krentsel, *J. Polym. Sci., C* **16**, 1383 (1967).

233. C. M. Paleou and M. M. Labes, *Mol. Cryst. Liq. Cryst.* **11**, 385 (1970).

234. E. Perplies, H. Ringsdorf, and J. H. Wendorff, *Makromol. Chem.* **175**, 553 (1974).

235. W. J. Toth and A. V. Tobolsky, *J. Polym. Sci.* **B8**, 289 (1970).

236. A. C. de Visser, J. Feyen, K. de Groot, and A. Bantjes, *J. Polym. Sci.* **B8**, 805 (1970).

237. H. Saeki, K. Iimura, and M. Takeda, *Polym. J.* **3**, 414 (1972).

238. C. A. Guymon, E. N. Hoggan, N. A. Clark, T. P. Rieker, D. M. Walba, and C. N. Bowman, *Science* **275**, 57 (1997).

239. C. A. Guymon and C. N. Bowman, *Macromolecules* **30**, 1594 (1997).

240. C. A. Guymon and C. N. Bowman, *Macromolecules* **30**, 5271 (1997).

241. S. I. Stupp, S. Son, H. C. Lin, and L. S. Li, *Science* **259**, 59 (1993).

242. S. I. Stupp, S. Son, L. S. Li, H. C. Lin, and M. Keser, *J. Am. Chem. Soc.* **117**, 5212 (1995).

243. S. I. Stupp, V. Lebonheur, K. Walker, L. S. Li, K. E. Huggins, M. Keser, and A. Amstutz, *Science* **276**, 384 (1997).

244. E. R. Zubarev, M. U. Pralle, L. Li, and S. I. Stupp, *Science* **283**, 523 (1999).

245. R. C. Smith, W. M. Fischer, and D. L. Gin, *J. Am. Chem. Soc.* **119**, 4092 (1997).

246. G. M. J. Schmidt, *Pure Appl. Chem.* **27**, 647 (1971).

247. H. Morawetz, *Science* **152**, 705 (1966).

248. I. C. Paul and D. Y. Curtin, *Acc. Chem. Res.* **6**, 217 (1973).

249. M. D. Cohen and B. S. Green, *Chem. Brit.* **9**, 490 and 517 (1973).

250. J. M. Thomas, *Pure Appl. Chem.* **51**, 1065 (1979).

251. N. B. Singh, R. J. Singh, and N. P. Singh, *Tetrahedron* **50**, 6441 (1994).

252. F. Toda, *Acc. Chem. Res.* **28**, 480 (1995).

253. K. Tanaka and F. Toda, *Chem. Rev.* **100**, 1025 (2000).

254. M. D. Cohen and G. M. J. Schmidt, *J. Chem. Soc.* 1996 (1964).

255. J. M. Thomas, *Phil. Trans. Roy. Soc.* **277**, 251 (1974).

256. M. Thakur, *Encyclopedia of Polymer Science and Engineering*, J. I. Kroshwitz, ed., Wiley, New York, 1989, Vol. 15, p. 362.

257. G. R. Desiraju, *Crystal Engineering: The Design of Organic Solids*, Elsevier, Amsterdam, 1989.

258. G. R. Desiraju, ed., *The Crystal as a Supramolecular Entity: Perspectives in Supramolecular Chemistry*, Wiley, Chichester, 1996, Vol. 2.

259. K. R. Seddon and M. Zaworotko, eds., *Crystal Engineering: The Design and Application of Functional Solids*, NATO ASI Series C, Kluwer, Dordrecht, 1999, Vol. 539.

260. D. Braga, F. Grepioni, and A. G. Orpen, eds., *Crystal Engineering: From Molecules and Crystals to Materials*, NATO ASI Series C, Kluwer, Dordrecht, 1999, Vol. 538.

261. J. W. Steed and J. L. Atwood, *Supramolecular Chemistry*, Wiley, Chichester, 2000, p. 389.

262. B. Tieke, *Adv. Polym. Sci.* **71**, 79 (1985).

263. B. Tieke and G. Chapuis, *Crystallographically Ordered Polymers*, ACS Symposium Series 337, D. J. Sandman, ed., American Chemical Society, Washington, DC, 1987, Chapter 5, p. 61.

264. B. Tieke, *Polymerization in Organized Media*, C. M. Paleos, ed., Gordon and Breach, Philadelphia, 1992, p. 105.

265. H. Ringsdorf and H. Schupp, *J. Macromol. Sci.—Chem.* **A15**, 1015 (1981).

266. K. Fukuda, Y. Shibasaki, and H. Nakahara, *Thin Solid Films* **133**, 39 (1985).

267. A. Laschewsky and H. Ringsdorf, *Macromolecules* **21**, 1936 (1988).

268. B. Tieke, *Colloid Polym. Sci.* **263**, 965 (1985).

269. B. Tieke and G. Wegner, *Makromol. Chem., Rapid Commun.* **2**, 543 (1981).

270. B. Tieke and G. Wegner, *Angew. Chem. Int. Ed. Engl.* **20**, 687 (1981).

271. B. Tieke, *J. Polym. Sci., Polym. Chem. Ed.* **22**, 391 (1984).

272. B. Tieke and G. Chapuis, *J. Polym. Sci., Polym. Chem. Ed.* **22**, 2895 (1984).

273. A. Blumstein, *J. Polym. Sci.* **A3**, 2653 (1965).

274. A. Blumstein, S. L. Malhotra, and A. C. Watterson, *J. Polym. Sci.* **A2**, 1599 (1970).

275. T. Kyotani, N. Sonobe, and A. Tomita, *Nature* **331**, 331 (1988).

276. K. Fukano and E. Kageyama, *J. Polym. Sci., Polym. Chem. Ed.* **13**, 1309 (1975).

277. K. Fukano and E. Kageyama, *J. Polym. Sci., Polym. Chem. Ed.* **13**, 1325 (1975).

278. J. P. Quaegebeur, T. Seguchi, H. Le Bail, and C. Chachaty, *J. Polym. Sci., Polym. Chem. Ed.* **14**, 2703 (1976).

279. S. M. Ng, S. Ogino, T. Aida, A. Koyano, and T. Tatsumi, *Macromol. Rapid Commun.* **18**, 991 (1997).

280. K. Moller, T. Bein, and R. X. Fischer, *Chem. Mater.* **10**, 1841 (1998).

281. C.-G. Wu and T. Bein, *Science* **266**, 1013 (1994).

282. P. Enzel and T. Bain, *Chem. Mater.* **4**, 819 (1992).

283. C.-G. Wu and T. Bein, *Science* **264**, 1757 (1994).

284. C.-G. Wu and T. Bein, *Chem. Mater.* **6**, 1109 (1994).

285. K. Kageyama, J. Tamazawa, and T. Aida, *Science* **285**, 2113 (1999).

286. M. Farina, *Encyclopedia of Polymer Science and Engineering*, J. I. Kroshwitz, ed., Wiley, New York, 1988, Vol. 12, p. 486.

287. K. Takemoto and M. Miyata, *J. Macromol. Chem., Rev. Macromol. Chem. Phys.* **C18**, 83 (1980).

288. M. Miyata, *Polymerization in Organized Media*, C. M. Paleos, ed., Gordon and Breach, Philadelphia, 1992, p. 327.

289. M. Miyata, *Comprehensive Supramolecular Chemistry*, N. D. Reinhoudt, ed., Pergamon, Oxford, 1996, Vol. 10, p. 557.

290. H. Clasen, *Z. Elektrochem.* **60**, 982 (1956).

291. J. F. Brown, Jr. and D. M. White, *J. Am. Chem. Soc.* **82**, 5671 (1960).

292. D. M. White, *J. Am. Chem. Soc.* **82**, 5678 (1960).

293. I. Sakurada and K. Nanbu, *Kogyo Kagaku Zasshi* **80**, 307 (1959).

294. M. Farina, *Tetrahedron Lett.* 2097 (1963).

295. M. Farina, G. Natta, G. Allegra, and M. Löffelholz, *J. Polym. Sci., Part C* **16**, 2517 (1967).

296. M. Farina, G. Audisio, and G. Natta, *J. Am. Chem. Soc.* **89**, 5071 (1967).

297. J. Finter and G. Wegner, *Makromol. Chem.* **180**, 1093 (1979).

298. H. R. Allcock, W. T. Ferrar, and M. L. Levin, *Macromolecules* **15**, 697 (1982).

299. H. R. Allcock and M. L. Levin, *Macromolecules* **18**, 1324 (1985).

300. M. Miyata, K. Morioka, and K. Takemoto, *J. Polym. Sci., Polym. Chem. Ed.* **15**, 2987 (1977).

301. M. Miyata, T. Tsuzuki, F. Noma, K. Takemoto, and M. Kamachi, *Makromol. Chem., Rapid Commun.* **9**, 45 (1988).

302. W. Goonewardena, M. Miyata, and K. Takemoto, *Polym. J.* **23**, 1405 (1991).

303. K. Nakano, K. Sada, and M. Miyata, *Polym. J.* **33**, 172 (2001).

304. K. Kamide, H. Yamazaki, K. Okajima, and K. Hikichi, *Polym. J.* **17**, 1291 (1985).

305. H. Yamazaki, Y. Miyazaki, and K. Kamide, *Polym. J.* **23**, 765 (1991).

306. M. Minagawa, H. Yamada, K. Yamaguchi, and F. Toishi, *Macromolecules* **25**, 503 (1992).

307. Y. Chatani, *Prog. Polym. Sci. Japan* **7**, 149 (1974).

308. M. Hasegawa, *Chem. Rev.* **83**, 507 (1983).

309. W. L. Dilling, *Chem. Rev.* **83**, 1 (1983).

310. K. Venkatesan and V. Ramamurthy, *Photochemistry in Organized and Constrained Media*, V. Ramamurthy, ed., VCH, New York, 1991, Chapter 4, p. 133.

311. M. Hasegawa, *Adv. Phys. Org. Chem.* **30**, 117 (1995).

312. G. Wegner, *Pure Appl. Chem.* **49**, 443 (1977).

313. R. H. Baughman and K. C. Yee, *J. Polym. Sci., Macromol. Rev.* **13**, 219 (1978).

314. D. Bloor, *Developments in Crystalline Polymers II*, D. C. Bassett, ed., Applied Science Publishers, London, 1982, Chapter 4, p. 151.

315. H. Bässler, *Adv. Polym. Sci.* **63**, 1 (1984).

316. H. Sixl, *Adv. Polym. Sci.* **63**, 49 (1984).

317. V. Enkelmann, *Adv. Polym. Sci.* **63**, 91 (1984).

318. M. Schott and G. Wegner, *Nonlinear Optical Properties of Organic Molecules and Crystals*, D. S. Chemla and J. Zyss, eds., Academic Press, New York, 1987, Vol. 2, Chapter 3-1, p. 3.

319. T. Ogawa, *Prog. Polym. Sci.* **20**, 943 (1995).

320. J. J. Kane, R.-F. Liao, J. W. Lauher, and F. W. Fowler, *J. Am. Chem. Soc.* **117**, 12003 (1995).

321. T. L. Nguyen, F. W. Fowler, and J. W. Lauher, *Mol. Cryst. Liq. Cryst.* **313**, 253 (1998).

322. B. Dinkelmeyer, J. W. Lauher, and F. W. Fowler, *Mol. Cryst. Liq. Cryst.* **313**, 259 (1998).

323. J. Kiji, J. Kaiser, G. Wegner, and R. C. Shulz, *Polymer* **14**, 433 (1973).

324. U. H. F. Bunz, *Angew. Chem. Int. Ed. Engl.* **33**, 1073 (1994).

325. V. Enkelmann, *Chem. Mater.* **6**, 1337 (1994).

326. J. Xiao, M. Yang, J. W. Lauher, and F. W. Fowler, *Angew. Chem. Int. Ed.* **39**, 2132 (2000).

327. A. Matsumoto, T. Matsumura, and S. Aoki, *J. Chem. Soc., Chem. Commun.* 1389 (1994).

328. A. Matsumoto and T. Odani, p. 93 in Ref. 6.

329. A. Matsumoto, *Prog. React. Kinet. Mech.* **26**, 59 (2001).

330. A. Matsumoto, T. Matsumura, and S. Aoki, *Macromolecules* **29**, 423 (1996).

331. A. Matsumoto, K. Yokoi, S. Aoki, K. Tashiro, T. Kamae, and M. Kobayashi, *Macromolecules* **31**, 2129 (1998).

332. K. Tashiro, T. Kamae, M. Kobayashi, A. Matsumoto, K. Yokoi, and S. Aoki, *Macromolecules* **32**, 2449 (1999).

333. A. Matsumoto, K. Katayama, T. Odani, K. Oka, K. Tashiro, S. Saragai, and S. Nakamoto, *Macromolecules* **33**, 7786 (2000).

334. K. Tashiro, A. N. Zadorin, S. Saragai, T. Kamae, A. Matsumoto, K. Yokoi, and S. Aoki, *Macromolecules* **32**, 7946 (1999).

335. A. Matsumoto and K. Yokoi, *J. Polym. Sci.; Part A: Polym. Chem.* **36**, 3147 (1998).

336. A. Matsumoto and T. Odani, *Polym. J.* **30**, 358 (1998).

337. D. Rabinovich and G. M. J. Schmidt, *J. Chem. Soc. B* 286 (1967).

338. S. E. Filippakis, L. Leiserowitz, and G. M. J. Schmidt, *J. Chem. Soc. B* 290 (1967).

339. S. E. Filippakis, L. Leiserowitz, and G. M. J. Schmidt, *J. Chem. Soc. B* 305 (1967).

340. M. Lahav and G. M. J. Schmidt, *J. Chem. Soc. B* 312 (1967).

341. S. E. Filippakis, L. Leiserowitz, and G. M. J. Schmidt, *J. Chem. Soc. B* 297 (1967).

342. B. S. Green, M. Lahav, and G. M. J. Schmidt, *J. Chem. Soc. B* 1552 (1971).

343. A. Matsumoto, T. Odani, M. Chikada, K. Sada, and M. Miyata, *J. Am. Chem. Soc.* **121**, 11122 (1999).

344. A. Matsumoto and T. Odani, *Polym. J.* **31**, 717 (1999).

345. T. Odani and A. Matsumoto, *Macromol. Rapid Commun.* **21**, 40 (2000).

346. A. Matsumoto, S. Nagahama, and T. Odani, *J. Am. Chem. Soc.* **122**, 9109 (2000).

347. T. Tanaka and A. Matsumoto, to be submitted.

348. A. Matsumoto, T. Kunisue, S. Nagahama, K. Inoue, K. Sada, and M. Miyata, *Mol. Cryst. Liq. Cryst.* (in press).

349. A. Matsumoto, T. Tanaka, T. Tsubouchi, K. Tashiro, S. Saragai, and S. Nakamoto, to be submitted.

350. S. Nagahama, A. Matsumoto, K. Inoue, K. Sada, and M. Miyata, to be submitted.

351. A. Matsumoto, K. Sada, K. Tashiro, M. Miyata, T. Tsubouchi, T. Tanaka, T. Odani, S. Nagahama, T. Tanaka, K. Inoue, S. Saragai, and S. Nakamoto, *Angew. Chem. Int. Ed.* (in press).

352. O. Matsumoto and S. Nagahama, *Proc. Jpn. Acad., Ser. B* **77**, 110 (2001).

353. S. Nagahama and A. Matsumoto, *J. Am. Chem. Soc.* **123**, 12176 (2001).

354. M. S. Whittingham and A. J. Jacobsen, eds., *Intercalation Chemistry*, Academic Press, New York, 1982.

355. A. W. Coleman, S. G. Bott, S. D. Morley, C. M. Means, K. D. Robinson, H. Zhang, and J. L. Atwood, *Angew. Chem. Int. Ed. Engl.* **27**, 1361 (1988).

356. M. Miyata, M. Shibakami, S. Chirachanchai, K. Takemoto, N. Kasai, and K. Miki, *Nature* **343**, 446 (1990).

357. K. Biradha, D. Dennis, V. A. MacKinnon, C. V. K. Sharma, and M. J. Zaworotko, *J. Am. Chem. Soc.* **120**, 11894 (1998).

358. J. A. Swift, A. M. Pivovar, A. M. Reynolds, and M. D. Ward, *J. Am. Chem. Soc.* **120**, 5887 (1998).

359. A. Matsumoto, T. Odani, K. Sada, M. Miyata, and K. Tashiro, *Nature* **405**, 328 (2000).

360. M. D. Ward, *Nature* **405**, 293 (2000).

14 Macromolecular Engineering by Controlled/Living Radical Polymerization

YVES GNANOU and DANIEL TATON

Laboratoire de Chimie des Polymeres Organiques, ENSCPB-CNRS,
Université Bordeaux I, Avenue Pey-Berland, 33607 Pessac, France

CONTENTS

14.1   INTRODUCTION

Radical processes are extensively utilized industrially; about 50% of all polymeric materials are produced by this chain polymerization. Compared to ionic polymerization techniques, free-radical processes offer the advantage of being applicable to a wide variety of vinylic monomers and are easier to handle experimentally. Indeed, free-radical techniques require very standard conditions and are not as demanding as other chain addition mechanisms regarding the purity of the reagents used.[1] They are therefore applied in emulsion, suspension, solution, or bulk. In addition, radical growing species are highly tolerant of many functional groups, including acid, hydroxyl, amino, and epoxide; hence functional monomers can undergo radical polymerization without the help of protection chemistry. Finally, radical polymerizations can be performed at moderate temperature, typically from room temperature to 140°C, depending on the monomer and the initiating system utilized.[1]

However, an essential feature of conventional free-radical polymerizations (RP) is the simultaneity of initiation, propagation and chain breaking termination steps, the latter occurring either by radical chain–chain coupling or by disproportionation, which seriously limits the relevance of RP in macromolecular synthesis.

Since the late 1990s, several families of vinylic monomers were demonstrated to undergo a "living"/controlled growth either by nitroxide-mediated polymerization (NMP)[2] [also called *stable free-radical polymerization* (SFRP) by some authors], atom transfer radical polymerization (ATRP),[3] reversible addition–fragmentation chain transfer (RAFT)[4] and other degenerative transfer methodologies,[5,6] or some other radical-based approaches,[7–10] paving the way for their use in macromolecular engineering. However, all these methodologies are not alike; for instance, NMP is unsuited to monomers that give tertiary radicals such as methacrylic esters and ATRP is inefficient for monomers that poison the catalytic system through coordination with the metal. In spite of these limitations, controlled/living free-radical polymerization (LRP) combines the advantages provided by truly "living" systems[11] for the quality of the polymeric structures formed, with the easiness of handling that characterizes RP.

For all these reasons, the 1990s–early 2000s has witnessed the renaissance of free-radical polymerization, which now appears as the most powerful and versatile tool for engineering macromolecular architectures. Three categories of materials can actually be distinguished, depending upon the feature considered: functionality, composition, and topology (Fig. 14.1). Indeed, well-defined homopolymers as well as miscellaneous copolymers (statistical, alternating, block, or gradient copolymers), but also branched architectures (stars, star block, and dendrimerlike
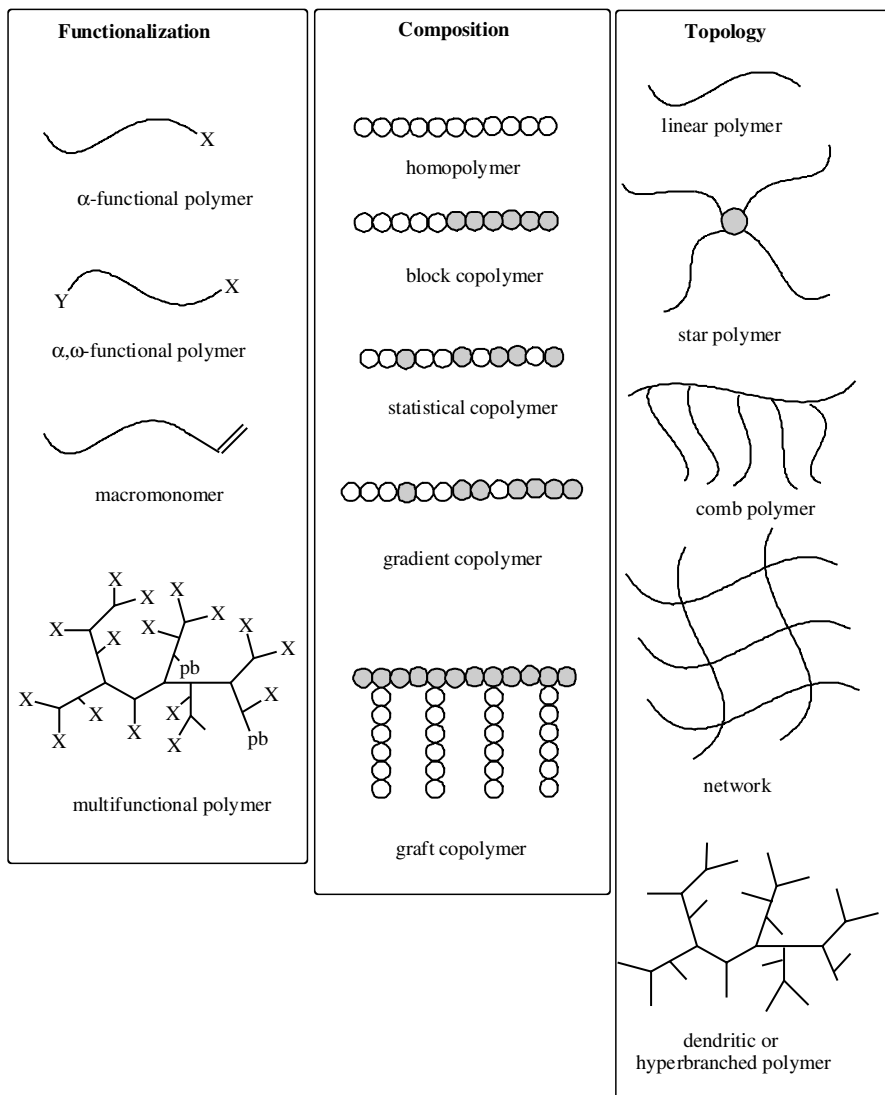
Figure 14.1 Macromolecular engineering by LRP.

copolymers, combs, densely grafted, hyperbranched polymers, etc.) whose synthesis was for long thought of unrealistic if not impossible, can now be easily derived by LRP. Macromolecular chains of various chemical composition and activity were also assembled in original topologies by combination of a LRP with another polymerization proceedure (that can be controlled/living or not) including step-growth, ring-opening, ring-opening metathesis, ionic, or conventional radical processes.

The following sections review the potential of LRP for macromolecular engineering, with particular emphasis on the scope and limitations associated with each

specific synthetic methodology. On the other hand, this chapter is organized according to the type of architectures derived by LRP rather than the LRP techniques themselves and the structures that were obtained through each of them.

14.2   ω-FUNCTIONAL POLYMERS AND MACROMONOMERS

Since radical reactions are tolerant of many functional groups such as hydroxyl and amine, LRP could be applied to numerous functional monomers belonging to the family of styrenics and alkyl (meth)acrylates.[4,12–13] These include glycidyl acrylate, hydroxyethyl (meth)acrylate, and (dimethylamino)ethyl methacrylate. More recently, N,N-dimethyl acrylamide could be successfully polymerized under controlled conditions either by NMP using a newly designed nitroxide as counter radical,[14] by RAFT,[4] or by ATRP.[15] The living/controlled polymerization of carboxylic acid containing monomers, such as (meth)acrylic acid, could also be achieved by ATRP under its neutralized form[16] or through RAFT with transfer agents based on the dithioesters or xanthates developed by the CSIRO team[4] and Rhodia,[17] respectively. For more details on LRP of functional monomers, the reader is invited to refer to the corresponding chapter of this handbook. A review article on functional polymers derived by ATRP is also available.[18]

This section focuses on the means that were developed to end-functionalize polymers grown by LRP. Before the emergence of LRP methodologies, terminal functions used to be incorporated into polymers through initiation by a functional generator of free radicals and via transfer with ω-functional telogens.[19] The corresponding ω-functional polymers then served as precursors for preparing macromonomers and block copolymers or were used as precursors for reactive blends as well. Following LRP routes, three main strategies were proposed to introduce functional groups at polymer ends:

1. The most convenient method is based on the use of initiators carrying reactive functions (e.g., alcohol, ester, epoxide) that do not require any protection.
2. Conversely, initiators containing specific functions such as thiol or carboxylic acid can be used only after a preliminary protection step, because of their participation in the polymerization process.
3. Finally, an alternative to access end-functionalized polymers is to modify the end groups corresponding to the "dormant" species carried by the chains into the desired functional groups by nucleophilic/electrophilic substitutions or addition reactions.

14.2.1   Functions Introduced in an Unprotected Form

14.2.1.1   Through Functional Initiators   Alkoxyamines containing functional groups such as hydroxyl, amino, and halide were successfully applied in NMP of styrenic monomers.[20–29] It should be noted, however, that functional alkoxyamines

(ref. 20, 21)

(ref. 20, 22, 24, 27)

X= (Br, COOEt, OMe, CH₂OH, CH=CH₂,...)

(ref. 25, 27)

(ref. 22, 23)

(ref. 26)

(ref. 28)

(ref. 29)

(ref. 28)
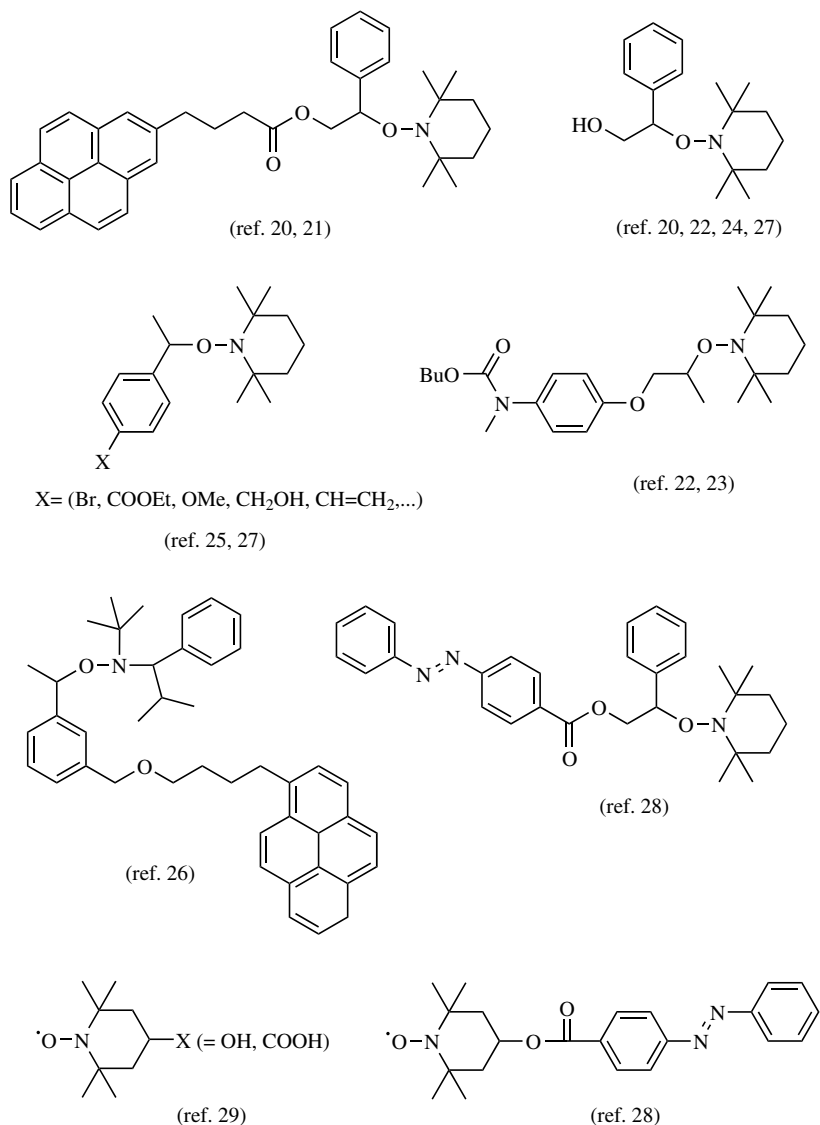
Figure 14.2 Examples of functional alkoxyamines and nitroxides.

or functional nitroxides (Fig. 14.2) were essentially meant to cap polymers with chromophores (e.g. pyrene, furazan) and probe the extent of functionalization as well as the degree of control achieved.[20,26,28] The chromophore were either attached to the initiating fragment or to the nitroxide moiety itself. For intance, it was shown that end-group purity decreases with the molar masses and the conversion when 2,2,6,6-tetramethylpiperidinyl-1-oxy (TEMPO) is used as the counterradical.[20] Much higher ''end-group fidelity'' could be achieved on making use of nitroxides

bearing a hydrogen on their α carbon or the corresponding alkoxyamines than in the case of TEMPO-derived polymers.[26] Indeed, the presence of these end groups could be ascertained for molar masses up to 100,000 g/mol. Of particular interest is the possibility of obtaining similar results with poly(alkyl acrylate)s for which the use of TEMPO was unsuccessful.

Hemery and colleagues associated a functional azo initiator, namely, 4,4′-azobis(4-cyanovaleric acid) with a functional nitroxide, namely, 4-hydroxy-TEMPO, to prepare α-hydroxy,ω-carboxy telechelic polystyrenes (PS), that were further subjected to an intramolecular cyclization; the efficiency of the latter reaction was close to 95%.[29] These authors thus reported the first example of cyclic PS derived by LRP.

Along the same line, initiators fitted with two reactive functions were also used in conjunction with a counterradical like TEMPO to generate ω-functional polymers. It is the way resorted by Mülhaupt et al. to end-cap their PS chains ($M_n \leq 50,000$ g/mol) with an oxazoline group via NMP.[30] These authors first synthesized bis(1,3-oxazoline-2-yl) azo compounds shown in Fig. 14.3 and further used them to initiate the polymerization of styrene at 130°C in the presence of TEMPO. These PS end-capped with an oxazoline moiety were chain-extended using monocarboxy-terminated PS.

Many halide-based functional initiators were employed for ATRP of vinylic monomers.[18] Figure 14.4 shows those based on alkyl halides that include a non-protected functional group. Although efficient and among the first initiatiors studied in ATRP, multihalogenated alkanes[31–33] such as $CHCl_3$ or CCl_4 do not enter in the category of functional initiating systems because the terminal fragments arising from them were generally not subjected to further chemical modifications.

Matyjaszewski's group demonstrated that ATRP of styrene and methyl acrylate (MA) is inert toward many functional groups carried by the initiator, including hydroxyl, cyano, allyl, epoxide, butyrolactone, or amide.[13,18] The corresponding end-functionalized polymers were prepared under controlled conditions from these initiators.

Haddleton reported the synthesis of hydroxy-terminated poly(methyl methacrylate) (PMMA) (M_n in the range 2,500–20,000 g/mol) from 2-hydroxyethyl-2′-methyl-2′-bromopropionate and the pyridine-2-carbaldehyde imine Cu(I) complex used as initiator and catalyst, respectively.[34]
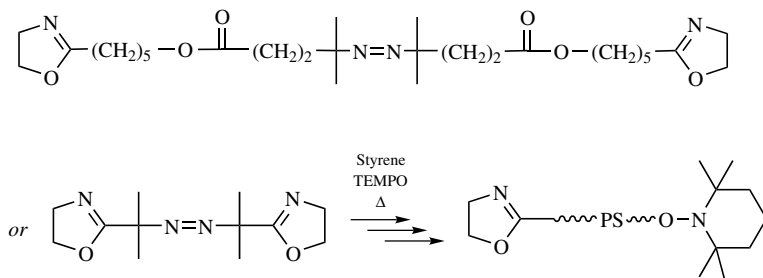
Figure 14.3   Functional azo initiators used in conjunction with TEMPO.[30]
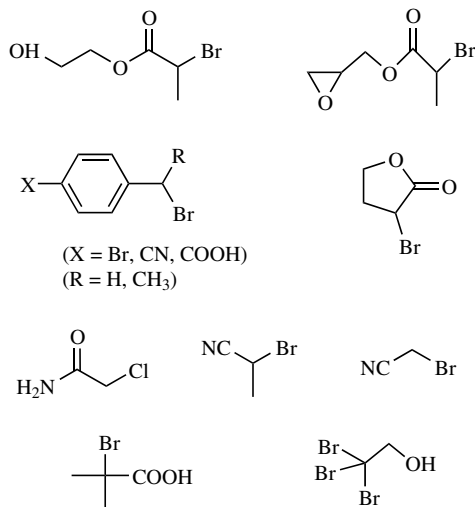
Figure 14.4   Examples of functional initiators for ATRP.[18,34–38]

Initiating ATRP with carboxylic acid-containing compounds was reported to be troublesome because of the risk of poisoning the catalytic system. However, the synthesis of carboxylic acid–terminated PS or PMMA was reported by different groups who used benzoic acid halide compounds in their unprotected form to initiate ATRP of styrene or MMA; a low initiation efficiency was sometimes noted.[35–38] The same approach was successfully applied for the preparation of anhydride, oxazoline, and hydroxy-terminated PS.[36]

Jérôme's group reported that both α-acid and α-hydroxy PMMA or poly(n-butyl acrylate) (Pn-BuA) could be derived, respectively, from 2-bromo-2-methyl propionic acid and 2,2′,2″-tribromoethanol used as initiator and NiBr$_2$(PPh$_3$)$_2$ as catalyst; the latter system was developed by these authors to bring about ATRP of the corresponding monomers.[38]

Figure 14.5 shows uridine and adenosine-derivatized initiators[39] as well as a cholesterol-based halide[40] used by the team of Haddleton to grow PMMA and PS chains from these biological moieties and thus functionalize them. The same group employed carbohydrates to prepare well-defined oligosaccharide-terminated polymers by ATRP.[41]

Miscellaneous substituted aliphatic and aromatic sulfonyl chlorides were found to be very efficient as initiators for ATRP, especially in the case of methacrylics (such compounds were even coined "universal class of initiators"), owing to their high rate of initiation as compared to that of propagation when employed in the presence of the CuCl/dipyridyl catalytic system.[42] By making use of aromatic sulfonyl chlorides including functional substituents in the para position (Fig. 14.6), the group of Percec prepared various end-functional polymers.[43]

(R = H, trimethylsilyl)   (R = H, trimethylsilyl)
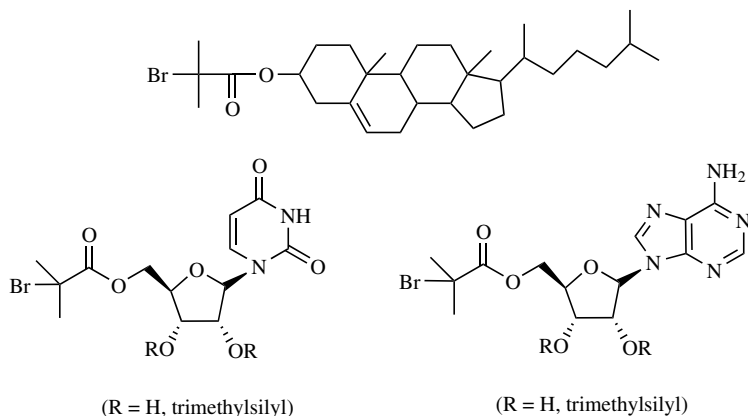
Figure 14.5   ATRP initiators containing a sugar or a natural residue.[39–40]
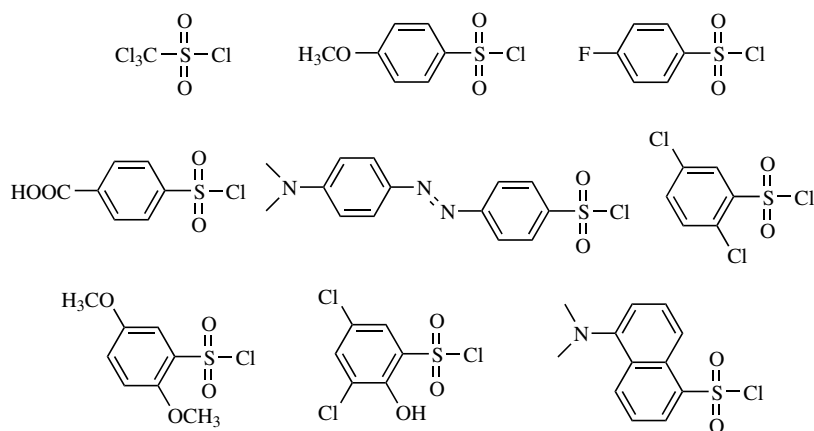
Figure 14.6   Examples of functional alkyl and aryl sulfonyl chloride initiators for ATRP.[42–43]

14.2.1.2   *Through Radical Postfunctionalization*

The use of radical addition reactions is an alternative route to functionalize polymers prepared by LRP. The substitution of allylic, hydroxyl or epoxide groups for halogens in ATRP-derived poly(methyl acrylate) could be achieved by using allyltri-n-butylstannate, allyl alcohol, and 1,2-epoxy-5-hexene, respectively.[18,44] If the allylation of organic halides is a well-known procedure, the introduction of epoxy and alcohol functions relied on the fact that the above monomers cannot homopolymerize by ATRP (Fig. 14.7).

In a similar manner, Kallitsis et al. prepared α,ω-bis-anhydride PS by reacting ATRP-derived PS with maleic anhydride (Fig. 14.8); the corresponding
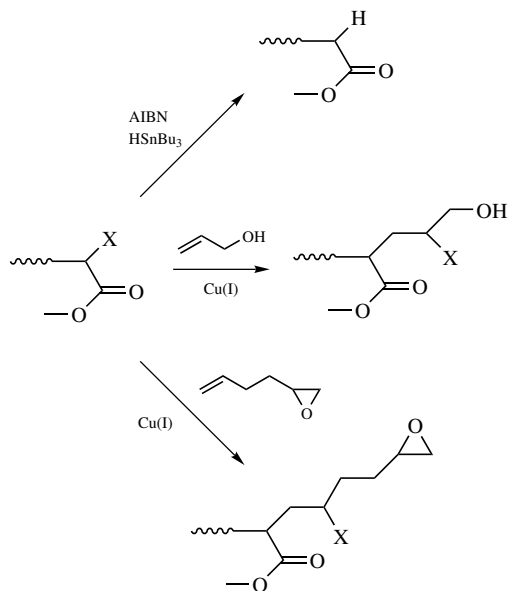
Figure 14.7   Radical postfunctionalization of ATRP-derived polymers.[44]
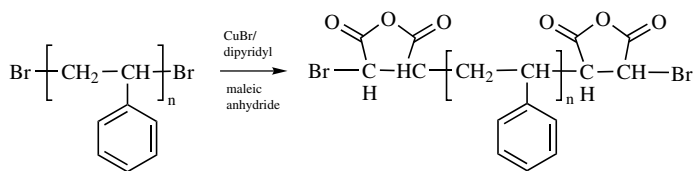
Figure 14.8   α,ω-Bisanhydride PS.[45]

functionalized polymers were further reacted with nylon 6 on blending the two polymeric materials in the molten state.[45]

Sawamoto et al.[46,47] as well as Haddleton and colleagues[48] incorporated ketone groups at the end of PMMA chains through a radical process that involved the reactions of polymeric radicals with silyl enol ethers (Fig. 14.9).
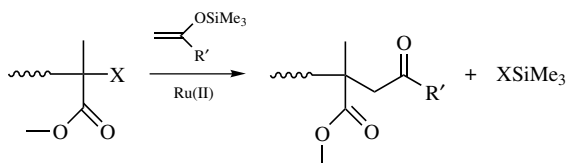
Figure 14.9   Reaction of silyl enol ethers with PMMA radicals.[46–48]

There are an increasing number of reports dealing with the synthesis of C_{60}- derivatized polymers.[49] One goal of the fullerenation of polymeric materials is to combine the processability of macromolecules with the interesting physical properties of C_{60}. Since fullerene exhibits a high reactivity toward radicals, LRP techniques were exploited to obtain tailor-made C_{60}-containing polymers, as described below.

Reaction of a 4-fold excess of C_{60} with PS radicals (M_n in the range 1,000–10,000 g/mol, PDI < 1.2) generated from TEMPO-based precursors in o-dichlorobenzene at 145°C was first reported by Fukuda et al.[50] This predominantly afforded a 1,4-bis-adduct, namely, 1,4-dipolystyryldihydro[60]fullerene, which is a C_{60} fitted with two well-defined PS arms, whose redox properties were similar to those oberved for pure C_{60}. Experimental evidence for the formation of the 1,4-bis-adduct was provided by UV–visible spectroscopy and by SEC as well.

No other products resulting from subsequent additions of PS radicals to this 1,4-bis-adduct were detected. Other authors carried out the same study but less information about the structures obtained was provided.[51] The team of Fukuda also showed that this (C_{60}-PS)$_2$ could be monomolecularly dispersed in a PS matrix but it could also form multimolecular micelles.[52] Incorporation of C_{60} at the ends of poly(p-vinylphenol) and of PS-b-poly(p-vinylphenol) diblock copolymers was also reported by the same team.[53] The vinylphenol units were generated after hydrolysis of poly(p-butoxystyrene) obtained by NMP of the corresponding monomer. Investigation of the solution behavior of these materials by light scattering showed that they formed stable multimolecular micelles at 25°C.

ATRP was also applied to synthesize PS and PMMA capped with C_{60}.[54] In this case, however, it was claimed that the monoadduct was the major product obtained: treating the bromo-terminated precursors with C_{60} in the presence of CuBr/dipyridyl at elevated temperature (90–110°C) in chlorobenzene afforded selectively PS-C_{60}-Br and PMMA-C_{60}-Br, as suggested by the characterization of these samples by SEC, UV–visible, fluorescence spectroscopy, and MALDI-TOF.[55] No further addition of PS chains onto PS-C_{60}-Br could be detected, unlike the case of the TEMPO-mediated reaction that gave rise to the (PS)$_2$-C_{60} 1,4-bis-adduct at 145°C. This difference in the selectivity likely originates from the nature of the dormant species carried by the monoadduct, namely, PS-C_{60}-TEMPO and PS-C_{60}-Br, which are more or less prone to homolytic cleavage in the experimental conditions used.

14.2.1.3 *Through Functional Reversible Transfer Agents* Figure 14.10 shows how Rizzardo and coll. used appropriate thiocarbonyl thio transfer agents to prepare polymers capped with functional groups (carboxylic, hydroxyl, etc.).[4] In addition, functional monomers such as the sodium salt of p-styrenesulfonic acid, acrylic acid, dimethylaminoethyl methacrylate, and N,N′-dimethyl acrylamide, were polymerized under controlled conditions using RAFT, affording the corresponding functional polymers.

14.2.2 Functions Requiring Protection

Thiols are typical examples of functions that require protection when placed in the presence of growing free radicals. To incorporate a thiol function at the chain end of
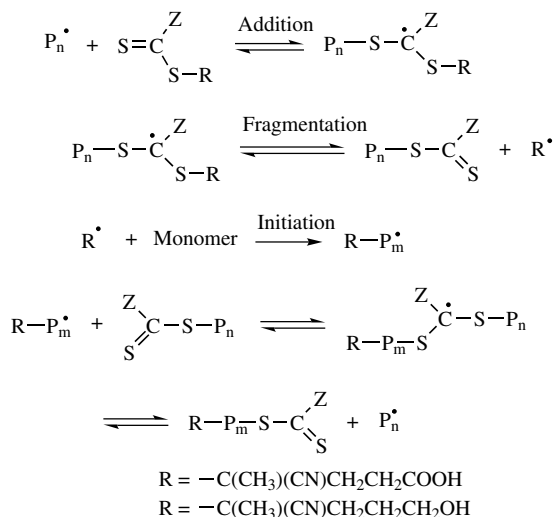
Figure 14.10   Use of functional transfer agents in the RAFT process.[4]

their PMMA obtained by ATRP ($\bar{M}_n$ = 6,000 g/mol), Hilborn and colleagues used a thiol containing initiator that was first reacted with the Sangers reagent (2,4-dinitro-fluorobenzene) for protection purpose.[56] The thiol function was easily removed by adding an excess of mercaptoethanol in the presence of triethylamine, affording, quantitatively, the desired thiol-functionalized PMMA.

As mentioned above, carboxylic acids also require protection when used in Cu-mediated ATRP. For instance, 2-bromopropionic acid exhibited a poor efficiency as initiator whereas its *tert*-butyldimethylsilyl-protected derivative gave better yields.[35] The best results were actually obtained with *tert*-butyl-2-bromopropionate whose deprotection could be accomplished by HCl treament.

14.2.3   Chemical Modification of LRP-Derived Polymers

LRP methodologies afford polymers capped with dormant species, giving one the opportunity to modify these end groups into specific functions or use them for the growth of a subsequent polymer block. However, the low concentration of these dormant species is a difficulty that mirrors in an incomplete conversion or the occurrence of side reactions. For instance, attempts to substitute alkoxides for the end-bromine groups of PS obtained by ATRP resulted in poor yields due to a significant elimination of hydrogen bromide.[36,57] However, ATRP-derived polymers were subjected to displacement of their halogen end groups by electrophilic or nucleophilic substitution. The dehalogenation of the chain ends as well as the introduction of azides or amines by nucleophilic or electrophilic substitutions, were described by Matyjaszewski (Fig. 14.11, route **a**).[58–60] On the other hand, the modification of the halogen end groups into hydroxyl functions could be achieved by using ethanol-amine and 4-aminobutanol in the case of ω-bomide PS and PMA, respectively
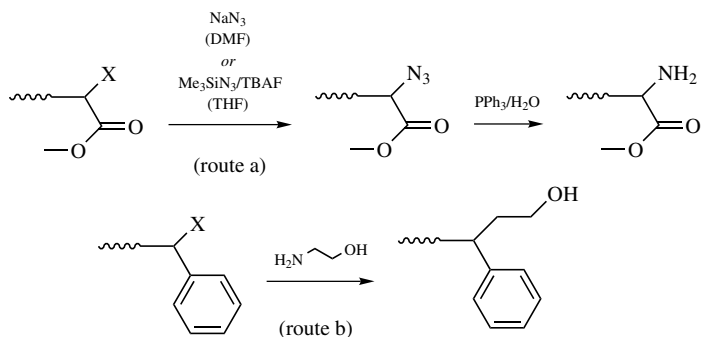
Figure 14.11   Chemical modification of CRP-derived polymers.[57]

(Fig. 14.11, route **b**).[57] The removal of the terminal halogen groups from hyper-branched polymers (see Section 14.7) with the help of potassium acetate, sodium ethyl sulfide, or potassium phtalimide was also reported.[61] Similarly, the thiocarbonylthio end groups of RAFT-derived polymers could be converted into thiol functions on treating them under basic conditions in the presence of an amine or a hydroxide.[4]

Less information about the chemical modification of NMP-derived polymers is available. Georges and colleagues showed how to transform alkoxyamines into ω-bromo and ω-benzoyloxy groups.[62] Chaumont and co-workers developed a methodology based on the use of thiuram disulfides to substitute dithiocarbamate groups for the end-standing nitroxide moieties of their NMP-derived PS chains.[63] More recently, Turro and colleagues demonstrated how to substitute newly designed photoactive functional nitroxides for TEMPO in a monodisperse PS-TEMPO, the reaction occuring by simple thermal exchange in chlorobenzene at 125°C (Fig. 14.12).[64]
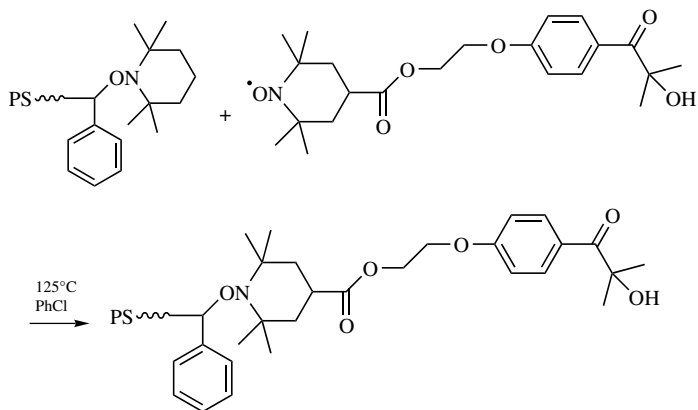
Figure 14.12   Chemical modification of TEMPO-derived PS.[64]

14.2.4   Synthesis of Macromonomers

Macromonomers are short macromolecular chains that are end-capped with a polymerizable group capable of copolymerizing with a low-molar-mass comonomer to give graft copolymers.[65] There are basically three methods for preparing such reactive polymers:

1. On choosing an initiator containing a polymerizable group, macromonomers can be derived provided this reactive group is totally inert toward the active species generated by its carrier (Fig. 14.13).
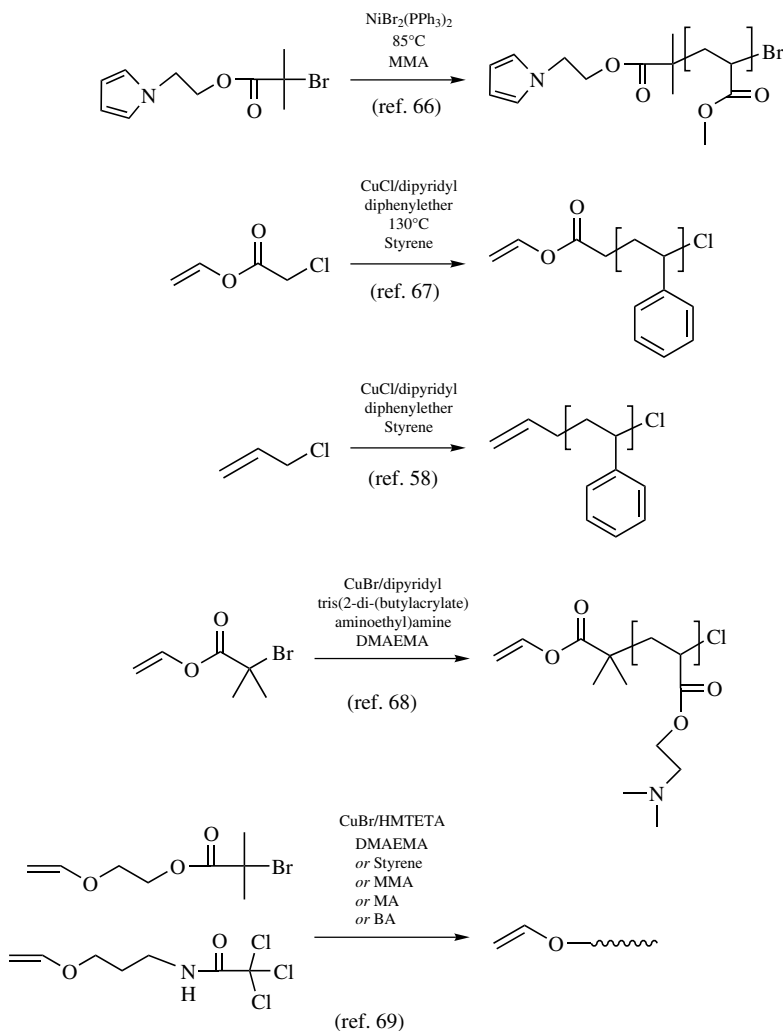
Figure 14.13   Synthesis of macromonomers by ATRP using functional initiators.

2. Macromonomers can also be obtained by functionalization of growing chains. Again, it is essential that the end-capping reaction does not involve the polymerizable group.

3. The last route consists in modifying ω-functional polymers into macromonomers using postfunctionalization methodologies. When chains are grown by free-radical polymerization, it is the easiest way to prepare macromonomers.

For instance, α-pyrrole macromonomers were prepared through the first route from pyrrole-functionalized initiators such as 2-pyrrolyethyl 2-bromo-2-methylpropionate, which subsequently served to trigger the ATRP of various monomers, including styrene, methyl methacrylate (MMA), tert-butyl acrylate (tBuA), n-butyl acrylate (n-BuA), (dimethylamino)ethyl methacrylate (DMAEMA), and methyloxyethylethyl methacrylate.[66] These macromonomers fitted with pyrrole end groups are expected to afford better processable polypyrrole graft copolymers on their chemical or electrochemical copolymerization with pyrrole.

Activated alkyl halides containing a double bond such as vinylchloroacetate, allyl chloride (or bromide), allyl 2-bromoisobutyrate, 2-vinyloxyethyl-2-bromoisobutyrate, and 3-vinyloxypropyl trichloroacetanamide also served to synthesize well-defined macromonomers by ATRP (Fig. 14.13).[67–69] This could be successfully achieved owing to the inability of vinyl acetate and allylic double bonds to copolymerize with either styrene or (meth)acrylic monomers. With vinyl ether derivatives, however, the terminal vinylic double bond was slowly consumed with increasing conversion during ATRP of acrylate monomers.[68] Water-soluble allyl-terminated poly(DMAEMA) were subsequently quaternized and the corresponding macromonomer was copolymerized with acrylamide, affording comb-shaped polyelectrolytes.[69]

The contribution of Rizzardo and his co-workers to the synthesis of macromonomers rests on the functionalization of growing chains using chain transfer agents or cobalt-mediated catalytic chain transfer.[70] These authors prepared macromonomers possessing a 1,1-disubstituted alkene end group by radical addition–fragmentation in the presence of alkyl sulfides. This particular class of macromonomers, which requires the presence of α-methyl vinyl monomers, was further used as precursors to the synthesis of block and graft copolymers. Chaumont and colleagues also described the synthesis of various macromonomers by addition–fragmentation.[71] Readers who are interested in these methods that do not require "living/controlled" systems can find more detail in Chapter 10 of this handbook.

As for macromonomers derived by postfunctionalization, an example was described by Haddleton and colleagues.[72] Starting from separately prepared ω-bromo PMMA that was activated using a CuBr/N(-n-octyl)-2-pyridylmethanimine catalytic system, they could derivatize the latter polymer and obtain ω-unsaturated macromonomers on addition of methyl(2-bromomethyl)acrylate (MBrMA), a monomer known to undergo addition–fragmentation. For a quantitative transformation of the ω-bromide polymers into macromonomers, they had to use a 5-fold excess of MBrMA and Cu(0).

14.3   RANDOM, GRADIENT, AND ALTERNATING COPOLYMERS

Most of the studies that compared the chemoselectivities in conventional and controlled/living copolymerization resulted in the conclusion that they are very similar and independent of the mechanisms used to create radicals.[73–92] However, it is notorious that conventional and LR copolymerizations lead to different copolymer structures. In conventional free-radical copolymerizations, the samples formed contain polymer chains with different comonomer composition, because comonomers are often consumed at different rates—unless being copolymerized under azeotropic conditions—and also because the lifetime of growing radicals is very short. As a result, a continuous drift occurs in the comonomer ratio during polymerization, and the polymers formed exhibit a first-order chemical heterogeneity. In LR copolymerizations, all chains grow simultaneously nearly at the same rate and therefore have the same chemical composition. The drift in the comonomer ratio that occurs is recorded in all individual chains; the composition in the copolymers formed continuously changes from one end to the other. Such copolymers exhibit a second-order heterogeneity and are also termed gradient copolymers.[82] They are expected to exhibit distinct physical properties as compared those of random or block copolymers of same composition.

From a practical point of view, two distinct strategies can be contemplated to synthesize such gradient copolymers. The first applies to monomers with dissimilar reactivity ratios; in that case, the copolymerization results in the formation of so-called spontaneous gradient copolymers. LR copolymerization also provides the opportunity to manipulate the spontaneous composition in such materials; in a semicontinuous process, one of the two monomers can be progressively added into the batch containing the second monomer and forced (or controlled) gradient copolymers can be obtained in this way.

In addition to monomers that are known to readily copolymerize, such as styrenics, alkyl (meth)acrylates, monomers that are unable to homopolymerize by any LRP process, such as isobutene, maleic anhydride, and vinylidene chloride, were also subjected to LR copolymerization with another comonomer. In the case of nitroxide-mediated copolymerizations, the use of TEMPO as counterradical necessarily implied that a styrene derivative be part of the comonomer mixture for a controlled propagation to occur; styrene was indeed successfully copolymerized with a wide variety of monomers, including acrylonitrile,[73] alkyl (meth)acrylates,[21] vinyl carbazole,[73–75] vinyl ferrocene,[76] chloromethylstyrene,[77] and epoxystyrene.[78] The difficulties in obtaining random copolymers including monomer units other than styrenics by NMP have been overcome by employing nitroxides containing a hydrogen in β position (see Fig. 14.16). Indeed, well-defined random copolymers of isoprene and (meth)acrylics (acrylic acid, 2-hydroxy-ethyl methacrylate, *tert*-butyl acrylate) and random copolymers of isoprene and styrenics (chloromethylstyrene, acetoxystyrene, styrene) could be derived thanks to these novel counterradicals.[79]

On the other hand, the Sawamoto[80] and Jérôme[38] groups gave further evidence of the versatility of ATRP by synthesizing forced and spontaneous gradient copolymers that were obtained by copolymerization of MMA with *n*BuA or with styrene, using

$RuCl_2(PPh_3)_2/Al$ or $NiBr_2(PPh_3)_2$ transition metals as catalytic system. Matyjaszewski and colleagues not only copolymerized styrene with nBuA, but they also succeeded to incorporate monomer units such as vinyl acetate.[81] Sawamoto and colleagues even attempted to sequentially polymerize mixtures of styrene and methyl methacrylate of different composition to synthesize the so-called ABC random block copolymers.[80] For additional information on gradient copolymers obtained by atom transfer radical copolymerization, the reader is invited to consult a review by Matyjaszewski and colleagues.[82]

Other pairs of monomers such as styrene and acetoxystyrene,[83] styrene and epoxystyrene,[78] methyl methacrylate and n-butyl methacrylate,[38,84–86] and N,N-dimethylacrylamide and methyl methacrylate[87] were copolymerized via atom transfer radical reactions. In this case, however, random copolymers were obtained as a result of the similar reactivity ratios of the two monomers. Of particular interest is the possibility shown by Matyjaszewski and co-workers of synthesizing waterborne statistical copolymers, such as those comprising styrene and butyl acrylate units.[88]

Less data are available regarding the synthesis of alternating copolymers by LR copolymerization. Maleic anhydride and styrene are examples of monomers that spontaneously undergo alternating copolymerization by RP, especially if the reaction temperature is kept below 80°C. The copolymerization of these two monomers in the presence of CuBr/dipyridyl was unsuccessful, likely because of the deactivation of the ATRP catalytic system by maleic anhydride.[89] The TEMPO-mediated copolymerization of this pair of comonomers did afford copolymer samples; the reaction proceeded even faster than for NMP of styrene.[90] However, random rather than alternating copolymers were obtained because of the elevated temperature of the process. This was also true for the samples obtained by Hawker and co-workers, who performed the copolymerization of maleic anhydride and styrene in the presence of a α-hydrido nitroxide.[91] As for Li and colleagues, they observed that the atom transfer radical copolymerization of maleimide derivatives—namely, N-(2-acetoxy-ethyl) and N-phenylmaleimide—with styrene produced well-defined copolymers with a predominantly alternating structure, whatever the comonomer feed ratio employed.[92]

14.4   BLOCK COPOLYMERS

Block copolymers enter in many applications as a result of the multifaceted role played by these species that can either serve as compatibilizers, viscosity modifiers, or dispersants to stabilize colloidal suspensions, and other compounds.[93] Before the advent of LRP, block copolymers obtained by RP required either the use of telomers or that of free-radical macroinitiators prepared beforehand.[19] Considering the number of contributions to the synthesis of block copolymers by LRP, it is currently one of the most active fields of research in polymer chemistry. All the methodologies of LRP (NMP, ATRP, RAFT, etc.) have been applied to prepare all sorts of block copolymers from those that were already obtained using other more demanding mechanisms to genuinely original ones.

It appears from these studies that the blocking efficiency is sensitive in NMP and ATRP to the experimental conditions (temperature, monomer conversion, use of additives, etc.) used to grow the first block; it is particularly essential to discontinue the polymerization of the first monomer before its total consumption so as to preserve intact its end functionality and thus prevent an excessive concentration of dead blocks. The second factor that plays a crucial role in the successful synthesis of block copolymers is the rate of cross-propagation as in any sequential polymerization; the achievement of an efficient cross-propagation is not only subordinated to the rate constant of cross-addition ($k_{a,b}$) and to the rate constant of propagation ($k_{p,b}$) of the second monomer but also depends on the equilibrium constants (K_a, K_b) between active and dormant species for the two kinds of monomer units. If the reactivity ratios of monomers and the rate constants of propagation are known, the equilibrium constant are not necessarily available in the literature, which introduces a further difficulty in such syntheses. A comprehensive description of block copolymers obtained by ATRP can be found in Chapter 11 of this handbook. In RAFT-mediated polymerizations, an efficient crossover requires that the rate of transfer to the terminal dithioester carried by a given precursor be higher than the rate of transfer to the dithioester generated at the end of the growing second block.[4] In other words, it is essential that the first block grown provide the better leaving radical. Also, the concentration of radical initiator in RAFT-mediated polymerization should be much lower than that of transfer agent, because the proportion of dead homopolymers is directly related to the concentration of the initiator consumed.

As a consequence of these features, monomers cannot be polymerized in an indiscriminate sequence, but they should be added in an order that privileges the fastest one. This general rule is valid for any of the three main LRP methodologies (NMP, ATRP, and RAFT). However, experimental ''tricks'' (e.g., ''halogen exchange'' in the case of ATRP[94]) can be used to increase the rate of cross-propagation relative to that of propagation, for a sequence of additions with an unfavorable rate of cross-propagation.

In addition to the traditional route based on the sequential addition of two radically polymerizable monomers, one can also get access to well-defined block copolymers by using a preformed polymer that can be used as a macroinitiator for the growth of the second block by LRP. This prepolymer can be derived from any of the LRP methodologies or from another chain addition polymerization—including conventional radical, cationic, anionic and ring-opening ones—or even step growth processes, before crossing over to LRP. One usually resorts to this synthetic strategy when the monomers to pair in a targeted diblock structure do not polymerize by the same mechanism. With bifunctional precursors, ABA triblock copolymers can be obtained in two steps but some of the latter were also derived by a three-step sequential polymerization of the A and B monomers.

14.4.1   Hard–Soft Block Copolymers

14.4.1.1   By Sequential LRP   ABA triblock copolymers whose central B blocks are soft, that is, with a low glass transition temperature (T_g); e.g., *n*-butyl acrylate,

methyl acrylate, 2-ethylhexyl acrylate) and outer B blocks are hard (high T_g); e.g., styrene, methyl methacrylate, acrylonitrile) attract interest because of their potential applications as thermoplastic elastomers.

In one of their first reports on ATRP in 1995, Matyjaszewski and co-workers described the synthesis of block copolymers based on styrene and methyl acrylate units that were obtained by sequential polymerization.[95] Other groups later showed how to take benefit of nickel(II) or ruthenium(II) catalytic systems to derive poly (methyl methacrylate)-b-poly(n-butyl methacrylate) (PMMA-b-Pn-BuMA) diblock copolymers as well as PMMA-b-Pn-BuMA-b-PMMA triblock copolymers.[96–97] Since then, miscellaneous hard–soft block copolymers were prepared by ATRP using various catalytic systems. The main characteristics of some of these materials are presented in Table 14.1 and relevant information can also be found in Chapter 11 of this handbook.

As emphasized above, there are golden rules to respect if one wants to access well-defined block copolymers that are free of any homopolymer contaminants by ATRP. For monomers that belong to the same family, their order of polymerization is less critical.[96–97] Interestingly, the same situation prevails for styrenics and alkyl

TABLE 14.1   Miscellaneous ATRP-Derived Hard–Soft Block Copolymers

A Block	B Block	Catalytic System	Type of Block Copolymers Synthesized	Ref.
n-BuA or MA	MMA	CuCl,CuBr/PMDETA CuCl,CuBr/HMTETA[a]	AB ($M_n = 21,000$ g/mol; PDI = 1.25)	107
n-BuA	MMA	CuCl,CuBr/PMDETA CuCl,CuBr/HMTETA[a]	BAB ($M_n = 90,000$ g/mol; PDI = 1.35)	107
MMA or n-BuA	MA or n-BuA	CuCl,CuBr/dNdipy[a]	AB ($M_n = 20,500$ g/mol; PDI = 1.15)	101
n-BuA	MMA	CuCl,CuBr/dNdipy[a]	ABA ($M_n = 37,200$ g/mol; PDI = 1.2)	101
MMA	n-BuMA	RuCl$_2$(PPh$_3$)$_2$ with Al(iPrO)$_3$	AB and ABA (PDI < 1.3)	97
n-BuA	MMA	NiBr$_2$(PPh$_3$)$_2$ or CuCl,CuBr /dNdipy[a]	BAB exhibiting microphase separation	102–105
S or n-BuA	n-BuA or S	CuCl/dipy with DMF[b]	ABA ($M_n = 104,000$ g/mol; PDI = 1.71)	98
S	MA	ReO$_2$I(PPh$_3$)$_2$ with Al(iPrO)$_3$	AB ($M_n = 16,000$ g/mol; PDI = 1.33)	106
MMA	n-BuA or MA	NiBr$_2$(nBu$_3$)$_2$ with Al(iPrO)$_3$[b]	AB ($M_n = 25,000$ g/mol; PDI = 1.5)	84

Key: n-BuA = n-butyl acrylate; N-BuMA = n-butyl methacrylate MA = methyl acrylate; MMA = methyl methacrylate; S = styrene; dipy = 2,2′-dipyridyl; dNdipy = 4,4′-di-(5-nonyl)-2,2′-dipyridyl; HMTETA = hexamethyltriethylenetetraamine; PMDETA = pentamethyltriethylenetriamine.

[a] Use of the "halogen exchange" technique.
[b] Random copolymers were also synthesized.

acrylates that can be sequentially polymerized in either order by ATRP (Table 14.1).[95,98–100] The situation is obviously different for monomers exhibiting a distinct reactivity. For instance, the rate of initiation of a PMMA block by a chlorine-terminated PMA is slow as compared with the rate of propagation of methyl methacrylate, which results in a poorly defined block copolymer.[101] One way to improve the blocking efficiency is to grow the PMMA block from a bromine terminated PMA precursor in the presence of CuCl so as to favor the initiation step over propagation. Thus, for the synthesis of block copolymers based on alkyl acrylate and alkyl methacrylate units, it is recommended to form the methacrylate-based block first and then cross over to the ATRP of the acrylate monomer, unless employing the "halogen exchange" technique previously described. For the same reason, polymethacrylate or polyacrylonitrile blocks should not be grown from a polystyrene or a poly(alkyl acrylate) macroinitiator because of a poor blocking efficiency.

The "halogen exchange" technique was also applied by Jérome and co-workers for the synthesis of narrowly distributed poly(methyl methacrylate)-*b*-poly(*n*-butyl acrylate)-*b*-poly(methyl methacrylate) (PMMA-*b*-P*n*-BuA-*b*-PMMA) triblock copolymers that were obtained from a difunctional P*n*-BuA macroinitiator.[102–105] The same triblock structures were also derived by these authors following a four-step procedure based on the sequential ligated anionic polymerization of MMA, *t*BuA, and again MMA, followed by the transalcoholysis of the *t*BuA units into the desired P*n*-BuA. Obviously, ATRP is more straightforward than anionic polymerization with respect to the easiness of the synthesis. On the other hand, the mechanical and rheological properties as well as the morphology of triblock copolymers of same molar mass and same composition, prepared either by anionic polymerization and ATRP were compared by the group of Jérôme.[102–105] It was clearly demonstrated that copolymers obtained by anionic polymerization exhibited better mechanical performances than those prepared by ATRP, although only minor differences could be detected by size-exclusion chromatography or ^{1}H NMR analysis. Therefore, the level of structural and molecular control of materials derived by LRP techniques can approach that delivered by traditional anionic procedures, but a thorough investigation of their physical behavior is required before their utilization in a particular application.

On a practical point of view, it is worth mentioning that the synthesis of water-borne hard–soft block copolymers was successfully achieved.[88,96] On the other hand, block and statistical copolymers of *n*-butyl acrylate and styrene were even derived in the presence of a limited amount of air by means of ATRP.[108]

Block copolymers containing styrene-rich statistical copolymer as a segment were also derived by NMP.[73] Provided the amount of styrene was sufficiently high in the initial monomer feed ratio, the statistical nitroxide-mediated copolymerizations of styrene with acrylonitrile, methyl acrylate, methyl methacrylate, or vinyl carbazole could be achieved under controlled fashion. On varying the composition of the statistical block, the morphology of these materials could be finely tuned. For instance, diblock copolymers (M_n in the range 3,600–6,800 g/mol and PDI < 1.3) were synthesized from a preformed ω-alkoxyamine PS that served as macroinitiator for the polymerization of an azeotropic mixture of styrene and acrylonitrile at 125°C.

Others[109,110] also described the synthesis of hard–soft block copolymers based on styrene and alkyl acrylate blocks. Either hydroxy-TEMPO or TEMPO were used as counterradicals, and in either cases the acrylic monomers could not be polymerized to complete conversion because of the lack of livingness of their propagation in the presence of this family of nitroxides. It was then suggested to use additives as a means to reduce the amount of free nitroxide resulting from irreversible termination and thus prevent the inhibition of acrylate polymerization.[111] This resulted in an increase of the rate of polymerization, and slightly better-defined polyacrylates could be prepared and chain-extended with styrene to yield Pn-BuA-b-PS block copolymers. However, the polydispersities of the copolymers formed were still in the range 1.5–1.9. Yousi et al.,[112] on one hand, and Catala and colleagues[113] on the other, followed the same approach resting on the use of TEMPO for the synthesis of a series of diblock copolymers based on styrenics for the first block and alkyl methacrylates for the second. These authors were also confronted to the occurrence of chain breaking reactions while growing the polymethacrylic block whose reaction with TEMPO resulted in the β-hydrogen abstraction from the growing chain end. Charleux and coll. clearly demonstrated that this side reaction is the main chain breaking event in their attempt to synthesize PS-b-Pn-BuA diblock copolymers.[114] The chain extension of a TEMPO-terminated PS in the presence of n-butyl methacrylate gave rise to diblock copolymers bearing a ω-methylene unsaturation (Fig. 14.14), as evidenced by MALDI-TOF mass spectroscopy and ^{1}H NMR. These authors even calculated the rate constant of this β-hydrogen abstraction reaction: $k_d = 1.4 \times 10^6$ L mol^{-1} s^{-1} at 130°C.

The Xerox group was also the first to report the synthesis of poly(styrene)-b-poly(isoprene) (PS-b-PI) copolymers by chain extension from a ω-alkoxyamine PS in the presence of 1,3-dienes.[110] The polymerization of isoprene had to be carried out at rather high temperature (145°C), and only moderate conversion could be achieved; the polydispersities were in the range of 1.4–1.5, indicating that these
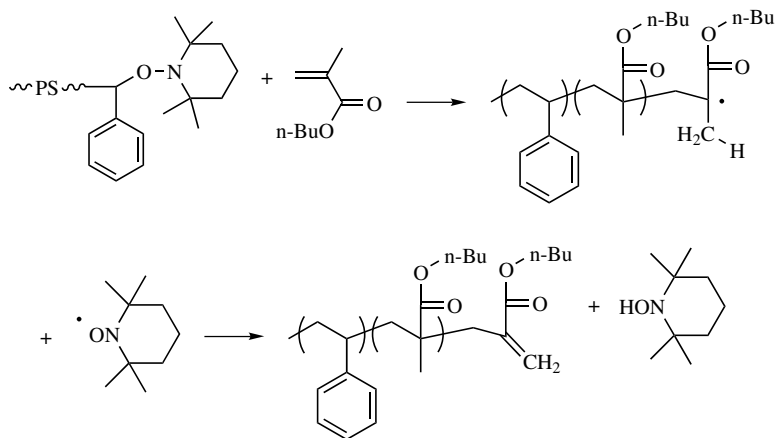
Figure 14.14   Synthesis of PS-b-Pn-BuA with TEMPO.[114]
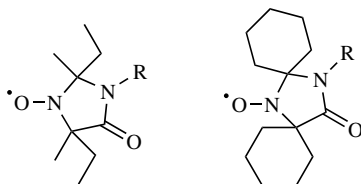
Figure 14.15   Structure of imidazolidone nitroxides.[115]

materials were rather ill-defined.[111] Following a three-step sequential polymerization procedure, poly(styrene)-*b*-poly(butadiene)-*b*-poly(styrene) (PS-*b*-PB-*b*-PS) triblock copolymer (M_n 43,000 g/mol; PDI = 1.24) were also obtained by the same team.[110,111]

Nitroxides based on imidazolidone (Fig. 14.15) developed by the group of Rizzardo offer a few advantages over TEMPO and its derivatives in terms of molecular control when synthesizing random and block copolymers;[115] for instance, soft–hard P*n*-BuA-*b*-PS.

The development of a novel generation of β-hydrogen-containing nitroxides developed by Elf-Atochem[116–117] and IBM,[14,79] such as those shown in Fig. 14.16, significantly improved the performances of NMP as compared to many of the nitroxides previously employed.

Indeed, these nitroxides are not only capable of bringing about a faster and yet controlled polymerization of styrenics but are also excellent at controlling the chain growth of alkyl acrylates, including functional monomers such as hydroxyethyl acrylate as well as dienes (butadiene and isoprene). A wide variety of well-defined random and block copolymers consisting of styrenic (chloromethyl styrene, acetoxystyrene, styrene, etc.), isoprene and alkyl (meth)acrylate blocks were synthesized. For instance, poly(*tert*-butyl acrylate-*b*-isoprene) (M_n = 10,000–40,000 g/mol and PDI ∼ 1.2) and poly(styrene-*b*-isoprene) ($M_n \leq$ 100,000 g/mol and PDI < 1.2) diblock copolymers were prepared by Hawker et al.[79] In addition, the use of such β-hydrogen-containing nitroxides allowed the same team to obtain poly[(styrene-*r*-maleic anhydride)-*b*-styrene)] random-block copolymers.[91] Gnanou and colleagues also resorted to a β-hydrogen-containing nitroxide [viz., *N*-*tert*-butyl-*N*-(1-diethylphosphono-2,2-dimethyl)propyl nitroxide, also referred to as DEPN
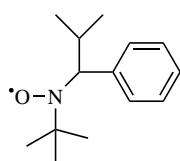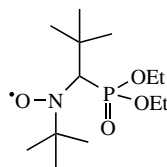
(ref. 14, 79)   (ref. 116, 117)

Figure 14.16   A novel generation of nitroxides containing β-hydrogen.

and patented by Atochem under the trademark of SG1] in association with AIBN to prepare di- and triblock structures containing soft and hard segments based on styrene and *N*-butyl acrylate units; they also employed novel dialkoxyamines based on this nitroxide to derive triblock copolymers.[118] They thoroughly discussed the factors that control the blocking efficiency in such syntheses, namely, the order of addition of monomers, the rate of crosspropagation, and so on and gave the key to obtain copolymers with a well-defined structure.

The synthesis of hard–soft block copolymer by sequential polymerization was also successfully achieved using the RAFT methodology.[4] However, to prepare well-defined methacrylate-*b*-acrylate diblock copolymers, one should sequentially polymerize the methacrylic monomer and then the acrylic one, this order of addition being imposed by the reasons previously discussed. ABA triblock copolymers constituted of a soft central block and two external hard segments all based on methacrylates could be derived by sequential polymerization from a molecule containing two dithiocarbonylthio groups that functioned as a bifunctional reversible transfer agent.[119] For instance, PMMA-*b*-P*n*-BuMA-*b*-PMMA of controlled molar mass ($M_n = 112,000$ g/mol) and narrow polydispersity (PDI = 1.14) were prepared using this transfer agent [Fig. 14.17 (i)]. Alternatively, trithiocarbonate-containing compounds [Fig. 14.17 (ii)] were also utilized to make PS-*b*-P*n*-BuA-*b*-PS triblock copolymers ($M_n = 161,000$ g/mol; PDI = 1.16).[120] Here also, the two dithio functions concomitantly served as transfering sites in the sequential LRP of two corresponding monomers. In this case, however, these dithio groups remained at the center of the final block copolymer whereas they were located at chain ends in the previous case.

Rod–coil-type copolymers can be viewed as a particular category of hard–soft materials. LRP was shown to be particularly dependable and efficient for the synthesis of rod–coil block copolymers of narrow molar mass distribution and precisely
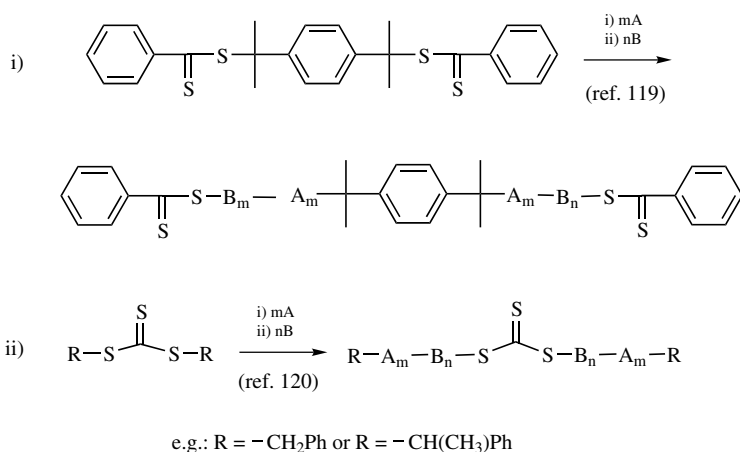
Figure 14.17   Synthesis of triblock copolymers by the RAFT process.[119,120]

(ref. 121)

(ref. 122)
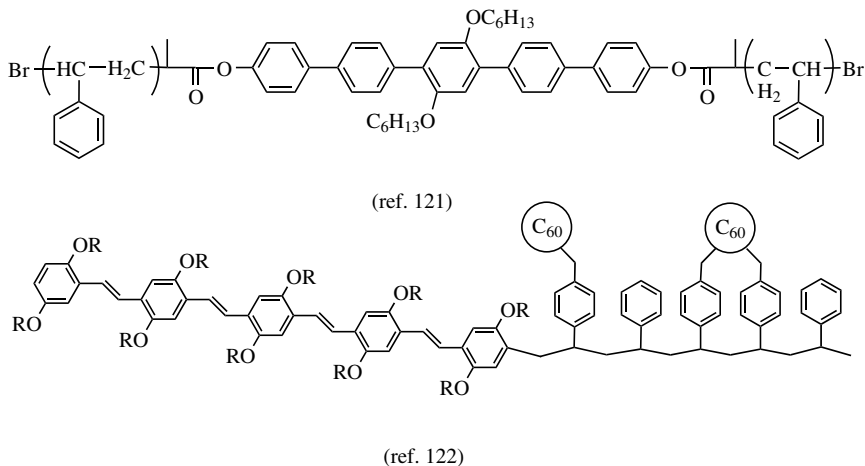
Figure 14.18   Rod–coil block copolymers by LRP.

tailored blocks (Fig. 14.18). Copolymers including amorphous segments and blocks carrying lateral mesogenic groups were for instance reported.[121] These AB block copolymers derived by sequential polymerization of 4-acetoxystyrene and a liquid crystalline styrenic monomer in the presence of TEMPO at 135°C exhibited, after annealing, a lamellar morphology with smectic layers. Another example of rod–coil diblock copolymer involving a NMP-derived poly(styrene-*co*-chloro-methylstyrene) block as the flexible coil and poly(*p*-phenylene vinylene) as the rigid rod (Fig. 14.18) was provided by Hadziioannou et al.[122] Such diblock copolymers were found to exhibit semiconducting properties and may find potential applications in photovoltaic devices. The subsequent grafting of C_{60} onto pendant chloromethyl groups through atom transfer radical addition afforded a diblock copolymer whose cast films from CS_2 solution exhibited honeycomblike morphologies.

***14.4.1.2   By Combination of LRP with Cationic Polymerization*[123]**   Excellent thermoplastic elastomers could be obtained on associating polymers of high T_g with a rubbery cationically derived polyisobutylene (PIB) in a triblock copolymer structure. The crossover from "living" carbocationic polymerization of isobutylene to ATRP of styrene, methyl acrylate, isobornyl acrylate, or *p*-acetoxystyrene was found to be efficient enough to prepare ABA as well as AB block copolymers.[124–128] Although belonging to this class of materials, Batsberg and colleagues engineered a slightly different triblock architecture (Fig. 14.19) made of a central rubbery PIB block flanked by two densely grafted poly(p-methylstyrene) segments.[129] The grafts in these outer blocks were grown by ATRP of styrene or acetoxystyrene after bromination of some of the pendant methyl groups of *p*-methylstyrene units. Gel formation could be avoided by an adequate choice of the experimental conditions

polystyrene or poly(acetoxystyrene)
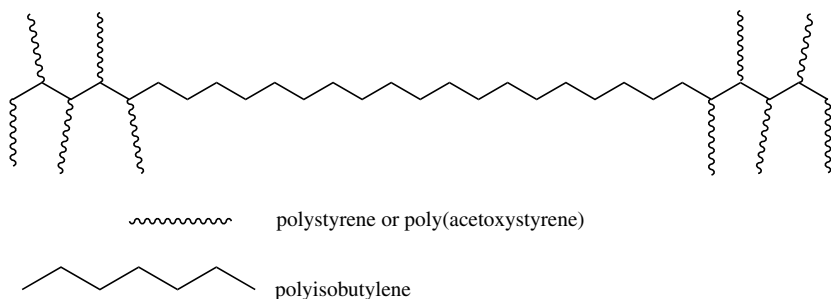
polyisobutylene

Figure 14.19   Block copolymers with densely grafted segments.[129]

(e.g., the type of ligand). A similar structure, a PIB-*g*-PS copolymer, was obtained using the same approach[130] starting from a commercially available poly(isobutylene-*co*-p-methylstyrene-*co*-p-bromethylstyrene) copolymer known as EXXPRO.

14.4.1.3   By Combination of LRP with Anionic Polymerization   The synthesis of hard–soft block copolymer through crossover from anionic polymerization to LRP was also contemplated. Polybutadiene (PB) or its hydrogenated derivative poly(ethylene-*co*-butylene) (PEB), polyisoprene (PI) and PS or a block copolymer of these two polymers were first obtained under "living" anionic conditions and then capped with halide functions (e.g., bromoisobutyrate, benzyl bromide).[131] From such precursors, various blocks based on methyl acrylate, styrene, butyl acrylate, and acetoxystyrene were grown by ATRP, allowing the synthesis of PI-*b*-PS, PS-*b*-PMA, PS-*b*-P*n*-BuA, PS-*b*-(P(S-*r*-AN)), PS-*b*-PI-*b*-PS, PEB-*b*-PS, PEB-*b*-PAS, PEB-*b*-PHS block copolymers. In a similar approach, the group of Haddleton prepared AB and ABA block copolymers from modified poly(butylene-*co*-ethylene).[40]

The combination of living anionic polymerization of isoprene and ATRP of styrene for the synthesis of PI-*b*-PS copolymers fitted with a fluorescent dye at the junction between the two blocks was also reported.[132] The same group applied an identical approach to derive block copolymers including methyl methacrylate and alkyl acrylate units.[133]

As an alternative route to PB-*b*-PS copolymers by sequential anionic polymerization, Priddy and colleagues proposed to associate the living anionic polymerization of butadiene and the LRP of styrene.[134] These authors used an epoxy-functionalized alkoxyamine to terminate "living" anionic PB chains[135] and initiate the polymerization of styrene from this alkoxyamine-functionalized PB. Rather well-defined PB-*b*-PS ($M_n = 15,000$–$27,000$ g/mol; PDI = 1.4) diblock copolymers were produced in this way. The samples obtained on blending these block copolymers with homo-PS chains were transparent to visible light.

14.4.1.4   By Combination of LRP with RP   NMP also allowed to prepare triblock copolymers consisting in hard and soft segments, such as styrene/butyl acrylate,

methyl methacrylate/isoprene, styrene-*alt*-acrylonitrile/isoprene blocks by combination of conventional radical technique with NMP.[136] Although poorly defined due to the contamination of the structure targeted by diblock copolymers, the resulting materials could however be used as emulsifiers in the corresponding blends. In contrast to the copolymer-free blends that formed opaque and brittle films due to macrophase separation, those emulsified by these copolymers exhibited much smaller phases (microphase separation).

14.4.2 Amphiphilic Block Copolymers

Amphiphilic copolymers made of hydrophilic and hydrophobic blocks are capable of self-aggregating into microdomains in the presence of a selective solvent of one of the two constituents.[93,137] This self-association can promote the formation of three-dimensional structures such as stable spherical or cylindrical micelles or even more organized assemblies such as vesicles; this aggregation phenomenon may be reversible depending on the concentration of the solution, its temperature, pH, and the ionic strength. Polymeric amphiphiles are exploited in dispersed media where they are currently used as emulsifiers, dispersants, or stabilizers but they are also applied as drug delivery devices. Moreover, in the solid state amphiphilic copolymers were shown to serve as templates for the crystallization of highly ordered inorganic structures.[138]

The emergence of LRP not only allows access to classic amphiphilic copolymers under nondemanding conditions and at low cost but also opens up the opportunity for designing original amphiphilic AB and ABA-type amphiphilic block materials.

14.4.2.1   By Sequential LRP   Monomers such as 2-(dimethylamino)ethyl methacrylate (DMAEMA)[4,139,140], hydroxyethyl (meth)acrylate (HEA and HEMA),[4,141–143] styrene sulfonate (NaSS),[4,144–146] dimethyl acrylamide (DMA),[15,87,147] and (meth) acrylic acid (AA and MAA)[4,79] could be directly polymerized to generate the hydrophilic blocks (Fig. 14.20). Noteworthy are the possibilities now offered to incorporate hydrophilic blocks in amphiphilic copolymers without resorting to protection chemistry via one of the LRP methodologies: NMP, in particular with the development of the β-hydrido-containing nitroxides for HEA, RAFT for AA, MAA, HEA, NaSS, DMAEMA, and so on and ATRP for HEA, HEMA, DMAEMA, and the neutralized form of MAA, and other compounds. The characteristics of the corresponding amphiphilic block copolymers are presented in Table 14.2.

Interestingly, DeSimone and Matyjaszewski demonstrated that ATRP performed in supercritical carbon dioxide could be conducted in a controlled fashion.[148] These authors synthesized block copolymers incorporating fluorinated CO_2-philic (meth)acrylate blocks and CO_2-phobic blocks (e.g., MMA or DMAEMA) that can also be viewed as amphiphilic ones. Moreover, ATRP of these monomers could be either carried out under homogeneous conditions or in dispersion. In the latter case, the fluorine-based block copolymers served as stabilizers to produce PMMA latex by dispersion polymerization in supercritical carbon dioxide.

poly(HEA) *or*
poly(HEMA)

(ref. 4, 79, 141-143)

poly(DMAEMA) *or*
poly(HEMA)

(ref. 4, 139-140)

poly(HEA) *or*
poly(HEMA)

(ref. 4, 144-146)

poly(AA) *or*
poly(MAA)

(ref. 4, 79, 91)

poly(DMA)

(ref. 87, 147)
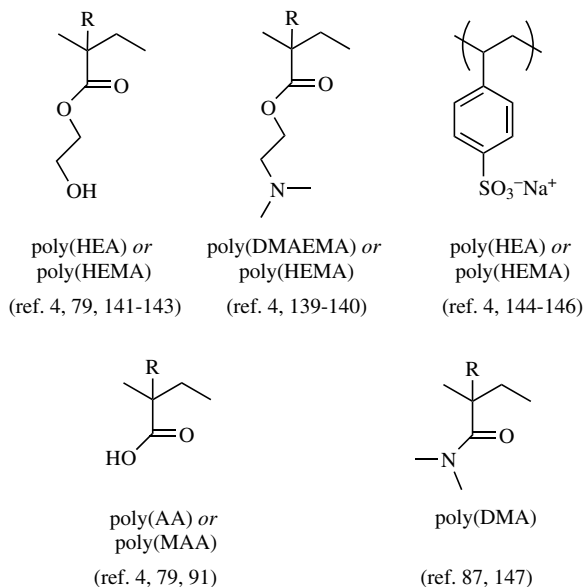
Figure 14.20   Hydrophilic monomer units in amphiphilic block copolymers obtained by LRP without protection chemistry.

TABLE 14.2   Examples of LRP-Derived Amphiphilic Block Copolymers Involving Nonprotected Hydrophilic Monomers (see Scheme 14.20)

Hydrophilic A Block	Hydrophobic B Block	Synthetic Route	Copolymers	Ref.
NaSS	S	NMP in water/ethylene glycol at 120°C (TEMPO)	AB and ABA	144,145
NaSS	Vinyl naphthalene	NMP in water/ethylene glycol at 125°C (TEMPO)	AB	146
MAA	MMA	RAFT	AB	4
DMAEMA	S or BzMA	RAFT	AB	4
DMAEMA	MMA or S or MA	ATRP (CuBr/4,4′-di-(5-nonyl)-2,2′-dipyridyl)	AB and ABA	140
HEA	MMA or S	ATRP (CuCl/dipyridyl)	AB	141
HEMA	MMA or S	ATRP (CuCl/dipyridyl)	AB	142,143
DMAEMA	S	NMP (TEMPO)	AB	139
DMAEA or DMA	S	NMP (TEMPO)	AB	112
AA, HEA	IP	NMP (α-hydridonitroxide shown in Scheme 14.16)	AB and (A-*r*-B)-*b*-B	79,91
AA	*n*-BuA	RAFT	AB	4
DMA	4VP	NMP (TEMPO)	AB	147

Key: AA = acrylic acid; *n*-BuA = *n*-butyl acrylate; BzMA = benzyl methacrylate; DMA = dimethylacrylamide; DMAEMA = (dimethylamino)ethyl methacrylate; HEA = hydroxyethyl acrylate; HEMA = hydroxyethyl methacrylate; IP = isoprene; NaSS = styrene sulfonate; MA = methyl acrylate; MAA = methacrylic acid; MMA = methyl methacrylate; 4VP = 4-vinyl pyridine; S = styrene.
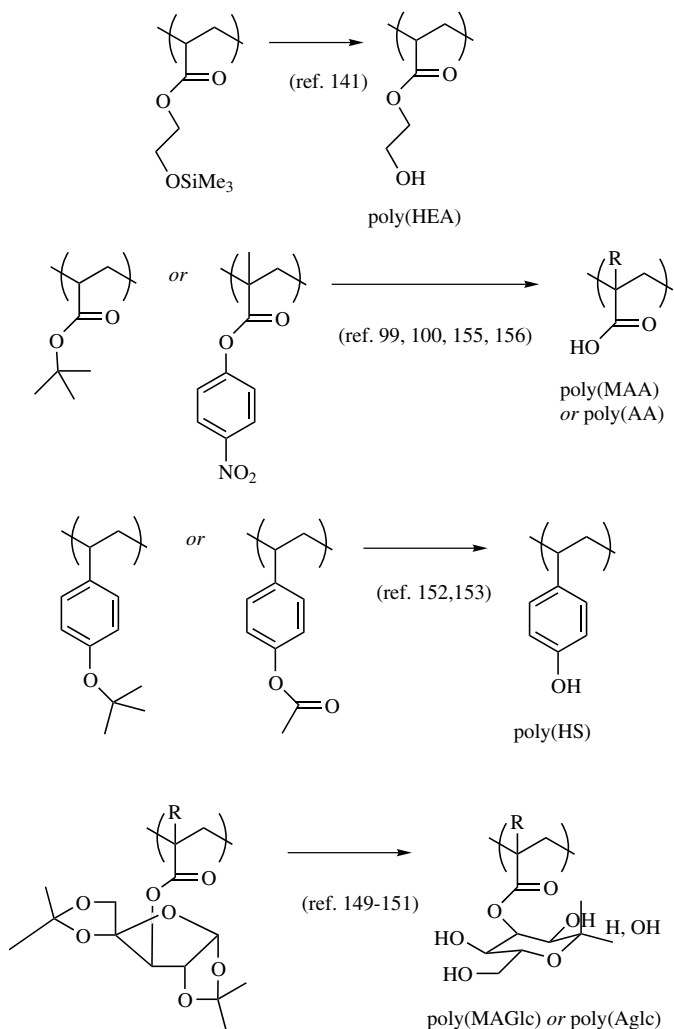
Figure 14.21 Hydrophilic monomer units of amphiphilic block copolymers obtained by LRP after a deprotection step.

Hydrophilic segments were also grown from monomers containing functional groups in their protected form, such as a sugar-containing (meth)acrylate,[149–151] butoxy- or acetoxystyrene,[152,153] phtalimide methylstyrene,[154] *tert*-butyl acrylate,[99,100,155] and miscellaneous[141,156] (Fig. 14.21). In this case, a subsequent step of hydrolysis was required to obtain the desired amphiphilic copolymer (Table 14.3).

The utilization of such amphiphilic copolymers to assemble nanoobjects was reported by Wooley and Ma.[155] These authors reported how amphiphilic PAA-*b*-PMA-*b*-PS triblock copolymers self-assemble in aqueous solution to form

TABLE 14.3   Examples of LRP-derived Amphiphilic Block Copolymers Involving Protective Groups^a

A Block^b	B (and C) Block	Synthetic Route (ATRP Catalyst or Nitroxide)	Comments	Ref.
HEA	n-BuA	(ATRP (CuBr/PMDETA)	AB and ABA	141
MAA	St	ATRP (CuBr/dipyridyl)	AB	156
n-BMADE	St	ATRP (CuBr/dipyridyl)	AB	156
MAGlc	St	ATRP in veratrole (CuBr/di-n-heptyl-dipyridyl)	AB	149
HSt	St	ATRP (CuBr/dipyridyl)	ABA and BAB	152–153
AGlc	St	NMP (di-tert-butyl nitroxide)	ABA	150-151
AA	St (and MA)	ATRP (CuBr/pentamethyltri-ethylenetriamine)	AB, ABA, BAB and ABC^c	99–100, 155

Key: AA = acrylic acid; AGlc = 3-*O*-acryloyl-1,2:5,6-D-glucofuranose; *n*-BuA = *n*-butyl acrylate; *n*-BMADE = *n*-butyl methacrylamide; HEA = hydroxyethyl acrylate; HS = *p*-hydroxystyrene; MA = methyl acrylate; MAA = methacrylic acid; MAGlc = 3-*O*-methacryloyl-1,2:5,6-D-glucofuranose; S = styrene.

^{a} See Scheme 14.21 for the structure of the hydrophilic blocks.
^{b} Hydrophilic block obtained after deprotection.
^{c} Triam star block copolymers (see Section 6) were also prepared.

nanostructures with either spherical or cylindrical morphologies that could be irreversibly preserved upon cross-linking their peripheral PAA units.

Lastly, cationic amphiphilic block copolymers were also obtained by NMP starting from poly(chloromethyl styrene-*b*-styrene) block copolymers; the chloromethyl styrene units were subsequently quaternized into hydrophilic polyelectrolytes with various amines (Fig. 14.22).[157–158] Following the same strategy, the preparation of poly(4-vinyl pyridine-*b*-styrene) diblock copolymers that were further converted to cationic polyelectrolytes by quaternization of the pyridine groups was described.[159]
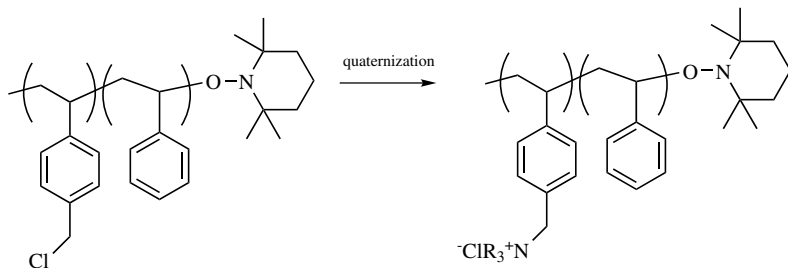
Figure 14.22   Cationic amphiphilic block copolymers.[157,158]

14.4.2.2   By Combination of LRP with Other Mechanisms   Among amphiphilic block copolymers, those based on poly(ethylene oxide) (PEO) segments are the most studied. Such materials can now be derived by combination of LRP techniques with anionic polymerization of ethylene oxide (Fig. 14.23). For instance, PEO-*b*-PS copolymers were obtained upon growing the PS blocks by NMP.[160] However, as the polymerization was carried out at 130°C for 14 h, homo-PS chains were formed by thermal self-initiation of styrene. A last step of selective extraction with cyclohexane was therefore required to get rid of these contaminants and isolate the expected amphiphilic compounds. A similar synthetic approach was followed by Huang and colleagues, who transformed a dimethylamino-terminated PEO into a hydroxy-TEMPO-ended one and used the latter to obtain PEO-*b*-PS copolymers.[161]

Better-defined diblock PEO-*b*-PS and triblock PS-*b*-PEO-*b*-PS structures were derived by ATRP of styrene from PEO macroinitiators ended with bromopropionate functions, in the presence of CuBr/dipyridyl system at 130°C.[162–163] ATRP was found more efficient than NMP since a lower amount of homopolystyrene chains formed by thermal polymerization was found than in the former case. Following the same route, Kubisa and colleagues prepared well-defined triblock P*t*BuA-*b*-PEO-*b*-P*t*BuA copolymers on polymerization of *t*BuA in the presence of CuBr/PMDETA as catalytic system.[164] When applied to the synthesis of PMMA-*b*-PEO-*b*-PMMA triblock copolymers, a lower initiation efficiency was observed. Höcker and colleagues synthesized a series of chlorotelechelic PEO that were employed as macroinitiators for ATRP of styrene or MMA, in order to evaluate the structural parameters that affect the efficiency of the initiation step.[165] These authors came to the conclusion that a fast initiation is observed when a phenyl group is employed in conjunction with an oxycarbonyl group at the end of PEO chains.
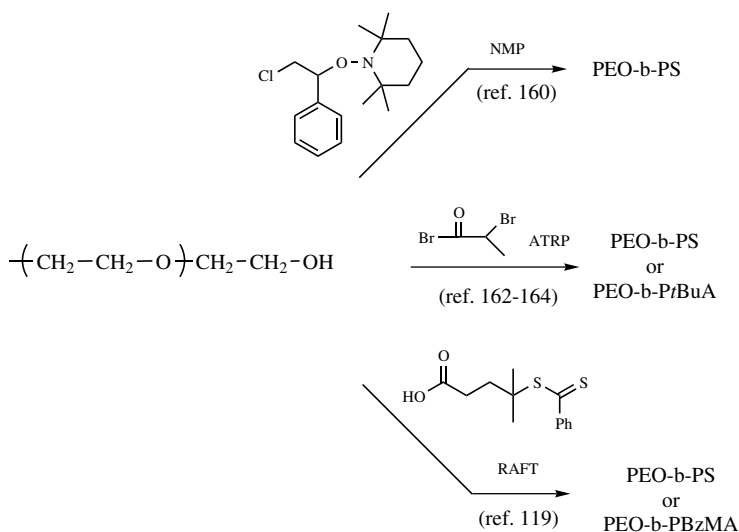
Figure 14.23   Amphiphilic block copolymers based on PEO.

Under these conditions, well-defined PEO/PS and PEO/PMMA-based copolymers could be obtained.

The RAFT methodology was also applied to the preparation of PEO-*b*-PBzMA and PEO-*b*-PS amphiphilic block copolymers.[119] The latter were readily synthesized from ω-dithioester PEO precursors; the hydrophobic blocks were grown by RAFT. The authors claimed that their block copolymers were of narrow polydispersity and did not contain any homo-PEO impurity.

The synthesis of amphiphilic block copolymers involving the chemical modification of a commercial monohydroxy-terminated hydrogenated polybutadiene—that is, a poly(ethylene-co-butylene) (PEB)—into the corresponding bromopropionate polymer that served as macroinitiator for ATRP of acetoxystyrene was reported.[166] The subsequent hydrolysis of the resulting block copolymer was carried out with hydrazine hydrate in xylene and yielded an amphiphilic poly(ethylene-*co*-butylene)-*b*-poly(hydroxystyrene) diblock copolymer.

Wooley and colleagues described the synthesis of amphiphilic block copolymers that involved the switch from anionic polymerization of ε-caprolactone to ATRP of *tert*-butyl acrylate (*t*BuA) followed by the complete hydrolysis of the *tert*-butyl groups of the acrylate blocks.[167] These compounds were found to self-organize into micelle-like structures, when put in the presence of water. The poly(acrylic acid)-based shell part of these micelles was subsequently crosslinked by adding a diamine to form "shell crosslinked knedel-like" nanoparticles containing, in this case, hydrolytically degradable crystalline core domains. Indeed, a last step of hydrolysis of the poly(ε-caprolactone) core yielded nanocage structures.

14.4.3 Double Hydrophilic Block Copolymers

Double hydrophilic block copolymers (DHBC) are water-soluble macromolecular compounds that usually result from the covalent pairing of a neutral block with a charged polyelectrolyte one, but they can also be constituted of two basic or two acidic blocks. This novel class of materials exhibit potential applications that are not necessarily similar to those found for amphiphilic block copolymers; they can be used as dispersants or as drug delivery systems, but they were also found of particular interest as templates for the growth of inorganic structures.[168] The group of Armes recently demonstrated that the ATRP of hydrophilic monomers such as ω-methacrylate-PEO macromonomer, sodium methacrylate, or sodium 4-vinylbenzoate can be conducted in water at ambient temperature.[16,169–171] These authors initiated the ATRP of the abovementioned monomers from a bromoester end-capped PEO macroinitiator and derived well-defined DHBC. The same group also derived zwitterionic as well as acidic block copolymers by sequential NMP of charged hydrophilic monomers in aqueous solutions.[172] Similar block copolymers and also dicationic block copolymers were synthesized by RAFT by McCormick et al.[173] To this end, these authors employed a water-soluble dithioester as a chain transfer agent (CTA).

Structures that could previously be obtained only by ionic polymerization techniques and laborious protection/deprotection step can now be prepared by either methodology of LRP (Fig. 14.24).
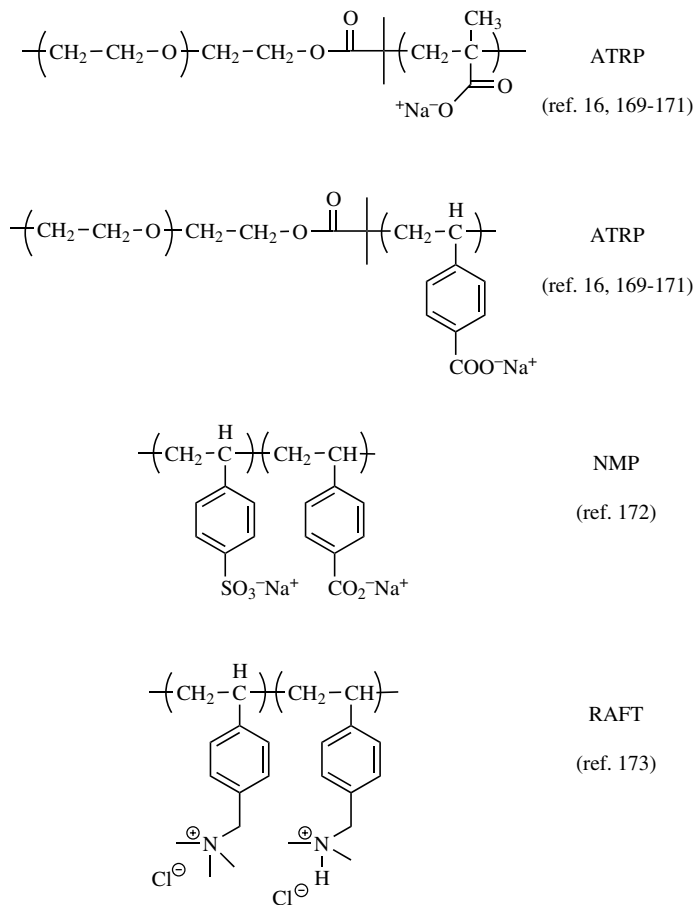
Figure 14.24 Double hydrophilic block copolymers.

14.4.4 Organic/Inorganic Block Copolymers

Poly(dimethylsiloxane) (PDMS) exhibits a very low glass transition temperature and is also the most widely utilized inorganic polymer. Coupling techniques were used to prepare copolymers based on PDMS blocks with the view of pairing them with hard blocks. The objectives of generating such copolymers were either to reinforce the mechanical properties of PDMS or improve the impact strength of the hard block. Such hybrid copolymers are also expected to find applications in the domain of pressure sensitive adhesives. The combination of ionic polymerization or step growth polymerization for the PDMS block with LRP for the formation of the hard block was contemplated for the synthesis of such copolymers.

For instance, Yoshida and colleagues obtained PS-*b*-PDMS-*b*-PS ($M_n = 30,000$ g/mol; PDI $= 1.9$) copolymers as follows. On polycondensing α,ω-diamino-PDMS with

a dichloroazo compound, these authors first obtained an azo-containing PDMS macroinitiator used to grow PS blocks by NMP at 130°C in the presence of methoxy-TEMPO.[174] Alternatively, α,ω-dihydrosilyl and divinylsilyl-terminated PDMS were derivatized by hydrosilylation and capped with either benzyl chloride or 2-bromoisobutyrate functions; the latter was subsequently used to initiate the ATRP of styrene or alkyl (meth)acrylates.[175–177] Well-defined ABA as well as ABC triblock copolymers and even graft copolymers (see Section 14.5) were produced in this way. Other hybrid block copolymers were synthesized by sequential ATRP of methacrylate-ended functional polyhedral oligomeric silsesquioxane (MA-POSS) and *n*-butyl acrylate.[178] The ATRP was carried out in toluene in the presence of CuBr/PMDETA catalytic system to afford triblock copolymers poly(MA-POSS-*b*-BuA-*b*-MA-POSS) ($M_n = 36,000$ g/mol by ^{1}H NMR; PDI = 1.20 by SEC). Star block copolymer analogues (see Section 14.6.) were even synthesized.[178]

Another class of hybrid inorganic/organic block copolymers are those including a polysilylene-based segment and a polystyrene one, as described by Jones et al.[179] A polymethylphenylsilylene precursor end-capped with two chloromethylbenzene groups was first synthesized by step-growth polymerization involving a reductive coupling reaction of dichloromethylphenylsilane followed by the addition of (4-chloromethylphenylethyl)dimethylchlorosilylene. The subsequent ATRP of styrene from the corresponding macroinitiator led to a mixture of diblock and triblock copolymers, as evidenced by SEC.

14.4.5 Miscellaneous Block Copolymers

In this part are described synthetic approaches to derive block copolymers that do not necessarily enter in the categories discussed above, although some of these materials may also be viewed as amphiphilic ones.

14.4.5.1 By Sequential LRP Block copolymers comprising styrene and methyl methacrylate units were, for instance, derived by different groups with a view of demonstrating the "living" character of the mechanism used.[80,142] The synthesis by Yoshida of poly(styrene-*b*-bromostyrene) in the presence of methoxy-TEMPO as counterradical provides another example of block copolymers being easily obtained by sequential polymerization of the corresponding monomers.[180]

Different was the case of poly(4-vinylpyridine) (P4VP) and the block copolymers derived from their synthesis by ATRP was a priori not straightforward since both monomer, and polymer may act as ligands for the catalytic system and thus saturate the coordination sites of the transition metal (Cu). On employing a strong coordinating ligand to copper such as tris[2-(dimethylamino)ethyl]amine (Me$_6$TREN), this potential difficulty could be overcome and well-defined P4VP chains be obtained, the latter being even chain extended to prepare P4VP-*b*-PMMA block copolymers ($M_n = 89,500$ g/mol; PDI = 1.35).[181]

In the category of nonordinary materials the preparation of copolymers by ATRP, including blocks of random nature and based on *para*-substituted styrenic units such as *p*-chlorostyrene, *p*-methylstyrene, *p*-acetoxystyrene, and *p*-acetoxymethylstyrene

was described by the group of Sawamoto who used Ni, Re, and Fe complex catalysts to this end; they reported the synthesis of ABC block copolymers (also named *terpolymers*) as well.[80]

Davis and Matyjaszewski also prepared miscellaneous linear and star-shaped ABC terpolymers based on monomers such as styrene, *tert*-butyl acrylate, methyl acrylate, methyl methacrylate, and 4-vinyl pyridine, using copper-based catalytic systems. In a systematic investigation, these authors optimized the experimental conditions to obtain linear and star–block architectures (see Section 14.7) with a well-defined character.[182] For instance, they stressed the necessity of selecting the proper ligand and/or solvent to achieve the homogeneity of the polymerization medium and recommended to add Cu(II) species as deactivators and/or vary the temperature to minimize the occurrence of termination reactions. They also showed how the "halogen exchange" technique could be useful to grow polymethacrylate blocks from polyacrylate macroinitiator and thus derive the corresponding block structures.

Because of the presence of terminal halogen atoms, ATRP-derived polymers were found to exhibit a thermal stability lower than that of polymers prepared under standard conditions. To increase the stability of these polymers, Novak and colleagues proposed using a bicyclodiolefin, namely, diethylbicyclo[2.2.1]hepta-2,5-diene-2,3-dicarboxylate, as end-capping agent for the PS chains.[183] These authors synthesized di- and triblock copolymers containing a short terminal poly(norbornadiene) block by ATRP; CuCl/dipyridyl was the catalytic system employed, and the reaction temperature was set at 130°C. The thermal stability of these PS-based copolymers was comparable to that of PS chains obtained by RP. It should be noted, however, that the homopolymerization of this bicyclic olefin was very slow as compared to that of standard vinylic monomers; it indeed took 2 weeks to reach 11% monomer conversion.

14.4.5.2 *By Combination of LRP with Cationic Polymerization*[123–130] Various types of block copolymers were prepared by associating LRP with a different mechanism (see also Ref. 184 for more detail). As mentioned above, this offers the opportunity to expand the variety of block copolymers accessible.

The combination of LRP with cationic polymerization was first attempted from polystyrene samples prepared by "living" cationic polymerization, which is known to generate chains ended with phenylethyl chloride groups on quenching.[127] The latter subsequently served to initiate the Cu-mediated ATRP of methyl acrylate, methyl methacrylate, or styrene, affording diblock copolymers with relatively well-defined structures, except for those involving methyl methacrylate units because of a too slow initiation. The crossover from the cationic ring opening polymerization of tetrahydrofurane[185–188] to LRP of vinylic monomers was also considered to derive block copolymers based on poly[oxy(tetramethylene], also termed *poly(tetrahydrofurane)* (PTHF) segments (Fig. 14.25).

If the switch from conventional living processes to LRP is rather common, the reverse was also contemplated.[188,189] For instance, block copolymers (M_n between 12,000 and 30,000 g/mol; PDI < 1.5) of styrene and 1,3-dioxepane (DOP) units have been prepared by combining ATRP of styrene first, then the cationic ring-opening
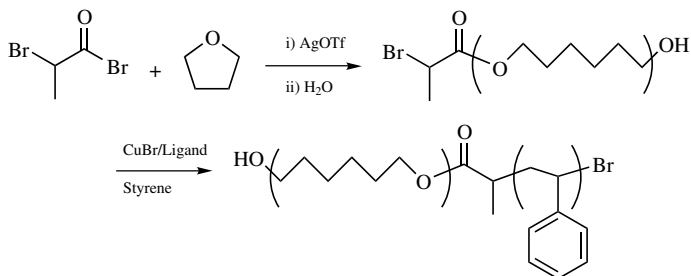
Figure 14.25   Synthesis of PTHF-*b*-PS by sequential LRP and cationic polymerization.[187]

polymerization of DOP.[189] Starting from α-hydroxy,ω-bromo PS precursor Pan and colleagues could cationically grow the poly(DOP) block, after adding triflic acid to trigger polymerization; contamination of the block copolymer with poly (DOP) chains was noted, however. The same team also derived PTHF-*b*-PS-*b*-PTHF by a similar site transformation technique. To this end, a α,ω-bis(bromo)-PS obtained by ATRP from a difunctional initiator was treated with silver perchlorate to trigger the ring opening cationic polymerization of THF.[190] The same strategy was applied for the preparation of star–block copolymers (see Section 14.7).

Yagci and colleagues also showed how to oxidize polymeric radicals produced by ATRP into cations that were subsequently used to initiate the cationic polymerization of cyclohexene oxide.[191]

14.4.5.3 *Block Copolymers by Combination of LRP with Anionic Polymerization* The quenching of "living" anionic polystyryl lithium chains by 1-oxo-4-methoxy-2,2,6,6-tetramethylpiperidinium salt in the presence of methoxy-TEMPO was reported to be an efficient way to prepare polystyrene capped with the corresponding alkoxyamine moiety.[192] It was proposed that the reaction proceeds via an electron transfer from the living carbanionic to the cationic species, forming a polymeric radical that was then trapped by the methoxy-TEMPO present in the reaction medium. The alkoxyamine-terminated PS obtained was then used to grow methyl, ethyl or butyl acrylate blocks, but the resulting block copolymers were poorly defined (PDI in the range 1.33–1.96), because of the limitations associated with the NMP of acrylics in the presence of TEMPO derivatives, as previously discussed.

14.4.5.4 *Combination of LRP with Step-Growth Processes* Prepolymers produced by step-growth polymerizations were also used as macroinitiators for LRP. For example, phenolic end groups of polysulfones were derivatized into 2-bromopropionate functions to trigger the polymerization of styrene or butyl acrylate by ATRP; this afforded the corresponding ABA triblock copolymers.[193] Examination of the physical properties of the latter showed that the styrene–sulfone copolymers formed optically clear but brittle films whereas the butyl acrylate–sulfone blends gave rubbery clear films. Another study described the use of difunctional

rigid oligophenylenes[194] that possess photoluminescent properties—prepared from the Suzuki reaction—for the preparation of ABA rigid–flexible triblock copolymers, where A consisted of styrene units.

14.4.5.5 Combination of LRP with Ring-Opening Metathesis Polymerization
Ring-opening metathesis polymerization (ROMP) of cycloolefins has been combined with ATRP to derive AB and ABA triblock copolymers. This approach was first described by Matyjaszewski and colleagues, who synthesized polynorbornene-*b*-PS and polynorbornene-*b*-PMA diblock copolymers as well as polycyclopentadiene-*b*-PS diblocks.[195] To this end, *p*-bromomethylbenzaldehyde was used in a Wittig reaction in order to cap the polycycloolefin precursors with benzyl bromide at one chain end; the latter function served to trigger ATRP. Grubbs and colleagues also contemplated the possibility of associating ATRP with ROMP to prepare block copolymers based on 1,4-polybutadiene;[196,197] after carrying out the ROMP of 1,5-cyclooctadiene in the presence of an appropriate difunctional transfer agent, these authors took advantage of the halides present at the ends of the polybutadienes formed to grow either PS or PMMA blocks by ATRP. These ABA triblock copolymers were found to exhibit thermoplastic elastomeric properties. Interestingly, this group also resorted to the concept of tandem polymerization (see Section 14.4.5.7) to obtain the same block copolymers, developing for that a novel dual ruthenium complex capable of initiating both ROMP and ATRP.[197]

14.4.5.6 Combination of LRP with RP
Janda and colleagues combined RP with NMP to build a "library" of block copolymers based on styrene, *tert*-butylstyrene, 3,4-dimethoxystyrene, *N*-vinylpyrrolidone, and isopropylacrylamide units.[198]

As for Matyjaszewki and colleagues, they resorted to RP and ATRP to make block copolymers including vinyl acetate units following four different strategies.[199] The first one (1) consisted in polymerizing vinyl acetate from a bishalogenated azo initiator and then growing a styrene block by ATRP. They also (2) polymerize *n*-BuA first by ATRP using the same azobis initiator and subsequently grew poly(vinyl acetate) blocks under standard conditions. Two other pathways were developed along the same line: (3) a redox-initiating system was used in combination with ATRP and (4) ATRP of vinyl acetate was attempted from a poly(*n*-BuA) macroinitiator. Although the formation of block copolymer was demonstrated, none of the four methods afforded well-defined materials.

An earlier study reported by Destarac and Boutevin had already described the consecutive use of RP and ATRP.[200–201] These authors initiated the RP of *n*-BuA from a trichloromethyl-containing azo initiator and then grew PS blocks from the trichloromethyl groups carried by the poly(*n*-BuA) macroinitiator. This resulted in a mixture of AB diblock and ABA triblock copolymers, because termination reactions of the first step occurred via either recombination or disproportionation. Block copolymers including a first block originating from a monomer that is not amendable to controlled polymerization (e.g., vinylidene fluoride, vinyl acetate) and a second grown by ATRP were described by the same team.[202–203] This could be achieved on telomerization of these monomers in the presence of chloroform, followed by

ATRP of various monomers (MMA, *n*-BuA, MA, styrene). Block copolymers of pre-determined molar masses could be prepared in this way, but the polydispersity index of the precursor was relatively large. Following the same strategy, poly(styrene-*b*-vinylidene fluoride-*b*-styrene) triblock copolymers (PDI in the range 1.4–1.7) were derived.[204] In the latter case 1,2-dibromotetrafluoroethane was used as transfer agent during the telomerization to prepare a dibromine-ended macroinitiator.

14.4.5.7 Block Copolymers from "Dual Initiators"   "Dual initiators" are compounds that contain at least two distinct sites for the potential initiations and controlled polymerizations of monomers by different mechanisms. Several groups[197,205–210] designed some of these dual initiators, which are shown in Fig. 14.26. This approach requires that each initiating site in such dual initiators be stable and inert while the

Figure 14.26   Block copolymers from "dual initiators."

other one is active, that is, during the growth of the other block. The two monomers can even undergo controlled polymerization process simultaneously, in a one-pot process without the need for a protection–deprotection step or functionalization of intermediates. This could be achieved on involving two different chain addition mechanisms (e.g., LRP and ring-opening polymerization) or LRP and a step-growth process.

Sogah developed such multifunctional initiators that were used in one-pot simultaneous block polymerization of three monomers, which are styrene by NMP, phenyloxazoline (PhOx) by cationic ring-opening polymerization, and ε-caprolactone by anionic ring-opening polymerization.[205] Block copolymers emanating from such syntheses exhibited well-defined structures ($M_n \sim$ 30,000–85,000 g/mol, PDI < 1.6). Hydrolysis of phenyl oxazoline units led to PS–b–polyethyleneimine amphiphilic block copolymers. The extension of this concept to the synthesis of graft copolymers was also proposed (see Section 14.5). Starting from a thiophene-containing initiator, Yagci and colleagues combined ATRP of MMA and electropolymerization of pyrrole to prepare block copolymers that were found to form thermally stable and electrically conducting films.[210] The same group also successfully synthesized block copolymers based on cyclohexene oxide and styrene (M_n in the range 22,000–40,000 g/mol; PDI 1.5–1.9), using an alkoxyamine containing a dihydroanthryl cation (see Fig. 14.26). This "double-head" initiator was capable of initiating the cationic polymerization of cyclohexene oxide (CHO) through its cationic site and the NMP of styrene through its alkoxyamine moiety.[209]

One requirement difficult to fulfill is that the mechanisms do not interfer each other. For instance, if NMP could be combined with aryl–aryl condensation in a one-pot procedure (Fig. 14.27), it was found more difficult to do so in the case of ATRP and aryl–aryl coupling, due to the instability of the halogenated ATRP species during the step-growth process.[208]
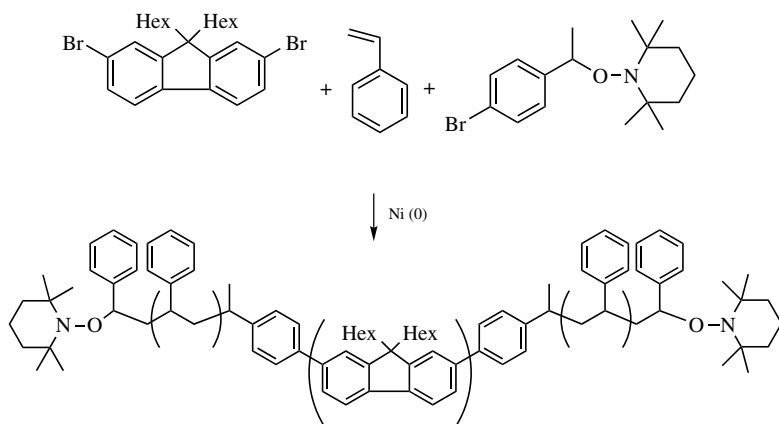
Figure 14.27   NMP combined with aryl–aryl condensation in a one-pot procedure.[208]

14.5   GRAFT COPOLYMERS AND POLYMER BRUSHES

The current interest in branched polymers that are molecularly well defined is fueled by the growing demand for structures exhibiting shape persistence; the role played by the branching points are to lower the conformational entropy of such objects.[211] Graft copolymers and polymer brushes[212] contain branching points that may be distributed along the polymer backbone either randomly or under a controlled manner. These materials may be useful in applications requiring surface modification and control of the surface properties. They can be generated by three distinct routes known as "grafting onto," "grafting from," or "macromonomer technique," but only the two latter were contemplated to synthesize graft copolymers by LRP.

14.5.1   Synthesis of Graft Copolymers by the "Grafting from" Method

The "grafting from" method was the most widely utilized to derive graft copolymers by LRP. As such architectures first involve the preparation of a backbone and then the growth of grafts, the synthetic routes that were chalked out either combined LRP with another method or relied on two consecutive LRP. As illustrated in Section 14.4.5, the association of LRP with another polymerization was extensively applied to obtain block copolymers, but it was also found very attractive to engineer graft copolymers. For instance, commercial poly(vinyl chloride) incorporating 1% of vinyl chloroacetate units served to grow PS, PMA, Pn-BuA, or PMMA grafts by ATRP using CuBr/4,4′-di-(5-nonyl)-2,2′-dipyridyl.[213] The copolymers obtained in this way were of high molar masses (M_n in the range 110,000–360,000 g/mol) and broad molar mass distribution (PDI in the range 2.4–4.9).

The metallocene-induced polymerization of styrene followed by ATRP of vinylic monomers was developed to make graft copolymers consisting of a syndiotactic PS backbone and either PS or poly[methyl (meth)acrylate] grafts.[214] In this case, the brominated initiating sites were introduced randomly by chemical treatment of the backbone with N-bromosuccinimide (NBS). The thermal properties of the corresponding graft copolymers were found to depend on the size of the grafts as well as on the branching density.

Backbone and grafts arising from identical or different LRP were also considered. For instance, the synthesis of well-defined densely grafted (so-called bottle–brush copolymers) copolymers could be accomplished by relying only on ATRP.[215] The multifunctional backbone was first prepared by homopolymerization of trimethylsilyl-protected 2-hydroxyethylmethacrylate and subsequent transformation of each hydroxyl of the repeating units into brominated functions. The corresponding polymer ($M_n = 55,500$ g/mol; PDI = 1.3) served to grow either PS or Pn-BuA grafts by ATRP (Fig. 14.28). To minimize the possibility for the growing grafts to undergo irreversible coupling, the concentration of Cu(I) as well as the temperature had to be reduced, while the polymerization had to be discontinued at low monomer conversion and performed under dilute conditions. Images of these copolymer brushes could be visualized by atomic force microscopy (AFM), and the dimension of the grafts (100 nm long, 10 nm wide, and 2 nm high) could be determined by this
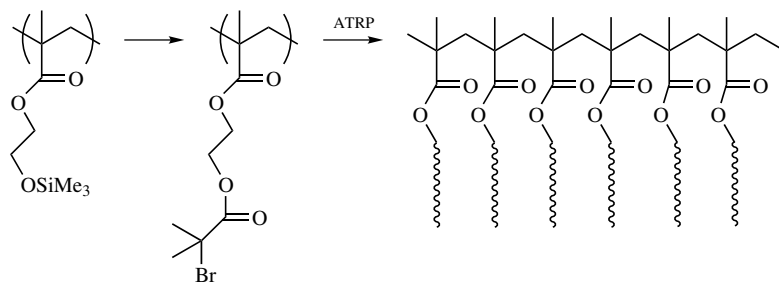
Figure 14.28 "Bottle-brush" copolymers by the "grafting from" method and ATRP.[215]

technique. Alternatively, conventional free-radical polymerization of 2-(2-bromo-propionyloxy)ethyl acrylate in the presence of CBr$_4$ afforded a poorly defined multi-functional macroinitiator ($M_n = 273{,}000$ g/mol PDI $= 2.3$), which was further used to grow grafts by ATRP.[215]

The synthesis of highly branched graft copolymers made of a polyolefin back-bone and PS or PMMA side branches grown by either ATRP or NMP was described by different teams.[216–218] These polyolefin-based graft copolymers may find appli-cation as compatibilizers in blends of polyethylene with other plastic materials. In 1998, the IBM team synthesized polymeric initiators by copolymerization of propylene or 4-methylpentene with an alkoxyamine-containing alkene using a metallocene/borate catalytic system.[216] The alkoxyamine-grafted polyolefins were used to initiate the NMP of styrene in a controlled fashion, affording polyolefins-g-PS. A similar TEMPO-based 1-alkene was copolymerized with ethylene via the so-called "migratory insertion" mechanism using a palladium catalyst (Fig. 14.29). This yielded a branched polyethylene whose branches carried side alkoxyamines; the latter were then used to initiate the NMP of either styrene or a mixture of styrene and acrylonitrile.[217] Rather well-defined graft-in-graft copolymers ($M_w \leq 100{,}000$ g/mol, PDI ~ 1.5) with large size branches of tunable polarity were thus obtained. Characterization of the latter by TEM (tunneling electronmicrography)
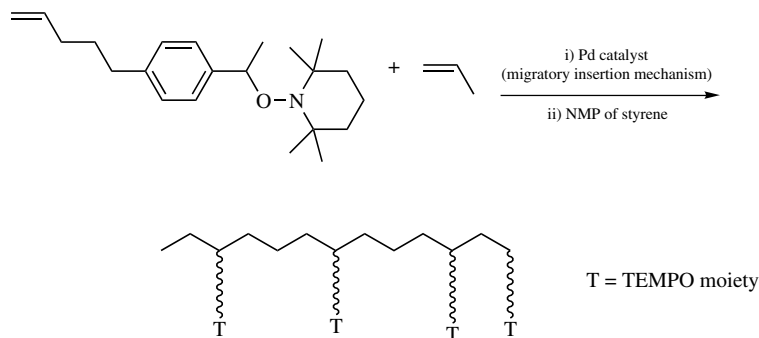
Figure 14.29 Graft copolymers with a polyolefine backbone.[216]

showed a microphase separation due to the incompatibility between the polyethylene precursor and the PS grafts.

Poly(ethylene-*g*-styrene) as well as poly(ethylene-*g*-methyl methacrylate) copolymers were derived by ATRP using commercially available poly(ethylene-*co*-glycidyl methacrylate) as precursor; for this, some of the pendant epoxide functions of glycidyl methacrylate units were first converted into ATRP initiating sites, although this chemical modification step was poorly controlled.[218] A similar strategy was followed to synthesize graft copolymers comprising an ethylene-propylene-diene terpolymer rubber as backbone and PMMA as side chains; the latter were grown by ATRP after bromination of the pendant allylic groups with NBS.[219] Likewise, the synthesis of block–graft copolymers consisted of poly(styrene-*b*-ethylene-*co*-propylene) (Kraton147, Shell co.) AB-type diblock as backbone and poly(ethyl methacrylate) grafts was also reported. The branches were grown by ATRP after chloromethylation of the styrene units.[220] Sen and Liu reported the first example of polyethylene-based graft copolymers possessing diblock grafts; poly(ethylene-*co*-styrene) backbone was first chemically modified with NBS before styrene (or methyl methacrylate), methyl acrylate, or 2-hydroxyethyl acrylate were sequentially polymerized by ATRP.[221]

Finally, as was already discussed in the section devoted to block copolymers synthesis, triblock architectures made of rubbery polyisobutylene blocks flanked with densely PS grafts were obtained via ATRP.[129–130] DSC analysis of the graft copolymers revealed two glass transition temperatures indicating the occurrence of a (micro)phase separation.

Another example utilizing the ''grafting from'' method consisted in growing pendant PS chains from an inorganic polysilylene backbone to generate hybrid graft copolymers.[222] In this case, the bromomethyl groups aimed at initiating ATRP of styrene were randomly introduced by a Friedel–Crafts reaction.

14.5.2 Synthesis of Graft Copolymers by the ''Macromonomer'' Technique

Both homo- and copolymerization of macromonomers are powerful tools to tailor well-defined graft copolymers.[65] The main difficulty is to obtain a complete conversion of macromonomers when copolymerizing the latter with a low-molar-mass comonomer, where the incompatibility between the macromonomer and the growing polymer was one of the reasons advanced to account for this feature. However, the controlled/living radical copolymerization of macromonomers was shown to occur efficiently and to be an excellent means to derive graft copolymers.

For example, ω-acryloyl polylactide and polylactone-based macromonomers obtained by ring-opening polymerization of the corresponding monomers were copolymerized with styrene and chloromethylstyrene using a TEMPO-based alkoxyamine.[223] The polyester grafts ($M_n \sim 40,000$ g/mol PDI ~ 1.25) were subsequently hydrolyzed to isolate the poly(styrene-*co*-acrylic acid) backbone. Characterization of the latter gave useful information about the efficiency of the grafting in the parent copolymers.

Müller and co-workers copolymerized MMA and *n*-BuA with a ω-methacryloyl macromonomer of PMMA by ATRP and observed that the reactivity of the latter was similar to that of the corresponding low-molar-mass monomer.[224–225] This unexpected result, which contrasts with those found in RP, could be accounted for by these authors, who argued that the frequency for monomer addition is in the range 10^{-3} s for RP and in seconds for ATRP. The graft copolymers obtained under such conditions exhibited a narrow molar mass distribution.[225]

In a recent (at the time of writing) contribution, Matyjaszewski and colleagues copolymerized a methacryloyl-terminated poly(dimethylsiloxane) macromonomer (PDMS-MA) with methyl methacrylate, under conventional and atom transfer radical conditions.[226] They determined a higher reactivity ratio for the PDMS macromonomer under ATRP conditions, which suggested that the incorporation of the macromonomer occurred more regularly in the latter case than in conventional copolymerization. In addition, they observed that the use of a PDMS-based macroinitiator helps improve the incorporation of the macromonomer into the copolymer, especially in experiments carried out in bulk. The role of the macroinitiator was to alleviate the incompatibility between the PDMS macromonomer and the growing PMMA radicals. The graft copolymers obtained by ATRP exhibited lower polydispersities and better compositional homogeneity than did those obtained under free-radical conditions.

On the other hand, Matyjaszewski and co-workers also copolymerized *N*-vinyl-pyrrolidone (NVP) by conventional means (using AIBN as the radical source at 60°C in dimethylformamide) with a macromonomer of PS that was prepared by ATRP.[67] Amphiphilic poly(NVP-*g*-styrene) graft copolymers of high molar masses were eventually obtained and found to highly swell in aqueous media, due to the formation of a physical gel. The coordination of NVP units to copper prevented the authors from applying ATRP for the copolymerization step.

The use of nitroxides as mediating agents for the copolymerization of a macromonomer was also considered; specifically, by copolymerizing an α-methacryloyl PEO macromonomer with styrene at 125°C in the presence of 4-hydroxyl-TEMPO as counterradical, amphiphilic graft copolymers with a rather well-defined structure were generated.[227]

Homopolymacromonomers are another class of branched architectures that are of great interest; they lead to structures of high branching density exhibiting unique behavior in both solution and the solid state. Polymacromonomers in the range of 20,000–100,000 g/mol molar mass (PDI < 1.2) were obtained by ATRP of ω-methacryloyl-poly(isobutyl vinyl ether) macromonomer; the latter was prepared by living cationic polymerization of the corresponding vinyl ether.[228]

14.5.3 Synthesis of Graft Copolymers from "Multireactive" Compounds (Tandem Mechanisms)

The concept of tandem polymerization involving two different controlled/living mechanisms occurring in one pot, such as LRP and ionic polymerization, was previously described for block copolymer synthesis, but it was also applied to the
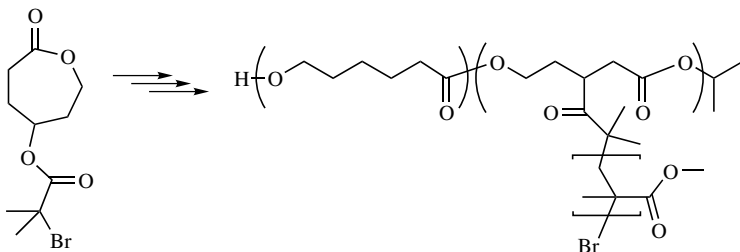
Figure 14.30   Synthesis of poly(ε-caprolactone-*g*-methyl methacrylate).[230]

preparation of graft copolymers, including poly(ethyleneimine-*g*-styrene).[229] The latter amphiphilic graft copolymer was obtained using a "double head" compound containing an alkoxyamine and an oxazoline function: PS chains were first grown by NMP, allowing the graft copolymer backbone to be subsequently built up by ROP of the oxazoline moiety.

An original approach was proposed by the Hedrick group for the preparation of poly(ε-caprolactone-*g*-methylmethacrylate) copolymers as shown in Fig. 14.30; starting from a bromofunctionalized lactone that served as monomer as well as initiator, these authors paired ATRP and ROP, which they carried out either in one-pot (concurrent) or sequential procedures.[230]

Indeed, three routes were developed to synthesize such graft copolymers. The first one consisted in the ROP of the lactone moiety followed by the ATRP of MMA from the pendant bromo groups of the backbone formed. Alternatively, ATRP of MMA could be initiated from the bromo group of the monomer shown in Fig. 14.30, thus affording a lactone-terminated PMMA that was subsequently copolymerized with ε-caprolactone. The third approach involved only one step; the nickel-mediated ATRP of MMA and the Al(iOPr)$_3$-initiated ROP of the monomer were performed at the same time. Both "grafting from" and "macromonomer" approaches resulted in the same kind of graft copolymer structure, but slightly differed by the molecular characteristics of the material formed: M_n revolved around 15,000 g/mol and PDI between 1.1 and 2.3, depending on the method utilized.

14.5.4   Polymer Brushes

Polymer brushes result from chains that are tethered to a solid surface and forced to adopt a stretched conformation because of an unusually high density.[212] On covalently anchoring appropriate initiating sites onto inorganic surfaces through their reactive functions, one can grow by LRP densely packed grafts, which will therefore adopt the conformation of brushes (Fig. 14.31). The dimensions of such tethered grafts are amenable to accurate control so that the thickness of the layer formed can be fine-tuned through LRP. In most of the studies described below, the grafts were subsequently cleaved from the solid particles for analysis purposes.

The first study on such polymer brush synthesis was reported by the group of Fukuda, who utilized the Langmuir–Blodgett technique to tether a well-organized
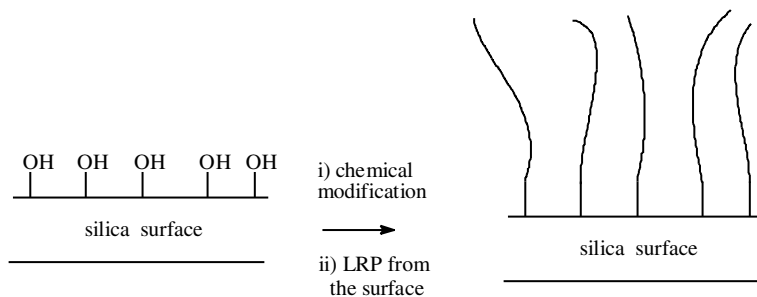
Figure 14.31   Polymer brushes.

set of arylsulfonyl chloride groups onto a silicon surface, the monolayer formed on water surface then being transferred for the subsequent growth of PMMA chains via ATRP.[231] This last step was performed in the presence of tosyl chloride as free initiator to increase the concentration in Cu(II). Since free linear chains were also created at the same time, several washings of the surface were necessary to dispose of these free linear contaminants. These authors then investigated the forces of interaction in their PMMA brushes by AFM and also examined the effect of chain length and that of grafting density.[232,233] AFM analysis confirmed that these structures were "exceptionnally" dense (0.4 chains/nm^2). The same team applied a similar methodology associating the Langmuir–Blodgett technique and surface initiation to grow by ATRP their sugar containing poly(methacrylate) grafts from modified silica gel.[234] On deprotection of the hydroxyl groups carried by the sugar substituent, a solid surface covered with polymer brushes of low polydispersity and carrying pendant saccharide residues could be obtained.

Zhao and Brittain were the first to describe the synthesis of diblock PS-*b*-PMMA copolymer brushes obtained from a silicon substrate by sequential carbocationic polymerization of styrene followed by ATRP of MMA.[235] These hybrid systems were found to exhibit dramatic changes in their surface organization and composition with the solvent used, particularly in the presence of a selective solvent for one block. This resulted in nanopattern formation, as evidenced by the characterization of these stimuli-responsive materials by AFM and X-ray photoelectron spectroscopy.[236] After an azo-functional trichlorosilane was attached to the surface of silica, the same team used "reverse ATRP"[3] to graft the same block copolymers.[237]

The IBM team derivatized silicon wafers into either alkoxyamines or brominated groups. Random copolymer-type brushes based on styrene and 2-hydroxy-ethyl methacrylate were subsequently grown, as well as block copolymers from styrene and methyl methacrylate.[238]

The surface modification of glass or silicon wafers with dithiocarbamate groups that were further used as photoiniferters was also proposed.[239] The thickness of the layer formed, which consisted of PS-*b*-PMMA block copolymer, was fine-tuned (up to 100 nm) through control of the photopolymerization of styrene and methyl methacrylate. The formation of a block copolymer bilayer was evidenced by a series of

characterizations such as contact-angle measurements and transmission and scanning electron microscopy, which confirmed the well-defined and dense character of the polymer brushes formed.

Silica gel was modified with benzyl chloride to grow from its surface polyacrylamide by ATRP.[240] Huang and Wirth showed that the polyacrylamide cleaved from the silica surface were of low polydispersity, suggesting that they were grown under controlled conditions. In addition, the thickness of the polymer layer could be varied as a function of concentration and conversion.

Silicon wafers were also modified into 2-bromoisobutyrate groups before growing PS, poly(fluoroacrylate), or PS-b-PtBuA block copolymers brushes.[241] The PtBuA blocks could be hydrolyzed into poly(acrylic acid) brushes, thus making it possible to vary the hydrophilicity of the surface and therefore its wettability. This was confirmed by the decrease of the contact angle from 86° to 18°. In contrast, a contact angle of 119° was obtained for polymer brushes based on poly(fluoroacrylate) grafts. Similarly, (11-chlorodimethylsilylundecyl)-2-chloro-2-phenylacetate was covalently bound to the surface of silica to grow PS grafts by ATRP.[242]

From all these studies, it appears that silicon substrates provide surfaces that are very appropriate for the growth of polymer brushes by LRP. Gold can also well serve to accomodate polymer brushes on its surface.[243] The IBM group even described the selective etching of gold in a three-step process.[244] Microcontact printing was first used to deliver at the gold surface a patterned monolayer of an ATRP initiator. Then ATRP of MMA was triggered to amplify the patterned monolayer into polymer brushes and, finally, the selective etching of regions of the substrates which were not protected by the polymer brushes could be achieved.

14.6   STARS AND STAR BLOCK COPOLYMERS

There are essentially two strategies to engineer star-branched polymers: one can either resort to the ''arm-first'' method or turn to the ''core-first'' route; the two approaches are complementary with their respective merits and drawbacks. Among all branched architectures, star polymers correspond to the simplest possible arrangement of macromolecular chains in a branched structure since they involve only one central branching point per macromolecule.[245]

14.6.1   Stars by the Convergent Approach

Although being known since the 1950s and developed in the context of anionic polymerization,[246] it is only relatively recently that the approach resting on the participation of a divinylic compound in the star formation was applied to LRP. The divinylic compound actually plays the role of a coupling agent. On its addition onto a solution containing a ''living'' polymer, one can trigger its polymerization and grow a short block-carrying pendant double bonds. Starlike polymers are formed in a second step through intermolecular reactions between the remaining
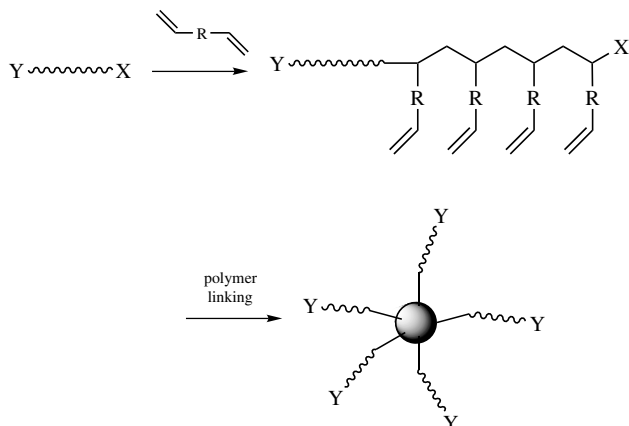
Figure 14.32   Star polymer synthesis through the use of a divinylic compound.[247–251]

"living" precursors and the pendant double bonds. Concomitantly to this mechanism of core formation, stars can also be built through intermolecular reactions involving the divinylic blocks themselves. Under these conditions, the number of chains attached to the core depends on several parameters such as the molar ratio (r) of the divinylic compound to the precursor, the molar mass of the latter, and the temperature. These features, which were established a long time ago for anionically derived star polymers also apply to stars derived by LRP (Fig. 14.32). The most recent studies on star synthesis by this convergent approach are described below.

To derive their PS stars, Matyjaszewski and colleagues used a preformed PS macroinitiator obtained by ATRP that was allowed to react with various divinylic monomers, in the presence of CuBr/PMDETA or CuBr/dipyridyl in anisole at 110°C.[247] A ratio of 5 : 15 between divinyl benzene and PS macroinitiator was found to be optimal for the star formation. Other experimental parameters such as the choice of solvent, the addition of Cu(II), and the reaction time were found to be crucial for the efficient star formation. However, the samples obtained were contaminated with residual linear chains and exhibited rather broad molar mass distribution due to star–star couplings. Following a similar route, the same group reported the synthesis of PtBuA stars.[248] Through the use of functional initiators from which the linear PtBuA precursors were grown, various functions such as epoxy, amino, cyano, or bromo could be introduced at the end of each branch of the stars. The SEC traces of such star samples also revealed their ill-defined character. More recently, the group of Sawamoto reacted a series of divinylic monomers with a bromo-terminated PMMA precursor in the presence of their ruthenium-based catalytic system. These authors also reported the star formation as being influenced by the parameters mentioned above.[249] Interestingly, they could prepare high-molar-mass PMMA stars in a one-pot procedure, by adding in situ the divinylic comonomer.

The synthesis of star polymers by NMP through a convergent approach was also described in two reports. Long and colleagues observed that a ratio of 67 between

divinylbenzene and their PS-TEMPO precursor is needed for obtaining PS stars.[250] In contrast, Hadjichristidis et al.[251] employed much smaller ratios (between 3 and 13) to obtain their PS stars. As such stars contained many TEMPO-based alkoxyamines at their core, a large number of arms (up to 600) could be grown outward by NMP, affording "miktoarm" stars with PDIs in the range of 1.15–1.56.[251]

It is worth pointing out that in most of the studies cited above, gel formation was observed above a critical value of the ratio between the divinyl monomer and the linear precursor.

An original study also based on the arm-first approach was reported by Fraser and colleagues, who synthesized 2,2'-dipyridyl-carrying PS and PMMA chains by ATRP, which they managed to chelate onto a hexadendate Fe(II)-based complex to form corresponding starlike polymers, thus containing a metallic core.[252] However, and as described below, the core-first method is certainly better suited to the synthesis of well-defined starlike polymers, particularly those of precise functionality.

14.6.2   Stars by the Divergent Approach: Use of Multifunctional Initiators

The core-first approach has come to maturity after it was shown in the 1990s that stars of precise functionality could be obtained from multiionic initiators.[253] Such well-defined stars of precise functionality are quite useful in providing acute insight into how branching affects the overall properties of polymers in solution or in the melt.[254] However, the main limitation of the core-first method is the development of suitable multifunctional initiators.

Its implementation in LRP conflicts with the possibility for growing radicals to undergo irreversible terminations. As in the case of the synthesis of densely grafted copolymers, it is essential to maintain the lowest possible concentration of propagating radicals because any irreversible recombination between growing arms would result in the loss of control of the star functionality. Each growing star indeed carries multiple active sites, and the probability for termination to occur is much higher in such multiarmed polymers. The extent of these side reactions is not correlated only with kinetic parameters such as the equilibrium constant (K_{eq}) between the radical active sites and the dormant species or the ratio between k_p/k_t, where k_p and k_t are the rate constant of propagation and that of termination but also to the actual concentration of stars in the reaction medium. It was observed, in particular, that the probability for intermolecular coupling is enhanced whenever the concentration of stars cross their overlapping concentration [C^*].

Hawker was the first to demonstrate the possibility of obtaining well-defined PS stars by the core-first methodology.[255] This author prepared a TEMPO-based trialkoxyamine (Fig. 14.33) that was designed to initiate the NMP of styrene in three directions and produce a triarm PS star ($M_n = 20,000$ g/mol; PDI = 1.2). The latter was characterized by comparing its molar mass with that of its hydrolyzed arms isolated after cleavage of the central core. Gnanou and co-workers also resorted to NMP to prepare triarmed PS and Pn-BuA stars of rather high molar mass; they
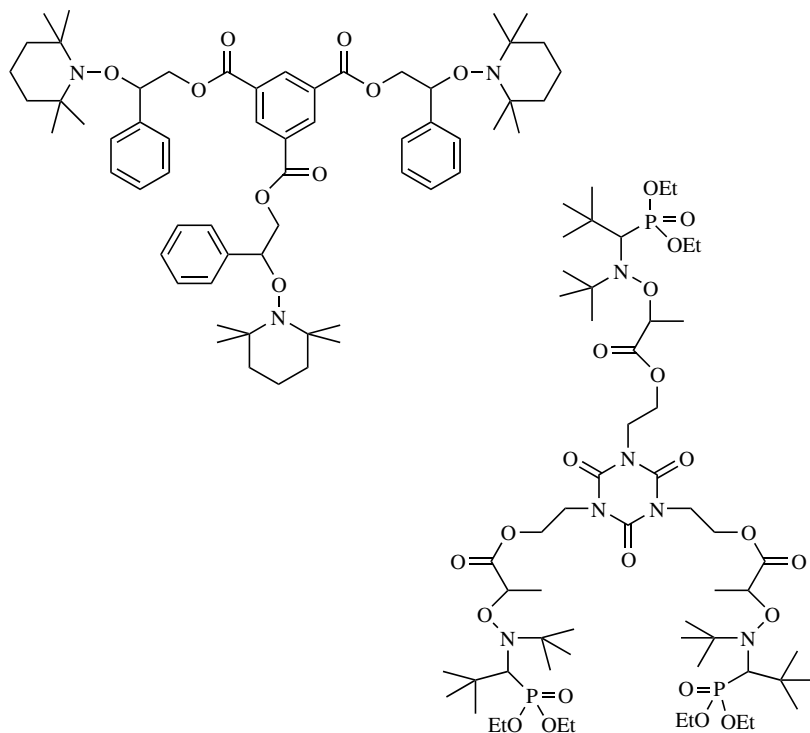
Figure 14.33 Trialkoxyamines for star polymer synthesis by NMP.[255,256]

used to this end an original trifunctional alkoxyamine (Fig. 14.33) on the basis of the β-hydrogen-containing nitroxide (SG1) of Atochem.[256]

Because it is easier to derive multihalides than multialkoxyamines, ATRP was preferred over NMP for the synthesis of starlike polymers. Matyjaszewski and colleagues were the first to explore the possibility of deriving six-arm stars by ATRP using hexakis(bromomethyl)benzene as initiator.[257] Later, Sawamoto and colleagues reported the synthesis of tri-arm poly(methyl methacrylate)s[258] and Pugh and colleagues described the synthesis of tri-arm liquid crystalline polyacrylates by ATRP using tris(bromomethyl)mesitylene as trifunctional initiator.[259] However, only few details were presented to demonstrate the star formation in these reports. In more systematic investigations, Sawamoto on one hand[260] and Gnanou on the other[261] first showed that stars with a high number of arms could be obtained using calixarene derivatized initiators (Fig. 14.34), with either Ru(II)/PPh₃ or Cu(I)/ dipyridyl as polymerization catalysts.

Many other groups have also resorted to ATRP to derive star polymers by the core-first method, using various families of multifunctional initiators (Fig. 14.35): the latter include inorganic heterocyclics such as cyclotetrasiloxanes[262,263] or cyclophosphazene,[262,263] activated phenol derivatives,[264–267] glucose,[268] sucrose,[48] or calixarene derivatives[260,261,269–271] with four to eight ATRP-initiating sites, tetrakis
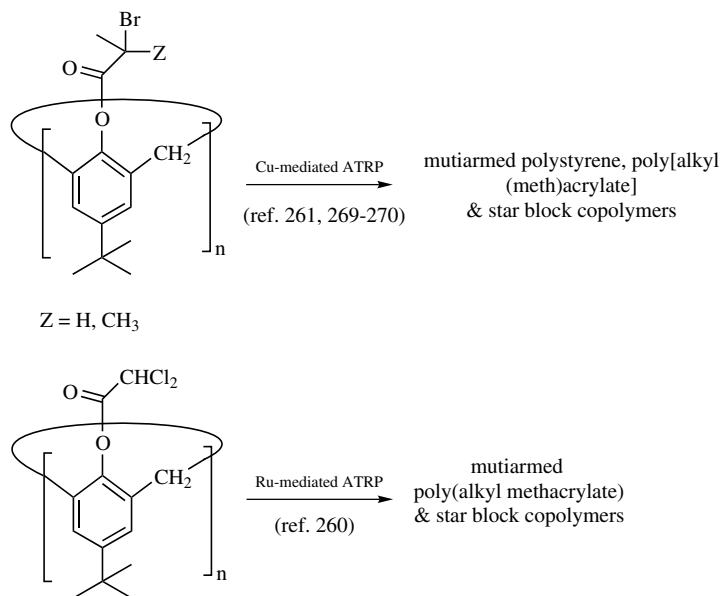
Figure 14.34   Calixarene-based initiators for ATRP.

(bromomethyl benzene),[272] hexa and dodecafunctional carbosilane-based dendritic cores[273] or other dendritic moities,[264–266] and various multifunctional aromatic sulfonyl chlorides[271] that were used in conjunction with various activators based on either copper, ruthenium or nickel halides, and miscellaneous ligands. Stars carrying polystyrene, polymethacrylate, or polyacrylate arms whose number ranged from 3 to 21 were synthesized via this route.

Fraser and colleagues used another approach based on coordination chemistry to obtain their multifunctional initiators; the halogeno-2,2′-dipyridyl-based complexes formed then served to initiate the ATRP of MMA and styrene by the core-first route.[274–278] Multiarm stars incorporating metallic cores were prepared in this way.

The scope and limitations of the CuBr/dipyridyl catalytic system, which is also the most commonly used one in ATRP, have been investigated by the Gnanou group in the context of star synthesis.[261,269–270] PS stars with predictable molar masses and polydispersity index close to unity, constituted of precisely four, six, and eight arms were synthesized, starting from calixarene-derived initiators. For instance, octafunctional PS stars exhibiting molar masses as high as 600,000 g/mol[−1] could be prepared by polymerizing styrene in bulk, discontinuing the polymerization to low conversion, typically below 15–20%, to prevent stars from mutually coupling. In the case of hexa- and tetrafunctional PS stars, well-defined samples could be obtained within a larger range of conversion because of the lower probability of such hexa- and tetraarmed species to get coupled, as compared to the case of the octafunctional system. Therefore, the lower the functionality of the stars prepared, the higher the conversion above which star–star coupling became detectable.

(ref. 257)

(ref. 274-278)

(ref. 267)

(ref. 264-266)

(ref. 262-263)

(ref. 271)
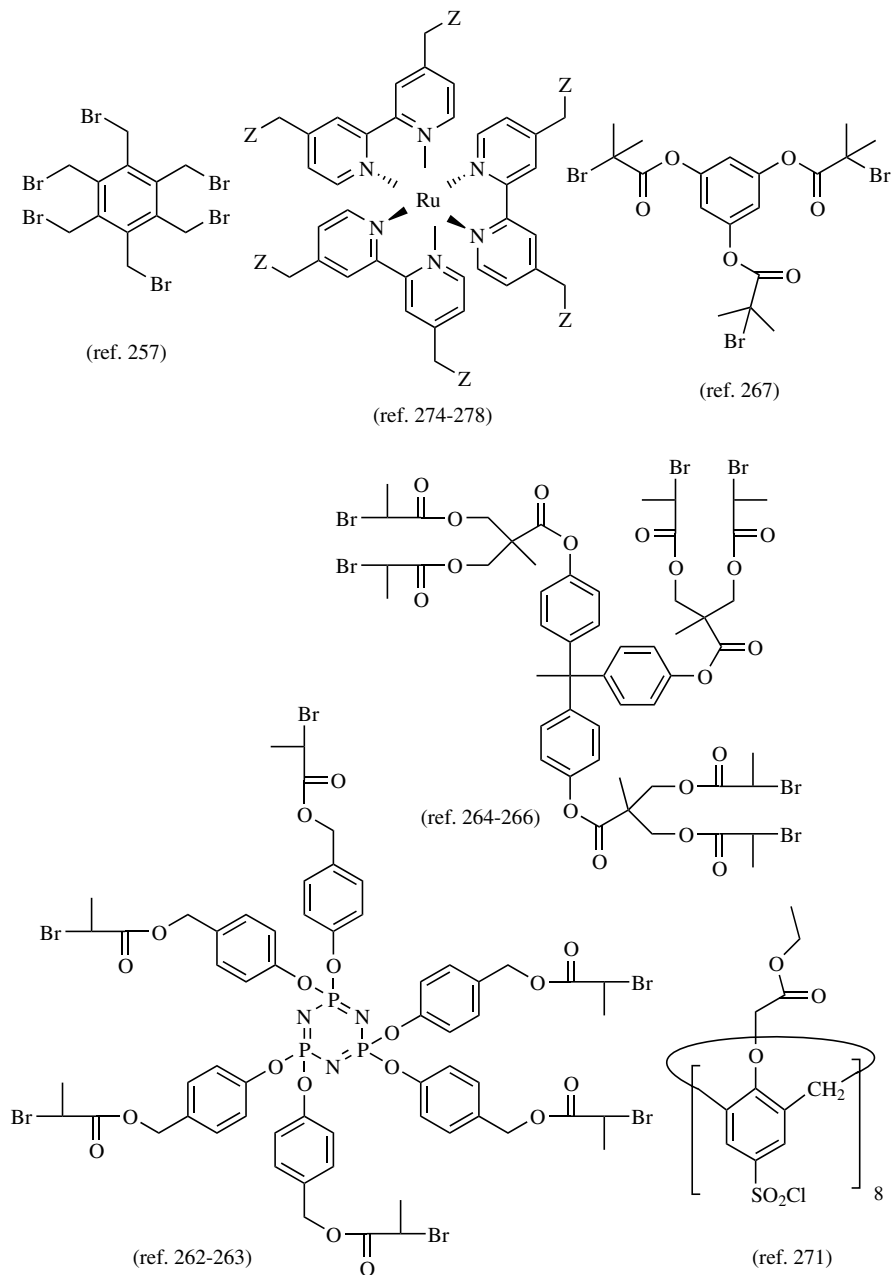
Figure 14.35 Other examples of multifunctional initiators for ATRP.

Eight-armed PMMA stars were also derived, using the octafunctional calixarene-based initiator. In the case of the Cu-mediated ATRP, the reaction also had to be discontinued at relatively low conversion (<25–30%) in order to isolate samples with the expected functionality of 8. Even though the ATRP of MMA is associated with a K_{eq} value larger than that for styrene, the probability for two stars to couple was lower than in the case of PS stars, just because k_p/k_t is higher for the former monomer. PMMA stars of high molar mass were thus obtained using large [M]/[I] ratios and restricting the polymerization to low conversion. In contrast, the multifunctional initiators developed by Percec and colleagues, which contain two, three, four, six, and eight sulfonyl chloride groups, allowed this team to carry out polymerization to high conversion (≤95%) and yet obtain well-defined PMMA stars.[271] No intermolecular couplings were detected while synthesizing poly(butyl acrylate) stars[263,269,270] with either ruthenium-based or copper-based catalytic systems, because the ATRP of acrylics is associated with a much lower equilibrium constant (K_{eq}) between dormant and active species. In this case, either CuBr/2,2'-dipyridyl[263,269] or CuBr/pentamethyl diethylenetriamine (PMDETA)[99,263,270] was used as catalyst in the presence of 10% in volume of ethylene carbonate. As expected, the use of PMDETA instead of dipyridyl as ligand led to a faster polymerization rate and narrower molar masses distribution, due to faster exchanges between active radicals and dormant halide species.

In many cases, the functionality of the multiarm stars obtained was checked by comparing their molar mass with that of their individual arms; the latter were isolated after hydrolysis of the ester functions of the central core.

Rizzardo's group[119] has described the synthesis of relatively well-defined tetra- and hexaarmed PS stars that were obtained by RAFT methodology, using transfer agents containing a precise number—either 4 or 6—of dithiocarbonyl thio groups (Fig. 14.36).
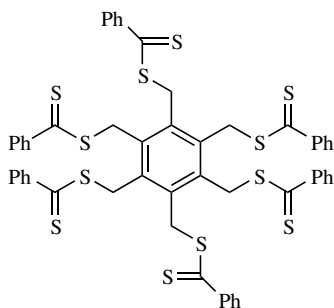
Figure 14.36   Hexafunctional transfer agent used in RAFT to synthesize hexaarmed PS.[119]

14.6.3   Star-Shaped Block Copolymers by the Core-First Approach

The possibility of derivatizing the arm tips and therefore deriving reactive stars is another reason for the attractiveness of the core-first method. Taking advantage of the presence of reactive end groups in core-first stars, different groups synthesized

star-shaped block copolymers (PS, PMMA, PTHF, PEO, PCL, etc.), either by sequential LRP[260,264,265,270] or by switching from one mechanism to LRP (or vice versa),[277–280] as was done for the block copolymer synthesis.

To obtain star block copolymers, the simplest method is, however, to sequentially polymerize two monomers by LRP; the restrictions mentioned in the section devoted to block copolymers also apply here. Few star block copolymers were derived in this way; for instance, hexaarmed poly(methyl acrylate-*b*-isobornyl acrylate), octaarmed poly(methyl methacrylate-*b*-*n*-butyl methacrylate)[263] stars, potentially useful as thermoplastic elastomers, or multiarmed poly(methyl methacylate-*b*-*tert*-butyl acrylate)[265,270] and poly(*tert*-butyl acrylate-*b*-methyl methacylate)[265] stars were reported. In the case of the two latter structures, the *tert*-butyl groups of the P*t*-BuA blocks were selectively hydrolyzed, affording dodecaarm starblock poly(acrylic acid)$_{12}$-*b*-PMMA$_{12}$ and PMMA$_{12}$-*b*-poly(acrylic acid)$_{12}$ copolymers.[265] Investigations by ^{1}H NMR showed that they responded to changes of the polarity of the solvent in which they were placed; these systems formed so-called stable unimolecular micelles owing to the precise topological arrangement of the chain units.

Star block copolymers were also engineered by combining two different mechanisms. Different teams paired PCL with poly(alkyl methacrylate) chains,[279] PS with PEO chains,[280] PTHF with PS and/or PMMA chains,[281] and PIB with PMA chains[282] in such star-shaped architectures. These star-shaped block copolymers with an inner PCL, PEO, PTHF, or PIB core surrounded by a corona grown by ATRP (PCL$_6$-*b*-PMMA$_6$, PEO$_f$-*b*-PS$_f$ with $f = 3$ or 4, and PTHF$_4$-*b*-PS$_4$, PTHF$_4$-*b*-PS$_4$-*b*-PMMA$_4$ or PIB$_3$-*b*-PMA$_3$) were obtained in three steps. At first, either PCL, PEO, PTHF, or PIB were initially synthesized using a multifunctional initiator that eventually became the star core. Then the end groups carried by the star arms were transformed into 2-isobutyrate or 2-bromopropionate functions. In a third step, ATRP of the vinylic monomer was carried out using either the Cu-mediated in the case of PEO/PS, PTHF/PS, and PIB/PMA star block copolymers or NiBr$_2$(PPh$_3$)$_2$ for the samples containing PMMA external blocks and PCL inner blocks. In all cases, the star structure of such block copolymers could be confirmed on hydrolysis of the ester functions linking the external blocks to the inner ones.

14.7 HYPERBRANCHED AND DENDRITIC POLYMERS

The search for simple methods to obtain highly branched macromolecules whose behavior would resemble that exhibited by dendrimers[283] resulted in the development of the so-called hyperbranched polymers.[284] Surprisingly, the latter compounds did not attract much interest until the 1990s; this was long after Flory theorized that AB$_x$ monomers should undergo self-condensation and afford soluble and highly branched materials with a three-dimensional globular shape for a sufficiently high degree of polymerization.[285] Hyperbranched macromolecules appear at first glance as an attractive alternative to regular dendrimers since they can be obtained at low cost by a convenient "one-pot" polycondensation of AB$_2$-type monomers. However, they generally exhibit a broad molar mass distribution and irregular structures with, in particular, numerous unreacted B sites that correspond

to linear units coexisting with dendritic and terminal units. Therefore, their properties (high solubility, low viscosity, absence of chain entanglement, thermal stability) are known to depend not only on their degree of branching but also on the type of their terminal functions.

14.7.1 Self-Condensing Vinyl Polymerization (SCVP)

Besides the "conventional approach" that consists in polycondensing AB_x-type monomers, progress has been made toward better controlling both the branching pattern and the molar mass distribution in hyperbranched polymers.[286] Among these new developments, the self-condensing vinyl polymerization (SCVP) of latent AB_2-type monomers was first described by Fréchet and colleagues for cationically polymerizing 3-(1-chloroethyl)styrene.[287] SCVP was later applied to the NMP of an alkoxyamine-containing styrenic, and then to ATRP of styrenics and (meth)acrylics. SCVP combines chain addition polymerization with self-condensation of chains, as shown in Fig. 14.37. It involves an AB* vinylic compound, where A represents a double bond and B*, a latent initiating site that can be activated by an external stimulus.

This AB* molecule is also termed inimer (for initiator + monomer) because it can undergo a vinyl polymerization (chain growth) through its double bond and, at the same time, initiate chain addition or condense with the double bond of larger branched species through its B group (the polymerization actually follows step growth kinetics). Such hyperbranched polymers exhibit a molar mass distribution much broader than that observed for regular dendrimers, and their degree of branching (DB) is usually lower than 1 (the characteristic value for dendrimers). Generally, indirect methods, such as viscometry and light scattering measurements are necessary to glean information about the shape taken by such hyperbranched objects in solution.[284–286]

Hawker derived highly branched polystyrenes starting from the inimer (**A**) (Fig. 14.38) containing both a styryl moiety and an alkoxyamine group.[288,289] Its SCVP, which was carried out at 130°C afforded a low T_g (45°C) solid that served to polymerize styrene through its multiple alkoxyamine nitroxide functions, thus producing a "hyperstar" polystyrene ($M_w = 300,000$ g/mol; PDI = 4.35). Figure 14.38 shows some other functional monomers that were later radically polymerized— essentially by ATRP—to obtain hyperbranched polymers by SCVP. Interestingly, compounds **D** and **E** were found to undergo photopolymerization; SCVP of these "photoinimers" led to hyperbranched polystyrenes, as evidenced by viscometric measurements.[290–292]

In SCVP-derived systems, the DB value depends on the relative reactivity of the two potential propagating species (**B** and **B'**) obtained after formation of the **ABB'** dimer. Indeed, a linear polymer (i.e., with a DB = 0) is obtained if $r_B \gg r'_B$ or $r'_B \gg r_B$ where r_B and r'_B are the reactivity ratios of the **B** and **B'** propagating sites, respectively. Conversely, a highly branched structure can be reached if **B** and **B'** exhibit similar reactivities.

The work of Fréchet et al.[61] offers an illustration of these features; these authors investigated the SCVP of chloromethyl styrene (**B** in Fig. 14.38) by ATRP (CuCl/2-
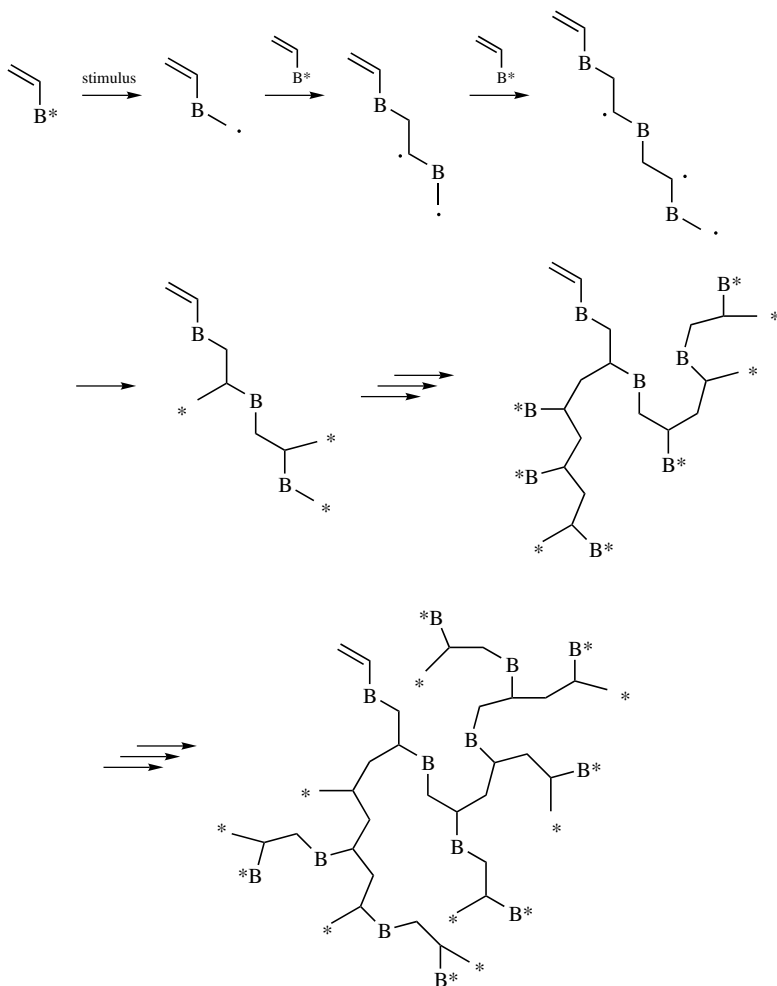
Figure 14.37 Mechanism of SCVP.[287]

2′-dipyridyl was used as the catalytic system) that was also studied by Matyjaszewski and colleagues.[293] The SCVP of such an inimer results in the formation of a dimer with a primary and a secondary benzylic halide of unequal reactivity. Fréchet and colleagues[61] showed that the experimental parameters (catalyst : monomer ratios, type of ligand employed, use or nonuse of a solvent reaction temperature, reaction time, etc.) have a dramatic influence on the rate of reaction, the molar masses, and the extent of branching (hence on the chain architecture) in the polymers formed. Because it involves two sites of contrasted reactivities, the SCVP of *p*-chloromethyl-styrene operates according to the following mechanism. At an early stage of reaction, the reactive sites initially formed (the primary chlorine in the case of chloromethylstyr-ene) slowly initiates a certain number of chains. On propagation, more reactive
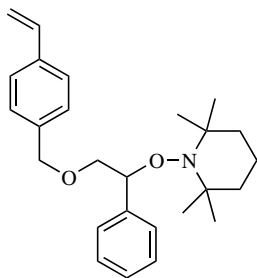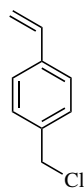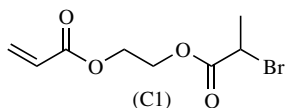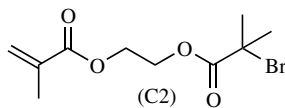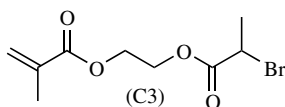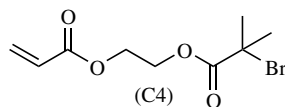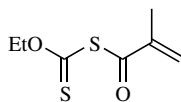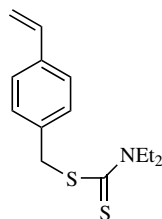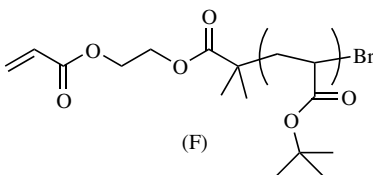
Figure 14.38   **AB* (macro)molecules used in SCVP.**

(secondary chlorine) sites are created that consume monomer faster than the primary chlorine; as a consequence, mainly linear units are produced. As the concentration of the inimer decreases in the reaction medium, there is more room for the linear oligomers formed during the initial stage to participate in the polymerization through their double bond; therefore the number of branching points increases.

As emphasized in the section devoted to star polymer synthesis, it is essential to maintain a very low concentration of propagating radicals when a given macromolecule carries more than one active species. Under such conditions only can irreversible recombination be minimized and crosslinking prevented.

On the other hand, Matyjaszewski and colleagues stressed the necessity to maintain a sufficiently high concentration in Cu(I) for the polymerization to carry on to completion because the concentration in Cu(II) continuously builds up with time, especially when homogeneous media and metal-solubilizing ligands were used.[294] These authors proposed to employ zerovalent copper to continuously regenerate Cu(I) species. Addition of Cu(0), indeed, allowed the polymerization of (meth)acrylic inimers to carry on to high conversion and afforded hyperbranched polymers that exhibited apparent molar masses below 10,000 g/mol (PDI = 2) and DB revolving around 0.5.

Müller and Matyjaszewski analyzed in detail the kinetics of SCVP of (meth)acrylate-based inimers (**C1**–**C4** in Fig. 14.38), as well as the molecular parameters such as the evolution of the molar mass distribution, the degree of branching, and the fraction of the various structural units, as a function of monomer conversion.[295–299] It was found that DB is slightly smaller (0.465) than in the case of the branched systems obtained by polycondensation of AB_2-type monomers at complete conversion, assuming that no side reaction such as intramolecular cyclization occurs. However, DB can be increased up to 0.66 by employing multifunctional initiators and the so-called "slow monomer addition" technique.

The presence of numerous terminal halide groups in the hyperbranched polymers obtained by ATRP offered the possibility of introducing various functionalities at the surface of these polymers by chemical modification. For instance, hyperbranched polystyrenes described by Fréchet and colleagues were subjected to different chemical modification of their branch ends; cyano, acetate, thioester, and maleimide groups were quantitatively incorporated at the surface.[61] Halogen end groups of hyperbranched polyacrylates and polystyrenes were subsequently modified into as many azides and crosslinked by heating.[300]

Hyperbranched polymers based on chloromethylstyrene even served as multifunctional macroinitiator for the ATRP of styrene and the synthesis of so-called "dendrigraft" polymers (see Section 14.7.2).[301] In the solid state, these materials were found to be more thermally stable than linear polystyrene, while in solution they exhibited a lower intrinsic viscosity. The switch from one mechanism to another was also considered to generate hyperbranched amphiphilic copolymers consisting of an inner hydrophilic core and an outer hydrophobic shell; hyperbranched polyglycerols—obtained by the so-called "ring-opening multibranching polymerization (ROMBP)" of glycidol—served to grow poly(methyl acrylate) blocks by ATRP, after chemical modification of their terminal hydroxy functions.[302]

Hyperbranched copolymers based on chloromethyl styrene and *N*-cyclohexyl-maleimide, which are respectively electron donor and acceptor, were also prepared by atom transfer radical SCVP with a view of generating charge-transfer complexes.[303]

The IBM team also proposed a versatile approach to hyperbranched polymers by "self-condensing vinyl and cyclic ester polymerization;" a bromide-containing lactone (shown in Fig. 14.30) and 2-hydroxyethyl methacrylate were either polymerized sequentially or used in concurrent copolymerizations combining ROP and ATRP.[304] The branching density of the copolymers produced in this way could be varied through the control of the composition of the comonomer ratio.

The group of Müller developed new hyperbranched poly(*tert*-butyl acrylate) by SCVP from a "macroinimer" (macromonomer + initiator), which is a short polymer fitted with a polymerizable acrylic double bond at one chain end and a bromine atom at the other end (**F** in Fig. 14.38).[305] ATRP of this macroinimer using CuBr/PMDETA at 40°C in ethyl acetate led to branched macromolecules that consisted of polymeric segments between the branching points, in contrast to the products derived from inimers. The branched character of these poly(*tert*-butyl acrylate)s ($M_n = 79,000$ g/mol; PDI = 2.6) was evidenced by viscometric measurements; a value of the Mark–Houwink exponent ($a = 0.49$) lower than that determined for linear poly(*tert*-butyl acrylate) ($a = 0.8$) indicated the compact nature of these samples.

Another way to access highly branched polymers consisted in the use of a trace amount of 4-methacryloyloxy-TEMPO (Fig. 14.39), which is a monomer containing the stable counterradical nitroxide, whose copolymerization with styrene led to hyperbranched polystyrene of high polydispersity, which were found to reversibly decompose into linear chains above 100°C.[306,307]

14.7.2   Dendrimerlike (Co)polymers

Branched architectures such as star block, H-type miktoarm stars, highly branched copolymers termed "dendrigraft" or dendrimerlike copolymers, were also covalently assembled by combination of two mechanisms. A distinction should be made here between "dendrigraft" and "dendrimerlike" copolymers. The former species resemble randomly branched macromolecules containing polymeric segments between the branching points.[308] They are obtained from the successive graftings of "living" linear polymers used as building blocks. The term "dendrimerlike" coined by the group of Hedrick[309] designates architectures that exhibit features similar to those of regular dendrimers (i.e., precise number of branching points and outer functions
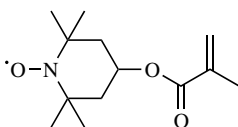
Figure 14.39   Structure of 4-methacryloyloxy-TEMPO.[306,307]

in all molecules, presence of a central core) but, unlike the latter, their successive generations consist of polymeric chains. They are obtained by combination of chain addition polymerization and functionalization of the chain ends.

Combining NMP of styrenics and ATRP of MMA (Fig. 14.40), Fréchet and colleagues covalently arrange PS and PMMA chains to form a "dendrigraft" structure, which is simply an irregular dendrimer whose branching points are randomly distributed along the chains.[308] However, it should be noted that the benzyl chlorides are slow initiators for the ATRP of MMA, which should likely result in the formation of grafts with a broad distribution in size.

The IBM team was the first to describe the synthesis of dendrimerlike copolymers, which resulted from the combination of the ring-opening anionic polymerization of ε-caprolactone for the inner part and ATRP of methyl methacrylate for the external branches.[309] In contrast to the formation of star block copolymer, the synthesis of these dendrimerlike copolymers requires the derivatization of the arm tips of the first generation into, at least, twice as many functions; the latter were then used to initiate the polymerization of the second monomer to subsequently form the second generation (Fig. 14.41). The presence of additional branching points in the dendrimerlike structure was found to bring about distinct properties as compared to those found for star block and linear homologs. As an extension of their work on PCL_6-b-$PMMA_6$ star block copolymers, Hedrick and colleagues described the synthesis of PCL_6-b-$PMMA_{12}$ and PCL_6-b-$PMMA_{24}$ dendrimerlike architectures.[309,310] Amphiphilic homologs, including HEMA units instead of MMA ones, have also been synthesized.

As for Gnanou and colleagues, they reported the synthesis of various well-defined amphiphilic dendrimerlike copolymers: PEO_f-b-PS_{2f} (with $f = 3$ or 4) as well as PEO_1-b-PS_2 miktoarm stars and PS_2-b-PEO-b-PS_2 H-type copolymers.[280] All these architectures have been prepared using the same sequence of reactions that is derivatization of chain ends of monohydroxy and bishydroxy PEOs and growth of the PS blocks by ATRP. Interestingly, investigations by ^{1}H NMR showed that these amphiphilic dendrimerlike copolymers exhibited self-associating properties and formed unimolecular micelles. For instance, it was observed that the hydrophilic arms of PEO_f-b-PS_{2f} branched compounds were able to wrap the hydrophobic parts, the latter preferring to stay within the core of the micellar structure. In THF, the PEO arms stayed in the inner part in a slightly more compact form than in chlorinated solvent, the dendritic and hydrophobic parts extending outward.

14.7.3   Hybrid Dendritic–Linear Macromolecules

On associating a dendritic structure with a linear chain, one can expect that the architecture formed exhibit properties specific to both moieties. In 1996, the group of Hawker[311] used a "unimolecular" dendritic initiator in LRP while the groups of Matyjaszewski and Fréchet[312] attached TEMPO to a dendritic precursor and initiated the polymerization of styrene in the presence of benzoyl peroxide. In the former case, a perfectly defined dendritic polyethers of generation 1 to 4 were connected at their "focal point" to a functional alkoxyamine before the growth of the PS chains
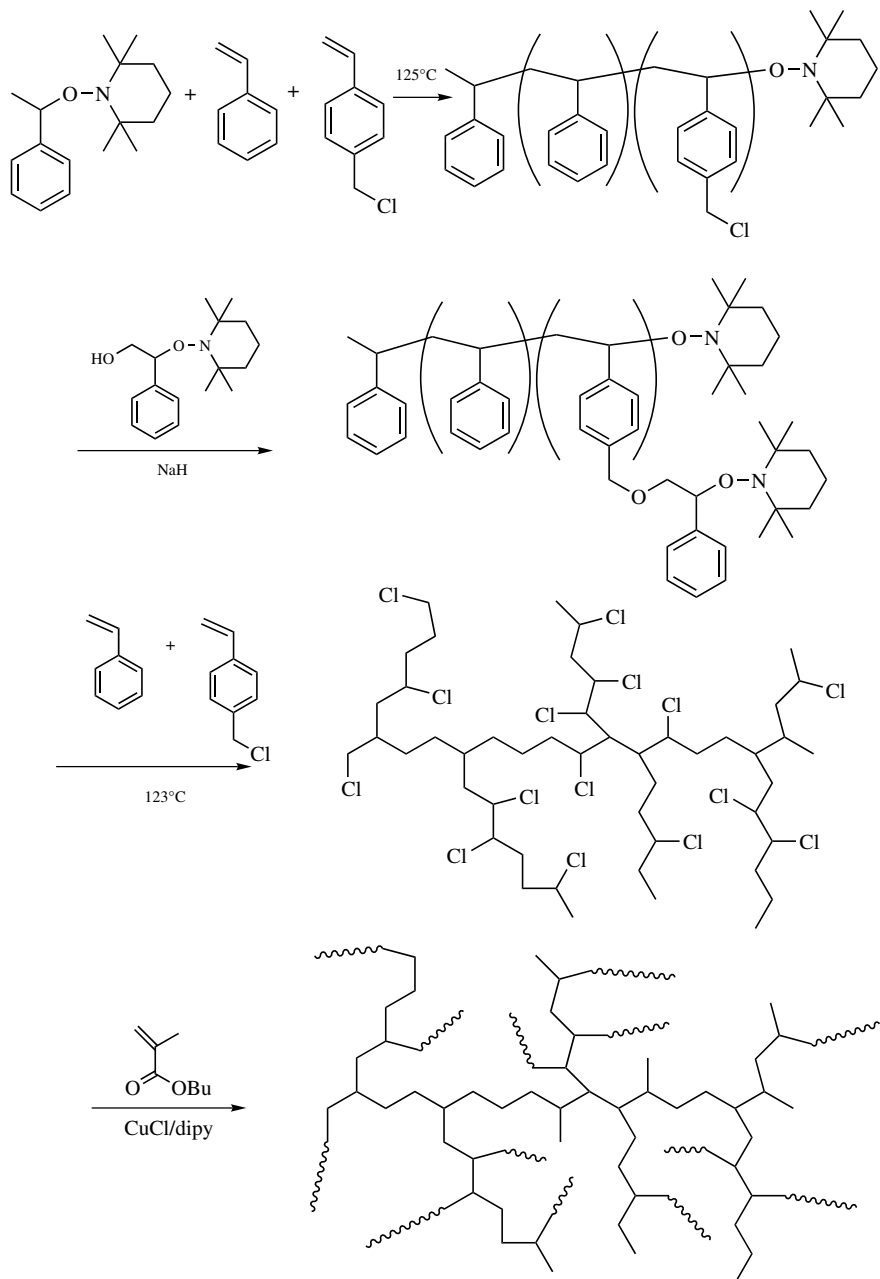
Figure 14.40   Synthesis of ''dendrigraft'' copolymers.[308]

central core

branching point

terminal group
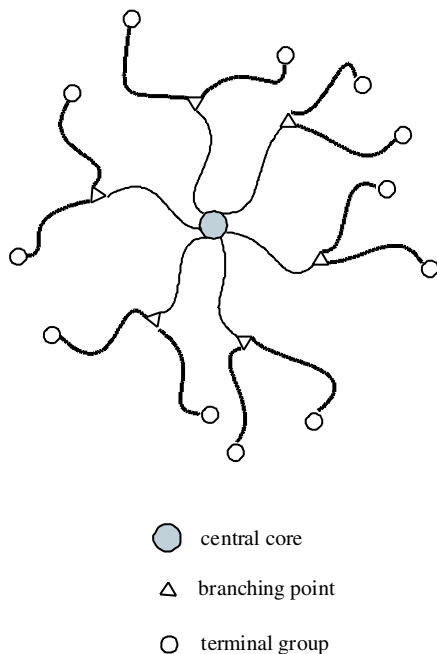
Figure 14.41   Dendrimerlike copolymers.[280,309–310]

by NMP. This gave rise to well-defined hybrid AB block copolymer. The same could be done via ATRP, the focal point being, in this case, a halogenated functionality.[311,312] The ATRP of styrene could not be controlled for molar masses higher than 30,000 g mol^{-1} L^{-1} (PDI < 1.3) when benzyl chloride groups were the initiating sites. Better control was obtained with the use of dendrons containing ethyl ester terminal units and benzyl bromides as initiating groups.[313] The chemical transformation of the peripheral ester groups of the dendritic moiety into various functional groups, including carboxylic acid, benzyl alcohol functions yielded, in some cases, hybrid amphiphilic materials exhibiting self-association properties. The thermal characterization of these hybrid block copolymers revealed only one glass transition temperature, indicating the miscibility of the two moieties. In contrast, the use of the TEMPO-carrying dendron to control the NMP of styrene led to poorly defined structures, probably due to a slow exchange between the growing PS radicals and the dendritic counterradical.

More recently, Fréchet and coll. combined the two previous approaches in their attempt to synthesize ABA triblock dendritic–linear hybrid copolymers.[314] These authors prepared a bisdendritic unimolecular initiator to be used in the NMP of styrene. However, the TEMPO-terminated dendron failed to adequately control the polymerization of styrene because of its size. Therefore, contamination of the ABA triblock structures with AB diblock copolymer was observed but the expected architecture could be isolated by column chromatography.

14.8 POLYMER NETWORKS

The synthesis of "model" networks using LRP-based end-linking processes was described by Chaumont et al.[315] Starting from a difunctional ATRP-derived PS sample, these authors obtained a network on addition of divinylbenzene under ATRP conditions. Earlier reports investigated the possibility of generating crosslinked PS by NMP, through the copolymerization of styrene with 4,4′-divinylbiphenyl using TEMPO-based alkoxyamine as initiating system.[316,317] On the other hand, Solomon and co-workers previously synthesized soluble microgels through the copolymerization of *tert*-butylstyrene with divinylbenzene by NMP.[318] Marked differences were observed between regular gels obtained by conventional free-radical polymerization and gels formed by LRP with respect to their homogeneity, soluble fraction, and swelling ratio for a same monomer conversion or crosslinking density.

14.9 APPLICATIONS AND PERSPECTIVES

ATRP as well as NMP and RAFT methodologies now allow a vast range of monomers to be (co)polymerized under "living"/controlled conditions. A wealth of tools based on LRP now exist to precisely control the end functionality and the composition of (co)polymers or direct their topology.

The patent literature[319] indicates that many of the products obtained by LRP target on the one hand segments of the specialty polymers market, covered until now by ionically produced materials, and on the other novel "niches." Also, processes that are currently used to produce certain materials can be replaced by methodologies based on LRP. For instance, block copolymers that are accessible only through solution anionic polymerization may be obtained via (mini)emulsion LRP. In contrast, there are little prospects for the commodity polymer industry to make use of LRP in its technologies.

In the case of the specialty polymers market are concerned applications such as thermoplastic elastomers, coatings, lubricants, and adhesives. Three conditions need to be met before substituting LRP methodologies for existing ones. The first points to address are a comprehensive evaluation of properties exhibited by the materials generated via LRP and a thorough comparison with those known for traditional products. For instance, Jérôme and colleagues compared the tensile properties of all-methacrylate-based thermoplastic elastomers prepared by ligated anionic polymerization and LRP: the latter were shown to exhibit poorer tensile properties than the anionic ones, likely because of the larger polydispersity of the PMMA outer blocks.[102–105] Should LRP materials demonstrate an improved behavior as compared to the traditional products and their utility confirmed then only criteria such as the manufacturing feasibility, environment concerns and cost can enter the picture. Even though the potential is very high for developing new technologies based on LRP and correspondingly new products to meet the demand of the market hurdles related, for instance, to the inertia factor cannot be ignored.

The "niche" market with, in some cases, its higher value application also looks, very promising. Sectors such as the microelectronics industry, which requires surface modification of inorganic materials at the nanoscale level, may soon benefit from the advances made in LRP. Obviously, such applications would not have been developed without the help of LRP methodologies. It is too early to predict how many applications will eventually arise out of LRP and whether they will replace old products and/or create new segments in the specialty polymers market. Research in LRP has come to maturity in less than 10 years' time (at the time of this writing), and its basic concepts are now being transferred to the hands of technologists.

REFERENCES

1. G. Moad and D. H. Solomon, *The Chemistry of Free-Radical Polymerization* Pergamon, Oxford (1995).

2. (a) M. K. Georges, R. P. N. Veregin, G. Kazmaier, and G. K. Hamer, *Macromolecules* **26**, 5316 (1993); (b) C. J. Hawker, *Trends Polym. Sci.* **4**, 183 (1994).

3. K. Matyjaszewski, *Chem. Eur. J.* **5**, 3095 (1999); T. E. Patten and K. Matyjaszewski, *Adv. Mater.* **10**, 901 (1998).

4. (a) J. Chiefari, Y. K. Chong, F. Ercole, J. Krstina, J. Jeffrey, T. P. Le, R. T. Mayadunne, G. F. Meijs, C. L. Moad, G. Moad, E. Rizzardo, and S. H. Thang, *Macromolecules* **31**, 5559 (1998); (b) E. Rizzardo, J. Chiefari, Y. K. Chong, F. Ercole, J. Krstina, J. Jeffrey, T. P. Le, R. T. Mayadunne, G. F. Meijs, C. L. Moad, and G. Moad, *Macromol. Symp.* **143**, 291 (1999).

5. D. Charmot, P. Corpart, H. Adam, S. Z. Zard, T. Biadatti, and G. Bouhadir, *Macromol. Symp.* **150**, 23 (2000).

6. K. Matyjaszewski, S. G. Gaynor, and J.-S. Wang, *Macromolecules* **28**, 2093 (1995).

7. B. B. Wayland, G. Poszmik, S. L. Mukerjee, and M. Fryd, *J. Am. Chem. Soc.* **116**, 7943 (1994).

8. M. Steenbock, M. Klapper, K. Muellen, C. Bauer, and M. Hubrich, *Macromolecules* **31**, 5223 (1998).

9. D. Braun, *Macromol. Symp.* **111**, 63 (1996).

10. T. Otsu, *J. Polym. Sci.; Part A: Polym. Chem.* **38**, 2121 (2000).

11. K. Matyjaszewski, *J. Phys. Org. Chem.* **8**, 197 (1995).

12. K. Matyjaszewski, *ACS Symp. Ser.* **768**, 2 (2000).

13. S. G. Gaynor and K. Matyjaszewski, *ACS Symp. Ser.* **768**, 347 (2000).

14. D. Benoit, V. Chaplinski, R. Braslau, and C. J. Hawker, *J. Am. Chem. Soc.* **121**, 3904 (1999).

15. M. Teodorescu and K. Matyjaszewski, *Macromol. Rapid Commun.* **21**, 190 (2000).

16. X.-S. Wang, S. F. Lascelles, R. A. Jackson, and S. P. Armes, *Chem. Commun.* 1817 (1999).

17. P. Corpart, D. Charmot, T. Biadatti, S. Zard, and D. Michelet, PCT Int. Appl. WO9858974 [*Chem. Abstr.* **130**, 82018 (1999)].

18. T. Pintauer, V. Coessens, and K. Matyjaszewski, *Progr. Polym. Sci.* **26**(3), 337 (2001).

19. B. Boutevin, *J. Polym. Sci.; Part A: Polym. Chem.* **38**, 3235 (2000).

20. E. E. Malmström, and C. J. Hawker, *Macromol. Chem. Phys.* **199**, 923 (1998).

21. C. J. Hawker, E. Elce, J. Dao, W. Volksen, T. P. Russell, and G. G. Barclay, *Macromolecules* **29**, 2686 (1996).

22. C. J. Hawker and J. L. Hedrick, *Macromolecules* **28**, 2993 (1995).

23. B. Frank, A. P. Gast, T. P. Russell, H. R. Brown, and C. J. Hawker, *Macromolecules* **29**, 6531 (1996).

24. C. J. Hawker, G. Barclay, A. Orellana, J. Dao, and W. Devonport, *Macromolecules* **29**, 5245 (1996).

25. J. Dao, D. Benoit, and C. J. Hawker, *J. Polym. Sci.; Part A: Polym. Chem.* **36**, 2161 (1998).

26. M. Rodlert, E. Harth, I. Rees, and C. J. Hawker, *J. Polym. Sci.; Part A: Polym. Chem.* **38**, 4749 (2000).

27. Y. Miura, K. Hirota, H. Moto, and B. Yamada, *Macromolecules* **31**, 4659 (1998).

28. Y. Zhu, Q. Li, B. A. Howell, and D. B. Priddy, *ACS Symp. Ser.* **685**, 214 (1998).

29. B. Lepoittevin, X. Perrot, M. Masure, and P. Hemery, *Macromolecules* **34**, 425 (2001).

30. M. Baumert, J. Zimmerman, J. Scherble, R. Mülhaupt, and J. Kressler, *Macromolecules* **32**, 2503 (1999).

31. J.-S. Wang and K. Matyjaszewski, *Macromolecules* **28**, 7901 (1995).

32. M. Destarac, J.-M. Bessière, and B. Boutevin, *J. Polym. Sci.; Part A: Polym. Chem.* **36**, 2933 (1998).

33. M. Destarac, K. Matyjaszewski, and B. Boutevin, *Macromol. Chem. Phys.* **201**, 265 (2000).

34. D. M. Haddleton, C. Waterson, P. J. Derrick, C. B. Jasieczek, and A. J. Shooter, *Chem. Commun.* 683 (1997).

35. X. Zhang and K. Matyjaszewski, *Macromolecules* **32**, 7349 (1999).

36. H. Malz, H. Komber, D. Voigt, I. Hopfe, and J. Pionteck, *Macromol. Chem. Phys.* **200**, 642 (1999).

37. D. M. Haddleton, A. M. Heming, D. Kukulj, D. J. Duncalf, and A. J. Shooter, *Macromolecules* **31**, 2016 (1998).

38. G. Moineau, M. Minet, Ph. Dubois, Ph. Teyssié, T. Senninger, and R. Jérôme, *Macromolecules* **32**, 27 (1999).

39. A. Marsh, A. Khan, D. M. Haddleton, and M. J. Hannon, *Macromolecules* **32**, 8725 (1999).

40. D. M. Haddleton, A. P. Jarvis, C. Waterson, S. A. F. Bon, and A. M. Heming, *ACS symp. ser.* **768**, 182 (2000).

41. D. M. Haddleton and K. Ohno, *Biomacromolecules* **1**, 152 (2000).

42. V. Percec, B. Barboiu, and H.-J. Kim, *J. Am. Chem. Soc.* **120**, 305 (1998).

43. V. Percec, H.-J. Kim, and B. Barboiu, *Macromolecules* **30**, 8526 (1997).

44. V. Coessens, J. Pyun, P. J. Miller, S. G. Gaynor, and K. Matyjaszewski, *Macromol. Rapid Commun.* **21**, 103 (2000).

45. E. G. Koulouri, J. K. Kallitsis, and G. Hadziioannou, *Macromolecules* **32**, 6242 (1999).

46. T. Ando, M. Kamagaito, and M. Sawamoto, *Macromolecules* **31**, 6708 (1998).

47. K. Tokuchi, T. Ando, M. Kamigaito, and M. Sawamoto, *J. Polym. Sci.; Part A: Polym. Chem.* **38**, 4735 (2000).

48. D. M. Haddleton, A. M. Heming, A. P. Jarvis, A. Khan, A. Marsh, S. Perrier, S. A. Bon, S. G. Jackson, R. Edmonds, E. Kelly, D. Kukulj, and C. Waterson, *Macromol. Symp.* **157**, 201 (2000).

49. K. E. Geckeler and S. Samal, *Polym. Int.* **48**, 743 (1999).

50. H. Okamura, T. Terauchi, M. Minoda, T. Fukuda, and K. Komatsu, *Macromolecules* **30**, 5279 (1997).

51. C. Wang, J. He, S. Fu, K. Jiang, H. Cheng, and M. Wang, *Polym. Bull.* **37**, 305 (1996).

52. H. Okamura, M. Minoda, T. Fukuda, T. Miyamoto, and K. Komatsu, *Macromol. Rapid Commun.* **20**, 37 (1999).

53. H. Okamura, N. Ide, M. Minoda, K. Komatsu, and T. Fukuda, *Macromolecules* **31**, 1859 (1998).

54. P. Zhou, G.-Q. Chen, H. Hong, F.-S. Du, Z.-C. Li, and F.-M. Li, *Macromolecules* **33**, 1948 (2000).

55. X. Shen, X. He, G. Chen, P. Zhou, and L. Huang, *Macromol. Rapid Commun.* **21**, 1162 (2000).

56. G. Carrot, J. Hilborn, J. L. Hedrick, and M. Trollsås, *Macromolecules* **32**, 5171 (1999).

57. V. Coessens and K. Matyjaszewski, *Macromol. Rapid Commun.* **20**, 127 (1999).

58. Y. Nakagawa and K. Matyjaszewski, *Polym. J.* **30**, 138 (1998).

59. V. Coessens, Y. Nakagawa, and K. Matyjaszewski, *Polym. Bull.* **40**, 135 (1998).

60. K. Matyjaszewski, Y. Nakagawa, and S. G. Gaynor, *Macromol. Rapid Commun.* **18**, 1057 (1997).

61. M. W. Weimer, J. M. J. Fréchet, and I. Gitsov, *J. Polym. Sci.; Part A: Polym. Chem.* **36**, 955 (1998).

62. C. H. Honeyman, K. A. Moffat, G. K. Hamer, and M. K. Georges, *PMSE* **80**, 88 (1999).

63. E. Beyou, Ph. Chaumont, F. Chauvin, C. Devaux, and N. Zydowicz, *Macromolecules* **31**, 6828 (1998).

64. N. J. Turro, G. Lem, and I. S. Zavarine, *Macromolecules* **33**, 9782 (2000).

65. Y. Gnanou, *Ind. J. Techn.* **31**, 317 (1993).

66. D. Mecerreyes, J. A. Pomposo, M. Bengoetxea, and H. Grande, *Macromolecules* **33**, 5846 (2000).

67. K. Matyjaszewski, K. L. Beers, A. Kern, and S. G. Gaynor, *J. Polym. Sci.; Part A: Polym. Chem.* **36**, 823 (1998).

68. F. Zeng, Y. Shen, S. Zhu, and R. Pelton, *Macromolecules* **33**, 1628 (2000).

69. Y. Shen, S. Zhu, F. Zeng, and R. Pelton, *Macromolecules* **33**, 5399 (2000).

70. J. Chiefari, J. Jeffrey, R. T. A. Mayadunne, G. Moad, E. Rizzardo, and S. H. Thang, *ACS Symp. Ser.* **768**, 297 (2000).

71. C. P. R. Nair, P. Chaumont, and D. Charmot, *J. Polym. Chem.* **33**, 2773 (1995).

72. S. A. F. Bon, S. R. Morsley, C. Waterson, and D. M. Haddleton, *Macromolecules* **33**, 5819 (2000).

73. T. Fukuda, T. Terauchi, A. Goto, Y. Tsujii, and T. Miyamoto, *Macromolecules* **29**, 3050 (1996).

74. H. Baethge, S. Butz, and G. Schmidt-Naake, *Macromol. Rapid Commun.* **18**, 911 (1997).

75. H. Baethge, S. Butz, C.-H. Han, and G. Schmidt-Naake, *Angew. Makromol. Chem.* **267**, 52 (1999).

76. M. Baumert, J. Fröhlich, M. Stieger, H. Frey, R. Mülhaupt, and H. Plenio, *Macromol. Rapid Commun.* **20**, 203 (1999).

77. P. M. Kazmaier, K. Daimon, M. K. Georges, G. K. Hamer, and R. P. N. Veregin, *Macromolecules* **30**, 2228 (1997).

78. R. G. Jones, S. Yoon, and Y. Nagasaki, *Polymer* **40**, 2411 (1999).

79. D. Benoit, E. Harth, P. Fox, R. M. Waymouth, and C. J. Hawker, *Macromolecules* **33**, 363 (2000).

80. Y. Kotani, M. Kamigaito, and M. Sawamoto, *Macromolecules* **31**, 5582 (1998).

81. S. V. Arehart and K. Matyjaszewski, *Macromolecules* **32**, 2221 (1999).

82. K. Matyjaszewski, M. J. Ziegler, S. V. Arehart, D. Greszta, and T. Pakula, *J. Phys. Org. Chem.* **13**, 775 (2000).

83. X. Chen, B. Ivan, J. Kops, and W. Batsberg, *Polym. Bull.* **39**, 559 (1997).

84. H. Uegaki, Y. Kotani, M. Kamigaito, and M. Sawamoto, *Macromolecules* **31**, 6756 (1998).

85. M. J. Ziegler and K. Matyjaszewski, *Macromolecules* **34**, 415 (2001).

86. D. M. Haddleton, M. C. Grossman, K. H. Hunt, C. Topping, C. Waterson, and K. G. Suddaby, *Macromolecules* **30**, 3992 (1997).

87. M. Seeno, Y. Kotani, M. Kamigaito, and M. Sawamoto, *Macromol. Symp.* **157**, 193 (2000).

88. K. Matyjaszewski, D. A. Shipp, J. Qiu, and S. G. Gaynor, *Macromolecules* **33**, 2296 (2000).

89. X. Jiang, P. Xia, W. Liu, and D. Yan, *J. Polym. Sci.; Part A: Polym. Chem.* **38**, 1203 (2000).

90. E.-S. Park, M.-N. Kim, I.-M. Lee, H. S. Lee, and J.-S. Yoon, *J. Polym. Sci.; Part A: Polym. Chem.* **38**, 2239 (2000).

91. D. Benoit, C. J. Hawker, E. E. Huang, Z. Lin, and T. P. Russel, *Macromolecules* **33**, 1505 (2000).

92. G.-Q. Chen, Z.-Q. Wu, J.-R. Wu, Z.-C. Li, and F.-M. Li, *Macromolecules* **33**, 232 (2000).

93. G. Riess and P. Bahadur, in *Encyclopedia of Polymer Science and Engineering*, H. F. Mark, N. M. Bikales, C. G. Overberger, and G. Menges, eds., Wiley, New York, 1989, p. 324.

94. K. Matyjaszewski, J. L. Wang, T. Grimaud, and D. A. Shipp, *Macromolecules* **31**, 1527 (1998).

95. J. S. Wang and K. Matyjaszewski, *J. Am. Chem. Soc.* **117**, 5614 (1995).

96. C. Granel, P. Dubois, R. Jerôme, and P. Teyssié, *Macromolecules* **29**, 8576 (1996).

97. Y. Kotani, M. Kato, M. Kamigaito, and M. Sawamoto, *Macromolecules* **29**, 6979 (1996).

98. M. Cassebras, S. Pascual, A. Polton, M. Tardi, and J. P. Vairon, *Macromol. Rapid Commun.* **20**, 261 (1999).

99. K. A. Davis, B. Charleux, and K. Matyjaszewski, *J. Polym. Sci.; Part A: Polym. Chem.* **38**, 2283 (2000).

100. K. A. Davis and K. Matyjaszewski, *Macromolecules* **33**, 4039 (2000).

101. D. A. Shipp, J. L. Wang, and K. Matyjaszewski, *Macromolecules* **31**, 8005 (1998).

102. G. Moineau, M. Minet, P. Teyssié, and R. Jérôme, *Macromolecules* **32**, 8277 (1999).

103. Ph. Leclère, G. Moineau, M. Minet, Ph. Dubois, R. Jérôme, J. L. Brédas, and R. Lazzaroni, *Langmuir* **15**, 3915 (1999).

104. G. Moineau, M. Minet, Ph. Dubois, Ph. Teyssié, and R. Jérôme, *Macromol. Chem. Phys.* **201**, 1108 (2000).

105. J. D. Tong, G. Moineau, Ph. Leclère, J. L. Brédas, R. Lazzaroni, and R. Jérôme, *Macromolecules* **33**, 470 (2000).

106. Y. Kotani, M. Kamigaito, and M. Sawamoto, *Macromolecules*, **33**, 6746 (2000).

107. K. Matyjaszewski, D. A. Shipp, G. P. McMurtry, S. G. Gaynor, and T. Pakula, *J. Polym. Sci.; Part A: Polym. Chem.* **38**, 2023 (2000).

108. (a) K. L. Beers, B. Woodworth, and K. Matyjaszewski, *J. Chem. Ed.* **78**, 544 (2001); (b) K. Matyjaszewski, K. L. Beers, and B. Woodworth, *J. Chem. Ed.* **78**, 547 (2001).

109. N. A. Listigovers, M. K. Georges, P. G. Odell, and B. Kheoshkerian, *Macromolecules* **29**, 8992 (1996).

110. M. K. Georges, G. K. Hamer, and N. A. Listigovers, *Macromolecules* **31**, 9087 (1998).

111. B. Kheoshkerian, M. K. Georges, M. Quinlan, R. Veregin, and B. Goodbrand, *Macromolecules* **31**, 7559 (1998).

112. Z. Yousi, L. J. Jian, Z. Rongchuan, Y. Jianliang, D. Lizong, and Z. Lansun, *Macromolecules* **33**, 4745 (2000).

113. S. Jousset, S. Oulad Hammouch, and J. M. Catala, *Macromolecules* **30**, 6685 (1997).

114. C. Burguière, M. A. Dourges, B. Charleux, and J. P. Vairon, *Macromolecules* **32**, 3883 (1999).

115. B. Y. K. Chong, F. Ercole, G. Moad, E. Rizzardo, S. H. Thang, and A. G. Anderson, *Macromolecules* **32**, 6895 (1999).

116. (a) D. Benoit, S. Grimaldi, J. P. Finet, P. Tordo, M. Fontanille, and Y. Gnanou, *Polym. Prep.* **38**(1), 729 (1997); (b) D. Benoit, S. Grimaldi, J. P. Finet, P. Tordo, M. Fontanille, and Y. Gnanou, *ACS Symp. Ser.* **685**, 225 (1998); (c) S. Grimaldi, J. P. Finet, F. Le Moigne, A. Zeghdaoui, P. Tordo, D. Benoit, M. Fontanille, and Y. Gnanou, *Macromolecules* **33**, 1141 (2000).

117. D. Benoit, S. Grimaldi, S. Robin, J. P. Finet, P. Tordo, and Y. Gnanou, *J. Am. Chem. Soc.* **122**, 5929 (2000).

118. (a) S. Robin, O. Guerret, J. L. Couturier, R. Pirri, and Y. Gnanou, *Macromolecules* **35**, 3844 (2000); (b) S. Robin and Y. Gnanou, *Macromol. Symp.* **165**, 43 (2001).

119. Y. K. Chong, T. P. Le, G. Moad, E. Rizzardo, and S. H. Thang, *Macromolecules* **32**, 2071 (1999).

120. R. T. A. Mayadunne, E. Rizzardo, J. Chiefari, J. Krstina, G. Moad, A. Postma, and S. H. Thang, *Macromolecules* **33**, 243 (1999).

121. M. C. Bignozzi, C. K. Ober, and M. Laus, *Macromol. Rapid Commun.* **20**, 622 (1999).

122. U. Stalmach, B. de Boer, C. Videlot, P. F. van Hutten, and G. Hadzoiiannou, *J. Am. Chem. Soc.* **122**, 5464 (2000).

123. K. Matyjaszewski, *Macromolecular Symposia* **132**, 85 (1998).

124. S. Coca and K. Matyjaszewski, *J. Polym. Sci.; Part A: Polym. Chem.* **35**, 3595 (1997).

125. K. Jankova, J. Kops, X. Chen, B. Gao, and W. Batsberg, *Polym. Bull.* **41**, 639 (1998).

126. X. Chen, B. Ivan, J. Kops, and W. Batsberg, *Macromol. Rapid. Commun.* **19**, 585 (1998).

127. S. Coca and K. Matyjaszewski, *Macromolecules* **30**, 2808 (1997).

128. B. Ivan, X. Chen, J. Kops, and W. Batsberg, *Macromol. Rapid Commun.* **19**, 15 (1998).

129. J. H. Truelsen, J. Kops, and W. Batsberg, *Macromol. Rapid. Commun.* **21**, 98 (2000).

130. T. Fonagy, B. Ivan, and M. Szestay, *Macromol. Rapid. Commun.* **19**, 479 (1998).

131. M. H. Acar and K. Matyjaszewski, *Macromol. Chem. Phys.* **200**, 1094 (1999).

132. J. Dong Tong, S. Ni, and M. A. Winnik, *Macromolecules* **33**, 1482 (2000).

133. J. Dong Tong, C. Zhou, S. Ni, and M. A. Winnik, *Macromolecules* **34**, 696 (2001).

134. S. Kobatake, H. J. Harwood, R. Quirk, and D. B. Priddy, *Macromolecules* **31**, 3735 (1998).

135. S. Kobatake, H. J. Harwood, R. Quirk, and D. B. Priddy, *Macromolecules* **30**, 4238 (1997).

136. I. Q. Li, B. A. Howell, M. T. Dineen, P. E. Kastl, J. W. Lyons, D. M. Meunier, P. B. Smith, and D. B. Priddy, *Macromolecules* **30**, 5194 (1997).

137. I. Piirma, in *Polymeric Surfactants*, Surfactant Science Series, Marcel Dekker, New York, 1992.

138. Y. Y. Won, H. T. Davis, and F. S. Bates, *Science* **283**, 960 (1999).

139. J. Lokaj, P. Viček, and J. Křž, *Macromolecules* **30**, 7644 (1997).

140. X. Zhang and K. Matyjaszewski, *Macromolecules* **32**, 1763 (1999).

141. A. Mühlebach, S. G. Gaynor, and K. Matyjaszewski, *Macromolecules* **31**, 6046 (1998).

142. X.-S. Wang, N. Luo, and S.-K. Ying, *Polymer* **40**, 4157 (1999).

143. K. L. Beers, S. Boo, S. G. Gaynor, and K. Matyjaszewski, *Macromolecules* **32**, 5772 (1999).

144. M. Bouix, J. Gouzi, B. Charleux, J. P. Vairon, and P. Guinot, *Macromol. Rapid Commun.* **19**, 209 (1998).

145. B. Kheoshkerian, M. Georges, and D. Boils-Boissier, *Macromolecules* **28**, 6381 (1995).

146. M. Nowakowska, S. Zapotoczny, and A. Karewicz, *Macromolecules* **33**, 7345 (2000).

147. A. Fischer, A. Brembilla, and P. Lochon, *Eur. Polym. J.* **37**, 33 (2001).

148. J. Xia, T. Johnson, S. G. Gaynor, K. Matyjaszewski, and J. DeSimone, *Macromolecules* **32**, 4802 (1999).

149. K. Ohno, Y. Yoshinobu, and T. Fukuda, *J. Polym. Sci.; Part A: Polym. Chem.* **36**, 2473 (1998).

150. K. Ohno, T. Fukuda, and H. Kitano, *Macromol. Chem. Phys.* **199**, 2193 (1998).

151. K. Ohno, Y. Izu, S. Yamamoto, T. Miyamoto, and T. Fukuda, *Macromol. Chem. Phys.* **200**, 1619 (1999).

152. K. Ohno, M. Ejaz, T. Fukuda, T. Miyamoto, and Y. Shimizu, *Macromol. Chem. Phys.* **199**, 291 (1998).

153. X. Chen, K. Jankova, J. Kops, and W. Batsberg, *J. Polym. Sci.; Part A: Polym. Chem.* **37**, 627 (1999).

154. M. Mariani, M. Lelli, K. Sparnacci, and M. Laus, *J. Polym. Sci.; Part A: Polym. Chem.* **37**, 1237 (1999).

155. Q. Ma and K. L. Wooley, *J. Polym. Sci.; Part A: Polym. Chem.* **38**, 4805 (2000).

156. Y. Liu, L. Wang, and C. Pan, *Macromolecules* **32**, 8301 (1999).

157. U. Wendler, J. Bohrisch, W. Jaeger, G. Rother, and H. Dautzenberg, *Macromol. Rapid Commun.* **19**, 185 (1998).

158. P. Lacroix-Desmazes, T. Delair, C. Pichot, and B. Boutevin, *J. Polym. Sci.; Part A: Polym. Chem.* **38**, 3845 (2000).

159. J. Bohrisch, U. Wendler, and W. Jaeger, *Macromol. Rapid Commun.* **18**, 975 (1997).

160. X. Chen, B. Gao, J. Kops, and W. Batsberg, *Polymer* **39**, 911 (1998).

161. Y. Wang, S. Chen, and J. Huang, *Macromolecules* **32**, 2484 (1999).

162. K. Jankova, X. Chen, J. Kops, and W. Batsberg, *Macromolecules* **31**, 538 (1998).

163. K. Jankova, J. H. Truelsen, X. Chen, J. Kops, and W. Batsberg, *Polym. Bull.* **42**, 153 (1999).

164. M. Bednarek, T. Biedron, and P. Kubisa, *Macromol. Rapid Commun.* **20**, 59 (1999).

165. B. Reining, H. Keul, and H. Höcker, *Polymer* **40**, 3555 (1999).

166. K. Jankova, J. Kops, X. Chen, and W. Batsberg, *Macromol. Rapid Commun.* **20**, 219 (1999).

167. Q. Zhang, E. E. Remsen, and K. L. Wooley, *J. Am. Chem. Soc.* **122**, 3642 (2000).

168. (a) M. Sedlak, M. Antonietti, and H. Cölfen, *Macromol. Chem. Phys.* **199**, 247 (1998); (b) H. Cölfen, *Macromol. Rapid Commun.* **22**, 219 (2001).

169. E. J. Ashford, V. Naldi, R. O. Dell, N. C. Billingham, and S. P. Armes, *Chem. Commun.* 1285 (1999).

170. X.-S. Wang, R. A. Jackson, and S. P. Armes, *Macromolecules* **33**, 255 (2000).

171. X.-S. Wang and S. P. Armes, *Macromolecules* **33**, 6640 (2000).

172. L. I. Gabaston, S.A. Furlong, R. A. Jackson, and S. P. Armes, *Polymer* **40**, 4505 (1999).

173. Y. Mitsukami, M. S. Donovan, A. B. Lowe, and C. L. McCormick, *Macromolecules* **34**, 2248 (2001).

174. E. Yoshida and S. Tanimoto, *Macromolecules* **30**, 4018 (1997).

175. Y. Nakagawa, P. J. Miller, and K. Matyjaszewski, *Polymer* **39**, 5163 (1998).

176. P. J. Miller and K. Matyjaszewski, *Macromolecules* **32**, 8760 (1999).

177. D. A. Brown and G. J. Price, *Polymer* **42**, 4767 (2001).

178. J. Pyun and K. Matyjaszewski, *Macromolecules* **33**, 217 (2000).

179. L. Lutsen, G. P.-G. Cordina, R. G. Jones, and F. Schué, *Eur. Polym. J.* **34**, 1829 (1998).

180. E. Yoshida, *J. Polym. Sci.; Part A: Polym. Chem.* **34**, 2937 (1996).

181. J. Xia, X. Zhang, and K. Matyjaszewski, *Macromolecules* **32**, 3531 (1999).

182. K. A. Davis and K. Matyjaszewski, *Macromolecules* **34**, 2101 (2001).

183. K. A. Ellzey and B. M. Novak, *Macromolecules* **31**, 2391 (1998).

184. K. Matyjaszewski, M. Teodorescu, M. H. Acar, K. Beers, S. Coca, S. G. Gaynor, P. J. Miller, and H-J. Paik, *Macromol. Symp.* **157**, 183 (2000).

185. E. Yoshida and A. Sugita, *Macromolecules* **29**, 6422 (1996).

186. E. Yoshida and A. Sugita, *J. Polym. Sci.; Part A: Polym. Chem.* **36**, 2059 (1998).

187. A. Kajiwara and K. Matyjaszewski, *Macromolecules* **31**, 3489 (1998).

188. Y. Yagci, A. B. Dütz, and A. Ohnen, *Polymer* **28**, 2861 (1997).

189. Y. Xu, C. Pan, and L. Tao, *J. Polym. Sci.; Part A: Polym. Chem.* **38**, 436 (2000).

190. Y. Xu and C. Pan, *J. Polym. Sci.; Part A: Polym. Chem.* **38**, 337 (2000).

191. A. B. Duz and Y. Yagci, *Eur. Polym. J.* **35**, 2031 (1999).

192. E. Yoshida, T. Ishizone, A. Hirao, S. Nakahama, T. Takata, and T. Endo, *Macromolecules* **27**, 3119 (1994).

193. S. G. Gaynor and K. Matyjaszewski, *Macromolecules* **30**, 4241 (1997).

194. P. K. Tsolakis, E. G. Koulouri, and J. K. Kallitsis, *Macromolecules* **32**, 9054 (1999).

195. S. Coca, H. J. Paik, and K. Matyjaszewski, *Macromolecules* **30**, 6513 (1997).

196. C. W. Bielawski, T. Morita, and R. H. Grubbs, *Macromolecules* **33**, 678 (2000).

197. C. W. Bielawski, J. Louie, and R. H. Grubbs, *J. Am. Chem. Soc.* **122**, 12872 (2000).

198. D. J. Gravert, A. Datta, P. Wentworth, Jr., and K. D. Janda, *J. Am. Chem. Soc.* **120**, 9481 (1998).

199. H. J. Paik, M. Teodorescu, J. Xia, and K. Matyjaszewski, *Macromolecules* **32**, 7023 (1999).

200. M. Destarac and B. Boutevin, *Macromol. Rapid Commun.* **20**, 641 (1999).

201. M. Destarac, B. Boutevin, and K. Matyjaszewski, *ACS Symp. Ser.* **768**, 234 (2000).

202. M. Destarac, B. Pees, and B. Boutevin, *Macromol. Chem. Phys.* **201**, 1189 (2000).

203. M. Destarac, K. Matyjaszewski, B. Boutevin, E. Silverman, B. Ameduri, and B. Boutevin, *Macromolecules* **33**, 4613 (2000).

204. Z. Zhang, S. Ying, and Z. Shi, *Polymer* **40**, 1341 (1999).

205. M. W. Weimer, O. A. Scherman, and D. Y. Sogah, *Macromolecules* **31**, 8425 (1998).

206. C. J. Hawker, J. L. Hedrick, E. E. Malmström, M. Trollsas, D. Mecerreyes, G. Moineau, Ph. Dubois, and R. Jérôme, *Macromolecules* **31**, 213 (1998).

207. D. Mecerreyes, G. Moineau, Ph. Dubois, R. Jérôme, J. L. Hedrick, C. J. Hawker, E. E. Malmström, and M. Trollsas, *Angew. Chem. Int. Ed.* **37**, 1274 (1998).

208. G. Klaerner, M. Trollsas, A. Heise, M. Husemann, B. Atthoff, C. J. Hawker, J. L. Hedrick, and R. D. Miller, *Macromolecules* **32**, 8227 (1999).

209. T. Girgin Yildirim, Y. Hepuzer, G. Hizal, and Y. Yagci, *Polymer* **40**, 3885 (1999).

210. S. Alkan, L. Toppare, Y. Hepuzer, and Y. Yagci, *J. Polym. Sci.; Part A: Polym. Chem.* **37**, 4218 (1999).

211. N. Hadjichristidis, S. Pispas, M. Pitsikalis, H. Iatrou, and C. Vlahos, *Adv. Polym. Sci.* **142**, 71 (1998).

212. A. Halperin, M. Tirrell, and T. P. Lodge, *Adv. Polym. Sci.* **100**, 31 (1992).

213. H. J. Paik, S. G. Gaynor, and K. Matyjaszewski, *Macromol. Rapid Commun.* **19**, 47 (1998).

214. S. Liu, and A. Sen, *Macromolecules* **33**, 5106 (2000).

215. K. L. Beers, S.G. Gaynor, K. Matyjaszewski, S. Sheiko, and M. Möller, *Macromolecules* **31**, 9413 (1998).

216. U. M. Stehling, E. E. Malmstrom, R. M. Waymouth, and C. J. Hawker, *Macromolecules* **31**, 4396 (1998).

217. M. Baumert, J. Heinemann, R. Thomann, and R. Mulhaupt, *Macromol. Chem. Phys.* **21**, 271 (2000).

218. K. Matyjaszewski, M. Teodorescu, P. J. Miller, and M. L. Peterson *J. Polym. Sci.; Part A: Polym. Chem.* **38**, 2440 (2000).

219. X.-S. Wang, N. Luo, and S.-K. Ying, *Polymer* **40**, 4515 (1999).

220. Q. Pan, S. Liu, J. Xie, and M. Jiang, *J. Polym. Sci.; Part A: Polym. Chem.* **37**, 2699 (1999).

221. S. Liu and A. Sen, *Macromolecules* **34**, 1529 (2001).

222. R. G. Jones and S. J. Holder, *Macromol. Chem. Phys.* **198**, 3571 (1997).

223. C. J. Hawker, D. Mecerreyes, E. Elce, J. Dao, J. L. Hedrick, I. Barakat, Ph. Dubois, R. Jérôme, and W. Volksen, *Macromol. Chem. Phys.* **198**, 155 (1997).

224. S. G. Roos, A. H. M. Müller, and K. Matyjaszewski, *Macromolecules* **32**, 8331 (1999).

225. S. G. Roos, A. H. M. Müller, and K. Matyjaszewski, *ACS Symp. Ser.* **768**, 361 (2000).

226. H. Shinoda, P. J. Miller, and K. Matyjaszewski, *Macromolecules* **34**, 3186 (2001).

227. Y. Wang and J. Huang, *Macromolecules* **31**, 4057 (1998).

228. K. Yamada, M. Miyazaki, K. Ohno, T. Fukuda, and M. Minoda, *Macromolecules* **32**, 290 (1999).

229. R. D. Puts and D. Y. Sogah, *Macromolecules* **30**, 7050 (1997).

230. D. Mecerreyes, B. Atthoff, K. A. Boduch, M. Trollsas, and J. L. Hedrick, *Macromolecules* **32**, 5175 (1999).

231. M. Ejaz, S. Yamamoto, K. Ohno, Y. Tsujii, and T. Fukuda, *Macromolecules* **31**, 5934 (1998).

232. S. Yamamoto, M. Ejaz, K. Ohno, Y. Tsujii, M. Matsumoto, and T. Fukuda, *Macromolecules* **33**, 5602 (2000).

233. S. Yamamoto, M. Ejaz, K. Ohno, Y. Tsujii, M. Matsumoto, and T. Fukuda, *Macromolecules* **33**, 5608 (2000).

234. M. Ejaz, K. Ohno, Y. Tsujii, and T. Fukuda, *Macromolecules* **33**, 2870 (2000).

235. B. Zhao and W. J. Brittain, *J. Am. Chem. Soc.* **121**, 3557 (1999).

236. B. Zhao, W. J. Brittain, W. Zhou, and S. Z. D. Cheng, *J. Am. Chem. Soc.* **122**, 2407 (2000).

237. R. A. Sedjo, B. K. Mirous, and W. J. Brittain, *Macromolecules* **33**, 1492 (2000).

238. M. Husseman, E. E. Malmström, M. MacNamarra, M. Mate, D. Mecerreyes, D. G. Benoit, J. L. Hedrick, P. Mansky, E. Huang, T. P. Russel, and C. J. Hawker, *Macromolecules* **32**, 1424 (1999).

239. B. de Boer, H. K. Simon, M. P. L. Werts, E. W. van der Vegte, and G. Hadziioannou, *Macromolecules* **33**, 349 (2000).

240. X. Huang and M. J. Wirth, *Macromolecules* **31**, 1694 (1999).

241. K. Matyjaszewski, P. J. Miller, N. Shukla, B. Immaraporn, A. Gelman, B. B. Luokala, T. M. Siclovan, G. Kickelbick, T. Vallant, H. Hoffmann, and T. Pakula, *Macromolecules* **32**, 8716 (1999).

242. H. Böttcher, M. L. Hallensleben, S. Nuss, and H. Wurm, *Polym. Bull.* **44**, 223 (2000).

243. J-B. Kim, M. L. Bruening, and G. L. Baker, *J. Am. Chem. Soc.* **122**, 7616 (2000).

244. R. R. Shah, D. Merreceyes, M. Husemann, I. Rees, N. L. Abbott, C. J. Hawker, and J. L. Hedrick, *Macromolecules* **33**, 597 (2000).

245. W. Burchard, *Adv. Polym. Sci.*, 143 (1998).

246. C. D. Thurmond and B. H. Zimm, *J. Polym. Phys.* **8**, 477 (1952).

247. J. Xia, X. Zhang, and K. Matyjaszewski, *Macromolecules* **32**, 4482 (1999).

248. X. Zhang, J. Xia, and K. Matyjaszewski, *Macromolecules* **33**, 2340 (2000).

249. K.-Y. Back, M. Kamagaito, and M. Sawamoto, *Macromolecules* **34**, 215 (2001).

250. T. E. Long and A. J. Pasquale, *J. Polym. Sci.; Part A: Polym. Chem.* **39**, 216 (2001).

251. T. Tsoukatos, S. Pispas, and N. Hadjichristidis, *J. Polym. Sci.; Part A: Polym. Chem.* **39**, 320 (2001).

252. X. Wu and C. L. Fraser, *Macromolecules* **33**, 4053 (2000).

253. (a) S. Jacob, I. Majoros, and J. P. Kennedy, *Macromolecules* **29**, 8631 (1996); (b) E. Cloutet, J. L. Fillaut, D. Astruc, and Y. Gnanou, *Macromolecules* **32**, 1043 (1999); (c) B. Comanita, B. Noren, and J. Roovers, *Macromolecules* **32**, 1069 (1999).

254. G. S. Grest, L. J. Fetters, J. S. Huang, and D. Richter, in *Advances in Chemical Physics*; Vol.XCIV I. Prigogine, and S. A. Rice, eds., Wiley, New York, 1996.

255. C. J. Hawker, *Angew. Chem. Int. Ed. Engl.* **34**, 1456 (1995).

256. S. Robin, O. Guerret, and J. L. Couturier, Y. Gnanou, *Macromolecules* **35**, 2481 (2002).

257. J.-S. Wang, D. Greszta, and K. Matyjaszewski, *PMSE* **73**, 416 (1995).

258. J. Ueda, M. Matsuyama, M. Kamigaito, and M. Sawamoto, *Macromolecules* **31**, 557 (1998).

259. A. M. Kasko, A. M. Heintz, and C. Pugh, *Macromolecules* **31**, 256 (1998).

260. J. Ueda, M. Kamigaito, and M. Sawamoto, *Macromolecules* **31**, 6762 (1998).

261. S. Angot, K. S. Murthy, D. Taton, and Y. Gnanou, *Macromolecules* **31**, 7218 (1998).

262. K. Matyjaszewski, P. J. Miller, E. Fossum, and Y. Nakagawa, *Appl. Organomet. Chem.* **12**, 667 (1998).

263. K. Matyjaszewski, P. J. Miller, J. Pyun, G. Kickelbick, and S. Diamanti, *Macromolecules* **32**, 6526 (1999).

264. A. Heise, J. L. Hedrick, M. Tröllsas, R. D. Miller, and C. W. Franck, *Macromolecules* **32**, 231 (1999).

265. A. Heise, J. L. Hedrick, C. Franck, and R. D. Miller, *J. Am. Chem. Soc.* **121**, 8647 (1999).

266. A. Heise, C. Nguyen, R. Malek, J. L. Hedrick, C. W. Franck, and R. D. Miller, *Macromolecules* **33**, 2346 (2000).

267. D. M. Haddleton and C. Waterson, *Macromolecules* **32**, 8732 (1999).

268. D. M. Haddleton R. Edmonds, A. M. Heming, E. J. Kelly, and D. Kukulj, *New J. Chem.* **23**, 477 (1999).

269. S. Angot, K. S. Murthy, D. Taton, and Y. Gnanou, *Macromolecules* **33**, 7261 (2000).

270. G. Hizal, S. Angot, K. S. Murthy, D. Taton, and Y. Gnanou, *Polym. Prep.* **40**(2), 348 (1999).

271. V. Percec, B. Barboiu, T. K. Bera, Van der Sluis, R. B. Grubbs, and J. M. J. Fréchet, *J. Polym. Sci.; Part A: Polym. Chem.* **38**, 4776 (2000).

272. P. Moschogianni, S. Pispas, and N. Hadjichristidis, *J. Polym. Sci.; Part A: Polym. Chem.* **39**, 650 (2001).

273. N. J. Hovestad, G. van Koten, S. A. F. Bon, and D. M. Haddleton, *Macromolecules* **33**, 4048 (2000).

274. J. E. Collins and C. L. Fraser, *Macromolecules* **31**, 6715 (1998).

275. C. L. Fraser and A. P. Davis, *J. Polym. Sci.; Part A: Polym. Chem.* **38**, 4704 (2000).

276. R. M. Johnson, P. S. Corbin, C. Ng, and C. L. Fraser, *Macromolecules* **33**, 7404 (2000).

277. X. Wu and C. L. Fraser, *Macromolecules* **33**, 7776 (2000).

278. X. Wu, J. E. Collins, J. E. McAlvin, R. W. Cutts, and C. L. Fraser, *Macromolecules* **34**, 2812 (2001).

279. J. L. Hedrick, M. Tröllsas, C. J. Hawker, B. Atthoff, H. Claesson, A. Heise, R. D. Miller, D. Mecerreyes, R. Jérome, and Ph. Dubois, *Macromolecules* **31**, 8691 (1998).

280. S. Angot, D. Taton, and Y. Gnanou, *Macromolecules* **33**, 5418 (2000).

281. Y. Xu and C. Pan, *Macromolecules* **33**, 4750 (2000).

282. B. Keszler, G. Fenyvesi, and J. P. Kennedy, *J. Polym. Sci.; Part A: Polym. Chem.* **38**, 706 (2000).

283. A. W. Bosman, H. M. Jannsen, and E. W. Meijer, *Chem. Rev.* **99**, 1665 (1999).

284. Y. H. Kim, *J. Polym. Sci.; Part A: Polym. Chem.* **36**, 1685 (1998).

285. P. J. Flory, *J. Am. Chem. Soc.* **74**, 2718 (1952).

286. B. Voit, *J. Polym. Sci.; Part A: Polym. Chem.* **38**, 2505 (2000).

287. J. M. J. Fréchet, M. Henmi, I. Gitsov, S. Aoshima, M. Leduc, and R. Grubbs, *Science* **269**, 1080 (1995).

288. R. B. Grubbs, C. J. Hawker, and J. M. J. Fréchet, *Angew. Chem. Int. Ed. Engl.* **36**, 270 (1997).

289. C. J. Hawker, J. M. J. Fréchet, R. B. Grubbs, and J. Dao, *J. Am. Chem. Soc.* **117**, 10763 (1995).

290. A. Ajayaghosh and R. Francis, *J. Am. Chem. Soc.* **121**, 6599 (1999).

291. R. Francis and A. Ajayaghosh, *Macromolecules* **33**, 4699 (2000).

292. K. Ishizu and A. Mori, *Macromol. Rapid Commun.* **21**, 665 (2000).

293. S. G. Gaynor, S. Edelman, and K. Matyjaszewski, *Macromolecules* **29**, 1079 (1996).

294. K. Matyjaszewski, J. Pyun, and S. G. Gaynor, *Macromol. Rapid Commun.* **19**, 665 (1998).

295. K. Matyjaszewski, S. G. Gaynor, A. Kulfan, and M. Podwika, *Macromolecules* **30**, 5192 (1997).

296. A. H. E. Müller, D. Yan, and M. Wulkow, *Macromolecules* **30**, 7015 (1997).

297. D. Yan, A. H. E. Müller, and K. Matyjaszewski, *Macromolecules* **30**, 7024 (1997).

298. K. Matyjaszewski, S. G. Gaynor, and A. H. E. Müller, *Macromolecules* **30**, 7034 (1997).

299. K. Matyjaszewski and S. G. Gaynor, *Macromolecules* **30**, 7042 (1997).

300. S. G. Gaynor and K. Matyjaszewski, *ACS Symp. Ser.*, **685**, 396 (1998).

301. X. Zhang, Y. Chen, A. Gong, C. Chen, and F. Xi, *Polym. Int.* **48**, 896 (1999).

302. S. Maier, A. Sunder, H. Frey, and R. Mülhaupt, *Macromol. Rapid Commun.* **21**, 226 (2000).

303. X. Jiang, Y. Zhong, D. Yan, H. Yu, and D. Zhang, *J. Appl. Polym. Polym. Sci.* **78**, 1992 (2000).

304. D. Mecerreyes, M. Trollsas, and J. L. Hedrick, *Macromolecules* **32**, 8753 (1999).

305. G. Cheng, P. W. F. Simon, M. Hartenstein, and A. H. E. Müller, *Macromol. Rapid Commun.* **21**, 846 (2000).

306. C. Li, J. He, L. Li, J. Cao, and Y. Yang, *Macromolecules* **32**, 7012 (1999).

307. A. Niu, C. Li, Y. Zhao, J. He, Y. Yang, and C. Wu, *Macromolecules* **34**, 460 (2001).

308. R. B. Grubbs, C. J. Hawker, J. Dao, and J. M. J. Fréchet, *Angew. Chem. Int. Ed. Engl.* **36**, 270 (1997).

309. M. Trollsas and J. L. Hedrick, *J. Am. Chem. Soc.* **120**, 4644 (1998).

310. J. L. Hedrick, M. Trollsas, C. J. Hawker, B. Atthoff, H. Claeson, A. Heise, R. D. miller, D. Mecerreyes, R. Jerome, and Ph. Dubois, *Macromolecules* **31**, 8691 (1998).

311. M. R. Leduc, C. J. Hawker, J. Dao, and J. J. M. J. Fréchet, *J. Am. Chem. Soc.* **118**, 11111 (1996).

312. K. Matyjaszewski, T. Shigemoto, J. M. J. Fréchet, and M. R. Leduc, *Macromolecules* **29**, 4167 (1996).

313. M. R. Leduc, W. Hayes, and J. M. J. Fréchet, *J. Polym. Sci.; Part A: Polym. Chem.* **36**, 337 (1998).

314. T. Emrick, W. Hayes, and J. M. J. Fréchet, *J. Polym. Sci.; Part A: Polym. Chem.* **37**, 337 (1999).

315. F. Asgarzadeh, P. Ourdouillie, E. Beyou, and P. Chaumont, *Macromolecules* **32**, 6996 (1999).

316. N. Ide and T. Fukuda, *Macromolecules* **30**, 4268 (1997).

317. N. Ide and T. Fukuda, *Macromolecules* **32**, 95 (1999).

318. S. Abrol, P. A. Kambouris, M. G. Looney, and D. H. Solomon, *Macromol. Rapid Commun.* **18**, 755 (1997).

319. J. Spanswick, E. A. Branstetter, and W. F. Huber, Jr., *Radical ACS Symp. Ser.* **768**, 427 (2000).

15 Experimental Procedures and Techniques for Radical Polymerization

STEFAN A. F. BON and DAVID M HADDLETON

University of Warwick, Coventry, United Kingdom

CONTENTS

15.1 INTRODUCTION

Radical polymerization has seen a revival with the development of controlled and living radical polymerization techniques, such as nitroxide-mediated living radical polymerization,[1] atom transfer radical polymerization (ATRP),[2,3] and the reversible addition fragmentation chain-transfer (RAFT) process.[4] Fascinating results on the synthesis of novel polymer materials are reported in the highest-ranked scientific journals, proving that polymer science plays a vast role in the development and innovation of current human society and prosperity. The science presented in the journals, however, focuses in general on explanation/discussion of the experimental

results, whereas elaboration of experimental procedures is often kept to a minimum. This can lead to confusion in how to repeat reported experiments. It is the goal of this chapter to present a number of radical polymerization experiments, both some traditional and novel experiments, in a ''this is how you do it'' way. Hopefully, the experimental procedures will be of guidance for both experienced people in the field and people who are at the dawn of their interest in radical polymer chemistry. We have attempted to cover as many processes as possible covering bulk, solution, emulsion, and suspension as well as a wide range of different chemistry. The examples chosen serve to illustrate the many types of polymerization processes, which propagate via heterolytic bond cleavage and a radical pathway. There are many more experiments, monomers, solvents, initiators, and so on, and the reader is advised to refer to the primary literature wherever possible.

In general, free-radical polymerization is inhibited or retarded by the presence of oxygen. However, limited amount of oxygen can be tolerated in ATRP in the presence of reducing agents, such as Cu(0). Thus all reactions are carried out under an inert atmosphere, usually nitrogen. All solvents, monomers, and other reagents are generally deoxygenated prior to use. This is achieved by either purging with inert gas for sufficient time, usually in excess of 30–60 min. or by freeze–pump–thaw degass cycles in a Schlenk line. Most monomers are supplied with an inhibitor, which helps prevent polymerization prior to controlled initiation. These inhibitors are usually phenolic in nature and are usually removed prior to polymerization by passing through a short column of basic alumina.

15.2   CONVENTIONAL RADICAL POLYMERIZATIONS

15.2.1   Bulk Polymerization

15.2.1.1   *Bulk Polymerization of Styrene by Spontaneous Self-Initiation*   An important phenomenon that may occur in radical polymerizations is that certain monomers may undergo spontaneous polymerization. In other words, radicals that will induce polymerization are created in absence of added initiator. One of the best-known monomers that is capable of generating free-radical species by itself, especially at elevated temperatures, is styrene. This thermal self-initiation of styrene is generally accepted to proceed via the mechanism proposed by Mayo[5] (outlined in Scheme 15.1) and has been confirmed by other investigations.[6,7] Since the Diels–Alder dimerization and the successive styrene-assisted homolysis of the cycloadduct is the pathway of the radical generation, the rate of the thermal self-initiation of styrene in bulk is likely to be third order in monomer concentration.

15.2.1.2   *Experiment*

Reagents

Styrene	50 g
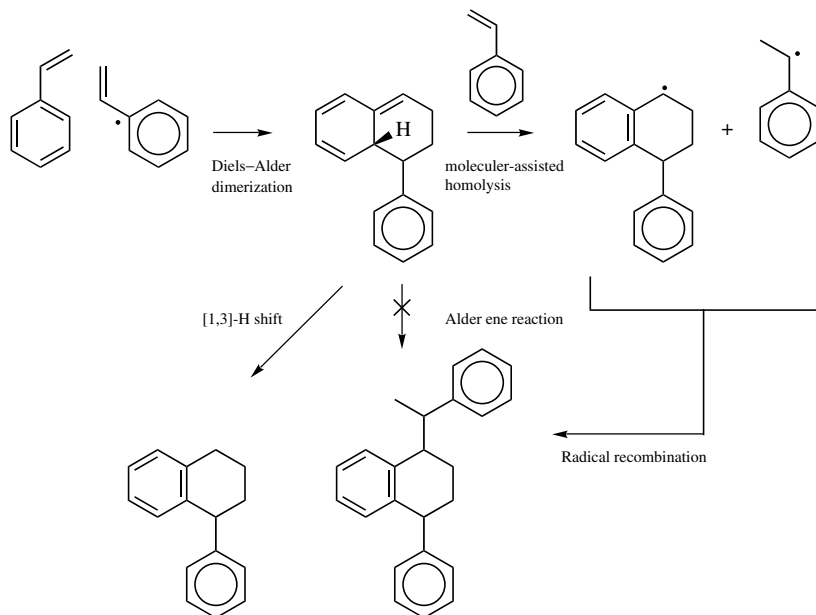
Scheme 15.1   Mechanism of thermal self-initiation of styrene.

Procedure   Styrene was distilled before use. This is done in order to remove contaminants such as oligomeric species. (Note that not all of the inhibitor is removed via distillation.) The distilled styrene was stored at $-18°C$. Prior to use, styrene was passed over a short column of inhibitor remover (Aldrich) and charged together with a magnetic stirrer bar into a Schlenk tube. Next the styrene was placed under an argon atmosphere via three freeze–pump–thaw cycles. (Note that the entire system is under a slight argon overpressure.) This means that styrene is frozen with the aid of a liquid nitrogen bath while the gas-inlet tab is closed. A vacuum $(< 10^{-3} \, \text{mbar})$ is applied to the frozen system for a few minutes, after which the liquid nitrogen bath is removed. The system is placed under argon via opening of the gas inlet tab and subsequently is allowed to defrost. This is repeated 2 times.

Polymerization was started by placing the styrene into an oil bath which was kept at 120, 130, or 140°C. Samples for the determination of monomer conversion were taken by syringe (∼2 mL).

15.2.1.2.1 Determination of Monomer Conversion by Gravimetry   To perform a valid gravimetric analysis an aluminium cup was weighed accurately. Next the reaction sample was added to the empty cup. Note that the amount of sample has to be measured fast as evaporation of styrene will occur rapidly. The sample was quenched with liquid nitrogen, after which ∼3 mL of methanol was added to the cup while swirling. This enhances the evaporation of styrene as a result of azeotrope

TABLE 15.1   Initial Overall Rates of Thermal Polymerization of Styrene in Bulk at Various Temperatures

		$R_{P, t=0} \times 10^4 \text{ mol L}^{-1} \text{ s}^{-1}$	
T (°C)	$[M]_0$ (mol/L)	Eq. (15.2)	Eq. (15.3)
120	7.860	1.3	1.6
130	7.776	2.3	3.0
140	7.692	4.1	4.7

formation. The sample was placed in the fume hood overnight. After this the "dry" sample was placed in a vacuum oven at 110°C (above the T_g of polystyrene) to remove the last traces of volatiles. Next the dry sample was weighed. Monomer conversion was calculated using

$$X_w = \frac{\text{dry cup} - \text{empty cup}}{(\text{sample} + \text{cup}) - \text{empty cup}} \tag{15.1}$$

15.2.1.2.2   Initial Rates of Polymerization   The results were as follows. The initial overall rates of polymerization were determined from the initial slopes of the conversion (X_w) versus time data using

$$X_w = \frac{R_{P, t=0}}{[M]_0} t + C \tag{15.2}$$

where C is a constant to account for the inhibition time.

A different way to fit monomer conversion data is to presume that the thermal self-initiation of styrene shows a third-order dependence on monomer concentration (see Scheme 15.1), then the X_w versus time data can be fitted with Eq. (15.3). The results obtained for $R_{P, t=0}$ are also given in Table 15.1:

$$-\ln(1 - X_w) = \frac{2}{3}\ln\left(1 + \frac{3}{2}\frac{R_{P, t=0}}{[M]_0}t\right) + C \tag{15.3}$$

The results for the average $R_{P, t=0}$ that were obtained from the thermal polymerizations of styrene at 120, 130, and 140°C are given in Table 15.1. In this table it is observed that systematically higher values of $R_{P, t=0}$ are obtained with Eq. (15.2), which is solely ascribed to the difference in the fitting procedure. The accuracy of the calculated values of $R_{P, t=0}$, however, was restricted, as the number of data points that could be used to obtain a decent fit was limited to 5–7 (see Figs. 15.1a and 15.1b for illustration).
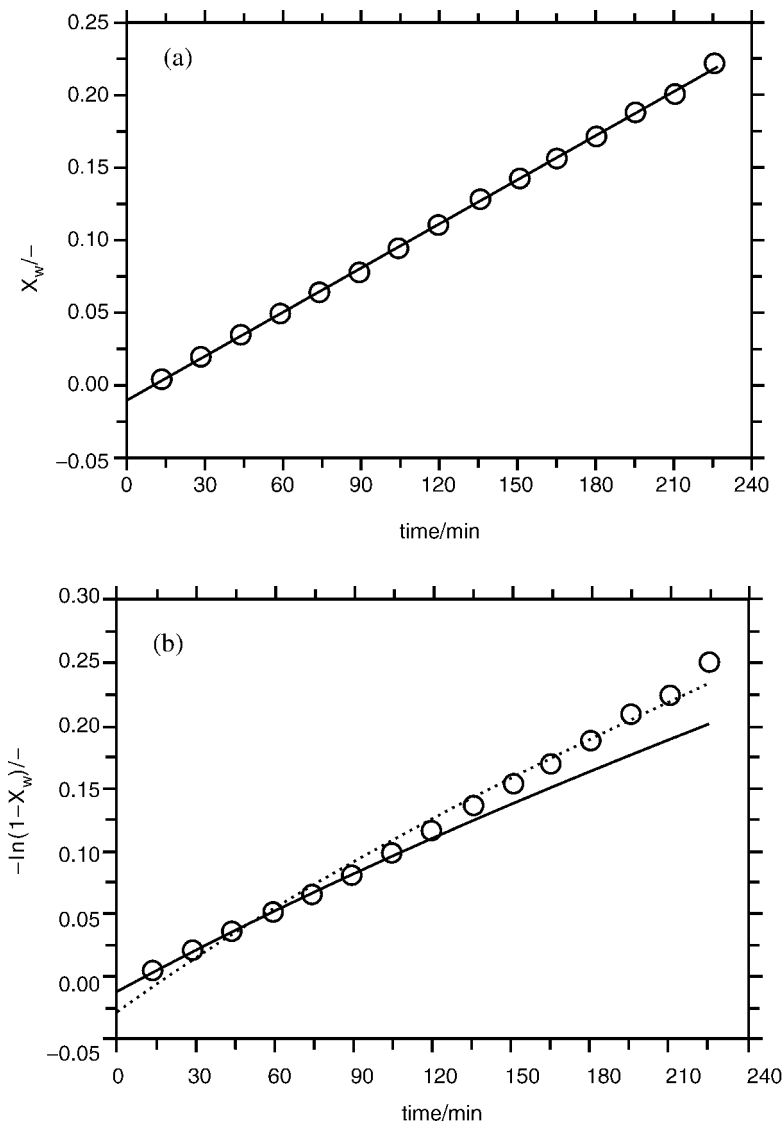
Figure 15.1 Initial polymerization rates: (a) X_w versus time for the thermal self-initiated polymerization of styrene at 393 K, where (——) represents the fit using Eq. (15.2) to yield $R_{P,t=0}/[M]_0 = 1.7056214 \times 10^{-5}$ s^{-1}, $C = -1.2314331 \times 10^{-2}$, $\langle r^2 \rangle = 0.999$, STD $= 1.730 \times 10^{-3}$; (b) $-\ln(1 - X_w)$ versus time for the thermal self-initiated polymerization of styrene at 393 K, where (·····) represents fit over all points using Eq. (15.3) to yield $R_{P,t=0}/[M]_0 = 2.3796285 \times 10^{-5}$ s^{-1}, $C = -2.8477918 \times 10^{-2}$, $\langle r^2 \rangle = 0.990$, STD $= 8.088 \times 10^{-3}$, where (——) represents the fit over the first 7 data points using Eq. (15.3) to yield $R_{P,t=0}/[M]_0 = 1.877407078 \times 10^{-5}$ s^{-1}, $C = -1.3053502 \times 10^{-2}$, $\langle r^2 \rangle = 0.998$, STD $= 1.609 \times 10^{-3}$.

An empirical expression for the temperature-dependent relationship for $(2k_t/k_p^2)$ at zero conversion has been reported by Hui and Hamielec:[9]

$$\left(\frac{2\,k_t}{k_p^2}\right)_{X_w=0} = 1.136 \times 10^{-5} \exp\left(\frac{6270}{T}\right) \tag{15.4}$$

From these equations the initial rate of polymerization, $R_{P,t=0}/\mathrm{mol\,L^{-1}\,s^{-1}}$, can be calculated by

$$R_{P,t=0} = [M]_0 \sqrt{\frac{\sigma}{(2\,k_t/k_p^2)}} \tag{15.5}$$

in which σ represents the radical flux.

This equation allows us to calculate values of k_i from our data for $R_{P,t=0}$ and $[M]_0$ at 120, 130, and 140°C, on the basis of a third-order dependence of σ on $[M]$ (data for $R_{P,t=0}$ obtained with Eq. (15.2) were used; see Eqs. (15.4) and (15.5) for calculation of k_i). Figure 15.2 represents the linearized Arrhenius plot for the rate coefficient of styrene self-initiation (k_i, $\mathrm{L^2\,mol^{-2}\,s^{-1}}$). The final empirical expression, obtained for the additional radical flux (σ) in our experiments, then equals

$$\sigma = 2.3_7 \times 10^4 \exp\left(\frac{-110._2 \times 10^3}{RT}\right)[M]^3 \tag{15.6}$$
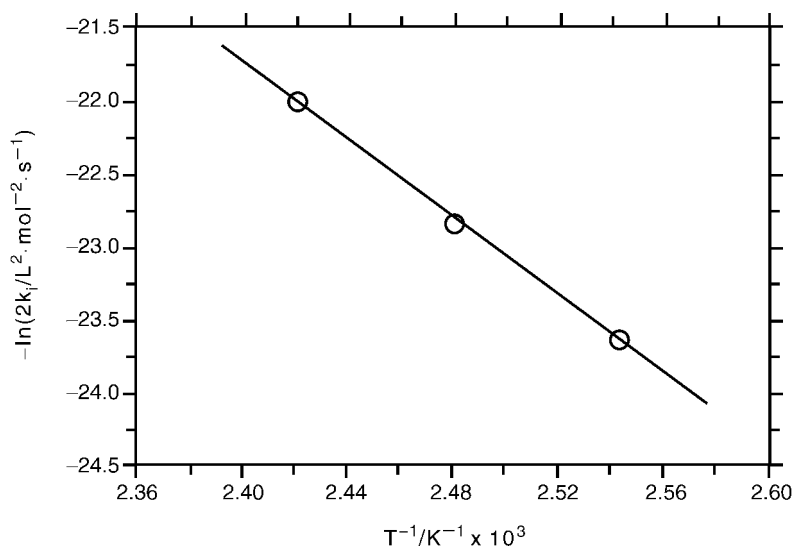
Figure 15.2   Linearized Arrhenius plot for the thermal-self initiation of styrene.

The process of radical generation via cycloadditions and subsequent molecular assisted homolysis via hydrogen atom transfer (see Scheme 15.1) may change on addition of a solvent, or a reactive species, resulting in a different dependence on monomer concentration. Therefore, the preceding equation for σ [Eq. (15.6)] is valid only for the polymerization of styrene in bulk.

15.2.2   Solution Polymerization

A downside of performing a polymerization in bulk is the restrictive heat transfer. This becomes an issue for monomers with a fast rate of propagation, such as acrylates. In conjunction with the increase in viscosity during polymerization and the possible occurrence of a gel effect (see later in section on TEMPO-mediated polymerization of styrene) a runaway of the polymerization reaction can occur. To overcome these problems bulk reactions are often stopped at intermediate stages of monomer conversion, or alternatively the polymerization is carried out in solution. The main prerequisite of the choice of solvent is that the solvent is a good solvent for both monomer and polymer. It is also important to be aware of the rate of chain transfer to solvent, which can dominate the termination process. Indeed, transfer to solvent is often used to control molecular weight of products. For example, chain transfer to isopropanol is used in polymerization in aqueous media in many commercial applications.

15.2.2.1   *Synthesis of Poly(vinyl acetate) (PVAc) in Toluene Solution*   Vinyl acetate together with its derivatives, often referred to as *VEOVA*'s, form an important class of monomers of commercial interest. When vinyl acetate is polymerized, it terminates almost exclusively by combination or transfer. However, under bulk conditions, unsaturated end groups and crosslinking occur as a result chain transfer to monomer and polymer. These events can be minimized under solution polymerization conditions. Solution polymerization of vinyl acetate can thus be exploited to prepare telechelic polymers by use of a functional initiator. Alternatively, monofunctional poly(vinyl acetate) (PVAc) may be prepared by use of a functional chain transfer agent. These relatively simple approaches give a trivial route into functional polymers and are illustrated here.

15.2.2.2   *Synthesis of Dihydroxy Telechelic PVAc*

Reagents

VA-086	3.58 g
Toluene	240 mL
Vinyl acetate	120 mL
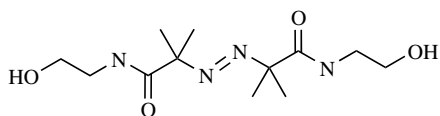
VA-086

Procedure   Toluene and vinyl acetate were purged with nitrogen gas for at least 30 min prior to use. In a 250-mL round-bottomed flask, were placed 3.58 g of initiator VA-086 (12 mmol, 1 equiv). The flask was flushed by nitrogen. Deoxygenated toluene (240 mL) and deoxygenated vinyl acetate (120 mL, 1302 mmol, 105 equiv) were then added via degassed syringes. The solution was refluxed under a nitrogen atmosphere overnight at 104°C, and the solvent was then removed in vacuo to give the product.

Results $M_n = 8350$, $M_w/M_n = 2.06$ (PMMA narrow-molecular-weight distribution standards).

15.2.2.3   Determination of Reactivity Ratios of the Copolymerization of Methyl Methacrylate and Butyl Methacrylate in Toluene

Experimentally determined average copolymer composition data are related to the composition of the feed. One of the simplest models that describes the copolymer composition is the ultimate or terminal copolymerization model[10,11] which uses the differential form of the copolymerization equation given by Eq. (15.7). The terms F_1 and f_1 represent the mole fraction of monomer: one in the polymer and monomer feed respectively. As Eq. (15.7) is the differential form of the copolymerization equation, its use is limited to low conversion copolymerizations (typically $<5\%$, but preferably as low as possible), where their symbols have their usual meanings when applied to copolymerization:

$$F_1 = \frac{r_1 f_1^2 + f_1(1-f_1)}{r_1 f_1^2 + 2f_1(1-f_1) + r_2(1-f_1)^2} \tag{15.7}$$

A number of assumptions are used in the derivation of Eq. (15.7).[10] One of these is the long-chain assumption, which states that the monomer incorporated into the chain by initiation, transfer, and termination reactions is negligible compared to the monomer incorporated by propagation. A second assumption is the equal reactivity assumption, which assumes that the relative rates of all the propagation reactions are independent of chain length and depend on the composition of the macroradical only through the terminal unit. Significant violation of these assumptions should show up as trends in the copolymer composition with chain length. This should be examined when reactivity ratios are being determined from relatively short polymer chain as is the case in living polymerization systems such as transition metal mediated radical polymerization.

A number of procedures have been developed for the estimation of r_1 and r_2 based on the Mayo–Lewis model. Most of these procedures have involved the linearization of Eq. (15.7) and are statistically unsound.[12] The popularity of these methods has contributed to the large variation in reactivity ratios reported in the literature. It has also resulted in poor estimates of reactivity ratios with misleading confidence intervals. Better estimates are obtained by the use of the error-in-variables-model (EVM) approach. This work used an implementation of the error-in-variables-model approach for estimating reactivity ratios from the differential form of the Mayo–Lewis

equation.[12] The EVM approach is a more satisfactory method of analyzing copolymerization data since it is statistically sound and allows for the major sources of experimental error to be properly accounted for and has thus been used in the present study.

One alternate approach is to use nonlinear least-squares (NLLS) data evaluation in conjunction with Tidwell–Mortimer criteria.[13] However, NLLS requires some prior knowledge of r_1 and r_2 and narrows confidence intervals quickly through an iterative process. It can be shown that using the D-optimal criterion, the initial optimal monomer feed compositions at which the low conversion experiments should be carried out, can be estimated by:

$$f_1' = \frac{2}{2 + r_1} \qquad f_1'' = \frac{r_2}{2 + r_2} \qquad (15.8)$$

Reagents

Butyl methacrylate	1600 g
Methyl methacrylate	1200 g
AIBN	0.05 g
Toluene	10 mL

Procedure   Three monomer mixtures were prepared with the following [MMA]/[BMA] ratios 75/25 (563.05 g MMA, 265.57 g BMA, [MMA]/[BMA] $=$ 3.011), 50/50 (374.90 g MMA, 533.89 g BMA, [MMA]/[BMA] $=$ 0.9973), and 25/75 (188.72 g MMA, and 799.28 g BMA, [MMA]/[BMA] $=$ 0.3353). In a typical reaction, 10 mL of each MMA/BMA mixture was degassed by three freeze–pump–thaw cycles in a Schlenk tube. 1 mL of AIBN stock solution (0.0467 g, 0.284 mmol AIBN in 10 mL toluene) was added. The solution was frozen, closed under vacuum, thawed to room temperature, and heated to 60°C for 60 min, after which the reaction was quenched by rapid cooling to 0°C. Duplicate experiments were carried out in each case. The sample was dried to constant weight in vacuo.

SEC was carried out using a Polymer Laboratories (PL) guard column (50 $\times$ 7.5 mm), and two Mixed-D columns (300 $\times$ 7.5 mm). THF was used as the eluent at a flow rate of 1 mL/min and data were collected at 1 point per second from a DRI detector. The system was calibrated with log molecular weight expressed as a third-order polynomial of elution volume based on Polymer Laboratories PMMA standards and pure samples of MMA dimer and trimer.

The copolymer composition (see data listed in Table 15.2) was determined in each case using ^{1}H NMR in CDCl$_3$ at 250 MHz by integration. The areas from the alkoxy region of the spectrum were used $\delta(-OCH_3, MMA) =$ approximately 3.50–3.65 ppm and $\delta(-OCH_2, BMA) = {\sim}3.80$–4.00 ppm. These data were used in the EVM program, assuming a 1% uncertainty in the monomer feed composition and a 5% uncertainty in the copolymer composition. All reactions were carried out to low conversion (Table 15.2). The resultant point estimates for the reactivity ratios

TABLE 15.2   Copolymerization Data

Composition MMA : BMA	M_n	M_w/M_n	Conversion (%)
75 : 25	487,900	2.07	4.65
75 : 25	458,700	2.07	6.19
50 : 50	544,500	1.80	4.69
50 : 50	535,600	1.75	6.40
25 : 75	515,800	1.96	7.82
25 : 75	457,900	2.01	7.83

were r_1 (MMA) $= 0.93$ and r_2 (n-BMA) $= 1.22$, respectively. These reactivity ratios compare very favourable with those reported by Manders[14] using a nonlinear least-squares analysis with NMR data with reactions taken to approx.0.5% conversion: r_1 (MMA) $= 0.91$ and r_2 (n-BMA) $= 1.09$.

15.2.3   Suspension Polymerization

A suspension polymerization is a heterogeneous process, in which a slurry of poly-mer particles/beads is formed by polymerization of a dispersed phase in a continu-ous medium. The dispersed phase consists of monomer, initiator, chain-transfer agent, and possibly solvent or blowing agent (porogen), the latter to control the por-osity of the beads. In general the continuous phase is water, which guarantees on reactor-scale basis proper heat and mass transfer due to its high heat capacity and thermal conductivity, and a low overall viscosity. This overcomes problems that are generally encountered in homogenous polymerization processes at higher mono-mer conversions, specifically, a runaway of the reaction as a result of the gel effect. Benefits of suspension polymerization over emulsion polymerization are that in gen-eral fewer additives are used and that the final product (average particle sizes $\sim$10 µm–5 mm) is easily recovered, after stripping of monomer, solvent/blowing agent, via centrifugation. Commercial important suspension polymerization pro-cesses include the preparation of poly(vinyl chloride), crosslinked polystyrene resins, and expandable polystyrene (EPS).

The difficulty of a suspension polymerization lies in the formation of a uniform a dispersion of monomer droplets as possible. A narrow particle size distribution is beneficial to processing as it assures more uniform properties, such as a lower den-sity of the polymer "powder." The dispersion is thermodynamically unstable and therefore the particle size distribution and success of the polymerization process depends on physical properties such as interfacial tension, viscosity and density of the two phases, volume fraction of dispersed phase (typical water:monomer, 1 : 1–4 : 1), geometric properties such as type of agitation and reactor/stirrer design, and operational conditions such as temperature and speed of agitation.

The stability of the dispersed droplets is enhanced by addition of stabilizers. These can be water-soluble, such as sucrose (40–80 wt% in water phase) or acacia gum (2–45 wt% in water phase),[15] or amphiphilic polymers, such as partly

hydrolyzed poly(vinyl acetate), or finely divided insoluble inorganic compounds, such as talc, calcium or magnesium carbonates, phosphates, and silicates, the latter often stabilized with the aid of ionic surfactants. The stabilizers increase the viscosity of the continuous phase and adsorb onto the droplets surface to create steric/electrosteric stabilization, and thus prevent coalescence and agglomeration. The latter becomes crucial in suspension polymerizations in which the polymer is soluble/swellable in its monomer/added solvent. At intermediate monomer conversion (approximately 20–60%) the so-called "tacky" stage exists, in which the suspension is most likely to coalesce and agglomerate irreversibly, thereby causing an overall process failure.

More recent innovations that enable the formation of a narrow particle size distribution are seeded or template suspension techniques and artificial or semisuspension polymerization techniques. In the first a monodisperse polymer colloid prepared via, for instance, emulsion or precipitation polymerization is used as template or seed. In the second option the organic phase is partly polymerized in a homogeneous manner (bulk or solution) before being dispersed into the aqueous phase. The latter has additional morphological advantages, for example, in composite applications such as pigment incorporation into the particles and/or in water-expandable polystyrene (WEPS). The pigment/emulsified blowing agent is more homogeneously distributed throughout the particles as a direct result of a higher viscosity in the dispersed phase, thereby restricting diffusion of pigment/emulsifier to the water/particle interface and exit/reentry events.

15.2.3.1   Preparation of Inorganic Stabilizing Slurry and Aqueous Phase

Reagents

Pentasodium triphosphate [Fluka: purum p.a. (per annum); >98%(T)]	1.0 g
β-Tricalcium phosphate [Fluka: purum p.a.; >96%(KT)]	50.0 g
Water	650 mL
Sodium dodecylbenzenesulfonate (Fluka: technical grade; ∼80% (CH) mixture of homologous Alkyl benzenesulfonates)	0.02 g

Procedure   First, 1.0 g of pentasodium triphosphate and 50 g of β-tricalcium was mixed with 150 mL of deionized water using ultrasound and/or agitation mill to yield a slurry. Next 2.0 g of slurry was mixed with 0.5 L of water and 0.02 g of sodium dodecylbenzenesulfonate to yield the final aqueous phase.

15.2.3.2   Suspension Polymerization of Styrene

Reagents

Styrene	250 g
n-Heptane	10 g
Lauroyl peroxide	1.25 g
Aqueous HCl	

A degassed mixture of 250 g of styrene, 10 g of heptane, and 1.25 g of lauroyl per-
oxide was added to the aqueous phase. This was stirred at room temperature for
30 min at 300 rpm, after which the temperature was raised to 80°C ($t_{1/2} = 1$ h
40 min) and kept there for 6 h. Next the mixture was cooled to room tempature, after
which aqueous HCl was added to dissolve the inorganic colloids. The beads were
isolated by filtration and washed with water and methanol.

15.2.4   Dispersion and Precipitation Polymerization

Dispersion and precipitation polymerizations start off as homogeneous systems con-
taining monomer, initiator, optionally solvent, and in case of dispersion polymeriza-
tion a steric/electrostatic stabilizer. During polymerization a stable polymer
colloidal solution is formed through phase separation from the continuous med-
ium.The phase separation is driven *enthapically*, where growing polymer chains
become insoluble because of poor polymer–solvent interactions; or *entropically*,
where crosslinking restricts the mixing of polymer and solvent to yield microgels.
A key requirement for precipitation polymerization is that the amount of polymer
produced has to be low, typical <5 w/v%, in order to maintain stability. Adding sta-
bilizers transforms the process into a dispersion polymerization and higher monomer
to solvent ratios can be used. The lack of colloidal stabilization in precipitation poly-
merization often leads to broad particle size distributions. However, the preparation
of monodisperse crosslinked microspheres has now been reported. The explanation
for the monodisperse particle size distribution, despite the absence of any added sta-
bilizers, is that by using a near-θ solvent the surface layer of the crosslinked particles
will be swollen, thereby providing sufficient steric stabilization to prevent coales-
cence and subsequent agglomeration.

15.2.4.1 Precipitation Polymerization of Divinylbenzene-55 in Toluene/Acet-
onitrile[16,17]

Reagents

Divinylbenzene (technical grade)	12.0 mL
AIBN	2.73 g
Toluene	120 mL
Acetonitrile	180 mL

Prior to use divinylbenzene (DVB) was passed over a short column of basic alumina
in order to remove the inhibitor. Both toluene and acetonitrile were purged with
nitrogen for at least 30 min prior to use.

Procedure   First, 12.0 mL of DVB was placed in a 500-mL round-bottomed flask
and subsequently degassed with three freeze–pump–thaw cycles. The degassed
amounts of toluene and acetonitrile were added by syringe. Next the amount of
AIBN was added. The mixture was stirred at room temperature until the AIBN

was dissolved completely, then the stirring speed was set at 40 rpm. Temperature was increased to 60°C for 1 h and then raised to 70°C, at which it was kept for 24 h. The monodisperse particles were isolated by filtration though a membrane, washed 3 times with tetrahydrofuran and acetone, and dried under vacuum at 50°C overnight. The filtrate containing the soluble polymer fraction was concentrated and precipitated into cold methanol.

15.2.4.2 Dispersion Polymerization of Styrene in Ethanol/Water

Reagents

Poly(*N*-vinyl pyrrolidone) (PVP-K30; Aldrich $M_n = 40,000$ g mol^{-1})	5.0 g
Ethanol p.a.	600 mL
Water	200 mL
Styrene	110 mL
AIBN	2.0 g

Prior to use styrene was passed over a short column of basic alumina in order to remove the inhibitor. Ethanol, water, and styrene were purged with nitrogen for at least 30 min prior to use.

Procedure   The dispersion polymerization was carried out in a baffled glass reactor (2 L) fitted with a gas supply (N$_2$), a condenser, and an overhead stirrer four-bladed turbine stirrer (200 rpm). Then 5.0 g of poly(N-vinyl pyrrolidone) was dissolved in 600 mL of ethanol and 200 mL water. The mixture was degassed further by purging with nitrogen for 10 min and was subsequently thermostated at 70°C. Then 100 mL of degassed styrene was added by syringe and after 10 min, 2.0 g of AIBN was added to the homogeneous mixture. The polymerization was proceeded for 24 h. The particles were isolated by filtration though a membrane, and were washed with ethanol.

15.2.5 Emulsion Polymerization

Emulsion polymerization[18] has developed as an important industrial scale method of producing a range of polymers. However, it also allows the efficient laboratory synthesis of a range of vinyl monomers. A simple recipe for emulsion polymerization involves water, surfactant, a water-insoluble monomer and a water-soluble initiator. The monomer in water is stirred to give an emulsion, and the droplets can be stabilized by the addition of the surfactant. Changing the amount of surfactant can alter particle size, more surfactant gives smaller particle size, and the rate of stirring, temperature, reaction time, and other factors can also influence the particle size. Initiation can be via thermal initiation or redox initiation, and the monomer may be present at the start of the reaction or alternatively fed in over the course of the reaction. The final form of the product in an emulsion polymerization is a latex where the size of the particles is typically in the range of 50–300 nm. Many monomers may be polymerized or copolymerized by emulsion polymerization, including

styrene, butadiene, vinyl acetate, tetrafluoroethene, alkyl methacrylates, butyl acrylate, and vinyl chloride, and so on. There are many recipes for emulsion polymerization. We have chosen to illustrate polymerization of styrene to give monodisperse particle size with and without surfactant. These are used in our laboratories when monodisperse particles are required for a range of applications.

Under normal emulsion polymerization reaction conditions, polymerization takes place in micelles and monomer is transferred to the locus of polymerization from monomer reservoirs across the aqueous phase. Polymerization does not take place in the original monomer droplets. Once the monomer reservoirs have been consumed, polymerization continues until the monomer is all reacted. An alternative method of producing the particles is to use a seed latex. When seed latex is used added monomer migrates into preformed particles and the particles grow in size. This can be useful for two purposes: (1) monodisperse particle of various sizes may be formed and (2) core–shell particles, as a result of phase separation, can be formed by addition of a second monomer. Particles, or selected layers of particles, may be crosslinked by addition of multifunctional monomers at the appropriate stage of the reaction. A few examples are given that have been used in our laboratories for a range of applications.

15.2.5.1   Feed Emulsion Polymerization of Methyl Methacrylate

Reagents

Water	450 mL
MMA	200 mL
Aerosol OT-100	2.00 g
ACVA	2.00 g

ACVA
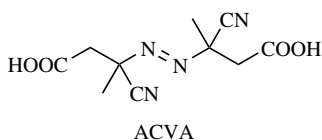
Water and MMA were degassed by purging with nitrogen for at least 30 min. A 1-L flange flask with a 100 mm bore, modified to have four baffles, was used as the polymerization reactor. The reaction was performed in an $80 \pm 0.5°C$ water bath and stirred at 150 rpm by a turbine impeller. Polymerizations using the above recipe (30% solids) show negligible coagulum.

Procedure   The AOT was placed in the reactor prior to the deoxygenated water, which was then allowed to come to reaction temperature. The ACVA, initiator, was added to the reactor immediately prior to starting the monomer feed. The monomer was added at 3.33 mL/min using an FMI metering pump so as to give a total feed time of 60 min. Temperature readings and samples were collected every 20 min for 2 h

TABLE 15.3   Feed Emulsion Polymerization of MMA

Time (min)	Reaction Temperature (°C)	Conversion		Molecular Weight Distribution			Particle Diameter (nm)[a]	
		Instant	Total	$M_n \times 10^{-3}$	$M_w \times 10^{-3}$	M_w/M_n	(1)	(2)
0	78.4	—	—	—	—	—	—	—
20	80.7	.916	.305	127	258	2.03	—	—
40	80.9	.970	.647	128	296	2.31	—	—
60	81.9	.979	.979	130	344	2.64	—	—
80	78.5	.998	.998	138	341	2.46	—	—
100	78.5	1.002	1.002	150	389	2.42	—	—
120	77.7	1.002	1.002	148	381	2.58	—	—
Final	—	.998	.998	143	367	2.57	65.9	12.5

[a]*Particle diameter*: (1) z average mean; (2) standard deviation.

and the reactions left to run overnight before a final sample was collected. All samples were analyzed for conversion, molecular weight, and particle size. The percent solids for each sample was corrected for the surfactant and initiator to obtain monomer conversions.

Results   The temperature, instantaneous and total monomer conversion, number and weight-average molecular weight and polydispersity, and the average particle size of the final latex are given in Table 15.3.

15.2.5.2   Soap-Free Emulsion Polymerization of Styrene to Monodisperse Particles

15.2.5.2.1   Particle Size 1.74 μm

Reagents

Water	4 L
Styrene	410 mL
Magnesium sulfate heptahydrate ($MgSO_4.7H_2O$)	2.51 g
Ammonium persulphate (($NH_4)_2S_2O_8$)	5.35 g

Procedure   Distilled water (4 L), magnesium sulphate (2.51 g), and styrene (410 mL) were placed in a flange flask (5000 mL) fitted with an overhead stirrer with turbine impeller and the solution deoxygenated through purging with nitrogen for one hour. After deoxygenating the reactor was placed in a water bath at 70°C. Once the solution had reached the required temperature, ammonium persulphate (5.35 g) was added and the reactor stirred at 250 rpm. The reaction was heated for 18 h before removing from heat and passing through a filter cloth. Solids = 5.64 wt %; average particle size from scanning electron microscope (SEM) = 1.74 μm.

15.2.5.2.2   Particle Size 1.0 μm

Reagents

Water	4 L
Styrene	410 mL
Magnesium sulfate heptahydrate (MgSO$_4$.7H$_2$O)	1.25 g
Ammonium persulfate ((NH$_4$)$_2$S$_2$O$_8$)	5.35 g

Procedure   Distilled water (4 L), magnesium sulfate (1.25 g), and styrene (410 mL) were placed in a flange flask (5 L) fitted with an overhead stirrer with turbine impeller and the solution deoxygenated through purging with nitrogen for one hour. After deoxygenating the reactor was placed in a water bath at 70°C. Once the solution had reached the required temperature, ammonium persulfate (5.35 g) was added and the reactor stirred at 250 rpm. The reaction was heated for 18 hours before removing from heat and passing through a filter cloth. Solids = 6.46 wt%; average particle size from SEM = 1.0 μm.

15.2.5.2.3   Particle Size 0.74 μm

Reagents

Water	4 L
Styrene	400 mL
Ammonium persulfate ((NH$_4$)$_2$S$_2$O$_8$)	9.00 g

Procedure   Distilled water (4 L) and styrene (400 mL) were placed in a flange flask (5 L) fitted with an overhead stirrer with turbine impeller and the solution deoxygenated through purging with nitrogen for one hour. After deoxygenating the reactor was placed in a water bath at 70°C. Once the solution had reached the required temperature ammonium persulphate (9.00 g) was added and the reactor stirred at 200 rpm. The reaction was heated for 72 h before removing from heat and passing through a filter cloth. Then 2 g sodium lauryl sulfate was added to stabilise the final latex. Particle size from SEM = 0.74 μm.

15.2.5.3   Synthesis of Core–Shell Particles by Emulsion Polymerization   This is usually a multistep synthesis. Although it is quite easy to carry out quite complicated feed profiles to form multilayer particles, we have illustrated this type of reaction with a relatively simple two-stage procedure

15.2.5.3.1   Synthesis of Styrene Seed Emulsions

Reagents

Sodium dioctylsulfosuccinate (SDOSS)	7.30 g
Water	808 mL

Styrene	183 g
Potassium persulfate	1.10 g
Sodium hydrogen carbonate	0.60 g

Prior to use styrene was distilled and passed over a column of basic alumina. Water and styrene were deoxygenated by purging with nitrogen for at least 1 h.

Procedure   SDOSS and Sodium hydrogen carbonate were placed into a sealed reactor (1.5 L) fitted with a water condenser and overhead stirrer guide. The water condenser was fitted to a nitrogen supply and the reactor then deoxygenated via purging with nitrogen for one hour. After this period the reactor was put under a low positive pressure of nitrogen at all times, which was controlled by placing a vent between the nitrogen supply and the condenser. Water (800 mL) and styrene were added to the reactor, and the reactor was placed into a constant temperature water bath (75°C) and stirred (200 rpm). Once the solution had reached equilibrium (~20 min) a degassed solution of the potassium persulphate (1.10 g) in 8 mL water was added by syringe. Stirring was maintained (200 rpm) throughout the reaction and the reactor removed from the water bath after 4 h. The warm emulsion was then filtered through a filter net to ensure that none of the small amount of coagulant that had formed was present. Solids content ~19%. Average Particle size (TEM) ~60 nm.

15.2.5.3.2   Synthesis of Core–Shell Emulsions: Poly(n-butyl acrylate/methacrylic Acid Shell)

Reagents

Polystyrene seed emulsion	383 g
Water	536 g
n-butyl acrylate	70 g
Methacrylic acid	7.4 g
Potassium persulfate	0.61 g
SDOSS	3.1 g

Water and monomers were deoxygenated by purging with nitrogen for at least 1 h.

Procedure

Preemulsion: SDOSS, *n*-BA, MAA and 50 mL of water were charged into a 200-mL flask fitted with a magnetic stirrer under a nitrogen atmosphere. The mixture was stirred rapidly at room temperature to create an emulsion.

Initiator solution: 0.61 g of potassium persulfate was dissolved in 10 mL of water.

Polystyrene seed and the remaining amount of water (476 mL) were charged into a sealed reactor (1.5 L) fitted with a water condenser and overhead stirrer guide. The reactor was purged with nitrogen for at least 1 h while stirring at 200 rpm and subsequently put under a low positive pressure of nitrogen at all times, which was controlled by placing a vent between the nitrogen supply and the condenser. Next the reactor was placed into a constant temperature water bath (75°C) and stirred (200 rpm). Once the solution had reached equilibrium (~20 min), both the preemulsion and the initiator were fed continuously to the reactor using FMI pumps over a dosing period of 3 h. After this the reaction was proceeded for another 2 h. The warm emulsion was then filtered through a filter net to ensure that none of the small amount of coagulant that had formed was present. Average Particle size (TEM) ~90 nm.

15.2.5.4 Butadiene Containing Emulsion Polymerization

One of the most important classes of commercially produced polymers by emulsion polymerization is diene-containing polymers. These synthetic rubbers and elastomers are used in many applications. A feature of diene polymerization is crosslinking due to reaction of the pendant vinyl groups formed by 1,2 addition. This is often desirable because of increases in mechanical performance. However, in the laboratory this can be a nuisance as it can hinder analysis by more routine methods, such as size-exclusion chromatography (SEC). Crosslinked polymer forms an insoluble gel, and the fraction of polymer gel increases with conversion (i.e., as the concentration of polymer relative to monomer increases in the reaction). Polymerizations were run at 10% solids. Sodium styrenesulfonate was added as a stabilizer. In order to reduce the gel content of the polymers, $0.15 \, cm^3$ of a chain transfer agent, tertiary dodecyl mercaptan, was added. Polymerizations have to be carried out in pressure vessels designed specifically for this purpose with appropriate safety measures including bursting disks and the use of blast shields.

Reagents

Sodium styrenesulfonate	0.1 g
tert-Dodecyl mercaptan	$0.15 \, cm^3$
Ammonium persulfate	0.167 g
Butadiene	9 g
Water	87.7 g
HCl	

All liquids were degassed by nitrogen purging for at least 1 hour prior to use. Distilled water (82.7 g) and sodium styrenesulfonate (0.1 g, 0.44 mmol) were added, was placed in a glass high-pressure reactor (up to 10 atm) under nitrogen and the solution nitrogen degassed. The pH was adjusted to pH $= 2$ with concentrated HCl. Butadiene (added as a liquid after being collected in a CO_2/acetone condenser directly from the cylinder) (9 g, 0.17 mol) was nitrogen degassed and added via syringe to the reactor, with tertiary dodecyl mercaptan ($0.15 \, cm^3$, 0.626 mmol). Ammonium

persulfate (0.167 g, 0.73 mmol) was dissolved in nitrogen degassed water (5.0 g) and the solution injected into the reactor. The mixture was then heated to 70°C under stirring, and allowed to react for 5 h. The product was formed as a stable latex. Particle size (DLS) $= 237$ nm, $M_w/M_n = 0.02$

15.2.6   Microemulsion Polymerization

The main difference in performing a micro-emulsion polymerization instead of a conventional emulsion polymerization is that when monomer, surfactant and water are mixed a thermodynamically stable emulsion of monomer in water is obtained. This is accomplished by using surfactants that are able to reduce the interfacial energy to values close to zero. This has drastic consequences for the mechanism and outcome of the polymerization process. Both polymerization systems show compartmentalization. In general the average particle sizes and the average number of chains per particle are smaller in a microemulsion polymerization process (i.e., 15–60 nm). A closer look at the mechanism of microemulsion polymerizations reveals that there are no monomer droplets; it is believed that particle nucleation occurs throughout the entire polymerization process, and chain-stopping events are dominated by chain-transfer reactions. As a consequence the overall rate of polymerization of a microemulsion polymerization will not have a constant interval (interval 2 in emulsion polymerization).

15.2.6.1   *Microemulsion Polymerization of Styrene*[19]

Reagents

Styrene	4 g
Dodecyltrimethylammonium bromide (DTAB)	16.94 g
V-50	0.04 g
Distilled and deionised Water	96 g
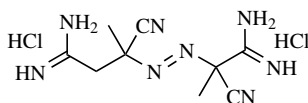
V-50

Styrene was distilled and passed over a short column of basic alumina prior to use. DTAB was recrystallised three times from 50 : 50 (v : v) acetone/ethanol to remove impurities. V-50 was recrystallised from methanol.

Procedure   The amounts of styrene, DTAB and 95.5 g of water were placed in a flange flask (250 mL) fitted with an overhead stirrer with turbine impeller (300 rpm) and the solution deoxygenated through purging with nitrogen for one hour. After

deoxygenating the reactor was placed in a water bath at 60°C. The amount of   V-50 was dissolved in 0.5 g of degassed water, and this solution was injected into the reactor. Polymerization was proceeded for 3 h.

Results   Final conversion was ∼85%. Monodisperse particle size distribution. Average particle size diameter (TEM) = 34.2 nm. $M_n = 1.6 \times 10^6$; $M_w/M_n = 2.3$.

15.3   LIVING AND/OR CONTROLLED RADICAL POLYMERIZATIONS

Since the early 1990s there has been a major development of living/controlled radical polymerization (LRP) techniques.

One of the first examples of a living radical polymerization was reported by Otsu et al.,[20,21] Who reported that radical photopolymerization of vinyl monomers with specific thiocarbamate compounds, including tetraethylthiuram disulfide, featured "living" polymerization characteristics, such as an increase of the molecular weight as a function of monomer conversion and the ability to prepare block copolymers. The thiocarbamate compounds were called *iniferters*, since they were capable of initiation, transfer, and termination. The mechanism of these controlled radical polymerizations was a combination of both reversible homolysis and degenerative transfer.
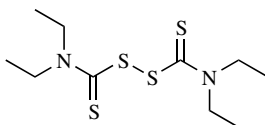
Tetraethylthiuran disulfide

Examples of living radical polymerizations operating via reversible homolysis include those mediated by persistent radicals based on arylmethanes,[22] organocobalt porphyrin complexes,[23,24] one-electron oxidation of arenediazoate,[25] nitroxides,[1] and atom transfer radical polymerization.[3,26–28] Examples of systems operating via degenerative transfer processes are the iodide-mediated polymerization of styrene,[30] polymerizations mediated by macromonomers of general structure $H_2C=C(Z)CH_2$ (A)$_n$ [where (A)$_n$ is a radical leaving group and Z is an activating group, e.g., CO_2R or Ph],[31] or polymerizations mediated by xanthates, referred to as the *MADIX process*.[29]

15.3.1   Catalytic Chain Transfer Polymerization

Catalytic chain transfer polymerization is an effective method for the synthesis of methacrylic oligomers which contain terminal unsaturation.[32–34]
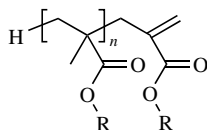
Polymerization is catalyzed by a family of Co(II) macrocycles, including cobaloximes,[35] cobalt porhyrins,[36] or more effectively BF$_2$-capped cobaloximes,[36,37] which may be introduced as either Co(II) or Co(III) alkyls.[31,38]

CoBF
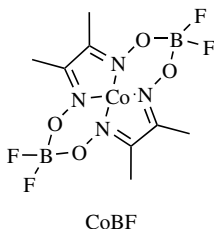
Chain transfer to Co(II) is extremely efficient where the propagating radical is α to a methyl group, as is the case in methacrylates and α-methyl styrene.[39] Chain transfer coefficients four orders of magnitude greater than for mercaptans are usually achieved for methacrylates resulting in extremely low concentrations of catalyst required achieving large reductions in mass. The catalysts are active under all radical polymerization conditions, including bulk, solution,[40] emulsion,[41] and suspension,[42] providing catalysts with the appropriate solubility characteristics are chosen. Solubility can be tuned by altering the ancillary ligands surrounding the macrocycle.[43] Many recipes covering a range of monomers and process conditions are available in the patent literature as well as the open literature.

15.3.1.1 Catalytic Chain Transfer of MMA in Emulsion Polymerization

Reagents

AOT-100	2.0 g
Water	450 mL
ACVA	2.00 g
MMA	200 mL
CoBF	0.030 g

All liquids were deoxygenated by purging with nitrogen for at least 2 h prior to use.

Procedure Surfactant, AOT-100 (2.0 g), was added to a 1-L quickfit flange flask glass reactor under a nitrogen atmosphere. Water (450 mL) was added to the reactor and then heated to the reaction temperature of 80°C. The mixture was stirred using a

turbine impeller at 150 rpm. 4,4′-azobis(4-cyanovaleric acid) (ACVA) (2.00 g) was added to the reactor immediately prior to the monomer/catalyst feed. A solution of catalytic chain transfer agent (CoBF) (0.030 g) in MMA (200 mL) was fed from a Schlenk tube via an FMI pump at a rate of 3.33 mL/min. The polymerization was left for a total of 240 minutes. Reactions can be sampled, for example, at 20-min intervals so as to follow conversion, M_n and M_w/M_n.

Results   This feed profile maintains an instantaneous conversion of approximately 50%, with 100% conversion reached after approximately 120 min. Final $M_n = 2120$ g/mol, $M_w/M_n = 1.65$ with an effective C_s of 1320, the M_n and M_w/M_n remain approximately constant throughout the polymerization.

15.3.1.2   Catalytic Chain Transfer of 2-Hydroxy Ethylmethacrylate (HEMA) in Aqueous Solution

Reagents

Distilled water	52 mL
Methanol	26 mL
HEMA	3.2 mL
4,4′-Azobis(4-cyanopentanoic acid)	0.14 g
CoBF	5 mg

Procedure   Distilled water (52 mL) and methanol (26 mL) were nitrogen-deoxygenated and added to 4,4′-azobis(4-cyanopentanoic acid) (ACVA) (0.14 g), CoBF, (4 mg) and HEMA (3.2 mL). The solution was heated to 80°C. Deoxygenated HEMA (30 mL) was added to CoBF (5 mg), this solution was fed into the aqueous solution of initiator and CoBF over 1 h. After the completion of the feed, additional CVA initiator was added (0.07 g). The reaction was left at 80°C for a further 2 h. Conversions and molecular mass information are calculated using ^{1}H NMR, $M_n = 2500$ g/mol, conversion $= 89\%$.

15.3.1.3   Determination of Chain Transfer Coefficient in Solution

Reagents

CoBF	2.2 mg
AIBN	60 mg
MMA	12 mL
Toluene	50 mL

Procedure   All reactions were carried out using standard Schlenk apparatus and closed ampoules in a 60°C (±0.5°C) constant temperature water bath. The reaction mixtures were deoxygenated by freeze–pump–thaw cycles. A stock solution of

TABLE 15.4 Data for C_s Determination

MMA	Solvent (mL)	[COBF]/[MMA] $\times 10^9$	M_n	M_w/M_n	% Conversion
2.00	4.00	0	97,000	2.05	7.43
2.00	4.00	261.0	11,800	2.03	6.37
2.00	4.00	522.0	6,980	1.99	5.86
2.00	4.00	1044	4,170	1.90	5.48
2.00	4.00	2088	2,210	1.71	5.24

CoBF was prepared by dissolving 2.2 mg of CoBF in 50 mL of toluene. A second initiator stock solution was prepared by dissolving 60 mg of AIBN in a mixture of 12 mL of MMA and 18 mL toluene. Five reaction mixtures were prepared, each containing 5 mL of the initiator solution and a mixture of toluene and the CoBF stock solution totaling 1 mL. The amounts of CoBF stock solution used in the five reactions were 0, 0.05, 0.10, 0.20, and 0.40 mL. After being deoxygenated and sealed, all five reactions were heated simultaneously at 60°C for 15 min prior to being cooled in ice. SEC (size-exclusion chromatography) was carried out on the reaction mixture to avoid fractionation on precipitation. Yields were determined by drying a known weight of the reaction mixture to constant weight in a vacuum oven at 60°C for 48 h, chain transfer coefficient in solution $C_s = 24,300 \pm 6730$ (see also Table 15.4).

15.3.2 Nitroxide-Mediated Polymerization

The concept of the nitroxide-mediated polymerization (NMP) was originally outlined and illustrated by many examples in an explorative study patented by Solomon et al. in 1985.[1] The power and capabilities of this novel type of polymerization did not draw worldwide attention until a decade later, in 1993, Georges et al.[44] reported that the TEMPO-mediated LRP of styrene in bulk and suspension at temperatures of 120–140°C featured "living" polymerization characteristics.
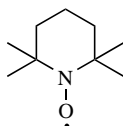
TEMPO

They[44] showed that it was possible to control the molar weight distribution (MWD), implying a low polydispersity of the MWD ($M_w/M_n < 1.3$) and an increase of the average molecular weights with conversion of monomer.

These "living" features of NMP can at first sight be explained with the concept of an elementary "living" radical polymerization system, consisting of a constant number of dormant species that can be reversibly activated, at a rate fast compared

to the overall rate of polymerization. In the activated form it undergoes propagation and as a result of the reversibility of the process this occurs via "stepwise" insertion of monomer. Obviously, insertion of one monomer unit at a time would give the best control, but this is not strictly necessary. A more generic statement would be that the number of monomer units inserted per step should be small with respects to the final chain length obtained.

15.3.2.1 Synthesis of Di-tert-butyl Peroxalate (DTBPO)
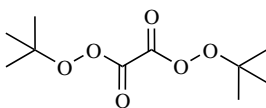
DTBPO

Reagents

Pyridine	12 mL
tert-Butyl hydroperoxide (3 M in *iso*-octane)	34.56 g
Pentane anhydrous	120 mL
Oxalyl chloride	9.75 g

Procedure   This compound was synthesized using the procedure reported by Bartlett et al.[45] Prior to use, all glassware was dried in an oven at 423 K for 24 h. Pyridine was dried over molecular sieves (4 Å). All other chemicals were used as received.

tert-Butyl hydroperoxide (3 M in *iso*-octane, 34.56 g), 12 mL of dry pyridine, and 120 mL of anhydrous pentane were charged into a 500-mL round-bottomed flask under argon and cooled below $-10°C$ with a saturated aqueous calcium chloride solution and liquid nitrogen. Next, a solution of oxalyl chloride (0.077 mol, 9.75 g) in 80 mL of anhydrous pentane was added dropwise to the mixture. Throughout the addition process the temperature was maintained under a maximum of $-5°C$ (about 1 h). After this the mixture was stirred for 1.5 h under these conditions, after which the cooling process was aborted and the mixture was allowed to gradually warm to room temperature (0.5–1 h). A clear solution of the product in pentane was obtained after removal of the pyridinium hydrochloride by filtration over a Büchner funnel.

The di-*tert*-butyl peroxalate (DTBPO) was obtained by crystallization from the pentane solution at -70–$60°C$ (using a mixture of liquid nitrogen and *n*-heptane) and isolated by filtration over a Büchner funnel. Yields are typically 50–65%.

A second portion of the compound can be obtained by dissolving the pyridinium hydrochloride and incorporated DTBPO with water and pentane. Extraction with pentane and isolation via the crystallization procedure mentioned above affords a relevant amount of product increasing the overall yield to about 90%. (*Caution*: This compound is an explosive hazard and, therefore, the use of metal equipment should be avoided to exclude possible induced decomposition. Moreover, the compound

should be handled with extreme care—avoid scratching and shaking—and should always be stored in the freezer ($T \pm -18°C$) immediately after use, preferably in a plastic container.)

Results are described in Section 15.3.2.1.1.

15.3.2.1.1   Rate Coefficient for Thermal Dissociation of di-tert-butyl Peroxalate (k_d)
Since DTBPO is used as a free-radical source in the synthesis of our alkoxyamine compounds, its rate coefficient for thermal dissociation [k_d (s^{-1})] is an important parameter in order to optimize experimental conditions. We, therefore, determined a set of Arrhenius parameters for k_d.

A number of groups have reported data for the k_d of DTBPO in various solvents.[45–48] In addition, we performed relative trapping experiments at 25°C, in which an equimolar mixture of two different nitroxides was used to evaluate their relative trapping coefficients in styrene with DTBPO as radical source. It was assumed that the rate of dissociation did not change noticeably on variation of the solvents used (i.e., benzene, saturated alkanes, bulk polypropylene, and styrene) and that the *tert*-butoxy radicals exclusively underwent the addition to monomer in our experiments. (Cage recombination of *tert*-butoxy radicals in toluene at 45°C amounts to 4.9% and would, therefore, be within the assumed experimental error of 5%). Therefore, the combined data for k_d provided the following Arrhenius expression (see also Fig. 15.3):

$$k_d = 2.9_1 \times 10^{15} \exp\left(\frac{-115._9 \times 10^3}{RT}\right) \qquad (15.9)$$
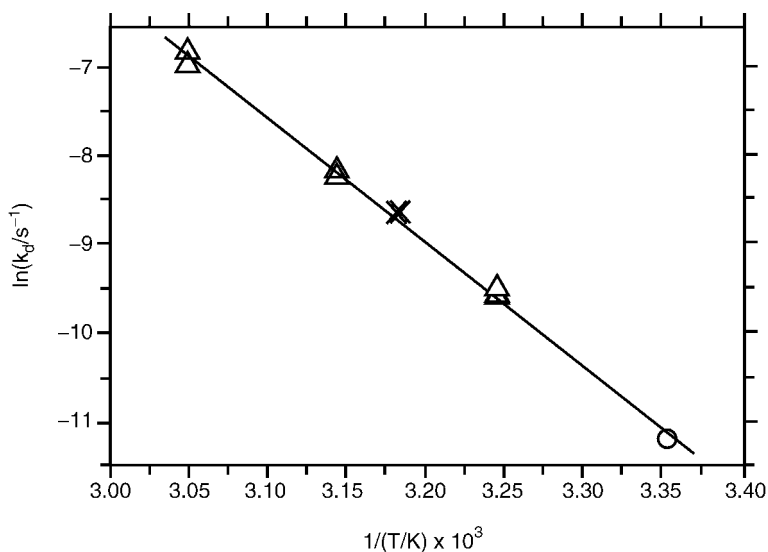
Figure 15.3   Linearized Arrhenius plot for the thermal dissociation rate coefficient (k_d) of di-*tert*-butyl peroxalate. Data include ($\bigcirc$, styrene), ($\triangle$, benzene), ($\times$, saturated alkanes), and ($+$, benzene and bulk polypropylene).

15.3.2.2   NMP of Styrene with In Situ Alkoxyamine Preparation

15.3.2.2.1   Preparation of Pyr-TEMPO
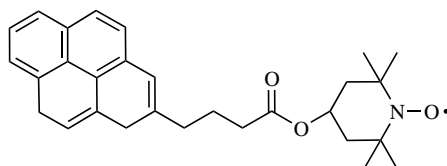
Pyr-TEMPO

Reagents

Pyrene butanoic acid	2.00 g
Dichloromethane dry	150 mL
DMF	3 drops
Oxalyl chloride	2.89 g
Hydroxy-TEMPO	1.91 g
Triethylamine dry	1.80 g
THF dry	200 mL

All reactions were carried out under dry conditions under an argon atmosphere. Dichloromethane was freshly distilled over calcium hydride, TEA was dried over KOH pellets, and THF was purchased as anhydrous.

Procedure   2.00 g of pyrene butanoic acid was suspended in 150 mL of dry CH_2Cl_2 with 3 drops of DMF to serve as catalyst. To this suspension 2.89 g of oxalyl chloride was added via syringe at room temperature. A yellow solution resulted, which was stirred under Argon for 4 h. Next the solvent was removed by vacuum distillation and the remaining solids were dried under high vacuum ($<10^{-3}$ mbar) for 3.5 h. Immediately after this, the resulting pyrene acyl chloride was dissolved in 100 mL of dry THF. This was added slowly to a solution of 1.91 g 4-hydroxy–TEMPO, 1.80 g TEA in 100 mL THF. The reaction mixture was left for 36 h. After this the solvents were removed by rotary evaporator and the residue was dissolved in 10 mL of dichloromethane. Flash chromatography over neutral alumina with CH_2Cl_2 as the eluent yielded 1.25 g of Pyr-TEMPO (40.6%).

15.3.2.2.2   In Situ Preparation of Alkoxyamine and Polymerization of Styrene in Bulk
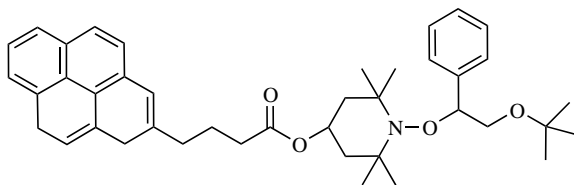
Alkoxyamine (**1**)

Reagents

Pyr-TEMPO	0.885 g
DTBPO	0.234 g
Styrene	40 mL

Prior to use styrene was distilled and passed over a short column of inhibitor remover (Aldrich).

Procedure The alkoxyamine was prepared in situ by adding 0.885 g of pyr-TEMPO, 0.234 g DTBPO to 40 mL of styrene into a 100 mL round-bottomed flask. The mixture was stirred until homogeneous and subsequently deoxygenated via three freeze–pump–thaw cycles to place the reaction mixture under an argon atmosphere. The flask was thermostated at 40°C and stirred for 24 h. After this time the alkoxyamines are formed, and no polymerization occurred. Next the reaction mixture was placed in an oil bath at 130°C.

Results The initial rate of polymerization was ~3.3×10^{-4} mol L^{-1} s^{-1}. Average molecular weights showed linear behavior versus monomer conversion with $M_w/M_n < 1.3$.

15.3.2.3 *Preparation of Alkoxyamine*
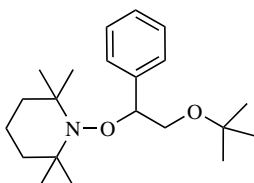
Alkoxyamine (**2**)

Reagents

TEMPO	1.56 g
Styrene	50 mL
DTBPO	1.17 g

Prior to use styrene was distilled and passed over a short column of inhibitor remover (aldrich).

Procedure TEMPO (10 mmol, 1.56 g) and styrene (50 mL, 45.5 g) were mixed in a 100-mL round-bottomed flask. Di-*tert*-butyl peroxalate (5 mmol, 1.17 g) was added. The mixture was stirred until all compounds were completely dissolved

and subsequently submitted to three freeze–pump–thaw cycles in order to remove the oxygen and to place the reaction mixture under an argon atmosphere. Next, the mixture was stirred and kept under argon for 3 days at 298 K. After this time period the excess of styrene was removed by vacuum distillation at room temperature. The crude alkoxyamine was purified by triple crystallization from methanol at 253 K. White crystals. Yield: 66%.

Spectral Data ^{1}H NMR (CDCl$_3$) δ 1.04 (s, 9 H, (CH_3)$_3$CO), 0.58, 1.02, 1.19, 1.37 (br. s, 3 H, CH_3 ring), 0.9–1.7 (br. m, 6 H, CH_2 ring), 3.41 (dd, 1 H, H_a), 3.89 (dd, 1 H, H_b), 4.74 (dd, 1 H, H_c), 7.18–7.35 (m, 5 H, Ph).

^{13}C NMR gated-decoupled (CDCl$_3$) δ 17.2 (t, 1 C, C(4) ring), 20.3 (q, 2 C, CH_3 ring), 27.3 (q, 3 C, (CH$_3$)$_3$CO), 33.9 (q, 2 C, CH_3 ring), 40.6 (t, 2 C, C(3) ring and C(5) ring), 60.0 (s, 1 C, C(2) ring), 62.0 (s, 1 C, C(5) ring), 65.0 (t, 1 C, CH$_a$H$_b$), 72.8 (s, 1 C, (CH$_3$)$_3$$C$O), 86.1 (d, 1 C, CH$_c$Ph), 127, 128, 129 (m, 5 C, Ph$_o$, Ph$_m$, Ph$_p$), 142.5 (s, 1 C, Ph).

15.3.2.4   Nitroxide Mediated Polymerization of Styrene in Bulk at 140°C

Reagents

Alkoxyamine (**2**)	0.75 g
Styrene	45.45 g
TEMPO	0.005 g

Procedure   Styrene was distilled and passed over a column of inhibitor remover (Aldrich) before use. Then styrene, alkoxyamine (**2**), and TEMPO were charged into a three-necked 100-mL round-bottomed flask equipped with a Teflon-coated magnetic stirrer. The reaction mixture was deaerated by three freeze–pump–thaw cycles in order to place the reaction mixture under an argon atmosphere. The flask was placed in a thermostated oil bath at 140°C. Conversion was determined gravimetrically.

SEC analysis proceded as follows. MWD of the polymers produced were determined by SEC. 0.1 w/v% Solutions in tetrahydrofuran (THF, stabilized, Biosolve, AR) were prepared of each sample, which was isolated by removal of solvent under reduced pressure at $T < 20°C$. The solutions were filtered through 0.2-μm syringe filters. The SEC analyses were carried out with two Shodex KF-80M (linear) columns, or two PL gel 10^3 and 500 columns, at 40°C. The eluent was THF at a flow rate of 1 mL/min. A Waters 410 differential refractometer and a Waters 440 UV detector (254 nm) were used for the detection. Narrow-molecular-weight-distribution polystyrene standards (Polymer Labs) with molar masses (M) ranging from 370 to 6.5×10^6 g/mol were used for calibration of the columns. After a baseline correction, the GPC chromatograms were converted to the differential log molar mass distributions [$x(M)$ vs. log(M)], weight MWD [$w(M)$ vs. M] and number MMD [$n(M)$ vs. M] according to the procedure described by Shortt.

The results are discribed in Section 15.3.2.4.1.

Figure 15.4 [M] versus time for both a thermal spontaneous polymerization of styrene (■) and a nitroxide mediated LRP with $[L]_0 = 4.40 \times 10^{-2}$ mol/L (○) in bulk at 140°C. The lines represent the theoretical values of [M] versus time in the absence of a Trommsdorff effect with $R_{P,t=0} = 4.7 \times 10^{-4}$ L mol^{-1} s^{-1} with (····) and without (—) volume contraction.

15.3.2.4.1 *Trommsdorff Effect* Figure 15.4 gives the concentration of monomer, [M], versus time for both a thermal spontaneous polymerization of styrene and a LRP with $[L]_0 = 4.40 \times 10^{-2}$ mol/L at 140°C. The data were corrected for volume contraction on the basis of their theoretical molar mass assuming an ideal "living" polymerization system.

The average molar mass produced in the TEMPO mediated polymerization is much lower than in a spontaneous thermal polymerization, as a result of the monomer distribution over the relatively large number of alkoxyamines. This difference is also reflected in the chain-length distribution of the propagating radicals (R•). Together with a lower microviscosity for a specific $R_i^{\bullet}$ in the LRP experiment in comparison with the thermal polymerization at the same X_w, the Trommsdorff effect is less pronounced in the LRP experiment.

This can be clearly observed from the theoretical [M] versus time of a thermal spontaneous polymerization of styrene in absence of the Trommsdorff effect (see Fig. 15.4). Therefore we use our value of $R_{P,t=0}$ at 140°C determined with a $[M]^{5/2}$ dependence: 4.7×10^{-4} mol L^{-1} s^{-1}. The [M]–time curves are calculated both with (····) and without (—) taking into account a volume contraction, which is linear as a function of X_w:

$$V = V_0(1 + \varepsilon X_w) \tag{15.10}$$

where $\varepsilon = -0.2003$ is the fractional change in volume of the system between zero and complete conversion.

Figure 15.5 $x(M)$ versus $\log(M)$ at different stages of conversion for a NMP of styrene in bulk at 413 K, with $[L]_0 = 4.40 \times 10^{-2}$ mol/L and $[T^\bullet]_0 = 1.0 \times 10^{-4}$ mol/L.

Figure 15.5 plots data for x(M) versus log (M) at different stages of conversion for this system. Figure 15.6 presents data for the number and weight average molar masses, $\langle M_n \rangle$ and $\langle M_w \rangle$, together with the corresponding polydispersity. The line represents the theoretical number molar mass development for an ideal living polymerization system $(\langle M_n^{\text{theor.}} \rangle)$.

As can be seen in Figs. 15.5 and 15.6, an excellent control of the MWD throughout the polymerization is reached. The broadening to the low-molecular-weight side of the MWD is less pronounced, indicating that indeed the undesired effect of a slow dissociation of the "initial" alkoxyamine compound has been overcome successfully. The measured values of $\langle M_n \rangle$ and $\langle M_w \rangle$ at the initial stages of polymerization are comparable to the theoretical values of an ideal "living" polymerization system and show a linear behavior up to high X_w. Furthermore, the molecular weights obtained are close to the values predicted for the ideal "living" polymerization and low values of ∼1.25 are obtained for M_w/M_n. These features all indicate that "stepwise" chain growth has been accomplished, so that proper control of the MWD can be achieved.

15.3.2.5 The Occurrence of Permanent Chain Stopping   In a nitroxide-mediated LRP system the cumulative fraction of the "dead" polymer chains has to be kept low to yield a uniform polymer material that is able to undergo further polymerization (e.g., to synthesize a block copolymer). The fraction of "dead" polymer material is higher in LRP systems with a lower number of alkoxyamines. A question that arises is how we are able to estimate the appropriate amount of alkoxyamines needed, based purely on this aspect.

Figure 15.6 $\langle M_n \rangle$ (■), $\langle M_w \rangle$ (○), and (×), together with the theoretical number molar mass development of an ideal living polymerization system (——) ($\langle M_n^{\text{theor}} \rangle$) versus X_w for a CRP of styrene in bulk at 413 K with $[L]_0 = 4.40 \times 10^{-2}$ mol/L.

A parameter p_D can be introduced that describes the probability of R• to undergo a permanent chain-stopping reaction, when it is deactivated. A value of p_D can be calculated using:

$$p_D = 1 - \left(\frac{v k_{\text{ed}} [L]_0}{R_{P, t=0}} \right) \tag{15.11}$$

The results of the determination of p_D for the TEMPO-mediated LRP of styrene at 140°C is presented in Table 15.5.

Now let us look at the total amount of "dead" polymer chains that is produced by the additional radical flux, which in our experiments was ascribed partly to the thermal self-initiation of styrene. All "additional" radicals produced must terminate in the end via disproportionation to yield two polymer chains, or via combination to yield one polymer chain.

For a hypothetical system in the absence of the Trommsdorff effect and volume contraction, the monomer conversion (X_w) can be described by assuming a third-order dependence for Ω on [M]. This enables us to derive an equation to calculate the total amount of radicals produced that is needed to reach complete conversion of monomer [Ω/(mol/L)]:

$$\Omega = \frac{2}{3} \left(\frac{2k_t}{k_p^2} \right) \frac{R_{P, t=0}}{[M]_0} \tag{15.12}$$
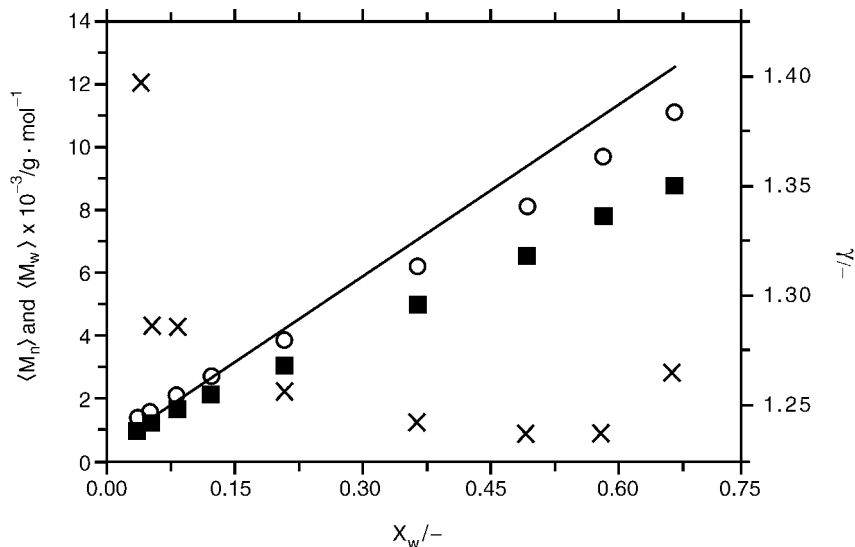
TABLE 15.5   Percentages of Permanent Chain Stopping for TEMPO-Mediated LRPs of Styrene in Bulk at 140°C

		p_D/%			
				$k_{ed} \times 10^3$ (s^{-1})	
[L]$_0$ (mol/L)	$R_{P,t=0} \times 10^4$ (mol L^{-1} s^{-1})	2.6[a]	1.6[b]	6.3[c]	15.7[d]
4.40×10^{-2}	4.1	0.31	0.51	0.13	0.05

[a] k_{ed} of (**2**) calculated from nitroxide exchange experiments.
[b] k_{ed} of (**2**) calculated from quantitative ESR.
[c] k_{ed} of polystyrene alkoxyamine (with $\langle M_n \rangle = 1.7 \times 10^3$ g/mol, $M_w/M_n = 1.11$ and $P_{dead} = 5\%$).
[d] k_{ed} of polystyrene alkoxyamine (with $\langle M_n \rangle = 7.6 \times 10^3$ g/mol, $M_w/M_n = 1.26$ and $P_{dead} = 5\%$).

The obtained values of Ω can be considered as maximum values to give a rough indication of the total amount of "dead" polymer chains produced. (Ω should be divided by 2 to yield the correct amount of "dead" polymer chains, if termination occurs exclusively by combination, as is the case for the polymerization of styrene.) The results for these hypothetical systems using data obtained from the experiments carried out at 120, 130, and 140°C are presented in Table 15.6.

From the above evaluation of the TEMPO-mediated CRP, however, it was inferred that chain transfer to monomer and to the Diels–Alder dimer was important as a chain-stopping process. This event leads to an extra amount of "dead" polymer chains. The amount of polymer chains produced in the hypothetical system described above via transfer to monomer at complete monomer conversion can simply be estimated with $C_{M,t=0}[M]_0$. These results are also given in Table 15.6.

The amounts of "dead" material obtained for this hypothetical system indicate that the initial alkoxyamine concentrations should be of the order of 10^{-2} mol/L to limit the fraction of "dead" polymer material in the final product. Therefore, it can be concluded that the TEMPO-mediated LRP of styrene will be successful only for the preparation of low-molecular-weight material ($M < 3.0 \times 10^4$), if an alkoxyamine end functionality is desired. Moreover, it is postulated that the total number of "dead" polymer chains produced at a certain overall polymerization time is equal

TABLE 15.6   Total Amount of "Dead" Polymer Chains Produced in Thermal Self-Initiated Polymerizations of Styrene

T (°C)	Termination by Combined (Ω/2) (mol/L)	Transfer to Monomer (mol/L)
120	5.3×10^{-4}	3.1×10^{-3}
130	6.4×10^{-4}	3.7×10^{-3}
140	7.9×10^{-4}	4.4×10^{-3}

or higher in the case of a nitroxide-mediated LRP in comparison with the polymerization process in the absence of the alkoxyamine/nitroxide species.

15.3.2.6 Emulsion NMP

Living radical polymerization techniques have emerged since the early 1990s as the most innovative development in the field of radical polymerization, allowing precise control, or design, of macromolecules. ATRP and NMP systems have proven to be successful mostly under conditions where "bulk" kinetics apply. A bottleneck in both of these techniques still seems to be emulsion polymerization. In order to achieve an optimal control of chain growth under the heterogeneous emulsion polymerization conditions certain guidelines need to be considered. These will now be addressed for NMP of styrene in emulsion.

Both the alkoxyamine and the nitroxide species need to have a high partitioning coefficient between the latex particles and the water phase. (The *partitioning coefficient* is defined as the ratio of the concentrations of a compound in the two phases in equilibrium.) It is essential that the alkoxyamine species be present and undergo chain growth in the latex particles and not in the monomer droplets, which is an extension of the general rule that polymerization in monomer droplets should be avoided in all cases in order to maintain colloidal stability. The alkoxyamines, therefore, need to have been distributed equally over the loci of polymerization, namely, the polymer particles, from the initial stages of the polymerization process.

In order to study the effect of the addition of the alkoxyamine on MWD of an emulsion polymerization, the latex produced must have a uniform particle size distribution throughout the entire process. A short particle formation period as well as the absence of coagulation during the stage of particle growth are required to rule out broadening of the MWD during the polymerization caused by a nonuniformity in the loci of polymerization. The easiest way to carry out a nitroxide-mediated living radical polymerization in emulsion would be based on an ab initio experiment, in which all components of the emulsion polymerization recipe are added from the start.

If we consider the basic rules given above for an ab initio process, there are two complicating problems to be solved. The first is that the presence of alkoxyamine species in the monomer droplets needs to be prevented. This can be indirectly achieved by using initially a water-soluble alkoxyamine species of low molecular weight. Chain-growth of this species via propagation in the water phase to its critical chain length for entry, micellization or precipitation will lead to proper distribution over the primary polymer particles, eventually yielding a uniform distribution over the mature latex particles after the stage of particle formation. In this case the presence of alkoxyamines in the monomer droplets is prevented. The second problem that needs to be accounted for in an ab initio experimental design is the partitioning of the free nitroxide between the latex particles, water phase, and monomer droplets throughout the entire polymerization process. This requires the use of a relatively large additional amount of nitroxide functioning as a buffer in the monomer droplets to guarantee the required concentration of free nitroxide in the latex particles needed for a "stepwise" growth of the alkoxyamines. This excess of free nitroxide in the system, however, has to be gradually destroyed in the polymerization, as its storage domains, that is, the monomer droplets, disappear on monomer conversion.

15.3.2.6.1 Seeded Emulsion NMP of Styrene Restricting ourselves to the TEMPO-mediated LRP of the styrene system, relatively high temperatures (in general exceeding 100°C) are required to achieve an acceptable rate of alkoxyamine C—O bond homolysis to guarantee a "stepwise" growth of the polymer chains. At these high temperatures a colloidally stable latex system is difficult to obtain, among other things, as a result of an increase in Brownian motion of the particles, the instability of various types of monomers toward hydrolysis, and the restricted temperature range of the surfactant as stabilizer. Furthermore, the thermal self-initiation of monomer, which is the secret behind the success of the TEMPO-mediated LRP of styrene in bulk, ironically complicates the polymerization process dramatically when transferred to the heterogeneous emulsion system. This can be ascribed to the limited water solubility of the radical species generated, which therefore will have no propensity for exiting the monomer droplets and thus cause polymerization herein.

Attempts to prepare a stable latex via conventional free-radical polymerization of styrene with thermal self-initiation required the addition of large amounts of surfactant to decrease the number of monomer droplets and to stabilize the particles formed. In this case, however, the stage of particle formation will continue throughout the major part of the polymerization process. Moreover, one should treat this process like a miniemulsion polymerization rather than a regular emulsion polymerization. Because of these considerations, the task to ab initio synthesize a monodisperse latex under these conditions appears to be impossible. The study on NMP of styrene in emulsion was, therefore, restricted to seeded emulsion polymerization systems.

15.3.2.6.2   Seed Latex Preparation

Reagents

Styrene	75.14 g
Water	0.156 L
Aerosol MA80	2.681 g
NaHCO$_3$	3.00 mmol/L
ACVA	0.90 mmol/L
DMEA	2.00 mmol/L
Water	0.010 L

Procedure   The experiment was carried out under argon in a jacketed all-glass reactor, thermostated at 90°C and equipped with a mechanical six-blade turbine stirrer. The stirring speed was kept at 250 rpm. Before polymerization, the reaction mixture was degassed and purged with argon 3 times. The polymerization was stopped after 12 h, and the product was filtered through a filter paper. The obtained latex was purified thoroughly by dialysis at ambient temperature. The average particle size and the polydispersity of its particle size distribution were determined with dynamic light scattering (DLS) and transmission electron microscopy (TEM) to yield

$D_n = 90$ nm and PD $= 1.1$, respectively. Its solids content had a value of 24.1 wt% after purification and was determined gravimetrically.

15.3.2.6.3   Seeded Emulsion NMP   We previously reported that in comparison with TEMPO mediated LRP of styrene in bulk, in general, higher values of the polydispersity for the MWD of the seeded emulsion experiments were found.[49] Possibly this was caused by both the heterogeneity of the system (e.g., partitioning and compartmentalization) and a possible increase in the additional radical flux caused by an enhancement of the thermal Diels–Alder reaction of styrene. An increase in temperature to 140°C, which resulted in a better control of chain-growth for the bulk polymerizations led to even broader MWD in the emulsion system.

   Novel experiments, which were carried out under similar conditions but this time in the absence of sodium hydrogen carbonate, revealed that the latter compound was the main source of the enhancement of the additional radical flux. Due to its nucleophilicity it steadily destroyed TEMPO at these elevated temperatures.

Reagents

Styrene	11.68 g
Seed latex	12.53 g
Alkoxyamine (**2**)	0.251 g
TEMPO	0.0026 g
Water	129.4 g
Aerosol MA-80	1.671 g

Procedure   The seeded emulsion polymerizations were carried out in a Teflon-jacketed high pressure reactor (0.25 L) under an argon atmosphere of 15 bar, thermostated at 125 ± 0.5°C, and equipped with a magnetic stirrer. The stirring speed was kept at 350 rpm. Prior to the polymerizations, all components were added to the seed latex in a laboratory bottle (0.5 L), and this was purged with argon. After the bottle had been sealed, the seed latex was allowed to swell for 24 h while shaking at ambient temperature. Then the reaction mixture was poured into the reactor, degassed and purged with argon 3 times.

Results   The results of these experiments are given both in Fig. 15.7 and Table 15.8, in which the log differential MMD are plotted and the theoretical molecular weights, the average molecular weights, and polydispersities of the polymer material produced under seeded conditions are given.

   From these results it can be concluded that a proper control of chain growth has been accomplished. Since online sampling to determine X_w and the MMD versus time was not possible with the current experimental setup, the question remains what the optimal overall reaction time is.

   In Table 15.7 it can be seen that in the last 12 h of polymerization the alkoxyamines underwent an average chain growth of only three monomer units. Therefore, one could argue whether these prolonged reaction times to reach ''complete''
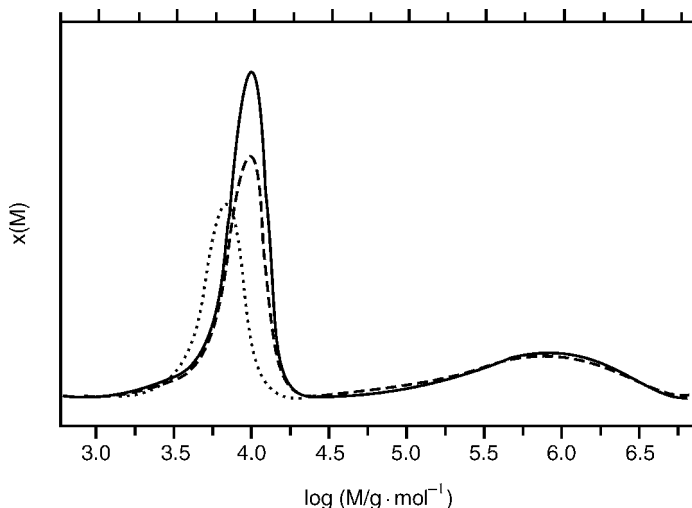
Figure 15.7 The differential log MWD obtained from the refractometric SEC spectra of latexes from a chain extension seeded emulsion CRP experiments after 12, 24, and 36 h of reaction at 125°C.

conversion are needed. The instability of the alkoxyamine C—O bond causes decomposition of the alkoxyamine species, which for the major part is ascribed to the nonreversible trapping by disproportionation. This resulted in an increase in the fraction of "dead" polymer chains, whereas it leaves the MMD relatively unaffected.

15.3.2.6.4 Chain Extension in Emulsion NMP The amount of permanently deactivated chains caused by this postpolymerization time, is clearly seen from a chain extension experiment. A new batch of styrene was added to the final polystyrene latex, which was obtained after 36 h of overall reaction time. The results of the MWD analyses after polymerization times of again 12, 24 and 36 h (see

TABLE 15.7 **Average Molecular Weights and Polydispersity for Seeded NMP of Styrene in Emulsion without Sodium Hydrogen Carbonate**

Overall Reaction Time $(M \times 10^{-3} \ g^{-1} \ mol^{-1})$	12 h	24 h	36 h
$\langle M^{\text{theor}} \rangle^a$	—	—	11.07
$\langle M_n \rangle$	5.75	7.00	7.42
$\langle M_w \rangle$	6.61	8.63	8.93
$M^{\text{top}\,b}$	6.76	9.27	9.63
PDI M_w/M_n	1.15	1.23	1.20

[a] $\langle M^{\text{theor}} \rangle$ is the theoretical value of the molecular weight that can be obtained in a living polymerization under recipe conditions at the specific monomer conversion.
[b] M^{top} is the maximum value of the $x(M)$ distribution as represented in Fig. 15.7.
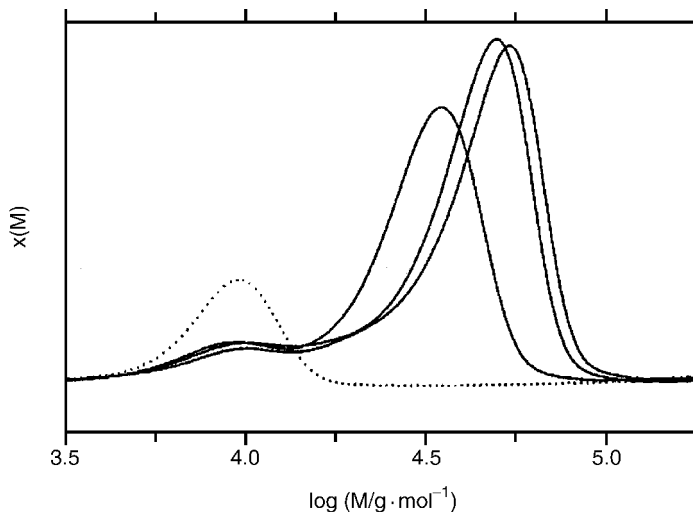
Figure 15.8 The differential log MWD obtained from the refractometric SEC spectra of latexes from a "chain extension" seeded emulsion NMP experiment after 12, 24, and 36 h of reaction at 125°C.

Fig. 15.8) revealed that indeed a considerable amount of "dead" polymer chains were present in the seed latex. On the basis of the extension of the average molecular weight observed it was calculated that about 16% of the chains was terminated permanently.

15.3.3   Atom Transfer Radical Polymerization (ATRP)

Living radical polymerization catalysed by transition metals has received tremendous interest following its inception in 1995. Two different research groups using two different catalyst systems published this chemistry independently. Matyjaszewski developed bipyridine and other N donor ligands[3,50,51] in conjunction with copper(I) halides (ATRP) while Sawamoto reported the use of $Ru(II)(PPh_3)_3Cl_2$ as catalyst.[2,28] A range of different initiators have been used mainly based on activated alkyl halides sulfonyl halides have been used to good effect.[52,53] A wide range of low-valence metals have subsequently been used as catalysts, including Ni(II),[54] Rh(I),[55] Pd(0),[56] and Fe(II).[57] The mechanism is via a radical pathway, although it has proved difficult to detect free radicals, and the possibility of caged radicals playing an important role in the mechanism cannot be excluded at present. The chemistry has been used with a range of monomers, including acrylates, methacrylates, and styrene to prepare many different controlled architecture polymers, and the subsequent examples serve to illustrate a small range of the work produced to date.

It is important to note at this point that the exact mechanism of this reaction is far from clear and the nature of the metallo species in solution quite complex. Thus the

exact reaction conditions and order of addition of reagents is very important. For example, in some cases all catalyst may not be dissolved at ambient temperature but will be dissolved at elevated reaction temperatures. Also in the case of copper(I)-mediated polymerization any oxygen- or nitrogen-containing monomers, solvents or additives will coordinate to the metal changing the nature if the catalyst often with dramatic effects on the rate of polymerization. This can result in an increase in the rate of termination and a subsequent loss of control when attempting to prepare block copolymers and other complex architectures. In such cases it may be necessary to change the temperature or change the levels of catalyst, even adding copper(II) in order to circumvent these problems. Even things that might appear trivial such as solubility of reagents can have large effects on the final polydispersity and level of termination observed. Thus it is necessary to be careful in carrying out experiments when trying to replicate procedures and especially on transferring reaction conditions from one monomer/solvent to another.

It is also important to realise that termination by radical–radical reaction is more likely at the start of the reaction when the species involved are relatively low molecular weight. Initiation and propagation will take place at low temperatures, especially ambient temperatures, albeit slow. Hence a way to achieve improved control over the reaction is to add all the reagents at ambient temperature and then place than in the heating bath so as to slowly increase the reaction temperature; this can improve the final polydispersities. However, it is noted that this procedure is not to be used if kinetic data are required. The reader is also encouraged to think about the order of reagent addition and consider this factor when designing experiments.

15.3.3.1 ATRP of Styrene with Bipyridine-Type Ligands[3]

Reagents

Cu(I)Br	0.0055 g
4,4′-Di(5-nonyl)-2.2′-bipyridyl (dNbpy)	0.314 g
Ethyl 2-bromoisobutyrate	0.035 g
Styrene	10 mL

Procedure Cu(I)Br 0.0055 g (3.8×10^{-4} mol) was placed in a oven-dried Schlenk tube. The tube was fitted with a rubber septum, and the tube was evacuated and flushed with dry N_2 3 times. Styrene 10 mL (9.6×10^{-2} mol) was transferred to the tube via degassed syringe. The mixture was stirred rapidly under nitrogen and 4,4′-di(5-nonyl)-2.2′-bipyridine (dNbpy) 0.314 g (7.68×10^{-4} mol) was added which imparted a deep red/brown color to the solution. Initiator ethyl 2-bromoisobutyrate (0.035 g, 4.8×10^{-5} mol (1.92×10^{-4} mol of initiating sites) was added and the resulting solution was degassed by three freeze–pump–thaw cycles. The resulting mixture was placed in a thermostatically controlled oil bath at 110°C for 4.5 h. The catalyst was removed from the samples by passing them through a column of activated basic alumina prior to SEC.

15.3.3.2   ATRP of MMA with N-Alkyl-2-pyridinalmethanimine Ligands   Many different alkyl pyridinalmethanimine ligands may be used in conjunction with copper(I) halides.[58] Most are prepared by the condensation of 2-pyridinecarbalde-hyde with the appropriate primary amine. The synthesis of the octyl variant is given as a representative example.

15.3.3.2.1   Synthesis of N-Octyl-2-pyridinalmethanimine

Reagents

2-Pyridinecarboxaldehyde	10 mL
Octylamine	17.35 mL
Diethyl ether	10 mL
Magnesium sulphate	2.5 g

Procedure   2-Pyridine carboxaldehyde (10 mL, 0.105 mol) and diethyl ether (10 mL) were added to a flask containing dried magnesium sulfate ($\sim$2.5 g). The flask was cooled to 0°C, and octylamine (17.35 mL, 0.105 moles) was added slowly. The mixture was stirred for two hours at 0°C prior to filtration. Diethyl ether was removed by rotary evaporation and the resulting yellow oil was purified by vacuum distillation.

The product was obtained as a yellow oil (bp 100°C at 7×10^{-2} mbar). Yield = 91%. Theoretical CHN 77.01, 10.16, 12.83, found 76.55, 10.06, 12.44.

Spectral Data ^{1}H NMR (CDCl$_3$, 298 K, 300 MHz) δ (ppm from TMS) = 8.49 (d, 1 H, $J = 4.89$ Hz), 8.24 (s, 1 H), 7.84 (d, 1 H, $J = 6.96$ Hz), 7.56 (td, 1 H, $J_1 = 7.53$ Hz, $J_2 = 1.5$ Hz), 7.13 (ddd, 1 H, $J_1 = 7.35$ Hz, $J_2 = 4.71$ Hz, $J_3 = 1.14$ Hz), 3.52 (td, 2 H, $J_1 = 6.99$ Hz, $J_2 = 1.32$ Hz), 1.58 (q, 2 H, $J = 7.35$ Hz), 1.15 (m, 14 H), 0.73 (t, 3 H, $J = 6.96$ Hz) ^{13}C NMR (CDCl$_3$, 298 K, 75 MHz) δ (ppm from TMS) = 161.3, 154.4, 149.1, 136.1, 124.2, 120.8, 61.3, 31.6, 30.4, 29.1, 29.0, 27.1, 22.4, 13.8

IR absorption ν (cm^{-1}) 3010, 2923, 2853 (alk. C—H stretch), 1650 (C=N stretch), 1587, 1567, 1467, 1435, 1366, 1331, 1291, 1144, 1043 (Ar C—C stretch)

Mass spectrometry (CI/EI): $m/z = 219$ (M + H), 203 (−CH$_3$).

15.3.3.2.2   ATRP of MMA with Octyl-2-pyridinal Methanimine Ligand ([M] : [I] : [Cu] : [L] = 100 : 1 : 1 : 2)

Reagents

Cu(I)Br	0.134 g
Toluene	10 mL
MMA	10 mL
N-$^{n−}$octyl-2-pyridinalmethanimine	0.453 mL
Ethyl-2-bromoisobutyrate	0.136 mL

Procedure   Cu(I)Br (0.134 g, 9.32×10^{-4} mol) and a dry magnetic follower were charged to a dry Schlenk tube. The tube was sealed with a rubber septum prior to three vacuum/N_2 cycles. Toluene (10 mL), MMA (10 mL, 9.36×10^{-2} mol) and N-$^{n-}$octyl-2-pyridinalmethanimine (0.453 mL, 1.872×10^{-3} mol) were added under N_2. The Schlenk tube was subjected to three freeze-pump thaw cycles and subsequently heated to 90°C with constant stirring. Once the reaction temperature had been reached, ethyl-2-bromoisobutyrate (0.136 mL, 9.36×10^{-4} mol) was added under N_2 (t = 0). Samples are removed periodically using a degassed syringe for molecular weight (SEC) and conversion (gravimetry) analysis.

15.3.3.3   ATRP of 2,2,2-Trifluoroethyl Methacrylate (TFEMA) ([M] : [I] : [Cu] : [L] = 100 : 1 : 1 : 2)   Many different methacrylates, acrylates, and styrene monomers may be polymerized by this type of polymerization. Polymerization of a fluorinated monomer is chosen as a representative example.

Reagents

Cu(I)Br	0.134 g
Toluene	13.3 mL
2,2,2-trifluoroethyl methacrylate	13.3 mL
N-$^{n-}$pentyl-2-pyridinalmethanimine	0.35 mL
Ethyl-2-bromoisobutyrate	0.136 mL

Procedure   Cu(I)Br (0.134 g, 9.32×10^{-4} mol) and a dry magnetic follower were charged to a dry Schlenk tube. The tube was sealed with a rubber septum prior to three vacuum/N_2 cycles. Toluene (13.3 mL), (TFEMA) (13.3 mL, 9.36×10^{-2} mol), and N-$^{n-}$pentyl-2-pyridinalmethanimine (0.35 mL, 1.872×10^{-3} mol) were added under N_2. The Schlenk was subjected to three freeze–pump–thaw cycles and then subsequently heated to 90°C with constant stirring. Once the reaction temperature was reached, ethyl-2-bromoisobutyrate (0.136 mL, 9.36×10^{-4} mol) was under N_2 (t = 0). Samples were removed periodically using a degassed syringe for molecular weight and conversion analysis.

The final sample was passed down a basic alumina column prior to precipitation into hexane. A sticky solid was collected, which was dissolved in dichloromethane. Solvent was removed by rotary evaporation to yield a faintly green-colored solid which contained 1% free monomer by ^{1}H NMR: $M_n = 24{,}400$, $M_w/M_n = 1.18$, $T_g = 73.5$°C; thermogravimetric analysis (TGA) revealed 70.9% loss at 200°C, 29.1% loss at 300°C.

15.3.3.4   Synthesis of Star Polymers Based on Simple Sugar Cores   ATRP offers an excellent route into a range of star polymers. This has been exploited by a number of research groups, including Sawamoto[59] and Gnanou[60] using derivitized calixarene cores. As described above, virtually any alcohol group may be transformed into an initiating site by esterification and used for subsequent polymerization. It must be noted that this approach can be used with the plethora of catalyst systems described and is not catalyst-specific. Virtually all simple multi functional alcohols may be utilized, and thus stars with virtually any number of arms

may be prepared. One very versatile class of multi-functional alcohols that have been used are the simple sugars, which offer almost every number of alcohol groups for derivitization. The example chosen is for glucose, a pentafunctional sugar, which gives rise to 5-arm star polymers. It is important to remember that, as in all living radical polymerization reactions, termination by combination will be present. When multifunctional initiators are used this inevitably leads to star–star coupling reaction, which can quickly give rise to crosslinking. It is thus often necessary to use quite dilute polymerization conditions and to stop the polymerization well short of 100% conversion. This is particary important when monomers that terminate predominantly be combination are being used, including styrene, acrylates, and vinyl acetate.

15.3.3.4.1   Synthesis of Pentafunctional Initiator Based on Glucose[61]

Reagents

2-Bromoisobutyryl bromide	38.6 g
α-D-Glucose	5.0 g
Pyridine (anhydrous)	30 mL
Chloroform (anhydrous)	50 mL
Diethyl ether	
0.1 M NaOH solution	
$MgSO_4$	
Methanol	

Procedure   1,2,3,4,6-Penta-*O*-isobutyrate-α-D-glucose initiator was synthesized by the slow addition of 38.6 g (0.17 mol) of 2-bromobutyryl bromide to a solution of 5.0 g (0.028 mol) of α-D-glucose refluxing at 80°C in a mixture of 30 mL anhydrous pyridine and 50 mL anhydrous chloroform. The solution was refluxed for 3 h under a dry atmosphere and then stirred at room temperature for 3 days. The solution was subsequently diluted in diethyl ether and washed with ice water, 0.1 M NaOH solution and water, respectively, prior to drying over anhydrous $MgSO_4$. The crude product was recrystallized from methanol to yield white crystals in 30% yield (7.3 g). Melting point was 211°C.

Spectral Data v(ATR)/cm^{-1} 1738; δ_H (CDCl$_3$, 300 MHz) 6.36 (d, $J = 3.78$, 1 H, anomeric), 5.64 (t, $J = 9.79$, 1 H, C*H*), 5.20 (dd, $J = 3.76, 9.89$, 2 H, C*H*), 4.4 (m, br, 3 H, C*H*, C*H*$_2$), 1.8 (m, br, 30 H, C*H*$_3$) [β anomer 5.78 (d, $J = 8.28$), 5.49 (t, $J = 9.51$)); δ_C (CDCl$_3$, 75.5 MHz) 171.5–163.9 (5 *C*O)], 89.8 (*C*H, anomeric resonance), 73.0–68.1 (4 *C*H), 62.5 (*C*H$_2$), 55.3–54.4 [5 *C*(CH$_3$)$_2$Br], 30.73–30.07 (10 (*C*H$_3$)$_2$Br); calc. for C$_{26}$H$_{37}$Br$_5$O$_{11}$: C 33.76; H 4.03%. Found: C 34.00; H 4.09%.

15.3.3.4.2   Synthesis of a 5-Arm Star Polymer Based on a Glucose Core

Reagents

1,2,3,4,6-Pentakis-*O*-2′-bromoisobutyrate-D-glucose	0.173 g
N-(*n*-pentyl)-2-pyridylmethanimine	0.347 g
CuBr	0.135 g

Toluene	10 mL
MMA	10 mL

Procedure   To a Schlenk tube was added 0.173 g of 1,2,3,4,6-pentakis-*O*-2′-bromoisobutyrate-D-glucose 0.347 g of *N*-(*n*-pentyl)-2-pyridylmethanimine, 10 mL of toluene, and 10 mL of MMA. The solution was freeze–pump–thawed 3 times. After this, 0.135 g of CuBr was added to the frozen solution, the flask was pump-thawed and subsequently freeze–pump–thawed for a final time. The flask was then placed in an oil bath at 90°C. The final polymer was precipitated into 40/60 petroleum spirit.

15.3.3.4.3   Hydrolysis of the Core of Polystyrene Star Polymers to Linear Polymers

Reagents

THF	30 mL
Water	1 mL
Ethanol	9 mL
KOH	2 g
Polystyrene star polymer	0.6 g

Procedure   Where polystyrene star polymers are prepared it is often informative to hydrolyze the core so that the linear arms may be analyzed be SEC. This can be carried out as follows. The polystyrene star polymer (0.6 g) was refluxed for 3 days in a solution of THF (30 mL), ethanol (9 mL), and water (1 mL) with 2 g of KOH. The final product was obtained by precipitation into water.

15.3.3.5   Synthesis of Block Copolymers Using Sequential Monomer Addition
In order to synthesise a true block copolymer by sequential monomer addition, it is necessary to prepare a macroinitiator. In anionic polymerization the normal practice would be to take a polymerization to high conversion prior to addition of the second monomer. However, in all types of living radical polymerization there will be significant termination by either disproportionation and/or combination, which increases at high conversion as the rate of propagation slows as a result of monomer depletion. A common way to circumvent this is to stop a polymerization at relatively low conversion (e.g., 70–90%) conversion to isolate the product by precipitation and other means and to then use this as a macroinitiator for a subsequent polymerization reaction. If the monomer is added directly into the first stage, then gradient copolymers are formed which themselves have some very interesting properties.[62]

15.3.3.5.1   Synthesis of Poly(n-butyl methacrylate)-block-poly(N,N-dimethylethylamino methacrylate)

15.3.3.5.1.1   SYNTHESIS OF POLY(N-BUTYL METHACRYLATE) A BLOCK

Reagents

Toluene	
n-butyl methacrylate (*n*-BMA)	

4-methoxyphenyl 2′-bromoioiobutyrate[63]
N-(n-propyl)-2-pyridylmethanimine
Basic alumina

Procedure P(n-BMA) macroinitiators were prepared in toluene (66% v/v) at 90°C. Purified n-BMA was degassed by bubbling dry nitrogen through it for 30 min just before polymerizations. Monofunctional macroinitiator was made using [n-BMA]/[4-methoxyphenyl 2′-bromoisobutyrate]/[CuBr]/[N-(n-propyl)-2-pyridyl-methanimine] = 32/1/1/2, The reactions were stopped after a suitable time. The products were isolated by passing through a column of basic alumina, precipitation in cold methanol, and drying under vacuum. Proporties: $M_n = 5100$, $M_w/M_n = 1.17$ (SEC, PMMA standards)

N-(n-propyl)-2-pyridylmethanimine
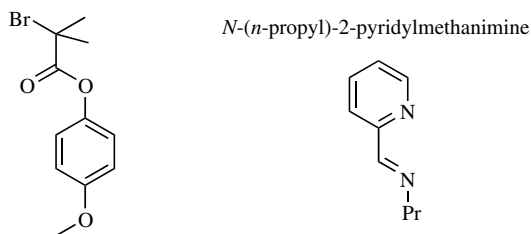
4-Methoxyphenyl-2′ bromo-2′-bromoisobutyrate

15.3.3.5.1.2 SYNTHESIS OF AB BLOCK COPOLYMER

Procedure DMAEMA was polymerized in the presence of the three P(n-BMA) macroinitiators in toluene using Cu^{I}Br complexed by N-(n-propyl)-2-pyridylmetha-nimine as catalyst. Purified DMAEMA was deoxygenated by three freeze–pump–thaw cycles just before injection into reaction vessels. The block copolymers obtained were purified by passing through a column of basic alumina, and drying under vacuum, and unreacted low molecular weight P(n-BMA) was removed by Soxhlet extraction using hexane as solvent. The final product was dried under reduced pressure for 24 h. Properties: $M_n = 15,900$, $M_w/M_n = 1.60$ (SEC, PMMA standards).

15.3.3.6 Synthesis of block copolymers using macroinitiators As most hydroxyl functional compounds may be converted into initiators for transition-metal-mediated polymerization by esterification this gives a facile route into AB and ABA copolymers. Many commercially produced polymers have either one or both termini hydroxyl functional, such as polymers from ring-opening polymerization (polyethers,[64] polylactones, etc.), condensation polymerization (polyurethanes, polyesters, etc.) and other specially prepared polymers, such as polybutadiene[65] and polysiloxanes.[66] This versatile method is becoming an increasingly popular method to synthesize a range of interesting molecules. Thus far nearly all commercially produced hydroxyl functional polymers have been utilized in this way. We have

chosen to include just one example where an ABA block is synthesized from a dihydroxyl functional poly(ethylene glycol). This approach avoids the inherent termination that complicates sequential monomer addition and is the approach always used in our laboratory if at all possible.

15.3.3.6.1 Synthesis of 2-Bromoisobutyryl Poly(ethylene glycol) Macroinitiator $M_n = 1000$

Reagents

Polyethylene glycol (PEG 1000)	20.33 g
Tetrahydrofuran	250 mL
Triethylamine	6.8 mL
2-Bromoisobutyryl bromide	5.5 mL
Na_2CO_3 solution	
Dichloromethane	
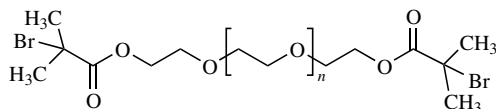
Procedure   Poly(ethylene glycol) (PEG 1000) 20.33 g (~0.02 mol) and 250 mL tetrahydrofuran (THF) (freshly distilled from sodium/benzophenone) were added to a oven, dried nitrogen-flushed 250 mL round-bottomed flask. Triethylamine, 6.8 mL (0.048 mol), was added to the solution and was allowed to stir to ensure mixing. 2-Bromoisobutyryl bromide 5.5 mL (0.044 mol) was slowly added to the mixture, triethylammonium bromide (TEABr) was formed as a white precipitate, and the reaction was left to react for 14 h. The TEABr was removed by filtration and the THF was removed by rotary evaporation, and the liquid products were dissolved in 150 mL of dichloromethane, and this solution was washed with 3×50 mL of saturated Na_2CO_3 solution. The dichloromethane layer was dried with $MgSO_4$, and the solution was filtered and the solvent removed under reduced pressure to give a pale yellow viscous liquid. The product was placed in a vacuum oven at 60°C for 2 days to remove any traces of residual dichloromethane. Yield 25.4 g.

Spectral Data ^{1}H NMR (CDCl$_3$, 298 K, 250.13 MHz) 3.69 (t, $J = 4.9$ Hz 4 H), 3.59 (m, 78 H) 1.89 (s, 12 H): ^{13}C{^{1}H} NMR (CDCl$_3$, 298 K 100.6 MHz) IR (liquid, ATR cell) 2865, 1733 (C=O), 1462, 1348, 1276, 1096, 947, 853, 748.

15.3.3.7   ATRP of N,N-Dimethylacrylamide (DMAA) Using a RuCl$_2$(PPh$_3$)$_3$ as Catalyst[67]   Although many monomers have been reported to be polymerized successfully by ATRP, the acrylamides and meth(acrylamides) have been reported to be problematic by both Brittain[68] and Matyjaszewski.[69] An alternative approach is the use of non-copper based systems as described by Sawamoto. This is probably as the amide functionality of the acrylamide is a good coordinator for copper(I) but less so for ruthenium, where the phosphine ligands are more strongly coordinated.

Reagents

RuCl$_2$(PPh$_3$)$_3$	0.098 g
Al(Oi-Pr)$_3$	0.084 g
Ethyl 2-bromoisobutyrate	0.040 g
Toluene	1 mL
DMAA	2.13 mL

Procedure   All preparations were carried out under dry nitrogen, and each solution was degassed individually by several freeze–pump–thaw cycles. RuCl$_2$(PPh$_3$)$_3$ (0.098 g) was dissolved with toluene (4.3 mL) in a Schlenk tube. DMAA (2.13 mL) was then added to this. Al(Oi-Pr)$_3$ (0.084 g) was dispersed in toluene (3.2 mL) and then degassed. Another solution of ethyl-2-bromoisobutyrate (0.040 g) in toluene (1 mL) was prepared in the same way, and then these two solutions were added sequentially in this order to the first solution. The solution was placed in an oil bath at 80°C. The polymerization was terminated after 5 h, by which time 90% conversion had been achieved, and monomer conversion was determined by ^{1}H NMR. The quenched reactions were purified by passing over basic alumina and then evaporated to dryness to give a brown solid product.

15.3.4   Reversible Addition–Fragmentation Chain Transfer (RAFT)

The CSIRO group showed that LRP system can be achieved on the basis of the principle of reversible addition fragmentation reactions. One of the first systems reported was based on nonhomopropagating methacrylate macromonomers. They reported the synthesis of poly(2-ethylhexylmethacrylate)-*block*-poly(methyl methacrylate) having a narrow molar mass distribution using a MMA macromonomer as chain transfer agent in emulsion polymerization, while adding 2-ethylhexyl methacrylate under starved feed conditions.[70]

The concept of reversible addition–fragmentation in the development of living radical polymerization techniques requires the use of efficient chain transfer agents. These were found in two forms of dithioesters, dithiocarbamates, xanthates, and trithiocarbonates.[4]

RAFT as a living radical polymerization technique looks promising, especially since controlled chain growth of vinyl acetate and its VEOVA analogs can be accomplished, which has not prove possible with other LRP techniques.

15.3.4.1   Synthesis of 4-Cyano-4((thiobenzoyl)sulfanyl)pentanoic Acid
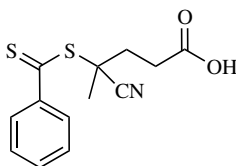
4-Cyano-4((thiobenzoyl)sulfanyl)pentanoic acid

Reagents

Bromobenzene	125.6 g
Magnesium turnings	20 g
THF dist.	600 mL
Anhydrous carbon disulfide	61 g
Iodine crystals	
Concentrated HCl, aqueous	
Dichloromethane	
Ethyl acetate	200 mL
Dimethylsulfoxide	53 g
4,4′-Azobis(4-cyanopentanoic acid)	132 g

Step 1: Synthesis of Dithiobenzoic Acid. This Grignard reaction was carried out under anhydrous conditions. A three-necked 2-L round-bottomed flask was fitted with two 500-mL dropping funnels and a thermometer. Then 100 mL of THF, a few crystals of iodine, and 20 g of magnesium turnings were charged into the round-bottomed flask, and 500 mL of THF was charged into one of the dropping funnels, while the other dropping funnel was filled with 125.6 g of bromobenzene. Approximately 10% of the bromobenzene was gently let into the reaction flask, which was carefully warmed until the reaction started (e.g., using a heat gun). Both bromobenzene and THF were added at such a rate that the temperature remained between 30 and 35°C. Excessive heat was removed via cooling with an ice bath. On completion of addition, the mixture was left to stir until completion of reaction, that is, no heat production. The mixture was allowed to reach room temperature, after which 50 mL of water was added slowly to neutralize the Grignard compound. The mixture was concentrated by removal of the solvent with a rotary evaporator, diluted with water, filtered to remove insoluble magnesium salts, and subsequently treated with concentrated HCl(aq) until the brown color had disappeared into a pink aquous layer and a purple oily layer of pure dithiobenzoic acid remained. The aqueous layer was extracted twice with dichloromethane, and the combined organic layers were put on a rotary evaporator in order to remove the dichloromethane. This yielded pure dithiobenzoic acid. Note that this compound is not stable on storage and should be transformed into its bis(thiobenzyl)disulfide derivative as soon as possible.

Step 2: *Synthesis of Bis(thiobenzyl)disulfide*. In this procedure 208 g of dithiobenzoic acid was mixed with 200 mL of ethyl acetate. A few crystals of iodine were added to the solution, and next 53 g of dimethylsulfoxide was added dropwise while stirring the mixture at room temperature. The mixture was kept in the dark overnight. The raw product was obtained in 90% yield by removal of ethyl acetate with a rotary evaporator. Recrystallization can be performed in ethanol.

Step 3: *Synthesis of 4-cyano-4((thiobenzoyl)sulfanyl)pentanoic Acid*. In this procedure 103 g of bis(thiobenzyl)disulfide and 132 g of 4,4′-azobis(4-cyanopentanoic acid) were dissolved in ethyl acetate (degassed prior to use by purging with

nitrogen) under an argon atmosphere. The mixture was refluxed for 30 min, after which time it was stirred overnight at 70°C. Next, ethyl acetate was removed under reduced pressure. The raw product was dissolved in a small amount of dichloromethane. Purification was done by column chromatography on silica gel. Eluent pentane : heptane : ethyl acetate (1 : 1 : 2). Product is red solid 65% yield, mp 94°C.

15.3.4.2 Reversible Addition Fragmentation Chain Transfer Polymerization of Styrene Using Cumyl Dithiobenzoate (CDB) as the RAFT Agent

Reagents

Styrene	10 mL
Cumyl dithiobenzoate (CBD)	6.8 mg

Procedure   First, 6.8 mg of cumyl dithiobenzoate (CDB, 2.5×10^{-3} mol L^{-1}) was placed in a 25-mL round-bottomed flask and mixed with 10 mL of purified styrene. Styrene was purified by passing over a column of basic alumina. The round-bottomed flask was then sealed with a rubber septum. The light violet reaction solution is subsequently purged for 15 min in a light argon or nitrogen stream (4.0). After purging, the reaction flask is placed in a water bath at 60°C for 24 h. After the 24 h have passed, the reaction vessel is placed into an ice bath and cooled to room temperature. The reaction mixture is subsequently slowly poured under stirring into a large excess of methanol (200 mL). The light pink polymer is collected by filtration and dried at 40°C in a vacuum oven. SEC analysis of the resulting polymer indicates the formation of narrowly distributed material ($M_w/M_n = 1.13$) of a weight average molecular weight $M_w = 77,000$ g/mol.

REFERENCES

1. D. H. Solomon, E. Rizzardo, and P. Cacioli, U.S. Patent 4,581,429 (1985).
2. M. Kato, M. Kamigaito, M. Sawamoto, and T. Higashimura, *Macromolecules* **28**, 1721–1723 (1995).
3. J. S. Wang and K. Matyjaszewski, *J. Am. Chem. Soc.* **117**, 5614 (1995).
4. PCT Int. Appl. Wo 9801478 A1 980115; *Chem. Abstr.* **128**, 115390 (1998).
5. F. R. Mayo, *J. Am. Chem. Soc.* **90**, 1289 (1968).
6. Y. K. Chong, E. Rizzardo, and D. H. Solomon, *J. Am. Chem. Soc.* **105**, 7761 (1983).
7. W. C. Buzanowski, J. D. Graham, D. B. Priddy, and E. Shero, *Polymer* **33**, 3055 (1992).
8. Y. Kotani, M. Kato, and M. Kamigaito, *Macromolecules* **29**, 6979 (1996).
9. A. W. Hui and A. E. Hamielec, *J. Appl. Polym. Sci.* **16**, 749 (1972).
10. A. Rudin, *The Elements of Polymer Science and Engineering*, Academic Press, New York, 1982.
11. G. Odian, *Principles of Polymerization*, 2nd ed., Wiley, New York, 1981.
12. M. Dube, R. A. Sanayei, A. Penlidis, K. F. O'Driscoll, and P. M. Reilly, *J. Polym. Sci.; Part A: Polym. Chem.* **29**, 703 (1991).
13. P. W. Tidwell and G. A. Mortimer, *J. Polym. Sci., Polym. Chem.* **3**, 369 (1965).

14. B. G. Manders, W. Smulders, A. M. Aerdts, and A. van Herk, *Macromolecules* **30**, 322 (1997).

15. C. Jégat, A. Bois, and M. Camps, *J. Polym. Sci.; Part B: Polym. Phys.* **39**, 201 (2001).

16. W. H. Li and H. D. H. Stöver, *J. Polym. Sci.; Part A: Polym. Chem.* **36**, 1543 (1998).

17. W. H. Li and H. D. H. Stöver, *Macromolecules* **33**, 4354 (2000).

18. R. G. Gilbert, *Emulsion Polymerization*; Academic Press, San Diego, 1995.

19. C. C. Co, P. Cotts, S. Burauer, R. D. Vries, and E. W. Kaler, *Macromolecules* **34**, 3245–3254 (2001).

20. T. Otsu and M. Yoshida, *Makromol. Chem., Rapid Commun.* **3**, 127 (1982).

21. T. Otsu, M. Yoshida, and T. Tazaki, *Makromol. Chem., Rapid Commun.* **3**, 433 (1983).

22. T. Otsu and T. Tazaki, *Polym. Bull.* (*Berlin*) **16**, 277 (1986).

23. B. B. Wayland, G. Poszmik, and S. L. Mukerjee, *J. Am. Chem. Soc.* **116**, 7943 (1994).

24. B. B. Wayland, L. Basickles, S. Murkerjee, M. Wei, and M. Fryd, *Macromolecules* **30**, 8109 (1997).

25. J. D. Druliner, *Macromolecules* **24**, 6079 (1991).

26. D. M. Haddleton, M. C. Crossman, B. H. Dana, D. J. Duncalf, A. M. Heming, D. Kukulj, and A. J. Shooter, *Macromolecules* **32**, 2110 (1999).

27. J. S. Wang and K. Matyjaszewski, *Macromolecules* **28**, 7901 (1995).

28. M. Sawamoto and M. Kamigaito, *Trends Polym. Sci.* **4**, 371 (1996).

29. M. Destarac, D. Charmot, X. Franck, and S. Z. Zard, *Macromol. Rapid Commun.* **21**, 1035–1039 (2000).

30. K. Matyjaszewski, S. Gaynor, and J.-S. Wang, *Macromolecules* **28**, 2093 (1995).

31. G. Moad, L. C. Moad, J. Krstina, E. Rizzardo, C. T. Berge, and T. R. Darling, WO/9615157 (1996).

32. A. Gridnev, *J. Polym. Sci.; Part A: Polym. Chem.* **38**, 1753 (2000).

33. T. P. Davis, D. Kukulj, D. M. Haddleton, and D. R. Maloney, *Trends Polym. Sci.* **3**, 365 (1995).

34. T. P. Davis, D. M. Haddleton, and S. N. Richards, *J. Macromol. Sci., Rev. Macromol. Chem. Phys.* **C34**, 243 (1994).

35. A. F. Burczyk, K. F. Odriscoll, and G. L. Rempel, *J. Polym. Sci.; Part A: Polym. Chem.* **22**, 3255 (1981).

36. A. A. Gridnev, S. D. Ittel, M. Fryd, and B. B. Wayland, *Organometallics* **12**, 4871 (1993).

37. A. H. Janowicz, L. R. Melby, and S. D. Ittel, Eur. Patent EP196783 (1986).

38. G. Moad, L. C. Moad, J. Krstina, E. Rizzardo, S. H. Thang, and M. Fryd, WO96/15158 (1996).

39. D. Kukulj, T. P. Davis, and R. G. Gilbert, *Macromolecules* **30**, 7661–7666 (1997).

40. K. G. Suddaby, D. R. Maloney, and D. M. Haddleton, *Macromolecules* **30**, 702 (1997).

41. K. G. Suddaby, D. M. Haddleton, J. J. Hastings, S. N. Richards, and J. P. O'Donnell, *Macromolecules* **29**, 8083 (1996).

42. S. G. Yeates and S. N. Richards, *Surf. Coat. Int.* **10**, 437 (1996).

43. D. M. Haddleton, D. R. Maloney, K. G. Suddaby, A. V. G. Muir, and S. N. Richards, *Macromol. Symp.* **111**, 37 (1996).

44. M. K. Georges, R. P. N. Veregin, H. Kazmaier, and G. K. Hamer, *Macromolecules* **26**, 2987 (1992).

45. P. D. Bartlett, E. P. Benzing, and R. E. Pincock, *J. Am. Chem. Soc.* **82**, 1762 (1960).

46. W. A. Pryor, E. H. Morkved, and H. T. Bickley, *J. Org. Chem.* **37**, 1999 (1972).

47. E. Niki, C. Decker, and F. R. Mayo, *J. Polym. Sci.; Part A: Polym. Chem.* 2813 (1973).

48. E. Niki and Y. Kamiya, *J. Am. Chem. Soc.* **96**, 2129 (1974).

49. S. A. F. Bon, M. Bosveld, B. Klumperman, and A. L. German, *Macromolecules* **30**, 324 (1997).

50. K. Matyjaszewski, J.-L. Wang, T. Grimaud, and D. A. Shipp, *Macromolecules* **31**, 1527 (1998).

51. T. E. Patten and K. Matyjaszewski, *Acc. Chem. Res.* **32**, 895 (1998).

52. V. Percec, H. J. Kim, and B. Barboiu, *Macromolecules* **30**, 8526 (1997).

53. V. Percec, B. Barboiu, and M. vanderSluis, *Macromolecules* **31**, 4053 (1998).

54. C. Granel, P. Teyssie, P. DuBois, and P. Jerome, *Macromolecules* **29**, 8576 (1996).

55. G. Moineau, C. Granel, P. Dubois, R. Jerome, and P. Teyssie, *Macromolecules* **31**, 542 (1998).

56. P. Lecomte, I. Drapier, P. DuBois, P. Teyssie, and R. Jerome, *Macromolecules* **30**, 7631 (1997).

57. K. Matyjaszewski, M. L. Wei, J. H. Xia, and N. E. McDermott, *Macromolecules* **30**, 8161 (1997).

58. D. M. Haddleton, M. C. Crossman, B. H. Dana, D. J. Duncalf, A. M. Heming, D. Kukulj, and A. J. Shooter, *Macromolecules* **32**, 2110 (1999).

59. J. Ueda, M. Kamigaito, and M. Sawamoto, *Macromolecules* **31**, 6762 (1998).

60. S. Angot, K. S. Murthy, D. Taton, and Y. Gnanou, *Macromolecules* **31**, 7218 (1998).

61. D. M. Haddleton, R. Edmonds, A. M. Heming, E. J. Kelly, and D. Kukulj, *N. J. Chem.* **23**, 477 (1999).

62. K. Matyjaszewski, *J. Macromol. Sci., Pure Appl. Chem.* **A34**, 1785 (1997).

63. D. M. Haddleton and C. Waterson, *Macromolecules* **32**, 8732 (1999).

64. K. Jankova, X. Y. Chen, J. Kops, and W. Batsberg, *Macromolecules* **31**, 538 (1998).

65. K. Jankova, J. Kops, X. Y. Chen, and W. Batsberg, *Macromol. Rapid Commun.* **20**, 219 (1999).

66. K. Matyjaszewski, P. J. Miller, E. Fossum, and Y. Nakagawa, *Appl. Organomet. Chem.* **12**, 667 (1998).

67. M. Senoo, Y. Kotani, M. Kamigaito, and M. Sawamoto, *Macromol. Symp.* **157**, 193 (2000).

68. J. T. Rademacher, R. Baum, M. E. Pallack, W. J. Brittain, and W. J. Simonsick, *Macromolecules* **33**, 284 (2000).

69. M. Teodorescu and K. Matyjaszewski, *Macromol. Rap. Commun.* **21**, 190 (2000).

70. J. Krstina, C. L. Moad, G. Moad, E. Rizzardo, and C. T. Berge, *Macromol. Symp.* **111**, 13–23 (1996).

16   Future Outlook and Perspectives

KRZYSZTOF MATYJASZEWSKI

Department of Chemistry, Carnegie-Mellon University, Pennsylvania, USA

THOMAS P. DAVIS

University of New South Wales, Sydney, Australia

CONTENTS

The outlook for conventional radical polymerization (RP) and controlled/''living'' radical polymerization (LRP) must take into account the current importance of RP but should also recognize developments in competing mechanisms of polymerization. Currently, RP is the most common method of making polymers, responsible for nearly 50% of all synthetic polymers. However, there is a constant pressure from coordination processes that are very well suited for olefin polymerization, especially in the preparation of stereoregular polymers. There has also been an increasing pressure from techniques that offer macromolecular control superior to conventional RP. Here, anionic polymerization, cationic polymerization and metathesis must be cited. These processes can be utilized to prepare unique (co)polymers with controlled composition, functionality and topology. Commercial products such as Kraton, i.e. polystyrene-*block*-polybutadiene-*block*-polystyrene may serve as a best example. Some new well-defined (co)polymers prepared via carbocationic methods have been recently introduced to the market. It took more than 15 years to reach commercialization since the discovery of ''living'' carbocationic polymerization. It is believed that the time from discovery of LRP to its commercialization will be much shorter. In fact there are already commercial products from catalytic

chain transfer (CCT) processes and it is anticipated that both nitroxide mediated polymerization (NMP) and atom transfer radical polymerization (ATRP) will be commercialized in 2002. Similarly, radical addition fragmentation chain transfer (RAFT) and other degenerative transfer processes can find many applications. Initial applications may be related to specialty products, such as coatings, adhesives, additives and materials for electronics and health/beauty products.

The renaissance of research in RP and LRP since the early 1990s has been fuelled by the prospect of making novel materials from established (and often cheap) building blocks. This approach often avoids excessive health and safety regulation and enables the development of new processes with minimum investment in plant and infrastructure. These drivers will still propel polymerization research into the next decade with control over a number of key areas elusive at present. Certainly a major goal remains increased stereocontrol over the propagation step and the ability to utilize kinetics to suppress or enhance propagation, termination or transfer relative to each other. LRP techniques are synthetic approaches that allow minimization of the bimolecular termination reaction but with some concomitant loss in rate, and refinement to minimize the loss of rate would be a significant improvement over the current synthetic methods. Enhancement of propagation relative to transfer would enable improvements both in LRP and RP systems.

This handbook covers fundamental information on conventional and controlled radical polymerization. It summarizes the state of art as of early 2001 with the appropriate literature citations till the end of 2000. What will happen in the future, what are remaining challenges for both RP and LRP systems?

16.1 RADICAL POLYMERIZATION

Despite seventy odd years of research and application of RP there still remains significant gaps in understanding. This can be largely attributed to the complexity of the chain process and the resulting elaborate mixture of products. A key to enhanced understanding of RP lies in the development of improved analytical techniques and new methods for evaluating kinetic parameters together with enhanced modeling procedures. Clearly, without improved understanding of RP the comprehension of LRP will be limited. It is also clear that by achieving better control over RP then enhanced processes and products can be achieved without recourse to LRP. This is best illustrated by an example from the CSIRO group[1] who used the backbiting reaction in acrylate polymerization at elevated temperatures to make macromonomers with terminal unsaturation. In what follows some personal insights are offered into the prospects for improved understanding of RP and possible improvements of control over processes and products in the next 5–10 years.

16.1.1 Initiation and Propagation

The process of initiation is fairly well understood. New initiation systems for specific applications are still being developed. New visible light systems are increasingly

required for specialist applications such as dental resins and lithography. The drive for new light initiated systems remains strong.

The process of propagation has seen a step change in understanding since the development of pulsed–laser polymerization by Olaj and colleagues in 1985–1987.[2,3] This technique whilst a vast improvement over the rotating sector experiment is still limited by the complexity of molecular weight analysis. Size exclusion chromatography is a mature technique and the columns have become almost commodity items (though too expensive) with little difference between the commercial suppliers. This means that the information extractable from the molecular weight distribution is limited by the analytical technique as the limits of resolution appear to have been reached using conventional gel packing. In addition the ability to measure absolute molecular weights by coupling with light scattering and viscometry detectors seems severely hampered by the difficulty in achieving simple and robust analyses. Any researcher who has been drawn into the purchase of these detectors will have been stung by the difficulty in achieving reliable results. The evidence is that only those groups that have made large investments of time and money have been able to acquire the expertise to utilize these detectors effectively.

It is clear that the need for a wider variety of propagation rate coefficients and their temperature dependencies is still required but the limited number of groups in the world with the equipment and expertise will limit the production of data over the next few years. Information is particularly sparse for copolymerization where the only Arrhenius parameters published across different comonomer feeds are for the 'fruit-fly' system of styrene/methyl methacrylate.[4] Historical evidence has already shown that the severe shortage of accurate kinetic data for copolymerization reactions resulted in significant ambiguity over copolymerization mechanism—this has only been resolved in recent years, with much more understanding over the complexity of the copolymerization process.[5,6]

Therefore future gains in understanding will be limited until enhanced resolution and detection–calibration can be developed. The advent of mass spectrometric methods still seems to offer the best prospects for overcoming the limitations of MWD analyses. Both MALDI and ESI methods offer improvements in both areas. However, these techniques are limited by a nonlinear detector response and the limited mass ranges for polydisperse samples. Despite this we believe that the use of rapidly pulsed lasers coupled with mass spectrometry will lead to significant understanding of initiation and propagation processes in the near future. Very fast pulsing can lead to control over initiation and termination reactions resulting in the generation of low molecular weight chains that can be resolved on current mass spectrometer instrumentation. The insertion of 'temporal markers' into chains using UV-lasers will allow for the design of new elegant methods of measuring rate coefficients.

The ESR method also has made limited advances over the last 15 years and it seems unlikely that enhanced measurement or calibrations will become available. In contrast the rapid rise in computational power and resources will underpin new strength in applying ab initio methods to RP processes. The potential power of this approach is clear from Chapter 1 and we would expect considerable advances in the use of these methods in near future. However, the complexity of radical chain

reactions and their sensitivity to media effects will always limit the applicability of ab initio methods. As with all approaches, awareness of limitations will be important in the application of comprehension achieved using such theoretical approaches.

16.1.2   Termination

The termination reaction is highly complex as it is sensitive to medium and chain-length effects. However, the single-pulse methods of analysis pioneered by Buback and his team[7] has led to a vast improvement of understanding and a wealth of kinetic data. Well-defined polymers prepared by LRP can be helpful in determining chain length dependence of termination. Once again the only limitation to insight will be the limited number of researchers equipped to undertake such work. Techniques for evaluating the disproportionation versus combination reaction have been less forthcoming and as pointed out by Moad and Solomon there is only limited information available.[8] It may be that increasing magnet strength of NMR and mass spectrometry will allow for some progress in this area.

16.1.3   Variation of selectivities in RP

Free radicals have limited selectivities because of relatively small variations in their electrophilic or nucleophilic nature. They lead to polymer microstructure with low stereocontrol (tacticity) and relatively random placement of repeating units in co-polymers. However, first successful attempts for controlling these parameters have been already reported (see Chapter 13) and are expected to continue to provide polymers with new properties. This could be accomplished by selective complexation, template synthesis, or polymerization in confined space. Probably LRP may give addition handle to control these systems by slowing down the chain growth.

16.2   CONTROLLED/"LIVING" RADICAL POLYMERIZATION

In LRP, future developments will require continuous research and correlation of structures and reactivities of the involved reagents.[9–13] This should include model and real macromolecular studies. Available information on how structure of nitroxides and the corresponding alkoxyamines affect the thermodynamics and kinetics of exchange reactions has been discussed in Chapters 9 and 10; similarly structure of alkyl halides and several organometallic complexes were correlated with their activities in Chapter 11; as well as structure of dithioesters, unsaturated esters and alkyl iodides in Chapter 12. More detailed information of this type is needed to extend the range of polymerizable monomers and reaction conditions, to increase selectivities of polymerization versus side reactions and prepare a variety of new materials.

The search for more efficient, selective and commercially more feasible reagents will continue. There are many unexplored areas. New stable free radicals may show better selectivities and reduced transfer–disproportionation in polymerization of methacrylates, new dithioesters may show lower retardation effects when low

MW oligomers are targeted. New more efficient ATRP catalysts may enable to reduce the amount of transition metals, their recovery and recycling.

At the same time, careful correlation of structure of new (co)polymers including their topologies, functionalities, and compositions as well as their uniformity (i.e. polydispersity) with macroscopic properties is urgently needed. Several of these novel materials have been reviewed in Chapter 14. Some of the new materials behave in the unexpected way and a comprehensive study of the effect of macromolecular structure on properties of the targeted materials is needed. This study may also include processing, since the properties depend on mechanical and thermal history, stresses, solvent removal, etc. The synthetic simplicity of LRP may offer a large number of samples which must be carefully studied to reach such a comprehensive correlation.

We realize that LRP is not a true living polymerization and there are always termination reactions which limit efficiency of blocking, end functionalities, etc. What is the effect of these and other side reactions on the properties? This still remains to be established.

There are a few important issues in LRP which have not yet been adequately addressed and may be easier approached in conventional RP systems. We just cite some of the most important points:

- How to increase k_p/k_t ratios? This would increase selectivities of propagation and allow to carry out LRP at a much faster rates. Perhaps both k_p and k_t should be separately studied. This area is clearly coupled with the earlier section on RP and enhanced understanding of the propagation process.

- What is the effect of chain length and viscosity on these rate constants? Can we change them in compartmentalized systems such as (micro/mini)-emulsions, zeolites or other inclusion complexes? In addition the use of RP and LRP in media such as supercritical and ionic liquids may result in new avenues for control.

- How charge on monomer and polymer units will affect them? How complexation with specific solvents and additives can affect not only these rate constants but even influence their chemo- and stereoselectivities? RAFT synthesis of well defined alternating copolymer of styrene and methyl methacrylate in the presence of Lewis acids by may serve here as a recent example.[14]

- Can exchange reactions enhance possibility to prepare stereoregular polymers?[15] Can chiral nitroxides or transition metal complexes with chiral ligand cleave selectively dormant species and affect stereo and chemoselectivities? Can slower rate of polymerization increase fidelity of the template synthesis?

- Can we increase chemoselectivity of olefin polymerization and compete with metallocene and Ziegler–Natta systems? Or if not, how can we combine polyolefins with polyacrylates and other polar monomers prepared by RP.

Perhaps not all of these questions will find positive answers in the next decade but we believe that they will stimulate broad research in RP and LRP and will provide

many avenues to new exciting materials. Therefore, continuation of fundamental kinetic, mechanistic and broad spectrum of characterization studies is required to reach these ambitious goals. The current renaissance of radical polymerization and the exponential increase of interest in this field owes to but also needs more fruitful collaborations of synthetic polymer chemists with theoreticians, organic chemists, inorganic/coordination chemists, kineticists, physical organic chemists, polymer physical chemists, physicists and engineers. We hope that this handbook will help to reach these goals and will stimulate further research and collaborative efforts.

REFERENCES

1. J. Chiefari, J. Jeffery, R. T. A. Mayadunne, G. Moad, E. Rizzardo, and S. H. Thang, *Macromolecules* **32**, 7700 (1999).

2. O. F. Olaj, I. Bitai, and F. Hinkelmann, *Makromol. Chem.* **188**, 1689 (1987).

3. O. F. Olaj, I. Bitai, and G. Gleixner, *Makromol. Chem.* **186**, 2569 (1985).

4. M. L. Coote, L. P. M. Johnston, and T. P. Davis, *Macromolecules* **30**, 8191 (1997).

5. M. L. Coote and T. P. Davis, *Prog. Polym. Sci.* **24**, 1217 (1999).

6. T. P. Davis, *J. Polym. Sci; Part A: Polym. Chem.* **39**, 597 (2001).

7. S. Beuermann and M. Buback, *Prog. Polym. Sci.* **27**, 191 (2002).

8. G. Moad and D. H. Solomon, The Chemistry of Free Radical Polymerization; Pergamon: Oxford, 1995.

9. H. Fischer, *Chem. Rev.* **101**, 3581 (2001).

10. C. J. Hawker, A. W. Bosman, and E. Harth, *Chem. Rev.* **101**, 3661 (2001).

11. K. Matyjaszewski and J. Xia, *Chem. Rev.* **101**, 2921 (2001).

12. M. Kamigaito, T. Ando, and M. Sawamoto, *Chem. Rev.* **101**, 3689 (2001).

13. G. Moad, J. Chiefari, Y. K. Chong, J. Krstina, R. T. A. Mayadunne, A. Postma, E. Rizzardo, and S. H. Thang, *Polym. Int.* **49**, 993 (2000).

14. B. Kirci, J. Lutz, and K. Matyjaszewski, *Macromolecules* **35**, 2448 (2002).

15. T. Nakano and Y. Okamoto, *Chem. Rev.* **101**, 4013 (2001).

INDEX